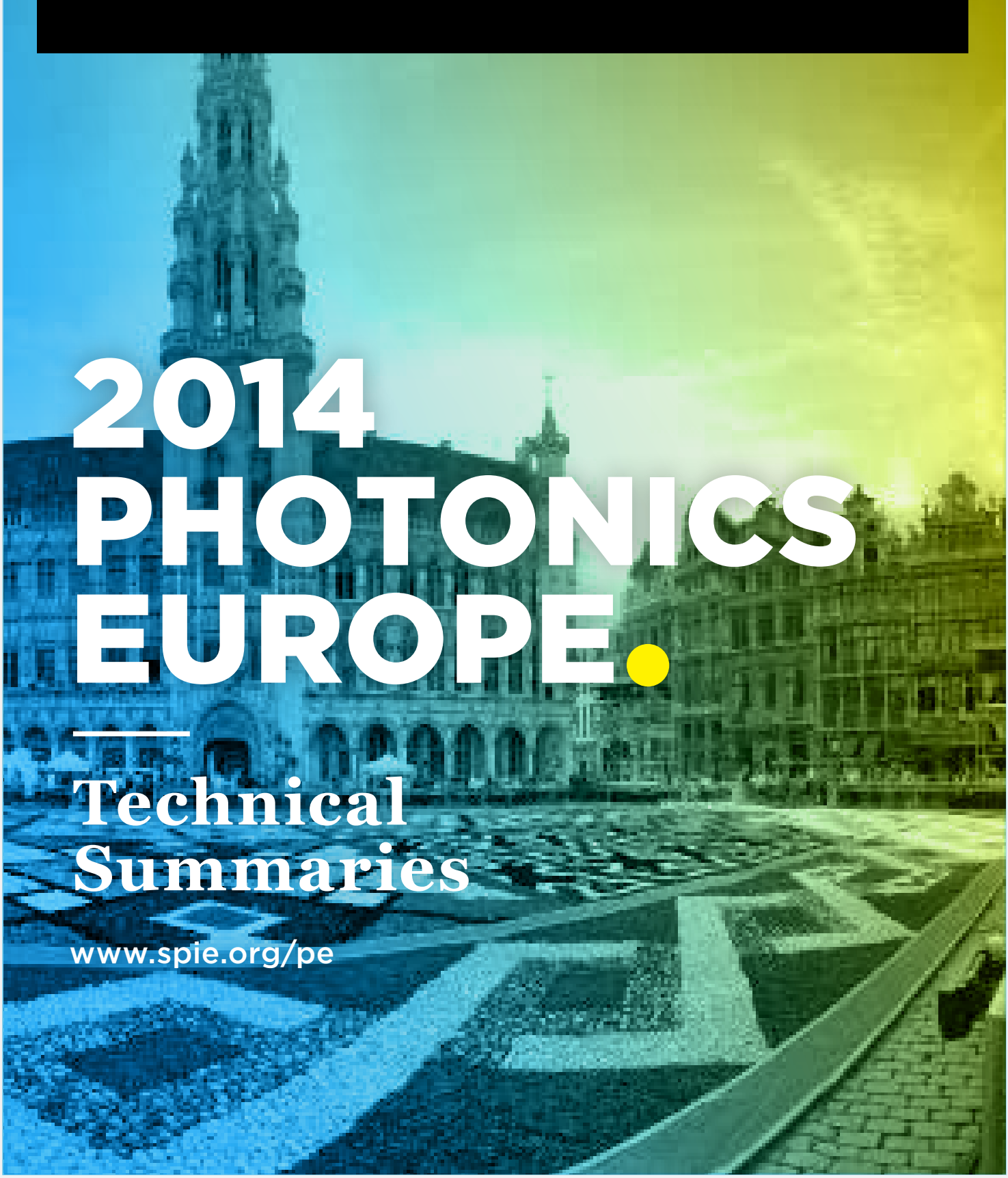

2014 PHOTONICS EUROPE.

Technical Summaries

www.spie.org/pe

SQUARE Brussels Meeting Centre
Brussels, Belgium

Exhibition: 15–16 April 2014

Conferences & Courses: 14–17 April 2014

SPIE. PHOTONICS EUROPE

GENERAL CHAIRS

Francis Berghmans
Vrije Univ.
Brussel (Belgium)

Ronan Burgess
European Commission Joint Research Ctr.
(Belgium)

Jürgen Popp
Institute of Photonic Technology Jena e.V. (Germany)

Peter Hartmann
Schott AG
(Germany)

HONORARY CHAIR

Hugo Thienpont
Vrije Univ.
Brussel (Belgium)

This programme is current as of
1 FEBRURAY 2014
See latest updates online:
www.spie.org/peconf

Registration fees increase after
16 MARCH 2014

Contents.

MANAGED BY
SPIE.EUROPE

SPIE Europe Ltd., a subsidiary of SPIE, is a not-for-profit UK-registered company serving SPIE constituents throughout Europe as an advocate and liaison to political and industry associations within the European optics and photonics community.

In addition to providing membership services, SPIE Europe Ltd. organises and manages internationally recognised conferences, education programmes, and technical exhibitions featuring emerging technologies in optics and photonics.

SPIE Europe
2 Alexandra Gate
Ffordd Pengam,
Cardiff, CF24 2SA
Tel: +44 29 2089 4747
Fax: +44 29 2089 4750
info@spieeurope.org

9125-1, Session 1

Enabling nanophotonics with plasmonics and metamaterials *(Keynote Presentation)*

Vladimir M. Shalaev, Purdue Univ. (United States)

Manipulating and controlling photons on nanoscale needed for the nanophotonic circuitry and other important applications requires novel plasmonic metamaterials with unique properties. Recent progress in the development of optical metamaterials allows unprecedented control over the flow of light on the nanoscales. Metamaterials (MMs) are rationally designed artificial materials with versatile properties that can be tailored to fit almost any practical need and thus go well beyond what can be obtained with “natural” materials. We review the exciting field of optical metamaterials and discuss the recent progress in developing tunable and active MMs, nanolasers, artificial optical magnetism, semiconductor-based and loss-free negative-index MMs, and a new means for engineering the photonic density of states with MMs. New plasmonic materials with superior properties based on transparent conducting oxides and ceramics will be also discussed. Finally, we review a new approach for controlling light by using meta-surfaces. Similar to the surface science that in the past revolutionized the physics and open up a family of new phenomena and applications unattainable with 3D systems, we envision that metasurfaces can make a difference for the fields of metamaterials and transformation optics as well as for the science of light in general.

9125-2, Session 1

Metamaterials with quantum gain *(Invited Paper)*

Ortwin Hess, Imperial College London (United Kingdom)

Optical metamaterials and nanoplasmonics offer extreme control and localization of light within nanovolumes that can be thousands of times smaller than a cubic light wavelength, but they suffer from significant dissipative losses. This weakness has been well appreciated for decades and it is thought to constitute the prime impediment before many of the envisaged applications can become practical for commercial products. However, recent breakthroughs in the theoretical understanding and experimental fabrication of gain-enhanced metamaterials and nanoplasmonic heterostructures, promise to overcome these hindrances, while allowing for new ways to control spontaneous and stimulated emission on the nanoscale [1, 2].

Ohmic losses in nanoplasmonic metamaterials arise from the interaction of the incident photons with the quasi-free conduction electrons of the metals, thereby constituting a rather inherent feature of the response of metal-based nanodevices. For truly subwavelength plasmonic structures, these losses follow universal laws, i.e. they do not depend on the particular geometric configuration but only on the deployed (usually noble) metal. Typical damping rates are thus of the order of ? ~ 100 ps-1, requiring gain coefficients ?/c ~ 104 cm-1 to compensate for the losses [3]. Meanwhile, there is an increased emphasis on two-dimensional metasurfaces, which are much more convenient to fabricate than their full-3D metamaterial counterparts but can steer light in equally dramatic ways, well below the fundamental diffraction limit and over broad, flat areas [4]. If the gain supplied by the active medium is sufficient to overcome both, dissipative and radiative losses, the structure can function as a coherent emitter of surface plasmons over the ultrathin 2D area, deep below the diffraction limit for visible light [1, 8]. Thereby, controlling the spontaneous emission (SE) rate is crucial [9] as both bright and dark plasmonic lasing states exist, giving rise to a strong, nonlinear competition. Which one eventually dominates can be controlled by the design and excitation of the metametaterial.

These 2D active nanostructures can function as powerful on-chip light sources, either coherent (nanolasers) or incoherent (LEDs), delivering intense optical power owing to the rapid relaxations of the excited molecules that arise from the nanolocalization-enhanced local density of optical states (LDOS). We note that although the typical plasmonic cavity Q-factors are rather small (~ 50), the attained Purcell factors (Fp Q/Vm) can still be large owing to extremely small mode volumes. A major fundamental goal in the field is, by enhancing the Purcell factor, to accelerate SE to the degree that it becomes faster than stimulated emissio, so that ultrafast, low-energy light-emitting diodes (LEDs) can be attained and integrated within nanoscale circuits [10]. Large Purcell factors can also be obtained close to zero-group-velocity (ZGV) points in plasmonic slow-light heterostructures [1]. Detailed computations reveal that at well-accessed ZGV points, full lasing operation can be reached in completely uniform (minimalistic) structures that do not require a ‘cavity’ to confine light (e.g., by reflections or Bragg scattering) because successive light pulses can be stopped and strongly localised. Importantly, because at the ZGV point the laser ?-factor tends to unity (? ? 1), spontaneous emission can be efficiently funnelled into the stopped-light mode, resulting in low-threshold operation.

Refereences

1. O. Hess, et al., Nature Materials 11, 573 (2012).

2. Y.-J. Lu, et al., Science 337, 450 (2012).

3. J. B. Khurgin, G. Sun, Opt. Express 20, 15309 (2012).

4. M. A. Kats, R. Blanchard, P. Genevet, F. Capasso, Nature Materials (2012), doi:10.1038/nmat3443.

5. S . Xiao, et al., Nature 466, 735 (2010).

6. S. Wuestner, A. Pusch, K. L. Tsakmakidis, J. M. Hamm, O. Hess, Phys. Rev. Lett. 105, 127401 (2010).

7. J. M. Hamm, S. Wuestner, K. L. Tsakmakidis, O. Hess, Phys. Rev. Lett. 107, 167405 (2011).

8. S. Wuestner, et al., Phys. Rev. B 85, 201406(R) (2012).

9. A. Pusch, S. Wuestner, J. M. Hamm, K. L. Tsakmakidis, O. Hess, ACS Nano 6, 2420 (2012).

10. E. K. Lau, A. Lakhani, R. S. Tucker, M. C. Yu, Opt. Express 17, 7790 (2009).

9125-3, Session 1

Surface plasmon polaritons in presence of dye molecules: stimulated emission, dispersion, and possible strong coupling *(Invited Paper)*

Thejaswi U. Tumkur, John K. Kitur, Mikhail A. Noginov, Norfolk State Univ. (United States)

Active plasmonic devices, in particular those with optical nonlinearity and gain, have promise to find applications in new generation nanocircuitry and sensors. In this talk, we will review our recent studies in the interrelated areas of stimulated emission of surface plasmon polaritons (SPPs), SPP dispersion, and hybridization of SPPs with ground state and excited state molecules in an adjacent dielectric. We find that in the presence of dye molecules, the SPP dispersion curves split and demonstrate the avoided crossing behavior, which is typical of strong coupling. Of particular interest are the modification of the dispersion curves in the presence of emission and gain and effect of SPP dispersion on the stimulated emission.

9125-4, Session 1

Nonlocal plasmonic response: from nano-gap dimers to hyperbolic metamaterials *(Invited Paper)*

N. Asger Mortensen, DTU Fotonik (Denmark)

Metallic nanostructures exhibit plasmonic response that we commonly address by classical electrodynamics with the plasma response treated in a Drude local-response approximation. Often such approaches are surprisingly successful in explaining experimentally observed phenomena and the formalism has over the years been instrumental for the prediction of a range of new phenomena.

On the other hand, the emerging field of quantum plasmonics will most likely need formalism beyond classical electrodynamics. Noble metal systems are being explored at the sub-nanometer to atomic scale which intuitively calls for quantum mechanical approaches. The pragmatic question is of course if some aspects can still be addressed with semiclassical electrodynamics?

My talk introduces a semiclassical nonlocal response theory that unifies nonlocal mechanisms representing both quantum aspects of the electron gas as well as more classical dynamics of the electron transport. The theory offers an explanation for frequency shifts and size-dependent damping observed in various experiments on metallic nanoparticles. Despite of its semiclassical starting point, the theory gives interesting predictions also for plasmonic systems which one would anticipate to be deep into the quantum regime, such as dimer configurations potentially supporting quantum tunneling currents across sub-nanometer gaps. Hyperbolic metamaterials represent another class of artificial materials where the nonlocal response poses fundamental limitations to the photonic density of states thus also having implications for quantum light-matter interactions and the emerging field of quantum plasmonics.

9125-5, Session 2

Advances in bottom-up crystal growth-based approach towards plasmonic materials and metamaterials *(Invited Paper)*

Dorota A. Pawlak, Marcin Gajc, Katarzyna Sadecka, Karolina Korzeb, Pawel Osewski, Andrzej Klos, Barbara Surma, Institute of Electronic Materials Technology (Poland); Alessandro Belardini, Grigore Leahu, Concita Sibilia, Univ. degli Studi di Roma La Sapienza (Italy)

Two novel bottom-up manufacturing methods of nanoplasmonic materials and metamaterials will be presented utilizing the crystal growth techniques: (i) directional solidification of eutectic composites [1], and (ii) direct doping of dielectric matrices with plasmonic nanoparticles (NanoParticles Direct Doping - NPDD) [2]. Eutectics are simultaneously monolithic and multiphase materials forming self-organized micro/nanostructures, which enable: (i) the use of various component materials including oxides, semiconductors, metals, (ii) the generation of a gallery of geometrical motifs and (iii) control of the size of the structuring, often from the micro- to nanoregimes. On the other hand, the novel method of direct doping of dielectric matrices with nanoparticles utilizing directional solidification provides three-dimensional nanoplasmonic materials enabling doping with nanoparticles of various chemical composition, various size and shape, as well as co-doping with other chemical agents. Materials with plasmonic resonances at visible and IR wavelengths, as well as materials with enhanced photoluminescence and with anomalous refraction [3] will be presented. Our new approach may lead to novel manufacturing solutions for photonic applications in areas such as metamaterials, plasmonics, as well as photovoltaics.

[1] D. A. Pawlak, S. Turczynski, M. Gajc, K. Kolodziejak, R. Diduszko, K. Rozniatowski, J. Smalc, I. Vendik, How far are we from making metamaterials by self-organization? The microstructure of highly anisotropic particles with an SRR-like geometry, Adv. Funct. Mat., 2010, 20, 1116-1124,.

[2] M. Gajc, B. H. Surma, A. Klos, K. Sadecka, K. Orlinski, A. E. Nikolaenko, K. Zdunek, Nanoparticle Direct Doping: novel method for manufacturing three-dimensional bulk plasmonic nanocomposites. Adv. Funct. Mat., 2013, 23, 3443-3451.

[3] A. Belardini, C. Sibilia, Evaluation of the negative refractive index by beam deviation measurements, Optoelectron. Adv. Mater.-Rapid Commun. 2013, 7, 184.

9125-6, Session 2

Gold mushroom array: a plasmonic refractive index sensor with an ultimate figure of merit *(Invited Paper)*

Chongjun Jin, Yang Shen, Sun Yat-Sen Univ. (China)

Localized surface plasmon resonance (LSPR) based on metal nano-particles has great applications in light harvesting, imaging and biosensing. Compared to commercially available sensors based on propagating surface plasmon resonances (PSPRs), LSPR sensors are simple, cost-effective and suitable for measuring local changes in the refractive index. However, the figure of merit (FOM) values of LSPR sensors are generally 1 to 2 orders of magnitude smaller than those of PSPR ones, which hinders the widespread use of LSPR sensors [1]. In this report, we will review the recent progress of LSPR sensors. Then we propose a novel method to improve the performance of the LSPR-related sensors, which is simultaneously improving its refractive index sensitivity and reducing its linewidth. Specifically, gold particles are lifted by dielectric pillars with a small refractive index. More spatial regions around the gold particles with plasmon-enhanced electric fields will be accessible by the surrounding environment. Therefore, the apparent refractive index sensitivity of the lifted metal particles will be increased [2]. Moreover, a Fano resonance caused by the interference between Wood's anomaly of the array and the LSPR of the individual gold units is simultaneously introduced. The presence of the Fano resonance results in a large reduction in the spectral linewidth. We developed submicrometer gold mushroom arrays (GMRA) with an ultimate FOM up to 108 resulted from the interference between Wood's anomaly and the LSPRs, which is comparable to the theoretically predicted upper limit (~108) for standard PSPR sensors [3]. The GMRAs can be fabricated via only two steps, which are two orthogonal two-beam interference lithography, and the following gold evaporation. This means that the GMRAs are easy to be fabricated. We further demonstrated these GMRAs as biosensors for detecting Cytochrome c and alpha-fetoprotein with detection limits down to 350 pM and 15 ng/mL respectively [1]. Our GMRA sensors can be a promising candidate for label-free chemical and biomedical sensing.

References:

1. Yang Shen, et al., Plasmonic gold mushroom arrays with refractive index sensing figures of merit approaching the theoretical limit, Nature Communications, 4, 2381(2013). DOI: 10.1038/ncomms3381.

2. Dmitriev, A. et al. Enhanced nanoplasmonic optical sensors with reduced substrate effect. Nano Lett. 8, 3893?3898 (2008).

3. Anker, J. N. et al. Biosensing with plasmonic nanosensors. Nat. Mater. 7, 442?453 (2008).

9125-7, Session 2

Tailoring of the circular dichroism produced by Au covered self ordered dielectric nanospheres

Alessandro Belardini, Alessio Benedetti, Marco Centini, Concita Sibilia, Univ. degli Studi di Roma La Sapienza (Italy); Davide Comoretto, Francesco Buatier de Mongeot, Univ. degli Studi di Genova (Italy)

Regular array of plasmonic nanoantennas (nanocrescents) can be easily produced by grazing evaporating gold on a self-ordered surface formed by hexagonal arrangements of polystyrene nanospheres [1], thus realising a hybrid plasmonic-photonics nanostructures (HPPN). In ref. [2], by using second harmonic generation (SHG) technique we

experimentally demonstrated that asymmetry in the shape of the nanoantennas induces an optical chiral response of the whole sample. Here we show how the geometrical induced chirality [3] of HPPN and the plasmonic anisotropic response can be controlled and tuned by changing different fabrication parameters such as the orientation (azimuth and tilt) of the Au flux deposition direction with respect the sample surface normal, the Au thickness, the nanosphere radius. As an example by changing the azimuth of the Au flux direction it is possible to obtain elongated rectangular nanoantennas that are non-chiral but are anisotropic (optical linear dichroism), asymmetric triangular antennas that presents either left-handed or right-handed optical chiral response or more squared antennas with no-chirality and few dichroism.

The contemporary presence of 2D Bragg resonances with plasmonic resonances leads to high SHG signal where different tensorial components of the nonlinear response can be activated by the corresponding chiral geometrical symmetry.

This kind of hybrid structures where 2D photonic crystals are combined with plasmonic resonant nanoantennas can be an innovative route in the field of nanophotonics where the artificial circular dichroism [4] is investigated for developing novel compact devices for optical signal manipulation or molecular sensing.

[1] V. Robbiano, M. Giordano, C. Martella, F. D. Stasio, D. Chiappe, F. Buatier de Mongeot, D. Comoretto, Advanced Optical Materials 1, 389 (2013).

[2] A. Belardini, A. Benedetti, M. Centini, G. Leahu, F. Mura, S. Sennato, C. Sibilia, V. Robbiano, M. C. Giordano, C. Martella, D. Comoretto, F. Buatier de Mongeot, Advanced Optical Materials, accepted (2013).

[3] E. Plum, X.-X. Liu, V. A. Fedotov, Y. Chen, D. P. Tsai, and N. I. Zheludev, Phys. Rev. Lett. 102, 113902 (2009).

[4] A. S. Schwanecke, A. Krasavin, D.M. Bagnall, A. Potts, A.V. Zayats, and N. I. Zheludev, Phys. Rev. Lett. 91, 247404 (2003).

9125-8, Session 2

Self-assembled lamellar metallo-dielectric nanocomposites with strong optical anisotropy

Clémence Tallet, Alexandre Baron, Kévin Ehrhardt, Ctr. de Recherche Paul-Pascal (France); Julien Vieaud, National Institute for Materials Science (Japan); Olivier Merchiers, Institut National des Sciences Appliquées de Lyon (France); Philippe Barois, Ctr. de Recherche Paul-Pascal (France); Marc Warenghem, Univ. d'Artois (France); Ashod Aradian, Virginie Ponsinet, Ctr. de Recherche Paul-Pascal (France)

Novel optical properties in the visible range are foreseen when organizing nanoresonators, which can be performed by the self-assembly of plasmonic nanoparticles prepared by wet chemistry. In this presentation, we describe the preparation and study of thin films of nanocomposites of polymers and gold nanoparticles. We relate the structure of the composites, and in particular the nature, density and spatial organization of the gold nanoparticles, with the optical index of the composites. The anisotropic nanocomposites are produced by the assembly of plasmonic nanoparticles templated by ordered matrices of diblock copolymers. Diblock copolymers are macromolecules made of two molecular chains of distinct chemical nature linked together, and present solid state spontaneous organizations with long-range order and tunable characteristic sizes between 40 and 140 nm. In particular, alternating lamellar structures are used here to spatially organize plasmonic nanoparticles. More precisely, using poly(styrene)-b-poly(2-vinylpyridine) pre-aligned lamellar thin films as templates, and in situ reduction of impregnated gold salts, we prepared nanocomposite films of thickness between 200 and 600nm on silicon wafers, with layered structures aligned parallel to the substrate surface. The structure of the nanocomposite films is studied by X-ray scattering and transmission electron microscopy. They consist in periodic lamellar stacks of alternating layers of pure polymer (dielectric) and layers of composite of polymer loaded with a high density of 10-nm gold nanoparticles. The layers have a thickness between 50 and 100 nm. The amount of gold in the composite layers can be varied in the preparation process. The optical properties of the films are determined by variable angle spectroscopic ellipsometry and analyzed by appropriately developed effective medium models. When the gold load is high enough, the composite layers present a metallic nature (? < 0) in a wavelength range close to the localized surface plasmon resonance of the gold nanoparticles, which can be accounted for by effective medium models derived from Maxwell-Garnett and modified in order to include couplings between disordered nanoresonators. The analysis of the optical properties of the lamellar nanocomposite films suggests the existence of a strong anisotropy of the dielectric permittivity, with Re(?//) < 0 < Re(??) in a limited range of wavelength. This property is studied with variable gold fraction, and the possible application towards hyperbolic materials is discussed.

We acknowledge the support of the Région Aquitaine, the French Agence Nationale de la Recherche (ANR-09-NANO-003), the European Union's 7th Framework Program (grant agreement FP7/2008/228762, METACHEM) and the LabEx AMADEus (reference ANR-10-LABX-0042-AMADEUS).

9125-9, Session 2

Threading plasmonic nanoparticle strings with light: large-scale metamaterials production

Ventsislav K. Valev, Lars O. Herrmann, Univ. of Cambridge (United Kingdom); Christos Tserkezis, Centro de Fisica de Materiales (Spain); Jon Barnard, Oren Scherman, Univ. of Cambridge (United Kingdom); Javier Aizpurua, Centro de Fisica de Materiales (Spain); Jeremy J. Baumberg, Univ. of Cambridge (United Kingdom)

Individual plasmonic nanoparticles (NPs) are the basic building blocks for bottom-up assembled nano- and meta-materials. At the most fundamental level these nanomaterials consists of NP chains, whereby the individual NPs are glued together with molecules. Here we demonstrate the next step towards achieving continuous bottom-up assembled meta- and nanomaterials. We show that ultrafast laser pulses can produce a continuous metal thread bridging the chains, thereby allowing charge transfer.[1] The process is characterised by the appearance of a new plasmon mode, exhibiting both chain- and rod-like features. Upon assembly, real-time monitoring of this plasmon mode allows highly precise control (±3 nm) over the width of the thread.

New optical materials are finding increasing applications in communications, healthcare, transport and sensing. Just as light is used to characterize optical materials, light can also be used to build them. Ultrafast lasers have so far been used to shape continuous metal surfaces with a variety of micro and nanostructures, such as needles, ripples, cavities, nanobumps and nanojets. Nanojets,[2] promising for such threading, are columns of liquid material, frozen in the process of surging from the metal surface in the direction opposite to that of the incoming laser pulse. However it is impossible to align individual nanostructures so nanojets from opposite nanostructures face each other. This can be circumvented with surface plasmon resonances – the coherent oscillation of surface electrons. Plasmons enhance even further the electric field of intense femtosecond pulses and localize it to sub-wavelength regions ('hotspots'). In dimers, or chains of plasmonic NPs, the plasmonic hotspots occur in the regions directly across the gap. It is therefore possible to form a continuous thread in such dimers or chains of nanoparticles, from first stage of nanoscale assembly[3].

Although threading nanowires or nanoparticles was attempted in the past, the number of nanoparticles involved was very small (a few dimers at most) and few could be characterized. Control on a large scale is the key aspect for this emerging nanotechnology.

In our work, assembly proceeds in water at an unprecedented large scale. Our results show that the width of the thread depends on the plasmon resonance wavelength of the chain modes, on the size of the nanoparticles, on the number of nanoparticles in the chains and on the peak-to-peak laser power, which can all be used to tune the optical properties of this novel type of material. Large-scale metamaterial production is thus in prospect.

[1] L. O. Herrmann, V.K. Valev, C. Tzerkezis, J. Barnard, O. Sherman, J. Aizpurua, J.J. Baumberg, Threading plasmonic nanoparticles with light. Nat. Mat submitted (2013).

[2] V. K. Valev, D. Denkova, X. Zheng, A. I. Kuznetsov, C. Reinhardt, B. N. Chichkov, G. Tsutsumanova, E.J. Osley, V. Petkov, B. De Clercq, A. V. Silhanek, Y. Jeyaram, V. Volskiy, P. A. Warburton, G. A. E. Vandenbosch, S. Russev, O. A. Aktsipetrov, M. Ameloot, V. V. Moshchalkov, T. Verbiest Plasmon-enhanced sub-wavelength laser ablation: plasmonic nanojets. Adv. Mater. 24, OP29 (2012).

[3] R.W. Taylor, T-C Lee, O. A. Scherman, R. Esteban, J. Aizpurua, F. Huang, J.J. Baumberg, S. MahajanPrecise subnanometer plasmonic junctions for SERS within gold nanoparticle assemblies using cucurbit[n]uril “Glue”. ACS Nano 5, 3878 (2011).

9125-14, Session 2

Plasmonics: going practical with transition metal nitrides *(Invited Paper)*

Nathaniel Kinsey, Marcello Ferrera, Purdue Univ. (United States); Viktoriia E. Babicheva, DTU Fotonik (Denmark); Urcan Guler, Justus C. Ndukaife, Clayton DeVault, Jongbum Kim, Naresh K Emani, Paul R. West, Gururaj V. Naik, Alexander V. Kildishev, Vladimir M. Shalaev, Alexandra Boltasseva, Purdue Univ. (United States)

Plasmonics and metamaterials have recently seen an explosion of novel ideas and device designs. However, transforming these concepts into practical devices requires a significant amount of effort. The main obstacle is the absence of robust, high performance, low cost plasmonic materials that can be easily fabricated using standard processing lines and integrated with established semiconductor technologies. In this talk alternative plasmonic materials (other than currently used silver and gold) for surface plasmon applications as well as plasmonic metamaterials will be discussed. This presentation will mainly focus on transition metal nitrides, in particular, titanium nitride and zirconium nitride, which are plasmonic materials having optical properties resembling gold. Titanium nitride is compatible with biological environments and semiconductor industry, and possesses superior properties compared to noble metals such as high temperature durability, chemical stability, and corrosion resistance, low cost and mechanical hardness. Additionally, titanium nitride can be grown in smooth, ultra-thin crystalline films, which are crucial in constructing high-performance, low loss plasmonic and metamaterial devices. Several examples of plasmonic structures and metamaterial devices using transition metal nitrides as the constituent plasmonic material will be shown including nanoparticles for localized surface plasmon applications, plasmonic waveguides as well as hyperbolic metamaterials. The prospects of using transition metal nitrides to enable the next generation of hybrid photonic devices based on low-loss optical metamaterials, CMOS-compatible plasmonic interconnects as well as novel devices for improved imaging, sensing, light harvesting and medical applications will be discussed.

9125-10, Session 3

Resonant dielectric nanostructures and metasurfaces *(Invited Paper)*

Arseniy I. Kuznetsov, A*STAR - Data Storage Institute (Singapore)

Resonant high-refractive index dielectric and semiconductor nanostructures are novel objects in nanophotonics, which may compliment or even substitute plasmonic particles for multiple applications in the nearest future. It has recently been shown that nanoparticles made of high-refractive index materials such as silicon can have strong resonant responses of both electric and magnetic nature, which spectral position scales linearly with particle size. Recently we have experimentally demonstrated strong magnetic and electric dipole resonances tuneable through the whole visible and near-IR spectral ranges in silicon nanoparticles with sizes ranging from 100 nm to 300 nm. Another unique peculiarity of high-refractive index dielectric nanoparticles is their ability to scatter light unidirectionally, i.e. mainly in a preferred direction. This property is a consequence of far-field Kerker-type interference of electric and magnetic dipoles simultaneously excited inside a single nanoparticle. In this lecture, I will review our recent results on resonant effects in single high-refractive index nanoparticles and dense nanoparticle arrays. Such resonant dielectric metasurfaces may have a huge promise for design of novel low-loss flat optics. Applications of these unique optical properties of resonant dielectric nanostructures to design of novel low-loss nanophotonic devices will also be discussed.

9125-11, Session 3

Dielectric sheet metamaterials with high quality factor

Aditya Jain, Iowa State Univ. (United States); Philippe Tassin, Chalmers Univ. of Technology (Sweden); Thomas Koschny, Costas M. Soukoulis, Iowa State Univ. (United States)

In this contribution, we present a solution to the loss problem of sheet metamaterials. Metamaterials are artificial, structured materials built from small electric or plasmonic resonators that constitute the basic units of interaction with electromagnetic radiation. They allow for optical media with properties that are not achievable or much weaker in natural materials, e.g., negative refraction, magnetism at terahertz and optical frequencies, or strong chirality. Many metamaterials are made out of metallic constituents, but they are plagued by dissipative loss due to conversion of energy to heat in the metal. It has been suggested to replace metallic electric circuits by Mie resonances in dielectric particles, but in general it is difficult to make such particles much smaller than the wavelength, resulting in periodicity effects as a result of working at the edge of the effective medium approximation. We propose a new type of meta-atoms in which we use a dark mode, i.e., a mode with negligible dipole moment, in a dielectric inclusion. We couple the electromagnetic energy of the incident wave to the dielectric meta-atom with secondary scatterers that otherwise do not significantly participate in the energy storage of the resonance. In this way, our metamaterial possesses a resonance with a much larger quality factor than what is normally observed in metal-based metamaterials. We present experimental results and computer simulations demonstrating dispersion-engineered metamaterials with quality factors over 1,000. Subsequently, we show that our dielectric meta-atoms can also be used to construct sheet metamaterials with negative permittivity or with negative permeability.

9125-12, Session 3

Light bending in a all-dielectric metamaterial

Benoit Cluzel, Univ. de Bourgogne (France); Eric Cassan, Institut d’Électronique Fondamentale (France); Jean Dellinger, Univ. de Bourgogne (France); Xavier Le Roux, Institut d’Électronique Fondamentale (France); Frédérique de Fornel, Lab. Interdisciplinaire Carnot de Bourgogne (France); Khanh Van Do, Institut d’Électronique Fondamentale (France)

Artificial materials at optical frequencies have raised a strong interest in the last years, including photonic metamaterial,

graded photonic crystals, and gradient index structures. The common objective of these approaches is achieving a tight control of the electromagnetic waves to play with light and propose versatile functionnalities. At the theoretical point of view, these new optical materials can be designed using the formalism of transformation optics or using Hamiltonian optics light ray propagation. At the experimental point of view, yet, very few techniques are available to directly investigate the underlying electromagnetic properties. In this context, to provide in situ observations of the electromagnetic fields behavior inside artificial optical structures, we have developed an original and versatile hyperspectral scanning near-field optical microscope (SNOM). In this communication, we will provide the complete and direct experimental observation of the light propagation, dispersion [1] and birefringence [2] within a two-dimensional Silicon on Insulator all dielectric metamaterial at near-infrared wavelengths. Then, the transition between the long-wavelength and the short-wavelength regimes of the light propagation will be discussed [3]. Our experimental results show an invariant quantity of only 1.78 times the lattice period as the criterion for the possible application of homogenization theories. These results will be discussed in light of Fourier decomposition of the electromagnetic Bloch waves and a physical interpretation of the observed transition between the two light propagation regimes will be proposed.

[1] J. Dellinger, K. Van Do, X. Le Roux, F. de Fornel, E. Cassan & B. Cluzel, App. Phys. Lett. 101, 141108 (2012)

[2] E. Cassan, K. Van Do, J. Dellinger, X. Le Roux, F. de Fornel & B. Cluzel, Opt. Lett. 38, 459 (2013)

[3] E. Cassan, J. Dellinger, X. Le Roux, K. Van Do, Frédérique de Fornel & Benoît Cluzel, Phys. Rev. B 88, 125138 (2013)

9125-13, Session 3

Semiconductor epsilon-near-zero nano-optics *(Invited Paper)*

Young Chul Jun, Inha Univ. (Korea, Republic of); John L. Reno, Ting-Shan Luk, Igal Brener, Sandia National Labs. (United States)

Epsilon-near-zero (ENZ) materials have attracted attention for their highly unusual and intriguing optical properties. For example, ENZ materials were employed for perfect coupling through a narrow channel, optical switing and bistability, and directivity control of antennas. More recently, it was also pointed out that a thin ENZ layer supports a new type of guided modes near the epsilon zero frequency, termed ENZ modes. In this talk, we will discuss our recent work on ENZ nano-optics based on ultra-thin, doped semiconductors: (i) Novel strong coupling between planar metamaterials and ENZ modes (ii) Narrowband thermal emission from an ENZ material (iii) Perfect absorption in an ENZ material.

9125-59, Session 3

Chirality and polarization-dependent characteristics of dielectric single gyroid metamaterials

Lung-Yu Chang Chien, Yu-Chueh Hung, National Tsing Hua Univ. (Taiwan)

Gyroid is a type of three-dimensional chiral structures, which have attracted much research attention recently. A dielectric single gyroid (SG) can be a candidate for providing new means of guiding light because it has been shown to exhibit complete photonic band gaps. Owing to the chiral nature, the SG metamaterials may exhibit circular polarization-dependent properties, leading to new types of polarization-sensitive devices. In this work, we present studies based on finite-difference time-domain (FDTD) method for analyzing the polarization-dependent characteristics of dielectric SG. We show that the operation frequency of SG metamaterials can be advanced from microwave to visible region by varying its material, lattice constant and volume fraction. The corresponding band structures, transmission spectra for right circularly polarized (RCP) light and left circularly polarized (LCP) light, and circular dichroism (CD) indices are examined. According to our analysis, a circular polarization gap is found in the visible region. In particular, the correlation between the volume fraction of dielectric SG and the frequency range of circular polarization band gaps is also investigated. These results are crucial for the design of functional polarization-sensitive devices at the visible wavelength based on dielectric single gyroid metamaterials.

9125-15, Session 4

Nanoplasmonic biosensors and photodetectors *(Keynote Presentation)*

Ekmel Özbay, Bilkent Univ. (Turkey)

In this talk, we will present our recent work on nanoplasmonic based biosensors and photodetec-tors. We will present a label-free, optical nano-biosensor based on the Localized Surface Plasmon Resonance (LSPR) effect that is observed at the metal-dielectric interface of silver nano-cylinder arrays located periodically on a sapphire substrate by E-Beam Lithography (EBL), which provides high resolution and flexibility in patterning. Firstly, the size and period dependency of the LSPR wavelength was studied. Secondly, the surface functionalization studies were carried out on an ar-ray with a selected size and period. Finally, the concentration dependency of the LSPR shifts was observed by changing the avidin concentrations to be sensed in the target solution. The sensing mechanism is based on the detection of refractive index change, due to the binding of biotin that is immobilized on the silver nano-cylinders to the avidin in the target solution, by observing the shifts in the LSPR wavelength. Our results show that such a plasmonic structure can be success-fully applied to bio-sensing applications and extended to the detection of specific bacteria species. A highly tunable design for obtaining double resonance substrates to be used in Surface Enhanced Raman Spectroscopy will also be presented. Tandem truncated nano-cones composed of Au-SiO2-Au layers are designed, simulated and fabricated to obtain resonances at laser excitation and Stokes frequencies. Surface Enhanced Raman Scattering experiments are conducted to compare the enhancements obtained from double resonance substrates to those obtained from single reso-nance gold truncated nano-cones. The best enhancement factor obtained using the new design is 3.86 x10E7. The resultant tandem structures are named after “Fairy Chimneys” rock formation in Cappadocia, Turkey. The integration of plasmonic structures with solid state devices has many po-tential applications. It allows the coupling of more light into or out of the device while decreasing the size of the device itself. Such devices are reported in the VIS and NIR regions. However, mak-ing plasmonic structures for the UV region is still a challenge. Here, we report on a UV plasmonic antenna integrated metal semiconductor metal (MSM) photodetector based on GaN. We designed and fabricated Al grating structures. Well defined plasmonic resonances were measured in the re-flectance spectra. Optimized grating structure integrated photodetectors exhibited more than eight-fold photocurrent enhancement.

9125-16, Session 4

Surface plasmon polariton waves onto graphene’s surface over an anisotropic metamaterial substrate

Stamatios A. Amanatiadis, Theodosios D. Karamanos, Nikolaos V. Kantartzis, Aristotle Univ. of Thessaloniki (Greece)

Graphene has, recently, attracted significant attention of the research community because of its outstanding properties at the microwave, millimeter-wave, and infrared frequencies. Specifically, at the far-infrared regime, graphene’s ability to support highly confined transverse magnetic (TM) surface

plasmon polariton (SPP) waves is leading to the development of various devices that can be utilized at several applications. One of the basic attributes of TM SPP waves supported on graphene is their considerably decreased wavelength compared to the free-space one, thus enabling the miniaturization of devices at the abovementioned frequencies. Although, this property is desirable for the majority of modern applications, there are some exceptions, such as the antenna design, where miniaturization affects not only the antenna compactness, but also its radiation efficiency that can be degraded enormously. In order to avoid this degradation, it is essential to control the SPP propagation properties effectively, by employing an epsilon near-zero (ENZ) material as graphene's substrate that can increase SPP wave's wavelength retaining the confinement.

However, a natural ENZ material cannot be easily encountered at the far-infrared spectrum and therefore a metamaterial should be applied. The basic advantage of this concept is the capability to efficiently tune material's properties at the desired frequency range. On the other hand, its major disadvantage is the anisotropic nature of artificial media that complicate the extraction of the SPP wave propagation properties. It is the purpose of the present work to investigate numerically these characteristics for the case of TM SPP waves onto graphene's surface over a theoretical anisotropic material and prove that their wavelength is able to be increased at normal levels for antenna applications. Furthermore, a more realistic scenario with a designed metamaterial as the graphene's substrate is implemented and analyzed by means of the finite-difference time-domain (FDTD) method.

9125-17, Session 4

High accuracy FDTD methods for computing scattering and propagation in photonics design *(Invited Paper)*

James B. Cole, Univ. of Tsukuba (Japan); Saswatee Banerjee, Sumitomo Chemical Co., Ltd. (Japan)

The finite difference time domain (FDTD) algorithm is derived from a second-order finite difference (FD) model of Maxwell's equations. For a grid spacing of h, the error of conventional FDTD is proportional to h**2, but the computational cost (C) rises as 1/h**4 (in three dimensions). Accuracy could be increased by using higher-order FD approximations, however this not only complicates the algorithm, but it has also been shown that when the order of the FD model is higher than that of the original differential equation, numerically unstable spurious solutions can arise.

Using what is called a nonstandard (NS) FD model, based on second-order FD approximations it is possible to reduce the error to h**6, without decreasing h. We introduce a high-accuracy version of the Yee algorithm based on a NS-FD model, with low computational cost.

In dispersive media the FDTD algorithm must be modified. Recursive convolution (RC) in conjunction with a dispersion model is widely used. It is common practice to input a pulse and then Fourier analyze the output to obtain a spectrum. There are two problems with this approach: (1) each frequency component has a different error, and (2) the dispersion model does not reproduce the tabulated values of complex permittivity over the entire spectrum. These latter errors, as we show are significant. In addition RC-FDTD is numerically unstable, unless the algorithm parameters are carefully chosen.

We show how to improve the accuracy of RC-FDTD by separately computing each frequency component of the desired spectrum, incorporating the tabulated values of complex (dispersive) permittivity. We have derived a set of stability criteria for implementing RC-FDTD.

RC-FDTD is computationally intensive because an extra field (besides electric and magnetic) must be computed to take dispersion into account. In two dimensions it can be shown that for the TE mode (electric field parallel to object boundaries), Maxwell's equations for the electric field reduce to the scalar wave equation (even in the presence of boundaries). We derived a two-dimensional form of RC-FDTD for the wave equation in TE mode, which is much less computationally costly than conventional RC-FDTD.

We verify the accuracy of our methodology by comparing our calculations with analytic solutions given by Mie theory. We have applied our new RC-FDTD methodology to investigate the optical properties of subwavelength metallic gratings and arrays of closely-spaced silver nanorods. We have verified that our computations can discriminate features of the reflection and transmission spectrum that other methods miss.

9125-18, Session 4

Nano-plasmonic sensors from asymmetric split-ring resonators (A-SRRs) *(Invited Paper)*

Nigel P. Johnson, Basudev Lahiri, Graham J. Sharp, Ifeoma G. Mbomson, Richard M. De La Rue, Univ. of Glasgow (United Kingdom); Scott G. McMeekin, Glasgow Caledonian Univ. (United Kingdom)

Nano-plasmonic arrays of asymmetric split-ring resonators (A-SRRs) can be used as sensor elements which produces a shift in their resonance spectra in the presence of analyte. The localized use of poly-methyl-methacrylate (PMMA), a well known electron beam lithography resist, as an organic probe, shows the relative hot spots and areas of maximum sensitivity. The phase and amplitude of a characteristic molecular Fano resonance associated with a carbonyl bond changes with its position relative to spectra peaks of the A-SRRs. The localization of blocks of PMMA at different positions on the A-SRR array also shows their relative sensitivity to position and corresponding hot spots in both experiment and simulation. Other organic materials such as the hormones progesterone and estradiol show similar Fano resonances and demonstrate the use of A-SRRs as sensors.

9125-19, Session 5

Metamaterials: optical properties on demand *(Keynote Presentation)*

Nikolay I. Zheludev, Optoelectronics Research Ctr. (United Kingdom)

No Abstract Available

9125-20, Session 5

Manipulation of light propagation with metasurfaces

Thomas Zentgraf, Univ. Paderborn (Germany); Shuang Zhang, Lingling Huang, The Univ. of Birmingham (United Kingdom); Holger Mühlenbernd, Univ. Paderborn (Germany); Xianzhong Chen, Heriot-Watt Univ. (United Kingdom); Jensen Li, The Univ. of Birmingham (United Kingdom); Hao Zhang, Tsinghua Univ. (China); Shumei Chen, The Univ. of Birmingham (United Kingdom); Cheng-Wei Qiu, National Univ. of Singapore (Singapore); Kok-Wai Cheah, Hong Kong Baptist Univ. (Hong Kong, China); Guofan Jin, Qiaofeng Tan, Benfeng Bai, Tsinghua Univ. (China)

One of the great benefits of metamaterials arises from the flexibility in engineering their optical responses to achieve control over the propagation of light to an unprecedented level. Plasmonic metasurfaces that consist only of a monolayer of planar metallic structures, have shown great promise for leveraging full control of light and low fabrication cost as they do not require complicated three dimensional nano-fabrication techniques. One of the interesting features of metasurfaces is the capability of generating abrupt interfacial phase changes

across the interface, and therefore provide a unique way of controlling the wave front locally at the subwavelength scale. Shaping the spatial phase and intensity distribution is very important for all applications that require a propagation of light like focusing, beam shaping, and 3D image reconstruction. Recently metamaterials were used to demonstrate wave plates for generating vortex beams, ultrathin metalenses and 2D holography. However, none of these techniques has achieved a more complex functionality like reconfigurable focusing or 3D image reconstruction in the visible range.

Here, we will experimentally demonstrate two new applications namely a switchable dual-polarity lens and 3D holography by using plasmonic metasurfaces. We utilize the abrupt phase change that occurs for circularly polarized light converted to its opposite helicity. The phase shift at the interface, ranging from 0 to 2pi, is realized by an array of plasmonic dipole antennas with spatially varying orientations. The local phase of light transmitting through the metasurface is geometrical and solely controlled by the orientation angle of the individual dipole antennas. With this technique we demonstrate an ultra-thin lens which can be altered from focusing to defocusing simply by changing the polarization state of the light. Furthermore, we will demonstrate a 3D computer generated holography image reconstruction by the same technique that will work over a large wavelength range.

9125-21, Session 5

Thermally induced switching of functionalities in DC electric cloak

Salvatore Savo, You Zhou, Harvard Univ. (United States); Giuseppe Castaldi, Vincenzo Galdi, Univ. degli Studi del Sannio (Italy); Shriram Ramanathan, Yuki Sato, Harvard Univ. (United States)

Transformation optics (TO) offers a powerful and systematic approach to design metamaterials with specific functionalities (e.g. cloak, concentrator, rotator) capable of precisely manipulating phenomena spanning beyond the domain of optics (e.g. acoustic waves, heat, DC electric currents). Materials capable of responding to environmental stimuli have been largely used to demonstrate the ability to control the response of metamaterials within the same functionality. Here we present the design of a thermally reconfigurable TO-based metamaterial engineered to convert its functionality from a reduced cloak to a concentrator for DC electric currents. Vanadium dioxide (VO2) thin film resistors combined with a resistor network designed according to TO theory is used to switch functionality as a function of the temperature. Our numerical and experimental results pave the way to a new paradigm for the design of self-regulating electrical and electronic systems.

9125-22, Session 5

Metamaterials enhancing optical forces *(Invited Paper)*

Vincent Ginis, Vrije Univ. Brussel (Belgium); Philippe Tassin, Chalmers Univ. of Technology (Sweden); Costas M. Soukoulis, Iowa State Univ. (United States); Irina Veretennicoff, Vrije Univ. Brussel (Belgium)

The interaction between light and matter involves not only energy transfer, but also the transfer of momentum. In everyday life, the linear momentum of light is too small to play a significant role. However, at nanoscale dimensions, the associated optical forces become increasingly important. These forces are, for example, large enough for exciting experiments in the fields of cavity optomechanics, laser cooling and optical trapping of small particles. Recently, it has been suggested that optical gradient forces can also be employed for all-optical actuation in micro- and nanophotonic systems. The typical setup consists of two slab waveguides positioned in each other's vicinity such that they are coupled through the interaction of the evanescent tails. Although the gradient forces between these waveguides can be enhanced considerably with electromagnetic resonators or slow-light techniques, the resulting displacements remain relatively small. In this contribution, we present an alternative approach to enhance optical gradient forces between waveguides by using a combination of transformation optics and metamaterials [Phys.Rev.Lett. 110,057401(2013)]. Our design starts from the observation that gradient forces decay exponentially with the separation distance between the waveguides. Therefore, we employ transformation optics to modify the apparent distance between the waveguides perceived by the light. Analytical calculations confirm that the resulting forces indeed increase when an annihilating cladding is inserted. Subsequently, we discuss the metamaterial implementation of the annihilating medium. Such lensing media automatically translate into anisotropic metamaterials with negative components in the permittivity and permeability tensors. Our full-wave numerical simulations demonstrate that the overall amplification is highly limited by the loss tangent of the metamaterial cladding. However, as this cladding only needs to operate in the near field for a specific polarization, it is sufficient to use a single-negative metamaterial implementation. We finally demonstrate that metamaterials can support optical forces enhanced by more than 200 times.

9125-51, Session PS2

THz spatial light modulators made with liquid crystals metamaterials absorbers

Salvatore Savo, David Shrekenhamer, Willie Padilla, Boston College (United States)

Tunability in terahertz (THz) metamaterials is of paramount importance for imaging and sensing applications where their exotic properties can be exploited for creating filters, phase modulators and spatial light modulators (SLM). The success of single pixel imaging techniques (e.g. compressive imaging) at terahertz strongly depends on the ability to develop a new generation of spatial light modulators specifically designed to work at these wavelengths. Here we experimentally demonstrate a terahertz spatial light modulator implemented with metamaterial absorbers (MMA) functionalized with isothiocyanate-based liquid crystals (LC). The device is designed to work in reflection mode and is arranged in a 6x6 pixel matrix where the response of each pixel is modulated by electronically controlling the orientation of the liquid crystals dimers covering the entire metamaterial absorber landscape. Experiments show that each pixel can be controlled independently and that pixelated absorption patterns can be created at will. The SLM shows an overall modulation depth performance of 75%. Our work demonstrates the viability of liquid crystal based reconfigurable metamaterials and highlights their great potential use for future state-of-the-art THz devices.

9125-52, Session PS2

Macroscopic characterization of metamaterials by means of spatial filters

Carlo A. Gonano, Francesco Grimaccia, Marco Mussetta, Riccardo E. Zich, Politecnico di Milano (Italy)

No Abstract Available

9125-53, Session PS2

Modelling angle resolved complex reflection and transmission coefficients from fishnet structures formed from nanoimprint lithography

Saima I. Khan, Graham J. Sharp, Richard M. De La Rue, Timothy D.

Drysdale, Nigel P. Johnson, Univ. of Glasgow (United Kingdom)

The evaluation of electromagnetic material parameters from metamaterial structures have received much attention in the literature. Among others, one method is to retrieve the material parameters from reflection and transmission measurements of the sample material. Assuming bianisotropic constitutive relations at oblique incidence, we describe an S-parameter retrieval method that allows us to obtain the full material parameter tensors from numerically calculated S parameters. The retrieval has been done for various angles of incidence, ranging from 0 to 85 degrees. It has been found that the electromagnetic material parameters depend on the angle of incidence, but this dependence is relatively small. Although based on the classical Nicholson-Ross-Weir technique, the proposed extraction technique has no limitations on the angle of incidence. The proposed extension of the NRW extraction technique is used to study a fishnet structure fabricated by nanoimprint lithography. Silver (Ag)-Magnesium fluoride (MgF2)-and silver (Ag) was deposited on the thick polymer, in this instance PMMA before directly imprinted by a stamp. Distinct resonance peaks are measured at both visible and infra-red frequencies. The effective material parameters have been found to characterise the imprinted fishnet structure.

9125-54, Session PS2

Enhanced cross-section of gold nanoparticles in the vicinity of a silicon substrate

Kévin Ehrhardt, Zhiqiang Zheng, Ctr. de Recherche Paul-Pascal (France); Julien Vieaud, National Institute for Materials Science (Japan); Olivier Merchiers, Institut National des Sciences Appliquées de Lyon (France); Yves Borensztein, Univ. Paris 6 (France); Ashod Aradian, Virginie Ponsinet, Ctr. de Recherche Paul-Pascal (France)

We report on the effect of the distance to a high index substrate on the absorption cross-section of simple spherical gold nanoparticles (NPs) in the visible range. Monolayers of 14-nm gold nanoparticles were deposited on a polymer layer (spacer), itself sitting on top of a silicon wafer. Four samples with polymer spacer layers of 1.3, 4.1, 9.8 and 18.4 nm-thickness, as determined by variable angle spectroscopic ellipsometry, were first produced by electrostatically controlled layer-by-layer spraying deposition technique. Nanoparticles were then sprayed onto the polymer layer in order to produce homogeneous monolayers.

In order to allow for a reliable extraction of the optical indices of the NP monolayer from the ellipsometric data, the mean NP surface density and the spacer thickness have been measured by atomic force microscopy and X-ray reflectivity.

The nanoparticle monolayer is treated as a homogeneous effective medium since the diameter of the nanoparticles is small compared to any wavelength of the explored spectrum range. The optical indices of this effective medium are determined using a ?-by-? inversion, whereby for each wavelength ?, n and k are numerically adjusted so as to obtain the best fit to the set of measured ellipsometric angles. Then, we use the classical Beer-Lambert law :

2ϖke/? = Ns ?_abs

where e is the thickness of the effective medium representing the NP layer (e = 2R = 14 nm), Ns is the NP

surface density, and ?_abs is the absorption cross-section of an individual nanoparticle. We can deduce the NPs individual absorption cross-section ?abs. For the thinnest spacer, we find an enhancement factor of the absorption of a factor close to two relatively to the other samples. This enhancement factor is not well reproduced by the image dipole theory which describes the NP-substrate coupling. This underestimation could be due to the presence of the dielectric spacer.

Preliminary numerical simulations have been performed using a Finite Element Method software. In a first step, these simulations allowed us to retrieve a qualitative enhancement to the NP absorption cross-section when the NP goes from free space to the close vicinity of a silicon substrate. Then, in a second stage, they seem to indicate that the presence of a dielectric spacer gives an additional increase to the NP absorption cross-section, compared with the situation of a NP floating in air at a given distance above the silicon wafer. We will discuss the comparison between our experimental and numerical results as well as possible more complex near-field effects.

We acknowledge the support of the Direction Générale de l'Armement, the Région Aquitaine and the French Agence Nationale de la Recherche (ANR-09-NANO-003).

9125-55, Session PS2

Optical properties of TiO2:Ag composites

Krzysztof Skorupski, Wroclaw Univ. of Technology (Poland)

The main goal of our work was to investigate the optical properties of nanocomposites, formed by combining titanium dioxide with noble metals. Our research was focused on silver (Ag), which reveals strong plasmonic effects in the visible spectrum, and rutile (TiO2), which is characterized by much lower imaginary part of the refractive index than the previous component. In the first step of our study, the central TiO2 particle, positioned in vacuum, was surrounded by non-intersecting, spherically-shaped Ag particles. They were randomly placed on the TiO2 surface and their number varied from 14 to 412. The diameter of the central (TiO2) particle was 72nm and the diameter of surrounding Ag spheres was assumed to be 5nm. Light scattering simulations were performed (and also compared) with two different algorithms to avoid any potential errors and inaccuracies. Our results show that Ag particles are responsible for the extinction peak that occurs at the wavelength of 350nm. Its location can not be easily shifted and its magnitude depends on the number of surrounding Ag spheres. No spectral effects were observed at the wavelength of 600nm and above - in this regime, the presence of Ag particles has negligible impact on the results. The main disadvantage of this approach is the computation time. On a standard PC simulations can last longer than 13h, especially when a large number of spheres is considered. Therefore, in the next step of our study, we tried to reduce this time by introducing an Ag layer instead of separate Ag particles. However, when coating is considered, the extinction efficiency changes drastically. Providing that the Ag layer is relatively thin, i.e. 1.3nm, only small aberrations occur in the non-visible spectrum from 1um to 2um. On the other hand, when the surrounding layer is thicker - the extinction peak appears. Its position can be easily controlled by the volume of the surrounding layer. For higher values, i.e. greater than 6.5nm, the peak is shifted to the visible spectrum. Our study show that these two approaches (separate Ag particles and coating) can not be used interchangeably because they lead to different results. However, it is possible to combine the optical properties of two different materials by creating proper composites. In similar cases, when the extinction peak mustbe positioned in a fixed position only, the central particle (e.g. TiO2) should be surrounded by small particles of the second material (e.g. Ag). Their amount can be used to control the magnitude of this peak. On the other hand, when the position of the extinction peak should be modified, it can be done by implementing an additional layer with an appropriate thickness. To get a better overwiew of the studied problem, similar calculations were performed for different composites, i.e. TiO2(rutile):Au, TiO2(anatase):Ag and TiO2(anatase):Au. Additionally, the simulations for TiO2(rutile):Ag were repeated in water, what can be useful for further comparison with experimental data.

9125-56, Session PS2

Dynamically tunable plasmonically induced transparency by graphene metamaterials

Shuqi Chen, Hua Cheng, Jianguo Tian, Nankai Univ. (China)

We present a highly wavelength-tunable plasmonically induced transparency (PIT) device composed of graphene nanostrips for the mid-IR region. We demonstrate that PIT can be achieved using a single layer of graphene nanostructures. Wavelength-shift active control of the PIT resonance is realized by varying the Fermi energy of the graphene without reoptimizing and refabricating the nanostructures. Meanwhile, the three-level plasmonic system is demonstrated to well explain the formation mechanism of PIT in the graphene nanostrips. This makes graphene PIT device more useful than metallic PIT devices. We believe that this method of actively tuning the wavelength of PIT may open up avenues for the development of compact elements such as tunable sensors, switchers and slow light devices.

9125-58, Session PS2

Internally twisted non-centrosymmetric optical metamaterials

Patrick Grahn, Andriy Shevchenko, Matti Kaivola, Aalto Univ. School of Science and Technology (Finland)

In optical metamaterials, the scatterers are usually aligned symmetrically with respect to the unit cells of the material. In this work, we consider metamaterials in which the "meta-molecules" can be non-centrosymmetric and have an arbitrary, but common, orientation in the unit cells, in analogy with the Smectic-C phase in liquid crystals. Such internally twisted crystalline structures are difficult to find in natural materials, but metamaterials of this type can easily be designed and fabricated. The twist itself does not lead to optical chirality. Here we present a detailed analysis of internally twisted non-centrosymmetric metamaterials, which are not chiral.

The analysis is performed by using our recently developed theoretical approach to the design and characterization of periodic optical metamaterials. The theory connects the optical properties of individual metamolecules with the properties of two- and three-dimensional arrays of the molecules. In this theory, the effective wave parameters, such as the refractive index and impedance, can be naturally retrieved also for internally twisted materials.

The approach was previously applied to the description of uniaxial bifacial nanomaterials [P. Grahn et al., Opt. Exp. 21, 23471 (2013)]. In the theory, one first calculates the transmission and reflection coefficients of a two-dimensional array of metamolecules. These coefficients depend on the polarization and propagation direction of the considered wave. From them, we calculate the effective wave parameters of the metamaterial by considering the waves that propagate between the metamolecular layers. In this work, we generalize the theory to treat also internally twisted materials, where these waves see different transmission and reflection coefficients at the metamolecular layers due to asymmetry. As a consequence, the resulting metamaterial exhibits significant spatial dispersion, e.g., the wave parameters depend judiciously on the propagation direction of light.

Using our generalized approach, we introduce and analyze a metamaterial design, in which for example (1) the k-surfaces are deformed by spatial dispersion, (2) counter-propagating optical waves with the same polarizations have very different impedances, and (3) the effective wave parameters depend on the orientation of the material's surface with respect to the metamolecules, while being fully independent of the size of, e.g., a metamaterial slab. We also illustrate the applicability of our model to metamaterials with misaligned or randomized molecular layers. The results of our analytical calculations are shown to be in perfect agreement with direct numerical calculations performed for metamaterial slabs containing several metamolecular layers.

9125-61, Session PS2

Existence conditions for bulk large-wavevector waves in metal-dielectric and graphene-dielectric multilayer hyperbolic metamaterials

Sergei V. Zhukovsky, Andrei Andryieuski, Andrei V. Lavrinenko, DTU Fotonik (Denmark); John E. Sipe, Univ. of Toronto (Canada)

We theoretically investigate general existence conditions for broadband bulk large-wavevector (high-k) propagating waves (such as volume plasmon polaritons in hyperbolic metamaterials) in arbitrary subwavelength periodic multilayers structures. Treating the elementary excitation in the unit cell of the structure as a generalized resonance pole of reflection coefficient and using the Bloch theorem, we derive analytical expressions for the band of large-wavevector propagating solutions. We apply our formalism to determine the high-k band existence in two important cases: the well-known metal-dielectric and recently introduced graphene-dielectric stacks. We confirm that short-range surface plasmons in thin metal layers can give rise to hyperbolic metamaterial properties and demonstrate that long-range surface plasmons cannot. We also show that graphene-dielectric multilayers tend to support high-k waves and explore the range of parameteres, where this is possible, confirming the prospects of using graphene for materials with hyperbolic dispersion. The suggested formalism is applicable to a large variety of structures, such as continuous or structured microwave, terahertz and optical metamaterials, optical waveguide arrays, 2D plasmonic and acoustic metamaterials.

9125-62, Session PS2

Homogenization of metamaterials through the singular analysis of scattering spectra

Jerome Wenger, Victor Grigoriev, Brian Stout, Guillaume Demesy, Nicolas Bonod, Institut Fresnel (France)

Homogenized descriptions of metamaterials as effective permittivity and permeability are required to fully exploit the unique electromagnetic material responses. However, homogenization is often challenging as the retrieved effective parameters can retain nonphysical values, especially close to spectral resonances. Here, we derive a new approach for homogenization of metamaterials based on the scattering properties of perfectly emitting and absorbing modes. We show how to uniquely convert the frequencies of these modes into the effective permittivity and permeability, and provide analytical formulas for their frequency dependence taking the reflection and transmission spectra as input data. Our approach avoids many diffculties caused by the branch discontinuities and always fulfills the passivity and causality constraints. It takes full advantage of a novel method based on Weierstrass factorization theorem applied to nanophotonics [Grigoriev et al, Phys Rev A (RP) 88, 011803(R) (2013)]. We apply the method to the fishnet structure, and expand the effective permittivity and permeability into explicit Drude–Lorentz formula. The retrieved effective parameters accurately describe the fishnet metamaterial properties over a broad spectral range, and stand in excellent agreement with finite-element numerical computations, especially near the spectral resonances.

9125-63, Session PS2

Gold asymmetric split ring resonators (A-SRRs) for nano sensing of estradiol

Ifeoma G. Mbomson, Univ. of Glasgow (United Kingdom); Scott G. McMeekin, Glasgow Caledonian Univ. (United Kingdom); Basudev Lahiri, Univ. of Glasgow (United Kingdom) and National Institute of Standards and Technology (United Kingdom); Richard M. De La Rue, Univ. of Glasgow (United Kingdom) and Univ. of Malaya (Malaysia); Nigel P. Johnson, Univ. of Glasgow (United Kingdom)

Recent advances have seen asymmetric split ring resonators (A-SRRs) developed as sensing elements to record a shift in their peaks when there is a corresponding change in the surrounding environment. These studies have led to the investigation of Fano resonances associated with the coupling of the resonances of the A-SRRs with the molecular resonances of the analyte. The hormone estradiol was dissolved in ethanol and evaporated, leaving thickness of a few hundreds of nanometres on top of gold A-SRRs on a silica substrate. The reflectance was measured and a red shift is recorded from the resonators plasmonic peaks. The geometric size of the ASRRs are calculated to tune the plasmonic resonances near the molecular resonance of the C-H stretch at nominally 3.31 microns. Corresponding Lumerical modelling of the experimental data is performed using only the intensity and wavelength to match the Fano resonance at a modified wavelength of 3.42 microns.

9125-23, Session 6

Guiding, switching and sensing with hyperbolic metamaterials *(Keynote Presentation)*

Anatoly V. Zayats, King's College London (United Kingdom)

Plasmonic metamaterials based on aligned nanorod and nanotube arrays hybridised with functional materials provide a very flexible photonic platform for controlling optical, magneto-optical, nonlinear and quantum optical properties. These metamaterials can be designed to achieve a nonresonant, broadband response based on the properties associated with the so-called hyperbolic dispersion when the permittivity tensor components have opposite sign. In this talk we will overview optical properties of nanorod metamaterials enabling high performance chemical sensing, ultrasound detection as well as nonlinear intensity and polarisation switching. These metamaterials can be incorporated in plasmonic or nanophotonic circuitry to provide high performance integrated metamaterial-based photonic devices.

9125-24, Session 6

Electromagnetic radiation and scattering in hyperbolic metamaterials *(Invited Paper)*

Ivan V. Iorsh, National Research Univ. of Information Technologies, Mechanics and Optics (Russian Federation); Alexander Poddubny, Ioffe Physico-Technical Institute (Russian Federation); Pavel Ginzburg, King's College London (United Kingdom); Pavel Belov, National Research Univ. of Information Technologies, Mechanics and Optics (Russian Federation); Yuri S. Kivshar, The Australian National Univ. (Australia)

First, we present our recent results for the spontaneous decay rate of point-dipoles in the metal-dielectric layered structures and the arrays of the grapheme sheets, and showed that these structures can be effectively described as hyperbolic media in the optical and THz range respectively [1,2] with the Purcell factor proportional to cube of the ratio of the wavelength and the period of the structure.

As a development of this research direction we present the recent results on the elastic and non-elastic electromagnetic scattering processes taking place in hyperbolic media. It is clear, that while many research efforts are currently dedicated to the study of the spontaneous emission and absorption of the quantum emitters in hyperbolic metamaterials, which from the mathematical point of view are described via the Fermi Golden Rule, which is the result of the first order perturbation expansion of the light-matter coupling, the sufficient changes to the higher order processes such as scattering, should arise due to peculiar eigenmode dispersion in hyperbolic media.

We have studied the Compton scattering in hyperbolic media. It is known that in vacuum Compton effect which is the red-shift of the photon scattered on the free electron, can be observed only for x-rays, since the magnitude of the red-shift is roughly proportional to the ratio of the photon energy and the electron rest mass energy. At the same it appears, that in hyperbolic media the red-shift can be greatly enhanced and depends drastically on the scattering angle. In the limit of the uniform hyperbolic media, for the certain angles the red shift diverges (frequency of the scattered photon goes to zero) as well as the differential cross-section. Moreover, we have studied the effect of losses and the composite nature of the hyperbolic metamaterial. Particularly, we have shown that for the case of layered hyperbolic metamaterial, the maximum value of the relative enhancement of the red-shift (the ratio of red-shift in hyperbolic media and the red-shift in vacuum) is proportional to the square of the ratio of the wavelength and the period of the structure.

Although the Compton effect in hyperbolic media is quite a superficial problem, since the hyperbolic metamaterial per se contains the free electrons which produce the currents leading to the negative dielectric permittivity, and thus it is not quite clear how to isolate these electrons from that which acts as the scattering centre, this model task can give us an insight on the scattering processes in hyperbolic media, and help in solving more sophisticated and at the same time more realistic problems. Particularly, we discuss how the developed formalism can be used to study the Raman scattering, as well as magnon scattering in hyperbolic media.

Together with inelastic scattering, elastic scattering mechanisms in hyperbolic media can be of great interest. Particularly, we have recently shown that if we take a subwavelength chiral scatterer, which can perform the polarization rotation of the scattered light, place it inside the hyperbolic media and illuminate with TE-polarized plane wave (these waves have elliptic isofrequency surface and small density of states), then the scattering cross-section of the scatterer can be greatly enhanced. This is again due to the large density of the final states which are the TM modes having the hyperbolic dispersion. The enhancement of the chiral scattering can in principle be used in the spintronic circuits.

[1] "Spontaneous emission enhancement in metal–dielectric metamaterials", I Iorsh, A Poddubny, A Orlov, P Belov, YS Kivshar, Physics Letters A 376 (3), 185-187, 2012

[2] "Hyperbolic metamaterials based on multilayer graphene structures", IV Iorsh, IS Mukhin, IV Shadrivov, PA Belov, YS Kivshar, Physical Review B 87 (7), 075416, 2013.

9125-25, Session 6

Photonic hyper-crystals *(Invited Paper)*

Evgenii Narimanov, Purdue University (United States)

In the present work, we introduce a new "universality class" of artificial optical media - the photonic hyper-crystals. These hyperbolic metamaterials with a periodic spatial variation of dielectric permittivity on a subwavelength scale, combine the features of optical metamaterials and photonics crystals within the same medium, and allow for an unprecedented degree of control of light propagation.

Metamaterials and photonic crystals currently represent the primary building blocks for novel nanophotonic devices. With the goal of ultimate control over the light propagation,

an artificial optical material must rely on ei- ther the effect of a subwavelength pattern that changes the average electromagnetic response of the medium, or on Bragg scattering of light due to a periodic variation that is comparable to the wavelength. By virtue of this inherent scale separation, the corresponding metamaterial- and photonic crystal paradigms, while complementary, are generally considered mutually exclusive within the same environment.

The situation is however dramatically different in the world of hyperbolic metamaterials, where the opposite signs of the dielectric permittivity components in two orthogonal directions lead to a hyperbolic dispersion of TM-polarized propagating waves, with the wave numbers unlimited by the frequency. As a result, a periodic variation in the dielectric permittivity, regardless of how small is its period, will necessarily cause Bragg scattering of these high-k waves, leading to the formation of photonic bandgaps in both the wavenumber and the frequency domains, with profound consequences on wave propagation and scattering in these photonic hyper-crystals.

9125-26, Session 6

Hyperbolic metamaterials for superresolution imaging and deep sub-wavelenth cavities *(Invited Paper)*

Junsuk J. Rho, Univ. of California, Berkeley (United States) and Lawrence Berkeley National Lab. (United States) and Argonne National Lab. (United States); Xiang Zhang, Univ. of California, Berkeley (United States) and Lawrence Berkeley National Lab. (United States)

Metamaterials, artificially structured nanomaterials, have enabled unprecedented phenomena such as invisibility cloaking and negative refraction. Especially, hyperbolic metamaterials also known as indefinite metamaterials have unique dispersion relation where the principal components of its permittivity tensors are not all with the same signs and magnitudes. Such extraordinary dispersion relation results in hyperbolic dispersion relations which lead to a number of interesting phenomena, such as super-resolution effect which transfers evanescent waves to propagating waves at its interface with normal materials and, the propagation of electromagnetic waves with very large wavevectors comparing they are evanescent waves and thus decay quickly in natural materials. In this abstract, I will discuss our efforts in achieving the unique optical property overcoming diffraction limit to achieve several extraordinary metamaterials and metadevices demonstration. First, I will present super-resolution imaging device called “hyperlens”, which is the first experimental demonstration of near- to far-field imaging at visible light with resolution beyond the diffraction limit in two lateral dimensions. [1] Second, I will show another unique application of metamaterials for miniaturizing optical cavity, a key component to make lasers, into the nanoscale for the first time. It shows the cavity array which successfully captured light in 20nm dimension and show very high figure of merit experimentally. [2] I believe our efforts in sub-wavelength metamaterials having such extraordinary optical properties will lead to further advanced nanophotonics and nanooptics research.

References

[1] J. Rho et al., “Spherical hyperlens for two-dimensional sub-diffractional imaging at visible frequencies,” Nature Commun., vol. 1, pp. 143, 2010

[2] J. Rho* et al., “Experimental realization of three-dimensional indefinite cavities at the nanoscale with anomalous scaling laws,” Nature Photon., vol. 6, pp. 450-454, 2012

9125-27, Session 7

Coherent control of metamaterial functionalities *(Invited Paper)*

Xu Fang, Seyedmohammad A. Mousavi, Jinhui Shi, Univ. of Southampton (United Kingdom); Eric Plum, Optoelectronics Research Ctr. (United Kingdom); Kevin F. MacDonald, Univ. of Southampton (United Kingdom); Nikolay I. Zheludev, Optoelectronics Research Ctr. (United Kingdom) and Nanyang Technological Univ. (Singapore)

Engaging the coherent interaction of electromagnetic waves on metamaterial nanostructures allows for the efficient and ultrafast optical control of a huge range of optical phenomena from absorption to refraction, from optical activity to anisotropy. We outline this new concept and provide a number of experimental demonstrations of coherent control phenomena alongside discussing their spectroscopic and optical data processing applications.

9125-28, Session 7

THz nonreciprocal guiding surfaces and structures based on InSb

Pavel Kwiecien, Ivan Richter, Czech Technical Univ. in Prague (Czech Republic); Vladimír Kuzmiak, Ji?í ?tyrok?, Institute of Photonics and Electronics of the ASCR, v.v.i. (Czech Republic)

We present the results of numerical modeling and analysis of one-way light propagation in special magnetooptic (MO) guiding InSb-based structures operating in THz range. In THz spectral region, such MO components have become of particular interest due to such characteristics as sub-wavelength confinement and nonreciprocal one-way-propagating properties, along with the increasing needs for functional devices (such as isolators, switches, splitters), controlled with the external magnetic field via the MO effect. Here, the unidirectional propagation can arise from a strong electromagnetic spectral asymmetry in the presence of that external magnetic field, based on the simultaneous breaking of space and time-reversal symmetry. Although many conventional nanostructures with metal surfaces, based on propagating surface plasmon polariton (SPP) modes, are easily excitable with the coupling methods, they cannot be directly applied in THz frequency range. On the other hand, unlike metals, the dielectric properties of semiconductors can be adjusted by controlling the dopant concentration, determining the degree of confinement and the losses.

Based on our work on RCWA/aRCWA techniques, to be able to analyze such MO structures, we have recently developed a 2D numerical technique based on the MO aRCWA (2D MOaRCWA), i.e. the method capable of analyzing fully anisotropic media described by a general form of permittivity and/or permeability tensors. The technique includes all key improvements of the method, taking into account both proper Fourier factorization rules as well as the adaptive spatial resolution techniques. Our technique also allows analyzing SPP, or rather magnetoplasmon (MSP) propagation in structures in the presence of the external magnetic field in all three possible MO configurations, i.e., transversal (or Voigt), longitudinal (Faraday), and polar configuration.

To study one-way properties in THz range, we applied both (quasi)analytical methods as well as numerical simulations with the 2D MOaRCWA technique. We focused on the structures containing highly-dispersive polaritonic InSb material, in the presence of the external magnetic field, and its interfaces with dielectric (air) / metal (gold) planar interfaces, for the transversal (Voigt) MO configuration, imposing nonreciprocity (one-way propagation). Specifically, we have studied three types of InSb structures, namely: InSb/dielectric (air) planar boundary guide, InSb/air/metal (gold) planar waveguide, and symmetric InSb/air/InSb planar waveguide. In particular, we have studied the dispersion diagrams and relative spectral transmittance characteristics, with nonreciprocity behavior with respect to the propagation direction for the one-way MO InSb waveguide structures of interest. Also, we have determined the influence of the design parameters on the cutoff frequencies of forward and backward propagating modes, such as e.g., the effect of external magnetic field B, the effect of the change in permittivity of the dielectric waveguide layer, and the effect of

the dielectric waveguide thickness.

Although we have not tried to fully optimize the designs of the proposed structures, their basic functionality in terms of one way nonreciprocal behavior was clearly demonstrated. We believe that these types of planar MO waveguides can find many interesting applications in THz spectral region.

9125-29, Session 7

Bulk photovoltaic effect in photoconductive metamaterials based on cone-shaped nanoparticles

Sergei V. Zhukovsky, Viktoriia Babicheva, DTU Fotonik (Denmark); Alexander V. Uskov, Igor E. Protsenko, P.N. Lebedev Physical Institute (Russian Federation); Andrei V. Lavrinenko, DTU Fotonik (Denmark)

Optical metamaterials are artificially engineered composites known to reproduce properties rare or absent in nature (such as negative permeability or refractive index), or to amplify naturally weak effects (such as giant optical activity in chiral metamaterials). Moreover, metamaterials and metasurfaces made of nanoparticles or nanoantennas have shown a variety of applications related to nanoscale light manipulation, subwavelength confinement, light trapping and beam steering.

However, most studies of optical metamaterials only take into account purely electromagnetic response of nanoparticles and nanoantennas. Plasmonic effects are brought into the picture by assuming that the conduction electrons in metals move freely, but only within each nanoparticle's boundaries.

In this paper, we relax this restriction and consider the scenario when electrons can leave nanoparticles by the process of "hot" electron photoemission as a result of resonant excitation of localized surface plasmon resonance in the nanoparticles [1-3]. These microscopic processes can then be averaged, the entire composite acquiring effective photoconductive properties attributable to the whole metamaterial. The considered plasmonic nanoparticle arrays can therefore be regarded as a new type of metamaterials – photoconductive metamaterials [4-5].

In particular, we study metamaterials made of cone-shaped, similarly oriented nanoparticles embedded in a homogeneous semiconductor matrix. We predict theoretically and demonstrate numerically that spatially asymmetric shape of such nanoparticles results in the existence of a preferred direction where "hot" photoelectrons are emitted from the nanoparticle surface under the action of the localized plasmonic resonance excited in the nanoparticles.

The resulting directional photocurrent flow occurring when nanoparticles are uniformly illuminated by a homogeneous plane wave is the direct analogy of the photogalvanic effect known to exist in naturally occurring non-centrosymmetric media. This plasmonic bulk photovoltaic effect is intermediate between the internal photoelectric effect in bulk media and the external photoelectric effect at macroscopic interfaces.

The results obtained are valuable for characterizing photoemission and photoconductive properties of plasmonic nanostructures. They constitute a new way to characterize light-matter interaction at the nanoscale, and can find many uses for photodetection-related and photovoltaic applications.

[1] M. W. Knight et al, Science 332, 702 (2011).

[2] M. W. Knight et al, Nano Lett 13, 1687 (2013).

[3] I. E. Protsenko and A. V. Uskov , Phys Usp 55, 508 (2012).

[4] A. Novitsky at al, Prog. Photovolt. Res. Appl., (2012, in press), doi: 10.1002/pip.2278

[5] S. V. Zhukovsky et al, Plasmonics (2013, in press), doi: 10.1007/s11468-013-9621-z

9125-30, Session 7

Excitation of trapped modes in single element planar metasurface composed of Z-shaped meta-atoms

Abdallah Dhouibi, Institut d'Électronique Fondamentale, Univ. Paris Sud (France); Shah Nawaz Burokur, Institut d'Électronique Fondamentale, Univ. Paris Sud (France) and Univ. Paris-Ouest (France); Anatole Lupu, Institut d'Électronique Fondamentale, Univ. Paris Sud (France) and CNRS, UMR 8622 (France); André de Lustrac, Institut d'Électronique Fondamentale, Univ. Paris Sud (France) and Univ. Paris-Ouest (France)

Metamaterials made of a periodic array of subwavelength inclusions have recently attracted considerable interests because of their capabilities which go beyond conventional materials [1]. Various forms of inclusions such as Split Ring Resonator (SRR) [2] or electric-LC (ELC) resonator [3] have been shown to be able to produce respectively a wide range of permeability or permittivity values in the vicinity of the resonance.

Recently, we have proposed a practical way to change the LC equivalent circuit topology in the effective medium regime of the conventional ELC resonator. It has been reported that our geometrical transformation can lead to a better material homogeneity [4]; in other words we can observe resonance at a lower frequency for similar geometrical dimensions. Transforming the LC topology of the resonator helps to facilitate transposition of geometrical parameters for the optical regime and also to improve the metamaterial homogeneity. We investigated numerically and experimentally the electromagnetic behavior of a Z-shaped resonator and we have shown that the latter resonator exhibits an electric resonance, with the real part of the permittivity ranging from positive to negative values in the vicinity of the resonance.

In this work, we discuss about the excitation of a dark or trapped mode in such Z-shaped meta-atom. The electromagnetic behavior of the meta-atom has been investigated through both simulations and experiments in the microwave regime. Our results show that the Z meta-atom exhibits a trapped mode resonance. Depending on the orientation of the polarized electromagnetic field with respect to the Z atom topology and the incident plane, the excitation of the dark mode can either lead to a narrowband resonance in reflection or to a very asymmetric Fano-like resonance in transmission, analog of electromagnetically induced transparency.

[1] R.A. Shelby, D.R. Smith, S. Schultz, Experimental verification of a negative index of refraction, Science 292: 77-79, 2001.

[2] J.B. Pendry, A.J. Holden, D.J. Robbins, W.J. Stewart, Magnetism from conductors and enhanced nonlinear phenomena, IEEE Trans. Microwave Theory Tech.: 47, 2075-2084, 1999.

[3] D. Schurig, J.J. Mock, D.R. Smith, Electric-field-coupled resonators for negative permittivity metamaterials, Appl. Phys. Lett.: 88, 041109, 2006.

[4] A. Dhouibi, S.N. Burokur, A. de Lustrac, A. Priou, Z-shaped meta-atom for negative permittivity metamaterials, Appl. Phys. A: 106, 47-51, 2012.

9125-31, Session 7

High Q quadrupole and Fano resonances in THz metamaterials *(Invited Paper)*

Ranjan Singh, Nanyang Technological Univ. (Singapore); Wei Cao, Oklahoma State Univ. (United States); Ibraheem A. I. Al-Naib, Institut National de la Recherche Scientifique (Canada); Weili Zhang, Oklahoma State Univ. (United States)

Losses in metamaterials arises from the Ohmic resistance of the materials used to fabricate the meta-atoms as well as the

radiation resistance. Metals are the most widely used material for fabricating the meta-atoms such as split-ring resonators (SRRs) due to their high conductivity. At optical and near infrared frequencies, even the highest conducting metals exhibit Ohmic losses, thus requiring a new plasmonic material to be discovered in order to overcome the large resistive losses in optical plasmonic metamaterials. However, at far infrared frequencies, the most commonly used metals for metamaterials like silver, aluminum and gold have very high conductivity. The ultra-high conductivity ensures much lower resistive losses at terahertz frequencies. In recent times, there have been several attempts to control the losses in SRRs by enhancing the metallic conductivities at cryogenic temperatures as well as by using superconductors. Though, these approaches succeeded in reducing the non-radiative losses to nearly zero but there has been no significant improvement in the quality factor (Q) of the metamaterial resonances due to the existing radiative loss channels in these planar resonators. The typical values of Q-factor in the terahertz, infrared and optical plasmonic metamaterials is less than 10. The Q-factor of any resonator is the measure of photon lifetime inside the structure. Higher Q-factor corresponds to longer lifetime and also determines the number of times a photon circumnavigates within the resonator. So far, it has been extremely difficult to achieve ultra-high Q-factors in planar metamaterial resonators due to excessive losses. In this talk, we report extremely high Q-factor quadrupole and Fano resonances in planar terahertz metamaterials by suppressing the radiative losses. The Q-factor values obtained is at least one order of magnitude higher than all the previous demonstrations and forms an ideal platform for high resolution ultrasensitive terahertz sensing.

9125-32, Session 8

Tunable THz metamaterials using liquid crystals *(Invited Paper)*

Volodymyr Tkachenko, CNR-SPIN (Italy); Mikhail Lisitskiy, Istituto di Cibernetica Eduardo Caianiello (Italy); Nassim Chikhi, CNR-SPIN (Italy); Antonello Andreone, Univ. degli Studi di Napoli Federico II (Italy)

Because of their inherent resonant nature, metamaterials (MMs) are naturally filtering devices, and their electromagnetic response (EM) can be tailored to transmit, reflect and absorb light in a narrow frequency band. Being their EM properties scale invariant, MMs can be scaled down and used at any wavelength of interest from microwaves to optics. They can be therefore successfully exploited in the Terahertz range to fill the so-called THz gap. Moreover, for many applications tunable metamaterials are desirable. Tunability in MMs has been already demonstrated in the frequency region ranging from microwaves to THz using different mechanisms, such as MEMS, Schottky gate, photoexcitation. We report here that strong tunability can be achieved also by combining a planar MM based on Split Ring Resonators (SRR) with a liquid crystal (LC) having a relatively high birefringence. The reorientation of nematic LC molecule is exploited to change the permittivity of different capacitors present in each SRR unit cell and, therefore, to control the resonance frequency of the metamaterial by applying a low frequency voltage. The whole system is designed to obtain a maximum resonance shift up to 8% around the operational frequency of 1 THz for a LC with birefringence up to 0.4. This results in about 20 dB transmittance modulation.

Time domain spectroscopy on the device will be compared with FDTD electromagnetic simulations. THz measurements on different LCs will be also presented, aiming at the choice of the best material in terms of high birefringence and small energy losses, which are critical for resonant devices.

The possible application of such tunable MM as a spatial light modulator (SLM), where each SLM pixel consists of a number of SRRs with controlled reorienting LC molecules, will be discussed.

9125-33, Session 8

Active liquid crystal-loaded metasurfaces for THz and IR applications

Oleksandr Buchnev, Optoelectronics Research Ctr. (United Kingdom); Jan Wallauer, Markus Walther, Albert-Ludwigs-Univ. Freiburg (Germany); Nina Podoliak, Optoelectronics Research Ctr. (United Kingdom); Malgosia Kaczmarek, Univ. of Southampton (United Kingdom); Nikolay I. Zheludev, Optoelectronics Research Ctr. (United Kingdom) and Nanyang Technological Univ. (Singapore); Vassili A. Fedotov, Optoelectronics Research Ctr. (United Kingdom) and Univ. of Southampton (United Kingdom)

One of the important steps towards practical application of the metamaterials is the implementation of an efficient active control over their optical response. This can be achieved by hybridising the fabric of these man-made photonic materials with naturally available functional media. Among such media liquid crystals possess arguably the largest and most broadband optical nonlinearity, while their properties can be readily controlled by light, temperature, electric and magnetic fields. Here we experimentally demonstrate active planar metamaterials (or metasurfaces) – artificially structured thin metal films loaded with liquid crystals, where the resonant response can be dynamically controlled both in terms of its magnitude and wavelength using externally applied electric field. The electric control has been implemented for THz and near-IR metasurfaces by engaging for the first time the in-plane switching of liquid crystals at micro- and nano-scale. As a result, it became possible to realise an optically thin large-area modulator of THz radiation with the absolute change in intensity and phase of correspondingly 20 % and 40 deg, achieved for a single pass transmission at only 20 V. For the near-IR metasurface we were able to bring the control voltage below 2 V demonstrating spectral tuning of its response by as larger as 100 nm.

9125-35, Session 8

THz and NIR metamaterials for sensing and switching in organics *(Invited Paper)*

Jeong-Weon Wu, Ewha Womans Univ. (Korea, Republic of)

Metamaterials are artificially structured materials in subwavelength scale, where the electromagnetic responses not readily available in nature are observed. In order to functionalize metamaterial, organics are introduced in metamaterial. Depending on the subwavelength size, the frequency regimes of functional metamaterial operation are determined. From a standard photolithography process, THz metamaterials are fabricated. By employing isotropic and anisotropic metamaterials with micron size linewidths, the orientation of nematic liquid crystal and carbon nanotube can be identified. The sensitivity of anisotropic sensing is significantly enhanced near the resonance of metamaterials. By use of a standard electron-beam lithography and focused-ion-milling, metamaterials with nano-sized linewidths are fabricated possessing near IR resonances. Two examples of switching in near IR metamaterials are introduced, namely, photonic and electric switchings. Photo-isomerization of azo-nematics allows for a photonic switching of transmission in positive near-IR metamaterial, while electric alignment of nematics provides an electric switching of reflection resonance in negative near-IR metamaterial.

9125-60, Session 8

Miniaturization of metamaterial electrical resonators at the terahertz spectrum

Theodosios D. Karamanos, Nikolaos V. Kantartzis, Aristotle Univ. of Thessaloniki (Greece)

During the past years, artificial media engineered to exhibit desired attributes, such as ?'<0 and ?'<0, represent an attractive research field in electromagnetism. These structures, also known as metamaterials, are composed of resonator arrays that operate at a wavelength much smaller than their largest dimension (usually smaller than ?0/3). Lately, metamaterials have entered the relatively unexplored area of the terahertz regime and are likely to contribute to the development of many interesting applications, like nano-antennas, extraordinary transmission devices, effective media with certain material parameters for surface wave propagation and combined graphene-metamaterial structures. A major challenge in the resonator design is its miniaturization, namely the technique that would allow them to operate at a lower frequency with minimal dimensions. The most popular algorithm is to consider the resonator in terms of an equivalent LC-circuit and attempt to lower the resonance frequency of the circuit by increasing the L or C of the resonator's inductive or capacitive elements, respectively.

In this work, we present a methodology for the efficient modification of electrical resonators in order to miniaturize their size for terahertz applications. For this purpose, we, firstly, employ the conventional OE1 resonator; a structure which without any change exhibits the lowest electrical resonance frequency for minimum dimensions. Furthermore, in order to increase C, we add interdigital capacitance elements and study their impact on the resulting device. Next, for the first time to the best of the authors' knowledge, spiral elements are incorporated to the electrical resonators to increase L and thus reduce the resonance frequency, while adding an extra degree of freedom in the design process. The proposed modifications are combined and their effect in the resonance position and quality is thoroughly investigated. Finally, the contribution of different dielectric substrates and metals is systematically assessed.

9125-36, Session 9

Nonlinear plasmonic metamaterials sustaining vortices and special guided waves *(Invited Paper)*

Allan D. Boardman, Peter Egan, Univ. of Salford (United Kingdom)

The fascinating world of structured material sustaining structured light, such as spinning light beams, is investigated with the aim of revealing new and exciting pathways to applications in modern digital control of our environment.. Vortex generation and propagation properties have a beautiful history, and the possibility of generating them together with magnetooptic control in plasmonic metamaterials will be discussed in detail. An emphasis will be placed on the fact that certain members of the soliton family have a lot of application possibilities, especially when placed into the context of materials being used in a light-controlling-light environment. The latter phenomenon is suitable for optical chips of the future. Both spatial and temporal solitons will be invoked with an emphasis upon narrow beams and extremely short pulses. It will be pointed out, very strongly, that detailed control of light-packets can also be introduced especially by the deployment of plasmonic metamaterials in the optical frequency range. In order to stimulate the main features of this kind of metamaterial activity, an exact study of wave propagation in waveguides is required. It is shown that such waveguides may need to be tapered, or simply just power controlled. It is an added advantage to be able to use magnetooptics, which is a, globally, very advanced technology. The detailed merits of magnetooptic control will be discussed and the positive ways that any potential disadvantages can be mitigated, for an integrated optics format, will be presented. All the complex structures that will be examined will include the kind of soliton-like channels available from modern experimental facilities. A special consideration will be given to neighboring interface interactions. Both optical linearity and nonlinearity will be compared, for a wide range of metamaterials, showing that the outcomes of the investigations given here will lead to a new range of exotic optical switching.

Sophisticated applications will be discussed in detail and it will be pointed out that they should now be entirely accessible. In addition, it will be emphasized, throughout the presentation, that isotropic metamaterials, with loss-free frequency windows, are within reach through composites containing certain types of nanospheres, especially since it is possible to make such composites using magnetooptic spheres. It will be made clear that it is evident that new portals are emerging, implying new frontiers that need to be addressed, urgently, especially on the transformation optics front, in a lot more detail. It is stressed that nonlinear systems are a vital part of this development, especially when coupled to tunability. Indeed, since taking into account nonlinearity, leads to very special properties when dealing with negative index metamaterials, it may well be the way forward when addressing potentially devastating loss windows. The work reported here ranges over a wide range of possibilities, and is supported by many fascinating, but achievable, magnetooptic manipulation and the role of solitons

Finally, vortices and vortex solitons can be important, especially if they are coupled to external control in plasmonic metamaterials, implying that important, future applications must be placed into the context of metamaterials being used in a light-controlling-light environment, and future research pathways must exploit light-packets and complex guides with a non-uniform thickness.

9125-37, Session 9

Optical channels for nonlinear metamaterials

Alexey P. Slobozhanuk, National Research Univ. of Information Technologies, Mechanics and Optics (Russian Federation); Polina V. Kapitanova, Saint Petersburg Electrotechnical Univ. "LETI" (Russian Federation); Dmitry S. Filonov, National Research Univ. of Information Technologies, Mechanics and Optics (Russian Federation); David A. Powell, Ilya V. Shadrivov, The Australian National Univ. (Australia); Mikhail Lapine, The University of Sydney (Australia); Pavel Belov, National Research Univ. of Information Technologies, Mechanics and Optics (Russian Federation); Ross C. McPhedran, The Univ. of Sydney (Australia); Yuri Kivshar, The Australian National Univ. (Australia)

We report a design and experimental implementation of an efficient scheme which yields a novel mechanism of nonlinear interaction between otherwise independent microwave signals via an optical channel. Our approach allows interaction to be imposed between otherwise independent signals with arbitrary frequencies, and therefore significantly widens the range of nonlinear processes possible in such optically-coupled systems.

To realise this goal, we provide a scheme where SRRs are actively involved in the optical control, serving as both receivers and sources of optical radiation. Our design comprises two varactor-loaded SRRs, which are arranged to be orthogonal to each other, so that there is no direct electromagnetic coupling between the two resonators. However, one of the SRRs is equipped with a photodiode (PD), and the other has a light-emitting diode (LED), resulting in an optical bridge between the LED and the PD.

At low power of the electromagnetic signal launched into the LED-SRR, there is insufficient voltage rectified by the varactor to light up the LED, so there is no interaction between the SRRs. At high power, the LED is lit and the emitted light is absorbed by the PD, providing a voltage across the varactor, thus changing its capacitance, which directly affects the resonance frequency of the PD-SRR. The higher the power, the brighter the LED, and the larger the voltage provided by the PD, causing a stronger change in the varactor capacitance. Thus, the resonant frequency of the PD-SRR is directly controlled by the signal power in the LED-SRR, despite having no direct electromagnetic coupling between the two.

To confirm our ideas, we have fabricated an experimental prototype, employing broadside-coupled SRRs, with one of the SRRs smaller then the other, so that the smaller one fits inside

the larger one. We report the experimental dependence of the frequency shift as a function of power and demonstrate a good agreement with the circuit calculations. We also experimentally confirm polarisation sensitivity of the non-reciprocal interaction. All the experiments were performed in the dark to prevent parasitic illumination of the PDs.

The designed meta-atom opens exciting opportunities to impose a novel control mechanism over microwave signals. For example, a chain of such elements supports two initially independent magnetoinductive waves with orthogonal polarisations, which can propagate along the chain without direct interaction: one of the waves only drives the sequence of PD-SRRs while the other one only drives the sequence of the LED-SRRs. However, by varying power of wave transmitted with the LED-SRR polarisation, we will launch an optical feedback onto the chain of PD-SRRs and thus alter its dispersion characteristics despite the lack of coupling between the two subsystems in the linear regime. This feedback mechanism is promising for applications in signal processing and filtering, as well as for tuning and sensing.

9125-38, Session 9

Static and dynamic properties of third harmonic generation in fishnet metamaterials

Alexander Shorokhov, Maxim Shcherbakov, Lomonosov Moscow State Univ. (Russian Federation); Jörg Reinhold, Christian Helgert, Thomas Pertsch, Friedrich-Schiller-Univ. Jena (Germany); Andrey A. Fedyanin, Lomonosov Moscow State Univ. (Russian Federation)

The angular dependence of third harmonic generation in fishnet metamaterials and its transient properties on the subpicosecond time scale were studied.

The proposed fishnet metamaterial was defined by e-beam-lithography and lift-off technique on a SiO2 substrate. It represents a multilayer structure of Au-MgO-Au films 20-35-20 thick. The structure has a period of 500 nm in both lateral directions.

Spectroscopy of the linear absorption for different angles of incidence with the angle varying from 0 to 50 degrees was carried out. The normal incidence IR absorption spectrum demonstrates an absorption peak at 1.54 ?m corresponding to the excitation of the magnetic plasmon mode, which position is blue-shifted as the angle of incidence is increased. For the nonlinear measurements a setup based on an optical parametric amplifier (OPA) was used operating at wavelengths of 1.49, 1.54, 1.56, and 1.60 ?m and having an average output power of 3 mW focused to a 300 ?m spot from the air side of the sample. The OPA was pumped by a Nd:YAG laser with a pulse duration of 5 ps and a repetition rate of 5 kHz. The resulting fluence took values up to 700 ?J/cm2 in the plane of the sample. The sample was placed on a six-axis positioning stage so that during the angular spectroscopy the beam was always focused into the same spot. The forwardly propagating third harmonic generation (THG) signal pulses were detected by a photomultiplier tube and gate-integrated by an oscilloscope. We used the p-p polarization configuration—illuminating with p-polarized light and selecting only the p-polarized part of forward propagating light before the detector. For all measurements spectral filtering before the detector was used for picking up the desired wavelength. The averaged THG signal from the pure SiO2 substrate measured outside the metamaterial area was at least one order of magnitude lower than that from the metamaterial area. Contributions from the substrate were therefore safely neglected.

For investigation of transient properties we use pump-probe technique. A laser beam from a femtosecond fiber laser with a central wavelength of 1.56 μm and pulse duration about 180 fs is split by the polarizing beam splitter into two channels, one of which allows us to bring time delay between two pulses by a mechanical translator. The average power of laser beam in two channels was up to 20 mW that corresponds to peak intensities up to 25 kW/cm2. Laser beams from two channels were focused by the objective lens onto the sample with waist about 25 μm and behind it were collected by the lens to the photon-multiply tube. To increase the ratio of signal to noise we use the lock-in technique with two modulation frequencies in two channels. It allows us to measure at summary frequency for separating only mutual influence of two pulses. Using the additional filters we determined that the spectral position of the detected signal corresponds to the triple frequency of the pump radiation.

9125-39, Session 9

Frequency-resolved optical gating of one-dimensional plasmonic crystals

Tatyana V. Dolgova, Varvara V. Zubyuk, Alexander I. Musorin, Andrey A. Fedyanin, Lomonosov Moscow State Univ. (Russian Federation)

The resonant interaction between the surface charge and the electromagnetic field of the light constitutes the surface plasmons polaritons and gives rise to its unique properties [1]. Oscillations of such nature allow one to use plasmonic nanostructures as devices that control the optical radiation on micro- and nanoscale. Femtosecond-scale polarization state shaping has been experimentally found recently in optical response of a plasmonic nanograting by means of time-resolved Stokes polarimetry [2] based on the intensity autocorrelation scheme that is the most common technique to examine ultrashort pulses because it is easy to set up and use. But the information of the electric field phase is lost in such a measurement. Frequency-Resolved Optical Gating (FROG) which was invented by R. Trebino et al. [3] is one of the technique for retrieving both the amplitude and phase of the field.

In this work ultrafast dynamics of surface plasmons in one-dimensional plasmonic crystals is studied experimentally by using FROG technique.

Several techniques can be used to excite surface plasmon. One of them is a periodic perforation of the metallic surface. One-dimensional perforated metal film fabricated by laser interference lithography is used to study the excitation of surface plasmon-polaritons. The sample is 50-nm-thick gold film sputtered onto the grating of the of 0.8-?m-thick photoresist on a quartz substrate. The reflectance spectra show two pronounced minima corresponding to the edges of the plasmonic band gap (792 nm and 842 nm), the distance between them increases with increasing the incidence angle.

For measurements of the surface plasmon dynamics the technique of frequency-resolved optical gating (FROG) was used. Spectrograms were measured for the pulses normally reflected from the sample. The wavelength was chosen near edges of the band gap (792 nm and 842 nm). The spectrograms show very distinctive peculiarities for the case of surface plasmon excitation configuration: for p-polarized incident light there are significant changes as the pulse width and spectral characteristics at wavelengths near edges of the plasmonic band gap. The features are associated with resonant excitation of surface plasmon polaritons. The amplitude and phase of the pulses are extracted from the spectrogram series. The phase sensitivity of the technique allows us to reconstruct non-symmetric plasmon-assisted reshaping of the femtosecond pulses.

[1] W. L. Barnes, A. Dereux, T. W. Ebbesen, “Surface plasmon subwavelength optics”, Nature 424 (2003) 824.

[2] M. R. Shcherbakov, P. P. Vabishchevich, V. V. Komarova, T. V. Dolgova, V. I. Panov, V. V. Moshchalkov, and A. A. Fedyanin “Ultrafast Polarization Shaping with Fano Plasmonic Crystals”, Phys. Rev. Lett. 108, 253903 (2012).

[3] R. Trebino, K.W. DeLong, D.N. Fittinghoff, J.N. Sweetser, M.A. Krumbügel, B.A. Richman, and D.J. Kane, “Measuring ultrashort laser pulses in the time-frequency domain using frequency-resolved optical gating”, Rev.Sci.Instrum. 68(9), 3277 (1997).

9125-40, Session 9

Controlling magnetism at the nanoscale with metamaterials *(Invited Paper)*

Nikitas Papasimakis, Evangelos Atmatzakis, Anagnostis Tsiatmas, Vassili A. Fedotov, Optoelectronics Research Ctr. (United Kingdom); Boris Luk'yanchuk, A*STAR - Data Storage Institute (Singapore); F. Javier Garcia de Abajo, ICFO - Institut de Ciències Fotòniques (Spain); Nikolay I. Zheludev, Optoelectronics Research Ctr. (United Kingdom)

Controlling magnetic fields at ever shorter time and length scales is important for both fundamental solid-state physics and technological applications such as spectroscopy, sensing, magnetic data recording. Here, we will present recent progress towards the generation and control of magnetic fields at the nanoscale. We will show that combining plasmonic and ferromagnetic metals in bimetallic nanorings leads to strong Kerr rotation enhancement. Moreover, when illuminated by femtosecond laser pulses, such arrays respond with transient thermoelectric currents of picosecond duration, which in turn induce Tesla-scale magnetic fields in the ring cavity. We will demonstrate that equivalent levels of confinement can be obtained at even higher frequencies by appealing to the deep sub-wavelength nature of plasmons in semi-metals, where strong, tunable magnetic response can be observed in electrically doped monolayers. Our results provide avenues to nanoscale magnetic fields and hold great potential for materials characterization, terahertz radiation generation, and data storage applications.

9125-41, Session 10

Terahertz graphene metamaterials *(Invited Paper)*

Philippe Tassin, Chalmers Univ. of Technology (Sweden); Nian-Hai Shen, Ames Lab. (United States); Thomas Koschny, Costas M. Soukoulis, Iowa State Univ. (United States)

Graphene, a one-atom-thick sheet of carbon atoms arranged in a honeycomb lattice, exhibits many interesting properties. In this contribution, we present a study of terahertz metamaterials made from patterned graphene [Science 341, 620, 2013]. Graphene is potentially useful for use in metamaterials, because (1) it allows for miniaturization down to the atomic length scale; (2) its tunable Fermi level allows for unprecedented tunability of electromagnetic structures made of this material; (3) it has a highly reactive response, resulting in strongly localized, deeply subwavelength plasmons and deep subwavelength resonators; and (4) it may provide broadband gain. We compare a series of experimental measurements for the dynamic terahertz conductivity of graphene with recently proposed terahertz graphene metamaterial structures. In addition, we compare split-ring resonators made from graphene versus gold and discuss the properties of the electric and magnetic dipole resonances of such split-ring resonators, as well as applications in tunable metamaterials.

9125-42, Session 10

Permittivity, specific resistivity and surface roughness of silver nanolayers for plasmonic applications

Tomasz Stefaniuk, Piotr Wróbel, Pawe? Trautman, Univ of Warsaw (Poland); Aleksandra A. Wronkowska, University of Technology and Life Sciences (Poland); Andrzej Wronkowski, University of Technology and Life Sciences, (Poland); Tomasz Szoplik, Univ of Warsaw (Poland)

We report on measurements of electrical, optical and morphological properties of silver nanolayers. The Ag films of thickness from 10 to 500 nm are deposited in e-beam evaporator. Fused silica and sapphire substrates are used with nominal root-mean-square (RMS) roughness equal 0.3 and 0.2 nm, respectively. Silver is deposited either directly on substrates or with Ge, Ni, or Ti wetting interlayer. The sheet resistivity of the Ag films is measured using two methods: the van der Pauw method with the electrical contacts located on perimeters of the samples and four probes contacting the samples at points lying in a straight line. Specific resistivity of Ag films on fused silica change from >109 to 1.80 [???cm] when thickness increases from 10 to 500 nm. Specific resistivity of 10, 30 and 50 nm Ag films on 1 nm Ge wetting layer are equal 14.01, 7.89, and 5.58 [???cm], respectively, and are about twice higher than those with Ti or Ni interlayers. The refractive index n and the extinction coefficient k of Ag films are derived from spectroscopic ellipsometry and reflectance measurements carried in air in the spectral range from 0.6 to 6.5 eV (193 – 2200 nm) using a rotating analyzer ellipsometer (V-VASE, J.A. Woollam Co.). At about 2 eV (620 nm) in both Ag/Ge/SiO2 and Ag/Ge/Al2O3 samples deposited at RT we observe strong maxima in imaginary part of permittivity. Increase of losses in silver on germanium samples results from segregation of Ge atoms to the Ag film surface, which is the low-coordination site. Segregation effect of Ge disappears when dielectric overlayer is added onto Ag film. Surface roughness is measured using AFM (Ntegra NT-MDT) under tapping mode in air with sharp etalon probes and 5:1 aspect ratio. Ag layers of 10 and 30 nm thicknesses have nearly the same RMS roughness at deposition temperatures from the range 180 – 350 K. The lowest RMS=0.2 nm is achieved for 10 nm film Ag/Ge evaporated at 295 K.

Acknowledgement: This work is supported by the Polish National Centre for R&D under the project PBS1/A5/27/2012.

9125-43, Session 10

Negative index fishnet structures with nanopillars formed by nanoimprint lithography

Graham J. Sharp, Saima I. Khan, Univ. of Glasgow (United Kingdom); Ali Z. Khokhar, Univ. of Southampton (United Kingdom); Nigel P. Johnson, Univ. of Glasgow (United Kingdom)

Metamaterial fishnet structures have long been used to exhibit a negative refractive index, owing to the ability to tune both the permittivity and permeability independently by changing the structural dimensions of their interlocking metal tracks. Conventionally, although other techniques exist, fishnets have been fabricated by employing e-beam lithography to pattern a mask and then either etch or deposit a series of metal and dielectric layers. In this paper we demonstrate the ability to fabricate fishnets by nanoimprinting directly into a pre-deposited three layer metal-dielectric-metal stack, enabling us to pattern the structures in less than two minutes. Patterning is achieved by imprinting an etched silicon carbide stamp into a tri-layer of Ag, MgF2 and Ag on top of a thick film of PMMA. We have designed and fabricated three different fishnets of varying dimensions using this method and measured their resonant wavelength in the near-infrared between 1.45 ?m and 3.28 ?m. FDTD simulations complement our measurements and suggest a negative refractive index at the resonant wavelength. A by-product of directly imprinting into the metal-dielectric stack is rectangular nanopillars that sit within the gaps, or "windows", between the fishnet tracks. Reflectance measurements at visible wavelengths show a plasmonic resonance that shifts accordingly with the size of the pillars.

9125-57, Session 10

Single photon excitation and entanglement transfer using hyperbolic metamaterials

Onur Danaci, Ozgur Müstecaplioglu, Koç Univ. (Turkey)

Quantum Information tasks such as entanglement generation/ transfer[1] and Quantum Imaging tasks such as subwavelength resolution[2] require single-photon sources and single-photon excitation of qubit. An efficient single-photon source requires enhanced spontaneous emission rate; increased Purcell Factor[3]. First noted by Agarwal et al[4], spontaneous emission rate of an atom is affected in the presence of absorbing dielectrics. Plasmonics community devised many setups to use this effect for Purcell factor engineering. In principle, reverse of this process, single-photon excitation of qubit, is possible. According to Choquette et al[5], however, a time-inverted pulse must be generated due to broken symmetry of plasmon-emitter system, hence strong directionality of emission, comparing to an emitter in vacuum. Numerous proposal have been made regarding plasmon-assisted transmission of entanglement[6-7-8]. However, we focus on Hyperbolic metamaterial(HMM) geometries due to their Purcell Factor enhancement [9-10-11] and high-k modes they support due to extreme anisotropy in dielectric tensor[10] leading to subwavelength resolution. We use stacked multilayer dielectrics geometry proposed by [12], and the model devised by Newman et al[9] where differing layers of Ag/Ti02 with thickness 10/30 nm are present. Newman et al [9] estimated greatest rate of high-k emission to far-field for 900nm, where a superstrate with real dielectric constant greater than 30 is needed for outcoupling to vacuum photonic modes and light is emitted to a cone of 34-degree half-angle. For the sake of engineering time-inverted pulse, we use this model with the same values predicted for greatest emission rate, and use Choquette et al's [5] suggestion of, which is proposed for Kreschmann configuration, using ring mirror to compensate conical spontanteous emission in HMM. A single photon, conical, time-inverted pulse is sent for single-photon excitation; two single-photon light modes are sent for qubit-qubit entanglement and checked if there is transfer between qubits or transmitted field modes similar to Cano et al[6]; second order coherence, g(2) for subwavelength imaging[2] is calculated. To predict quantum optical statistics, we utilize Green's Tensor formalism for QED in Absorbing media that was developed by Knöll et al[13], input-output formalism for incoming and transmitted field modes[13], conical field envelope and small-frequency range approximation by Choquette [5], an open-quantum two-level system with Jaynes-Cumming model, and Classical Green's Dyad calculations oh HMM by Z.Jacob[10] and Potemkin[12] et al as analytical foundations. For numerics, Fresnel transmission&reflection coefficients for Green's Tensor are calculated by Scipy, master-equation solutions and entanglement measures like Wootter's[14] concurrence for qubit-qubit and Hillery et al's [15] genuine mode entanglement for photon-photon correlations are managed by QuTIP packages of Python. Our results indicate that excitation probability is highly directional and converges to unity as it goes by predicted 34-degree half-cone angle, entanglement transfer between qubits and fields are possible if dissipation is manipulated by changing dipole orientation due to directionality, and even sharper g(2) for subwavelength resolution due to multipath interference in anisotropic dielectrics.

[1]: Phys. Rev. A 73, 042319 (2006)

[2]: PhysRevLett.99.133603

[3]: Phys. Rev. 69, 681 (1946)

[4]: Phys. Rev. A 11, 230 (1975)

[5]: Phys.Rev. A 85, 063841 (2012)

[6]: Phys. Rev. B 84, 235306 (2011)

[7]: E. Altewischer et al., Nature (London) 418, 304 (2002)

[8]: Phys. Rev. Lett. 94, 110501 (2005)

[9]: JOSA B, Vol. 30, Issue 4, pp. 766-775 (2013)

[10]: J. Opt. 14 (2012) 063001

[11]: Phys. Rev. A 84, 023807 (2011)

[12]: PhysRevB.74.075103.pdf

[13]: Ludwig Knöll and Stefan Scheel and Dirk-gunnar Welsch; "QED in Dispersing and Absorbing Media"

[14]: Phys. Rev. Lett. 80, 2245–2248 (1998)

[15]: Phys. Rev. A 74, 032333 (2006)

9125-45, Session 11

Polarization control with transformation optics and metasurfaces *(Invited Paper)*

Jensen Li, The Univ. of Birmingham (United Kingdom)

Transformation optics is mainly enabled by metamaterials with varying indices and anisotropies. For two dimensional propagation, the TE and TM polarizations are usually decoupled and manipulated separately. By using anisotropic media with non-trivial principal axes, we show how polarizations can be coupled and controlled within a framework using field transformation, in addition to the conventional coordinate transformation approach. For example, we can design a device to achieve complete cross-polarization conversion between TE and TM waves. We can mimic a perfect magnetic conductor of arbitrary shape. In a related context of metasurfaces consisting of a mono-layer of spatially varying metamaterial atoms, we will discuss how geometric phase elements constructed from anisotropic metamaterial atoms can be used to manipulate spin-orbit interaction on structured light with both orbital angular momentum (OAM) and spin angular momentum. We will show spin-induced effect on the OAM, as a manifestation of optical spin Hall effect and orbital rotation.

9125-46, Session 11

Trapping light by mimicking gravitational lensing

Hui Liu, Chong Sheng, Shining Zhu, Nanjing Univ. (China); Dentcho A. Genov, Louisiana Tech Univ. (United States)

According to Einstein's theory, the presence of matter energy results in curved spacetime and the complex motion of matter and light along geodesic trajectories that are no longer straight lines. On the other hand, given the analogy between the macroscopic Maxwell's equations in complex inhomogeneous media and the free-space Maxwell's equations on the background of an arbitrary spacetime metric, the study of light propagation in artificially engineered optical materials and the motion of massive bodies or light in gravitational fields are closely related.

In particular, the transformation optics approach can be used to mimic black holes, Minkowski spacetimes, electromagnetic wormholes, cosmic strings, the Big Bang and cosmological inflation, as well as Hawking radiation. Although the theoretical foundations behind the design of "toy" models of general relativity are now sufficiently well understood, the experimental validation of the transformation optics approach to mimic the scattering of electromagnetic radiation in close proximity to actual celestial objects remains a challenge, especially for visible light.

In this work, we propose a flexible experimental methodology that allows the direct optical investigation of light trapping around a microsphere, which simulates the gravitational lensing due to power law mass–density/pressure distributions, including light trapping at the photon sphere similar to that around compact neutron stars and black holes. Our approach uses a microsphere that is embedded into a planar polymer waveguide that is formed during a controlled spin-coating process. Given the surface tension effects, the waveguide around the microsphere is distorted resulting in a continuous change in the waveguide effective refractive index, which under certain conditions can mimic the curved spacetimes caused by strong gravitational fields. Based on direct fluorescence imaging, we observe the lensing and asymptotic capture of the incident light at an unstable circular orbit that corresponds to the photon sphere of a compact stellar object. These observations clearly demonstrates that the proposed experimental methodology provides a useful "toy" model to study both near- and far-field electromagnetic effects under a controlled laboratory environment, similar to the gravitational lensing described in general relativity. The experimental observations are in excellent agreement with the developed theory, validating both the derived exact solution of the Einstein field equations and the

predicted geodesic trajectories of massless particles in the inherent curved spacetime. Our method may also be applied to control light propagation in integrated optoelectronic elements, light splitters and benders, omnidirectional absorbers and energy harvesting devices.

9125-47, Session 11

Transformation multiphysics metamaterials

Massimo Moccia, Giuseppe Castaldi, Univ. degli Studi del Sannio (Italy); Salvatore Savo, Yuki Sato, The Rowland Institute at Harvard (United States); Vincenzo Galdi, Univ. degli Studi del Sannio (Italy)

Metamaterials can be used to manipulate physical quantities spanning beyond the traditional realm of optics. Transformation optics offers an unprecedented tool to design anisotropic, spatially inhomogeneous artificial materials capable of controlling the propagation of electromagnetic, acoustic and mechanical waves, DC electrical currents as well as diffusion-based phenomena like heat flow.

Here we address the simultaneous manipulation of multiple physical phenomena in independent fashions. As a proof of principle of this "transformation multiphysics" framework, we design and synthesize (in terms of realistic material constituents) a metamaterial shell that simultaneously behaves as a thermal concentrator and an electrical "invisibility cloak". Our numerical results open up intriguing possibilities in the largely unexplored phase space of multi-functional metastructures, with a wide variety of potential applications to electrical, magnetic, acoustic, and thermal scenarios.

9125-48, Session 11

Metasurfaces applications at terahertz and infrared frequencies: flat lenses, directive antennas and planar modulators *(Invited Paper)*

Tahsin Akalin, IEMN, Lille 1 University (France)

Metasurfaces offer new degrees of freedom for the realization of fundamental functions for the control of electromagnetic waves. Recent results that we have obtained at different frequency ranges, from millimeter waves to terahertz and infrared frequencies, will be presented and compared to the state of the art in this research topic. These different metallic structures can be combined with materials as well for their fundamental study but also for their own properties in order to improve the performances of these metasurfaces.

9125-49, Session 11

Chiral metamaterials for THz polarization control *(Invited Paper)*

Maria Kafesaki, G. Kenanakis, Eleftherios N. Economou, Foundation for Research and Technology-Hellas (Greece); Costas M. Soukoulis, Iowa State Univ. (United States) and Foundation for Research and Technology-Hellas (Greece)

Chiral metamaterials operating in the THz regime, due to their great potential for polarization control, can provide a valuable tool for the polarization manipulation of THz waves, where natural materials show limited possibilities. In this talk we demonstrate, both theoretically and experientially, a variety of THz chiral structures based on the bi-layer conductor configuration and fabricated on flexible substrates. Our structures show giant optical activity and negative index of refraction for both left- and right-handed circularly polarized waves. Incorporating properly photoconducting Si in some of the structures, we demonstrate also tunable chiral response, represented by tunable optical activity and circular dichoroism.

9125-50, Session 11

Controlling coherence in epsilon-near-zero metamaterials *(Invited Paper)*

Humeyra Caglayan, Univ. of Pennsylvania (Turkey)

The extreme-parameter metamaterials, such as epsilon-near-zero (ENZ) have attracted a great deal of attention recently. Manipulating electromagnetic waves and fields by spatially and temporally tailoring the material parameters such as permittivity and permeability offer unprecedented tools in the design of devices and components. ENZ structures "stretch" the effective wavelength inside the structure and as a result physical distances in such structures, although physically large, may behave as electrically small lengths. Coherent electromagnetic waves incident on multiple randomly placed scatterers in a conventional medium may be given some degree of incoherence. In this talk, I am going to present how an ENZ medium can be used to mitigate this effect by comparing the incoherence introduced by scatterers in a conventional medium to that in an ENZ medium.

9126-1, Session 1

Enhancement of second-harmonic generation from silicon nitride with gold gratings

Tingyin Ning, Chunlei Tan, Tapio Niemi, Janne Simonen, Goëry Genty, Martti Kauranen, Tampere Univ. of Technology (Finland)

Both metallic and dielectric nanostructures can concentrate optical energy to strong local electromagnetic fields that can enhance optical interactions. Such local-field enhancement is particularly beneficial for nonlinear optical effects. We have previously shown that resonance waveguide gratings fabricated into silicon nitride (SiN) films can enhance second- (SHG) and third (THG)-harmonic generation for TM-polarized light by factors of 1000 and 2000, respectively. In this paper, we show that gold gratings covered with SiN waveguide layer can lead to similar enhancements of SHG for both TE and TM-polarized light.

The structures were designed by solving the coupled equations for the fundamental and SHG waves using the finite element method. The design for the wavelength of 1064 nm resulted in a gold grating with a period of 565 nm, fill factor of 0.67, gold thickness of 30 nm, and SiN film thickness of 450 nm. The results predicted that SHG should be enhanced by a factor of 2000 for both TE- and TM- polarized incident light with the SHG signal being always TM-polarized.

The gold grating was fabricated by nanoimprint lithograph on silica substrates. The SiN film was then deposited on top of the grating by plasma-enhanced chemical vapor deposition. The resonant angle of the structure was determined from the linear transmission of 1064 nm light through the structure as a function of the angle of incidence. SHG from the structure was subsequently measured as a function of the angle of incidence and an enhancement exceeding two orders of magnitude was observed for both incident polarizations at the resonant angle.

Our results show that hybrid structures with plasmonic resonance and waveguide mode can lead to new concepts for nonlinear nanophotonic devices. The present fabricated structures are not yet optimized, leaving room for significant further enhancement.

9126-2, Session 1

Fabrication and spectral tuning of standing gold infrared antennas using single fs-laser pulses

Martin Reininghaus, RWTH Aachen (Germany) and Fraunhofer-Institut für Lasertechnik (Germany); Dirk Wortmann, Fraunhofer-Institut für Lasertechnik (Germany); Zhao Cao, Jon M. Hoffmann, RWTH Aachen (Germany); Thomas Taubner, RWTH Aachen (Germany) and Fraunhofer-Institut für Lasertechnik (Germany)

Optical antennas are nanostructures that exhibit strongly localized field enhancement and are thus suited to enhance optical spectroscopies, for example vibrational spectroscopies such as surface enhanced infrared absorption spectroscopy (SEIRA) [1, 2]. While the first SEIRA results on IR antennas have been performed with chemically grown nanowires [1], these IR antennas are nowadays usually fabricated in arrays with electron-beam lithography on planar substrates and are then subsequently characterized with far-field and near-field methods such as scanning near-field optical microscopy (SNOM) [3].

In this talk, we present a simple method for producing upright standing nanoantennas with a high aspect ratio and a tunable resonance frequency by single pulses of femtosecond laser radiation [4]. Irradiation of a thin gold film on a silicon substrate with a single fs-laser pulse results in the formation of a “nanojet”, a nanoscaled needle or nanoantenna with a diameter in the 100nm-range and a height of up to 3 micrometers The resulting antennas exhibit extinction resonances in the mid infrared spectral rage for p-polarized light under grazing incidence. Due to the free charge carriers in the surrounding gold film of the antenna, the resonance condition of the thin-wire monopole antenna can be explained by introducing image charges yielding an observable resonance wavelength of four times the antenna length.

The antenna length, and therefore the resonance frequency can be coarsely tuned over a broad wavelength range by varying the numerical aperture of the focusing objective used for the focusing of the fs-laser radiation for the structure manufacture. A fine tuning of the resonance wavelength is enabled by a slight variation of the pulse energy used for structuring. An additional ultrafine tuning of the resonance wavelength with a sub-10 nm resolution is realized by an additional coating process subsequent to the laser structuring.

[1] F. Neubrech et al., „Resonant Plasmonic and Vibrational Coupling in a Tailored Nanoantenna for Infrared Detection“, Physical Review Letters, 101, 157403, (2008).

[2] R. Adato, et al.,“ Ultra-sensitive vibrational spectroscopy of protein monolayers with plasmonic nanoantenna arrays“ PNAS, 106, 19227–19232, (2009).

[3] J.M. Hoffmann, et al., „Antenna-enhanced infrared near-field nanospectroscopy of a polymer“, Applied Physics Letters, 101, 193105, (2012).

[4] M. Reininghaus, et al., Optics Express (accepted).

9126-4, Session 1

Fano resonant nanoantenna for unidirectional side scattering of light

Niels Verellen, Katholieke Univ. Leuven (Belgium) and IMEC (Belgium); Dries Vercruysse, IMEC (Belgium) and Katholieke Univ. Leuven (Belgium); Yannick Sonnefraud, Fabian B. Fuchs, Giuliana Di Martino, Imperial College London (United Kingdom); Victor V. Moshchalkov, Katholieke Univ. Leuven (Belgium); Liesbet Lagae, IMEC (Belgium) and Katholieke Univ. Leuven (Belgium); Stefan A. Maier, Imperial College London (United Kingdom); Pol Van Dorpe, IMEC (Belgium) and Katholieke Univ. Leuven (Belgium)

In recent years, nanotechnology and nanoscience have been expanding their toolbox dramatically. Plasmonic resonators (also referred to as nanoantennas) can be considered as one of these novel tools providing an effective route to couple photons in and out of nanoscale volumes.

The higher the level of control over the way a plasmonic resonator interacts with light, the more effective this tool becomes and the further its applications will reach. Essential to this end is a detailed knowledge of its scattering characteristics and one can ask the—what appears to be—simple question: in which way does the antenna influence the directionality of the light flow?

Recent studies have demonstrated that proper antenna designs can result in scattering patterns strongly deviating from the trivial dipole distribution, allowing one to route light in specific directions. Left-to-right directionality or unidirectional side scattering (i.e. preferential scattering in a single direction perpendicular to the incident wave) has so far only been possible with multi-nanoparticle arrangements. [1,2] Our work demonstrates the unidirectional side scattering phenomenon with only a single nanoparticle geometry, namely a V-antenna. [3] We show that the directionality is the result of phase and amplitude matching that occurs at the Fano interference between two localized surface plasmon modes in the V-shaped nanoparticle. A detailed analysis of the V-antenna modeled as a system of two coherent point-dipole sources explains how the Fano interference gives rise to a tunable directivity. This model is confirmed experimentally by back focal plane microscopy where left-to-right directionality up to 15 dB is observed.

Additionally, we demonstrate directional tunability by varying the opening angle of the V-antenna allowing further structural optimization. The understanding of Fano-based directional scattering opens a way to develop new directional optical antennas for sub-wavelength color routing and self-referenced directional sensing.

[1] T. Kosako, et al. Nat. Photonics (2010) 4(5), 312–315

[2] T. Shegai, et al., Nat. Commun. (2011) 2(481)

[3] D. Vercruysse, et al. Nano Lett., 2013, 13 (8), 3843–3849

9126-142

Nonlinear nanophotonics solar cells

Jean-Michel Nunzi, Somayeh M. Mirzaee, Queen's Univ. (Canada)

Nonlinear absorption is investigated in a poly (3-hexylthiophene) (P3HT) PCBM fullerene blend, one of the most popular organic solar cell's materials. Three-photon absorption is recorded in the bulk hetero junction photodiode configuration. The output photocurrent of the photodiode is interpreted in terms of the three-photon absorption properties of the P3HT:PCBM blend at 1550 nm. Extrapolated of the concept to high efficiency solar cells would allow to exceed the Shockley–Queisser limit. We currently develop arrays of plasmonic optical antennas which should permit the development of an ultra-high efficiency PV technology that is compatible with large-area fabrication and low-cost technologies.

9126-6, Session 1

Photoluminescence dynamics at fast and slow time scale in PbSe nanocrystals

Rafael Quintero-Torres, Univ. Nacional Autónoma de México (Mexico); Jeff F. Young, The Univ. of British Columbia (Canada)

Photoluminescence as a function of time, wavelength and temperature is used to elucidate the relaxation of energy in PbSe as a function of the structural arrangement of the nano-crystals. The contribution of radiation emission, Förster exchange and non-radiative relaxation are accounted in processes from 77 to 300 K and in the wavelength from 1.65 to 1.20 um and in temporal scales from 1 ns to 10 us. Important contribution to the nonradiative relaxation with the mesoscopic arrangement of the nanocrystals and evidence of the Föster exchange independent of temperature and around 25 ns is measured. The general description of relaxation is used as well to correlate with the complex interaction between nanocrystals.

9126-141, Session 1

Plasmonic waveguide coupled ring cavity for non-resonant type refractive index sensor

Soon-Hong Kwon, Chung-Ang Univ. (Korea, Republic of)

Sensitive refractive index sensors with small footprint have been studied for high integration of numbers of sensors into a tiny chip as bio/chemical applications. In particular, the resonant-type index sensors based on various micro/nanocavities, which use a resonant wavelength dependence on the index of the environmental materials, have been developed. However, the spectral linewidth of the resonance, which becomes the resolution limit, is considerably large in the plasmonic cavities due to large absorption loss in metals. Therefore, it is demanded new type of plasmonic refractive index sensors that are not limited by the linewidth of the cavity. Here, we propose a new-type plasmonic index sensor consisting of a channel waveguide and a ring cavity, as shown in Fig. 1. Two emissions from a ring cavity into both arms of the waveguide couples with a phase difference depending on the length of the right arm. Therefore, the output power changes as a function of the refractive index of the analyte filling the waveguide.

9126-7, Session 2

Nanoplasmonics: an interface technology for opto-electronics devices *(Invited Paper)*

Alexandre Bouhelier, Ctr. National de la Recherche Scientifique (France)

The research steps presented here seek at developing a new class of miniature devices to interface a plasmonic platform to an electronic control layer. Two key components shall be discussed in this presentation. We will first discuss the integration of an electrical source of surface plasmons based upon the opto-electrical properties of a single carbon nanotube field-effect transistor. We show that depending on the electrical stress applied to the transistor, the electroluminescent activity of the semiconducting channel can be coupled to the electrical leads in the form of propagating surface plasmons. Our results demonstrate that SWNTs can act as SPP sources making them promising candidates for integration in plasmonic and nanophotonic circuits.

We will then describe the development of a novel optical antenna-based photonic device: the optical rectenna. Optical gap antennas are electromagnetic wave-vector converters used for interfacing optical radiation with nanoscale emitters. However, the size of these components and their ultrafast responses suggest that optical gap antennas may play a significant role at interfacing an electronic control device layer with an optical circuitry. In this framework, we investigated a transduction mechanism based on photon-assisted tunneling for converting photons to transported electrons in optical gap antennas by introducing a method for electrically contacting the feed area. Our approach enables nanometer-scale self-aligned spatial overlap between region of strong electromagnetic coupling required for enhanced light-matter interaction, and region where electronic transport is dictated by the applied static bias. Under pulsed laser illumination, the conversion mechanism and the material response become 2? dependent and are linked by the nonlinear electrical susceptibility ?(2). We experimentally demonstrate that the feed-gap of optical antennas are responsible for an enhanced second harmonic generation concomitant to a rectifying property. Nature of the transduction process is deduced from the evaluation of the work function at each electrode.

9126-8, Session 2

Quantum effects in plasmonics: electron tunneling, nonlocality and nonlinear effects *(Invited Paper)*

Ruben Esteban, Centro de Fisica de Materiales (Spain); Asier Zugarramurdi, Institut des Sciences Moléculaires d'Orsay (France); Garikoitz Aguirregabiria, Centro de Fisica de Materiales (Spain); Andrei G. Borissov, Institut des Sciences Moléculaires d'Orsay (France); Javier Aizpurua, Centro de Fisica de Materiales (Spain)

Metallic nanoparticles can support strongly localized, broadband plasmonic modes, with possible applications that range from spectroscopy to photovoltaics. Typically, the optical response is obtained using a classical electrodynamic framework that describes particles by a bulk local permittivity.

However, for the nanometer and subnanometer gaps achieved in recent experiments[1] novel physical phenomena can emerge and a different approach is necessary. For example, a non-local hydrodynamic description is often used to account for the nonlocal screening of electrons and the gradual variation of the electron charge distribution near the interfaces. The validity of these nonlocal approaches can be tested against conveniently

modified local models[2]. Furthermore, a more dramatic effect can be observed when electron tunneling in a gap becomes relevant. Time-Dependent Density Functional Theory (TDDFT) calculations allow for analyzing this situation in gaps formed by small particles. When tunneling is triggered out, charge transfer changes the resonant wavelength and the modal structure of the structure, strongly quenching the fields at the gap.

Here we discuss the interplay between non-locality and electron tunneling, and how the latter effect becomes dominant for very narrow gaps. We further describe the Quantum Corrected Model (QCM)[3], which allows to introduce electron tunneling into a classical formalism, making possible to treat the large particles typical of experiments. The method is in good agreement with TDDFT calculations of small particles, and correctly interprets recent experimental results tracing the linear plasmonic response of subnanometer gaps. Last, we also describe how electron tunneling can modify strongly the non-linear response of plasmonic systems.

[1] K. J. Savage et al, Nature 491, 574 (2012)

[2] T. V. Teperik et al, PRL 110, 263901 (2013)

[3] R. Esteban et al., Nature Communications 3, 825 (2012)

9126-9, Session 2

The magic of nanoplasmonics: from superhydrophobic and 3D suspended devices for SERS/TERS-like applications to hot-electrons based nanoscopy

Alessandro Alabastri, Andrea Toma, Istituto Italiano di Tecnologia (Italy); Andrea Giugni, Bruno Torre, Istituto Italiano di Tecnologia (Italy) and King Abdullah Univ. of Science and Technology (Saudi Arabia); Mario Malerba, Ermanno Miele, Francesco de Angelis, Carlo Liberale, Gobind Das, Istituto Italiano di Tecnologia (Italy); Enzo Di Fabrizio, King Abdullah Univ. of Science and Technology (Saudi Arabia); Remo Proietti Zaccaria, Istituto Italiano di Tecnologia (Italy)

The presentation will mainly focus on three kinds of devices all having plasmonics as common ground:

1) Superhydrophobic nanostructures for single/few molecules detection. The working principle is based on the possibility of beating the diffusion limit owing to the superhydrophobicity mechanism. In fact, it will be shown that Raman spectrum can be collected, in short time, from samples having concentrations down to atto-molar.

2) The next introduced device focuses on the possibility of performing SERS analysis on three dimensional (3D) metallic standing structures. In fact, even though in this case we cannot exploit the advantages offered by superhydrophobicity (this characteristic was not implemented in the present device), the 3D peculiarity leads to an extraordinary local field enhancement, therefore to strong SERS signal. The result is, once again, the capability of reading samples concentrations down to pico/femto molar in relatively short time.

3) Finally, we shall introduce a new kind of nanoscopy based on the combination of plasmonics and hot electrons. In particular, we will show that by means of an adiabatic metallic concentrator, under the appropriate conditions it is possible to obtain hot electrons production, to the extend of realizing an extremely localized “current reading” capable of reproducing the topological/material characteristics of the investigated substrate. A comparison with standard AFM analysis will be shown.

9126-10, Session 2

Coherent surface plasmon polariton emission from a nanodiode

Dmitry Y. Fedyanin, Moscow Institute of Physics and Technology (Russian Federation); Alexey V. Krasavin, King’s College London (United Kingdom); Aleksey V. Arsenin, Moscow Institute of Physics and Technology (Russian Federation); Anatoly V. Zayats, King’s College London (United Kingdom)

Surface plasmon polaritons (SPPs) being surface electromagnetic waves propagating along the interface between a metal and an insulator offer a unique opportunity to break the diffraction limit and localize electromagnetic energy at the subwavelength scale. This makes SPPs extremely attractive for many optical applications ranging from biosensing to integrated optics and optoelectronics. The mode size in plasmonic waveguides can be several orders of magnitude smaller than in their all-dielectric counterparts that results in higher sensitivity, integration density and stronger light-matter interaction. However, the propagation length of an SPP is fundamentally limited by ohmic loss in the metal and is typically less than 10 ?m for metal-semiconductor structures, which are vitally important for nanophotonic circuitry providing simultaneously high mode confinement and compatibility with electronics. The later is crucial for active nanophotonic components, since electrical injection provides an undisputed edge over the optical control in terms of energy efficiency, ultimate device size and integration density.

Since presently there are no materials in plasmonics, which can beat silver and gold in terms of ohmic loss, only loss compensation can bring SPPs into the practical domain. In this regard, efficient SPP amplification under electrical pumping is needed.

In this work, we propose a novel surface plasmon amplification scheme based on a double-heterostructure tunneling Schottky-barrier diode and for the first time present an on-chip subwavelength coherent SPP source based on this scheme. Unlike most of the nanolasers, our device does not merely emit light into the free-space in a dipole-like fashion, but efficiently couple radiation into in-plane plasmonic (or photonic) waveguides. The proposed scheme ensures steady state room temperature operation at feasible current densities. Furthermore, the temperature decrease reduces the threshold current below 1kA/cm2. Thus, the presented concept creates the backbone for the realization of active components for the next generation of nanophotonic circuitry.

9126-11, Session 2

Field emission of super-focused plasmons

Julia H. Majors, Alejandro Rodriguez Perez, Vartkess A. Apkarian, Univ. of California, Irvine (United States)

Field emission takes place upon focusing propagating surface plasmon polaritons (SPP) at the apex of a sharp metal tip. The effect is most clearly demonstrated with remotely launched SPPs on a silver tip. We couple femtosecond laser pulses through a grating inscribed on the taper of a smooth, silver wire, separated by 30um from the apex. The tips are first electrochemically etched and then shaped by a focused ion beam (FIB) of gallium ions to a final apex of <40nm. The grating is also etched using the FIB. The tip is mounted in a vacuum chamber facing a DC-biased copper rod for electron collection. Field-emitted current measured is directly correlated with the radiation of super-focused surface plasmons (SFSP) at the apex, captured by a 60x magnified backscatter image. Both current and radiation at the apex are measured as a function of polarization of the grating incident light. In the absence of a locally incident laser at the apex, the coherent collective oscillations of the surface charge density (plasmon) are responsible for the local electric field that lowers the work function, enabling tunneling into vacuum.

Currently, due to low grating coupling efficiency and non-adiabatic losses of the propagating plasmon along the tip, an applied DC bias is used to partially suppress the work function. The oscillating plasmon field then reduces the tunneling barrier sufficiently for Fermi electrons to tunnel into vacuum. Experimental data was fitted to a dynamic Fowler-Nordheim

model, incorporating both the local DC and AC fields, to demonstrate field regimes of dominant electron emission contributions from the Fermi level. Even in the regime of emission above Fermi level, the plasmon decays to e-h pairs by Landau damping and tunnel through a coherently gated barrier, driven by the superfocused field. These spatially confined currents, driven by a coherent process, present a novel opportunity for electron imaging at the limit of space-time resolution.

9126-12, Session 3

Ultrafast nanooptics: Using strong laser fields to control the motion of electrons in and around metallic nanotstructures *(Invited Paper)*

Christoph Lienau, Carl von Ossietzky Univ. Oldenburg (Germany)

Sharp metallic nanotapers irradiated with few-cycle laser pulses are emerging as a source of highly confined coherent electron wavepackets with attosecond duration and strong directivity [1-6]. The possibility to steer, control or switch such electron wavepackets by light is expected to pave the way towards direct visualization of nanoplasmonic field dynamics and real-time probing of electron motion in solid state nanostructures. Such pulses can be generated by strong-field induced tunneling and acceleration of electrons in the near-field of sharp gold tapers within one half-cycle of the driving laser field. Here, we study for the first time the effect of the carrier envelope phase of few cycle laser pulses on the motion of electrons emitted from metallic nanostructures by strong-field tunneling.

We illuminate very sharp, single-crystalling gold tips with CEP-stable few-cycle near-infrared pulses at 1.5 μm and record angle-resolved kinetic energy spectra of the photoemitted electrons. Our experiments give first evidence for the effect of absolute phase of the laser pulses on the emission direction and kinetic energy distribution of the photoemitted electrons. We observe pronounced modifications of the photoelectron spectra when varying the CEP phase, paving the way towards a light-driven control of motion of electrons in the near field of metallic nanostruuctures on sub-femtosecond time scales and nanometer length scales. In my talk, I will give an introduction into this emerging field, discuss our own recent experimental observations and their interpretation within simple theoretical models and will give an outlook, illustrating possible applications of such electron sources.

References

[1] P. Hommelhoff, Y. Sortais, A. Aghajani-Talesh, M. A. Kasevich, Phys. Rev. Lett. 96, 077401 (2006).

[2] C. Ropers, D. R. Solli, C. P. Schulz, C. Lienau, T. Elsaesser, Phys. Rev. Lett. 98, 043907 (2007).

[3] M. Krüger, M. Schenk, P. Hommelhoff, Nature 475, 78 (2011).

[4] G. Herink, D. R. Solli, M. Gulde, C. Ropers, Nature 483, 190 (2012).

[5] D. J. Park et al., Phys. Rev. Lett. 109, 244803 (2012).

[6] B. Piglosiewicz et al., Nature Photonics, doi:10.1038/NPOTON.2013.288 (2013).

9126-13, Session 3

Purcell effect and directional emission in a plasmonic patch antenna *(Invited Paper)*

Agnès Maître, Univ. Pierre et Marie Curie (France); Chérif Belacel, Univ. Pierre et Marie Curie (France) and Lab. de Photonique et de Nanostructures (France); Amit Raj Dhawan, Univ. Pierre et Marie Curie (France); Benjamin Habert, Florian Bigourdan, François Marquier, Institut d'Optique Graduate School (France); Laurent Coolen, Univ. Pierre et Marie Curie (France); Xavier Lafosse, Lab. de Photonique et de Nanostructures (France); Benoit Dubertret, Ecole Supérieure de Physique et de Chimie Industrielles (France); Jean-Jacques Greffet, Institut d'Optique Graduate School (France); Pascale Senellart, Lab. de Photonique et de Nanostructures (France)

Plasmonic nano-antennas provide broadband spontaneous emission control by confining light on highly sub-wavelength volumes. This property assures efficient coupling and spectral matching of spectrally broad emitters like defects in diamonds or colloidal quantum dots with nanostructures. Precise positioning of emitters inside the nanostructures has been a limitation for efficient coupling and remains a key parameter to control for efficient light nanostructures interaction. In this paper, we propose to optimise the interaction of nanoemittors with antennas by assuring spatial and spectral matching. Although spontaneous emission acceleration ensuring large coupling to the mode has been evidenced in antennas, this property has not been combined with high emission directionnality.

Here, we control both the spontaneous emission rate and radiation pattern of nanocrystals in a plasmonic antenna. We use a patch antenna, as proposed in [1], consisting in a thin gold microdisk 30 nm above a thick gold layer, with a emitter positioned in the dielectric spacer. The small 30 nm separation between the disk and the gold film provide a large confinement of the electromagnetic field. The emitters are clusters of CdSe/CdS colloidal nanocrystals. A deterministic positioning of clusters inside each antenna with a precision of 25nm is provided by an optical in situ lithography technique as demonstrated in [2] for quantum dots in micropillars. The emitters are shown to radiate through the entire patch antenna in a highly directional mode. The theory predicts an acceleration of dipole emission up to 70 for a dipole perpendicular to the gold layers, and much lower for a dipole parallel.

For an antenna with a gold disk diameter ranging from 1.4 to 2.2mm, emission is directive in accordance with the theory. The average cluster lifetime is reduced by a factor ranging from 5 to 15 which correspond, taking into account the 2D dipole transition of the emitters, their orientation and distribution of lifetime inside the cluster, to accelerations consistent with an acceleration of 70 for vertical dipoles , in good agreement with our theoretical calculations

In a second step, we develop a protocol in order to couple a single emitter to a patch antenna by controlling deterministically its location in middle of the patch antenna and the orientation of the dipole. The optical properties of the antenna are qualified as a single photon source.

References:

[1] R. Esteban, T. V. Teperik, and J. J. Greffet, Optical Patch Antennas for Single Photon Emission Using Surface Plasmon Resonances Phys. Rev. Lett. 104, 026802 (2010)

[2] A. Dousse et al. Controlled light-matter coupling for a single quantum dot embedded in a pillar microcavity using far-field optical lithography, Phys. Rev. Lett. 101, 267404 (2008).

[3] C. Belacel et al. Controlling spontaneous emission with plasmonic optical patch antennas, nanoletters 13 1516 (2013)

9126-14, Session 3

Vector polarization states of vortex light generated from electronically excited nanoscale molecular arrays

Mathew D. Williams, David S. Bradshaw, David L. Andrews, Univ. of East Anglia (United Kingdom)

It has recently been shown possible to directly generate an optical vortex (a beam of light endowed with orbital angular momentum) by spontaneous emission from a molecular exciton array. This contrasts with most established methods, which typically rely on the modification of a conventional beam by an appropriate optical element (for example, a q-plate) to impose the requisite helical twist of a vortex. The new procedure

is achieved by nanofabricating a chiral arrangement of chromophores into a ring of specifically configured symmetry, supporting a doubly degenerate (conjugated) exciton with the appropriate azimuthal phase progression. It emerges that the symmetry elements present in the phase structure of the optical field, produced by emission from these degenerate excitons on a propeller-shaped array, exhibits precisely the sought character of an optical vortex. The highest order of exciton symmetry, including the corresponding splitting of the electronic states, dictates the maximum magnitude of the topological charge. The latest developments, based on the analysis of computer simulations, now reveal the detailed pattern of polarization behaviour in the emitted light, in which the vector character of the beam progresses around the phase singularity along the beam propagation axis. This effect arises not only in the plane of the nanoantenna ring, but also in the far-field reach of an optical detector. Significantly, this analysis points to the emission of radiation with polarization varying over the beam profile. These principles offer scope for the development of a vortex laser, enabling radiation with a helical wave-front to be tailor-made by creation from the vacuum.

9126-15, Session 3

Dynamic polarization modulation of tailored light fields

Christian Schlickriede, Christina Alpmann, Cornelia Denz, Westfälische Wilhelms-Univ. Münster (Germany)

Tailored light fields with complex polarization states are of growing interest in theory as well as in experimental investigations. In the last years, especially solutions of the Helmholtz equation have been investigated intensively, including Hermite-, Laguerre-, and Ince-Gaussian beams, which are related to Cartesian, polar and elliptical coordinates, respectively. We now introduce an experimental system capable of tailoring complex light fields including a spatial modulation control of linear states of polarization. Therefore we modify the polarization, phase and amplitude distribution of the light field without any mechanical moving parts by means of a single reflective phase only spatial-light-modulator operating in split screen mode. Our concept leads to new kinds of complex vector fields with interesting propagation properties, which will be characterized in a conjugated object plane of the SLM as well as in its Fourier plane. To verify the accurateness of the light field generation, we employ intensity, phase and polarization measurements. We will show the generation of even, odd and helical Laguerre-Gaussian beams and combine their spatial intensity and phase structure with different polarization states. Furthermore we investigate the propagation behavior and stability of different modes in dependence of the polarization. The possibility to arbitrarily control the spatial polarization and phase distribution of a beam covers a broad range of applications, for example in high-NA microscopy or laser machining, where these properties can be used to shape the focal field in three dimensions. Another field of application for these beams is optical micromanipulation, where they could be used in order to manipulate the orientation of micro and nano particles.

9126-16, Session 3

Complementary optical Yagi-Uda antenna

Chang-Won Lee, Samsung Advanced Institute of Technology (Korea, Republic of)

Plasmonic nanoantennas are key elements in nanophotonics capable of directing radiation or enhancing the transition rate of a quantum emitter. The magnetic-dipole-type nanoantennas, which are the Babinet complementary structures of typical electric-dipole-type, have received little attention leaving their antenna properties largely unexplored. We present a multi-slot nanoantenna with a magnetic dipole feed exhibiting highly unidirectional free-space radiation. We find our antenna can avoid directivity limit arising from a natural tendency to radiate into high-refractive-index substrates upon irradiation from the substrate side. Its geometry is engineered to achieve an optimal front-to-back (FB) ratio by adjusting the phase of the plasmon field and couplings between slot elements. We present antennas with two-, three-, and five-slots and find FB ratio increases with increasing number of slots. We achieve a maximum FB ratio of 8.5 (9.2 dB) with a five-slot structure at 664 nm. A multi-slot nanoantenna provides a new possibility of an electrically excitable feed and of energy transfer from one waveguide to another by working as a future “optical via.”

9126-3, Session PS1

Surface-plasmon-polariton wave guided by the periodically corrugated interface of a metal and a columnar thin film

Francesco Chiadini, Univ. degli Studi di Salerno (Italy); Vincenzo Fiumara, Univ. degli Studi della Basilicata (Italy); Antonio Scaglione, Univ. degli Studi di Salerno (Italy); Akhlesh Lakhtakia, The Pennsylvania State Univ. (United States)

Surface plasmonics deals with the excitation and propagation of electromagnetic surface waves guided by metal/dielectric interfaces [1]. These waves are called surface-plasmon-polariton (SPP) waves. Current research interest in surface plasmonics is boosted by multiple potential applications: from near-field microscopy to sensors, from realization of planar optical circuitry to photovoltaic energy conversion supported by the fascinating perspective of improving the efficiency of solar cells [2, 3, 4].

In this work we have analyzed the excitation of SPP waves when the partnering materials are silver and a columnar thin film (CTF) [5] made of Ta2O5. To excite the SPP wave, a grating ruled onto a silver substrate has been considered. Since a CTF is fabricated by means of physical vapor deposition, when the substrate is topographic instead of being flat, a superlattice structure is formed when the vapor flux impinges on the silver grating. This grating-coupled configuration has been analyzed using the Rigorous Coupled-Wave Analysis (RCWA) to calculate the absorptance of the structure as a function of the incidence angle of a linearly polarized plane wave [6, 7].

The absorptance angular spectra are explored to find peaks with angular locations that remain about the same regardless of the average thickness of the CTF layer above athreshold value. Analysis has been done for various directions of the vapor flux (that is, for CTFs with different permittivity dyadics), finding that only one SPP wave can be excited in each case.

References

[1] J. A. Polo, Jr., T. G. Mackay, and A. Lakhtakia, Electromagnetic Surface Waves: A Modern Perspective (Elsevier, 2013).

[2] M. E. Stewart, C. R. Anderton, L. B. Thompson, J. Maria, S. K. Gray, J. A. Rogers, and R. G. Nuzzo, “Nanostructured plasmonic sensors,” Chem. Rev. 108, 494–521 (2008).

[3] S. Kawata, Y. Inouye, and P. Verma, “Plasmonics for near-field nano-imaging and superlensing,” Nat. Photon. 3, 388–394 (2009).

[4] S. Mokkapati and K. R. Catchpole, “Nanophotonic light trapping in solar cells,” J. Appl. Phys. 112, 101101 (2012).

[5] A. Lakhtakia and R. Messier, Sculptured Thin Films: Nanoengineered Morphology and Optics (SPIE Press, 2005).

[6] A. Marini, A. V. Gorbach, and D. V. Skryabin, “Coupled-mode approach to surface plasmon polaritons in nonlinear periodic structures,” Opt. Lett 35, 3532–3534 (2010).

[7] V. Fiumara, F. Chiadini, A.Scaglione, and A. Lakhtakia, “Theory of thin-film, narrowband, linear-polarization rejection filters with superlattice structure,” Opt. Commun. 268, 182–188 (2006).

9126-65, Session PS1

Design of plasmonic nanoantenna for total internal reflection fluorescence microscopy

Eun-Khwang Lee, Jung-Hwan Song, KAIST (Korea, Republic of); Kwang-Yong Jeong, Korea Univ. (Korea, Republic of); Min-Kyo Seo, KAIST (Korea, Republic of)

There have been many research conducted in bioimaging, chemical sensing or biophysical applications to visualize or sense biological phenomenon. Among various branches in such research areas, the improvement of signal quality as well as selective excitation has been an issue. Total internal reflection fluorescence (TIRF) microscopy was introduced for advanced spatial resolution and signal-to-noise ratio (SNR). It uses evanescent wave generated right above substrate within a few hundreds of nanometers when illumination source is incident above a critical angle. However, it still lacks spatial resolution in vertical direction as well as in lateral direction in order to detect target specimen in the very proximity of substrate.

In this study, we have designed a plasmonic gold nano-antenna that can be integrated into TIRF microscopy system strengthening the deficiencies of the sensing capability stated above. The designed antenna has a symmetric bowtie shape merged with a rod so that external electromagnetic field can be confined between its sharp tips at multiple wavelengths. Using finite-difference time-domain (FDTD) simulation in aqueous environment, we have analyzed the near-field plasmonic characteristics as well as the far-field properties of the modified bowtie antenna. Having the total length of 450 nm with a 30-nm-gap, it shows fundamental plasmonic resonance at ~1150 nm and 3rd mode resonance at ~670 nm. With such well-separated resonant modes, both excitation and radiation of a quantum emitter placed at the nano-gap can be fully enhanced twice. Due to the confinement characteristic of incident electric field, evanescent wave is generated within the gap having shorter tail than in the absence of the antenna when the external field is incident over a critical angle. This phenomenon enables selective excitation of target molecules lying near substrate (≤ 100 nm), immersed in aqueous media. By reducing unwanted signals from the rest of the molecules suspended in media, an SNR can be increased. Besides the near-field advantages, the far-field radiation pattern of respective 1st and 3rd resonance modes has little overlap each other, leading to high collection efficiency using objective lenses. This can also contribute to the reduction of background signals by differentiating excitation and detection paths.

We have shown that our designed, plasmonic gold modified bowtie antenna is capable of electric field confinement within ultra-small volume resulting in deep subwavelength scale illumination and highly enhanced both absorption and radiation process of a quantum emitter using multiple resonances. By investigating far-field properties, strong correlation between the enhancement in the incident excitation light intensity and far-field radiation patterns was confirmed. Employing such advantages of the designed antenna with TIRF microscopy system, we expect detection sensitivity and precision can be improved.

9126-66, Session PS1

Interlevel transitions and light absorption in cylindrical quantum dot with Morse potential in the presence of external magnetic field

David B. Hayrapetyan, Eduard M. Kazaryan, Tigran Kotanjyan, Russian-Armenian State Univ. (Armenia)

Progress in semiconductor nanoelectronics has made it possible to fabricate zero-dimensional structures, so-called quantum dots (QD) or “artificial atoms”. These structures are interesting because of the fact that charge carrier (CC) motions are restricted in all three directions, which gives the possibility for physical characteristics effective control of those structures. A strong dependence of the energy spectrum of CC on the geometrical shape and sizes of QD allows to manipulate the energy spectrum and consequently, the physical characteristics of QD. The controlling QD physical properties are attractive not only from the fundamental science point of view, but also because of its potential application in the development of semiconductor optoelectronics devices.

A correct approximation of quantum dots confinement potential plays the relevant role at the investigation of physical characteristics of such systems. It is important to note that modeling of this potential in many aspects depends on the method of size-quantized semiconductor growth. Various approximations of confinement potential were proposed in the literature. As a result of diffusion, the confining potential, formed during the growth process, in most cases can be approximated with a high accuracy by a parabolic potential. It should be mentioned that the parabolic approximation of the confinement potential of QD introduced in works of Maksym, Chakraborty and Peeters enables to carry out detailed analytic analysis of the one-particle energetic spectrum and wave functions at the presence of codirected electric and magnetic fields.

However, in reality, the parabolic potential is realized only for the lowest energy levels. It is obvious that with increase of quantum number the course of confining potential diverge from the parabolic potential. For a more successful and realistic approximation of the formed confining potential in Z direction the use of the Morse potential have been proposed. In the radial direction the parabolic confining potential have been used.

Investigations of the optical absorption spectrum of various semiconductor structures are a powerful tool for determination of many characteristics of these systems: forbidden band gaps, effective masses of electrons and holes, their mobilities, dielectric permittivities, etc. There are many works devoted to the theoretical and experimental study of the optical absorption in size-quantized systems. The presence of size quantization essentially influences the absorption mechanism. In fact, the formation of new energy levels of the size quantization makes possible new interlevel transitions.

In this work the interlevel transitions and direct interband light absorption in cylindrical QD with Morse potential are studied. For the regime of strong size quantization analytical expressions for the particle energy spectrum, absorption coefficient and dependencies of effective threshold frequencies of absorption on the geometrical sizes of QD and magnitude of magnetic field are obtained. Blue-shift occurs for effective threshold frequencies of absorption in the presence of external magnetic field. The selection rules corresponding to different transitions between quantum levels are found. Interlevel transitions and absorption coefficients are calculated for ensemble of cylindrical QDs by the geometrical size dispersion distribution. The dependence of absorption coefficient on the magnitude of magnetic field is revealed.

The controlling QDs’ absorption properties by means of magnetic field are attractive not only from the fundamental science point of view, but also because of its potential application in the development of semiconductor optoelectronics devices.

9126-67, Session PS1

Raman spectroscopy and periodic surface structures of Mg:ZnO thin film fabricated by femtosecond laser pulses

Hongying Wang, Vrije Univ. Brussel (Belgium); Zhen Cheng, Xi’an University of Arts and Science (China); Guanghua Cheng, Xi’an Institute of Optics and Precision Mechanics of Chinese Academy of Sciences (China); Fei Ma, Xi’an Jiaotong University (China); Yuanyuan Li, Xi’an University of Arts and Science (China)

Intensively increasing research activities in the field of laser-induced periodic surface structures (LIPSS) have been

studied for past several decades and observed on many types of materials. These structures, also termed as ripples, are usually divided into Low Spatial Frequency LIPSS (LSFL) and High Spatial Frequency LIPSS (HSFL). LSFL are observed with a period ?LSFL close to or somewhat smaller than the irradiation wavelength ? and an orientation perpendicular to the laser beam polarization. These LSFL ripple formation is attributed to surface and bulk plasma wave interference as the key mechanisms underlying the nanostructuring process. HSFL spatial periods significantly is smaller than the irradiation wavelength (?HSFL<?? /2). These HSFL are always predominantly for transparent materials and their orientations often perpendicular and sometimes parallel to the polarization. The main different mechanisms are mainly involved in interference effects along with transient changes in the optical properties during laser irradiation, second harmonic generation (SHG), excitation of surface plasmon polaritons, or self-organization.

Magnesium oxide (MgO) is a promising material for controlling the optical band gap engineering of the ZnO crystal system. Mg-doped ZnO (MZO) thin films formed by alloying ZnO with MgO showed that the band gap energy varies with the Mg concentration. The crystal structure of MZO thin films can be changed from hexagonal to cubic structure when the Mg concentration exceeds 40 at% and the optical band gap energy of MZO varies from3.3 to 4.0 eV without changing crystal structure.

In this work, high repetition rate femtosecond (fs) laser pulses were employed to produce various nanostructures on MZO thin film. These MZO films were fabricated by radio-frequency magnetron sputtering. By using different laser parameters and irradiation conditions, it is possible to manipulate the shapes and sizes of the nanostructures. Here, surface ripples at a period of approximately 250 nm-570 nm oriented perpendicular to the laser polarization as well as ripples at a period of about 2.2 ?m-2.5??m running parallel to the polarization are observed. Morphological ripple features measured by scanning electron microscope (SEM) demonstrate that these structures originate from melting and rapid resolidification. In order to investigate the vibrational properties of the LIPSS MZO nanostructures at room temperature, the corresponding Raman study were made for optical characterization.

9126-68, Session PS1

Emission properties of square-shaped organic microlasers

Stefan Bittner, Clément Lafargue, Ecole Normale Supérieure de Cachan (France); Eugene Bogomolny, Univ. Paris-Sud 11 (France); Iryna Gozhyk, Nadja Djellali, Ecole Normale Supérieure de Cachan (France); Christian Ulysse, Lab. de Photonique et de Nanostructures (France); Joseph Zyss, Mélanie Lebental, Ecole Normale Supérieure de Cachan (France)

Microlasers have attracted great attention in the past two decades as microscopic coherent light sources. One of the key requirements for applications is a directional far-field emission. Here we report on the measurement and modeling of the highly directional far-field emission from square-shaped microlasers.

The microcavities used in the experiments are made of a polymer matrix (PMMA) doped with a conventional laser dye (DCM) acting as the active medium and deposited on a silicon/silica wafer. The cavity shape, a square in the case considered here, is defined by electron beam lithography which allows a precise fabrication with sub-wavelength accuracy. In particular, sharp corners and edges are ensured. Typical cavities have a side length in the range of 100-200 μm but a thickness of only 700 nm. Hence, they can be treated in most respects as two-dimensional systems with an effective refractive index of n=1.5. The microlasers are pumped by a frequency-doubled pulsed Nd:YAG laser (532 nm, 500 ps pulse width, 10 Hz repetition rate) with the pump beam impinging perpendicularly to the plane of the cavity. The laser emission around 600 nm is collected by a lens and fed via a fibre to a spectrometer. The sample is placed on a rotational stage in order to collect the emission in the plane of the cavity as a function of the observation angle. Furthermore, the emission out of the plane of the cavity is measured with a so-called solid angle scanner [1].

The square microlasers exhibit a multimode lasing spectrum consisting of 20-30 equidistant resonances. The free spectral range of the resonances corresponds to the length of the so-called diamond orbit [2], i.e., a ray trajectory impinging on all four sides of the cavity with an angle of incidence of 45°. The measurement of the far-field intensity showed that the emission is concentrated in four beams that are parallel to the sides of the cavity and that have an angle of 7° with respect to the cavity plane. All four emission lobes are very narrow with a widths of about 8°. We explain this strongly directional emission with the help of a ray-based based model for the modes of the dielectric square resonator [3]. The model calculations show good agreement with the measured far-field under the assumption that the lasing modes are localized on ray trajectories with an angle of incidence just below the critical angle for total internal reflection (~42°). We therefore conclude that the observed far field patterns stem from rays escaping refractively into the directions parallel or close to parallel to the side walls. This is also confirmed by camera images of the lasing cavities.

[1] C. Lafargue, S. Bittner, S. Lozenko, J. Lautru, J. Zyss, C. Ulysse, C. Cluzel, and M. Lebental, Appl. Phys. Lett. 102, 251120 (2013).

[2] M. Lebental, N. Djellali, C. Arnaud, J.-S. Lauret, J. Zyss, R. Dubertrand, C. Schmit, and E. Bogomolny, Phys. Rev. A 76, 023830 (2007).

[3] S. Bittner, E. Bogomolny, B. Dietz, M. Miski-Oglu, and A. Richter, arXiv:1305.2049 (2013).

9126-69, Session PS1

Efficient side-coupling into the slow light modes of photonic crystal slot waveguides

Yameng Xu, Dingshan Gao, Xinliang Zhang, Wuhan National Lab. for Optoelectronics (China); Eric Cassan, Institut d'Électronique Fondamentale (France)

Silicon hybrid photonics has attracted in the last years a growing interest due to its great potential for integrating various active materials within the strong index contrast silicon photonics platform for light amplification, nonlinear optics, or sensing. In this picture, the so-called empty-core slot waveguides play an important role as they allow an efficient overlap between the electromagnetic density of propagating modes and the introduced materials. Adding to the lateral slot waveguide geometry the slow light properties of photonic crystal waveguides (PCW) has led to the concept of slow light slot PCW, making such unusual waveguides ideal candidates for the strengthening of light-matter interactions. Besides this potential advantage, part of the cost to pay is that light coupling into such PCW from strip access waveguides becomes difficult.

In this context, we will propose a strategy in order to efficiently side-couple light into the slow light modse of PCW leading to a typical 80% efficiency for nG=35. The adopted approach makes use of the possible phase-matching between the fundamental PCW mode and a sub-wavelength corrugated strip waveguide. We will show that tuning the parameters of the sub-wavelength lateral waveguide, like the etching duty cycle, offers a simple path for controlling the phase-matching wavelength and thus the light group index of excited Bloch modes. As a whole, the proposed approach describes a new efficient method for light injection into the slow light modes of slot photonic crystal waveguides that may be used for the development of silicon hybrid photonic circuits.

9126-70, Session PS1

Femtosecond laser-induced controlled avalanche polymerization for 3D micro-/nanostructuring of non-photosensitized polymers

Mangirdas Malinauskas, Sima Rek?tyte, Albertas ?ukauskas, Vilnius Univ. (Lithuania); Saulius Juodkazis, Swinburne Univ. of Technology (Australia)

The direct laser writing technique is becoming a part of wider field of additive manufacturing. Here, we employ it for 3D nanostructuring of polymers [1]. We show that ultra-short pulses at ~TW/cm2 irradiance intensity in the focal volume enable creation of cross-linkable species by direct and multiphoton absorption followed by avalanche ionization. A well-controlled local heating of high pulse repetition pulse rate finishes polymerization on much longer time scales < 0.1 s. This unique feature of ultra-short pulsed irradiation is an efficient use of light energy for localized polymerization within femtoliter volume [2]. We apply it for direct laser structuring of non-photosensitized polymers (containing no photoinitiators). It enables creation of optically transparent and biocompatible micro/nano-objects and widens their possible applications in photonics and biomedicine [3].

In our experiments we used 300 fs pulse width 200 kHz repetition rate 1030 nm and 515 nm central wavelengths of laser irradiation ("Pharos", Light Conversion Ltd.). SZ2080 (IESL-FORTH), PEG-DA (Mw = 700, Sigma-Aldrich) and PDMS (Sylgard 184, Dow Corning) polymer materials non-doped with photoinitiators were applied for micro/nano-structuring in 3D. Various NA (0.95; 1.25; 1.4) objectives were used and the intensity in the focal spot was within the range of ~1 – 10 TW/cm2 at 0.1 – 5 mm/s scanning speed. Linear motion stages combined with galvo-scanner were employed for sample translation and beam deflection. A comparison with photosensitized materials was also performed. Obtained results confirm the fact that photoinitiators, especially more efficient ones, increase processing fabrication window width (Idamage–Ithreshold/Ithreshold, up to ~11 times in SZ2080 material [4]) and improve reproducibility. Yet, does not increase spatial resolution or are necessary for high definition 3D structuring of cross-linkable materials. In this paper, we show that accumulative dose is important for structuring of polymers. This proves a linear and thermal absorption plays a dominant role next to multiphoton absorption. Micro/nano-structuring of pure polymers via avalanche ionization adds more flexibility for 3D direct laser writing in the meaning of choice of materials and processing parameters.

[1] M. Malinauskas et al., Ultrafast-laser micro/nano-structuring of photopolymers: a decade of advances, Phys. Rep., http://dx.doi.org/10.1016/j.physrep.2013.07.005 (2013).

[2] R. Buividas et al., Nano-structuring of materials by controlled avalanche using femtosecond laser pulses, Opt. Mat. Express, 3(10), 1674 (2013).

[3] S. Rekstyte, M. Malinauskas and S. Juodkazis, Three-dimensional laser micro-sculpturing of silicone: towards bio-compatible scaffolds, Opt. Express, 21(14), 17028 (2013).

[4] M. Malinauskas et al., Mechanisms of three-dimensional structuring of photo-polymers by tightly focussed femtosecond laser pulses, Opt. Express 18(10), 10209 (2010).

9126-71, Session PS1

Multipolar second-harmonic generation from films of chalcogenide glasses

Abdallah Slablab, Kalle O. Koskinen, Robert Czaplicki, Martti Kauranen, Tampere Univ. of Technology (Finland); S. Mathew, Padmanabhan Radhakrishnan, Pradeep Chandran, Indu Sebastian2, Cochin Univ. of Science & Technology (India); M Kailasnath, International School of Photonics, Cochin University of Science and Technology, (India)

Chalcogenide glasses are amorphous semiconductors with a number of interesting properties required for photonic devices. Such glasses contain one or more of the chalcogenide (group 16) elements, such as sulfur, selenium, or tellurium. By tailoring the composition of such materials, their optical properties can be widely tuned. Such glasses are known to have high third-order nonlinear optical response.

Second-order nonlinear optical properties however are forbidden in centrosymmetric materials within the electric-dipole approximation of the light-matter interaction. However, at the surface or interface, the symmetry is broken giving rise to ,e.g,., second–harmonic generation (SHG). In addition to that, the higher-multipole (magnetic-dipole and electric-quadrupole) interactions allow SHG even in centrosymmetric materials. In this paper, we address the role of the dipole and higher-multipole contributions to the second-order response of the thin films of chalcogenide glasses, consisting of the Ge-Se-Sb system.

The separation of dipole and higher-multipole effects is possible by SHG using two non-collinear fundamental beams. Very direct evidence of the higher-multipole contributions can be obtained by detecting s-polarized SGH light and modulating the polarization of one of the incident beams.

The Ge-Se-Sb films were fabricated by the thermal evaporation technique. Such samples were studied by two-beam SHG experiments using 70 ps pulses at 1064 nm and 1 kHz repetition rate. The transmitted s-polarized SHG signal was measured as a function of polarization of the incident fundamental beams. Our results show that the higher multipole effects are present and contribute significantly to the second-harmonic response of Ge-Se-Sb films. In our presentation, we will report a detailed analysis of the results.

9126-72, Session PS1

Analysis and synthesis of arbitrary polarization states of light with a single nanoantenna

Francisco J. Rodríguez-Fortuño, Daniel Puerto, Amadeu Griol, Alejandro Martínez, Univ. Politècnica de València (Spain)

Nanoantennas generally have a fixed polarization of radiated light determined by their geometrical structure. In this work we demonstrate a universal method to achieve the analysis and synthesis of any arbitrary polarization state of radiated light, spanning the full Poincare sphere, from a single nanoantenna or scattering element by feeding it with two different waveguides.

The intuitive explanation of the phenomenon is straight forward and can be put in terms of simple symmetry considerations: Although the proposed method works in more general cases, consider a specially simple case of a mirror-symmetric nanoantenna fed by two waveguides at either side of the symmetry plane, designed so that the light introduced by one waveguide is radiated in a spatial direction within the mirror symmetry plane, with a polarization that is at 45 degrees to that plane. Simple symmetry considerations demand that feeding the nanoantenna with the other waveguide will radiate in the same direction but with an orthogonal polarization, at -45 degrees to the plane. Therefore, by feeding the nanoantenna simultaneously with the two waveguides with a given amplitude and phase relation, the superposition of two orthogonal polarizations in the radiated light allows the synthesis of any arbitrary radiated polarization within the full Poincare sphere.

We experimentally demonstrate the synthesis of linearly, circularly and elliptically polarized light using this method. The reciprocal situation, in which impinging light in the nanoantenna excites its two output waveguides, allows the analysis of the polarization of light by looking at the amplitude and phase of the output waveguide excitations. We demonstrate the sorting of different incoming polarizations into the two waveguides. By designing different nanoantennas, we experimentally demonstrate the sorting of different incident polarizations, such as opposite circular polarizations or orthogonal linear

polarizations, into the two different output waveguides of the nanoantenna.

Although the method can be extended to any wavelength and technology, we perform our demonstrations in a silicon photonics platform using a silicon nanoantenna built into a standard silicon waveguide, potentially allowing the fast electrical modulation of its amplitude and phase to achieve a tuneable polarization synthesizer/analyser, with a myriad of applications for compact polarization scramblers, compact ellipsometers, polarization multiplexed communications, and control of polarization-encoded qubits. In particular, the possibility of synthetizing and analysing circularly polarized light, which carries spin angular momentum, has exciting applications such as the generation of torque in rotating objects, the detection of spinning objects via the rotational Doppler effect, and novel magnetic storage applications based on ultrafast circularly polarized laser pulses.

9126-73, Session PS1

Analysis of structural and chemical features of CdHgSe nanocrystals via resonance Raman spectroscopy

Sergey A. Cherevkov, National Research Univ. of Information Technologies, Mechanics and Optics (Russian Federation); Anatoly V. Prudnikau, Belarusian State Univ. (Belarus); Elena V. Ushakova, Aleksandr P. Litvin, Anatoly V. Fedorov, Alexander V. Baranov, National Research Univ. of Information Technologies, Mechanics and Optics (Russian Federation); Mikhail V. Artemyev, Belarusian State Univ. (Belarus)

In this work, the Raman scattering is applied to control the formation of ternary nanocrystal CdxHg1-xSe with different values of x in the chemical substitution of cadmium atoms by mercury atoms in the CdSe quantum dots and nanorods of cubic and hexagonal crystal structure.

Recently, semiconductor nanocrystals are widely used to create various types of optoelectronic devices. This is due to the possibility of purposeful control the optical properties of nanocrystals by changing their size. Additional possibilities for controlling the optical parameters provide nanocrystals based on semiconductor ternary compounds like AxB1-xC , where 0≤x≤1 - proportion of component A in the semiconductor. In this case, electrical, optical and structural properties of the nanocrystals also depend on their chemical composition.

Nanocrystals based on ternary compound CdxHg1-xSe are of particular interest and have great potential for use as a photosensitive elements in a wide spectral region because of the potential significant change in the band gap as due to size effects, and because of changes in the chemical composition. So the chemical substitution of cadmium by mercury in colloidal CdSe quantum dots and nanorods has been examined by Raman spectroscopy.

The spectrum of original CdSe demonstrates the well-known Raman bands of surface (SO) and longitudinal (LO) optical phonons, and 2LO overtone. The Raman spectrum of HgSe shows the bands of TO, LO and 2LO phonons which are in good agreement with the energies of corresponding phonons in a bulk HgSe. The chemical substitution of cadmium by mercury atoms results in the appearance of new 1-st and 2-nd order Raman bands with wavenumbers in the region expected for the TO, LO and 2LO bands of HgSe. Importantly, positions and relative intensities of these band as well as the LO and 2LO bands attributed to CdSe depend on Hg content in the CdHgSe. The dependency of wavenumbers of bands in 1-st order Raman spectra of CdxHg1-xSe from Hg content is clearly demonstrate classic two-mode behavior of lattice vibrations and therefore indicate the formation of Cd?Hg?-1Se ternary compound.

9126-74, Session PS1

Weak measurement of the Goos-Hanchen shift

Gaurav Jayaswal, Michele Merano, Univ. degli Studi di Padova (Italy)

It is well known from quantum Physics that weak measurements offers a platform of amplifying and detecting very small signals. In this letter we present the first experimental observation of the Goos-Hanchen(GH) shift.

Generally the measurements of these optical shifts are challenging task because they are tiny phenomena. A weak measurement approach is consider to be a successful methods for the observations of these effects. A weak measurement is one in which the coupling between the measuring device and the observable to be measured is so weak that the uncertainty in a single measurement is large compared with the separation between the eigenvalues of the observable.

In this article we present the first experimental observation of the GH effect by a weak measurement scheme. The ”weak measurement device” is a prism which introduces a small lateral displacement Dp (Ds) for the p(s) polarization of a Gaussian beam in total internal reflection (TIR) .A polarizer and an analyzer selects the initial and the final linear polarizations to be an angles ? and ? with respect to the horizontal in the xy plane. The weak measurement scheme works as follows, if the polarizer and the analyzer are set to ?=ϖ/4 and ?=?+ϖ/2+? (?<<1) respectively, the emerging beam is laterally shifted of a quantity ? .?GH. cot (?) where ?GH=Dp –Ds.We measure the GH shift for different angle of incidence. Our experimental results have a good agreement with the theoretical prediction.(Ref: “ Weak measurement of the Goos-Hanchen shift” Optics letters vol 38, issue 8, pp 1232-1234 (2013)).

In summary, we have demonstrated that the weak measurement is a valuable approach for observing the GH shift in TIR. Furthermore they can be extended, experimentally and theoretically, to the case of metallic mirrors

9126-75, Session PS1

Self-organization of PbS quantum dots with different sizes

Elena V. Ushakova, National Research Univ. of Information Technologies, Mechanics and Optics (Russian Federation); Valeriy Golubkov, Institute of Silicate Chemistry (Russian Federation); Aleksandr P. Litvin, Peter S. Parfenov, Sergey A. Cherevkov, Anatoly V. Fedorov, Alexander V. Baranov, National Research Univ. of Information Technologies, Mechanics and Optics (Russian Federation)

Monodisperse colloidal nanoparticles (NPs) can self-assemble into ordered arrays, so-called superlattices. The assembly of nanoparticles in a periodically ordered superlattice has led to the creation of a new class of functional materials with remarkable optical, electronic, and vibrational properties. This type of materials possesses either the quantum size effects of NPs, or “collective” properties of ordered array. The establishment of the fundamental principles that rule the process of nanoparticles self-assembly into mono- and multi-component superlattices is critical for the creation and improvement the devices based on NPs arrays, such as LEDs, solar cells, photodetectors, and thermoelectric converters.

In this study we investigate the structure, obtained by self-organization of nanoparticles - lead sulfide (PbS) quantum dots (QDs) of different sizes deposited on a glass substrate or embedded in a porous organic matrix. To produce PbS nanocrystals a high-temperature organometallic synthesis in organic solution is applied. For further research obtained QDs are redispersed in tetrachlormethane. The test samples of PbS QDs are prepared by drying a drop of QD stock solution on a glass substrate, as well as by the soaking the strips of matrix into QD solution. Peak positions in PL spectra of

obtained samples with PbS QDs of different sizes are situated in the range of 0.8 - 1.9 micron. To study the nanometer scale inhomogeneities, including investigation of NPs size distribution as well as their relative positions on the substrate and in the volume of the matrix, the methods of X-ray structural analysis, wide-angle and small-angle X-ray scattering, are used.

Obtained data suggest that the nanostructures obtained by both methods represent ordered close-packed structures of the nanoparticles. The SAXS patterns show the decreasing of scattered intensity near zero angle and the appearance of peak caused by interference between close-packed QDs. Interference peak position depends on QDs diameter, with decreasing their size the peak angle increases. This dependence is typical for a dense packing of spheres in which the structure period and, hence, the angular peak position are determined by the diameter of spheres. The peak position in the SAXS patterns allows us estimate the distance between QDs in obtained structures. It is found that these distances in all samples depend on QD diameter linearly.

We conclude that by droping PbS QD solution on the glass substrate and by PbS QDs embedding into the porous matrix the ordered assemblies of QDs are formed. The configuration of obtained structures does not depend on the nanoparticle size and type of substrate and matrix. However, at this stage of study it is not possible to determine whether obtained structures are amorphous also called «glassy solids» or they are 2D and 3D superstructures. To answer this question we must receive evidence of long-range order in the formed QDs assemblies.

9126-76, Session PS1

Förster resonant energy transfer in lead sulfide QD assemblies

Aleksandr P. Litvin, Elena V. Ushakova, Peter S. Parfenov, Sergey A. Cherevkov, Anatoly V. Fedorov, Alexander V. Baranov, National Research Univ. of Information Technologies, Mechanics and Optics (Russian Federation)

The growing interest to close-packed semiconductor quantum dot (QD) induces investigations of assemblies made of lead chalcogenide QDs, which may find an application for solar energy and light detection in the near infrared. An ability to create self-organized superstructures of lead sulfide QDs on different substrates and in matrices may improve performance of many devices for near infrared photonics.

In the current study concentration-dependent optical properties of lead sulfide (PbS) QDs embedded into a porous matrix are investigated. Samples of filter paper porous matrix were dipped into colloidal solutions of 4.6 nm PbS QDs in carbon tetrachloride. After infiltration into the matrix QD close-packed assemblies are formed. A red shift of luminescence peak position depends on QD concentration and evidences for Förster resonant energy transfer (FRET) inside the quasi-monodispersed assemblies.

Size-selective photoluminescence (PL) kinetics measurements are used to study FRET in quasi-monodispersed PbS QD assemblies in details. PL decay curves recorded in narrow spectral bands inside PbS QD PL spectrum show significant influence of FRET process on QD optical properties. PL lifetime size-dependencies are founded to be dependent on the QD concentration. Smaller QDs in quasi-monodispersed assemblies play role of donors of energy and their luminescence is quenched. At the same time larger QDs can act as both acceptors and donors and their PL lifetimes weakly depend on QD concentration. Thus, the growing impact of FRET process with increasing QD concentration leads to transformation of anomalous size-dependence of PL lifetimes to the inverse.

FRET efficiency gradually increases with QD concentration and saturates at 35% that corresponds to the average donor-acceptor distance of 6.3 nm. The raise of the FRET efficiency corresponds to the formation and growing of clusters of several QDs, while the saturation of the FRET efficiency may relate with formation of an ordered QD superstructure, when optical properties cannot further depend on QD concentration. Formation of an ordered PbS QD superstructure is confirmed by X-ray analysis for more concentrated samples, while calculated interdot distance in the superstructure coincides with the one obtained by FRET technique. The obtained result may be used for determination of superstructure's lattice constant without X-ray analysis.

9126-77, Session PS1

Josephson surface plasmons in spatially confined cuprate superconductors

Filippo Alpeggiani, Lucio C. Andreani, Univ. degli Studi di Pavia (Italy)

A generalization of the well-known theory of localized surface plasmons to the case of high-Tc cuprate superconductors is presented [1]. At variance from ordinary metals, cuprate superconductors are strongly anisotropic materials whose structure is characterized by conductive CuO2 planes stacked along the c-axis. They support two kinds of plasma waves [2-4]: quasi-2D plasmons, resulting from plasma oscillations of the carriers along the conductive planes, and the so-called Josephson plasma wave (JPW), a low-frequency excitation arising from interlayer Josephson tunnelling of the condensate along the c-axis. In compounds with multiple planes per unit cell, inequivalent intra- and inter-multilayer couplings give rise to both acoustic and optical JPWs.

The complexity of bulk electromagnetic modes is reflected in a broad spectrum of localized surface excitations, which we calculate analytically for the benchmark example of a cuprate superconductor spatially confined in the form of a small spherical particle [1]. The effect of the JPW is revealed in the presence of low-frequencies surface modes in the terahertz range, which we call "Josephson surface plasmons". Our results can be applied to the interpretation of far-infrared experiments with the sphere-resonance method [5,6] or electron-energy-loss spectroscopy, the latter involving the whole spectrum of multipolar surface modes, with delicate coupling and mixing effects. Moreover, spatial confinement of the JPWs could represent a new degree of freedom to explore the link between interlayer tunnelling and high-Tc superconductivity, especially in the light of the fact that the plasma frequency of optical JPWs has been shown to correlate with the critical temperature [6].

References:

[1] F. Alpeggiani and L. C. Andreani, arXiv:1305.4579, to be published in Phys. Rev. B.

[2] D. van der Marel and A.A. Tsvetkov, Phys. Rev. B 64 024530 (2001); D. van der Marel, J. Supercond. 17, 556 (2004).

[3] A. Bill et al, Phys. Rev. B 68, 144519 (2003).

[4] S. Savel'ev et al, Rep. Prog. Phys. 73, 026501 (2010).

[5] T. W. Noh et al, Phys. Rev. B 41, 307 (1990).

[6] Y. Hirata et al, Phys. Rev. B 85, 054501 (2012).

9126-78, Session PS1

Performance improvements in vertical-type GaN LEDs using silicon-nitride-based transparent conductive electrodes

Kyeong Heon Kim, Su Jin Kim, Hee-Dong Kim, Suk Won Kim, Ju Hyun Park, Byeong Ryong Lee, Tae Geun Kim, Korea Univ. (Korea, Republic of)

Gallium nitride (GaN)-based light emitting diodes (LEDs) have been extensively researched as optoelectronic devices for illumination applications, such as automotive headlights, full color displays and interior/exterior lighting because of their recent considerable progress external quantum efficiency. However, for the realization of next-generation solid-state lightning, we must further improve the performance of LEDs, particularly, vertical-type LEDs (VLEDs) because of their advantages including larger emitting areas, better current

spreading and heat dissipation, as compared to traditional lateral-type LEDs. However, under a high current operation, the current injected into the n-GaN layer does not sufficiently spread over the entire surface, which causes the non-uniform light emission and the reduction of luminous efficiency.

To overcome these drawbacks, several approaches have been proposed to enhance current injection and distribution, including the use of carefully designed n-type electrode patterns, embedded insulating current blocking layers in p-GaN, and the ITO and indium–zinc-oxide (IZO) transparent conductive electrodes (TCEs) below the n-type metal electrode. However, the increase of the light absorption due to the narrow bandgap of the ITO, IZO and ZnO-based TCEs limited the light extraction from the chip surface. Graphene films on LEDs have been reported but they showed poor electrical properties because of their high contact barrier and high sheet resistance. Here, we introduce a novel method1 to obtain both high electrical conductivity and high optical transmittance, by introducing an electrical breakdown (EBD) process into the wide-bandgap materials such as Si3N4; during which nano-scale conducting filaments (CFs) can be formed within the wide-bandgap films to provide a current path (or channel) between the n-type metal pad and N-face n-GaN layers.

In this study, four samples (reference VLED, VLED with metallic ITO, VLED with insulating ITO, and VLED with Si3N4 TCE) are fabricated and characterized for comparison.

First, we observed low specific contact resistivities of 1.15?10-4 ?•cm2 and 8.39?10-5 ?•cm2 for the insulating ITO and Si3N4, while the transmittances of the metallic ITO, insulating ITO and TCEs are measured to be 86.9, 93.2, and 97.7 % at 450 nm, respectively. We then fabricated and demonstrate the validity of this concept on a device level using VLED structures. Interestingly, the output power of the VLED with proposed Si3N4 TCEs (after EBD) at 1A increased by 9.0 %, 21.7 %, and 10.2 %, respectively, compared with those of the conventional VLED and VLEDs with metallic and insulating ITO (after EBD). Furthermore, the forward voltage at an injection current of 350 mA was found to be 4.0, 4.55, 3.76, and 3.42 V, respectively, for the conventional VLED and VLEDs with TCEs such as metallic ITO, insulating ITO, and Si3N4 TCE after EBD. More details including a new ohmic mechanism via EBD will be presented at the conference.

1 “A Universal Method of Producing Transparent Electrodes Using Wide-Bandgap Materials”, Advanced Functional Materials, 2013 (in press)

9126-79, Session PS1

Light extraction improvements in nitride-based light-emitting diodes using optimized conical nanopillar structures

Su Jin Kim, Kyeong Heon Kim, Ho Young Chung, Hee Woong Shin, Byeong Ryong Lee, Kie Young Woo, Suk Won Kim, Korea Univ. (Korea, Republic of); Tak Jeong, Korea Photonics Technology Institute (Korea, Republic of); Tae Geun Kim, Korea Univ. (Korea, Republic of)

Recently, demands for GaN-based vertical light-emitting diodes (VLEDs) have increased since they can provide a solution for high-brightness power LEDs. VLEDs provide many advantages compared to conventional LEDs, including larger emitting area, better current spreading, excellent heat dissipation and simple packaging. However, although the tremendous progresses related to such LEDs have been achieved, the light output efficiency of LEDs should be further improved to meet such requirements and to replace traditional light sources. One of the advantages of VLEDs can be found from their high extraction efficiency through various methods of surface engineering. It is well known that most of the light is lost in the semiconductor materials and only about 4% of the light emission radiates through the top and bottom in a flat-surface LED structure. However, the light extraction efficiency has been greatly improved using various methods of surface texturing, together especially with VLED structures. Some of the texturing methods include nanoimprint lithography, laser interference lithography and nanosphere lithography (NSL), etc. Among these, the NSL technique has been paid attention since it is a simple and low-cost process and suitable for mass production.

In this work, we investigated the fabrication of GaN-based vertical light-emitting diodes (VLEDs) with periodic and conical nanopillar arrays using NSL to maximize the light output efficiency. The influence of the different geometrical features such as a diameter and a height of the conical nanopillar arrays on the light output efficiency of VLEDs was studied using two types of dry etching conditions. For this study, the finite-difference time-domain (FDTD) simulation was performed to understand the influences of the features such as diameter and height of conical nanopillars on the light extraction behavior and the emission characteristics. In order to confirm the simulation result, SiO2 nanospheres ranging from 100 to 500 nm in size were synthesized and then single layered SiO2 nanospheres were coated onto the n-GaN layer by a simple spin-coating method. After that the inductively coupled plasma reactive-ion etching (ICP-RIE) was applied to make conical nanopillar patterns with the different diameter and size. It was experimentaly shown that among the different patterns, the maximum enhancement of the light output was achieved from VLEDs incorporating conical nanopillar arrays with optimized pattern diameter of 500 nm and height of 0.8-0.9 ?m. At the injection current of 350 mA, the VLEDs with conical nanopillar arrays with diameter of 500 nm and height of 0.8-0.9 ?m was exhibited no significant degradation of electrical properties and an increase in light output power by 253 and 5.1 %, respectively, compared to the flat-surface and the surface-roughened VLEDs. These improved optical properties could be attributed to the optimized conical nanopillar structures on the n-GaN surface, which increase the effective photon escape cone and reduced total internal reflection at n-GaN/air interface. More details on the experimental results and discussion will be presented at the conference.

9126-80, Session PS1

Investigation of the slot mode enhancement of erbium-doped polymer silicon on insulator waveguide amplifiers

Samuel F. Serna Otalvaro, Weiwei Zhang, Institut d’Electronique Fondamentale (France); Yonggan Zhang, Meiling Zhang, Dingshan Gao, Daming Zhang, Wuhan National Lab. for Optoelectronics (China); Eric Cassan, Institut d’Électronique Fondamentale (France)

The feasibility of a hybrid silicon SOI (Silicon on Insulator) slot waveguide scheme filled with Erbium highly doped polymers is studied by solving the coupled pump and signal propagation equations, including a realistic description of the slot waveguide cross-section and the rate equations of a four level model, respectively, for a 1480 nm pumping wavelength excitation and considering the ion-ion interactions and the transition rates through the co-propagative signal and pump beams. Starting from realistic slot waveguide losses (around 10dB/cm) and spectroscopic parameters (e.g. absorption and emission cross-sections, up-conversion parameter, etc), different possible situations are explored depending on the beam powers as well as on the Erbium ion concentration.

The adopted approach brings a clear estimation of the slot-mode enhancement factor on the gain and shows that with high Erbium ion concentration around 10^26 ions/m^3, optical gains ranging from 0 to 15dB can be obtained for propagation lengths in the range of 10 to 20 mm. Additionally, in contrast to most waveguide amplifier models, the influence of Excited State Absorption (ESA) that establishes a limit for the input pump power is included. Doing so, it is predicted that the optical gain is significantly suppressed for large pumping powers, leading to the counterintuitive result that there is an optimum pumping power of only about 10 mW and 30 mW for 100 nm and 200 nm slot widths, respectively. As a whole, these works bring a new theoretical insight into the possible design of Erbium Doped Waveguide Amplifiers (EDWA) in silicon photonics.

9126-81, Session PS1

Temporally shaped femtosecond laser pulses as direct patterning method for dielectric materials in nanophotonic applications

Tamara Meinl, Nadine Goette, Yousuf Khan, Thomas Kusserow, Cristian Sarpe-Tudoran, Jens Köhler, Matthias Wollenhaupt, Univ. Kassel (Germany); Arne Senftleben, University of Kassel, Institute of Physics and CINSaT (Germany); Thomas Baumert, Harmut H. Hillmer, Univ. Kassel (Germany)

Dielectric materials have great potential for usage in photonic devices. Implementation of nanophotonic structures like photonic crystals with dimensions smaller than the used wavelength enable the utilization of specific effects and they are of great interest, especially in the visible and UV spectral range. A big variety of dielectric materials, e.g. oxides and nitrides, can be chosen and they offer good chemical and mechanical stability and processing properties. Additionally they offer a low-cost fabrication when compared to semi-conductors. However, to tap the full potential of these advantages, it is a big challenge to overcome charging effects of the dielectrics, which occur in conventional processing techniques based on electron beam lithography or focused ion beams.

We present a direct patterning method via temporal shaped femtosecond laser pulses. A thin-film waveguide with a 2D periodic pattern of photonic crystals with circular base elements is investigated. Although, the refractive index contrast is low, we show by numerical design results that normal incident of light to the plane of periodicity couples into the waveguide to a waveguide mode and can excite Fano resonances. That makes the device extremely interesting as narrow-band optical filter. To produce optical filters in the visible and UV spectral range photonic crystal structures in the sub-100nm range are required.

Temporal shaped infrared femtosecond laser pulses are applied as a novel method for very high precision laser processing of wide band gap materials to create photonic crystal structures in dielectrics. Shaping temporal asymmetric pulse trains enable the production of structures well below the diffraction limit with best results <100 nm. We combine this process with deposition of a high index layer by ion beam sputtering to achieve the targeted resonant waveguide structure.

9126-82, Session PS1

Transient pump-probe absorption spectroscopy of semiconductor nanodumbbells

Mikhail Y. Leonov, National Research Univ. of Information Technologies, Mechanics and Optics (Russian Federation); Ivan D. Rukhlenko, Monash Univ. (Australia); Anvar S. Baimuratov, National Research Univ. of Information Technologies, Mechanics and Optics (Russian Federation); Yurii K. Gun'ko, Trinity College Dublin (Ireland); Alexander V. Baranov, Anatoly V. Fedorov, National Research Univ. of Information Technologies, Mechanics and Optics (Russian Federation)

The creation of semiconductor nanostructures of complex geometries is a hot topic in photonics research and technology. Of particular interest, owing to their inherently strong optical anisotropy, are nanodumbbells made of quantum dots that are connected by quantum rods. The nanodumbbell's topology offers quite a few degrees of freedom (associated with the possibility to alter the sizes and shapes of the dots, the length and diameter of the rod, as well as the composition of both dots and rods) for flexible manipulation of the nanodumbbell's optical response. Despite the many advantages of using nanodumbbells in photonics devices, their physical properties and electronic dynamics are still poorly understood. A better understanding of these features may be achieved via the analysis of the nanodumbbell's optical response measured using the time-resolved pump–probe spectroscopy.

In this work, we develop a first unified theory of transient pump–probe absorption spectroscopy of a semiconductor nanodumbbell. We treat the physical process underlying this spectroscopic method, which constitutes the absorption of the probe pulse induced by the pump pulse resonant to some interband transition of the nanodumbbell, using the density matrix formalism. We ascertain the physical conditions under which the dependence of the absorbed probe energy on the delay time between the pump and probe pulses is described by one or two exponential functions with exponents proportional to the energy relaxation rates of the nanodumbbell's electronic states. Furthermore, we show that the transient absorption spectroscopy allows one to reliably determine the energy relaxation rates of the nanodumbbell's electronic states. The derived analytical expressions for the absorbed energy of the probe's pulse can be used for studying the dynamics of quantum transitions in semiconductor nanodumbbells, whereas the novel approaches for the determination of energy relaxation rates suggested in our work may prove useful for developing advanced optical methods of nondestructive analysis of relaxation processes in quantum nanostructures.

9126-83, Session PS1

Thermalization and cooling of plasmon-exciton polaritons: towards quantum condensation

Said R. K. Rodriguez, FOM Institute for Atomic and Molecular Physics (Netherlands); Johannes Feist, Univ. Autónoma de Madrid (Spain); Marc A. Verschuuren, Philips Research (Netherlands); Francisco J. García-Vidal, Univ. Autónoma de Madrid (Spain); Jaime Gomez Rivas, FOM Institute for Atomic and Molecular Physics (Netherlands) and Cobra Research School (Netherlands)

Bose-Einstein Condensation (BEC) – the ground state accumulation of particles with integer spin (bosons) at low temperature and high density – has been reported for atoms, photons, and solid-state quasi-particles such as exciton-polaritons. In a recent publication, we presented the first experiments towards the quantum condensation of bosonic quasi-particles in a plasmonic system [1]. The system studied comprises a periodic array of metallic nanorods covered by a polymer layer with organic dye molecules at room-temperature. The nanorod array sustains collective resonances arising from the diffractive coupling of localized surface plasmons. These are known as surface lattice resonances (SLRs), and their narrow linewidth and steep dispersion enables to access the strong coupling regime with molecular excitons. The resultant hybrid quasi-particles, known as plasmon-excicton-polaritons (PEPs), have an extremely small effective mass (~7 orders of magnitude lighter than the electron rest mass). Both their ground-state energy and the Rabi frequency are well above kT at room-temperature, thereby making PEPs ideal for room-temperature quantum condensation.

Here we present new experimental results in an effort to reach quantum condensation in a plasmonic system. By varying the lattice constant of the array we probe different detunings between the underlying plasmonic, photonic, and excitonic states underlying the PEPs. Furthermore, by varying the dimensions of the metallic nanostructures we induce pronounced modifications in the PEP mass, lifetime, and composition. Thermalization and cooling of PEPs as function of their density, which is in turn increased through optical pumping, is observed in the emission dispersion relation. Our results elucidate the challenges and opportunities that plasmonic systems face with respect to other systems in their way towards the quantum degeneracy threshold, wherein a single quantum state becomes macroscopically populated.

[1] S.R.K. Rodriguez et al., Phys. Rev. Lett. 111, 166802 (2013).

9126-84, Session PS1

Giant enhancement of spin hall effect of light in an exotic optical system

Ankan Bag, Shubham Chandel, Chitram Banerjee, Debashis Saha, Mandira Pal, Ayan Banerjee, Nirmalya Ghosh, Indian Institute of Science Education and Research Kolkata (India)

Spin orbit interaction (SOI) of light, which refers to intrinsic coupling between the spin (polarization) and orbital angular momentum (topological phase vortex) of photons, has evoked intensive investigations in the past few years owing to fundamental interests and potential nano-optical applications [1]. SOI is associated with two distinct effects – (a) evolution of geometric (topological) phase due to the effect of trajectory of light on polarization and (b) spin hall effect of light (SHEL) arising due to the effect of polarization on the trajectory itself [1-3]. The former has led to observation of a number of interesting effects associated with spatial polarization characteristics as manifestation of topological phase evolution [2]. The latter on the other hand, has been observed in various micro / nano systems involving light-matter interactions. For refraction, reflection, or total internal reflection from inhomogeneous isotropic media, such Spin Hall (SH) shifts have been typically observed via breaking the symmetry of the system, either by employing oblique incidence of light or by using oblique detection geometry. In most cases the SHEL effect have been rather small –shifts are typically of sub-wavelength magnitudes [1-3]. Here, we report giant enhancement of SH shift even for normal incidence in an exotic optical system, an inhomogeneous anisotropic medium having complex spatially varying birefringent structure. We unravel the reason for such large enhancement of SH shift by performing rigorous three dimensional analysis of polarization evolution in such complex anisotropic medium.

The system employed in our study is a twisted nematic liquid crystal spatial light modulator (TNSLM), whose individual pixels are electronically addressed to form complex spatially varying birefringence effect. The spatial variation of birefringence is obtained by changing the three dimensional orientation of local liquid crystal director (tilt and twist angle of the director axis), by modulating the pixels with user-controlled spatial maps. The polarization dependent spatial variation (in a plane transverse to the direction of propagation of light) of the transmitted light beam (for incident fundamental Gaussian beam lacking any intrinsic angular momentum) through such inhomogeneous anisotropic medium was recorded using an Eigenvalue calibrated Stokes-Mueller imaging system. Giant SH shift was manifested as distinctly different spatial distribution of the recorded output Stokes vector elements for two orthogonal (left and right) input circular polarization states. The theoretical analysis revealed that generation of large magnitude of transverse energy flow (quantified via the Poynting vector evolution inside the medium) originating from SOI in the inhomogeneous birefringent medium leads to the observation of such a large spin dependent deflection of the trajectory of light beam. The details of the experimental results of SH shift in inhomogeneous anisotropic media and the corresponding theoretical results will be presented. The significance of the observed SH shifts in context to optical nano-probing applications will be highlighted.

References

1. K. Y. Bliokh, A. Niv, V. Kleiner, and E. Hasman, Nat. Photonics 2, 748 (2008).

2. L. Marrucci, C. Manzo, and D. Paparo, Phys. Rev. Lett. 96, 163905 (2006).

3. K. Bliokh, Y. Gorodetski, V. Kleiner, and E. Hasman, Phys. Rev. Lett. 101, 030404 (2008)

9126-85, Session PS1

Nonlinear properties of plasmonic metamaterials studied using femtosecond z-scan technique

Andres Neira, Gregory A. Wurtz, Anatoly V. Zayats, Nicolas Olivier, Mazhar Nasir, King's College London (United Kingdom)

Metamaterials are new kinds of artificial materials which are engineered to control propagation of light. In a plasmonic metamaterial, light is usually coupled as surface plasmon-like modes to allow for the modification of not only linear response, but also to enhance the metamaterial's optical nonlinearity. Our research reports on the investigation of the third-order nonlinear optical properties of the metamaterials based on arrays of metallic nanorods using the z-scan. Polarisation and pulse compression effects have been studied. The results are compared to the modelling of nonlinear response of electron plasma component of the metamaterial. It is shown that as a consequence of the epsilon-near zero condition achieved in the metamaterial the nonlinear properties of gold can be enhanced and studied in more detail at wavelengths where the actual bulk nonlinear response is very small.

9126-86, Session PS1

Analytical expression of dipolar interactions in subwavelength plasmonic nanoparticles

Jan Fiala, Ivan Richter, Czech Technical Univ. in Prague (Czech Republic)

Recently, by utilizing our experience with the analysis of interactions at the nanoscale of the periodic subwavelength hole array structures, our interest has been turned into characterization of resonances for the case of 'inversed' structures, being those e.g. periodical arrays of metallic nanoparticles. Such subwavelength-scaled plasmonic nanostructures have gained much interest for their applications in surface plasmon resonance (SPR) biosensing as well as surface-enhanced Raman scattering (SERS) spectroscopy activities since the optical fields associated with nanoparticles can be effectively enhanced and confined locally.

Here, we investigate, first, the surface plasmon polariton assisted interaction between two dipoles and, subsequently, a revelation of an interplay between resonances localized in individual particles and lattice resonances originating in the periodic array of such naoparticles. It has been observed that such metallic nanoparticles can sustain localized plasmon excitations which travel across neighbors. This effect can be utilized to transmit light energy along chains of subwavelength particles, thus e.g. providing some basic constituents for plasmonic sensors. In fact, the phenomena of field enhancement and spatial confinement are related to dipolar fields and resonances, being governed by the generation of localized surface plasmons and their mutual coupling [1,2].

In order to describe and utilize the underlying physics, a simple analytical model of the two coupled nanoparticles is proposed. Polarizabilities and cross-sections are calculated under the action of a monochromatic plane wave which exhibits resonances indicating light trapping and field enhancement. Within the model, modes of coupled oscillations and the corresponding eigenfrequencies are computed as well as the prediction of a shift in the resonance frequency with the change of the mutual distance of two interacting particles is made.

Under a proper periodicity of the nanoparticle lattice, such nanoparticle arrays can exhibit narrow resonances with asymmetric Fano-type spectral line shapes in the transmission and reflection spectra [3]. In order to reveal the interplay between resonances localized in individual particles and lattice resonances, a simple model that characterizes an isolated building block in terms of equivalent induced dipoles of both magnetic and electric character, and lattice resonances

originating in coupling of such dipoles, is developed, inspired with the work of Garcia de Abajo [4]. A final formula of particle polarizability is achieved which describes the pronounced asymmetric resonance character of a Fano resonance, as well as the reflection coefficient of the whole periodic structure.

[1] Apostol M., Ilie S., Petrut A., Savu M., Toba S.: Coupled nano-plasmons, Proceedings of Meta 2013 Conference, United Arab Emirates, 2013. [2] Zhou F., Liu Y., Li Z.: Surface-plasmon-polariton-assisted dipole–dipole interaction near metal surfaces, Opt. Lett., Vol. 36, 1969-1971, 2011.

[3] Miroshnichenko A. E., Flach S., Kivshar Y. S.: Fano resonances in nanoscale structures, Rev. Mod. Phys., Vol. 82, 2257-2289, 2010. [4] Garcia de Abajo F.J.: Colloquium: Light scattering by particle and hole arrays, Rev. Mod. Phys., Vol. 79, 1267-1290, 2007.

9126-87, Session PS1

Photo-voltage in InGaAs/GaAs Heterostructures with One-Dimensional Nanostructures

Marianna Kovalova, National Taras Shevchenko Univ. of Kyiv (Ukraine); Sergey V. Kondratenko, National Taras Shevchenko Univ. of Kyiv (???????)

The work is devoted to the study of mechanisms of photovoltage generation in p-i-n InGaAs/GaAs heterostructures with nanoobjects, which are among the most attractive materials optoelectronics. Studied low-dimensional heterostructures showes perspectives for design a novel solar cells, photodetectors and transistors. Through the use of optical transitions involving low-dimensional states such structures are able to work in a wider optical range in comparison with the structures without quantum objects.

The photovoltage spectra for the InGaAs/GaAs structure with nanoobjects and GaAs reference structure without the nanoobjects were measured. The dependencies of photovoltage signal from illumination intensity were found to be nonlinear, which gives possible to estimate the contact potential difference for p-i-n barrier.

Photovoltage spectra were studied for structures InGaAs/GaAs with nanoobjects and for reference sample without InGaAs using different intensities and modulation frequency of exciting radiation at room temperature. As a result, it was shown that the structure with InGaAs nanoobjects have higher photosensitivity as compare with the structure without the nanoobjects in the spectral region from 1.25 to 1.37 eV. It was shown that photovoltage generation of the structures is caused by spatial separation of photoexcited electron-hole pairs inside electric field of p-i-n structure.

9126-88, Session PS1

Effect of matrix on Raman scattering and luminescence in 2D gold nanorod arrays

Signe Damm, Univ. College Dublin (Ireland); Antony Murphy, Mark McMillen, Robert J. Pollard, Queen's Univ. Belfast (United Kingdom); James H. Rice, Univ. College Dublin (Ireland)

Nanoscale structures made from coinage metals such as gold or silver possess localized surface plasmon-polariton (LSP) excitations when the material interacts with light of the correct frequency and polarization [1]. When LSPs are formed, strongly enhanced electromagnetic near-fields are generated at the surface of the supporting nanostructure. This property has attracted considerable research interest due to its potential applications in sensors, photonic circuits and medical diagnostics and therapeutics. Modern nanofabrication methodologies enable the creation of a number of different nanostructures with precisely controlled shapes, sizes, and spacing's. One particular area of active research within plasmonic's is to investigate the effect of nanostructure substrate geometry on the optical properties of materials in the near-field of the LSP.

Fluorescence and Raman spectroscopies are established methods that enable selective detection of bioanalytes. The presence of LSPRs on plasmonic metal nanostructures can enhance the fluorescence signal from locally situated fluorophores, a process known as metal enhanced luminescence (SEL) or Raman (SER) [2]. Few reports have studied SERS and SEL together which is potentially attractive for sensor applications. One challenge to this approach is to fabricate conditions that enable SERS and/or SEL responsive from nanoprobes as the optimum distance for enhancing fluorescence emission and Raman scattering with respect to the nanoprobe-metal separation distance. A direct contact between molecule and metal surface is detrimental to SEL due to enhanced non-radiative decay in the probe molecule, while a noncontact attachment of molecule to metal could be detrimental to SERS.

Metallic nanorod arrays with reproducible nanorod diameter and location are known to support SERS and SEL [1-3]. Anisotropic nanorods exhibit two surface plasmon resonances, with large and controllable tunability across the visible and near-infrared (NIR) region as outlined above [1-3]. In addition gold nanorods possess good chemical stability and biocompatibility under biological conditions. Self-standing Au nanorod arrays have been demonstrated to support SERS. These substrates have the potential also to support SEL. Here we study the conditions that optomise SERS and SEL from self-standing Au nanorod arrays. Specifically in regard to the conditions that optimise SERS and SEL from self-standing Au nanorod arrays in regard to the presence of aluminium matrix present around the Au nanorod array. We show that there is an inverse relationship between SERS and SEL from a rhodamine 6G probe molecule.

REFERENCES

1. A. Murphy, Y. Sonnefraud, A.V. Krasavin, P. Ginzburg, F. Morgan, J. McPhillips, G. Wurtz, S.A. Maier, A.V. Zayats, R. Pollard, App. Phys. Lett. 102, 103103, 2013.

2. M.D. Doherty, A. Murphy, R.J. Pollard, P. Dawson, Phys. Rev. X. 3, 011001, 2013.

3. G.A. Wurtz, R. Pollard, W. Hendren, G.P. Wiederrecht, D.J. Gosztola, V.A. Podolskiy, A.V. Zayats, Nat. Nanotech. 6, 106-110, 2011.

9126-89, Session PS1

Intraband optical transitions in a semiconductor nanocrystal with a degenerate valance band

Vadim K. Turkov, Anvar S. Baimuratov, National Research Univ. of Information Technologies, Mechanics and Optics (Russian Federation); Ivan D. Rukhlenko, Monash Univ. (Australia); Alexander V. Baranov, National Research Univ. of Information Technologies, Mechanics and Optics (Russian Federation); Yurii K. Gun'ko, National Research Univ. of Information Technologies, Mechanics and Optics (Russian Federation) and Trinity College Dublin (Ireland); Anatoly V. Fedorov, National Research Univ. of Information Technologies, Mechanics and Optics (Russian Federation)

We present a theoretical study of intraband optical transitions in a direct-bandgap semiconductor nanocrystal of a cubic lattice structure and an 8-fold degenerate valance band. We calculate analytically the matrix elements of the hole–photon interaction by assuming the nanocrystal to be in the regime of strong spatial confinement and have surface that is impenetrable for holes. The obtained matrix elements are then used to study the dynamics of holes upon optical excitation of the nanocrystal. In particular, we calculate the radiative lifetimes of the hole states and analyze their dependencies on the size and material of the nanocrystal.

9126-90, Session PS1

Quantum dots-graphene hybrid structures: interplay of optical and electrical properties

Yulia A. Gromova, National Research University of Information Technologies, Mechanics and Optics (Russian Federation); Andrei V. Alaferdov, Univ. Estadual de Campinas (Brazil) and N.I. Lobachevsky State Univ. of Nizhni Novgorod (Russian Federation); Victor A. Ermakov, Univ. Estadual de Campinas (Brazil); Kirill V. Bogdanov, National Research Univ. of Information Technologies, Mechanics and Optics (Russian Federation); Irina V. Martynenko, ITMO University (Russian Federation); Anna O. Orlova, Vladimir G. Maslov, National Research Univ. of Information Technologies, Mechanics and Optics (Russian Federation); Stanislav A. Moshkalev, Univ. Estadual de Campinas (Brazil); Alexander V. Baranov, Anatoly V. Fedorov, National Research Univ. of Information Technologies, Mechanics and Optics (Russian Federation)

We investigate electrical photoresponse of multilayer graphene decorated with CdSe/ZnS quantum dots (QDs), QD/graphene hybrid structures. It was found that photoresponse of these hybrid structures depends on QD photoluminescence (PL) quantum yield.

The hybrid structures based on CdSe/ZnS QDs and multilayer graphene were formed on Ti microelectrodes. Photocurrent appears in samples under direct voltage and laser radiation. We found that a quenching of QD PL intensity leads to dramatic decreasing of photocurrent in our hybrid structures.

The studied hybrid structures are very attractive as highly sensitive chemical sensors. We discovered that exposure of QD/grapheme structure with ammonia vapor leads to QD PL quantum yield decreasing accompanied by dramatic reduction of photocurrent. Further, under radiation ammonia molecules desorb from QD surface that leads to rising QD PL accompanied with photocurrent increasing.

Thus, our research shows that the electrical properties of QD/graphene structures are in pronounced correlation with QD PL quantum yield. It should be taken into account during development of optoelectronic devises. This feature could be used for sensor design also.

9126-91, Session PS1

Strong light-matter coupling mediated by surface plasmons in metallic nanostructures

Filippo Alpeggiani, Univ. degli Studi di Pavia (Italy); Stefania D'Agostino, Istituto Italiano di Tecnologia (Italy); Lucio C. Andreani, Univ. degli Studi di Pavia (Italy)

Light-matter interaction can be effectively enhanced by the confinement of the electric field due to the excitation of plasmonic modes at metal-dielectric interfaces [1]. In this work we give a theoretical formulation of the interaction between a radiating dipole and the localized surface plasmons of metallic nanoparticles, which is particularly suitable for studying strong-coupling effects beyond perturbation theory, such as the appearance of a vacuum Rabi splitting in the emission spectrum of the dipole [2,3]. In the case of a Drude-like electromagnetic response from the metal, the threshold for entering the strong-coupling regime can be expressed with a formalism analogous to that of cavity-quantum-electrodynamics [4], upon defining some characteristic properties of the plasmonic modes, such as the effective volume and the linewidth, which can be analytically calculated for simple geometries.

The procedure is applied to the analysis of a spherical metallic nanoshell, deriving a spectrum of sphere-like and cavity-like surface plasmon excitations [5]. By suitably tuning the geometry of the nanoshell and by choosing the optimal surface plasmon mode, a vacuum Rabi splitting can occur in emission spectra for dipole oscillator strengths as small as a few units, which can be easily achieved with organic molecules or quantum dots [6]. Our framework can be extended in a straightforward way to a fully computational approach in order to investigate the strong-coupling regime of light-matter interaction involving more complex geometries and with more realistic metal dielectric functions, as done, for instance, with the configurations of a single and double metallic nanocone [7].

References:

[1] S. Gaponenko, Introduction to Nanophotonics (Cambridge University Press, 2010).

[2] S. Savasta et al., ACS Nano 4, 6369 (2010).

[3] C. Van Vlack, P. T. Kristensen, and S. Hughes, Phys. Rev. B 85, 075303 (2012).

[4] L. C. Andreani, G. Panzarini, and J.-M. Gérard, Phys. Rev. B 60, 13276 (1999)

[5] E. Prodan and P. Nordlander, Chem. Phys. Lett. 352, 140 (2002).

[6] F. Alpeggiani, S. D'Agostino, and L. C. Andreani, Phys. Rev. B 86, 035421 (2012).

[7] S. D'Agostino, F. Alpeggiani, and L. C. Andreani, to be published in Opt. Express.

9126-92, Session PS1

Defect-rich zinc oxide nanoparticles by laser fragmentation

Marcus Lau, Kyra Kujawski, Stephan Barcikowski, Univ. Duisburg-Essen (Germany)

Optical fabrication of nanoparticles in liquid environment by pulsed laser sources is a versatile and straight forward method firstly shown by Henglein and Fojtik [1]. These nanoparticles are known to show high stability without surface-attached ligands, compared to chemical routes. By varying the geometry of target material (e.g. ablation of a thin metal wire) productivity can be enhanced [2]. Another approach is the laser fragmentation where fabrication of nanoparticles takes place from suspended microparticles [3]. We show the opto-physical fabrication of defect-rich zinc oxide nanoparticles by laser fragmentation in water. These laser-generated zinc oxide nanoparticles show an enhanced green fluorescence when irradiated with UV light. This shows that laser fragmentation is not only a mechanical top-down comminution process, but can also change material composition.

From nanoparticles prepared by laser processes it is known that laser and material parameters have a crucial influence to the amount and properties of produced nanoparticles [4]. The idea of a free liquid jet, initially shown by Wagener and Barcikowski, was used to design an experimental set up enabling to determine energy input and laser fluence thresholds for nanoparticle generation [5].

[1] A. Fojtik, A. Henglein, Laser Ablation of Films and Suspended Particles in a Solvent: Formation of Cluster and Colloid Solutions, Berichte der Bunsengesellschaft für physikalische Chemie, 1993, 97, 252-254

[2] G. Messina, P. Wagener, R. Streubel, A. De Giacomo, A. Santagata, G. Compagnini, G. S. Barcikowski, Pulsed laser ablation of a continuously-fed wire in liquid flow for high-yield production of silver nanoparticles, Physical Chemistry Chemical Physics, 2013, 15, 3093-3098

[3] Philipp WAGENER, J. J. & BARCIKOWSKI, S. Organic Nanoparticles Generated by Combination of Laser Fragmentation and Ultrasonication in Liquid, Journal of Laser Micro/Nanoengineering, 2011, 6, 59-63

[4] Vincenzo Amendola and Moreno Meneghetti, Controlled size manipulation of free gold nanoparticles by laser irradiation and their facile bioconjugation, Journal of Material Chemistry, 2007, 17, 4705–4710

[5] P. Wagener, S. Barcikowski, Laser fragmentation of organic

microparticles into colloidal nanoparticles in a free liquid jet, Applied Physics A, 2010, 101, 435–439

9126-93, Session PS1

Two band superlinear luminescence from GaSb-based nanostructures with AlSb/InAsSb/AlSb deep quantum well

Maya P. Mikhailova, Eduard V. Ivanov, Leonid V. Danilov, Andrey A. Petukhov, Karina V. Kalinina, Nikolay D. Stoyanov, Sergei I. Slobozhanyuk, Georgy G. Zegrya, Yury P. Yakovlev, Ioffe Physico-Technical Institute (Russian Federation); Alice Hospodková, Jirí Pangrác, Jirí Oswald, Markéta Zíková, Eduard Hulicius, Institute of Physics of the ASCR, v.v.i. (Czech Republic)

We report on study of the two-band superlinear electroluminescence (EL) in nanoheterostructures with deep AlSb/InAs1-xSbx/AlSb quantum well (QW) (d=5 nm)MOVPE grown on n-GaSb substrate.

Narrow-gap InAs1-xSbx well considered 15% of Sb. Two band El was measured in the photon energy range 0.5-0.8 eV with emission energy h?1=0.635 and h?2=0.695 eV at 300 K.

According to theoretical calculation there are two electron levels in QW in the QW and three hole levels at room temperature. Photon energy of the radiative transitions from the first electron level corresponded to the participation of the first hole level h?1=0.76 eV and the second hole level h?2=0.704 eV at T=300 K. At low temperature there are 2 electron levels and only 1 heavy hole level. It agrees with EL band maximum h?1=0.73 eV. Superlinear behavior of EL and the optical power dependence on drive current P=A?TB was found for both bands at T=300 K, where B=1.72-2.

These effects were explained by the contribution into radiative recombination of the additional electron-hole pairs which were created due to impact ionization by electron heated at high band offset Ec=1.284 eV between AlSb barrier and the first electron level Ee1 (inverse Auger-effect [1]). Temperature dependence of the two-band EL was measured in the range of 90-300 K. It was shown that with temperature decreasing a ratio between energy of the valence band offset ΔEv and the second heavy hole level position Eh2 changes due to temperature transformation of the energy band diagram. It was found that radiative transition on the second hole level “disappears” at T≤200 K, and we can see only one band in the EL spectrum.

[1] M.P. Mikhailova, E.V. Ivanov, L.V. Danilov et al., J.Appl.Phys., 112, 023108 (2012).

9126-94, Session PS1

Photoinduced polarized luminescence enhancement and darkening in an ensemble of CdSe/ZnS quantum rods

Maria V. Mukhina, Vladimir G. Maslov, Alexander V. Baranov, Anatoly V. Fedorov, National Research Univ. of Information Technologies, Mechanics and Optics (Russian Federation)

Colloidal semiconductor nanocrystals, or quantum dots, have become efficient light-emitting or energy-transferring elements in a range of applications from sensors, labels and lasers to solar cells, optical storage and quantum computing. In all of these applications it is very important to understand properly, how the optical, first of all, luminescent, properties of the nanocrystals will change under continuous irradiation with light. Therefore, the photoinduced processes, occurring on the surface of irradiated nanocrystal, have attracted considerable attention in recent years. Different photoinduced effects such as photoinduced luminescence enhancement (PLE), photooxidation, photoionization, photoannealing are well known for spherical nanocrystals. In this research PLE and photooxidation effects have been used to induce the photoluminescence (PL) anisotropy in initially disordered Quantum Rod (QR) ensemble under continuous irradiation with polarized light. Quantum rods, elongated nanocrystals with axial symmetry, absorb and emit light anisotropically because dipole moments of their lowest excitonic transitions are directed along their long axes. Therefore, if disordered QR ensemble is irradiated with polarized light, the incident radiation will be absorbed mainly by the nanocrystals whose dipole moments coincides with the direction of polarization of the light. The surface of these QRs and their luminescent characteristics are modified due to selective photochemical reaction (photoinduced effect), but the luminescent properties of the other part of a QR ensemble do not change. This is the reason of an appearance of the PL polarization. In experiment QRs were embedded in pores (12-15 μm) of filter paper from toluene solution to achieve disordered ensemble. Next, the sample was irradiated through a polarizer. An orange light emitting diode, with a centre wavelength of 595 nm and a converted power 23 mW, was used for sample exposure. The observation of photoinduced PL polarization in a QR ensemble was carried out by comparing of the intensities of the luminescence components with vertical and horizontal polarization that were recorded separately. PL polarization appeared as a result of photochemical reactions in the initially isotropic sample. The polarization direction coincided with the polarization direction of the light initiating the photoreaction. A photoinduced process led to a blue shift of the PL band around 15 nm (for 80 hrs irradiation). The PL as a function of time is well fitted by a double exponential with time constants 35-40 min and 2-18 hrs, indicating that two processes are occurring in the system. Using the previously published and obtained experimental data, the photoprocess with time constant 35-40min was identified as PLE due to photopassivation of surface defects, and the photoprocess with time constant 2-18 hrs was attributed to photooxidation. The observed degree of polarization was calculated to be 16%. Investigation of the relaxation process in the QR ensemble in darkness after continuous irradiation allowed to reveal the depolarizing factor attributed to rotational diffusion of the QR in the pores of matrix.

9126-95, Session PS1

Split-ball resonator

Arseniy I. Kuznetsov, A*STAR - Data Storage Institute (Singapore); Andrey E. Miroshnichenko, The Australian National Univ. (Australia); Yuan Hsing Fu, A*STAR - Data Storage Institute (Singapore); Vignesh Viswanathan, National Univ. of Singapore (Singapore); Mohsen Rahmani, Vytautas Valuckas, Zhenying Pan, A*STAR - Data Storage Institute (Singapore); Yuri Kivshar, The Australian National Univ. (Australia); Daniel S. Pickard, National Univ. of Singapore (Singapore); Boris Luk’yanchuk, A*STAR - Data Storage Institute (Singapore)

We introduce a new concept of split-ball resonator as a nontrivial generalization of more familiar split-ring resonator composing electromagnetic metamaterials. We realize this novel concept experimentally by employing the laser-induced transfer method to produce near-perfect spheres and helium ion beam milling to make cuts with the nanometer resolution. Due to high quality of the spherical particle shape, governed by strong surface tension forces during the laser transfer process, and the clean, straight side walls of the cut made by helium ion milling, magnetic resonance is observed at 600 nm in gold and at 565 nm in silver nanoparticles. We demonstrate a strong omnidirectional magnetic dipole response, for both gold and silver spherical plasmonic nanoparticles with nanometer-scale cuts, and also realize tunability of the magnetic dipole resonance throughout the visible spectral range by a change of the depth and width of the nanoscale cut. Structuring arbitrary features on the surface of ideal spherical resonators with nanoscale dimensions provides new ways of engineering hybrid resonant modes and ultra-high near-field enhancement.

9126-96, Session PS1

Randomization of two-dimensional photonic structures showing transverse Anderson localization

Sebastian Brake, Martin Boguslawski, Patrick Rose, Falko Diebel, Cornelia Denz, Westfälische Wilhelms-Univ. Münster (Germany)

Anderson localization (AL) is one of the most intriguing effects in solid state physics [1], describing an increased probability of a wavefunction in randomly affected potential to be localized in the vicinity of its initial position. This effect was primarily predicted for electron waves in condensed matter. However, since the effect is based on wave phenomena, AL has recently been discovered for light waves in several systems as e.g. random granular media or photonic band gap materials [2-3].

In this contribution, we demonstrate light localization in optically induced two-dimensional photonic random lattice structures. Using the so-called optical induction technique [4], we are able to create reconfigurable refractive index patterns in a nonlinear optical medium. In contrast to previous realizations, our approach is based on a computer- controlled spatial light modulator that is used to generate structured nondiffracting beams with a tremendous flexibility.

This particular class of beams that provides complex transverse intensity structures while being invariant in the direction of propagation is the foundation of our flexible approach for the generation of complex random structures.

Consequently, analyzing statistically whole sets of hundreds of different potentials we observe AL connected with different localization behaviors in terms of a changing localization length. We demonstrate how to manipulate the strength of localization by varying fundamental parameters, as e.g. the correlation length of the randomized potential and the momentum distribution of the probe beam.

In combination with nondiffracting beams of regular symmetries such as periodic, quasi-periodic as well as curvilinear transverse intensity modulations, we developed a tool to reversibly induce complex photonic refractive index landscapes of various shapes and degrees of randomness.

Due to the universal nature of Anderson localization our results are relevant for all wave systems containing disorder.

References:

[1] P.W. Anderson, “Absence of Diffusion in Certain Random Lattices,” Phys. Rev. 109, 1492 (1958).

[2] D.S. Wiersma, P. Bartolini, A. Lagendijk, and R. Righini, “Localization of light in a disordered medium,” Nature 390, 671 (1997).

[3] T. Schwartz, G. Bartal, S. Fishman, and M. Segev, “Transport and Anderson localization in disordered two-dimensional photonic lattices,” Nature 446, 52 (2007).

[4] P. Rose, M. Boguslawski, and C. Denz, “Nonlinear lattice structures based on families of complex nondiffracting beams,” New J. Phys. 14, 033018 (2012).

9126-97, Session PS1

Self-reconstructing singular beams

Geo M. Philip, Nirmal K. Viswanathan, Univ. of Hyderabad (India)

An optical beam which reconstructs itself after partial obstruction, reported first in Bessel beams, has enabled a variety of applications in microscopy and nanoscopy [1], beam propagation through scattering and turbid media [2] and in optical manipulation [3]. The self-reconstruction of optical beams have been demonstrated, apart from in Bessel-type beams, in caustic beams, Airy beams, Parcey beams, non-paraxial Mathieu and Weber accelerating beams and in ring lattice beams [4]. Until now only the intensity self-reconstruction process has been demonstrated behind intensity and phase obstruction, leaving the polarization obstruction and transverse energy flow during the reconstruction of the beam open for further investigation.

In the recent times a family of optical beams with spatially inhomogeneous polarization structure, known as vector beams has caught the attention of researchers for their applications in optical science and engineering, ranging from classical to quantum optics experiments [5, 6]. It was theoretically proposed that the vector Bessel-Gauss and Laguerre-Gauss beams self-reconstruct under tight focus conditions at the focal plane [7].

Phase singular or optical vortex beams with orbital angular momentum (AM) and polarization singular optical beams with entangled spin (?) and orbital (l) AM contribution has opened entirely new avenues for researchers [8]. Phase and polarization obstruction and the total reconstruction of the class of singular optical beams are experimentally studied and presented here. The singular optical beam with desired characteristics is generated using a polarization Sagnac interferometer with a spiral phase plate (SPP) wherein the counter rotating beams have opposite helicities (± l) and linear orthogonal polarization. The interferometer output when passed through a quarter-wave plate generates vector (V-) singular beam and for the generation of circular (C-) singular beams an additional SPP is used. Paraxial focusing of the output beam from the interferometer using an axicon with 179o cone angle results in the corresponding Bessel-Gauss beam. Introducing a phase or polarization modifying obstruction at the center of the non-diverging range modifies the beam characteristics. Measurements are made along the propagation direction to study the transverse energy flow during the beam reconstruction using interferometric and polarimetric methods. Our results confirm that the intensity, phase and polarization of the obstructed singular beams reconstruct itself completely. The implications of the complete reconstruction of singular beams in the context of emerging applications in nano photonics and plasmonics are significant.

References:

1. F.O. Fahrback et al., Nat. Photonics 4, 780, 2010

2. V.G-Chavez et al., Nature 419, 145, 2002

3. J. Baumgartl et al., Nat. Photonics 2, 675, 2008

4. N. Hermosa et al., Opt. Lett., 38, 383, 2013 for related references

5. Q. Zhan, Adv. Opt. Photon. 1, 1, 2009

6. A. Holleczek et a., Opt. Expr. 19, 9714, 2011

7. S. Vyas et al., J. Opt. Soc. Am. A 28, 837, 2011

8. The angular momentum of light ed. D.L. Andrews and M. Babiker, Cambridge University Press, 2013

9126-98, Session PS1

Study of quantum dots interaction with human serum albumin and heavy metal ions

Vyacheslav I. Kochubey, Julia G. Konyukhova, Elena K. Volkova, N.G. Chernyshevsky Saratov State Univ. (Russian Federation); Andrey G. Melnikov, Ekaterina V. Naumova, Gennady V. Melnikov, Saratov State Technical Univ. (Russian Federation)

The use of quantum dots (nanoparticles) as fluorescent probes is promising in medical diagnostics, since they are photochemically stable.

We have studied the interaction of quantum dots (QDs) based on semiconductor nanocrystals ZnCdS with proteins and heavy metals ions. When studying the interaction of the quantum dots with molecules of human serum albumin (HSA), we observed an increase in fluorescence intensity with increasing in concentration of HSA to 2 mM.

It is suggested that this is due to the formation of aggregates of nanoparticles – protein macromolecule, which increases the fluorescence intensity of the nanoparticles. The binding of protein macromolecules with nanoparticles may change the photo-physical properties of nanoparticles surface. This can change the number of surface defects or energy loss and

increase the quantum yield of nanoparticles luminescence. As a result, the luminescence intensity of the nanoparticles at the wavelength of 655 nm increases.

We studied the processes of interaction of several heavy metals ions with nanoparticles bound to HSA.

It is established that the addition of the nanoparticles to the protein solution leads to quenching of nanoparticles fluorescence. In the work [1] the quenching of nanoparticles (cadmium selenide) fluorescence by cuprum ions in BSA.

We determined the constant of quenching of nanoparticles fluorescence by cuprum ions in water and HSA. An increase in the value of Stern-Folmer constant in HSA in contrast of aqueous solutions can be explained by concentrating of cuprum ions in protein- nanoparticles complex which significantly increase the probability of diffusion encounters of cuprum ions and nanoparticles.

We have carried out studies of the interaction of cadmium ions with nanoparticles in phosphate buffer of HSA. The increase in fluorescence intensity can be explained by binding of the cadmium ions to the surface of the nanoparticles. Also we observed the increase in luminescence intensity of nanoparticles in aqueous solution of nanoparticles.

We have carried out investigations of the interaction of nanoparticles with zinc ions.

With the increase of zinc ions concentration up to 0.2 mM nanoparticles fluorescence intensity almost unchanged, which is consistent with the results of [2] obtained in the study of the interaction of nanoparticles with zinc ions formed during salt dissociation. When the concentration of zinc was greater than 0.2 mM, we have observed the decrease in fluorescence intensity. We assume that this is due to protein denaturation under the effect of ions of heavy metal - zinc. Protein- heavy metal-nanoparticle complexes were precipitated. Similar results were obtained in [3]. As a result, the intensity of the scattered light increases, and the intensity of the nanoparticles fluorescence decreases.

Conclusion

The obtained results showed that the quenching of nanoparticles fluorescence by heavy metal ions is determined by the solubility of used salts in the aqueous media and by interaction with the surface of the ZnCdS nanoparticles.

The interaction of nanoparticles with heavy metal ions leads to both an increase (cadmium ions) and a reduction (copper ions) of fluorescence intensity of nanoparticles that determines the possibility of applying ZnCdS nanoparticles for selective determination of heavy metals in aqueous media.

9126-99, Session PS1

In-situ fabrication of nanoparticle-loaded microgels by ultrashort pulsed laser ablation in monomer solutions and their future application in burn wound healing

Nina Million, Univ. Duisburg-Essen (Germany); Philipp Nachev, RWTH Aachen (Germany); Vincent Coger, Kerstin Reimers, Peter M. Vogt, Medizinische Hochschule Hannover (Germany); Andrij Pich, RWTH Aachen (Germany); Stephan Barcikowski, Univ. Duisburg-Essen (Germany)

The medical use of microgels loaded with bioactive nanoparticles for drug delivery or agent transport is highly interesting. Ion-release initiated by nanoparticles could be used for instance for the treatment of thermal injuries, as it could be shown that different healing stages benefit from different concentrations of particular metal-ions. Beside chemical synthesis strategies, water-based laser-ablation techniques are a promising alternative for the generation of totally surfactant-free nanoparticles. Due to the absence of surfactants, this method yields nanoparticles with outstanding purity and is very flexible concerning the used materials, hence multiple materials may be synthesized applying the same protocol. Therefore multi-element microgels parallel containing e.g. magnesium, iron, zinc and copper may be easily synthesized by this strategy leading to polymer systems which support all wound healing stages, due to their metal-specific properties concerning the biochemistry of wound healing. Microgels, consisting of N-vinylcaprolactam (VCL) as basic-monomer and different comonomers loaded with laser-generated ZnO-nanoparticles were prepared by an in-situ synthesis route.[1] Subsequently, these nanocomposites were processed via electrospinning to obtain microfibers to fabricate wound-coverages. These microgels loaded with ZnO-nanoparticles show a thermal stability in nitrogen atmosphere up to 300°C which benefits further thermal sterilization processes. Due to their cell-stimulating effect and support of wound healing [2], the ion-release kinetics of zinc-ions from ZnO-nanoparticles were studied using ICP-MS. Preliminary results indicate a fast release of ions in the first day of the experiment. To achieve higher nanoparticle concentrations required for long term treatment, the synthesis was transferred from a Batch- to a Flow-through setup. Furthermore it could be possible to influence the release kinetics by metal-combinations as it was shown by Hahn et al. [3] for nanocomposites with different metal combinations. The successful embedding of bioactive nanoparticles in a polymer matrix using a completely water-based laser-ablation process enables the utilization of these systems in various fields of medicine by using the peculiar properties of different metals applying multi-element microgels.

[1] Nachev, P., van't Zand, D.D., Coger, V., Wagener, P., Reimers, K., Vogt, P.M., Barcikowski, S., Pich, A., "Synthesis of hybrid microgels by coupling of laser ablation and polymerization in aqueous medium", Journal of Laser Applications 24(4), 042012 (2012).

[2] Agren, M. S., Chvapil, M., Franzén, L., "Enhancement of Re-epithelialization with Topical Zinc Oxide in Porcine Partial-Thickness Wounds", Journal of Surgical Research 50(2), 101-105 (1991).

[3] Hahn, A., Günther, S., Wagener, P., Barcikowski, S., "Electrochemistry-controlled metal ion release from silicone elastomer nanocomposites through combination of different metal nanoparticles", Journal of Materials Chemistry 21, 10287-10289 (2011).

9126-100, Session PS1

Using MoO3 quantum-wells as buffer layer in organic light emitting diodes and its effect on reducing threshold voltage

Hamid Reza Fallah, Gholamreza Rahimi, Univ. of Isfahan (Iran, Islamic Republic of)

Organic Light Emitting diode (OLED) is one of the important devices that attracts a lot of attention. In this work we have used quantum-wells of MoO3 and NPB as buffer layers in the OLED structure and investigate its effect on the characteristics of the fabricated device. We have used thermal evaporation deposition method to form the layers and then measured the J-V cureve of the device. Structures with one and triple quantum wells are deposited on top of an ITO substrate and their characteristics are compared. One of our results shows that we can reduce threshold voltage of the device by using a triple quantum-well of MoO3 and NPB as the bufer layer.

9126-101, Session PS1

Induced symmetry breaking in a bulk-type metal-silica nanocomposite

Mariusz R. Zdanowicz, Juha Harra, Jyrki M. Mäkelä, Tampere Univ. of Technology (Finland); Esa Heinonen, Univ. of Oulu (Finland); Tingyin Ning, Martti Kauranen, Goëry Genty, Tampere Univ. of Technology (Finland)

The optical properties of metal nanoparticles are dominated by their localized surface plasmon resonances. Such resonances

give rise to strong local fields, important for nonlinear optical effects. Second-order nonlinear effects, however, require non-centrosymmetry, which is difficult to achieve in bulk nanocomposites. Here, we present a bulk-type nanocomposite fabricated using aerosol synthesis, which leads to an overall non-centrosymmetric structure.

Our material consists of alternating layers of pure silica and silica nanoparticles decorated with silver nanodots. The silica nanoparticles were synthesized by chemical vapor synthesis from liquid tetraethyl orthosilicate. Their silver decoration was achieved by evaporation and condensation from a bulk material. The fabricated nanoparticles were deposited on a glass substrate. The layer was then covered with pure silica in an electron beam coater. The whole cycle was repeated to fabricate the desired number of layers and results in linear relation between the maximum extinction and the number of layers. More importantly, the manufactured multilayer structures preserve the narrow plasmon resonance of the nanodots even for high optical densities. This behavior arises from the fact that our fabrication process separates the metal inclusions from each other and they do not agglomerate.

The second-order response was characterized by second-harmonic generation (SHG) in a Maker-fringe setup. The 70 ps pulses at 1 kHz repetition rate from a Nd:YAG (1064 nm wavelength) generate SHG radiation at the 532 nm wavelength. The results show that the SHG signal amplitude scales with the number of layers. This occurs because the differences between the alternating particle-silica and silica-particle interfaces break the overall centrosymmetry of the whole structure.

Aerosol techniques are flexible with regard to the size of the carrier particles and the decorative nanodots. Our results thus open new opportunities for the fabrication of nanocomposites with a wide range of linear and nonlinear optical properties.

9126-103, Session PS1

Optical characterization of lifted-off thin film crystalline InGaN microdisks

Ahmed Ben Slimane, Tien Khee Ng, Ahmad Al-Jabr, Damian P. San-Roman-Alerigi, Mohammed Abdul Majid, Boon S. Ooi, King Abdullah Univ. of Science and Technology (Saudi Arabia)

We report on optical analysis of lifted off thin InGaN layer synthesized using selective ultraviolet (UV) assisted electroless photo chemical etching (EPCE) of GaN, which shows promising application for fabrication of flexible optical devices and optically pumped micro phosphor. The initial epitaxial structure consisted of a 200 nm undoped InGaN on 4 μm unintentionally doped GaN grown on sapphire, we investigated three different indium compositions of 20%, 30% and 40%. We then fabricated micro-columns of diameters ranging from 5 to 100 μm via inductively coupled plasma (ICP) etching process. Scanning electron microscopy (SEM) measurements performed on the pillars, after etching in a HF:CH3OH:H2O2 (2:1:2) solution under UV illumination, show the porous GaN selectively etched. We explain in detail the selective EPCE mechanism which relies on holes generated from UV emission and band bending effect in the interface between GaN and electrolyte. The weak bond between InGaN and porous GaN facilitate microdisks lift-off via flexible polydimethylsiloxane (PDMS) material. For optical study, thin InGaN microdisks were then transferred onto Si substrate and blue LED structure.

Micro photoluminescence (μPL) measurements of different InGaN microdisks revealed typical strong peaks in the visible range dependent on the indium composition. We performed excitation power dependent analysis on the InGaN layers to study wavelength tunability and attributed it to the localized potential fluctuation present within the matrix. After InGaN lift-off, we observed a large shift in phonon frequency in micro Raman spectroscopy, corresponding to a relaxation of strain with respect to the as-grown InGaN. Further study of microdisk size dependent strain effect was carried out via μPL and micro Raman spectroscopieswith results in good agreement. Samples with high indium composition were then transferred onto blue LED structure and were optically pumped. Spectral characteristics show prominent blue and green peaks. These observations confirm the promising application of this technique to fabricate inorganic micro phosphor. We also successfully lifted off quantum well structures using the EPCE process. The presented lift-off process is also a compelling candidate for next generation flexible optical devices, confined photonic membrane, template for transferred substrate devices and InGaN micro lasers.

9126-104, Session PS1

Electro-optical effects in porous PET films filled with liquid crystal: new possibilities for fiber optics

Anton P. Chopik, Sergey V. Pasechnik, Denis Semerenko, Dina V. Shmeliova, Alexander V. Dubtsov, Moscow State Univ. of Instrumentation Engineering & Computer Science (Russian Federation); Vladimir G. Chigrinov, Hong Kong Univ. of Science and Technology (Hong Kong, China)

We have studied the dynamic electro-optical response of porous PET films filled with a nematic liquid crystal (5CB) which essentially differs from response that usually registered for conventional LC cells fig.1. In particular, at relatively low frequencies (f < fc~500Hz) a short (about some ms) peak of a transmitted light intensity I(t) arises as a result of very fast (some nanoseconds) change of the field polarity. In this case the total time of arising and decay of an optical response is essentially smaller than the total duration of the electric voltage pulse. The amplitude of the peak changes it's sign (from plus to minus) at increasing of electric voltage. For higher frequencies (f > fc) it does not hold and overall steady decreasing of intensity takes place. The peculiarities in I(t) dependences at low frequencies were understood and explained after comparison with the non-monotonic temperature dependence I(T) of light intensity induced by corresponding monotonic dependence of the effective refractive index. The variations of the latter parameter with time can be explained by the corresponding time variations of the polar angle of a director with the initial decreasing and further increasing to the initial state (our dielectrical experiments have confirmed initial state as homeotropic to the inner surface of the pore) for the time shorter than the electric pulse duration. The small intensity of the light registered in this case is probably connected with scattering caused by breaking the waveguide mode of light propagation due to almost complete orientation of LC molecules along the pore axis as the value of n0 =1.535 of 5CB at room temperature is slightly smaller than the minimal refractive index of the polymer film in amorphous state (np = 1.576).

Such unusual behavior was assigned to the orienting action of the electrically induced shear flow, which changes it's direction at changing of the field polarity and can be stopped by capillary forces arising inside pores. The physical background of electro-kinetic phenomena is connected with absorption of polar molecules by the internal surface of a capillary which results in polarization of the surface and appearance of the electric Debye layer with thickness of order some nanometers. [1] It produces non homogeneous radial distribution of ions inside a capillary and as a result overall steady (or oscillating) flow of a liquid under application of a static (or low frequency) axial electric field. The experimental results and estimations confirm the electro-kinetic mechanism for the low frequency optical response. The overall flow of 5 CB (both in nematic and isotropic phase) through the porous film under the action of DC voltage (60V) was also registered by us. It arose for some seconds in the small parts of the film with wetted outer surfaces (no meniscuses inside the pores) and further was spreading inside the gap between the porous film and the surface substrate. The direction of such flow changed after changing the field direction. These observations are in accordance with the proposed electrokinetic mechanism. Electro-optical response of the samples at higher frequency can be explained by standard dielectric torque acting on a director which tends to align it along the pore axis.

9126-105, Session PS1

Nanocarbons and quantum dots formation in new hybrid materials

Kirill V. Bogdanov, Yulia A. Gromova, National Research Univ. of Information Technologies, Mechanics and Optics (Russian Federation); Victor A. Ermakov, Andrei V. Alaferdov, Univ. Estadual de Campinas (Brazil); Anna O. Orlova, National Research Univ. of Information Technologies, Mechanics and Optics (Russian Federation); Anatoly V Fedorov, ITMO University (Russian Federation); Stanislav A. Moshkalev, Univ. Estadual de Campinas (Brazil); Alexander V. Baranov, National Research Univ. of Information Technologies, Mechanics and Optics (Russian Federation)

Nanostructured carbon materials, such as nanotubes and graphene, have a great potential for applications in many scientific and technological fields. They are regarded as “building blocks” for electronics and photonics devices, such as nanotransistors, power converters, energy storage devices, sensors for various substances, as well as part of a variety composite materials.

The study demonstrated the possibility of obtaining complex hybrid structures of nanocarbons and quantum dots. The object of this study was synthesis technique of hybrid structures nanocarbon-nanocrystal, where the nanocarbon used multi-walled carbon nanotubes or multi-layer graphene, and as the nanocrystal - luminescent carbon nanotubes of CdSe (ZnS).

Initial samples of carbon nanotubes and quantum dots were prepared in 2 versions of solvent: isopropanol and toluene, which are among the most suitable for them, respectively. Since the dissolution in isopropanol is not allowed to dissolve quantum dots complexes, and completely extinguished the luminescence of these samples in the future as a solvent was used only toluene.

Structures with multi-layer graphene where prepared in two ways: deposition of hybrid structures quantum dots / multi-layer graphene prepared in toluene solution or successive precipitation components of hybrid structure in toluene solutions. Deposition were produced on microelectrodes for further dielectrophoresis which allows better positioned samples of multi-layer graphene for optical characterization and is a preparation for further study electrical conductivity.

To obtain data of distribution hybrid materials where made scans on the surface of the sample. Scans was recorded as two-dimensional maps of Raman spectra with excitation wavelength 633 nm - for the of nanocarbon materials and luminescence spectra of quantum dots with excitation wavelength 473 nm. Maximum intensity of quantum dots luminescence and intensity of the Raman signal from nanocarbon materials were obtained from the same area at the sample. This correlations shown that large number of nanocarbon materials lying on a substrate provides a good grip of quantum dots, while a small number (even like single carbon nanotube) and the complete lack of them, causes less grip of quantum dots, resulting in the weakening of the luminescence signal. Additional SEM photos from hybrid structures with multi-layer graphenes also shown good correlations with Raman and luminescent spectra. In addition to the correlation between Raman and luminescence spectra detailed study of the results shows weak traces of the interaction between nanocarbons and quantum dots. For multi-layer graphene it is shown in shift of maximum in luminescent spectra and for multi-walled carbon nanotubes in additional peaks in Raman spectra which is not belong to any of starting materials.

9126-106, Session PS1

Light trapping structures fabricated by low cost and scalable techniques

Barbara Brudieu, Ecole Polytechnique (France); Jérémie Teisseire, Saint-Gobain Recherche (France); Arthur Le Bris, Ecole Polytechnique Fédérale de Lausanne (Switzerland); Géraldine Dantelle, Ecole Polytechnique (France); François Guillemot, Saint-Gobain Recherche (France); Fabien Sorin, Ecole Polytechnique Fédérale de Lausanne (Switzerland); Thierry Gacoin, Ecole Polytechnique (France)

Light management schemes have known a steady development in the past decade as a solution envisioned to enhance the performance of optical and optoelectronic systems. However, to avoid additional processing costs, it is important to propose simple and scalable fabrication techniques to integrate such schemes within functional devices. In this project, we demonstrate highly efficient and tunable light trapping structures prepared using simple and scalable Sol-Gel chemistry, spin coating processing, and Nanoimprint lithography techniques. First, Distributed Bragg Mirrors in the form of periodic dielectric stacks are fabricated with dense TiO2 layers as the high index material (2.08 in the visible range), and macroporous silica layers as the low index counterpart. A homogenous latex of PMMA is used to create the porosity in the silica layer by leaving pores of prescribed size that appear after calcination of the deposited layer. The 60nm-diameter macropores allow to have a stable layer with a refractive index as low as 1.24 with 50% of porosity. This leads to a high refractive index contrast of 0.84 that should allow a large Full Width at Half Maximum (FWHM) and a high maximum reflectivity for a limited number of layers. The final stack is obtained by depositing alternatively the TiO2 sol and the SiO2-PPMA latex mixture followed by a single annealing step of the full stack. This simple process leads to a stable and repeatable system for a wide range of fabrication conditions. A defect-free semi-transparent 9-layer stack is obtained and shows a high specular reflectivity up to 96% at normal incidence in its prescribed bandwidth. We also demonstrate the flexibility of our process by making highly reflective DBRs with a tunable reflection range from UV to IR (from 400nm to 1300nm). The mirrors exhibit a wide reflectivity band from 170nm to 360nm depending on the resonance wavelength. Thanks to the closed porosity, our DBRs are robust over time and in harsh conditions (good optical properties after 6h at 120°C, 2 bars and 100% RH) compared to open-porous reflectors made with colloids, which makes them a perfect candidate for a wide range of optics and photonics applications. To demonstrate the versatility of our approach, we optimized a 8-layer DBR and integrated it within in a a-Si:H thin-film solar cell, which resulted in an increase of efficiency by 14.6%. More over, we demonstrated an enhancement of the light emission from an Europium-doped luminescent silica layer that is deposited on a Bragg reflector.

Our approach allows us to obtain back reflectors with high optical performance, low absorption given the all-dielectric nature of our structure, with tunable reflection range within the solar spectrum and negligible scattered reflection. This is achieved by using a simple and scalable technique amenable to industrial development. We will also present our latest results on the possibilities opened by the integration of diffraction gratings fabricated by soft Nanoimprint Lithography, with our DBR structures.

9126-107, Session PS1

Synthesis and characterization of Ti1-xZrxO2:Eu3+ nanotube core-Au shell particles

Kwang-Cheol Lee, So-Ra Gang, Deok Gi Kim, Korea Photonics Technology Institute (Korea, Republic of)

A nanotube particle structure comprised of a Eu3+ doped Ti1-xZrxO2 nanotube core and a gold shell is presented. 2 mol% Eu3+ doped Ti1-xZrxO2 nanotubes were synthesized by a two-step approach of hydrothermal method and heat process. Gold nanoshells were prepared using the combination of self-assembly method and seed growth technique from colloidal chemistry. (3-aminopropyl) triethoxysilane (APTES) was used to modify the surface of Ti1-xZrxO2:Eu3+ nanotubes to allow attachment of small gold nanocolloids from tetrachloroauric

acid (HAuCl4·3H2O) to their surface. More gold ions, using sodium borohydride (NaBH4), were further reduced to grow the gold shell on the seeded particles. XRD, SEM, TEM, UV/Vis spectroscopy as well as photoluminescence (PL) were the characterization methods employed to monitor the synthesis process of the composite particles. Compared with the Zr un-doped TiO2:Eu3+ nanotubes, Zr doped Ti1-xZrxO2:Eu3+ nanotubes exhibit stronger photoluminescence of 615nm under the excitation of 465nm. Furthermore, the PL intensity increases with the increasing of Zr concentration in Ti1-xZrxO2:Eu3+ nanotubes, and concentration quenching occurs when Zr concentration exceeds about 3 mol%. By gradually growing the Au shell, the surface plasmon resonance (SPR) position was shifted from green region to red region of visible spectrum. It is expected that the Ti1-xZrxO2:Eu3+ nanotube core-Au shell particles can be used as novel luminescence materials.

9126-108, Session PS1

Optical and nonlinear optical effects in 1D magneto-plasmonic structures

Alexander L. Chekhov, Aleksey I. Shaymanov, Victor L. Krutyanskiy, Lomonosov Moscow State Univ. (Russian Federation); Alexander I. Stognij, Institute of Solid State and Semiconductor Physics (Belarus); Tatyana V. Murzina, Lomonosov Moscow State Univ. (Russian Federation)

Optical properties of magneto-optical structures is a topic of rapidly growing interest in recent years. This interest is caused by unique properties of such structures, which allow for the resonant enhancement of optical and magneto-optical effects due to the excitation of surface plasmon-polaritons (SPP) at the boundary of the magnetic medium. Metal film with a spacial periodicity allows excitation of SPP using the grating method. Linear transmission spectra and magnetic response of such structures were reported recently, while the spectroscopy of nonlinear optical and magneto-optical effects has not been studied yet. At the same time, resonant increase of the local field due to SPP excitation can lead to the appearance of new effects in the nonlinear-optical response.

Here we present the first experimental results on optical second harmonic generation (SHG), on optical and magneto-optical effects in one-dimensional magneto-plasmonic structures consisting of 1D gold stripes arrays with different spatial periods deposited on iron garnets (IG). The period of the gratings was varied from 700 to 800 nm, the thickness of Au layer was 100 nm. Linear frequency-angular transmission spectra reveal resonant structure of SPP excitation on two interfaces: gold-air and IG-gold. An increase of linear magneto-optical effects up to the values of 0.5% is attained close to these resonances. The spectroscopy of the SHG intensity and of nonlinear magneto-optical Kerr (NOMOKE) effect were studied using the output of a tunable femtosecond Ti:sapphire laser. SHG maxima that change their spectral position with angle of incidence are observed. An increase of the transversal NOMOKE up to 15% is detected close to the SHG spectral peaks. These effects are attributed to the magnetic field induced shift of SPP wavelength and to the resonant enhancement of local optical field near the SPP resonances.

9126-109, Session PS1

A simple technique to create thermally stressed thin metal film on glass and Fourier plane fluorescence microscopy of localized surface plasmons enhanced collection efficiencies

Ankit Arora, Pankaj Arora, Ananth Krishnan, Indian Institute of Technology Madras (India)

We report (i) a simple technique to create Nano-islandic Metal coated Glass substrate (NMG) and (ii) Fourier Plane Fluorescence Microscopy (FPFM) of localized surface plasmons in these samples. Thin gold (Au) film (~6 nm) was deposited on a glass slide using a low end sputter coater designed for scanning electron microscopes, followed by heating on a hot plate at 250° C, until the color of the glass slide changed from blue to red. An 80 nm thick dye doped PMMA was spin coated on the sample. Characterization of the sample was performed before and after heating, using FPFM. These images were compared to Bare Glass slide (BG) and a glass slide coated with 50 nm thick evaporated Au film (AG), both coated with the same dye.

FPFM image of BG was disk shaped with outer and inner radii limited by NA of objective and critical angle (at glass/dye/air interface) respectively. FPFM of AG was a thin ring corresponding to the leakage of surface plasmon mode. The propagation length of the fundamental surface plasmon mode was extracted from the FPFM image as 32 ?m. The NMG sample showed the emission for all angles smaller than the NA of objective and hence the propagation lengths could not be accurately determined, nevertheless, since the range of momentum (k) values of emission were much higher than AG, the propagation lengths were estimated to be much smaller. The large range of k values in FPFM confirmed that localized surface plasmons were excited. It was observed that for the same exposure times, the light collection efficiency in NMG was higher by a factor of 2.2 over BG and 7 over AG. This increase in collection efficiency was attributed to the scattering by the nano-islandic metal layer in NMG. This simple technique of creating a substrate for brighter fluorescent image can be used in long duration imaging of fluorescent samples using low illumination and prevent the photo-bleaching of the dye, in laboratories equipped with a low end sputter coater and a hot plate (typical of biological labs).

9126-110, Session PS1

Characterization of polymer nanowires fabricated using the nanoimprint method

Charusluk Viphavakit, Frederick Univ. (Cyprus); Nithi Atthi, Thai Microelectronics Center (TMEC) (Thailand); Sakoolkan Boonruang, National Electronics and Computer Technology Ctr. (Thailand); Christos Themistos, Frederick Univ. (Cyprus); Waleed S. Mohammed, Bangkok Univ. (Thailand); Kyriacos Kallie, Cyprus University of Technology (Cyprus); B.M.Azizur Rahman, City University (United Kingdom); Michael Komodromos, Frederick Univ. (Cyprus)

Polymer nanowires are alternatively used as optical waveguides in sensing applications due to their unique optical properties and mechanical flexibility over the semiconductor nanowires such as silicon nanowires. In this paper, an ormocomp nanowire is presented including the fabrication process and the characterization. The fabrication process in this work is based on the nanoimprint technique. The nanoimprint technique promises a simpler, less time consuming, and lower cost compared to other fabrication techniques of polymer nanowires. The method assumes a silicon nanowire as an original pattern, and polydimethylsiloxane (PDMS) as a soft mold. The PDMS mold is directly imprinted on the ormocomp layer cured by UV light to form the polymer based nanowire. The ormocomp nanowires are fabricated to have various dimensions of width and length at a fixed 500nm thickness. The length of the nanowires is varied from 250 ?m to 2 mm, whereas the width of the structures is varied between 500nm and 1?m. In the characterization part, the optical field profile and the intensity at the output are the main focus of this paper. The various lengths of the nanowires show different characteristics in term of output intensity. The ormocomp nanowires are designed and intended to be used as integrated optics devices. Therefore, the nanowires are attached to tapered waveguides at both ends. The tapered waveguides reduce the optical loss occurring in an alignment process. In order to characterize these polymer nanowires a (variable intensity tunable LED is used as a light source. The output signal is detected by a CCD camera and the image of the

optical field is obtained. A MatLab program is used to process the image to obtain the intensity of the output signal. A comparison of the optical field and intensity output for each polymer nanowire is also demonstrated in this paper.

9126-111, Session PS1

Leakage radiation spectroscopy of organic nanofibers on metal films: influence of SiO2 coverage of metal film on exciton-surface plasmon polariton interaction

Leszek Józefowski, Jagiellonian Univ. in Krakow (Poland); Jacek Fiutowski, Univ. of Southern Denmark (Denmark); Tomasz Kawalec, Jagiellonian Univ. in Krakow (Poland); Horst-Günter Rubahn, Univ. of Southern Denmark (Denmark)

Leakage radiation spectroscopy of organic para-Hexaphenylene (p-6P) molecules has been performed in the spectral range 420-675 nm which overlaps with the p-6P photoluminescence band. The p-6P was deposited on a 40-60 nm silver (Ag) film covered with SiO2 layer prepared on the BK7 glass substrate. Several samples were used with the SiO2 layer thickness in the 5-20 nm range. The p-6P was used in two different forms: either of a thin 40-60 nm film or a domain of nanofibers. In the first case the p-6P was directly evaporated onto the sample. In the latter case domains of mutually parallel oriented organic nanofibers were initially grown under high-vacuum conditions by molecular beam epitaxy onto a cleaved muscovite mica substrate and afterwards transferred onto the sample – a soft transfer technique. The sample placed on a flat side of a hemisphere fused silica prism with an index matching liquid was illuminated under normal angle by a He-Cd 325 nm laser. Two orthogonal linear polarizations were used, both parallel and perpendicular to the detection plane. The leakage radiation was observed on the opposite side of the Ag film (i.e. at the hemisphere prism) at the phase matching angle. The spectrally resolved intensity of the scattered radiation was measured as a function of the scattering angle. Each spectrum contains a distinct peak at a wavelength dependent angle above the critical one. This way the dispersion curve was measured, originating from a hybrid mode, i.e. the interaction between the p-6P excitons and surface plasmon polaritons (SPPs) of the metal/dielectric boundary. The presence of the SiO2 layer considerably changes the dispersion curve in comparison to the one of the Ag/p-6P/air system. On the other hand the Ag/SiO2/p-6P/air stack forms a stable structure allowing construction of organic plasmonic devices like nano-lasers.

9126-112, Session PS1

A simple theoretical analysis of sum-frequency generation spectroscopy of molecules adsorbed on 3D nano-structures with plasmon resonances

Yves Caudano, Dan Lis, Francesca Cecchet, Univ. of Namur (Belgium)

Infrared-visible sum-frequency generation spectroscopy (SFG) probes surfaces and interfaces of centro-symmetric materials. As a result, this nonlinear optical spectroscopy is particularly well-adapted to probe vibrations of adsorbed molecular layers. In SFG, two laser beams, an infrared one (?IR) and a visible one (?vis), are focused on the sample surface to generate a new beam at the sum of the incident beam frequencies (?SFG = ?IR + ?vis). Usually, the infrared laser frequency is scanned over the frequency range of the molecular vibrations of interest. A resonant increase of the intensity of the generated SFG beam can be observed when ?IR matches the frequency of an adsorbate vibration that is both infrared and Raman active.

The intensity of the generated SFG beam depends also on the optical properties of the interface. In particular, for a flat surface, the SFG yield is proportional to the square of the total electric field at the interface for the IR, vis, and SFG beams [1]. (These three factors are called the Fresnel factors.) Essentially, when the molecules sense a stronger electric field at any of the three ?IR, ?vis, or ?SFG frequencies, the intensity of the emitted SFG beam increases. Therefore, by optimizing the optical properties of the substrate, it is possible to increase the sensitivity of SFG spectroscopy. This effect has been recently demonstrated using nano-structured substrates. In this experiment, the localized surface plasmon resonances of vertical metallic nano-cylinders grown on flat metal surfaces are exploited to enhance by two orders of magnitude the SFG signal of dodecanethiol self-assembled monolayers [2]. The transverse (TM) and longitudinal (LM) localized plasmons of the nano-cylinders are excited by tuning adequately either the visible, or the SFG beam frequency to one of the plasmon frequencies. An unexpected result of this experimental work is the observation of a strong enhancement when the TM plasmon is excited with the ssp polarization set (s-SFG, s-vis, p-IR). Indeed, ssp SFG signals are usually much weaker than their ppp counterparts on metallic substrates because the metal electrons screen efficiently the electric fields parallel to the surface (thus, they reduce substantially the Fresnel factors for s-polarization).

In this work, we investigate from the theoretical point of view how the three-dimensional component of the nano-structured substrate affects the SFG yield. Therefore, we adapted T. F. Heinz's two-dimensional model [1] to predict the expected SFG intensity produced by molecules adsorbed at different heights along the nano-cylinders, above the flat substrate supporting the vertical pillars. Our model explains why the experimental SFG signal is strongly enhanced with the ssp polarization set (s-SFG, s-vis, p-IR) when exciting the transverse mode.

[1] Tony F. Heinz, in Non-linear surface electromagnetic phenomena, H.-E. Ponath and G.I. Stegeman eds, Elsevier Science 1991, p.356.

[2] Dan Lis, Yves Caudano, Marie Henry, Sophie Demoustier-Champagne, Etienne Ferain, and Francesca Cecchet, "Selective plasmonic platforms based on nanopillars to enhance vibrational sum-frequency generation spectroscopy", Advanced Optical Materials 1, 244–255 (2013).

9126-113, Session PS1

Changes in the optical properties of two gold nanoparticles caused by different connection types

Krzysztof Skorupski, Wroclaw Univ. of Technology (Poland)

In our work we investigate the impact of the necking phenomenon on the optical properties of gold particles. The initial structure was composed of two spherically-shaped particles, with the radius Rp=25nm, and a single connector. Simulations were performed with a light scattering code based on the DDA theory. The structure was decomposed into min. 240000 volume elements (dipoles) and the results were averaged over 125 orientations (5x5x5). The Filtered Couple Dipole Method (FCDM) was used and the reference wavelength was 532nm. To avoid potential errors, the results for touching spheres (without any connector) were compared to other light scattering techniques. The structure was positioned in vacuum, i.e. the refractive index of the surrounding medium was 1+0i. In the first step of our study the total volume of the structure was constant - the spheres were positioned in fixed positions and their radii were decreased. To keep the same volume, the neck size was adjusted accordingly. Such approach can model e.g. the early stages of the sintering process. Our results show that there is almost no difference between various connection types. Therefore, they can be used interchangeably. This effect seems to be universal and is also valid when other materials are used (e.g. carbon black). On the other hand, the extinction cross section decreases slightly with the neck size and the asymmetry parameter is at its maximum for intermediate necks (i.e when the value of the neck radius is ca. 70% of the particle radius). In the next step of our study we repeated the simulations, but this time the volume of the structure was not

conserved. The particle radii were constant and only the size of the neck was increased. The aim of this approach was to reveal potential errors that can arise when a modeled structure is devoided of interparticle connections. When this condition is satisfied (i.e. particles are positioned in point contact only) much faster light scattering simulation codes can be used. In many studies it might be crucial, because the DDA method is very time consuming and can be problematic when high values of the imaginary part of the refractive index are used (e.g. when noble metals are considered). Our results show that the necking phenomenon can be omitted, but only when connections are not too large (i.e when the value of the neck radius is less than 20% of the particle radius). Otherwise, they may have significant impact on the results. In the final step of our study we modeled the necking phenomenon by changing the overlap factor only (no additional connectors were implemented). This is the most basic approach which can also be found in other studies. This time the changes are much more significant and should not be omitted. This statement applies for both cases - when the volume of the structure is conserved and when the distance between particle centers is diminished only (what leads to decreased volume).

9126-115, Session PS1

Formation and evolution of ultrashort pulse-induced nanogratings in Borofloat glass

Felix Zimmermann, Friedrich-Schiller-Univ. Jena (Germany); Anton Plech, Karlsruher Institut für Technologie (Germany); Sören Richter, Friedrich-Schiller-Univ. Jena (Germany); Andreas Tünnermann, Stefan Nolte, Friedrich-Schiller-Univ. Jena (Germany) and Fraunhofer-Institut für Angewandte Optik und Feinmechanik (Germany)

The versatility of ultrashort laser pulses as a tool for laser materials processing has augmented particular interest in the past decade. Especially birefringent modifications, so-called nanogratings, have found to exhibit tremendous potential for manifold photonic functionalities. These self-assembling structures, orienting always perpendicular to the laser polarization, have been up to now extensively studied in bulk fused silica. Commonly it is assumed that the formation of nanogratings is actually limited to anomalous glasses like silica or slightly doped silica. However, we recently found that even in glasses like borofloat or BK7 nanogratings can be observed within certain parameter regimes.

Here we report on an extensive study of the fundamental constituents of nanogratings in bulk borofloat glass using the noninvasive technique of small angle x-ray scattering (SAXS) in combination with focussed ion beam milling (FIB) and scanning electron microscopy (SEM). By analysing the data we found that slightly anisotropic nanopores with diameters of about (30 x 40) nm are formed which do not change in size with varying number of pulses and laser pulse energy. However, in agreement with the SAXS measurements, SEM images of the nanograting samples show that the total number of pores increases when the number of laser pulses applied increases, which finally leads to fusing of pores and thus forming of individual grating planes. Interestingly, we observe nanograting periods of about 60 nm at an inscribing laser wavelength of 800 nm which strongly differs from the theoretical prediction of the period (?/2n, n-refractive index) as observed in fused silica. Furthermore, the period remains constant with prolonged laser exposure as well as when using different laser pulse energies. Moreover, in the direction of the laser polarization fine anisotropic cracks with diameters of about 10 nm arise with increasing number of pulses incident which can also be observed in images of samples prepared by FIB milling.

9126-116, Session PS1

Generation of standard and elegant Gaussian beams for optical micromanipulation

Christoph Schöler, Christina Alpmann, Cornelia Denz, Westfälische Wilhelms-Univ. Münster (Germany)

In the field of optical manipulation various kinds of higher order light fields with different propagation behavior have been proposed like nondiffracting Bessel and Mathieu beams, self-similar Laguerre- and Ince-Gaussian beams or accelerating Airy beams. Here we present the holographic generation of standard and elegant Gaussian beams of different families and their implementation into an optical tweezers setup. The well known families of Gaussian modes arise as complete solutions of the paraxial Helmholtz equation in Cartesian, polar and elliptical coordinates, respectively, and have mostly been used for the description of stable laser resonator modes. As a remarkable property they show structural stability under propagation due to their self-similarity. Apart from the common standard Gaussian beams alternative solutions of the paraxial Helmholtz equation exist, known as ‘elegant beams’, which comprise polynomials of complex arguments. The associated loss of self-similarity and emergence of distinct propagation behavior of the intensity and phase distribution leads to interesting application potentials. The generation of higher order modes is accomplished by the use of a spatial light modulator with which we can arbitrarily tailor the phase and amplitude of an incident fundamental Gaussian laser beam by means of computer generated Fourier holograms. The modulated beam is imaged to the back aperture of a high N.A. microscope objective and focused into the sample plane of an inverted microscope, where its optical potential landscape provides a high degree of order that can be transferred to micro and nano particles. We show the experimental realization of micron sized beams of different kinds of Hermite-, Laguerre-, and Ince-Gaussian modes and compare their transverse structure during propagation by intensity and phase measurements.

9126-117, Session PS1

Field enhancement and funneling of light in combinations of MIM resonators

Paul Chevalier, Patrick Bouchon, ONERA (France); Fabrice Pardo, Lab. de Photonique et de Nanostructures (France); Riad Haïdar, ONERA (France)

Plasmonic metal-insulator-metal resonators can nearly totally absorb an incident light (P. Bouchon et al., Appl. Phys. Lett. 98, 191109 (2011)). It has been shown on a subwavelength grating of gold grooves that the incoming energy is funneled towards the resonators aperture thanks to the magneto-electric interference between the incident wave and the evanescent field escaping from the resonator (F. Pardo et al., Phys. Rev. Lett. 107, 93902 (2011)).

Indeed, the Poynting vector could be split into three terms, each of them being flux-conservative, corresponding to the incident flux, the evanescent field flux, and the flux of the magneto-electric interference. The latter contributes mostly to the funneling mechanism by redistributing the incident energy into the apertures of the resonator.

This energetic analysis can also be applied to more complex antennas geometries, in particular to periodic combinations of grooves or MIM ribbons (C. Koechlin et al., Appl. Phys. Lett. 99, 241104 (2011), P. Chevalier et al. J. N). For instance, we show the funneling of light in a structure made of the superposition of three MIM cavities tuned at three different resonance wavelengths. At each resonance wavelength, the photons are funneled towards the apertures of the corresponding MIM cavity. The combination of resonators in the same

subwavelength period leads to two remarkable phenomena: first, the photons are sorted as a function of their energy and second, there is a widening of the absorption band. Such structures permit to conceive surfaces with customizable absorption. These results also give promising design rules for complex antennas.

In another domain, the funneling of light is a convenient way of reaching strong field intensity enhancement. Indeed, the total Poynting vector is shrunk from a large space to a tiny aperture. This contraction leads to very high field intensity enhancement in structure with an adapted design.

References:

P. Bouchon et al., Total funneling of light in high aspect ratio plasmonic nanoresonators. Applied Physics Letters, 98(19), 191109-191109 (2011).

F. Pardo, P. Bouchon, R. Haïdar, & J. L. Pelouard, Light funneling mechanism explained by magnetoelectric interference. Physical review letters, 107(9), 093902 (2011).

P. Chevalier, P. Bouchon, R. Haïdar, & F. Pardo, Funneling of light in combinations of metal-insulator-metal resonators. Journal of Nanophotonics, 6(1), 063534-063534. (2012).

9126-118, Session PS1

Femtosecond multi-level phase switching in chalcogenide thin films for all-optical data and image processing

Qian Wang, Univ. of Southampton (United Kingdom) and A*STAR Institute of Materials Research and Engineering (Singapore); Jonathan S. Maddock, Ben Mills, Christopher Craig, Edward T. F. Rogers, Tapashree Roy, Kevin F. MacDonald, Daniel W. Hewak, Univ. of Southampton (United Kingdom); Nikolay I. Zheludev, Univ. Southampton (United Kingdom) and Nanyang Technological Univ. (Singapore)

We report on the non-volatile switching of amorphous chalcogenide glass thin films to the crystalline phase through a through a number of reproducible, discrete, optically distinguishable intermediate states, and on the re-amorphization of these films using femtosecond laser pulses. Potential applications lie in high-base (>binary) all-optical signal modulation, high-density data storage, image processing and non-Von Neuman computing.

Chalcogenide phase-change media such as Ge2Sb2Te5 (GST) are commercially established as a platform for both optical and electronic data storage (re-writable CDs, DVDs and Blu-Ray discs; Phase-change RAM). These technologies harness non-volatile amorphous-crystalline (binary) transitions in the chalcogenide induced by nanosecond optical or electronic excitations, which have also recently been applied to the realization of metamaterial electro- and all-optical transmission/reflection modulators for near- to mid-IR wavelengths providing switching high-contrast in device structures only a fraction of a wavelength thick. However chalcogenides offer a much richer pallet of transitional behaviours that can be exploited to enhance all of these functionalities and to open up new computational and image processing paradigms: they retain a 'memory' of sub-threshold excitations, such that transitions ordinarily initiated by single excitation pulses can be reproducibly stimulated by sequences of arbitrarily timed shorter/lower energy pulses cumulatively delivering the required energy.

Here we demonstrate multi-level switching of GST films down to 30 nm thick using femtosecond optical pulses. Domains ranging in size from 100 down to 1 μm2 are progressively converted through at least eight distinct partially crystalline states using 85 fs pulses. Intermediate states are distinguished and their progressively changing optical properties characterised using white light reflectivity, transmission/reflection microspectrophotometry and spectroscopic ellipsometry measurements.

Applications potential is demonstrated to high-density data storage - encoding/read-out of multiple bits per (semi-) crystalline mark with micron-level pixellation, the performance of optical arithmetic operations, and progressive tuning of chalcogenide hybrid metamaterial resonances.

9126-119, Session PS1

Plasmonic antenna for wideband and nearly total linear polarization conversion

Quentin Levesque, Patrick Bouchon, ONERA (France); Fabrice Pardo, Jean-Luc Pelouard, Lab. de Photonique et de Nanostructures (France); Riad Haïdar, ONERA (France)

Capasso group has presented V-shaped metallic nano-antennas to create gradual phase shifts, in order to design planar polarization converters or lenses [1]. These nanostructures have been experimentally demonstrated but with a low efficiency, that can be expressed in two figures of merit: (1) the extinction ratio of the incident radiation ER and (2) the conversion ratio into the emitted radiation CR. In [1], ER and CR demonstrated values are less than 10%.

We propose an alternative planar design based on resonant plasmonic nano-antennas with similar ease of process but exhibiting a high efficiency. This design has been confirmed by a technological realization in the infrared domain (3 to 5 μm wavelength range). Experimental results corroborate the high efficiency of our design, which is summarized as ER and CR values close to 100% and 80% respectively.

Furthermore, the angular acceptance was studied. We will show how multiresonant designs are able to expand the bandwidth while keeping a high efficiency.

[1] N. Yu et al., "Light Propagation with Phase Discontinuities: Generalized Laws of Reflection and Refraction", Science, 334, 333 (2011).

9126-120, Session PS1

Direct injection in organic SU8 nanowires and nanotubes for waveguiding properties investigation

John Bigeon, Nolwenn Huby, Univ. de Rennes 1 (France); Jean-Luc Duvail, Institut des Matériaux Jean Rouxel (France); Bruno Bêche, Univ. de Rennes 1 (France) and Institut Univ. de France (France)

Sub-wavelength waveguides are the subject of numerous publications and applications (Mach-Zehnder, add-drop filter, etc...). Among the nano-objects, 1D-nanostructures are of particular interest in integrated optics due to by the ability to control their aspect ratio.

We report photonic concepts related to two milestones in integrated photonics : light injection and sub-wavelength propagation in organic nanotubes. These are fabricated by the wetting template method, allowing the creation of 1D nanostructures with aspect ratio larger than 100, a diameter ranging from 50 nm to 250 nm and length up to 100 μm typically. This method achieves fine control dimensions while providing the possibility of large-scale production.

At first, laser injection (675nm) into nanotubes of SU8, a photoresist used for integrated photonics, was successfully achieved by using polymer microlensed fibers with sub-micronic radius of curvature. This is a powerful alternative to evanescent coupling which is usually applied for optical injection in sub-micronic structures. When the microlens is judiciously located close to the SU8 nanotube, a spot at the opposite end of the nanotube is visible. The presence of this spot is the proof of a significant injection into the nanotube while the absence of light scattering along the nanotube is an indicator of low roughness of the surface and the absence of morphological defects.

In parallel, theoretical simulation by finite domain time-dependent (FDTD) method was used to corroborate this coupling phenomena.

Regarding propagation behavior, the optical losses are fundamental interest. To estimate the attenuation coefficient during sub-wavelength propagation in SU8 nanotubes, we developed a strategy inspired from the cut-back method and transposed to such nanostructures.

For SU8 nanotubes of 240 nm outer diameter and 60 nm wall thickness, it leads to a loss value of about 1.25 dB/mm. These results confirm the interest of these organic 1D-nanostructures as the prototypical element of highly integrated nanophotonics and validate the innovative injection process.

9126-122, Session PS1

ZnSe/ZnS quantum dots-photosensitizer complexes: optical properties and cancer cell photodynamic destruction effect

Irina Martinenko, National Research Univ. of Information Technologies, Mechanics and Optics (Russian Federation); Vera Kuznetsova, SAMSON-MED, Pharmaceutical Co., Ltd. (Russian Federation); Anna O. Orlova, National Research Univ. of Information Technologies, Mechanics and Optics (Russian Federation); Pavel Kanaev, SAMSON-MED, Pharmaceutical Co., Ltd. (Russian Federation); Yulia Gromova, University ITMO (Russian Federation); Vladimir G. Maslov, Anatoly V. Fedorov, Alexander V. Baranov, National Research Univ. of Information Technologies, Mechanics and Optics (Russian Federation)

For past decade semiconductor quantum dots were widely investigated as energy donors in complexes with photosensitizer molecules. In these complexes efficient photoexcitation energy transfer from quantum dots to molecules provides probability of increasing the efficiency of singlet oxygen generation compared with the free molecules as well as broadening of the photoexitation spectral range of the molecules. In this study we develop complexes between non-toxic ZnSe/ZnS quantum dots and chlorine e6 molecules, that are widely used as photosensitizers in photodynamic therapy. The spectroscopic properties of these hybrids have been studied in detail. Spectroscopic methods have been applied to evaluate the energy transfer pathways. It was found that in aqueous solution cationic ZnSe/ZnS quantum dots form stable complexes with chlorine e6 molecules that exhibit efficient photoexcitation energy transfer from quantum dots to molecules. Stoichiometry of these complexes was studied.

Additionally, the photodynamic therapy efficacy of the quantum dots/chlorin e6 complexes has been in vitro assessed against Ehrlich ascites carcinoma cancer cell line using a trypan blue assay. We have found that complex offers an improved cancer cell photodynamic destruction as compared to free chlorine e6 molecules. This effect can be caused by the singlet oxygen generation enhancement due to the efficient photoexcitation energy transfer as well as essentially enhancing intracellular uptake of photosensitizer in complex with quantum dots.

9126-123, Session PS1

Synthesis and characterization of glutathione passivated Mn--doped ZnS quantum dots suitable for bio-imaging applications

Mojde Taherian, Ali A. Sabbagh Alvani, Amirkabir Univ. of Technology (Iran, Islamic Republic of); Mohammad A. Shokrgozar, Pasteur Institute of Iran (Iran, Islamic Republic of); Reza Salimi, Shima Moosakhani, Hassan Sameie, Farzaneh Tabatabaee, Amirkabir Univ. of Technology (Iran, Islamic Republic of)

Manganese doped zinc sulfide nanoparticles were successfully synthesized at room temperature through ?chemical precipitation method. Glutathione (GSH) is used as a biocompatible capping agent to stabilize and ?passivate the surface of the particles in aqueous medium. The nanocrystals have been characterized using a ?combination of experimental techniques including X-ray diffraction (XRD), transmission electron microscopy ??(TEM), UV-Vis and photoluminescence (PL) spectroscopy, energy dispersive analysis of X-rays (EDAX) and ?Fourier transform infrared spectrometry (FTIR). The XRD patterns showed a cubic zinc blende crystal structure ?and a crystallite size of about 2 - 3 nm using Scherrer's equation that the TEM observations confirm it. ?According to PL spectra, two emission bands were observed in doped nanoparitcles and attributed to the defect-?related emission of ZnS and the Mn2+ emission, respectively. With the increase of Mn2+ concentration up to 3%, ?the luminescence intensity of Mn2+ emission increased. Higher dopant concentrations resulted in quenching of ?PL intensity. The results based on optical analysis yield enhancement of optical band gap values as 3.93, 4.26 ?and 4.33 eV for ZnS, GSH capped ZnS and ZnS:Mn nanoparticles, respectively. In addition, it was found that ?compared with the bulk zinc sulfide, the absorption band-edge is blue-shifted, suggesting the quantum ?confinement effect in the developed nanoparticles of size below the Bohr diameter. The average ZnS ?nanoparticle size, deduced from the absorption spectra by an Effective Mass Approximation (EMA), is 2.7, 1.9 ?and 1.81 nm for ZnS, GSH capped ZnS and ZnS:Mn nanoparticles, respectively. EDAX spectra confirmed the ?presence of Mn in the samples with expected stoichiometry. Also, the FT-IR spectrum indicated the interaction ?of the capping agent groups with ZnS nanoparticles. Consequently, as-prepared GSH capped ZnS:Mn ?nanoparticles with a small size, satisfactory biocompatibility and luminescent characteristics can be considered ?as a suitable candidate to be coupled with anti-bodies for bio-imaging applications.?

9126-124, Session PS1

Unidirectional emission of light mediated by a single-element nanoantenna

Dries Vercruysse, Niels Verellen, IMEC (Belgium) and Katholieke Univ. Leuven (Belgium); Yannick Sonnefraud, Giuliana Di Martino, Imperial College London (United Kingdom); Victor V. Moshchalkov, Katholieke Univ. Leuven (Belgium); Liesbet Lagae, IMEC (Belgium) and Katholieke Univ. Leuven (Belgium); Stefan A. Maier, Imperial College London (United Kingdom); Pol Van Dorpe, IMEC (Belgium) and Katholieke Univ. Leuven (Belgium)

Plasmonic resonators, or nanoantennas, provide an effective route to couple photons in and out of nanoscale volumes. This unique ability makes them excellent tools to study and manipulate light-matter interaction at the nanoscale. For instance, the antenna's high electric field enhancement and nanoscale confinement of light can result in strong enhancement of fluorescence and SERS signals. Not only the emission efficiency of a quantum emitter, but also its direction of emission can efficiently be manipulated by a properly designed nanoantenna configuration, such as, e.g., an optical Yagi–Uda antenna. [1 2]

In contrast, here, we study the interaction of a quantum emitter with only a single-element directional plasmonic antenna, the V-shaped antenna. [3] Using FDTD simulations, the quantum efficiency and directionality of an emitter is evaluated at different positions around the antenna. These simulations show that the directionality is highly dependent on the placement of the emitter, and allow us to identify specific regions around the antenna where the emission will be directional. These results are tested experimentally by depositing fluorescently doped PMMA at different regions on the antennas, using e-beam lithography. The direction of the light emitted by the dyes is mapped experimentally by back focal plane microscopy, revealing directional emission for dye located in the directional regions, in good agreement with simulations. The directional behavior of the V-antenna is the result of Fano interference between two localized surface plasmon modes, as we have shown for the case of directional scattering of a plane wave. [3] Such small (<?3/100) directional nanoantennas based on Fano interference are a promising tool to increase detection efficiencies of

fluorescence and surface enhanced Raman scattering in a variety of applications.

[1] T. Kosako, et al. Nat. Photonics (2010) 4(5), 312–315

[2] A. G. Curto, et al. Science (2010) 329(5994), 930–933

[3] D. Vercruysse, et al. Nano Lett., 2013, 13 (8), 3843–3849

9126-125, Session PS1

Prediction of the behavior for fullerene C20 inside the icosahedral outer shell of C240

Olga E. Glukhova, Anna S. Kolesnikova, Mikhail M. Slepchenkov, Vladislav V. Shunaev, N.G. Chernyshevsky Saratov State Univ. (Russian Federation)

In this work, we study the behavioral regularity of fullerene C20 inside the icosahedral outer shell of fullerene C240. The feature of such two-shell fullerenes is that the internal fullerene will move at low temperatures in a certain way: between the potential wells. The aim of this work is to reveal the regularities for motion of small fullerenes in nanospace of large external icosahedral fullerene, including the identification of the spatial configuration for a multi-well potential of interaction between two objects and prediction of possible tunneling for the internal object between potential wells.

To study the behaviour of the carbon nanoclusters C20@?240 we applied the molecular dynamics method. Within this method the total energy of a system is calculated using bond-order potential developed by Brenner. The total energy is described by the sum of the binding energy Eb , the torsional energy Etors and the van der Waals energy EvdW. We have applied velocity scaling thermostat. Each atomic velocity is multiplied by a factor that creates the desired temperature. The scaling has been done at every step.

For the fullerene C20 it was found twenty potential wells in the direction of the fifth order axes for icosahedron of fullerene C240 cage, thirty towards in the direction of the middle of the ribs and twenty potential wells towards centers of the faces of the icosahedron. The prediction of possible tunneling for the internal object between potential wells and the regularities of this tunneling were made based on the relief analysis of the interaction energy surface of fullerenes.

The numerical simulation of C20 motion in the field of C240 was carried out to test the prediction of tunneling. As results of the experiment, it was found that the fullerene C20 is easy to jump between the potential wells even at low temperatures up to 300K. Molecular dynamics simulations confirmed our conclusions about regularities of C20 tunneling between potential wells. Thus, one can conclude that the analysis of the topology of the energy surface of van der Waals interaction between the components of nanoparticles gives a true predictive picture of the regularities of the internal molecule behavior. Probably, the phenomenon of fullerene C20 tunneling in a cell of another fullerene can be used in modern technologies, such as determining a local temperature by increase of jumping velocity.

9126-126, Session PS1

Extraction length determination in patterned luminescent sol-gel films

Lucie Devys, Géraldine Dantelle, Viacheslav O. Kubytskyi, Ecole Polytechnique (France); Henri Benisty, Institut d'Optique Graduate School (France); Thierry Gacoin, Ecole Polytechnique (France)

One of the main challenges for light emitting devices (Light Emitting Diodes (LEDs), Organic LEDs, Plasma displays...) is efficient light extraction. Due to the different refractive indices (especially for those technologies using semiconductors), light emitted in solids undergoes internal reflections and a significant amount of the "useful" light is thus trapped within the device, limiting its external efficiency. In the case of thin film devices, for which guiding effects are often limiting, extraction through surface structuration by a photonic crystal (PhC) presents the unique advantage of providing explicit control of light propagation as compared to other strategies such as disorder scattering. In this case, in addition to the directionality of the emitted light, optimization of the structure should be performed in order to limit the guided light optical path, thus reducing absorption losses or uncontrolled defects scattering. For that purpose, the key parameter to be controlled is the so-called guided mode extraction length, which corresponds to the average distance of light propagation in the device main mode before extraction. In the literature, only a few papers are devoted to the measurement of the extraction length in PhC-patterned emitting devices. Here we investigate two different methods for the quantitative evaluation of the extraction length in the case of luminescent sol-gel films patterned with a 2D photonic bandgap structures. For that purpose, we chose a model system made up of two successive TiO2 layers obtained by sol-gel chemistry: the first one contains a dispersed luminescent non-scattering europium molecular complex, chosen for its large Stokes shift. The second TiO2 layer, deposited on top of the first one, is patterned on its surface by nanoimprint lithography. The patterning has a square lattice with a period of 400 nm and variable depth controlled by the viscosity of the TiO2 sol. In the first method, we use an optical microscope to measure the extraction length. By fitting the experimental results with the corresponding simulation, the extraction length is deduced. The second method demonstrates the possibility to use simple absorption measurements by routine spectrometers to evaluate the efficiency of the process of guided light extraction. Indeed, absorption spectra of the patterned systems show extinction peaks, evidencing the coupling by the photonic crystal structure of free-space light with light guided within the film. Furthermore, using RCWA simulations, we show that it is possible to evaluate the extraction length, characteristic of the efficiency of light extraction, from the absorption spectra. Those methods are illustrated through the study of the pattern depth dependence of extraction, from 20 to 61 nm. They are both in agreement and confirm that, in this range, the deeper the surface structure, the shorter the light extraction. Moreover they are complementary, the first one taking into account the contributions of the extraction due to the photonic crystal and to the isotropic scattering linked to the imperfections of the layer, while the second one only characterizes the effect of the photonic crystal.

9126-129, Session PS1

Plasmon-enhanced tilted fibre Bragg gratings with oriented silver nanowire coatings

Jean-Michel Renoirt, Marc Debliquy, Univ. de Mons (Belgium); Jacques Albert, Anatoli I. Ianoul, Carleton Univ. (Canada); Christophe Caucheteur, Univ. de Mons (Belgium)

We demonstrate the proof of concept of a plasmonic-enhanced refractometer based on a tilted fibre Bragg grating (TFBG) covered by silver nanowires aligned perpendicularly to the fibre axis. TBFGs are a convenient way to measure surrounding refractive index, as they provide intrinsic temperature-insensitivity and preserve the optical fibre structural integrity. With bare TFBGs, sensitivity is about 60 nm/RIU (refractive index unit) while when coated with a gold thin film, surface plasmon resonance can be excited leading to a sensitivity about 600 nm/RIU. In our case, we show that localized plasmon resonances can be excited on silver nanowires. These nanowires (100 nm diameter and about 2.5 μm length) were synthetized by polyol process (ethylene glycol reducing silver nitrate in the presence of poly(vinyl pyrrolidone) and sodium chloride). The nanowires were aligned and deposited perpendicularly to the fibre axis on the gratings using the Langmuir-Blodgett technique in order to maximise the coupling between azimuthally polarized light modes and the localized

plasmons. Excitation of surface plasmons at wavelengths around 1.5 μm occurred, leading to a dip in the polarization dependent losses of the grating. This dip is highly dependent of the surrounding refractive index, leading to a sensitivity of 650 nm/RIU, which is a 10-fold increase compared to bare gratings. We obtain results equal or slightly higher than those obtained using a gold layer on TFBGs. In spite of the comparable bulk refractometric sensitivity, the use of these oriented nanowire layers provide significantly higher contact surface area for biochemical analysis using bioreceptors, and benefit from stronger polarization selectivity between azimuthal and radially polarized modes.

9126-130, Session PS1

Localized plasmons in sub-nanometre gaps

Daniel Sigle, Jan Mertens, Lars O. Herrmann, Ventsislav K. Valev, Jeremy J. Baumberg, Univ. of Cambridge (United Kingdom)

Recent progress in nanofabrication methods allows precise structuring of metals on a scale comparable to the wavelength of light, with dramatically new properties. Here we report the capability to produce plasmonic systems with sub-nm gaps containing semiconductors and semimetals, which produce completely new optical properties and extreme field confinement.[1,2]

Suitably shaped metallic nanostructures support the optical excitation of electron oscillations along their surface, called surface plasmons. In metallic nanoparticles, the plasmonic resonance conditions can be precisely tuned via variations in size, shape and surrounding environment. Adjacent nanoparticles spaced apart by only few Angstroms lead to a capacitive charge build-up and subsequent extremely localized and strongly enhanced optical fields inside the gap between them. Such plasmonic gaps are a powerful tool to investigate traces of substances and even single molecules via methods such as surface enhanced Raman spectroscopy.

We report our latest results on the nature of plasmonic sub-nanometre gaps. Graphene spacers are used to provide robust gaps down to less than 0.4nm, which enables control of the system`s plasmonic resonance and direct observation of quantum tunnelling between nanoparticles. Using semiconductor spacers, we investigate the spectral tunability of gap plasmon resonances by variations of the optical properties of the gap material and morphology changes of the nanoparticles. We further demonstrate that nanometre gaps are a suitable environment to study spatially confined phonons via surface-enhanced Raman scattering.

The ability to concentrate light into areas far below the diffraction limit is of interest for a wide range of sensing applications and allows detecting traces of substances with highest levels of sensitivity. Accurate control over the plasmonic frequency opens up possibilities for new classes of ultra-compact optical switches, accounting for the current need in numerous technologies.

[1] Nano Lett, DOI 10.1021/nl4018463 (2013); Controlling Sub-nm Gaps in Plasmonic Dimers using Graphene, J Mertens et al.

[2] Nature Mat submitted (2013), Optical-tuning plasmonics with nano-gap semiconductors, D Sigle et al.

9126-131, Session PS1

Photocurrent spectroscopy of Ge nanoclusters grown on oxidized silicon surface

Anastasiia A. Mykytiuk, Sergey V. Kondratenko, National Taras Shevchenko Univ. of Kyiv (Ukraine); V. S. Lysenko, V.E. Lashkaryov Institute of Semiconductor Physics (Ukraine); Yu. N. Kozyrev, Institute of Surface Chemistry (Ukraine)

Germanium or silicon nanoclusters grown on silicon dioxide have been successfully applied in the novel nanoelectronic, optoelectronic, or memory devices due to the quantum confinement effect and the possibility of integration within the Si-based technology. The Ge nanocluster structures were grown using a molecular beam epitaxy (MBE) technique on boron-doped (N_{a} ~ 10^{17} cm^{-3}) p-Si(100) substrates with the resistivity of 7.5 ?•cm containing 2-nm-thick SiO_{2} layer.

X-ray diffraction and photocurrent spectroscopy demonstrate that the nanoclusters have the local structure of body-centred tetragonal Ge, which exhibit an optical absorption edge at 0.48 eV. The usual diamond-like crystal structure of Ge nanoclusters appears to be completely absent due to isolation from Si(100) substrate. Further deposition of silicon on the surface with Ge nanoclusters leads to the surface reconstruction and formation of polycrystalline diamond-like Si coverage, while nanoclusters core becomes tetragonal SiGe alloy. Intrinsic absorption edge for nanoclusters with silicon coverage is shifted to 0.73 eV due to Si-Ge intermixing.

Optically induced changes of persistent conductivity in structures with Ge NCs grown on silicon oxide is observed at low temperatures. Selective excitation of Ge-NCs or Si by photons with different energy results in recharging of interface and NC's states leading to local-field effect on surface conductivity of underlying Si. Intrinsic absorption in Si at low temperatures induces residual conductivity due to reducing of downward band bending as a result of decreasing of positive charge trapped by NC's and SiO_{2}/Si interface. Infrared illumination in the range from 0.6 eV to 1.0 eV results in selective photoexcitation of Ge NCs, trapping of excess holes by NCs and interface states, and observation persistent conductivity lower than equilibrium value.

9126-132, Session PS1

Synthesis and characterization of Fe3O4-cys-naphthoquinone complex for biomedical applications

Pravin A. Patil, Manipal Univ. (India) and Defence Institute Of Advanced Technology (India); Shaibal Banerjee, Defence Institute Of Advanced Technology (India)

Nanotechnology is a multidisciplinary field with diverse biomedical applications. Recently, iron oxide nanoparticles have attracted much attention in magnetic resonance imaging (MRI), in biotechnology, in ferrofluids and biosensing etc. One of the features of magnetic nanoparticles is their tendency to aggregate due to their magnetic attractive forces. An important prerequisite for such applications is functionalization of these nanoparticles with some suitable moieties so as to result into biocompatible nanoparticles. We describe here a simple method to functionalized Fe3O4 nanoparticles with phenol complexes using cysteine as a linker to produce Fe3O4-Cys-naphthoquinone nanocomplex. These complexes are completely characterised by FTIR, SEM, XRD, TGA, VSM and TEM to know about the various properties such as size, shape, magnetisation etc. The FTIR spectrum of the complex shows a slight shift in the C=C and C=O stretching bands, confirming the interaction of the biomolecule with iron oxide nanoparticles. The method adapted to synthesized Fe3O4 nanoparticles is very simple and produce stable particles at very less temperature and time as compared to other conventional chemical synthesis methods. The synthesized nanocomplex was used in study of anti-microbial activity and was found to show interesting responses.

9126-133, Session PS1

Experimental characterisation of holographic optical traps for microbubbles

Chris Fury, National Physical Lab. (United Kingdom) and Univ. College London (United Kingdom); Caroline Harfield, National Physical Lab. (United Kingdom) and Univ. of Oxford (United

Kingdom); Philip H. Jones, Univ. College London (United Kingdom); Eleanor Stride, Univ. of Oxford (United Kingdom); Gianluca Memoli, National Physical Lab. (United Kingdom)

Microbubbles, which have found use in the medical field through the improved contrast they provide for ultrasound imaging, are now showing high potential as targeted drug delivery vectors. The characterisation of the acoustical properties of these microbubbles is important in order to validate simulations and devise improvements to their medical applications, thereby leading to safer, more clinically effective and cost-effective medical products. In order to perform this characterisation a system has been constructed based upon simultaneous use of optical and acoustical trapping (NPL "sono-optical tweezers"), with the former providing the reference force calibration and a finer manipulation than the latter.

Here we present results of a study of the characteristics of the optical trap on low-refractive index microbubbles. The microbubbles are trapped in three dimensions in a custom-built microfluidic slide using holographically generated Laguerre-Gaussian beam optical tweezers, propagating in direction opposite to buoyancy.

While similar techniques have already been used by other authors to manipulate microbubbles, this is the first time this type of trap is fully characterised in a metrological environment, with its peculiar characteristics highlighted. To this aim, Wwe track the Brownian motion of the trapped microbubble via back focal plane interferometry using a separate probe laser beam.

The optical potential is then characterised as a function of trapping laser power and trapping beam diameter (i.e. the user controlled parameters) using the trap spring constant in the planar and vertical direction, obtained from the decay of the autocorrelation of position fluctuations and its relation to the known hydrodynamics of the microbubble. We find that:

1. microbubbles are held at the equilibrium position of buoyant and optical forces, at a distance from the focus of the beam that increases with laser power;

2. optical trapping of microbubbles in this configuration is only possible within a limited range of the user controlled parameters, with a limited number of optimal configurations.

A ray optics model of optically trapped microbubbles in a Laguerre-Gaussian beam will be also presented. The model calculates spring constants and equilibrium trapping position as a function of the different parameters, highlighting key physical behaviours.

9126-135, Session PS1

Integrated coupled multi-stage plasmonic resonator for on-chip sensing

Rehab K. Abd-Allah, Zewail City of Science and Technology (Egypt) and The American Univ. in Cairo (Egypt); Yehea Ismail, Zewail City of Science and Technology (Egypt); Mohamed A. Swillam, The American Univ. in Cairo (Egypt)

A sharp resonance and narrow bandwidth plasmonic cascaded nanofilter is proposed. The resonator based on Metal-Insulator-Metal (MIM) configuration plasmonic waveguide which has the ability to confine light at sub-wavelength scale. The proposed inline resonator has low loss, compact size, and good sensing characteristics which opens the door for many nanophotonic applications. An analytical model to the filter behavior is provided and investigated. The model depends on the circuit model and the physical parameters of optical waveguides and gives a good understanding to the filter resonance response. Despite the fact that the proposed model is simple, it is accurate and shows a good agreement with FDTD simulations. This structure can be used in many applications such as sensing, biomedical diagnostics and on-chip optical interconnects. For example, it can be used as a highly effective integrated sensor with sensitivity up to 3000 RIU-1.

9126-136, Session PS1

Surface ligands affect photoinduced modulation of the quantum dots optical performance

Victor A. Krivenkov, Pavel S. Samokhvalov, Pavel A. Linkov, Daria O. Solovyeva, Gennadiy E. Kotkovskiy, Alexander A. Chistyakov, National Research Nuclear Univ. MEPhI (Russian Federation); Igor R. Nabiev, Univ. de Reims Champagne-Ardenne (France) and National Research Nuclear Univ. MEPhI (Russian Federation)

Due to their unique luminescence features, semiconductor quantum dots (QDs) are a promising material for photovoltaics, medicine and biology. Yet there is evidence that the QD fluorescent properties degrade upon strong irradiation above the band gap [S. F. Lee and M. A. Osborne, ChemPhysChem, 2009, 10, 2174–2191], which poses the problem of long-term stability of QDs under their operational conditions. This is normally explained by photoinduced oxidation of the nanocrystal surface in the presence of free oxygen, whereas the involvement of the organic ligands covering the surface of the synthesized nanocrystals is usually not taken into account.

We have studied the changes in the optical properties of CdSe/ZnS QDs coated with trioctylphosphine oxide (TOPO) ligands in air-saturated solutions under pulsed laser irradiation (??=266 nm). It has been shown that, under the influence of the laser irradiation, the fluorescence quantum yield (QY) of QDs coated with TOPO decreases progressively. The QY drops by more than an order of magnitude when the radiation dose is close to 2 ? 10-15 J per particle. In addition, when the radiation dose rises, the luminescence decay kinetics changes, and its decay time decreases. The observed decrease in the QY of QDs is accompanied by a blue shift of both the photoluminescence spectrum and the first excitonic absorption peaks. With increasing irradiation dose to 7.2 ? 10-15 J per particle, these shifts exceed 23 nm. The increase in the total amount of TOPO in the solution leads to slowdown of the decline of the QY and fluorescence decay time. Surprisingly, when ???? ligands are replaced with n-hexadecylamine (HDA), no changes in the QY at doses lower than 6 ? 10-15 J are observed. At much higher doses (up to 2.4 ? 10-14 J), we observed only a 5-nm red spectral shift of fluorescence and a decrease in the decay time from 14 to 11 ns, which is most likely to be related to slight aggregation of nanoparticles. This assumption is supported by an increase in the scattering component of the extinction spectrum.

Due to the specific HOMO energy of TOPO [Z. Ning, M. Molnar, Y. Chen, P. Friberg, L. Gan, H. Agrena and Y. Fu, Phys. Chem. Chem. Phys., 2011, 13, 5848–5854], which is slightly above the CdSe valence band energy Ev, TOPO may act as an effective hole scavenger. We assume that the described changes in the QD optical properties are related to photoinduced oxidation of TOPO ligands by the excited QDs. Upon oxidation, TOPO+ may either desorb from the surface of QDs or decompose with release of oxygen. Moreover, the TOPO desorption would probably facilitate the oxidation of QDs by oxygen molecules under irradiation. These processes are less probable for the HDA ligand due to its different HOMO energy, which is lower than that for TOPO and Ev of the CdSe core of QDs.

The described effects pave the way for new approaches to improvement of the photostability of QD-based photonic and photovoltaic devices under extreme operational conditions with laser irradiation.

9126-137, Session PS1

Photoluminescence of CdSe/ZnS quantum dots in a porous silicon microcavity

Dmitriy S. Dovzhenko, Igor L. Martynov, Pavel S. Samokhvalov, Igor S. Eremin, National Research Nuclear Univ. MEPhI (Russian Federation); Gennadii E Kotkovskii, Department of the Physics of

Micro- and Nanosystems, National Research Nuclear University "MEPhI" (Russian Federation) and Laboratory of Nano-Bioengineering, National Research Nuclear University "MEPhI" (Russian Federation); Igor P Sipailo, National Research Nuclear University "MEPhI" (Russian Federation); Alexander A. Chistyakov, National Research Nuclear Univ. MEPhI (Russian Federation)

It is known that manufacturing and application of photonic crystals is currently an area of much interest. One of the focuses of special attention in this area is various microcavity (MC) devices. They have implications for photonics, laser physics, biology, and other fields. Porous silicon is one of the most promising materials for manufacturing such devices because it is simple to prepare, its optical parameters are precisely controllable, and it has an enormous surface area. This allows us to inject different kinds of luminophores into porous silicon MC devices. Apparently, quantum dots (QDs) are among the most interesting of them. Semiconductor QDs are characterized by a wide absorbance spectrum, which enables using a wide range of sources for their excitation; a large absorption cross-section; a high quantum yield; and an excellent photostability.

To date, there have been few studies on QD injection into porous silicon photonic structures. In addition, many structures used lack the desired characteristics; the depth of QD penetration also remains a question. This is the first study to analyze the photoluminescence spectrum of QDs in a high-quality porous silicon MC. Porous silicon samples were fabricated by electrochemical etching in a hydroalcoholic HF solution from a highly doped monocrystalline p-type <100> orientation silicon wafer. The microcavity has a single eigenmode at a wavelength of 619 nm with a width smaller than 10 nm. For injection, we used CdSe/ZnS QDs with a quantum yield of about 70%, a luminescence spectrum peak at 617 nm, and a width at half-height of about 30 nm. The QD photoluminescence decay time was 19 ns; the average diameter of QDs capped with TOPO was about 5.5 nm. QDs were injected into the structure as a 0.024 mg/ml toluene solution. The volume of the injected solution was 2 ?l. To prevent dramatic QD luminescence quenching in the MC, the MC surface was oxidized by immersing the sample in a solution of hydrogen peroxide. A drastic narrowing of the luminescence spectrum was observed after QD injection. The width of the QD luminescence peak in a porous silicon MC corresponds to the mode width in the reflectance spectrum. We have found that the MC morphology considerably affects the penetration of QDs. It has been demonstrated that the luminescence spectrum pattern reflects the penetration of QDs into the structure. The kinetics of photoluminescence has also been investigated. Measurements have shown a twofold decrease in the QD characteristic photoluminescence decay time after injection into a porous silicon MC compared with the QD photoluminescence decay time in the toluene solution. However, we have not observed a significant difference between the photoluminescence decay times of QDs in an MC and in single-layer porous silicon. The decay time linearly depends on the photoluminescence wavelength, which agrees with the data on the photoluminescence kinetics of CdSe QD films and solutions. This indicates independent radiative recombination of individual nanoparticles in a porous silicon microcavity.

9126-138, Session PS1

A consideration of silver nanoparticle aggregates with a view to SERS

Sam Mehigan, Eithne McCabe, Trinity College Dublin (Ireland)

It has been well documented that ideal SERS conditions occur in the nano sized gaps between metal nanoparticles. Aggregation of the nanoparticles is required to form these gaps. We have investigated the 2 salts most commonly used throughout the literature as aggregating agents. Their absorption spectra were measured over time as the nanoparticles gradually aggregate and fall out of suspension, as well as their effects on SERS spectra.

It was found that adding these salts to colloidal silver nanoparticles causes them to form large clusters which provide huge enhancement to the SERS spectra. This is due to the analyte molecules being situated in newly formed "hot spots" between the nanoparticles. This method is shown to be a cheap and simple way to achieve very large SERS enhancement.

9126-139, Session PS1

Theoretical analysis of metallic nanohole filled with dispersive material

Shaymaa I. H. Ibrahim, Zewail City of Science and Technology (Egypt) and Mansoura Univ. (Egypt); Salah S. Obayya, Zewail City of Science and Technology (Egypt); Mohamed A. Swillam, The American Univ. in Cairo (Egypt) and Univ. of Toronto (Canada)

In this work we present the theoretical analysis of metallic hole filled with dispersive material with dielectric function modeled by Drude model. Dispersion curve of the fundamental mode supported by the metallic nano-hole shows interesting features that can be used in numerous applications including sensing, backward wave propagation and slow light transmission. Previous work in the literature either analyze only air-filled holes or just deals with the dielectric materials filling the metallic nano-hole as non-dispersive materials. However, at a certain range of frequencies commonly used in sensing and other applications even the most common dielectrics show a dispersive nature. The actual behavior of the supported mode is fundamentally different when considering the dispersive nature of material in the analysis.

In this study, we consider a hole with width and depth of 50 nm and 200 nm, respectively. The hole is etched inside a silver plate. The hole is filled with silicon which shows extremely dispersive nature in the wavelength range from 100 nm to 1000 nm.

Critical points on the dispersion curve are essential to understand the behavior of the modes supported by the nano-hole. Below a certain critical wavelength (?c1), silicon has a complex dielectric constant (?r) with negative real part while the silver has a positive real part of its own dielectric constant. This is the required condition for a surface plasmon polarition (SPP) to be exited, although reversed, so we have confined SPP modes in the first region of operation. Above ?c1, silicon possesses a positive real part of ?r, however, with significantly high values for the imaginary part. This leads to highly leaky core modes in this region with very high losses. At another important critical wavelength (?c2), the real part of the dielectric constant of the silver is equal to the negative real part of the dielectric constant of the silicon. At this condition the propagation constant of the guided mode reaches a maximum value and the dispersion curve slope becomes negative.

Therefore, it is important to accurately analyze this problem to take the dispersion of both the metal and dielectric into account. A full vectorial finite element method (VFEM) along with perfectly matched layer (PML) is being used to find the propagation characteristics of the metallic nano-hole structure. Incorporating PML as boundary conditions, leaky mode can be accurately calculated. The effective index method (EIM) is commonly used to solve this kind of problems for its simplicity and low computational cost required. However, we noticed there is a relatively large error when we compared the results obtained using VFEM and EIM, especially near critical points.

The theoretical analysis of the metallic hole filled with a dielectric material highlights the importance of considering the dispersive nature of the materials as it changes the nature of the guided mode from SPP to core modes and vice versa. The results obtained can hence be used in various applications such as sensing devices, slow light transmission and backward wave propagation.

9126-17, Session 4

Quantum enhanced photonic force microscopy *(Invited Paper)*

Michael A. Taylor, The Univ. of Queensland (Australia); Jiri Janousek, Vincent R. Daria, The Australian National Univ. (Australia); Joachim Knittel, Univ. of Queensland (Australia); Boris Hage, H. A. Bachor, The Australian National Univ. (Australia); Warwick P. Bowen, The Univ. of Queensland (Australia)

Biology is an important and longstanding frontier for quantum metrology, with quantum enhanced sensitivity allowing optical intensities to be lowered and a consequent reduction in specimen damage[1]. Here we report the first demonstrations of biological measurement with precision surpassing the quantum noise limit[2], and of sub-diffraction limited quantum imaging in biology[3]. These results are enabled through the development of a new photonic force microscopy system that extends the applicability of non-classical light from the realm of macroscopic mirrors to measurements of microscopic particles with non-paraxial fields (see Fig. 1). Biological dynamics in the critical Hz-kHz frequency range were made accessible by applying a quantum optical lock-in technique for the first time. This straightforward technique allowed quantum enhancement at frequencies as low as the best previous results in the literature, reported after over a decade of effort within the gravity wave detection community[4].

[1] K. C. Neuman, E. H. Chadd, G. F. Liou, K. Bergman, and S. M. Block, “Characterization of photodamage to Escherichia coli in optical traps,” Biophys. J. 77, 2856-2863 (1999).

[2] M. A. Taylor et al. “Biological measurement beyond the quantum limit” Nature Photonics 7 229 (2013)

[3] M. A. Taylor et al. “Sub-diffraction limited quantum imaging in a living cell”, In print, Physical Review X (2014). ArXiv:1305.1353.

[4] J. Abadie et al, “A gravitational wave observatory operating beyond the quantum shot-noise limit,” Nature Phys. 7, 962–965 (2011).

9126-18, Session 4

Electroluminescence of single-atom and single-molecule contacts *(Invited Paper)*

Guillaume Schull, Institut de Physique et Chimie des Matériaux de Strasbourg (France)

No Abstract Available

9126-19, Session 4

Local low-energy electrical excitation of localized and propagating surface plasmons with a scanning tunnelling microscope *(Invited Paper)*

Elizabeth Boer-Duchemin, Univ. Paris-Sud 11 (France); Tao Wang, RWTH Aachen (Germany); Eric Le Moal, Benoît Rogez, Geneviève Comtet, Gérald Dujardin, Univ. Paris-Sud 11 (France)

The highly confined nature of the fields from surface plasmons makes them excellent candidates for future nano-optical devices. Most often, optical excitation is used to excite surface plasmons. However, a local, low energy, electrical method for surface plasmon excitation would be preferable for device applications.

The scanning tunnelling microscope (STM) is an ideal, low energy, local source of electrons that can excite both localized (LSP) and propagating surface plasmons (SPP). Its local nature, along with the ability to precisely position the excitation source and the absence of any background light from the excitation are essential for our experiments. We have used this technique to locally excite surface plasmons on a variety of metal structures. In our setup, the STM is coupled to an inverted optical microscope and the resulting emitted light is collected through the glass substrate. In such a configuration, both the light emitted from localized plasmons as well as the leakage radiation from propagating surface plasmons may be recorded. Both real plane (spatial information) and Fourier plane (angular information) images may be obtained, as well as emission spectra.

Recently, it has been shown that the direction of the emitted radiation from gold nanotriangles may be controlled by changing the excitation position of the STM tip on the triangle. This may be understood as selectively exciting different modes of the particle. The scattering of SPPs by single and double holes has been another topic of study. For the single hole experiments it was found that the larger the hole diameter, the more directional the scattered radiation. A type of SPP-Young’s experiment was realized with the two-hole pairs. From these experiments it was shown that the SPP polarization is maintained upon scattering and that the effective size of our electric-STM surface plasmon source has an upper bound of ~200 nm.

9126-20, Session 4

Tuning tip-enhanced Raman spectra by the bias voltage in an STM

Alfred J. Meixner, Dai Zhang, Kai Braun, Eberhard Karls Univ. Tübingen (Germany)

We report on tip-enhanced Raman spectroscopy of surface bound molecules in a laser illuminated Au-tip Au-sample tunneling junction of an STM and investigate the influence of the applied bias voltage on the TERS-spectra. For efficient optical access the tunneling junction is centered in the focus of a parabolic mirror. Tip illumination and optical signal collection are performed in reflection under perfect diffraction and polarization conditions with a radially polarized laser beam. No restrictions apply with respect to the conductivity or transparency of the samples.

For low bias voltage the TERS-spectra look similar to those recorded with shear-force tip-sample distance control. As the bias voltage increases we observe reversible mode specific enhancement and suppression of bands. These changes depend also on the molecular structure and the polarity of the applied voltage and can be explained by the interplay of molecular orientation and charge transfer through the molecule.

9126-21, Session 4

Imaging nano-objects by tip-induced second harmonic generation (SHG)

Patrick Hsia, Céline Fiorini-Debuisschert, Sylvie Marguet, Fabrice Charra, CEA-SACLAY (France)

The miniaturization of optoelectronics components and the promising applications of nanoscience require better techniques for characterizing the optical properties of nano-objects. Techniques like SNOM (Scanning Near-Field Optical Microscopy) have been developed in order to circumvent the inherent limitation of conventional microscopy, which is related to the diffraction limit. With near-field techniques, the resolution is no longer limited by the wavelength but by the size of the probe.

We have developed a new “active probe” near-field technique which couples a sharp gold tip (tip radius of curvature about 20 nm) to a conductive substrate and a solution of non-linear “push-pull” molecules exhibiting both a high dipolar moment together with a high second order polarizability. Following the application of a static electric field between the tip and the sample, the molecules under the tip orient along the direction of this static electric field, thus breaking locally the

centrosymmetry. By focusing a pulsed femtosecond laser beam of frequency ? on this nanovolume of oriented molecules via a microscope objective, a non-linear polarization at 2? is then generated locally, creating a nanosource of light.

We have showed that this nanosource of light can be used to image nanometer-wide gold nanowires made by electronic lithography. Optical resolutions down to 60 to 100 nm could be evidenced . Our goal is now to study more in detail the potentialities of such “tip-induced-SHG” technique, as a new background-free nanoscale characterization tool to map field enhancement effects in nano-objects. We are currently working on gold nanowires made by colloidal chemistry. We will more particularly discuss and compare results from tip-induced SHG microscopy of colloidal nanowires to their mapping simultaneously associating topography and two-photon luminescence.

9126-22, Session 4

Superresolution optical fluctuation imaging (SOFI) aided nanomanipulation using AFM for novel artificial arrangements of chemically functionalized colloidal quantum dots and plasmonic structures

Katja Dopf, Sebastian Heunisch, Patrick Schwab, Carola Moosmann, Uli Lemmer, Hans-Juergen Eisler, Karlsruher Institut für Technologie (Germany)

The controlled assembly of artificial tailor-made nanostructures comprised of colloidal quantum dots (Qdots) and plasmonic particles well below the diffraction limit of light is crucial for a fundamental understanding of dipole-dipole interactions and for a new class of hybrid nanoplasmonic devices. Especially the dedicated positioning of single emitters and the precise placement with respect to enhanced local states close to plasmonic nanostructures still represent open challenges from an experimentalist’s point of view. Most techniques reach the necessary precision even at the current technological limit but require extensive expertise together with expensive equipment. They are therefore not favorable for prototype structures where we focus on a sufficiently high precision that is efficiently reachable on a short timescale.

In this work, we suggest the combination of atomic force microscopy (AFM) with wide-field fluorescence microscopy improved by superresolution optical fluctuation imaging (SOFI) for manipulation and characterization of Qdots. Although the high spatial resolution topography information gained from AFM measurements provides detailed localization of single Qdots, the analysis is slow and the fluorescence images are diffraction limited. Qdots that are arranged closer together than the width of the point-spread-function cannot be optically distinguished as separated by conventional means. These limitations can be overcome by applying superresolution techniques which exploit the blinking behavior of Qdots. We showed a significant improvement and speed enhancement in the precision of Qdots positioning as we can now mechanically manipulate and localize Qdots with the AFM and, as a key fact, additionally overlay the topography information with the fluorescence emission pattern improved by SOFI. With our approach we do not only determine the local spatial coordinate of Qdots, but we also discriminate between single Qdots that are optically active and “dark” Qdots, even in densely packed clusters.

To demonstrate the utility of this setup we moved single Qdots in order to arrange well defined clusters. Simultaneously, the optical behavior of the emitters, e.g. lifetimes, fluorescence spectra, blinking statistics and directionality, can be analyzed with the fluorescence microscope by using either an attached spectrograph equipped with an EMCCD camera and the possibility for Fourier imaging or confocal TCSPC spectroscopy. We evaluated the fluctuating fluorescence signals recorded with the EMCCD camera by applying SOFI schemes before and after we mechanically pushed Qdots to specific assemblies. The experiments resulted in high resolution images of combined topography and fluorescence information. Additionally, the method is adaptable to the exact combination of substrate surface, type of cantilever and Qdots.

In summary, our findings represent an easily adaptable, highly reproducible and comparatively cheap sub-diffraction limit imaging and manipulation method in a standard lab environment for proof-of-principle nanostructures. The multi-functional setup is a significant tool toward the realization of novel devices with tailored optical features.

9126-23, Session 5

Trapping, unfolding, identifying, and binding single proteins using the double-nanohole optical trap *(Invited Paper)*

Reuven Gordon, Univ. of Victoria (Canada)

Optical trapping of dielectric nanoparticles is typically limited by the third-power scaling of the polarizability, which requires large damaging laser powers. To overcome this limitation, we have been investigating apertures in metal films since 2009. Particles smaller than 10 nm in size, such as the protein bovine serum albumin, can be trapped with a double-nanohole structure, which has two sharp cusps where the double-nanoholes overlap. Using this approach, we have trapped, unfolded, and demonstrated binding of single proteins. We have also used this approach to measure particle size and concentration. More recently, we have begun to investigate the high-speed response of the double-nanohole trap in an attempt to learn more about the dynamics of the trapped particle, for example, to witness the speed of protein folding.

With the dynamic analysis, we have verified that the double-nanohole trap is 1000 times more efficient than conventional diffraction-limited optical tweezers. We have also been working towards identifying the trapped particle by in-situ Raman analysis. The double-nanohole approach uses low optical powers, typically less than 10 mW, and also gives negligible heating because of the presence of a gold film that efficiently removes heat from the region of trapping. It should be stressed that our trapping approach is non-resonant, and so this also helps to reduce the local heating and optical damage.

Our approach is of particular interest applications including biomolecular sensing and investigating the dynamics of proteins. Unlike typical works in these areas, we do not use binding sites to immobilize the analyte, since it is held in place by optical forces. This allows for studying interactions with all binding sites available. Furthermore, we do not require the use of fluorescence, and so no molecule attachment of fluorescent labels is required. Hence, we can study the intrinsic properties of the analyte, and not a hybridized form of the analyte. The aperture provides a large background free signal, therefore, we can detect single protein trapping and binding with signal-to-noise ratios >30, which is well above the limit of detection.

9126-24, Session 5

Sculpting optical energy landscapes for multi-particle nanoscale assembly

David S. Bradshaw, Kayn A. Forbes, David L. Andrews, Univ. of East Anglia (United Kingdom)

To understand the forces and dynamics of two or more neutral particles trapped within an optical beam, careful consideration of the influence of inter particle forces is required. The well-known, field-independent intrinsic force is known to derive from the Casimir-Polder interaction. However, the magnitude of this force may be over ridden by the effect known as optical binding, in cases when the laser beam is of sufficient intensity. This binding interaction is completely independent of optomechanical effects relating to optical tweezers, and involves a stimulated (pairwise) forward-scattering process. Unlike the Casimir-Polder coupling, optical binding is not always

an attractive force when both particles are in their ground state. Associated with optical binding are potential energy surfaces, which reveal intricate patterns of local minima – sets of positions in which one of the particles will sit at equilibrium (with the other notionally set at the origin). These optical energy landscapes, which can be illustrated by use of contour diagrams, have mostly been considered for systems in which spherical particles are optically bound. The effect of different particle shapes, for example tube-like structures, can now be explored. Moreover, although the theory of conventional optical binding generally assumes situations in which both particles reside in their ground states, new results arise when either (or both) particles are excited to a higher electronic state. Finally it emerges that although, in the experimentally most convenient structural configuration (for tumbling spherical particles), pairwise optical binding vanishes in the short-range region, novel effects can arise as a result of non-zero optical binding between three neighbouring particles.

9126-25, Session 5

Optical fiber tip-based nano-tweezers for dielectric particle trapping

Jean-Baptiste Decombe, Serge Huant, Jochen Fick, Institut NÉEL (France)

Optical fiber tweezers attract increasing attention as a highly flexible tool for particle trapping. They do not require any substrates or bulky high numerical aperture objective and they provide easy access to the trapped particle, which is useful for the implementation of further manipulation or characterization elements.

In this context we are developing a fiber tip-based optical nano-tweezers for trapping of micro- and nanoparticles. In the present communication we will report on optical trapping of commercial 1 μm size dielectric particles using two optical fiber tips. In this dual-beam configuration, the particle is confined on the common optical axis by the transverse gradient forces and stabilized at a point on the optical axis where the two repulsive scattering forces are canceled.

The fiber tips were elaborated by chemical etching of standard pure silica core single mode optical fibers. The obtained tips are reproducible with smooth surfaces, full angle of about 15°, and apex diameters of 60 nm. The fiber tip light emission is of circular Gaussian shape with 900 nm minimal spot size and an emission angle of 8°.

A homemade microscope with a x50 long working distance objective coupled to a CMOS camera was used for visualizing the trapped particles. Automatic particle tracking software was developed in order to exploit videos with more than 300000 frames. The program detects the center of the particle surface in each frame with an estimated resolution of 50 nm. The longitudinale (coaxial to the fiber tips) and transverse position fluctuations were determined separately, thus allowing to calculate the corresponding forces independently.

Stable trapping for several hours was observed for one sphere with light power at each fiber tip of down to 2 mW. The sphere position along the optical axis could be controlled by varying the relative optical intensity inside the two fibers. We were also able to trap 2 and 3 spheres at the same time during few minutes.

Boltzmann statistics was used to determine the trap stiffness. For a harmonic trapping potential, the probability density for finding the particle at a certain position is of Gaussian shape and the trap stiffness can be directly obtained by numerical fitting without free parameters.

We will present two series of trapping experiments, which were conducted in one go using a pair of identical fiber tips. The first series was recorded at a fixed fiber distance and variable light powers. The seconds series was recorded at fixed power and variable fiber tip distances. Harmonic trapping potentials wer found in all cases. The calculated trap stiffnesses are of the order fN/nm with a maximal value of 1 fN/nm for 6.2 mW and tip-to-tip distance of 6 μm. The trapping forces increase linearly with increasing light intensities and decrease with increasing tip-to-tip distance. The longitudinal stiffness was about 2.5 times smaller in respect to the transverse one, according to the conformity of the optical trap.

The presented results are promising for ongoing work on fiber tip-based nanoparticle trapping.

9126-26, Session 5

Photonic-force microscopy of radiation forces generated by surface mode of one-dimensional photonic crystals

Irina V. Soboleva, Lomonosov Moscow State Univ. (Russian Federation) and A.N. Frumkin Institute of Physical Chemistry and Electrochemistry (Russian Federation); Daniil A. Shilkin, Evgeny V. Lyubin, Andrey A. Fedyanin, Lomonosov Moscow State Univ. (Russian Federation)

Optical tweezers are scientific instruments that use a highly focused laser beam to provide an attractive or repulsive force to physically hold and move microscopic dielectric objects. In the case of the small displacements of the test particle from the center of the trap the particle was shown to be exerted by a force generally proportional to the gradient of the electric field. Force measurements performed with the help of optical tweezers are called photonic-force microscopy. The high sensitivity of this technique allows the use of optical tweezers to study the electromagnetic fields properties, for example, radiation pressure exerted on a single microparticle within an evanescent field of total internal reflected light, as well as the forces acting on the test particle near the surface plasmon localized close to the surface. Surface electromagnetic waves and guided modes in photonic crystals also provide the localization. In this paper the radiation forces of surface and guided modes in one-dimensional photonic crystals are studied using photonic-force microscopy technique.

Optical trap was formed by single-mode diode infrared laser beam focused by 100x immersion objective (N.A. 1.3). Laser power in trap was estimated to be in between 1 to 2 mW. Sample consisted of 1 ?m fluorescence particles suspension in water placed between cover glass and photonic crystal on the glass substrate. The forward scattered light of infrared trapping laser was collected by a 10X objective and detected using quadrant photodiods (QPD). The photonic-crystal surface mode was ecxited using Nd-YAG laser with wavelength of 532 nm. Radiation of the green laser was passed though the single-mode optical fiber and focused in 50 ?m spot at the photonic crystal surface. An attenuated total internal reflection prism configuration was used to couple the incident s-polarized light to the surface mode of photonic crystal because p-polarized light did not excite the surface mode in the studied samples. The intensity of the exciting radiation is estimated to be 1 kW/cm2. Displacements of the trapped particle were extracted from the changes in the QPD photocurrent. The shape of the potential energy function was obtained from the histogram of the positions of the bead. In the presence of surface mode experimental results show a significant changes of the positions of potential energy minima.

The angular dependence of forces of the photonic-crystal surface and guided mode acting on the bead is obtained. At angles of incidence that are far from resonance of the photonic-crystal surface mode the radiation force acting on the particle is close to zero. As angle of incidence increases the radiation force increases both in the direction to the surface of the photonic crystal and along the surface in the direction of the surface mode propagation. Besides, the radiation-force value is enhanced with surface-bead distance decrease. The force growth is due to the increase of the gradient of the electromagnetic field near the surface related to the excitation of the surface mode of photonic crystal.

9126-27, Session 5

Near-field enhanced optical nanotweezers based on laser-structured substrates

Domna G. Kotsifaki, National Hellenic Research Foundation (Greece); Pavlos G. Lagoudakis, Univ. of Southampton (United Kingdom); Maria Kandyla, National Hellenic Research Foundation (Greece)

Optical tweezers are widely employed for trapping micron- and nanometer-size particles for various applications, however the trapping efficiency of conventional optical tweezers is limited when dealing with nanometer-size specimens. We present an optical nanotrapping setup that exhibits enhanced efficiency, based on near fields around sharp metallic nanotips. The trapping substrates consist of laser-structured silicon wafers with quasi-ordered nanospikes on the surface, covered by a thin Ag or Cu/Au layer. The resulting optical traps show significant enhancement of the trapping force and the effective quality factor.

Polystyrene beads of 400 nm diameter were trapped near the focal point of a CW fiber laser beam (1074 nm wavelength), focused through an oil immersion objective lens (NA = 1.4) near the coated nanostructured substrates. The nanostructured substrates were prepared by irradiating silicon wafers with femtosecond laser pulses in distilled water. The silicon surface was irradiated by a 20 KHz train of 200 fs pulses at 400 nm wavelength from a frequency doubled, Ti:sapphire laser system. The average power of the frequency-doubled laser beam was 25 mW. The pulses were tightly focused by a 10x objective lens and traveled through 4 mm of water before striking the sample at normal incidence. Columnar, quasi-ordered nanospikes were formed on the irradiated wafers with average tip diameter ~220 nm and height ~1.75 ?m. The nanostructured wafers were covered by a 50-nm Ag layer or a 3-nm Cu/50-nm Au layer using thermal evaporation.

The particle solution was imaged by fluorescence excitation with a blue laser diode that was focused on the solution through the trapping objective lens, forming an inverted fluorescence microscope. We determined the effective optical trap force by escape velocity measurements. The nanostructured substrates were placed on a piezo-controlled stage, on which a continuous triangular function with a variable frequency was applied. By determining the minimum frequency at which a trapped bead escapes the trap, we are able to calculate the trapping force, using Stokes' law. The particles were trapped at various distances above the nanostructured substrates and the corresponding trapping forces and quality factor were determined for each distance.

The nanostructured silicon substrates coated with Ag or Cu/Au resulted in trapping quality factors, which were 30 and 40 times higher than the quality factors obtained with nanostructured substrates without metallic coating, respectively. In the case of metallic-coated nanostructured substrates, the quality factor decreases exponentially with the distance of the trap from the substrate surface, indicating near-field enhancement of the optical trapping force. For uncoated nanostructured substrates the quality factor does not depend significantly on the distance of the trap from the substrate surface. Strong bubble formation was observed in the presence of the trapping laser beam near the Ag coated nanostructured substrates, hindering measurements very close to the surface. The bubbles did not appear with the Cu/Au coated nanostructured substrates, due to more efficient thermal transport into the substrate.

9126-28, Session 6

Nanoplasmonics meets bio *(Invited Paper)*

Jochen Feldmann, Ludwig-Maximilians-Univ. München (Germany)

I will report on our recent efforts to utilize some of the unique plasmonic properties of noble metal nanoparticles for sensing and controlling nano- and microscale processes in aqueous solution. The use of optical forces and of local optothermal heating is in the focus of our investigations. Examples range from controlled laser printing with nanoscale precision via the study of DNA-binding events to the direct optical monitoring of flow generated by bacterial flagellar rotation.

Recent publications:

Optically trapped gold nanoparticle enables listening at the microscale, A. Ohlinger et al., Phys. Rev. Lett. 108, 018101 (2012)

Tuning DNA Binding Kinetics in an Optical Trap by Plasmonic Nanoparticle Heating, L. Osinkina et al., Nano Lett. 13, 3140 (2013)

Two-Color Laser Printing of Individual Gold Nanorods, J. Do et al., Nano Lett. 13, 4164 (2013)

9126-29, Session 6

Improving the detection limit of plasmonic biosensors: manipulation of field distribution in nano-structures

Mitradeep Sarkar, Maha Chamtouri, Julien Moreau, Mondher Besbes, Michael T. Canva, Lab. Charles Fabry (France)

Most biochip systems based on surface plasmon resonance (SPR) with conventional flat metallic surface, have limited performance for detection of trace concentrations of target molecules when total surface coverage is not reached. The signal (reflectivity or wavelength variation) can then remain below the minimum detectable signal of SPR detectors. Our approach is based on enhancing the signal above the detectable limit of the detector while using trace concentrations of target molecules, by nano-structuration of the biochip surface. To evaluate the performance of these structures we introduce the Sensitivity Enhancement Factor (SEF), which directly relates to the reduction in the minimum detectable concentration of target molecules.

We have studied numerically and experimentally three families of structures for which local electric field enhancement is observed, due to confinement of the plasmon modes by the nano-metric structures. By selective localization of target molecules in areas with field enhancement, we have demonstrated that an improvement of sensitivity with respect to the required target molecule concentrations can be achieved.

For the first family we have studied an array of metallic ribbons with propagating plasmon (PP) excitation perpendicular to the ribbons. For the second family we have studied the similar structure, but with plasmon excitation parallel to the ribbon arrays. For the first group of structures we have coupling between the PP and the excited localized plasmons (LP). For the second group, we have new transverse PP modes which propagate along the sides of the metallic ribbons. For these structures the minimum detectable concentration can be improved by a factor of 2 (SEF~2). Because the modes studied and optimized in these structures are strongly confined close to the metal surface, the effect of background refractive index changes are also reduced appreciably thus making the detection of target molecules more robust and less sensitive to noise.

For the third family we have studied a 3D periodic array of metallic nano-cylinders where the PP interacts with the cylinders to excite new plasmonic modes with field enhancement close to the cylinders. The interaction gives rise to hybrid modes with various characteristics depending on structural parameters such as the cylinder diameter, the height of the cylinders and the period of the array. We have also observed the appearance of plasmonic band-gaps which is a result of interference between contra-propagating plasmons. By optimizing the different plasmonic modes excited in the structure, we have achieved a SEF of around 10, thus increasing the limit of detection of the SPR sensor by at least an order of magnitude.

9126-30, Session 6

Biochemical component identification by plasmonic improved whispering gallery mode optical resonance based sensor

Vladimir A. Saetchnikov, Elina A. Tcherniavskaia, Anton V. Saetchnikov, Belarusian State Univ. (Belarus); Andreas Ostendorf, Gustav Schweiger, Ruhr-Univ. Bochum (Germany)

New opportunity to improve a sensitivity of a label-free biomolecule detection in sensing systems based on microcavity evanescent wave optical sensors has been recently found and is being under intensive development. Novel technique based on combination of optical resonance on microring structures with plasmon resonance. Recently developed tools based on neural network data processing can realize real-time identification of biological agents. So combining advantages of plasmon enhancing optical microcavity resonance with identification tools can give a new platform for ulta sensitive label-free biomedical sensor.

Our developed technique used standard glass and polymer microspheres as sensitive elements. They are fixed in the solution flow by spin - coating techniques in adhesive layer on the surface of substrate or directly on the coupling element being in the field of evanescence wave. Sensitive layer was integrated into developed fluidic cell with a digital syringe. Light from tuneable laser strict focusing on and scattered by the single microsphere was detected by a CMOS camera. The image was filtered for noise reduction and integrated on two coordinates for evaluation of integrated energy of a measured signal.

To improve a sensitivity of a sensor layer it has been treated by gold nanoparticle solution. Another technique used thin film gold layers deposited previously on the substrate below adhesive. Normalized by free spectral range resonance shift of whispering gallery modes and a relative efficiency of their excitation were used as input data for biomolecule classification. Hydrophily of a sensitive element was obtained and investigated can disturb drastically measured parameters. So the sort of microspheres and suitable their material have been selected experimentally on the basis of previous calibration of a sensitive layers in pure water.

Experimental data on detection and identification of variety of biochemical agents, such as proteins (albumin, interferon, C reactive protein), microelements (Na+, Ca+), antibiotic of different generations, in both single and multi component solutions under varied in wide range concentration are represented. As the entrance data following signal parameters were used: relative (to a free spectral range) spectral shift of frequency of whispering gallery mode optical resonance in microsphere and relative efficiency of whispering gallery mode excitation obtained within a free spectral range which depended on both type and concentration of investigated agents. Multiplexing on parameters and components has been realized using spatial and spectral parameters of scattered by microsphere light with developed data processing. Biochemical component classification and identification of agents under investigation has been performed by network analysis techniques based on probabilistic network and multilayer perceptron. Developed approach is demonstrated to be applicable both for single agent and for multi component biochemical analysis.

Both biomolecules and gold nanoparticle injection was obtained caused whispering gallery mode spectra modification. But after gold nanoparticle treatment spectral shift and intensity of whispering gallery mode resonances in biomolecule solutions increased. Whispering gallery mode resonances in microspheres fixed on substrate with gold layer in biomolecule solutions also had higher intensity and spectra modification then without gold layer. The effect can be effective under optimized layer thickness.

9126-31, Session 6

Surface plasmon amplification without inversion in plasmonic nanogaps

Vladimir G. Bordo, Univ. of Southern Denmark (Denmark)

The field of plasmonics has been considered as holding promise for developing diverse optical and optoelectronic nanodevices for subwavelength waveguiding, light energy concentration, ultra-sensitive sensing, high-resolution microscopy, ultra-fast computations and many other applications. However, it faces a serious obstacle preventing from its wide utilization in photonic circuits originating from high metallic losses which lead to short surface plasmon polariton (SPP) propagation lengths in the optical spectral range. As a solution to this problem, it has been suggested to introduce optical gain in the dielectric material bordering the metal surface. It has been also proposed that in such systems Surface Plasmon Amplification by Stimulated Emission of Radiation (SPASER) can occur if the gain medium undergoes a strong enough pumping. However, currently available gain materials put limits for possible spaser characteristics, such as spasing threshold and output intensity, and for its operation conditions.

In this talk, we propose a principally new avenue to SPP amplification. It is based on the consideration of the SPP field generated in the plasmonic nanostructure from first principles. The approach suggests that under certain conditions the field emitted in the active medium undergoes a positive feedback from the plasmonic waveguide/cavity walls. This interaction introduces loop gain in the system which amplifies the polarization of the active medium. In a plasmonic gap cavity such gain can lead to a parametric instability to any weak incoherent perturbation which develops in generation of SPPs. The considered loop gain does not imply stimulated emission in the active medium and hence it does not require a population inversion in the active centers. In this sense, the predicted here effect of Surface Plasmon Amplification Without Inversion (SPAWI) is principally different from spaser. Such an effect is essentially classical which means that the active medium can be comprised of highly polarizable particles, for example, metal nanoparticles.

In this talk, we consider the SPAWI effect in a metal-insulator-metal (MIM) waveguide structure. Basing on the dyadic Green's function of this structure we derive the SPP gain coefficient. We demonstrate that the gain is possible for an even SPP mode and it is not achievable for the fundamental odd SPP mode. Then we discuss the case of a MIM cavity and obtain the SPP generation condition. The general theory is illustrated by the calculations for gaps between Ag and Au surfaces.

9126-32, Session 6

On the controllable optical beam direction by means of nanopatterened plasmonics device

Fabio A. Bovino, SELEX Sistemi Integrati S.p.A. (Italy); Alessio Benedetti, Concita Sibilia, Univ. degli Studi di Roma La Sapienza (Italy)

The field of plasmonics has become a widespread research topic with myriad applications in many are of science. Further development of plasmonic applications relies on the emergence of advanced passive and active plasmonic devices that can control the propagation of plasmonic fields. In particular, directional beaming, splitting, and focusing of plasmonic signals are prerequisites for plasmonic circuiting and plasmonic sensing applications. The key element is a metallic slit milled into a thin metallic film: when illuminated, the subwavelength slit converts the incident light into SPPs propagating toward the top of the metal structure and then the radiation is coupled out, giving conditions for enhanced light transmissions. Positioning and focusing surface plasmon polariton (SPP) waves in a controlled way is important for nanophotonic applications. To date, plasmonics offers only a limited flexibility in the control of light

fields. As with the conventional lens the geometry is typically fixed, so for a given optical frequency the locations of optical field enhancement are also fixed. Recently, some breakthroughs have been made regarding active control, in which the intensity of the light fields is influenced in time, either through pump–probe or coherent control.

In the present work we systematically analyzed different methods of emission radiation pattern control from suitable patterned slits. The analysis has been performed for a fixed geometry, and we considered an Au film, on a transparent dielectric substrate, of thickness ranging from 240 nm to 360 nm , with an input radiation of 532 nm impinging on the sample from the dielectric side. We first considered a difference of thickness to the slit's opposite sides, in order to achieve different localization effects in the output corners and consequently a modified emission pattern for the propagating wave (PW). The slit ranging from 30 up to 180 nm has been simulated in many different configurations including parallel and non parallel walls.

Another approach adopted a Bragg's diffraction grating, which is grown upon the slit's upper surface in order to convert the outcoming SPP into a PW. The need of a stable output pattern respect to the input polarization and angle of incidence provides a high output SPP-to-PW ratio, thus the effects of the Bragg's grating, enhanced with the aid of a proper chirped profile, allows a strong control for the emission pattern.

The analysis has been performed by FDTD numerical method. Realization of samples and experiments are in progress.

-T.W. Ebbesen, H.J. Lezec, H.F. Ghaemi, T. Thio, P.A. Wolff, "Extraordinary optical transmission through sub-wavelength hole arrays", Nature 931, 667-669 (1998).

-Z. Sun, H.K. Kim, "Refractive transmission of light and beam shaping with metallic nano-optic lenses", App. Phys. Lett. 85, 642-644 (2004).

- E. Çetin, A. Sennaroglu. ?.E. Mustecaplioglu, "Nanoscale plasmonic devices for dynamically controllable beam focusing and scanning", Phot. Nano. Fund. Appl. 8, 7-13 (2010).

9126-33, Session 6

Formation of ferroelectrically defined Ag nanoarray patterns

Signe Damm, N. Craig Carville, Univ. College Dublin (Ireland); Katia Gallo, Michele Manzo, KTH Royal Institute of Technology (Sweden); Brian J. Rodriguez, James H. Rice, Univ. College Dublin (Ireland)

Ferroelectric lithography is an approach based on patterning the spontaneous polarisation inside ferroelectric crystals so to engineer static electric field distributions, suitable for driving bottom-up assembly of nanomaterials [1,2]. Besides electric field poling the spontaneous polarization in materials such as LiNbO3, can be modified through the chemical process of proton exchange. This method accounts for a change in crystal lattice of the ferroelectric substrate creating a modification to the polarization and charge at the surface. This is an approach that enables directed self-assembly, which potentially offers a cost effective way to create arrays of metallic nanostructures. This approach has the potential to enable control of surface self-assembly processes with nanoscale precision over mm to cm lateral sample sizes and beyond, making such an approach applicable to engineer plasmonic devices.

Ferroelectric lithography potentially offers a method to create substrates that support reproducible surface enhanced Raman scattering spectroscopy (SERS) via arrays of nanopatterns made from silver nanoparticles [3-5]. Damm et al. demonstrated using a molecular probe 4-Aminothiophenol (4-ABT) absorbed onto a silver nanostructured array that SERS can be obtained. The authors showed that the observed SERS spectra show peaks arising from b2 modes, which occur for plasmon enhanced Raman scattering from 4-ABT, in place of a1 modes, which occur in normal Raman scattering [4]. We study here Ag nanopattern arrays formed using Ferroelectric lithography and demonstrate that the resulting metal nanoarrays support both SERS and SEL (surface enhanced luminescence). Fluorescence lifetime imaging revealed that fluorescence intensity is greatest on silver and that the molecular probes lifetime was reduced in line with a plasmon enhanced luminescence mechanism. Studies showed that the substrate simultaneously supports plasmon enhanced luminescence and Raman scattering. Fluorophores emitting near the plasmon absorption maxima were enhanced 4-fold. Fluorphores that emit to the red of the plasmon absorption band were 'blue-shifted' potentially via a dipolar coupling mechanism. We also show that these plasmon active substrates are applicable for bioimaging eg fluorescence imaging of cells.

REFERENCES

1. D. Li and D. A. Bonnell, Annu. Rev. Mater. Res. 38, 351-366 (2008)

2. S.V. Kalinin, D.A. Bonnell , T. Alvarez , X. Lei , Z. Hu, J. H. Ferris, Nano Letters, 2, 589 (2002)

3. S. Damm, N.C. Carville, B.J. Rodriguez, M. Manzo, K. Gallo, J.H. Rice. Applied Physics Letters. Submitted, 2013.

4. S. Damm, N.C. Carville, B.J. Rodriguez, M. Manzo, K. Gallo, J.H. Rice. J. Phys. Chem. C. 116, 26543–26550, 2012.

5. N.C. Carville, M. Manzo, S. Damm, M. Castiella, L. Collins, D. Denning, S.A.L. Weber, K. Gallo, J.H. Rice B.J. Rodriguez, ACS Nano, 6, 7373–7380, 2012

9126-34, Session 7

Local Energy transfer in hybrid nanoplasmonics *(Invited Paper)*

Renaud Bachelot, Xuan Zhou, Jérôme Plain, Pierre-Michel Adam, Anne-Laure Baudrion, Univ. de Technologie Troyes (France); Stephen K. Gray, Gary P. Wiederrecht, Argonne National Lab. (United States)

Incorporating resonant optical properties of metal nanostructures into nanoscale applications such as ultrahigh density storage devices, nanoelectronics, and nanophotonics has gained considerable interest within the last years.

Recent advances in hybrid and molecular plasmonics will be presented. The approach relies on near-field energy transfer between metal nanoparticles and photosensitive organic materials, and is not diffraction-limited.

Optical nanosources supported by metal nanoparticles can be used for controlling/triggering photochemical and photo physical processes involving photons, charges and motion transfers at the nanoscale. In particular, three examples of local energy transfer will be presented and commented: free radical photopolymerization [1,2], photo isomerization [3,4] and nanoscale strong coupling [5].

Free-radical photopolymerization

The metal nanoparticles are coated with a liquid polymerizable formulation, and optically excited close to their plasmon resonance. By using an incident dose below the threshold of photopolymerization, the polymer is produced only at the points where local optical electric field of the metal nanoparticles is plasmon-enhanced to exceed the threshold. The resulting metal/polymer is characterized by atomic force microscopy and optical spectroscopy. this method presents many interests including the developpement of new nano-emitters of hybrid and nano-quantification of plasmonic fields based on molecular probing.

Photoisomerization

Azobenzene derivatives containing polymers deform when exposed to light with a wavelength in the absorption band associated with trans-cis isomerization of the azobenzene molecules. In that way, each molecule acts as an optical nano-motor able to mechanically perturb the surrounding polymer matrix.

When such copolymers cover a metallic nanoparticle exposed to light, the resulting surface deformations lead to novel ways of probing plasmonic near-field intensity and provide new information about the local optical vectorial sensitivity

of the azobenzene molecules. In other words, the molecular nanomators are driven / activated by plasmonic nanosources.

Strong coupling

Surface plasmon resonances can couple with molecular excitons leading to so-called weak or strong coupling regimes. The latter is always observed wherever either the plasmon or the molecular exciton presents large oscillator strength (high-Q plasmonic cavities or J-aggregates). We will present the observation of a strong coupling regime between the surface plasmon resonance of a nanoparticle array and the molecular excited state of photochromic molecules, both of them presenting weak oscillator strength. This strong coupling leads to plasmons-mode hybridizing and coupled nano-systems presenting controllable optical properties.

These threes examples open new routes for controlling and exploiting energy transfer in nanooptics.

[1] PRL 98, 107402 (2007).

[2] ACS Nano 4, 4579 (2010).

[3] Nano Lett. 5 615-619 (2005)

[4] ACS Nano 6, 1299 (2012).

[5[Nano Lett. 13, 282 (2013).

9126-35, Session 7

Plasmonics for enhanced Raman spectroscopy: From SERS to TERS *(Invited Paper)*

Francois Lagugné-Labarthet, The Univ. of Western Ontario (Canada)

1-The limit of detection of 4-nitrothiophenol adsorbed onto the surface of a platform fabricated by nanosphere lithography is investigated by surface-enhanced Raman spectroscopy. Critical factors, such as the functionalization time and the change of sharpness of the gold nanostructures upon annealing are studied. Platforms for surface-enhanced Raman spectroscopy provide detection ranging from monolayers down to isolated molecules. For a functionalization time of twenty four hours, a limit of detection of 10-16 M (100 aM) is achieved. Furthermore, by shortening the functionalization time to thirty minutes, a significant higher limit of detection is determined ranging from 10-6 to 10-9 M. By altering the shape of the nanotriangles via annealing, a loss in signal intensity occurs. Optimizing the factors that enable a lower limit of detection is critical for many applications where SERS can be considered as a promising analytical alternative.

2-The behavior of the electromagnetic field interaction with gold nanotriangles organized in bow-tie arrays is investigated. A side-by-side comparison between the absorbance of the array and the electric field resonance confined around the gold structures is presented and discussed to explain the spectral shift between both parameters. We show the importance of tuning the absorbance spectra of the structure carefully in order to optimize SERS platforms. FDTD calculations and Raman measurements of gold triangles of different sizes and periodicity are systematically performed. Numerical calculations show that the spectral maximum of the electric field varies in distinct areas over the metallic structures.

9126-36, Session 7

Thermally controlled photocatalytic coalescence of functionalized gold nanoparticles

Moshik Cohen, Zeev Zalevsky, Bar-Ilan Univ. (Israel); Salvador Pocoví-Martínez, Univ. de València (Spain); Asaf Shahmoon, Bar-Ilan Univ. (Israel); Julia Perez-Prieto, Univ. de València (Spain)

Gold nanoparticles (GNPs) have recently fashioned rapid expansion of interest from both fundamental and applicative perspectives, owing to their unprecedented optical and chemical properties[1]. These properties might lead to applications including quantum plasmonics[2] biological and chemical sensors, spectroscopic enhancers, quantum dots and nanostructure fabrication, and micro imaging methods[3–5]. Hence, the selective synthesis of metal GNPs of any desired size is of high interest. Here we introduce a new strategy for thermally controlled photocatalytic growth of functionalized GNPs. Irradiated benzophenone (BP) in THF can act as an efficient photocatalyst for growing GNPs [6] . We explored now the effect of applied thermal energy to control the process. Our findings provide the pass for high resolution growth of GNPs tailored for specific applications. The benzophenone triplet excited state (3BP) is of an nϖ* nature and efficiently abstracts hydrogen atoms from good hydrogen donors[7]. As a consequence, the irradiation of BP in THF leads to ketyl radicals (BPH) that can act as electron donors (Eox=-0.25 Vvs SCE)[8,9]. This property has been previously used for the synthesis of Ag and Au NPs from their corresponding salts[10,11] as well as in the size reduction of CdSe NPs [12]. In our experiments, GNPs were synthesized based on a modified version of the methodology described by Qi and Hegmann[13]. We analyzed samples containing Au@DCT and BP in THF, as well as Au@DCT, BP and gold salt in THF. The samples were irradiated using a photoreactor at UVA (Lamps: LCZ-UVA), as the samples were kept at constant - controlled temperature at range of 120 - 450. Measurements were carried out for different temperatures and irradiation timeframes. To characterize the samples, we measured the absorption spectra and obtained TEM images of the nanoparticles for the timeframes times and temperatures. To measure the UV-Vis absorption spectrum a spectrophotometer Agilent 8543 equipped with UV-Vis scanning ChemStation software was used. Quartz cuvettes of 1 x 1 x 4 cm3 where used to irradiate and measure the samples. TEM images were registered with a JEOL JEM-1010 microscope operating at 100 kV and equipped with a digital camera (Megaview III). To prepare TEM samples, a few drops of the gold nanoparticles suspension were deposited on a carbon film supported on a copper grid, which was subsequently dried. We observed truthfully and broadly controllable growth of GNPs, which size can be tuned via irradiation times and temperature. In the presence of gold salt, bigger nanoparticles are observed due to the additional Au contribution. In conclusion, we introduce a thermally controlled photocatalytic based synthesis process of GNPs. This process requires mild conditions and achieves narrow size distribution, which may be of considerable interest for variety of new applications.

References

[1] C. A. Mirkin, R. L. Letsinger, R. C. Mucic, and J. J. Storhoff, “A DNA-based method for rationally assembling nanoparticles into macroscopic materials,” Nature 382(6592), 607–609 (1996) [doi:10.1038/382607a0].

[2] K. J. Savage, M. M. Hawkeye, R. Esteban, A. G. Borisov, J. Aizpurua, and J. J. Baumberg, “Revealing the quantum regime in tunnelling plasmonics,” Nature 491(7425), 574–577 (2012) [doi:10.1038/nature11653].

[3] M. A. Hayat, Colloidal gold: principles, methods, and applications, Academic Press, San Diego (1900).

[4] G. J. Bassell, C. M. Powers, K. L. Taneja, and R. H. Singer, “Single mRNAs visualized by ultrastructural in situ hybridization are principally localized at actin filament intersections in fibroblasts.,” J. Cell Biol. 126(4), 863–876 (1994) [doi:10.1083/jcb.126.4.863].

[5] M. Brust, D. J. Schiffrin, D. Bethell, and C. J. Kiely, “Novel gold-dithiol nano-networks with non-metallic electronic properties,” Adv. Mater. 7(9), 795–797 (1995) [doi:10.1002/adma.19950070907].

[6] M. Consuelo Cuquerella, S. Pocovi?-Marti?nez, and J. Pe?rez-Prieto, “Photocatalytic Coalescence of Functionalized Gold Nanoparticles,” Langmuir 26(3), 1548–1550 (2010) [doi:10.1021/la9040503].

[7] K. Okada, M. Yamaji, and and H. Shizuka, “Laser photolysis investigation of induced quenching in photoreduction of benzophenone by alkylbenzenes and anisoles,” J. Chem. Soc. Faraday Trans. 94(7), 861–866 (1998) [doi:10.1039/A707900A].

[8] T. Lund, D. D. M. Wayner, M. Jonsson, A. G. Larsen, and K.

Daasbjerg, “Oxidation Potentials of ?-Hydroxyalkyl Radicals in Acetonitrile Obtained by Photomodulated Voltammetry,” J. Am. Chem. Soc. 123(50), 12590–12595 (2001) [doi:10.1021/ja011217b].

[9] D. Dondi, M. Fagnoni, and A. Albini, “Tetrabutylammonium Decatungstate-Photosensitized Alkylation of Electrophilic Alkenes: Convenient Functionalization of Aliphatic C H Bonds,” Chem. – Eur. J. 12(15), 4153–4163 (2006) [doi:10.1002/chem.200501216].

[10] M. Sakamoto, T. Tachikawa, M. Fujitsuka, and T. Majima, “Acceleration of Laser-Induced Formation of Gold Nanoparticles in a Poly(vinyl alcohol) Film,” Langmuir 22(14), 6361–6366 (2006) [doi:10.1021/la060304k].

[11] K. L. McGilvray, M. R. Decan, D. Wang, and J. C. Scaiano, “Facile Photochemical Synthesis of Unprotected Aqueous Gold Nanoparticles,” J. Am. Chem. Soc. 128(50), 15980–15981 (2006) [doi:10.1021/ja066522h].

[12] R. E. Galian, M. de la Guardia, and J. Pe?rez-Prieto, “Photochemical Size Reduction of CdSe and CdSe/ZnS Semiconductor Nanoparticles Assisted by nϖ* Aromatic Ketones,” J. Am. Chem. Soc. 131(3), 892–893 (2009) [doi:10.1021/ja807454u].

[13] H. Qi and T. Hegmann, “Postsynthesis Racemization and Place Exchange Reactions. Another Step To Unravel the Origin of Chirality for Chiral Ligand-Capped Gold Nanoparticles,” J. Am. Chem. Soc. 130(43), 14201–14206 (2008) [doi:10.1021/ja8032444].

9126-37, Session 7

Raman spectroscopy and optical trapping of 20 nm polystyrene particles in plasmonic nanopores

Sarp Kerman, Chang Chen, Yi Li, Liesbet Lagae, IMEC (Belgium) and Katholieke Univ. Leuven (Belgium); Tim Stakenborg, IMEC (Belgium); Pol Van Dorpe, IMEC (Belgium) and Katholieke Univ. Leuven (Belgium)

The detection and identification of single or a few nanoparticles has caught the attention in the last decade due to its potential application on small bio-particles. Nanopores are efficient platforms for this purpose as they provide mechanical confinement for such particles. Surface Enhanced Raman Spectroscopy (SERS) stands out as a technique that can identify the fingerprints of the surface molecules of the nanoparticles and can be integrated in/near nanopores[1]. However, nanoparticles are highly mobile due to Brownian motion and usually their dwell time is too short compared to the time it takes to obtain their SERS spectrum. In order to increase the observation time of individual particles, optical trapping can be used by exploiting the high gradient of the plasmonic hot spot that is already present for SERS detection [1,2]. Besides optical trapping benefiting SERS, SERS also allows us to observe trapping of small nanoparticles. As the particles get smaller, it gets harder to observe optical trapping of nanoparticles by common techniques such as transmission or reflection from nanopores due to decrease in signal to noise ratio [3]. Since SERS has been proven to be able to detect even a few molecules, it can provide information about the optical trapping of nanoparticles in nanopores[3]. Here, we present our work on the SERS and optical trapping of 22 nm surface modified polystyrene particles in plasmonically optimized gold coated nanopores as described by Chen et al [1,2]. The optical field intensity enhancement can reach up to around 10^3 at the hot spot of a 30 nm x 200 nm nanopore illuminated by 785 nm laser according to simulations. As the amplitude of SERS signal is roughly proportional to the square of the optical intensity, roughly 10^6 times enhanced SERS signal can be observed for a single particle/molecule at the hotspot. The field decays in a few nanometers away from the hot spot. However, this is mainly true when the molecule only brings a small perturbation to the local refractive index. Numerical simulations show that in the case of a particle with a higher refractive index than the medium, which is the case for the polystyrene particles, the field is confined mostly between the particle and the nanopore surface and the enhanced volume is essentially only a few A s thick. We show that this happens due to near-field scattering from the particle. Therefore, the SERS signal obtained depends on the surface modification of particle. We initially used a 22 nm carboxyl modified polystyrene bead. The SERS signal merely consists of a peak around 830 cm-1, which can be attested to the carboxyl-gold interaction according to the literature [4,5], rather than the polystyrene’s well known benzene breathing ring mode at 1000cm-1 [6]. We also acknowledged this 830+-20 cm-1 peak on a roughened gold substrate. Using this peak, we show that 22 nm carboxyl modified particles can be trapped up to a few seconds depending on the incident intensity in nanopores with no adsorption. Particles with different surface modifications are also tested and gave a different SERS signal. We expect that this phenomenon will be beneficial for studying and identifying single or a few bio-particles in the near future.

References:

[1] Chen, C., Hutchison, J., Van Dorpe, P., Kox, R., De Vlaminck, I., Uji-I, H., Hofkens, J., Lagae, L., Maes, G., Borghs, G. (2009). Focusing Plasmons in Nanoslits for Surface-Enhanced Raman Scattering. Small, 5 (24), 2876-2882

[2]Enhanced Optical Trapping and Arrangement of Nano-Objects in a Plasmonic Nanocavity, Chang Chen, Mathieu L. Juan, Yi Li, Guido Maes, Gustaaf Borghs, Pol Van Dorpe, and Romain Quidant, Nano Letters 2012 12 (1), 125-132

[3]Plasmon nano-optical tweezers,Mathieu L Juan, Maurizio Righini, Romain Quidant, Nature Photonics 5, 349–356 (2011)

[4] Michota, A. and Bukowska, J. (2003), Surface-enhanced Raman scattering (SERS) of 4-mercaptobenzoic acid on silver and gold substrates. J. Raman Spectrosc., 34: 21–25.

[5]Jiao Gao, Yongjun Hu, Shaoxin Li, Yanjiao Zhang, Xue Chen, Adsorption of benzoic acid, phthalic acid on gold substrates studied by surface-enhanced Raman scattering spectroscopy and density functional theory calculations, Spectrochimica Acta Part A: Molecular and Biomolecular Spectroscopy, Volume 104, March 2013, Pages 41-47, ISSN 1386-1425

[6]Raman Spectrum of Polystyrene, Ann Palm, The Journal of Physical Chemistry 1951 55 (8), 1320-1324

9126-38, Session 8

Charge transfer and quantum coherence in solar cells and artificial light harvesting system

Christoph Lienau, Carl von Ossietzky Univ. Oldenburg (Germany)

In artificial light harvesting systems the conversion of light into electrical or chemical energy happens on the femtosecond time scale [1], and is thought to involve the incoherent jump of an electron from the optical absorber to an electron acceptor. Here we investigate the primary dynamics of the photoinduced electronic charge transfer process in two prototypical structures: (i) a carotene-porphyrin-fullerene triad, a prototypical elementary component for an artificial light harvesting system and (ii) a polymer:fullerene blend as a model system for an organic solar cell. Our approach [2] combines coherent femtosecond spectroscopy and first-principles quantum dynamics simulations. Our experimental and theoretical results provide strong evidence that the driving mechanism of the primary step within the current generation cycle is a quantum-correlated wavelike motion of electrons and nuclei on a timescale of few tens of femtoseconds. We furthermore highlight the fundamental role played by the flexible interface between the light-absorbing chromophore and the charge acceptor in triggering the coherent wavelike electron-hole splitting.

Experimentally, we perform ultrafast nonlinear spectroscopy with 10-fs time resolution using a two-color pump-probe spectrometer providing independently tunable ultrashort pump and probe pulses from two non-collinear optical parametric amplifiers. We study a supramolecular triad consisting of three functional units, a porphyrin ring acting as the primary light absorber in the center of the molecule, a fullerene (C60) electron acceptor and a carotene unit serving as hole stabilizer.

Impulsive excitation of the porphyrin Q-band with a 7-fs pulse centered at 550 nm reveals rich transient transmission (?T/T) dynamics. Specifically, we observe a short-lived and spectrally red-shifting transient emission band in the region between 540 nm and 580 nm. The red-shifting band displays both temporal and intensity oscillations, which are attributed to stimulated emission from a photoexcited intermediate charge-transfer state whose population coherently oscillates between donor and acceptor state. This interpretation is supported by detailed TDDFT quantum-dynamical simulations of the system. Photoexcitation of the porphyrin unit leads to an almost complete electron transfer to the fullerene moiety within about 70 fs displaying moreover strong oscillations with a period of 30 fs (Fig. 1(b)). Both the time scale of the charge build-up and the oscillation period of the electronic wavepacket derived from the simulation are in striking agreement with the experimentally observed dynamic evolution of the charge transfer band (Fig. 1(c)). These conclusions are corroborated by a recent study of the ultrafast nonlinear optical of a thin-film blend of the conjugated polymer poly-3-hexylthiophene (P3HT) and [6,6]-phenyl-C61 butyric acid methyl ester (PCBM), a prototypical organic solar cell material. In brief, we observe that an impulsive excitation of the polymer moiety results in coherent vibrational motion of the non-excited PCBM moiety. This points to an ultrafast and coherent charge transfer across the interface of this non-covalently bonded hybrid system. Detailed TDDFT simulations support this conclusion.

Our experimental and theoretical data provide strong evidence that the correlated, quantum-coherent motion of ions and electrons not only governs the first steps of the photoinduced electron dynamics but also the yield of the charge separation in these prototypical photovoltaic systems, in stark contrast to prevailing statistical models for electron transfer reactions.

[1] C. J. Brabec et al., “Tracing photoinduced electron transfer process in conjugated polymer/fullerene bulk heterojunctions in real time,” Chem. Phys. Lett. 340, 232 (2001).

[2] C. A. Rozzi et al., “Quantum coherence controls the charge separation in a prototypical artificial light-harvesting system”, Nature Communications 4, 1602 (2013).

9126-39, Session 8

Strong coupling with localized surface phonons

Ruben Esteban, Javier Aizpurua, Centro de Fisica de Materiales (Spain); Garnett W. Bryant, Joint Quantum Institute (United States) and National Institute of Standards and Technology (United States)

The coupling between low volume electromagnetic modes and single emitters can be large. In particular, it is possible to reach the strong coupling regime characterized by coherent transfer of energy, as has been demonstrated for dielectric cavities and metallic particles supporting plasmonic resonances. In the latter case, the very small modal volumes achievable, not limited by the diffraction limit, can compensate the large plasmonic losses.

Here, we show theoretically that it is also possible to reach the strong coupling regime when a single emitter interacts with a Localized Surface Phononic Polariton[1]. The phononic mode is supported by a SiC bowtie antenna and has a extremely low modal volume. We demonstrate the presence of anti-crossing and vacuum Rabi Oscillations. The latter depend on the population of the phononic mode, as expected. We also describe the possibility to excite complex hybrid modes to which several phononic modes contribute. We finally discuss different aspects of relevance for experimental implementation, such as the difficulty to obtain appropriate emitters.

[1] R. Esteban et al, Submitted

9126-40, Session 8

Designing media for the local control of nanoscale absorption, transmission and energy transfer

Jamie M. Leeder, Matt M. Coles, Jack S. Ford, David L. Andrews, Univ. of East Anglia (United Kingdom)

Interactions between light and molecular matter featuring photon absorption are commonly associated with excitation of individual chromophores. Subsequent relaxation is achieved through numerous mechanisms, including fluorescence emission and/or energy transfer to neighbouring chromophores. The efficiency of such processes depends on many factors including the intensity and wavelength of the optical input, the absorption cross-section of the molecule and the relative orientation of molecular components. New photonic materials are developed on the principle that such factors are controllable, duly tailoring the system to suit new technological applications.

Parameters determining the linear response in multi-component materials are typically assessed within the theoretical framework of classical optics. However, with improved interest and capability in fabricating nanoscale structures (especially those that exhibit quantum effects), it is becoming increasingly relevant to develop theory that more faithfully represents how individual photons engage with matter. In such constructs, the interaction of materials with optical waves and photons is highly dependent on local molecular environment, therefore surrounding structures and ancillary species generally exert forms of influence on the photophysical processes inherent within dielectric media. At optical wavelengths where the secondary structure displays little intrinsic optical absorption, the role of such components is often interpreted as modifying the input through a corrective local index of refraction. Although expedient in the discussion of bulk properties of a macroscopic medium, it is reasonably supposed at a local chromophore-photon level that optical mechanisms operate in a different fashion.

Using a fully quantized approach to the representation of local molecular electronic structure and electrodynamics, this research develops rigorous theory and a corresponding physical interpretation of how photon absorption, scattering and energy transfer are modified by vicinal, non-absorbing chromophores. The results provide insight into the mechanisms achieved within multi-chromophore systems, highlighting factors that can assist in the optimization of optical characteristics in designer materials.

9126-41, Session 8

Theoretical investigation of energy transfer in the presence of Au nanoparticles

Cristian A. Marocico, Xia Zhang, A. Louise Bradley, Trinity College Dublin (Ireland)

We present a theoretical investigation of the energy transfer (ET) rate between donor-acceptor quantum dots (QDs) in the presence of Au nanoparticles (NPs). The localized surface plasmon of the Au NPs can enhance the ET rate between the donor and acceptor QDs. This can lead to an enhancement of the acceptor emission and has potential applications in light-emitting devices.

We have used a Green’s tensor formalism to numerically calculate the ET rate between the donor and acceptor QDs in the presence of Au NPs. Considering a donor/acceptor pair placed near a Au NP, we have calculated the ET rate and efficiency as a function of their separation and relative position from the Au NP. We find that the ET rate and efficiency are more sensitive to the donor-Au NP distance than to the acceptor-Au NP distance, when the Au NP is placed between the donor and acceptor.

We have also considered the dependence of the energy transfer on the size of the Au NP. In this case both donor and acceptor are on the same side of the NP and the energy transfer between them is enhanced as the particle size increases up to a certain value dependent on the distance from the donor to the Au NP.

Finally, we have also calculated the ET rate between monolayers of donor and acceptor QDs, separated by a monolayer of Au NPs. The corresponding experiments have been performed in our lab, and we have found good agreement between the numerical and experimental results.

The energy transfer efficiency and rate, in the case of monolayers, will also depend on the concentration of Au NP in the monolayer, and we find that it increases with the concentration.

The enhancement of the ET rate effectively extends the interaction range over between donor and acceptor, which can have uses as an extended optical ruler or for sensing applications.

9126-42, Session 8

Resonant energy transfer in rigid solutions of semiconductor quantum dots with concentration gradient

Anna O. Orlova, Margarita A. Kurochkina, Yulia A. Gromova, Vladimir G. Maslov, National Research Univ. of Information Technologies, Mechanics and Optics (Russian Federation); Evgeny N. Bodunov, Petersburg State Transport Univ. (Russian Federation); Alexander V. Baranov, Anatoly V. Fedorov, National Research Univ. of Information Technologies, Mechanics and Optics (Russian Federation)

A resonant energy transfer between particles is a powerful tool to control an optical response of systems on external light. Förster Resonant Energy Transfer (FRET) is a widely used in systems with semiconductor quantum dots (QDs). A size quantization of QD energy structure allows an easy control of their photoluminescence (PL) properties. A quantum confinement effect in QDs combines with their broad absorption spectrum and their high PL quantum yield. Optical properties of QDs make them an ideal photoexcitation donor in different sensitized processes.

There are number of systems using QDs as energy donors based on complexes of quantum dots with organic molecules. However, rigid solutions, where the efficient FRET between QDs and molecules could be realized without a QD/molecule complex formation, are of undoubted interest. Polyethylene terephthalate (PET) membranes can be utilized as matrices for such systems. These matrices have local special areas bordering with track pore walls with monotonically changing material density and a number of broken polymer chains. Utilizing this feature of PET membranes, we have formed a hybrid structure based on hydrophobic semiconductor CdSe/ZnS QDs and hydrophilic porphyrin molecules. We found that in QDs/porphyrin structures energy transfer from QD to molecule accompanied with both quenching of QD photoluminescence and enhancement of porphyrin PL.

An analysis of our data has shown, that in these systems, energy transfer efficiency depends on QD size and it correlates with overlapping power between QD PL and porphyrin absorption spectra. At the same time, a noticeable deviation of an experimental FRET efficiency dependence on an acceptor concentration from the theoretical ones was observed for all donor-acceptor pairs. The most probable reason of this deviation is a gradient of donor and/or acceptor concentration in these matrices. A theoretical model describing FRET in a rigid solution with gradient of particles concentration is proposed.

9126-43, Session 9

Cryogenic single nanocrystal spectroscopy: reading the spectral fingerprint of individual CdSe quantum dots *(Invited Paper)*

Brahim Lounis, Univ. Bordeaux 1 (France)

Spectroscopically resolved emission from single nanocrystals at cryogenic temperatures provides unique insight into physical processes that occur within these materials. At low temperatures the emission spectra collapse to narrow lines revealing a rich spectroscopic landscape and unexpected properties, completely hidden at the ensemble level. Since these techniques were first used, the technology of nanocrystal synthesis has matured significantly and new materials with outstanding photostability have been reported. In this talk, I will discuss how cryogenic spectroscopy of single nanocrystals probes the fundamental excitonic structure of the band edge, revealing spectral fingerprints that are highly sensitive to a range of photophysical properties as well as nanocrystal morphology. In particular, spectral and temporal signatures of biexciton and trion emission will be presented and their relevance to emerging technologies discussed. Overall I will show how cryogenic single nanocrystal spectroscopy can be used as a tool for understanding fundamental photophysics and guiding the synthesis of new nano crystals.

9126-44, Session 9

Chiral quantum dot based materials

Joseph Govan, Trinity College Dublin (Ireland); Alexander V. Baranov, Anatoly V. Fedorov, National Research Univ. of Information Technologies, Mechanics and Optics (Russian Federation); Yurii K. Gun'ko, Alexander Loudon, Trinity College Dublin (Ireland)

Over last years the area of chiral metal nanoparticles (e.g. Au and Ag) has received a great deal of attention due to the range of potential applications offered by these materials in chiral sensing and as metamaterials in advanced optical devices. Recently, the use of stereospecific chiral stabilising molecules has also opened another avenue of interest in the area of quantum dot (QD) research. The main goal of our research is to develop new types of technologically important quantum dot materials containing chiral defects, study their properties and explore their applications. For the first time chiral QDs (penicillamine stabilised) have been prepared by us using microwave induced heating with the racemic (Rac), D- and L-enantiomeric forms of penicillamine as stabilisers. Circular dichroism (CD) studies of these QDs have shown that D- and L-penicillamine stabilised particles produced mirror image CD spectra, while the particles prepared with a Rac mixture showed only a weak signal. It was also demonstrated that all three types of QDs (D-, L-, and Rac penicillamine stabilised) show very broad emission bands between 400 and 700 nm due to defects or trap states on the surfaces of the nanocrystals. The utilisation of chiral penicillamine stabilisers also allowed the preparation of new water soluble white emitting CdS nano-tetrapods, which demonstrated circular dichroism in the band-edge region of the spectrum. Biological testing of chiral CdS nanotetrapods showed a chiral bias for uptake of the D-Pen stabilised nano-tetrapods by cells. The chiral CdS nanostructures have also been doped by various metal ions. It was found that copper doping had a strong effect at low levels in the synthesis of CdS nano- structures. We expect that this research will open new horizons in the chemistry of chiral nanomaterials and their application in biotechnology, sensing and asymmetric synthesis.

9126-45, Session 9

Optical properties of coupled three-dimensional Ge quantum dot crystals

Yingjie Ma, Zhenyang Zhong, Quan Lu, Fudan Univ. (China); Xinjun Wang, Shanghai Institute of Technical Physics (China); Tong Zhou, Yongliang Fan, Zuimin Jiang, Fudan Univ. (China)

Correlation and coupling of quantum dots (QDs) have been extensively studied [1]. The coupling can be clearly observed and modulated when the QDs are laterally or vertically close enough, which allows for strong excition wave-function overlapping. High-density, homogeneous and three-dimensional (3D) ordered QD arrays have been refered to as quantum dot crystals (QDCs) [2]. In 3D artificial QDCs, the QDs play a role similar to that of atoms in real crystals. The band offsets at the interfaces between the QD and the matrix in the QDCs also play a role analogous to the periodic potential in real crystals. Minibands are formed in QDCs due to the 3D coupling. Maximum density of states (DOS) peaks of electrons or holes will emerge in each miniband and will significantly change the optical and transport properties of the QDCs [3]. Few works have been reported on the coupling effect of 3D ordered QDs, especially of dense ordered QDCs. Extensive study of the optical properties of the Ge QDCs with the formation of minibands is in demand.

In this paper, In this paper, we present the realization of high density and 3D ordered Ge QDCs by multilayer growth of QDs on pit-patterned silicon (001) substrates via nanosphere lithography [4, 5]. The QDs are arranged laterally in a hexagonal lattice with a periodicity of 100 nm. The vertical period of the QDCs is ~7 nm. A systematic investigation of the photoluminescence (PL) and photoreflectance (PR) properties of this QDCs is performed. The observed unique PL and PR features, including the changes in spectral linewidth, peak energy blueshift caused by increasing excitation power, weight of phonon component in entire PL spectrum and a much more reduced optical reflectivity at the interband transition energy for the QDCs, are interpreted by a coupling model in which the localized hole ground state of each Ge QD couples and extended into delocalized hole minibands [6].

[1] A. I. Yakimov, et al. Appl. Phys. Lett. 93, 132105 (2008).

[2] D. Grützmacher, et al. Nano. Lett. 7, 3150 (2007).

[3] O. L. Lazarenkova, et al. Phys. Rev. B 66, 245319 (2002).

[4] Y. J. Ma et al., Appl. Phys. Lett. 100, 153113 (2012).

[5] Y. J. Ma et al., Nanotechnology 24, 015304 (2013).

[6]Y. J. Ma et al., Opt. Express 21, 6053-6060 (2013).

9126-46, Session 9

Laser cooling of CdSe quantum dots

Galina A. Nemova, Raman Kashyap, Ecole Polytechnique de Montréal (Canada)

We consider process of laser cooling of CdSe quantum dots (QDs) based on anti-Stokes fluorescence. The physical mechanism of radiation cooling of solids by anti-Stokes fluorescence was originally proposed in 1929 [1] and experimentally observed for the first time in ytterbium-doped ZBLANP glass in 1995 [2]. In 2013, the first laser cooling of semiconductor using group II-VI cadmium sulphide (CdS) nanobelts starting from 290K was announced [3].

We present a detailed study of laser cooling of CdSe QDs, which are technologically well developed and can demonstrate relatively high (up to 85%) quantum efficiency at the present time. Contrary to isolated atoms, carriers in QD are coupled to the vibration modes of the crystal lattice and interact with phonons broadening the optical linewidth with temperature. In our scheme high purity surface passivated colloidal CdSe QDs are laser pumped with photon energy less than the mean fluorescence photon energy. In this case the thermalization process is accompanied by phonon absorption. The subsequent radiative recombination of the exciton removes energy from the system. The laser power and QD concentration are set to ensure that only a single exciton is excited per QD, since multiexciton decay on the picoseconds time scale caused by Auger recombination is a source of unwanted heat generation in the system. It is shown experimentally that anti-Stokes photoluminescence exhibits a linear dependence on excitation intensity as a result of energy transfer to the excited electron-hole pair from the phonon ensemble. Thermally stimulated increase in anti-Stokes photoluminescence is almost independent on the QD sizes. The efficiency of this process increases for the QDs with better passivated surface. The anti-Stokes photoluminescence energy shift is about the energy of optical phonons in CdSe crystal. Using the rate equations we have simulated the cooling process in the system of passivated QDs taking into account the temperature dependences of all parameters of the system. The energy of the pump photons is 2.03eV. The core diameter for CdSe QDs is ~4nm. The overall diameters of QDs, which include the CdSe core and the thickness of passivation, are in the range 7-11nm. It is shown that the temperatures down to 100K can be reached in CdSe QDs. We have investigated how the “dark” level ±2, which participates in the spin-flip process and does not participate in the radiative decay of the excitons, influences the cooling process. It is shown that the nano size of the sample is the key parameter on the way of experimental realization of laser cooling in semiconductors today. QDs of group II-VI as well as nanobelts of group II-VI are very promising material for laser cooling of semiconductors.

1. P. Pringsheim, Z. Phys. 57, 739-746 (1929).

2. R. I. Epstein, M. I. Buchwald, B. C. Edwards, T. R. Gosnell, C. E. Mungan, Nature (London) 377, 500-502 (1995).

3. J. Zhang, D. Li, R. Chen, Q. Xiong, Nature 493, 504-508 (2013).

9126-47, Session 10

Strong-field phenomena in Si-based nanoplasmonic guides *(Invited Paper)*

Abdulhakem Y. Elezzabi, Univ. of Alberta (Canada)

We investigate silicon-based plasmonic devices as a platform for high-non-linear field effects at telecommunication wavelengths of 1550nm. The Silicon-based nanoplasmonic devices are fabricated on silicon-on-insulator (SOI) substrates using processing techniques that are largely CMOS compatible, thus, allowing an ease of integration with electronic and silicon photonic devices. The strong nonlinear filed confinement at the metal-Si interface allows for the generation of third harmonic (TH) 516nm radiation at unprecedented conversion efficiency that is two orders of magnitude higher than any observed to date in Silicon. This demonstrates the potential for compact visible light sources for integrated photonics or hybrid photonic-electronic nanocircuitry. We show also that electrons excited, via two photon absorption, are accelerated to energies up to several eV by the ponderomotive potential that exists in the highly confined nanoplasmonic field. Subsequent collisions with valence electrons enable the observation of new phenomena, such as field-driven electron impact ionization, strong white light emission, and ultrafast electron-hole sweeping. These findings uncover a new strong-field interaction that can be used in sensitive nanoplasmonic modulators and hybrid plasmonic-electronic transducers. As an example, I will propose a CMOS-compatible ultrafast silicon nanoplasmonic ballistic triode capable of switching high current in less than 100fs.

9126-48, Session 10

Hybrid fibers for nanophotonic applications *(Invited Paper)*

Markus A. Schmidt, Institut für Photonische Technologien e.V. (Germany)

Cylindrical nanophotonic devices in fiber form are a new class of integrated components which can overcome several limitations of state-of-the-art planar devices such as insufficiently small aspect ratios or significant insertion loss when coupled to single-mode fibers. Our approach to overcome these essential bottlenecks and to realize such functionalized fiber waveguide structures is based on pressure-assisted melt-filling of holey photonic crystal fibers (PCFs). This method gives PCF new functionalities and opens up new ways for applications of optical fiber. The structures I will discuss here are modified PCFs including metallic nanowire, giving rise to so-called plasmonic PCFs. I will discuss the basics of plasmonic excitation on metallic nanowires and show that the propagating plasmons can be described as planar plasmons spiraling around the wire circumference. Also I will introduce ultralong range plasmons, which reveal much longer propagation lengths than their planar counterparts. After that I will focus the talk onto several experimental implementations of plasmonic fiber by showing plasmonic molecules, local near field polarizations of plasmonics supermodes and broadband azimuthal polarizers. As last point I will introduce a new type of fiber-integrated near field probe, which can be used to locally measure the evanescent fields of all kind of excitations. This probe, which operates by a local propagation plasmonic nanoresonator at the front end of the tip, has the potential for a real world implementation and to replace commonly used tips.

9126-49, Session 10

Experimental demonstration of plasmonic switching via optical cavity resonances

Cillian McPolin, Jean-Sebastien G. Bouillard, King's College London (United Kingdom); Daniel P. O'Connor, Univ. of North Florida (United States); Alexey V. Krasavin, Wayne Dickson, Gregory A. Wurtz, Anatoly V. Zayats, King's College London (United Kingdom)

The ability to control and manipulate electromagnetic energy at the nanoscale, both dynamically and in real-time through low-energy external control signals is a missing link in our aim to develop a fully integrated sub-wavelength optical platform. To date, plasmonic systems demonstrating active functionalities, incorporating thermo- and electro-optic media, quantum dots, and photochromic molecules, are achieving incremental progress in switching and modulation applications. However, long switching times (>nanosecond) or the need for relatively strong control energy (~?J/cm2) to observe sensible signal modulation (35% to 80%) limit the practical use of such structures as signal processing or other active opto-electronic nanodevices. In order for active plasmonics to offer a viable technological platform, both the magnitude and the speed of the employed nonlinearity, as well as the spectral/spatial tunability of the effect must be improved.

In this context, we experimentally demonstrate plasmonic signal extinction in the presence of optical cavity modes using leakage radiation microscopy, with a change in transmission of above 60%. We also numerical demonstrate modulation via a change in gold permittivity with temperature, yielding extinction ratios of up to 3dB. Here we provide a detailed discussion on the underlying switching mechanism and possible device integration.

9126-50, Session 10

Design of large scale plasmonic nanoslit arrays for arbitrary mode conversion and demultiplexing

Pierre Wahl, Vrije Univ. Brussel (Belgium); Takuo Tanemura, The Univ. of Tokyo (Japan); Jürgen Van Erps, Nathalie Vermeulen, Vrije Univ. Brussel (Belgium); David A. B. Miller, Stanford Univ. (United States); Hugo Thienpont, Vrije Univ. Brussel (Belgium)

Over the last decade, surface plasmon polaritons have generated a substantial amount of research interest because of their unique property of being confined to a metallic surface and the associated ability of metallic structures to confine light to sub-wavelength volumes. Also the problem of mode splitting or conversion has recently become very topical because of the possibility of using multiple modes in optical fibers and various techniques have been explored in the literature to separate modes optically. While most work on plasmonic couplers and demultiplexers has made use of periodic arrays of metallic slits, aperiodic arrays can have a much richer behavior which is not readily attainable with periodic approaches [1]. We present an iterative design method for the coupling and the mode conversion of arbitrary modes to focused surface plasmons using a large aperiodic array of randomly located slits in a thin metal film. As the distance between the slits is small and the number of slits is large, significant mutual coupling occurs between the slits, which makes an accurate computation of the field scattered by the slits difficult. Recently, we have developed a novel semi-analytic model, namely the modal source radiator model, which allows us to compute the mutual coupling among arbitrarily located apertures with a significantly reduced computational cost [2]. We present a design method based on this modal source radiator model that, in contrast to commonly used schemes used in [1], can account for the scattering by the slits of both the direct excitation wave and the surface plasmons generated by all the slits. This knowledge allows us to calculate the optimal position of slits that scatter the surface plasmon waves more than they scatter the excitation beam. In addition, we are able to detect when a slit is ``blocking'' a focused surface plasmon and is basically scattering the field one is trying to focus, and hence a better device is achieved by removing this particular slit. We apply this method to the design of various types of couplers for arbitrary fiber modes and a mode demultiplexer that focuses three orthogonal fiber modes to three different foci and validate our design results using fully vectorial 3D finite-difference time-domain (FDTD) simulations. Our designs contain more than 1000 randomly located slits the scattering pattern of which we calculate in less than 50 seconds. Also, our design method could be used for most designs that aim at achieving a certain optical functionality using a large number of randomly located apertures or grooves in a metal film.

[1] T. Tanemura, K. C. Balram, D.S. Ly-Gagnon, P.Wahl, J.S. White, M.L. Brongersma, and D.A.B. Miller, "Multiple-wavelength focusing of surface plasmons with a nonperiodic nanoslit coupler", Nano Letters 11, 2693--2698 (2011).

[2] T.Tanemura, P.Wahl, S.Fan, and D.A.B. Miller, Modal source radiator model for arbitrary two-dimensional arrays of subwavelength apertures on metal films, Journal Of Selected Topics in Quantum Electronics, 19 4601110 (2013).

9126-51, Session 10

Magnetoplasmonics going 3D

Kristof Lodewijks, Chalmers Univ. of Technology (Sweden); Nicolo Maccaferri, CIC nanoGUNE Consolider (Spain); Irina Zubritskaya, Addis Mekonnen Adamu, Chalmers Univ. of Technology (Sweden); Randy K. Dumas, Johan Akerman, Univ. of Gothenburg (Sweden); Paolo Vavassori, CIC nanoGUNE Consolider (Spain); Alexander Dmitriev, Chalmers Univ. of Technology (Sweden)

In recent years the magnetoplasmonic response of ferromagnetic nanoparticles has been studied extensively. Nowadays it is well established that ferromagnetic nanoparticles show pronounced plasmonic resonances that can be exploited to obtain very broadband tunability of the magneto-optical Kerr effect (MOKE) response. In this work we show how the third dimension plays a critical role in the observed effects and how it can be exploited in order to enhance the effects observed before in largely two-dimensional nanostructures. We study various 3D ferromagnetic nanoparticles with longitudinal spectral MOKE and show how light phase retardation becomes a crucial parameter when the particle geometries are changed from mostly flat 2D structures to full 3D geometries. As such, the nanoparticles

support localized surface plasmon resonances (LSPRs) along all three major axes, each having specific contribution to the observed MOKE behavior. In combination with applied magnetic field, these three axes form various conditions to observe and exploit 3D magnetoplasmonic anisotropy. All of these 3D magnetoplasmonic modes can be easily excited in p-polarization, where one directly couples to the out-of-plane and one of the in-plane nanoplasmonic modes, while orthogonal in-plane nanoplasmonic axis is engaged by means of the spin-orbit interaction that couples it to the out-of-plane mode. Simultaneously, the magnetic behavior of the nanostructures is altered substantially, as depending on the particle dimensions along all the axes, the magnetic easy/hard axes can be arbitrarily changed to be in- or out-of-plane, allowing for active control over the magnetoplasmonic response by means of the applied external magnetic field.

9126-52, Session 11

Ultrafast and nonlinear plasmon dynamics: for strong coupling to coherent control *(Invited Paper)*

Markus B. Raschke, Univ. of Colorado at Boulder (United States)

Plasmonics provides for sub-diffraction limited optical confinement and control, with the surface plasmon polariton excitation related to the underlying elementary electronic excitations in the supporting metal being well understood. The corresponding ultrafast and nonlinear plasmon interactions could provide further enhanced plasmonic functionalities for imaging, spectroscopy, sensing, or switching. However, while the ultrafast and nonlinear optics of metals is an advanced field, the understanding of the related plasmonic properties is less developed. Here we discuss ultrafast and nonlinear properties of metals and metallic nanostructures in terms of the elementary optical interactions under of electronic band structure, plasmon resonances, and geometry-sensitive selection rules. We will provide recent results from measurements of nonlinear plasmon dynamics and focusing and nonlinear control, which aid in the understanding of these properties, the nonlinear plasmonic light-matter interaction, and in particular the measurement and control of the intrinsically fast dephasing times. This insight is important for the development of applications such as spatio-temporal nano-imaging, coherent control of individual quantum systems, or strong light-matter interaction.

9126-53, Session 11

Nonlinear superchiral meta-surfaces *(Invited Paper)*

Ventsislav K. Valev, Jeremy J. Baumberg, Univ. of Cambridge (United Kingdom); Nuno Braz, Univ. College London (United Kingdom); Jan Mertens, Claire Blejean, Univ. of Cambridge (United Kingdom); Paul A. Warburton, Univ. College London (United Kingdom); Victor V. Moshchalkov, Katholieke Univ. Leuven (Belgium); Nicolae-Coriolan Panoiu, Univ. College London (United Kingdom); Thierry Verbiest, Katholieke Univ. Leuven (Belgium)

We demonstrate a surprising direct relationship between a key linear optical property (superchiral light) and a nonlinear one (second harmonic generation).[1] By tuning the superchiral light in our meta-molecules, we identify material dimensions for optimal nonlinear optical response. We then build such optimized meta-surfaces and use their strong response to reveal a fundamental physical property, i.e. non-reciprocity with respect to space-time reversal.

Chirality is the handedness of Nature, the property where the mirror image of an object cannot be superimposed on the object itself. Although often associated with biochemistry because of the large number of chiral bio-molecules, recently chirality has attracted considerable attention in relation to metamaterials,[2] which consist of metallic nanostructures with substantially sub-wavelength features. Chiral metamaterials are highly promising because they can achieve negative refractive index, large optical activity and repulsive Casimir forces that can lead to nano-levitation and frictionless nano-motors. Moreover, chiral metamaterials can compress the helical pitch of circularly polarized light thereby achieving superchiral light. Just as plasmonic near-field enhancements can be used to enlarge the interaction of light with molecular (10^14 in the case of Raman scattering), superchiral light can enlarge the interaction within chiroptical (chiral optical) effects. Due to the favorable power-law scaling of near-field enhancements, the nonlinear optical properties of chiral nano- and metamaterials are of prime fundamental and practical interest.

In optical second harmonic generation (SHG) two photons at a fundamental frequency are annihilated to generate a single photon at twice the frequency (half the wavelength). The chiroptical effects in SHG are typically 10^3 larger than their linear optical counterparts. Nonlinear metamaterials and meta-surfaces are expected to achieve record-high chiroptical values compared to those of natural materials and consequently to serve as highly sensitive probes for exploring chiral molecular chemistry. Presently though, very little has been done towards fulfilling these high expectations. Basic understanding of the nonlinear chiroptical properties of meta-surfaces is also lacking; for instance, fundamental physical properties, such as reciprocity, have not yet been investigated. The question of reciprocity in meta-surfaces is crucial as they are the basic building blocks of bulk metamaterials.

Our work brings together expertise from physics, chemistry, material science and engineering domains. We combine state of the art linear and nonlinear experimental probes with cutting edge theoretical developments to piece together a comprehensive an coherent picture of SHG chiroptical properties. This work provides a framework for exploiting the benefits of chiral nonlinear meta-surfaces.

[1] V. K. Valev, J. J. Baumberg, B. De Clercq, N. Braz, X. Zheng, E. J. Osley, S. Vandendriessche, M. Hojeij, C. Blejean, J. Mertens, C.G. Biris, V. Volskiy, M. Ameloot, Y. Ekinci, G. A. E. Vandenbosch, P. A. Warburton, V. V. Moshchalkov, N. C. Panoiu, T. Verbiest Nonlinear superchiral meta-surfaces: tuning chirality and disentangling non-reciprocity at the nanoscale. Nat. Mat. Submitted (2013).

[2] V. K. Valev, J. J. Baumberg, C. Sibilia, T. Verbiest, Chirality and chiroptical effects in plasmonic nanostructures: fundamentals, recent progress and outlook. Adv. Mater. 25, 2508-2628 (2013).

9126-54, Session 11

Nonlinear optics of magnetoplasmonic resonance in Co nanodisks

Ilya Razdolski, Sergey Semin, Radboud Univ. Nijmegen (Netherlands); Kristof Lodewijks, Alexander Dmitriev, Chalmers Univ. of Technology (Sweden); Andrei Kirilyuk, Theo Rasing, Radboud Univ. Nijmegen (Netherlands)

Surface plasmon resonance (SPR) has been demonstrated to greatly modify magneto-optical effects [1,2]. However, the nonlinear magnetooptical response of structures capable of exhibiting SPR has received much less attention, leaving many open questions regarding, for example, multipole contributions to the second harmonic generation (SHG) [3]. In this work we study spectral properties of the magnetic SHG response from ferromagnetic nanostructures in the vicinity of their SPRs. The Co nanodisks and nanoellipses of 60-210 nm in lateral size and 30 nm-thick, prepared by hole mask colloidal lithography, are studied in the visible and near-IR spectral ranges. Measurements of the nonlinear-optical magneto-optical Kerr effect in the transverse geometry reveal distinctive spectral behaviour for the s- and p-polarised fundamental beams. The magnetic contrast ? is shown to reach up to 10% and changes sign near the SPR wavelength, which shifts noticeably with the size of the nanostructures. For large nanodisks the magneto-optical hysteresis measured by means of SHG demonstrated the presence of a vortex state, which manifests itself in a characteristic shape of the magnetic SHG signal. These results

are complemented with phase measurements thus allowing to unambiguously distinguish magnetic and non-magnetic SHG contributions. A comparison between circular and elliptical nanostructures is performed, providing important insights into the mechanisms of the enhancement of the magneto-optical SHG effects.

[1] G. Armelles et al., Adv. Opt. Mater. 1, 10 (2013);

[2] V. Bonanni et al., Nano Lett. 11, 5333-5338 (2011);

[3] I. Razdolski et al., Phys. Rev. B 88, 075436 (2013).

9126-55, Session 11

Imaging of polarization rotation in transmission resonances of periodic plasmonic structures

Ananth Krishnan, Pankaj Arora, Indian Institute of Technology Madras (India)

Polarization rotation of reflected light from metallic grating has been studied extensively in recent past [1,2]. We imaged TE to TM polarization rotation of transmitted light in 1D and 2D Periodic Plasmonic Structures (PPS) fabricated on thin metal coated dielectric substrate. Several PPS of 50% duty cycle and extremely low aspect ratio (height to width ratio) of 0.1 were designed using rigorous coupled wave analysis to exhibit transmission plasmonic resonances at optical wavelengths (400 nm to 700 nm). 1D and 2D PPS were fabricated using electron beam lithography, evaporation and lift-off process on glass substrates coated with thin metal. The PPS were characterized using normally incident broadband visible light and cross-axis Polarizer Analyzer (PA) setup, with the transmitted light imaged in direct and momentum space using a camera. When the cross axis PA were positioned at +45° & -45° respectively w.r.t. plane of incidence, bright emissions of Green, Yellow or Red colors corresponding to transmission plasmonic resonances of the PPS with different periods, were observed in both direct and Fourier planes, instead of completely dark images. From the measured emission momentum in Fourier plane images and spectra of collected light, the emissions were attributed to the excitations of surface plasmons and the reason for surface plasmon excitation in this arrangement is strong coupling of hybrid modes with each other caused by the anisotropy introduced by grating which strongly enhances the efficiency of PC. In the direct image plane, the PPS appeared brightly colored in a dark background. The presented structures behave as frequency selective half wave plates in transmission configuration and could also be used to eliminate the effect of direct beam while imaging the coupling to surface plasmons in periodic structures.

References :

1. G.P. Bryan-Brown, J. R. Sambles and M.C. Hutley, “Polarization conversion through the excitation of surface plasmons on a metallic grating”, J. Mod. Opt. 37, 1227-1232 (2007)

2. L. Feng, A. Mizrahi, S. Zamek, Z. liu, V. Lomakin and Y. Fainman “Metamaterials for enhanced polarization conversion in plasmonic excitation”, ACS Nano 5, 5100-5106 (2011)

9126-56, Session 11

Study of surface plasmons at the metal/semiconductor interface

Ray-Hua Horng, Shih-Hao Chuang, Cheng-Sheng Tsung, Dong-Sing Wuu, National Chung Hsing Univ. (Taiwan); Ching-Ho Chen, Cheng-Yi Lin, National Chung Hsing University (Taiwan); Feng-Yeh Chang, National Chung Hsing University, (Taiwan)

The brightness of GaN-based light-emitting diode (LED) was successfully enhanced using surface plasmons (SPs) excited at the metal/semiconductor interface. Normally, SPs excited by the interaction between light and metal surfaces were known to enhance the internal quantum efficiency of LEDs via the quantum-wells (QW) and SPs coupling. Thus, the distance between the QWs and metallic nanoparticles was critical for SP-QW coupling. The penetration depth of SPs fringing field for the silver nanoparticle was calculated as 43.0 nm at an emission wavelength of 460 nm. However, the p-GaN layer in blue emissive GaN-based LEDs, which is a sandwich layer between the active and p-type conducting layers, must has a thickness of over 120 nm to ensure the sufficient mobility of carriers. In this study, a silver nanoparticle layer was deposited on p-GaN top layer as the grating structure. The light extraction efficiency of lateral conducting blue LED is expected to be enhanced by the surface plasmon-TM light mode (SP-TM) coupling during the localized surface plasmon resonance (LSPR). Compared to the optoelectronic performance of the conventional LED, the SP-enhanced LED shows the superior performance, even though the silver nanoparticles were placed at least 250 nm away from the quantum-well active layer. The output power of the SP-enhanced LED exhibited over 1.2 times in magnitude as compared with that of the conventional LED at 350 mA, while still keeping nearly the same current-voltage characteristic. Especially, the transmittance of silver nanoparticles on the glass substrates is higher than 85%. This indicates that the increase in output power intensity is not due to the optical reflection by the silver nanoparticle layer.

9126-57, Session 12

Single gold nanoparticles to enhance the detection of single fluorescent molecules at micromolar concentration using fluorescence correlation spectroscopy *(Invited Paper)*

Jerome Wenger, Deep Punj, Herve Rigneault, Ctr. National de la Recherche Scientifique (France)

Sensors able to detect a specific type of molecules in real-time and with high sensitivity represent a major drive for nanophotonics. In this framework, optical antennas are receiving a large interest to interface light with molecules on dimensions much beyond the optical wavelength. In this contribution, we report the use of plasmonic nanoantennas especially designed for enhanced single molecule analysis in solutions at high concentrations. Several antenna designs are investigated, including nanoparticles, nanoapertures, and antennas-in-box. Fluorescence Correlation Spectroscopy is implemented to quantify the volume reduction and the fluorescence enhancement factor. Using the dominant fluorescence emission from the nanoantenna gap region, we report detection volumes down to 58 zL, enabling the observation of a single fluorescent molecule di?using within a solution of concentration exceeding 10 micromolar along with a large enhancement of the single molecule fluorescence, up to 1100-fold. The large fluorescence enhancement and detection volume reduction combine to make nanoantennas a highly parallel platform for studying single molecule dynamics at the biologically relevant micromolar concentration regime.

References:

* D. Punj, M. Mivelle, S. B. Moparthi, T. van Zanten, H. Rigneault, N. F. van Hulst, M. F. Garcia-Parajo, J. Wenger, A plasmonic ‘antenna-in-box’ platform for enhanced single-molecule analysis at micromolar concentrations, Nature Nanotech. 8, 512-516 (2013).

* D. Punj, H. Rigneault, J. Wenger, Gold nanoparticles for enhanced single molecule fluorescence analysis at micromolar concentration, Opt. express, in press (2013).

* M. P. Busson, B. Rolly, B. Stout, N. Bonod, J. Wenger, S. Bidault, Photonic engineering of hybrid metal-organic chromophores, Angew. Chem. Int. Ed. 51, 11083-11087 (2012).

* E. Bermúdez Ureña, M. P. Kreuzer, S. Itzhakov, H. Rigneault, R. Quidant, D. Oron, J. Wenger, Excitation enhancement of a quantum dot coupled to a plasmonic antenna, Adv. Mater. 24, OP314-OP-320 (2012).

* H. Aouani, O. Mahboub, E. Devaux, H. Rigneault, T.W. Ebbesen, J. Wenger, Plasmonic antennas for directional sorting of

fluorescence emission, Nano Lett. 11, 2400-2406 (2011).

* H. Aouani, O. Mahboub, N. Bonod, E. Devaux, E. Popov, H. Rigneault, T.W. Ebbesen, J. Wenger, Bright unidirectional fluorescence emission of molecules in a nanoaperture with plasmonic corrugations, Nano Lett. 11, 637-644 (2011).

9126-58, Session 12

Development of a new optical nanobiosensor for disease diagnosis *(Invited Paper)*

Marc Lamy de la Chapelle, Univ. Paris 13 (France)

The development of reliable, sensitive and specific biosensors is a very active research field. Among all the technique, the Surface Enhance Raman Scaterring (SERS) is one of most sensitive way to detect protein [1]. It has been widely used for ultrasensitive chemical analysis down to single molecule detection. Its field of applications now includes chemical-biochemical analysis, nanostructure characterization and biomedical applications. In this work, we present the SERS detection of specific proteins and more especially specific disease biomarkers in serum, using a functionalizion layer.

To investigate the protein detection, the arrays of metallic nanoparticles were made by electron-beam lithography (EBL) to control the Localized Surface Plasmon Resonance (LSPR) position in order to obtain the best enhancement and optimise the SERS signal [2-3]. The nanoparticles were in gold with different shapes: cylinders and rods. The optimization of plasmonic nanostructures to improve their sensing properties such as their sensitivity and their easy manipulation is of first importance in order to develop highly sensitive sensor. The key point is then the optimization of the localized surface plasmon resonance (LSPR) properties especially for surface-enhanced Raman scattering (SERS). Several aspects can be considered in order to optimize the sensing performance: size and shape of the nanoparticles, nanoparticle coupling, molecular adhesion layer between gold nanostructures and glass...[4] By controlling all these aspects, we are able to produce a highly sensitive sensor. To be specific, the surface was functionalized with aptamer or anti-bodies to catch selectively the targeted protein. We have determined the sensor characterisrics such as its detection limits and its selectivity. We have determined that such sensor could be highly sensitive by reaching some detection limits lowest than the pico-molar.

In conclusion, we report that we can detect the disease biomarkers using the LSPR and the SERS. Moreover, we demonstrate that the functionalization surface assure the specificity of the biosensor and allow to detect the target protein in the serum.

The authors want to acknowledge the Nanoantenna collaborative European project (HEALTH-F5-2009-241818) for financial support.

[1] K. Kneipp, Y. Wang, H. Kneipp, L. Perelman, I. Itzkan, R. Dasari, and M. Feld, Phys. Rev. Lett. 78/9 (1997) 1667-1670

[2] J. Grand, M. Lamy de la Chapelle, J.-L. Bijeon, P.-M. Adam, A. Vial, and P. Royer, Phys. Rev. B 7, (2005) 033407, 2005.

[3] N. Guillot , H. Shen , B. Fremaux , O. Péron , E. Rinnert , T. Toury, M. Lamy de la Chapelle, Applied. Phys. Lett. 97 (2010) 023113

[4] H. Shen , N. Guillot, J. Rouxel, M. Lamy de la Chapelle, T. Toury, Optics express 20(19) (2012) 21278

9126-60, Session 12

Heat-free non-plasmonic optical nanoenhancers

Pablo Albella Echave, Imperial College London (United Kingdom); Rodrigo Alcaraz de la Osa, Univ. de Cantabria (Spain); Tyler R. Roschuk, Aliaksandra Rakovich, Mohsen Rahmani, Heykel Aouani, Imperial College London (United Kingdom); Fernando Moreno, Univ. de Cantabria (Spain); Stefan A. Maier, Imperial College London (United Kingdom)

Plasmonic structures enable control and manipulation of light in the nanoscale, allowing for strong enhancements of the electric field for interaction with molecules and materials in their vicinity. The primary materials for plasmonics are, however, metals that can inherently suffer from high losses. The effect of those losses, inherent to plasmonic structures and leading to the local heating of the particle due to the absorption of incident radiation, is an aspect often neglected despite to the fact that it is of critical importance when seeking to perform unperturbed molecular spectroscopy. In fact, theoretical and experimental studies have reported temperature increases ranging from 50K under continuous excitation to as high as 1000K using pulsed sources. This increase in the nanoparticle temperature and in turn in the temperature of the surrounding medium can directly disrupt the response of the system, due to changes in its optical properties and in the nanoparticle itself. Numerous attempts to design plasmonic materials with improved losses are being performed without clear success, by using unconventional plasmonic materials to control the permittivity of the structures. In a recent work (J. Phys. Chem. C 2013, 117, 13573), we showed that high refractive index dielectric nanoparticles, often called magnetodielectrics (MD), can enhance the electric and magnetic near- and far-field. This enhancement together with the absence of quenching of radiative emission and high quantum efficiency shown by an emitting molecule coupled to the electromagnetic modes of a dielectric nanoantenna, make these structures promising building blocks to develop surface enhanced applications.

These MD materials have at the same time established compatibility with photonic fabrication methods and more importantly they exhibit low losses, and therefore low-heat generation over broad wavelength ranges depending on the choice of material. Here we show how structures made of GaP for the visible and of GaAs for the IR offer a new way to approach applications that require near and far field enhancements, such as SERS or SEIRA, but with the peculiarity of not perturbing the response of the sample being analysed. In particular, we have compared the near and far field enhancing performance of plasmonic dimers with that of magnetodielectric ones, as well as the heat radiated from each of them, finding that even though the near field-enhancing capability of GaP nanoparticles is comparatively less intense than that provided by metallic nanoparticles, the stronger far field enhancement together with the absence of losses and therefore of heat radiation, make the proposed heat-free structures clear candidates to overcome losses and heat generation issues associated with plasmonic nanostructures for a range of applications in nanophotonics and metamaterials.

9126-114, Session 12

Investigation of the correlation between the bulk and surface sensing performance in plasmonic crystals

Jiaqi Li, Chang Chen, IMEC (Belgium) and Katholieke Univ. Leuven (Belgium); Yi Li, IMEC (Belgium) and KULeuven (Belgium); Niels Verellen, Liesbet Lagae, Pol Van Dorpe, IMEC (Belgium) and Katholieke Univ. Leuven (Belgium)

In the investigation of the sensing performance based on localized surface plasmon resonance (LSPR), the bulk sensitivity, which is the spectral shift per refractive index unit upon the change of the surrounding index to spatial infinite, is often measured and considered as the indication of the sensing ability. To the contrary, in biosensing applications only the refractive index in the confined region close to the metal nanostructure surface is altered due to the attachment of the recognition and target molecules. The correlation between the bulk and surface sensitivity is nevertheless ambiguous, especially in strongly coupled plasmonic systems, and rarely discussed in the literature. In this paper, we examine the bulk

and surface sensing performance of periodic Au nanodisk arrays on quartz substrates. By means of diffractive coupling of LSPR in the periodic arrays, the bulk sensitivity and the figure of merit (FoM) could be varied by engineering the coupling strength and adjusting the size of the Au nanodisk and the array pitch. Measured using refractive index matching oil, a bulk sensitivity of ~250 nm/RIU and a FoM as high as 30 have been achieved. The surface sensing performance is also explored by sequential atomic layer deposition of Al2O3 up to 60 nm, and the electric field decay from the Au nanodisk surface could thus be extracted using an exponential function. It is demonstrated that in these substrates the surface and bulk sensitivity have opposite dependence on the coupling strength. In spite of the high bulk sensitivity and FoM in systems with strong coupling, the low surface sensitivity is shown due to the large electric field decay length. Therefore, detailed and careful design of the coupling strength and the surface electric field to match the size of the target biomolecule is very critical for the best sensing performance. Moreover, we propose a second-order derivative to the size and the refractive index of the target molecules, and provide a more reliable biosensor design protocol based on the surface sensing performance by considering the exponentially decaying electric field.

9126-61, Session 13

Probing the radiative transition and determining the fluorescence quantum yield of a single molecules in a tunable microresonator *(Invited Paper)*

Alfred J. Meixner, Alexander Konrad, Eberhard Karls Univ. Tübingen (Germany); Alexey I. Chizhik, Jörg Enderlein, Georg-August-Univ. Göttingen (Germany)

Small optical microresonators are structures which confine light to volumes with dimensions on the order of one wavelength and hence have become increasingly important for controlling light-matter interaction in integrated optics . The ultimate limit of miniaturization for generating laser radiation is e.g. a single quantum system enclosed in an optical microresonator. While it is well known from quantum electrodynamics nowadays that the spontaneous emission is not an intrinsic process of an atom but can be modified by tailoring the electromagnetic environment, the situation for a molecule is more complex since the radiation rate and relaxation path of a molecule depend on the balance between the radiative (the far-field) and non-radiative (the near-field) relaxation paths, the later being sensitively dependent on the interaction of the molecule with the local chemical environment. Hence, by controlling the electromagnetic environment of a single molecule we select the vibronic transition where fluorescence will mostly occur and we can tune its radiative transition and determine its fluorescence quantum yield. Using a tunable optical microresonator with subwavelength spacing, we demonstrate controlled modulation of the radiative transition rate of a single molecule, which is measured by monitoring its fluorescence lifetime. Variation of the cavity length changes the local mode structure of the electromagnetic field, which modifies the radiative coupling of an emitting molecule to that field. By comparing the experimental data with a theoretical model, we extract both the pure radiative transition rate as well as the quantum yield of individual molecules. We observe a broad scattering of quantum yield values from molecule to molecule, which reflects the strong variation of the local interaction of the observed molecules with their host environment.

9126-62, Session 13

Enhanced fluorescence emission from resonant DNA assembled plasmonic nanoantennas loaded with single dye molecules

Jerome Wenger, Petru Ghenuche, Vincent Maillard, Nicolas Bonod, Sebastien Bidault, Ctr. National de la Recherche Scientifique (France)

Because of homogeneous broadening effects, single organic molecules exhibit weak absorption cross-sections at room temperature even though they feature large dipolar transition moments for their electronic excited states. We recently demonstrated, by a conjunction of time-resolved luminescence and fluorescence correlation spectroscopy, that gold nanoparticle (AuNP) dimers can be used to enhance reproducibly the excitation cross-sections and decay rates of organic dyes by more than one order of magnitude (M. P. Busson et al, Angew. Chem. Int. Ed. 51, 11083, 2012). We use 40 nm diameter AuNPs linked by a single DNA strand as short as 10 nm and electrophoretic purification to obtain a stable suspension of dimers (M. P. Busson et al, Nano Lett. 11, 5060, 2011). By controlling the number of DNA linkers, we ensure that only one quantum emitter is attached per nanostructure, allowing single photon emission with lifetimes as short as 30 ps (M. P. Busson et al, Nat. Commun. 3, 962, 2012). These nanostructures behave as the optical equivalent of a dipolar antenna driven by a single photon source. In order to optimize the quantum yield and excitation probability of these emitters, we increase the size of the AuNPs and the scattering cross-sections of the antenna in order to reach an average 44 times enhancement of the fluorescence count rate with picosecond lifetimes. We discuss thoroughly the influence of the antenna resonance on the dye fluorescence emission by considering antennas of different dimensions and different emission wavelenghts. These results correspond to unprecedented dipolar transition moments of isolated quantum emitters at room temperature, picosecond lifetimes, and bright single photon emission.

9126-63, Session 13

Terahertz emitter based on single-walled nanotube filled with fullerenes C60

Olga E. Glukhova, Anna S. Kolesnikova, Mikhail M. Slepchenkov, N.G. Chernyshevsky Saratov State Univ. (Russian Federation)

It is well known that obtaining terahertz radiation is necessary for the creation of medical diagnostic devices of new generation, scanning luggage on transport, search for explosives on their spectral composition, as well as for nanomikroskopii. There are currently developed sources of terahertz time has two significant drawbacks: they have very little power, they are very bulky size.

In this paper we were carried out simulation of terahertz emitter operating in the gigahertz and terahertz frequency ranges, based on single-walled nanotube (length 10.3 nm and a radius of 1.35 nm) filled with fullerenes C60 and spend defining the technical parameters of the radiation device. The presence of chemically bonded to each other and to the tube wall is the requirement for fullerene nanotube. These fullerenes creates a potential well for the free charged fullerene. Free fullerene can not get out of the potential well without external driving force, but it can oscillate in the potential well under the influence of an external electric field. The deformation of a carbon nanotube is observed during the formation of chemical bonds between the nanotube and polymerized fullerene. Shape of the profile of the potential well is largely determined by the degree of deformation of carbon nanotubes. Fullerene is moving with some acceleration on power lines, radiating electromagnetic waves in an external electric field.

It is found a regime in which the nanoemitter will emit terahertz

waves (C60 is charged +3e and an external electric field intensity 106 V/ cm). The oscillation frequency is 0.36 THz.

9126-64, Session 13

Absence of mutual polariton scattering for strongly coupled surface plasmon polaritons

and dye molecules with a large Stokes shift

Jussi Toppari, Univ. of Jyväskylä (Finland); Ulrich Hohenester, Karl-Franzens-Univ. Graz (Austria); Tommi K. Hakala, Aalto Univ. School of Science and Technology (Finland); Mikko Koponen, Univ. of Jyväskylä (Finland)

During the last decades surface plasmons polaritons (SPP) have attracted vast interest because of their strongly enhanced light-matter interactions, which opens routes towards optical devices beyond the diffraction limit allowing thus nanoscale integration of photonics. Of particular interest is also strong coupling between SPPs and molecular excitations (ME), which manifests itself through a formation of new SPP-ME hybrid modes exhibiting Rabi splitting even up to several hundreds of meV depending on the molecular species and concentration. These new hybrid modes could provide the missing non-linearity to enable interactions between photons/plasmons, needed for active all optical components. Also the dynamics of these modes can differ dramatically from the dynamics of either SPP or ME, and they can significantly affect the chemical properties of the molecules involved.

We have demonstrated strong coupling between SPPs and various molecules, and in all of them the fluorescence of the MEs reveals the coexistence of the strongly coupled hybrid polariton modes and non-coupled MEs. As the molecular fluorescence is directly related to the ME occupation, it provides an ideal tool for studying the polariton dynamics. Here we have utilized dye molecules with an especially large Stokes shift, i.e. Nile Red (NR), to demonstrate the absence of scatterings among the polariton branches and to show that the modes decay directly via dephasing and internal relaxation of the molecules to a fluorescing state of the dye.

The samples consisted of a thin layer of silver (Thickness ~50 nm) on a glass substrate with a polymer film (~50 nm) on top with the NR embedded in. The reflectance measurements were carried out in Kretchmann configuration with linearly polarized collimated white light as an excitation for SPPs. The reflected signal (D1) and the luminescent light (D2), i.e., out-scattered polaritons and SPPs as well as fluorescence of the MEs, were measured by a spectrometer with different excitation angles. An extra polarizer was utilized in front of the D2 measurement to separate the luminescence due to out-scattered polaritons (TM-polarized) and ME fluorescence (non-polarized). The absorption of the polymer layers on three samples with the NR/SU-8 mass ratios of ?0.2, ?0.45, and ?1, were measured separately, i.e., without the silver layer. Dispersion curves were experimentally derived for all the samples and to study the scattering dynamics via ME occupation, the fluorescence data were measured as a function of the SPP excitation angle.

We use a transfer matrix approach to compute the electromagnetic fields in the layered system, as well as the reflection and transmission coefficients, which agreed well with the measured ones. For the calculation of the molecular excitation probability we employ the Poynting vector at the interface between the silver film and the NR-doped polymer layer, which describes the transfer of energy into the molecular film. Since for the Kretschmann geometry no light can propagate on the air side, the energy transported into the molecular layer must be absorbed by the molecules, whose subsequent decay can be monitored in fluorescence. To understand better the physics of the increased energy transfer around the excitation angle of 55 degree, we employ a generic quantum mechanical three-level coupled oscillator model for the fluorescence. The model agrees well with the measurements – but only if one assumes absence of polariton scatterings.

M.A. Koponen, U. Hohenester, T.K. Hakala, J.J. Toppari, Phys. Rev. B 88, 085425 (2013).

9127-1, Session 1

Observation and use of internal water in silica photonic structures *(Invited Paper)*

Alvaro Blanco, Consejo Superior de Investigaciones Científicas (Spain)

Recently, it has been shown that silica artificial opals possess a PBG controlable by simple heating on a hot plate [1]. Submicrometer silica spheres easily form high-quality face-centered-cubic (fcc) structures displaying a Bragg peak (the lowest energy PBG) in the visible range. Given the hydrophilic character of silica, these opals inherently contain a substantial amount of molecular water (as much as 8 wt.% in as-grown samples) physisorbed on the silanol groups at the spheres surface. This water is partially placed between the spheres forming necks, leading to a nonclose-packed arrangement, so that the opal lattice parameter directly depends on the amount of water. Thus, controlled desorption of this water upon moderate opal heating induced large effects in the opal photonic properties, mostly due to shrinking of the lattice parameter in up to ~ 12 nm. Complete water removal (achieved at ~ 120 ºC) leads to a pronounced blueshift of the Bragg peak of 25 nm. PBG changes are reversible upon cooling down to room temperature (RT) by virtue of spontaneous water re-adsorption. By in situ measuring PBG behavior with temperature one can extract relevant fundamental knowledge regarding water morphology and adsorption in silica colloidal systems [2], [3]. Further, this internal water plays an important role in Azo-Molecules photo-alignment [4] or in the mechanical properties of these systems [5]. Furthermore, we have recently succeeded in observing this water by standard electronic microscopy as shown in figure 1 [6].

Once the presence of water is characterized we are able to use it for different means. The amount of adsorbed water and its distribution can be controlled by modifying the chemistry of the silica surface, from hydrophilic to hydrophobic through thermal annealing. By doing this we can acquire deep knowledge on silica chemistry and use it to tune the structure photonic response. Further, although thermal effects regarding the whole structure (sample size around some square centimeters) are usually rather slow (seconds) we can bring this response to the millisecond range by inducing local heating [7]. The opal was photoirradiated with a focused 488-nm Ar+-laser while measuring the opal reflectance spectrum in order to monitor in situ the PBG changes. Photoirradiation significantly affected the spectrum of the infiltrated opal in a reversible fashion. Under light exposure the Bragg peak shifted to shorter wavelengths (up to 13 nm) within a few milliseconds and rapidly shifted back to the original position after turning the light off. Simultaneously, the bandgap width decreased (up to 5%) during irradiation, also reversibly. Thus, the photoinduced PBG changes were fast and, without external stimulus, fully reversible, and the shift distance directly depended on the irradiation intensity I. Additionally, the overall performance was reproducible over millions of cycles. All these issues are greatly relevant for switching applications demanding not only spontaneous reverse effect but also accurate response and fidelity in a fast fashion.

References

[1] F. Gallego-Gómez, A. Blanco, V. Canalejas-Tejero and C. López, Small 2011, 7, 1838.

[2] F. Gallego-Gómez, A. Blanco, and C. López, Langmuir 2012, 37, 13992.

[3] F. Gallego-Gómez, A. Blanco, and C. López, J. of Phys. Chem. C 2012, 116, 18222.

[4] F. Gallego-Gómez, A. Blanco, D. Gomayo, and C. López, Adv. Funct. Mater. 2011, 21, 4109.

[5] F. Gallego-Gómez, V. Morales-Flórez, A. Blanco, De la Rosa-Fox, N. and C. López, Nano Letters 2012, 12, 4920.

[6] A. Blanco, F. Gallego-Gómez, and C. López, J. Phys. Chem. Lett. 2013, 4, 1136.

[7] F. Gallego-Gómez, A. Blanco, and C. López, Adv. Mater. 2012, 24, 6204

9127-2, Session 1

Optimization of LOPA-based direct laser writing technique for fabrication of submicrometric polymer three-dimensional structures

Mai Trang Do, Qinggele Li, Thi Thanh Ngan Nguyen, Isabelle Ledoux-Rak, Ngoc D. Lai, Ecole Normale Supérieure de Cachan (France)

Confocal laser scanning microscopy has been used as an ideal way to fabricate submicrometric structures. Two excitation ways have been adopted for photo-induced fabrication, namely one-photon absorption (OPA) and two-photon absorption (TPA), involving different excitation mechanisms and aiming at specific applications. The OPA excitation method is a very convenient technique to fabricate 1D and 2D thin structures, based on a simple and low-cost laser source operating at a wavelength located within the absorption band of the thin film material. 3D fabrication however requires the use of a pulsed laser (femtosecond) to induce TPA effect, which is rather expensive and complicate. However, it should be borne in mind that resist exposure is also per se a highly nonlinear process. Hence, the exposure localization by TPA is not essential to resolution. Rather, a genuine analysis reveals that the linear absorption is the true limiting factor of current OPA. In this work, we demonstrate a new way to benefit of the respective advantages of these two excitation techniques, by using a simple, low-cost one-photon elaboration method operating in a low absorption regime [1]. Indeed, on one hand, when the material presents very low linear absorption at a chosen excitation laser wavelength, the light intensity of a collimate light beam keeps almost unchanged through the propagation inside the material. On the other hand, by using a high a numerical aperture objective lens (NA OL), the light beam will be tightly focused, resulting in a very high intensity at the focusing spot. We have demonstrated that by using a photosensitive polymer (SU8) possessing an ultralow one-photon absorption (LOPA) coefficient at the exciting laser wavelength (532 nm) and a high NA OL, various 2D and 3D submicrometric structures with feature size as small as 150 nm have been successfully fabricated [2]. We have further investigated the energy accumulation effect in LOPA direct laser writing when the structures lattice constant approaching the diffraction limit. In this case, a proximity correction, i.e., a compensation of the dose between different voxels, is applied, allowing to create uniform and submicrometric structures with lattice constant as small as 400 nm. As compared to commonly used two-photon absorption microscopy, the LOPA method allows to simplify the experimental setup and also to minimize the photo-damaging or bleaching effect. The idea of using LOPA also opens a new and inexpensive way to address optically 3D structures, namely 3D fluorescence imaging.

1. Q. Li, M. T. Do, I. Ledoux-Rak, and N. D. Lai, “A novel concept for three-dimensional optical addressing by ultralow one-photon absorption method,” Opt. Lett. 38, in press (2013).

2. M. T. Do, T. T. N. Nguyen, Q. Li, H. Benisty, I. Ledoux-Rak, and N. D. Lai, “Sub-micrometer three-dimensional structures fabrication enabled by one-photon absorption direct laser writing,” Opt. Express 21, 20964 (2013).

9127-3, Session 1

Fabrication of polymer inverse opals with linear and nonlinear optical functionalities using a sandwiching approach

Pieter-Jan H. M. Demeyer, Stefaan Vandendriessche, Stijn van Cleuvenbergen, Sophie Carron, Tatjana N. Parac-Vogt, Thierry Verbiest, Koen Clays, Katholieke Univ. Leuven (Belgium)

Three-dimensionally (3D) ordered macroporous materials combine interesting structural and optical properties. Accessible and economic fabrication is essential to fully explore the unique possibilities these materials present. A common method to fabricate 3D ordered macroporous materials is by self-assembling colloids, resulting in so-called opals. A templating strategy is often used to introduce additional functionality inside the porous structure, giving rise to inverse opals.

In this work, we developed an easy and versatile method to fabricate highly uniform polymer inverse opals without overlayers. Briefly, our approach consists of sandwiching a resin melt between two opal templates, forcing all material inside or between the macroporous structures. The opal voids are fully filled and the superfluous melt material is extruded before curing the resin. Finally, the opal templates are removed by chemical etching. The resulting structures are freestanding 3D macroporous films with large-area uniformity, displaying strong photonic properties due to their structural order. Additionally, many applications require specific optical functionalities. The versatility of our templating method is uniquely suited for this purpose as it allows doping of the melt before infiltration. Therefore, we can incorporate a large variety of optical functions in the inverse opals using a single approach.

We believe this method will help the systematic investigation and improvement of existing effects in these structures, while providing a platform for the discovery and demonstration of novel effects. As this method combines 3D ordered macroporous materials with linear and nonlinear optical materials, it is even possible to tune optical interactions, which could be technologically relevant for OLEDS, solar cells, lasers, electro-optical modulators and optical switches.

9127-4, Session 1

Development of photonic crystal structures for on-board optical communication

Umar Khan, John Justice, Tyndall National Institute (Ireland); Arjen Boersma, TNO (Netherlands); Judith Wijnhoven, Utrecht Univ. (Netherlands); Maurice C. D. Mourad, Renz J. van Ee, TNO (Netherlands); Alfons van Blaaderen, Utrecht Univ. (Netherlands); Brian Corbett, Tyndall National Institute (Ireland)

In recent years 3D colloidal crystals have been made and assessed for use in all kinds of optical applications. Several manufacturing strategies have been evaluated ranging from controlled drying to slow sedimentation and spin coating. Although the possible applications are promising, many processes lack the manufacturing speed and flexibility in crystal structures to make implementation into optical communication feasible. In this paper, we present the modelling, manufacturing and characterization of colloidal crystals grown from silica and titania dispersions on structured seed layers. Particular attention is given to Photonic Crystal (PhC) based stuctures suitable for compact on-board optical functions implemented using single mode polymer waveguides at a wavelength of ?=1.55 μm. The use of polymer waveguide materials, with typical refractive indices of ~1.5, guides the choice of colloidal crystals.

In order to manipulate light appropiately in optical structures, the PhC must be manufactured with sufficient refractive index contrast between particle and matrix with careful control of the orientation of the crystal planes.Polymers necessitate the use of high refractive index titiana particles (n~2.4) in PhCs. The titania “core” particles are surrounded by a silica “shell”, n~1.45, allowing independent variation of both the diameter of the high refractive index particle and PhC lattice constant.

Dispersions of monodisperse nanoparticles left to sediment freely, cannot control the crystal type since the first two layers will be stacked hexagonally, but the third can grow in either of two ways leading to a combination of two crystal forms: ABABAB (=HCP) and ABCABC (=FCC). We present a method for the controlled colloidal crystallization through a combination of a well defined structured surface and two deposition techniques: a slow sedimentation process and a relatively fast “printing” process in which a dispersion of nanoparticles is moved over the seed layer, leaving the particles in the cavities of the structure, thus creating multilayer arrays. The structured surface or “seed”layer is manufactured using nanoimprint lithography. The depth and pitch of this seed layer guides the deposition and crystallization of the particles in the required crystal structure: which is FCC in our case, but using a square base layer. Initial work focuses on the controlled growth of PhCs made of Silica particles with subsequent work focusing on titania-silica core shell particles.

Finite-Difference Time-Domain (FDTD) modelling of a Titania-Silica core-shell PhC based on an FCC structure has been used to design a PhC for a compact in-plane reflector. Core-shell diameters are optimised to maximise reflectance for the wavelengths of interest. Simulations predict reflection of 80% at a wavelength of 1.55 μm. The effects of incident light polarisation were noted. Colloidal crystals grown on the seed layers have been characterized using optical (fluorescent) microscopy and SEM, in order to see the stacking of the particles. These analyses showed that the pitch of the seed layer imprint should match the size of the monodisperse particles within a few %. Interrogation of optical characterisics (reflection, polarisation dependance, etc) using larger (mm) and smaller spot-sizes, on the order of the domain, was carried out on the constructed PhCs.

9127-5, Session 1

Rolled-up TiO2 microtubes for photonics applications

Silvia Giudicatti, Sonja M. Marz, Stefan Böttner, Barbara Eichler, Matthew R. Jorgensen, Leibniz-Institut für Festkörper- und Werkstoffforschung Dresden (Germany); Oliver G. Schmidt, Leibniz-Institut für Festkörper- und Werkstoffforschung Dresden (Germany) and Technische Univ. Chemnitz (Germany)

In the last decades, great attention has been focused on titania (TiO2) because of its unique properties, including high chemical stability, high refractive index, optical transparency in the visible, semiconducting behavior, photocatalytic activity, high photoelectric conversion efficiency, and biocompatibility. While titania has been widely explored in many different fields, it has been only recently introduced to the world of rolled-up nanotechnology.[1, 2] We systematically investigated the behavior of titania within this context. In particular, we show how the structural parameters (tube diameter and tightness of the windings) of the titania microtubes, as well as the titania phase and refractive index, can be controlled by properly tuning the microfabrication parameters and via post-rolling processes. The etching of titania deposited under different conditions is also under investigation.

The fabrication of microtubes via rolling of several different materials has already been successfully applied to the development of sensors, micromotors, batteries, as well as in the fields of electronics and photonics. The combination of titania with rolled-up nanotechnology paves the way for interesting novel applications. For example, high refractive index tight microtubes represent a promising candidate as high performance 3D microresonators. Another exciting application is related to the field of photonic crystals. 3D photonic crystals promise to offer unprecedented opportunities in controlling light. However, their fabrication requires

sophisticated techniques mainly resulting in devices operating in the near IR or longer wavelengths. In the visible, examples are limited to partial band gap devices and systems achieved via biotemplating. Although biotemplating represents an interesting alternative to conventional fabrication techniques, it is limited by the inherent defects and small size of natural photonic crystals. Recently, we proposed a novel method for the fabrication of 3D photonic crystals operating in the visible based on the rolling of pre-patterned 2D membranes. [3] A combined control of the structural parameters such as membrane thickness, geometry of the 2D lattice and rolling direction allows to access a variety of architectures, including diamond and diamond-like structures. Band structure and DOS calculations were performed to identify the structural parameters resulting in the best band gap. A full band gap was found in a <100> stacked diamond lattice with a refractive index larger than 2.3. This value has been proven to be accessible using titania. The influence that finite size and bending have on a band gap was also explored.

[1] V. Y. Prinz, V. A. Seleznev, A. K. Gutakovsky, A. V. Chehovskiy, V. V. Preobrazhenskii, M. A. Putyato and T. A. Gavrilova, Physica E 2000, 6, 828.

[2] O. G. Schmidt and K. Eberl, Nature (London) 2001, 410, 168.

[3] M. R. Jorgensen, S. Giudicatti and O. G. Schmidt, Phys. Rev. A 2013, 87, 041803.

9127-6, Session 2

Photonic topological insulators *(Invited Paper)*

Mikael C. Rechtsman, Technion-Israel Institute of Technology (Israel); Julia M. Zeuner, Friedrich-Schiller-Univ. Jena (Germany); Yonatan Plotnik, Yaakov Lumer, Mordechai Segev, Technion-Israel Institute of Technology (Israel); Alexander Szameit, Friedrich-Schiller-Univ. Jena (Germany)

Abstract: I will present the experimental demonstration of topological insulators (TIs) where the propagating field is electromagnetic (in this case, visible light), rather than electronic. In solid-state TIs, topological protection is achieved by virtue of the Kramers degeneracy, which doesn't apply to photons (since they are bosons). Therefore, another mechanism is required. Theoretical proposals for achieving photonic TIs have included: aperiodic coupled resonator arrays; coupled optical cavities; birefringent metamaterials; and temporally modulated photonic crystal slabs. Our system, which is quite distinct from the previously proposed structures, is composed of an array of evanescently-coupled helical waveguides arranged in a honeycomb lattice. In this system, light diffracts according to the Schrödinger equation, where the time coordinate is replaced by the distance of propagation, and the waveguides act as potential wells. The helicity of the waveguides induces a fictitious, time-varying electric field, and the structure thus becomes equivalent to a Floquet TI. The resulting 2+1-dimensional "photonic lattice" exhibits topologically protected edge states, and we demonstrate their presence and probe their properties experimentally. I will show a number of consequences of topological protection, such total absence of backscattering at sharp corners, and scatter-free propagation around edge defects. Our setting can potentially allow for the study of mean-field interactions (through optical nonlinearity), and the effects of highly tunable disorder in TIs. Photonic TIs have been suggested for a number of applications, including highly robust optical delay lines, on-chip optical diodes, and spin-cloaked photon sources.

9127-8, Session 2

Influence of external electric field on laser-induced wave process occurring in semiconductor under the femtosecond pulse acting

Vyacheslav A. Trofimov, Mariya M. Loginova, Vladimir A. Egorenkov, Lomonosov Moscow State Univ. (Russian Federation)

We analyze laser-induced periodic structure developing in a semiconductor under both femtosecond pulse and external electric field acting. Optical bistability appears because of nonlinear dependence of semiconductor absorption coefficient on charged particles concentration caused by both the Fermi energy level renormalization and the Burstein-Moss effect. The electron mobility, diffusion of electrons, and laser-induced electric field are taken into account for laser pulse propagation analyzing in semiconductor.

We found out that an external electric field could induce complicate motion of a high absorption domain in semiconductor. In certain case, it causes the charged particles drops developing.

9127-9, Session 2

Coherent Cerenkov emission from electrons streaming through a photonic crystal

Peter J. M. van der Slot, Thomas Denis, Joan H. H. Lee, Marc W. van Dijk, Klaus J. Boller, Univ. Twente (Netherlands)

Cerenkov radiation is usually incoherent radiation emitted by charged particles when they pass through a medium with sufficiently high, usually relativistic velocity. It has recently been shown that in photonic crystals Cerenkov emission is possible without a velocity threshold, however emission from electrons streaming through the crystal typically remains incoherent.

Here we show that sufficiently strong feedback between the electrons and the Cherenkov radiation results in coherent emission. The coherent amplification results in a growth of the power by many orders of magnitude, from incoherent emission to saturation in the kW-range. This concept to directly generate coherent radiation with free-electrons in a photonic crystal forms a novel type of coherent radiation source, which can be termed a photonic free-electron laser. The required increase in feedback is obtained via properly designing the photonic crystal. Specifically, the structure is chosen to strongly reduce the phase velocity of a low order spatial harmonic of the radiation field to match it to the electron velocity. Additionally, the structure is chosen to maximize the electric field component in the propagation direction, to provide maximum bunching of the electrons and thereby generate strong stimulated emission.

This laser has several unique properties. First, the laser output frequency can be continuously tuned by varying the electron velocity. Second, as the photonic crystal has many natural channels for the electron beam in parallel, adding more electron beams increases the output power while still maintaining full transverse coherence. Finally, due to the scale invariance of Maxwell's equations, downsizing the photonic crystal structure by a certain factor scales up the frequency of the laser by the same factor, without requiring a change in velocity of the electrons.

Here, we demonstrate the principle physics behind this device and illustrate this with numeric results obtained with a so-called particle-in-cell simulation code for a device working in the microwave spectral region.

9127-10, Session 2

Shape-memory effect for self-healing and biodegradable photonic systems

André Espinha, Instituto de Ciencia de Materiales de Madrid (Spain); Maria Concepción Serrano, Hospital Nacional de Parapléjicos (Spain) and Instituto de Ciencia de Materiales de Madrid (Spain); Álvaro Blanco, Cefe López, Instituto de Ciencia de Materiales de Madrid (Spain)

Photonic systems with the ability to respond to different stimuli are more and more desirable for achieving high levels of performance. They demand materials with high responsivity that may eventually be used for integrating sensing and actuating functions, a feature highly pursued in technological applications.

A notable property which is being gradually incorporated in this kind of multifunctional materials is the shape memory effect (SME), especially due to the fact that it allows the development of self-healing devices. This effect is particularly useful in polymers (shape memory polymers – SMPs), that present the ability to switch from a temporary to a permanent shape as a response to an external action.

Although it has been previously shown that the shape memory effect can be induced at nanoscale, and thus it is possible to control the topology of a surface, only few studies have addressed the application of this effect for the development of photonic applications.

In this work, a material system consisting of a two-dimensional photonic crystal (PC) imprinted in the surface of a SMP is reported. It integrates several interesting features such as thermoresponsivity, elasticity, shape memory and read/write capability. The referred PC consists of a hexagonal lattice of nanobowls, transferred to the SMP's surface using a replica molding based procedure. Good quality and large extensions of photonic crystal were achieved. They were characterized with atomic force and scanning electron microscopies from the structural point of view. From the optical point of view, the characterization of the first order Bragg diffraction angle was carried out.

The as fabricated system presented programmable character, the responsible mechanism triggering SME being the temperature. By heating the sample above the SMP transition temperature and applying mechanical deformation, it is possible to induce a temporary shape which on its turn is conserved after cooling below the transition temperature. Re-heating of the sample allows the recovery of the initial state.

In this way, two proofs of concept are introduced that demonstrate the direct impact of SME on the photonic properties of the sample. The first one shows that it is possible to configure the lattice parameter of the nanostructure, which translates as a change in the diffraction angle of the radiation impinging the PC. The behavior of the diffraction angle as a function of the strain imposed to the sample is well described by a simple theoretical model. The second proof of concept shows that it is possible to temporarily erase the nanopattern by compressing the sample between two surfaces. The topological periodic modulation of the surface becomes much smaller than the wavelength and thus Bragg diffraction is precluded.

The reported system presents some interesting additional features. The SMP selected for replicating the PC was a polydiolcitrate which are known to be biocompatible and biodegradable. Thus we expect that the system described herein might find application in biophotonics or in the development of disposable devices with minimum environmental impact.

9127-55, Session 2

Partial cloaking by graded index photonic crystals

Bilgehan B. Oner, Melih G. Can, Hamza Kurt, TOBB Univ. of Economics and Technology (Turkey)

Since the first proposal of the idea of cloaking, huge research effort has been spent to implement hiding objects by various methods.We propose a broad band all-dielectric partial (single-way) cloaking device that hides an arbitrary shaped object. The cloaking structure is designed utilizing graded index (GRIN) photonic crystals (PCs). Refractive index distribution of the structure is chosen as hyperbolic secant profile. In order to generate the desired GRIN profile, both high (n=3.46) and low (air) dielectric backgrounds are chosen. The lattice types of the GRIN PC profiles are determined to consist of hexagonal symmetry (triangular lattice) for high dielectric and square lattice for air background.The transmission efficiencies of both GRIN PC cloaking devices without inserting any additional layers is about 80%. Therefore, anti-reflection coating (ARC) is implemented for both input and output sides of the devices in order to increase the transmission efficiency over 90%. The radii of the ARC air holes (for dielectric background) and locations of the ARC dielectric rods (for air background) are determined with respect to quarter wave coating method.

The main principle of the cloaking in the study is separating the beam into two main parts while propagating through the composite device. Each part of the separated beam focuses at the center of the stacked GRIN devices. Then these beams converge again without deteriorating the planar input field profile. This mechanism dramatically reduces the intensity at the center of the device. Therefore, existence of an object at the cloaked region almost does not affect wavefront of the exiting beam due to this light manipulation mechanism. In this manner, an observer can not detect the hidden object.

The complementary design to hide an object in air background can be realized by incorporating dielectric rods in air background. GRIN medium is a special type of inhomogeneous environment and light propagation is greatly affected by the presence of GRIN. Any partial solution as long as being practical and broadband in nature can be preferred. In this case, material selection and easy transferring the design to other electromagnetic regions become crucial. Therefore, the proposed idea in this work collects these desirable features.

9127-11, Session 3

Analysis and global optimization of photonic crystal structures *(Invited Paper)*

Vincenzo Savona, Ecole Polytechnique Fédérale de Lausanne (Switzerland)

No Abstract Available

9127-12, Session 3

High-Q filled slot photonic crystal cavities on SOI for hybrid photonics

Charles Caer, Xavier Le Roux, Eric Cassan, Institut d'Électronique Fondamentale (France)

Photonic crystals cavities have the unique property of confining light in wavelength-size volumes with very small losses. This remarkable property has led to a wide span of applications, such as dynamic control of light trapping in high-Q nanocavities, Raman lasing in photonic crystal cavities or quantum ground state cooling in optomechanical crystals. The tightly confined optical field is also beneficial for low-power operations, illustrated by optical RAM in photonic crystal cavities. In the same time, silicon is a widely used material for photonics thanks to its CMOS compatibility, but suffers from large nonlinear losses, particularly in enhanced optical field devices such as waveguides and cavities. Several works based on the concept of slot waveguide have overcome this limitation by confining the light in a low index material and exploiting this feature to strongly enhance nonlinearities.

In this context, we report the design, fabrication, and the experimental realization of high-Q slot photonic crystal cavities on SOI infiltrated by a liquid as a proof-of-concept towards hybrid silicon photonic devices based on such nanoscale resonators. Loaded Q-factor of 23,000 is measured at telecom wavelengths. The intrinsic quality factor inferred from the transmission spectrum is higher than 200,000 whereas the maximum of intensity of the cavity is as high as 20% of the light transmitted in the waveguide in the bandpass wavelength range. This result makes the demonstrated filled slot photonic crystal cavities very promising for the integration of various active materials for light amplification, nonlinear optics, or sensing.

9127-13, Session 3

Phase shift multiplication effect in coupled photonic crystal cavities system

Boyun Wang, Tao Wang, Wuhan National Lab. for Optoelectronics (China)

In the last decades, a great effort has been devoted to the integration of optical components on a single chip. The miniaturization of non-reciprocal devices, key elements to reduce the power consumption and allow serial integration of active and passive photonic components, is very challenging and has attracted a great deal of attention.

Quantum coherence in atomic systems has led to fascinating and counterintuitive outcomes, such as laser cooling, trapping of atoms, and Bose-Einstein condensates. In electromagnetically induced transparency (EIT), the quantum destructive interference between excitation pathways to the upper level in three-level atomic systems has led to sharp dips of absorption in the medium, resulting in phenomena such as lasing without inversion and freezing light, and dynamical storage of light in a solid state system. EIT was originally observed in atomic vapors, yet the narrowness of the EIT window and the complexity of constructing atomic systems restrict the practical use of the EIT effect.

To make better use of the EIT effect, classical all-optical EIT-like has been realized on various platforms, including photonic crystal waveguides and micro-cavities, coupled resonance induced transparency (CRIT) systems, and plasmonic nanostructures. For EIT-like, the narrow transparency peak in the transmission spectrum is associated with a large group delay, which has been experimentally measured in a two-microcavity system. For optical analog to EIT of two micro-cavities side coupled to a waveguide system, each optical resonance with frequency of ?A and ?B from two optical resonators is analog to the transitions between the energy levels in the atomic EIT system. The coupling strength ?c between the two resonators acts as the control laser field, which is determined by the frequency detuning (?A-?B). The coherent interference between two optical pathways will introduce EIT transparency region between two resonances ?A and ?B. Recently, the different phase shifts of the transmission spectrum in 2-D photonic crystal two micro-cavities have been obtained. However, phase shift multiplication effect in two micro-cavities side coupled to a waveguide system is found in our work. This effect can be applied to microstructure integration photonic devices to solve the problem of the high power consumption.

In this paper, we propose phase shift multiplication effect of all-optical analog to electromagnetically induced transparency (EIT) in coupled photonic crystal cavities system through external optical pump beams. With dynamically tuning the propagation phase of the line waveguide, the phase shift of the transmission spectrum in coupled photonic crystal cavities system is doubled along with the phase shift of the line waveguide. ϖ-phase shift and 2ϖ-phase shift of the transmission spectrum are obtained when the line waveguide is tuned to 0.5ϖ-phase shift and ϖ-phase shift, respectively. Phase shift multiplication effect and the all-optical Mach-Zehnder Interferometer (MZI) switch are combined to verify a novel all-optical switch. We show that the energy of all-optical switch for yielding ϖ-phase shift is reduced by 55.13% compared with the situation without phase shift multiplication effect. All observed schemes are analyzed rigorously through finite-difference time-domain simulations and the coupled-mode formalism. These results show a new direction to the low power consumption of microstructure integration photonic devices in optical communication and quantum information processing.

This paper is organized as follows. Section I gives an introduction. Section II gives the simplified model to realize EIT-like effect and analyzes the related theory. Section III proposes phase shift multiplication effect in coupled photonic crystal cavities system and demonstrates an all-optical MZI switch based on phase shift multiplication effect of EIT-like. Conclusions are given in Section IV.

9127-14, Session 3

A Bloch modal approach for engineering waveguide and cavity modes in two-dimensional photonic crystals

Jakob R. de Lasson, Philip Trøst Kristensen, Jesper Mørk, Niels Gregersen, Technical Univ. of Denmark (Denmark)

In micro- and nanostructured media, such as micropillars and photonic crystals (PhCs), characteristic feature sizes are on the order of the wavelength of light which makes analysis of light propagation in these systems intricate. Analysis and design of such structures therefore rely on an interplay between theory, computations and fabrication, and to avoid design and analysis based on trial-and-error transparent and efficient numerical methods are indispensable. Popular choices include spatial discretization techniques like the finite-difference time-domain (FDTD) and the finite element method (FEM).

In this work, we present an optical modeling scheme based on the Fourier Modal Method (FMM) [1] and a scattering matrix approach (SMA) [2]. As opposed to the aforementioned spatial discretization methods, the FMM and SMA provide direct physical insight into the reflection and transmission between different optical modes, and as an example these techniques have successfully been applied to design efficient single-photon sources [3]. In periodic structures like distributed Bragg reflectors (DBRs) and PhCs, Bloch modes obeying the periodicity may readily be computed with the FMM and SMA framework [4], giving both the associated Bloch mode field distributions and their dispersion relations.

We employ the FMM and SMA techniques to study two-dimensional PhCs, both with rectangular and triangular lattices. Specifically, we analyze W1-waveguides in PhCs and by introducing a cavity in the bulk of the PhC, in the vicinity of the W1-waveguide, a frequency dependent mirror is created. The high reflection of this mirror is associated with the excitation of a cavity mode, and we present a scheme for determining this cavity mode and its associated complex mode frequency and Q-factor. The scheme uses no external excitation and an outgoing wave boundary condition (BC) and determines the cavity mode as a unity eigenvalue of the associated cavity roundtrip matrix [5]. Analytic spatial dependence in the propagation direction and the periodic Bloch mode condition allow to satisfy the outgoing wave BC in an infinitely extended PhC without using artifical absorbing BCs, and to the best of our knowledge cavity modes in PhCs have not been determined as presented in this work before. The analysis of complex frequency modes in PhCs using a Bloch modal approach may also be used for analyzing lossy or active structures, e.g. for understanding and designing slow light devices [6].

References:

[1]: M. G. Moharam et al., J. Opt. Soc. Am. A 12, 1068-1076 (1995)

[2]: L. Li, J. Opt. Soc. Am. A 13, 1024-1035 (1996)

[3]: N. Gregersen et al., IEEE J. Sel. Top. Quantum Electron. 19, 9000516 (2013)

[4]: Q. Cao et al., J. Opt. Soc. Am. A 19, 335-338 (2002)

[5]: N. Gregersen et al., IEEE J. Quant. Electron. 46, 1470-1483 (2010)

[6]: J. Grgi? et al., Phys. Rev. Lett. 108, 183903 (2012)

9127-15, Session 3

Room-temperature continuous wave operation of nanobeam laser on sapphire substrate

Indra Karnadi, Jaehyun Son, Ju-Young Kim, Bumki Min, Yong-Hee Lee, KAIST (Korea, Republic of)

In this work, we demonstrate RT CW operation of PhC laser based on nanobeam structure. The nanobeam was fabricated on 280-nm-thick InGaAsP slab which contained of three quantum wells in the middle as an active medium. By using transfer printing processes, the nanobeam was integrated on sapphire substrate. From this structure, single mode lasing at 1570 nm with threshold pump power of ~150 ?W was achieved. The integrated structure has theoretical Q-factor and mode volume of 200,000 and 0.2(?/n)^3, respectively. This high Q-factor and small mode volume are beneficial for reducing the threshold pump power. The present of sapphire, which has superior thermal conductivity at room-temperature, as the substrate gives better heat dissipation for the nanobeam. As a result, CW operation of the nanobeam at RT was achieved.

9127-46, Session PS2

The linear and nonlinear optical properties of ZnS-PMMA composite

Abderrahmane Chaieb, Abdelhamid Chari, Univ. Constantine 1 (Algeria); Bouchta Sahraoui, Univ. d'Angers (France)

In this paper we report linear and non linear properties of thin films based on ZnS, nanocrystals dispersed into centro symmetric and transparent polymer matrix the Polymethyl-Methacrylate (PMMA). Samples were prepared from colloidal solution and deposited in glass substrate by spin coating technique .The resulting samples are characterized by UV?visible spectroscopy, the absorption spectrum exhibit a blue shift equal to 0.82 eV compared to the gap of respective bulk material. The nonlinear optical properties are also exploited by the techniques of SHG using Nd: YAG laser at 1064 nm in picoseconds regime and transmission mode. It follows from this analysis an increase of nonlinear parameters represented by the second order effective susceptibility (?2eff,) due to the size reduction that induces a quantum confinement effect and also due to the surface effect.

9127-47, Session PS2

Improvements to crystal quality of sapphire grown by the Kyropoulos method

John P. Ciraldo, Rubicon Technology Inc. (United States)

High quality sapphire demonstrates properties that are of great interest to a wide range of industrial and academic applications. For example, relatively flat transmission across a wide range of wavelengths makes sapphire very useful in optical applications. As one of the hardest material in nature, sapphire is also quite useful in applications where resistance to chemical decomposition, radiation damage, and mechanical wear are important concerns.

While the past few decades have seen great strides in improving the quality of synthesized sapphire, the material still tends to suffer from quite high defects as compared to silicon, for example. To address this concern, Rubicon Technology has been diligently working on methods to improve not only the crystal growth process, but also to gain better control over the alumina source material that is being utilized to produce sapphire boules. To achieve the latter goal, Rubicon has moved away from the industry standards, creating an integrated approach to sapphire production where we control the entire process from alumina purification to polishing the finished substrates. This unified approach allows for much better control of impurities and final material quality.

In this talk I will demonstrate advances that Rubicon Technology has made in sapphire quality that far exceed what is currently available through other manufacturers. Improvements to the growth process, as well as increased control over supply material have allowed Rubicon to consistently grow sapphire demonstrating rocking curves with FWHM values less than 9 arc-seconds, as verified by Argonne National Laboratory. Moreover, etch pit density and x-ray topography results verify near defect free crystals. Optical characterization confirms transmission near or at maximum theoretical values across a broad range of wavelengths from deep UV to far IR. Additionally, comparisons to other industry leaders will be presented in order to provide further confirmation that Rubicon is currently creating material that is of significantly better quality that what is currently available elsewhere. In fact, the dramatic improvements in crystal quality achieved by Rubicon are already allowing for sapphire to be used in sensor technologies where sapphire was previously unusable due to high defects.

9127-48, Session PS2

Wideband slow light with improved NDBP values in asymmetric photonic crystal waveguides

Bo Liu, Tao Wang, Wuhan National Lab. for Optoelectronics (China); Boyun Wang, Wuhan National Laboratory for Optoelectronics,Huazhong University of Science and Technology (China)

Slow light has recently regained vitality for it's extensive potential applications, such as ultrafast all-optical signal processing, quantum computing, and enhancement of light-matter interactions. Photonic crystal, particularly constructed in a silicon-on-insulator (SOI) slab, is among the most optimal structures for achieving slow light in a waveguide formation. The slow light in photonic crystal waveguide (PCW) enhances the light-matter interaction, and reduces either the active length or the optical energy required for obtaining the same linear and nonlinear effect compared with the fast light regime. However, as the group velocity decreases, the pulse shape envelop will become broader and more asymmetric. This effect is called group velocity dispersion (GVD). In order to reduce the effect of GVD and obtain a wider bandwidth, many structures have been studied recently, such as chirping the waveguide property, infiltrating dielectric material, changing the holes size, and adjusting the holes positions. From the aspect of fabrication processes, adjusting the holes position is the best choice. Firstly, it is important to emphasize the concept of the normalized delay-bandwidth product (NDBP), which characterizes the compromise between the light slowing down factor and bandwidth.

In our study, asymmetric slotted photonic crystal waveguides (SPCW) are proposed to achieve slow light with improved normalized delay-bandwidth product (NDBP) and low group velocity dispersion. The slow light performance of our structures is improved for both the W1 defect mode and the slot mode, whereas previous studies only optimized for one of the modes. The basic structure of SPCW is constructed in a SOI substrate (n=3.46) by replacing the central row of air holes (radii r=0.34a) with a narrow air slot (slot width ?s=0.28a) in a triangular lattice photonic crystal. We employ the 2D plane wave expansion method to study the structure and the effective index of 2.9 is used for the 210nm thick slab. In numerical simulation, supercell size is set to 2a?11a and waveguide width is √3a, where a is the lattice constant (a=430nm). The mechanism for the slow light effect can be explained from a simple 1D grating perspective. The holes on each side of the line defect can be understood as period constrictions; the waveguide is narrow where there is a hole and is wider where there is not. A standing wave forms at the Brillouin zone boundary where the Bragg condition(i.e.?/2=a,where a is the period) occurs. In

our simulations, the asymmetry is obtained by shifting the two rows of air holes and results in a redistribution of the effective index of the waveguide and the electromagnetic field. The modification of the first row of air holes has a strong effect on the index guided mode. While the displacement of the second row has a stronger effect on the gap guided mode. Thus the modifications influence the position and strength of the anticrossing between the index guided mode and gap guided mode. Before we use asymmetry, we also studied some symmetric cases in our simulations. The influence of the symmetric case to the distribution of the effective index along the waveguide is not as efficient as the asymmetric case, and can not satisfy our needs of both the W1 and slot mode. So we fix the asymmetric procedure to achieve slow light of both the W1 mode and slot mode.

By using 2-D plane wave expansion (PWE) with a resolution of 36 pixels/a (a is the lattice constant), we engineer the dispersion curves of both the W1 defect mode and the slot mode , among which the former has received more interests for its easier coupling from/to a photonic nanowire. The slow light performances are shown here comparing with the previous published results in terms of the NDBP and bandwidth values. The conversion of the “flat band” from band-up slow light to band-down slow light is achieved for W1 defect mode. The group index curves of W1 defect mode are changed from U-like to step-like and high NDBP values of 0.223, 0.21, and 0.192 are obtained, respectively. For a special configuration, the NDBP value has been improved by 163% compared to previous results of W1 mode. Then, we engineer the band curves of the slot mode and also obtain a high NDBP of 0.168, 0.163, and 0.133, respectively. The slow light performance is optimized for both the W1 mode and the slot mode in our asymmetric SPCW. Then the low dispersion slow light performance is numerically demonstrated by 2D finite-difference time-domain method. The results in our study reveal powerful potential for further practical applications such as optical sensors, optical switches and dispersion compensation.

9127-50, Session PS2

Redistributed photon density of states influence on Raman scattering enhancement in hybrid metal-dielectric photonic crystals

Sriram Guddala, Univ. of Hyderabad (India); Vijaya P. Gaddam, Indian Institute of Technology Delhi (India); Narayana R. Desai, Univ. of Hyderabad (India)

The rate of spontaneous emission or the probability of elastic/inelastic scattering is defined by the dependency on the density of electromagnetic modes (photon density of states (DOS)) of a given quantum system [1]. The photon DOS can be defined as number of energy states per unit volume per unit energy interval (?E). The role of such photon-DOS influence on various physical mechanisms has been studied to a wide extent in various confined structures, like microcavities, dielectric slabs, etc, [2].

The photonic crystal (PhC) structures, called periodic dielectric materials with the intriguing photonic band gap (PBG) property, are well-known with enhanced photon DOS for the frequencies of PBG edge and embedded defect state [1]. Here in our studies we focused in detail to probe enhanced optical field strengths, resulted from these redistributed photon DOS of 3D and 1D hybrid metal-dielectric PhCs and microcavities respectively, through wavelength scanned and angle resolved Raman scattering studies [3]. We adopted simple sol-gel and electrochemical etching techniques to fabricate new class of hybrid metal-dielectric PhCs: one of this kind are gold nanoparticles (Au NPs) dispersed inverse silica opal structures for the band edge studies and the second are multilayered porous silicon microcavity structures with Au NPs dispersion for defect state studies. The intense optical field strengths and enhanced Raman signals are explained through photon-photon, photon-plasmon and photon-phonon interaction mechanisms. These results are further supported by electric field confinement simulations from transfer matrix method.

References:

[1] S. V. Gaponenko, “Effects of photon density of states on Raman scattering in mesoscopic structures,” Phys. Rev. B 65(14), 140303 (2002).

[2] P. R. Berman, Cavity quantum electrodynamics, Academic Press, Boston (1994).

[3] S. Guddala, S. A. Kamanoor, A. Chiappini, M. Ferrari, and N. R. Desai, “Experimental investigation of photonic band gap influence on enhancement of Raman-scattering in metal-dielectric colloidal crystals,” J. Appl. Phys. 112(8), 084303–084303–7 (2012).

9127-51, Session PS2

Silicon dioxide nanoporous structure with liquid crystal for optical sensors

Orest Sushynskyi, Lviv Polytechnic National Univ. (Ukraine); Maria Vistak, Lviv National Medical Univ. (Ukraine); Zenon Gotra, Zinoviy Mikityuk, ANDRIY FECHAN, Lviv Polytechnic National Univ. (Ukraine)

Nanoporous materials are characterized by pores with different size and shape depending from technology. The nanopores size changes from 10 to 100 nanometers, and shape changes from spherical to cylindrical. Such nanoporous materials can be used as host matrix. As guest the organic and inorganic materials can be doped in such pores, and optical characteristics are changed of these porous materials. It is permits to use nanoporous materials doped by organic or inorganic materials as primary transducer for optical sensors.

In paper we demonstrate the results of spectral characteristics studies of nanoporous silicon dioxide doped by liquid crystal. As nanoporous matrix we used the silicon dioxide with native 0D structural holes of different topology and size. For doping of porous material we use the direct intercalation of liquid crystal in pores by means of placed in liquid crystal the nanoporous matrix with next processing in ultrasonic bath.

Nanoporous silicon dioxide is transparent in visible range of spectrum. Cholesteric liquid crystal EE1 has a wavelength transparent minimum on 550 nm. In nanoporous structure of silicon dioxide doped liquid crystal the transparent minimum shift in short range to 366 nm.

The interaction features and forces, which leads to changes of cholesteric liquid crystal pitch in pores of silicon dioxide are anylased.

9127-52, Session PS2

Light extraction analysis of GaN-based light-emitting diodes with nano-patterned AlN interlayers

Sang-Mook Kim, Hee-Sung Ku, Kwang Cheol Lee, Su Chang Ahn, Jae Bum Kim, Korea Photonics Technology Institute (Korea, Republic of)

Nanopatterned aluminum nitride (NP-AlN) templates were used to enhance the light extraction efficiency of the light-emitting diodes (LEDs). Here, the NP-AlN interlayer between the sapphire substrate and GaN-based LED was used as an effective light outcoupling layer at the direction of bottom side and as a buffer layer for growth of GaN LEDs. The cross-sectional transmission electron microscopy (TEM) analysis showed that the formation of stacking faults and voids could help reduce the threading dislocations. Micro Raman spectra also revealed that the GaN-based epilayer grown on the NP-AlN template had smaller residual stress than that grown on a planar sapphire substrate. The normalized electroluminescence (EL) spectra at the top and bottom sides of device revealed that the enhancement of the bottom side emission of the LED with the NP-AlN interlayer was more notable than a planar

sapphire substrate due to the graded-refractive-index (GRIN) effect of the NP-AlN.

9127-56, Session PS2

PBG structures as substrates to improve the performance of patch antennas

Nawel Mohammedi, Sabrina Zaiter, Rachid Oussaid, Univ. des Sciences et de la Technologie (Algeria)

Artificial photonic crystals exhibits Photonic Band Gap (PBG), i.e. totally reflect the incident field in a certain frequency range. Photonic crystals (PC) or photonic band gap structures are extensively used nowadays for both fundamental research and applications in the optical range as well as at microwaves. PBG structures in the microwave range (Stop-Band Structures) are widely applied in antenna systems with the aim to increase the antenna gain and improve the pattern. A new method of miniaturization of the antennas consists to use the EBG materials which are able to synthesize artificial physical properties. To improve the performance of printed antennas, new models incorporating artificial structures, such as metamaterial structures have been studied and developed. In this work, we present a study on the performance of patch antennas based on photonic crystals. The introduction of a substrate layer made of this kind of materials can improve the performance of a normal patch antenna.

The PBG structure is composed of a network of rods placed in the air of square mesh of finite size. Deferent PBG structures in one and two dimensions have been considered. In this study, we have performed numerical simulations using the commercial full-wave software CST, in order to show the increasing of the performance of the antenna. The numerical simulation results obtained on the antenna structure based on these both geometries of PBG structures have enabled us to have better performances. To see the impact of the size of rod's network and their radius on the operating of the antenna, several simulations were performed to meet best requirements imposed in terms of gain and directivity. Indeed, the gap between the cylinders is a very important criterion to consider as it directly affects the gain including directivity. A comparison of simulated results between the antennas alone and in the presence of PBG structure and shaped metamaterials has been presented. We note that the addition of the metamaterial substrate based on photonic crystals, above the antenna increases the simulated gain and contribute to improving the directivity. We can also conclude that the PBG structures contributes significantly to improving the directivity, gain and angular width and provides a better matching of the antenna compared to the shaped metamaterial patterns. We present thus the antenna performance and comment on the results.

9127-57, Session PS2

A finite difference time domain study of the Mie plasmon modes in 2D photonic crystals composed by metallic shell rods

Brayan F. Diaz, Ricardo Mejía, Univ. del Valle (Colombia)

In the present work, we study the properties of Mie surface plasmon-polariton modes in 2D photonic crystals com- posed by metallic shell rods. Numerical calculations were performed within the finite difference time-domain (FDTD) technique, and by using the Z-transform method in order to avoid complicated numerical convolution integrals. The importance of such Mie plasmon modes in the present work is the harnessing of absorption in such plasmonic struc- tures for their possible application in the design and development of a new era of plasmonic sensors and photovoltaic cells. As a result, we have observed that Mie plasmon modes in shell rods increase in comparison with its solid rods counterparts, and such a behavior is reflected within the photonic band structure (PBS) of the system.

9127-58, Session PS2

Continuously tunable opal based microcavity

Anirban Sarkar, B. N. Shivakiran Bhaktha, Indian Institute of Technology Kharagpur (India)

Opals, 3D photonic crystals (PCs)[1] of silica particles assembled in a face-centered-cubic form, exhibit photonic band gap due to the periodic variation of dielectric constant along the direction of propagation of light. Opals can be fabricated by different techniques such as evaporation-assisted sedimentation (EAS) deposition[2], vertical deposition[3] and Langmuir-Blodgett (LB)[4] methods. Opal based microcavities which inhibit the spontaneous emission of photons in an optically-engineered environment can lead to low-threshold micro-lasers[5]. Also, dye-doped polymer based lasers[5] are of great interest due to their low threshold, cost effectiveness and ease of fabrication. Here we present the emission properties of a continuously, mechanically tunable opal based microcavity. Rhodamine-6G (Rh6G) dye dissolved in ethylene glycol (2??10?^(-3) mol/l) is mixed with polydimethylsiloxane (PDMS) polymer and spin-coated on a glass substrate. The film is heated at 85? C for 2 hours and then peeled off the substrate to form an active, tunable microcavity. Controlled growth of opals on either side of the dye-doped microcavity is achieved by LB technique using monosized silica spheres of ~250 nm diameter synthesized by Stober method[6]. The active microcavity surrounded by the PC is pumped with pulsed 532 nm laser source and the emission spectra are studied. A complete study of the mechanically-tunable emission properties of the opal based microcavity related to the lattice parameter of the opal structure will be presented.

References:

[1] E. Yablonovitch, Phy. Rev. Lett. 58, 2059 (1987).

[2] S-Y. Hsiao, D. S. H. Wong, and S-Y. Lu, J. Am. Ceram. Soc. 88, 974 (2005)

[3] P. Jiang, et al. Chem. Mater.11, 2132 (1999).

[4] S. Reculusa, S. Ravaine, Chem. Mater. 15, 598 (2003).

[5] J. R. Lawrence, Y. Ying, P. Jiang, and S. H. Foulger, Adv. Mater. 18, 300 (2006).

[6] W. Stober, A. Fink, E. Bohn, J. Colloid Interface Sci. 26, 62 (1968).

9127-16, Session 4

Light control with 3D photonic media leads to new concepts and uses *(Invited Paper)*

Willem L. Vos, Univ. Twente (Netherlands)

No Abstract Available

9127-17, Session 4

Transformation of light polarization in thin film opal photonic crystals

Christian Wolff, Max-Born-Institut (Germany); Jens Küchenmeister, Karlsruher Institut für Technologie (Germany); Kurt Busch, Humboldt-Univ. zu Berlin (Germany) and Max-Born-Institut für Nichtlineare Optik und Kurzzeitspektroskopie (Germany); Sergei G. Romanov, Ulf Peschel, Friedrich-Alexander-Univ. Erlangen-Nürnberg (Germany)

Transformation of the polarization state of light is a tool for material characterization and is the aim of signal processing. This assignment is fully applicable to photonic crystals owing to their unique property of transforming plane waves into Bloch modes.

Opals are model 3-dimensional photonic crystals possessing well-documented properties, but opal's response to linearly and circularly polarized light continues to unveil secrets of light-matter interaction.

Thin film opals were prepared by vertical crystallization from a suspension of monodisperse polymer beads with film thickness varied from 1 to 30 bead monolayers.

Generally, the linear polarization state cannot be ascribed to Bloch modes, but theoretical analysis revealed that under certain constrains on the type of field distribution, the energy exchange may occur between opal eigenmodes of comparable k-vectors. Experimentally and numerically obtained spectra are in close agreement regarding the spectral range and the propagation direction, where the maximal polarization conversion occurs.

Theory predicts that polarization conversion varies between 0 and 100% depending on the film thickness. In real-life samples the outcome is strongly affected by lattice defects. If N<5, the cross-polarization coupling survives, but appears radically different in terms of the frequency range and the directionality compared to that of opals with face-centred cubic lattice.

Under circular polarized light the transparency of opal films appears different for opposite rotations for the oblique light incidence. The dispersion of bands of difference spectra correlates that of opal eigenmodes, but these spectra are dissimilar to those in co- and cross-polarized light. In contrast to cross-polarized transmission showing the even dependence on the incidence angle sign, the transparency of circular polarized light shows the odd one.

Summarizing, the transformation of light polarization in photonic crystals originates from the field distribution in Bloch modes and can be engineering by purposive design of the crystal structure.

9127-18, Session 4

Improvement of spatial filtering phenomenon in chirped photonic crystal structures

Vytautas Purlys, Vilnius Univ. (Lithuania); Lina Maigyte, Univ. Politècnica de Catalunya (Spain); Darius Gailevi?ius, Martynas Peckus, Mangirdas Malinauskas, Roaldas Gadonas, Vilnius Univ. (Lithuania); Kestutis Staliunas, Univ. Politècnica de Catalunya (Spain) and Institució Catalana de Recerca i Estudis Avançats (Spain)

Spatial filtering plays an important role in optics as a tool for improving the spatial quality of the light beams. Usually a confocal system of two lenses and diaphragm is used, which is however a bulky and sensitive to mechanical positioning system. It is well known that photonic crystals (PhCs) can exhibit photonic bandgaps in frequency domain, meaning that the light of certain wavelengths can not pass through. Such type PhCs works as frequency filters. In analogy to the frequency bandgaps, the angular bandgaps could be also obtained in PhCs as recently proposed. In particular, the larger angle spatial radiation components are reflected or deflected to diffraction maxima, and the lower angle components pass unaffected. Such PhC spatial filters could be an attractive alternative due to their tiny size and mechanical stability.

The first proof-of-principle experiments demonstrated the angular filtering [L.Maigyte et al., Phys.Rev.A 82, 043819 (2010)], however the filtering efficiency was very small and the filtered-out angular areas were very narrow, of less than 1 degree. The depth of filtered out lines can be increased by elongating the PhC, but the width is limited fundamentally as the radiation from deflected components starts to return back. Here we extend the idea by using chirped PhCs, where the longitudinal period of the PhC linearly varies along the structure and the return of filtered out components is suppressed by longitudinal period mismatch. Such linear chirp results in broadening of the angular bandgaps, and in much wider filtered angles. According to our calculations the performance of angular filters increase several times for proper chirp parameters.

We inscribed chirped PhCs into soda lime glass slides using direct laser writing technique. This technique is based on point by point modification of refractive index induced by tightly focused femtosecond laser beam. We used 1030 nm wavelength and 50 kHz repetition rate laser source. We chose 1 μm traversal and 6 μm longitudinal periods of woodpile geometry. Such particular geometry corresponds to central filtering angle of 4 degrees. The angular spectrum of inscribed PhCs was measured for 633 nm wavelength. Chirped PhCs exhibited up to 4 degrees wide filtering angle, which is around 10 times wider compared to the regular ones. In addition, we support the experimental data with theoretical calculations which are in very good agreement with experimental results and show that PhC filtering performance could be improved even more.

9127-19, Session 4

Optical characterization of active photon cages

Artinyan Rémy, Aziz Benamrouche, Chérif Belacel, Institut des Nanotechnologies de Lyon (France); Marina Kozubova, ILM (France); Alice Berthelot, Anne-Marie Jurdyc, Lab. de Physique de la Matiére Condensée et Nanostructures (France); Guillaume Beaudin, Vincent Aimez, Institut Interdisciplinaire d'Innovation Technologique (3IT) (Canada); Pedro Rojo-Romeo, Jean L. Leclercq, Peretti Romain, Xavier Letartre, Ségolène Callard, Institut des Nanotechnologies de Lyon (France)

Recently, we developed a new family of 3D photonic hollow resonators which theoretically allow tight confinement of light in a fluid (gaz or liquid). These new resonators could be ideal for sensing applications since they not only localize the electromagnetic energy in a small mode volume but also enforce maximal overlap between this localized field and the environment (i.e. a potential volume of nano-particles). They are based on an original photonic concept [1,2] where a photonic crystal membrane, acting as a non absorbing mirror, is folded to enclose a hollow micrometric volume in which light is efficiently trapped. The first attempt to use these membranes has led to the fabrication of rigid cylindrical microcavities, called "photon cages", with top down technique, including delicate steps of deep Reactive Ion Etching [2]. A remaining milestone on the way towards further developments of these objects lies in their optical characterization.

In this work, we will present numerical and experimental studies of a photon cage optical mode interaction with internal nano-emitters embedded in a low index matrix. For this, PbS quantum dot emitters in a PDMS host matrix have been introduced in the 3D resonator. Far-field and near-field optical characterization techniques have been used to demonstrate the photon cage abilities to confine and enhance quantum dots emission.

References

[1] C. Sieutat C et al., 3D harnessing of light with photon cage, Proceedings of SPIE-The International Society for Optical Engineering, 77120E (2010)

[2] C. Sieutat et al., Strong confinement of light in low index materials: the Photon Cage, Opt. Ex. 21, 20015 (2013)

Acknowledgements

We thank L.Lalouat and B.Gonzalez-Acevedo for their help and advice regarding FDTD computing.

We acknowledge iMust and Région Rhône-Alpes for the funding of this research.

9127-20, Session 4

Balancing ballistic and hopping light transport by purposive arraying of colloidal particles

Sergei G. Romanov, Friedrich-Alexander-Univ. Erlangen-Nürnberg (Germany); Sergej Orlov, Max-Planck-Institut für die Physik des Lichts (Germany); Nicolas Vogel, Harvard School of Engineering and Applied Sciences (United States); Karina Bley, Katharina Landfester, Max-Planck-Institut für Polymerforschung (Germany); Clemens K. Weiss, Fachhochschule Bingen (Germany); Ulf Peschel, Friedrich-Alexander-Univ. Erlangen-Nürnberg (Germany)

One of the most important issues in designing optical materials for light emitting and harvesting devices, lasing and signal processing is to control the light-matter interaction. Such functionality is a property of nanomaterials with slow light propagation. The alternative to the mode dispersion engineering is the weak coupling of resonators that exploits the scattering of evanescent waves. Disappointingly, such materials cannot provide sufficient light throughput. Our idea is to engineer collective modes via hybridization of local excitations of purposively arranged resonators.

We prepared monolayers of polystyrene spheres on glass substrates and gold-coated glass substrates and experimentally and theoretically studied their optical properties. In densely packed arrays of spheres their Mie resonances are hybridized and familiar photonic bandgap structures appear. In such arrangements no local resonators can be distinguished and light is guided along the monolayer. However, when the light leakage to metal-coated substrate is reduced, the strength of high-order Mie resonances achieves that of Bragg modes, i.e., improving light confinement reduces the hybridization. In this regime one can expect energy exchange between localized and Bloch optical modes.

Further isolation of resonators was achieved by increasing their spacing either via reducing the size of the polymeric spheres by plasma etching or via randomizing the sphere lattice. The former approach allows shifting the dipole Mie resonances towards the Bragg ones. Their interaction manifests itself in strongly uneven transmission spectra due to Fano resonances. The latter one allows reducing the strength of Bragg resonances and shifting them to longer wavelengths. Hence, the administered positional disorder decreases the hybridization of resonator modes and increases the overlap range of local and extended states.

Concluding, purposive structuring of the colloidal materials allows tuning the strength of mode hybridization and thus controlling the mechanism of in-plane light propagation.

9127-7, Session 5

Tantalum-tungsten alloy photonic crystals for high-temperature energy conversion systems

Veronika Stelmakh, Veronika Rinnerbauer, Walker R Chan, Jay J. Senkevich, John D. Joannopoulos, Marin Soljacic, Ivan Celanovic, Massachusetts Institute of Technology (United States)

A tantalum tungsten (Ta-W) solid solution alloy, Ta 3%W, based 2D photonic crystal (PhC) was designed and fabricated for high-temperature energy conversion applications. Metallic PhCs are promising as high performance selective thermal emitters for solid-state thermal-to-electricity energy conversion concepts including thermophotovoltaic (TPV) energy conversion, as well as highly selective solar absorbers/emitters for solar thermal and solar TPV applications due to the ability to tune their spectral properties and achieve highly selective emission. The mechanical and thermal stability of the substrate was characterized as well as the optical properties of the fabricated PhC. The Ta 3%W alloy presents advantages compared to the non-alloys as it combines the better high-temperature thermo-mechanical properties of W with the more compliant material properties of Ta, allowing for a direct system integration path of the PhC as selective emitter/absorber into a spectrum of energy conversion systems. Furthermore, the thermo-mechanical properties can be fine-tuned by the W content. A 2D PhC was designed to have high spectral selectivity matched to the bandgap of a TPV cell, using numerical simulations and fabricated using standard semiconductor processes. The emittance of the Ta 3%W PhC was obtained from near-normal reflectance measurements at room temperature before and after annealing at 1200C for 24h in vacuum with a protective coating of 40nm HfO2, showing high selectivity in agreement with simulations. SEM images of the cross section of the PhC prepared by FIB confirm the structural stability of the PhC after anneal, i.e. the coating effectively prevented structural degradation due to surface diffusion.

9127-21, Session 5

Photonic structures for light trapping in thin-film solar cells *(Invited Paper)*

Lucio C. Andreani, Angelo Bozzola, Piotr Kowalczewski, Marco Liscidini, Univ. degli Studi di Pavia (Italy)

Light trapping is crucial to increase efficiency in thin-film solar cells and to reduce the cost of advanced photovoltaic devices. It is especially important to enhance light absorption in the spectral region close to the electronic band gap of the semiconductor, where material absorption is low – and to approach the ultimate limit to absorption, which is usually taken to be the Lambertian limit. Light trapping at the wavelength-scale can be performed with ordered photonic lattices (photonic crystals, diffraction gratings), or with disordered structures, or with a combination of both.

In this work we report on a theoretical study of thin-film silicon solar cells with various types of photonic structures: fully ordered lattices [1], photonic lattices with correlated disorder [2], fully randomly rough surfaces [3,4], and hybrid (ordered+disordered) structures [4]. Light trapping capabilities of these structures are analyzed by means of rigorous coupled-wave analysis and compared with the Lambertian limit.

Ordered photonic lattices are 1D or 2D photonic crystals, and are characterized by the lattice constant as well as the filling fraction. They allow achieving a substantial improvement of the short-circuit current with respect to the unpatterned structure with anti-reflection coating, but the increase in Jsc is still about 50% of the required value for reaching the Lambertian limit. Photonic lattices with correlated randomness (size or position disorder) yield a further improvement of Jsc and can still be realized with top-down procedures based on lithography (possibly nanoimprint lithography for large-scale exploitation) and etching.

Randomly rough surfaces are described by a Gaussian disorder, which is characterized by the root mean square (RMS) deviation of the height and the lateral correlation length. We show that this model describes very well the scattering properties of actual rough substrates in terms of angular distribution function and haze, and we demonstrate that optimization of the disorder parameters allows to reach the Lambertian limit for absorption. However, this requires values of the RMS deviation (>200 nm) that are too high for growth of good-quality microcrystalline silicon. To avoid this problem, we introduce hybrid structures that combine Gaussian disorder with moderate roughness together with a photonic crystal: such structures have still a Jsc close to the Lambertian limit, and are amenable to fabrication on rough substrates.

[1] A. Bozzola, M. Liscidini, and L.C Andreani, Opt. Express Vol. 20, A224 (2012)

[2] A. Bozzola, M. Liscidini, and L.C Andreani, Progr. Photov. Res. Appl. (2013), DOI: 10.1002/pip.2385

[3] P. Kowalczewski, M. Liscidini and L.C. Andreani, Opt. Letters 37, 4868 (2012).

[4] P. Kowalczewski, M. Liscidini and L.C. Andreani, Opt. Express 21, A808 (2013).

9127-22, Session 5

Plasmonic LED devices

Manuela Lunz, Dick de Boer, Philips Research (Netherlands); Gabriel Lozano, Said R. K. Rodriguez, Jaime Gomez Rivas, FOM Institute for Atomic and Molecular Physics (Netherlands); Marc A. Verschuuren, Philips Research (Netherlands)

Plasmonic nanostructures are known to influence the emission of near-by emitters. They can enhance the absorption and modify the external quantum efficiency of the coupled system. In regular plasmonic arrays of aluminum nanocylinders with a diameter of ca 140nm combined with a thin (650 nm) layer of luminescent material, the authors have observed very narrow resonances, which lead to large enhancement in a small spectral range for particular angles (G. Lozano et al, Light: Science & Applications 2 e66 doi:10.1038/lsa.2013.22 (2013)). In particular, enhancements of up to a factor of 60 and 20 for excitation with a directional blue laser source and a lambertian LED respectively have been reported for non-polarized light. The measured resonances agree very well with calculations by finite-difference time-domain numerical simulations.

In this contribution we further investigate these regular plasmonic arrays to evaluate the possibility of using plasmonics to enhance the light emission of a phosphor converted LED device and create an efficient directional light source. In a first step, the focus lies on modifying the angular emission profile of a red dye and to spectrally shape its emission to better fit the eye sensitivity curve. To determine the spectral features of different plasmonic arrays, e.g. with different sized nanoparticles and different lattice constants, the angular dependent extinction as well as photoluminescence enhancement are evaluated under white light and blue laser excitation respectively. Choosing samples with emission enhancement at ca 610 - 620nm in forward direction, the samples are further investigated by Fourier spectroscopy with a blue LED as excitation source. Comparing to reference samples without plasmonic nanostructures, clear modifications of the angular emission profile as well as spectral shaping are observed for these plasmonic LED devices.

9127-23, Session 5

Solution-processed distributed Bragg reflectors and optical microcavities using high-index organic/inorganic molecular hybrid material

Andrew Strang, Manuela Russo, Imperial College London (United Kingdom); Walter R. Caseri, ETH Zürich (Switzerland); Donal D. C. Bradley, Natalie Stingelin, Paul Stavrinou, Imperial College London (United Kingdom)

Solution-processed photonic structures are attracting increasing interest in the scientific and industrial community due to the advantages straight-forward deposition methods adapted from the bulk “plastic” manufacturing offer compared to current technologies which are predominantly based on inorganic materials. Key to realising photonic structures from solution, and at low temperatures, is the development of versatile, high refractive index, low loss material systems. In this work we employ an organic/inorganic hybrid material that was developed by Russo et al.[1-3] and processable from an aqueous solution: titanium oxide hydrate cross-linked polyvinyl alcohol (PVA). The material’s refractive index in solution-cast architectures can be tuned from 1.5 to greater than 1.8 by controlling the inorganic content of the material (from 0 to >99vol% titanium), yet without inducing significant optical losses. The refractive index can be further increased if required to over 2.1 by thermal annealing, showing that the refractive index of these hybrids can be tuned over a similar window as the best materials previously reported[4], but without reducing the material’s transparency. We attribute this highly beneficial feature of these novel materials to the fact that they are molecular hybrids rather than nanocomposites that suffer from nanoparticle aggregation, and ultimately scattering of light, even at relatively low loadings.

We present solution-processed distributed Bragg reflectors (DBRs), fabricated to a desired optical response, which achieve close to 100% reflectance over a pre-designed optical stop-band. We demonstrate the versatility of the material system in the production of DBRs in the optical and infrared, which can be tuned after deposition by thermal annealing to change the position of the reflectance band. Through modeling of the optical response of these DBR structures we prove that the hybrid material exhibits unprecedentedly low optical losses and excellent interfacial quality when integrated in multilayer stacks using deposition techniques commonly employed in the manufacturing of commodity “plastic” products. Finally, we show the production of optical microcavities, processed from solution, which present a whole host of future applications for this novel material system.

1. Russo, M., et al., Pronounced photochromism of titanium oxide hydrates (hydrous TiO2). Journal of Materials Chemistry (2009). 20(7): p. 1348-1356

2. Russo, M., et al., One-Pot Synthesis of Polymer/Inorganic Hybrids: Toward Readily Accessible, Low-Loss, and Highly Tunable Refractive Index Materials and Patterns. Journal of Polymer Science Part B: Polymer Physics (2011). 50(1): p. 65-74

3. Russo, M., et al., Versatile Chromism of Titanium Oxide Hydrate/Poly(vinyl alcohol) Hybrid Systems. Advanced Materials (2012). 24(22): p. 3015-3019

4. Liu, J.G.a.M.U., High refractive index polymers: fundamental research and practical applications Journal of Materials Chemistry (2009). 19(47): p. 8907-8919

9127-24, Session 5

Optics and mechanics of stretchable DBRs and DBR balloons

Gen Kamita, Jeremy J. Baumberg, Ullrich Steiner, Univ. of Cambridge (United Kingdom)

Elastically-deformable Distributed Bragg Reflector (DBR) membranes are “Rubbery mirrors” that can be reversibly colour-tuned across the full visible spectrum by stretching, compressing or any other kind of deformation that changes the thickness of the membrane. Starting from an initial bilayer consisting of two rubbers, the multifolding Origami manufacture process multiplies the number of layer stacks, leading to an enhancement of reflectance at a wavelength set by the layer thicknesses.

In this work, the optics and mechanics of “DBR balloons” were investigated. The DBR balloons were inflated from initially flat DBR membranes into a hemispherical shape by pressure difference. Upon deformation, the hemispherical balloons displayed a colouration effect similar to Papilio Blumei, a butterfly well known for their brilliant colour produced by the multilayer concavity arrays on their wing scales, but with their hue arrangements being inverted compared to the butterfly. In the butterfly, the concavities displayed a blue colour at their rim and green colour at the centre due to the angular variation of colour produced by multilayer interference. In contrast, the deformed DBR showed a red shifted colour in the centre of the balloon compared to the edge, which indicates a significant thickness gradient along the radius.

The arrangement of the colours during tuning of the DBR was studied in relation with the axisymmetric geometry and the mechanical properties of the deformed DBR. Numerical analysis was used to model the deformed DBR assuming that the DBR behaves as a Mooney-Rivlin material. The hue arrangements of the deformed DBR balloons were able to be reproduced when the ratio of the two Mooney-Rivlin constants, C2/C1, was set to negative. This indicates that the interplay of the viscoelastic property of the DBR and the geometrical configuration of the inflation process enhances the radially inhomogeneous strain distribution, which creates the inverted hue arrangement. This device can be utilised as tunable flexible security printing feature and other novel optical devices.

9127-25, Session 6

Genetically optimized photonic crystal cavities

Momchil Minkov, Vincenzo Savona, Ecole Polytechnique Fédérale de Lausanne (Switzerland)

Optical cavities in a photonic crystal slab are a promising versatile platform for various photonic applications, from optical circuits to quantum devices and sensing. Some very specific designs in particular have been conceived to have an enormous theoretical quality factor of up to one billion. These values, however, are never experimentally measured, due to a limitation set by disorder and/or absorption losses. On the other hand, for most research and application purposes, more elementary cavity designs – such as the L3, H0 and H1 design – are commonly adopted for various reasons, including compactness, small mode volume, and, in the case of the H1, the presence of two degenerate modes. However, the theoretical quality factors of those designs – even for the (previously) most optimized structures – are at best in the moderate range of a few hundred thousand, which is in many cases well below the limit set by e.g. disorder losses. This essentially means that improving the theoretical Q of such cavities is of tremendous practical benefit. Previous attempts to do so relied on computationally heavy first-principle methods, which unavoidably led to a heuristic search for an optimal design, exploring few structural variations. In our work, we use a highly effective mode-expansion method to simulate such structures, which greatly decreases the computational time while only slightly compromising on accuracy, and allows for the first time for a global optimization algorithm to be used. We apply the genetic optimization procedure to the L3, H0 and H1 cavities, using a very restricted number of variational parameters (typically the spatial shifts of a few holes). The procedure consistently returns quality factors higher than one million, thus improving previous designs by, in some cases, more than one order of magnitude. In particular, we demonstrate an L3 design with Q = 2.1x106 (8 times the previously highest), an H1 design with Q = 1.05x106 (15 times the previously highest), and several H0 designs with Q going as high as 8.9x106 (30 times the previously highest, and entering the disorder-limited region even for state-of-the-art manufacturing techniques). We further perform a disorder analysis and find that these new designs are as robust to fabrication imperfections as any of the other well-known cavities, meaning that values close to the quoted theoretical quality factors can be reached experimentally. This has direct practical implications in view of the various uses of those cavities, and perhaps more importantly, sets the standard for future optimization of photonic crystal structures in general by highlighting the importance of exploring the full parameter space.

9127-27, Session 6

Photonic crystals for optical interconnects *(Invited Paper)*

Liam O'Faolain, Univ. of St. Andrews (United Kingdom)

No Abstract Available

9127-28, Session 7

Cellulose biomimetic: a new prospective for smart materials *(Invited Paper)*

Ahu G. Parry Dumanli, Gen Kamita, Jeremy J. Baumberg, Ullrich Steiner, Silvia Vignolini, Univ. of Cambridge (United Kingdom)

The mimicry of biological species to produce photonic materials has raised increasing interest in the scientific community [1,2]. Plants, like animals, develop nanostructured tissues with a strong photonic response [3,4], as an example the colour of Pollia fruit is the results of chiral multilayered structures composed of cellulose micro-fibrils, which from a layered structures. In each component layer, cellulose micro-fibrils lie parallel to one another, with successive layers offset from each other at a small angle, so that the direction of the parallel-aligned micro-fibrils changes consistently, rotating from one layer to another and producing an intense colour-selective reflection [5-6].

Biomimetics with cellulose-based architectures enables us to fabricate novel photonic structures using low cost materials in ambient conditions [7-8]. Importantly, it also allows us to understand the biological processes at work during the growth of these structures in plants.

In this work the route for the fabrication of cellulose-base architecture will be presented and the optical properties of the fabricated structures will be analyzed and compared with natural photonic structures.

[1] M. Kolle, et al. Nat. Nanotech. 5, 511 (2010).

[2] H. Noh et al. Phys. Rev. Lett. 106, 183901 (2011).

[3] H. M. Whitney et al. Science 325, 449 (2009).

[4] S.Vignolini et al. PNAS 109, 15712 (2012).

[5] A. C. Neville & S Levy. Biochemistry of plant cell walls. Cambridge Univ. Press (1985).

[6] H. De Vries, Acta Cryst. 4, 219(1951).

[7] S. Beck et al., Biomacromol. 12, 167 (2011).

[8] S. N. Fernandes 1, 25 (2013).

9127-29, Session 7

Hoplia coerulea: a porous natural photonic structure as template of optical vapour sensor

Sébastien R. Mouchet, Olivier Deparis, Univ. of Namur (Belgium)

Natural photonic structures found on the cuticle of insects are known to give rise to astonishing structural colours. These ordered porous structures are made of biopolymers, such as chitin, and some of them possess the property to change colour according to the surrounding atmosphere composition. This phenomenon is still not completely understood.

We investigated the structure found on the cuticle of the male beetle Hoplia coerulea (Scarabaeidae). The structure, in this case, consists in a 1D periodic porous multilayer, reflecting incident light in the blue. The colour variations were quantified by reflectance spectral measurements under controlled atmosphere, as well as environmental ellipsometry using different vapours (e.g., water, ethanol, acetone, toluene...). A rigorous coupled wave analysis method was used for modelling light reflection on the photonic multilayer. An effective medium approximation was applied in order to calculate the refractive index of the porous layers.

The colour variations were explained by studying three mechanisms: capillary condensation inside the pores, vapour adsorption on the inner surface of the pores due to Van der Waals interactions and swelling of the structure. The origin of the reported colour changes has therefore to be tracked in variations of the effective refractive index and of the dimensions of the photonic structure. This remarkable phenomenon observed for a natural porous multilayer could be very interesting for vapour sensing applications.

9127-30, Session 7

Optical biosensing with slottted cavities in diamond photonic crystals

Candice Blin, CEA LIST (France) and Univ. Paris-Sud (France); Xavier Checoury, Institut d'Électronique Fondamentale (France); Hugues A. Girard, Céline Gesset, Samuel Saada, CEA LIST (France); Philippe Boucaud, Institut d'Électronique Fondamentale (France); Philippe Bergonzo, CEA LIST (France)

Diamond is currently emerging as a novel material for photonic devices thanks to its high refractive index, a quasi-transparency from UV to far IR, high thermal conductivity and low thermo-optic coefficient. Besides, diamond is also an ideal oxide free interface for covalent functionalization thus for the realization of chemical and biological sensors. We here propose a novel approach which consists in combining the sensitivity of 2D slotted photonic crystals (PhC) to the versatility and biocompatibility of diamond interface for the development of innovative diamond-based photonic biosensors taking advantage of the covalent grafting of proteins, and namely of nucleic acids.

We first developed a fully integrated planar photonic platform, with a design consisting of a narrow slot in a width-modulated line defect. Cavities with Q factors up to 6500 around 1550nm, among the highest reported on diamond, were fabricated in polycristalline diamond films deposited on two-inch Si wafers. Standard nanotechnology techniques were used, thus allowing large scale processing. As proof of concept, we demonstrated the possibility to perform label-free molecule detection with 2D-slotted diamond-PhC using the biotin/streptavidin recognition system. The efficiency of the functionalization on such nanostructured interfaces was assessed via the use of streptavidin molecules terminated with gold nanoparticles. Combined with microscopy investigations, we were also able to reveal that the functionalization of such large molecules is effective even in the 130nm-slot and that they maintain their activity, allowing the selective capture of target molecules.

Finally, slotted PhCs were used to detect streptavidin with concentrations up to 100µg/mL. After recognition, the resonance of the cavity mode is shifted by 5 nm towards longer wavelengths showing a clear evidence of the detection by the structure of the refractive index change induced by the protein capture. We believe this truly opens up the route towards diamond based PhC for ultra-high sensitivity biosensing.

9127-31, Session 7

3D photonic crystal based biosensor functionalized with quantum dot based aptamer for thrombine detection

Chae Young Lim, Eunpyo Choi, Sogang Univ. (Korea, Republic of); Youngkyu Park, Agency for Defense Development (Korea, Republic of); Jungyul Park, Sogang Univ. (Korea, Republic of)

Photonic crystal (PC) based biosensors have been attracted more attention due to their advantages, such as sensitivity, real time monitoring and low-cost realization. PC based sensors have been reported to measure various environmental changes, such as pH, temperature and glucose. In this study, we characterize enhancement of intensity in quantum dots (Qdot) whose emission is guided by 3D photonic crystal (PC) structures for protein detection. We design that the emitted light from the PC based sensor can be recovered, when the chemical antibody (aptamer) conjugated with guard DNA (g-DNA) labeled with a quencher (Black FQ), detects the target proteins. The quencher has broad light absorbance property ranging from 500 to 700 nm (its maximum absorbance is 531 nm). It induces the quenching effect of fluoresce intensity in the Qdot-aptamer. In presence of target protein (thrombin), the Qdot-aptamer complex prefers to form the thrombin-aptamer complex: this results in the release of Black FQ-g-DNA and the quenched light intensity recovers into the original high intensity with Qdot. The intensity recovery varies quantitatively according to the level of the target protein concentration. This proposed sensor shows much higher detection sensitivity than the general fluorescent detection mechanism, which is functionalized on the flat surfaces because of the light guiding effect from 3D photonic crystal structures. Also, the end user can detect the target directly and easily without any sample preparation like a ELISA kit.

9127-32, Session 7

On the effect of broadband, multi-angular excitation and detection in guided-mode resonance biosensors

Daniela Threm, Sabrina Jahns, Yousef Nazirizadeh, Martin Ziegler, M. Hansen, Hermann Kohlstedt, Christian-Albrechts-Univ. zu Kiel (Germany); Jost Adam, Christian-Albrechts-Univ. zu Kiel (Germany) and Univ. of California, Los Angeles (United States); Martina Gerken, Christian-Albrechts-Univ. zu Kiel (Germany)

Guided mode resonance biosensors are of emerging interest as they allow integration on chip with fabrication on mass scale. The guided mode resonances (GMRs) observed in the transmission or reflection spectrum are sensitive to refractive index changes in the vicinity of the photonic crystal (PhC) surface.

Standard measurement setups, however, utilize a macroscopic collecting lens focussing the extracted light intensity to a single-point photo detector. In order to achieve a higher grade of device integration, we consider the integration of planar emitting and detector structures, such as organic light emitting diodes (OLEDs) and organic photo detectors (OPDs), together with the PhC based biosensors on a single chip. This approach consequently leads to a broadband, multi-angular light excitation as well as to a multi-angular contribution to the photon count on an OPD. This lens-less setup enables highly integrated devices.

While guided mode resonance effects in photonic crystal slabs with directional light sources have been widely studied, this particular scenario requires a deeper understanding of the broadband and the angular influence of both incident and reflected or transmitted light.

In this contribution, we present finite-difference time-domain (FDTD) calculations for guided mode resonance effects in two-dimensional (2D) linear photonic crystal slabs. We study the effects for broadband emission in the visible spectrum, together with a spatial incident beam divergence of up to 80°. Furthermore, we differentiate between two different detector scenarios. In the FDTD simulation single-point transmission detection is sufficient for representing the collecting lens setup. Simulation of a lens-less experimental setup requires a near-to-far field transformation with successive angular superposition of the reflected or transmitted intensities.

We verify the simulation results with two different measurement setups using an LED and an OLED as excitation source, respectively. We measure the GMRs in a reflection setup with different distances to the detector.

9127-33, Session 8

Gain/loss modulated photonic structures: PT-symmetry and slow-light-inspired functional devices *(Invited Paper)*

Anatole Lupu, Institut d'Électronique Fondamentale (France); Henri Benisty, Institut d'Optique Graduate School (France); Aloyse Degiron, Institut d'Électronique Fondamentale (France)

The aim of the present work is to explore the potential of the concept of Parity-Time symmetry (PT) in optics [1-3] toward new types of functional photonic devices. We examine how the concept of gain/loss modulation, which is the basis of PT-symmetry-based devices [4-6] can be combined with the exploitation of slow light based on a periodic perturbation of the refractive index profile.

In particular we consider the example of a Bragg-grating-assisted forward directional coupler [7,8] where the implementation of a gain/loss modulation can be used to change grating's dispersion. We show how an efficient switching or modulation can be achieved with this type of PT-symmetric structures where gain/loss alternation is implemented along the direction of light propagation. In the

spirit of our recent work [4-6], we demonstrate that operation compatible with practical applications can be achieved also with an imperfect PT-symmetry design, where only the gain is variable while the losses are fixed (e.g. plasmonics [6]).

This reported result provides a distinct difference with those previously reported on PT- symmetry grating-assisted devices. The essential feature is that in our case operation is based on a four-wave interaction, marking thus a step in the further development of PT-symmetry devices, which, currently, are nearly always based on two-waves interactions. We shall present some other prospects for PT-symmetry devices based on four-waves interaction.

1. C. M. Bender and S. Boettcher, "Real spectra in non-Hermitian Hamiltonians having PT symmetry," Phys. Rev. Lett. 80, 5243 (1998).

2. A. Guo, G. J. Salamo, D. Duchesne, R. Morandotti, M. Volatier-Ravat, V. Aimez, G. A. Siviloglou, and D. N. Christodoulides, "Observation of PT-symmetry breaking in complex optical potentials," Phys. Rev. Lett. 103, 093902 (2009).

3. C. E. Rüter, K. G. Makris, R. El-Ganainy, D. N. Christodoulides, M. Segev, and D. Kip, "Observation of parity–time symmetry in optics," Nature Phys. 6, 192–195 (2010).

4. A. Lupu, H. Benisty, and A. Degiron, "Switching using PT symmetry in plasmonic systems: positive role of the losses," Opt. Express 21, 21651-21668 (2013).

5. H. Benisty, C. Yan, A. Degiron, and A. T. Lupu, "Healing near-PT-symmetric structures to restore their characteristic singularities: Analysis and examples," J. Lightwave Technol. 30, 2675-2683 (2012).

6. H. Benisty, A. Degiron, A. Lupu, A. De Lustrac, S. Chénais, S. Forget, M. Besbes, G. Barbillon, A. Bruyant, S. Blaize, and G. Lérondel, "Implementation of PT symmetric devices using plasmonics: principle and applications," Opt. Express 19, 18004-18019 (2011).

7. K. Muhieddine, A. Lupu, E. Cassan, J-M. Lourtioz, "Proposal and analysis of narrow band transmission asymmetric directional couplers with Bragg grating induced phase matching," Opt. Express 18, 23183-23195 (2010).

8. A. Lupu, K. Muhieddine, E. Cassan, J-M. Lourtioz, "Dual transmission band Bragg grating assisted asymmetric directional couplers," Opt. Express 19, 1246-1259 (2011).

9127-34, Session 8

Optimizing 2D photonic crystals in silicon-on-oxide for high performance polarization diversity couplers in integrated Si-photonic circuits

Lee B. Carroll, Dario Gerace, Ilaria Cristiani, Lucio C. Andreani, Univ. degli Studi di Pavia (Italy)

Polarization Diversity Couplers are a low-cost, CMOS-compatible, and industrially scalable means of coupling light from single-mode telecom fibers to the Silicon-on-Insulator (SOI) platform for integrated Si-Photonic circuits. Unlike 1D-Grating Couplers, which typically only couple the TE-polarization of the fiber-mode into the SOI waveguide, the two-dimensional Photonic Crystal Array of lithographically-etched holes in a Polarization Diversity Coupler provide a coupling efficiency that is nearly independent of the fiber-mode polarization, making it ideal for practical telecom-SOI coupling. Until now, the efficiency of such Polarization Diversity Couplers has lagged behind state-of-the-art of 1D-Grating Couplers. However, using 3D Finite Difference Time Domain (3D-FDTD) calculations for a global optimization of the Photonic Crystal Array and other design parameters, we demonstrate a significant performance enhancement beyond state-of-the-art. Specifically, we show that it is possible to essentially eliminate the "performance gap" between Polarization Diversity Couplers and their corresponding uniform 1D-Grating Couplers. The globally optimized fully CMOS-compatible design has a coupling efficiency of -1.8dB (66%) at 1550nm and a polarization dependent loss of less than 0.3dB. This design offers between -1dB and -2dB higher coupling efficiency than state-of-the-art Polarization Diversity Couplers, while simultaneously offering a lower polarization dependent loss. The semi-infinite Photonic Crystal slab, on which the optimized Polarization Diversity Coupler is based, is studied using Guided Mode Expansion (GME) calculations, to describe the photonic band structure and identify the resonances giving rise to the high coupling efficiency. The same 3D-FDTD optimization scheme and GME calculations are also used to investigate Polarization Diversity Couplers that incorporate a back-reflector (Distributed Bragg Reflector or metallic-layer) in their design to further improve performance to -1dB, albeit at the cost of more complicated materials and device fabrication.

9127-35, Session 8

Managing spatial diffraction trough a periodic modulation of loss

Muriel Botey, Nikhil Kumar, Lina Maigyte, Ramon Herrero, Kestutis Staliunas, Univ. Politècnica de Catalunya (Spain)

Structured dielectric materials allow a precise control over both temporal and spatial dispersion of light; enabling the possibility to engineer the propagation of light beams, managing diffraction. Among the reported novel effects are nondiffractive propagation with no guiding boundaries or line defects [1], or negative diffraction which provides lenses with flat surfaces and hence insensible to alignment [2]. More recently, attention was paid to analogous artificial materials with a periodic Gain/Loss Modulation (GLM) on the wavelength scale, but with no refractive index contrast. It was predicted that such structures could hold sub-diffraction propagation, self-collimation or beam focusing [3]. As in the case of Photonic Crystals (PhC), such effects are accounted by the distortion of isofrequency contours of propagating modes in the wave-vector space. Additionally, in GLM, a strong anisotropic dependence of the wave amplification/attenuation arises, which could be used for applications such as beam spatial filtering [4].

Note, however, that both PhC and GLMs are two ideal limiting cases since, in general, the refractive index and the gain/loss variations are intrinsically related via the Kramers-Kronig relations. Therefore, we here consider two different structures: a 2-dimensional slab made of a periodic distribution lossy cylinders embedded in air with flat-flat interfaces, and a similar arrangement of gold cylinders in air. For the pure lossy structure we show the predicted self-collimation and flat lensing effects. Besides, contrary to what would be expected for a PhCs, the light intensity map of a Gaussian beam exiting the structure does not show a bandgap but a high transmission window, for frequencies close to the edges of the first Brillouin Zone; resulting from the anisotropic attenuation provided by the periodicity. A significant focusing after the thin crystal slab is confirmed by a deeper analysis on the phase profile curvature of the beam exiting the structure, which confirms negative diffraction for given frequencies. The accumulated phase-shifts within the crystal are then compensated by normal diffraction behind the structure, determining the focal distance from the flat lens. Moreover, the phase curvature follows analytical estimations based on the spatial dispersion diagrams [5]. We also show that metallic PhCs supports both nondiffractive propagation and focusing, associated to zero and negative diffraction, respectively. Finally, we also demonstrate that metallic PhCs are able to spatially filter noisy beams, due to the anisotropic attenuation of light.

The predicted phenomena are expected to be generic for spatially modulated materials and other kinds of waves. Indeed, we extend our work to acoustics and obtain similar results from phononic crystals with periodically distributed losses.

[1] H. Kosaka, et al. APL 74, 1212 (1999). K. Staliunas, R, Herrero, PRE 73, 016601 (2006)

[2] J. B. Pendry, PRL 85, 3966 (2000). P. V. Parimi, et al., Nat. 426, 404 (2003)

[3] K. Staliunas, et al. PRA 80, 013821 (2009). M. Botey, et al. PRA 82, 013828 (2010).

[4] N Kumar, et al. Phot. and Nanostr.-Fundamentals and

Applications 10, 644 (2012). M. Radziunas, et al. APL, 103, 132101 (2013).

[5] N Kumar, et al. JOSA B 30, 2684 (2013).

9127-36, Session 8

Nondestructive readout of photonic lattices recorded by Bessel beam technique in photochromic LiNbO3:Fe:Cu crystals

Rafael K. Drampyan, Tigran Dadalyan, Ruben K. Hovsepyan, Paytsar Mantashyan, Varsenik Nersesyan, Institute for Physical Research (Armenia)

Investigations of the time evolution of the readout erasure of 1D and 2D annular symmetry photonic lattice structures optically induced by nondiffracting Bessel beam technique [1] were performed. The lattices were recorded with the use of cw single mode 532 nm, 17 mW laser beam in photorefractive LiNbO3:Fe:Cu crystals having also photochromic properties. Bessel beam was formed by an axicon. For the formation of Bessel standing wave the back-reflecting mirror was situated in the Bessel beam zone. The counter propagating Bessel beam geometry builds up the Bessel standing wave with periodic annular structure in each anti-node. The intensity distributions formed by traveling Bessel beam and Bessel standing wave can be imparted into the photorefractive crystal via electro-optic effect thus creating 1D photonic Bessel lattices and 2D complex annular-planar photonic lattices. While the 1D Bessel-like annular refractive lattice induced by traveling Bessel beam had micrometric scale modulation in the radial direction, the 2D complex lattices inducted by Bessel standing wave were a combination of annular and planar refractive gratings with ~10 ?m period in the radial direction and half-wavelength standing wave 266 nm period in the axial direction.

The study of photochromic properties of LN:Fe:Cu crystal at 532 nm showed 1.6 times increase of absorption coefficient with increase of illuminating intensity from 12.5 to 96.8 mW/cm2, which opened a new direct approach of essential decrease of the erasure of the stored lattices during readout by weaker probe beam at the recording wavelength. The optical testing of recorded photonic lattices was performed by observing the forward diffraction of the probe beam from the lattices in the far field. The readout erasure of the photonic lattices was studied by measuring the decrease of the power of the far field light ring during readout process. The polarization of the readout beam was in the plane (e-polarization) defined by C-axis of the crystal and wave vector of the beam. The annular diaphragm was used to separate out the diffraction ring which was converged by lens into photo-detector of the power meter. Power meter was connected to PC which allowed the study of the dependence of diffracted power Pdif on the illumination time. The 1D and 2D lattices readout by homogeneous 1.2 mW 532 nm probe beams are characterized by erasure constants of 6150 sec and 5150 sec, respectively.

The suggested method is easier compared to the non-volatile two-center holographic recording performed in [2] by two-beam interference technique using 633 nm light under incoherent UV sensitizing illumination in LN:Fe:Mn crystal.

The nondestructive refractive lattices recorded by Bessel beam technique will assist the different applications for all optical devices, telecommunications, optical storage, and have particular interest for experiments on light localization and spatial soliton formation in structured nonlinear media.

References:

1. A. Badalyan, R. Hovsepyan, P. Mantashyan, V. Mekhitaryan, R. Drampyan: J. Modern Optics, 60, 617 (2013).

2. A. Adibi, K. Buse, D. Psaltis, JOSA B, 18, 584 (2001).

9127-37, Session 8

Fano resonances in high-index dielectric photonic structures *(Invited Paper)*

Mikhail Rybin, Ivan Sinev, Kirill Samusev, Ioffe Physico-Technical Institute (Russian Federation) and National Research Univ. of Information Technologies, Mechanics and Optics (Russian Federation); Andrey E. Miroshnichenko, The Australian National Univ. (Australia); Yuri Kivshar, National Research Univ. of Information Technologies, Mechanics and Optics (Russian Federation) and The Australian National Univ. (Australia); Mikhail Limonov, Ioffe Physico-Technical Institute (Russian Federation) and National Research Univ. of Information Technologies, Mechanics and Optics (Russian Federation)

Fano resonance is a fundamental physical phenomenon known across many different disciplines including optics and nanophotonics [1-3]. It is associated with a characteristic asymmetric line-shape (profile) caused by resonant wave interference. Here we reveal new remarkable manifestations of Fano resonance in high-index all-dielectric photonic structures. First, we study Mie scattering by an infinite dielectric rod, and we reveal cascades of Fano resonances in the optical cross-section which we investigate both numerically and analytically. Our analytical study is based on the exact solution of the Maxwell's equations for the Mie scattering by spatially homogeneous bodies of revolution, and the subsequent derivation of the Fano formula. Next, we revisit the study of the photonic bandgap structure and transmission spectra of two-dimensional square lattices of dielectric circular rods (a two-dimensional photonic crystal). We vary the refractive index of the rods from low to high values, and find a remarkable evidence for the existence of a novel type of Fano resonances arising due to interplay between resonant Mie scattering from individual rods and the Bragg scattering from the photonic lattice.

This work was supported by the Ministry of Education and Science of the Russian Federation, the Russian Foundation for Basic Research, and the Australian Research Council.

[1] A.E. Miroshnichenko, S. Flach, and Yu.S. Kivshar, Rev. Mod. Phys. 82, 2257 (2010).

[2] Optical properties of photonic structures: interplay of order and disorder, Eds: M.F. Limonov and R.M. De La Rue (CRC Press, 2012).

[3] A.N. Poddubny, M.V. Rybin, M.F. Limonov, and Yu.S. Kivshar, Nat. Comm. 3, 914 (2012).

9127-38, Session 9

Using small photonic crystal cavities or waveguides for all-optical signal processing *(Invited Paper)*

Alfrédo De Rossi, Thales Research & Technology (France)

No Abstract Available

9127-39, Session 9

Slow light SOI slot photonic crystal waveguides with low loss

Charles Caer, Institut d'Électronique Fondamentale (France); Sylvain Combrié, Thales Research & Technology (France); Xavier Le Roux, Institut d'Électronique Fondamentale (France); Alfrédo De Rossi, Thales Research & Technology (France); Eric Cassan, Institut d'Électronique Fondamentale (France)

Slot Photonic Crystal Waveguides (SPCW) combine strong optical confinement, arising from the giant dispersive effect of the photonic crystal, and sharp discontinuities in the electric

filed distribution at the slot sidewalls. This induces a large optical intensity in the low index material, which is very useful for a wide range of applications, from sensing to nonlinear optics. However, slow light devices are known to suffer from disorder-induced backscattering losses, which is particularly sensitive in slow light SPCW. Here we address this crucial issue, namely and we consider the propagation losses with respect to the group index by probing different infiltrated SPCW using an interferometric technique similar to Optical Coherent Tomography (OCT). OCT provides transmission or reflectance maps in time and wavelength. That provides an insightful view over the scattering mechanismsoccuring inside the waveguides. State-of-art clean room processes resulted into group velocity down to c/20 over a millimeter-long devices. We infer from these OCT measurements moderate propagation losses in fast light regime (nG<10), about15 dB.cm-1 and an efficient coupling to slow modes. We show that the transmission is strongly affected by stitching errors at the e-beam write field boundaries,, indicating that devices shorter than a write field (i.e. <300 μm) are comparable to W1 standard photonic crystal waveguides (e.g. around 100 dB.cm-1 for nG~20-25).

These results demonstrate the feasibility of slow light SPCW and shows that these devices are a promising route towards silicon organic hybrid photonics.

9127-41, Session 9

On-chip photonic tweezers: from optical trapping to manipulation of microparticles

Christophe Pin, Claude Renaut, Emmanuel Picard, Emmanuel Hadji, CEA Grenoble (France); David Peyrade, Ctr. National de la Recherche Scientifique (France); Frédérique de Fornel, Lab. Interdisciplinaire Carnot de Bourgogne (France); Benoit Cluzel, Univ. de Bourgogne (France)

In order to design future lab-on-a-chip, integrated optofluidic tools for trapping and manipulation of micro- and nano-objects are needed [1-4]. In this work, optofluidic chips with integrated photonic tweezers are fabricated by adding a polydimethylsiloxane (PDMS) microfluidic chanel on top of silicon-on-insulator (SOI) photonic “nanobeam” cavities [5].

The light resonance inside such photonic crystal cavities leads to a high spectral and spatial confinement of the electromagnetic field. Spectral and spatial characteristics of resonant modes can be tuned by coupling several cavities. The light confinement in these nanocavities generates strong and localized near-field gradient forces. First, we will show how these optical forces are used to trap, detect, assemble and manipulate microparticles [6, 7]. We will then focus on the characterisation of the studied on-chip photonic tweezers. Trap stiffnesses are deduced from the trajectory of trapped polystyrene microparticles. In the case of particles 1?m in diameter, a lateral stiffness of 5 pN.?m-1 is measured, whereas it is found to decrease to 0.5 ± 0.1 pN.?m-1 along the waveguide axis. In addition, the trap is proved to resist to lateral fluidic forces of typically 10-1pN. Corresponding particle displacements are consistent with the above measured trap stiffness.

Eventually, we also propose a new characterisation method for on-chip photonic tweezers. Indeed, designing photonic nanocavities directly within the optical waveguide enables to precisely record the influence of a trapped particle on the cavity resonance. The transmitted signal shows for instance a different correlation time depending on the particle motion. This property is used to distinguish particles 1?m and 2?m in diameter. Moreover, the analysis of the transmitted signal is investigated as a valuable method to characterise the trapping efficiency of photonic tweezers.

REFERENCES:

[1] X. Serey, S. Mandal and D. Erickson, “Comparison of silicon photonic crystal resonator designs for optical trapping of nanomaterials”, Nanotechnology 21, 305202 (2010)

[2] S. Lin, W. Zhu, Y. Jin and K.B. Crozier, “Surface-Enhanced Raman Scattering with Ag Nanoparticles Optically Trapped by a Photonic Crystal Cavity”, Nanoletters 13, pp.559-563 (2013)

[3] N. Descharmes, U.P. Dharanipathy, Z. Diao, M. Tonin and R. Houdré, “Single particle detection, manipulation and analysis with resonant optical trapping in photonic crystals”, Lab on a Chip 13, 3268 (2013)

[4] T. van Leest and J. Caroa, “Cavity-enhanced optical trapping of bacteria using a silicon photonic crystal”, Lab on a Chip 13, 4358 (2013)

[5] P. Vehla et al., “Ultra-high Q/V Fabry-Perot microcavity on SOI substrate”, Optics Express 15, pp.16090-16096 (2007)

[6] C. Renaut et al., “Assembly of microparticles by optical trapping with a photonic crystal nanocavity”, Applied Physics Letters 100, 101103 (2012)

[7] C. Renaut et al., “On chip shapeable optical tweezers”, Scientific Reports 3, 2290 (2013)

9127-54, Session 9

Polarization independent nanobeam cavity tuning using annular photonic crystals

Melih G. Can, Bigehan B Oner, Hamza Kurt, TOBB Univ. of Economics and Technology (Turkey)

Nanobeam cavity waveguides have drawn attention of the researchers due to being a useful tool for several applications, e. g. optical switching [1]. Almost all of the past studies investigated high quality (Q) factors without considering polarization independency. In the literature Loncar et. al. proposed a device that enables high Q for both transverse electric (TE) and transverse magnetic (TM) modes for a specific frequency [2]. In our study we demonstrate a three-dimensional study of polarization independent nanobeam cavity waveguide that consists of annular photonic crystals (PCs) showing similar optical properties for both TE and TM modes [3]. Also a detailed analysis of the shift of the overlapped frequency is investigated with respect to height and width variation of the nanobeam structure. The designed waveguide is composed of 12 air holes and 4 annular PCs located in the Silicon (nSi=3.46). Radii of all air holes in the structure are 0.36a. The annular PCs at the interior section have inner dielectric radius of 0.18a and the outer ones have inner dielectric radius of 0.20a. Silica (nSilica=1.52) is used as substrate. The width and height of the waveguide may be tuned in order to obtain high Q factors at the desired frequency for both polarizations.

In our analysis, we investigated the relation between width, height and cavity frequency for both TE and TM cases. Obtained frequencies are fitted to cubic polynomials of the structural parameters width and height. Overlapped frequency curve is revealed by an equalization of the polynomials of TE and TM resonant frequencies. Curve elucidates the effect of the parameters on overlap mechanism.

9127-42, Session 10

Plasmon excitation and induced emission with a plasmonic self-organized crystal *(Invited Paper)*

Agnès Maître, Univ. Pierre et Marie Curie (France) and Institut des NanoSciences de Paris (France); Hugo Frederich, Clotilde Lethiec, Institut des NanoSciences de Paris (France); Julien Laverdant, Univ. Claude Bernard Lyon 1 (France); Traian Popescu, CEA-IRAMIS (France); Catherine Schwob, Univ. Pierre et Marie Curie (France); Ludovic Douillard, CEA-IRAMIS (France); Laurent Coolen, Univ. Pierre et Marie Curie (France)

Surface Plasmon Polariton (SPP) offers the opportunity to accelerate efficiently spontaneous emission of nanoemitters located close to a metallic surface, but as SPP modes are not coupled to far-field radiative modes, they induce loss of

radiation. As metallic gratings radiate SPP modes in far field, they can be used to enhance the fluorescence of nanoemitters coupled to SPP. Moreover a periodically corrugated metallic surface offers the opportunity to absorb light with an efficiency close to 100% with applications in fields such as bio-imaging, light-emitting diodes (LED), photovoltaics or single-photon sources.

We fabricated a plasmonic crystal of centimetric size, by evaporating a thick layer of gold on an artificial silica opal used as a periodic template. By optical specular reflection spectra, we evidenced a dip of almost complete absorption due to coupling to SPP. We demonstrated a broad continuum of coupled wavelengths and perfect complete absorption over the visible spectrum whatever the direction of illumination is, illustrating a crystallographic arrangement at the microscopic scale and disorder at the macroscopic scale. The theoretical interpretation rely on a semi-analytical model based on the phase matching condition between wave vectors of propagating modes and SPP modes mediated by the metallic grating characteristic vectors. This opens new possibilities in fields where light-plasmon coupling is required over a broad range of wavelengths and incidence orientations [1].

Complementary photo-emission electron microscopy (PEEM) measurements gives a non-linear image of the excited plasmons. It demonstrates the coupling of propagating light modes to SPP and localized plasmon modes. The arrangement of the hot spots is discussed as a function of the crystallographic quality of the opal.

To study the fluorescence of nanoemitters coupled to the gold corrugated surface, we sputtered an intermediate 80 nm silica layer to avoid quenching. We then deposited colloidal CdSe/ZnS nanocrystals on silica and performed angle and polarization-resolved emission spectra. We observed a p-polarized wavelength-dependent increase of emission for the angles corresponding to previous phase matching condition (bare plasmonic crystal). As SPP are TM waves, this evidences excitation of plasmon modes by nanocrystals and re-emission of plasmons to far field p-polarized radiation.

In order to quantize the extraction and re-emission of SPP, we compared the obtained spectra to the one obtained in the case of nanocrystals on a plane gold surface. We obtained a reliable estimation of the SPP radiation rate (ratio between radiated and excited SPP) (fig2b) which shows a real improvement of the fluorescence intensity. The experimental method developed here can be generalized to other systems and provides an interesting tool for designing light-extracting devices.

References:

[1] H. Frederich, F. Wen, J. Laverdant, L. Coolen, C. Schwob, A. Maître, Isotropic broadband absorption by a macroscopic self-organized plasmonic crystal, Optics Express 19, 24424(2011).

[2] H. Frederich, F. Wen, J. Laverdant, W. Daney de Marcillac, C. Schwob, L. Coolen, A. Maître, Determination of the Surface Plasmons Polaritons extraction efficiency from a self-assembled plasmonic crystal, http://arxiv.org/abs/1311.2269, submitted(2013)

9127-43, Session 10

Lasing from Penrose quasicrystal made by holographic polymer-dispersed liquid crystals

Dan Luo, Xiao Wei Sun, South Univ. of Science and Technology of China (China)

Quasicrystals, which possesse only long-range order and orientation symmetry but not translation symmetry, was firstly observed by D. Shechtman in Al-Mn metallic alloy. Lasing, generated from photonic quasicrystals (PQCs) fabricated by semiconductor materials, have been reported to generate possible unlimited lasing modes due to the arbitrary order of their rotational symmetry while only limited mode existing in photonic crystals (PCs) .

Due to electrically switchable/tunable optoelectronic properties, liquid crystals/polymer composite have received substantial attention. Different kinds of periodic/non-periodic structures such as grating, photonic crystals and photonic quasicrystal have been realized through holography lithography based on holographic polymer dispersed liquid crystals (H-PDLCs). Despite the low index contrast, which forbids the exist of complete bandgaps, lasing from photonic crystals made by H-PDLCs is still possible due to low group velocity dispersion and local field enhancement .

In this paper, we report the lasing from photonic Penrose quasicrystal made by H-PDLCs. The lasing presented here shows excellent linear polarization property and relative low pumping threshold comparing to that from photonic crystal made by H-PDLCs. A wide directional dependence of lasing is also achieved. These properties make laser based on H-PDLC photonic quasicrystal promising for a new type of an all organic tunable miniature lasers.

9127-44, Session 10

Enhancing light emission with periodic arrays of metallic nanoparticles: near-field versus far-field phenomena

Said R. K. Rodriguez, Gabriel Lozano, FOM Institute for Atomic and Molecular Physics (Netherlands); Marc A. Verschuuren, Philips Research Nederland B.V. (Netherlands); Jaime Gomez Rivas, FOM Institute for Atomic and Molecular Physics (Netherlands) and Technische Univ. Eindhoven (Netherlands)

Periodic arrays of metallic nanoparticles constitute a versatile system for enhancing light emission from near-field sources. At the heart of this approach lies the collective oscillation of conduction electrons driven by light, known as surface plasmon polaritons (SPPs). While individual nanoparticles sustain localized SPPs (LSPPs), an array of such particles can also sustain delocalized plasmonic-photonic states due to the coupling of LSPPs to diffracted or refractive-index guided photons. In the case of diffractive coupling, collective states known as surface lattice resonances (SLRs) emerge [1-8]. In the case of waveguide coupling, waveguide-plasmon polaritons (WPPs) emerge [9,10]. Both SLRs and WPPs can lead to strong electromagnetic field enhancements extending several unit cells (>30) while still preserving subwavelength confinement out of the plane of the periodicity. Thus, in contrast to LSPPs for which emission enhancements are highly restricted spatially (typically <40 nm), these delocalized modes can collectively enhance the emission from extended sources such as thin luminescent layers [1,3,6-10].

Herein, we demonstrate how various plasmonic structures coupled to diffraction and dielectric waveguides can tailor the luminescence of both organic and inorganic materials. In particular, we show large directional enhancements (>60-fold in certain wavelength and angles for emitters with near unity quantum efficiency), polarizaton control, and unconventional discrepancies between the far-field and near-field spectra. We present light extinction and emission experiments, numerical simulations, and analytical results, for systems in both in the strong- and weak-coupling regimes. We discuss the impact of the coupling strength on the luminescence enhancements, and the dependence of the latter on the degree of light localization. Our results therefore elucidate a design strategy for enhancing the performance of solid-state lighting-emitting devices with plasmonics, and we conclude that even for emitters with near-unity quantum efficiencies, and despite the losses in the metals, plasmonics is a convenient platform for efficient and designed solid-state lighting.

[1] G. Vecchi et. al, Phys. Rev. Lett. 102, 146807 (2009).

[2] G. Vecchi et. al, Phys. Rev. B (R) 80, 20401 (2009).

[3] V. Giannini et. al., Phys. Rev. Lett. 105, 266801 (2010).

[4] S.R.K. Rodriguez et al., Phys. Rev. X 1, 021019 (2011).

[5] S.R.K. Rodriguez et. al., Phys. B 407, 4081 (2012).

[6] S.R.K. Rodriguez et. al., Appl. Phys. Lett. 100, 111103 (2012).

[7] G. Lozano et. al., Light: Science & Applications 2, e66 (2013).

[8] S.R.K. Rodriguez et al., Phys. Rev. Lett. 111, 166802 (2013).
[9] S.R.K. Rodriguez et. al., Phys. Rev. Lett. 109, 166803 (2012).
[10] S. Murai et. al., Opt. Exp. 21, 4250 (2013).

9127-45, Session 10

Tamm plasmon-polariton induced second-harmonic generation enhancement in photonic crystal structure

Vladimir O. Bessonov, Lomonosov Moscow State Univ. (Russian Federation) and A.N. Frumkin Institute of Physical Chemistry and Electrochemistry (Russian Federation); Boris I. Afinogenov, Andrey A. Fedyanin, Lomonosov Moscow State Univ. (Russian Federation)

Tamm plasmon-polaritons (TPP) in photonic crystals (PC) are optical analogues of electronic density localization at the boundary of periodic atomic potential [1]. These states manifest themselves experimentally as narrow peaks in transmittance spectra of metal/photonic crystal (Me/PC) systems [2]. Electromagnetic field is localized at the boundary of metal and PC in the presence of Tamm plasmon-polariton. Thus TPP-induced optical second-harmonic (SH) generation enhancement is expected.

The studied sample consists of 6 pairs of ZrO2/SiO2 (average thicknesses 110 nm and 145 nm, respectively) quarter-wavelength-thick layers deposited on fused quartz substrate using thermal evaporation. The thickness of the topmost layer was 225 nm. The resultant photonic crystal was covered with a semitransparent 30-nm-thick gold film allowing good field localization in the TPP mode. Bare photonic crystal of the same parameters and a 30-nm-thick gold film on fused quartz substrate were reference samples. A Ti:sapphire laser with a pulse duration of approximately 150 fs, a repetition rate of 80 MHz, and the output wavelength tunable from 720 to 860 nm was used as the radiation source. The average laser power on the sample was 20 mW. The beam was focused to the 20-?m-wide spot at the sample. Generated second-harmonic radiation was collimated to a photomultiplier tube through 9-mm-thick BG 39 filter to reject fundamental light. Gated photon counter was used for signal detection. Second-harmonic intensity spectra were measured with 1-nm resolution. Measurements of transmittance spectra were performed together with SH spectra ones to provide the control of TPP excitation.

According to the theory and numerical calculations, electromagnetic field is localized at the interface of metal and photonic crystal in the presence of TPP. As main part of SH in metals is generated by the surface, enhancement of local electromagnetic field leads to enhancement of the SH signal from the metal film. The SH intensity spectra of the reference samples demonstrated no features. The average SH signal level generated by the Au/PC sample out of the TPP transmittance resonance corresponds to the signal level from the reference samples. Sharp peak in the SH intensity spectrum of the Au/PC sample is observed in the vicinity of the TPP transmittance resonance. The maximum achieved SH enhancement factor is 50 in the maximum of the TPP resonance. With increasing the angle of incidence the position of the SH resonance redshifts which coheres with the behavior of the TPP dispersion curve. The experimental results are in good agreement with numerical calculations.

The experimental proof of SHG enhancement in Au/PC system in the presence of TPP is obtained. The 50-times TPP-induced enhancement of the SH signal is shown. This is an unambiguous experimental evidence of the electromagnetic field localization in the TPP mode at the boundary of metal and photonic crystal.

[1] I.E. Tamm, JETP 3, 34 (1933).
[2] M. Kaliteevski et al. Phys. Rev. B 76, 165415, (2007).

9128-28, Session PS1

New possibilities of higher-order mode filtering in large-mode-area photonic crystal fibers

Vladimir Demidov, Egishe Ter-Nersesyantz, S.I. Vavilov State Optical Institute (Russian Federation)

Large-mode-area photonic crystal fibers (PCFs) have proven themselves as powerful optical elements on the way of suppressing undesirable nonlinear processes in fiber-based lasers and high-intensity beam delivery systems. However, extremely high bending sensitivity restrains noticeably the effective mode area expansion. We provide theoretical and experimental analysis of a few phenomena affecting higher-order mode discrimination toward pure single-mode propagation (beam quality factor M squared insignificantly exceeds 1.0) and improved bending properties (exploitation of a PCF on a spool of small radius) in very-large-core structures. Firstly, the core was comprised of 7 elements instead of 1 in order to reduce the pitch (hole-to-hole spacing), since smaller pitches correspond to lower bend-induced losses in the structures with conventional C6V cladding symmetry. That measure aided to realize a set of PCFs with a core of 35-75 μm in diameter (which means comparatively small pitch varying from 10 to 23 μm) propagating a single transverse mode due to embedded leakage channels for the higher-order mode which losses were rated to be above 1 dB/m in a straight fiber and approximately 10 dB/m in a bent fiber. The ability of the fibers to maintain robust single-mode operation far beyond the phase higher-order mode cutoff condition enables exceptional bending resistance characteristics even for cores of greater diameter giving the effective mode area of 5000 square μm. Secondly, we studied and implemented a PCF having C3V cladding symmetry with intentional alternation of large and small air holes, especially in the first air-hole ring, relying on the discrepancy in spatial higher-order mode distribution and organized geometrical configuration. As predicted, owing to increase in the ratio of large/small air holes the excited higher-order mode split to three uneven parts leaking from the core with an overall attenuation coefficient of about 2 dB/m. The efficient higher-order mode delocalization process allowed to obtain single-mode propagation in a core of 35-50 μm in diameter. Furthermore, when the ratio exceeds 2 there is almost no need in bending, but if the fiber is bent the created leakage channels only enhance the higher-order mode losses to tens of dB/m. Thirdly, we drawn a series of PCFs with a core of 35-60 μm in diameter which was shifted from its usual location in the center of the structure. Initially, we started from the typical 4-ring PCF and then shifted the core for a single-pitch, double-pitch and triple-pitch values. The aim was to provoke an enhancement of the higher-order mode leakage losses, as it has a larger field near to the air-hole silica interfaces compared to the fundamental mode. At the same time, the most substantial part of experiment lied in the ability to control higher-order mode filtering by choosing a certain bending plane, since the core was placed closer to the outer fiber cladding than in a classical structure. Those PCFs have distinguished bending resistance properties and can be bent on a spool of 5 centimeters in diameter.

9128-1, Session 1

Electrostatic actuation of nanomechanical optical fibres with integrated electrodes *(Invited Paper)*

Nina Podoliak, Zhenggang Lian, Martha Segura-Sarmiento, Wei H. Loh, Peter Horak, Univ. of Southampton (United Kingdom)

We are investigating theoretically and experimentally the possibility of integrating microelectromechanical systems (MEMS) functionality into microstructured optical fibres. In previous work [1] we have demonstrated a nanomechanical optical fibre that can be mechanically reconfigured by controlling the gas pressure inside an air hole of the microstructure. However, for various applications e.g. in telecommunications, sensing, or imaging, a faster and more robust actuation method is desirable.

Here we study electrostatic actuation of a nanomechanical optical fibre having two optically guiding cores suspended in air by thin flexible membranes. The electrostatic forces are generated by electrically charged electrodes embedded in the fibre cladding. We first present a simplified analytical model to qualitatively describe the electrostatic actuation. Two mechanisms are found to contribute significantly: (i) The electrodes induce electrical dipoles in the fibre cores which subsequently experience gradient forces due to the non-uniform background field; (ii) the induced dipoles of the two cores also interact directly through dipole-dipole interaction. Fibre designs with one to four electrodes are analysed and, in particular, a quadrupole geometry is shown to allow for all-fibre optical switching in a 10cm fibre with an operating voltage of 35V. The analytical model is also supported by full numerical simulations.

First fibres have been successfully fabricated via a co-draw technique from a glass preform with the corresponding parts filled by tin to form the electrodes. Tens of metres of fibre were fabricated with relatively uniform cores with good optical guidance; the electrodes were demonstrated to be continuous. The supporting membranes in these first fabricated fibres, however, turned out to be too stiff to allow for measurable electromechanical actuation. Optimisation of the fabrication method and experimental demonstration of nanoelectromechanical fibre functionality are therefore still ongoing.

[1] Z. Lian et al., Opt. Express 20, 29386 (2012).

9128-2, Session 1

Integration and excitation of microsphere optical resonators inside microstructured optical fibers *(Invited Paper)*

Kyriaki Kosma, Gianluigi Zito, Foundation for Research and Technology-Hellas (Greece); Kay Schuster, Institute of Photonic Technology Jena (IPHT) (Germany); Stavros Pissadakis, Foundation for Research and Technology-Hellas (Greece)

Light localisation into transparent microspheres, in the form of so-called whispering-gallery modes (WGM) has been of high interest in the area of photonics during the last fifteen years. Excitation is commonly achieved through planar waveguides, prisms, fiber tips and tapers, placed at evanescent-field proximity with the spherical microcavity. We report here on a new, integrated in-fiber microresonator coupler, which is a combination of a microstructured optical fiber (MOF) and a microsphere; the last is encapsulated into one of the capillaries of the MOF. In such a scheme, the light guided into the MOF core excites WGMs inside the encapsulated microsphere, manifested in out-scattering or transmission mode. Microspheres being made of polystyrene (n=1.59) or BaTiO3 glass (n~2.1) and having a variable diameter between 4.7 – 10.4?m, have been infiltrated inside silica and germanosilicate core MOFs and their spectral response was measured. The operation of this composite light coupler has been investigated under two different launch/collection schemes, i.e. the core-input/sphere-output and the sphere-input/core-output modes, for TE and TM polarisations, leading to Q-factors 3.5?103 for a single microsphere. Results related to the infiltration of several

polystyrenes microspheres inside a single MOF capillary and their spectral scattering characterisation will be shown; focusing on improved Q-factors obtained. Furthermore, the tuning of the WGM spectral behaviour of a BaTiO3 glass microsphere infiltrated inside a MOF by exploiting photorefractivity effects while using C.W. 532nm laser radiation will be presented.

9128-3, Session 1

Effect of the coverage density of noble metal nanoparticles on the performance of SERS-active microstructured fibers

Jiri Kanka, Institute of Photonics and Electronics of the ASCR, v.v.i. (Czech Republic); Polina Pinkhasova, Massachusetts Institute of Technology (United States); Henry H. Du, Stevens Institute of Technology (United States)

Surface functionalization of air channels of a microstructured fiber imparts the functionality of surface-enhanced Raman scattering (SERS) in the functionalized microstructured fiber for chemical and biochemical sensing and detection. To realize a SERS-active microstructured fiber, noble metal nanoparticles are immobilized in the fiber air channels with a controlled surface coverage density. Our experiments with different types of microstructured fibers and nanoparticles revealed that a higher SERS signal is generated in a longer fiber with a low nanoparticle density. To provide a deeper understanding of phenomena behind the coverage density effect and also guidelines for the SERS-acttive fiber design, the optical properties of a collection of nanoparticles, and possible coupling events between them, are numerically investigated. For the modeling of nanoparticles, the Finite Element Method (FEM) and Generalized Multi-particle Mie (GMM) solution are implemented.

9128-35

The role of specialty fi bers in fi ber optic sensors (Presentation Only)

Alexis Mendez, MCH Engineering LLC (USA)

As optical fibers cemented their position in the telecommunications industry and its technology and commercial markets matured, parallel efforts were carried out by a number of different groups around the world to exploit some of the key fiber's features and utilize them in sensing applications. The requirements imposed by the broad variety of these new applications have resulted in the evolution of a new subset of custom-tailored optical fibers commonly known as "specialty fibers", which have their material and structure properties manipulated to render them with new properties and characteristics.

This talk will review the basic principles, applications, and specialty fiber needs for optical fiber sensors. Key technical trends will be identified along with relevant commercial opportunities and challenges.

9128-4, Session 1

Hollow core photonic crystal fibers for biological recognition processes

Alessandro Candiani, Sara Giannetti, Univ. degli Studi di Parma (Italy); Hussein T. Salloom, Univ. of Baghdad (Iraq); Michele Sozzi, Univ. degli Studi di Parma (Italy); Ahmad K. Ahmad, Al Nahrain Univ. (Iraq); Annamaria Cucinotta, Univ. degli Studi di Parma (Italy); A. Hadi Al-Janabi, Univ. of Baghdad (Iraq); Stefano Selleri, Univ. degli Studi di Parma (Italy)

The recent advent of Hollow-Core Photonic Crystal Fibers (HC-PCF), which consist of a hollow (air) core surrounded by air holes running down the length of the fiber, provide a unique opportunity for chemical and biological application. HC-PCF potential efficiency as a biosensor is due to the large overlap between the propagating field and the sample. Moreover very small volumes are required to fill the holes of HC-PCF, which is highly advantageous in the case of hazardous or expensive substance.

In this work, theoretical and experimental bio-functionalized all silica HC-PCFs has been investigated for label free DNA detection. The approach is based on layer-by-layer self-assembly Peptide Nucleic Acid (PNA) probes, which is an oligonucleotide mimic that is well suited for specific DNA target recognition, allowing the recognition of specific sequences of DNA. Two kinds of HC-PCFs have been considered: a one dimension photonic Bragg fiber and a two dimension photonic hollow core (HC-1060) fiber. After spectral characterization and internal surface functionalization using PNA probes, genomic DNA solutions from soy flour were infiltrated into the fibers. The hybridization of the complementary strand of target DNA increased the optical thickness of the silica internal surface. This led the generation of surface modes, resulting in a significant modulation of the transmission spectra. Theoretical investigations will also be presented to support the experimental results, demonstrating the feasibility of this approach for biosensing applications.

9128-5, Session 1

Flavin and porphyrin-micro optical fibre biosensor: analysis and design

Jesús S. Velázquez-González, Ctr. de Investigación en Ciencia Aplicada y Tecnología Avanzada (Mexico); Saúl Mújica-Ascencio, Ctr. de Investigación e Innovación Tecnológica (Mexico); Alfredo I. Aguilar-Morales, Sigifredo Marrujo-García, José A. Álvarez-Chávez, Fernando Martínez-Piñón, Instituto Politécnico Nacional (Mexico)

Micro Optical Fibre Biosensors (MOFBS) are emerging as one of the most sensitive bio-detection system technologies which do not require of labelling or amplification of the analyte. In these devices, a short region of the fibre core is exposed to the external environment, so that the evanescent field can interact with biological species such as cells, proteins, and DNA. In order to increase the sensitivity and selectivity, MOFBS are often used in combination with other optical transduction mechanisms such as changes in refractive index, absorption, fluorescence and surface plasmon resonance. In this work we present the full characteristics, analysis and design of a MOFBS for Flavin and Porphyrin detection.

9128-6, Session 2

Low loss chalcogenide microstructured optical fibers for IR applications *(Invited Paper)*

Laurent Brilland, David Méchin, PERFOS (France); Perinne Toupin, Celine Caillaud, Institut des Sciences Chimiques de Rennes (France); Pascal Besnard, CNRS-Fonctions Optiques pour les Technologeis de l'information (France); Thierry Chartier, Ecole Nationale Supérieure des Sciences Appliquées et de Technologie (France); Guillaume Canat, ONERA (France); Gilles Renversez, Institut Fresnel (France); Johann Trolès, Institut des Sciences Chimiques de Rennes (France)

The chalcogenide glasses are among the most nonlinear glasses with a Brillouin gain and an index of nonlinear refraction n2, 2 orders of magnitude larger than that of silica. Microstructured optical fibers (MOF) have been developed since 20 years and are well known to enhance the nonlinear effects. During the 2000's, the main challenge was to reduce the losses in chalcogenide MOF. Recently, in 2010, a casting method has

been developed to produce chalcogenide microstructured preforms leading to the fabrication of low loss fibers. We will describe this method and will show the different designs that can be achieved. This breakthrough has opened the way to the studies of optical functions for Infrared applications. Some results of these works will be presented. At telecom wavelengths, the chalcogenide MOFs enables the enhancement of nonlinear effects at low power threshold. For applications based on Brillouin fiber laser, a 4 μm core of a single mode chalcogenide MOF has been developed. A threshold pump power of only 6 mW and 30 mW respectively was necessary to generate the first and second stock component. In the middle infrared, supercontinuum generation is one of the most exciting optical functions but it is still a challenge to achieve. We will discuss about the importance of the glass composition and the MOF design to generate efficiently a supercontinuum. In addition, a chalcogenide exposed core acting as a sensor has been made and we will present some preliminary chemical sensing measurements.

9128-7, Session 2

Striving towards a periodicity breaking of the photonic crystal fibers microstructuration for an unprecedented singlemode robustness

Romain Dauliat, Institut für Photonische Technologien e.V. (Germany) and XLIM Institut de Recherche (France); Aurélien Benoit, XLIM Institut de Recherche (France) and EOLITE Systems (France); Raphaël Jamier, XLIM Institut de Recherche (France); Kay Schuster, Institut für Photonische Technologien e.V. (Germany); François Salin, EOLITE Systems (France); Philippe Roy, XLIM Institut de Recherche (France); Stephan Grimm, Institut für Photonische Technologien (Germany)

The reliability of optical fibers for high power laser/amplifier operation is nowadays manifest with optical powers reaching up to 10 kW in continuous wave while maintaining a good beam quality. However non-linear phenomena commonly impact the emitted spectrum, leading to a strong infatuation for the development of Large-Mode-Area (LMA) fibers. To date, a singlemode operation was evidenced in Large Pitch Fibers (LPF) exhibiting a Mode Field Area (MFA) exceeding 10,000μm? [1].

Nevertheless, it has been highlighted recently that these LMA LPFs are subjected to modal instabilities [2]. This mechanism, occurring when the pump power exceeds a certain threshold, stems from the inherent ability of LMA LPFs to sustain several core modes. In this context, we have proposed novel kinds of microstructured LPFs exhibiting much lower core modes content [3]. As presented in [4], our opto-geometrical considerations are dictated by the selected manufacturing process based on the stack and draw of sintered and vitrified doped powders [4]. Then, a full-vector finite-element-method based software was used to compute the first 300 guided modes for each proposed fiber structure. In this way, we evidenced and took care of the resonant and disturbing LP31 mode.

In this communication, we will discuss a thorough investigation of all-solid triple-clad microstructured LPFs aiming to provide a robust singlemode emission. First, we will demonstrate an efficient discrimination of unwanted High-Order Modes (HOM) by resorting to beneficial modes couplings. This was made possible thanks to a judicious introduction of low-index inclusions into the inner cladding microstructuration. These low-index rods influence then the effective indices of the guided modes and act on the modes couplings dynamic. Following this approach, several optimized LPFs have been developed. However, these fibers are not scalable contrary to air/silica LPFs. Thence; we have devised aperiodic microstructured LPFs structures favouring the HOMs delocalization out of the gain region. Indeed, the confinement of high-order symmetric modes into the active core was avoided because of the cladding aperiodicity. Moreover, the mode leakage was improved as only five low-index inclusions surround the gain region. For instance, a Spiral-like LPF was designed, exhibiting stronger singlemode robustness than that of the state-of-the-art air/silica LPF. In this case, the standard 6-fold symmetry of conventional microstructured LPFs was fully removed. To go further, a robust singlemode operation was also noticed in fully aperiodic microstructured fibers. The scalability (from 40 to 100 μm core) and wavelength independent behaviour in the near-IR range (from 400 to 2200 nm) of aperiodic microstructured LMA LPFs is also discussed.

[1] Limpert et al., “Yb doped large-pitch fibers: effective singlemode operation based on higher-order modes delocalization”, Light: Science & applications 1, e8 (2012).

[2] Eidam et al., “Experimental observation of the threshold-like onset of modal instabilities in high power fiber amplifier”, Optics Express 19, 13218-24 (2011).

[3] Dauliat et al., “Inner cladding microstructuration based on symmetry redcution for improvement of singlemode robustness in VLMA fibers”, Optics Express 21 (16), 18927-36 (2013).

[4] Dauliat et al., “Ytterbium doped all-solid Large-Pitch Fiber made from powder sintering and vitrification”, International conference in fiber optics and photonics, TPo.7 (2012).

9128-8, Session 2

Double-cladding photonic crystal fibers with reduced cladding symmetry for Tm-doped lasers

Enrico Coscelli, Carlo Molardi, Federica Poli, Annamaria Cucinotta, Stefano Selleri, Univ. degli Studi di Parma (Italy)

High-intensity sources, capable of delivering several Watts of output power at ~2?m are currently required by many applications, such as soft-tissue medicine, communication, material processing and sensing. To this aim, Thulium-doped fiber lasers appear to be a valuable option, being able to combine high-brightness and beam quality together with compactness and emission on a wide band between about 1.9?m and 2.1?m, when pumped with commercially-available diodes at 790nm.

One of the key-factors to improve the laser performances beyond the current state-of-art, especially for what concerns operation in the short-pulse regime, is the development of large mode area double-cladding Tm-doped fibers capable of operating in the Single-Mode (SM) regime under high heat load. Indeed, due to the remarkable quantum defect of Tm ions, a large fraction of the pump power is converted into heat, which leads, through thermo-optic effect, to an increase of the index contrast that allows guidance of high-order modes.

In this paper, innovative Photonic Crystal Fibers (PCF) with optimized air-hole matrix, designed to break the C6? symmetry of the inner cladding while preserving their feasibility through the well-established stack-and-draw technique, are presented. The possibility to provide stable SM guiding at ? ~ 2?m with core diameter up to 100?m and a coupled pump power exceeding 300W is analyzed by means of a full-vector modal solver based on the finite-element method with embedded thermal model, to account for the effects of heating on the mode confinement. Simulation results have been used to carefully trim the PCF parameters, such as the cladding hole-to-hole spacing and air-hole diameter, to achieve the highest possible discrimination between the fundamental mode and the most-confined high-order mode during laser operation. Effective suppression of the high-order modes under a heat load of 350W/m, while keeping an effective area exceeding 2500 ?m2 has been demonstrated.

9128-9, Session 2

Influence of core diameter and Cladding-Core-ratio on light-guidance in specialty step-index fibers

Karl-Friedrich Klein, Hannah Ohlmeyer, Tim Tobisch, Technische Hochschule Mittelhessen (Germany); Mathias Belz, World Precision Instruments (Germany); Maarten A. J. Voncken, Leonhard Prechtel, ASML Netherlands B.V. (Netherlands)

Multimode fibers with a core and step-index core/cladding profile are commonly used from 185 nm (DUV) up to 2300 nm (NIR). The core diameters of such fibers range from 100 to 600 μm and the clad-to-core-ratios (CCR) typically are 1.1 and larger.

Fibers with smaller core diameter and thinner cladding thicknesses are interesting candidates for bundle applications in the UV-region. Such mono fibers offer reduced coupling losses due to the fact that the light acceptance surface area is relatively larger. However, using these bundles at higher wavelengths, e.g. in the VIS- or even NIR-region, different light-guiding properties including total transmission can be observed.

In this work, the numerical aperture (NA) of such specialty fibers will be determined in dependence of wavelength, using the inverse far-field method at two separate laser wavelengths and with a broadband source from 190 nm up to > 2000 nm. Further, the spectral fiber attenuation with UMD-illumination and mode-selective illumination will be discussed and compared with the experimental NA results. Finally, bending losses are included in this study. As expected, the ratio of cladding thickness and wavelength is the most important parameter reducing the NA and transmission in short-length applications with increasing wavelength. As a consequence, an upper wavelength limit for e.g. sensing applications is presented and discussed in respect to the geometrical data of these specialty fibers with reduced cladding-thickness.

9128-10, Session 2

New design of multicore nonlinear photonic crystal fiber for mid-IR supercontinuum generation

Amira Baili, Rim Cherif, Mourad Zghal, SUP'COM (Tunisia)

Supercontinuum (SC) generation is a nonlinear optical phenomena characterized by the dramatic spectral broadening of intense light passing through a nonlinear material. The SC is useful in a diverse range of fields, including frequency metrology, optical coherence tomography, fiber laser and gas sensing. For mid-infrared applications, broadband, coherent, and low energy spectra are required.

In order to increase the expansion of coherent supercontinuum generated in photonic crystal fibers (PCF), we propose a new design of six-core As2Se3-based chalcogenide PCF having an effective mode area equal to 5.4 μm2. We use chalcogenide glasses because they offer a high refractive index, large nonlinearities, and excellent transmission at IR wavelengths. Several simulations are performed and optimized results are found for ? equal to 1 μm and different filling ratios varying from 0.6 to 0.9 thus, leading to a normal dispersion with a flat top profile at -3 [ps/(nm.km)]. The full-vectorial finite element method is used to determine the mode field distribution and calculate the optical fiber properties of the multicore (MC) PCF e.g. chromatic dispersion D, nonlinear coefficient ? and effective mode area Aeff. The energy of the generated spectrum in the MC-PCF is two times greater than that generated in the single core PCF having the same air hole diameter and hole to hole distance. We find a coherent, flat and smooth SC extending over 4000 nm, from 1700 to 5925 nm by pumping the fiber at ?p=3.4 μm with a femtosecond laser having 50 fs as pulse width with a relatively low energy of E=100 pJ in only 1 cm fiber length. We examine the interplay of the nonlinear effects leading to the construction of the SC while optimizing the injected energy, the pulse duration and the fiber length. These results will be helpful in the future design of MC-PCF with proper guidance properties for high power supercontinuum generation.

9128-26, Session PS1

Defining single-mode regime of double-cladding large mode area optical fibers

Enrico Coscelli, Federica Poli, Masruri Masruri, Annamaria Cucinotta, Stefano Selleri, Univ. degli Studi di Parma (Italy)

Recent years have seen an outstanding improvement of the performances of fiber lasers and amplifiers, both in the continuous-wave and pulsed regimes. Today's high-power, premium-beam quality, highly-efficient systems rely on constant innovations of the double-cladding fiber technology, which led to the development of several Single-Mode (SM), large mode-area fiber designs with high pump absorption. Among them, Photonic Crystal Fibers (PCFs) appear to be the most promising solution for future ultrafast lasers, being able to overcome the limits of step-index technology concerning the control of core/cladding index contrast. In most cases, the PCFs exploit the differential leakage between the Fundamental Mode (FM) and the High-Order Modes (HOMs) to strip the latter ones from the active core, effectively suppressing them during amplification.

One preliminary issue in the development of double-cladding fibers is the possibility to define in which conditions effectively single-mode operation is achieved, and to be able to numerically assess it through simulations. Several definitions of the single-mode condition have been given in literature, which, in most cases, are not directly comparable with each other. Moreover, some of them are based on the assumption of either an infinite cladding or on the removal of the low-index outer cladding to allow calculation of the confinement losses. Recent works have shown that these approximation cause significant changes in the expected mode properties and do not provide reliable information on the SM regime.

In this work the modal properties of several PCF designs have been studied numerically with the aim to compare the different definitions of SM regime currently used, and to infer the limits of their applicability. Moreover, a spectral and spatial amplifier model has been applied to account for the effects of other system parameters, such as fiber length and input coupling, on the effectiveness of HOM suppression through gain competition.

9128-27, Session PS1

Higher order dispersion measurement using the stationary phase point method

Tímea Grósz, Attila P. Kovács, Univ. of Szeged (Hungary)

Chirped pulse amplification (CPA) is the current state of the art technique on which the vast majority of high power laser systems are based on. In CPA systems where pulse compression is required the aim is to cancel the group-delay dispersion (GDD) out. Doing so, the third and the higher order terms in the spectral phase of the pulse become significant. A similar effect occurs in the case of specialty, more and more widespread photonic crystal fibers, as their GDD can be reduced by tailoring the geometry of the fiber. As it is well known certain pulse distortions can be associated with given dispersion terms, thus monitoring and precise measurement of the higher order dispersion is crucial.

Spectral interferometry is a commonly used technique for dispersion characterization. There are more evaluation methods suitable for spectral phase retrieval. For instance the applicability of the so-called stationary phase point (SPP) method has already been demonstrated in measuring the dispersion of various optical elements. To the best of our knowledge up until now this method was used only on optical

elements and fibers where the highest decisive dispersion term was the GDD.

In this work we present a detailed study of the applicability of the SPP method when other higher order dispersion terms become significant. We did a simulation to demonstrate the effects of given dispersion terms on the movement and shape of the SPP. First of all we assumed that the GDD is the only decisive term the spectral phase, using the values for fused silica. As expected, in this case one SPP is formed in the interferogram which simply travels along the wavelength axis as the delay between the reference and sample arm of the interferometer is changed. Since the GDD can be reduced at the expense of an increment in the third order dispersion (TOD), either by prism or grating pairs or a specially designed fiber, we performed a simulation to analyze this case. Now two SPPs appear in the interferogram which symmetrically travel toward each other as the delay between the arms of the interferometer decreases. By following the movement of the SPPs the group delay as a function of the wavelength is easily measured along the whole domain, thus the dispersion coefficients describing the spectral phase can be retrieved from a simple polynomial fit. We also investigated the case when the fourth order dispersion (FOD) became the most significant term. At a first glance this case resembles the case of dominant GDD, except here the SPP becomes too broad at some delays making the evaluation impossible in a certain wavelength domain. It can be concluded that while the SPP method is suitable for dispersion measurement up to the third order, it is less sensitive if fourth order dispersion is dominant. Having the measurements performed on a TOD-dominant fiber sample (HC-800, NKT Photonics) we found good agreement between simulations and the measurements.

9128-29, Session PS1

Dispersion limits of the small mode area photonic crystal fibers designed as a broadband compensator

Richard Zeleny, Michal Lucki, Czech Technical Univ. in Prague (Czech Republic)

Nonlinear photonic crystal fibers with the small effective mode area allow one to control chromatic dispersion in the near-infrared region. This paper investigates dispersion limits in a nonlinear photonic crystal fiber with hexagonal geometry and nondoped silica core. Chromatic dispersion is controlled entirely by structural parameters and the influence of each structural parameter on the chromatic dispersion is examined and described in detail. An understanding of these influences not only permits fiber design and dispersion tailoring, but it also predicts the potential manufacturing tolerances. As a consequence, the fiber structural parameters are modified to found the balance between the operating bandwidth and the high negative dispersion parameter. It should be noticed that the structural parameters are adjusted with respect to the confinement loss being below the Rayleigh scattering loss. Taking these facts into account, a novel fiber, which exhibits desirable residual dispersion property from 1410 to 1700 nm, is considered. In spite of the fact that the relative dispersion slope is in good agreement over the large range of operating wavelengths with the relative dispersion slope of standard single mode fibers, the negative dispersion parameter is not higher than in commercially available dispersion compensating fibers. Therefore the structural parameters are optimized to increase the confinement of the fundamental mode in the core, which, in fact, leads to smaller effective mode area and lower chromatic dispersion. As a result, the desired dispersion slope is achieved in the narrower band of wavelengths of about 120 nm. More specifically, waves with shorter wavelengths are confined more in the core than those with longer wavelengths. Therefore, the chromatic dispersion decreases with the smaller effective mode area, which is more significant for longer wavelength waves. The effective mode area cannot be smaller due to the confinement loss, which significantly grows with it. It is also necessary to increase number of air-hole rings. The chromatic dispersion parameter is minimal, while the bandwidth in which the chromatic dispersion can be compensated is kept maximal. The limit value for the dispersion parameter is of about -1600 ps/(nm.km). We predict that the negative dispersion parameter cannot be higher in the small mode area photonic crystal fibers operating over the bandwidth larger than the one considered in our paper. The results are calculated by applying the full-vectorial finite difference frequency domain method on the fiber cross-section bounded by anisotropic perfectly matched layers.

9128-30, Session PS1

Dispersion nonlinear refractive index on multiwavelength generation through mismatch photonic crystal fibre from transmission wavelength

Mohd Nizam Abdullah, Sahbudin B. H. Shaari, Abang Annuar Ehsan, Susthitha Menon, Univ. Kebangsaan Malaysia (Malaysia); Osman Zakaria, SIRIM Berhad (Malaysia)

This paper proposes a measurement of nonlinear refractive index in the course of multi wavelength technique. We have generated a multi wavelengths formation by utilising a photonic crystal fibre (PCF) which mismatches zero dispersion wavelength from transmission wavelength at 1550 nm. We provide an experimental set-up in generating the multi wavelength phenomenon. A fibre ring laser configuration consists of erbium doped fibre amplifier (EDFA) set up and arrangement of FBGs is described. Encouraging results obtained from the set up proves the relations of signals generated through FBGs and new wavelengths. These findings shows, multi wavelengths able to present valuable inputs in determination of nonlinear refractive index parameter.

9128-31, Session PS1

Insights into microstructure and chemistry of active fiber core material produced by the granulated silica method

Hossein Najafi, Berner Fachhochschule Technik und Informatik (Switzerland); Dereje Etissa, Univ. Bern (Switzerland); Valerio Romano, Berner Fachhochschule Technik und Informatik (Switzerland)

The production of special fibers relies on new methods and materials to incorporate new functionalities into optical fibers by virtues of dopants and structure. In particular, the granulated silica method allows to rapidly produce active fibers with high dopant content and with virtually any microstructure.

The implementation of this production method requires a multitude of process steps at various temperatures and temperature gradients that can significantly influence the optical properties of the produced preforms and fibers.

To better understand and optimize the processes of active material production and fiber drawing parameters we have done a thorough analysis of microstructure, phase development, cristallinity and chemical mapping of active fiber cores produced by the granulated silica method. The microstructure of fibers have been analyzed with a diverse suite of techniques in Transmission Electron Microscopy (TEM), revealing formation of various silica polymorphs and distribution of active elements into the core structure. Our results show the presence of another polymorph of silica with low crystallinity dispersed in the amorphous main polymorph (i.e. quartz). We conclude that in spite of importance of homogeneous distribution of Yb and P into the core, the formation of various silica polymorphs resulting from materials processing has to be considered.

9128-32, Session PS1

High spatial resolution optical time domain reflectometer (HROTDR) for the characterization of doped optical fibers

Ali F. El Sayed, Manuel Ryser, Univ. Bern (Switzerland); Valerio Romano, Univ. Bern (Switzerland) and Berner Fachhochschule Technik und Informatik (Switzerland)

To measure fiber losses, the methods of choice are the cut-back method and the optical time domain reflectometry (OTDR). These methods are optimized for telecommunication fibers of tens of km length. Here we present an adapted version that allows to measure the losses of special fibers, e.g. of short active fibers of few meters length. Our HROTDR allows to measure the overall attenuation in short optical fiber pieces, to locate big scatterers, defects and faults, and to estimate the fiber length. Various types of high resolution photon-counting OTDR's at different wavelengths have already been demonstrated, using various kinds of detectors. However, the spatial resolution is in most cases limited by the laser pulse duration, as the dynamic range decreases with shorter duration and by the detector response time. Our purpose in this experiment is to characterize short optical fibers with a high spatial resolution of few centimeters. Therefore, we built a HROTDR based on time-correlated single-photon-counting technique (TCSPC) that has the advantage that the time resolution of TCSPC is not limited by the impulse response of the detector and the dynamic range can be increased by longer measurement times. However, the limiting factor is in our case the timing accuracy of our TCSPC system which is limited by the timing uncertainty the detector introduces in the conversion from a photon to an electrical pulse. However, this timing error can be as much as 10 times smaller than the detectors impulse response. By using a single-photon counting avalanche diode with a timing resolution of 55 ps and a pulsed diode laser with short pulse duration of 60 ps, we are able to characterize a fiber of several meters length with a spatial resolution of 2 cm (200 ps).

9128-33, Session PS1

All-glass leakage channel fibers with large mode area

Jonas Scheuner, Manuel Ryser, Univ. Bern (Switzerland); Valerio Romano, Univ. Berne (Switzerland) and Berner Fachhochschule Technik und Informatik (Switzerland); Thomas Feurer, Univ. Bern (Switzerland)

Power scaling in fiber lasers and amplifiers is inherently linked with fiber designs and fabrication concepts that target an increase of core size without losing beam quality. The leakage channel fiber (LCF) is a very promising approach to achieve this goals. Among the different implementations of this type of fiber, the all-glass variant is advantageous with respect to production and operation at high power: Using a low-index glass instead of air holes simplifies the production and increases the damage threshold. The greatest difficulty in the realization of this concept, is the precise control of the refractive indices in the structure: Namely, the low-index structure elements and the index-matching between active core and passive cladding.

The granulated silica method potentially solves this problem, since the composition of silica powder which constitutes the bulk material, can be controlled accurately. Furthermore, this method facilitates the control over the realization of the aimed geometry. With this method at disposition, it is possible to implement structures preliminarily examined in simulations in a fast and accurate way.

First results of our work in this field will be presented.

9128-34, Session PS1

Highly nonlinear birefringent tellurite photonic crystal fiber

Amr Abdelghani, Electronics Research Institute (Egypt); Mohamed F. Hameed, Zewail City of Science and Technology (Egypt); Maher Abdelrazzak, Mansoura Univ. (Egypt); Moataza Hindy, Electronics Research Institute (Egypt); Salah S. Obayya, Zewail City of Science and Technology (Egypt)

In this paper, a novel design of tellurite photonic crystal fiber (PCF) is presented and analyzed. The proposed design offers high birefringence, high nonlinearity and low confinement losses for the two fundamental polarized modes. The cladding air holes of the suggested PCF are arranged on a triangular lattice on the corner of a triangle shape. A bigger hole of diameter d1 is located at the top corner of the triangle shape while the two holes at the bottom side have a diameter of d2. The distance between the two holes at the bottom side is equal to x-hole pitch ?x. In addition, to achieve good field confinement through the core region, small hole of diameter d3 is located at the midpoint between the two holes at the bottom side of the triangle. The distance between any two holes in the y-direction is called y-hole pitch ?y. In order to study the modal characteristics of the reported design, the use of full vectorial numerical approaches is mandatory. In this investigation, the full-vectorial finite-difference method (FVFDM) with nonuniform meshing capabilities is used to study the optical properties of the reported deign. In order to calculate the leakage property of the modes, a perfectly matched layer (PML) boundary condition is considered at the edges of the computational window. The analyzed parameters are the birefringence, effective mode area, nonlinearity and the dispersion for the two fundamental polarized modes. The effects of the structure geometrical parameters on the modal properties are studied in detail. The numerical analysis reveals that the proposed design has high birefringence of 0.10568 and high nonlinearity ? of 4784 W-1 Km-1 and 4030 W-1 Km-1 for the quasi transverse electric (TM) and quasi transverse magnetic (TE) modes, respectively at the operating wavelength of 1.55 μm with low losses for the two fundamental polarized modes. Also, the dispersion can be tailored to achieve flat or zero dispersion. The fabrication tolerances of the structure geometrical parameters and their effects on the modal properties of the suggested PCF are also investigated in detail. The suggested PCF can be fabricated by stack and draw technique which can realize various lattice structures and fiber core designs. Through careful process control, the air holes retain their arrangement all through the drawing process and even fibers with complex designs and high air filling fraction. In addition, complex PCF structures can now be fabricated due to recent dramatic improvements in the fabrication of PCFs. Moreover, other techniques such as drilling and extrusion can offer alternative approaches for fabrication of complex non-silica PCFs with low potential cost and thus availability to a large number of users.

9128-11, Session 3

Optical frequency stabilization using gas-filled hollow-core photonics crystal fibers *(Invited Paper)*

Marco Triches, Jan Hald, Danish Fundamental Metrology Ltd. (Denmark); Jens K. Lyngsø, NKT Photonics A/S (Denmark); Ole Bang, Jesper Lægsgaard, DTU Fotonik (Denmark)

During the last decade, the vapor cells [1, 2] and the gas-filled hollow-core (HC) fibers [3] have been investigated as portable standard frequency references, using the saturated absorption spectroscopy (SAS) technique. A SAS setup is used to investigate the different HC fibers. A sealed box with anti-reflective coated windows is used and two laser beams are coupled into the fiber with free-space optics. One (pump beam) is modulated with an AOM at 35 MHz, meanwhile the other (probe beam) is AOM-modulated at 40 MHz. The probe

is modulated with an EOM at 35 MHz to create the sidebands needed for frequency modulation (FM) spectroscopy. Finally, the AOM is used to chop on the pump, modulating the amplitude at 10 kHz. A feedback-loop is used to stabilize the detected probe power via the AOM, while a second loop is used to lock the laser at the Acetylene resonance. The box is temperature controlled through a Peltier cell deployed underneath, and two temperature probes (sensitivity 3mK) monitor the temperature variation. This configuration allows testing the fibers both in a stable and varying temperature environment, in order to investigate how fiber temperature affects the frequency instability.

The four types of fiber are tested for 22h: the system runs with a stable temperature inside the box (25°C, 10h), then the Peltier cell forces a temperature variation inside the box. The locked-frequency fluctuates within 25 kHz and 4 kHz. In the long-term, the frequency instability is clearly visible for almost the fibers and the behavior is enhanced by the thermal stress. The instability is more evident in the fibers with larger core. The fractional frequency instability is calculated for the best fiber. It has an Allan deviation <8x10^-12 (corresponding to 1.5 kHz) and better behavior in a controlled temperature environment (< 3x10^-12 in the 1< t<1000 s range).

The fibers tested behave differently with respect to the core size. These results indicate that fibers with a core <10 μm are desirable, although a lower limit on the core diameter is needed to reduce the additional short-term noise due to the transit-time broadening [4]. Also, the presence of asymmetric structures that create the PM properties seems to introduce an additional cause of instability. The best fiber tested shows a fractional frequency instability <5x10^-12 (1< t < 100s), better than previously published [5] and with an frequency offset accuracy <4 kHz [2], that encourage to develop a stand-alone all-fiber optical frequency reference system in the 1.5 μm range.

References

1. J. Hald, L. Nielsen, J. C. Petersen, P. Varming, and J. E. Pedersen, “Fiber laser optical frequency standard at 1.54 mm,” Opt. Express 19, 2052–2063 (2011).

2. K. Knabe, S. Wu, J. Lim, K. A. Tillman, P. S. Light, F. Couny, N. Wheeler, R. Thapa, A. M. Jones, J. W.Nicholson, B. R. Washburn, F. Benabid, and K. L. Corwin, “10 khz accuracy of an optical frequency reference based on 12c2h2-filled large-core kagome photonic crystal fibers,” Opt. Express 17, 16,017–16,026 (2009).

3. F. Benabid, F. Couny, J. Knight, T. Birks, and P. S. J. Russell, “Compact, stable and efficient all-fibre gas cells using hollow-core photonic crystal fibres,” Nature 434, 488–491 (2005).

4. J. Hald, J. C. Petersen, and J. Henningsen, “Saturated optical absorption by slow molecules in hollow-core photonic band-gap fibers,” Phys. Rev. Lett. 98, 213,902 (2007).

5. C. Wang, N. V. Wheeler, C. Fourcade-Dutin, M. Grogan, T. D. Bradley, B. R. Washburn, F. Benabid, and K. L. Corwin, “Acetylene frequency references in gas-filled hollow optical fiber and photonic microcells,” Appl. Opt. 52, 5430–5439 (2013).

9128-12, Session 3

Fiber Bragg grating-based shear strain sensors for adhesive bond monitoring

Sanne Sulejmani, Camille Sonnenfeld, Thomas Geernaert, Danny Van Hemelrijck, Vrije Univ. Brussel (Belgium); Geert Luyckx, Univ. Gent (Belgium); Pawel Mergo, Univ. of Maria Curie-Sklodowska (Poland); Waclaw Urbanczyk, Wroclaw Univ. of Technology (Poland); Karima Chah, Christophe Caucheteur, Patrice Mégret, Univ. de Mons (Belgium); Hugo Thienpont, Francis Berghmans, Vrije Univ. Brussel (Belgium)

The increasing demand for structural health monitoring has motivated the development of dedicated strain sensors. Multi-axial strain sensing has been a challenge for the fiber optic community, but promising results have been achieved for axial and transverse strain sensors. On the contrary, little research has been conducted on fiber optic-based shear strain sensing. Shear strain monitoring is in particular of high importance in adhesive bonds, which are, for example, used in composite repair patches. Adhesive bonding is preferred over fastening with rivets, bolts or by welding because these techniques can weaken the structure locally. However, at present no adequate techniques exist to control the manufacturing quality of an adhesive bond or to monitor its quality during operation.

We present an overview of the state-of-the-art of fiber optic shear strain sensors. Earlier results either feature a low measurement resolution or the interrogation of the output signal is complex. We propose to use fiber Bragg grating-based sensors fabricated in dedicated highly birefringent microstructured optical fibers and to embed them in the adhesive of a single lap joint. The orientation angle of the fiber is carefully chosen such that their polarization axes are aligned parallel with the direction of maximum shear stress. The fabricated samples are subjected to tensile tests and the results are verified with two dimensional finite element modelling. These tests demonstrate a shear strain sensing resolution of 0.01 pm/μ?. We study the influence of the adhesive material on the sensor response, as well as the influence of sensor orientation and location in the bond line. Our results demonstrate the potential of Bragg grating-based sensors for shear strain sensing, and emphasize the added value of dedicated microstructured optical fiber sensors for adhesive bond monitoring.

9128-13, Session 3

Fiber Bragg grating inscription in novel highly strains sensitive microstructured fiber

Karol Stepien, Military Univ. of Technology (Poland) and InPhoTech Ltd. (Poland); Tadeusz Tenderenda, Michal Murawski, Michal Szymanski, Military Univ. of Technology (Poland); Lukasz Szostkiewicz, InPhoTech Ltd. (Poland); Martin Becker, Manfred Rothhardt, Hartmut Bartelt, Institut für Photonische Technologien e.V. (Germany); Pawel Mergo, Krzysztof Poturaj, Univ. of Maria Curie-Sklodowska (Poland); Leszek R. Jaroszewicz, Military Univ. of Technology (Poland); Tomasz Nasilowski, InPhoTech Ltd. (Poland)

Microstructured fibers (MSF) became one the most attractive research topics in the optic fiber technology domain in the last years. This is due to their unique properties and parameters which are frequently superior to traditional fibers’ parameters (i.e. lower bending losses, better chromatic dispersion compensation, endlessly single mode light propagation for a very broad wavelength range). Furthermore by appropriate selection of fibers’ microstructure: hole size, distance between holes – lattice pitch, geometry and the air holes position MSFs can obtain specific properties. On the other hand Fiber Bragg Grating (FBG) have also played a major role in many applications. A FBG in the simplest application is a selective spectral filter that reflects a particular wavelength (called the Bragg wavelength) of light and transmits all others. Furthermore changes of a physical quantity (e.g. temperature, pressure or strain) shift the Bragg wavelength, therefore FBGs are widely used in sensor applications. In this paper we present the results of an experimental analysis of the influence of the novel special structure MSF on the high strain sensitivity of the propagation modes’ effective refractive index. As the Bragg wavelength is a function of the effective refractive index and longitudinal stretching, the external strain changes can be monitored through the Bragg wavelength shift with an optical spectrometer. Moreover, since the MSF is also optimized for low loss splicing with standard single mode fiber, our novel sensor head can be used with standard components in complex multiplexed sensing arrays, with the measured signal transmitted to and from the sensor by standard telecom fibers, which significantly reduces costs. High sensitivity and low cost makes our sensor very useful for industrial applications.

9128-14, Session 3

Polymer optical fiber grating as water activity sensor

Wei Zhang, David J. Webb, Aston Univ. (United Kingdom)

Controlling the water content within a product has long been required in the chemical processing, agriculture, food storage, paper manufacturing, semiconductor, pharmaceutical and fuel industries. Traditionally, discussions about water in products focus on moisture or water content, which is a quantitative or volumetric analysis that determines the total amount of water present. The limitations of water content measurement as an indicator of safety and quality are attributed to differences in the strength with which water associates with other components in the product. The water content of a safe product varies from product to product and from formulation to formulation. Using only water content values, it's impossible to know how "available" the water in the product is to support microbial growth or influence product quality. Water activity describes the energy status or escaping tendency of the water in a sample. It indicates how tightly water is "bound," structurally or chemically, in products. Water activity is the ratio of the vapor pressure of water in a material to the vapor pressure of pure water at the same temperature. When vapor and temperature equilibrium are obtained, the water activity of the sample is equal to the equilibrium relative humidity of air surrounding the sample in a sealed measurement chamber. In this work we report, to the best of our knowledge, the first optical fiber water activity sensor.

Bragg gratings have been successfully inscribed into poly(methyl methacrylate) (PMMA) based plastic optical fiber in both step-index and microstructured geometries. Water absorption in PMMA is a function of the equilibrium relative humidity. Water absorption introduces changes in the volume and refractive index of PMMA. Therefore for a grating made in PMMA based optical fiber, its wavelength is an indicator of water absorption and PMMA thus can be used as water activity sensor. In this work we have investigated the performance of a PMMA based optical fiber grating as a water activity senor in sugar solution, saline solution and Jet A-1 aviation fuel. Samples of sugar solution with sugar concentration from 0 to 8%, saline solution with concentration from 0 to 22%, and dried (10ppm), ambient (39ppm) and wet (68ppm) aviation fuels were used in experiments. The corresponding water activities are measured as 1.0 to 0.99 for sugar solution, 1.0 to 0.86 for saline solution, and 0.15, 0.57 and 1.0 for the aviation fuel samples. The water content in the measured samples ranges from 100% (pure water) to 10 ppm (dried aviation fuel). The PMMA based optical fiber grating exhibits good sensitivity and consistent response, and Bragg wavelength shifts as large as 3.4 nm when the sensor operates in from dry fuel to wet fuel. This particular feature of water activity measurement allows PMMA based optical fiber gratings to detect very tiny amount of water in some solutions that have a low water saturation limit (such as aviation fuel).

9128-15, Session 3

Periodically tapered photonic crystal fibre based stain sensor fabricated by a CO_2 laser technique

Gerald T. Farrell, Lin Bo, Dublin Institute of Technology (Ireland); Chunying Guan, Harbin Engineering Univ. (China); Yuliya Semenova, Pengfei Wang, Dublin Institute of Technology (Ireland)

The properties and applications of Photonic Crystal Fibre (PCF) have been widely studied, mostly for sensing, owing to their potential for realizing special optical fibres with unique properties, such as singlemode operation over a wide wavelength range, very large mode area, and unusual dispersion characteristics. Long Period Fibre Gratings (LPFGs) fabricated in PCFs have demonstrated promising behavior as sensing elements due to their strong wavelength dependency and strong evanescent field. The wave propagating inside a PCF has a particularly strong evanescent field compared with a standard optical fibre owing to a much closer proximity of the guided mode to the holes of the cladding than to the exterior of the fibre. A focused CO2 laser beam has been previously used in the fabrication of LPFGs in PCFs. However existing fabrication methods require a CO2 laser scanning over the PCF and this makes the fabrication more complicated and time consuming.

In this paper, we present a fibre heterostructure stain sensor consisting of a singlemode fibre (SMF) - periodically tapered photonic crystal fibre – SMF. This structure utilises a series of periodic tapers in place of a traditional LPFG. Because of this it is possible to use a novel CO2 laser fabrication technique which does not require a time consuming CO2 laser scanning process as presented in previous reports. A further difference between the work presented in this paper and the previous work on PCF LPFGs written by a CO2 laser is that the periodically tapered PCF is sandwiched between two SMFs, in a manner similar to traditional Singlemode-Multimode-Singlemode (SMS) structures. The light is delivered by one SMF and collected by the other SMF and importantly the second splice between the tapered PCF and SMF acts as a spatial filter. Because of the multimode interference in the periodically tapered PCF structure, the effective transmission spectrum of the device is strongly dependent on the spatial filtering.

We experimentally demonstrate a competitive strain sensitivity of -68.4 pm/μ? over a microstrain range from 0 to 100 μ? compared with other existing fibre-optic sensors. Most importantly we also demonstrate that such a fibre stain sensor also has a low temperature dependence down to circa 8.4 pm/°C, therefore a corresponding temperature correction technique is not needed to overcome potential temperature induced fluctuations during strain measurement in many applications.

Generally speaking the mechanisms for refractive index modulation in this structure under tensile strain are complex but here may be regarded as a combination of stress-relaxation, strain-induced and tapering-induced refractive index perturbations over the length of the tapered PCF. A physical insight into the operation of the hybrid fibre heterostructure we present here combines the interference between high-order cladding modes and the evanescent fields of the periodical tapers along the sandwiched PCF section, which allows the structure to achieve a higher sensitivity, compared with previously published work in relation to a PCF LPFG based sensors.

9128-16, Session 4

Palladium particles embedded into silica optical fibers for hydrogen gas detection *(Invited Paper)*

Stéphanie Leparmentier, Jean-Louis Auguste, Georges J. Humbert, XLIM Institut de Recherche (France); Gaëlle Delaizir, SPCTS (France); Sylvie Delepine-Lesoille, Johan Bertrand, Stéphane Buschaert, ANDRA (France); Jocelyn Perisse, Jean Reynald Macé, AREVA (France)

Hydrogen gas is a dangerous colorless and odorless gas due to its high detonation tendency at low concentration in air. Hydrogen monitoring is important in nuclear activity for energy production and radioactive waste storage. Optical fiber sensors are passive components useful for efficient local or distributed measurements in explosive and/or severe conditions (temperature, pressure and gamma radiations). Optical fiber hydrogen sensors, made with palladium coatings, have shown a great interest these last 30 years giving rise to high performances such as response time lower than 10 seconds for H2 gas rate lower than 4% [1-4]. Sensitive layers can be deposited either around silica standard optical fibers core [1] or cladding [2], either at the end face of the fiber [1], or on fiber tapers [3]. Palladium reacts with hydrogen to form palladium hydride PdHx involving in particular bulk refractive index variation and volume increase [4]. Low contents of H2 gas are then detectable and measurable with such optical fiber sensors by using interferometric, spectral or reflectometric techniques.

Nevertheless, palladium coatings are sensitive to temperature [2], several gases (cross-sensitivity) [5] and deteriorate rapidly after several hydrogenation/dehydrogenation cycles decreasing to sensor efficiency.

Here, we propose the insertion of palladium in the form of metallic particles inside optical fibers, in the silica cladding, to prevent from non-expected gas sensitivity, palladium layer damage and to allow long length distributed gas sensing. Optical fibers are fabricated thanks to an original process developed at XLIM research institute, based on the use of high purity powders as the raw materials and on specific heat-treatment of the powdered preforms before drawing. This technique allowed us to realize step index, graded index and air/silica microstructured optical fibers with Pd particles embedded in the silica cladding.

It is the first time to our knowledge that this kind of process is optimized and applied to the fabrication of palladium doped optical fiber. Palladium oxide PdO and silica SiO2 powders are used to elaborate the preform cladding material. The preform is then heat-treated in specific conditions to control the oxidation state of palladium into the silica cladding. X-ray diffraction measurements have indeed demonstrated that PdO has totally been reduced during the heating process to form metallic Pd particles.

Numerical modelling has also been performed to design different fiber topologies. We have studied more specifically the mode field distribution into the fiber core, its weak interaction with the absorptive cladding and potential mode coupling between core and cladding. These last two phenomena are harmful to fiber losses and then for sensing applications over long fiber length. Numerous results and optical characterization results of different kind of fabricated optical fibers will be presented and discussed.

[1] M. TABIB AZAR et al., Sensors and Actuators B, 56(1-2), p 158-63, 1999.

[2] M.A. BUTLER, Applied Physics Letters 45(10), p 1007-9, 1984.

[3] J. VILLATORO et al., Optics Express 13(13), p 5087-93, 2005.

[4] RRJ. MAIER et al., Pure Applied Optics 9, p 545?59, 2007.

[5] R.D. SMITH et al., Fuel Chemistry Division Preprints 47(2), p 825-8, 2002.

9128-17, Session 4

Latest progress in the production of active fibers by the granulated silica method

Dereje Etissa, Manuel Ryser, Valerio Romano, Thomas Feurer, Univ. Bern (Switzerland); Woojin Shin, Gwangju Institute of Science and Technology (Korea, Republic of)

The granulated silica method, as an alternative to the MCVD technique, significantly simplifies the manufacturing of fibers with respect to geometry and composition. However, fibers fabricated with this method suffer from higher scattering losses (up to 1dB/m) as compared to fibers drawn from preforms that are produced by the conventional MCVD technique. Although the granulated-silica method targets the production of optical fibers for special applications where only a few meters are needed, e.g. highly doped active fibers for high power fiber lasers, amplifiers and sensing applications, in some cases lower losses are necessary.

In our previous work, we were able to improve the quality of Ytterbium doped and Al2O3-P2O5 co-doped samples by the Sol-Gel process1. Furthermore, the sol-gel based method eases the incorporation of the dopants at high concentrations and appropriate heat treatment of the sol-gel material reduces the amount of (micro-) bubbles that are a source of scattering centers in the core. In such a way we were able to fabricate optical fibers that, piecewise (between individual strong scatterers), exhibited attenuation losses as low as 0.35 dB/m at 633 nm.

In ongoing work we have further succeeded in reducing the losses of optical fibers produced by the granulated silica method to below 0.2 dB/m at 633 nm. This is being achieved by i) iteratively milling and melting the doped granulated silica and by ii) applying a CO2 Laser based “travelling small zone vitrification” procedure to produce the cores of the preforms.

First results obtained with this new method will be presented.

9128-18, Session 4

Photonic crystal lenses for transverse focusing of laser illumination in microstructured optical fibers

Tigran Baghdasaryan, Thomas Geernaert, Hugo Thienpont, Francis Berghmans, Vrije Univ. Brussel (Belgium)

Transverse light propagation through the air holed cladding of microstructured optical fibers (MOFs) has recently attracted interest owing to its importance for several applications such as fiber grating writing, particle trapping in hollow core fibers, all optical switch devices, etc. The air holes in the MOF cladding region impede efficient delivery of transversely propagating light to the core region when the fiber is illuminated from the outside. To overcome this problem we designed MOFs with a gradient air holed cladding structure that will actually focus transversely propagating light to the fiber core.

We used photonic crystal Mikaelian lenses (PCML) as focusing gradient media in the holey cladding. First, we considered and compared several PCML types with varying air hole diameter and air hole pitch, in both hexagonal and rectangular lattices. We studied the design rules of those structures and we carried out a frequency response analysis to identify the most efficient operational regions of the PCMLs. The polarization properties of the considered structures were investigated as well. Finally, we analyzed the transverse coupling properties of the MOF equipped with such a PCML structure in the cladding and we obtained a fiber that clearly focuses transversely incident light to its core region with a normalized focal intensity up to 20, whilst exhibiting good guiding properties.

9128-19, Session 4

Synthetically generated fiber pixilated image database

Anant B. Shinde, Vadakke M. Murukeshan, Ctr. for Optical and Laser Engineering (Singapore) and Nanyang Technological Univ. (Singapore)

Visual access to the physically inaccessible parts has become the prime requirement of the tools for medical diagnostics, biomedical research and industrial applications. Flexible and thin endoscope with fiber bundle as image conduit serves this purpose. Thousands of fiberlets are closely packed in a diameter of a millimeter or less to form a coherent bundle in such image fiber conduits. However, while light passes through the core of the fiberlet, it is blocked by the inter fiber gap. This phenomenon creates special honeycomb like pattern overlaying the image captured with the fiber probe, known as comb structure or fiber pixelation. It obstructs the perception of original image and inhibits the use of object recognition and tracking algorithms on the images obtained.

Generally, comb structure removal or depixelation methods were employed to remove honeycomb pattern from an image. In the recent past, several depixelation techniques have been proposed albeit using different set of pixelated images by different researchers. It is quite difficult to make a performance comparison based on such images as they adopted different images for different particular framework of their study. In this context, a basic database of such images is the need of the hour to meet growing diagnostic needs in the medical and industrial arena.

Through this paper, we propose a Comb Structure Affected Image database (CSAI) to meet such an objective. Images

are generated considering the image fiber specifications and characteristics at different targeted optical imaging modalities delineated by resolution scales. The proposed database designed to have a set of synthetically generated pixelated images of test patterns of different scale, size and shapes. Further, for each instance, both the original image and pixelated image will be statistically analyzed for further referencing.

9128-20, Session 4

Enhanced polarization and dispersion properties of double cladding photonic crystal fiber usig dual lattice structure

Soeun Kim, Yong Soo Lee, Chul-Sik Kee, Gwangju Institute of Science and Technology (Korea, Republic of); Chung Ghiu Lee, Chosun Univ. (Korea, Republic of)

We propose double cladding photonic crystal fiber using dual lattice structure for control polarization and dispersion properties. The outer cladding structure is made of conventional square lattice by removing 6 air holes around its center. The inner cladding of triangle lattice structure is made of two layered small size air holes and the shape of form the triangle lattice is isosceles triangle. This induces asymmetric core. Previously, there had been a research about structure of having double cladding structure. But, the size of small hole of inner cladding is very small about 0.1 ?m. In this scale, there has a problem such as a incorrect result or difficulty of making. Because the whole size of the inner cladding was small, it was hard to determine whether a changing optical property by having a double cladding structure is by structure or simply adding small air hole. In this study, the proposed double cladding structure of having lattice structure of triangle and square has merit that transmission mode become to efficiently confine at core. So, about this structure, we analyze polarization and dispersion properties by using Finite Element Method (FEM) and Eigenmode solver. According to increase layers of inner cladding using small size air hole at core, the shape of mode profile becomes to have highly asymmetry. This result can expect that proposed PCF get to have high birefringence. And dispersion value of proposed PCF becomes small with taking a place microstructure at core and get to have negative dispersion on type 3. In this study, proposed structure of PCF enhance birefringence and dispersion property since increasing asymmetry of core of PCF and confinement of transmission mode by using double lattice structure of triangle and square.

9128-21, Session 5

Factors the influencing temperature sensitivity of PMMA based optical fiber Bragg gratings *(Invited Paper)*

Wei Zhang, David J. Webb, Aston Univ. (United Kingdom)

PMMA based polymer optical fiber Bragg gratings (POFBGs) have been used for temperature sensing. They are particularly appealing in medical devices as polymers are biologically compatible with human tissues and already routinely put in the human body in many applications. POFBGs have been shown to be more sensitive to temperature than is the case for silica FBGs. Another interesting feature of polymer fiber gratings is the negative refractive index change over temperature rise. It offers a well-conditioned response for overcoming the cross sensitivity issues existing in silica fiber gratings. Whilst there have been many reports on polymer fiber grating temperature sensing applications, the reported results are quite inconsistent. This inconsistency has not been addressed and causes great uncertainty in POFBG's performance and applicability. In this work we have investigated the factors that influence the temperature sensitivity of PMMA based optical fiber gratings.

The Bragg wavelength of a PMMA based fiber grating is determined by the effective core index and the grating pitch, which depend on the thermo-optic and thermal expansion coefficients of PMMA, respectively. These two coefficients are not constant. Instead, they are a function of surrounding temperature and humidity. As a consequence a PMMA based fiber grating shows much larger temperature sensitivity in a high relative humidity environment than in a dry environment and a nonlinear temperature response. On the other hand the measured temperature sensitivities usually are larger than those calculated even though the varying coefficients have been considered. The reported thermal expansion coefficient of PMMA is measured by using optical interference methods or estimated from the volume change by using a dilatometer. In both cases PMMA was assumed to be isotropic so the linear thermal expansion coefficient is a third of the volume coefficient. However, amorphous polymers including PMMA exhibit a known degree of anisotropic thermal expansion. The anisotropic nature of expansion mainly depends on the polymer processing history. The expansion coefficient is believed to be lower in the direction of the molecular orientation than in the direction perpendicular to the draw direction. Such anisotropic behavior of polymers can be expected in drawn PMMA optical fiber, and will lead to a reduced thermal expansion coefficient and larger temperature sensitivity than would be the case were the fiber to be isotropic.

Extensive work has been carried out to identify these factors. The temperature responses of gratings have been measured at different relative humidity. Gratings fabricated on annealed and non-annealed PMMA optical fibers are used to compare the sensitivity performance as annealing is considered to be able to mitigate the anisotropic effect in PMMA optical fiber. Furthermore an experiment has been designed to examine the assumption of anisotropic thermal expansion in the fiber, in which the thermal expansion contribution to the grating wavelength change is eliminated and much increased temperature sensitivity is achieved.

9128-22, Session 5

Effect of peaks splitting in fiber-optic Bragg gratings fabricated using phase mask method

Karol Tarnowski, Waclaw Urbanczyk, Wroclaw Univ. of Technology (Poland)

First successful inscription of fiber Bragg gratings (FBGs) was reported in 1978. Since that time several fabrication methods have been developed, including the phase mask method, interferometric method and point by point inscription method. Splitting of reflection peaks due to fiber misalignment in Bragg gratings fabricated using a phase mask was observed by Dyer et al. [1]. In 2012 Wade et al. [2] presented valuable experimental data showing the influence of possible misalignments of the phase mask inscription system on the grating characteristics. Very recently theoretical description of the observed effects has been presented [3]. The splitting of certain Bragg peaks reported in earlier experiments is caused by formation of the gratings with different periodicities in the waveguide tilted with respect to the phase mask plane due to the interference of non-symmetrical diffraction orders.

In our work we compare analytical predictions for spectral separation of the split peaks derived in [3] with numerical simulations of reflection spectra. Using a finite element method we modeled a mode propagation through a planar waveguide with the gratings inscribed with different tilt angles and obtained reflection spectra with multiple Bragg reflection peaks.

The work was supported by Wroclaw Research Centre EIT+ within the project "The Application of Nanotechnology in Advanced Materials" - NanoMat (POIG.01.01.02-02-002/08) co-financed by the European Regional Development Fund (Operational Programme Innovative Economy, 1.1.2). K. Tarnowski acknowledges Foundation for Polish Science START Program.

[1] P. E. Dyer, R. J. Farley, R. Giedl, K. C. Byron, and D. Reid, Electron. Lett. 30(11), 860–862 (1994).

[2] S. A. Wade, W. G. A. Brown, H. K. Bal, F. Sidiroglou, G. W.

Baxter, and S. F. Collins, J. Opt. Soc. Am. A 29(8), 1597–1605 (2012).

[3] K. Tarnowski, W. Urbanczyk, Opt. Express 21(19): 21800-21810 (2013).

9128-23, Session 5

PMMA mPOF Bragg gratings written in less than 10 min

Ivan-Lazar Bundalo, Kristian Nielsen, Christos Markos, Ole Bang, DTU Fotonik (Denmark)

Since the inscription of the first Bragg grating in a micro-structured polymer optical fiber (mPOF), the time required to inscribe a strong grating has been reported to be between 40 min and 60 min. In this paper we report on our efforts towards reducing the required writing time.

The mPOF is of the PCF design and is fabricated on our polymer draw tower. The mPOF fabrication is a two-step process; in the first step the preform is scaled down 10 times using the draw tower. In the second step the scaled down preform is stacked inside extra tubes, in order to increase the diameter, and then drawn down to a 125 micron in diameter fiber. The preform is made of a PMMA cylinder with a hole pattern drilled into it and the final optical fiber has a hole size of 1 μm and the hole to hole distance, the pitch, is 3.75 μm. The hole to pitch ratio is 0.27 ensuring that the fiber is endlessly single mode.. The hole to pitch ratio is 0.27 ensuring that the fiber is endlessly single mode. The fiber has a propagation loss at 630 nm of around 10 dB/m.

The grating inscription is made using a HeCd 30 mW 325 nm laser; the laser light is directed to the fiber using mirrors and is focused on to the fiber, through the phase mask, using a cylindrical lens with a focal length of 25 mm. An Ibsen phase mask with a pitch of 424.84 nm is used to create the diffraction pattern needed to write a 630 nm grating into the PMMA mPOF. The mPOF is interrogated using the light from a SuperK white light source and a 3 dB fiber coupler, the light is launched into the mPOF using an SMF28 fiber, the space between both fibers is filled with index matching oil to reduce reflections. Reflected light from the grating is fiber coupled from the 3 dB coupler to the spectrum analyzer. With this setup we can write a 28 dB grating in a 3-ring PMMA mPOF in less than 10 min. The grating is centered at 632.6 nm and has a FWHM of 0.3 nm.

We attribute the low writing time to the high light intensity due to the short focal length of our lens together with accurate alignment of the setup. The low hole to pitch ratio of the fiber also makes it possible for the UV light to reach the core of the fiber.

Previously, our setup had a second cylindrical lens used to expand the laser spot to 1.2 cm in the direction of the fiber axis; this was done in order to write long gratings. We have removed this lens from the setup in order to increase the intensity of the light hitting the fiber and as a consequence the length of the grating is reduced from 1.2 cm to 2-3 mm.

9128-24, Session 5

Increase of the photosensitivity of undoped poly(methylmethacrylate) under UV radiation at 325 nm

David Sáez-Rodríguez, Aston Univ. (United Kingdom); Kristian Nielsen, Ole Bang, DTU Fotonik (Denmark); David J. Webb, Aston Univ. (United Kingdom)

The photosensitivity of polymers to UV radiation is a key factor in the fabrication of optical devices, such as gratings and waveguides. For this reason it is important to understand the different mechanisms involved in such index changes. One of the most common polymers in the fabrication of such optical devices is poly(methylmethacrylate) (PMMA) because of its good optical properties. It has been used to fabricate both waveguides in films and fibre Bragg gratings in polymer optical fibre (POF) using UV radiation. The first study of the photosensitivity of undoped PMMA prepared under special oxidative conditions was done by Tomlinson et al. in 1970 and later by Bowden et al. in 1974. Both authors achieved similar results, getting an increase of the density in the irradiated areas under CW UV radiation at 325 nm. However, each proposed different mechanisms responsible for this density increase. Tomlinson proposed an increase of the density because of the photo-crosslinking effect and Bowden explained it as a consequence of the polymerization of the residual monomers, using as initiator peroxides produced during the fabrication process of the PMMA films studied.

The photosensitivity of these PMMA films was low and the inscription time long, which is why the PMMA was doped to increase photosensitivity and reduce fabrication time with a different range of dopants such as photoiniciators or photoisomers. However, doping PMMA can lead to the loss some of the good optical properties, such as the transparency, besides complicating the fabrication process of the devices due to the doping process.

The first study of PMMA photo-degradation was done by Torikai et al. in 1990 and 1993 in air and vacuum, respectively. They demonstrated that photo-degradation of PMMA occurs at the lower wavelength of 320 nm. Furthermore, they showed that for longer wavelengths the oxygen did not contribute to the photo-degradation effect. No evidence of photo-degradation has been reported before in PMMA under UV radiation at 325 nm. However, in the scope of polymer science it is well-known that stress in the sample produces an increase of the photo-degradation effect which could be used to reduce the wavelength threshold for photodegradation under UV radiation.

In this paper we report, for the first time in our knowledge, an increase of the photosensitivity of a microstructured polymer optical fibre (mPOF) made of undoped PMMA due to the applied strain during the fabrication of the gratings. In the work fibre Bragg gratings (FBGs) have been fabricated in undoped PMMA mPOFs with an hexagonal structure of three rings in the inner cladding. Two sets of FBGs were inscribed at two different resonant wavelength (827 nm and 1562 nm) at different strains using an UV He-Cd laser at 325 nm focused by a lens and scanned over the fibre. We observed an increase of the reflection of the fibre Bragg gratings when the fabrication strain is higher. The photosensitivity mechanism is discussed in the paper along with the chemical reactions that could underlie the mechanism. Furthermore, the resolution limit of the material was investigated.

9128-25, Session 5

Investigations on birefringence effects in polymer optical fiber Bragg gratings

Xuehao Hu, Univ. de Mons (Belgium); David Sáez-Rodríguez, Aston Univ. (United Kingdom); Ole Bang, DTU Fotonik (Denmark); David J. Webb, Aston Univ. (United Kingdom); Christophe Caucheteur, Univ. de Mons (Belgium)

Bragg gratings photowritten in step-index polymer optical fibers and microstructured polymer optical fibers, commonly referred to as POFBGs and mPOFBGs, respectively, present several attractive features, especially for temperature, tension and humidity sensing purposes. In comparison to FBGs written in standard silica fibers, they are more sensitive to temperature and pressure because of the larger thermo-optic coefficient and smaller Young's modulus of polymer materials. (M)POFBGs are most often manufactured in poly(methylmethacrylate) (PMMA) materials using a continuous-wave 325 nm HeCd laser with an average optical power of a few tens of mW. The phase mask technique is largely used to obtain the refractive index modulation in the fiber core.

In this paper, for the first time to the best of our knowledge, we study photo-induced birefringence effects in (m)POFBGs arising from both the lateral inscription process and the application of a transverse force. To achieve this, highly reflective gratings (few millimetres in length) were inscribed

with a 1044 nm period uniform phase mask in two kinds of PMMA optical fibers. They were then monitored in transmission with polarized light. For this, (m)POF sections a few cm in length containing the gratings were glued to angled silica fibers to minimise the insertion loss. Then, measurements were made of two specific polarization properties, namely polarization dependent loss (PDL) and differential group delay (DGD). They were both computed from the Jones matrix eigenanalysis method using an optical vector analyser (OVA CTe from Luna Technologies). The latter was chosen for both its wavelength resolution (1.25 pm) and its fast scanning rate (less than 1 s to analyse a range of a few tens of nm). Maximum values exceeding several dB and a few tens of ps were obtained for the PDL and DGD, respectively, confirming that important birefringence effects result from the lateral photowriting process. The response to lateral force was finally investigated with a set-up permitting the application of controlled transverse loads on the gratings. As it induces mechanical birefringence in addition to the photo-induced one, an increase of the PDL and DGD values were noticed. The obtained results confirm that polarization metrology can be used with (m)POFBGs for transverse strain sensing purposes.

9129-1, Session 1

Single protein identification based on SERS active raspberry-like nanoparticles

Thibault Brulé, Lab. Interdisciplinaire Carnot de Bourgogne (France); Hélène Yockell-Lelièvre, Lab. Interdisciplinaire Carnot de Bourgogne (France) and Univ. de Montréal (Canada); Alexandre Bouhelier, Lab. Interdisciplinaire Carnot de Bourgogne (France); Jérémie Margueritat, Lab. Interdisciplinaire Carnot de Bourgogne (France) and Univ. Claude Bernard Lyon 1 (France); Laurent Markey, Alain Dereux, Eric Finot, Lab. Interdisciplinaire Carnot de Bourgogne (France)

The Surface Enhanced Raman Spectroscopy (SERS) is a powerful measurement technique to obtain vibration modes of single biomolecules. Existing SERS spectra result from a cumulative contribution of these multiple vibrations. Using a specific experimental approach combining microfluidic with Chebychev gold nanoparticles (raspberry-like surface structure), the dynamics of rare events characterizing the Raman activity of single Bovin Serum Alumin protein (BSA) was monitored.

The observed large amplitude fluctuations [1] of the spectra both in wavenumber and intensity require a careful and extensive multivariate analysis. We propose a detailed description of the available statistical tool for SERS response of individual proteins with different statistical tools [2]. Principal Components Analysis (PCA) [3] coupled with a kinetic analysis proved to be a robust and systematic technique to provide a unique spectral differentiation between the different states of the BSA proteins.

This method highlights four sites of interaction for BSA with gold. Coupling with a theoretical DFT-calculation of amino-acids interacting with gold using Gaussian 03 and based on the spectral identification of amino-acids in BSA spectra, a localisation of these sites and the folding-unfolding forms differentiation are able.

The understanding of these protein-gold interactions is also an important point of the practical outcome of this nanobiochip in monitoring specifically biomarkers. In fact, a comparative study should be applied on Heat Shock Protein-70 (HSP-70), which protein has a good interest in the early-stage cancer detection in blood (SPEDOC European project www.spedoc.eu).

Bibliography:

[1] J.Margueritat et al., ACS Nano., 5, 1630 (2011)

[2] J.Margueritat et al. J. of Phys.Chem. C, 116 (2012)

[3] P.G.Etchegoin et al, Anal.Chem., 79, 8411 (2007)

9129-2, Session 1

3D flower-like nanostructures as an efficient and reproducible surface enhanced Raman spectroscopy substrate (SERS) using ultra-thin film techniques

Sezin Yüksel, Friedrich-Schiller-Univ. Jena (Germany); Mario Ziegler, Institut für Photonische Technologien e.V. (Germany); Dana Cialla, Friedrich-Schiller-Univ. Jena (Germany) and Institut für Photonische Technologien e.V. (Germany); Uwe Hübner, Institut für Photonische Technologien e.V. (Germany); Karina Weber, Jürgen Popp, Friedrich-Schiller-Univ. Jena (Germany) and Institut für Photonische Technologien e.V. (Germany)

Surface enhanced Raman spectroscopy (SERS) is a versatile tool in chemical and biological sciences due to not only its unique surface properties at nano-scale but also its performance with high specificity and sensitivity [1]. However, this technique is restricted by several parameters of metallic substrates such as size, shape, and material of the nanoparticle which plays an important role in plasmon resonance [2]. Thus, an easy and efficient approach is used for modeling the SERS substrates in this work. Enzymatically generated silver-nanoparticles (EGNPs) [3, 4] are produced by silver deposition on a modified glass surface. Different layer thicknesses of SiO2 are applied onto EGNPs with low temperature of plasma enhanced atomic layer deposition (PE-ALD). The growth of 3D flower-like nanostructures used as template, is observable after the deposition of 10 nm SiO2. In order to meet with different working spectral ranges and applications, 3D flower-like template nanostructures are coated with silver, gold or aluminum using chemical vapor deposition (CVD). The morphological studies, optical properties as well as the SERS response of these metallized 3D nanostructures are introduced. Additionally, we demonstrate silver coated nanoflowers which are promising to afford large SERS enhancement for quantitative analysis with the detection limit of riboflavin down to 10-7 M. Furthermore, this flower like templates can be stored easily until needed and be employed for tuning the spectral range for appropriate chemical and biochemical applications.

[1] S. Pahlow et.al., Eng. Life Sci., 12, 2, 131-143 (2012)

[2] D. Cialla et. al., ABC, 403, 27-54 (2012).

[3] H. Schneidewind et. al., Beilstein J. Nanotechnol., 3, 404-414 (2012).

[4] K.K. Strelau, et. al., ChemPhysChem, 42, 3, 1-6 (2010).

Acknowledgement: Funding of research projects “QuantiSERS” and “Jenaer Biochip Initiative 2.0” within the framework “InnoProfile Transfer – Unternehmen Region“ the Federal Ministry of Education and Research, Germany (BMBF) is gratefully acknowledged.

9129-3, Session 1

Lab-on-a-chip-SERS for bioanalytical applications

Karina Weber, Friedrich-Schiller-Univ. Jena (Germany) and Institut für Photonische Technologien e.V. (Germany); Anna Hauser, Friedrich-Schiller-Univ. Jena (Germany); Izabella Hidi, Institut für Photonische Technologien e.V. (Germany) and Friedrich-Schiller-Univ. Jena (Germany); Dana Cialla, Jürgen Popp, Friedrich-Schiller-Univ. Jena (Germany) and Institut für Photonische Technologien e.V. (Germany)

A fast and easy to handle approach combined with high sensitivity as well as specificity are the key properties of modern analytical methods. Based on the optical characteristics of metal nanostructures for advanced optical biosensing application, our research on a variety of innovative lab-on-a-chip (LOC) based techniques applying in bioanalytics will be introduced [1]. The resonant excitation of surface plasmon polaritons modes of nanostructured metal surfaces leads to a strong electromagnetic field enhancement, which can be utilized to amplify the intrinsic weak but molecular specific Raman signals of analyte molecules in close vicinity to the metal surface by several orders of magnitude. This so called surface enhanced Raman spectroscopy (SERS) is of major interest for answering a broad range of bioanalytical questions based on its high sensitivity and fingerprint specificity [2]. However, to establish SERS as a reliable routine detection method within this field, suitable and powerful SERS active substrates have to be developed. Within this contribution, the implementation of silver nanoparticles in a droplet-based LOC-SERS device [3] is introduced as well as discussed in context to both fundamental investigations on the binding sites and orientation of molecules towards the silver surface and drug monitoring in complex media (e.g. urine, blood).

[1] Anne März, Thomas Henkel, Dana Cialla, Michael Schmitt, Jürgen Popp, Lab on a Chip, 11(21), 3584-3592 (2011).

[2] Dana Cialla, Anne März, René Böhme, Frank Theil, Karina Weber, Michael Schmitt, Jürgen Popp, Analytical and Bioanalytical Chemistry, 403(1), 27-54 (2012).

[3] Anne März, Thomas Bocklitz, Jürgen Popp, Analytical Chemistry, 83(21), 8337-8340 (2011).

Acknowledgements

We thank Dr. Thomas Henkel and his entire team (IPHT Jena) for providing the microfluidic chip platform. Funding of research projects “QuantiSERS” and “JBCI 2.0” within the framework “InnoProfile-Transfer, Unternehmen Region” from the Federal Ministry of Education and Research, Germany (BMBF) is gratefully acknowledged.

9129-4, Session 1

Strategies for determining food purity and quality by using SERS as analytical tool

Dana Cialla, Friedrich-Schiller-Univ. Jena (Germany) and Institut für Photonische Technologien e.V. (Germany); Martin Jahn, Andreea Radu, Sophie Patze, Friedrich-Schiller-Univ. Jena (Germany); Karina Weber, Jürgen Popp, Friedrich-Schiller-Univ. Jena (Germany) and Institut für Photonische Technologien e.V. (Germany)

Despite the strong progress made in the fields of diagnostics and treatment of diseases, prevention remains the better solution. To realize this approach, one of the most important factors is to guarantee a healthy diet. To that end it is essential to obtain information about food quality, food composition and vitamin content. In addition an important factor concerning food quality concerns the presence of certain food additives like dyes, which are often used to mislead the customer and to deceive him about the actual quality of the food product. Within this contribution, we present a method of detecting low-molecular weight substances like vitamins, carotenoids and food dyes (extracted from food) by using surface enhanced Raman spectroscopy (SERS) as molecular specific and highly sensitive detection scheme [1]. As SERS-active substrate enzymatically generated silver nanoparticles (EGNP) are applied [2]. Moreover, a self-assembled layer of aliphatic hydrocarbons on the nanostructures was prepared to allow additionally the detection of water-insoluble substances by enrichment these molecules on the surface and repel water-soluble substances.

[1] Dana Cialla, Anne März, René Böhme, Frank Theil, Karina Weber, Michael Schmitt und Jürgen Popp, Surface-enhanced Raman spectroscopy (SERS): progress and trends. Analytical and Bioanalytical Chemistry, 403(1), 27-54 (2012).

[2] Katharina K. Strelau, Thomas Schüler, Robert Möller, Wolfgang Fritzsche und Jürgen Popp, Novel bottom-up SERS Substrates for Quantitative and Parallelized Analytics. ChemPhysChem, 11(2), 394-398 (2010).

Acknowledgement:

Funding of research projects “QuantiSERS” and “Jenaer Biochip Initiative 2.0” within the framework “InnoProfile Transfer – Unternehmen Region“ the Federal Ministry of Education and Research, Germany (BMBF) is gratefully acknowledged.

9129-6, Session 1

Recognition of SERS labelled tumour cells in a microfludic continuous flow experiment

Isabel Freitag, Claudia Beleites, Sebastian Dochow, Christoph Krafft, Institut für Photonische Technologien e.V. (Germany); Jürgen Popp, Institut für Photonische Technologien e.V. (Germany) and Abbe Ctr. of Photonics (Germany)

Rapid recognition of single circulating tumour cells is an important goal in medical diagnostics. Compared to fluorescence labelling, Raman spectroscopy offers much better multiplexing capabilities. Raman spectra allow not only to distinguish cancer cells from normal blood cells but also to identify different cancer cell lines. This is also possible on a single-cell basis in a microfluidic chip [1]. However, Raman measurements are slow. In order to speed up the measurements, surface enhanced Raman spectroscopic (SERS) labels attached to antibodies can be used to sensitively mark specific cell types, allowing a very fast recognition of these cells while unlabelled cells are still subject to normal Raman measurements.

We use specific multicore SERS labels consisting of gold nanoparticle aggregates marked with reporter molecules and covered with a thin silver layer for further enhancement of the SERS signal [2]. The nanoparticles are stabilized with a further silica layer which facilitates their use. Conjugation with antibodies leads to specific binding of the nanoparticles to the target cells.

We show results on a mixture of leukocytes with MCF-7 breast cancer cells and polystyrene beads measured in a continuous flow regime in a microfluidic chip. Our anti-EpCAM-tagged nanoparticles label the MCF-7 cells. Our results also show that the Raman spectra acquired with 25ms exposure time allow to distinguish polystyrene beads from the 3-mercaptobenzoic acid reporter molecule even though the most intense band of both is the aromatic ring breathing vibration at 1000cm^-1, demonstrating the excellent multiplexing capabilities of the approach.

The presented multicore SERS labelling strategy allows fast recognition of known cell types, while cells of unknown type are not labelled and can still be studied by normal Raman spectroscopy.

The authors gratefully acknowledge financial support by the BMBF via the project RamanCTC (13N12685).

[1] Dochow, S. and Beleites, C. and Henkel, T. and Mayer, G. and Albert, J. and Clement, J. and Krafft, C. and Popp, J.: Quartz microfluidic chip for tumour cell identification by Raman spectroscopy in combination with optical traps, Anal Bioanal Chem, 2013, 405, 2743-2746.

[2] Freitag, I. and Neugebauer, U. and Csaki, A. and Fritzsche, W. and Krafft, C. and Popp, J.: Preparation and characterization of multicore SERS labels by controlled aggregation of gold nanoparticles, Vib Spec, 2012, 60, 79-84.

9129-96, Session 1

Chip-based isolation of microorganisms with subsequent Raman spectroscopic identification

Susanne Pahlow, Sandra Kloss, Friedrich-Schiller-Univ. Jena (Germany); Konstantin Kirsch, Uwe Hübner, Institut für Photonische Technologien e.V. (Germany); Dana Cialla, Petra Rösch, Karina Weber, Jürgen Popp, Friedrich-Schiller-Univ. Jena (Germany)

Raman spectroscopy is a powerful tool for the fast and reliable detection of analytes. The specific spectroscopic fingerprint of each Raman active molecule enables the investigation and identification of a broad range of substances, including single bacteria cells. Due to characteristic features in the Raman spectra of each bacteria species, it is possible to identify bacteria on species level with this approach. [1]

Within this contribution, a Raman compatible chip for isolation of microorganisms from complex media is introduced. [2] The system allows performing the isolation and the subsequent Raman identification on the same platform. The chip was designed to be integrated into a microfluidic chamber for future automatization of the system. The chip surface is modified with capture probes for bacteria. Antibodies against analogue cell wall surface structures of Gram-positive and Gram-negative bacteria were employed as capture molecules. Since the identification of the bacteria is achieved later on via Raman

micro-spectroscopy it is not necessary to employ antibodies against each bacteria species of interest. For capturing the bacteria on the chip surface the sample is guided over the chip using the microfluidic setup. Due to specific interactions of the antibodies the microorganisms are immobilized on the chip and become available to be identified via Raman micro-spectroscopy. The capability of our system was demonstrated for several Gram-positive and Gram-negative species.

[1] S. Meisel, S. Stöckel, M. Elschner, F. Melzer, P. Rösch, J. Popp, Appl Environ Microbiol, 2012, 78, 5575-5583.

[2] S. Pahlow, S. Kloß, V. Blättel, K. Kirsch, U. Hübner, D. Cialla, P. Rösch, K. Weber, J. Popp, ChemPhysChem, 2013, 14, 3600–3605.

Acknowledgement: Funding of the research project 'FastDiagnosis' and the young research group 'Jenaer Biochip Initiative 2.0' within the framework 'Unternehmen Region – InnoProfile Transfer' from the Federal Ministry of Education and Research, Germany (BMBF) is gratefully acknowledged.

9129-14, Session 2

Correlating Raman and MALDI-TOF imaging of cell layers and tissue sections

Christian Matthäus, Institut für Photonische Technologien e.V. (Germany); Anna C. Crecelius, Thomas W. Bocklitz, Nico Tarcea, Friedrich-Schiller-Univ. Jena (Germany); Ferdinand von Eggeling, Universitätsklinikum Jena (Germany); Michael Schmitt, Ulrich S. Schubert, Friedrich-Schiller-Univ. Jena (Germany); Jürgen Popp, Institut für Photonische Technologien e.V. (Germany)

Currently various imaging techniques have been established that combine conventional microscopy or other optical settings with spectroscopic methods. The combination offers spatially resolved information about chemical composition of very small sample volumes. Different spectroscopic techniques often provide complementary information, which requires a multimodal approach. Here, we introduce first results to combine Raman microscopic imaging with MALDI-TOF-MS. Principally; both techniques can be applied to thin-sectioned biopsies as well as to cell monolayers grown in vitro. One challenging aspect to correlate the spectral information is the discrepancy of the spatial resolution. Whereas Raman microscopy can reach the resolution of confocal fluorescence microscopy, MALDI-TOF-MS imaging is limited by the spot size of the ionization process, which is estimated to be about 50 ?m. For the analysis of cells grown in vitro Raman microscopy can provide very detailed information about individual cells, but is limited with respect to the number of cells that can be investigated, due to the weakness of the effect and the associated imaging time per cell. MALDI-TOF-MS on the other hand can not image individual cells, but provide statistically more reliable data. Raman spectroscopy can shed light on the general composition of the sample, whereas MALDI-TOF-MS would allow further characterization of individual subspecies. Both techniques require different sample preparations. Raman spectroscopy can potentially be applied in vivo. MALDI-TOF-MS on the other hand is too invasive for application on live samples. However, the spectral information obtained from both techniques can be correlated. For the correlation we employ a statistical analysis based on a partial least square algorithm, which can be used in a predictive manner. Spectral information from MALDI-TOF experiments can be utilized to interpret Raman spectra. The reverse application may allow the search for MALDI-TOF-MS marker signals under in-vivo conditions by utilizing Raman spectroscopy. With this contribution we would like to introduce first results correlating the spectroscopic information obtained from both methodologies from cell cultures as well as mouse brain tissue samples.

Acknowledgements:

Financial support of the German Research Foundation (DFG) for the research projects PO 563/13-1, PO 563/16-1, EG 102/5-1 and SCHU 1229/15-1 are gratefully acknowledged. The authors A. C. Crecelius, and U. S. Schubert wish to thank the Thüringer Kultusministerium (grant no. B515-07008) for the financial support of this study.

9129-15, Session 2

Confocal Raman imaging for cancer cell classification

Evelien Mathieu, Pol Van Dorpe, IMEC (Belgium) and Katholieke Univ. Leuven (Belgium); Tim Stakenborg, Chengxun Liu, IMEC (Belgium); Liesbet Lagae, IMEC (Belgium) and Katholieke Univ. Leuven (Belgium)

Traditional cancer therapy is based on the biology of the primary tumor. However, metastasis is responsible for over 90% of cancer related deaths. Cancers undergoing metastasis may change biology and biochemical marker expression, resulting into tumors that are significantly different from the primary tumor. Knowledge about the identity and characteristics of patients' tumors is crucial for diagnosis, effective therapy and prognosis. Present-day, biomarker-based single cell characterization techniques require labels and long incubation times. For these reasons, it would be interesting to differentiate cells based on their physical properties and characteristics, rather than the biomarkers they express. Confocal Raman microscopy is used as a single cell characterization technique that does not require labeling or specific sample preparation [1-3].

We report on a study with different cancer cell lines, cell lines originating from healthy tissue and blood cells. Raman spectra of single living cells are recorded with a confocal Raman microscope (alpha300R, WITec GmbH, Germany), equipped with an excitation laser at 785 nm with a maximum power of 200 mW. Cell suspensions are imaged in between a glass slide and a glass coverslip, using a 100x oil-immersion objective with NA 1.25. For each cell, the laser beam is focused on the middle of the cell and spectra are taken at different focus depths, sweeping the complete cross-section of the cell, with an integration time of 5 s for each single spectrum.

Cosmic ray removal and normalization [4] are performed on all Raman spectra. For further preprocessing principal component analysis is employed [5]. The resulting features are plugged into typical classification methods [6]: i.e. linear discriminant analysis and K-means clustering. These data processing methods are implemented using in-house written algorithms in MATLAB (The MathWorks inc. USA). Application of these algorithms on the single cell Raman spectra results into the classification of the different cell types based on their principal components. Additionally, new cell samples can successfully be classified under the correct cell type using the previously obtained categorization criteria.

Next to this, we are working towards identification of the biological molecules that cause the variations in the Raman spectra of various cell types. On the one hand, important features in the spectra are identified using the classification algorithms and related back to biological molecules. On the other hand, biological changes are induced into cells and the changes in the corresponding Raman spectra are assessed.

These results show the potential of Raman microscopy for single tumor cell identification and recognition of circulating tumor cells in blood samples. Also, these results prove the ability of Raman spectra to give useful information about the tumor cells, which could result into diagnosis of the primary tumor or metastases.

[1] Hawi, Campbell, Kajdacsy-Balla, Murphy, Adar and Nithipatikom, "Characterization of normal and malignant human hepatocytes by Raman microspectroscopy", Cancer Letters, vol. 110, iss. 1-2, pp. 35-40, December 1996

[2] Krafft, Knetschke, Siegner, Funk and Salzer, "Mapping of single cells by near infrared Raman microspectroscopy", Vibrational Spectroscopy, vol. 32, iss. 1, pp. 75-83, August 2003

[3] Dochow, Krafft, Neugebauer, Bocklitz, Henkel, Mayer, Alberta and Popp, "Tumour cell identification by means of Raman spectroscopy in combination with optical traps and microfluidic environments", Lab on a Chip, vol 11, iss. 8, pp.

1484-1490, 2011

[4] Krishna, Majumder and Gupta, "Range-independent background subtraction algorithm for recovery of Raman spectra of biological tissue", Journal of Raman Spectroscopy, vol. 43, iss. 12, pp. 1884-1894, December 2012

[5] Chan, Taylor, Lane, Zwerdling, Tuscano and Huser, "Nondestructive identification of individual leukemia cells by laser trapping Raman spectroscopy", Analytical Chemistry, vol. 80, iss. 6, pp. 2180-2187, March 2008

[6] Becker-Putsche, Bocklitz, Clement, Rösch and Popp, "Toward improving fine needle aspiration cytology by applying Raman microspectroscopy", Journal of Biomedical Optics, vol. 18, iss. 4, no. 047001, April 2013

9129-16, Session 2

From micro- to nanometer: chasing single pathogens via biophotonics

Stephan Stöckel, Evelyn Kämmer, Konstanze Olschewski, Susann Meisel, Friedrich-Schiller-Univ. Jena (Germany); Mandy Elschner, Friedrich-Loeffler-Institut (Germany); Petra Rösch, Roland Zell, Friedrich-Schiller-Univ. Jena (Germany); Dana Cialla, Karina Weber, Institut für Photonische Technologien e.V. (Germany); Volker Deckert, Institut für Photonische Technologien e.V. (Germany) and Institut für Photonische Technologien e.V. (Germany); Jürgen Popp, Institut für Photonische Technologien e.V. (Germany) and Friedrich-Schiller-Univ. Jena (Germany)

The search for cost-effective and appropriate technologies to control infectious disease is a major component in the pursuit of global health. The socioeconomic burden of infections is enormous, as pathogenic agents, like virions, bacteria, or fungi, pose dangers in human health, agriculture and food, as well as in bioterrorism. Unfortunately, most of the current methods to identify pathogens rely on a time-consuming pre-cultivation step.

Several biophotonic approaches allow an analysis on a single-cell level making a pre-cultivation redundant. Two examples shall be shown here:

(i) Raman microspectroscopy was employed to detect and identify the causative agent of anthrax, the spore-former B. anthracis, in household powders[1]. Raman spectra of single endospores were recorded and used as "fingerprints" to determine the endospore's species via a two-step algorithm. These models (two support vector machines, SVM, and a linear discriminant analysis, LDA) were backed up by a database of more than 10.000 Raman spectra of various Bacillus spp.

(ii) In case of virion diagnostic on single-cell level, a nanoscale resolution is needed. Here, the tip-enhanced Raman spectroscopy (TERS), which combines the specificity of Raman spectroscopy with the high lateral resolution of scanning probe microscopy, was the method of choice[2]. Single virions of different species (e.g. herpes simplex, Influenza A) were probed via TERS and classified according their intrinsic Raman fingerprint of viral components (lipids, proteins, nucleic acids). Again, model-assisted classification methods were the centerpieces of data evaluation.

Funding of the project FastVirus by the Thüringer Aufbaubank is gratefully acknowledged.

References

[1] S. Stöckel, S. Meisel, M. Elschner, P. Rösch, J. Popp, Angew. Chem., Int. Ed. 2012, 51, 5339-5342.

[2] a) D. Cialla, T. Deckert-Gaudig, C. Budich, M. Laue, R. Möller, D. Naumann, V. Deckert, J. Popp, J. Raman Spectrosc. 2009, 40, 240-243; b) T. Deckert-Gaudig, V. Deckert, Curr. Opin. Chem. Biol. 2011, 15, 719-724.

9129-17, Session 2

A review of Raman and FTIR for multicomponent analysis

Sinead J. Barton, Bryan M. Hennelly, National Univ. of Ireland, Maynooth (Ireland) and Callan Institute (Ireland)

Raman spectroscopy is based on the inelastic scattering of monochromatic light. Radiation from a laser is incident on the sample and interacts with the component molecules; the emitted photons that result from this interaction have a different energy to the incident photons and can be measured in terms of the shift in wavelength compared to that of the laser. Only about 1 in 10 million photons undergo Raman scattering [1], the rest will undergo Rayleigh scattering. Raman spectroscopy is a powerful tool for analysing the composition of biological samples in terms of biomolecular content. Over the past two decades there has been considerable interest in the application of Raman to measuring the concentration of the various constituents in a multicomponent mixture [2-4]. This is achieved by first building up a database of the Raman spectra of the individual components in a pure form. Following this a least squares algorithms is applied to find a best fit that accounts for the spectrum of the mixture. The weights returned by the least squares algorithm indicate the relative concentration of each component. Of particular interest has been application of the method to estimate the concentration of various analytes in blood and urine samples, including glucose. In this paper we briefly review the subject of multicomponent analysis by Raman Spectroscopy in terms of experimental methodology, limits of measurement, and applications. We include in this review a comparison with a related inelastic scattering process, Fourier Transform Infrared Spectroscopy.

[1] Saleh BEA, Teich MC. Fundamentals of Photonics. 2nd ed. John Wiley & Sons; 2007.

[2] M.J. Goetz Jr., G.L. Cot´e, R. Erckens, W. March, M. Motamedi, "Application of a Multivariate Technique to Raman Spectra for Quantification of Body Chemicals" IEEE Trans. Biomed. Eng. 42(7), 728 (1995)

[3] Andrew J. Berger, Tae-Woong Koo, Irving Itzkan, Gary Horowitz, and Michael S. Feld, "Multicomponent Blood Analysis by Near-Infrared Raman Spectroscopy," Appl. Opt. 38, 2916-2926 (1999)

[4] Andrew J. Berger, "Raman Spectroscopy of Blood and Urine Specimens," Emerging Raman Applications and Techniques in Biomedical and Pharmaceutical Fields Biological and Medical Physics, Biomedical Engineering, 2010, 385-404

9129-18, Session 2

Mathematical methods to deconvolve and monitor important biomarkers from Raman spectra of biomedical samples

Mónica Marro Sánchez, ICFO - Institut de Ciències Fotòniques (Spain); Alice Abernathy, Claudia Nieva, Angels Sierra, Pablo Villoslada, Institut d'Investigacions Biomèdiques Agustí Pi Sunyer (Spain); Dmitri Petrov, ICFO - Institut de Ciències Fotòniques (Spain) and ICREA- Institució Catalana de Recerca i Estudis Avançats (Spain); Pablo Loza-Alvarez, ICFO - Institut de Ciències Fotòniques (Spain)

Although Raman spectroscopy (RS) has the maximum specificity among all optical techniques for detecting molecular changes, the interpretation of Raman spectra is complex. Biomolecules have many Raman bands and some of them have similar molecular structures. Consequently, they share groups of bands, making difficult to deconvolve the contributions of pure molecular components from the Raman spectra. During the past decades applications of Raman spectroscopy have been focused to discriminate several groups of samples by means of multivariate analysis. However, little information can be

obtained from those methods to extract meaningful molecular components from the Raman spectra that could be assigned to pure molecules constituting the sample. For this reason we proposed to apply Multivariate Curve Resolution (MCR) to deconvolve pure molecular components from the Raman spectra and monitor its content in the tissue or cell over the illness or biological process under study. MCR requires minimal a priori knowledge of the system providing objective and chemically meaningful information. We present two successful biomedical applications of our approach.

First, the retina is a distinctive component of the central nervous system (CNS) in which retinal ganglion cells from the ganglion cell layer (GCL) project their axons to the brain through the optic nerve and is frequently damaged in several diseases such as Glaucoma and Multiple Sclerosis (MS). Therefore, the analysis of molecular changes at the retinal level will increase our understanding of neuronal loss and axonal transection and would aid the development of new neuroprotective strategies for brain and retina diseases. In this study we assess the molecular changes along time of the GCL during retina inflammation by means of RS. We made use of an in vitro model of neuroinflammation using murine retinal organotypic cultures, which preserve cellular composition and tissue architecture while allowing direct in vivo imaging analysis. By using MCR analysis, we deconvolved 6 molecular components suffering dynamic changes along the inflammatory process. Those include the increase of immune mediators, changes in molecules involved in energy production and decrease of Phosphatidylcholine. RS combined with MCR allows monitoring the evolution of retina inflammation based in a number of molecular components sensible to inflammation. It can become a useful technology for studying and monitoring for MS and other brain and retina diseases.

Second, in breast cancer the presence of cells undergoing the epithelial-to-mesenchymal transition (EMT) is indicative of metastasis progression. Since metabolic features of breast tumour cells are critical in cancer progression and drug resistance, we hypothesized that the lipid content of malignant cells might be a useful indirect measure of cancer progression. In this study, MCR was applied to RS to assess the metabolic composition of breast cancer cells undergoing EMT. MCR analysis led to the conclusion that the EMT process affects the lipid profile of cells, increasing tryptophan but maintaining a low fatty acid content in comparison with highly metastatic cells.

In addition, we also study the bone metastasis progression. Our approach permitted to deconvolve and track biomarkers for cancer cell aggressiveness and prognosis at the first stages of malignancy.

Thus, the combination of RS and MCR represents a novel methodology that will push forward the applicability of RS for non-invasive monitoring of the biochemical content in vivo.

9129-19, Session 2

Classification of bladder cancer cell lines using Raman spectroscopy; A comparison of excitation wavelength, sample substrate and statistical algorithms

Laura T. Kerr, Aine Adams, Shirley O'Dea, National Univ. of Ireland, Maynooth (Ireland); Katarina Domijan, Department of Maths and Statistics, National University of Ireland Maynooth (Ireland); Ivor Cullen, University College London Hospitals NHS Foundation Trust (United Kingdom); Bryan M. Hennelly, National Univ. of Ireland, Maynooth (Ireland)

Bladder cancer is the fourth most common cancer in men and ninth in women, with approximately 28 new cases diagnosed every day in the UK. [1, 2] With the continual growth of patients being diagnosed with bladder cancer every year, early detection of the disease is essential for providing the best treatment possible. Detection often requires invasive procedures such as a cystoscopy or biopsy. However, Raman micro-spectroscopy can be combined with multivariate diagnostic algorithms to discriminate between healthy and cancerous tissue non-invasively, as well as identifying the exact grade/stage of bladder cancer present. This is achieved by monitoring the inelastic scattering of photons from bladder tissue, preferably from cells obtained from voided urine, and using this information to determine the biochemical differences between normal and cancerous tissue. Experiments to date have shown promising results but there appears a high degree of variability across different experiments, which has stalled the advancement of the technique into a clinical setting. The main objective of this study is to optimise the materials and methods involved in the diagnosis of bladder cancer using Raman spectroscopy in order to further improve diagnostic accuracy, diagnostic accuracy, thus having the potential to further improve patient outcome afterwards. In this investigation we vary the following parameters in order to find the optimum combination for providing the highest accuracy for diagnostics: (I) a variety of different excitation wavelengths are investigated including 488 nm and 532 nm, (II) different sample substrate are also investigated including calcium fluoride, glass and fused silica, (III) various multivariate statistical techniques are also tested including principal components analysis, discriminant function analysis and neural networks. The sensitivity and specificity of classifying two different bladder cancer cell lines are compared across all of these variables.

References:

[1]: Cancer Research UK. Available from: http://publications.cancerresearchuk.org/downloads/Product/CS_KF_BLADDER.pdf

[2] Jemal A, Siegal R, Ward A, Murray T, Xu J, Smigal C, et al. Cancer Statistics 2006. CA Cancer J Clin. 2006;56:106-130

9129-8, Session 3

Morphological and functional imaging of the mouse cochlea with phase-sensitive optical coherence tomography *(Invited Paper)*

Brian E. Applegate, Jesung Park, Texas A&M Univ. (United States); Simon S. Gao, Rice Univ. (United States); Hee Yoon Lee, John S. Oghalai M.D., Stanford Univ. (United States)

Our best understanding of the mechanical function of the cochlea is derived from complex mathematical models designed to account for the experimental observations of cochlear structure and vibratory response. Unfortunately, experimental measurements of the vibratory response in the soft tissues of the living mammalian cochlea are confounded by the mass of dense bone encapsulating the organ. The predominant approach is to create a hole in the bone exposing the soft tissues and enabling vibratory measurements via laser Doppler vibrometry at the surface of the basilar membrane. However, this procedure can potentially change the mechanical properties of the cochlea and often results in damage to the soft tissues leading to unreliable results. We have recently overcome this issue by using a technique called phase-sensitive optical coherence tomography (PhOCT) that enables imaging through the intact bone of the mouse cochlea. The mouse is an important model for hearing research with models for noise induced loss, blast induced loss, as well as genetic mutants with progressive hearing loss. PhOCT can generate detailed morphological images resolving the substructures of the entire organ of Corti including the tectorial membrane, inner hair cell region, outer hair cell region, and the basilar membrane. At each spatial point, the vibratory response can be measured with subnanometer sensitivity. This exquisite sensitivity is achieved without using any active phase stabilization or common-mode interferometry. Instead working in the frequency domain we are able to achieve shot-noise limited performance for vibrational frequencies above ~ 2 kHz. Using this technology we have been able to make detailed measurements of the cochlear soft tissues under tonal stimulation. Tuning curves measured near the apex of the cochlea at the basilar membrane demonstrate the nonlinear response due to the active gain of the outer hair cells. Spatially resolved measurements of the amplitude and

phase of the vibratory response along the entire organ of Corti suggest how the outer hair cells both generate gain and narrow the frequency response in a normal healthy cochlea.

9129-9, Session 3

Localized measurement of flow and diffusion using Fourier-domain optical coherence tomography

Nicolas Weiss, Ton G. van Leeuwen, Academisch Medisch Ctr. (Netherlands); Jeroen Kalkman, Academisch Medisch Ctr. (Netherlands) and Technische Univ. Delft (Netherlands)

Quantifying total blood flow is an important functional parameter to describe the supply of blood to tissue. Various studies have demonstrated that optical coherence tomography (OCT) can accurately determine the longitudinal component of the local flow velocity [1,2]. One approach to measure the transverse flow velocity is based on the quantification of the intensity fluctuations due to the motion of the scattering particles through the transverse point-spread function [3-7].

In a recent study, we have shown that the autocorrelation function of the OCT signal allows for the localized measurement of the transverse and longitudinal flow velocities [7] and of Brownian motion [8]. In principle the autocorrelation function allows for a simultaneous measurement of the flow velocities and the diffusion coefficient [7]. However, the choice of the imaging optics determines the sensitivity to both diffusion and/or flow measurement.

We report on the simultaneous and localized measurement of the diffusion coefficient and the transverse flow velocity. We show how the quantification depends on the imaging optics beam waist. The choice of a smaller beam waist increases the sensitivity towards the lower range of transverse flow velocities, but decreases the sensitivity of the measurement of the diffusion coefficient. We demonstrate this at micrometer scale in a single measurement in a flow/diffusion phantom. We anticipate that the proposed method opens up new opportunities for the study of complex rheological systems, such as, blood dynamics in the microvasculature.

[1] M. D. Kulkarni, T. G. van Leeuwen, S. Yazdanfar, and J. A. Izatt, Opt. Lett. 23, 1057 (1998).

[2] J. Kalkman, A. V. Bykov, D. J. Faber, and T. G. van Leeuwen, Opt. Express 18, 3883 (2010).

[3] H. Ren, K. M. Brecke, Z. Ding, Y. Zhao, J. Stuart Nelson, and Z. Chen, Opt. Lett. 27, 409 (2002).

[4] Y. Wang and R. Wang, Opt. Lett. 35, 3538 (2010).

[5] J. Lee, W.Wu, J. Y. Jiang, B. Zhu, and D. A. Boas, Opt. Express 20, 22262 (2012).

[6] A. Bouwens, D. Szlag, M. Szkulmowski, T. Bolmont, M. Wojtkowski, and T. Lasser, Opt. Express 21, 17711 (2013).

[7] N. Weiss, T. G. van Leeuwen, and J. Kalkman, Phys. Rev. E. 88, 042312 (2013).

[8] J. Kalkman, R. Sprik, and T. G. van Leeuwen, Phys. Rev. Lett. 105, 198302 (2010).

9129-11, Session 3

The offbeat optics of fat tissue in norm and at ICG/NIR light processing

Irina Y. Yanina, N.G. Chernyshevsky Saratov State Univ. (Russian Federation) and Saratov State Medical Univ. (Russian Federation); Valery V. Tuchin, N.G. Chernyshevsky Saratov State Univ. (Russian Federation) and Institute of Precise Mechanics and Control (Russian Federation) and Univ. of Oulu (Finland); Valery A. Doubrovsky, Saratov State Medical Univ. (Russian Federation); Alexander V. Bykov, Univ. of Oulu (Finland)

The offbeat optical properties of adipose tissues in norm and at NIR irradiation with Indocyanine Green (ICG) sensitizing were found and investigated in detail using 3D OCT and digital microscopy imaging. It was found three major features of optical transmission change of fat tissue slices: 1) initially transmittance was not smooth with bright and dark spots on the image, 2) it became smooth within image area with some mid transmittance at ICG/NIR light treatment, and 3) the multiple “dynamic structures” were registered within each cell image area. These structures were hypothesized to be lipid droplets of cell cytoplasm flowed out through the pores in the membranes. The number and size of “dynamic structures” on the cell surface with time elapsed after laser irradiation were measured.

The 100-150 ?m fat tissues slices and thicker were used in in vitro experiments. Water-ethanol solution of ICG (1 mg/ml) was used for fat tissue staining. CW diode laser (LS-2-N-808 -10000, 808 nm) was used for irradiation of tissue slices with exposure time of 1 min. The studies were conducted at room temperature or physiological temperatures. After laser irradiation the tissue slice was imaged in transmittance mode by a CCD camera of the microscope periodically with the period 5 - 10 min during 40-60 min. The obtained images presented the distribution in time and space of the optical transmittance T for an adipose tissue specimen induced by laser exposure.

It was demonstrated that number of “dynamic structures” was growing with time after light exposure. A strong correlation between the optical transmittance spatial equalizing through the image of a fat tissue slice and the number of “dynamic structures” (cell membrane pores) was found. This result proves our earlier hypothesis about mechanism of light-induced fat cell lipolysis via increased cell membrane porosity and will allows us to hypothesize further that these “dynamic structures” are the cell membrane pores via which adiposomes are secreting under photochemical stress produced by ICG/NIR light action.

9129-12, Session 3

Combining the correlation-stability approach to OCT elastography with the speckle-variance evaluation for quantifying the stiffness differences

Lev A. Matveev, Vladimir Y. Zaitsev, Alexandr L. Matveyev, Institute of Applied Physics (Russian Federation) and Nizhny Novgorod Medical Academy (Russian Federation); Grigory V. Gelikonov, Institute of Applied Physics (Russian Federation) and Nizhny Novgorod State Medical Academy (Russian Federation); Valentin M. Gelikonov, Institute of Applied Physics (Russian Federation) and Nizhny Novgorod Medical Academy (Russian Federation)

Elasticity imaging in optical coherence tomography attracts much attention since the first publication in 1999 [1]. Methods based on quasistatic tissue straining continue to attract much attention, because they do not need any auxiliary system for excitation of vibrations or waves. It is well known that in such compression-based methods, OCT signals have to be specially processed to reconstruct the spatial strain distribution in the tissue. In parallel during the last decade, several OCT signal and image processing techniques were developed for visualization of blood microcirculation in the matrix “rigid” tissue. The latter case can be viewed as an ultimate variant of elastography (differentiation between “rigid” and liquid tissues).

The corresponding processing techniques proposed for solving these problems can be divided in two main categories:

1. Processing of OCT images aimed at reconstruction of the displacement field at the first stage and its subsequent numerical differentiation for obtaining local strains. The development of this approach has led to phase-sensitive OCT elastography based on processing of full OCT signals, as well as methods based on advanced digital image correlation or digital volume correlation (DIC or DVC) techniques in application to OCT;

2. Another significantly different group of methods is based

on statistical analysis of sequences of OCT images, which is the basis of the speckle-variance approach developed for visualization of blood microcirculation using OCT [2] and the correlation-stability (CS) approach to elasticity mapping [3,4].

An important advantage of the statistical (CS) approach to elastographic mapping is that it allows one to directly visualize local strains and avoid the stage of its reconstruction via error-sensitive numerical differentiation of experimentally determined displacements. Besides, CS-methods are applicable at the larger strain range in comparison with displacement-based approaches. Since better tolerance of the CS approach to significant decorrelation of the compared frames determines a much wider strain range of its operability, the CS approach opens attractive prospects for its free-hand implementation, in which the OCT probe itself can be used for deforming the tissue [3]. The CS approach can be implemented using either the image elements reflecting the morphological structure [3] of the tissue or performing the speckle-level cross-correlation [4].

The main disadvantage of the straightforward CS mapping [3,4] is that the values of the correlation function give us only qualitative visualization of the stiffness inhomogeneity. However, in order to quantify the stiffness differences, the CS approach can be modified into a form, which is closely related to the speckle-variance approach proposed for visualization of blood microcirculation using OCT. In this report, we introduce a natural combination of these approaches. The presented results show that the speckle-variance form of the CS approach is promising for quantifying the relative stiffness in OCT.

[1] Schmitt, J., "OCT elastography: imaging microscopic deformation and strain of tissue," Optics express 3, 199211 (1998)

[2] Mariampillai, A., Standish, B. A., Moriyama, E. H., Khurana, M., Munce, N. R., Leung, M. K. K., Jiang, J., Cable, A., Wilson, B. C., Vitkin, I.A., and Yang, Y. X. D., "Speckle variance detection of microvasculature using swept-source optical coherence tomography," Optics Letters 33, 1530 (2008)

[3] Zaitsev, V. Yu., Matveev, L. A., Gelikonov, G. V., Matveyev, A. L., and Gelikonov, V. M., "A correlation-stability approach to elasticity mapping in optical coherence tomography," Laser Physics Letters 10(6), 065601 (2013)

[4] Zaitsev, V. Yu., Matveev, L. A., Matveyev, A. L., Gelikonov, G. V., and Gelikonov, V. M., "Elastographic mapping in optical coherence tomography using an unconventional approach based on correlation stability," Journal of Biomedical Optics 19(2), 021107 (2014)

9129-13, Session 3

Towards free-hand implementation of OCT elastography: displacement-based approaches versus correlation-stability ones

Vladimir Y. Zaytsev, Institute of Applied Physics (Russian Federation) and Nizhny Novgorod Medical Academy (Russian Federation) and State Univ. of Nizhny Novgorod (Russian Federation); Lev A. Matveev, Institute of Applied Physics (Russian Federation) and Nizhny Novgorod Medical Academy (Russian Federation); Grigory V. Gelikonov, Institute of Applied Physics (Russian Federation) and Nizhny Novgorod State Medical Academy (Russian Federation); Alexandr L. Matveyev, Institute of Applied Physics (Russian Federation) and Nizhny Novgorod Medical Academy (Russian Federation); Valentin M. Gelikonov, Institute of Applied Physics (Russian Federation)

Elasticity imaging in OCT has attracted much attention over the last 15 years since the first publications by Schmitt [1], in which the use of speckle-tracking by correlation processing of images of quasi-statically deformed tissue was proposed. Since then a number of dynamic methods have also been studied, which require auxiliary excitation of vibrations or shear-wave fields and evaluation of their characteristics by OCT means.

However, most of elastography-related works were focused on using the OCT probe itself to produce quasistatic tissue deformation, which looks especially promising for free-hand implementation by analogy with medical ultrasonics. Following the initial idea considered by Schmitt, almost all methods from the latter group are based on the initial reconstruction of the displacement field in the inspected region of the tissue, where approximately uniform strain is created by the OCT probe. Then the reconstructed displacement field should be differentiated to evaluate local strains that are inversely proportional by the tissue stiffness.

Independently of different particular techniques of the displacement-filed reconstruction (e.g., digital image correlation, phase-resolved approaches, and their modifications), generically all such methods can be viewed as displacement-based approaches. Recently, an alternative, the so-called correlation-stability approach to OCT elastography has been proposed in which the difference in the local strains is visualized without the intermediate stage of the displacement-field reconstruction [2,3]. Usually elastographic OCT methods of different types are discussed independently and the differences/similarities or limitations on their operability conditions are insufficiently understood.

Here, we perform the corresponding comparison of the above-mentioned methods, which is indispensable in the context of their practical implementation for clinical applications. In particular, it can be noted that despite the recent progress in phase-resolved techniques for measuring particle displacements (e.g. [4,5]), the initial Schmitt's approach [1] based on correlation processing for speckle tracking is still often discussed. Furthermore, it is widely accepted that for sufficiently small strains (for which speckles do not yet demonstrate pronounced blinking/boiling), speckle tracking is always feasible. However, we show that in general this statement is incorrect unless rather special requirements to the OCT system parameters and observation depth are satisfied. We also elucidate how the specific requirements to the frame rates and strain ranges are related for the above-mentioned different elastographic approaches. In the report, we present corresponding analytical arguments, as well as numerical/experimental examples. Special attention is paid to the advantages of the correlation-stability approach [2,3] which are favorable for its free-hand implementation. Further prospects of this approach for stiffness-difference quantification in the context of alternative methods are pointed out.

1. J. Schmitt, OCT elastography: imaging microscopic deformation and strain of tissue, Opt. Express 3, 199–211 (1998).

2. Zaitsev, V. Yu., Matveev, L. A., Gelikonov, G. V., Matveyev, A. L., and Gelikonov, V. M., "A correlation-stability approach to elasticity mapping in optical coherence tomography," Laser Physics Letters 10(6), 065601 (2013)

3. Zaitsev, V. Yu., Matveev, L. A., Matveyev, A. L., Gelikonov, G. V., and Gelikonov, V. M., "Elastographic mapping in optical coherence tomography using an unconventional approach based on correlation stability," Journal of Biomedical Optics 19(2), 021107 (2014)

4. R. K. Wang, S. Kirkpatrick, and M. Hinds, Phase-sensitive optical coherence elastography for mapping tissue microstrains in real time, Appl. Phys. Lett. 90, 164105 (2007).

5. B. F. Kennedy, S. H. Koh, R. A. McLaughlin, K. M. Kennedy, P. R. T. Munro, and D. D. Sampson, Strain estimation in phase-sensitive optical coherence elastography, Biomed. Opt. Express 3, 1865–79 (2012).

9129-20, Session 4

Pseudo-spectrum reconstruction algorithm for reducing saturation artifact in fourier-domain optical coherence tomography *(Invited Paper)*

Cheng-Kuang Lee, Chiung-Ting Wu, Meng-Tsan Tsai, Chang Gung Univ. (Taiwan)

Optical coherence tomography is a novel medical imaging

technique. Fourier-domain optical coherence tomography draws much attention with its advantages of high imaging speed and high sensitivity. Saturation artifact is one of the common image noises in fourier-domain optical coherence tomography. This artifact is caused by that the received light spectrum is partly over the dynamic range of the detector. Saturation artifact produces obvious spot noise or stripe noise that blocks the real image and makes the diagnosis difficult. As we know that Y. Huang and J. U. Kang proposed a method in Opt. Engineering (2012) to reduce the artifact with interpolation of nearby non-saturated A-scans. However, this method cannot preserve the real structure information of the sample and the error would be serious when the saturation A-scans successively appear. We propose a pseudo-spectrum reconstruction algorithm to estimate the real number of saturation part based on nearby non-saturated measured data. The artifact is significantly reduced with this proposed method and the real structure information of the sample is preserved.

We demonstrate this method with spectral-domain OCT scheme. The center wavelength of the light source is 890 nm with FWHM about 150 nm. In the detection arm, the spectrometer is constructed with a collimator, a grating, a set of focusing lenses, and a line-scan CCD camera. The image acquisition device is set as 12-bit. The intensity keeps 4095 when the saturation occurs. The line-scan CCD camera captures the spectrum. Each acquired interference spectrum is checked if there exist successive 4095 data points. If the number of successive 4095 data points is more than 2, the pseudo-spectrum reconstruction processing was performed. The parabolic curve fitting is made based one the two edged saturation points and the two nearby non-saturation points. Next, the “guess” numbers of the the saturated part are evaluated with the parabolic curve. The test sample is is 3M post-it with five layers semi-opaque tape. Original OCT image with saturation artifact is compared with the images under artifact reducing algorithm. The results show that the saturation artifact is reduced. And we compare the results with that based on the other method proposed by Y. Huang et al. in Opt. Engineering in 2012. Both methods can reduce the saturation artifact. However the real structure information remains under the pseudo-spectrum reconstruction algorithm.

9129-21, Session 4

Advances in tumor diagnosis using OCT and Raman spectroscopy

Valery P. Zakharov, Ivan A. Bratchenko, Samara State Aerospace Univ. (Russian Federation); Sergey Kozlov, Alexander A. Moryatov, Samara State Medical Univ. (Russian Federation); Dmitry V. Kornilin, Oleg O. Myakinin, Dmitry Artemyev, Samara State Aerospace Univ. (Russian Federation)

Diagnosis of the first stage malignant tumors by medical staff is successful only in every second case. Taking into account that biopsy and histological tests are not suitable in some tumors study, instrumental diagnosis methods should be used. Complex investigation of malignant tumors was performed involving combined optical coherence tomography (OCT) and Raman spectroscopy (RS) setup. Combined the OCT and RS setup for the main skin and lung malignant tumors analysis may be used for precise tissue topology visualization and simultaneous tissue type determining. Combined OCT and RS system used in current research was used in ex vivo and in vivo experiments and allowed to register OCT images with 3.7 um resolution. The system comprises of a broadband superluminescent laser diode (840 ± 25nm wavelength range, 20mW output power) at the source end, Michelson interferometer with 50/50 split ratio to the sample and reference arms and a spectrometer at the detector end. The spectrograph Sharmrock SR-303i (diffraction grating 1200 grooves/mm) with integrated camera ANDOR DV-420A-OE was used. For Raman spectrums registration thermally stabilized laser based on the semiconductor laser module LML-785.0RB-04 (providing lasing power of 100 - 200 mW, wavelength of 785 nm) was used. Diffusely scattered light from the sample was registered by Sharmrock spectrograph. Use of this spectrograph provided a resolution of 0.05 nm at a low noise level. Raman scattering was obtained with a narrow-band filter to cut off fluorescent and Raman contribution of fiber, and broadband filters and dichroic mirror for prevention of excitation laser radiation registration.

The OCT may be useful in BCC diagnosis while the RS allows determining other malignant tumors (malignant melanoma of skin, adenocarcinoma and squamous cell carcinoma of lung). Raman spectra researches of lesions allow us to formulate the criteria for determining the phase-type human tissue lesions. A phase method for skin and lung tumors type determining, based on changes in Raman spectral intensity in 1300-1340 cm-1 and 1640-1680 cm-1 bands in relation to the intensity of 1450 cm-1 was proposed. The bands in these regions correspond to the CH3CH2 twisting, wagging vibrations (protein and nucleic acids), to the amide I vibrations (protein) and to the bending vibration mode CH2 (protein and lipid deformation), respectively. In vivo experiments on skin tumors were performed for 23 samples (9 melanomas, 9 basal cell carcinoma, 1 squamous cell carcinoma, 2 pigment nevi, 2 benign tumours); ex vivo experiments on lung tissue 22 samples (11 adenocarcinomas and 11 squamous cell carcinomas) were tested. Experimental in vivo and ex vivo researches were approved by ethical committee of Samara State Medical University. The phase method could identify: malignant melanoma with 88,9% of sensitivity and 87,8% of specificity; adenocarcinoma with 100% of sensitivity and 81,5% of specificity; squamous cell carcinomas with 90,9% of sensitivity and 77,8% of specificity.

9129-22, Session 4

Real-time data processing for in-line monitoring of a pharmaceutical coating process by optical coherence tomography

Daniel Markl, Jakob Ziegler, Research Ctr. Pharmaceutical Engineering GmbH (Austria); Günther Hannesschläger, RECENDT GmbH (Austria); Stephan Sacher, Research Ctr. Pharmaceutical Engineering GmbH (Austria); Andreas Buchsbaum, Research Center for Non-Destructive Testing GmbH (Austria); Michael Leitner, RECENDT GmbH (Austria); Johannes G. Khinast, Research Ctr. Pharmaceutical Engineering GmbH (Austria) and Technische Univ. Graz (Austria)

Coating of tablets is a widely applied unit operation in the pharmaceutical industry. Thickness and uniformity of the coating layer are crucial for efficacy as well as for compliance. Not only due to different initiatives it is thus essential to monitor and control the coating process in-line. Optical coherence tomography (OCT) was already shown in previous works to be a suitable candidate for in-line monitoring of coating processes. However, to utilize the full potential of the OCT technology an automatic evaluation of the OCT measurements is essential. The main requirements on such an algorithm are to be fast and efficient as well as to provide reliable and accurate results. The speed of the evaluation is very critical since the data is acquired continuously and has to be processed in real-time. Therefore, this study presents an efficient approach allowing the use of the graphical processing unit (GPU) in future. The automatic evaluation is currently implemented in MATLAB and includes several steps: (1) extraction of features of each A-scan, (2) classification of A-scan measurements based on their features, (3) detection of interfaces (air/coating and coating/core), (4) correction of distortions due to the curvature of the bi-convex tablets and the oblique orientation of the tablets, and (5) determining the coating thickness. The algorithm is tested by OCT measurements acquired by moving the sensor head of the OCT system across a static tablet bed. The multiple direct measurement of the coating thickness on a tablet basis allows the analysis of the inter- and intra-tablet coating uniformity. Specifically, the information about those parameters emphasizes the high capability of the OCT technology to improve process understanding and to assure a high product quality.

9129-23, Session 4

Color high resolution full-field optical coherence microscopy for enhanced contrast imaging

Antoine Federici, Eliot De-Toldi, Arnaud Dubois, Institut d'Optique Graduate School (France)

Full-field optical coherence microscopy (FF-OCM) is an established optical technology based on low-coherence interference microscopy for high-resolution non invasive three-dimensional imaging of semi-transparent samples. We present an extension of the technique setting up an achromatic imaging system over a spectral range extending from 530 nm to 1700 nm, to provide tomographic images in three distinct bands centered at 635 nm, 870 nm and 1170 nm. Image contrast enhancement as well as sample characterization is performed using the conventional RGB color channel representation.

Light is emitted by a halogen lamp and then separates into two arms of a Linnik-type interferometer with microscope objectives placed in each arm. Three illumination bands within the spectral response of the camera are selected by inserting three sets of filters in a Köhler illumination system. The images are projected onto a visible to short-wavelength infrared detector based on an InGaAs photodiode array by two different 400 mm-focal length doublet lenses, one optimized for the 600-1000 nm wavelength range and the other one for 1000-1600 nm, depending on the filter combination. En-face oriented tomographic images are obtained by arithmetic combination of four phase-shifted interferometric images. Because refractive microscope objectives cannot function efficiently over such a broad spectral band, reflective microscope objectives (x15, 0.28 NA), coated with gold, are employed, providing good reflectivity, zero chromatic aberration and negligible coma, spherical, and astigmatic aberrations over the three bands.

Great care was taken to reach similar performances in the three bands for good superposition of the three images. In FF-OCM systems, the larger the mean wavelength, the broader the spectrum must be to keep the axial resolution constant. The width of each of the three spectral bands is then adjusted so that the latter is quasi-constant over the three imaging bands. In order to obtain a constant transverse resolution over the three bands, the PSF is scaled by convolving every pixel of the acquired image with a suited Gaussian function. An axial resolution of ~1.9μm and a transverse resolution of ~2.4μm are achieved while the detection sensitivity is close to 85dB in the three bands. A dynamic dispersion compensation system is set up to preserve axial resolution and signal intensity level when the imaging depth is varied. To do so, the optical path length of the reference arm is adjusted by rotating a glass plate, while an identical plate is placed at a fixed angle in the other arm. Theoretically, a perfect compensation is achieved if the group velocity dispersion of the glass plate is equal to the one of the sample. Assuming that biological samples are mainly made of water, fused silica appears well suited with regard to its dispersion properties. Images of biological samples revealing their spectral properties are shown as illustration of improved detection capability with enhanced contrast.

9129-24, Session 4

Photon mayhem: OCT for structural and functional assessment of biological tissues and treatment response monitoring *(Invited Paper)*

I. Alex Vitkin, Ontario Cancer Institute (Canada)

Measuring of pH in tumor is an important task for basic researches and successful treatment. This work is aimed at the development of the method of pH registration in the tumor models. The study was performed using 3D tumor spheroids and xenografts expressing new genetically encoded sensor for pH. Measuring of pH was based on a radiometric analysis of fluorescence intensity at two different wavelengths. The data of fluorescence microscopy and whole-body imaging were confirmed by morphological investigation and hypoxia analysis in the tissue sections. The possibility of using the unique genetically encoded sensor for ratiometric pH imaging in the tumors in vitro and in vivo was shown for the first time.

9129-25, Session 5

Optical imaging of intracranial hemorrhages in newborns: modern strategies in diagnostics and direction for future research *(Invited Paper)*

Alexey Pavlov, Saratov State University (Russian Federation) and Saratov State Technical University (Russian Federation); Oxana Semyachkina-Glushkovskaya, Vladislav V. Lychagov, Olga Bibikova, Sergey Sindeev, N.G. Chernyshevsky Saratov State Univ. (Russian Federation); Olga Pavlova, Elena Shuvalova, Saratov State University (Russian Federation); Valery V. Tuchin, N.G. Chernyshevsky Saratov State Univ. (Russian Federation) and Institute of Precise Mechanics and Control (Russian Federation) and Univ. of Oulu (Finland)

Intracranial hemorrhage (ICH) in newborns is an important but poorly studied problem. Even recently, it was believed that in term newborns ICH is relatively uncommon because most infants with ICH are asymptomatic and cannot be readily detected with the most widely used neuroimaging procedures. However latest prospective magnetic resonance imaging (MRI) studies of asymptomatic term newborns suggest that ICH is much more frequent that previously thought. Cranial ultrasound is often used as the first imaging modality for newborns. But ultrasonography is not enough sensitive for detection of subarachnoid, subdural hemorrhage – most common types of ICH in term newborns. Cranial ultrasound can be effective when clinical symptoms suggest that intracranial hemorrhage has occurred. Therefore, cranial ultrasound is used predominantly for prediction of severity infants in post-hemorrhagic period. Computed tomography and MRI are more sensitive than ultrasonography but currently impractical as a routine investigation in newborns due to ionizing radiation, sedation, difficulties with transportation of sick newborns to an imaging suite. Over the past decade, many new technologies that can be used to monitor brain physiology have been introduced into intensive care units. These include brain-tissue oxygen monitoring, transcranial Doppler ultrasound and near-infrared spectroscopy. An area of interest in pediatrics has been the use of neuromonitoring to describe cerebral hemodynamics and cerebral autoregulation following brain injury. However, it remains unclear if impaired autoregulation and cerebral blood flow (CBF) are a simply markers of injury severity or an independent causal factors.

A small number of animal studies have examined the mechanisms of ICH in neonatal period. There is no experimental method which is closest to the natural origin ICH. We developed the new original model for inducing of ICH in newborn rodent using harmful effects of infrasound on the brain. The results of MRI and histological analysis of the brain tissue of stressed newborn rats showed multiple ICH in the cortex in next day after infrasound action. Notice, that the clinical works have been shown that term neonates have superficial ICH. The results of DOCT and speckle imaging studies of CBF in sagittal sinus through fontanel (dura left intact) in newborn mice/rats show that the low CBF is key reason for development of cerebral hypotension and hypoxia, as well as it is important criteria of severity and consequences of ICH. We also obtained that the loss reactivity of cerebral vessels to adrenaline (it is used in clinics for prevention of cerebral hypotension in newborns with ICH) can be a diagnostic criteria of risk of ICH in newborns. Using pharmacological modulation of activity of different types of vascular adrenoreceptors in the brain we found that the high activation of non-innervated beta2-adrenoreceptors which stimulate ATP-sensitive K+-channels and Gs-protein-dependent activation of protein kinase A and ?-arrestin-mediated signalling

pathways, trigger stress-induced rupture of cerebral vessels. These findings can be useful for better understanding the symptoms and mechanisms of ICH in newborns and also for the further study of sensitive markers of predictability of ICH in infants during the first days after birthday.

9129-26, Session 5

Measuring fast fluorescence-lifetime changes by fluorescence lifetime-transient scanning (FLITS)

Hauke Studier, Vladislav I. Shcheslavskiy, Wolfgang Becker, Becker & Hickl GmbH (Germany)

Abstract: We present a technique that records transient fast changes in the fluorescence lifetime of a sample with spatial resolution along one scanned line. The technique is based on building up a photon distribution over the distance along a selected line, the arrival times of the photons after the excitation pulses of the laser, and the total experiment time after starting with any kind of stimulation of the sample. The maximum resolution at which lifetime changes can be recorded is given by the line scan time. With repetitive stimulation and triggered accumulation transient effects of changing the fluorescence lifetime can be resolved at a resolution of about one millisecond. Potential applications of FLITS are experiments of plant physiology, electro-physiology, and Ca++ imaging of neuronal tissue.

9129-27, Session 5

Correlative two-photon and light sheet microscopy

Ludovico Silvestri, Anna Letizia Allegra Mascaro, Irene Costantini, Univ. degli Studi di Firenze (Italy); Leonardo Sacconi, National Institute of Optics (Italy); Francesco S. Pavone, Univ. degli Studi di Firenze (Italy)

One of the unique features of the brain is that its activity cannot be framed in a single spatio-temporal scale, but rather spans many orders of magnitude both in space and time. A single imaging technique can reveal only a small part of this complex machinery. To obtain a more comprehensive view of brain functionality, complementary approaches should be combined into a correlative framework. Here, we describe a method to integrate data from in vivo two-photon fluorescence imaging and ex vivo light sheet microscopy, taking advantage of blood vessels as reference chart [1]. We show how the apical dendritic arbor of a single cortical pyramidal neuron imaged in living thy1-GFP-M mice can be found in the large-scale brain reconstruction obtained with light sheet microscopy. Starting from the apical portion, the whole pyramidal neuron can then be segmented. The correlative approach presented here allows contextualizing within a three-dimensional anatomic framework the neurons whose dynamics have been observed with high detail in vivo.

This work has received funding from LASERLAB-EUROPE (grant agreements n° 228334 and 284464, EC's Seventh Framework Programme) and has been supported by the Italian Ministry for Education, University and Research in the framework of the Flagship Project NANOMAX, by Italian Ministry of Health in the framework of the 'Stem Cells Call for proposals'. This work has been supported by Regione Toscana in the framework of POR-CreO 2007-2013 action (SMAG project). This work has been carried out in the framework of the activities of ICON foundation supported by "Ente Cassa di Risparmio di Firenze". This work is part of the activities of the European Flasghip Human Brain Project (grant agreement n° 604102). Part of this work was performed in the frame of the Proof of Concept Studies for the ESFRI research infrastructure project Euro-BioImaging at the PCS facility LENS.

References:

1. L. Silvestri et al. Correlative two-photon and light sheet microscopy, in press

9129-28, Session 5

A translational paradigm for quantitative multiplexed fluorescence image guidance for brain tumor surgery

Pablo A. Valdes, Dartmouth College (United States); Valerie L. Jacobs, Dartmouth Hitchcock Medical Ctr. (United States); Frederic Leblond, Dartmouth College (United States); Brian C. Wilson, Univ. of Toronto (Canada); Keith D. Paulsen, Thayer School of Engineering at Dartmouth (United States); David W. Roberts M.D., Dartmouth Hitchcock Medical Ctr. (United States)

Intraoperative fluorescence image guidance during brain tumor surgery - specifically, the use of 5-aminlevulinic acid-induced protoporphyrin IX (ALA-PpIX) as a fluorescent biomarker - has been shown as a useful adjunct for maximizing the extent of tumor resection and concomitant improved clinical outcomes. Nevertheless, current state-of-the-art clinical technologies demonstrate significant limitations. First, their diagnostic performance is limited in accuracy and sensitivity at detecting non-visible yet diagnostic levels of PpIX, leaving significant amounts of tumor tissue undetected in high and low grade gliomas. Second, current techniques provide subjective non-quantitative assessments of fluorophore levels, and finally, they do not perform simultaneous resolution of multiple fluorophores in vivo. We have previously demonstrated using a point spectroscopy handheld probe system that quantitative, spectrally resolved measurements significantly improve the diagnostic accuracy of PpIX for tumor tissue, including in low-grade gliomas. These results are encouraging for support of using a quantitative technique for PpIX detection in clinical practice. Further, the rise of new fluorescent markers for intraoperative applications provides support for the development of an imaging technique that enables simultaneous quantitative measurements of fluorescent biomarkers across the full surgical field of view. Here we present a translational paradigm – from bench-to-bedside – in the development of a quantitative, spectrally-resolved intraoperative fluorescence imaging technique. We present the system design composed of a liquid crystal tunable filter in the visible or near-infrared region for fast, automated wavelength selection, a highly sensitive CMOS camera detector, and custom optics that enable seamless integration unto commercial surgical microscopes. Full 3-dimensional spectral image cubes (x,y,lambda) of the diffuse white light reflectance and fluorescence emissions are collected in near real time. A light attenuation correction algorithm is applied to correct for the distorting effects of tissue optical properties on the emitted fluorescence, and a spectral decomposition algorithm is used to individually extract the distinct fluorescent components under investigation. We present tissue simulating phantom studies with varying concentrations of scatterer medium using intralipid and absorber dye, demonstrating spectrally-resolved and quantitative estimates (i.e., attenuation corrected) of protoporphyrin IX concentration, as well as simultaneous imaging of multiple visible and near-infrared fluorophores. We further demonstrate in vivo pre-clinical studies in rodent models implanted with the CNS-1 glioma cell line and grown for 2-3 weeks. For surgery the animals were given a dose of 5-aminolevulinic acid, fluorescein sodium, and/or near-infrared activatable dyes and imaged under appropriate conditions for single and multiple biomarker imaging of tumor and brain parenchyma anatomy using our spectrally resolved, quantitative intraoperative fluorescence imaging system. This technique provides improved tumor tissue detection, quantitative estimates of fluorophore concentration in tissue, and spectrally-resolved imaging for simultaneous resolution of multiple biomarkers in vivo. We finally conclude with translation into the clinical neurosurgical suite for our first in-human results of our quantitative intraoperative imaging system for improved guidance of human brain tumor resection. This quantitative imaging technique has potential use with a broad range of

fluorescent biomarkers in multiple additional tumor sites, including breast, prostate and lung cancer.

9129-29, Session 5

The method of intraoperative analysis of structural and metabolic changes in the area of tumor resection

Tatiana A. Savelieva, Victor B. Loshchenov, Vladimir V. Volkov, Kirill G. Linkov, A. M. Prokhorov General Physics Institute (Russian Federation); Sergey A. Goryainov M.D., Alexander A. Potapov M.D., N.N. Burdenko Neurosurgical Institute (Russian Federation)

Background and Objective. The method of intraoperative analysis of tumor markers such as structural changes, concentrations of 5-ALA induced protoporphyrin IX (Pp IX) and hemoglobin (Hb) in the area of tissue resection was developed. The theoretical and clinical rationales of this method were published earlier [1, 2]. A device for performing this method is a neurosurgical aspiration cannula coupled with the fiber optic probe. The configuration of the optical fibers at the end of this tool provides the most accurate estimation of tumor marker concentrations. The aim of this study was to demonstrate the accuracy of data recovery in the tests on optical phantoms with optical properties imitating optical properties of studied tumor.

Materials and Methods. The configuration of fibers at the end of cannula was developed according to the results of numerical modeling of light distribution in biological tissues. The optimal distance between the illuminating and receiving fiber was found for biologically relevant interval of optical properties. On this particular distance the detected diffuse reflectance depends on scattering coefficient almost linearly. Array of optical phantoms containing hemoglobin, protoporphyrin IX and fat emulsion (as scattering media) in various concentrations was prepared to verify the method.

Results. The recovery of Hb and Pp IX concentrations in the scattering media with an error less than 10% has been demonstrated. The fat emulsion concentration estimation accuracy was less than 12%. The first clinical test was carried out during glioblastoma multiforme resection in Burdenko Neurosurgery Institute and confirmed that sensitivity of this method is enough to detect investigated tumor markers in vivo.

Conclusion. This method will allow intraoperative analysis of the structural and metabolical tumor markers directly in the zone of destruction of tumor tissue, thereby increasing the degree of radical removal and preservation of healthy tissue.

1. Tatiana A. Savelieva; Nina A. Kalyagina; Maria N. Kholodtsova; Victor B. Loschenov; Sergey A. Goryainov; Aleksander A. Potapov; Numerical modelling and in vivo analysis of fluorescent and laser light backscattered from glial brain tumors. Proc. SPIE 8230, Biomedical Applications of Light Scattering VI, 82300L (February 9, 2012); doi:10.1117/12.907444.

2. A.A. Potapov et al. Intraoperative combined spectroscopy (optical biopsy) of cerebral gliomas. Voprosy nejrokhirurgii imeni N.N. Burdenko, 2013, 77(2), 3-10.

9129-30, Session 6

High content-high throughput hyperspectral imaging of cell populations *(Invited Paper)*

Ewa M. Goldys, Martin E. Gosnell, Ayad G. Anwer, Saabah Mahbub, Sandeep M. Perinchery, Macquarie Univ. (Australia)

Biological cells are very heterogeneous and significant subpopulations have been uncovered in stem, neural, cancer, immune, and other cell cultures. The understanding of these biochemically and functionally different cell subpopulations will revolutionise biology and medicine.

We report the development of specialised characterization hardware and analysis tools using hyperspectral imaging able to identify cells within a population with different biochemistry. Crucially, the method is label free, avoiding biochemical interference with cells. We explain how our method responds to commercial and clinical needs across a broad spectrum of medicine and the life sciences.

Our approach uses only native characteristics of cells without extraneous fluorescent labels and it can be used alongside established methods of fluorescent labeling. We analyse all acquired cell images in a fully automated way without subjective choices. The process aims to derive maximum quantitative information from cell images using statistics to assess population properties and differences. Our approach is also fully compatible with standard biochemical methods used in cell biology and it can be naturally combined with them.

We present four examples of applicability of the hyperspectral method (1) for differentiation of healthy control cells, cells with a mitochondrial disorder and treated cells, which show a return to normalcy; (2) for biochemically mapping key fluorophores in cell populations, including statistics of fluorophore content; (3) for the detection of cell subpopulations answering the question of whether cells form distinguishable clusters; (4) for finding label-free signatures of cell subpopulations, which demonstrate that, in some cases, antibody labeling may in some cases be replaced by measurements and analysis of autofluorescent characteristics. These methods have been applied to several cell types including olfactory neuronal cells, adipose-derived stem cells, induced pluripotent stem (IPS) cells, motor neuron disease cells, various cancer cells, animal embryos and diabetic tissue.

The results of our analysis reveal abundant new information about cell behaviour. We have been able to detect osteogenic differentiation of stem cells in a label-free fashion. The results of therapies have been clearly observed in two different classes of cells (olfactory neuronal cells and motor neurone disease cells). We have been able to distinguish healthy from diseased cells in all cased under investigation (mitochondrial disease MELAS, motor neurone disease, diabetes). Early breast cancer (MCF10) and advanced cancer cells (MCF7) have been extremely well separated. Environmental factors such as smoking for 1 day and for 20 days are clearly apparent in tissue samples. Biochemistry of an embryo can be detected and monitored. Cell confluence, different passages and also different individuals had a visible effect on the observed hyperspectral characteristics. The method has also been able to distinguish specific cell subpopulations, such as a diseased cell subpopulation in the mitochondrial disease MELAS and a highly performing adipose-derived stem cell subpopulation that differentiates into bone more rapidly than the remaining cells in the sample.

9129-31, Session 6

Fractal anisotropy in tissue refractive index fluctuations: potential role in precancer detection

Nandan K. Das, Subhasri Chatterjee, Prasanta K. Panigrahi, Indian Institute of Science Education and Research Kolkata (India); Asima Pradhan, Indian Institute of Technology Kanpur (India); Nirmalya Ghosh, Indian Institute of Science Education and Research Kolkata (India); Semanti Chakraborty, IISER K (India)

Tissue exhibits multifractality [1] which can be inferred from the analysis of refractive index (RI) fluctuation within tissue. Our present study is aimed to quantify the fractal anisotropy present in human cervical tissues having different orders of dysplasia. Differential interference contrast images (DIC) are the direct representation of this RI fluctuation. In this present study, we have performed multi-fractal de-trended fluctuation analysis (MFDFA) on RI fluctuation series obtained by unfolding images horizontally and vertically to get the information about anisotropic self-similarity. Results of our statistical analysis on several samples reveal the presence of anisotropy in fractality in tissue-structures.

We have taken DIC images of the human cervical pre-cancerous tissue-sections (histopathologically characterized as Grade I and III dysplastic) of 5.0 micron thickness prepared on glass

slide using DIC microscopy. The area under observation are unstained connective tissue sections near basal layer which were biopsy samples of human cervical tissues. DIC images are unfolded horizontally and vertically to get 1 D refractive index fluctuation series in orthogonal direction and subject to MFDFA analysis to get fractal parameter like Hurst exponent [hq(q=2)], width of the singularity spectra (Δ?) [1, 2] .

The Hurst exponent values for self-similar fluctuation remains in the range between 0.0 < hq(q=2) < 1.0. The Hurst exponent hq(q=2) = 0.5 indicates that the fluctuation is random but if hq (q=2) > 0.5 indicates correlated fluctuation and < 0.5 indicates anti-correlated fluctuation. A general trend of decreasing Hq (Hurst exponent) as the progress of cancer increases is observed. This is expected considering the fact that as cancer progresses, collagen fibre in stromal region breaks which in turn decrease the correlations such that Hurst exponent get reduced. Also, the width of singularity spectrum (WSS) increases with increase grade of cancer indicates of the increase of multi-fractality [1]. Horizontal as well as vertical unfolding is done on the image samples, difference in Hurst exponent as well as width of singularity spectrum is observed in same tissue DIC image. This shows signature of anisotropy in the human cervical cancer tissue and anisotropy reduced as cancer progress. More detailed study is under way and which might enable us to detect cancer in early stage from the information of the change in anisotropic multi-fractality in DIC images of the cervical cancer tissue. The Hurst exponent for a grade I and Grade III tissue of the horizontal r. i. fluctuation are 0.53 and 0.47 respectively. But, for same samples, the Hurst exponent of vertical r.i. fluctuation is 0.5 and 0.46 respectively.

References

[1] Nandan Das et al, “Probing multifractality in tissue refractive index: prospects for precancer detection”, Vol. 38, No. 2 / OPTICS LETTERS.

[2] H. Eugene Stanley et al, “Multifractal detrended $uctuation analysis of nonstationary time series” A 316 (2002) 87 – 114.

9129-32, Session 6

Analysis of mixed cell cultures with quantitative digital holographic phase microscopy

Björn Kemper, Jana Wibbeling, Steffi Ketelhut, Univ. of Münster (Germany)

In order to study, for example, the influence of pharmaceuticals or pathogens on different cell types under identical measurement conditions and to analyze interactions between different cellular specimens a minimally-invasive quantitative observation of mixed cell cultures is of particular interest. Quantitative phase microscopy (QPM) provides high resolution detection of optical path length changes that is suitable for stain-free minimally-invasive live cell analysis. Due to low light intensities for object illumination, QPM minimizes the interaction with the sample and is in particular suitable for long term time-lapse investigations, e.g., for the detection of cell morphology alterations due to drugs and toxins [1,2]. Furthermore, QPM has been demonstrated to be a versatile tool for the quantification of cellular growth [3,4], the extraction morphological parameters [5,6] and cell motility. Thus, we studied the feasibility of QPM for the analysis of mixed cell cultures. It was explored if quantitative phase images provide sufficient information to distinguish between different cell types and to extract cell specific parameters. For the experiments quantitative phase imaging with digital holographic microscopy (DHM) [7] was utilized. Mixed cell cultures with different types of human pancreatic tumor cells were observed with quantitative DHM phase contrast up to 80 h. The obtained series of quantitative phase images were evaluated by adapted algorithms for image segmentation. From the segmented images the cellular dry mass and the mean cell thickness were calculated and used in the further analysis as parameters to quantify the reliability of the measurement principle. The obtained results demonstrate that it is possible to characterize the growth of cell types with different morphologies in a mixed cell culture separately by consideration of specimen size and cell thickness in the evaluation of quantitative DHM phase images.

[1] A. Bauwens, M. Bielaszewska, B. Kemper, P. Langehanenberg, G. von Bally, R. Reichelt, D. Mulac, H.-Ulrich Humpf, A. W. Friedrich, K. S. Kim, H. Karch, J. Müthing, “Differential cytotoxic actions of Shiga toxin 1 and 1 Shiga toxin 2 on microvascular and 2 macrovascular endothelial cells”, Thrombosis and Haemostasis 105, 515-528 (2011).

[2] J. Kühn, E. Shaffer, J. Mena, B. Breton, J. Parent, B. Rappaz, M. Chambon, Y- Emery, P. Magistretti, C. Depeursinge, P. Marquet, G. Turcatti. ASSAY and Drug Development Technologies11, 101-107 (2013).

[3] B. Rappaz, E. Cano, T. Colomb, J. Kühn, V. Simanis, P. J. Magistretti, P. Marquet, C. Depeursinge, “Noninvasive characterization of the fission yeast cell cycle by monitoring dry mass with digital holographic microscopy”, J. Biomed. Opt. 14, 034049 (2009).

[4] B. Greve, F. Sheikh-Mounessi, B. Kemper, I. Ernst, M. Götte, H. T. Eich, “Survivin, a target to modulate the radiosensitivity of Ewing-Sarcoma”, Strahlenther. Onkol. 188,1038–1047 (2012).

[5] B. Kemper, A. Bauwens, A. Vollmer, S. Ketelhut, P. Langehanenberg, J. Müthing, H. Karch, G. von Bally, “Label-free Quantitative Cell Division Monitoring of Endothelial Cells by Digital Holographic Microscopy”, J. Biomed. Opt. 15, 036009 (2010).

[6] P. Girshovitz, N. Shaked, “Generalized cell morphological parameters based on interferometric phase microscopy and their application to cell life cycle characterization”, Biomed. Opt. Express, 3, 1757-1773 (2012).

[7] B. Kemper, G. von Bally, “Digital holographic microscopy for life cell applications and technical inspection”, Appl. Opt. 47, A52-A61 (2008).

9129-33, Session 6

Laser double Doppler flowmeter

Luiz Poffo, Jean-Marc Goujon, Ronan Le Page, Jonathan Lemaitre, Univ. Européenne de Bretagne (France); Mohammed Guendouz, Nathalie Lorrain, Dominique Bosc, Université européenne de Bretagne, CNRS, Laboratoire FOTON (France)

The Laser Doppler flowmetry (LDF) is a non-invasive method for estimating the tissular blood flow and speed at a microscopic scale (microcirculation). It is used for medical research as well as for the diagnosis of diseases related to circulatory system tissues and organs including the issues of microvascular flow (perfusion). It is based on the Doppler effect, created by the interaction between the laser light and tissues.

The Laser Double Doppler Flowmeter (FL2D) aims at improving this technique by bringing a major breakthrough in the measurement method. Current developments of the LDF are focused on the use of always more complex and sophisticated methods for the detected signal processing. With FL2D, we propose to change the principle of generation of the measurement volume by using two laser sources. This volume would be perfectly stable and localized at the intersection of the two laser beams.

Indeed, the major disadvantage of LDF is the inaccuracy of the measurement volume (MV), which is normally a cone or a cylinder of about 1 mm3. Its size mainly depends on the way that light is absorbed in the probed tissue, which changes for each individual and for each tissue. The inaccuracy of the MV does not provide a measurement of the velocity of blood on a specific capillar but a mean value of this quantity resulting from all the capillaries present in the MV at the time of measurement. For this reason, an estimation of the blood perfusion requires the LDF signal but also a mathematical model of the MV in the tissue analysed. It is then impossible to determine an absolute value for the blood flow (e.g. in ml/s) with LDF method: measurements are then expressed in arbitrary units such as PU (Perfusion Unit). These arbitrary units prevent the use of LDF for real-time medical supervision on Humans.

In order to measure blood perfusion in an artery and to obtain the absolute blood perfusion, it is mandatory to control the MV. To do so, this work will use a micro velocimeter, originally developed for fluid mechanic measurements, that presents a MV of about 30 x 30 x 30 μm3 delimited by the interference pattern of two laser beams. This device will allow measuring on one hand the velocity of the blood in a specific capillary; on the other hand the size of erythrocytes that passes through it. Moreover, building arrays of micro velocimeters would enable the velocity profile measurement in larger arteries, such as aorta. With more accurate information concerning blood flow, it will be possible to use the FL2D in the daily medical supervision opening hence new perspectives for research in the field of cardiovascular diseases.

9129-34, Session 6

Sensorless adaptive optics and the effect of field of view in biological second harmonic generation microscopy

Stefaan Vandendriessche, Maarten K. Vanbel, Thierry Verbiest, Katholieke Univ. Leuven (Belgium)

In light of the population ageing in many developed countries, there is a great economical interest in improving the speed and cost-efficiency of healthcare. Clinical diagnosis tools are key to these improvements, with biophotonics providing a means to achieve them. Standard optical microscopy of in vitro biological samples has been an important diagnosis tool since the invention of the microscope, with well known resolution limits. Nonlinear optical imaging improves on the resolution limits of linear microscopy, while providing higher contrast images and a greater penetration depth due to the red-shifted incident light compared to standard optical microscopy. It also provides information on molecular orientation and chirality. Adaptive optics can improve the quality of nonlinear optical images. We analyzed the effect of sensorless adaptive optics on the quality of the nonlinear optical images of biological samples. We demonstrate that care needs to be taken when using a large field of view. Our findings provide information on how to improve the quality of nonlinear optical imaging, and can be generalized to other in vitro biological samples. The image quality improvements achieved by adaptive optics should help speed up clinical diagnostics in vitro, while increasing their accuracy and helping decrease detection limits. The same principles apply to in vivo biological samples, and in the future it may be possible to extend these findings to other nonlinear optical effects used in biological imaging.

9129-35, Session 6

Wavelet and multi-fractal based analysis on DIC images in epithelium region to detect and diagnose the cancer progress among different grades of tissues

Sabyasachi Mukhopadhyay, Nandan K. Das, Nirmalya Ghosh, Indian Institute of Science Education and Research Kolkata (India); Asima Pradhan, Indian Institute of Technology Kanpur (India); Prasanta K. Panigrahi, Indian Institute of Science Education and Research Kolkata (India)

Differential Interference Contrast Image (DIC) provides well-known technique to achieve high contrast image of spatial refractive index fluctuation. DIC images of cervical cancer tissues are taken from epithelium region, on which wavelet transform and multi-fractal analysis are applied. Discrete wavelet transform (DWT) through Daubechies basis are done for identifying fluctuations over polynomial trends for clear characterization and differentiation of tissues. A systematic investigation of denoised images is carried out through the continuous Morlet wavelet. The scalogram reveals the changes in coefficient peak values from grade-1 to grade-3. Wavelet normalized energy plots are computed in order to show the difference of periodicity among different grades of cancerous tissues. Using the multi-fractal de-trended fluctuation analysis (MFDFA), it is observed that the values of Hurst exponent decrease and width of singularity spectrum increases as cancer progresses from grade-1 to grade-3 tissue.

9129-42, Session 7

Second-harmonic generation microscopy of collagen-bearing structures

Maarten K. Vanbel, Tom W. Callewaert, Thierry Verbiest, Katholieke Univ. Leuven (Belgium)

Nonlinear optical phenomena cover a broad research area. The emphasis is mostly on the generation of higher harmonics to be used in laser designs or on the characterization capabilities of nonlinear optics. The latter ability of nonlinear optics is important when combined with a microscope to detect simultaneously multiphoton fluorescence and second-harmonic generation. Submicron size features can then be investigated separately and information on their structure can be revealed by second-harmonic generation. For example, the point group symmetry can be determined in situ and in vivo in complex media. Moreover, nonlinear optical microscopy has several additional advantages: the generation and detection of nonlinear signals is intrinsically confocal and degradation, if present, only occurs at a localized places in the structure. In biological structures, multiphoton fluorescence and second-harmonic generation do not necessarily occur in the same type of the structure. This can be exploited to visualize different structures in one sample by simultaneous detection of two-photon fluorescence and second-harmonic generation. Also, the incident beam can be tuned to fit in the biological window of biological structures, which gives second-harmonic generation microscopy a significant advantage over linear microscopy due to absorbance issues in the visible wavelength range. We exploit these advantages to characterize collagen-bearing biological structures. Collagen is the dominant structural protein in connective tissue in mammals. Being the most abundant protein in the mammal clade, it is essential for the very existence of it. Collagen is a protein with a very strict quaternary structure. The most simple Ramachandran model states that a amino-acid sequence of Glycine-prolin-hydroxyprolin leads to a right-handed helical structure. The inherent stability is such that a sole helix cannot exist for a prolonged period of time, it will therefore combine with 2 near identical helices, resulting in the formation of the superhelical structure tropocollagen. Subsequently tropocollagen will align in a linear direction forming the fibers composing collagen-tissue. Due to the superhelical nature of collagen, this structure is ideal to be probed by second-harmonic generation.

9129-43, Session 7

Glare-free optical system for fundus visualization

Viktor K. Salakhutdinov, Smetanin G. Yuriy, Institute of Optical Neural Technologies (Russian Federation); Jasser Doroshenko, Posterior Eye Section Diagnostics and Surgery Ctr. (Russian Federation); Eugene A. Sivachenko, Joint Institute for Nuclear Research (Russian Federation)

For a particular class of optical systems, it is impossible to reduce the glare to the required level using nothing but antireflection the fee for the solution to the problem is a substantial degradation of the technical characteristics. An illustrative example is the optical system of a fundus camera where glare suppression is achieved by a wide-angle objective glass with a lens whose relative aperture is more than one. In modern ophthalmology, fundus cameras are principle means of diagnostics.

A matrix method of computation the parameters of a glare-free

optical system is presented. The idea of eliminating reflections (Fig. 1): the light reflected by the optical surface (dotted line) is focused and completely absorbed by a low-sized absorber.

The computation of the characteristics of an arbitrary complex optical system is reduced to the solution of a particular system of equations.

The results for a new optical system of fundus camera with two confocal two-lens objective glasses O1, O2 (Fig.2) are presented. These objective glasses are used simultaneously for forming the light beam that brightens the fundus and for registering the image by a TV camera.

For illuminating the fundus, the light from the source is collimating by a two-lens objective O1 and after that is focusing on the pupil of the eye by a two-lens objective O2. For registering the image of the fundus, the optical system transfers the light that is scattered on the fundus from the pupil of the eye to the pupil of the TV camera. For the registration with the field of approximately 20?, the relative aperture 1:5 for each objective (O1, O2) is sufficient.

The results of mathematical modeling of optical characteristics are presented. It is shown that, taking into account average statistical aberrations of the eye, the resolution near the optical axis of the eye is more than 40 lines/mm; when the angles with the axis are more then 30?, the resolution decreases to 20 lines/mm. The main reason of this decrease is the individual specificity of the aberrations in the eye. The results of the investigation of the laboratory version of a fundus camera are presented together with the results of the video registering using this camera. The experiments demonstrated that the proposed method reduces the glare by more than 56 db

9129-44, Session 7

Second and third NIR optical windows for imaging of bone micro-fractures

Laura A. Sordillo, Yang Pu, Peter P. Sordillo M.D., Yury Budansky, Robert R. Alfano, The City College of New York (United States)

Near-infrared (NIR) light can give deeper depth penetration in high scattering tissue media than does light in the visible wavelength range and can produce higher quality images. An optical image of turbid media, such as biological tissue, can be blurred due to the molecular process of Rayleigh/ Mie scattering. The penetration of light into tissue is limited due to absorption by biomolecules such as collagen and elastin, lipids, and, in particular, by water. The limitations on light penetration into tissue are expressed in the absorption and scattering coefficients. There exist, however, spectral NIR regions of minimal water absorption between peak NIR water maxima (~900 nm, ~1,200 nm, ~1,400 nm and ~1,900 nm) which can help minimize detection of diffusive photons, and thus can highlight ballistic and snake photons that produce clearer images. The region from 650 nm to 1,000 nm (or the first NIR therapeutic window) is conventionally used for most optical studies of tissue. Limited work has been done utilizing other NIR spectral regions between water peak maxima. Microfractures in bone, secondary to repetitive stress, particularly in the lower extremities, are an important problem for military recruits and for athletes. They also may occur in those with weakened bones, such as the elderly, or in patients taking bisphosphonates for osteoporosis or for treatment of bone metastases from solid tumors or multiple myeloma. Microfractures can be early predictors of major bone fracture and may be as important as changes in bone density in predicting where and how likely a major fracture will occur. We explore a second spectral window from 1,100 nm to 1,350 nm, and introduce a third spectral window from 1,600 nm to 1,870 nm. Employment of these windows may allow for deeper penetration into tissue and higher contrast images. We have used these new spectral windows to measure optical attenuation properties and, due to reduction in scattering, to obtain high contrast images of microfractures and non-displaced fractures with and without overlying tissue. These results may be useful in aiding in the development of a more advanced non-invasive NIR imaging system.

9129-45, Session 7

SPADnet: a fully digital, scalable and networked photonic component for time-of-flight PET applications

Edoardo Charbon, Ecole Polytechnique Fédérale de Lausanne (Switzerland) and Technische Univ. Delft (Netherlands); Claudio E. Bruschini, Ecole Polytechnique Fédérale de Lausanne (Switzerland); Chockalingam Veerappan, Technische Univ. Delft (Netherlands); Leo H. C. Braga, Nicola Massari, Matteo Perenzoni, Leonardo Gasparini, David Stoppa, Fondazione Bruno Kessler (Italy); Richard Walker, Ahmet T. Erdogan, Robert K. Henderson, The Univ. of Edinburgh (United Kingdom); Steve East, Lindsay A. Grant, STMicroelectronics (R&D) Ltd. (United Kingdom); Balázs Játékos, Ferenc Ujhelyi, Gabor Erdei, Emöke Lörincz, Budapest Univ. of Technology and Economics (Hungary); Luc André, CEA-LETI (France); Laurent Maingault, Commissariat à l'Énergie Atomique (France); Vincent Reboud, Loick Verger, Eric Gros d'Aillon, CEA-LETI (France); Peter Major, Zoltan Papp, Gabor Nemeth, Mediso Medical Imaging Systems (Hungary)

The SPADnet FP7 European project is aimed at a new generation of fully digital, scalable and networked photonic components to enable large area image sensors, with primary target gamma-ray and coincidence detection in (Time-of-Flight) Positron Emission Tomography (PET). SPADnet relies on standard CMOS technology, therefore allowing for MRI compatibility.

SPADnet innovates in several areas of PET systems, from optical coupling to single-photon sensor architectures, from intelligent ring networks to reconstruction algorithms. It is built around a natively digital, intelligent SPAD (Single-Photon Avalanche Diode)-based sensor device which comprises an array of 8x16 pixels, each composed of 4 mini-SiPMs with in situ time-to-digital conversion, a multi-ring network to filter, carry, and process data produced by the sensors at 2Gbps, and a 130nm CMOS process enabling mass-production of photonic modules that are optically interfaced to scintillator crystals. The sensor operates on a 100 MHz clock, which divides the sensor counting function in time bins. At each clock cycle, the sensor is able to generate its total counts value, which is then output in real-time. This stream of data, which represents the digitized photon flux, is also used by the on-chip discriminator. The SPADnet sensor has been fully characterised, achieving for example a 10.8% energy resolution at 20C for a LYSO crystal of 3x3x5mm3, and a Coincidence Resolving Time (CRT) of 288ps using two sensors and a crystal of the same size as above.

A few tens of sensor devices are tightly abutted on a single PCB to form a so-called sensor tile, thanks to TSV (Through Silicon Via) connections to their backside (replacing conventional wire bonding). The sensor tile is in turn interfaced to an FPGA-based PCB on its back. The resulting photonic module acts as an autonomous sensing and computing unit, individually detecting gamma photons as well as thermal and Compton events. It determines in real time basic information for each scintillation event, such as exact time of arrival, position and energy, and communicates it to its peers in the field of view. Coincidence detection does therefore occur directly in the ring itself, in a differed and distributed manner to ensure scalability. The selected true coincidence events are then collected by a snooper module, from which they are transferred to an external reconstruction computer using Gigabit Ethernet.

We will detail the SPADnet core technologies as well as the latest project achievements in all project areas, including a new measurement technique that makes it possible to excite our experimental PET modules in a single point at a time (relying on

UV excitation instead of the conventional collimated gamma-source to generate POIs), as well as the development of a number of optical concentrator geometries.

9129-46, Session 7

Retroreflective imaging systems for enhanced optical biosensing

Mark H. Bergen, Jacqueline A. Nichols, Christopher M. Collier, Xian Jin, Jonathan F. Holzman, UBC Okanagan (Canada)

Biosensing technologies play an important part in the detection and characterization of microorganisms. These biosensing technologies are often facilitated by electrical, magnetic or chemical sensing techniques, each of which has its own distinct capabilities. When the detection and characterization of targeted microorganisms require micron-scale resolutions, however, optical biosensing techniques have proven to be especially beneficial.

Optical biosensing can be applied through direct optical sensing techniques (e.g., standard microscopy) or indirect optical sensing techniques (e.g., fluorescence microscopy), but it is the indirect optical sensing techniques that have demonstrated especially high sensitivities for the detection of targeted microorganisms. Indirect optical sensing techniques make use of labeling to enhance the detection process. A well-known example of this is molecular labeling in fluorescence microscopy. Unfortunately, such fluorescence systems must rely on high-resolution microscopy with microscopic sampling areas to image the fluorescence from targeted microorganisms. This can lead to especially long characterization times when operating with macroscopic sample sizes, for applications such as pathogen detection in water quality monitoring, as it is necessary to scan the micron-scale sampling areas across the millimeter- or even centimeter-scale sample sizes.

Given the benefits of optical biosensing, and the challenges of contemporary indirect optical sensing techniques such as fluorescence microscopy, the work that follows introduces retroreflector (RR) labels for the detection and characterization of microorganisms. The retroreflective imaging system that is demonstrated makes use of a laser source to illuminate the sample, in lieu of the fluorescent excitation source, and micron-scale RR labels, in lieu of fluorescent stains/proteins. The RRs are bound to targeted microorganisms by way of antibodies, and the presence of these microscopic RR-microorganism pairs is monitored in a retroreflected image that is captured by a distant image sensor. The retroreflected image shows a well-localized retroreflected beamspot for each RR-microorganism pair that is present on the sample. An appropriately-designed retroreflective imaging system will therefore provide a quantifiable record of microorganism-coupled RRs across macroscopic sample sizes. The characteristics of the full retroreflective imaging system are presented here, with the operation analyzed in terms of directionality, collimation, and contrast. The system is used to investigate both corner-cube RRs and spherical RRs (of varying refractive indices). It is ultimately found that such a system can be an effective tool for the detection and characterization of microorganism targets, down to a single-target detection limit.

9129-47, Session 7

A Blue Optical Filter for Narrow-band Imaging in Endoscopic Capsules

Manuel F. R. Silva, Univ. do Minho (Portugal); Mohammadamir Ghaderi, Technische Univ. Delft (Netherlands); Luis Goncalves, Univ. do Minho (Portugal); Ger de Graaf, Reinoud F. Wolffenbuttel, Technische Univ. Delft (Netherlands); Jose Higino Gomeo Correia, Univ. do Minho (Portugal)

This paper presents the design, simulation, fabrication and characterization of a thin film Fabry Perot resonator composed of titanium dioxide (TiO2) and silicon dioxide (SiO2) thin films. The optical filter is developed to integrate with a light emitting diode (LED) for narrow band imaging (NBI) technique in endoscopy. The NBI is a high resolution imaging technique that uses spectrally centered blue light (415 nm) and green light (540 nm) to illuminate the target tissues. The light at 415 nm enhances the imaging of superficial veins due to their hemoglobin absorption, while the light at 540 nm penetrates deeper into the mucosa, thus enhances the sub-epithelial vessels imaging. Typically the endoscopes and endoscopic capsules use white light for acquiring images of the gastrointestinal (GI) tract. However, implementing the NBI technique in endoscopic capsules enhances their capabilities for the clinical applications. A commercially available blue LED with a maximum peak intensity at 402 nm and Full Width Half Maximum (FWHM) of 20 nm is integrated with a narrow band blue filter as the NBI light source. The thin film simulations show a maximum spectral transmittance of 36 % centered at 415 nm with FWHM of 13 nm for combined the blue LED / Fabry Perot resonator system. A custom made deposition scheme was developed for the fabrication of the blue optical filter by RF sputtering. RF powered reactive sputtering at 200 W with controlling the gas flows of argon and oxygen at 5:1 ratio gives the optimum optical conditions for TiO2 thin films, while for SiO2 thin films, a non reactive RF sputtering at 150 W with argon gas flow at 15 sccm results in the best optical performance. The TiO2 and SiO2 thin films were fully characterized by an ellipsometer in the wavelength range between 250 nm to 1700 nm. Finally, the optical performance of the filter is measured and will be presented.

9129-36, Session 8

Lensless microscopic diagnostics of human skin *(Invited Paper)*

Rainer Riesenberg, Institut für Photonische Technologien e.V. (Germany); Jürgen Schreiber, Nuga Lab. GmbH (Germany); Andreas Wuttig, Mario Kanka, Institut für Photonische Technologien e.V. (Germany)

We present a new digital inline holographic setup. It is characterized by a lensless arrangement working in reflection mode. With this arrangement the inline holography is not restricted by the extension of the sample and is suitable for the point of care investigation of the skin of a human body.

A micro-coherent illumination with a length of coherence of 10 ... 200 μm avoids disturbing interferences caused by reflections. A very efficient algorithm for image reconstruction of the samples based on the so called tile superposition propagation allows a spatial resolution below 1 μm, corresponding to a numerical aperture of 0.8.

With this set-up we take images as well as speckle pattern of the human skin. A lot of information like roughness in dependence of the age and correlation functions is derived.

9129-37, Session 8

Organic solvent-free sugar-based nanopatterning transparency material derived from biomass for eco-friendly optical biochips using green lithography

Satoshi Takei, Toyama Prefectural Univ. (Japan); Akihiro Oshima, Osaka University (Japan); Tomoko G. Oyama, Japan Atomic Energy Agency (Japan); Kenta Ito, Kigenn Sugahara, Toyama Prefectural Univ. (Japan); Miki Kashiwakura, Takahiro Kozawa, Seiichi Tagawa, Osaka University (Japan)

A organic solvent-free water-developable sugar-based nanopatterning transparency material derived from biomass was investigated in a method of producing optical biochips for organic solvent toxicity, safety, environmental affair, easiness of handling, and health of the working people, instead of the common developable process such as trimethylphenylammonium hydroxide and cyclohexanone. This emphasizes the use of plant products instead of conventionally used aqueous alkaline developer and organic solvents. The images of 60-100 nm line and space pattern with exposure dose of 5.0-7.0 ?C/cm2, a real refraction index of 1.45-1.53 at

350-800 nm and an imaginary refractive index of less than 0.005 at 350-800 nm and great O2 Gas barrier properties were provided by specific process conditions in the organic solvent-free processes using the green lithography. The sugar-based nanopatterning transparency material were also indicated highly efficient crosslinking and lower film thickness shrinkage, and was also applicable to future fabrications of eco-friendly optical biochips using green lithography, which will potentially benefit low-carbon societies.

9129-38, Session 8

Real-time protein aggregation monitoring with a Bloch surface wave-based approach

Sara Santi, Elsie Barakat, Ecole Polytechnique Fédérale de Lausanne (Switzerland); Emiliano Descrovi, Politecnico di Torino (Italy); Reinhard Neier, Univ. of Neuchâtel (Switzerland); Hans Peter Herzig, Ecole Polytechnique Fédérale de Lausanne (Switzerland)

The misfolding and aggregation of amyloid proteins has been associated with incurable diseases such as Alzheimer's or Parkinson's disease. In the specific case of Alzheimer's disease, recent studies have shown that cell toxicity is caused by soluble oligomeric forms of aggregates appearing in the early stages of aggregation, rather than by insoluble fibrils. Research on new strategies of diagnosis is imperative to detect the disease prior to the onset of clinical symptoms.

In this work, we exploit the unique properties of an optical label-free refractometric sensing platform to propose a novel approach for investigating the initial lag-phase of Ab(1-42) aggregation. Our sensing approach allows the real-time optical detection of local refraction index changes occurring as aggregation takes place. The method is based on the optical interrogation of a dielectric multilayer (one-dimensional photonic crystal) sustaining an electromagnetic surface wave. The sensing technique is reminiscent of surface plasmon resonance (SPR). Instead of having a surface plasmon propagating on a thin metallic film, an evanescent wave called "Bloch surface wave" (BSW) is coupled on a purely dielectric multilayer structure. Depending on the materials used and the layout of the periodic dielectric multilayer, the BSW can be produced in a wide spectral range, from the visible to the near-infrared. This spectral tunability represents one of the main advantages of BSW-based optical transduction systems, as compared to SPR. In addition, BSWs present very narrow resonances that can increase the resolution and improve the limit of detection in label-free detection schemes. BSWs generated on dielectric multilayers are sensitive to external perturbations of the refractive index close to the surface of the photonic multilayer. In the following, we report on a proof of principle of the BSW-based detection technique for sensing protein aggregation by monitoring in real time the refractive index variation of an aqueous solution containing the Ab(1-42) peptide during early aggregation and fibril formation. The multilayer surface is directly contacted with the probed aqueous medium and the sensing chamber is positioned vertically. Hence, we exploit BSWs to locally probe the refractive index variations of a solution wherein the Ab(1-42) peptide is initially injected in a monomeric form and is progressively aggregating to form fibrils. During this process, the Ab(1-42) peptide tends to precipitate away from the multilayered surface, therefore, the measurements using BSWs monitor a local variation of the refractive index of the solution, which is directly related to the depletion of the concentration of the Ab(1-42) monomeric form during aggregation.

We demonstrate the efficacy of the BSW approach by monitoring in real-time the first crucial steps of A?42 oligomerization. Furthermore, we provide new insights into the complex mechanism of aggregation of this protein system in the presence of small molecular probes able to interfere with the dynamics of amyloid formation. As a control method, Transmission Electron Microscopy has been used to morphologically characterize the sample during aggregation.

9129-39, Session 8

Specific biosensing with an oligofluorene truxene distributed feedback laser

Anne-Marie Haughey, Benoit Guilhabert, Martin D. Dawson, Glenn A. Burley, Nicolas Laurand, Univ. of Strathclyde (United Kingdom)

Distributed-feedback (DFB) laser sensors are a class of evanescent sensor that enable the detection of interactions occurring at the device surface as laser emission wavelength varies with changes in the refractive index. Such lasers can be used for biosensing by functionalising the device surface with probe molecules that selectively bind to an analyte of interest. A number of attributes make DFB lasers based on organic or 'plastic' materials especially well-suited for biosensing applications, including their capacity for multiplexing, incorporation into standard labware and high-throughput measurements.

In this paper, we present a plastic DFB laser biosensor made with pi-conjugated oligofluorene truxene macromolecules. In addition to the attributes already mentioned this sensor has the potential to provide a compact and portable sensing system, as low lasing thresholds make optical pumping with a laser diode a possibility. Furthermore, the high refractive index of the truxene macromolecules (relative to that of dye-doped polymers) enables high laser mode confinement, which is desirable for sensitivity. The capabilities of our DFB laser sensor are demonstrated by the specific detection of a range of different concentrations of the protein avidin, using a biotin-functionalised laser. The minimum detectable avidin concentration is 100 ng.mL-1. Our intention is to develop a biosensor that can be used with biologically relevant samples, therefore, we have also investigated the effect of non-specific binding of albumin, a protein found in abundance in blood samples, as a potential source of interference. Results from a competition assay with avidin and albumin show no interference from albumin at biologically relevant concentrations (50000 ?g.mL-1).

9129-40, Session 8

Time-stretched spectrally encoded angular light scattering for high-throughput real-time diagnostics

Jost Adam, Christian-Albrechts-Univ. zu Kiel (Germany) and Univ. of California, Los Angeles (United States); Ata Mahjoubfar, Eric D. Diebold, Brandon W. Buckley, Bahram Jalali, Univ. of California, Los Angeles (United States)

The angular light scattering profile of microscopic particles significantly depends on their morphological parameters, such as size and shape. This dependency is widely used in state-of-the-art flow cytometry methods for particle classification. We recently introduced spectrally encoded angular light scattering (SEALS) method, with potential application in scanning flow cytometry (SFC). We show that a one-to-one wavelength-to-angle mapping enables the measurement of the angular dependence of scattered light from microscopic particles over a wide dynamic range. Improvement in dynamic range is obtained by equalizing the angular scattering dependence via spectral equalization. The resulting continuous angular spectrum is obtained without mechanical scanning, enabling single-shot measurement. Using this information, particle morphology can be determined with improved accuracy. We derive and experimentally verify an analytic wavelength-to-angle mapping model, facilitating rapid data processing. As a proof of concept, we demonstrate the method's capability of distinguishing differently sized polystyrene beads.

The combination of SEALS with time-stretch dispersive Fourier transform (TS-DFT) offers real-time and high-throughput (high frame rate) measurements and renders the method suitable for integration in standard flow cytometers: By transforming the spectrum into time and slowing the time scale, using group velocity dispersion (GVD), single-shot spectra can be obtained

at high throughput using a photodiode and a real-time digitizer. We achieve the necessary GVD by using a high-dispersion low loss optical fiber. In order to improve the signal to noise ratio (SNR), the fiber is pumped with diode pump lasers to create distributed optical amplification via stimulated Raman scattering. The amount of group velocity dispersion is chosen to time-stretch the optical pulses, that is, to slow them down, such that they do not overlap and may be digitized in real-time.

9129-41, Session 8

Particle detection from spatially modulated fluorescence signals

Siegfried W. Kettlitz, Sebastian Valouch, Uli Lemmer, Karlsruher Institut für Technologie (Germany)

Flow cytometry relies on the detection of cells selectively stained with markers. Optically, they can be detected as fluorescent particles. The use of microfluidics offers a wide range of benefits over traditional flow cytometer designs but when replacing expensive components with inexpensive counterparts the sensitivity of the instrument suffers [1]. To increase the sensitivity of the detection system, spatial modulation has been proposed [2]. The spatial modulation is implemented via fine pitched shadow masks close to the microfluidic channel which generate a signal pattern when a fluorescent particle passes by. Using a fine pitch and long total length for the pattern a high spatial resolution and long total exposure time are combined. The proposed benefit is that the high spatial resolution allows for a high particle throughput and the long exposure time increases the instrument sensitivity significantly. Compared to systems with only a single measurement aperture [2], the particle detection, however, is much more complicated since overlapping spatially modulated signals generate a complex pattern containing many local signal peaks.

We compare the performance of particle detection using different approaches. Matched filtering is known to provide the highest signal-to-noise ratio but in this case suffers from low spatial resolution. To remedy this, the use of the derivative of the filtered signal has been proposed. While this method provides high spatial resolution for a single particle detection it suffers from side maxima interfering with particles nearby. We model the system, analyse the signal and derive a minimum-mean-square-error (MMSE) solution closely related to a Wiener filter. Our approach provides both a high spatial resolution together with tuneable suppression of signal noise and side maxima allowing for a sensitive detection and high particle throughput.

[1] Kettlitz, S. et al., IEEE Trans. Instrum. Meas., 62 (2013), 1960-1971

[2] Kiesel, P. et al., Appl. Phys. Lett., 94 (2009), 041107

9129-91, Session PS2

Hollow core photonic crystal fiber probes for Raman and fluorescence spectroscopy with photonic nanojet focusing

Jerome Wenger, Hervé Rigneault, Petru Ghenuche, CNRS (France)

Current optical fiber probes for Raman and/or fluorescence spectroscopy struggle with large luminescence background and low detection sensitivities. The use of conventional fibers is severely limited by the high luminescence background generated in silica, which complicates the signal processing and/or the probe implementation. We solve this issue by using a new type of hollow core photonic crystal fiber probe for Raman spectroscopy and endoscopy. Compared to earlier work, our approach combined several novel key features: (i) the very simple optical configuration, (ii) the two orders of magnitude reduction in silica background noise, and (iii) the large spectral bandwidth. We apply further this technical breakthrough to bring the sensitivity of fluorescence endoscopy to the single molecule level. Our solution uses a hollow core photonic crystal fiber probe combined with a polystyrene microsphere. As compared to the previous state-of-the-art, we report a 200x improvement of the signal-to-noise ratio for single molecules detection events, together with a 1000x gain on the minimum detectable concentration. The applications for fluorescence imaging and direct laser writing will also be described. We believe that this device offers new opportunities for remote or in vivo optical characterization together with a miniaturization of microscope setups. Applications include inspection of semiconductor wafers, photolithography, laser surgery, and fluorescence sensing.

References:

- P. Ghenuche, H. Rigneault, J. Wenger, Hollow-core photonic crystal fiber probe for remote fluorescence sensing with single molecule sensitivity, Opt. Express 20, 28379-28387 (2012).

- P. Ghenuche, H. Rigneault, J. Wenger, Photonic nanojet focusing for hollow-core photonic crystal fiber probes, Appl. Opt. 51, 8637-8640 (2012).

- P. Ghenuche, S. Rammler, N. Y. Joly, M. Scharrer, M. Frosz, J. Wenger, P. St. J. Russell, H. Rigneault, Kagome hollow-core photonic crystal fiber probe for Raman spectroscopy, Opt. Lett. 37, 4371-4373 (2012).

9129-92, Session PS2

Polarization effects in cutaneous autofluorescence spectra

Ekaterina G. Borisova, Liliya P. Angelova, Alexandra Z. Zhelyazkova, Tsanislava I. Genova, Institute of Electronics (Bulgaria); Elmira P. Pavlova M.D., Petranka P. Troyanova M.D., Univ. Hospital “Queen Jiovanna-ISUL” (Bulgaria); Latchezar A. Avramov, Institute of Electronics (Bulgaria)

The light-induced autofluorescence spectroscopy is a very useful tool for early detection and differentiation of skin pathologies, including neoplasia. It has the potential to provide real-time diagnosis of malignant and premalignant skin tissue, but as the skin is a very complex multilayered and inhomogeneous organ with spatially varying optical properties that complicate the analysis of cutaneous fluorescence spectra.

Polarization fluorescence spectroscopy has the potential to increase our knowledge for the origins of endogenous fluorophore content in normal and diseased skin and to be used for initial diagnostics and differentiation of the cutaneous neoplasia investigated, thus increasing the diagnostic accuracy of fluorescence technique for clinical investigations. Used polarized light for excitation of the skin samples one could obtain response related to the anisotropy features of extracellular matrix of the tissue and namely to structural proteins fluorescence dependable from the polarization of incident excitation light. The fluorophore anisotropy is attenuated during lesions’ growth and level of anisotropy demolition could be correlated with the stage of tumor development.

Our investigations presented here are based on in vivo point-by-point measurements of excitation-emission matrices (EEM) from volunteers skin on different anatomical places using linear polarizer and analyzer for excitation and emission light detected. Measurements were made using spectrofluorimeter FluoroLog 3 (HORIBA Jobin Yvon, France) with fiber-optic probe in steady-state regime of work using excitation in the region of 280-440 nm with step of 10 nm. Three different situations were evaluated and corresponding excitation-emission matrices were developed – with parallel and perpendicular positions for linear polarizer and analyzer, and without polarization of excitation and fluorescence light detected from the samples. Normal skin polarized fluorescence in vivo was investigated on six different volunteers. These results are compared with twelve freshly surgically removed skin non-melanoma tumours and normal skin samples from so called “safety area” used in surgical removal to evaluate the polarization effects observed in case of tumours detected.

Fluorescence spectra obtained reveal differences in spectral intensity, related to general attenuation of the signal, due to filtering effects of used polarizer/analyzer couple. Significant spectral shape changes were observed for the complex autofluorescence signal detected, which correlated with collagen and protein cross-links fluorescence, that could be addressed to the tissue extracellular matrix and general condition of the skin investigated, correlating with tissue morphological destruction due to the lesions' growth. The initial results obtained and their interpretation will be presented in our report. Our next step is to increase our database and to evaluate all sources of intrinsic fluorescent polarization effects and found if they are significantly altered from normal skin to cancerous state of the tissue, to obtain useful for development non-invasive diagnostic tool for dermatological practice.

Acknowledgements: This work is supported by the National Science Fund of Bulgarian Ministry of Education, Youth and Science under grant #DMU-03-46/2011.

9129-93, Session PS2

Nonlinear and nonmonotonic nature of the intensity of fluorescence emission on a surface of turbid fluorescing biotissues

Dmitry A. Rogatkin, Ludmila G. Lapaeva, Irina Guseva, MONIKI (Russian Federation)

Many researchers during the past 20 years have used the laser fluorescence spectroscopy (LFS) for in vivo tissue diagnosis. But in the up-to date medical in vivo LFS there is a problem of quantification of fluorophores concentrations in optically-turbid biotissues basing on measurements of the laser induced fluorescence on a surface of the tissues. The purpose of our work is both experimental and theoretical study of the character of dependences of measured fluorescence intensities on tissues' optical properties and on fluorophores concentrations in tissues. In the experimental part of the study the laboratory measurements of the superficial fluorescence on phantoms at different known concentration of fluorophores in them were carried out. As a result the experimental dependences of the registered intensities of the laser induced fluorescence emission on concentration of fluorophores were plotted. In the theoretical part of our study the analytical solution for fluxes of fluorescence emission on a tissue surface by Kokhanovsky's method (J. Opt. Soc. Am. A., 2009, v.26. No.8. P.1896–1900) based, in its turn, on the well-known Kubelka-Munk approach (KMA) was used. Though it is considered that KMA is very simplified, not rigorous and accurate, nevertheless it allows anyone to receive the strict and analytical equations convenient for the further detailed analysis. Besides that, in our study the Kokhanovsky's method was cardinally improved by its association with new improved KMA (Biomed. Engineering, 2007, v.41, No. 2, P.59-65), allowing us to receive exact solutions for boundary intensities collected by an optical probe on surfaces of the inspected tissue. As a result a set of theoretical curves describing the influence of tissues' optical properties and concentration of fluorophores in tissues on the registered intensities was obtained as well. Both experimental and theoretical results show a good qualitative similarity between each other. Moreover, all these results show that the dependence of the fluorescence intensity from tissues' optical properties and from the concentration of fluorophores is both nonlinear and non-monotonic. Thus, these results show a number of difficulties which a doctor can meet at the laser fluorescence diagnostic data analysis. From the doctor's point of view the concentrations of different fluorophores, for example, in a tumorous tissues are the most important parameters. But only having the information of fluorescent emission fluxes on boundaries of the inspected tissues he cannot make a correct interpretation of the registered data. To do that he needs the additional information about the optical properties of the tissue, because the changing in fluxes can be caused by changing of the concentrations of fluorophores as well as by complex changing of tissue's optical properties due to the intensive blood filling, for example. And this dependence is not linear and not monotonic in the general case. It cannot be predicted; therefore it should be measured by the diagnostic equipment at the same time and from the same tissue's area as the fluorescent fluxes are measured. The research is supported by RFBR grant No. 14-02-00733.

9129-94, Session PS2

Wearable photoplethysmography device prototype for wireless cardiovascular monitoring.

Edgars Kviesis-Kipge, Zbignevs Marcinkevics, Univ. of Latvia (Latvia); Viktorija Mechnika, Riga Technical Univ. (Latvia); Andris Grabovskis, University of Latvia, Faculty of Biology, Department of Human and Animal Physiology (Latvia)

Over last decade physical activity has become a popular as an effective rehabilitation method for elderly population and cardiovascular patients as an active lifestyle and regular physical activity can reduce the stress and improve the health. This seemingly simple activity can be ineffective or even dangerous without an assistance of experienced fitness instructor. Though very often irregularly exercising and inadequate intensity led to over-training and health related problems. The affordable solution can be the monitoring of hemodynamic during exercise and post exercise recovery period. Recent consumer market proposes a variety of inexpensive personal heart rate monitors; however they register electrical potential difference of myocardium and thus do not provide information regarding hemodynamics. Photoplethysmography (PPG) is a simple and affordable non-invasive optical technique which is very promising for monitoring of the hemodynamics during exercise and post-exercise period. Conventional PPG recording approach requires expensive analogue circuitry, which increases system complexity and cost. There was an attempt to use simplified techniques such as the "pulse duration-based signal conversion technique" which is similar to the well-known single-slope A/D converter technique. The LED-LED technique was first proposed by Stojanovic et al in 2007, and then implemented by others. Although being attractive it provides PPG recording in a relatively small DC range, which is not suitable when registering signal during exercise and post exercise recovery when DC component rapidly changes in large range.

Therefore the present study is addressing two questions- the alternative technique for "pulse-duration-based signal conversion" and improved PPG sensor which is more suitable for signal recording from different parts of the body during an exercise.

The prototype system for integration into smart garment for real time telemetric monitoring of human cardiovascular activity has been developed. The operation principle of device prototype is based on modification of "pulse-duration conversion" principle. Electronic setup consists of PPG sensor (either single PD or multiple PDs), a main electronic circuit, and a Li-polymer battery integrated into the garment. The pulse-duration signal conversion circuit of the sensor is rather simple and resembles well known single-slope A/D converter technique. It consists of two Field Effect Transistors and four resistors. The ceramic capacitor is connected in parallel to the photodiode. Capacitor charging time is constant - 30μs, which is the maximum required to charge such capacitor. Each charging cycle is followed by the discharge cycle and time of each discharge cycle is measured. Using the pulse duration technique, the signal resolution decreases at higher light intensities on the photodiode due to faster discharge of the capacitor, and vice versa.

The developed prototype and two types of PPG reflectance sensors were evaluated both on bench and in vivo conditions, comparing the data to those recorded by reference ECG monitor. Overall, both types of PPG sensors showed acceptable signal quality SNR 86.56+/-3.00 dB, dynamic range 89.84 dB. However, in-vivo condition tests revealed lower noise and higher accuracy for the multiple photodiode in comparison to single photodiode sensor.

There was a high correlation between the heart rate values

obtained by our prototype and referent ECG monitor (r=0.94+/-0.15; p<0.001). We concluded that the proposed PPG device prototype is simple and reliable, and therefore, can be utilized in low-cost smart garments for cardiovascular monitoring during exercise and post exercise recovery period.

9129-95, Session PS2

Clostridium spp. discrimination with an easy to use bead-based fluorescence assay

Barbara Seise, Susanne Pahlow, Sibyll Pollok, Institut für Photonische Technologien e.V. (Germany); Christian Seyboldt, Friedrich-Loeffler-Institut (Germany); Karina Weber, Jürgen Popp, Institut für Photonische Technologien e.V. (Germany)

C. chauvoei is an endogenous bacterial infection and the causative agent of blackleg. Typically cattle and other ruminants are affected. The symptoms of blackleg are very similar to the phenotype malignant oedema caused by an infection with C. septicum. Therefore, a reliable differentiation of C. chauvoei from other Clostridium spp. is required. Traditional microbiological detection methods are time consuming and laborious. When both species are within a clinical sample, the correct specification is hindered by the overgrowing tendency of swarming C. septicum colonies. Thus, an improved and simplified specific detection of C. chauvoei and C. septicum is needed.

In this contribution we present an easy and fast Clostridium spp. discrimination method combining magnetic beads with fluorescence spectroscopy. Functionalized magnetic particles exhibited numerous advantages, like their simple manipulation in combination with huge binding capacity of biomolecules. A specific sequence of the pathogen's DNA is amplified and labelled with biotin by polymerase chain reaction (PCR). These PCR products were used to generate single-stranded capture probe DNA, which were immobilized on magnetic beads via a biotin-streptavidin interaction. A hybridization reaction allows the binding of fluorescence-labelled detection probe to the immobilized single-stranded PCR products. Finally, the successful binding was verified by means of fluorescence spectroscopy.

Acknowledgement

Funding of the research projects "FastDiagnosis" (13N11350), "WK Basis" (03WKCB01H), "JBCI 2.0" (03IPT513Y) and ATLAS (13N9520) by the Federal Ministry of Education and Research (BMBF), Germany, is gratefully acknowledged.

9129-97, Session PS2

Identification of vessel wall anomalies in thoracic aortic aneurysms through optical coherence tomography and gradient-based strategies

Alma Eguizabal, Univ. Paderborn (Germany); Eusebio Real, Univ. de Cantabria (Spain); Alejandro Pontón, Marta Calvo, J. Fernando Val-Bernal, Marta Mayorga, José M. Revuelta, Univ. Hospital Marques de Valdecilla (Spain); José M. López-Higuera, Olga M. Conde, Univ. de Cantabria (Spain)

Optical Coherence Tomography is a natural candidate for imaging biological structures just under tissue surface. Human thoracic aorta from aneurysms reveal elastin disorders and smooth muscle cell alterations when visualizing the media layer of the aortic wall, which is only some tens of microns in depth from surface. Therefore, OCT technology is here presented as a real-time intraoperative diagnostic test and an alternative to traditional histopathology where, in addition, no stains of cuts are needed. A strategy must be defined to automatically acquire a diagnosis from OCT tissue measurements and improve their usability. Thus, the resulting images require a suitable processing to enhance interesting disorder features and use them as indicators for wall degradation, converting OCT into a hallmark for diagnosis of risk of aneurysm under intraoperative conditions. In this work we propose gradient-based digital image processing approaches to achieve this. These techniques are believed to be useful in this applications, as aortic wall disorders directly affect the refractive index of the tissue, having an effect on the gradient of the OCT image. Specimen data set consists in 76 images from 15 different patients from aneurysmatic thoracic aorta and control aorta from donors. After being OCT-measured, a gold standard histopathological analysis is performed to be used later in validation framework: all samples were stained with H&E, EVG, AB and ?-SMA, and the specimens were graded according to a semi quantitative grading scheme that accounts for fibrosis, medionecrosis, cystic medial change, smooth muscle cell orientation and elastic fiber fragmentation. For the OCT image interpretation, the automatic diagnostic study is divided in several steps: pre-processing, segmentation and classification. The segmentation step is the keystone of the analysis and if it is optimized it allows the design of a very simple and fast classification step, and it also permits estimating the dimension of the aortic disorders. OCT measurements reveal that interesting features often occur between adjacent A-scans, so two dimensional segmentation approaches, based on Computer Vision strategies, are then faced. The goal is then to separate images into various regions in which the pixels have similar characteristics. A comparative study of the diagnostic ability of each technique over the OCT aortic images is then presented. Different gradient-based techniques are compared in the study: Sobel operator, Prewitt Compass, Laplacian of Gaussian filter and Canny algorithm. Preliminary results show that the direction of the gradient contains information to estimate the position and size of the tissue abnormalities. Detecting the edges of the OCT image can be done straightaway after thresholding the gradient as, for instance, Canny algorithm performs. Furthermore the threshold-based performance of the edges permits to tune those thresholds in order to make only the desired features to show up, isolating the abnormalities before computing a quantification. Finally the classification step is performed with a leave-one-out validation, using the histopathological results as comparison. Automatic results from gradient-based strategies are finally compared to the histopathological global aortic score, which accounts for each risk factor presence and seriousness.

9129-98, Session PS2

The cultivation independent identification of mycobacteria on a single cell level by Raman microspectroscopy

Anja Silge, Susann Meisel, Petra Rösch, Friedrich-Schiller-Univ. Jena (Germany); Jürgen Popp, Friedrich-Schiller-Univ. Jena (Germany) and Friedrich-Schiller-Univ. Jena (Germany)

The genus Mycobacteria includes a variety of pathogens like the M. tuberculosis complex known to cause serious diseases in humans like tuberculosis and leprosies. But also the incidence of diseases caused by mycobacteria other than tuberculosis (MOTT) increase in the last years [1-2]. It is imperative to separate the former (M. tuberculosis complex) from the later (MOTT), because the treatment and the epidemiology of MOTT- derived infections differs significantly, since the MOTT bacteria are highly resistant against tuberculosis (TB) drugs [1-2]. Present approaches for the correct identification of mycobacterial infections are not optimal for a point-of-care diagnosis. They bases on cultivation methods which are complex and difficult and for some species an appropriate culture technique doesn't exist [1].

Here we present a Raman microspectroscopic characterisation of mycobacteria species on a single cell level. Raman microspectroscopy, which is the combination of Raman spectroscopy with a conventional light microscope, allows investigating single bacterial cells. A preceding culture step is not needed The identification of single bacterial cells requires a reference database, which has to include some variations

because Raman spectra of single bacterial cells, even of the same bacterial strain, differ according to their growth conditions and possible pre-treatments like inactivation [3-6].

The presented results are important to evaluate the combination of Raman microspectroscopy with chemometrical methods for the identification of mycobacterial pathogens in patient samples.

Acknowledgement: We gratefully acknowledge the Free State of Thuringia and the European Union (EFRE) for financial support under support code 2013FE9057 (Fast-TB).

1. Hahn, Helmut. Medizinische Mikrobiologie und Infektiologie. Springer DE, 2009.

2. Leung, Janice M., and Kenneth N. Olivier. "Nontuberculous mycobacteria: the changing epidemiology and treatment challenges in cystic fibrosis." Current opinion in pulmonary medicine (2013).

3. Meisel, Susann, et al. "Identification of meat-associated pathogens via Raman microspectroscopy." Food Microbiology, Volume 38, (2014): 36–43

4. Kloß, Sandra, et al. "Culture independent Raman spectroscopic identification of urinary tract infection pathogens–A proof of principle study." Analytical Chemistry 2013 85 (20), 9610-9616.

5. Stöckel, S., et al. "Raman spectroscopy-compatible inactivation method for pathogenic endospores." Applied and Environmental microbiology 76.9 (2010): 2895-2907.

6. Meisel, Susann, et al. "Raman spectroscopy as a potential tool for detection of Brucella spp. in milk." Applied and Environmental Microbiology 78.16 (2012): 5575-5583.

9129-99, Session PS2

Laser bonding with ICG-infused chitosan patches: preliminary experiences in suine dura mater and vocal folds

Francesca Rossi, Paolo Matteini, Roberto Pini, Istituto di Fisica Applicata Nello Carrara (Italy); Maurizio Iacoangeli, Univ. degli Studi di Ancona (Italy); Luca Giannoni, Damiano Fortuna, Emiliano Di Cicco, Sylwia Corbara, El.En. S.P.A. (Italy); Stefano Dallari, Ospedale A. Murri (Italy)

Laser bonding is a promising minimally invasive approach, emerging as a valid alternative to conventional suturing techniques. It shows widely demonstrated advantages in wound treatment: immediate closuring effect, minimal inflammatory response and scar formation, reduced healing time. This laser based technique can overcome the difficulties in working through narrow surgical corridors (e.g. the modern "key-hole" surgery as well as the endoscopy setting) or in thin tissues that are impossible to treat with staples and/or stitches. We recently proposed the use of chitosan matrices, stained with conventional chromophores, to be used in laser bonding of vascular tissue. In this work we propose the same procedure to perform laser bonding of vocal folds and dura mater repair.

Laser bonding of vocal folds is proposed to avoid the development of adhesions (synechiae), after conventional or CO2 laser surgery. Laser bonding application in neurosurgery is proposed for the treatment of dural defects being the Cerebro Spinal Fluid leaks still a major issue.

Vocal folds and dura mater were harvested from 9-months old porks and used in the experimental sessions within 4 hours after sacrifice.

In vocal folds treatment, an IdocyanineGreen-infused chitosan patch was applied onto the anterior commissure, while the dura mater was previously incised and then bonded. A diode laser emitting at 810 nm, equipped with a 600 μm diameter optical fiber was used to weld the patch onto the tissue, by delivering single laser spots to induce local patch/tissue adhesion. The result is an immediate adhesion of the patch to the tissue.

Standard histology was performed, in order to study the induced photothermal effect at the bonding sites. This preliminary experimental activity shows the advantages of the proposed technique in respect to standard surgery: simplification of the procedure; decreased foreign-body reaction; reduced inflammatory response; reduced operating times and better handling in depth.

9129-100, Session PS2

Nanoplasmonic biosensor for cancer diagnosis: design and fabrication

Yong-Beom Shin, Korea Research Institute of Bioscience and Biotechnology (Korea, Republic of); Na-rae Cho, Univ. of Science & Technology (Korea, Republic of); Ki-Joong Lee, Korea Research Institute of Bioscience and Biotechnology (Korea, Republic of)

The optical biosensors based on the nano-plasmonics, have been considered as one of the promising tools for bio-medical diagnosis and environmental monitoring because of their high sensitivity, label-free detection, small sample volumes, simple instrumentations and real-time detection.

In this study, gold nanoplasmonic biosensors using localized surface plasmon resonance (LSPR) were designed and fabricated for the diagnosis of cancer. We optimized the structures of the metal nanoparticle-array (MNA) via the electro-dynamic calculation. In addition, the nanoimprint lithography was employed for realizing MNA structures, which is a more efficient technique for mass production than nanolithography such as electron beam lithography (EBL) or focused ion beam (FIB) lithography that is a quite intricate, time-consuming and expensive process.

After the UV nanoimprinting process using a film stamp and the removal of residual layer via oxygen plasma etching, metal films were deposited using an electron-beam evaporator, followed by the lift-off step. Consequently, the nanoplasmonic MNA was realized on 5-inch glass wafer and the pitch, diameter and height of MNA were 300nm, 150 nm and 20 nm, respectively. The wavelength of nanoplasmonic resonance peak represented from the MNA sensors was about 750nm.

The capture antibodies of the lung and the pancreas cancer marker, respectively, were immobilized on the surfaces of MNA sensor. Using a compact fiber-optic spectrometer and a reflection optical probe, we were able to confirm the binding of cancer markers with their antibodies due to the immunoreactions between each cancer marker and its corresponding antibody on the sensor surfaces. The amount of the cancer markers in serum were analysed through the observation of nanoplasmonic resonance wavelength-shift on the reflection spectra. To amplify a sensitivity of detection demonstrated by the nanoplasmonic resonance peak shift, we applied enzyme-precipitation reaction on the surface of MNA biosensor. The enzyme-catalyzed precipitation method in the MNA biosensor could be extended to detect other clinical biomarkers at extremely low concentrations in actual clinical samples.

9129-101, Session PS2

Three-dimensional characteristics of alveolar macrophages in vitro observed by dark field microscopy

Dominic Swarat, Fachhochschule Dortmund (Germany); Martin Wiemann, IBE GmbH (Germany); Hans-Gerd Lipinski, Fachhochschule Dortmund (Germany)

Alveolar macrophages (AM) are motile cells inside the lung which engulf particles in vacuoles formed from the outer membrane. To characterize the particle uptake by AM in the context of toxicological in vitro studies, data on dynamic volume and surface parameters of AM are highly desirable. AM protrude numerous fine filopodia and flat lamellipodia and change their overall shape within a few seconds. Volume and surface of unrestrained AM are, therefore, hard to obtain by confocal laser scanning microscopy, which is commonly used

to generate 3D-images of fluorescence labeled cells. Especially in case of AM the fluorescence labeling of fine processes (e.g. with DiO) proved to be is weak and long scan times were not applicable to moving cells.

As an alternative method we imaged AM (NR8383 cell line) using dark field microscopy (DFM). This method delivers contrast rich gray tone or color images not only of the finest fibrillar processes of the vital AM, but also of the enclosed vesicles or engulfed particles. To this aim unstained AM were observed under cell culture-like conditions using a temperature-controlled observation chamber. As an optical system we used a CytoViva dark field condenser, and a 100x oil immersion iris objective (N.A.=1.3, Olympus). Digital images were taken with a CMOS camera (Pixelfly USB) mostly operated at 1920 x 1020 pixel. AM adhering to the substrate were selected for imaging and image z-stacks were taken at 0.5 or 1 μm intervals. Regular z-stacks were obtained by means of a 30DV50 system (Piezojena). Typically, image stacks from a single AM consisted of up to 30 images. All images were pre-processed with a Gaussian filter for denoising and an unsharp mask filter which served for contour enhancement. The 3D reconstruction of AM was then carried out with improved images. The well known “Marching cube” algorithm was applied which allowed to visualize the volume data of a vital macrophage on a stereoscopic screen (Tridelity MV2600va monitor) and volume and surface data from the spatial model of the macrophage was calculated.

First data derived from DFM images showed that the cell volume of an NR8383 cell was 1050 μm3 with a corresponding surface of 1500 μm2. These values are fairly in line with values found for macrophages in the literature.

We conclude that the DFM-based approach may be used as a rapid and versatile method to measure volume and surface data of vital macrophages in vitro.

9129-102, Session PS2

Simultaneous optical manipulation of multiple particles inside microfluidic channels using one rectangular-shaped VCSEL

Rainer Michalzik, Univ. Ulm (Germany); Marwan Bou Sanayeh, Notre Dame Univ., Louaize (Lebanon); Anna Bergmann, Univ. Ulm (Germany)

Optical trapping for isolation and sorting of cells and particles inside microfluidic channels is an efficient non-destructive manipulation technique in the field of biophotonics. The examination of biological samples in microfluidic channel structures with widths below 100 μm enables the drastic reduction of the used sample volume, parallel cycles, and exact timing. Combining microfluidics and optical tweezers is the ultimate tool to efficiently manipulate particles and cells without the usage of extensive equipment.

In recent years, vertical-cavity surface-emitting lasers (VCSELs) have been proven to be excellent light sources for particle manipulation inside microfluidic channels. The small dimension and low power consumption of these devices enable direct integration with the channels. Furthermore, due to their vertical emission, VCSELs can be arranged in two-dimensional arrays, which can be employed for simultaneous optical trapping and movement of several particles. Commercial VCSEL arrays used in optical communication typically have a large device pitch of 250 μm. For miniaturized optical trapping without using external optics, however, these arrays need to be densely packed, with a center-to-center distance in the range of 20 μm and a gap between mesas of only 2 μm. This makes their fabrication process more expensive and more complicated.

We present an innovative optical technique for simultaneous multi-particle manipulation using one rectangular-shaped top-emitting AlGaAs-GaAs VCSEL. The emission wavelength is about 850 nm, which is suitable for usage in biophotonics, as biological materials present very little absorption in the near-infrared spectral range. Unlike circular VCSELs, the laser used in this work has a rectangular 100 μm times 14 μm active aperture area. It has a threshold current of about 20 mA and a roll-over current of about 90 mA, at which a maximum output power of 39 mW is reached. The near-field intensity exhibits a relatively homogeneous distribution along the surface of the laser, whereas the far-field parallel to the long axis of the VCSEL aperture is dominated by two peaks with angles between plus/minus10 degrees with respect to the optical axis. Being oblong, this VCSEL can replace the linear array of circular VCSELs which is usually used to simultaneously trap more than one particle, and it has the advantages of being cheaper and easier to fabricate. The results show the excellent multi-particle trapping ability of this VCSEL, where trapping and sorting of single and multiple polystyrene particles inside PDMS microfluidic channels with widths between 60 and 75 μm were achieved. The particles used have sizes between 1 and 10 μm. Moreover, this VCSEL, like its VCSEL array predecessors, can be integrated directly underneath the microfluidic channel without the need of external optics. Therefore, portable and inexpensive microfluidic chips for biological particle manipulation can be designed.

9129-103, Session PS2

Dynamics and morphometric characterization of hippocampus neurons using digital holographic microscopy

Saeid Elkatlawy, Univ. Miguel Hernandez de Elche (Spain); María Gomariz Clemente, Cristina Soto-Sánchez, Gema Martínez-Navarrete, Eduardo Fernandez, Antonio Fimia-Gil, Univ. Miguel Hernández de Elche (Spain)

Excitable biological specimens, such as neural and muscular tissues, are highly active and dynamic structures. Moreover, their biophysical and morphological attributes are continuously changing and adapting in response to the surrounding environment. Visualization and imaging of biological structures as neural structures and neural networks in cultures can reflect cellular dynamics and morphological changes (Fox & Schott 2004; Langehanenberg et al. 2009). These dynamical changes and their responses can be affiliated with the cellular functions providing us a significant analytical information (Gobel et al. 2007). This information is really useful to study the degenerative origin of neural dysfunctions that arise in neural structures and result in neurodegenerative diseases.

On the other hand, digital holographic microscopy (DHM) has recently attracted much attention in the field of biomedical imaging (Kemper & Von Bally 2008; Kou & Sheppard 2007). DHM is a label-free quantitative phase imaging technique, based on refractive index contrasting (Cuche et al. 1999; Marquet et al. 2005). It works noninvasively and it doesn’t require antibodies’ labeling or photochemical dyeing.

In this paper we report on the use of digital holographic microscopy for 3D real time imaging of neural cells and networks, in vitro. Our study consists in morphological characterization of cellular bodies and neural processes. The average size and thickness of the soma were 21 and 13 ?microns, respectively. Furthermore, the average size and diameter of some randomly selected neural processes were 4.8 and 0.89 ?microns, respectively. In addition, the spatiotemporal growth process of cellular bodies was fitted to by a non-linear behavior of the nerve system. Remarkably, this non-linear process represents the relationship between the growth process of cellular body with respect to the different neural processes of the axon and the dendrites of a nerve cell.

9129-104, Session PS2

Raman spectroscopy and SERS analysis of ovarian tumour derived exosomes (TEXs): a preliminary study

Laura T. Kerr, National Univ. of Ireland, Maynooth (Ireland); Luke

Gubbins, Karolina Weiner Gorzel, Shiva Sharma, Univ. College Dublin School of Medicine and Medical Sciences (Ireland) and Conway Institute (Ireland); Malcolm R. Kell, Department of Surgery, Mater Misericordiae Hospital (Ireland); Amanda Mc Cann, Univ. College Dublin School of Medicine and Medical Sciences (Ireland) and Conway Institute (Ireland); Bryan M. Hennelly, National Univ. of Ireland, Maynooth (Ireland)

Exosomes are tiny microvesicles (40–100 nm in diameter) released into the extracellular environment by different cell types. It is thought that exosomes have a significant role in cell signalling and communication, and are therefore linked with disease progression. [1] A recent study by Tirinato et al. [2] based on analysing exosomes using Surface Enhanced Raman Spectroscopy (SERS) showed that there was a significant difference in the biochemistry of exosomes derived from healthy cells in comparison to those from tumour cells. It has also been shown that cells grown in hypoxia (1% O2 conditions, which mimic the conditions often found within malignant tumours) produce more exosomes in comparison to cells grown in normal oxygen conditions (normoxia). [3]

In this study, we have used Raman micro-spectroscopy and SERS to investigate the biomolecular differences between exosomes isolated from ovarian carcinoma cells (cell line A2780) grown in (i) normoxia, (ii) hypoxia and (iii) from A2780 cells stably expressing the microRNA miR-433. Raman micro-spectroscopy is an optical tool which can be used to analyse the biomolecular composition of biological vesicles. This technique is based on the inelastic scattering of laser light whereby the scattered photons have a different wavelength to the incident photons, which is dependent on the molecular bonds in the sample. By comparing Raman spectra it is possible to detect the molecular differences between each group of exosomes. SERS is a similar method to Raman micro-spectroscopy with the exception that the Raman signal is amplified by the presence of metallic nanoparticles, which allows for an analysis of smaller concentrations of exosomes with shorter acquisition times. SERS however is less reproducible. The overarching goal of this study is to investigate the possibility of using Raman based profiling of exosomes as signatures for specific tumour types.

References:

[1] Carr B, Malloy A, Warren J. Nanoparticle tracking analysis. NTA Review of Applications and Usage, Nanosight. 2013

[2] Tirinato L, Gentile F, Di Mascolo D, Coluccio ML, Das G, Liberale C, et al. SERS analysis on exosomes using super-hydrophobic surfaces. Microelectronic Engineering. 2012;(97):337–340

[3] King HW, Michael MZ, Gleadle JM. Hypoxic enhancement of exosome release by breast cancer cells. BMC Cancer. 2012;12(421)

9129-105, Session PS2

Spectral analysis of tissues from patients with cancer using a portable spectroscopic diagnostic ratiometer unit

Laura A. Sordillo, Yang Pu, Peter P. Sordillo M.D., Yury Budansky, Robert R. Alfano, The City College of New York (United States)

The use of a novel spectroscopic ratiometer device (S3-LED) for the detection of the emission spectra of key native organic biomolecules such as tryptophan, collagen, nicotinamide adenine dinucleotide (NADH) or flavins in tissue is presented. This compact, portable, unit with no moving parts and no external power utilizes a fixed light emitting diode (LED) excitation source and an optical fiber probe to excite the tissue sample. LEDs offer greater lifetimes over conventional lamp light sources. A selection of LEDs is available with wavelengths ranging from 280 nm to 520 nm (ultraviolet to blue-green region). The emission signal is detected using an Ocean Optics spectrometer which includes a linear silicon array detector. The Ocean Optics detector has a wavelength range of 200 nm to 1,100 nm. This S3-LED ratiometer unit was used in the investigation of the spectral fingerprints of paired (normal and malignant) breast samples from breast cancer patients with different cancer histologies. The samples were excited at a selective ultraviolet (UV) wavelength of 280 nm. From a single scan done in seconds, the absorption and emission spectra were displayed and recorded by the S3-LED ratiometer unit, and information on the state of each tissue sample was obtained. Multiple spectral profiles were acquired and used to evaluate the ratios of intensity peaks from biomolecules in each of the samples. Linear Discriminant Analysis (LDA) was applied to separate Principle Component Analysis (PCA) analyzed results into two groups (normal and malignant) in order to highlight the spectral differences between paired malignant and normal breast tissues caused by key fluorophores. In all cases, greater intensity peak ratios from 340 nm over 440 nm and 340 nm over 460 nm were found in the malignant breast sample compared to its paired normal sample. This likely represented increased ratios of tryptophan to NADH in the malignant as compared to the normal samples. This was true regardless of the histologic, hormone receptor or HER-2-Neu receptor status. This difference between the paired malignant and normal breast tissues appeared to be greater in cancers that had more aggressive characteristics, such as very large tumor size or hormone receptor negativity. The S3-LED ratiometer unit may be useful as part of the evaluation for determining the presence of residual cancer after surgery, in locating margins during surgery, or in assessing recurrence and thus making repeat biopsies unnecessary. Investigation into the spectral fingerprints of tissues from patients with breast cancer may lead to better identification of breast cancer sub-types, potentially resulting in more individualized therapies.

9129-106, Session PS2

635nm diode laser biostimulation on cutaneous wounds

Hakan Solmaz, Murat Gülsoy, Yekta Ülgen, Bogaziçi Üniv. (Turkey)

Biostimulation is still a controversial subject in wound healing studies. The effect of laser depends of not only laser parameters applied but also the physiological state of the target tissue. The aim of this project is to investigate the biostimulation effects of 635nm laser irradiation on the healing processes of cutaneous wounds by means of morphological and histological examinations.

3-4 months old male Wistar Albino rats weighing 330 to 350 gr were used throughout this study. Low-level laser therapy was applied through local irradiation of red light on open skin excision wounds of 5mm in diameter prepared via punch biopsy. Each animal had three identical wounds on their right dorsal part, at which two of them were irradiated with continuous diode laser of 635nm in wavelength, 30mW of power output and two different energy densities of 1 J/cm2 and 3 J/cm2. The third wound was kept as control group and had no irradiation. In order to find out the biostimulation consequences during each step of wound healing, which are inflammation, proliferation and remodeling, wound tissues removed at days 3, 7, 10 and 14 following the laser irradiation are morphologically examined and than prepared for histological examination. Fragments of skin including the margin were embedded in paraffin and 6 to 9 um thick sections cut are stained with hematoxylin and eosin.

Histological examinations show that 635nm laser irradiation accelerated the healing process of cutaneous wounds while considering the changes of tissue morphology, inflammatory reaction, proliferation of newly formed fibroblasts and formation and deposition of collagen fibers. The data obtained gives rise to examine the effects of two distinct power densities of low-level laser irradiation and compare both with the non-treatment groups at different stages of healing process.

9129-107, Session PS2

The investigation of hemagglutinating sera color influence on the resolving power of the acousto-optical method for human blood typing

Valeri A. Doubrovski, Maria F. Medvedeva, Stanislav O. Torbin, Saratov State Medical Univ. (Russian Federation)

The present work is devoted to the further development of the previously proposed acousto-optical method for blood typing of human AB0 system. From physical point of view the method is based on ultrasonic action upon RBC agglutination and aggregation for the blood sample investigated by means of turbidimetric method. From the point of view of the life sciences in the paper the cross-method for blood typing is treated: the direct approach (the interaction of blood sample investigated with agglutinating serum), inverse approach (the interaction of blood sample plasma investigated with standard erythrocytes). The aim of this work is the study of the effect of agglutinating serum coloring upon the resolving power of acousto-optical method and, hence, the reliability of sample blood typing. Indeed, the turbidimetric approach for RBC agglutination registration the serum coloring may lead to the significant distortion of the blood typing results.

The spectroscopic studies of four sera system AB0 and also of the blood samples after positive or negative reactions of RBC agglutination using ultrasonic action were carried out in the work. The experiments had shown, that optical densities of anti-A and anti-0 sera are significant and they differently depend on the wavelength of optical radiation in the visible range. Especially the influence of sera coloring upon the resolution of acousto-optical method is more significant for the possitive reactions of agglutination, when due to the sedimentation of agglutinates the clearing of medium under investigated takes place. Besides it changes the relation between the magnitudes of resolving powers for different types of serum.

Blood typing was carried out by cross-method using experimental apparatus where the samples were tested by the light beam which spectrum was in green range, it corresponded to the spectrum of light absorption by hemoglobin. In order to improve the resolution and to reduce its dependence on the type of serum it was proposed and experimentally tested in the apparatus the use of neutral light filters with their preliminary optimization individually for each agglutinating serum used. It was shown, that such a measure made possible to increase the resolving power of the acousto-optical method, to equalize it in respect to different types of serum and, hence, to increase the reliability of blood typing.

The comparison of blood typing results obtained by direct and inverse approaches of the cross-method was carried out for two cases: after adjustment of the testing light energy flux by neutral density filters and without it. It was shown that light flux adjustment by means of filters individually for each type of serum increases the resolving power of acousto-optical method significantly both for the direct and inverse approaches of the cross-method of blood typing, makes it more stable. It reduces the possibility of incorrect interpretation of the results measured in the case of real blood typing. It should be noted that the increase of acoustic-optical method resolution and the use in parallel of both approaches of the diagnostic biomedical cross-method for blood typing are of particularly importance in the cases of weak erythrocytes agglutination, when the mistake in blood typing becomes more possible.

This study may be used to develop the apparatus for instrumental determination of human blood group.

9129-108, Session PS2

Scaling Monte Carlo simulation implemented in CUDA

Fang-Wei Hsu, National Taiwan Univ. (Taiwan)

Diffuse reflectance spectroscopy has been used to detect tissue absorption and scattering properties associated with dysplasia, which may be a precursor for epithelial cancer. Our model includes a fiber bundle probe which consists of a source fiber and several detector fibers, all fibers are perpendicularly or obliquely placed upon the tissue. We use hemoglobin as absorbers and polystyrene microspheres as scatters to make tissue phantoms which help us predict how light propagates in tissue. No matter our spectroscopy system is applied to tissue phantom or real tissue, a corresponding Monte Carlo simulation is essential for analyzing the error between experimental and theoretical value or inversely extracting optical properties.

Monte Carlo simulation is an algorithm that strongly relies on random sampling to obtain the numeric results. Massive computation is inevitable in Monte Carlo simulation if we want the simulation to approach the reality. Typically, we need to simulate about one million photons for normal fiber configuration and about ten million photons for oblique one. The simulation for oblique fiber configuration needs more photons to achieve the same amount of signal intensity as normal fiber configuration because smaller portion of photons are detected by the oblique detection fibers on the surface.

The previously proposed scaling Monte Carlo method can dramatically reduce the simulation time. Briefly, its fundamental concept is to use the results of a single baseline Monte Carlo run for scaling the photon propagation length at each propagation step by the ratio of total interaction coefficients between the baseline tissue model and the tissue of interest, and adjusting the photon exit weight by a factor equal to the albedo of the tissue of interest raised to the exponent N where N is the total number of photon-tissue interactions. In order to obtain a whole spectrum, we have to do Monte Carlo simulations at multiple wavelengths. By scaling, we can only do the Monte Carlo simulation at one specific wavelength and then scale the result to other wavelengths. Furthermore, parallel computing implemented by CUDA is also able to significantly reduce the simulation time. The key idea of CUDA is to distribute each photon in each thread in GPU architecture. Instead of serially processing every photon like a typical Monte Carlo simulation, each thread in GPU architecture is like an independent work unit and in which photon's propagation path is calculated parallelly. If we combine the two approaches, scaling Monte Carlo algorithm and parallel computation by CUDA, it will be a much more efficient way to simulate the propagation path of a large number of photons.

9129-109, Session PS2

Effect of LED light stimulation on sleep latency in night shift people

Jih-Huah Wu, Ming Chuan Univ. (Taiwan); Yang-Chyuan Chang, Hui-Ling Chiu, Min-Sheng Hospital (Taiwan); Wei Fang, Yi-Chia Shan, National Taiwan Univ. (Taiwan); Ming-Jie Chen, Yu-Ting Chang, Ming Chuan University (Taiwan)

Sleep problems are getting worse and worse in modern world. They have a severe impact on psychological and physical health, as well as affect social and academic performance. From our previous study, the brain ? rhythm?? wave and ? wave were affected by radiating the palm of the subject with low-level laser array. In addition, from our other experiment, the LED array also has the similar effect. In this study, a LED array stimulator (6 pcs LEDs, central wavelength 850nm, output power 30mW, operation frequency: 10 Hz) was designed to be the light source. Thus, in this study, LED light was used to radiate the left palm of the subjects, and the effect was assessed with the multiple sleep latency test (MSLT). The "double-blind randomized trial" was used in this study. The result revealed that it doesn't have significant meaning between these two groups. Most of university students always stay up late in Taiwan. Therefore, we do believe night-shift working is an important factor that affects the experimental results. However, from the experimental results, the trend of reduction of MSLT seems happened in the active group. In the future, we will consider this factor and rearrange the experiment.

9129-110, Session PS2

PAMAM modified PpIX generations in experimental photodynamic therapy induce a antitumoral effect on stomach cancer cells

Tugba Kiris, Hasim O. Tabakoglu, Mehmet N. Burgucu, Fatih Univ. (Turkey)

1.Introduction: PDT is a minimally invasive succesfully applied procedure for treatment solid tumors on cancer patient without harmfull effects to compare other traditional methods. PDT consist of three essential components photosensitizer, light and oxygen. A photosensitizer absorbs light which it transfers to moleculer oxygen to create an activated form of oxygen called singlet oxygen(1O2). And photosensitizer can target tumor cells induces apoptosis by distrupting protein structure of the cell membran or rarely necrosis.

Using the photosensitizers which modified with PAMAM is fairly new application. PAMAM which confined in dendrimer structure of the molecule is enable to easily uptake in cells and this way it shows effects.

Some photosensitezers which aren't targeting specific cell groups may can show toxicant effect and can lead to transformed healthy cells to cancer cells. With this aspect dendrimer structures enable advantages and can penetrate in tumor tissue easily.

Aim of the this study; to investigate PAMAM modified porphyrin mediated PDT effects on stomach cancer cells wtih new developed LED based light source.

2.Materials and Methods:Light source is composed of a 12x8 LED array and every well is paired with a LED which is fixed on a perforated plate. LED system is connected to ARDUINO® control card that can be controlled by a computer. LEDs irradiate at 465 nm peak wavelength and have 21 mW optical powers.In order to synthesize polyamidoamine (PAMAM) dendrimer on porphyrin core, carboxylic acid functional porphyrin was reacted with SOCl2 to obtain acyl chloride. Acyl chloride functional porphyrin was dissolved in dichlorometane and mixed slowly with solution of trietilamine and ethilendiamine which was also dissolved in dichlorometane. This mixture was stirred about eight hours at room temperature. Than, excess etilenaiamin and solvent was removed by rotary evaporator. The amine-terminated porphyrin cored PAMAM dendrimers was synthesized divergently by initial Michael addition of methanolic solution of ferrocene amine with excess methyl acrylate (1:10 molar ratio). The reaction mixture was stirred for three days at room temperature. The excess methylacrylate was removed under vacuum at 40–50 °C temperature to afford the ester-functionalized derivative. The reaction mixture was next submitted to the reaction sequence leading to the next generation porphyrin-PAMAM dendrimer, consisting of the exhaustive amidation of the ester functionalized porphyrin-PAMAM dendrimers to ethylenediamine (1:30 molar ratio), followed by Michael addition of the resulting amine with methylacrylate (20 equiv of G0.5). Excess reagents were removed under vacuum at 60–70 °C temperature. Repetition of this two-step procedure ultimately leads to the next generations of porphyrin-PAMAM dendrimer (G1, G2 and G3).

AGS human stomach cancer cells (1 x 104) were seeded in 96-well plate and incubated overnight for cells to settle down. Plates were divided into 2 groups (Control (C) and PDT). Control group was replaced with fresh complete media. PDT group was incubated in dilution ratio of 1:1, 1:10, 1:25, 1:50 and 1:100 to 4 generation of synthesized material (P0,P1, P2, P3) for 24 hour. The next day Control group was kept at dark for 20 minute and PDT group was treated under 465 nm LED for 20 minute with a power density 21 mW.

3.Results : It can be said that:

I- 25 and 50 micromolar are the best density amounts for PDT applications on in vitro AGS stomach cancer cell lines.

II- Increasing the step of amination of molecule lead to cell death and increases the PDT effect. Poly(amido amine) can increase porphyrin uptake in cell more easily.

Future studies with different wavelenghts and different output power light sources which can be modulated will performed on different cancer cell lines.

9129-111, Session PS2

Evaluation of the Doppler component contribution in the total backscattered flux for noninvasive medical spectroscopy

Denis Lapitan, Dmitry A. Rogatkin, MONIKI (Russian Federation)

The widespread introduction of modern optical (laser) noninvasive diagnostic techniques in biology and medicine gave rise interest to theoretical description of light propagation in turbid media. One of the purposes for that is the preliminary simulation of incoming radiation for diagnostic equipment based on the backscattered or transmitted fluxes detection. In particular, for complex diagnostic devices combining the Laser Doppler Flowmetry (LDF), pulse oximetry (PO) and/or tissue reflectance oximetry (TRO) it is necessary to know a ratio of signals in each diagnostic channel. It is necessary for a proper choice of the radiation power for laser sources, sensitivity of photodetectors, dynamic range of the instrument, etc. at a stage of the device projecting. For example, in the LDF the signal from moving scatterers – the red blood cells (RBC) - is the useful signal only, while in TRO and PO both signals from static and moving scatterers are registered. So, the aim of our study was an estimation of the typical ratio between flux with the Doppler shifted signal available for LDF and a total backscattered flux registered in TRO. For this purpose the simple analytical model describing the backscattered radiation for a two-layered biological tissue with different levels of blood volume in that was under consideration. The physical model was based on the improved Kubelka-Munk two-fluxes approach (Biomed. Engineering, 2007, v.41, No.2, P.59-65) to obtain the strict analytical solution available for the detailed analysis. This model involves an additional parameter of the density of scatterers, so it is useful for the Doppler signal intensity calculation as well. In our two-layered tissue model the first layer had no blood vessels and had a finite width (like a stratum corneum or epidermis of the skin), while the second layer was an infinite width tissue filled with blood (like derma). Thus, the backscattered by the tissue radiation was a function of optical properties of both layers as well as of the blood fraction in the second layer. So, the key parameter among all other actual optical and physics properties of layers was the level of blood volume in the second layer. In our study the full spectra of backscattered light for different theoretical levels of blood volume (Vb=0...100%) were simulated in the waveband 370-950 nm. To assess the intensity of the Doppler component in total detected fluxes the single-scattering approximation inside the second tissue's layer was used. The backscattered radiation from the RBC was computed as increase in the total backscattered flux with growth of the density of RBC in the second layer of the tissue. It was found that the fraction of the Doppler component in the total backscattered flux can vary in the range of 1-5% for the normal blood volume of 5-20%. The dependence of the Doppler component contribution in the total backscattered flux on the blood volume of the second layer is quite linear and can have different spectral shapes depending on optical properties of both layers. This work is supported by the RFBR grant No.14-08-31637.

9129-112, Session PS2

A complex noise reduction method for improving visualization of SD-OCT skin biomedical images

Oleg O. Myakinin, Valery P. Zakharov, Ivan A. Bratchenko, Dmitry V. Kornilin, Samara State Aerospace Univ. (Russian Federation);

Alexander G. Khramov, Samara State Aerospace Univ. (Russian Federation) and Image Processing Systems Institute (Russian Federation)

In this paper we consider the original method of solving noise reduction problem for visualization's quality improvement of SD-OCT skin and tumors biomedical images. The principal advantages of OCT are high resolution and possibility of in vivo analysis. We propose a two-step algorithm: 1) process of raw one-dimensional A-scans of SD-OCT and 2) remove a noise from the resulting B(C)-scans. The general mathematical methods of SD-OCT are unstable: if the noise of the CCD is 1.6% of the dynamic range then result distortions are already 25-40% of the dynamic range. We use at the first stage a resampling of A-scans and simple linear filters to reduce the amount of data and remove the noise of the CCD camera. The efficiency, improving productivity and conservation of the axial resolution when using this approach are showed. At the second stage we use an effective algorithms based on Discrete Wavelet Transform and Hilbert-Huang Transform for more accurately noise peaks removal. The effectiveness of the proposed approach for visualization of malignant and benign skin tumors (melanoma, BCC etc.) and a significant improvement of SNR level for different methods of noise reduction are showed. Also in this study we consider a modification of this method depending of a specific hardware and software features of used OCT setup. The basic version does not require any hardware modifications of existing equipment. The effectiveness of proposed method for 3D visualization of tissues can simplify medical diagnosis in oncology. Effective ways to implement a parallel version for high performance systems was considered.

9129-113, Session PS2

A study of human knee articular cartilage by using multiphoton microscopy for potential diagnosis of osteoarthritis

Rajesh Kumar, Norwegian Univ. of Science and Technology (Norway); Kirsten M. Grønhaug, Levanger Hospital (Norway); Elisabeth I. Romijn, Norwegian Univ. of Science and Technology (Norway); Jon O. Drogset?, St. Olavs Hospital (Norway); Magnus B. Lilledahl, Norwegian Univ. of Science and Technology (Norway)

Osteoarthritis is one of the most prevalent joint-bone diseases in the world. Surprisingly, to date, there are neither biomarkers for early diagnosis nor any effective therapies available, other than symptomatic treatment and replacement surgery. It affects cartilage, bone, synovial fluid and associated tissue simultaneously, which makes it complex in diagnosis and treatment. Although the cause of osteoarthritis is not exactly clear but it is believed that the disease process results in degradation of quality of articular cartilage (covering the bone) and other extra-cellular matrix.

We have investigated alterations in the structure of collagen fibers in the cartilage tissue of human knee. Based on the quality of cartilage by visual inspection of experienced surgeons, osteoarthritis is classified into different grades (Grade I to IV). Due to inherent high nonlinear susceptibility, ordered collagen fibers present in the cartilage tissue matrix produces strong second harmonic generation (SHG) signals. Significant morphological differences are found in different grades of cartilage by SHG microscopy. While splitting starts in the superficial layer of cartilage, it continues down to a depth of 200 μm approximately in the form of micro-splitting. Based on the analysis of many locations of tissue, we hypothesize that micro-splitting starts in early stage of osteoarthritis and size of splits increases as we move towards the upper surface of the cartilage. These large size splits joins adjacent lacunae and eventually creating whole fragments which may detach as degradation progresses to higher grade of osteoarthritis. Based on the intensity difference, we also find that a few locations of hyaline cartilage (mainly type II collagen) is being replaced by fibrocartilage (mainly type I cartilage), which is in agreement with earlier literature. Another interesting feature is the appearance of bright peri-cellular lacuna in two-photon excited fluorescence (TPEF) image, probably indicating collagen VI; a potential early biomarker of osteoarthritis.

To quantify the different types of collagen fiber we are incorporating polarization-SHG microscopic analysis, also referred as ?-tensor imaging. The differences in the ?-tensor element can be used as contrast mechanism to distinguish different types of molecules producing SHG. The image analysis of ?-tensor image obtained by excitation polarization measurements would represent different tissue constituents in different colors at pixel level resolution.

9129-114, Session PS2

Gold nanostructures for optical coherence tomography imaging of blood flow

Olga Bibikova, Univ. of Oulu (Finland) and N.G. Chernyshevsky Saratov State Univ. (Russian Federation); Alexey P. Popov, Univ. of Oulu (Finland); Artur Prilepskyi, Institute of Biochemistry and Physiology of Plants and Microorganisms (Russian Federation); Alexander V. Bykov, Matti Kinnunen, Krisztian Kordas, Univ. of Oulu (Finland); Vladimir A. Bogatyrev, Nikolai G. Khlebtsov, Institute of Biochemistry and Physiology of Plants and Microorganisms (Russian Federation) and N.G. Chernyshevsky Saratov State Univ. (Russian Federation); Valery V. Tuchin, N.G. Chernyshevsky Saratov State Univ. (Russian Federation) and Univ. of Oulu (Finland) and Institute of Precision Mechanics and Control (Russian Federation)

Plasmon-resonant gold nanoparticles have attracted particular interest as a novel platform for nanotechnology and medicine because of their unique optical properties, related to the localized plasmon resonance resulting in an enhanced electromagnetic field at the metal nanoparticle surface, low toxicity, convenient surface bioconjugation with molecular probes, stability in solvents and ideal size for delivery within the body. Gold nanostars and nanocomposites, based on nanostars, because of strong absorptions and high electric field intensities at the tips, hold much promise as optical agents for optical coherence tomography (OCT) that allowed distinguishing normal from cancer tissue.

Nanostars were fabricated as described by Yuan et al [1]. The nanostars had an average size of about 60 nm and possessed a number of thin sharp beams. The resulting nanostars after PVP-coating proved to be stable at least for 3 months and allowed multiple centrifugation-redispersion cycles in different media. We used the method of silica coating presented by Khlebtsov et al [2]. A silica shell around a nanostar core is synthesized due to base-catalyzed hydrolysis of tetraethyl orthosilicate (TEOS). The silica shell thickness was about 60 nm and could be simply varied by changing the reaction time and TEOS concentration. Gold nanostars and nanocomposites were applied as contrast agents for visualization of capillaries in tissue-mimicking phantoms (model liquid) and heterogeneous structures (blood vessels) by OCT. In experiments with model liquid nanostars with plasmon resonance maximum at 700-900 nm corresponds to central emission wavelength of the light source (superluminescent diode) of the employed OCT system (Thorlabs, USA). The capillaries were filled in with 4% water solution of Intralipid (in the field of biomedical optics, this liquid is frequently used for the fabrication of tissue phantoms) with or without gold nanostars. For blood experiments we used suspensions of red blood cells with and without gold nanostars, pumped through a glass capillary with fixed velocity. In-depth distribution of the registered intensity and velocity profile was retrieved from measured data and 2D images of the capillary with the suspensions. Nanostructures significantly increase visibility of capillaries and allowed obtain clearer picture of the velocity profile of blood.

1. Yuan, H., Khoury, C. G., Hwang, H., Wilson, Ch. M., Grant, G. A., Vo-Dinh, T., "Gold nanostars: surfactant-free synthesis, 3D modelling, and two-photon photoluminescence imaging" Nanotechnology 23(7):075102 (2012).

2. Khlebtsov, B., Panfilova, E., Khanadeev, V., Bibikova, O., Terentyuk, G., Ivanov , A., Rumyantseva, V., Shilov, I., Ryabova, A., Loshchenov, V., Khlebtsov, N. G., "Nanocomposites containing silica-coated gold–silver nanocages and Yb–2,4-Dimethoxyhematoporphyrin: Multifunctional capability of IR-luminescence detection, photosensitization, and photothermolysis" ACS Nano, 5 (9), 7077–7089 (2011).

9129-115, Session PS2

Dielectrophoresis microjets: A merging of electromagnetics and microfluidics for on-chip technologies

Kyle A. Hill, Christopher M. Collier, Jonathan F. Holzman, UBC Okanagan (Canada)

Microfluidic technologies are of growing importance due to their fluid-handling characteristics. Especially high throughputs and sensitivities have been exhibited with such on-chip microfluidic systems, and this has supported applied technologies, including proteomics, clinical diagnostics, and DNA analyses, to name only a few.

Contemporary microfluidic technologies make use of on-chip continuous flow channels, however, these continuous flow channels are known to suffer from practical issues, such as clogging, which can cause complete chip failure. In response to these challenges, digital microfluidics has been introduced and developed over recent years. Digital microfluidic systems apply electromagnetic characteristics as the fundamental mechanism for fluid actuation. Such electromagnetic systems can be readily implemented in two-dimensional architectures, to overcome many of the practical issues for one-dimensional continuous flow channels, and can be adapted via software for a variety of fluid flow applications.

The fundamental operation mechanism for digital microfluidics relies upon the creation of an electric field distribution, and the use of this distribution for the desired fluid actuation. The electric field distribution would typically be nonuniform, to allow for the creation of a net dielectrophoresis (DEP) force. The magnitude of the DEP force is proportional to the difference between the complex dielectric constant of the microdroplet and the surrounding medium, as well as the gradient of the square of the electric field magnitude, and the sign/direction of the force can be manipulated to bring about a force towards regions of higher electrostatic energy (positive DEP) or lower electrostatic energy (negative DEP). The magnitude and directions of these DEP forces are applied in this investigation for well-controlled and high-speed microdroplet actuation. The control and speed characteristics come about by the use of significant differences in the microdroplet/medium conductivity and the use of a micropin architecture with strong electric field gradients. The implementation, referred to here as a DEP microjet, establishes especially strong axial propulsion forces. It is found that both single-micropin and double-micropin topologies achieve this strong axial propulsion force, but only the double-micropin topology achieves the transverse converging forces needed for stable and controlled microdroplet actuation. The electric fields distributions for each topology are investigated and linked to the axial and transverse forces. Experimental results are presented for both topologies and the double-micropin topology is tested with biological fluids. Microdroplet actuation speeds up to 25 cm/s are achieved—a result which is comparable to the fastest microdroplet speeds to-date.

9129-116, Session PS2

Optoelectrowetting for continuous microdroplet actuation

Christopher M Collier, Kyle A. Hill, Mark A. DeWachter, Alexander M. Huizing, Jonathan F. Holzman, UBC Okanagan (Canada)

Recently, there has been great attention on microfluidics technologies. Conventional laboratory analyses can be performed on these microfluidics lab-on-a-chip devices and this technology offers many practical advantages. The advantages of microfluidics systems include high throughput, increased portability, and low consumption of power. These many benefits are brought about because of the micron device scale and nanolitre/microliter reactant volumes. These microfluidics devices are now used in bioanalyses applications such as DNA analysis, proteomics, and clinical diagnostics.

A subset of microfluidics that has recently emerged is droplet-based microfluidics or digital microfluidics (DMF). Here, microdroplets are manipulated two-dimensionally using electric fields, in contrast to the one-dimensional pressure-based channel flow of continuous microfluidics. The fundamental benefit of DMF systems is that they are offer reconfigurability, whereby a single device can perform many bioanalysis tasks.

A subset of droplet-based DMF systems called optoelectrowetting (OEW) is of particular interest to applications seeking intricate microdroplet routing processes (such as merging or splitting) in an on-chip plane. For a chip employing OEW, the DMF structure is modified so that the electrodes are triggered with arrayed photoconductive switches. The arrayed photoconductive switches are light-activated so that microdroplets in the vicinity are routed into the illuminated switch. Unfortunately, such systems still require intricate electrode arrays, and the resolution of microdroplet actuation is limited by the electrode size.

In this work, we propose a device that makes use of a continuous and planar semiconductor layer as the photoconductive mechanism. An illuminated section of the semiconductor layer acts as a transient electrode, with photogenerated charge-carriers attracting microdroplets in the vicinity. Given this planar topology, the illuminating beam can be used to move the microdroplets continuously with precise control. The ultimate resolution is limited only by the diffusion of charge-carriers. Given this diffusion-dependence, an unusual semiconductor material, based upon Si nanoparticles, is used in this investigation to control the diffusion length. This gives an approximate diffusion length that is on the nanometer-scale of the nanoparticles (being 20 nm in diameter). Our work provides a thorough analysis of diffusion and introduces experimental results showing the device operation. This technology can be beneficial for microfluidic bioanalyses.

9129-118, Session PS2

Common path optical coherence tomography probe in dentistry by using lensed-patch cord and PZT bender

Joo Beom Eom, In Hee Shin, Jae Seok Park, Hyung Joo Paek, Byeong-il Lee, Korea Photonics Technology Institute (Korea, Republic of)

We proposed a practical common path optical coherence tomography probe which uses a LC type fiber patch cord, an anti-reflection coated ball lens for dental optical coherence tomography 2D imaging. By simply placing a ball lens directly in front of a LC type fiber patch cord. The probe has benefits of compactness and disposable lens for patient's hygiene. To achieve a sufficiently ling working distance and good transverse resolution, the proper ball lens diameter and the distance between the ball lens and the fiber patch cord were investigated. With the line scan probe which consists of PZT bender and LC type lensed fiber patch cord, a common path swept source OCT system was implemented and used to demonstrate the feasibility as dedicated probe for dentistry.

9129-119, Session PS2

Closed-loop optical stimulation & recording system with GPU-based real-time spike sorting

Ling Wang, Thoa Nguyen, Katholieke Univ. Leuven (Belgium) and Neuro-Electronics Research Flanders (Belgium); Henrique Cabral, Neuro-Electronics Research Flanders (Belgium) and Radboud Univ. Nijmegen (Netherlands); Barbara U. D. Gysbrechts, Katholieke Univ. Leuven (Belgium) and Neuro-Electronics Research Flanders (Belgium); Francesco P. Battaglia, Radboud Univ. Nijmegen (Netherlands) and Neuro-Electronics Research Flanders (Belgium); Carmen Bartic, Katholieke Univ. Leuven (Belgium) and Neuro-Electronics Research Flanders (Belgium)

Closed-loop brain computer interfaces are rapidly progressing due to their application in fundamental neuroscience and prosthetics implemented. For optogenetic experiments, the integration of optical stimulation and electrophysiological recordings is emerging as an imperative engineering research topic. Optical stimulation does not only bring the advantage of cell-type selectivity, but also provide an alternative solution to the stimulation-induced artifacts, a challenge in electrical stimulation. A closed-loop system must identify the neuronal signals in real-time such that a strategy is selected immediately (within a few milliseconds) for delivering stimulation patterns. Real-time spike sorting poses important challenges especially when a large number of recording channels are involved.

Here we present a prototype allowing simultaneous optical stimulation and electro-physiological recordings in a closed-loop manner. The prototype is implemented with online spike detection and classification capabilities for selected cell-type stimulation. Our experimental setup is comprised of an animal headstage, a LED light source, a purpose-designed data acquisition platform and a workstation armed with a GPU card for signal processing. The headstage connects to the implanted microwires via a Neuralynx electrode interface and an micro-drive. The drive host 8 active tetrodes, each consisted of a twisted bundle of 4 microwires and coupled to a guiding unit with a micro screw, allowing vertical displacement of the tetrode. The total 32 data acquisition channels have an acquisition speed of 12.5 kSps/channel. We interface GPU computation using the ArrayFire Library instead of programming directly through the NVIDIA's CUDA platform. The signal processing sequences including acquisition, detection, classification, and pulse delivery are operated online. The processing accuracy and speed of the integrated software was demonstrated first with recorded data and later with recordings in the awake animals. The LED light is delivered through the optical fiber to trigger neural cells based on the sorting results. Our implementation is fast enough to process at least 8 integrated tetrodes (32 channels) with a controlling frequency of 8 ms. The prototype offers a platform to enhance the study of brain dynamics in optogenetic experiments.

9129-120, Session PS2

Two-step Raman spectroscopy method for tumor diagnosis

Valery P. Zakharov, Ivan A. Bratchenko, Samara State Aerospace Univ. (Russian Federation); Sergey Kozlov, Alexander A. Moryatov, Samara State Medical Univ. (Russian Federation); Oleg O. Myakinin, Dmitry Artemyev, Samara State Aerospace Univ. (Russian Federation)

The problem of noninvasive monitoring of human tissues cancer detection requires innovate diagnosis method with high precision. In current work we used a Raman spectroscopy (RS) method which allowed determine malignant changes in tissue. For Raman spectrums registration thermally stabilized laser was used based on the semiconductor laser module LML-785.0RB-04 (providing lasing power of 100 - 200 mW, wavelength of 785 nm). Diffusely scattered light from the sample was registered by Sharmrock spectrograph. Use of this spectrograph provided a resolution of 0.05 nm at a low noise level. Raman scattering was obtained with a narrow-band filter to cut off fluorescent and Raman contribution of fiber, and broadband filters and dichroic mirror for prevention of excitation laser radiation registration. Biological tissues are characterized by high autofluorescence level with NIR laser radiation interaction. For autofluorescence removal from raw data and pure Raman spectrum acquiring the method of polynomial approximation.

More than 60 human cancer tumors samples were researched by the RS method. Experimental researches were approved by ethical committee of Samara State Medical University. Raman spectra researches of lesions allowed us to formulate the criteria for human tumors type determining. A two-step phase method for skin cancer type diagnosis was developed based on the localization changes in the spectral intensity of Raman bands in the 1300-1340, 1430-1460 and 1640-1680 cm-1. The bands in these regions correspond to the CH3CH2 twisting, wagging vibrations (protein and nucleic acids), to the bending vibration mode CH2 (protein and lipid deformation) and to the amide I vibrations (protein) respectively. At the first step we analysed spectral intensity changes of the Raman bands in 1300-1340 and 1640-1680 cm-1 in relation to the intensity of the 1450 cm-1 in a phase plane. At the second step of the phase method we analysed absolute changes in the intensities of the 1320, 1450, 1660 cm-1 bands of healthy tissue and pathologies in the non-normalized Raman spectra. For classification tumors type at the phase plane we used Linear Discriminant Analysis (LDA), Quadratic Discriminant Analysis (QDA) and Principal Components Analysis (PCA). In current work we used the QDA for obtaining results, which was about 10% more precisely than PCA. Every tumor type was controlled by histological analysis to get the final diagnosis. Proposed two-step phase method allows to reach 88,9% of sensitivity and 87,8% specificity for malignant melanoma (skin cancer); 100% of sensitivity and 81,5% specificity for adenocarcinoma (lung cancer); 90,9% of sensitivity and 77,8% specificity for squamous cell carcinoma (lung cancer).

9129-121, Session PS2

Fluorescence particle detection using microfluidics and planar optoelectronic elements

Siegfried W. Kettlitz, Sebastian Valouch, Uli Lemmer, Karlsruher Institut für Technologie (Germany)

Detection of fluorescent particles is an integral part of flow cytometry for analysis of selectively stained cells. Established flow cytometer designs achieve great sensitivity and throughput but require bulky and expensive components which prohibit mass production of small single-use point-of-care devices. The use of a combination of innovative technologies such as roll-to-roll printed microfluidics with integrated optoelectronic components such as printed organic light emitting diodes and printed organic photodiodes enables tremendous opportunities in cost reduction, miniaturization and new application areas. In order to harvest these benefits, the optical setup requires a redesign to eliminate the need for lenses, dichroic mirrors and lasers.

We propose a thin planar design of the whole microfluidic chip and integrate a high power LED as planar light source and a PIN-photodiode as planar detector [1]. For fluorescence detection, filters are required to separate excitation light from the fluorescence. These filters are implemented by using low-cost plastic foil filters with absorbing dyes. To block out unwanted light and for sharper definition of the detection region a shadow mask on a foil is integrated closely to the microfluidic channel. Since optical considerations advocate a minimized device thickness, the microfluidic channel is molded in very thin PDMS. Mask and optical filter foils are used as supporting substrate thereby eliminating any unnecessary components between the light source and the detection area. The resulting device is thin and bendable. Therefore the whole

production process can be performed by roll-to-roll-machines. The detection setup is powered and data is recorded via a single USB-port thus making it very portable. We characterize the optical performance of the setup for the application as flow cytometer using fluorescence calibration particles.

[1] Kettlitz, S. W et al., Lab on a Chip, 12 (2012), 197-203

9129-122, Session PS2

Improvement of the healing process in superficial skin wounds after treatment with EMOLED

Riccardo Cicchi, Istituto Nazionale di Ottica (Italy); Francesca Rossi, Francesca Tatini, Istituto di Fisica Applicata Nello Carrara (Italy); Stefano Bacci, Gaetano De Siena, Univ. degli Studi di Firenze (Italy); Domenico Alfieri, Light4Tech Firenze S.r.l. (Italy); Roberto Pini, Istituto di Fisica Applicata Nello Carrara (Italy); Francesco S. Pavone, Univ. degli Studi di Firenze (Italy)

In this study, 10 Sprague Dawley rats were mechanically abraded in four regions of their back: two regions were used as a control and the other two were treated with EMOLED. The EMOLED instrument consists of a compact handheld photocoagulation device, useful for inducing coagulation in superficial abrasions. The illumination is provided by a high power blue LED. Blue light is selectively absorbed by haemoglobin and converted into heat through a photothermal effect that was monitored real-time by an infrared thermocamera. Visual observations, histopathological analysis and non-linear microscopic imaging performed after 8 days from the treatment showed no adverse reactions and no thermal damage in both treated areas and surrounding tissues. Moreover, a faster healing process and a better-recovered morphology was evidenced in the treated tissue with respect to the untreated tissue. Compared to the control regions, a reduced inflammatory response, a higher collagen content, and a skin morphology more similar to normal skin were observed in the treated regions. Collagen organization in the two regions was characterized using image pattern analysis algorithms on SHG images, demonstrating a fully recovered aspect of dermis as well as a faster neocollagenesis in the treated regions. This study demonstrates that the selective photothermal effect we used for inducing immediate coagulation in superficial wounds is associated to a minimal inflammatory response, which provides reduced recovery times and improved healing process.

9129-123, Session PS2

Line field off axis swept source OCT utilizing digital refocusing

Daniel Fechtig, Abhishek Kumar, Branislav Grajciar, Amardeep S. G. Singh, Wolfgang Drexler, Rainer A. Leitgeb, Medizinische Univ. Wien (Austria)

OCT is a promising tool for performing fast and cheap noninvasive biopsies. High speed imaging helps to reduce motion artifacts that cause decreased sensitivity and resolution. Using a point scanning configuration one is ultimately limited in sensitivity. Parallel configurations are a potentially attractive solution to further enhance the speed capabilities of future OCT systems, since either more power can be distributed over a large area or the exposure time can be increased without reducing acquisition speed. Even more, if full field configurations are employed one can exploit the intrinsic phase correlation over the field of view for digital wavefront correction techniques. Full field OCT has nevertheless limitations concerning the missing confocal gating. The sensitivity and dynamic range is decreased in the presence of specular reflexes from optical interfaces, furthermore light scattering cross talk between pixel causes additional signal degradation. A good compromise between parallel detection capabilities and confocal gating seems therefore line field swept source OCT. One important advantage of parallel line detection is that mechanical jitter from the remaining single axis scanner affects all parallel channels the same way. Phase jitter can therefore easily corrected by phase referencing to the first tomogram. In comparison to spectrometer based line field OCT, line field swept source OCT provides longer depth range, is free of spectral crosstalk and more flexible in designing the optical detection path.

We built a line field system employing a swept source enabling 2D/3D imaging at up to 100 kA-scans/s with an axial/lateral resolution of 5.6/5.2 ?m and a depth range of 3.53 mm in air. The swept source provides an output power of 20mW centered at 840nm. To prevent specular reflexes reaching the line scan camera, an off axis configuration of the optical path together with spatial filters placed in conjugate planes of the system was used. To the best of our current knowledge, off axis design of the sample arm and detection arm optics is the only way to effectively suppress reflections emanating from lenses, mirrors, filters and other bulk media in parallel OCT systems. A simple phase calibration technique that corrects defocus error was used to achieve uniform lateral resolution in the full imaging range. The technique uses numerical Fresnel wave propagation combined with the geometrical optics information of the system to yield defocus corrected images in a single step. Digital refocusing through the full depth range was shown on a sample target containing FeO particles. The imaging performance and the importance of spatial and spectral phase stability were analyzed in biological samples. Furthermore, we assessed the regime where line field has an advantage over point scanning OCT in terms of sensitivity. As a future perspective we present a novel scanning scheme enabling larger field of view and promising superior phase stability as compared to conventional scanning techniques. Instead of using a single axis galvo scanner, a rotating dove prism integrated into the sample arm is used to scan the object.

9129-124, Session PS2

Non-invasive tissue diagnostics using a multimodal spectroscopic device based on fiber probe

Riccardo Cicchi, Istituto Nazionale di Ottica (Italy); Suresh Anand, Alessandro Sturiale, Univ. degli Studi di Firenze (Italy); Flavio Giordano, Azienda Ospedaliera Univ. Anna Meyer (Italy); Gabriella Nesi, Anna Maria Buccoliero, Francesco Tonelli, Univ. degli Studi di Firenze (Italy); Renzo Guerrini, Azienda Ospedaliera Univ. Anna Meyer (Italy); Francesco S. Pavone, European Lab. for Non-linear Spectroscopy (Italy)

Two different optical fiber probes for combined Raman and fluorescence spectroscopic measurements were designed, developed and used for tissue diagnostics. Two visible laser diodes were used for fluorescence spectroscopy, whereas a laser diode emitting in the NIR was used for Raman spectroscopy. The two probes were based on fiber bundles with a central multimode optical fiber, used for delivering light to the tissue, and 24 surrounding optical fibers for signal collection. Both fluorescence and Raman spectra were acquired using the same detection unit, based on a cooled CCD camera, connected to a spectrograph. The two probes were successfully employed for diagnosing neoplastic, dysplastic, and healthy tissue on ex vivo fresh tissue biopsies of brain and colon. The obtained results demonstrated that the multimodal approach is crucial for improving diagnostic capabilities. In particular, the combination of fluorescence and Raman improves the diagnostic capabilities compared to the results obtained using the two techniques separately. The system presented here can improve diagnostic capabilities on a broad range of tissues and has the potential of being used for endoscopic inspections in the near future.

9129-125, Session PS2

Clinical measurements analysis of multi-spectral photoplethysmograph biosensors

Lasma Asare, Edgars Kviesis-Kipge, Janis Spigulis, Univ. of Latvia (Latvia)

The developed portable multi-spectral photoplethysmograph (MS-PPG) optical biosensor device intended for analysis of peripheral blood volume pulsations at different vascular depths has been clinically proofed. Multi-spectral monitoring was performed by means of a four – wavelengths (454 nm, 519 nm, 632 nm and 888 nm) light emitted diodes and photodiode with multi-channel signal output processing. Two such sensors can be operated in parallel and imposed on the patient's skin. The clinical measurements confirmed ability to detect PPG signals at four wavelengths simultaneously and to record temporal differences in the signal shapes (corresponding to different penetration depths) in normal and pathological skin. This study analyzed rising time difference at systole maximum, wavelengths relations between systole and diastole peak difference at various tissue depths in normal and pathological skin. The difference between parameters of healthy and pathological skin at various skin depths could be explain by oxy- and deoxyhemoglobin dominance at different wavelengths operated in sensor. The proposed methodology and potential clinical applications in dermatology for skin assessment are discussed.

9129-126, Session PS2

Imaging of macrophages incubated with deuterated fatty acids using Raman microscopy

Clara Stiebing, Christian Matthäus, Christoph Krafft, Institut für Photonische Technologien e.V. (Germany) and Friedrich-Schiller-Univ. Jena (Germany); Stefan Lorkowski, Friedrich-Schiller-Univ. Jena (Germany); Jürgen Popp, Institut für Photonische Technologien e.V. (Germany) and Friedrich-Schiller-Univ. Jena (Germany)

During the development of atherosclerotic plaques the uptake and metabolism of lipids by macrophages play an important role. Macrophages derive from monocytes which circulate in the bloodstream and can enter the subendothelial layer of arteries in case of an inflammation. Lipids are taken up by macrophages through receptor mediated processes and get stored in lipid droplets in the cytoplasm. Through the uncontrolled scavenger pathway an elevated lipid concentration in the blood can lead to a high lipid content in the cell. Eventually the cells reach toxic lipid levels and undergo necrosis or apoptosis. The cell content is then deposited within the arterial wall and forms lipid-rich plaque depositions. The blood flow in the arteries can be disturbed or blocked completely by thickening of the wall and rupture of the plaque, leading to myocardial infarction or stroke.

Raman microscopy is a powerful tool, to learn more about cellular lipid droplets in macrophages by combining microscopic information with chemical characterization. Incubated with different fatty acids, Raman images of THP-1 macrophages have been conducted. The cells were incubated with a deuterated fatty acid complexed to serum albumin for certain time points and arrested by chemical fixation. To be able to distinguish between the fatty acid of interest and the cellular lipids, deuterium labels were introduced. To further investigate the formation of lipid droplets, live cell experiments were performed. Over a period of several hours Raman images of the same macrophage were taken. With the help of Raman microscopy, it is possible to see the increase of lipid content in fixed and living macrophages and specify the location of the fatty acid of interest through deuterium labeling.

Acknowledgements:

This work is financially supported by the Carl-Zeiss-Stiftung.

9129-127, Session PS2

Cell morphology studied using an off-axis digital holographic microscope with a quasi-monochromatic partially spatially coherent illumination in transmission

Yana Tarakanchikova, Anton A. Grebenyuk, N.G. Chernyshevsky Saratov State Univ. (Russian Federation); Vladimir Ryabukho, Valery V. Tuchin, N.G. Chernyshevsky Saratov State Univ. (Russian Federation) and Institute of Precision Mechanics and Control (Russian Federation)

Analysis of biological cells in vitro and in vivo using optical microscopy is a widespread technique in medical and biological studies. Digital holographic microscopy provides the ability of quantitative phase imaging and follow up analysis of various biological structures. The phase image carries valuable information for diagnostics of the status of the biological cell. In particular digital holographic microscopy has the ability to study the morphology of red blood cells, which can be specifically altered with the development of hematological diseases and syndromes. Digital holographic microscopy techniques allow for monitoring of individual cells as well as cell populations.

Recently we have proposed an off-axis digital holographic microscopy technique with a quasi-monochromatic partially spatially coherent illumination in transmission mode. In this paper we use this novel digital holographic microscopy technique for dynamic studies of cell morphology. This technique allowed us to provide dynamic phase imaging of cells, including red blood cells, with reduced coherence noise. The phase images characterizing cell morphology have been investigated and analyzed.

9129-128, Session PS2

Measurement of the optical properties of rat brain tissue using contact spatially resolved spectroscopy

Barbara U. D. Gysbrechts, Nghia Nguyen Do Trong, Ling Wang, Katholieke Univ. Leuven (Belgium); Henrique Cabral, Neuro-Electronics Research Flanders (Belgium); Zaneta Navratilova, NERF (Belgium); Francesco P. Battaglia, Donders Ctr. for Neuroscience (Netherlands); Wouter Saeys, Carmen Bartic, Katholieke Univ. Leuven (Belgium)

Local illumination of the brain is used in optogenetics, a popular technology allowing precise optical activation and inhibition of specific cell populations on a millisecond timescale. Understanding photon-tissue interactions is important to estimate light distribution in animal brains under different illumination strategies and wavelengths. In this study, photon propagation in brain tissue in the visible and near infrared spectrum was investigated. A 3D model for multi-layered brain tissue allowing simulation of photon distribution for fibers with different sizes and numerical apertures has been developed. Since the model can predict the volume of perturbed neural activity, it is helpful in the design of new fiber optic probes in optogenetics.

In order to estimate the photon distribution by numerical simulation, knowing optical properties of the brain is crucial. Large variations in the optical absorption and scattering coefficients are presented in literature [Yaroslavsky2002, Heureux2009]. Therefore, we adopted the technique of spatially resolved spectroscopy (SRS) to determine the optical absorption and scattering coefficients of the rat brain in the spectral range between 500 and 1000nm. SRS is a versatile technique with applications ranging from biomedical research to nondestructive evaluation of food quality [NguyenDoTrong2013]. Scattering and absorption coefficients are estimated by simultaneously measuring multiple reflectance Vis/NIR spectra on the brain samples at different distances

from the light source. A purpose-designed optical fiber array for SRS is of small size and non-destructive, suitable for both in vitro and in vivo experiments. In this study, experimental measurements have been performed on rat brains with and without fixative. The estimated optical properties of the brains were compared to find differences. Thereafter, the optical properties obtained by the SRS measurements were used as inputs for the Monte Carlo model to simulate photon distribution in the brain.

Finally, the bioheat equation was solved using a finite element method in order to calculate local temperature rises in the brain due to photon absorption.

References:

Yaroslavsky, A. N., N, Schulze, P. C., Yaroslavsky, I. V, Schober, R., Ulrich, F., & Schwarzmaier, H. J. (2002). Physics in medicine and biology, 47(12), 2059–73.

Heureux, B. L., Gurden, H., & Pain, F. (2009). Optics Express, 17(12), 9477–9490.

Nguyen Do Trong, N., Erkinbaev, C., Nicolaï, B., Saeys, W., Tsuta, M., & De Baerdemaeker, J. (2013). SPIE Proceedings, 8881.

9129-129, Session PS2

Platelet aggregates registration in vitro by digital microscopy method

Valeri A. Doubrovski, Stanislav O. Torbin, Olga E. Tsareva, Saratov State Medical Univ. (Russian Federation); Igor V. Zabenkov, N.G. Chernyshevsky Saratov State Univ. (Russian Federation)

The potentialities of digital microscopy method to register platelet aggregation in vitro are demonstrated experimentally on the example of plasma interaction with inductors ADP and collagen.

Two approaches to prepare the tests were examined: 1) platelets aggregates formation according to the traditional technology, when aggregometers are used for analyzes, 2) the preparation of diagnostic smear, which contains platelets and their aggregates only, no other types of blood cells.

In the first case, the solution of platelets and their aggregates were deposited on the glass and digital images were made.

In contrast to the first case in the second one the platelets and their aggregates were stained by means of standard solution of eozinmetilen blue by Mayu-Grunwald and then they were visualized also.

To increase the contrast in imaging of platelets and their aggregates on the smear different spectral regimes of bioobjects light illumination were selected.

Two approaches to computer processing of digital photo images received were examined.

In the study of unstained specimens the gradient approach to binarize photo images was used followed by the calculation of the metrological characteristics of platelet aggregates.

It was shown, that the staining of platelets and their aggregates permits to apply to the spectral approach for the aims of images binarization followed by its RGB decomposition besides the gradient one.

Both approaches to computer processing of photo images investigated were compared.

The dependence of the number and sizes of PLT aggregates on blood plasma status was analyzed: normal quantity of platelets in plasma, thrombocytosis, thrombocytopenia and the samples of plasma with weak platelets aggregation activity.

The experiment had shown, that digital microscopy method has a high level of sensitivity and wide dynamic range - it is capable to detect as small aggregates which contain few platelets only and those that include hundreds of cells.

The paper shows, that digital microscopy permits directly to define such a metrological parameters of aggregates as their individual mean sizes, aria, occupied by each unit and the sizes distribution of aggregates.

The study may be treated as the base to develop the new types of aggregometers based on the principles of digital microscopy.

9129-130, Session PS2

Time-resolved imaging system for fluorescence-guided surgery with lifetime imaging capability

François Powolny, Claudio E. Bruschini, Ecole Polytechnique Fédérale de Lausanne (Switzerland); Eugene I. Grigoriev, FORIMTECH S.A. (Switzerland); Olivier Michielin, Ctr. Hospitalier Univ. Vaudois (Switzerland); Katja Muehlethaler, Univ. de Lausanne (Switzerland); John O. Prior, Ctr. Hospitalier Univ. Vaudois (Switzerland); Donata Rimoldi, Univ. de Lausanne (Switzerland); Riccardo Sinisi, Elena Dubikovskaya, Ecole Polytechnique Fédérale de Lausanne (Switzerland); Edoardo Charbon, Ecole Polytechnique Fédérale de Lausanne (Switzerland) and Technische Univ. Delft (Netherlands)

We present a novel camera based on digital Single Photon Avalanche Diodes (SPADs) that we are developing for clinical applications in cancer detection and treatment using fluorescent markers. From secondary fluorescence photons, it provides both intensity imaging, which can give physicians anatomical information for localizing cancer tissues, and an image of the marker's photoemission lifetime, which may yield useful molecular information about the presence of metastatic cells.

Indeed, lifetime imaging may offer increased discrimination capability between bound and unbound states of ICG and real-time monitoring of the molecular and chemical environment.

With this camera we show the possibility to determine sub-nanosecond fluorescence mechanisms with a resolution better than 100ps.

As a first step towards the study of biologically relevant samples, the camera was used to characterize in-vitro cultured melanoma cells labeled with indocyanine green (ICG).

It was also used to characterize ICG conjugated with cyclic pentapeptide (RGDfK). This second contrast agent was studied in this work so as to target tumors with better specificity. In particular our objective is to target the integrin alpha-vbeta-3.

The alpha-vbeta-3 integrin is an attractive marker for diagnostic of tumor angiogenesis due to its high expression on activated and proliferating endothelial cells during tumor angiogenesis and metastasis, in contrast to resting endothelial cells and most normal organs.

In-vitro studies were carried out with two cell lines, one expressing the integrin alpha-vbeta-3 at the cell surface (SK-Mel-37 melanoma cells), and one negative for the marker (HEK-293T embryonic kidney cells).

Preliminary results obtained in-vivo should also be available by the time of the conference.

The first envisioned clinical application would be in image-guided surgical oncology to help the surgeon to remove metastatic lymph node and tumoral tissue by a better discrimination from normal tissues.

9129-131, Session PS2

Combination of near infrared (808 nm) laser and selective gold nanorods in antimicrobial action on Staphylococcus aureus

Elena S. Tuchina, Kristina V. Kozina, N.G. Chernyshevsky Saratov State Univ. (Russian Federation); Fulvio Ratto, Istituto di Fisica Applicata Nello Carrara (Italy); Valery V. Tuchin, N.G. Chernyshevsky Saratov State Univ. (Russian Federation)

We investigated action of near infrared laser irradiation on two S. aureus strains (meticillin-sensitive and meticillin-resistance) threated with cojugates of gold nanorods and anti-staphylococcal antibodies. Microbial cells were targeted using suspension of gold nanorods in PEG or conjugated with anti-protein A antibodies (IgG and IgA) in concentration 0.4 mM. For radiaton NIR laser (808 nm, 100 mW/cm2) in the CW mode with exposures 5, 10, 15 and 30 min was used.

It was shown that combination of NIR laser light and gold nanorods with IgG effectively supress growth of bacterial population: after 30 min irradiaton reduction in number of S. aureus colony forming units on 94% was noted.

9129-132, Session PS2

Spectral imaging microscope on acousto-optical filter for biology and medicine

Alexey V. Perchik, Bauman Moscow State Technical Univ. (Russian Federation)

Spectral imaging techniques are widely used in medical and biological research for example in skin cancer diagnostics. In this paper methods and equipment for spectral imaging of micro objects such as cells, their structure and histological samples are discussed.

AOTF based spectral imaging microscope consist of Carl Zeiss Axio Imager m2M microscope, double acousto – optical tunable filter (AOTF), and black and white CCD camera. AOTF with receiver is mounted on microscope instead of standard camera.

Acousto-optical tunable filters are based on crystals, generally tellurium dioxide or quartz, with optical properties that changes in the presence of an acoustic wave (elasto-optical effect).

When an acoustic wave propagates through the crystal it induces regions of compression and relaxation in lattice structure of crystal that causes fluctuations of refractive index. This induced structure plays a role of diffraction grating for incident light, controlled by frequency of sound wave. Changing frequency of RF signal on piezoelectric transducer bonded to acousto-optical crystal allows selection of wavelength of light that passes through filter.

Software development was made using virtual instruments technique by National Instruments in LabView environment with NI Vision module. This technique allows building modular software, which can be rapidly modified for any desirable algorithm, utilizing unique random spectral access property of AOTF.

9129-134, Session PS2

Joint photoplethismography system for early sepsis diagnostics and clinical course monitoring

Andris Grabovskis, Zbignevs Marcinkevics, Uldis Rubins, Univ. of Latvia (Latvia); Sigita Kazune, Hospital of Traumatology and Orthopaedics (Latvia)

According to data from the European Health Organization, the European Society of Critical Care Medicine and the Surviving Sepsis Campaign, incidence of severe sepsis (sepsis-induced organ dysfunction) in the European Union has been estimated at 90.4 cases per 100?'000 population, as opposed to 58 per 100'000 for breast cancer. The documented incidence of sepsis worldwide is 1.8 million cases annually, but this figure reflects low rates of recognition and diagnosis. Recent estimations give an incidence of sepsis requiring intensive care admission of 0.25–0.38 per 1000 population, suggesting about 2 million admissions to intensive care units (ICUs) alone.

Physicians report about an extremely rapid dynamics of septic shock and subsequent organ dysfunction syndrome, while existing bio-array based diagnostic techniques are often delayed and insufficiently effective. Clinical outcome and mortality risk are primary dependent on timely launched treatment. This leads to the necessity for technique for an early and comprehensive diagnostic and disease course stratification. Our previous study confirmed photoplethysmography (PPG) method to be promising in sepsis monitoring. Continuing early studies, within the present study the exploitation of joint PPG approach for sepsis monitoring has been demonstrated using both contact-manner arterial PPG and contact-less PPG skin imaging (PPGI) techniques for the first time.

The aim of present pilot study is to develop and evaluate joint PPG system in order to improve reliability and specificity of sepsis monitoring.

By combining contact manner and imaging technique hemodynamic data (conduit artery PPG waveform parameters and microcirculation perfusion index) from both arterial and microcirculatory vascular beds were obtained, providing the more reliable assessment of sepsis impaired endothelial function.

In order to assess the effectiveness of the proposed methodology and improved experimental protocol, clinical measurements were performed on septic patients (n=10) and control group of healthy volunteers (n=5). Two contact manner PPG probes (880 nm) placed on the skin over brachial and radial arteries, and multispectral PPGI device were focused on forearm. The data acquisition was performed during rest conditions and following post-occlusion test (arterial occlusion on biceps proximal to brachial a. PPG sensor @ 220 mmHg for 5 minutes). During entire joint PPG recording systemic hemodynamic parameters (heart rate, Arterial pressure, SpO2) were acquired invasively from vital sign monitor. Further data processing encompassed the extraction of PPG indexes (sepsis impaired endothelial parameters) and their comparison to the same indexes obtained from healthy volunteers. In addition the relationship between magnitude of indexes and clinical outcome and SOFA score dynamics have been performed.

The present study demonstrates advantages of joint PPG approach over the use of single contact manner PPG in terms of more extensive hemodynamic information, in particularly regarding microcirculatory alterations which are considered to be the early marker of systemic inflammatory response syndrome.

We conclude that joint PPG approach can be promising solution for noninvasive optical sepsis diagnostics and monitoring. However to bring this technology to the healthcare market more extensive further investigation is required.

9129-135, Session PS2

Simultaneous high-resolution morphologic and biochemical optical imaging of atherosclerosis

Javier A. Jo, Paritosh Pande, Jesung Park, Sebina Shrestha, Fred Clubb, Texas A&M Univ. (United States); Brian Walton, The Texas Heart Institute (United States); Brian E. Applegate, Texas A&M Univ. (United States)

Improving the understanding of atherosclerotic plaque development will require in-vivo monitoring of morphological and biochemical changes accompanying plaque formation. Optical Coherence Tomography (OCT) generates high-resolution 3D images of plaque morphology. Endogenous Fluorescence Lifetime Imaging Microscopy (FLIM) characterizes plaque biochemical composition. Both methods rely on intrinsic optical characteristics of the plaque, thus contrast agents are not required. A multimodal OCT/FLIM system has been developed to generate morphological and biochemical maps of the plaque, composed of a high-resolution (7/13 ?m axial/lateral) structural volumetric image superimposed with a luminal biochemical map (100 ?m lateral resolution). Fresh postmortem human coronary segments were imaged. On the basis of the histopathologic evaluation, each section was classified as either intimal thickening (IT, n=11), pathologic intimal thickening (PIT, n=2), collagen-rich PIT having >50% of collagen content (CLG-PIT, n=7), PIT with superficial lipid accumulation (LIP-PIT, n=11), fibroatheroma (FA) with a cap

having >50% of collagen content (CLG-FA, n=3), FA with a lipid-rich cap (LIP-FA, n-2), thin-cap fibroatheroma (TCFA, n=2), calcified FA (CA, n=4), or CA with a collagen-rich cap (CLG-CA, n=4). In addition, the collagen-rich plaques (CLG-PIT, CLG-FA, CLG-CA) were grouped in a high-collagen (HC) category, the lipid-rich plaques (LIP-PIT, LIP-FA, TCFA) were grouped in a high-lipid (HL) category, and the other plaques (IT, PIT, CA) were grouped in a low-collagen/lipid (LCL) category. Following a methodology recently validated by our lab, the endogenous FLIM signal was analyzed to classify the tissue based on its biochemical composition as HC, HL or LCL plaques. The OCT B-scans (cross-sectional images) were reviewed by an interventional cardiologist with clinical experience in the use of intravascular imaging (B.W.). Following standard criteria for intravascular OCT reading, each plaque was classified as IT (showing 2 or 3 well-defined layers), PIT (showing a homogeneous signal-rich region), FA (showing a signal-poor region with diffuse borders corresponding to a necrotic-core or a lipid-pool), or CA (showing a signal-poor region with sharp borders). An FA was considered TCFA if the cap thickness was <100 ?m. To apply an integrated OCT and FLIM plaque evaluation, the FLIM-derived biochemical map was superimposed on the surface of the OCT volumetric image. The classification results were compared with the histopathology evaluation and the overall classification accuracy was computed. All the LCL plaques correctly classified by FLIM were further correctly identified as IT, PIT or CA based on their OCT evaluation. From all the 14 HC plaques correctly identified by FLIM, 12 were further correctly identified as CLG-PIT, CLG-FA or CLG-CA based on their OCT evaluation; however, one CLG-PIT was misclassified as CLG-FA, and one CLG-FA was misclassified as CLG-PIT. From all the 15 HL plaques correctly identified by FLIM, 14 were further correctly identified as LIP-PIT, LIP-FA or TCFA based on their OCT evaluation; however, one LIP-PIT was misclassified as LIP-FA. Overall, 93.5% of the plaques (43/46) were correctly identified using the combined OCT-FLIM evaluation. Based on the success of this study an intravascular OCT/FLIM imaging system is being developed for the in vivo study of mechanisms of atherosclerosis development.

9129-136, Session PS2

Computational modelling of cerebrovascular haemodynamics for non-invasive laser diagnostics of neuronal diseases

Alexey Goltsov, Univ. of Abertay Dundee (United Kingdom); Anastasia Anisimova, Maria Zakharkina, Pirogov Russian National Research Medical Univ. (Russian Federation); Alexander I. Krupatkin M.D., Priorov's Central Institute of Traumatology and Orthopedics (Russian Federation); Victor V. Sidorov, SPE LAZMA Ltd. (Russian Federation); Sergei G. Sokolovski, Edik U. Rafailov, Univ. of Dundee (United Kingdom)

WHO prognoses that the number of stroke events in Europe countries will increase from 1.1 million per year in 2000 to more than 1.5 million per year in 2025. This will create a serious challenge for national health systems bringing to the agenda a development of diagnostic technologies for monitoring of brain haemodynamics in normality and pathology. Recent well-developed magnetic resonance angiography (MRA) allows reliable diagnosis of cerebrovascular diseases. However, the cost of MRA for routine monitoring of cerebrovascular condition is high and requires highly trained personnel only available in hospital. Recent progress on compact laser diodes emitting in wide range of electromagnetic spectrum brought a new opportunity to biomedical engineering, e.g. diagnostics. Here we describe an application of laser Doppler flowmetry (LDF) to pilot research of patient haemodynamic at post-acute ischemic stroke (AIS) conditions. LDF measurements were carried out using LAKK-M device (SPE LAZMA Ltd.) in patients with AIS from left and right over brow skin areas corresponding to branch of the internal carotid (ophthalmicus) arteries showed asymmetry in perfusion levels between "healthy" and stroke-affected hemispheres of 9.5 and 3.9 p.u., respectively, and same myogenic oscillation amplitudes around 0.14 Hz.

3D morphologic and hemodynamic model of cerebrovasculature was developed bringing together the state-of-the-art of electronic human brain atlas projects and LDF data analysis of AIS patients. This voxelized model is used to describe the response of cerebral hemodynamics to vascular lesions observed in MRA. Comparison of LDF signals calculated in the model and measured in patients allows us to calibrate and validate the model. It is proposed to explore the developed model as a supportive tool in non-invasive laser diagnostics and prediction of deferent cerebrovascular diseases.

9129-138, Session PS2

On characterization of human pancreatic tissue using diffuse reflectance spectroscopy: an ex vivo observational study

Paulien L. Stegehuis, Charlotte W. J. Roeloffs, Leiden Univ. Medical Ctr. (Netherlands); Nicola Debernardi, Par Dunias, TNO (Netherlands); Alexander L. Vahrmeijer, Jouke Dijkstra, Leiden Univ. Medical Ctr. (Netherlands)

In this study we use diffuse reflectance spectroscopy to characterize pancreas tissue non-invasively. The diffuse reflectance signal depends on the absorption and the scattering properties of the illuminated tissue. For pancreas cancer, the only cure is complete resection of the tumor. However, currently in up to 79% of pancreatic surgeries positive margins are found. The aim of this study is to test the feasibility of diffuse reflectance spectroscopy to recognize different tissue types found during pancreatic surgery.

Patients that were scheduled for a resection of a lesion in the pancreas were included. After surgery, the excised specimen was assessed by a pathologist who removed pieces of macroscopically appearing normal, tumorous and/or inflamed pancreas tissue, as well as gallbladder and duodenal tissue. Later, this was microscopically confirmed with hematoxylin and eosin stained coupes. Wide band (350nm-1830nm, with 1 nm resolution) spectra were collected using an custom built optical fiber probe with one central receiving fiber tip, surrounded by 7 illuminating fibers. The spectral data was mathematically analyzed using total principal component regression [1].

So far we measured 26 sites from 8 patients, of the 20 patients we plan to include, and we obtained a total of 254 spectra. Unfortunately this is not yet enough data to both make a training and study set. Although further analysis and a bigger sample size are required to get significant results, the obtained results obtained up to now seem promising. After proving the feasibility of characterizing pancreas tissue using diffuse reflectance spectroscopy, the following step will be to test the technique in vivo, during surgery.

[1] Yongxi Tan, Leming Shi, Weida Tong and Charles Wang. Multi-class cancer classification by total principal component regression (TPCR) using microarray gene expression data. Nucleic Acids Research, Vol. 33, Issue 1, pp. 56-65. (2005)

9129-139, Session PS2

Raman spectroscopy for diagnostics of bone implant

Larisa A. Taskina, Valery P. Zakharov, Elena V. Timchenko, Pavel E. Timchenko, Samara State Aerospace Univ. (Russian Federation); Larisa T. Volova, Samara State Medical Univ. (Russian Federation); Arthur G. Leshenko, Samara State Aerospace Univ. (Russian Federation)

The use of allogeneic implants with different extent of demineralization is necessary for an optimization of regenerative processes, such as for replacing bone defects of patients. Furthermore, the control of implant's demineralization

is an important constituent at production and performed using biochemical methods. However, biochemical methods have not widespread due to prolonged time of data processing.

The demineralization extent analysis of implant by Raman spectroscopy was performed. The samples were prepared from a native allogeneic cancellous bone formation. Raman spectroscopy has been implemented by a high-resolution digital spectrometer Shamrock sr-303i with a cooling camera ANDOR DV420A-OE, Raman probe InPhotonics RPB785 and laser module LuxxMaster Raman Boxx of PD-LD's firm. The system was provided a spatial resolution up to 1 mkm; the registration error was +0.2 nm. Moreover, the processing of Raman spectra using «Wolfram Mathematica»'8 was performed.

This review focuses on evaluation for the distribution of organic substance by stretching vibrations ?s (PO), ?s (?O) and amide I. The characteristics (the Raman shift, the ratio of carbonate/phosphate and mineral/organic matrix) of Raman spectra were calculated for not-demineralized, partially demineralized and demineralized allogeneic implants. Thereafter, taking into account of the Raman shift for phosphate-ion was established that the mineral phase of all samples is substituted for B-type carbonate-hydroxyapatite. In additional, the relative content of phosphate was depended on the demineralization extent of bone tissue. The highest value of mineral/organic matrix was characterized for not-demineralized samples. Also, as the demineralization extent was increasing, we were observed the decrease of the phosphate-ions content (and the integrated intensity).

Thus, Raman spectroscopy assists to evaluate the demineralization extent of bone implants in very short time.

9129-140, Session PS2

Fiber-optically integrated cost-effective spectrometer for optical coherence tomography

Christoph Meier, Stefan Remund, Anke Bossen, Berner Fachhochschule Technik und Informatik (Switzerland); Xianfeng Chen, Bangor Univ. (United Kingdom); Ling Wang, Katholieke Univ. Leuven (Belgium); Boris Pova?ay, Berner Fachhochschule Technik und Informatik (Switzerland)

A tilted fiber Bragg grating (TFBG) was integrated as the dispersive element in a high performance biomedical imaging system. Based on the 45° UV-written PS750 TFBG a compact refractive spectrometer with 1.8 radiant/μm dispersion and 0.1 numerical aperture was set up and tested. The spectrum emitted by the 23 mm long active region of the fiber is projected through custom designed optics consisting of a cylindrical lens for vertical beam collimation and successively by an achromatic doublet onto detector array. The spectrometer was calibrated in order to linearize the non-equidistant sampling in k-space resulting in a sensitivity drop of – 3dB/0.4 mm. Two line cameras with different pixel size (8, 14 μm), pixel numbers (3648, 2048) and read out rates up to 70 kHz were deployed for investigation of sensitivity, resolution and measurement range. The optics of the fine adjustable and rigid device was numerically optimized for broadband operation to maximize throughput and minimize chromatic error. Covering 740 nm to 860 nm the device was interfaced to a galvanometric-mirror assembly and an electronic acquisition and control unit. High resolution tomograms of biomedical samples were successfully acquired by the frequency domain OCT-system. For video rate display of tomographic cross-sections the time consuming OCT post processing was performed in real time on a graphic processing unit (GPU).

The dense integration as a compact fiber-optical device, builds on an existing opto-electronic infrastructure and overcomes mechanic limitations of bulk systems. This miniaturization reduces costs and has the potential to further extend the field of application for OCT-systems in biology, medicine and technology.

9129-141, Session PS2

Diffuse reflectance and fluorescence multispectral imaging system for assessment of skin

Inga Saknite, Dainis Jakovels, Janis Spigulis, Univ. of Latvia (Latvia)

The diffuse reflectance multispectral imaging technique has been used for distant mapping of in vivo skin chromophores (hemoglobin and melanin) and oxygenation level. The fluorescence multispectral imaging is not so common for skin applications due to complicity of data acquisition and processing, but could provide additional information about skin fluorophores. Both techniques are compatible, and could be combined into a multimodal solution.

The multispectral imaging system Nuance based on liquid crystal tunable filter was adapted for diffuse reflectance and fluorescence spectral imaging of in vivo skin. Uniform illumination was achieved with LED ring light. Combination of four LEDs (warm white, 770 nm, 830 nm and 890 nm) was used to support diffuse reflectance mode in spectral range 450-950 nm. 405 nm LEDs were used for excitation of skin autofluorescence. Multispectral imaging system was adapted for spectral working range 450-950 nm with scanning step 10 nm and spectral resolution 15 nm. An average field of view was 50x35 mm in size with spatial resolution 0.05 mm (the pixel size). White reflectance was integrated into the field of view, so speeding-up the image acquisition procedure. Due to spectrally different illumination intensity and system sensitivity various exposure times (form 7...500 ms) were used for each image acquisition.

The proposed approach was tested for different skin provocations, for example, arterial occlusion and heat test. Spectral image cubes of different skin lesions (pigmented and vascular) were acquired and analyzed to test its diagnostic potential.

9129-142, Session PS2

Implementation of laser speckle contrast analysis as connection kit for mobile phone for assessment of skin blood flow

Dainis Jakovels, Inga Saknite, Janis Spigulis, Univ. of Latvia (Latvia)

Laser speckle contrast analysis (LASCA) offers a non-contact, full-field, and real-time mapping of capillary blood flow and can be considered as an alternative method to Laser Doppler perfusion imaging. LASCA technique has been implemented in several commercial instruments. However, these systems are still too expensive and bulky to be widely available. Several optical techniques have found new implementations as connection kits for mobile phones thus offering low cost screening devices.

In this work we demonstrate simple implementation of LASCA imaging technique as connection kit for mobile phone for primary low-cost assessment of skin blood flow. Stabilized 650 nm and 532 nm laser diode modules were used for LASCA illumination. Dual wavelength illumination could provide additional information about skin hemoglobin and oxygenation level.

Blood flow maps of injured and provoked skin were demonstrated. The proposed approach was tested for arterial/venous occlusion and heat test.

9129-143, Session PS2

Comparison of image reconstruction methods for structured illumination microscopy

Tomas Lukes, Czech Technical Univ. in Prague (Czech Republic); Guy M. Hagen, Pavel Krízek, Charles Univ. in Prague (Czech Republic); Zdenek Svindrych, Institute of Cellular Biology and Pathology, First Faculty of Medicine, Charles University in Prague (Czech Republic); Karel Fliegel, Milos0 Klíma, Czech Technical Univ. in Prague (Czech Republic)

The resolution of conventional fluorescence microscopy is limited by diffraction. Therefore, its optical resolution is not sufficient for the investigation of subcellular structures. Structured illumination microscopy (SIM) is a recent microscopy technique that enables one to go beyond the diffraction limit using different patterned excitation light. Usually unobservable high frequency information of a sample is shifted inside the region of support of the optical transfer function of a microscope with the help an amplitude-modulated illumination. The high frequency information is encoded through aliasing into the observed image. By acquiring multiple images with different illumination patterns aliased components can be separated and a high-resolution image reconstructed.

There are several methods able to perform this task, but very little has been written about objective comparisons of their performance under various conditions. It is becoming especially important when considering super-resolution microscopy for live cell imaging which has higher requirements on the image reconstruction algorithms. They should be simple to implement, preferably computationally inexpensive and provide good results without disturbing artifacts even for low signal levels. The main contribution of the paper is a performance evaluation of five methods under different noise level conditions, different spatial frequencies of illumination patterns and various number of images used for the reconstruction.

The paper investigates five image processing methods that perform the task of high-resolution image reconstruction, namely the two methods of Neil, et al., (square-law detection and homodyne detection), scaled subtraction, the Gustafsson-Heintzmann method, and Bayesian estimation. Optical sectioning and lateral resolution improvement abilities of these algorithms were tested under various noise level conditions on simulated data and on fluorescent microscopy images of a pollen grain test sample.The microscopy set up is based on an Olympus IX71 equipped with 100 ? /1.4 NA and 60 ? /1.35 NA objectives. We used an Andor Neo sCMOS camera. The desired illumination patterns were produced by a high speed ferroelectric liquid crystal microdisplay (type 3DM, Forth Dimension Displays).In order to compare the performance of the algorithms, the following objective criteria were evaluated: Signal to Noise Ratio (SNR), Signal to Background Ratio (SBR) and Full Width at Half Maximum (FWHM) of sub-diffraction features. The results show that the Gustafsson-Heintzmann method and Bayesian estimation combine illumination patterned images more effectively and provide better lateral resolution in exchange for a more complex image processing. The Gustafson-Heintzmann method requires one to precisely shift the separated spectral components to their proper positions in reciprocal space. High noise levels in the raw data can cause inaccuracies in the shifts of the spectral components which seriously degrade the super-resolved image. Bayesian estimation has proven to be more robust to changes in noise level and illumination pattern frequency.

9129-144, Session PS2

Low power laser and LED irradiation effect on proliferation and differentiation of Wistar rats mesenchymal stem cells

Diana L. Mancera Zapata, Efrain Solarte-Rodriguez, William Criollo, Univ. del Valle (Colombia)

The cell functions could be affected through interaction with photons from a laser source. In the case of stem cells, the application of low-power laser irradiation stimulates cell proliferation and differentiation. The aim of this work is to exploit the effect generated by photons in the cell functions to also to develop strategies allowing cell therapy, contributing to cure diseases like Alzheimer's, Parkinson's, diabetes, permanent neurological lessons among others. The cells obtained from bone marrow of Wistar rats are isolated and characterized for further cultivation. We evaluate the cell proliferation and differentiation induced by low power light irradiation in these cell cultures of mesenchymal cells. Roche® XTT and LDH tests were used to assess proliferation and cytotoxicity. Cellular differentiation was determined by optical microscopy and using specific fluorescent markers. We have found laser cellular proliferation enhancement by 532 and 473 nm laser irradiation, and the best response of the cell culture has been found at a 2 Jcm-2 dose. Although the cultures underwent a three day irradiation protocol they have grown up well and no cytotoxicity was detected. The differentiation and the production of cardiomyocytes were stimulated, promoted and enhanced by low power laser irradiation. The next step is to find out if these light effects on the proliferation and differentiation cellular processes are related to the light coherence, and other sources such as LED's will be used.

9129-145, Session PS2

Active eye-tracking for AOSLO imaging with a tracking SLO

Christy K. Sheehy, Ramkumar Sabesan, Pavan Tiruveedhula, Austin Roorda, Univ. of California, Berkeley (United States)

The human eye is constantly in motion, even during fixation, preventing repeated imaging and stimulation of individual retinal cells. Image-based eye-tracking methods in software have been incorporated in Adaptive Optics Scanning Laser Ophthalmoscopes (AOSLO), but are restricted to tracking amplitudes of roughly 1°. Although this is sufficient for normal trained observers, repeated high-resolution retinal imaging in patients with retinal disease becomes prohibitive in AOSLO since they exhibit significantly larger eye motion, falling beyond the range of current software-based methods. Here, we incorporated a tracking SLO (tSLO) into an AOSLO to achieve active hardware-based eye tracking for real-time image acquisition. Both systems are modular and described in detail previously. For illumination, the AOSLO used 840 nm wavelength and the tSLO used 730 nm wavelength, both of which were optically combined using a dichroic filter. Eye-tracking was achieved via a 2-step process. First, the tSLO used image-based eye tracking methods (previously published) over a 3.5° FOV image and generated two 14-bit voltage outputs that were proportional to the x and y motion of the eye. These actively steered a tip-tilt mirror in the pupil plane of the AOSLO to keep the imaging raster on target. Next, any residual, high spatial resolution eye motion artifacts in the retinal image were corrected in the smaller 1°- 2° FOV high-resolution AOSLO image using the same image-based methods. In this way, the active eye-tracking system allowed the AOSLO to effectively capture high-resolution retinal images over a larger range of motion than previously possible.

9129-146, Session PS2

Development of optical near-infrared spectroscopy instruments for human skin sebum measurement

Mohd Zubir Mat Jafri, Aisyah Ruqayyah Mohd Sabbri, Mastura Mohamad, Univ. Sains Malaysia (Malaysia); Ahmad Fairuz Omar, Univ Sains Malaysia (Malaysia)

There are many techniques and instruments that are currently available to give better results for measuring the quality of human skin. In this study, two non-invasive Near-Infrared

spectroscopy instruments namely NIRQuest spectrometer, ASD FieldSpec® 3 Spectroradiometer) were used to find the correlation between the clinical instruments (DermaLab® USB Sebum Module). Firstly, the experiment was conducted to find the intensities peak of the absorption peak of the oleic as a part of the sebum composition. From the spectra peak of the absorbance, the wavelength will determine. Next step was to measure the reflectance of human skin sebum by using two spectroscopic instruments. The analysis will carry on at the wavelength that have been choose from the previous study and also from the wavelength of the fatty acid to find the best wavelength that contribute in sebum composition. From, the result of the best wavelengths that obtained from this research were at 1208 nm, 1414 nm, 1726 nm and 1758 nm. Lastly, two spectroscopic instruments were compared to determine the best spectroscopic instruments that give the better responds for human skin sebum measurement. The best spectroscopic instrument was ASD FieldSpec® 3 Spectroradiometer because of its specification and detector responds. For future research this non- invasive techniques can be used in dermatology field for the use of various skin analysis. Besides that, the less wavelength used is an advantage for develop instruments with less amount of wavelength sensor. It can reduce the cost of development.

9129-147, Session PS2

Multimodal Raman-fluorescence spectroscopy of formalin fixed samples is able to discriminate brain tumors from dysplastic tissue

Suresh Anand, European Lab. for Non-linear Spectroscopy (Italy); Riccardo Cicchi, Istituto Nazionale di Ottica (Italy) and Univ. degli Studi di Firenze (Italy); Flavio Giordano, Azienda Ospedaliera Univ. Anna Meyer (Italy); Anna Maria Buccoliero, Univ. degli Studi di Firenze (Italy); Francesco S. Pavone, European Lab. for Non-linear Spectroscopy (Italy) and National Institute of Optics (Italy) and Univ. degli Studi di Firenze (Italy)

In the recent years, there has been a considerable surge in the application of spectroscopy for disease diagnosis. Raman and fluorescence spectra provide characteristic spectral profile related to biochemical and morphological changes when tissues progress from normal state towards malignancy. Spectroscopic techniques offer the advantage of being minimally invasive compared to traditional histopathology, real time and quantitative. In biomedical optical diagnostics, freshly excised specimens are preferred for making ex-vivo spectroscopic measurements. With regard to fresh tissues, if the lab is located far away from the clinic it could pose a problem as spectral measurements have to be performed immediately after dissection. Tissue samples are usually placed in a fixative agent such as 4% formaldehyde to preserve the samples before processing them for routine histopathological studies. Fixation prevents the tissues from decomposition by arresting autolysis. In the present study, we intend to investigate the possibility of using formalin fixed samples for discrimination of brain tumours from dysplastic tissue using Raman and fluorescence spectroscopy. Formalin fixed samples were washed with phosphate buffered saline for about 5 minutes in order to remove the effects of formalin during spectroscopic measurements. In case of fluorescence spectroscopy, changes in spectral profile have been observed in the region between 520-650 nm between a representative set of freshly excised and formalin fixed samples. For Raman measurements we did not see any significant change in the spectra but a reduced intensity when compared with freshly excised samples. The outcomes of this study and the discrimination capability between dysplastic and tumour tissues using principal component analysis will be presented further. In conclusion, formalin fixed samples can be potentially used for the spectroscopic discrimination of tumour against dysplastic tissue in brain samples.

9129-148, Session PS2

Characterization of the unique human liver cell line HepaRG by Raman microspectroscopy

Katharina Bräutigam, Thomas W. Bocklitz, Friedrich-Schiller-Univ. Jena (Germany) and Abbe Ctr. of Photonics (Germany) and Institute of Photonic Technology (Germany); Esther Fröhlich, Universitätsklinikum Jena (Germany); Ute Neugebauer, Institut für Photonische Technologien e.V. (Germany) and Universitätsklinikum Jena (Germany); Andreas Kortgen, Alexander Mosig, Universitätsklinikum Jena (Germany); Ferdinand von Eggeling, Institut für Humangenetik (Germany) and Universitätsklinikum Jena (Germany); Michael Bauer, Universitätsklinikum Jena (Germany); Jürgen Popp, Friedrich-Schiller-Univ. Jena (Germany) and Institut für Photonische Technologien e.V. (Germany)

Due to their hepatotoxicity several drugs were withdrawn from the market during the last decades. Thereby, the animal based studies failed as a result of a lack of correlation between the xenobiotic metabolism and hepatic toxicity between humans and animals [1]. In addition, primary human hepatocytes, as the gold standard model for investigations concerning metabolism and toxicity, can only be obtained invasively, require surgical operation of patients, and liver cell lines often lose liver-specific functions as enzyme activities. In contrast, the unique human liver cell line HepaRG, which forms hepatocyte-like as well as biliary epithelial-like cells, is capable to express most of these liver-specific functions, including cytochrome P450, which is involved in most of drug metabolic pathways. Thus, the HepaRG cell line is well suited for toxicity and metabolism studies and much easier to handle than animal based investigations [1].

Furthermore, these cell-drug-interaction assays need sensitive detection methods as an important step towards an understanding on a cellular and subcellular level. Raman spectroscopy is considered as such an innovative method allowing answering a broad range of biomedical questions. In combination with optical microscopy, Raman spectroscopy is characterized by its non-invasive character, its high molecular specificity and the minimal sample preparation. The great potential of Raman imaging to retrieve biochemical information from single cells in combination with a high spatial resolution has been demonstrated within the last years [2-4].

Here, we show the Raman spectroscopic characterization of HepaRG cells as well as several drugs including the determination of their detection limits, e.g. for the antibiotic rifampicin.

Furthermore, investigations of the interaction between HepaRG cells and drugs as well as enzyme activity assays are applied. As advancement matrix-assisted laser desorption/ ionization (MALDI) imaging will be utilized.

[1] A. Guillouzo et al., Chemico-Biological Interactions, 168, 66–73 (2007).

[2] K. Hartmann and M. Becker-Putsche et al., Anal. Bioanal. Chem., 403, 745-753 (2012).

[3] K. Bräutigam and T. Bocklitz et al., ChemPhysChem, 3, 550-553 (2013).

[4] U. Neugebauer et al., J. Biophotonics, 3, 579-587 (2010).

The authors thank the Federal Ministry of Education and Research, Germany (BMBF) for financing (FKZ 01EO1002). K.B. gratefully acknowledged the Carl-Zeiss Stiftung for financial support.

9129-149, Session PS2

Far-field ocular microtremor measurement system

James P. Ryle, National Univ. of Ireland, Maynooth (Ireland); Brian Vohnsen, John T. Sheridan, Univ. College Dublin (Ireland)

Ocular Microtremor (OMT) is the smallest of the three fixational movements described by Adler and Fliegelman in the 1930's. Unlike microsaccades and drift, OMT has a much finer amplitude range between 150 nm and 2500 nm peak-to-peak while the relative frequency content, in terms of physiological signals is much higher with a peak component around 88 Hz for clinically normal human beings. It originates in the oculomotor nuclei in the reticular formation. Owing to the low amplitude of the movement, OMT measurement has to date been mainly achieved using the piezoelectric contact method. Despite being clinically uncomfortable and dampening low frequency motions, this method is sensitive enough to measure displacements on a nanometer scale. In this paper we review the clinical significance of the smallest and least measured, and thus least understood of the three, OMT. Using modern ultrafast digital cameras as well as digital processing techniques, in-plane measurements of fixational human eye movements in both horizontal and vertical directions are obtained. Detailed analysis and examination of the extracted results are presented from our noncontact far-field OMT measurement system. Such camera based methods for far-field measurement of the three involuntary eye movements has not been achieved since the 1950's.

9129-150, Session PS2

Strategy for high recovery of fluorescence from quencher assembled quantum-dot donor

Joong Hyun Kim, Daegu-Gyeongbuk Medical Innovation Foundation (Korea, Republic of); Mihri Ozkan, Univ. of California, Riverside (United States)

Since the target specific controllable signal generation with less background fluorescence resonance energy transfer (FRET) has been widely implanted in developing novel probes for specific and sensitive detection of biological and medically important target substance such as DNA/RNA, protein, enzymes, and so on. The superior optical properties of quantum dots (QDs) such as broad excitation spectrum, narrow and stable emission have allowed the nanoparticles as fluorescent donors. However high signal recovery from QD is main challenge in use of QDs because FRET is only effective in extremely short distance between the donor and accepter molecules. Therefore, in this report, we will discuss our experimental and theoretical investigation of fluorescence energy transfer of quantum dots by considering several parameters such as acceptor's extinction power, number of immobilized acceptors and mechanical principles of the energy transfer and strategy to improve signal recovery by overcoming the size of QDs but sustaining the superior optical properties.

9129-151, Session PS2

Laser-activated nanocomposite biomaterials for biomedical applications

Paolo Matteini, Fulvio Ratto, Rossi Francesca, Francesca Tatini, Roberto Pini, Istituto di Fisica Applicata Nello Carrara (Italy)

Stimuli-responsive biomaterials have attracted much attention for their prospective application in several fields including biomedicine, biotechnology and biosensing. As a rule of thumb a stimuli-responsive system is capable of undergoing conformational and chemical changes on receiving an environmental signal. Here we discuss the exploitation of a light stimulation produced by a laser source to "activate" biomaterials doped with nanosized photothermal enhancers. We will present into more details two laser-activated biomaterials, which we have recently developed and characterized as viable solutions to critical issues in tissue repair and drug delivery applications.

Laser-assisted tissue repair or laser welding has been proposed to close chronic, accidental and surgical wounds. Typically, laser light is delivered 1) to a wound site to be repaired which has been stained with an exogenous optical absorber or 2) to a photoresponsive medical dressing (e.g. patches, stents, etc) placed in intimate contact with the tissue to be repaired, in order to produce a photothermal effect. The endogenous tissue or the externally applied dressing respond to the thermal stimulus producing different chemostructural modifications such as denaturation and fusion, which can mediate the repair of the wound. We have recently engineered an hybrid bioadhesive consisting in a chitosan film doped with gold nanorods (GNRs) that can be activated by NIR laser light [1]. These films (0.8 cm diameter, 40 ?m thickness) are insoluble, flexible, resistant and stable in a physiological environment. Upon laser irradiation a well-localized photothermal effect can thus be produced in the film, which is in turn stimulated to produce adhesion with a proximal tissue surface (e.g. arterial wall, tendon, lens capsule).

Capitalizing on this previous experience, we have succeeded in fabricating an implantable device for on demand chemical release in the form of a light-activated sponge-like nanocomposite scaffold [2]. The sponge (0.8 cm diameter, 300 ?m thickness) consists of a porous chitosan scaffold containing a dispersion of GNRs, which acts as an absorber of the incoming laser light, and of thermosensitive polymeric micelles, which serve as a reservoir for the drug molecules to be released. The photothermal response of the nanoparticles contained inside the sponge triggers a contraction in proximal micelles, thus promoting the expulsion of the drug that in turn is released from the sponge to the external environment. The peculiar physiochemical and structural properties of the nanocomposite sponges impart a number of interesting features to this drug release system, including the possibility of spatially confining the therapeutic treatment as well as of precise control of the amount of released drug as a function of duration and power of the excitation light.

[1] Matteini P, Ratto F, Rossi F, Centi S, Dei L, Pini R. 'Chitosan films doped with gold nanorods as laser-activatable hybrid bioadhesives'. Adv Mater 22 4313-4316 (2010)

[2] Matteini P, Tatini F, Luconi L, Ratto F, Rossi F, Giambastiani G, Pini R 'Photothermally activated hybrid films for quantitative confined release' Angew Chem Int Ed 52 5956-5960 (2013)

9129-152, Session PS2

Multimodal label-free in vitro toxicity testing with digital holographic microscopy

Christina E. Rommel, Christian Dierker, Westfälische Wilhelms-Univ. Münster (Germany); Angelika Vollmer, Steffi Ketelhut, Björn Kemper, Univ. Münster (Germany); Juergen Schnekenburger, Westfälische Wilhelms-Univ. Münster (Germany)

Common in vitro toxicity tests of drugs, chemicals or nanomaterials involves the measurement of cellular endpoints like stress response, cell viability, proliferation or cell death. The assay systems determine enzyme activity or protein expression by optical read out of enzyme substrates or marker protein labeling. These standard procedures have several disadvantages. Cellular processes have to be stopped at a distinct time point for the read out, where usually only parts of the cells were affected by the treatment. Only one parameter is analyzed and detection of cellular processes requires several time consuming incubations and washing steps.

Here we have applied digital holographic microscopy (DHM) for a multimodal label-free analysis of drug toxicity. NIH 3T3 cells were incubated with 1 µM Taxol for 24 h. The recorded quantitative phase images were analyzed for cellular refraction index, cell thickness, cell volume, dry mass and cell migration. Taxol treated cells showed rapidly decreasing cell motility as measure of cell viability. A short increase in cell thickness and dry mass indicated cell division and growth in control cells, whereas Taxol treatment resulted in a continuous increase in cell height followed by a rapid decrease and a decrease of dry mass as indicators of cell death.

Multimodal DHM analysis of drug treatment by multiple parameters allows direct and label-free detection of several toxicity parameters in parallel. DHM can quantify cellular reactions minimally invasive over a long time period and analyze kinetics of delayed cellular responses. Our results demonstrate digital holographic microscopy as a valuable tool for multimodal toxicity testing.

9129-153, Session PS2

Metal capped polystyrene nanotubes arrays as super-hydrophobic substrates for SERS applications

Pierre P. Lovera, Niamh Creedon, Hanan Alatawi, Alan O'Riordan, Tyndall National Institute (Ireland)

We present a low-cost and rapid fabrication and characterisations of polymer nanotubes based substrates inspired by a Gecko's foot, and demonstrate its suitability for Surface Enhanced Raman Scattering (SERS) applications. Substrates are fabricated in a simple, scalable and cost efficient way by melt wetting of polystyrene (PS) in an anodised alumina (AAO) template, followed by silver evaporation. Scanning electron microscopy reveals the substrates are composed of a dense array of free-standing polystyrene nanotubes topped by silver nanocaps. The gaps (electromagnetic hot spots) between adjacent nanotubes are measured to be 30nm +/-15nm. SERS characterisation of the substrates, employing a monolayer of 4-aminothiophenol (4-ABT) as a model molecule, exhibits an enhancement factor of ~1.6 ? 106. This value is consistent with the one obtained from 3D-Finite Difference Time Domain (3D-FDTD) simulations of a simplified version of the sample. The contact angle of the substrates is measured to be 150˚, making them super-hydrophobic. This later property renders the samples compatible to very low sample volumes and highly sensitive detection (down to 408ppt) of the environmental pollutant crystal violet in water is demonstrated.

9129-154, Session PS2

Nonlinear optical properties of GFP-like proteins

Louis Vanpraet, Evelien De Meulenaere, Peter Dedecker, Johan Hofkens, Koen Clays, Katholieke Univ. Leuven (Belgium)

We have determined the first-order hyperpolarizability of GFP-like proteins using Hyper-Rayleigh Scattering (HRS) in order to establish a baseline for optimization for use in nonlinear optical microscopy.

Second Harmonic Imaging Microscopy (SHIM) is used to visualize non-centrosymmetrical biological structures in cells and membrane-related events, like the visualization of membrane potentials, using exogenous dyes. Moreover, it allows simultaneous measurement of the Two-Photon Excited Fluorescence (TPEF) signal, adding orientation information to the localization data obtained from TPEF. Despite numerous exogenous probes under developed, only few reports can be found on successful endogenous labeling systems for SHIM, both expressed by the cell as free proteins and fusion proteins. The use of fluorescent proteins in biological samples is superior to the use of exogenous labels in terms of specificity, invasiveness and toxicity of the labeling method on live samples.

GFP-like proteins have become a well-established tool for genetic labeling of living organisms, e.g., for protein localization and research into enzymatic pathways. They also have a proven track record as a labeling tool in TPEF microscopy. Over the years numerous variants has been developed, spanning the whole visual range and catered to specific functional needs, while maintaining a uniform overall structure. This, coupled to the relative ease at which they can be expressed in both prokaryotic and eukaryotic systems has resulted in a very versatile labeling platform.

In the determination of the first-order hyperpolarizability of a whole range of these proteins in correlation to their structural and spectral characteristics, we can determine what influences the first-order hyperpolarizability, and perhaps more importantly, to what degree. Moreover, suitable candidates for optimization, produced either by (semi-) random mutagenesis or through rational design, can be identified which can be developed in to endogenous SHIM, or hybrid SHIM/TPEF probes.

9129-155, Session PS2

Obesity in Mice and Low Laser Stimulated Wound Healing Study

Andrea A. Calmon N Gama, IPEN Nuclear Energy Research Institute (Brazil); Silvia Nunes, Martha S. Ribeiro, Instituto de Pesquisas Energéticas e Nucleares (Brazil)

Several articles can be found in the literature indicating the use of low level laser therapy (LLLT) to accelerate scarring. These studies showed satisfying results, allowing the introduction of variants in test subjects. Meanwhile, for the correct application of light parameters, some variables must be taken into account in order to understand how laser radiation at lower power levels acts in these processes, it is necessary to understand the normal structure of the tissues involved in the injury and the stages involved in its mending, keeping in mind that the final result must be a completely mended wound. When an organism is hit by obesity, the metabolism changes and studies show that there is a greater incidence of complications in tissue regeneration. Our objective is to investigate this mending process in surgical wounds made in the tissue of obese female mice and eutrophics, introducing body mass as a variable for the correct use of LLLT. To the best of our knowledge there are no studies in the literature that report obesity as being a relevant factor for the establishment of a different dosage scale. We used 40 female Balb/c type mice from IPEN's bioterium that where severed from breast feeding at the same time, 20 were feed with a specific ration in order to reach obesity and the other 20 received a normal ration. After a period of 6 months, during which we kept track of weight, glycemia and C-reactive protein levels, an evaluation by optical coherence tomography consolidated the diagnose of obesity (group 1),The second group was eutrophics animals. cut was performed on the skin of each animal in the dorsal region in a U shape, and 1.2mm of depth. The animals from the first group received irradiation from an infra-red laser (?=780nm) for a total of 1,2J/cm? of energy density, applied in 6 points around the wound. The final evaluation was done through images and measured by (Image J) and after the animals were euthanized, after shape her the tissue was studied through hystomorfométric analysis. To evaluate infiltration of lymphocytes over adypocytes and collagen fiber orientation. We concluded that the model of obesity was successfully developed after ingestion of the offered diet. The C-reactive protein, in accordance with the literature, as a stage for inflammatory disease. When analyzing the standard glycemics of the sample we noticed that the obese and eutrophic animals had the same glycemic trend, without showing signs of diabetes. The difference presented by the use of laser at the applied parameters between the obese and eutrophic groups demonstrates that the interaction between light and obese animal tissue is different and that with the applied parameters we obtained results that confirmed this fact.

9129-156, Session PS2

Nonlinear optical microscopic and spectroscopic changes in 7,12-Dimethylbenz-alpha-anthracene induced carcinogenesis in murine skin

Giju Thomas, Erasmus MC (Netherlands); Johan van Voskuilen, Hoa H. Truong, Hans C. Gerritsen, Utrecht Univ. (Netherlands);

Henricus J. C. M. Sterenborg, Erasmus MC (Netherlands)

Nonlinear optical imaging has immense potential in biomedical diagnostics due to its advantages like deeper tissue penetration and minimal photo bleaching. Among the various applications of non-linear optical imaging, its utility is the most significant in the field of cancer diagnostics. Nevertheless it would be interesting to see if the first signs of cellular transformation during carcinogenesis could be detected using nonlinear optical microscopy as compared to conventional histopathology. This could be useful in predicting the onset and progress of carcinogenesis, especially skin cancer.

In this study, 16 hairless female mice were treated topically with 7, 12-dimethylbenz-alpha-anthracene (DMBA) once every week. For comparison, additional two control groups of 16 mice each were added. While the first control group comprised of untreated mice, the second control group consisted of mice treated with acetone once every week. These mice were followed through till 25 weeks from the first application of DMBA or acetone. At specified intervals of week 4, 8, 11, 14, 17, 20, 22 and 25, these mice were anaesthetized and assessed by in vivo nonlinear optical imaging using a femto-second pulsed laser. The imaging was performed at the wavelength of 765 nm and an average laser power of 15 mW. The mice were imaged on at least two separate regions. At each region, the imaging regime involved a stack of 20 consecutive scans at depth intervals of 3 micrometer in the XY dimension and a single scan in the XZ dimension. Post imaging, the mice were euthanized and skin punch biopsies were obtained from the imaged region. These biopsies were later subject to histological evaluation after Haematoxylin and Eosin staining. Based on the histological observation, the skin specimens were broadly categorised into the following categories – (i) Normal (ii) Hyperplastic (iii) Benign Papillomas (iv) Carcinoma in situ and (v) Malignant squamous cell carcinoma. Following this, the nonlinear optical microscopic findings of the corresponding specimens were assessed. Upon analysis, it was seen that in untreated and acetone treated mice skin, autofluorescence pertaining to epidermal components was present upto a depth of 15-18 micrometer, following which second harmonic generation of collagen from dermis begins to appear at subsequent deeper scans. In contrast, autofluorescence from epidermal components in DMBA treated mice skin was present even upto depth of 35-40 micrometer. In addition, the emission spectral data recorded from various fluorophores present in murine skin – keratin, NADH, FAD, elastin and collagen – were evaluated and compared for the respective specimens. The results suggest that nonlinear optical imaging is indeed a useful tool to aid in diagnostic pathology.

9129-48, Session 9

Porphyrin involvement in redshift fluorescence in dentin decay *(Invited Paper)*

Amel Slimani, Ivan Panayotov, Bernard Levallois, Univ. Montpellier 1 (France); Thierry Cloitre, Univ. Montpellier 2 (France); Nicole Bec, Christian Larroque, Institut de Recherche en Cancérologie de Montpellier (France); Csilla Gergely, Univ. Montpellier 2 (France); Herve Tassery, Frédéric J. G. Cuisinier, Univ. Montpellier 1 (France)

The aim of this study is to understand the porphyrin involvement in the red fluorescence observed in dental decay with SoproLife® and VistaCam® intraoral cameras.

Methods: Ex vivo fluorescence spectral characteristics of 9 teeth cross sections, ranked according to ICDAS classification, were examined by an epi-fluorescence microscope (Nikon Eclipse TE2000, spectrometer Acton SP215i-CCD PIXI400B) with an excitation wavelength range of 380-450 nm and the same experiments were applied to Protopophyrin IX, Porphyrin I and Pentosidine solutions. Micro-Raman spectra of the dentin samples were measured with LabRAM ARAMIS IR2 confocal micro-Raman spectrometer and Matrix-assisted laser desorption/ionization time-of- flight imaging mass spectrometry (MALDI-TOF IMS) was also experimented. Excitation wavelength of SoproLife® was 450nm and VistaCam® was 405nm respectively. Pictures of dentin decay according the ICDAS classification were taken and analyzed in the RGB color model with ImageJ Software.

Results: Enamel fluorescence spectra had lower relative intensities than dentin fluorescence and show significant porphyrins-like peaks between 580-750nm. VistaCam® fluorescence images overlayed a number of samples fluorescence pattern but signals varied according to the sample working distance, background color and picture focus. SoproLife® fluorescence images correlated also with the fluorescence results and seemed to be sensitive to Maillard reaction (Pentosidine). Raman spectra revealed a high autofluorescence level and a very low relative intensities ratio of Porphyrin I and Protoporphyrin IX except for one specific sample (ICDAS score 6) that gives an explicit Protoporphyrin IX spectrum. A spatial distribution of porphyrins (Protoporphyrin IX, Porphyrin I) and AGEs (Pentosidine) in teeth cross-section was revealed for the first time thanks to the mass spectroscopy experimentation. The highest signal was observed with Protoporphyrin IX (ICDAS 5) and on the contrary no Protoporphyrin, Porphyrin and Pentosidine signals were detectable in sound dentin.

Conclusions: Understanding the specific role of porphyrins and Maillars reaction in the caries process brings additional elements to this complex biological reaction. These new biological approaches of the dentin decay introduce new concepts in restorative dentistry and specially in minimally invasive dentistry and could totally change the clinical paradigm of dentin decay. Further work is ongoing to establish the biochemical characteristics of porphyrins and derivates involved in the dental caries process.

9129-49, Session 9

Fluorescence image guided oncologic surgery using a wearable goggle based imaging system

Suman B. Mondal, Shengkui Gao, Washington Univ. in St. Louis (United States); Nan Zhu, College of Optical Sciences, The Univ. of Arizona (United States); Gail P. Sudlow, Walter J. Akers, Washington Univ. School of Medicine in St. Louis (United States); Rongguang Liang, College of Optical Sciences, The Univ. of Arizona (United States); Viktor Gruev, Washington Univ. in St. Louis (United States); Samuel Achilefu, Washington Univ. School of Medicine in St. Louis (United States)

Cancer surgery is often the only curative option available for most solid tumors. However, cancer surgery often suffers from positive margin resection, which implies incomplete removal of tumor tissue. This increases the risk of cancer recurrence for the patient and often requires repeat surgery. The issue of positive margin resections stems from the difficulty in identifying the exact tumor boundary during surgery. Preoperative diagnostic images are not adequate in guiding intraoperative detection of exact tumor boundaries. Therefore there is a need for intraoperative image guidance which can allow the surgeon to interrogate the tumor boundaries. Towards this goal we have developed a wearable, goggle based imaging system which can intraoperatively image tumors and provide fluorescence image guidance during cancer surgery. Our system can detect fluorescence from near infra-red (NIR) contrast agent that selectively accumulates in tumors. This information is displayed directly to the head mounted display worn by the surgeon, without hindering the normal surgical workflow. This facilitates intraoperative visualization of tumor boundaries and tumor nodes which may not be apparent otherwise to the surgeon. Based on this intraoperative guidance the surgeon can decide surgical margins which may allow complete tumor removal while conserving healthy tissue. Our system can potentially improve outcomes in oncologic surgery and reduce the chances of cancer recurrence.

9129-50, Session 9

Handheld multispectral fluorescence lifetime imaging system for in vivo applications

Javier A. Jo, Shuna Cheng, Rodrigo Cuenca, Bilal H. Malik, Joey Jabbour, Kristen C. Maitland, Texas A&M Univ. (United States)

There is an increasing interest in the application of multispectral fluorescence lifetime imaging (FLIM) for medical diagnosis. Central to the clinical translation of FLIM technology is the development of compact and high-speed clinically compatible systems. We present a novel multispectral FLIM handheld rigid endoscope based on the point scanning direct pulse recording implementation. The system consists of a handheld box (volume: 7?13?5 cm3, mass: 450 g) fitted with a custom-designed rigid endoscope (length: 14 cm, diameter: 1.7 cm). A frequency-tripled Q-switched Nd:YAG laser (355 nm, 1 ns pulse width, 100 kHz max. rep. rate) is used as the excitation source. A multimode fiber with core diameter of 25μm or 50 μm delivers the excitation light to the handheld box. Inside the handheld box, the excitation light is collimated and scanned by a pair of galvo mirrors on the proximal end of the rigid endoscope. The rigid endoscope was built using standard 0.5'' lens tubes and consists of three lenses. The first two lenses (L3, L4: f = 25 mm) work as a relay, while the third lens (L4: Near UV achromat doublet; f = 30 mm, 50 mm or 60 mm) works as the objective. In this configuration, the excitation fiber core diameter and the objective lens focal length determine the lateral resolution and the field of view (FOV) of the system. The range for lateral resolution and maximum FOV were tested to be ~35 ?m to 140 ?m and ~6.5 mm to 13 mm, respectively. The time-resolved fluorescence emission is spectrally divided in three emission bands and multiplexed in time following a strategy previously reported. Thus, for a single excitation pulse, multiple decays corresponding to different spectral bands can be recorded using a single detector. The multispectral fluorescence signal is detected by an MCP-PMT and digitized at 6.25 GS/s. In addition, to demonstrate real-time estimation and visualization of the multispectral FLIM maps, an online deconvolution method was applied, in which the recorded time-resolved decay for each pixel was compared against a lookup table of pulses generated by convolving the instrument response with single exponential decays. For all the validation experiments performed, the following working parameters were used. The laser pulse energy at the sample was set at ~1 μJ/pulse, resulting in sufficient signal-to-noise ratio (SNR ≥ 30 dB). Since only one pulse is required per pixel, the pixel rate equates to the laser repetition rate. The laser repetition rate was set at 30 kHz and the total number of pixels per frame was set at 150?150, corresponding to an acquisition speed of ~1.3 Hz. The 50 μm excitation fiber and the 50 mm focal objective lens were used, corresponding to a lateral resolution of ~110 μm and a FOV od ~11 mm. The system was validated by imaging in vivo both the hamster cheek pouch and the oral mucosa of a human volunteer, using safe and permissible exposure levels. Such a design can greatly facilitate the evaluation of FLIM for in vivo oral cancer imaging.

9129-51, Session 9

Collagen organization in perilesional skin dermis of melanocytic lesions studied by combined SHG and FLIM microscopy

Riccardo Cicchi, Istituto Nazionale di Ottica (Italy); Cristina Giubani, Vincenza Maio, Daniela Massi, Francesco S. Pavone, Univ. degli Studi di Firenze (Italy)

SHG microscopy an ideal tool for imaging collagen and probing its organization at various scale levels. In particular, SHG microscopy is able to highlight morphologic changes in collagen structure, which indicate particular disease states, such as tumor invasiveness, as well as indicators of collagen remodeling in tumor stroma, which is playing a key-role in the tumor development from in-situ to invasive stage. Although its capabilities for collagen imaging have been already largely demonstrated, SHG is not the only microscopic technique able to probe collagen organization. In fact, the cross-linking of collagen fibrils into fibers affects not only SHG emission pattern but also the fluorescence lifetime of collagen, making FLIM a potential imaging tool for probing collagen organization. In this study, we used SHG and FLIM microscopy, in a combined-correlative approach, aimed at characterizing collagen organization in the perilesional dermis of melanocytic lesions of different grades. Thin ex vivo tissue slices with skin lesions of various grades, including melanocytic naevi, dysplastic naevi, and malignant melanomas, were imaged and characterized using combined SHG-FLIM microscopy. Particular attention was devoted to the analysis of the collagen within the lesion-connective tissue border, finding differences in terms of both architectural organization and fluorescence lifetime of collagen. This novel approach, based on combined SHG-FLIM microscopy, can provide additional understanding of the collagen role in the tumor development, and has the potential of being applied to other connective and collagen-rich tissues.

9129-52, Session 9

PH measuring in tumor models in-vitro and in-vivo using new genetically encoded sensor and fluorescence imaging *(Invited Paper)*

Elena V. Zagaynova M.D., Nizhny Novgorod State Medical Academy (Russian Federation); Marina V. Shirmanova, N.I. Lobachevsky State Univ. of Nizhni Novgorod (Russian Federation); I. N. Druzhkova, Nizhny Novgorod State Medical Academy (Russian Federation); Maria M. Kuznetsova, N.I. Lobachevsky State Univ. of Nizhni Novgorod (Russian Federation); Ludmila B. Snopova M.D., N. N. Prodanetz, Nizhny Novgorod State Medical Academy (Russian Federation); Vsevolod V. Belousov, Konstantin A. Lukyanov, Shemyakin-Ovchinnikov Institute of Bioorganic Chemistry (Russian Federation)

Measuring of pH in tumor is an important task for basic researches and successful treatment. This work is aimed at the development of the method of pH registration in the tumor models. The study was performed using 3D tumor spheroids and xenografts expressing new genetically encoded sensor for pH. Measuring of pH was based on a radiometric analysis of fluorescence intensity at two different wavelengths. The data of fluorescence microscopy and whole-body imaging were confirmed by morphological investigation and hypoxia analysis in the tissue sections. The possibility of using the unique genetically encoded sensor for ratiometric pH imaging in the tumors in vitro and in vivo was shown for the first time.

9129-53, Session 10

Collagen bioengineered systems: in situ advanced optical spatiotemporal analysis *(Invited Paper)*

Yu Jer Hwang, Xuye Lang, Joseph Granelli, Cassandra C. Turgman, Julia G. Lyubovitsky, Univ. of California, Riverside (United States)

The architecture of collagen is important in maintenance and regeneration of higher vertebrates' tissues. We had been studying the changes to this architecture with in situ multi-photon optical microscopy that combines nonlinear optical phenomena of second harmonic generation (SHG) and two-photon fluorescence (TPF) signals from collagen hydrogels prepared from different collagen solid content, polymerized at different temperatures, with different ions as well as modified with reducing sugars. For example, we incubated 2 g/l collagen hydrogels with 0.1 M fructose at 37 C and after about 20 days observed a significant induction of in situ fluorescence. The

two-photon fluorescence emission was centered at about 460 nm for 730 nm excitation wavelength and shifted to 480 nm when we changed the excitation wavelength to 790 nm. The one-photon fluorescence emission was centered at about 416 nm when excitation was 330 nm. It red shifted and split into two peaks centered at about 430 nm and 460 nm for 370 nm excitation; 460 nm peak became predominant for 385 nm excitation and further shifted to 470 nm for 390 nm excitation. SHG and TPF imaging showed restructuring of hydrogels upon this modification. We will discuss these findings within the context of our ongoing dermal wound repair research.

9129-54, Session 10

Simultaneous recording of t-tubular electrical activity and Ca2+-release in heart failure

Claudia Crocini, Raffaele Coppini, Cecilia Ferrantini, Univ. degli Studi di Firenze (Italy); Ping Yan, Leslie M. Loew, Univ. of Connecticut Health Ctr. (United States); Chiara Tesi, Corrado Poggesi, Elisabetta Cerbai, Francesco S. Pavone, Leonardo Sacconi, Univ. degli Studi di Firenze (Italy)

T-tubules (TT) are invaginations of the surface sarcolemma (SS) that mediate the rapid propagation of the action potential (AP) to the cardiomyocyte core. We employed the advantages of an ultrafast random access multi-photon (RAMP) microscope (Sacconi et al., PNAS 2012) with a double staining approach to optically record t-tubular AP and, simultaneously, the corresponding local Ca2+-release in different positions across the cardiomyocytes. Despite a uniform AP between SS and TT at steady-state stimulation, in control cardiomyocytes we observed a non-negligible be variability of local Ca2+-transient amplitude and kinetics. This variability was significantly reduced by applying 0.1?M Isoproterenol, which increases the opening probability of Ca2+-release units. In the rat heart failure model (HF), we previously demonstrated that some tubular elements fail to propagate AP. We found that the tubules unable to propagate AP, displayed a reduced correspondent Ca2+-transient amplitude as well as a slower Ca2+ rise compared to electrically coupled tubules. Moreover variability of Ca2+-transient kinetics were increased in HF. Finally, TT that did not show AP, occasionally exhibited spontaneous depolarizations that were never accompanied by local Ca2+-release in the absence of any pro-arrhythmogenic stimulation. Simultaneous recording of AP and Ca2+-transient allows us to probe the spatio-temporal variability of Ca2+-release, whereas the investigation of Ca2+-transient in HF discloses an unexpected uncoupling between t-tubular depolarization and Ca2+-release in remodeled tubules. This work was funded by the European Union 7th Framework Program (FP7/2007- 2013) under grant agreement n° 284464, 241526, by the Italian Ministry of University and Research (NANOMAX), and by Telethon-Italy (GGP13162).

9129-55, Session 10

High speed microscopy techniques for signaling detection in live cells

Claudio de Mauro, Domenico Alfieri, Carlo A. Cecchetti, Light4Tech Firenze S.r.l. (Italy); Giulia Borile, Andrea Urbani, Marco Mongillo M.D., Venetian Institute of Molecular Medicine (Italy); Francesco S. Pavone, Univ. degli Studi di Firenze (Italy)

High-speed multiphoton microscopy techinques, such as multispot and random access, allow for the collection of information on fast cellular phenomena with high spatial resolution and with upreceded acquisition rate.The multiphoton excitation also provides optcal sectioning to hundreds of micorons i ndepth in biological tissues.

We develop both these techniques in user friendly arrangements: the MCube system and the RAMP system. The first one can acquire full field images at tens of frames per second, while the seconf one, based on extremely fast scanning technology, can detect localized signals at kilohertz rate.

With these two microscopes, we investigated animal models with inherited and acquired arrhythmias to assess the role of Ca2+ and voltage signals as arrhythmia triggers in cell and subcellular components of the intact heart and correlate these with electrophysiology. In fact, Ca2+ signaling in arrhythmogenesis has been mainly studied in isolated cardiomyocytes and given that the extracellular matrix influences both Ca2+ and membrane potential dynamics in the intact heart and underlies environmentally mediated changes, understanding how Ca2+ and voltage are regulated i

9129-56, Session 10

Plasmon enhanced vibrational nonlinear spectroscopy for surface specific analysis

Dan Lis, Yves Caudano, Univ. de Namur (Belgium); Marie Henry, Sophie Demoustier-Champagne, Univ. Catholique de Louvain (Belgium); Etienne Ferain, it4ip s.a. (Belgium); Francesca Cecchet, Univ. de Namur (Belgium)

Metallic nanostructures such as nanopillars and nanoantennas are capable of confining the energy of an incident radiation into volumes much smaller than the wavelength of incoming waves through localized surface plasmon resonance (LSPR).[1] This electromagnetic-field enhancement, attributed to the collective motion of free electrons, has been extensively used for surface-enhanced Raman scattering (SERS) and other surface-enhanced spectroscopic processes. This has drive nanoparticles to become a powerful tool for chemical and biological optical sensing experiments.[2]

In this work, we coupled such localized electromagnetic-field enhancement effect to a nonlinear second-order optical spectroscopy to obtain high molecular signal intensity and sensitivity. The technique is based on a three waves mixing process in which one infrared (?1) and one visible (?2) photons interact together with matter to generate a new coherent photon at the sum frequency (?sfg = ?1 +?2). The whole process relying on ?(2), the sum frequency generation (SFG) signal can be emitted only where the centrosymmetry is broken, that is at surfaces and interfaces separating two SFG inactive bulk media. [3,4] In fine, SFG spectroscopy is a background free vibrational surface-sensitive spectroscopy able to retrieve accurate informations on molecular thin films such as conformation, orientation, dynamics, bio-recognition, phase transition, these at any kind of interfaces accessible by light.

Practically, we report a strong enhancement of the vibrational SFG signal from molecules adsorbed on metallic nanopillars when those latter are excited at their localized plasmon resonance frequencies.[5] Gold nanopillars, sizing around 100 nm in height and 60 nm in diameter, stand vertically on a substrate of gold or platinum. The nanopillars exhibit two plasmon modes that can be excited selectively by the incident visible laser beam or by the generated SFG beam itself. At the best until now, the molecular SFG signal obtained on such nanostructured surfaces is more than 100 times larger that what can be achieved on unstructured flat surfaces. Besides, because of the directional profile of the two plasmon modes, an adequate choice of the beam polarizations and frequencies leads to a spatial selectivity of the SFG emission. It is indeed likely possible to selectively probe the molecules adsorbed onto the nanopillar side wall, the nanopillar top part, or the flat region of the substrate in-between the pillars. This gives promising issues to set up label free vibrational bio-recognition platforms with “multi-zone” enhanced sensitivity.

References

[1] L. Novotny and N. van Hulst, Nat. Photon. 5 (2011) 83

[2] Willets, K. A.; Van Duyne, R. P., Annu. Rev. Phys. Chem., 58 (2007) 267-297.

[3] Shen, Y. R., Nature, 337 (1989) 519-525.

[4] Vidal, F.; Tadjeddine, A., Rep. Prog. Phys. 68 (2005) 1095-1127.

[5] Lis, D., Caudano, Y., Henry, M., Demoustier-Champagne, S., Ferain, E. and Cecchet, F., Advanced Optical Materials, 1 (2013) 244–255.

9129-58, Session 11

Biomarkers, microenvironment and tropism: opportunities to actively target plasmonic particles to malignant cells *(Invited Paper)*

Fulvio Ratto, Francesca Tatini, Istituto di Fisica Applicata Nello Carrara (Italy); Sonia Centi, Ida Landini, Stefania Nobili, Ewa Witort, Franco Fusi, Sergio Capaccioli, Enrico Mini, Univ. degli Studi di Firenze (Italy); Roberto Pini, Istituto di Fisica Applicata Nello Carrara (Italy)

Plasmonic particles such as gold nanorods are gaining relevance as contrast agents for the near-infrared photoacoustic imaging and the photothermal ablation of cancer. Selective targeting of malignant cells may rely on complementary biochemical and biological strategies, including the use of specific probes or the exploitation of cellular vehicles.

Here we move from a platform of PEGylated gold nanorods with plasmonic bands around 800 nm, good biological profiles, stability and efficiency of photoacoustic and photothermal conversion as well as potential to passively accumulate into solid tumors by their enhanced permeability and retention. In order to enhance this potential, we implemented different approaches for active delivery by functionalization with (i) antibodies against cancer antigen 125 (CA125), which is a common biomarker for ovarian lesions; (ii) inhibitors of carbonic anhydrases 9 and 12 (CAIX and CAXII), which are expressed by hypoxic cells such as those found in solid tumors; and (iii) by introducing macrophages as a versatile model of cellular vehicles that would phagocytose the particles and home to inflammatory lesions.

We challenge these alternatives in vitro under relevant conditions and discuss issues and perspectives behind their optimization and synergy.

9129-59, Session 11

Quantification of tissue texture with photoacoustic spectrum analysis

Xueding Wang, Guan Xu, Zhuoxian Meng, Jiandie Lin, Paul L. Carson, Univ. of Michigan Medical School (United States)

Biopsy has been regarded as the reference standard for many diseases, as the method directly reveals the histological changes in biological tissues. However, the invasive nature as well as the long procedure of biopsy makes it less desirable for many conditions. Ultrasound spectrum analysis (USSA) has been employed extensively to study the intensity attenuation and frequency or phase shift of the ultrasound (US) waves backscattered from tissues, as well as periodicities captured by the spectrum, and has shown ability to discriminate tissue microscopic features. Our group has for the first time demonstrated that the frequency domain power distribution of the broadband photoacoustic (PA) signals encode the texture information within the regions-of-interest (ROI). Following the similar method of USSA, photoacoustic spectrum analysis (PASA) could evaluate the relative concentrations and, more importantly, the dimensions of microstructures of the optically absorbing materials in biological tissues, including lipid, collagen, water and hemoglobin. By providing valuable insights into tissue pathology, PASA should benefit basic research and clinical management of many diseases, and may help achieve eventual “noninvasive biopsy”.

This study investigated the feasibility of differentiating fatty and normal livers by PASA. Six and nine pairs of normal and fatty liver tissues from mice were scanned ex vivo with our PA system working at 1200 nm and 532 nm, respectively. To explore the feasibility of this technique for future study on mouse model in vivo, an additional pair of normal and fatty mouse livers was scanned in situ with an US and PA dual-modality imaging system. The PA signals acquired were analyzed by the proposed PASA method, resulting three quantitative spectral parameters including the intercept, the midband fit and the slope. The spectral parameters from the fatty livers were compared to those from the normal livers using the student t-test. Prominent differences between the fatty and the normal mouse liver tissues were observed. The analysis of the PASA parameters from six normal and six fatty mouse liver tissues indicates that there are differences of up to 5 standard deviations between the PASA parameters of the normal and the fatty livers at 1200 nm; whereas for parameters from nine normal and nine fatty mouse liver tissues at 532 nm, the differences are approximately 2 standard deviations $P<0.05$ for each PASA parameter. The results support our hypothesis that the PASA can quantitatively identify the microstructure changes in liver tissues for differentiating normal and fatty livers. Compared to that at 532 nm, PASA at 1200 nm is more reliable for fatty liver diagnosis. This study suggests that PASA holds promise to provide, in an in vivo and noninvasive manner, the identification of the microstructures in biological tissues for the purposes of diagnosis and treatment monitoring.

9129-60, Session 11

Human epithelial cancer cells studied using combined AFM-IR absorption nanoimaging

Eamonn Kennedy, Rasoul Al-Majomaie, Dominic Zerulla, Mohammed Al-Rubeai, James H. Rice, Univ. College Dublin (Ireland)

Chemical heterogeneity on the micro and nanometer length scales is a key feature of living systems. On the cell membrane, the spatiotemporal confinement of proteins and lipids which govern cell adhesion, signaling, antigen presentation and cell-cell interactions occur in specific, sub-micron geometries. Quantifying the underlying biochemical heterogeneity and cytomorphology of subcellular features is of key interest in understanding disease and realizing advances in diagnostics and therapeutics [1].

Probe-based multimodal, tip-hybridized and force mapping methods enable cellular analysis on the scale of fully resolved cell substructures [2]. Atomic Force Microscopy (AFM) has successfully been applied to advance the understanding of biology. AFM studies have detected malignant transformation and discriminated between the different mechanical properties of tumour and control cell populations. Despite having demonstrated imaging of pathogens and cancer, scanning probe based tools have not seen wide use in mainstream biological research, in part due to the persistent difficulties associated with imaging soft, live cells in situ and also in part due to an inability to be chemical specific.

One such emerging method is infrared (IR) nanospectroscopic absorption imaging based on detection of photothermal induced resonance (PTIR), which can perform spectroscopic mapping and label free chemical identification of cell components on the nanoscale [2-5]. The technique is based on the fact that a small, sensitive cantilever placed in contact with the sample surface during pulsed photothermal excitation will be displaced with a magnitude proportional to the material absorption coefficient at the excitation wavelength. PTIR spectroscopic imaging is capable of pure infrared absorption measurements, namely on those properties which depend on the imaginary, and not the real component of the material’s dielectric function. This has led to the use of AFM-IR for absorption imaging and spectroscopy of numerous biomaterials indicating the advantage of AFM-IR for heterogeneous chemical detection at a nanoscale resolution [2-5].

Here we apply AFM-IR (ie photothermal induced resonance imaging in combination with topographic imaging), to study human epithelial cells. We study (with sub-50nm resolution) membrane and nuclei boundaries, via creating cell chemical

complexity maps. We outline how by normalizing for cell height, infrared absorption nanoimaging can also quantify local chemical complexity by image analysis with Minkowski functions. In this way, combined AFM-PTIR absorption imaging can uniquely assess and map biochemical inhomogeneity in mammalian cancer cells on the nanoscale. As many cell processes related to disease are governed by the position, orientation and dynamics of subcellular features on this scale, we utilize the chemical complexity maps to quantify the nanoscale biochemical inhomogeneity of cancer cells with a view to understanding the subcellular biomechanics underlying carcinogenesis.

REFERENCES

1. T. Xia, L. Rome, A. Nel, Nature Materials 7, 519 - 520 (2008)

2. E. Kennedy, R.I Al-Majmaie, M. Al-Rubeai, D. Zerulla, J.H. Rice. RSC Advances, 29, 11311-11904, 2013.

3. E. Kennedy, R.I Al-Majmaie, M. Al-Rubeai, D. Zerulla. J. Biophotonics, in press, 2013.

4. E. Kennedy, F. Yarrow, J.H. Rice. J. Biophotonics, 4, 588, 2011.

5. F. Yarrow, F. Salaun, E. Kennedy, J.H. Rice. Biomed. Optics Express, 2, 37-43, 2011.

9129-61, Session 11

Multidepth illuminating photoacoustic microscopy with a tunable focus lens

Kiri Lee, Tae Joong Eom, Gwangju Institute of Science and Technology (Korea, Republic of)

Optical-resolution photoacoustic microscopy (OR-PAM) systems have been studied to improve its imaging resolution and speed. However the imaging depth range of OR-PAM is limited by its short depth of focus due to a high numerical aperture (NA) objective lens. In order to obtain photoacoustic (PA) images of different layers, we need to change an imaging sample position with the depth direction or to change a focusing depth of an objective lens with mechanical movements. This mechanical movement of the specimen or the objective lens limits PA image scanning speed and the precision of the depth direction, and may be harmful to the sample. In this study, we proposed a multi-depth illuminating PAM with a tunable focus lens. We could electrically tune the focal length of the tunable lens with the depth direction and extend the imaging depth range. Furthermore, the proposed multi-depth illuminating PAM can increase scanning speed with the depth direction and the PAM system can avoid distortions during PA signal acquisitions, because there is no mechanical scanning with the depth direction.

In the experimental setup, a diode pumped solid state pulsed laser (FQS-200-1-Y-532, Elforlight Ltd.) has 280 Hz pulse rate and 13 mW averaged output power at 532 nm wavelength. The laser pulses were attenuated by a neutral density filter. The attenuated beam was collimated by a condenser lens. An objective lens with 35mm focal length focused on a sample. A photodiode was also added to monitor the fluctuations of the laser pulse intensity. The PAM system consisted of an electrically tunable lens (EI-10-30-C, Optotune Inc.) to control focal plane and a relay lens with 50 mm focal length to expand beam size. The tunable lens composed of liquid crystals is based on local changes in the refractive index that enable the implementation of a Fresnel lens. The focal length can be adjusted from 50 mm to 200 mm with changing the driving current of the tunable lens. The maximum response time of the tunable lens is 2.5 msec. The PA signals were detected by an ultrasonic transducer with a central frequency of 25 MHz and the focal length of 20 mm. The measured PA signals were amplified by a low noise amplifier and filtered unwanted high frequency noise by a low pass filter with 55 MHz cutoff frequency. We controlled the driving current of the tunable lens by LabVIEW software (National Instruments corp.), and acquired the PA signals using a high speed digitizer (PXI-5122, National Instruments corp.) with 100 MS/sec sapling rate. To investigate the performance of the PAM system, we imaged a phantom made of a black ink in a water tank to reduce loss of the PA signals. The moving stages scanned the sample in the x-y plane except for z-axis with a stage moving speed of 3 mm/sec. The obtained PA signals were processed by low pass filtering and achieved the maximum intensity values. Then, we rendered the signal processing data of the phantom. In the future work, we expect the scanning speed improvement of the entire system to obtain in-vivo PA imaging.

9129-62, Session 12

Light-induced autofluorescence and diffuse reflectance spectroscopy in clinical diagnosis of skin cancer *(Invited Paper)*

Ekaterina G. Borisova, Institute of Electronics (Bulgaria); Elmira P. Pavlova M.D., Univ. Hospital 'Queen Jiovanna-ISUL' (Bulgaria); Todor Kundurjiev, Medical Univ.-Sofia (Bulgaria); Petranka P. Troyanova M.D., Univ. Hospital 'Queen Jiovanna-ISUL' (Bulgaria); Tsanislava I. Genova, Latchezar A. Avramov, Institute of Electronics (Bulgaria)

This report generalized our four-year efforts on accumulation and development of autofluorescence and diffuse-reflectance spectral database for skin cancer diagnosis and differentiation for clinical practice. We investigated more than 500 clinical cases to receive the spectral properties of basal cell (136 patients) and squamous cell carcinoma (28), malignant melanoma (41) and different cutaneous dysplastic and benign lesions. Excitation at 365, 385 and 405 nm using LEDs sources is applied to obtain autofluorescence spectra, and broad-band illumination in the region of 400-900 nm is used to detect diffuse reflectance spectra of all pathologies investigated. USB4000 microspectrometer (Ocean Optics Inc, USA) is applied as a detector and fiberoptic probe is used for delivery of the light.

In the case of in vivo tumor measurements spectral shape and intensity changes are observed that are specific for a given type of lesion. Autofluorescence origins of the signals coming from skin tissues are mainly due to proteins, such as collagen, elastin, keratin, their cross-links, co-enzimes – NADH and flavins and endogenous porphyrins. Spectral features significant into diffuse spectroscopy diagnosis of different cutaneous tumours are related to the effects of re-absorption of hemoglobin and its forms as well as melanin and its concentration in different pathologies. The spectral features in both spectroscopic modalities used depend from the lesion type and growth stage of the tumor and could be applied for differentiation algorithms and cancer diagnosis. Based on our results, we develop significant database and revealed specific features for a large class of cutaneous neoplasia, using about 30 different spectral pecularities to differentiate cutaneous tumor and to evaluate the diagnostic accuracy, when optical spectroscopy of skin is applied in clinical environment. Sensitivity and specificity obtained exceed 90%, which make optical biopsy very useful tool for clinical practice.

These results are obtained in the frames of clinical investigations for development of significant "spectral features" database for the most common cutaneous malignant, dysplastic and benign lesions. In the forthcoming plans, our group tries to optimize the existing experimental system for optical biopsy of skin, and to introduce it and the diagnostic algorithms developed into clinical practice of University hospital "Queen Jiovanna-ISUL"- Sofia, based on the high diagnostic accuracy achieved under these investigations.

Acknowledgements: This work is supported by the National Science Fund of Bulgarian Ministry of Education, Youth and Science under grants #DMU-03-46/2011 and #DO-02-112/2008.

9129-63, Session 12

Optimal source to detector separation for extracting sub dermal chromophores in fiber optic diffuse reflectance spectroscopy: a simulation study

Narayanan U. Sujatha, Bala Nivetha K., Akshay Singhal, Indian Institute of Technology Madras (India)

Localization and determination of blood region parameters in skin tissue can serve as a valuable supplement to standard non invasive techniques, especially in accessing the degree of depth of burns on skin and for the classification of vascular malformations. Quantitative optical examination of skin local blood region requires the use of depth sensitive techniques and preferential probing for assessment of data from specific layers of skin tissue. Diffuse reflectance spectroscopy (DRS) is a proven method facilitating quantitative optical examination of tissues with respect to their biochemical information. Additionally, DRS have the potential of being clinically viable due to its non invasiveness and portability. This work incorporates the depth sensitivity of diffuse reflectance and optimal source to detector fiber separation for maximum reflectance collection efficiency from local blood region in skin. Monte Carlo simulation for diffuse reflectance was performed on a multi layered skin tissue model consisting of epidermis, perfused dermis and localized blood region. It was found that the slope of the spatially resolved reflectance curve plotted with respect to the source to detector separation distance in semi log scale varies with the depth of the local blood region at specific wavelengths corresponding to the absorption wavelengths of hemoglobin. From the depth information obtained from the spatially resolved reflectance data, the optimum source to detector separation is determined for maximum collection efficiency from the chromophore layer. The results obtained from simulation suggest the design of a linearly variable source to detector separation probe for preferential analysis of the depth of a specific tissue layer and subsequent determination of optimal source to detector separation for extracting the layer information.

9129-64, Session 12

Pre-processing method to improve optical parameters estimation in Monte Carlo-based inverse problem solving

Maria Kholodtsova, Univ. de Lorraine (France) and A. M. Prokhorov General Physics Institute (Russian Federation) and CNRS (France); Christian Daul, CNRS (France) and Université de Lorraine (France); Viktor B. Loschenov, A. M. Prokhorov General Physics Institute (Russian Federation); Walter C. Blondel, Univ. de Lorraine (France) and CNRS (France)

Introduction: Estimating optical properties of biological tissues using spatially resolved diffuse reflectance measurements is still a challenge in pre-cancer diagnosis. Widely used Monte Carlo (MC) simulations are flexible and may be fasten through multithread calculation approaches. Inverse problem solving to estimate optical parameters still has a problem of local minima which may lead to convergence difficulties and error. The aim of our work is to analyze the features of cost function in the parameter variation space of interest and hence to define some data preprocessing step for improving the robustness and precision of the optical property estimation scheme.

Methods: The simulation of light propagation into tissue (forward problem) using MC was written in CUDA code (GPU) for accelerated calculations. The geometrical configuration of our model was based on the characteristics of our experimental setup: one central excitation and 6 detection fibers (NA = 0.22, d = 200 μm) at different radial distances, ri (i = 1:6). The number of photons I(r) received by each fiber was simulated depending on optical properties of media, (μs, μa, g).

Optimization algorithm (Levenberg-Marquardt in the present work) aims at finding the optimal values of the optical parameters vector (μs, μa) by comparing experimental I0(r), to simulated I(r) data.

The cost function evaluated is a quadratic error:

Error=∑(i=1:6) [I(ri; μs,μa)-I0(ri)]^2.

Here, I0 corresponds to simulated data (for fixed values) serving as known reference data set.

Analysis of the error variation space: The variation space for (μs, μa) parameters with values (10:10:1000, 1:0.1:10) [cm-1], g = 0.8, shows that statistical noise in I(r) results in the error space's noise. Along μs axis, wide variation of the error function is observed while for μa axis this variation is very low. The low gradient in this direction implies, in presence of noise, local minima are numerous thus leading to error in global minimum achieving. In contrast, the similar variation space analyzed with diffusion equation approximation show global minimum easy achievement.

Solution: We tried to reduce the influence of statistical noise inherent to MC simulation, using several combinations of smoothing and fitting of the modeled curves. 500 curves were simulated with the same parameters μs = 500 cm-1, μa = 5 cm-1, g = 0.8. These curves were also smoothed and fitted with the same functions. Then for 500 error spaces' minima were found.

Results and Discussion: The minima of the error spaces were projected on the (μs, μa) plane. They are distributed along the exponential decay curve. All the values of (μs, μa) along this curve are the probable correct optical properties, derived for the curve simulated with same optical properties. After we found the best pair of fit and smooth to concentrate the correct optical properties near real values. It was shown that smoothing with weighted local regression and fitting with double exponential decay are optimal: its mean values give correct optical properties (μs, μa). Suggested processing before using the LM algorithm leads to the correct optical properties recovery and to the way of postulated task proper solution.

9129-65, Session 12

Measurement and quantification of fluorescent changes in ocular tissue using a novel confocal instrument

Kim K. Buttenschoen, Durham Univ. (United Kingdom) and Lein Applied Diagnostics Ltd. (United Kingdom); John M. Girkin, Durham Univ. (United Kingdom); Daniel J. Daly, Lein Applied Diagnostics Ltd. (United Kingdom)

We report on the development of a non-invasive instrument based on scanning confocal microscopy that simultaneously measures reflected and fluorescent light from ocular tissues and humours to quantify the distribution and concentration of fluorescent compounds such as ocular medication or autofluorescence within the eye. The reflected light is being used as a position reference for the fluorescence signal, thus guaranteeing that the concentration of the compound of interest can be located accurately within the eye. The measurement concept has been proven by monitoring the diffusion of Sodium Fluorescein and a pharmaceutical compound for treating open angle glaucoma in vitro in a cuvette as well as in ex vivo porcine eyes. Furthermore we measured the natural change in corneal and crystalline lens autofluorescence in human volunteers of different ages over the course of a week. Results will be presented that show the capability of the instrument to measure the location and concentration of the compound of interest with high axial and temporal resolution of 124 μm and 0.6 s respectively, and with a precision of 5 μm. We demonstrate that the instrument has high sensitivity and can accurately measure 2 nM Fluorescein in aqueous solution at an excitation wavelength of 402 nm (equivalent to 530 pM Fluorescein at its peak excitation wavelength) as well as being able to measure concentrations below 1 μM of compounds with quantum yields as low as 0.01 with high specificity for the compound of interest over competing background signals. The instrument is now being

adapted for broader exploitation and applications and is compact, portable and affordable. We believe that this instrument has a large number of applications in fields such as, but not limited to, in vitro and in vivo assessment of the diffusion of fluorescent compounds through the eye and skin, measuring auto-fluorescence of tissues such as the lens and cornea (e.g. for diabetes monitoring) and reducing the number of animals needed for drug development and general research. Furthermore we will discuss the potential use of this technology in the clinical and home care environment.

9129-66, Session 12

Construct a new method accurately extracting parameters associate with absorption and scattering coefficients of epithelium and stroma: using perpendicular and oblique fiber bundle probes

Hong-po Hsieh, Kung-Bin Sung, Fang-Wei Hsu, National Taiwan Univ. (Taiwan)

Diffuse reflectance spectroscopy has been applied to detect tissue absorption and scattering properties associated with dysplasia, which is a potential precursor of epithelial cancers. We propose a beveled fiber bundle probe consisting of a source fiber and multiple detection fibers parallel to each other and oriented obliquely to the tissue surface and investigate the sensitivity of reflectance measured with the probe to optical properties of a two-layered normal oral mucosa model. In our previous work, we analyzed the influence of changes in absorption and scattering coefficients and it showed that the influence of changes in scattering or absorption coefficient to reflectance varied with the source-detector separation(SDS), the wavelength, the fiber-bundle probe used(perpendicular or oblique) and the SDS alignment on oblique probes. In general, oblique probes are more sensitive to coefficient in epithelium while perpendicular probes are more sensitive to those of stroma.

We use perpendicular and oblique fiber bundle probes to measure reflectance spectra from patients with oral dysplasia as well as healthy volunteers, and using scaling Monte Carlo work with iterative curve fitting tool to extract parameters related to tissue properties. However, we found that the iterative curve fitting method aimed at minimizing the RMS-error is not accurate enough. By searching for the uniqueness of each parameter in a spectrum, we can establish a new method to extract the parameters. To solve this problem, we try to develop a method that can extract a unique value for each parameter separately. Using scaling Monte Carlo method as the simulation tool, we search for the uniqueness for each parameter on a spectrum. Once we have enough knowledge for all parameters, we can develop a protocol, which decides a unique value for each parameter step by step. The determined parameter is then set to constant so that we have less unknown parameters for next step.

From the results of our previous work, perpendicular probes are less sensitive to the upper layer parameters. The simulation showed that parameters related to upper layer scattering have negligible effects compared to those of lower layer, which indicates that the two probes could be use simultaneously to extract upper and lower layer scattering parameters separately. The scattering coefficient, modeled by Zonios et al as A*?^(-k), affect the spectra on almost every wavelengths from 400nm to 700nm. The parameter A affects the amplitudes without changing the shapes, whereas k affect relative values between wavelengths. On the other hand, parameters related to absorption coefficient only affect wavelengths shorter than 600nm. The blood oxygen value decides the number and locations of absorption peaks around 420nm and between 530~580nm. The concentration of hemoglobin affects the amplitudes without changing the shape, but its value can be decided by comparing the relation between the intensities on both sides of around 600nm.

In our research, we found out how the parameters affect the shape or amplitude of a spectrum. By using these features, we can build an innovative method with more accuracy and efficiency to extract tissue parameters from spectra measured in vivo.

9129-67, Session 13

Gold nanoparticles for cell optoporation and transfection

Olga Bibikova, Univ. of Oulu (Finland) and N.G. Chernyshevsky Saratov State Univ. (Russian Federation); Alexey P. Popov, Prateek Singh, Ilya Skovorodkin, Zuomin Zhao, Univ. of Oulu (Finland); G. G. Akchurin Jr., Institute of Precision Mechanics and Control (Russian Federation) and N.G. Chernyshevsky Saratov State Univ. (Russian Federation); Ivan V. Fedosov, N.G. Chernyshevsky Saratov State Univ. (Russian Federation); Ksenia Maximova, Aix-Marseille Univ. (France); Matti Kinnunen, Univ. of Oulu (Finland); Marc L. Sentis, Andrei V. Kabashin, Aix-Marseille Univ. (France); Vladimir A. Bogatyrev, Nikolai G. Khlebtsov, Institute of Biochemistry and Physiology of Plants and Microorganisms (Russian Federation) and N.G. Chernyshevsky Saratov State Univ. (Russian Federation); Seppo Vainio, Univ. of Oulu (Finland); Valery V. Tuchin, N.G. Chernyshevsky Saratov State Univ. (Russian Federation) and Univ. of Oulu (Finland) and Institute of Precision Mechanics and Control (Russian Federation)

Plasmon-resonant gold nanoparticles are novel structures with the unique property of plasmon resonance resulting in an enhanced electromagnetic field at the metal nanoparticle surface. One of the new areas of application of gold nanoparticles is the use of nanostructures as probes and carriers for cell transfection and bioimaging. Transfection of molecules is among of the most important research tools in modern molecular biology. Optoporation, or treatment of cell with light can significantly enhance membrane permeabilization. This promising technique is an efficient, relatively high throughput and virus-free method having potential for cell transfection and wide applications in both in vivo and in vitro. We investigated possibility to increase efficiency of this method by implementing a new feature – gold nanostructures.

For our experiments, we used colloidal gold nanospheres with diameter of 25 nm, and gold nanocomposites, with diameter of 100 nm, consisted of nanostars as a core and silica shells. The methods of synthesis nanospheres imply the use of ultra-short laser radiation to ablate a solid target (a peace of gold) in aqueous environment in order to produce ultrapure nanomaterials. Water-dispersed fabricated nanospheres have superior purity compared to chemically synthesized counterparts and exhibiting promising optical properties. Silica-gold nanocomposites were fabricated by covering nanostars with an average size of about 50 nm with silica shells synthesized via base-catalyzed hydrolysis of tetraethyl orthosilicate (TEOS). The silica shell thickness was about 50 nm and could be simply varied by changing the reaction time and TEOS concentration.

In laser-assisted cell optoporation experiments a laser with a tunable central wavelength corresponding to the plasmon resonance wavelength of the used nanostructures was applied to irradiate nanostructure-incubated living cells.

Assessment of optoporation efficiency was performed by staining the cells with propidium iodide or incubation with red fluorescent plasmids. The MTT test was applied to reveal viability of the treated cells. The results show enhanced membrane permeabilization upon laser irradiation in presence of gold nanostructures, with cells remaining alive.

9129-69, Session 13

Investigation on cytoskeleton dynamics for no-adherent cells subjected to point-like stimuli by digital holographic microscopy and holographic optical trapping

Lisa Miccio, Pasquale Memmolo, Francesco Merola, Istituto Nazionale di Ottica (Italy); Martina Mugnano, Sabato Fusco, Paolo A. Netti, Istituto Italiano di Tecnologia (Italy); Pietro Ferraro, Istituto Nazionale di Ottica (Italy)

Guiding, controlling and studying cellular functions are challenging themes in the biomedical field, as they are fundamental prerequisites for new therapeutic strategies from tissue regeneration to controlled drug delivery. In recent years, multidisciplinary studies in nanotechnology offer new tools to investigate important biophysical phenomena in response to the local physical characteristics of the extracellular environment, some examples are the mechanisms of cell adhesion, migration, communication and differentiation. Indeed for reproducing the features of the extracellular matrix in vitro, it is essential to develop active devices that evoke as much as possible the natural cellular environment. Our investigation is in the framework of studying and clarifying the biophysical mechanisms of the interaction between cells and the microenvironment in which they exist.

We implement an optical tweezers setup to investigate cell material interaction and we use Digital Holographic Microscopy (DHM) as non-invasive imaging technique. We exploit the Holographic Optical Tweezers (HOT) arrangement to induce cell deformation. HOT arrangement allows to generate different numbers and configurations of trapping sites, in order to trap and manage functionalized micrometric latex beads to induce mechanical deformation in suspended cells. A lot of papers in literature examine the dynamics of the cytoskeleton when the cell adhere on substrates and nowadays well established cell models are based on such research activities. Actually, the natural cell environment is made of a complex extracellular matrix and the single cell behavior is due to intricate interactions with the environment and are strongly correlated to the cell-cell interactions. Our investigation is devoted to understand the inner cell mechanism when it is mechanically stressed by point-like stimulus without the substrate influence. HOTs are exploited to induce cellular response to specific stimuli and DHM imaging allows to measure such responses in a quantitative, label free and not invasive way.

9129-70, Session 13

3D visualization and biovolume estimation of motile cells by digital holography

Francesco Merola, Lisa Miccio, Istituto Nazionale di Ottica (Italy); Pasquale Memmolo, Istituto Italiano di Tecnologia (Italy) and IIT-CRIB (Italy); Paolo A. Netti, Istituto Italiano di Tecnologia (Italy); Giuseppe Di Caprio, Giuseppe Coppola, Istituto per la Microelettronica e Microsistemi (Italy)

Three-dimensional morphology and shapes estimation of micro-samples is an important information in many fields of application, such as bio-technologies and medicine. In this context, the universally recognized approach for micro-sample characterization is tomography, where a full 3D information can be obtained gathering projection data from multiple point of view. At same time, biovolume and biomass are significant parameters involved in several research areas from taxonomy to the study of ecosystem health. The most common and well-established methods to calculate biovolume are based on more or less complicated geometrical models. Procedures for measuring biovolumes need isolation and sorting of the cells and observation at microscope.

We propose here a non-contact as well as all-optical approach based on an optical coherent microscopy apparatus able to select the cell, to induce rotation along its main symmetrical axis, and to measure and display its volume. The method is especially suited for non-spherical micro-samples such as spermatozoa cells. The apparatus includes a combination of the Optical Tweezers (OT) and Digital Holographic (DH) techniques. OT by a simple Gaussian beam allows to select and to induce self-rotation of the cell whereas quantitative phase-contrast maps (QPMs) are obtained through DH microcopy. In this context, the well-known features of DH allow quantitative, label-free, phase-contrast imaging that is essential in visualization of low-amplitude contrast objects.

Quantitative phase-contrast images are processed using a special algorithm, for the first time adopted in case of micrometric and phase-contrast objects. We obtain the biovolume estimation of a population of 80 sperm cells, both X and Y-types. To validate the technique, we compare it with a standard biovolume measurement method, starting from the measurement of the sample's linear dimensions.

The experimental setup can be implemented in a microfluidic chip, and is able to optically trap motile cells while they are flowing into microfluidic channels and perform a controlled rotation. Demonstration of simultaneous measurements on more cells by Holographic Optical Tweezers (HOTs) is also presented.

9129-71, Session 13

Mechanics of protein-DNA interaction studied with ultra-fast optical tweezers

Carina Monico, European Lab. for Non-linear Spectroscopy (Italy); Alessia Tempestini, Univ. degli Studi di Milano-Bicocca (Italy); Francesco Vanzi, Francesco S. Pavone, European Lab. for Non-linear Spectroscopy (Italy) and Univ. degli Studi di Firenze (Italy); Marco Capitanio, Univ. degli Studi di Firenze (Italy) and European Lab. for Non-Linear Spectroscopy (Italy)

The lac operon is a well known example of gene expression regulation, based on the specific interaction of Lac repressor protein (LacI) with its target DNA sequence (operator). LacI and other DNA-binding proteins bind their specific target sequences with rates higher than allowed by 3D diffusion alone. Generally accepted models predict a combination of free 3D diffusion and 1D sliding along non-specific DNA. We recently developed an ultrafast force-clamp laser trap technique capable of probing molecular interactions with sub-ms temporal resolution, under controlled pN-range forces. With this technique, we tested the interaction of LacI with two different DNA constructs: a construct with two copies of the O1 operator separated by 300 bp and a construct containing the native E.coli operator sequences. Our measurements show at least two classes of LacI-DNA interactions: long (in the tens of s range) and short (tens of ms). Based on position along the DNA sequence, the observed interactions can be interpreted as specific binding to operator sequences (long events) and transient interactions with nonspecific sequences (short events). Moreover, we observe continuous sliding of the protein along DNA, passively driven by the force applied with the optical tweezers.

9129-72, Session 13

Raman tweezers on bacteria: following the mechanisms of bacteriostatic versus bactericidal action

Silvie Bernatova, Ota Samek, Zdenek Pilat, Mojmir ?er?, Jan Jezek, Petr Jakl, Jan Ka?ka, Pavel Zemanek, Institute of Scientific Instruments of the ASCR, v.v.i. (Czech Republic); Filip R??i?ka, Masaryk Univ. (Czech Republic)

The main goal of our investigation is to use Raman tweezers

technique so that the response of Raman scattering on microorganisms (bacteria, yeast and algae cells) suspended in liquid media can be used to identify different species. The presented investigation includes identification of bacteria strains (biofilm-positive and biofilm-negative) by using principal component analysis (PCA). On top of being able to distinguish the bacterial strain (or biofilm positive and negative bacteria of the same strain), we are able to detect antibiotic effect on bacteria, bacterial growth or viability. Antibiotics can be divided into two groups on the basis of effect they have on microbial cells, which is either bactericidal or bacteriostatic. Bactericidal antibiotics kill the bacteria and bacteriostatic antibiotics suppress the growth of bacteria by keeping them in the stationary phase of growth. One of many factors to predict a favorable clinical outcome of the potential action of antimicrobial chemicals may be provided using in vitro bactericidal/bacteriostatic data from MICs (MICs - minimum inhibitory concentrations). Consequently, MICs are used in clinical situations mainly to confirm resistance, and to determine the in vitro activities of new antimicrobials. We report on the combination of data obtained from MICs with information on microorganism´s "fingerprint" (e.g., DNA/RNA, and proteins) provided by Raman tweezers. Thus, we could follow mechanisms of the bacteriostatic versus bactericidal action simply by detecting the Raman bands corresponding to DNA and their changes in fingerprint of trapped bacteria. The Raman spectra of Staphylococcus epidermidis treated with clindamycin and chloramphenicol (a bacteriostatic agent) indeed shows little effect on DNA which is in contrast with the action of ciprofloxacin (a bactericidal agent), where the Raman spectra shows a decrease in strength of the signal assigned to DNA, suggesting DNA fragmentation.

9129-73, Session 13

A compact optoelectronic tweezers tool for cell manipulation

Abigail Jeorrett, Univ. of Strathclyde (United Kingdom); Steven L. Neale, Univ. of Glasgow (United Kingdom); David Massoubre, Griffith Univ. (Australia); Enyuan Xie, Owain R. Millington, Keith Mathieson, Erdan Gu, Martin D. Dawson, Univ. of Strathclyde (United Kingdom)

Manipulation of cells and other biological particles is an essential technique in biomedical research to understand cellular and molecular interactions, as well as to develop novel therapeutics. Many of the tools available to perform these studies are large, expensive and labour-intensive, incorporating lasers and complex optics [1]. There is therefore a demand for devices to provide bio-compatible manipulation in a compact and high-throughput format.

We demonstrate a novel integrated photonics device capable of cell manipulation within a single chip. Gallium nitride on sapphire micro-LED arrays are utilised to provide a compact, incoherent light source to create dynamic, programmable light patterns [2]. The micro-LED array is coated with a layer of indium tin oxide (a conductor) and a layer of amorphous silicon (a photoconductor) which combine with an ITO coated electrode placed directly on top of the deposited layers to form an optoelectronic tweezers (OET) chamber. OET is a recently established technique where an AC voltage is applied across the upper and lower electrodes to generate a uniform electric field within the chamber. Illuminating the photoconductor with the micro-LED array generates an electric field gradient, along which particles suspended in low conductivity solution move [3].

In this study, two micro-LED/OET integrated devices were developed. The first device incorporates an array of square micro-LED pixels with which particles could be corralled at low velocity, demonstrating the potential of the compact format. The second device consisted of a micro LED pixel pattern in the form of a light chamber for the selection and transport of particles. The integrated format of these devices provides a simple tool for cell manipulation which can be easily adopted with no need for optical alignment. Finally, live immune cells were collected and controllably brought into contact and separated, demonstrating the application to biomedical research and drug discovery.

[1] D. J. Stevenson, F. Gunn-Moore, and K. Dholakia, "Light forces the pace: optical manipulation for biophotonics.," J. Biomed. Opt., 15, 041503, 2011.

[2] J. J. D. Mckendry, R. P. Green, A. E. Kelly, Z. Gong, B. Guilhabert, D. Massoubre, E. Gu, and M. D. Dawson, "High-Speed Visible Light Communications Using Individual Pixels in a Micro Light-Emitting Diode Array," IEEE Photonics Technol. Lett., 22, 1346–1348, 2010.

[3] M. C. Wu, "Optoelectronic Tweezers," Nat. Photonics, 5, 322–324, 2011.

9129-157, Session 13

Optical tweezers experiments for fibroblast cell growth stimulation

Remy Avila, Univ. Nacional Autónoma de México (Mexico); Norma Medina-Villalobos, Univ. de Guadalajara (Mexico); Jose Victor Tamariz Flores, Univ. Veracruzana (Mexico); R. Chiu, Univ. de Guadalajara (Mexico); L. M. Lopez, A. Acosta, V. Castaño, Univ. Nacional Autónoma de México (Mexico)

Optical tweezers constitute an increasingly used tool for the study of biomechanical properties of cells. Here we report experiments for the projection induction of NIH3T3 fibroblast cells, using a single-trap optical tweezers. The system is based on a 1064-nm, 50mW infrared gaussian laser beam, a 100x microscope objective with 1.25 numerical aperture and a temperature-controlled warming plate to maintain cell viability. Eighteen cells were exposed to the focussed laser beam in different cell zones and another 18 cells were observed without laser stimulation as a control population. The results show that the probability of lamelipodia growth increases on exposed cells by a factor 1.5.

9129-74, Session 14

Direct imaging of singlet oxygen luminescence generated in blood vessels during photodynamic therapy *(Invited Paper)*

Buhong Li, Lisheng Lin, Huiyun Lin, Defu Chen, Fujian Normal Univ. (China); Long-Chao Chen, Fujian Normal Unv. (China); Min Wang, Shusen Xie, Fujian Normal Univ. (China); Ying Gu, Chinese PLA General Hospital (China); Brian C. Wilson, Ontario Cancer Institute (Canada)

Singlet oxygen (1O2) is the major phototoxic component in type II photodynamic therapy (PDT). In this study, a novel spatially-resolved imaging system was developed for imaging photodynamically generated 1O2 luminescence, which has a near-infrared InGaAs camera that employs 320?256 focal plane array detectors. Green diode laser emits at 532 nm was used as excitation light source. After the intravenous administration of the photosensitizer rose bengal (25 mg/kg body weight), the images of 1O2 luminescence that generated in blood vessels via a dorsal skinfold window chamber model were directly recorded. Moreover, the photosensitizer fluorescence and biological response of blood vessels were monitored, respectively. In addition, the influence of light dose on 1O2 luminescence image and PDT efficiency was quantitatively evaluated. Our obtained results indicate that the image of 1O2 luminescence generated in blood vessels can be successfully acquired. The arteriole vasoconstriction correlated well with local 1O2 luminescence intensity, which was determined from the 1O2 luminescence image. This study suggests that the 1O2 luminescence imaging system may has great potential for elucidating the mechanisms for vascular targeting PDT.

9129-75, Session 14

Conformable, Low Level Light Therapy platform

Michal Jablonski, Frederick Bossuyt, Jan Vanfleteren, Thomas Vervust, Herbert De Smet, Univ. Gent (Belgium)

Well-being applications demand unobtrusive treatment methods in order to reach user acceptance. In the field of light therapy this needs to be carefully addressed because, in most cases, light treatment system size has to be significant with respect to human body scale. At the same time we observe the push is to make wearable devices that deliver the treatment "on the go". Once scaled up, standard flexible electronics (FPC) must fail to conform to body curvatures leading to decrease in comfort. A solution to this problem demands new or modified methods for fabrication of the electronic circuits that fulfils the conformability demand (flexing, but also stretching). Application of SMI (Stretchable Molded Interconnect) technology, that attempts to address these demands, will be discussed. The unique property of SMI is that its manufacturing draws mainly from standard PCB and FCB technologies to inherit the reliability and conductivity. At the same time, however, it allows soft, flexible and stretchable circuits with biomimetic haptics. In this work a demonstrator device for blue light therapy of RSI is presented that illustrates the strengths as well as challenges ahead of conformable light circuits.

Juvenile jaundice treatment, melatonin suppression effect, wound healing acceleration and disinfection or pain relief are among the applied and researched effects of the blue light on the human body. The treatments have the great benefit of triggering body own protection mechanisms, drug-fee. This however, comes at the cost of rather long, continuous exposures for treatments to take effect. The ability to make the light sources wearable is therefore of evident benefit to user comfort, but also to treatment efficiency (less light spilling out).

In this work an RSI (Repetitive Strain Injury) wrist-wrap demonstrator will be presented that uses SMI technology to interconnect a matrix of power LEDs in a soft, flexible and stretchable manner. We have been able to demonstrate that the technology of the stretchable interconnect delivers up to 60% one-time elongation, and up to 100 000 cycles of MTTF at 10%, repeated elongation. The next challenge is to maximize the light flux toward the skin to meet the irradiance target for the treatment. This must be achieved while maintaining skin thermal comfort. In order to achieve this we combine a number of PDMS materials that allow high blue transmission, tear strength or increased thermal conductivity. Resulting system efficiencies are reported.

9129-76, Session 14

Is there a stimulation of blood microcirculation at low level laser irradiation?

Dmitry A. Rogatkin, MONIKI (Russian Federation); Andrey Dunaev, State Univ. Scientific-Educational Ctr. (Russian Federation)

In 1980-2000 besides a laser surgery the intensive evolution of Low Level Laser Therapy (LLLT) had started in medicine, especially in Russian medicine as well as in medicine of a number of other East-European countries. At the same time in serious scientific literature, especially of developed European countries, USA, Japan, etc., the biophysical mechanisms and a real clinical effect of LLLT are still the subject of disputes. Today one may speak of at least 4-5 existing initial mechanisms of LLLT: thermal effect (heating of tissue), photodynamic one (activation of singlet oxygen), photochemical effect (direct photo-destruction of organic molecules), placebo effect and so on. One of the most popular biomedical effects at Low Level Laser Irradiation (LLLI) being mentioned in medical literature for justification of the healing outcome of LLLT is a stimulation of blood microcirculation in irradiated tissues. It is assumed that underneath the threshold of heating of the tissue at LLLI, there is the blood microcirculation stimulation due to different non-thermal photochemical processes. It was declared a priori at a dawn of LLLT and is now a basis of medical interpretation of the healing mechanisms of LLLT at least in Russia. But in past 20 years a lot of investigation was carried out on in vivo optical registration of microhemodynamics parameters as well as a number of noninvasive diagnostic tools was developed and created for that. So, today it is possible to check experimentally the hypothesis of the blood microcirculation stimulation at LLLI. Our study was aimed on that during the past 10 years. The more precision and accurate experiments we have carried out recently using simultaneously three different noninvasive diagnostic techniques: Laser Doppler Flowmetry (LDF), Tissue Reflectance Oximetry (TRO) and Infrared Thermography (IRT). A multifunctional noninvasive laser diagnostic system "LAKK-M" and the medical thermograph "IRTIS ME-2000" were used for that in our study. To carry out the LLLT procedures we used both the laser therapeutic device "ULAN-BL-20" (?=890 nm, the pulse mode up to 30 kHz pulse rate) and the physiotherapy laser system "ULF-1" (?=632 nm, continuous power mode of 20 mW). Both 10 healthy volunteers (authors of the paper in that number) and a number of real clinical patients with skin and mucosa blood microcirculation disorders were involved in the study. The main majority of the experiments were carried out at external LLLI of the skin and mucosa, but the intravenous laser irradiation of blood was explored as well. As a result, all these three diagnostic methods – LDF, TRO and IRT - didn't confirm that LLLI has unequivocal stimulating effect on the blood microcirculation system in skin or mucosa at irradiation with a power density below 50 mW/cm2 and irradiation time up to 5-6 minutes. Above this threshold the heating on 0,8...1,0 C of tissue in the field of irradiation and the corresponding synchronous increase of all parameters of microhemodynamics were observed authentically. So, today we have a quite proved opinion that the heating is the dominant mechanism of the LLLI actions on the blood microcirculation system.

9129-77, Session 14

Hypericin mediated photodestruction of collagen-based systems studied by multiphoton microscopy and fluorescence spectroscopy

Vladimir A. Hovhannisyan, Chen-Yuan Dong, National Taiwan Univ. (Taiwan)

Collagen is the main structural protein in higher vertebrates, and the key determinant of mechanical and functional properties of tissues and organs. Proper balance between synthesis and degradation of collagen molecules is critical for maintaining normal physiological functions. The importance of collagen is also mentioned in cancer treatment due to collagen-influenced tumor development and drug delivery. The damage and alteration of collagen in blood vessels can change delivery of the photosensitizer and molecular oxygen to tumor tissue, therefore the outcome of cancer photodynamic therapy (PDT). In PDT of superficial malignant tumors, such as skin and oral cancer, collagen-rich skin and oral mucosa determine the penetration depth of the photosensitizer and excitation light. Thus, the qualitative and quantitative characterization of collagen organization is important factor to optimize the treatment strategy of therapy of collagen-related disorders. Hypericin (Hyp), a natural pigment synthesized in plants of the Hypericum genus, has recently received increasing attention due to its high phototoxicity against viruses and its anti-tumor photoactivity. The PDT effect of Hyp has been demonstrated both in vitro and in vivo studies. The photophysical and photochemical properties of Hyp allow considering this pigment as a potent photosensitizer and fluorescent marker for PDT and clinic tumor diagnosis, respectively. Furthermore, Hyp exhibits a stronger affinity to collagen and may be an effective photosensitizer in collagen-rich tissues such as cornea or skin. Using second harmonic generation (SHG), two-photon excited fluorescence (TPEF) microscopy, and spectrofluorometry,

we show that Hyp induces a photosensitized destruction of collagen-based tissues. Spectrofluorimetric measurements reveal that UV (337 nm) and visible (532 nm) light can induce irreversible changes in Hyp-sensitized collagen from bovine Achilles tendon, chicken skin and artery. Dose-dependent decay and shift of maximum from 390 nm to 435 nm in collagen fluorescence spectrum indicat a photo-induced damage in the collagen-Hyp systems. Furthermore, it is demonstrated that the spectral profile of Hyp-photosensitized collagen is similar to that of gelatin and denatured collagen.

SHG and TPEF imaging provide additional evidence about Hyp-photosensitized modification of collagen. Very efficient generation of the SHG signal is observed in non-irradiated collagen that decreases under the light action. It must be stressed that no SHG is observed in gelatin due to its completely irregular coil structure. Spatially-resolved multiphoton imaging of Hyp-collagen interaction and the dynamic of light induced modification of Hyp-collagen system are studied for purified collagen and native collagen-based tissues (skin, tendon, and aorta). We demonstrate that Hyp–mediated changes in collagen fibers are irreversible and may be used for the treatment of cancer and collagen-related disorders. These properties of Hyp suggest that it can be considered as a native collagen photosensitizer for the treatment of cancer and collagen-related diseases. In addition, our results show that time-lapsed multiphoton imaging is capable of monitoring collagen photomodification. Also, results we obtained may be applied to research and development of new approaches in clinical areas such as skin resurfacing, wound healing, cancer treatment, and destruction of atherosclerotic plaques, as well as diagnostics and therapy of other collagen-related disorders.

9129-78, Session 14

Photophysical properties and antimicrobial activity of new metalloporphyrins

Anna G. Gyulkhandanyan, Institute of Biochemistry (Armenia); Elena S. Tuchina, N.G. Chernyshevsky Saratov State Univ. (Russian Federation); Robert K. Ghazaryan, Yerevan State Medical Univ. (Armenia); Marina H. Paronyan, Science and Production Ctr. 'Armbiotechnology' (Armenia); Grigor V. Gyulkhandanyan, Institute of Biochemistry (Armenia); Valery V. Tuchin, N.G. Chernyshevsky Saratov State Univ. (Russian Federation) and Univ. of Oulu (Finland)

Photodynamic inactivation of microorganisms by photosensitizers is one of the most promising areas for the destruction of antibiotic-resistant microorganisms. Previously, we studied a wide range of new cationic porphyrins, investigated their photophysical characteristics and identify the most promising of them to be used in biomedical applications. Generation of singlet oxygen is the determining criterion for the effective functioning of the porphyrins. It was found that the highest values of quantum yield of singlet oxygen (97%) possess Zn-containing metalloporphyrins.

Antibiotic-resistant strain of the microorganism Staphylococcus aureus (St. aureus) is the most dangerous microorganisms. In the U.S., the number of deaths due to methicillin-resistant strain St. aureus is equivalent to the total number of deaths from AIDS, tuberculosis and viral hepatitis. Two strains St. aureus 209 P and methicillin-resistant St. aureus were tested in this work. We have studied the effectiveness of four types of porphyrins: meso-tetra [4-N-(2'-oxyethtyl) pyridyl] porphyrin (TOEt4PyP)-(I); Zn-TOE4PyP-(II); Zn-meso-tetra [4-N-butyl pyridyl] porphyrin (Zn-TBut4PyP)-(III) and Zn-TBut3PyP-(IV).

It was found that against both strains of St.aureus the highest activity has metalloporphyrin (IV) when the concentration of metalloporphyrins was 0.01 ug/ml, which correlates with the received values of the quantum yields of singlet oxygen (97% for compounds III and IV). Destruction efficiency of microorganism St. aureus 209 P by compound (IV) in comparison with compound (I) was higher more than 8 times that would be expected from the values of quantum yield of singlet oxygen generation (for the compound (I) is 77%). Close results were also obtained for methicillin-resistant strain of St. aureus: in the same conditions, the highest efficiency was of the compound (IV) - 2.5 times higher than for the compound (I). Considering that the compounds (III) and (IV) are practically non-toxic, these compounds can be recommended for studies in vivo, with the aim of further clinical application.

9129-79, Session 14

Effect of near-infrared diode laser and indocyanine green to treat infections on different wound models

Nermin Topaloglu, Sahru Yueksel, Murat Gulsoy, Bogaziçi Üniv. (Turkey)

The emergence of antibiotic resistant bacteria causes significant increase in deaths due to wound infections around the world. Nowadays, it could be impossible to find appropriate antibiotics to treat some bacterial strains, especially multidrug resistant types. The aim of this study is to use photodynamic therapy that destroys these kinds of bacteria with the interaction of Indocyanine green (ICG) and 808-nm diode laser.

In this study, antibacterial Photodynamic Therapy technique that we call ICG-IR Laser PDT was applied on antibiotic-resistant strains of Staphylococcus aureus that infected two different types of wound model (excisional and abrasion wound model) in vivo. The main motivation to test ICG and 808-nm diode laser is that the near infrared laser has more penetration depth in the biological tissue than the other lasers have. Therefore it is supposed that it may show more antibacterial effect through the deeper tissue. However, laser light which irradiates in this spectrum may cause thermal destruction. Laser power, application duration have to be well-predicted and controlled.

Wistar albino rats were used to create animal wound models. Excisional or abrasion wounds were formed on the dorsal skin of the rats. They were infected with Staphylococcus aureus. 300 mW and 500 mW of 808-nm diode laser were applied on the wounds for 30 minutes and 15 minutes of exposure duration, respectively. ICG concentration applied topically was 1000 ug/ml. Then the tissue was dissected properly and homogenized in buffer solution. From this solution, bacterial cell count was determined by serial dilution method. 1-2 log reduction in viable cell count was observed after these applications. The temperature increase in the tissue was between 6-8 oC during these applications.

From these findings, it was understood that this method with 808-nm and ICG is promising but it must be improved by further dosimetry studies.

9129-80, Session 14

Determination of pulse energy dependence for skin denaturation from 585 nm fibre laser

Saúl Mújica-Ascencio, Jesús S. Velázquez-González, Ctr. de Investigación e Innovación Tecnológica (Mexico); César Mújica-Ascencio, IPN-ESCOM (Mexico); José Alfredo Álvarez-Chávez, Ctr. de Investigación e Innovación Tecnológica (Mexico)

In this paper, simulation and mathematical analysis for the determination of pulse energy from a Q-switched Yb3+-doped fiber laser that would be required in Port Wine Stain (PWS) treatment is presented. The pulse energy depends on average power, gain volume, repetition rate and pulse duration employed in some treatments such as Selective Photothermolysis (SP) and the peak power at the end of the optical fibre. Pulse duration and peak power can be obtained and modified from such an optical fibre laser. For that purpose, a 585 nm optical fibre laser full design which considers all of the above besides the average losses through the optical devices

proposed for the design and the Ytterbium optical fiber overall gain will be presented.

9129-81, Session 15

Improving performances of surface plasmon resonance imaging biosensors: real-time multi-spectral interrogation *(Invited Paper)*

Alexandra Sereda, Institut d'Optique Graduate School (France) and HORIBA Scientific (France); Julien Moreau, Michael T. Canva, Institut d'Optique Graduate School (France); Emmanuel Maillart, HORIBA Scientific (France)

Surface plasmon resonance (SPR) sensing is a powerful tool for biomedical applications, where real-time and label-free detection, as well as high throughput screening, are particularly needed. To meet these requirements, most SPR-based systems operate in a reflectivity interrogation mode (RIM), which provides real-time information on multiple biomolecular interactions in parallel on a biochip format. More precisely, the RIM is performed at a fixed wavelength and angle of incidence both chosen so to be close to the optimum sensitivity for one specific probe-target binding interaction. However, since several interactions are to be monitored simultaneously in practice, the choice of a unique operating point does not provide a homogeneous and optimal response over the entire bio-array analyzed. Therefore, some significant data dispersion can be observed, especially when different families of probes are spotted on the same biochip. Moreover, the response in the RIM is no longer linear for important buffer index changes, when working at a single operating point, which limits the dynamic of detection.

To overcome these limitations, SPR-based systems have turned to either angular or spectral interrogation modes, both offering accurate measurements through the monitoring of the plasmon dip shift. The resolution is then independent of the sample or the injected target solutions, and related directly to the experimental setup used to acquire the resonance profile as well as to the data processing performed to extract the plasmon dip position. In order to achieve a good precision on the plasmon dip position, several measurements have to be performed to acquire sufficient data on the angular or spectral resonance profile. In the case of spectral interrogation, the resonance profile can be obtained either by scanning the incident wavelength or using a spectrometer as the detector. However, while the former configuration allows maintaining a 2D imaging capability at the expense of the measurement rate, the latter provides instantaneous spectral information, but only for a limited portion of the biochip (1D-arrays). Therefore, combining spectral interrogation with an imaging system allowing high data throughput, while keeping a real-time measurement capability, is still a challenge.

In this contribution, we introduce a SPR multi-spectral imaging system combining spectral interrogation with both real-time and 2D imaging capabilities. Based on only five interrogation wavelengths, the presented method achieves a resolution of 2.10^(-6) RIU (or a minimum surface coverage detectable of around 1 pg.mm^(-2)), which equals some of the best SPR imaging systems. Moreover, the performances, both in terms of resolution and accuracy, are constant within a dynamic range of ±5.10^(-3) RIU of the surrounding media. We demonstrate experimentally that this allows significant gain in data quality compared to the RIM, where the optimal conditions are strongly dependent on the buffer index variations and the surface chemistry inhomogeneity. We believe that the developed technique would be particularly useful in multichannel fluidic experiments where target molecules are simultaneously delivered onto the gold surface in different buffer conditions. Furthermore, nanostructured gold biochips which usually exhibit broad plasmonic resonances leading to low RIM signals could take advantage of such an interrogation technique.

9129-82, Session 15

Measuring tissue oxygen saturation using NIR spectroscopy

Aslinur Sircan-Kucuksayan, Akdeniz Üniv. (Turkey); Mehmet Uyuklu, Bezmiâlem Vakif Üniv. (Turkey); Murat Canpolat, Akdeniz Üniv. (Turkey)

Tissue oxygen saturation (StO2) is known quite useful parameter for medical applications. A spectroscopic method has been developed to diagnose pathologic tissues due to lack of normal blood circulation by measuring tissue oxygen saturation. In the study, human blood samples with different level of oxygen saturations have been prepared and spectra were taken using an optical fiber probe to investigate correlation between the oxygen saturations and the spectra. The experimental set up for the spectroscopic measurements was consists of a miniature NIR light spectrometer, an optical fiber probe, a halogen-tungsten light source and a laptop. Spectra were acquired from the blood samples with a hematocrit of 40% and oxygenized 0, 30, 60, 90, 150 and 210 s to change their oxygen saturation level. A linear correlation between the oxygen saturation of the blood samples and the ratio of the light of wavelengths 660 nm to 790 nm has been found from the spectra. Then, oxygen saturations of the blood samples were estimated from the spectroscopic measurements within an error of 2.9%. Furthermore, it has been shown that the linear dependence between the ratio and the oxygen saturation of the blood samples was valid for the blood samples with different hematocrits. Tissue oxygen saturation has been estimated from the spectroscopic measurements were taken from the fingers of healthy volunteers using the correlation between the spectra and blood oxygen saturation. The tissue StO2 measured as 80% as expected. The technique developed to measure tissue oxygen saturation has potential to diagnose premalignant tissues, follow up prognosis of cancerous tissues, and evaluation of ischemia reperfusion tissues.

9129-83, Session 15

In-vivo continuous glucose monitoring using a chip based near infrared sensor

Lhoucine Ben Mohammadi, Susanne Sigloch, Ines Frese, Knut Welzel, Michael Goeddel, Thomas Klotzbuecher, Institut für Mikrotechnik Mainz GmbH (Germany)

Diabetes is a serious health condition considered to be one of the major healthcare epidemics of modern era. An effective treatment of this disease can be only achieved by reliable continuous information about the rate of change of blood glucose levels. In this work we present a minimally invasive, chip-based near infrared (NIR) sensor, combined with microdialysis, for continuous glucose monitoring (CGM). The sensor principle is based on difference absorption spectroscopy in the 1st overtone band of the near infrared spectrum. The device features a multi-emitter LED and InGaAs-Photodiodes, which are located on a single electronic board (non-disposable part), connected to a personal computer via Bluetooth. The disposable part consists of a chip containing the fluidic connections for microdialysis, two fluidic channels acting as optical transmission cells and total internally reflecting mirrors for in- and out-coupling of the LED light to the chip and to the detectors. The sensor is combined with an intravascular microdialysis to separate the glucose from the cells and proteins in the blood and operates without any chemical consumption. In vitro measurements showed a linear relationship between glucose concentration and the integrated difference signal with a coefficient of determination of 99 % in the relevant physiological concentration range from 0 to 400 mg/dl.

In vivo measurements on 10 patients showed that the NIR-CGM sensor data reflects the blood reference values adequately, if a proper calibration and signal drift compensation is applied. The MARE (mean absolute relative error) value taken over all

patient data is 13.8 %. The best achieved MARE value is at 4.8 %, whereas the worst is 25.8 %, with a standard deviation of 5.5 %.

9129-84, Session 15

Ex vivo optical characterization of in vivo grown tissues on dummy sensor implants using Double Integrating Spheres measurement

Sandeep Sharma, Mohammad Goodarzi, Ben Aernouts, Katholieke Univ. Leuven (Belgium); Karolen Gellynck, Lieven Vlaminck, Ronny Bockstaele, Maria Cornelissen, Univ. Gent (Belgium); Herman Ramon, Wouter Saeys, Katholieke Univ. Leuven (Belgium)

A glucose implantable sensor based on near infrared (NIR) spectroscopic measurements is expected to produce reliable glucose levels in human body for the long term to justify the surgical implantation procedure. Once implanted in body, the sensor will be influenced by surrounding biological environment. In context of glucose sensor, examples of such influences may include the growth of wound healing tissue encapsulating the sensor, and/or gradual growth of a thin tissue layer in the optical path of sensor over time. The former issue can be tackled by using bio-compatible polymeric materials which do not produce aggressive reaction in the body. Furthermore, the surface of such materials can be activated using antibodies which help to attract blood vessels and promote vascularization. However, no such remedy is available at hand to handle the growth of tissue layer in optical path of the sensor which might result in large variation in optical output. In a perfect world situation, this issue can be handled by increasing the input light signals, but for an implantable sensor, there are restrictions from power budget point of view ruling out the option of increasing light input. Most importantly, the output light signals depend on optical properties (especially scattering) of tissue layer grown in the optical path. In view of above, ex vivo optical characterization of wound healing tissues will be carried out.

For the purpose, the in vivo grown tissues were obtained from dummy implants placed surgically in selected animals (goats). Once the sensors were explanted, tissues grown on implant surface were removed and frozen rapidly using liquid nitrogen to preserve the tissue microstrcture. Immediately before measurement, the tissues were cut in thin slices of 1100 ?m, and 550 ?m thicknesses at -18°C. The samples were placed in a cuvette (30 mm diameter), and few drops of biological water (0.9% NaCl) was added to reduce the refractive index mismatch between sample and glass. The Double Integrating Spheres measurements were performed on these samples, and the values of total reflectance, and total transmittance were measured. A transmission setup was used to measured unscattered transmittance of samples. From these measurements, the bulk optical properties of tissues were estimated using Inverse Adding Doubling procedure. The results indicated that the tissues were non-homogenous, and there was high variation for tissue layers cut from the same tissue sample. From measuring glucose concentration, the combination band (2050-2400 nm) was found to be preferred choice than the first overtone wavelength range (1500-1850 nm).

9129-85, Session 15

Localized biomolecular sensing enabled through plasmonic nanocavities

Gaël D. Osowiecki, Elsie Barakat, Ali Naqavi, Hans Peter Herzig, Ecole Polytechnique Fédérale de Lausanne (Switzerland)

In sensor development, the sensitivity S is an important parameter to evaluate the sensor performance. Fundamentally, sensitivity is determined by the strength of the light-matter interaction. It is defined as the change of the magnitude of the sensor transduction signal in response to the change of the analyte. Another important parameter, the sensor Detection Limit (DL), expresses the sensor performance. It is defined as the ratio of the minimum detectable signal and the sensitivity. The sensitivity can be enhanced by increasing the light-matter interaction or the interaction length and the detection limit can be reduced by reducing the noise of the system.

In the case of a resonator, the effective light-matter interaction length is not only determined by the sensor's physical size, but also by the resonator quality factor (Q-factor) defined as the number of revolutions of the light contained in the resonator. There is a trade-off between the size of the cavity, the Q factor and the localization. We will show the scaling properties of photonic nanocavities (size versus performance) considering the factors Q and the sensing volume as well as the investigation of the coupling mechanisms of light into such nanostructures which are related to the coupling strength and coupling length.

We are using the property of light to travel as a bound electromagnetic mode along metal-dielectric interfaces. Surface plasmon polariton (SPP) have the ability to confine the light in the sub-wavelength regime thus beating the diffraction limit. Our experiences in integrated optical sensors using dielectric waveguides led us to a new type of hybrid photonic-plasmonic structure. The latter is a silicon strip waveguide vertically coupled to a cavity based on a plasmonic slot waveguide or also called metal-dielectric-metal (MDM) waveguide and separated by a silicon dioxide spacer. We will show the theoretical study of this sensor and explain the key elements needed to understand and optimize the strong coupling from the dielectric waveguide to the plasmonic slot waveguide cavity, thus enabling the ability to locally sense the change in refractive index with a very high sensitivity of around 600nm/RIU in femtoliter volume. These results are complete 3D FDTD simulations made with CST MWS. The sensing performance of the experimental devices produced to date will also been presented and compared to the theoretical results and the practical needs to achieve localized biomolecular sensing.

9129-86, Session 16

Development and potential applications of microarrays based on fluorescent nanocrystal-encoded beads for multiplexed cancer diagnostics *(Invited Paper)*

Kristina Brazhnik, National Research Nuclear Univ. MEPhI (Russian Federation); Regina Grinevich, Laboratory of Nano-Bioengineering, National Research Nuclear University "MEPhI (Russian Federation); Anton Efimov, SNOTRA, LLC. (Russian Federation); Igor R. Nabiev, Univ. de Reims Champagne-Ardenne (France) and National Research Nuclear Univ. MEPhI (Russian Federation); Alyona Sukhanova, Univ. de Reims Champagne-Ardenne (France) and National Research Nuclear Univ. MEPhI (Russian Federation)

Common approaches to multiplex analysis of biological samples employ solid-state two-dimensional planar arrays or liquid-state suspension arrays based on encoded microparticles. Both detection systems have their specific advantages and shortcomings. The liquid-state suspension arrays are easily modifiable to fit the analyzed target profiles and are characterized by fast binding kinetics and high sensitivity and quality of analysis. The development of multiplex suspension arrays is currently of particular interest for clinical diagnostics. This technology uses combinations of fluorophores incorporated into microbeads to obtain individual spectral codes. Fluorophore-encoded beads can be rapidly analyzed using classical flow cytometry. Specific characteristics of conventional organic dyes considerably restrict the number of their possible combinations, limiting the number of color sets in a detection array.

QDs have unique advantages over classical organic

fluorophores. These are, e.g., high extinction coefficients and, hence, a high brightness; narrow, symmetrical fluorescence peaks; the possibility to excite QDs of different colors with a single light source and a rock-stable photostability. Due to the unique spectral characteristics, QDs can act as efficient donors for Förster resonance energy transfer (FRET) to a suitable acceptor. This significantly improves the detection quality and increases the sensitivity of diagnostic assays. We have recently developed diagnostic suspension arrays for identification of specific autoantibodies in serum samples from systemic sclerosis patients. These benefits of FRET-based suspension arrays have been demonstrated experimentally.

In this study, we have designed a new, highly sensitive and specific diagnostic system based on QD-encoded microbeads to detect specific markers of prostate cancer and breast cancer. Preparation of optically encoded fluorescent microbeads suitable for immunodiagnostics is based on layer-by-layer electrostatic deposition of charged polymers onto the charged surface of polystyrene latex beads. Different molar ratio of water-soluble CdSe/ZnS QDs emitting in green (510-520 nm) and orange (570-590 nm) regions were used to deposit them between polymer layers. A huge amount of individual spectral codes of microbeads for biomolecule tagging could be obtained with this technology by using multiple color combinations.

We prepared multicolor sets of QD-encoded microbeads and bound capture Abs against different cancer biomarkers (PSA, CEA, and CA15-3) to their surfaces in a highly oriented manner. These biomarkers are generally found in serum of patients with prostate cancer and breast cancer. The capture Ab is bound to protein A or an adapter molecule chemically conjugated with the polymer shell of the microbead. Protein A binds the monoclonal Ab molecule in a highly oriented manner due to specific interaction with the Ab Fc-fragment. The proposed protocol prevents nonspecific binding and decreases the false positive signal in the case of using the Fc-specific F(ab)2-fragment as a labeled visualization agent. Microbeads linked to specific Abs have been calibrated with the recombinant antigens and used to test serum samples from cancer patients and compare results obtained for healthy donors. About 150-200 serum samples from patients with different stages of cancer and healthy donors were collected for quantitative analysis of cancer serum antigens. The data have been validated by comparison with the results of the “gold standard” ELISA.

The results obtained pave the way to development of multiplexed arrays based on QD-encoded beads as an advanced alternative to the conventional diagnostics of cancer markers, especially for very early diagnosis.

9129-87, Session 16

Photonic based teledentistry

Nicolas Giraudeau, Clément Roy, Bernard Levallois, Univ. Montpellier 1 (France); Herve Tassery, Univ. Montpellier 1 (France) and Aix-Marseille Univ. (France); Nicolas Molinari, CHRU de Montpellier (France); Frédéric J. G. Cuisinier, Univ. Montpellier 1 (France)

Use of Photonics systems increases in dentistry to help practitioners in caries and gingival inflammations diagnostics. Intraoral camera, specially the Soprocare® devices use fluorescence light excitation around 450nm to diagnose and treat dental caries and gingival inflammation. Fluorescent pictures or videos, recorded in real time in the Soproimaging software with high level of magnification, increase the quality and precision of the diagnostic steps and treatment procedures. Theses new technologies adapted for oral health policy can be applied and extend to a new paradigm in dentistry called teledentitry.

In order to validate teleconsultation versus classical consultation using visual inspection, 100 patients were recruited in Montpellier’s dental health center (ethic committee agreement). First step, visual dental consultation was run by one experimented practitioner (gold standard) who noted all decay, except wisdom teeth and gave oral health recommendations if needed. Second steps the same patient was observed and recorded by a second practitioner, with the intraoral camera device specially the occlusal, vestibular and palatal surfaces of each tooth in Cario and Perio modes. Third steps the last practitioner completed the oral exam thanks to the pictures and videos recorded. Comparison of visual inspection and teleconsultation were then performed the patient needs and both diagnostics compared.

In France, residents of medico-social establishments, with reduced mobility or not, have limited access to a dental practitioner. Indeed, different public investigations validated that around 86,2% of residents had no oral consultation since 12 months (South of France) and nearly 42% had no oral consultation since 5 years (Essonne department). On the national level, 35% of residents with residual teeth need conservative dentistry, without including the others needs in oral health. Teledentistry was developed specially for these populations and others medical applications should be expanded.

9129-88, Session 16

New strategies for luminescence thermometry in the biological range using upconverting nanoparticles

Oleksandr A. Savchuk, Joan J. Carvajal Marti, Maria Cinta Pujol Baiges, Jaume Massons, Univ. Rovira i Virgili (Spain); Patricia Haro-González, Daniel Jaque Garcia, Univ. Autónoma de Madrid (Spain); Magdalena Aguilò Diaz, Francesc Díaz, Univ. Rovira i Virgili (Spain)

Upconversion (UC) is a process in which the sequential absorption of two or more photons with short energies, typically in the near infrared (NIR), leads to the emission of light, typically in the visible, at shorter wavelengths than the excitation wavelengths, through mechanisms of excited state absorption (ESA) or energy transfer upconversion (ETU) using physically existing intermediary energy states of lanthanide ions, principally. This method encompasses benefits of high conversion efficiency without the need for intense coherent excitation sources, with the inherent advantages of large anti-Stokes shifts, sharp emission bandwidths, and long excited-state lifetimes. For these reasons has attracted interest in the fields of physics, chemistry, materials and life sciences because of their broad potential applications, including color displays, optoelectronics, sensor technology, laser cooling, data storage, solar cells, biological labelling, in-vivo imaging, and therapeutics, among others, and also more recently temperature determination through luminescence thermometry techniques.

The only luminescence thermometry technique used up to now involving upconversion nanoparticles covering the biological range of temperatures has been the fluorescence intensity ratio (FIR) technique. This technique consists in analyzing the change of intensity of the emission originating from two thermally coupled electronic levels of lanthanide ions as the temperature changes. For determination of temperature in the biological range only two lanthanide ions, and two materials have been used: Er3+, Yb3+ codoped NaYF4 nanoparticles and Tm3+, Yb3+ codoped CaF2 nanoparticles, providing a good relative sensitivity of the order of 2.3 % K-1.

Here we analyze alternative luminescence thermometry techniques to FIR, such as lifetime luminescence nanothermometry and intensity ratio luminescence thermometry between the emission arising from two electronic levels that are not necessarily thermally coupled, but that show different evolutions with temperature in (Er, Yb):NaYF4, (Er, Yb):NaY2F5O and (Ho, Tm, Yb):KLu(WO4)2 nanoparticles. This is the first time that lifetime luminescence nanothermometry has been demonstrated using upconverting nanoparticles. The thermal sensitivity achieved is similar to that one achieved when quantum dots are used, which demonstrate the potentiality of these materials in this kind of thermometry. We proved the practical applications of this technique by determining the temperature in ex-vivo experiments in chicken breast. The

second technique tested shows higher sensitivity values than conventional FIR, and a linear evolution with temperature, which facilitates calibration procedures. Also, by testing non-halide based nanoparticles, we want to present suitable alternatives to halide-based materials, which are usually hygroscopic and show relatively poor chemical and photophysical stabilities compared with oxide matrices. This is especially important when dealing with biological samples, for which the release of harmful chemical elements has to be prevented. Furthermore, most of the preparative routes for lanthanide-doped halide-based upconverting nanoparticles are complex and often environmentally harmful. Instead, (Ho, Tm,

Yb):KLu(WO4)2 nanoparticles can be prepared by a simple sol-gel method. By combining these nanoparticles with graphene nanosheets we provide multiple functionalities in which graphene nanosheets act as nanoheaters, while (Ho, Tm, Yb):KLu(WO4)2 nanoparticles act as luminescent nanothermometers.

9129-90, Session 16

Quantifying immune deficiency at the primary health care level

Anil Prabhakar, Indian Institute of Technology Madras (India);
Taslimarif Saiyed, National Ctr. for Biological Sciences (India)

Understanding and quantifying immune deficiencies in rural and semi-urban areas in India has many potential benefits. A low cost indigenous point-of-care (PoC) device can quickly decide whether the individual must seek assistance at a secondary or tertiary care centre. The CD4+T cell count, more commonly called the white blood cell count, is a measure of the human immune system. CD4 is glycoprotein that is found on the surface of immune cells, and we propose using an opto-fluidic flow analyzer to count the number of CD4 molecules in a blood sample. When compared to a conventional flow analyzer system, the opto-fluidic system has the advantage of being able to act as a PoC device, easy to maintain and with simple usage protocols.

Flow analyzers typically use a combination of forward scatter (FSC) and side scatter (SSC) to differentiate between different types of cells. Molecules that are tagged with fluorophores are then used to study the chemistry of the cells. We have designed an opto-fluidic system that combines all three functionalities (FSC, SSC and fluorescence), while using hydrodynamic focusing of the sample liquid to ensure single cell excitation and minimize false positives. Key optical technologies that have been incorporated into the design include the use of high power pulsed lasers, gated avalanche photodetection for improved signal to noise ratio, lensed fibres for better excitation and capture of photons, and fibre Bragg grating filters for excitation wavelength rejection. A PIC microcontroller based digital board is used to control the different functionalities of the device, and also to estimate cell velocities in the flow channel. Most of the optoelectronics used are commonplace in the world of telecommunications, and adapting them to healthcare systems provides the necessary cost advantages while ensuring reliability in the measurement.

9130-1, Session 1

Thermally tunable optical aperture based on a segmented thin-film resonator

Hendrik Block, Philipp Metz, Jost Adam, Martina Gerken, Christian-Albrechts-Univ. zu Kiel (Germany)

Apertures are basic elements found in almost any optical system. Since optical systems are continuously being miniaturised and integrated, there is a need for small and inexpensive apertures to control beam shape and intensity. Scaling down macroscopic lamella apertures has led to micro-electro-mechanic (MEMS) lamella systems moved by electrostatic forces. However, MEMS apertures still consist of moving parts and therefore space for their operation has to be provided in the system. We demonstrate an aperture concept for single-wavelength operation based on thermal tuning of a segmented thin-film resonator. Thermal tuning changes the optical thickness of the elastomer cavity material. This allows for adjusting the intensity to any level between constructive and destructive interference in a specific aperture segment.

The optical cavity is formed by a polydimetylsiloxane (PDMS) thin film sandwiched between semi-transparent silver layers on top of a glass substrate. The top silver mirror layer is structured in separate sections. Applying an electric current to a specific section generates resistive losses in the silver and causes thermal expansion of the PDMS. Section shaping and the amount of electric current in each section determine the light beam's shape and the intensity distribution, respectively. In order to demonstrate the aperture operation, we simulate thermal, mechanical, and optical properties of the apertures using finite-element-method (FEM) and transfer-matrix-method (TMM) calculations. We confirm our simulation results by experimental beam shape measurements as well as spatially-resolved spectral transmission and light intensity measurements.

The segmented thin-film aperture allows for on-chip integration for beam shaping and intensity control in future laser applications. This approach combines a rugged design due to deformations only in wavelength dimensions with the possibility of wafer-level fabrication with standard thin-film processes.

9130-2, Session 1

3D optimization of a polymer MOEMS for active focusing of VCSEL beam

Sami Abada, Thierry Camps, Benjamin Reig, Jean-Baptiste Doucet, Lab. d'Analyse et d'Architecture des Systèmes (France) and Univ. de Toulouse (France); Emmanuelle Daran, Lab. d'Analyse et d'Architecture des Systèmes (France); Veronique Bardinal, Lab. d'Analyse et d'Architecture des Systèmes (France) and Univ. de Toulouse (France)

Active control of laser beam is a key issue to improve the integration of VCSELs in optical interconnects or in compact sensors. With this aim, the authors previously reported the fabrication of a new type of polymer-based actuator that can be directly integrated on a VCSEL for vertical beam scanning. Its operation principle is based on the vertical displacement of a SU-8 membrane including a polymer microlens. Under an applied thermal gradient, the membrane is shifted vertically due to thermal expansion in the actuation arms induced by Joule effect. This leads to a modification of microlens position and thus to a vertical scan of the laser beam. Membrane vertical displacements as high as 8μm for only 3V applied were recently obtained [1]. To explain these outstanding performances, we have developed a comprehensive tri-dimensional thermo-mechanical model that takes into account SU-8 material properties and precise MOEMS geometry.

As a vertical displacement is involved, SU-8 transverse anisotropy in terms of Young modulus, Poisson coefficient and thermal expansion coefficients had to be considered [2]. Out-of-plane mechanical coefficients and thermal conductivity were thus integrated in our 3D model (COMSOL Multiphysics) as well as their thermal variation. Thanks to these refinements, exact calculation of heat distribution and deformation profile in the complete structure was performed. Vertical displacements extracted from these data for different actuation powers were successfully compared to experimental values, validating this modeling tool. Thereby, we have exploited it to further increase MOEMS performances and to reduce design sensitivity to possible misalignments. Finally, hysteresis of displacement due to thermal inertia has been also minimized.

[1] B Reig "2012 J. Micromech. Microeng. 22 065006.

[2] R. Feng, R. J. Farris, Journal of Material Science 37 (2002) 4793 – 4799

9130-3, Session 1

An endoscopic microscope with liquid-tunable aspheric lenses for continuous zoom capability

Pengpeng Zhao, Albert-Ludwigs-Univ. Freiburg (Germany)

Continuous optical zoom is an enabling feature for an endoscopic microscope system designed to combine high resolution and large field-of-view (FOV) imaging. However, it is very challenging to implement such zoom optics within an endoscopic system due to the stringent size limitations. Conventional zoom microscopes employ translating lenses to modify the effective focal length of the system. One or more of these active lenses might be necessary to attain the desired zoom range. The tight area budget of an endoscopic probe is therefore shared between the footprint of the actuator and the optical aperture. In recent years, there have been several efforts to implement zoom microscope modules using liquid tunable lenses to overcome this limitation. Comprised of a chamber sealed with an elastic membrane and a fluidic interface, these lenses combine the optical functionality within the actuator itself and allow optically efficient use of the available system aperture. However, despite their great potential, little work has been devoted to the study and improvement of the optical quality of these lenses, which usually suffer from spherical and other optical aberrations. In principle, aspherical tunable lenses can correct for these effects and also help reduce the total length of the optical system. On the other hand, a systematic approach to design tunable aspherical optical components has hitherto not been attempted.

In this paper, we propose a miniaturized continuous zoom microscope design with an optical aperture of 1.5 mm featuring two liquid-tunable aspheric lenses for optical zoom and two fixed lenses for aberration and color dispersion correction. The continuous magnification range of the system is from 1.5 to 3.5 using a 1x1 mm CCD as the imaging element. With a fixed object distance smaller than 5 mm, the total length of the system is less than 8mm. All of the optical components are compatible with the micro-optical bench technology previously developed in our group. This technology allows alignment and assembly of complex optical systems with < 5 μm accuracy while maintaining optical and microfluidic interfaces to the individual components.

The aspherical tunable lens is formed by a liquid-filled cavity which is sealed with a PDMS membrane of non-uniform thickness. The main opto-mechanical challenge in the lens design is the determination of the precise membrane thickness profile that deforms into the desired lens shape under uniform load exerted by the liquid pressure. This is achieved through an iterative process. Once the aspherical lens shape is determined after the system optimization with Code V, the corresponding membrane thickness function is analytically calculated. This profile is then analyzed using finite element analysis simulations, and the results are imported back into Code V to re-optimize the optical system using the actual lens profiles. In this paper, we will present a detailed account of the tunable aspherical

lens design procedure, and system optimization through optical simulations. The zoom system performance will be compared with that achievable using conventional designs to illustrate the effectiveness of the novel approach. Microfabrication methods to implement the tunable aspherical lenses will also be discussed.

9130-4, Session 1

Design and fabrication of multiple airgap-based visible filters

Mohammadamir Ghaderi, Reinoud F. Wolffenbuttel, Technische Univ. Delft (Netherlands)

The efficiency in the design of Bragg mirrors for implementation in optical resonators is strongly dependent on the ratio between the high-index material and the low-index material (i.e. the index of refraction contrast) used for the quarter wavelength (QWOT) layers. A higher contrast implies that fewer layers are required for achieving a specified spectral selectivity. The reduced total thickness of the filter stack in turn reduces the effect of optical absorption in the layers. The research presented here is focused on implementation of filters on top of silicon detectors that are already fabricated in a CMOS process. This implies that the constraints of process compatibility, such as materials to be used, process temperature and cleanroom re-entrance related to contamination are applicable.

The set of materials available for optical filters is limited. Silicon-dioxide is often used in CMOS-compatible designs, which has an index of refraction n~ 1.5, thus limiting nHi/nLo to about 2. This value can be improved by 50% when using air-films as the low-n material. Surface micromachining has been used for the fabrication of such mirrors. Multiple layers of TiO2 and SiO2 have been alternatingly deposited, and subsequently the SiO2 layers are selectively removed in a sacrificial etch. The width of the Lambda/4 air-gaps is about 150 nm, which is well within the range of layer thickness that can be fabricated in surface micromachining. Since the number of stacked layers is significantly higher as compared to the conventional MEMS applications, fabricating such filters is a challenge. However, the fact that, the optical application does not require electrical contact to the structural layers, eases the fabrication of such filters unlike conventional MEMS devices.

The generic air-gap filter has already been demonstrated in the near-IR, where wider air-gaps are required. This paper presents the design of several 4-layer structures for use in the visible spectral range, along with the fabrication sequence and optical measurement results.

9130-5, Session 1

Integrated electrochromic aperture diaphragm

Tobias Deutschmann, Egbert Oesterschulze, Technische Univ. Kaiserslautern (Germany)

In recent years, the triumphal march of handheld electronics with integrated cameras has opened great possibilities for small high performing optical systems. For this purpose miniaturized iris apertures are of practical importance because they are essential to control both the dynamic range of the imaging system and the depth of focus. Therefore, we invented a micro optical iris based on an electrochromic (EC) material. This material changes its absorption in response to an applied voltage. A coaxial arrangement of rings of the EC material is used to establish an iris aperture without the need of any mechanical moving parts. The advantages of this device do not only arise from the space-saving design with a thickness of the device layer of 50μm. But it also benefits from low power consumption. In fact, its transmission state is stable in an open circuit, phrased memory effect. Only changes of the absorption require a voltage of up to 3V. In contrast to mechanical iris apertures the absorption may be controlled on an analog scale offering the opportunity for apodization. These properties make our device the ideal candidate for battery powered and space-saving systems.

We present optical measurements concerning control of the transmitted intensity and depth of focus, and studies dealing with switching times, light scattering, and stability. While the EC polymer used in this study still has limitations regarding color and contrast, the presented device features all functions of an iris aperture. In contrast to conventional devices it also offers some special features. Owing to the variable chemistry of the EC material, its spectral response may be adjusted to certain applications like color filtering in different spectral regimes (UV, optical range, infrared). Furthermore, all segments may be switched individually to establish functions like spatial Fourier filtering or lateral tunable intensity filters.

9130-6, Session 1

Analysis of effect of single and multiple micro-ring resonators as an optical filter using the Mason's gain formula

Santosh Kumar, Ajay Kumar, Sanjeev Kumar Raghuwanhsi, Indian School of Mines (India)

Micro-ring resonators are the most important devices applicable for optical filtering phenomena. The paper provides the detailed description of general characteristics of serially coupled multiple ring resonator (SMRR). The identical perimeters and coupling coefficients provides the pass band characteristics with flatter top. The paper includes the concept of Masons gain formula and its application in order to analyze the transfer characteristics of single and multiple ring resonator structures. The graphical approach provides the fast derivation of transfer function of SMRR. We have implemented the graphical method for the analysis of transfer function of serially coupled ring resonator structures. The paper describes the transfer characteristics of single, double and ripples ring resonator structures as optical filters. Graphical method with signal flow graph (SFG) is applied for analysis, which provides the fast derivation of optical transfer function. A flatter top is achieved for serially coupled double ring resonator (SDRR) and serially coupled triple ring resonator (STRR) filters. The influence of optical loss in SDRR and STRR is studied and we found that it deforms the box like shapes in the pass band and resonant peaks. The results are properly verified with the MATLAB simulation.

9130-7, Session 2

Wide band, wide angular width wire-grid polarizer using galvanic growth technology

Yves Jourlin, Lab. Hubert Curien (France) and Univ. de Lyon (France); Markus Guttmann, Karlsruher Institut für Technologie (Germany); Frédéric Lacour, Exxelia Group Eurofarad (France); Janne Laukkanen, Univ. of Eastern Finland (Finland); Koceila Yadel, Frédéric Celle, Colette Veillas, Thomas Kämpfe, Lab. Hubert Curien (France) and Univ. de Lyon (France); Olivier Parriaux, Lab. Hubert Curien (France) and Univ. de Lyon (France); Barbara Mathis, Karlsruher Institut für Technologie (Germany)

Functional demonstration of a wide band, wide angular width "wire-grid polarizer" has been made in the frame work of a User Project of the European project ACTMOST (Access To Micro-Optics Expertise, Services and Technologies). The polarization function relies upon linear polarizers using the "wire-grid" polarizer principle by means of a metal grating of unusually large period, exhibiting a large extinction of the transmission of the TE polarization in the 850 nm wavelength range. This grating achieves a broadband and especially high angular aperture reflection with low loss and permits resorting

to very low cost incoherent light sources of the transmitted TM polarization.

The paper will describe the design, the modeling optimization, and the complete technological process chain which has been used: from the photoresist grating printing using lithography to the uniform galvanic growth of very shallow gold grating on transparent conductive layer on glass substrate. Transmission curves for both polarizations on the first demonstrators will be presented.

9130-8, Session 2

Complex refractive index measurements of double-cylinder structures found in natural spider silks

Douglas J. Little, Deborah M. Kane, Macquarie Univ. (Australia)

The silk of certain spider species is a compelling protein-based material for research into its fundamental optical properties. This is due to the self assembly and biocompatibility properties, and the potential for such study to lead to approaches for customizing optical properties of self assembled protein-based material more generally. Most photonics research on silk to date has been based on silk fibroin solution; however the use of naturally spun silks have been earmarked for potential use as well. Using natural silks eliminates many of the processing steps required with silk fibroin, and the spun silk has a diameter ranging from 1-10 microns, making it useful for miniaturized optical interconnects and sensing.

One challenge of using natural silks may be the natural variability in optical properties from silk-to-silk, which needs to be characterised. To facilitate the use of natural silks in micro-optical components, we have developed a technique for determining the complex refractive index of silks by refracting light through the silk (which is immersed in a liquid of known refractive index) and observing the resultant irradiance pattern using a standard optical microscope. A measurement precision of 0.0005 is demonstrated for the real component of the refractive index. Measurements can be made across any wavelength provided the intensity of the illumination and the response of the camera is sufficient. The technique is also applicable to micro-optics more generally.

The particular interest in certain spider silks is also because they possess remarkable mechanical properties in addition to excellent optical properties. Spider silks are highly extensible and possess high tensile strength and so are incredibly robust optical materials. Spider silks are characteristically birefringent and possess a double cylinder structure, so we have tailored the above approach to be able to measure both principal birefringent refractive indices for each cylinder. Variation in the real and imaginary refractive indices with wavelength and contrasts in the properties between the two cylinders will be presented and discussed. The power of the technique for application to micro-optics more generally will be demonstrated.

9130-9, Session 2

Determination of thermo-optic properties of atomic layer deposited thin TiO2 films for athermal resonant waveguide gratings by spectroscopic ellipsometry

Muhammad Rizwan Saleem, Rizwan Ali, Seppo K. Honkanen, Jari Turunen, Univ. of Eastern Finland (Finland)

The environmental conditions, e.g., temperature and moisture have significant effects on the performance of today's miniaturized Photonics devices. These devices utilize various types of thin films, e.g., TiO2 thin films in our case. Although TiO2 thin films feature excellent optical properties, they are unfortunately affected by these environmental conditions, which subsequently deteriorate the functionality of the devices. TiO2 thin films fabricated by Atomic Layer Deposition (ALD) are hydrophilic and adsorb water molecules on the near surface region of the films. Due to temperature change they vaporize, causing the reduction of density and refractive index of the film.

We have earlier reported that ALD–TiO2 films with thicknesses < 200 nm exhibit negative dn/dT values, i.e., the decrease in film's refractive index with temperature. This kind of TiO2 films' behavior has certain advantages and disadvantages: an advantage in a sense that it can be employed in sensing devices where a change in material's refractive index/density with temperature is required; a disadvantage as an instability of the spectral shift of the resonance reflectance peak, due to change in temperature, in guided mode resonant (GMR) gratings. On the other hand, ALD–TiO2 films with thicknesses > 200 nm have positive dn/dT values, which means that there is no significant effect on the optical properties of these films with temperature. They can act as impermeable barrier layers and play a key role in the functioning of various optical devices.

We demonstrate improvements in thermo-optical properties of ultra-thin ALD–TiO2 films (thicknesses < 200 nm) and corresponding functionality of different optical devices by exploring the thermo-optical properties of inorganic ALD–Al2O3 barrier layers of various thicknesses. We show that the amorphous ALD–Al2O3 films of different thicknesses have positive dn/dT values and have the ability to withstand harsh conditions and find applications in different regimes of Photonics. We show improvement in the performance of various optical devices in terms of their operation stability by exploring the concept of ALD–TiO2 and ALD–Al2O3 bi-layers. The ALD–Al2O3 films act as impermeable inorganic barrier layers and fill not only the pores/holes or any other defects on ALD–TiO2 films' surface, but they also help in turning the negative thermo-optic behavior to positive. In our study, we fabricated three different sets of ALD–TiO2 and ALD–Al2O3 films, consisting of two bi-layers and one single layer set. We utilized variable angle spectroscopic ellipsometry for the characterization of three different sets of samples by employing a wide spectral range 380 ≤?≤ 1800, two angles of incidence, 65° and 75°, and a wide temperature range from room temperature to 155 °C. We used Cauchy model to extract the wavelength and temperature dependent optical data n=n(?,T) and subsequent modeling with Lorentz-Lorenz relation for calculating the temperature-dependent optical (dn/dT) and density (d?/dT) coefficients. Based on the results obtained, we propose that thickness controlled combinations of ultra-thin ALD–TiO2 and ALD–Al2O3 bi-layers can be used in a variety of applications where permeable behavior of unwanted components has significant effects.

9130-10, Session 2

Printing on demand of polymer micro lenses array

Sara Coppola, Istituto Nazionale di Ottica (Italy); Immacolata A. Grimaldi, Fausta Loffredo, ENEA (Italy); Fulvia Villani, Istituto Nazionale di Ottica (Italy); Giuseppe Nenna, Carla Minarini, ENEA (Italy); Veronica Vespini, Lisa Miccio, Simonetta Grilli, Pietro Ferraro, Istituto Nazionale di Ottica (Italy)

Microlenses are nowadays being incorporated in many devices with a large area of application fields. In fact in the recent years, a lot of commercial applications such as optoelectronics, photonic and biomedical devices, as well as image processing require the fabrication of adaptive and adjustable microlens array. For that reason a lot of attempts have been conducted in order to support the growing interest in the production of lens arrays for sensors or optical communications devices for parallel data transmission. Several fabrication techniques and a large variety of process have been proposed for polymer based microlenses but the preparation of moulds, masks or metal layers with very accurate dimensions and shapes is generally required. The drawbacks and the rigidity of template-based manufacturing processes strongly stimulated the investigation of alternative and direct approaches such as those based on printing techniques. In this work a novel nozzle-less approach

is applied for the fabrication of tunable size microlens arrays exploiting the pyro-electrohydrodynamic (Pyro-EHD) effect activated onto a ferroelectric crystal (Lithium Niobate). Different polymer solvent mixtures were investigated for the realization of the microstructures. Experiments were conducted in order to improve the printing process in terms of precision and ink properties. The pyro-dispensing process show great flexibility making possible the formation of polymer microlens arrays overpassing the viscosity border of the conventional ink-jet printing systems and working in a nozzle-less modality. Controlling the experimental parameters tunable arrays of microlenses were produced in a direct way; the experiments were carried out at room temperature and in air atmosphere. Their optical quality and the geometrical features were investigated by profilometric and interferometric analysis.

9130-11, Session 2

Wavefront sensor sampling plane fabricated by maskless grayscale lithography

Giuseppe A. Cirino, Univ. Federal de São Carlos (Brazil); Felipe T. Amaral, UFMG (Brazil); Sergio A. Lopera, Univ. de São Paulo (Brazil); Arlindo N. Montagnoli, UFSCAR (Brazil); Aparecido Arruda, Independent Consultant (Brazil); Ronaldo D. Mansano, Univ. de São Paulo (Brazil); Tayeb Mohammed-Brahim, Univ. de Rennes 1 (France); Davies W. de Lima Monteiro, UFMG (Brazil)

In this work we report on the design and characterization of Shack-Hartmann wavefront sampling plane based on a microlens array (MLA) with 12 X 12 hexagonal contiguous diffractive lenslets, a pitch of 355 ?m, a focal length of 4.5 mm, and lateral dimensions 4.3 X 4.3 mm2. The device was fabricated by maskless grayscale lithography. Preliminary optical characterization was carried out using a He-Ne laser source (? = 633 nm), by evaluating the intensity distribution of all spots generated at the MLA focal plane, IMAX, as well as their sharpness by measuring full width at half maximum (FWHM) intensity values. The average resulting values were FWHM_AVG = 16 ± 1.4 ?m and IMAX_AVG = 0.83 ± 0.05 a.u. AFM characterization was performed within a region 10 X 10 ?m2 comprising the center of a microlens and the resulting RMS roughness was 6.87 nm (? / 92). A comparison between theoretical and measured intensity profiles at the MLA focal plane was also carried out. A good correspondence between the results was found. An effective optical characterization was carried out (also at ? = 633 nm) in order to determine wavefront aberrations from Zernike polynomials by introducing a wavefront with a well-known induced aberration, such as defocus or spherical aberration. For the wavefront reconstruction, the modal approach was used, in which the first derivatives of Zernike polynomials are used as the set of orthogonal basis functions. The corresponding polynomial coefficients up to the first 10 Zernike terms were obtained and the resulting reconstructed wavefront presents an RMS reconstruction error compliant to most optical systems of interest. These results are acceptable for most applications including lens aberrations characterization and adaptive optics for astronomical studies.

9130-12, Session 2

Microfabrication and characterization of single-mask silicon microlens arrays for the IR spectra

Pablo Nunes Agra Belmonte, Davies W. de Lima Monteiro, UFMG (Brazil); Rodolfo Felipe de Oliveira Costa, Mediphacos Researcher (Brazil) and UFMG (Brazil); Paddy French, Gregory Pandraud, Technische Univ. Delft (Netherlands)

Microlenses Arrays in Silicon are suitable for an important range within the IR spectrum, since silicon features relatively high refractive index and is transparent at the aimed wavelengths [1,2,3], leading to microlenses with focal length short enough to allow compact systems [4], offering an alternative for applications where miniaturization and reduction of alignment and packaging costs are necessary [1]. The Microlenses are meant to sample and focus an IR beam on a focal plane array, which might be an image sensor, or a dedicated IR sensor, as for instance Lab-on-chip, or selective gas detection system. Nowadays refractive microlenses are manufactured using sophisticated techniques with relatively high costs and complexity of well controlled steps, like thermal reflow [5,6], and grayscale lithography [7]. We hereby propose a new solution for microfabrication of Silicon Microlens Arrays, with one single-mask step using KOH anisotropic etching of Si [8]. The proposed technique solves many current demands, like achieving high reproducibility, fill-factor close to 100%, and higher precision of focal axis alignment. We have made optical profilometric measurements to estimate the shape, roughness and the focal distance. We have also observed the focal points imaging in the IR spectrum, proving that the silicon microlenses actually yield the results expected.

[1] SUSS MicroOptics. (2013). Retrieved from SUSS MicroOptics: http://www.suss.com/fileadmin/user_upload/brochures/SMO_catalog.pdf

[2] A. Ghosh, P. B. (2004). Broad band antireflection coating on silicon from 1.5 to 6?m spectral band. Infrared Physics & Technology, pp. 408-411.

[3] Ipek Girgin KAVAKLI, K. K. (2002). Single and Double-Layer Antireflection Coatings on Silicon. Turk J Phys, 349 – 354

[4] Yan Jianhua(???), O. W. (2012). Fabrication of a 100% fill-factor silicon microlens array. Journal of Semiconductors, pp. Vol. 33, No. 3.

[5] Popovic Z D, Sprague R A, Connell G A N. Technique for mono-lithic fabrication of microlens arrays. Appl Opt, 1988, 27: 1281

[6] Yan Jianhua, Ou Wen, Ou Yi. Fabrication of a 100% fill-factor silicon microlens array. Journal of Semiconductors, Vol. 33, No. 3, 034008

[7] Yao J, Su J, Du J, Zhang Y, Gao F, Gao F, Guo Y and Cui Z 2000 Coding grey-tone mask for refractive microlens fabricationMicroelectron. Eng.53531–4

[8] D. W. de Lima Monteiro, O. Akhzar-mehr, P. M. Sarro and G. Vdovin, Single-mask microfabrication of aspherical optics using KOH anisotropic etching of Si, Optics Express, 18 ,11 (2003).

9130-37, Session PS1

Approach of pullulan derivatives to resist polymers for green lithography in eco-friendly optical NEMS and MEMS

Satoshi Takei, Toyama Prefectural Univ. (Japan); Akihiro Oshima, Osaka University (Japan); Kenta Ito, Kigenn Sugahara, Toyama Prefectural Univ. (Japan); Miki Kashiwakura, Osaka University (Japan); Tomoko G. Oyama, Japan Atomic Energy Agency (Japan); Takahiro Kozawa, Seiichi Tagawa, Osaka University (Japan); Makoto Hanabata, Toyama Prefectural Univ. (Japan)

This presentation reported an approach of glucose derivatives to resist polymers for eco-friendly optical NEMS and MEMS. The material design concept to use the water-soluble resist material with highly efficient crosslinking, water development, and lower film thickness shrinkage was proposed for green lithography. The lithographic properties due to the glucose derivatives, and the low film thickness shrinkage due to distinctive bulky chemical structure were proposed in the resist material, and then demonstrated to be effective for creating high resolution, excellent patterning dimensional accuracy, and low line edge roughness in EB lithography. Mixing or blending of glucose and cellulose derivatives was a valuable approach to the design of resist formulations for eco-friendly optical NEMS and MEMS.

9130-38, Session PS1

Progressive phase conjugation and its application in reconfigurable spatial-mode extraction and conversion

Atsushi Okamoto, Tomohiro Maeda, Yuki Hirasaki, Akihisa Tomita, Hokkaido Univ. (Japan); Kunihiro Sato, Hokkai-Gakuen Univ. (Japan)

We develop a new technology, which is referred to as progressive phase conjugation (PPC), in which phase conjugation is electrically performed without requiring a coherent reference beam by fusion using a reference-free spatial phase detection and spatial phase modulation. Unlike the conventional digital phase conjugation, the PPC can obtain a phase-conjugate beam by only preparing the signal beam to be phase reversed; thus, the PPC can electrically realize a function similar to the self-pumped optical phase conjugator using a photorefractive crystal. This method enables remote setting of a phase detector from the signal transmitter without an additional transmission line for the reference beam. It also enables realization of high-speed and dynamic wavefront compensation owing to its open-loop architecture using the single-shot phase detection method. Therefore, the PPC is applicable to a wide range of optical communication technologies, including the reconfigurable spatial-mode extraction and conversion of mode transmission in a multi-mode fiber (MMF).

In our PPC experiment, first, a reference-free spatial phase detector is constructed by combining a spatial filtering method with holographic diversity interferometry (HDI), a system that combines information from two spatially dispersed image sensors to detect the complex amplitude of light signals. In HDI, the optical phase is measured in the signal at the same observation time and location, thus enabling high-speed and highly accurate phase detection in a single measurement without spatial interpolation. Next, the spatial phase modulation is applied to the signal by a spatial light modulator (SLM) using the detection results obtained from the reference-free HDI.

In our optical setup, spatial modes are generated by directing a 532-nm-wavelength laser beam into a MMF with a 50-micron core diameter. At the output side of the optical fiber, the phase distributions of the spatial modes are detected using the HDI constructed using two CCD imagers with a 1280 x 960 pixel array. Then, the phase conjugate distribution of the detected phase pattern is displayed on a LCOS-type SLM with 800 x 600 pixels. In this case, only when the same phase pattern that emerges from the optical fiber is incident on the SLM, the wavefront of the mode beam is converted into a plane wave. The plane wave converges into an optimal point on the other optical fibers to be coupled. In this experiment, three different mode patterns are selectively excited in the MMF by changing the excitation pattern using another SLM. We confirm that the PPC system can extract a specific mode pattern with a considerably low crosstalk of less than 1% by displaying the corresponding phase-conjugation pattern on the SLM. These results revealed that multiplex signal transition can be realized by modulating multiple independent signals over different spatial-mode patterns. In addition, we demonstrated a reconfigurable spatial-mode conversion using the PPC technology. By applying the spatial phase modulation to an optical beam incident on the mode converter, the spatial mode of the output beam is flexibly changed. For example, mutual eigenmode conversions between the fundamental mode (LP01) and higher order modes (LP11 and LP21) are successfully performed.

9130-39, Session PS1

Laser-induced damage of photopolymer thin films induced by ns and fs laser pulses at various wavelengths

Albertas ?ukauskas, Gintar? Batavi?i?t?, Mindaugas ?ciuka, Andrius Melninkaitis, Mangirdas Malinauskas, Vilnius Univ. (Lithuania)

Manufacturing of diverse microoptical components (MOCs) by direct laser writing (DLW) of photopolymers technology namely known as two-photon photopolymerization was implemented since the advent of it in 1997. Up to now, a large number of MOCs and arrays of them were reported and broad range of the applications were demonstrated. Much effort has been devoted to improve the fabrication process in terms of manufacturing duration and surface roughness. Nevertheless, the field of the MOCs applications in the industry remains limited and unexplored. The reason of it could be the photopolymer as the material itself, more precisely – optical resistance to the laser radiation as it is critical parameter at high intensities.

In this paper, we report extensive measurements of laser-induced damage threshold (LIDT) for thin film photopolymers widely used in DLW micro/nano-lithography. Several types of commercial and laboratory sensitized photosensitive materials are investigated: epoxy based photoresists (SU-8), hybrid organic-inorganic photopolymers (SZ2080 and OrmoComp), thermo polymer (PDMS) and pure acrylate (PMMA). The presence and influence of the photoinitiators molecules (Irgacure 369) at 2 wt. % concentration within the host of the SZ2080 photopolymers matrix to the LIDT is revealed. Photosensitization of the pure photopolymer SZ2080 leads to the decreased damage threshold for the second harmonics (515 nm and 532 nm wavelengths) both in ns and fs regimes while it has no influence for the first harmonics (1030 nm and 1064 nm wavelengths). LIDT damage testing was performed in 1-on-1 as well as and in S-on-1 (1000-on-1) conditions in order to evaluate the accumulation effects. Optical breakdown measurements were carried out under ns (11 ns) and fs (300 fs) pulse duration laser irradiation at the fundamental and second harmonics and at different repetition rates (50 Hz and 50 kHz respectively for ns and fs regimes). Nd:YAG and Yb:KGW laser systems and fully automated test station were used to perform the measurements according to ISO 11254-2 certified standard. Several different damage morphologies were observed (delamination of thin films, thermal and femtosecond melting and defect induced breaks) and it was used for the qualitative analysis of the photopolymers optical breakdown mechanisms. Significant reduce of the damage threshold due to local absorption centers and impurities was observed. Attained LIDT values of the various photopolymers were approximately in 2 – 14 J/cm2 fluency range at ns regime and in 0.1 – 1 J/cm2 fluency range at fs regime. Obtained results prove that pure hybrid organic-inorganic photopolymer is the most resistant in comparison to other photosensitized polymers used in DLW at ns regime while in fs regime LIDT values are similar. All of the same experimental LIDT values were directly compared to reference materials. They were of the same order as the common dielectric coatings used in laser optical systems. Attained results may pave the way for the new avenue of the MOCs applications in industry [1].

[1] A. ?ukauskas, G. Batavi?i?t?, M. ??iuka, T. Jukna, A. Melninkaitis and M. Malinauskas, Laser induced damage threshold (LIDT) of photopolymers used in 3D laser micro/nano-lithography, submitted (2013).

9130-40, Session PS1

Preliminary investigation in optical resonators based on carbon nano-tube and coupling for optoelectronics

Patrice Salzenstein, FEMTO-ST (France); Taron Makaryan, Yerevan State University (Armenia)

In this work we present how we improve theoretically and experimentally the problem of the coupling between a high quality factor (Q-factor) resonator and its external coupler. Oscillations of ringing are observed. There are induced by the sweeping of the excitation frequency of an active micro sphere. Thanks to this approach, quality factor of optical resonators are measured. Obtained Q-factors are up to 10^9.

9130-41, Session PS1

Design and analysis of beam splitters and GRIN lenses using 2D photonic crystals in silicon for telecommunications

Uday M. Bangavadi, Manipal Univ. (India); Prita Nair, SSN College of Engineering (India)

Fiber to planar waveguide interconnects and planar beam modifiers are crucial for the implementing efficient silicon photonic devices for communication applications. In this work, broadband performance in the 1300nm-1600nm region is ensured by appropriately controlling the spatial variation of the effective index of silicon to realize a beam splitter (1x2) and a quarter wave GRIN lens. Sub wavelength (?/10) 1D periodic array of low-index air holes in the high index host silicon, along the propagation direction of the optical beam, is repeated, with decreasing or increasing periodicities in the transverse direction to form a 2D photonic crystal(PhC) structure to realize a beam splitter or GRIN lens respectively. The lowest wavelength of 1300nm is used as the design wavelength to ensure less than ?/10 periodicities for all useful wavelength ranges. The transverse width of the 2D PhC structure is tailored to match the mode field diameter of the incoming beam and optical confinement in the third dimension is ensured by air on top and bottom of the silicon layer. A decreasing transverse periodicity of 1D hole arrays from the horizontal axis at the centre along the direction of propagation results in formation of 2 high index wave guiding structures towards the edges of the crystal separated by low effective index central region thus leading to formation of a beam splitter. On the other hand increasing transverse periodicity of the defect array leads to lowering of effective index gradually to the edges of the device resulting in the formation of a GRIN lens. FEM analysis of the propagation of electromagnetic field through these structures show that GRIN lens focuses the input beam to a mode field diameter (MFD) of 1.5?m and that MFD of each output arm of the 1x2 splitter is 1.75?m. The decrease in intensities at the focal point of the GRIN lens with increasing input wavelength in the 1300-1600nm is found to be within 6% and that in the two arms of the beam splitter is found to be less than 13%. Relationship between analytical expressions representing the geometry of the and the effective index profile is also presented.

9130-42, Session PS1

Tailoring the optical and rheological properties of an epoxy acrylate based host-guest system

Uwe Gleißner, Albert-Ludwigs-Univ. Freiburg (Germany); Thomas Hanemann, Karlsruhe Institute of Technology (KIT) (Germany)

Polymers with individually adjusted optical and rheological properties are gaining more and more importance in industrial applications like information technology. To modify the refractive index n, an electron-rich organic dopant is added to a commercially available reactive polymer based resin. Changes in viscosity for applications like ink-jet printing can be achieved by using a comonomer with suitable properties.

Therefore we used a commercially available epoxy acrylate based UV-curable polymer matrix to investigate the influence of both ethylene glycol dimethacrylate (EGDMA) on the viscosity and phenanthrene on the refractive index. First, EGDMA was added to pure polymer to achieve lower viscosity. Second, phenanthrene was added with 5 and 10 wt% to the mixtures which contained 0, 20, and 40 wt% EGDMA, whereas 10 wt% of phenanthrene was close to solubility limit. Additionally, both a photo and a thermal initiator were added. All components were mixed and then polymerized by irradiation with UV light for 10 minutes and with a 2 hours postcure at 80 °C. The viscosity of the uncured mixtures was measured at different shear rates and temperatures. The refractive index was measured at a wavelength of 589 nm and 20 °C using an Abbe refractometer.

As a result the change in viscosity went linearly from 47 Pa•s (pure resin) to 4 mPa•s (pure EGDMA) (@20 °C, shear rate = 60 1/s), which is a more suitable region for inkjet printing. However, the refractive index decreased at the same time from 1.548 to 1.514. Adding phenanthrene to the pure resin the refractive index increased linearly from 1.548 up to 1.561 and for the 20 wt% EGDMA mixture the lowered refractive index increased from 1.546 up to 1.563.

It was shown that both, viscosity and refractive index can be successfully adjust in a wide range depending on requirements.

9130-43, Session PS1

Photoactivation and optogenetics with micro mirror enhanced illumination

Florian Rückerl, Institut Pasteur (France); Jörg Heber, Fraunhofer-Institut für Photonische Mikrosysteme (Germany); Spencer L. Shorte, Institut Pasteur (France)

Photoactivation and “optogenetics” require precise control over of the illumination path in optical microscopes. It is equally important to restrict the illumination spatially as well as to have control over the intensity and the duration of the illumination.

In order to maximize the illumination control of the objects under observation we use unique programmable, ultra-fast Micro Mirror Arrays (MMA) as high-resolution spatial light modulators. Using two 256x256 MMAs our illumination setup allows for fast angular-spatial control at a wide range of wavelength (260-1000nm). Illumination times can be as short as 1 ms, but can also extend to several seconds. Additionally, the illumination intensity can be controlled at high resolution allowing simultaneous illumination of multiple, discrete regions at different intensities. The continuous illumination of the individual areas results in a precise control over the light dose to the sample, giving significant advantage when investigating dosage dependent activation inasmuch as both the duration and the intensity can be controlled distinctly.

The setup is integrated to a microscope and allows selective illumination of regions in the sample, enabling the precise, localized activation of fluorescent probes and the activation and deactivation of cellular and subcellular signaling cascades using photo activated ion channels. The high reflectivity in the UV range (up to 260nm) further allows gene silencing using UV activated constructs (e.g. caged morpholinos).

9130-13, Session 3

Proof-of-concept demonstration of a Total Internal Reflection based module for fluorescence and absorbance detection using a 3D-printed syringe pump

T. Verschooten, Heidi Ottevaere, Jürgen Van Erps, Michael Vervaeke, Hugo Thienpont, Vrije Univ. Brussel (Belgium)

In the past decades the development of microfluidic systems for biochemical analysis has evolved rapidly. Since the start, detection has been one of the main challenges and very sensitive techniques must be employed to detect the limited amount of molecules available in the nanoliter detection volumes. Optical detection is one of the techniques capable of providing sufficient sensitivity but is commonly still accomplished by bulky and expensive microscopes located off-chip. Miniaturized and integrated optical detection systems are therefore needed to fully exploit the potential advantages of microfluidic devices.

We have developed a miniaturized detection unit for UV-VIS laser-induced fluorescence (LIF) and absorbance (ABS) analysis. This kind of optical detection module was already shown to work using fused silica capillaries with an inner diameter of 150μm [Van Overmeire et al.]. To provide a sufficiently large optical path length we have increased the

inner diameter of the glass tubing, that contains the sample, to 3mm. This allows for more interaction between the excitation light and the sample, thus increasing sensitivity. The more "macroscopic" sample container opens the opportunity towards the study of fluorescence in larger biological cells and organisms (e.g. zebrafish embryos).

In a first step, we have improved the optical design proposed by [Van Overmeire et al.] by replacing the original refractive optics by a reflective system which is built upon the principle of total internal reflection (TIR). Even though our implementation shares the idea of using "air mirrors" with that of [Llobera et al.], our design does not only use these mirrors to capture the fluorescent light, but also to expand and collimate the excitation light. This excitation light is supplied by a multimode fiber through a side-facet of the optical chip. All excitation light not absorbed by the sample is collected at the other side of the system by a curved refractive facet onto a photodetector. Any fluorescent light, emanating from the illuminated sample volume, is at the same time contained by two spherical air mirrors and guided towards a photodetector to quantize the amount of fluorescent light.

We have designed this detection module using non sequential ray tracing software (ZemaxTM). In these simulations we have studied and optimized the efficiency of the excitation delivery, the collection of fluorescence and non-absorbed light and the uniformity of the excitation light field inside the sample tubing. The microfluidic device was fabricated with Deep Proton Writing (DPW) [Van Erps et al.] in 2mm thick PMMA and afterwards quantitatively characterized using a 3D coordinate measurement machine. Next we compared the results of this geometrical characterization to our original design parameters. We obtained optical collection efficiencies of 45% and 7% for absorbance and fluorescence detection respectively.

In addition to developing miniaturized Lab-On-Chip (LOC)-devices, we also target to increase the portability of the lab-equipment needed to operate these devices. Therefore we have developed a low-cost compact syringe pump consisting of standard commercial cage mechanics and 3D printed objects. At the conference we will show the results of the proof-of-concept demonstration of the proposed detection module using literature standard reference substances where the goal of the syringe pump is to get repeatable sample transport.

Bibliography

Van Erps, J., & Vervaeke, M. (2011). "Deep Proton Writing: a rapid prototyping tool for polymer micro-optical and micro-mechanical components. Rapid Prototyping .... Retrieved from http://www.intechopen.com/source/pdfs/20729/InTech-Deep_proton_writing_a_rapid_prototyping_tool_for_polymer_micro_optical_and_micro_mechanical_components.pdf

Llobera, A., Demming, S., Wilke, R., & Büttgenbach, S. (2007). Multiple internal reflection poly(dimethylsiloxane) systems for optical sensing. Lab on a Chip, 7(11), 1560–1566. Retrieved from http://www.ncbi.nlm.nih.gov/pubmed/17960286

Van Overmeire, S. (2008). Miniaturized detection system for fluorescence and absorbance measurements in chromatographic applications. IEEE Journal of Selected Topics in Quantum Electronics, 14(1), 140–150. Retrieved from http://ieeexplore.ieee.org/xpls/abs_all.jsp?arnumber=4451133

9130-14, Session 3

Electrically tunable Fabry-Pérot interferometer with inherent compensation of the influence of gravitation and vibration

Marco Meinig, Steffen Kurth, Fraunhofer-Institut für Elektronische Nanosysteme (Germany); Karla Hiller, Technische Univ. Chemnitz (Germany); Mario Seifert, Martin Ebermann, Norbert Neumann, InfraTec GmbH (Germany); Elvira Gittler, JENOPTIK Optical Systems GmbH (Germany); Thomas Gessner, Fraunhofer-Institut für Elektronische Nanosysteme (Germany)

Small-sized, fast and robust analyzers for volatile organic compounds are facing a great marked perspective in the near future. Applications ranging from industrial multicomponent gas analysis to the detection of toxic gases in personal protective equipment. The analyzers are based on the principle of infrared absorption spectroscopy and can be constructed very cost efficient by using highly miniaturized spectrometer modules. The key component of these modules is a tunable infrared filter that is fabricated reliable, reproducible, with high yield in an efficient MEMS wafer batch process. This contribution reports on a Fabry-Pérot interferometer (FPI) consisting of two movable reflectors of equal size and mass to stabilize the optical resonator and hence the central wavelength of the filter against vibration and gravitation induced forces. Two identical wafers are combined by silicon fusion bonding to build the FPI between two movable reflectors. The movable reflector carries are structured with a combination of wet and dry etching using the whole wafer thickness. The reflectors are made of dielectric layer stacks deposited on the 300 µm thick reflector carries and have a size of 2 mm x 2 mm giving the FPI a large aperture. The optical performance is improved with an anti-reflection coating (ARC) on the outer sides of the FPI. The chip is symmetric and compensated against mechanical stress, as well as the dielectric layer stack and the ARC. In comparison to previous designs the chip size is reduced significantly to 7 mm x 7 mm. With voltages lower than 35 V the FPI can be tuned over the spectral range from 3.1 µm to 4.8 µm using the 2nd and 3rd interference order. Depending on the central wavelength the measured FWHM bandwidth is between 40 nm and 70 nm in the 2nd interference order and between 25 nm and 35 nm in the 3rd interference order. The peak transmittance is between 70 % and 90 %. The filters are robust against mechanical shocks according to Mil-Std-883 test condition B.

9130-15, Session 3

Design of a MEMS-based retina scanning system for biometric authentication

Franziska Woittennek, Jens Knobbe, Uwe Schelinski, Heinrich Grüger, Fraunhofer-Institut für Photonische Mikrosysteme (Germany)

There is an increasing need for reliable authentication for a number of applications such as e commerce. Common authentication methods based on ownership (ID card) or knowledge factors (password, PIN) are often prone to manipulations and may therefore be not safe enough. Various inherence factor based methods like fingerprint, retinal pattern or voice identifications are considered more secure. Retina scanning in particular offers both low false rejection rate (FRR) and low false acceptance rate (FAR) with about one in a million. Images of the retina with its characteristic pattern of blood vessels can be made with either a fundus camera or laser scanning methods. The present work describes the optical design of a new compact retina laser scanner which is based on MEMS (Micro Electric Mechanical System) technology. The use of a dual axis micro scanning mirror for laser beam deflection enables a more compact and robust design compared to classical systems. The scanner exhibits a full field of view of 15° which corresponds to an area of 4mm? surrounding the optical disc. The system works in the near infrared and is designed for use under ambient light conditions, which implies a pupil diameter of 1.5mm. Furthermore it features a long eye relief of 40mm so that it can be conveniently used by persons wearing glasses. The optical design requirements and the optical performance are discussed in terms of spot diagrams and ray fan plots of the system are presented in detail.

9130-16, Session 3

Curved artificial compound-eyes for autonomous navigation

Robert Leitel, Andreas Brückner, Wolfgang Buß, Fraunhofer-Institut für Angewandte Optik und Feinmechanik (Germany); Stéphane Viollet, Aix-Marseille Université, CNRS, ISM (France);

Ramon Pericet-Camara, Laboratory of Intelligent Systems, EPFL (Switzerland); Hanspeter Mallot, Laboratory of Cognitive Neuroscience, Department of Biology, University of Tübingen (Germany); Andreas Braeuer, Fraunhofer-Institut für Angewandte Optik und Feinmechanik (Germany)

Natural compound-eyes consist of a large number of ommatidia that are arranged on a curved surface and thus are able to detect signals from a wide field of view. We present an integrated artificial compound-eye sensor system with enhanced field of view of 180° x 60° due to the introduction of curvature. The system bases on an array of adaptive logarithmic wide-dynamic-range photoreceptors for optical flow detection and compound-eye optics for increasing sensitivity and expanding the field of view. Its assembling is mainly done in planar geometry on a flexible printed circuit board. The separation into smaller ommatidia blocks by dicing enables flexibility and finally allows for mounting on curved surfaces. The signal processing electronics of the presented system is placed together with further sensors into the concavity of the photoreceptor array, and facilitates optical flow computation for navigation purposes.

9130-17, Session 3

Packaged micro-integrated semiconductor laser modules for quantum optical sensor applications in space

Ahmad I. Bawamia, Christian Kuerbis, Anja Kohfeldt, Martin Heyne, Mandy Krueger, Andreas Wicht, Goetz Erbert, Ferdinand-Braun-Institut (Germany); Max Schiemangk, Humboldt-Univ. zu Berlin (Germany); Achim Peters, Ferdinand-Braun-Institut (Germany) and Humboldt-Univ. zu Berlin (Germany)

We present the design and implementation of compact, robust and energy-efficient semiconductor laser modules that are suitable for deployment in space. We concentrate on GaAs-based laser chips engineered for emission at 780 nm, which aim at meeting the requirements for Rubidium-atom interferometry experiments in space.

We discuss different laser module concepts (master oscillator power amplifier module concept, low power local oscillator module, high power dual stage amplifier module) and compare them w.r.t. electro-optical performance, power and mass budget, and form factor.

We report on the integration of two arbitrary laser chips, micro-optics, DC and HF electronics plus fiber-coupling into a single-mode, polarization maintaining fiber on a structured AlN-substrate within a footprint of 80 x 30 mm?. Moreover, we present the packaging of the AlN-Substrate into a hermetically sealed housing including custom-made feedthroughs for all DC, HF and optical signals. Emphasis is put on the choice of CTE-matched and low-outgassing materials and packaging processes, such that the laser modules are ready to undergo a complete cycle of mechanical and thermal stress tests in view of qualification for space missions.

We present the electro-optical performance of a master oscillator power amplifier (MOPA) module with a distributed feedback laser (DFB) as master oscillator. The results of mechanical and thermal stress tests according to the ESA evaluation test program for laser diodes (ESCC Basic Specification No. 91) are also presented.

We further outline the next step in the development of the laser technology discussed above in order to extend the accessible wavelength spectrum to the UV. The laser technology is directly transferred to semiconductor chips emitting at a wavelength of 1070 nm to form the local oscillator of the UV-laser system. The wavelength of 267 nm is then achieved through two frequency-doubling stages, at least one of which consisting of a micro-integrated monolithic enhancement cavity.

9130-18, Session 3

Design, fabrication and characterization of miniaturized high resolution camera modules

Matthias Kuehn, Albert-Ludwigs-Univ. Freiburg (Germany); Maximilian Goetz, Albert-Ludwigs-Univ. Freiburg (Germany) and HSG-IMIT (Germany); Claas Müller, Albert-Ludwigs-Univ. Freiburg (Germany); Holger Reinecke, Albert-Ludwigs-Univ. Freiburg (Germany) and HSG-IMIT (Germany)

Nowadays the miniaturization of electro opto mechanical systems becomes more and more important for many applications particularly in the medical and industrial field. Within this transition there are many challenges that have to be overcome concerning optical calculations, tolerance analysis, materials, mounting and environmental conditions.

There are many miniaturized systems such as WLCs (Wafer Level Cameras) available in higher quantities but with a limited optical quality caused by the type of optical elements that are often used within those systems. However, many applications show a need for high optical quality objectives concerning chromatic and spherical aberrations and also impose high requirements for mechanical stability during use or conditioning. This leads to specific requirements for the design and implementation of a miniaturized camera module concerning mechanics, optics, electronics and their adjustment and assembly. After comparing conventional objectives of known reflex cameras or video cameras consisting out of more than ten lenses for the correction of spherical and chromatic aberrations, we focused on a triplet system for reasons of cross section, adjustment, assembly and sensitivity to environmental impact (e.g. temperature). After the optical calculation with ZEMAX® based on specifications like opening angle, working distance, depth of field and resolution a tolerance analysis is necessary. On the one side the tolerance analysis are based on the manufacturing tolerances of the lenses, spacers and the fittings, while on the other side the behavior of the parts at different temperatures and the influence of the alignment during assembly has to be considered. With the help of tolerance analysis the elements with the highest impact on the entire performance were figured out. Simulating the mechanical behavior at higher temperatures due to thermal dissipation loss of the electronic components or environmental conditions resulted in the choice and implementation of suitable materials, geometries, entire design, assembly fixtures and their tolerances. With the new defined tolerances the loss of optical quality is simulated by changing the parameters to the analyzed thresholds. After the characterization of the optical performance values with respect to vignetting, distortion and chromatic aberrations compared to the specified values, the tolerances were adjusted. Issues like spherical and chromatic aberrations should be minimized in order to reduce any quality loss. However, the effort for a detailed optimization of the aberrations is very high and can be lowered to a certain extent by image processing algorithms. Important for the optical design of small objectives is the ratio of the lens diameter and the radius of the spherical structures. The smaller the diameter of lenses and the smaller their spherical radius, the higher are the requirements to be placed upon manufacturing and mounting of the optical elements.

The approach is necessary to develop high performance miniaturized camera modules. With the help of this technical expertise we calculated, manufactured and assembled small objectives with a diameter smaller than 2,5 mm suitable to high resolution.

9130-19, Session 4

Self-centering fiber alignment structures for high-precision field installable single-mode fiber connectors

Jürgen Van Erps, Evert Ebraert, Fei Gao, Michael Vervaeke,

Francis Berghmans, Vrije Univ. Brussel (Belgium); Stefano Beri, Jan Watté, TE Connectivity Ltd. (Belgium); Hugo Thienpont, Vrije Univ. Brussel (Belgium)

There is a steady increase in the demand for internet bandwidth, primarily driven by cloud services and high-definition video streaming. Europe's Digital Agenda states the ambitious objective that by 2020 all Europeans should have access to internet at speeds of 30Mb/s or above, with 50% or more of households subscribing to connections of 100Mb/s. Today however, internet access in Europe is mainly based on the first generation of broadband, meaning internet accessed over legacy telephone copper and TV cable networks. In recent years, Fiber-To-The-Home (FTTH) networks have been adopted as a replacement of traditional electrical connections for the 'last mile' transmission of information at bandwidths over 1Gb/s. However, FTTH penetration is still very low (<5%) in most major Western economies, mainly due to the high deployment cost of FTTH networks. Indeed, the success and adoption of optical access networks critically depend on the quality and reliability of connections between optical fibers. In particular a further reduction of insertion loss of field installable connectors must be achieved without a significant increase in component cost. More demanding optical performance levels of field installable connectors force carriers to move from C-grade to B-grade and from B-grade to A-grade. This requires precise alignment of fibers that can differ in terms of ellipticity, eccentricity or diameter and seems hardly achievable using today's widespread ferrule-based alignment systems.

In this paper, we present an alignment methodology for the alignment of ferrule-less connectors, based on deflectable/compressible spring structures, providing a self-centering functionality for the fiber. This way, it can accommodate for possible fiber cladding diameter variations (the tolerance on the cladding diameter of G.652 fiber is typically ±0.7?m). The mechanical properties of the cantilever are derived through an analytic approximation and a mathematical model of the spring constant, and finite element-based simulations are carried out to find the maximum first principal stress as well as the stress distribution in the fiber alignment structure. Elastic constants of the order of 30kN/m are found to be compatible with a proof stress of 70MPa. We show the successful prototyping of a 3-spring fiber alignment structure using deep proton writing while taking into account their compatibility with replication techniques such as hot embossing and injection moulding. Fiber insertion in our self-centering alignment structures is achieved by means of a dedicated interferometric setup allowing assessment of the fiber facet quality, of the fiber's position in relation to the connector's front and of the spring deformation during fiber insertion. These self-centering structures have the potential to become the basic building blocks for a new generation of field installable connectors to further increase optical performance levels. In combination with robust operator-independent installation equipment they can ultimately break the current paradigm of ferrule-based connectivity requiring extensive pre-engineering and highly specialized manpower for field deployment.

9130-21, Session 4

Opto-mechanical design of a buckling cavity in a novel high-performance outside-plant robust field installable fiber connector

Evert Ebraert, Jürgen Van Erps, Vrije Univ. Brussel (Belgium); Stefano Beri, Jan Watté, TE Connectivity Ltd. (Belgium); Hugo Thienpont, Vrije Univ. Brussel (Belgium)

Internet based-applications, like cloud computing and HD-streaming, give rise to an increased demand for connection bandwidth. For this reason the European Union states as a goal for 2020 that at least 50% of all European households should have at least a 100Mb/s Internet connection. To satisfy this demand, Fiber-to-the-home (FTTH) networks would be ideal, providing a future-proof infrastructure that can accommodate even more than 100Mb/s connections. However, FTTH penetration is still very low (<5%) in most major western economies, mainly because of the high deployment cost of FTTH networks.

An optical connector designed for the FTTH market must endure severe climatic and environmental conditions, including thermal excursion from -40°C to +70°C. Differences in thermal expansion between glass and cable material are known to result in fiber grow-outs especially when tighter-jacket cables are deployed. Even in the absence of a dramatic failure, the need to accommodate extra length of optical fiber within the cable results in the formation of bends and in decreased optical performance. These detrimental effects can be further increased when field-installed rather than factory-assembled connectors are used to terminate the cables. The need for solving these connectivity issues via truck rolls results in high operational costs of optical networks and ultimately delays the achievement of the above-mentioned European 2020 objectives for broadband connectivity.

We tackle this problem by incorporating a cavity inside the optical connector in which the optical fiber can buckle in a controlled way. With this design approach, variations of the fiber length will not be accommodated inside the cable, but rather in the buckling cavity. This concept will be robust against the unavoidable installation tolerances and variations when field termination is considered. However, bending losses may incur during buckling, especially at longer wavelengths, and hence careful design is required in order to mitigate this. To this end, we present the use of finite element analysis simulations to investigate the shape of the formed buckle and the mechanical stability of the fiber for various buckling cavity lengths. The results show that the shape of the buckle can be accurately approximated by a cosine function. They also suggest that if the buckling cavity is longer than 17mm, the first principal stress values in the buckled SMF will not exceed 700MPa, at which G.652 telecom fibers were proof-tested. In the proposed connector design, with a buckling cavity of 20mm long, the maximum first principal stress in the buckled SMF is 550MPa in the worst-case scenario and is thus well below the tensile strength of G.652 telecom fibers.

In addition, the optical performance of a buckled SMF is investigated by bending loss calculations and simulations. To this end, we use Marcuse's analytic formula and a fully vectorial mode solver respectively. We show a good agreement between the analytical and the simulated bending loss results of G.652 fiber at 1310nm, 1550nm, 1625nm and 1650nm wavelength. In the analytical model, a cosine shape of the buckle is used. We show that in the worst-case scenario buckling cavity lengths smaller than 20mm length should be avoided to keep the optical bending loss due to the formed buckle below 0.05dB.

9130-22, Session 4

Three dimensional fabrication of optical waveguiding elements for on-chip integration

Vijay Vittal Parsi Sreenivas, Univ. Bremen (Germany); Mike Bülters, Martin Schröder, Bremer Institut für angewandte Strahltechnik GmbH (Germany); Ralf B. Bergmann, Bremer Institut für angewandte Strahltechnik GmbH (Germany) and Univ. of Bremen (Germany)

We present micro polymer optical waveguide (POW) elements fabricated using femtosecond lasers and a two-photon absorption (TPA) process. The POWs are constructed by tightly focussing a laser beam in PMMA based SU-8 resists transparent to the laser wavelength for one-photon absorption. The TPA process enables the patterning of the resist in 3D at a resolution of 100-200 nm, which provides a high degree of freedom for POW designs. Using the 3D lithographical capabilities provided by TPA in polymers such as PMMA, we present a novel approach to 3D polymer optical waveguide (3D-POW) fabrication and a coupling with single mode fibres in the optical wavelength region. Our research is currently focussed on fabricating 3D-POW and other passive micro optical devices,

such as Y-splitters and simple logical elements. For this reason, we are aiming to achieve optimum coupling efficiency and optimize the coupling technique between 3D-POWs and single mode fibres as well as 3D-POWs and CMOS dies. This technology facilitates 3D-POWs and optical interfaces fabrication independent of the substrate material.

Presently, the waveguide is designed to enable structural stability and optimal in- and -out coupling regions. It is supported by a row of stilts that are ~50 μm tall, also realised via TPA process. This ensures that the waveguide has minimal contact to the substrate and the losses are minimised. The waveguide itself is curved at the input and output ends by an angle of 45 degrees parallel to the surface of the substrate, so that the errors arising from a direct measurement between the fibre optics are eliminated. Furthermore, to enhance the coupling efficiencies, we have fabricated coupling lenses at the end-facets of the POW with tapered waveguide transition, from the same polymer material. With this technique, we make the POW and the lenses as one homogenous unit, thereby reducing a couple of interface mismatch losses. The POW is coupled with the single mode fibres that are mounted at 45 degrees angles on high precision motion stages. Index matching liquid is used to further minimise losses at the POW-fibre interfaces. We use a broadband white light source as the input to characterise the POW. At the output end, we measure the spectral response of the POW as well as the mode field distribution.

We present results on 3D-POWs fabrication with integrated optics for optimum waveguiding and coupling properties optimised by numerical simulations and report our initial results on the transmission properties of the 3D-POWs. With a length of 270 μm, a polymer core diameter of 9 μm and air cladding, the waveguides possess a total loss of 12 dB. This value includes the external in and out mode coupling and is continuously being improved upon and backed up by the simulation results. We verify the overall feasibility of the design and coupling mechanisms that can be exploited to execute complex 3D waveguide based optical functions such as filters and logical operations.

9130-23, Session 4

Three-dimensional buried polymer waveguides via femtosecond direct laser writing with two-photon absorption

Ho Hoai Duc Nguyen, Kerstin Kaleta, Stefan Hengsbach, Uwe Hollenbach, Jürgen Mohr, Karlsruher Institut für Technologie (Germany); Ute Ostrzinski, Karl Pfeiffer, micro resist technology GmbH (Germany)

Integrated optics has emerged as a promising solution to the electronic interconnect bottleneck, enabling high bandwidth density and low power consumption. Recently, confining photochemical and physical reactions in a volume has given an extra dimension to optical interconnection using glass or polymer. Three-dimensional waveguides can then connect, combine, or split the optical signal among any blocks in all dimensions. However, the refractive index increase is still a challenge to fabricate free-form, stable and single-mode three-dimensional buried waveguides.

This paper presents a new concept to tackle this challenge using the combination of femtosecond direct laser writing (FsDLW) in polymer and external diffusion of lower-index monomer. The host polymer consists of an oligomer based on a bisphenol-A diglycidylether with a refractive index of 1.57 at 1550 nm. The refractive index is only slightly changed by cross-linking (delta_n ≈ 0.003). The aliphatic guest monomer applied for diffusion has a refractive index of 1.445 at 1550 nm.

FsDLW with two-photon absorption was used to initiate cross-linking in a cross-section of ~8 x 8 μm2 following a programmed trajectory to form the waveguide core. Post exposure baking at 80°C for 10 minutes then completed the cross-linking of the core. Afterwards, lower-index monomer from a gas atmosphere was diffused into the uncross-linked cladding. It has to be mentioned that this diffusion hardly occurred into the locally exposed, cross-linked pattern. Subsequently, the diffused monomer and host oligomer were cross-linked by UV flood exposure at 365 nm to decrease the refractive index of the cladding. Finally, the whole structure was hard-baked at 140°C for 10 minutes for polymerization and stabilization. Our fabrication method requires only one layer of a single material with no wet processing and could be easily transferred to industrial production.

We used Photonic Professional, a commercially available system offered by Nanoscribe GmbH, for laser writing. The system uses Erbium-doped fiber emitting 100 fs pulses at 780 nm wavelength with 80 MHz repetition frequency. The objective has high numerical aperture of 0.75 producing tightly focused Gaussian beam, while its long working distance of 1.7 mm assures high depth of the writing field. Writing speed varies between 100-1000 μm/s. Laser intensity falls in the range of 5-40 mW.

The peak refractive index change of ~0.01 was measured using refractive near field method. Measured near-field intensity at the end facet of waveguides showed single-mode Gaussian profiles. We further demonstrated how voxel size and refractive index profile can be adjusted using scanning speed and laser intensity. Moreover, changing the voxel shape by a field aperture in front of the objective was investigated. The waveguide length is several cm which is suitable for on-board interconnection. Some potential applications of this method are three-dimensional arrays of optical waveguide network routers, optofans, pitch converters or splitters.

9130-24, Session 4

Development of laser non-linear lithography technique for fiber end-face microoptical components

Albertas ?ukauskas, Vilnius Univ. (Lithuania); Etienne Brasselet, Univ. Bordeaux 1 (France); Mangirdas Malinauskas, Vilnius Univ. (Lithuania)

A large variety of the fiber tip microoptical components (MOCs) were demonstrated over last forty years. Nevertheless, fabrication of microoptical elements, precisely aligned according to the fiber core center, still remains challenging. Several techniques and methods were proposed to avoid this issue. Chemical etching and free-radical photopolymerization technologies are used to achieve automatically centered MOCs, but in this way only symmetrical elements can be produced. For complex shaped MOCs, point-by-point writing techniques, such as electron beam lithography, focused ion beam milling and direct laser writing non-linear lithography (known as two-photon polymerization), are desirable. However, the fabrication process becomes more tricky and impractical to use. The solution to it, is the expansion of mode field coming out from the fiber. It is realized by splicing a coreless silica fiber or by fusion splicing a photonic crystal fiber. In practice, this cannot be realized easily and adds an extra step in the fabrication procedure.

The purpose of this research is to implement a method to improve the fabrication procedure of the well centered fiber tip microoptical elements. The suggested approach is based on the fabrication of the MOC at the proper distance from the single mode fiber (SMF) in a single procedure in order to exploit the larger beam waist emerging out of the fiber. It is realized by exploiting the advantages of the laser photopolymerization (MPP) technology. Here, the peculiarities of the fabrication process of fiber tip microoptical elements are discussed in details. Hybrid microoptical element is manufactured on the end-face of the cleaved SMF (0.35 NA, ?0=3.3 ?m). It is designed as a monolithic element consisting of the aspherical and conical microlenses which shares the common basis and is attached to the fiber with the four 10x10 μm2 pillars at the 35 ?m distance from the fiber end-face. Aspherical lens is used for the beam collimation while the conical lens (inclination angle ?=15°) – for the Bessel beam generation. According to the measured emerging light's divergence coming out of the fiber, the radius and the focal length of the aspherical lens is set to 20 μm and 35 ?m, respectively. Beam waist as a function

of the propagation distance is measured in three cases: laser beam (?=633 nm) propagates only through SMF (i), SMF and aspherical lens (ii) and SMF with the hybrid MOC on the tip (iii). Besides, the propagation distance of the Bessel beam is increased ≈5 times by realizing the suggested fabrication method. Additionally, the spiral phase plate (SPP) with the topological charge l=1 and radius R=20 ?m is structured directly and at the 35 μm distance from the fiber tip in order to demonstrate the generation of the optical singularities and compare two different strategies for the fabrication of the fiber tip MOC. The optical performance of the fiber tip SPP is measured and obtained experimental results are compared to the theoretical calculations by considering the paraxial approximation of the Fresnel diffraction of a Gaussian beam. Potential applications are discussed and preliminary results are presented. Implementation of the presented development of the MPP technology allows to minimize the discrepancy of the MOC centering and to manufacture high quality integrated microoptical systems.

9130-25, Session 5

Fabrication of refractive freeform array masters for artificial compound eye cameras

Jens Dunkel, Frank C. Wippermann, Andreas Brückner, Andreas Reimann, Andreas Bräuer, Fraunhofer-Institut für Angewandte Optik und Feinmechanik (Germany); Martin Müller, Fraunhofer IOF (Germany)

There is a huge demand on miniaturized cameras in the field of mobile consumer electronics. These cameras are currently based on miniaturized single aperture optics that are often fabricated by a UV-replication process on wafer scale in order to ensure minimum fabrication costs in combination with large quantities. According to the applied imaging principle, the miniaturization of these systems is physically limited. In order to further decrease the thickness of the camera systems, a multichannel imaging principle needs be used. These artificial compound eye cameras permit a further decrease in thickness by a factor of two in comparison to miniaturized single aperture optics with same resolution and pixel size. Their fabrication process is currently based on the reflow of photoresist.
This technique is used to fabricate the microlens arrays of a multitude of camera systems in parallel on a master wafer. This master wafer is subsequently transferred into a polymer stamp that permits the replication in a mask aligner. Due to physical limitations of the reflow of photoresist, only spherical and ellipsoidal surface shapes of the single lenslets are achievable. Consequently, the potential for correcting optical aberrations is restricted leading to limited image quality and resolution. This can be improved significantly by the use of refractive freeform arrays. Due to the non-symmetrical and aspherical surface shapes of the single lenslets, the fabrication by the reflow of photoresist is no longer possible. Therefore, we propose a new approach for the fabrication of these structures based on a step and repeat process using a modified nano imprint stepper. First, a single refractive freeform array was fabricated by an ultra-precision diamond machining process. Subsequently, this structure was used as a master structure in order to generate a copy in PDMS which conducts as a stamp in the final step and repeat process. A sequence of polymer dispensing, positioning of the PDMS stamp, imprinting, UV-curing and demolding is applied in order to replicate the master structure several hundred times on a glass substrate. The approach is demonstrated by fabricating the master wafers for an artificial compound eye camera with a resolution above one megapixel. The fabricated master wafers permit the replication of 253 single freeform arrays in parallel on an adopted mask aligner. The arrays itself consist of 135 single lenslets with a pitch of 500 μm and sag heights up to 160 μm. Several process conditions like polymer volume, dispense pattern, UV-exposure time, and intensity had to be carefully adopted in order to compensate for inevitably occurring surface artifacts due to the shrinkage of the used polymers. A white light interferometer in combination with a tactile surface profilometer was used to characterize the fabricated structures.

9130-26, Session 5

Polymer self-assembling of light converting microlense arrays

Sara Coppola, Biagio Mandracchia, Istituto Nazionale di Ottica (Italy); Giuseppe Nasti, Consiglio Nazionale delle Ricerche (Italy); Veronica Vespini, Istituto Nazionale di Ottica (Italy); Paola Pareo, Istituto Italiano di Tecnologia (Italy); Luigi Carbone, Consiglio Nazionale delle Ricerche (Italy); Michele Manca, Istituto Italiano di Tecnologia (Italy); Giuseppe Gigli, Consiglio Nazionale delle Ricerche (Italy); Pietro Ferraro, Istituto Nazionale di Ottica (Italy)

Brightness and electroluminescence efficiency (ELE) are two critical factors to consider for the diffusion of devices based on organic light emitting diodes (OLEDs) with the scope of lighting and display applications. Thereby, with the aim at improving the ELE, the gathering of the wave-guided light trapped within an OLED device and, more in general, within an electroluminescent flat multilayer-device has become one of the major point in question to be investigated. In the last few years, the interest in polymer-based microlenses and devices has increased specially motivated by the possibility of embedding active media like colloidal inorganic nanocrystals (NCs) into polymers thus transforming originally passive micro-optical elements into active components.

In the specific case of light emitting semiconducting polymers different techniques have been used for the fabrication of electroluminescent devices. Experiments and characterization have been carried out at different operating voltages and for voltage dependent emission color1,2 also combining the processability of organic materials with efficient luminescence displayed by inorganic nanocrystals.3 In fact, the experimental perspective to disperse emitting colloidal NCs into polymers has allowed to further engineer hybrid organic-inorganic materials introducing innovative functionalities as for instance photoluminescence conversion capabilities. This has proved of great interest for novel applications such as the fabrication of photonic crystals4 and, notably, of innovative solar cells showing enhanced efficiency.5-8 With this in mind, we have been developing new active micro-optical elements made by a mixture of rod-shaped inorganic NCs dispersed into poly-dimethylsiloxane. As inkjet printing procedure a nozzle-less approach exploiting a pyro-electro-hydrodynamic effect (Pyro-EHD) activated onto a lithium niobate crystal has been employed.9 By applying the Pyro-EHD pressure and using micro-engineered crystals, polymeric and size-tunable micro-lens arrays have been produced in a direct and simple way. Herein we detail on the fabrication and optical characterization of nanorod-incorporating and light-converting micro-lens arrays of different shapes and heights as down as 4 microns.

9130-27, Session 5

Soft-thermal printing of thick polymer layers for microoptics and MOEMS fabrication

Sami Abada, Benjamin Reig, Lab. d'Analyse et d'Architecture des Systèmes (France) and Univ. de Toulouse (France); Emmanuelle Daran, Lab. d'Analyse et d'Architecture des Systèmes (France); Jean-Baptiste Doucet, Thierry Camps, Veronique Bardinal, Lab. d'Analyse et d'Architecture des Systèmes (France) and Univ. de Toulouse (France)

We report on a new method, that we call "soft thermal printing" able to improve the uniformity of SU-8 polymer thick layers (>100μm) deposited on small samples such as III-V wafers. The aim is to enable a high yield integration of polymer high aspect-ratio microlenses on GaAs-based VCSELs [1] whatever the

sample size (1cm? up to 2"). This achievement is not possible using direct spin-coating due to large edge beads appearing on such small wafers (30% of the targeted thickness) leading to a detrimental lack of reproducibility in pattern definition.

The principle of our method is the following: the SU-8 layer is first deposited by spin-coating on a 4" flexible plastic film that is already glued on a silicon wafer serving as a temporary mechanical support. This way, the layer thickness is uniform over a surface much larger than the final one (maximal variation lower than 10% over 3"). After removal from the Si wafer, this flexible film is reported on the III-V wafer using a nano-imprint lithography equipment ("Nanonex NX-2500") originally dedicated to thermal or UV NIL. This set-up is equipped with a double membrane system that allows for a "soft" film transfer thanks to the homogeneous hydrostatic pressure applied to the substrate. Temperature, pressure and printing duration were optimized to achieve a good adhesion on the wafer (flat or already micro-patterned) without any film crushing. Micro-patterns were then fabricated by standard photolithography and were found to be well-defined, with a low variation in height, reproducing the initial uniformity profile of the film. This new method was successfully applied for uniform fabrication of polymer MOEMS for VCSELs beam focusing and can also be applied to other types of substrates (glass, silicon) or using commercial SU-8 films.

[1] B Reig et al 2012 J. Micromech. Microeng. 22 065006.

9130-28, Session 5

Toolchain concept for the automated assembly of micro-optical systems

Sebastian Haag, Tobias Müller, Fraunhofer-Institut für Produktionstechnologie (Germany); Christian Brecher, RWTH Aachen (Germany)

Today, the assembly of high-technology micro-optical systems is dominated by manual or semi-automated processes. Due to the high ratio of manual processes, companies in high-wage countries experience a disadvantageous competitive situation. Technical feasibility of assembly automation has been proven in previous research work as well as in a few industrial use cases. [1,2] Still, automation of micro-optical assembly is economically challenging because of high initial invest and high complexity of process development and therefore long planning and commissioning efforts. In case of many high-technology applications, production volumes stay below the critical amount when automation is profitable – even in high-wage countries. [3] In recent years flexible and reconfigurable assembly systems have been set up in order to increase machine utilization by producing several products or product variants on a single machine. [3,4]

In micro-optical assembly, the mastering of the steps of passive and active alignment, bonding, and part feeding as well as their interdependencies are crucial to the success of an automation solution. In a flexible scenario, sensor systems like cameras are integrated to support each of those process steps. Process development is therefore complex and time consuming. Separation of assembly process planning and assembly execution decouples both phases so that production and process development can take place in parallel and even in spatially separated stations. The work presented in this paper refines the concept of flexible assembly systems by separating the phases of assembly process planning and assembly execution by providing a dedicated process development platform on the one hand and by providing automatisms regarding the transfer from the development platform into industrial production on the other.

For this purpose, two key concepts are being developed by the research carried out at Fraunhofer IPT. The first concept comprises formal descriptions of the product and its individual components as well as constraints on their spatial relations. The notation for mechanical assemblies in [5] is extended to meet the demands of optical assembly. The formalism introduced allows the derivation of hardware-independent assembly flow control logic without extra programming efforts. The second concept achieves transferability of the assembly flow control logic between different production platforms through a hardware abstraction layer combined with a plugin-concept for device drivers implementing standardized interfaces. The combination of both concepts leads to reduced times for assembly process planning and commissioning.

The paper introduces the overall approach and formalisms as well as a form of notation based on part lists, product features and key characteristics and it shows industrial use cases the approach has been applied to. Key characteristics are constraints on spatial relations and they are expressed in terms of optical functions or geometric constraints which need to be fulfilled. In the paper, special attention is paid to the illustration of the end-user perspective. The approach has the clear goal to enable non-automation experts to plan and commission automated assembly processes for micro-optical systems. As a development platform a robot-based system will be depicted. As production platform a professional industrial micro-assembly solution will be shown.

References:

[1] Miesner, Jörn; Timmermann, Andre; Meinschien, Jens; Neumann, Bernhard; Wright, Steve; Tekin, Tolga et al. (2009). In: Mark S. Zediker (Hg.): High-power diode laser technology and applications VII. 26-27 January 2009, San Jose, California, United States. Bellingham, Wash: SPIE (v. 7198), S. 71980G–71980G-11.

[2] Pierer, J.; Lützelschwab, M.; Grossmann, S.; Spinola Durante, G.; Bosshard, Ch.; Valk, B. et al. (2011). In: Mark S. Zediker (Hg.): High-power diode laser technology and applications IX. 23-25 January 2011, San Francisco, California, United States. Bellingham, Wash: SPIE (v. 7918), S. 79180I–79180I-8.

[3] Brecher, Christian (2012): Integrative production technology for high-wage countries. Berlin, New York: Springer.

[4] Garlich, Torsten; Guerrero, Vicente; Hoppen, Martin; Müller, Tobias; Pont, Pere; Pyschny, Nicolas et al. (2012): SCALAB. Scalable Automation for Emerging Lab Production. Final report oft the MNT-ERA.net research project. 1. ed. Aachen: Apprimus-Verl.

[5] Whitney, Daniel E. (2004): Mechanical assemblies. Their design, manufacture, and role in product development. New York: Oxford University Press.

9130-29, Session 5

Design, fabrication and characterization of LVOF-based IR microspectrometers

N. Pelin Ayerden, Mohammadamir Ghaderi, Technische Univ. Delft (Netherlands); Manuel F. R. Silva, Univ. do Minho (Portugal); Arvin Emadi, Maxim Integrated (United States); Peter Enoksson, Chalmers Univ. of Technology (Sweden); José Higino Gomeo Correia, Univ. do Minho (Portugal); Ger de Graaf, Reinoud F. Wolffenbuttel, Technische Univ. Delft (Netherlands)

This paper presents the design, fabrication and characterization of an IC-compatible LVOF-based (Linear Variable Optical Filter) microspectrometer that operates in the infrared spectral range and intended for measuring the composition of natural gas. An LVOF-based microspectrometer is a tapered-cavity Fabry-Perot optical filter placed on top of a linear array of detectors. The filter transforms the optical spectrum into a lateral intensity profile, which is recorded by the detectors.

The IR LVOF has been fabricated in an IC-compatible process flow using a resist reflow step and is followed by the transfer etching of resist into the optical resonator layer. This technique provides the possibility to fabricate a small, robust and high-resolution micro-spectrometer in the IR spectral range directly on a detector chip. In these designs, the LVOF uses thin-film layers of sputtered Si and SiO2 as the high and low refractive index materials respectively. By tuning the deposition conditions and analyzing the optical properties with a commercial ellipsometer, the refractive indexes for Si and SiO2 thin-films were measured and optimized for the intended spectral range. Two LVOF microspectrometers, one operating

in the 2.0-3.0 μm, and the other in the 3.0-4.5 μm wavelength range, have been designed and fabricated on a silicon wafer. The filters consist of a Fabry-Perot structure combined with a band-pass filter to block the out of band transmission. Finally, the filters were fully characterized with an FTIR spectrometer. The measured transmittance curves were in agreement with theory. The preliminary characterization shows a spectral resolution better than 20 nm, which can be further improved using signal processing algorithms.

9130-30, Session 5

Arrays of millimeter-sized glass lenses for miniature inspection systems

Jorge Albero, Stephane Perrin, Sylwester Bargiel, Maciej Baranski, Nicolas Passilly, FEMTO-ST (France); Ludovic Gauthier-Manuel, Institut FEMTO-ST (France); Christophe Gorecki, FEMTO-ST (France)

In this paper, we adapt a technique employed for glass microlenses fabrication in order to obtain matrices of millimeter size lenses having high quality. The use of microfabrication processes and Micro ElectroMechanical Systems (MEMS) compatible materials allow the integration of lenses larger than usual in microsystems. Since the presented lenses can have 2 mm in diameter or more, some aspects apparently irrelevant when diameters are lower than 500 μm must be reviewed and taken into account. Indeed, when the lenses are in the millimeter range, problems such as size non-uniformities within a matrix and asymmetric shapes of each lens are dependent on parameters such as mask design, depth of the silicon cavities, enclosed vacuum control after anodic bonding, reflow temperature and even position of the lenses on the substrate. In the fabrication process, a mask formed of circular shapes is patterned with positive photoresist on a silicon wafer by standard UV photolithography. Then, cylindrical cavities about 300 μm deep are obtained in silicon by deep reactive ion etching (DRIE). After removing the photoresist mask, the silicon cavities are sealed under vacuum with a borosilicate glass wafer by anodic bonding. When placing the silicon-glass stack inside a furnace at high temperature, the glass melts with spherical shape by getting aspired into the cavity thanks to the pressure differences between the sealed cavity and the outer environment. After melting, the glass backside is polished in order to obtain a flat surface with optical quality. Silicon can be afterwards selectively removed by dry or wet etching and the plano-convex lenses are then released. Issues related to this fabrication flow-chart are addressed in this paper and few solutions are proposed. Results consecutive to optimization are shown to prove the pertinence of this technique to fabricate MEMS-compatible millimeter-sized lenses to be integrated in miniature microscopes.

9130-31, Session 6

High-performance embedded transmission gratings for spectrometric applications

Frank Fuchs, André L. Matthes, Torsten Harzendorf, Fraunhofer-Institut für Angewandte Optik und Feinmechanik (Germany); Uwe D. Zeitner, Fraunhofer-Institut für Angewandte Optik und Feinmechanik (Germany) and Friedrich-Schiller-Univ. Jena (Germany); Roman Windpassinger, Kayser-Threde GmbH (Germany)

Spaceborne spectroscopic instrumentation has become an important tool for the study of Earth's atmospheric composition. Future missions such as Sentinel-4/5 - monitoring the air quality, stratospheric ozone, solar radiation, and climate - favor grating spectrometers due to their demand for highly sensitive instruments with high spectral resolution.

In this contribution we report on the design, fabrication, and characterization of a grating tailored for the NIR channel of ESA's Sentinel-5 mission. Designed for the NIR band between 750 nm ... 775 nm the grating features a line-density of about 2268 lp/mm, while still delivering a highly polarization insensitive diffraction efficiency of greater 90%. The design is based on a novel grating concept, forming a high index grating on the template of a structured fused-silica substrate. The gratings have been realized by the Fraunhofer IOF by a genuine technological approach based on the combination of electron-beam lithography, reactive ion-etching, and atomic-layer-deposition (ALD). Efficiencies in good agreement with the grating design are demonstrated.

9130-32, Session 6

Linear to radial/azimuthal polarization converter in transmission using form birefringence in a segmented silicon grating manufactured by high productivity microelectronic technologies

Thomas Kämpfe, Lab. Hubert Curien (France); Pierre Sixt, Denis Renaud, Armelle Lagrange, Fabrice Perrin, MINATEC (France); Yves Jourlin, Olivier Parriaux, Lab. Hubert Curien (France)

A rotation of the polarization of a laser-beam can be achieved by a subwavelength 0th order binary grating using the phase-shift between the TE and TM 0th order grating modes. If the corrugation is etched directly into the substrate surface, i.e. the ridges and substrate consist of the same material, a very high ridge aspect ratio (3 to 4 for a half-wave phase-shift of pi) is required, which is difficult to fabricate and furthermore imposes an undesired compromise between the desired 100% transmission and the required phase-shift of pi. An inventive design based on the phase management of the grating modes involved in a high index corrugation on a low index substrate permits to simultaneously achieve close to 100% TM transmission, maximum TE Fabry-Perot resonant transmission and close to pi phase-shift between the TE and TM transmitted fields in a corrugation which has the minimum depth, requiring an comparatively smaller ridge aspect ratio of 2.1, being therefore more easily manufacturable.

A segmented polarization rotating element for a 1030 nm Yb:YAG laser beam converting a linearly polarized incidence to a radial polarization distribution was realized wafer-scale on 200 mm diameter borofloat glass wafers. The high index layer was first deposited by the well developed PECVD of amorphous silicon solar cells followed by the deposition of a 250 nm thick TEOS hard mask on top. The microstructuring starts with the projection of a chromium reticle by means of a 248 nm KrF stepper with a 4x reduction factor. An ICP dry etching transfers the photoresist corrugation into the hard mask; the needed 113 nm ridge width of the 613 nm period grating is controlled by ICP trimming in a post-process. Finally, the amorphous silicon layer is etched through and the remnants of the TEOS mask removed. The fabricated subwavelength gratings show locally a transmission >95% through crossed polarisers for a 90° polarization turning functionality, indicating a very high transmission for TE as well as for TM combined with a phase shift of pi between the two polarizations. The efficient creation of radially polarized light at 1064nm was demonstrated by analyzing the intensity distribution of the transformed beam after passing through an additional linear polarizer.

The presentation will give the technical characteristics of the obtained polarization converters and of the uniformity achieved wafer-scale. Beyond this, the presentation will give an evaluation of the general potential of microelectronic technology for the batch manufacturing of wavelength-scale diffractive elements for the processing of free space waves. We will also discuss the general formalism of the novel design scheme, based on normalized grating parameters, allowing the easy adaption to applications deeper into the visible range and at 10.6 μm wavelength.

9130-33, Session 6

Fast character projection electron beam lithography for diffractive optical elements

Torsten Harzendorf, Frank Fuchs, Fraunhofer-Institut für Angewandte Optik und Feinmechanik (Germany); Michael Banasch, Vistec Electron Beam GmbH (Germany); Uwe D. Zeitner, Fraunhofer-Institut für Angewandte Optik und Feinmechanik (Germany) and Friedrich-Schiller-Univ. Jena (Germany)

Electron beam lithography becomes attractive also for the fabrication of large scale diffractive optical elements by the use of the character projection (CP) technique. Even in the comparable fast variable shaped beam exposure approach for conventional electron beam writers optical nanostructures may require very long writing times exceeding 24 hours per wafer because of the high density of features, as required by e.g. sub-wavelength nanostructures. Using character projection, the writing time can be reduced by more than one order of magnitude, due to the simultaneous exposure of multiple features. The benefit of character projection increases with increasing complexity of the features and decreasing period. In this contribution we demonstrate the CP technique for a grating of hexagonal symmetry at 350nm period. The pattern is designed to provide antireflective (AR) properties, which can be adapted in their spectral and angular domain for applications from VIS to NIR by changing the feature size and the etching depth of the nanostructure. This AR nanostructure can be used on the backside of optical elements e.g. gratings, when an AR coating stack could not be applied for the reason of climatic conditions or wave front accuracy.

9130-34, Session 6

Chromatic confocal microscopy using hybrid aspheric diffractive lenses

Mathieu Rayer, AMETEK Taylor Hobson Ltd. (United Kingdom) and Heriot-Watt Univ. (United Kingdom); Daniel Mansfield, AMETEK Taylor Hobson Ltd. (United Kingdom)

A chromatic confocal microscope is a high dynamic range non-contact distance measurement sensor; it is based upon a hyper-chromatic lens. Currently the vast majority of commercial chromatic confocal microscope use refractive-based chromatic dispersion in such a lens. The performance of refractive, diffractive and Hybrid Aspheric Diffractive are compared. Hybrid aspheric diffractive lenses combine the low geometric aberration of a diffractive lens with the high optical power of an aspheric lens [1]. Hybrid aspheric diffractive lenses can significantly reduce the number of elements in an imaging system or create large hyper-chromatic lenses for sensing applications [2]. In addition, if the lenses are designed for large diffraction order, the modes both are overlap spatially and spectrally [2]. Hence, the surface signature is carried by multiple peak rather that one. Therefore, by averaging the positions by the number of mode the resolution is enhanced by the square root of the number of mode. Consequently, such multi-order diffractive lenses can improve the resolution of a chromatic confocal microscope by 2.23 for 5 modes [2]. However, the optical power carried by the diffractive side of a hybrid aspheric diffractive lens is limited by the manufacturing process and the diffraction efficiency. It is shown that a special hybrid aspheric diffractive arrangement permits a diffraction efficiency exceeding 95 % over the visible spectrum [3]. Such diffraction efficiency is reached by carefully selecting the dispersion curve of the chosen materials.

However, a theoretical and experimental study of the manufacturing losses has revealed that the hybrid aspheric diffractive configuration with the highest diffraction efficiency is a step diffractive surface. Step diffractive surface [4] lenses have the potential to reduce light losses associated with the manufacturing limits by five without increasing the surface roughness allowing scalar diffraction-limited optical design with a diffractive element. Using such lenses, the dynamic range of the chromatic confocal microscope has been improved by a factor 3 to reach 100,000.

1. G. J. Swanson, Binary optics technology: the theory and design of multi-level phase diffractive optical elements, MIT Tech. Rep. 854 (MIT, Cambridge, Mass., 1989).

2. M. RAYER, “Metrological apparatus,” Patent WO2013093459 A2 (June 27, 2013).

3. B. H. Kleemann, M. Seeßelberg, and J. Ruoff, “Design concepts for broadband high-efficiency DOEs,” Journal of the European Optical Society-Rapid publications 3, (2008).

4. J. M. Sasian and R. A. Chipman, “Staircase lens: a binary and diffractive field curvature corrector,” Appl. Opt. 32, 6066 (1993).

9130-35, Session 6

Optimizing the fabrication of diffractive optical elements using a focused ion beam system

Vijayakumar Anand, Indian Institute of Technology Madras (India); Ulrike Eigenthaler, Kahraman Keskinbora, Max-Planck Institut für Intelligente Systeme (Germany); Gayathri M. Sridharan, Vayalamkuzhi Pramitha, Indian Institute of Technology Madras (India); Michael Hirscher, Joachim P. Spatz, Max-Planck Institut für Intelligente Systeme (Germany); Shanti Bhattacharya, Indian Institute of Technology Madras (India)

In the past, UV lithography has been used extensively for the fabrication of diffractive optical elements (DOEs). While UV lithography has the advantage of fabrication of the entire structure at one time, however, the minimum feature size is limited to about 1 ?m. Many 1-d and 2-d periodic grating structures may not need such fine details but it is essential for DOEs with circular structures since the spacing between features typically decreases further away from the optical axis of the element. Therefore, the smallest feature size can easily be well below 1 ?m. Also, 1-d sub-wavelength gratings will have smaller features sizes for wavelengths in the infra-red region. In such cases, advanced techniques such as Focused Ion Beam and Electron-beam Lithography are required for the fabrication of finer structures. In this paper, we present results of DOEs fabricated with a focused ion beam system (Nova Nanolab 600 from FEI) directly on a single mode fiber tip. The ability to write DOEs directly on fiber tip is of great importance in fields such as endoscopy and optical trapping. The DOE itself, transforms the laser beam to a phase and intensity profile that matches the requirement. Because it is located directly on the fiber, no extra alignment is required. In addition, the system becomes more compact, which is especially important for applications in the field of endoscopy.

The main goal of the present work was to develop the most accurate method for creating the desired pattern (that is, the DOE structure) into an actually working element. Different exposure strategies for writing test structures directly with the ion beam on the fiber tip have been tested and carefully evaluated.

The paper will present in detail the initial fabrication and optical test results for blazed and binary structures of 1-d and circularly symmetric Fresnel axicons on single mode fibers.

9130-36, Session 6

Sub-wavelength grating as phase retarder: design using modal method and modeling by finite element method

Gayathri M. Sridharan, Shanti Bhattacharya, Indian Institute of Technology Madras (India)

Sub-wavelength dielectric gratings can be used to achieve phase retardation. Due to the vector nature of the devices,

scalar theory is not applicable and rigorous calculation methods are required. The modal method proves to be a simple but powerful compromise, between rigorous techniques that are computationally expensive and the scalar theory that is inadequate, for design of such elements. As a proof of concept, a quarter wave plate (QWP) was designed and its behavior compared against previously published data. Wave plate design requires that the orthogonal polarizations travel in the same direction with appropriate phase delay. It is assumed that light is incident normally on the grating. Floquet-Bloch periodicity ensures that discrete modes get excited within the grating. The number of propagating modes and the propagation constant of the modes can be controlled by the angle of incidence, the ratio of period to the incident wavelength and the fill factor. Modal method characterizes the underlying eigen modes (/ effective indices) of the orthogonal field components in the sub-wavelength structure. Based on the indices obtained by modal method, height of the grating ridge is deduced. The design gives a high aspect ratio of about 8 for a quarter wave phase retarder. The design is also numerically evaluated by the finite element method. The solver COMSOL was used to visualize how polarization direction evolves with time. The designed QWP could convert linearly polarized light into circularly polarized light and vice versa. This result proves the validity of the design procedure.

9131-1, Session 1

Spatial and angular color and luminance distribution of phosphor-converted white LEDs, modeling and experiments *(Invited Paper)*

Hugo J. Cornelissen, Philips Group Innovation (Netherlands); Shu-Li Hsiao, Binq-Qi Chen, National Taiwan Univ. of Science and Technology (Taiwan)

A new way of dual phosphors-converted white LED modeling is established and demonstrated. We use near-field chromatic luminance measurement data to investigate the effect of modeling parameters in LightTools and propose some key parameters to predict characteristics of LEDs accurately. In dual phosphors LEDs, there are many parameters in the simulation. It is not only overloading LightTools but also inefficient. Our novel approach is that we use phosphors without scattering, and add Mie particles to describe scattering specifically. It's an equivalent phosphors model which can predict characteristic of dual phosphors-converted LEDs very well. For example, there is a strong dependence of the luminance and the color as a function of position on the LED surface of a phosphor-converted medium-power LED. Our method can accurately predict this phenomenon. Another example is that we can predict the experimental finding that the LED color changes when the LED is coated with a TiO2-filled silicone layer. When adding a higher concentration of TiO2, higher backscattering and subsequently higher wavelength conversion occurs. This trend of decreasing correlated color temperature with increasing TiO2 concentration is predicted well.

9131-2, Session 1

Taking the spectral overlap between excitation and emission spectra of fluorescent materials into account with Monte Carlo simulations

Sven Leyre, Katholieke Univ. Leuven (Belgium); Jana Ryckaert, KU Leuven (Belgium); Paula Acuña, Jan Audenaert, Youri Meuret, Guy Durinck, KAHO Sint-Lieven (Belgium); Johan Hofkens, Geert Deconinck, Katholieke Univ. Leuven (Belgium); Peter Hanselaer, KAHO Sint-Lieven (Belgium)

Monte Carlo ray tracing is an importing simulation tool in many applications where fluorescence is present, e.g. in bio-medical applications, for luminaires or luminescent solar concentrators. In most commercial Monte Carlo ray tracing packages, it is possible to attribute absorption properties to a volume and to save the (partially) absorbed rays as a volumetric distribution. Using this volume distribution, it is possible to create a new fluorescent emission file.

A frequently used ray tracing procedure for fluorescence is a 'dual stage' approach. In this approach, first, all sources are traced through the system and the rays absorbed in the fluorescent components are stored. Next, the emission from the fluorescent components is traced, based on the information stored in the volumetric distribution files. This approach does not allow subsequent re-absorption and re-emission effects in fluorescent materials with a spectral overlap between excitation and emission spectra.

In this work, a 'multi stage' ray tracing procedure for fluorescence is presented. In this approach, wavelengths are traced from short to long separately and no distinction is made regarding the origin of emission (either a fluorescent component or a source). This allows accurate simulation of fluorescent materials with a spectral overlap between excitation and emission spectra. Moreover, the presented approach can be easily implemented in existing commercial ray tracing software packages. This reduces the programming efforts for the new ray tracing algorithm and takes advantage of the strength of the selected ray tracing package concerning the implementation of complex geometrical systems and the treatment all other optical effects (reflections at surfaces, absorption and volume scattering in materials, emission from sources...).

Both techniques are compared to investigate the influence of the selected ray tracing approach on the colour characteristics and efficiency prediction of a remote phosphor light source. A clear deviation on the prediction of the colour characteristics and efficiency is found.

9131-3, Session 1

Near-field and far-field goniophotometry of focused LED arrays

Valéry A. Jacobs, Vrije Univ. Brussel (Belgium); Stefaan Forment, Peter Hanselaer, Katholieke Univ. Leuven (Belgium); Patrick Rombauts, Vrije Univ. Brussel (Belgium)

Luminaires are conventionally modeled using a far-field representation. This representations describes the radiation pattern of a light source as if it originates from a single point. To calculate a far-field representation, a photometer revolves a light source at fixed distance and illuminances are measured in a set of angular directions. Using the inverse-square-law, the far-field intensity, also termed luminous intensity distribution (LID) is then calculated. However, this method is only valid in the far-field region and literature is unclear when defining a near-field and far-field zone. Traditionally, the far-field starts from a distance of five times the maximal dimension of a light source; which is called the limiting photometric distance. The advent of luminaires composed of LED arrays with narrow beams have shown that this limit is no longer valid and far larger distances (up to 15 times the maximal diameter) are suggested by the lighting community. This problem is even more outspoken when the individual LEDs are focused at close distance, as in e.g. surgical luminaires. To overcome these problems, we exploit the use of a near-field representation to describe an array of two narrow beam LEDs that are focused at close distance. For such a test source, this paper shows how a near-field luminance goniometer is able to construct ray-data and compares this near-field representation to a far-field representation using a photometer. The near-field representation allows us to construct accurate illuminance maps at any distance to the source, irrespective of the dimension of the array and the beam angle of the individual components. It is validated using a simple analytical model to describe the emission of the individual LEDs and it shows where the far-field representation fails to provide correct illuminances. This near-field approach makes discussions to determine the far-field photometric distance superfluous.

9131-4, Session 1

Design of refractive laser beam shapers to generate complex irradiance profiles

Meijie Li, Vrije Univ. Brussel (Belgium); Youri Meuret, KAHO Sint-Lieven (Belgium); Fabian Duerr, Vrije Univ. Brussel (Belgium); Michael Vervaeke, Brussels Photonics Team (B-PHOT), Vrije Univ Brussel (Belgium); Hugo Thienpont, Vrije Univ. Brussel (Belgium)

Laser beam shaping is widely used in many industrial and medical applications. In most cases, a laser beam with a Gaussian irradiance profile is reshaped to have a uniform output profile, usually called a flat-top profile. Some applications (e.g. laser additive manufacturing) require complex irradiance profiles in order to ensure optimal system performance. One example of such a complex irradiance profile is a Dark Hollow Gaussian (DHG) irradiance profile. There are many optical approaches that can be used for laser beam shaping, including apertures, filters, integrators, refractive lenses, reflective mirrors

and diffractive optical elements. Refractive laser beam shapers are commonly used due to their high optical efficiency and simple structure. Such refractive laser beam shapers typically consist of either two plano-aspheric lenses or one thick lens with two aspherical surfaces. The first aspherical surface redistributes the beam irradiance while the second aspherical surface recollimates the beam. Ray mapping is a general optical design technique for irradiance reshaping based on geometric optics. This approach in principle allows the design of lenses for any type of irradiance profile, yet it is typically used to transform a Gaussian beam into a beam with a flat-top profile. In order to generate more complex irradiance profiles especially with low intensity in the on-axis region (e.g. a DHG profile), this method is not directly applicable in practice. Due to the complexity of the desired irradiance profile, the numerical effort of calculating the aspherical surfaces increases. In addition, high accuracy of the designed aspherical surfaces is needed to obtain good results. This work presents a comprehensive numerical approach on how to efficiently design refractive laser beam shapers for different complex irradiance profiles, based on the geometric ray mapping method. There are two essential design steps involved in our approach. First, a "smart" sampling method is developed to calculate the mapping function between the radial positions on the two aspherical surfaces. Considering the complexity of the desired irradiance profile, we have found that the numerical calculation effort can be reduced considerably by sampling the radial position on the second aspherical surface with equidistant points, compared with sampling the encircled power directly as is usually done. Taken the DHG profile for example, it requires at least 10.000 points for the usual sampling method, whereas our proposed sampling method needs only 100 points or less. Second, an accurate surface reconstruction with either polynomials or splines is described. In case of polynomial fitting, it is necessary to use a polynomial function with both odd and even orders to fit to the calculated data points of the surface profile. Another option is spline fitting which fits piecewise polynomial functions with lower orders to the data points. Spline fitting is found to be able to describe the surface more precisely than polynomial fitting. Ray tracing analysis for several complex irradiance profiles demonstrates excellent performance of the designed lenses and the versatility of our design procedure.

9131-5, Session 1

Obsidianus lapis rugosity and hardness determination: fibre laser craftsmanship

Alfredo I. Aguilar-Morales, Jesús S. Velázquez-González, Jesus Ivan Reyes Sanchez, Sigifredo Marrujo-García, José Alfredo Álvarez-Chávez, Instituto Politécnico Nacional (Mexico)

Obsidian is a volcanic rock that has been worked into tools for cutting or weaponry by Teotihuacan people for hundreds of years. Currently it is used in jewelry or for house decorative items such as elaborated sculptures. From the physico-chemical properties point of view, obsidian is considered a glass as its composition is 80% silicon dioxide. In México there are different kinds of obsidian according to its colour: rainbow, black, brown, red, silver, golden and snowflake. The traditional grinding process for working with obsidian includes fixed grinders and sandpaper for the polishing process, where the craftsman grinds the stone manually obtaining a variety of shapes. Laser processing of natural stones is a relatively new topic. We propose the use of an Yb3+-doped fibre laser for cutting and ablating obsidian into spherical, rectangular and oval shapes. By means of a theoretical analysis of roughness and hardness, which affect the different surfaces and final shapes, and considering the changes in material temperature during laser interaction, this work will focus on parameter determination such as: laser fluence, incidence angle, laser average power and peak pulse energy, from the proposed Q-switched fibre laser design. Full optical, hardness and rugosity, initial and final, characterization will be included in the presentation.

9131-6, Session 2

Design and optimization of compact freeform lens array for laser beam splitting: a case study in optimal surface representation

Milan Maksimovic, Focal 2.0 (Netherlands)

We present a design study concerning freeform surface representation suitable for optimization of a compact freeform lens array for laser beam spitting.

Main emphasis of our paper is theoretical analysis of possible freefrom surface representations that can replace usual description of lens array by compact continuous freeform surface. We concentrate our study on some recently introduced and in this context less explored freeform surface representations such as Q-polynomials, Chebyshev polynomials, Linear Combination of Gaussians and Bernstein polynomials.

We use standard ray-tracing code available in Zemax software for optimization. We implemented customized merit function based on energy balance conditions and use both available surface representations implemented in the software and efficient implementations by means of User Defined Surfaces. We concentrate on the designs well described with geometrical optics. Final results are also simulated using wave propagation tool.

We start with the examples where lenses in the array are individually optimized and subsequently whole array is approximated with selected global freeform surface. Next, we introduce global freeform surface in the optimization procedure from the start. Optimization results obtained with the compact freeform surface representation are compared to the solutions obtained by the usual approach of arraying individually optimized freeform lenses. Important aspect of surface representations investigated in this way is a support of local deformations, lower and higher order rotationally symmetric and non-symmetric surface shapes. Further, we analyze merit function landscape with respect to complexity, order of surface representation and robustness to perturbations.

Presented design examples perform well for both Gaussian and multimodal input beams. Possible applications of similar designs are in laser fiber coupling and off-axis multi-spot generation where power splitting ratio can be arbitrarily predefined.

9131-7, Session 2

Design of freeform optics for an ophthalmological application

Ingo Sieber, Karlsruher Institut für Technologie (Germany); Allen Yi, Likai Li, The Ohio State Univ. (United States); Erik Beckert, Ralf Steinkopf, Fraunhofer-Institut für Angewandte Optik und Feinmechanik (Germany); Ulrich Gengenbach, Karlsruher Institut für Technologie (Germany)

Optical freeform surfaces are gaining increasing importance in different optical applications. A huge demand arises in the fields of automotive and defence technologies, consumer applications, and medical engineering. Among the optical systems requiring freeform optics are LED headlights and head-up displays.

Such innovative systems often need high-quality and high-volume optics. Injection-molded polymer optics represents a cost-efficient solution. However, it has to be ensured that the tight requirements with respect to system's performance are met by the replicated freeform optics.

To reach this goal, it is not sufficient to only characterize the manufactured optics by means of peak-to-valley (pv) or root mean square (rms) data describing a deviation from the nominal surface. To be able to determine the effect of this deviation in surface shape from the nominal shape, optical performance of the manufactured freeform optics has to be

analyzed and compared with the performance of the nominal surface. This can be done by integrating the measured surface data of the manufactured freeform optics into the optical simulation model.

The feedback of the measured surface data into the model allows for a simulation of the optical performance of the optical subsystem containing the real freeform optics manufactured. Hence, conclusions can be drawn as to whether the specifications with respect to e.g. imaging quality are met by means of the real manufactured optics.

Another important issue in system's design is to ensure the manufacturability of the optical component. This is achieved by a consequent application of a design for manufacturing approach called the comprehensive modeling approach. All constraints and requirements specific to the chosen manufacturing process as well as the process related design rules are acquired prior to modeling and considered in the design process.

This approach will be presented using an Alvarez-Humphrey optics as an example of a tunable optics of an ophthalmological application, the Artificial Accommodation System. Two different manufacturing technologies are used: on the one hand ultra precise diamond turning and on the other hand the replication method injection molding. Four different variants of the freeform optics are manufactured by means of the method injection molding, only differing in the choice of their surface parameters.

A comparative analysis of these variants by means of optical simulation allows for an evaluation of the manufactured parts on basis of the optical performance.

The focus of this article will be on design for manufacturing of the freeform optics, the integration of the measured surface data into the optical simulation model, the simulation of the optical performance, and the analysis in comparison to the nominal surface.

After introducing the concept and implementation of the comprehensive modeling approach, the concept of integration of the measured surface data in the model will be presented along with its application to the tuneable optics of the Artificial Accommodation system currently under development in the KD Optimi programme funded by the German Federal Ministry of Education and Research.

9131-8, Session 2

Optimization of the spectral performance of multilayer coatings on curved optics in plasma assisted deposition processes

Dirk Isfort, Diana A. Tonova, Stephane Bruynooghe, Carl Zeiss Jena GmbH (Germany)

The performance of optical components is usually improved by optical coatings. Some of these optical components exhibit complex geometrical shapes and are therefore very difficult to coat in a homogeneous way. The spectral performance of the optical coatings on such substrates will vary as a function of its geometry making it very difficult to keep the spectral performance within customer specifications all over the substrate.

Examples for optics with complex geometries are half sphere lenses, freeform surfaces, diffraction gratings, microlense arrays etc.

We developed a simulation tool that can calculate and optimize the spectral performance of a given multilayer stack on arbitrarily shaped optics as a function of the processing parameters of the coating plant. This tool will obviously reduce the risk and the development costs.

The spectral performance of a multilayer stack is given in general by the coating design, that means by the individual layer thicknesses and the refractive indices of the different layer materials. On curved optics different coating materials exhibit different thickness and refractive index distributions. Consequently the optical layer stack will exhibit varying spectral performance at different positions on the substrate.

Empirical models for thickness and refractive index distributions have been developed as a function of the most important processing parameters (e.g., deposition rate, deposition angle, ion impingement rate and temperature).

Finally the spectral performance of an AR-coating on a half spherical lens is simulated and optimized and then compared with the experiment.

9131-9, Session 2

New vistas in refractive laser beam shaping with an analytic design approach

Fabian Duerr, Hugo Thienpont, Vrije Univ. Brussel (Belgium)

Many commercial, medical and scientific applications of the laser have been developed since its invention. Materials processing applications, like cutting or welding; and medical applications, like corneal surgery are just a few examples. Many of these applications require a specific beam irradiance distribution to ensure an optimal performance. There are a number of optical technologies that can be used for laser beam shaping, including simple apertures, diffractive optical elements, lenses and mirrors. The right choice depends on the optical design problem.

Often, it is possible to apply geometrical methods to shape a laser beam profile. This common design approach is based on the ray mapping between the input plane and the output beam which takes into account conservation of energy, a constant optical path length of the geometric wave-front between the input and output planes, and the ray trace equations. Geometric ray mapping designs with two plano-aspheric lenses have been thoroughly studied in the past. Even though analytic expressions for various ray mapping functions do exist, the surface profiles of the lenses are still calculated by numerical integration.

In this work, we present a novel design approach that allows an analytic description of the entire optical design problem: including the rotational symmetric lens profiles. This design approach is related to an analytic design method for optimal imaging that enables the coupling of three ray-bundles with only two free-form lens profiles

[Opt. Express 20, 5576-5585 (2012)].

The example of a Gaussian to flat-top irradiance beam shaping system is used to establish a set of functional differential equations derived from Fermat's principle. The transformation of these functional differential equations into an algebraic linear system of equations allows a successive calculation of the Taylor series coefficients up to very high order. The implemented solution scheme makes it possible to calculate the exact lens profiles. For obvious reasons, it is only possible to calculate a finite (but high) number of initial terms of the Taylor series. Such a function is called a Taylor polynomial and will be the only approximation made.

To demonstrate the versatility of this new approach, a second design problem is solved to generate a more complex dark hollow Gaussian (doughnut-like) irradiance profile with zero intensity in the on-axis region. In this case, the problem arises that it is not possible to find a closed-form analytic expression for the ray mapping function, which is needed for the analytic design. However, by working with the inverse mapping function for which a closed-form expression does exist, we show that Lagrange inversion theorem can be applied to provide a Taylor series expansion of the original mapping function. The original mapping function is then given by a fractional Taylor series. The presented ray tracing results confirm the high accuracy of both calculated solutions and indicate the potential of this design approach for refractive beam shaping applications.

9131-10, Session 2

Single optical surface imaging designs with unconstrained object to image mapping with non-rotational symmetry

Jiayao Liu, Juan Carlos Miñano, Pablo Benítez, Univ. Politécnica de Madrid (Spain)

In this work, novel imaging designs with a single freeform optical surface (either refractive or reflective) are presented. In these designs, not only the mapping is obtained in the design process, but also the shape of the object is found. In the examples considered, the image is virtual and located at infinity and is seen from known pupil, which can emulate a human eye.

In the first introductory part, 2D designs and 3D designs by rotation using the differential equation method for the limit case of small pupil have been reviewed. As an advanced variation, the differential equation method is used to provide the freedom to control the tangential rays and sagittal rays simultaneously.

In the second part, according to the study of astigmatism of different types of design with rotational symmetry, the differential equation method for 3D rotational design without astigmatism (at the small pupil limit) on a curved object surface has been extended to 3D freeform design. The result of the extended method has been proved to coincide with the former 3D design by rotation which is a special case of 3D freeform design. Finally, the initial condition has been used as an additional freedom to control the shape of the object surface. As a result, a reflective design with a much flatter object surface has been obtained.

9131-11, Session 3

Design, alignment and applications of optical systems for parallel processing with ultra-short laser pulses

Lasse Buesing, RWTH Aachen (Germany); Stephan Eifel, Fraunhofer Institute for Laser Technology (Germany); Peter Loosen, RWTH Aachen (Germany) and Fraunhofer-Institut für Lasertechnik (Germany)

During the last years, the average power of commercial ultra-short pulsed laser sources increased significantly. The utilization of high average laser power in the field of material processing requires an efficient distribution of the laser power onto the work piece to reduce the thermal load for the work piece. One approach to increase the efficiency is the application of beam splitting devices to enable parallel processing. Especially for manufacturing periodic structures this method will provide a substantial technical progress. However, the shaping and steering of multiple beams requires particular optical systems which are not state of the art today.

Limitations for large spot arrays are evaluated and considered for the design concept of appropriate optical systems. During larger spot separations are capable to decrease the thermal load for a work piece, they will also increase aberrations as the whole field is increasing. So a convenient spot separation and total number of spots has to be determined, to keep both aberrations and thermal load sufficiently small but to guaranty a most efficient process at the same time.

For the purpose of micro structuring with high demands on the spatial accuracy, an optical system based on a diffractive 14x14 beam splitter (DOE) is designed and set up. All partial beams are coupled into a scanner device by using a relay lens system. Furthermore, this relay lens system offers a practicable solution to remove higher diffraction orders of the DOE. Due to the scanner a highly dynamic, simultaneous deflection of all partial laser beams can be achieved.

In comparison to optical systems for single laser beams, distortion effects become highly important. The distortion compensation for a single laser beam can be realized by correction files. But in case of a two dimensional spot array only the centroid position of the array can be corrected in this way. Therefore the distortion of the complete optical system has to be matched with the angular distribution of the beam splitter to attain the target distribution of the laser spots in the focus plane. Furthermore a reduction of the field curvature is essential for homogeneous processing results all over the spot array and all over the scan field.

For the alignment and the experimental evaluation of the complex optical system appropriate measurement devices are necessary. The simultaneous determination of several spot positions is realized by a camera system and adapted evaluation software. First experiments of large-area processing metal foils show promising results. Presented are recent design and alignment methods as well as application examples.

9131-12, Session 3

Effcient position tolerancing of optical components for precision adhesive bonding

Tobias Müller, Sebastian Haag, Josef Schleupen, Fraunhofer-Institut für Produktionstechnologie (Germany); Hansruedi Moser, Thomas Gisler, FISBA OPTIK AG (Switzerland); Christian Brecher, Fraunhofer-Institut für Produktionstechnologie (Germany)

Laser systems have become integral parts of highly diverse applications in the field of industrial, medical or consumer goods. Still, what many of these systems from the differing fields share is a complex optical design process aiming at the best tradeoff between optical efficiency, manufacturing costs and last but not least the complexity and equivalently the cost of the assembly process. Extensive research efforts are being made in matters of bonding methods, whilst the challenges of the state-of the art UV-curing adhesive bonding still provide opportunities for improvement as identified in several recent research projects and contributions.

In most cases, optical systems are designed according to the optical function only. However, optical systems often turn out to be highly sensitive to misalignments or positioning tolerances causing design reviews often linked to major changes in the optical design. Another way to face this challenge is to take a closer look at the end of the process chain in advance, and establish a link between the optical function of the system, spatial flexibility and the resulting positioning uncertainty which will still be acceptable in the production process. Therefore, an extensive examination of the bonding process is necessary.

Micro-optics, such as fast-axis collimators for diode lasers (FACs) have demanding positioning tolerances often within a sub-micron range. Additionally, FACs require active alignment in five degrees of freedom (DoF). In case of multi-DoF problems mechanical references cannot be used for alignment making a gap between the optical component and the mounting surface unavoidable. To bridge this gap UV-curing adhesive bonding is the state of the art method. The adhesive gap plays a crucial role in the tolerancing of the optical system as shrinkage effects in the curing process may cause misalignments.

Accordingly, the system design begins with the selection of a suitable adhesive matching temperature, outgassing, shrinkage and curing time requirements specified. While temperature and outgassing requirements are unalterable, shrinkage and curing time have a target conflict: Fast curing often leads to increased shrinkage. Also, the shrinkage rate is not constant over the shelf life of an adhesive. At Fraunhofer IPT a measurement setup to quantify the shrinkage of UV-curing adhesives has been setup. A number of common adhesives have been characterized in order to quantify the positioning uncertainty that results from the bonding process.

In order to determine the sensitivity of the single DoF modeling tools like Radiant Zemax® are used. However, the results obtained from simulation differ with those from reality due to manufacturing tolerances and misalignments in prior assembly processes. Accordingly, a certain flexibility in positioning is mandatory. This flexibility is provided by the glue gap and

limited by the uncertainty due to shrinkage in matters of direction and quantity.

Based on the results from the characterization of the adhesive the maximum acceptable tolerance limited by the assembly process is known answering the question of assembly process limitations for the optical system by specifying three values: The nominal value of the components position, the tolerance of the optic's ideal position and the sensitivity of this ideal position.

Answering these questions is enhancing an efficient product development process in preparation of a robust automated production process.

9131-13, Session 3

Methods for compensation of thermal lensing based on thermo-optical (TOP) analysis

Alexander Gatej, RWTH Aachen (Germany); Peter Loosen, RWTH Aachen (Germany) and Fraunhofer-Institut für Lasertechnik (Germany)

Thermal lensing in optical systems for laser beam guiding and shaping is an important topic touching many fields of application. Even laser powers of about 100 W can produce significant thermal effects and deteriorate the position of and the beam quality in the focus. Thereby, inhomogeneous temperature distributions in combination with occurring stresses influence the local refractive index and diminish imaging properties. Moreover, these effects overlay with surface deformations and thickness variations which additionally manipulate the optical behavior. Hence, high-loaded optical systems require thermally compensated system designs.

In a previous publication numerical algorithms have been demonstrated, enabling the integration and evaluation of arbitrary temperature profiles in the context of optical simulation: First, ray information from the optical simulation are being used in a finite-element analysis (FEA) as a heat source. Second, the resulting discrete FEA output is approximated into a continuous function. Third, the approximated function is integrated into the optical simulation for tracing.

Based on the generated software, thermal effects can be analyzed and strategies for the passive compensation of thermo-optic instabilities can be developed. The compensation of thermal lensing is based on three pillars:

• modelling and simulation of thermally aberrated optical systems

• methodologies for the compensation (design) and the validation (metrology)

• precise information on material data, particularly the absorptivity in bulk and coatings

The focus of the presentation will be on the methodology for compensation and the generation of material data. Therefore, experimental measurements can be used in combination with the simulation model to derive the required absorption data and thus generate the necessary data basis to transfer compensation methodologies into realized thermally stable optical systems.

Besides methodologies also experimental data will be presented as a basis of validation. Moreover, besides the stationary impact also the transient behavior can be analyzed and considered in the compensation process.

9131-14, Session 3

Shaping the effective focal volume inside dielectrics upon fs laser processing with complex beam wavefronts

Jesus del Hoyo Muñoz, Marcial Galvan-Sosa, Alexandro Ruiz de la Cruz, Consejo Superior de Investigaciones Científicas (Spain); Edward J. Grace, Imperial College London (United Kingdom); Andres Ferrer, ETH Zürich (Switzerland); Jan Siegel, Javier Solis, Consejo Superior de Investigaciones Científicas (Spain)

Integrated optical elements have revolutionized the perspectives of usage and deployment of optical devices. Non-linear laser processing of dielectrics with ultrafast lasers has been extensively studied over the last years and successfully applied to the production of photonic and micro-fluidic 2-D surface and 3-D subsurface devices.

For any application, a well-defined focal volume of the focused laser beam is of key importance in order to ensure optimum processing conditions. In fact, the ability of shaping the effective focal volume (EFV), i.e. the volume in which the laser energy is actually deposited, would strongly enhance device quality for industrial production Yet, problems related to the presence of strong optical non-linearities and spherical aberration make it difficult to optimize the EFV. Given the non-linear nature of the problem and the complexity of the material response, the input beam capable of producing the desired EFV cannot be easily calculated. For that reason, methods providing a rapid estimate of these effects, even approximately, are required for optimizing the processing parameters.

We have developed a new method for calculating the non-linear propagation of laser beams based on a generalized adaptive fast-Fourier evolver. The code has been successfully tested by comparing its results with experimental results of spatial soliton formation and also with results obtained for "usual" conditions in subsurface processing of dielectrics. Non-linear refraction, non-linear absorption and spherical aberration effects are explicitly considered in the calculations. The most attractive features are the calculation speed (typically a few minutes of computer time per irradiation) and the capability of propagating beams with non-flat wavefronts.

In this work we demonstrate the capability of using the code for designing EFVs using highly complex wavefronts, like those that can be generated with spatial light modulators (SLM). For this purpose the beam wavefront is codified using Zernike polynomials before being propagated inside the material.

We start with the EFV of a linearly propagated beam (choosing beam radii and focal length). Depending on the application, we may introduce an ad-hoc wavefront to produce a desired effect, such as the splitting of the focal volume (calculated with a Gerchberg-Saxton algorithm, for instance). Then, the effects of non-linear absorption and refraction, and spherical aberration are introduced considering the pulse duration and energy to calculate the EFV. Then we compare the difference between the desired and the non-linear and spherical-aberrated EFV. With that information, we can choose a number of Zernike polynomial to be the basis of a new wavefront we add to the old one to obtain the desired EFV. This can be done either by visual inspection of the so calculated EFV or by using an optimization algorithm to match the desired result.

The results obtained show that under certain conditions, non-linearities can be controlled and exploited to produce optimized EFVs. Simulations producing different effects are compared to in-situ laser-induced plasma emission and/or post-irradiation microscopy images to show the effectiveness of the approach.

9131-15, Session 3

Optical choppers with high speed rotating elements

Virgil-Florin Duma, Dorin Demian, Aurel Vlaicu Univ. of Arad (Romania); Octavian Cira, Aurel Vlaicu Univ of Arad (Romania)

Choppers are optomechatronic devices used for the modulation of light: to attenuate or eliminate certain wavelength ranges or to generate series of laser impulses. We have previously made a detailed study on choppers with rotating wheels with different configurations – and for different types of laser beams (i.e., top-hat, Gaussian and Bessel). In this paper we report a novel configuration of optical choppers with fast rotating elements (patent pending). The possible configurations of the device are discussed, and four chopper types are presented. The modulation functions of one of the types of choppers

newly introduced (i.e., the functions of the transmitted flux) are deduced and studied with regard to the geometry of the device. Comparison with other types of choppers – classical and eclipse (the latter introduced by us) – are being made. Aspects like chop frequency, attenuation coefficient, and profile of the light impulses transmitted by the device are taken into account.

Selected references: [1] Duma, V. F., "Theoretical approach on optical choppers for top-hat light beam distributions," Journal of Optics A: Pure and Applied Optics 10, 064008 (2008). [2] Duma, V. F., "Optical choppers with circular-shaped windows: Modulation functions," Communications in Nonlinear Science and Numerical Simulation 16, 2218-2224 (2011). [3] Duma, V. F., "Prototypes and modulation functions of classical and novel configurations of optical chopper wheels," Latin American Journal of Solids and Structures 10(1), 5-18 (2013).

9131-16, Session 4

Optical glass: refractive index change with wavelength and temperature

Marion Englert, Hochschule Darmstadt (Germany); Peter Hartmann, Steffen Reichel, SCHOTT AG (Germany)

With the catalog of 1992 SCHOTT introduced two formulae each with six parameters for a better representation of the refractive index of optical glasses. The Sellmeier-equation improved the characterization of dispersion at room temperature and the Hoffmann equation that of its temperature dependence. Better representation had been expected because both formulae were derived from general dispersion theory. The original publication of Hoffmann et al. from 1992 contains first results on the accuracy of the fits. The extended use of the formulae has led to a collection of data allowing reviewing the adequacy of the Sellmeier-equation approach on a much broader basis. We compare fitted refractive index values with measured values for all wavelengths used at our precision refractive index goniometer. Data sets are available for specific melts of the four representative glass types N-BK7, N-FK5, LF5 and IRG2.

For some materials, the optical glass N-LAF21, the IR glass IRG2 and the crystal CaF2, several sets of data for the temperature dependence of the refractive index are available thus giving evidence for the variation of these properties among melts of the same material.

9131-17, Session 4

Measuring reflective index of glass by using two captures under speckle field illumination

Changliang Guo, Dayan Li, Univ. College Dublin (Ireland); Damien P. Kelly, Technische Univ. Ilmenau (Germany); John T. Sheridan, Univ. College Dublin (Ireland)

Measurement of the reflective index of regular shaped glass by speckle correlation is reported. Two intensity images in the diffraction field of a speckle-illuminated sample are captured by a CCD before and after the presence of glass sample. As the position of peak correlation coefficient is quantitatively related to the change in optical path length arising due to the presence of glass, the reflective index of the glass can be evaluated by the correlation of the two intensity images. The theoretical correlation function is first derived that describes the relationship between optical path length change and speckle decorrelation. In experiment, various regular shaped glasses are measured to demonstrate the accuracy and robustness of the proposed technique.

9131-18, Session 4

The influence of a lightpipe on the coherence properties in laser projectors

Stijn Roelandt, Vrije Univ. Brussel (Belgium); Jani Tervo, Univ. of Eastern Finland (Finland); Youri Meuret, Katholieke Univ. Leuven (Belgium); Guy Verschaffelt, Hugo Thienpont, Vrije Univ. Brussel (Belgium)

Lightpipes are key optical components used in projection systems to transport and homogenize light from the source towards the light valve. They can provide a uniform light distribution at their output as a result of multiple internal reflections. Also in laser projection systems, such lightpipes are useful in combination with a laser-light module consisting of one or more single-mode lasers and a rotating diffuser. The partially coherent light emanating from the rotating diffuser is transported and homogenized towards the end of the light pipe. Consequently, propagation through the lightpipe will also modify the coherence properties of the laser light. In this paper, a computationally efficient simulation model is presented to propagate partially coherent light through a homogenizing rectangular light pipe. The resulting coherence function clearly differs from that of free-space propagation over the same optical path length. The implications of these results on, for example, the appearance of speckle are discussed in further detail. The simulation results are experimentally verified using a reversing wavefront Michelson interferometer. The approach described in this paper can be extended further to investigate other types of lightpipes, such as tapered lightpipes or even more complex ones.

9131-19, Session 4

Analysis of birefringence effects in laser crystals by full vectorial beam propagation method

Rainer Hartmann, Christoph Pflaum, Thomas Graupeter, Friedrich-Alexander-Univ. Erlangen-Nürnberg (Germany)

Modern laser technology demands powerful numerical tools to predict the efficiency of laser configurations. Birefringence has a strong influence on the beam quality and output power of a laser amplifier. To analyze this effect, we developed a complex physical model for simulating laser amplifiers. This model includes a model of the pump configuration, thermal lensing effect, birefringence, and beam propagation in the laser amplifier. The pump configuration is simulated by a complete 3-dimensional ray tracing or by an approximation based on super Gaussian functions. For an accurate modeling of the thermal lensing effect, the deformation of the end faces and the polarization dependent index of refraction is taken into account. To this end, temperature, deformation and stress inside the laser crystal are calculated by a 3-dimensional finite element analysis (FEA). In particular the index of refraction is accurately calculated including it's temperature dependency and the photoelastic effect. This index of refraction is used to propagate a laser beam through a laser amplifier. These simulations are performed by a completely 3-dimenional vectorial beam propagation method (VBPM). The advantage of VBPM is that it can be applied to polarization dependent index of refraction, which is important for taking into account birefringence obtained by the photoelastic effect inside the laser crystal. The beam propagation method is based on a finite elements on block structured grids and a Crank-Niccolson approximation in propagation direction (FE-BPM). The number of unknowns for a beam propagation method with stepping in propagation direction is relatively small compared to a fully three-dimensional system. Direct solvers are used as well as iterative Krylov subspace methods and multi grid methods. Reflecting boundaries are eliminated by introducing a perfect matching layer (PML).

Simulation results show that a complete 3-dimensional simulation model is useful to analyze and optimize high power

laser amplifiers. In particular, our model can take into account the crystal cut direction.

9131-20, Session 4

A new design approach to innovative spectrometers. Case study: TROPOLITE

Jean-Baptiste Volatier, Stefan Baümer, Bob Kruizinga, TNO (Netherlands); Rob Vink, Technisch Physische Dienst-TNO (Netherlands)

Designing a novel optical system is a nested iterative process. The optimization loop, from a starting point to final system is already mostly automated. However this loop is part of a wider loop which is not. This wider loop starts with an optical specification and ends with a manufacturability assessment.

When designing a new spectrometer with emphasis on weight and cost, numerous iterations between the optical- and mechanical designer are inevitable. The optical designer must then be able to reliably produce optical designs based on new input gained from multidisciplinary studies.

This paper presents a procedure that can automatically generate new starting points based on any kind of input or new constraints that might arise. These starting points can then be handed over to a generic optimization routine to make the design tasks extremely efficient. The optical designer job is then not to design optical systems, but to meta-design a procedure that produces optical systems paving the way for system level optimization.

This procedure is based on an original combination of well-known computational and theoretical tools. On the theoretical side combining plate and yybar diagrams provides an efficient yet detailed formalism of an optical system starting point. Efficient because of its dimensional parsimony, and detailed because characteristics usually only assessable at the latest stage of the design are available early on. Volume, sensitivity to manufacturability tolerances are examples of tradeoff that this procedure can take into account from the beginning.

On the computational side, instead of locally optimizing such a model, one can leverage present day computing technologies and combine brute force search with a clustering algorithm to identify the available solutions.

We present here this procedure and its application to the design of TROPOLITE a lightweight push broom imaging spectrometer.

9131-21, Session 5

Formalizing the procedure of structural synthesis on reflective and reflective-refractive optical systems design *(Invited Paper)*

Irina L. Livshits, Victor Zverev, National Research Univ. of Information Technologies, Mechanics and Optics (Russian Federation)

The idea of formalizing of procedure of structural synthesis on reflective and reflective-refractive optical systems is described. Classification of such systems and design examples are given.

At design of any optical systems the choice of the initial optical system which is often called its starting point is very important. Next step is a procedure of a structural synthesis which is understood as selecting the elements and putting them in a certain sequence in reflective and reflective-refractive objectives. Classification of optical elements and definition of their functional purpose is necessary for realization of this procedure in optical system.

It is obvious that in reflective system the basic element creating its optical power could be the concave mirror located by a concave surface towards the object. The role of correction element in purely mirror system is realized only due using coefficients of aspherical surfaces, i.e. changing the shape of the basic element. As the angular field of mirror systems is limited and can't usually reach great values, we will exclude from consideration elements for development of an angular field. As elements for development of the aperture in reflective objective have the same sign of optical power as basic elements (positive), they are located after the basic element in the converging beams.

In case of reflective-refractive optical systems in addition to this theory application of lens elements both as for aberrations correction, and as elements for development of an aperture in an objective (so called "fast" elements) is supposed. Structure of reflective and refractive-reflective system depends of type of optical scheme selected: Cassegrain, Ritchey Chre?tien, Mersenne, Newton, Maksutov, etc.

So, general equation of structural synthesis for reflective system is:

Pm + nCm+nFPm

And for reflective-refractive system is:

Pm+nC(m-l)+nF(m-l)

Where:

Pm – mirror with positive optical power;

Cm – mirror-corrector;

FPm – fast element with positive power;

n - number of elements on a certain place.

After the structure of optical system is decided, we go to the next stop which is parametrical synthesis of the objective where we calculate all the values of optical systems parameters: radii, distances between the mirrors and material type in case some refractive elements are presented in the system. The most difficult is to deal with the obscuration in mirror system. To solve it we propose to use an obscuration as a parameter which depends on general structure of the optical system and depend on optical scheme type, as well as of its overall length calculated as a sum of all distances between mirrors, lenses (if applicable) and back focal length.

Reflective optical systems have a long story of design, this is why we have so many design examples which we studied and created general rules on the design process based on heuristic rules. These rules were extracted from literature, patents and personal experience in optical systems design and transferred to heuristic algorithm for future CAD for reflective and reflective-refractive. Modern tendencies of using free-form, tilted and decentered mirrors are also included into consideration.

9131-22, Session 5

Comparison of off-axis TMA and FMA telescopes optimized over different fields of view: applications to Earth observation

Lionel Clermont, Yvan G. Stockman, Wouter Dierckx, Jérôme J. D. Loicq, Univ. de Liège (Belgium)

The aim of this paper is to present a comparison between off-axis TMA and FMA, with applications in wide field Earth observation.

TMA, or three mirror anastigmats, are widely used for applications such as space and earth observation. They indeed provide high image quality over large fields of view (FOV). Because such systems are purely reflective, they are achromatic and can operate over a wide spectral domain. Moreover, TMA made of material such as aluminum are lightweight and thus suit well for space missions. For larger FOV FMA, or four mirror anastigmats, are suspected to provide better image quality than TMA, as a fourth mirror would allow better correction of the optical aberrations. At identical focal length and pupil size, larger field of view could be achieved with good optical quality for FMA than for TMA. As a drawback, FMA are less tolerant to alignment and manufacturing errors. It might furthermore present more stray light than for TMA.

In the frame of earth observation, TMA have already been

used successfully on the ProbaV satellite (daily monitoring of the vegetation reflectivity all over the Earth). Three TMA, with individual field of view of 34 °, are used in a fan-like configuration to cover a total 102 ° field of view. On a heliosynchrone orbit at 800 km from earth, it provides daily images of the earth with resolution of 100 meters at the center of the FOV, 330 meters at the edge. For a successor mission, there is a need of increasing the resolution while keeping the same total field of view.

Increasing the resolution requires to increase the instrument size, thus increasing the geometrical aberrations. This would result in a decrease of image quality, especially at the edge of the individual instruments field of view. More than 3 TMA with a smaller individual field would thus be required. In order to minimize the total number of instruments, FMA could be used as they provide good image quality over higher FOV than TMA.

TMA and FMA have been optimized over different fields of view. MTF and distortion, as a function of total FOV, are compared for both designs. A preliminary tolerance analysis is performed and shows that more compensators are required for FMA. Advantages and drawbacks of FMA over TMA are discussed, and specific applications to earth observation are presented.

9131-23, Session 5

Imaging and analysis of biostructures using digital holographic microscopy (DHM)

James P. Ryle, National Univ. of Ireland, Maynooth (Ireland); John O'Connor, Univ. College Dublin (Ireland); Nazim Dugan, National Univ. of Ireland, Maynooth (Ireland); Susan McDonnell, John T. Sheridan, Univ. College Dublin (Ireland); Bryan M. Hennelly, National Univ. of Ireland, Maynooth (Ireland)

Scaffolds in tissue engineering are porous structures made from biocompatible artificial materials. They have an important role to support and structure cells to form and promote new tissue growth (e.g. artificial skin). Scaffolds are complex formations, often with random porous structures that optimizes cell seeding and adherence.

Microscopy offers enhanced spatial resolution which allows for microscopic structures to be imaged with a theoretical limit of half a wavelength of light. However, as a result of the high numerical aperture (NA) of the imaging optics, the depth of focus is proportionally decreased. Digital Holographic Microscopy (DHM) enables the recording of the full complex wavefront emanating from the object. It is possible to numerically reconstruct both intensity and phase (shape) information at various depths beyond that of the DOF limit of conventional microscopy. This can be achieved by capturing as little as a single intensity hologram of the object using a standard digital camera (CCD or CMOS sensor).

In the case of thick specimens with small gradient changes, DHM produces phase images or two dimensional surface profiles of the object under investigation. This phase reconstruction ability is useful in tissue engineering where surface features are of importance for quality analysis and to obtain specimen parameters such as shape information and an estimate of surface roughness and porosity.

In this paper, we apply DHM to obtain the surface profile of biostructures to determine this imaging technique's ability and feasibility of quickly imaging such objects.

9131-24, Session 5

Achieving super resolution using a dielectric spherical geodesic waveguide

Hamed Ahmadpanahi, Dejan Grabovickic, Juan Carlos González, Pablo Benítez, Juan Carlos Miñano, Univ. Politécnica de Madrid (Spain); Paul Urbach, Technische Univ. Delft (Netherlands)

In this paper we investigate super-resolution properties of a dielectric SGW in NIR spectrum. Since the losses in a dielectric waveguide can be much lesser than a metallic waveguide, the maximum resolution of the system can be improved significantly. In this work the SGW is made of three concentric hollow spheres with different thickness. The first and the third layers (claddings) have the thickness of 0.165?m and are made of air. The second layer (middle, core), which has a thickness of 0.11?m and outer radios of 0.835?m, is made of silicon with refractive index of 3.48. A spectrum of wavelength (in vacuum) that range from 1.562?m to 1.692?m has been used to excite the SGW and we study the super-resolution properties of the dielectric SGW in this wavelength range. The central wavelength of the spectrum which falls approximately around 1.624?m (in vacuum) is used as the reference wavelength. The reference wavelength inside the dielectric is around 0.471 ?m which is almost 11 times shorter than the guide's circumference. Our recent results show that we have achieved a sub-wavelength resolution of ?/209 (resolving power of about 8 nm).

The SGW contains a source and a drain which are located on two poles of the sphere, source at ? =0 and the drain at ? = pi (considering spherical coordinate). When the drain is shifted from its initial position a sudden drop in the transmitted power happens at a certain wavelength which we will call notch wavelength (frequency). This shift can be as small as a portion of the wavelength. This means that our receiver senses a small shift, which is much smaller than the wavelength. We define the "resolution" as the arc length (in wavelength units) that a drain port needs to be shifted so the transmitted power drops to 10% (not far from the Rayleigh criteria in Optics, which refers to the first null). With this criteria we have achieved the resolution power of ?/209 (~8nm) for a notch wavelength of 1.652 ?m.

9131-25, Session 5

Three-dimensional optical addressing by ultra low one-photon absorption microscopy

Qinggele Li, Trang M. Do, Isabelle Ledoux-Rak, Diep N. Lai, Ecole Normale Supérieure de Cachan (France)

Light microscope based on far field light focusing is an important tool for imaging and fabrication due to its easy accessible and noninvasive properties. For instance, it can be used for in-vivo bio-imaging or fabrication of photonic structure with micro or even nano scale. Basically, diffraction and penetration depth are the main factors for affecting the capability of optical microscope. Especially for 3D addressing, the axial resolution of light microscope based on one-photon absorption mechanism is pronounced problematic. Here, a novel method for three-dimensional (3D) optical addressing based on low one-photon absorption (LOPA) is theoretically and experimentally demonstrated. We investigated for first time the intensity distribution of point spread function (PSF) taking into account the absorption of material in which the light propagates. It is shown that the intensity and focusing spot shape strongly depend on the absorption coefficient and the numerical aperture (NA) of the used objective lens (OL). Indeed, on one hand, when the material presents very low linear absorption at a chosen excitation laser wavelength, the light intensity distribution of a collimated light beam keeps almost unchanged through the propagation inside the material. On the other hand, by using a high NA OL, the light beam will be tightly focused, thus resulting in a very high intensity in focal region. Combining low linear absorption effect and high NA OL, sub-micrometric focusing spot has highly contrast intensity distribution at any position inside the studied material. The axial sectioning capability of light microscope has been remarkably enhanced. This combination thus allows to optically address 3D object, equivalent to those achieved by using two-photon absorption technique. By solving the new evolution of mathematic representation of electromagnetic field distribution in focal region, it shows that for instance, in the case of high NA =1.35 oil immersion objective, with presenting low absorption coefficient 800 cm-1 , the derived penetration depth up to 300 ?m without any significant deformation [1]. The theoretical

calculations are also experimentally verified by focusing a laser beam, with different excitation wavelengths, inside a Rhodamine 6G solution. The experimental results show great enhancement of penetration depth, similar to what obtained by two-photon absorption microscopy, but this LOPA technique presents many advantages, since it requires only a simple setup and a low-cost and low power continuous laser. This LOPA based microscopy is very promising for submicrometric 3D imaging and 3D fabrication [2], as well as 3D photonic crystal.

1. Q. Li, M. T. Do, I. Ledoux-Rak, and N. D. Lai, "A novel concept for three-dimensional optical addressing by ultralow one-photon absorption method," Opt. Lett. 38, in press (2013).

2. M. T. Do, T. T. N. Nguyen, Q. Li, H. Benisty, I. Ledoux-Rak, and N. D. Lai, "Sub-micrometer three-dimensional structures fabrication enabled by one-photon absorption direct laser writing," Opt. Express 21, 20964 (2013).

9131-26, Session 6

3D-PSTD applied to the resolution in time and space of the time reversal of an image transmitted through a scattering medium

Fabrice Devaux, Eric Lantz, Univ. de Franche-Comté (France)

Recently we have reported experimental results in which infrared images transmitted through ex-vivo biological tissues were restored by back propagation in the biological tissues of a phase-conjugate wave obtained in a quadratic ???crystal by three-wave mixing phase conjugation (TWMPC) in a type II configuration [1]. Our results suggest that the scattering process in such biological samples is more or less independent of the polarization state of the light and that a polarization change of the phase conjugated wave with respect to the incident wave does not preclude the image restoration process.

In order to confirm this hypothesis, we have developed a numerical model of our experiment based on a Pseudo-Spectral Time Domain (PSTD) algorithm.

Stemming from the traditional FDTD method, the PSTD applies the Fast Fourier Transform, instead of the finite difference method, to calculate the spatial derivatives in Maxwell's equations [2]. In comparison with the FDTD, the PSTD method has higher order accuracy, smaller numerical dispersion errors and enhancing computational efficiency even with the use of a relatively coarse grid mesh (at least two cells per wavelength). Then, it allows considering larger scale problems than FDTD and allows 3D sampling of a scattering medium with realistic dimensions.

As the 3D-PSTD simulation gives access to the full vector components of the electromagnetic fields, it first allowed us to analyse the polarization state of the scattered light with respect to the characteristics of the scattering medium and the polarization state of the incident light [3]. In this conference, we will present new numerical results where the time reversal process by TWMPC has been implemented and we will show how the phase conjugate wave retraces the scattering path and gives a restored image.

[1] F. Devaux et al. J. of Biomed. Opt. 18 (2013) 111405.

[2] Q. H. Liu, Microwave Opt. Technol. Lett. 15 (1997) 158–165.

[3] F. Devaux et al. Opt. Express 21 (2013) 24969-24984.

9131-27, Session 6

Simulation-based investigation of the three-dimensional distribution of fluorescence and photobleaching in multi-photon excited samples

Imre B. Juhász, Árpád I. Csurgay, Peter Pazmany Catholic Univ. (Hungary)

In this paper, a numerical study is presented on the spatial distribution of fluorescence and photobleaching occurring in samples subject to multi-photon excitation.

We developed a simulation model and implemented a simulator program. The quantitative predictions enabled by our program can help to find the optimal operating parameters (such as laser power, pulse length, pulse repetition rate) of the two-photon microscope in order to reach higher image quality, to reduce undesired photobleaching, and to pave the way for optimized photoswitching-based super-resolution imaging. Conversely, the simulator might also be useful when photodynamic parameters are searched for. Furthermore, such simulations are able to promote the evaluation of the results of other fluorescence based techniques (e.g. fluorescence recovery after photobleaching [FRAP] measurements).

The photodynamic model of the fluorophore contains a ground state, an excited state, a triplet state, and several photobleached states; the state transitions are characterized by absorption cross sections and life times. The sample is modelled as a fluorophore solution divided into cubic cells among which diffusion takes place. In each cell the number of fluorophore molecules is stored state by state. The illumination is simulated as a focused laser pulse train described by a pulsed Gaussian beam profile, which is a more realistic approach than the continuous wave Gaussian beam function commonly used in former publications. Exploiting the cylindrical symmetry of the modelled region, calculations can be limited to a two-dimensional array of cells instead of a three-dimensional one, which significantly reduces the computation complexity. The appropriate dimensions of the simulation volume and the cell size were determined by simulations. Each laser cycle corresponds to one simulation step as it can be assumed that each fluorophore molecule can be excited at most once during a laser pulse since the life time of the excited state is assumed to be much longer than the pulse duration. Our simulator calculates probabilities; i.e. it determines expectation values that are real numbers, which eliminates oscillations originating from the fact that in reality only molecules and photons as a whole exist.

As a demonstration of the capabilities of the simulator, an example is presented that reveals the spatial distribution of photon emission in the sample investigated by a two-photon microscope in case of different laser and photobleaching parameters, assuming one-photon absorption induced photobleaching. The simulation demonstrates quantitatively how photobleaching affects the spatial distribution of fluorescence and the resolution of the microscope. As photobleaching progresses, the most photons are not emitted from the focus but from an ellipsoid or in more expressed cases, from a surface with an 8-shape cross section situated around the focus. In other words, a "dark hole" evolves at the focus. The unusual spatial distribution of the fluorescence is the consequence of the interplay of a second order and a first order process, namely the two-photon excitation and the one-photon absorption induced photobleaching. This effect is to be taken into account when the inverse problem (i.e. the reconstruction of the fluorophore distribution based on two-photon microscope measurements) is addressed.

9131-28, Session 6

Investigation of autofocus algorithms for brightfield microscopy of unstained bladder cancer cells

Shuyu Wu, Nazim Dugan, Bryan M. Hennelly, National Univ. of Ireland, Maynooth (Ireland)

In the past decade there has been significant interest in image processing for brightfield cell microscopy. [1] Much of the previous research has focused on image processing for fluorescence microscopy, including cell counting, cell tracking, cell segmentation and autofocusing. Fluorescence microscopy provides functional image information that involves the use of labels in the form of chemical stains or dyes. For some applications, where the biochemical integrity of the cell is

required to remain unchanged so that sensitive chemical testing can later be applied, it is necessary to avoid staining. For this reason it is the challenge of image processing of unstained, often "invisible" cells has become a topic of increasing attention. Brightfield microscopy is the most universally available and most widely used form of optical microscopy and for this reason we are interested in investigating image processing of unstained cells recorded using a standard brightfield microscope. In this paper we investigate the application of a range of different autofocus metrics [2-3] applied to unstained bladder cancer cell lines using a standard inverted bright field microscope with microscope objectives that have high magnification and numerical aperture. We present a number of conclusions on the optimum metrics and the manner in which they should be applied for this application.

[1] Rehan Ali, Mark Gooding, Tünde Szilágyi, Borivoj Vojnovic, Martin Christlieb, Michael Brady, "Automatic segmentation of adherent biological cell boundaries and nuclei from brightfield microscopy images," Machine Vision and Applications, Volume 23, Issue 4, pp 607-621

[2] Feimo Shen, Louis Hodgson, and Kluas Hahn "Digital Autofocus Methods for Automated MicroscopyVol. 414, No. 06. (2006), pp. 620-632

[3] Rafael Redondo et al. "Autofocus evaluation for brightfield microscopy pathology," Journal of Biomedical Optics 17(3), 036008 (March 2012)

9131-29, Session 6

Novel approach to modeling spectral-domain optical coherence tomography with Monte Carlo method

Maciej Kraszewski, Michal Trojanowski, Marcin Str?kowski, Jerzy Pluci?ski, Bogdan Kosmowski, Gdansk Univ. of Technology (Poland)

Theoretical modeling Optical Coherence Tomography (OCT) systems is needed for optical setup optimization, development of new signal processing methods and assessment of impact of different physical phenomena inside the sample on OCT signal. Monte Carlo method has been often used for modeling Optical Coherence Tomography, as it is a well established tool for simulating light propagation in scattering media. However, in this method light is modeled as a set of energy packets traveling along straight lines. This reduces accuracy of Monte Carlo calculations in case of simulating propagation of gaussian beams. Since such beams are commonly used in OCT systems, classical Monte Carlo algorithm need to be modified. In presented research, we have developed model of SD-OCT systems using combined Monte Carlo and analytical method. Our model includes properties of optical setup of OCT system, which is often ommited in other research. We present applied algorithms and comparison with SD-OCT scans of optical fantoms. We have found that our model can be used for determination of level of OCT signal comming from scattering particles inside turbid media placed in different positions relatively to focal point of incident light beam. It may improve accuracy of simulating OCT systems.

9131-30, Session 7

Advanced simulation tool for optical time-domain reflectometry (OTDR) with arbitrary pulse shapes

Benjamin Feigel, Jürgen Van Erps, Mulham Khoder, Michael Vervaeke, Vrije Univ. Brussel (Belgium); Stefano Beri, Kristof Jeuris, Danny Van Goidsenhoven, Jan Watté, TE Connectivity Ltd. (Belgium); Hugo Thienpont, Vrije Univ. Brussel (Belgium)

Optical time-domain reflectometry (OTDR) is used to characterize optical fiber systems in a non-intrusive way. Typical fiber systems contain fiber sections, fiber jumpers, splices, connectors and bends. By injecting a series of laser pulses into an optical fiber system and detecting the time-dependent Rayleigh backscattered and the Fresnel reflected power coming out of the system, OTDR allows the detection, localization and quantization of faults (e.g. fiber breakage), losses (e.g. from a splice) and reflections (e.g. from a connector). An OTDR trace shows the time-dependent detected power versus the distance in the fiber system, by converting this time dependence into a distance dependence via the time-of-flight of the laser pulses.

OTDR simulations, enabling the numerical generation of OTDR traces of well-defined fiber systems, are a very valuable – yet currently unavailable – tool to verify if OTDR is a suitable technique to monitor, test or characterize an optical system. This way, one can determine through simulations whether OTDR is usable for a certain application. Indeed, by simulating OTDR traces of a system containing a studied component, one can determine the component's influence on the system performance, without the need to build an experimental setup of this system and to run actual OTDR measurements. In addition, such a simulator is a powerful tool to analyze measured OTDR traces by fitting simulated traces to the measured ones and applying (advanced) statistical analysis.

Although much literature is found on how to model OTDR traces, these "simple" models do not include the influence of the actual pulse shape on the traces, but instead usually only consider ideal narrow rectangular pulses. Therefore, we present a comprehensive mathematical formalism, together with its numerical implementation, for OTDR simulations with arbitrary pulses. In our approach, the optical fiber network under test is treated as a linear time-invariant (LTI) single-input/single-output (SISO) system, which allows us to include the effects of the pulse shape. More specifically, the fiber system is modeled through its LTI system impulse response, while the incident OTDR pulse is considered as the input of the LTI system, and the OTDR trace as its output. The output signal is then calculated as the convolution of the impulse response with the input signal. The OTDR simulations take into account the attenuation and fiber backscattering coefficient of each separate fiber section. A discrete non-reflective event is simulated through its position and insertion loss (IL), while for the simulation of a discrete reflective event, its position and return loss (RL) is used. Moreover, the limitations of current OTDR equipment such as (nonlinear) power saturation of the OTDR detector, and limited dynamic range due to detector noise are also incorporated in the simulation model. Finally, simulated traces can be averaged to minimize the influence of noise, as is done in most OTDR devices.

To demonstrate the ability of the proposed simulator to accurately generate traces of fiber sections, splices and connectors, we verify our simulation results with an experimental setup and OTDR measurement. We show an excellent agreement between the measured and simulated traces.

9131-31, Session 7

Modal propagation and imaging characteristics of a custom designed coherent fiber bundle for endomicroscopy with proximal wave front shaping

Stefaan Heyvaert, Heidi Ottevaere, Vrije Univ. Brussel (Belgium); Ireneusz Kujawa, Institute of Electronic Materials Technology (Poland); Ryszard Buczynski, Institute of Electronic Materials Technology (Poland) and Univ. of Warsaw (Poland); Marc Raes, Herman Terryn, Hugo Thienpont, Vrije Univ. Brussel (Belgium)

For conventional endoscopes, the bijective relationship between each pixel in the image of interest and each sensing element (a core in a fiber bundle or a photosensitive element in a CCD chip) does not allow for a straightforward scaling of the diameter below 1-mm without a prohibitive deterioration in image quality. In recent years, several groups have investigated the use of Proximal Spatial Light modulation (PSML) as an

alternative fiber optic imaging technique. In PSLM, the light exiting the distal end of the fiber optic endoscope can be focused, without any distal micro-optics or micro-mechanics, on any point within the Field Of View (FOV) via spatial modulation of the light before it is coupled in at the endoscope's proximal end.

Since PSLM does not require any distal micro-optics or micro-mechanics, the outer diameter of the endoscope would only be limited by the diameter of the fiber optics waveguide. In previous work, we reported on the custom design of an ultra-high NA (0.928 at 850-nm) Coherent Fiber Bundle made of soft glasses (custom developed NC21 for the cladding and Schott SF6 for the cores) to be used with PSLM (as opposed to the commercially available optical fibers used by other groups). In this paper we present the results of the numerical characterization of the Coherent Fiber Bundle fabricated according to our design. We investigate the CFB's modal propagation characteristics as well as its imaging properties (FOV and point spread function). Our numerical characterization also takes into account fabrication induced defects such as variations in core size, core shape (ellipticity) and lattice constant. Realistic values for the defects were obtained via SEM images of the fabricated CFB's cross section. We find that noise on the wave front of the field exiting the distal end of the CFB causes a much larger deterioration of the point spread function than amplitude noise. And while we find that variations in core shape have the largest impact on the CFB's propagation characteristics, our results indicate that this negative impact could be negated if the elliptical cores were to be aligned along a common axis.

9131-32, Session 7

A new design of a directional coupler for high order mode multiplexing in few mode fiber

Abderrahmen Trichili, Amine Ben Salem, Rim Cherif, Univ. of Carthage (Tunisia); Mourad Zghal, Univ of Carthage (Tunisia); Andrew Forbes, CSIR National Laser Ctr. (South Africa)

Mode Division Multiplexing (MDM) over a few mode fiber (FMF) is considered to be one of the promising techniques to increase the overall transmission capacity for telecommunication systems. One of the key elements of the MDM is the mode multiplexer which is suitable for selective excitation of high order modes. However, existing mode multiplexers demonstrate high multiplexing loss exceeding 5 dB mainly introduced by holography-based mode conversion components such as tunable spatial light modulators (SLM) or liquid crystal on display (LCOS) panels.

In this paper, we design a low loss fiber-based directional coupler multiplexer capable of selectively exciting five linearly polarized (LP) modes and multiplexing them in a FMF. The designed device is assembled with five single mode fibers (SMF) which are positioned parallel to a FMF with optimized angles in order to convert the fundamental mode generated in each SMF into a selected high order mode in the FMF. The lengths of the SMFs are chosen of the order of few centimeters to ensure a complete coupling of all the modes. The finite element method (FEM) is applied to calculate the coupling coefficients. We find a total coupler insertion loss (CIL) less than 3 dB and a mode dependent loss (MDL) around 1 dB is obtained at the telecommunication wavelength ?=1550 nm. The impact of the angular positions of the SMFs with respect to the FMF on the extinction ratio of the generated high order mode is examined. The effect of the wavelength on the coupling efficiency as well as the coupling length is investigated too. Our results show that the proposed device is very promising for low loss high order mode multiplexers for high bit-rate optical communication systems.

9131-33, Session 7

On the design of few-mode Er-doped fiber amplifiers for space-division multiplexing optical communications systems

Adolfo Herbster, Murilo A. Romero, Univ. de São Paulo (Brazil)

Optical communications technologies based on space-division multiplexing use space as the final degree of multiplexing freedom, either by exploring the modal orthogonality in a few-mode fiber (FMF) or by using the multiple fiber cores (multi-core fiber, MCF) [1]. For long-haul transmission, optical amplification is required. However, in conventional EDFAs, each mode will experience a different value of optical gain, on account of distinct field profile configurations. This lack of gain equalization imposes difficulties for mode demultiplexing and may impair the system performance.

The FMF-EDFA designer should define Er doping and/or refractive index profiles, as well as the pumping configuration, to provide the best possible mode equalization of optical gain and noise figure. Conventional EDFA design usually requires solving a set of coupled propagation and rate differential equations for the HE11 fundamental mode [2]. In the case of the FMF-EDFA, the problem is much more involved because each mode contributes with its own set of coupled differential equations. To use this approach to carry out a rigorous optimization procedure is not feasible and the FMF-EDFAs designs proposed in the literature are either empirical, resulting in optical fiber cross-sections very complex to fabricate [3], or based on multiple (often high-order) pumps and pre-selected fiber doping profiles, limiting the available solution space [4].

A novel optimization method is proposed here. The definition of a figure of merit related to the equalization of the pump-mode signal overlap integral significantly reduces computation time, allowing the implementation of a multiobjective Non-dominated Sorting Genetic algorithm. The results obtained were validated against the solution provided by the full set of rate and propagation equations. Next, we conducted a FMF-EDFA optimization case-study. Our double-ring Er doping profile design requires a single 350 mW LP11,p pump to provide a mean gain of 21.6 dB, within 0.6 dB for each of the four modes considered, to the best of our knowledge the most promising result reported in the literature to date.

References:

[1] R. Essiambre and A. Mecozzi, "Capacity limits in single-mode fiber and scaling for spatial multiplexing," Optical Fiber Communication Conference, OFC 2012.

[2] C.R. Giles and E. Desurvire, "Modeling erbium-doped fiber amplifiers," Journal Lightwave Technology, vol.9, no.2, pp.271-283, February 1991.

[3] E. Ip, "Gain Equalization for Few-Mode Fiber Amplifiers Beyond Two Propagating Mode Groups", IEEE Photonics Technology Letters, Vol. 24, no. 21, pp 1933-1936, November 2012.

[4] Q. Kang, E. Lim, Y. Jung, F. Poletti, S. Alam, and D. Richardson, "Design of Four-Mode Erbium Doped Fiber Amplifier with Low Differential Modal Gain for Modal Division Multiplexed Transmissions," Optical Fiber Communication Conference, OFC 2013, paper OTu3G.3.

9131-48, Session PS3

Study on wavefront precompensation of thermal deformation aberrations in the beam path by FEM and Zernike polynomials

Qiong Zhou, Wenguang Liu, Zongfu Jiang, National Univ. of Defense Technology (China)

We present a new method to calculate wavefront pre-

compensation of the thermal deformation aberrations based on the finite element method (FEM) and Zernike polynomials. Firstly, The thermal deformation aberrations of a plat circular Si mirror are theoretically analyzed in detail. In order to study the influence of laser beam properties on thermal deformations aberration, we choose total absorption power P? as variable and define the radio ?nm as Anm=?nm P?. The result shows that the astigmatism becomes one of the main Zernike aberration terms and the value of astigmatism ratio ?2-2 is depend on the incident angle ? under the same absorption power. Then, Model of the beam path with 4 reflective mirrors and a uniform incident laser source is established. With the above model, performances of outgoing laser in the beam path with wavefront pre-compensation using the new method were calculated. It is shown that the Strehl ratio of the outgoing laser beam is increased from 0.13 to 0.66 with wavefront pre-compensation using the new method. Finally, The influence of Fresnel number on the ability of wavefront pre-compensation was also studied. The value of SR increases to 0.83 as the Fresnel number is 257. The result shows that the ability of the wavefront pre-compensation is limited when the Fresnel number is small which means that the wavefront pre-compensation cannot effectively coreected the thermal distortion aberrations of outgoing laser beam.

9131-49, Session PS3

Dynamic modeling of slow-light in a semiconductor optical amplifier including the effects of forced coherent population oscillations by bias current modulation

Michael J. Connelly, Univ. of Limerick (Ireland)

The slow light effect in semiconductor optical amplifiers has many potential applications in microwave photonics such as phase shifting and filtering. In an SOA the principle mechanism causing the slow light effect is coherent population oscillations, whereby beating between two lightwaves leads to carrier density oscillations at the beat frequency. This in turn leads to a change in the group index and so the beat signal at the SOA output is phase shifted relative to the SOA input beat signal. Most slow light models, while they give reasonably good predictions, use a linearized theory which assumes that the carrier density oscillations are small, use simple gain coefficient models and also ignore amplified spontaneous emission. Such models usually only apply to a single wavelength; the use of a different wavelength requires the model parameters to be adjusted to enable agreement between experiment and theory. In this paper we develop a dynamic model of a tensile-strained SOA and use it to predict slow light in such an SOA. The model includes full band-structure based calculations of the material gain, bimolecular recombination and spontaneous emission, a detailed carrier density rate equation and traveling-wave equations for the amplitude modulated signal and amplified spontaneous emission. The model predicts that the slow-light transfer function, defined as the ratio between the SOA output and input beat signal electrical signals, has a high-pass filter characteristic with a rapid decrease in the beat signal gain at frequencies less than the inverse of the carrier recombination lifetime (typically < 5 GHz). This leads to a poor signal-to-noise ratio at such frequencies. This limitation can be overcome, if the optical input and SOA drive current are simultaneously modulated. The current modulation leads to forced population oscillations that can greatly enhance the beat signal gain at low frequencies. The dynamic model is used to determine the improvement in gain and the phase response, in particular the dependency on input optical power, bias current, modulation index and the relative phase between the SOA input optical and current modulation signals. A further advantage of using current modulation is that it allows greater control over the achievable phase shift. The input optical signal is a double-sideband unsuppressed carrier amplitude modulated lightwave and the SOA drive current is amplitude modulated at the same frequency. The model shows that it is possible to obtain beat signal gain improvements of more than 15 dB from DC to 5 GHz. The model predictions show good agreement with experimental trends reported in the literature.

9131-50, Session PS3

Coping with diffraction effects in protein-based volumetric memories: a possible solution for the case of completely random data

Dragos Trinca, SC Piretus Prod SRL (Romania); Sanguthevar Rajasekaran, Univ. of Connecticut (United States)

Much of the current research effort in biological nanotechnology is directed toward protein-based memories [1,2]. Although there are quite many proteins that have been explored, bacteriorhodopsin has received the most attention. This protein, with its unique properties (nanoscale size, cyclicity > 10000000, etc.), provides for protein-based memories that have a comparative advantage over magnetic and optical data storage devices. However, there are a number of problems associated with protein-based memories, such as diffraction effects and scaling. Previous work dealing with the diffraction effects in protein-based memories has reported that these effects can be reduced if one can reduce the differences between the refractive indices within the same page [3]. In terms of binary representations, this can be achieved if the number of 0's is equal to the number of 1's.

Most of the binary representations don't have an equal number of 0's and 1's. One way of ensuring an equal number of 0's and 1's is to replace a 0 with 01 and a 1 with 10. However, this would reduce the available memory by a factor of 2 (which means that the utility factor would be 50% in this case). There are many algorithms that have been proposed and shown to achieve utility factors of 100% or even more. However, for completely random data, the best utility factor provided by previously proposed algorithms is about 99.9%, and can be obtained by using the APPROXv3 algorithm [4], which works as follows. Let I be completely random data. Let bI be the its corresponding binary representation, of length L. We also have an input parameter sl such that L is a multiple of sl. Let NofZs be the number of 0's in bI, and NofOs the number of 1's in bI. Suppose that NofZs> NofOs. Let Zs[i] be the number of 0's in bI_{1:i}, that is, the number of 0's in the first i bits of bI. For each i, 1≤i≤(L/sl), let us define the following numbers: a_{i}=Zs[i·sl-sl+1]-(i·sl-sl+1-Zs[i·sl-sl+1]) and b_{i}=Zs[i·sl]-(i·sl-Zs[i·sl]). Then, it has been proved [4] that there is at least one i, 1≤i≤(L/sl), such that a_{i}≤(NofZs-NofOs)/2≤b_{i}. Let j be the smallest index such that a_{j}≤(NofZs-NofOs)/2≤b_{j}. Then, the APPROXv2 [4] algorithm is applied to search for the position q, j·sl-sl+1≤q≤ j·sl, with the property that C(bI_{1:q})bI_{q+1:L} has an equal number of 0's and 1's, and the output of APPROXv3 is xC(bI_{1:q})bI_{q+1:L}, where x is binary string of length 62 that stores the position q (x has an equal number of 0's and 1's; for a binary string s, C(s) is the complement of s).

In this work-in-progress, we propose the following algorithm that could provide an utility factor of at least 100% in the case of completely random data.

1. Compress bI_{1:8000} using a compression algorithm (there is no particular reason for choosing the first 8000 bits, just that this value seems reasonable in practice). Let Y be the output, also binary.

2. Apply the APPROXv3 algorithm for the binary string YbI_{8001:L}.

If Y is of length at most 8000-62=7938, then clearly the output in the above algorithm has length at most L, which means that in such a case the above algorithm would provide an utility factor of at least 100%. However, applying a common compression algorithm leads to a length of Y of more than 8000, because bI_{1:8000} is a portion that corresponds to completely random data. So, the challenge is to develop a compression algorithm that would be guaranteed to compress a binary string of length 8000 into a binary string of length at most 7938, which would lead to an utility factor of at least 100%. This is our current main focus.

REFERENCES:

[1] R.R. Birge (1990) Annual Review of Physical Chemistry 41:683-733.

[2] R.R. Birge, N.B. Gillespie, E.W. Izaguirre, A. Kusnetzow, A.F. Lawrence, D. Singh, Q.W. Song, E. Schmidt, J.A. Stuart, S. Seetharaman, and K.J. Wise (1999) Journal of Physical Chemistry B 103:10746-10766.

[3] S. Rajasekaran, V. Kumar, S. Sahni, and R. Birge (2008) Efficient algorithms for protein-based associative processors and volumetric memories, Proc. of IEEE NANO 2008, pp 397-400.

[4] D. Trinca and S. Rajasekaran (2013) Journal of Computational and Theoretical Nanoscience 10:894-897.

9131-51, Session PS3

Lamp system with a new single second lens designed by using the least square method for 4 LEDs

Jae Heung Jo, Hannam Univ. (Korea, Republic of); Jae Myung Ryu, Kumoh National Institute of Technology (Korea, Republic of)

It use recently a multiple LED for many companies to increase the brightness of LED lamp and they mainly is recommended and applied four LEDs to LED lamp systems. Also, it has to always use a second-lens to achieve a straight uniform illumination from LED lights. In case of four LEDs, it produce and assemble conventionally four second-lens for four LEDs by creating four assemble configuration from a single mold. In this paper, we suggest a new method using a least square method about to create a straight uniform illumination with the divergence angle of 40 degrees by a new single lens molded with a single injection. Because of optical design with a single lens, the assemble process of LED lamp system have simplified without any complex procedure. In case of this designed lamp system, the uniformity of illumination is less than 14.1%.

9131-52, Session PS3

Miscalibration detection in phase-shifting algorithms by applying Radon transform

Tania A. Ramirez-Delreal, Univ. de Guadalajara (Mexico) and Univ. Politécnica de Aguascalientes (Mexico); Miguel Mora-González, Univ. de Guadalajara (Mexico); Marco A. Paz, Univ. Politécnica Autonoma de Aguascalientes (Mexico); Jesús Muñoz-Maciel, Univ. de Guadalajara (Mexico); Ulises H. Rodriguez-Marmolejo, Univ. de Guadalajara (Mexico) and Instituto Tecnológico de Aguascalientes (Mexico)

The phase shifting algorithms are a widespread method in the technical and scientific literature for relatively non-invasive measurements of a variety physical variables. PSI (phase-shifting interferometry) techniques consist in acquiring at least three interferograms to obtain the wrapped phase. It is important to emphasize that if these acquired intensity images are inadequate, the measurement would have an error associated. The presence of miscalibration or mechanical vibrations in an interferogram can cause an inaccurate measurement; it is possible to design a phase shifting algorithm with a better performance. The present work proposes a novel methodology in order to determine the existence of a miscalibrated interferogram in a four steps phase shifting algorithm by applying the Radon transform.

9131-53, Session PS3

Influence of the set-up in the diffractive optical elements recorded into photopolymers

Sergi Gallego, Roberto Fernández, Andrés Márquez, Cristian Neipp, Jorge Francés, Inmaculada Pascual, Augusto Beléndez, Univ. de Alicante (Spain)

Photopolymers are often used as a base of holographic memories displays. Recently the capacity of photopolymers to record diffractive optical elements (DOE's) has been demonstrated. Depending on each particular application, different photopolymers are used. For each composition the main parameters should be determined previously. To fabricate diffractive optical elements we use a hybrid setup that is composed by three different parts: LCD, optical system and the recording material. The DOE pattern is introduced by a liquid crystal display (LCD) working in the amplitude only mode to work as a master to project optically the DOE onto the recording material. The main advantage of this display is that permit us modify the DOE automatically, we use the electronics of the video projector to send the voltage to the pixels of the LCD. The LCD is used in the amplitude-mostly modulation regime by proper orientation of the external polarizers (P); then the pattern is imaged onto the material with an increased spatial frequency (a demagnifying factor of 2) by the optical system. The use of the LCD allows us to change DOE recorded in the photopolymer without moving any mechanical part of the set-up. Nevertheless the size of the pixel of this LCD limits the minimum value of the spatial period to 168 μm (high pixels to reproduce a period). A diaphragm is placed in the focal plane of the relay lens so as to eliminate the diffraction orders produced by the pixelation of the LCD. It can be expected that the final pattern imaged onto the recording material will be low filtered due to the finite aperture of the imaging system and especially due to the filtering process produced by the diaphragm. In this work we analyze the effect of the visibility achieved with the LCD and the high frequency cut-off due to the diaphragm in the final DOE recorded into the photopolymer. To simulate the recording we have used the fitted values parameters obtained for PVA/AA based photopolymers and the 3 dimensional models presented in previous works.

9131-54, Session PS3

Comparison of software for numerically approximating the Wigner distribution function

John J. Healy, Bryan M. Hennelly, National Univ. of Ireland, Maynooth (Ireland)

The Wigner distribution function (WDF) has been used as a tool in wave optics for more than forty years. It is desirable to numerically simulate the WDF for a variety of situations; we argue that the reasons this is not more commonly done are the difficulty in defining the discrete transform appropriately and the size of the computation. In this paper, we examine a number of software packages freely available online, each purporting to calculate the WDF. We present results on their speed and accuracy. Optical engineers desiring to make use of the WDF in optical analysis and design will find our results useful in choosing which package to use in their simulations.

9131-55, Session PS3

Use of Costas arrays in subpixel metrology

John J. Healy, National Univ. of Ireland, Maynooth (Ireland); Gavin Sweeney, Univ. College Dublin (Ireland); David Mas, Univ. de Alicante (Spain); John T. Sheridan, Univ. College Dublin (Ireland)

Subpixel methods increase the accuracy and efficiency of image detectors, processing units, and algorithms and provide very cost-effective systems for object tracking. A recently proposed method permits micropixel and submicropixel accuracies providing certain design constraints on the target are met. In this paper, we explore the use of Costas arrays – permutation matrices with ideal auto-ambiguity properties – for the design of such targets.

9131-56, Session PS3

Two-wavelength phase shift interferometry for the 3D imaging of ballistics shell cartridge cases

Glenn W. Pagano, Christopher J. Mann, Northern Arizona Univ. (United States)

We apply two-wavelength phase shifting interferometery to generate 3D surface profile images of spent bullet cartridge cases. From the captured interferograms, an optimized algorithm was used to calculate a phase profile from which a precise digital surface map of the cartridge casing may be produced. This 3D surface profile is used to enhance a firearms examiners ability to uniquely identify distinct features or toolmarks imprinted on the casing when the weapon is fired. These features play a key role in the matching process of ballistic forensic examination.

9131-57, Session PS3

Design of autocollimation systems by modelling an illumination distribution of a vignetted image

Igor Konyakhin, Andrey A. Smekhov, National Research Univ. of Information Technologies, Mechanics and Optics (Russian Federation)

During an installation and maintaining industrial large-scale constructions there is a necessity in controlling their deformations caused by different reasons like weather conditions such as wind or deformations under their own weight or other man-made reasons controlling of which is the purpose. Anyway there is a necessary of usage angular measuring devices such as autocollimation systems which are used in the cases of measurement tiny angular displacements of an object or its parts.

However autocollimation systems have some principal disadvantage. Errors caused by incoming radiation vignetting is one of them. Due the light (radiation) transition through the system slanted beams could be reduced by entrance pupil. This corresponds to incomplete transition and energy losses at matrix photo-receiver

Moreover, variety of vignetted beams causes insufficient illumination distribution at the sensitive area ?f photomatrix, which is the reason of incorrect image centre.

Despite this the errors of such vignetting could be eliminated being systematical ones. Because of each point of the resulting emitting diode image is the focused intersection of entrance pupil and light beam, its energy proportional to integrated (by energy) intersection's area.

Implemented software model traces emitted rays through the simulated autocollimation system, predicts the illuminance distribution and calculates vignetting errors. The amount of precalculated vignetting errors for each reflecting element position which is fixed at the object to control are saved at any database. Due to the simple recovery algorithm this amount gives the possibility to reconstruct the real object position and eliminate vignetting error.

In this simulation model the energy field at each point between emitting and detecting is represented by 2-dimentional vector field, which is changed by some operators corresponding to the optical system parts (including empty space). The idea of such representation gives us ability to enhance the optical system complexity to further researches. The ability to model different types of apertures, reflecting elements and emitter's radiation patterns incorporated into the software gives the opportunity to apply one at much more complicated systems and decrease the time and exps of a design process.

Because of quite complicated array calculation, MatLab software package was chosen as the development environment.

Results of modeling the vignetting error for type autocollimation system are discussed.

The parameters of the optic components are following. The focal length of objective is 250 mm and diameter of purple is 40 mm; the size of emitting diode is 0,5 mm. As results the range of angle measurement with small error is the 7 minutes of arc at distance L = 1000 mm and 1 minutes of arc at distance L = 5000 mm. The error of angular measurement can be reduced by using the result of its modeling and precalculation.

The ability to model many different types of apertures, reflecting elements and emitter's radiation patterns incorporated into the software gives the opportunity to apply one at much more complicated systems and decreases the time of a design process.

9131-58, Session PS3

An integrable high resolution all-optical analog-to-digital conversion scheme

Shile Wei, Jian Wu, Beijing Univ. of Posts and Telecommunications (China); Lingjuan Zhao, Dan Lu, Institute of Semiconductors (China); Jifang Qiu, Beijing Univ. of Posts and Telecommunications (China)

Nowadays, photonic-based ADCs have received considerable attention as an alternative approach to providing increased resolution and speed in high-performance applications, such as phased array antenna systems, medical imaging, radio astronomy, and electronic instrumentation. The first integrable all-optical ADC scheme was proposed in, and much work following the idea has been carried out by researchers. But all of these photonic ADCs suffer from the drawbacks that either complexity (one modulator per bit) or distribution of the high-voltage analog signal applied to many electrodes. To overcome these disadvantages, a phase-shifted optical quantization ADC scheme was demonstrated, which had been followed by many other researchers. In these schemes, additional mechanical adjustment is needed and they are difficult to be integrated, thus increasing the costs and causing poor mechanical stability.

In this paper, a novel photonic analog-to-digital conversion system at high resolution is proposed, in which wavelength division multiplexing idea is applied, 4?4 multimode interference (MMI) couplers are used as a quantizer and multi-wavelength mode locked pulse lasers (MLL) as sampling source. The whole scheme can be integrated on a InP-based chip. Higher quantization resolution ADCs can be easily obtained by inducing more 4?4 MMI couplers to the basic low resMuch hlution ADC element or replacing 4?4 MMI couplers with 8?8 MMI couplers. Quantization resolution can be also improved as the number of the used MLLs increases.

The whole progress of the signal process is carried out in waveguides, so the system is ultra-stable.

9131-59, Session PS3

Design of the coded aperture imaging spectrometer system based on the double amici prism

Linlin Pei, Qunbo Lv, Yangyang Liu, Jianwei Wang, Lulu Qian, Academy of Opto-Electronics (China)

A compact imaging spectrometer spreading from visible

wavelength to near infrared wavelength range with a spectral resolution of 10 nm, is introduced. The system mainly includes a front telescope objective, coded aperture, double Amici prism, collimator and the imaging lenses, obtaining high diffraction efficiency. In this paper, we analyze the principle and characteristics of the imaging spectrometer system based on the double Amici prism, design a complete imaging spectrometer system.This design possesses characteristics of small size, compact structure, low mass as well as little spectral line curve (smile) and spectral band curve (keystone or frown). The whole system is coaxial and simple.The optical design layout of the spectrometer is presented, and the performance evaluation of this design, including spot diagram and MTF, is analyzed.Therefore, this paper can offer theoretic guide for imaging spectrometer of the same kind.

9131-60, Session PS3

Optic-electronic system for deformation measurement of radio-telescope counter-reflector computer modeling

Andrey Petrochenko, National Research Univ. of Information Technologies, Mechanics and Optics (Russian Federation); Nina Tolochek, National Research Univ. of Information Technologies, Mechanics and Optics (Russian Federation); Igor Konyakhin, National Research Univ. of Information Technologies, Mechanics and Optics (Russian Federation)

The metrological maintenance of many measurement tasks requires measuring spatial position of some control objects relative to rigid base. The microwave radio-telescope development requires high-precision control for the position of the counter-reflector. The construction elements weight and thermal deformation leads to changes of position and linear shift of each planar section relative to theoretical parabola. In this case it is necessary to realize special control system for controlling these deformation. The triangulation method is chosen to solve this problem. This method means CMOS camera, placed on the base object. On the control object there are placed elements, determining its spatial position. The special construction element – the base ring – acts as a base object. The rigid base ring is placed in the top of the main mirror and is a motionless measurement base. In accordance to the method video camera measures the LED vision angles. For the system errors research it is effective the computer modeling. The experimental research of the structure of the system error was made with the realized computer model. The result of the taken analysis are the primary errors influencing the error of linear and angular position measurements of control object.

The way of investigation of a measuring techniques, concerned with definition of spatial and angle position of object is actual and upcoming. The development of production technology, aircrafts, ships, scientific labs requires precise controlling the elements positions during the assembling and justifying ship-ways, test benches, ground-based radio-telescopes, synchrophasotrons.

In particular the microwave radio-telescope development requires high-precision control for the position of the counter-reflector. The counter-reflector diameter is 3 meters; the distance from the base to counter-reflector is 40 meters. The microwave range requires the error from the theoretical parabola not bigger than 0.1 mm. The construction elements weight and thermal deformation leads to changes of position and linear shift of each planar section relative to theoretical parabola. In this case it is necessary to realize special control system for controlling these deformations.

The triangulation method is chosen to solve this problem. This method means CMOS camera, placed on the base object. On the control object there are placed elements, determining its spatial position. The special construction element – the base ring – acts as a base object. The rigid base ring is placed in the top of the main mirror and is a motionless measurement base. The measurement channel uses the triangulation method.

The spatial position changing is our considered metrological task. To build a measurement system designed to measure spatial position of controlled object we consider three effective methods called “linear localization”, “intersection” and “resection”.

With the method “Intersection” we measure viewing angle of controlled point in vertical and horizontal surfaces. Viewing angle is the angle between optic axis of objective and point direction. XYZ-coordinates of controlled point are defined with known base interval B and measured viewing angle ?1, ?2, n1, n2:

Z = B * [1 + sin(?1- ?2) / sin(?1+ ?2)] / 2;

X = B * sin j1 * sin ?2 / sin(?1+ ?2);

Y = [Y + B * (tg n1 * sin ?2 + tg n2 * sin ?2) / sin(?1 + ?2)] / 2.

Optic-electronic theodolite serves as a base of devise realization of this method.

Using the third type method we must have three LEDs (at known distances from each other) on the controlled object and one static observation point to take measurements. If we knew control points images coordinates on the matrix of CMOS and objective focal length, we can to define rotation angles of the surface assigned with three control points and coordinates of there control points. We can see the controlled object with three control points: X1Y1Z1, X2Y2Z2 and X3Y3Z3 and measuring system includes the objective and the CMOS matrix.

Error in realization of intersection or resection method requires 2-3 times smaller base intervals B1B2B3 then the realization of linear-location method with equal measurement errors (in that case base intervals are commensurable with distance L from the base to the object). Intersection and resection methods provides for greater precision then linear-location method, because we use a reference ring as a static basis. Intersection and resection methods provide equal precision, but the system working with resection method have lower price. This circumstance determines the measuring system development with the resection method.

Error of targets image X and Y coordinates measurement is acceptably, when error is smaller then 0.6 matrix element, or 3.6 mkm (X-coodinate) and then 0.75 matrix element, or 4.2 mkm (Y-coodinate). It is possible.

Computer modeling uncovers complexity with one parameter - error of targets image Z-coordinates measurement. As a whole, this original research shows high effectiveness of methods, using computer-aided design.

9131-61, Session PS3

Automation of data pre-processing at the control of optical systems by the Hartmann technique

Nadezhda D. Tolstoba, National Research Univ. of Information Technologies, Mechanics and Optics (Russian Federation); Vladimir E Malutin, ITMO University (Russian Federation); Grigory V. Yakopov, Edward V. Emelianov, Special Astrophysical Observatory (Russian Federation)

During the quality control of the optical systems by the Hartmann technique it is often necessary to analyze the picture using an unknown number and placement of spots.

This report examines the stage of hartmanogramm spots separation.

For reliable automatic operation of the Hartmann method with various images it is necessary to be able to identify any patterns with an unknown number of scattering spots.

This in turn requires the division into separate hatrmanogramm spots for search for information about the energy centers of spots in other ways.

We consider methods of finding spots on hatrmanogramm.

This report will examine several methods which are compared to each other in the performance and reliability of positioning spots. During the analysis it was developed several ways to find the location of the scattering spots. It will show examples

of different gartmanogramm and results are on the proposed algorithms.

9131-62, Session PS3

Effect of keystone on coded aperture imaging spectrometer

Lulu Qian, Qunbo Lü, Min Huang, Linlin Pei, Yuan Ma, Qisheng Cai, Yang Li, Academy of Opto-Electronics (China)

Compared to conventional imaging spectrometry, coded aperture imaging spectrometer?CAIS? has the advantages of high throughput snapshot imaging etc. In CAIS, a coded mask which modulates and compresses the 3D spatial-spectral data-cube about the scene is imported appropriately in the light path. The 3D spatial-spectral information about a scene of interest is first encoded and captured with one snapshot at the two-dimensional (2D) detector array. Compressed sensing (CS) theory is then used to reconstruct the 3D data-cube from the 2D aliasing image. But because of the presence of the dispersive element, CAIS system suffers the effect of the same optical aberration as traditional single slit spectrometer. To study the effect of keystone on signal acquisition, the model of spatial-spectral aliasing and the reconstructed result in CAIS system, combined with the principle of code aperture imaging spectrometer and the reconstruction algorithm, the relative peak signal-to-noise ratio(PSNR) of the reconstructed image and the maximal error of the reconstructed spectral curve at different spectral band bending were calculated and analyzed. The experimental result showed that spectral band offset of the signal acquired by the detector will change the degree of spatial-spectral aliasing. The reconstructed results with spectral band bending exhibit distinct errors compared with no spectral band bending. And the reconstructed spectral curve tends to be smooth on either hand. In order to reconstruct the object scene with high accuracy, spectral band offset should be no more than half a pixel.

9131-63, Session PS3

Study of the total light flux measurement of wafer-level LED in a multichannel LED measuring system with nonimaging concentrator array

Yi-Jiun Chen, Yao-Chi Peng, National Taiwan Univ. (Taiwan); Yu-Tang Chen, Chen-Chin Cheng, Industrial Technology Research Institute (Taiwan); Hoang Yan Lin, National Taiwan Univ. (Taiwan)

To raise the speed of characterizing wafer-level LEDs, simultaneous measurement for both electrical and optical properties in parallel is a necessity. The total light flux measurement is commonly performed using integrating sphere, however the physical size of most of the existing integrating sphere is too large for parallel characterization of multiple points on the wafer.

To concentrate as much light as possible from LEDs and miniaturize the light collector, a non-imaging concentrator is used in our measurement system, instead of an integrating sphere. For the sake of meeting the requirements for the numerical aperture of sensing fiber (?NA) and the angle (?in) for collecting 70 % emitting flux from a Lambertian source, a reversed angle transformer (RAT) is used with exit and entrance angles ?1 and ?2, which correspond to ?NA and ?in, respectively. The simulation is conducted using the commercial software LightTools®, based on the Monte-Carlo ray-tracing method. According to the simulation, the entrance port can collect approximately 94% of radiance from a Lambertian source, and the concentration ratio of RAT is approximately 99%.

In practice, the manufacturing process limits the design freedom of the RAT, which in turn makes ?1 larger than ?NA, and this results in less radiance into the fiber. Regarding the effect of tolerances on the manufacturing and alignment between the target and concentrator, the optical model of the LEDs and probes is built to examine and calibrate the measurement results.

The novelty of this measurement method with RAT array lies in that, unlike traditional integration sphere calibration, no effective standard of specifications and comparisons exist for RAT. A demonstrated prototype is in the process of being built and experimented to validate our design.

9131-64, Session PS3

Designing and researching of the virtual display system based on the prism elements

Vladimir V. Vasilev, Wyacheslav A. Grimm, Galina E. Romanova, Sergey A. Smirnov, Alexey V. Bakholdin, Natalya Y. Grishina, National Research Univ. of Information Technologies, Mechanics and Optics (Russian Federation)

In the paper the questions of the designing of the systems for virtual display system for augmented reality placed near the observer's eye (so called head worn displays) with the light guide prismatic elements are considered. A system of augmented reality is the complex consists of the image generator (most often it's the microdisplay with the illumination system if the display is not self-luminous), the objective which forms the image of the display practically in infinity and the combiner which organizes the light splitting so that the observer could see the information of the microdisplay and the surrounding environment as the background at the same time. This work deals with the system with the combiner based on the composite structure of the prism elements. The prismatic compound screen consists of several elements with special profile coating so the light is partially reflected and partially transmitted depend on the incidence angle. The slope angle of layer could not be equal to 45 degrees because in the latter case there ghost images could appear. So with different slope angle the results of transmission of the light will be different. In the work three cases of the prism combiner design are considered and also the results of the modeling using the optical design software are presented. In the model the question of the large pupil zone was analyzed and also the discontinuous character (mosaic structure) of the angular field while transmitting the information from the microdisplay to the observer's eye with the prismatic structure are discussed

9131-65, Session PS3

Analysis of aberration properties of two-component zoom lenses

Kseniia Ezhova, National Research Univ. of Information Technologies, Mechanics and Optics (Russian Federation); Victor Zverev, Nguen V. Luen, National Research Univ. of Information Technologies, Mechanics and Optics (Russian Federation)

The calculation of the zoom-lenses in the paraxial region comes down to the choice of optical powers of the components of the system and the definition of the law of movement, for which predetermined lateral magnification is achieved. The range of movement of components is determined by the initial position of the components. However, the choice of the initial positions of the components cannot always be the most favorable for the conservation constant correction of aberrations. Therefore, the development of the aberration analysis method for selected component's starting position and the range of movement of components for a predetermined changing of multiplicity image magnification is a very actual task.

In the two-component zoom-lenses object and image are located at a finite distance from the first and second components, respectively, and modifying the lateral magnification image is longitudinal movement of the components, but the distance between the object and image

planes is unchanged. The optical powers of components are constant, and the optical power of the system is changed.

In a first approximation, components of the zoom-lenses are thin components. Basic parameters of thin component are defined only on its internal constructive elements of components and functionally are related to the parameters, which define aberrations of the image formed by any arbitrary position of the components relative to the object plane.

In the case of a two-component zoom-lenses, we have four main parameters and one parameter that should remain unchanged for five values of the lateral magnification.

The result is a system of five linear equations with five unknowns.

Any zoom-lenses can exist only for a finite distance between the object and image. If the object is at an infinite distance, the optical conjugation between the object plane and the plane of the object for zoom-lenses needs to additional optical system ?_0. In this case, we have five basic parameters and one parameter that should remain unchanged for five values of the transverse magnification. The result is a system of six equations with six unknowns. If the two-component zoom-lenses forms a virtual image, then the description system is necessary to supplement the optical image transfer system (ITS), which is placed behind a zoom-lenses.

The ITS is consist of two components ?_01 and ?_02. If the optical system consisting of an additional system ?_0, zoom-lenses and component ?_01, forming an afocal system, then in case of independent aberration correction, afocal system in combination with the component ?_02 forms an optical system of the zoom. The optical power and the lateral magnification of the ITS are constant. In this case we assume that the ITS aberration coefficient is not changed. Thus we have five basic parameters and one parameter which is the coefficient of aberration ITS. The result is a system of five linear equations with six unknowns. Solving a system of equations, we obtain values for basic parameters.

The present approach to the analysis of the aberration properties of two-component zoom-lenses allows you to choose the best combination of aberration characteristics.

9131-66, Session PS3

A Performance evaluation of WDM-Nyquist systems generated by optical flat comb source and based on POLMUX-QPSK, POLMUX-DQPSK, POLMUX-16QAM and POLMUX-64QAM

Hraghi Abir, National Engineering School of Communication of Tunis (Tunisia); Mourad Menif, SUP'COM (Tunisia)

The bandwidth demand is growing at staggering rates driven by multimedia services, such as cloud, mobile, high-definition television (HDTV) and video. However, to cope with forecasted increase data traffic, it will be necessary to deploy a new generation of optical systems. As a possible solution, WDM-Nyquist system could be employed in order to transmit spectral efficient super-channels with bit rates beyond 1 Tbit/s [1].

In this work, we implement a WDM-Nyquist transmission system with 12.5 GHz channel spacing generated through an Optical Flat Comb Source (OFCS). Each channel could carry one of four different modulation format as Polarization Multiplexing-Quadrature Phase Shift Keying (POLMUX-QPSK), Polarization Multiplexing-Differential Quadrature Phase Shift Keying (POLMUX-DQPSK), Polarization Multiplexing-Quadrature Amplitude Modulation based on 16 (POLMUX-16QAM) and 64 (POLMUX-64QAM) with Return-to-Zero (RZ) pulse carving and 33% duty cycle.

A 1 Tbit/s WDM-Nyquist system could be made up of 20 subcarriers using POLMUX-QPSK and POLMUX-DQPSK, operating at 12.5 Gbaud and carrying each 50 Gbit/s. For instance only 7 subcarriers using POLMUX-64QAM, delivering 150 Gbit/s each, are needed to achieve the same capacity. Intermediate solutions using 10 subcarriers are possible with POLMUX-16QAM. The subcarriers are generated by an OFCS. The difference in intensity between the upper and the lower subcarrier is around 1 dB.

Numerical simulations have been carried out, in order to evaluate the performances of the different modulation format using appropriate metrics at a bit rate of 1 Tbit/s. Indeed, we discuss their back-to-back receiver sensitivity and the required Optical-to-Noise Signal Ratio (OSNR) for 3.8 10-3 and 10-9 Bit Error Rate (BER). We find that 33RZ-POLMUX-QPSK has the best receiver sensitivity and the lower OSNR penalty compared to the other modulation formats. With 33RZ-POLMUX-64QAM sensitivity as reference, we can observe a benefit of 13.4 dB (for a BER equal to 3.8 10-3) for 33RZ-POLMUX-QPSK. In addition, we can observe a benefit of 21 dB in OSNR for 33RZ-POLMUX-QPSK compared to 33RZ-POLMUX-64QAM modulation format for a BER equal to 3.8 10-3.

We study also the robustness of these four optical modulation formats for transmission of 1 Tbit/s in dispersion compensated WDM-Nyquist systems using two kinds of transmission fibers: SMF (Single Mode Fiber) and NZDSF (Non-Zero Dispersion Shifted Fiber). We find that 33RZ-POLMUX-QPSK is the suitable modulation format in dispersion compensated WDM-Nyquist systems using NZDSF fiber.

Finally, we study the nonlinear effect tolerance by considering self-phase modulation (SPM), cross-phase modulation (XPM) and four-wave mixing (FWM) of the different modulation format. We observe that 33RZ-POLMUX-QPSK modulation format has the best robustness against the cited nonlinear fiber effects in NZDSF fiber.

[1] J. Hoxha, G. Cincotti, N.P. Diamantopoulos, P. Zakynthinos, I. Tomkos, "All-optical implementation of OFDM/NWDM Tx/Rx", Proc ICTON 2013, paper Tu.P.9, (2013).

9131-67, Session PS3

Determination of parameters and research autoreflection scheme to measurement errors relative position of the optical elements of the space telescope

Fedor Molev, OAO Avangard (Russian Federation); Igor Konyakhin, Kseniia Ezhova, National Research Univ. of Information Technologies, Mechanics and Optics (Russian Federation)

The paper has consideration the main principles for the development autoreflection scheme to build the measuring channel, designed to control the relative position of the optical elements of the Space Telescope.

Autoreflection scheme is based on the scheme of measuring angles by autoreflection method, according to which the radiant stamp that was registered in the plane of the analysis is at a finite distance from the front of the lens.

The main advantages of the autoreflection scheme is less clear aperture of the optical elements for large distances of measurement and for range the measured angles in contrast to the classical autocollimating scheme, which standard is used to the control of optical elements position in complex electro-optical systems.

Also in the paper, we consider dimensional relations for determining the parameters of the autoreflection scheme for position elements control of the optical system by rotation and shifting the controlled element.

Simulation results of the measuring autoreflection scheme modelihg by Zemax are described. The simulation results showed that the method is sensitive to the quality of manufacturing elements of the control system. When we using a single lens, not adjusted for minimum spherical aberration, as a lens of the control system, we can to obtain the scattering spots with a size commensurate with the magnitude of the measured displacement of the controlled element.

9131-68, Session PS3

Aberration properties of thin lenses and composition of optical systems

Vasilisa Ezhova, Victor Zverev, Kseniia Ezhova, National Research Univ. of Information Technologies, Mechanics and Optics (Russian Federation)

Research aberration properties of a thin lens in narrow and wide beams of rays showed that there are two pairs of positions of input (output) of the pupil, in which the image of an infinitely distant object formed by a thin lens, there is no astigmatism. Research aberration properties of a thin lens in the wide beams of rays showed that, for the subject, which is located at an infinite distance from the lens, the image will be present spherical aberration and coma. Afocal optical system (damper), consisting of two thin lenses in a plane anastigmatic pupil, will not make the astigmatism in the image. Using the “bend” lens system as a correction parameter can be compensated for the residual spherical aberration and coma.

The image formed by this optical system has a residual curvature. To address this shortcoming thin compensator replace Galilean afocal system type of two thin lenses in the long distance between them. If pupils anastigmatic combine all three lenses, the astigmatism of the image formed by them will be omitted. Possible mutual compensation of astigmatism by “bending” lens when moving the entrance pupil relative to the lens along the optical axis.

The resulting system is a variant of the system of “triplet”. From an analysis of the location in the system pupil that the latter must have a deflection lens which is unfavorable for correction of spherical aberration. Image aperture any optical system is achieved by improving the correction of the spherical aberration and coma. To solve this problem the last lens is replaced with glued components, forming a system of “INDUSTAR.”

Knowledge of the properties of the thin lens aberration, chosen as a base, allows to correctly complement its required corrective elements.

9131-69, Session PS3

Alignment control optical-electronic system with duplex retroreflectors

Maksim A. Kleshchenok, National Research Univ. of Information Technologies, Mechanics and Optics (Russian Federation); Andrey G Anisimov, Oleg U Lashmanov, ITMO University (Russian Federation); Alexandr N. Timofeev, National Research Univ. of Information Technologies, Mechanics and Optics (Russian Federation); Valery V Korotaev, ITMO University (Russian Federation)

Reconciliation of alignment - one of the most complex and demanding operations carried out during the maintenance of turbine unit and other mechanisms.

Alignment largely determines the duration and complexity of major repairs.

On the quality of these works depends largely on the duration of start-up, as well as the reliability and efficiency of turbine repaired.

Misalignment of shafts in a machine can cause following negative effects:

1) Emergence of moment causes generation forces reaction in the bearings of the machine

2) Overload of bearing shafts which leads to increase of distortions by 20% reduces bearing life estimated by 50%

3) Wear of seals, which in turn increases bearing damage risk due to penetration of dirt and grease leakage

4) Overload and vibration, those cause damage of couplings (overheating, weakened or broken bolts) and shafts

5) Power consumption engine may rise up to 20%, as a result of machine shafts warps.

For proper work of complex technological equipment its components need to be spatially positioned relative to assembly axis with high accuracy.

As a result, the problem of contactless control of the position of objects relative to the extended linear base is relevant in many areas of technology.

The task of object positioning is offer performed by means of optical – electronic measuring systems (OEMS), because of its high accuracy, remoteness and high level of automatization.

OEMS determine the offset of basic parts of cylinders relative to the stage of turbine rotor axis with accuracy of 0.05 mm in the vertical and horizontal planes.

The axis of the engine defined in the base bores (BB) during the measurement.

OEMS allows recalculating measurements relative to its own sighting line (SL) to given rotor axis, whereby there is no need “align” SL at predetermined coordinates, which is significantly automated of the measurement process.

In OEMS task of spatial positioning is implemented using the autoreflection and autocollimation techniques convergent beams, which allows for highly accurate measurement of linear offsets without determining the distance to the controlling element and provide power to the test object.

In this paper, we consider the influence of various factors and the noise on the invariant transformation of measurement information in autoreflection alignment control schemes. Theoretical and experimental research carried out for basic errors on bidiods and biprizms schemes.It is shown that the main influencing factors are non-linear transformations in optical systems and the impact of air path.

Experimental studies were carried out on the basis of two opto-electronic control systems alignment, in which the control element is in the form of one or two corner-cube prisms.

9131-70, Session PS3

Numerical investigation of noise chracteristics of telecommunication laser sources for various modulation formats

Ján Litvik, Daniel Benedikovic, Michal Kuba, Univ. of ?ilina (Slovakia); Jozef Dubovan, University of Zilina (Slovakia)

In this paper, we present numerical investigation of noise properties of lasers for telecommunication purposes with emphasis on widely used distributed feedback (DFB) lasers and its influence on novel kinds of modulation formats. DFB lasers can be used in optical transmitters with internal and external modulation, as well as in optical receivers employing coherent detection, where they act as local oscillator. The main noise factors influencing signal characteristics of lasers are intensity and phase noise. These random impairments cause degradation of fundamental output characteristics of laser signals such as power and phase fluctuations. In case of implementation of new modulation formats in transmission systems, these stochastic processes play important role and have significant impact on transmission properties of modulated signals and total performance and quality of fiber-optic transmission systems. The quality of optical systems is usually evaluated by optical signal-to-noise ratio (OSNR) and bit-error rate (BER). In case of high-order modulation schemes is more suitable to use error vector magnitude (EVM) as figure of merit due to the complex nature of modulated signals and EVM is directly related to BER and OSNR. The obtained results are described and discussed with the aim to determine the impact of stochastic properties of investigated laser on different modulation formats in context of optical system parameters such as moderate symbol rate, average symbol power and order of modulation format.

9131-71, Session PS3

Holographic transmission gratings stored with high spatial frequency in PVA/AA photopolymers

Elena Fernández, Rosa Fuentes, Manuel Ortuño, Augusto Beléndez, Inmaculada Pascual, Univ. de Alicante (Spain)

Holography is the physical mechanism from which holograms can be stored by exposing a photosensitive material to the interference of two light beams. In this way the amplitude and phase of a waveform can be stored when this waveform interfere with a coherent light background. When the material where the interference pattern is stored is illuminated a diffracted beam is observed that is an exact reproduction of the original waveform. In the last decade holography has acquired great importance since holographic devices can store information throughout the volume of the material, thereby increasing the storage capacity in comparison with two-dimensional devices that only store information on the surface.

One way to increase the storage capacity of these devices is to store objects with a higher spatial frequency as this could store more information. Conventional recording materials studied reach diffraction efficiencies close to 100%, but only for spatial frequencies not much higher than 1000 lines / mm. However, when objects with higher spatial frequencies are tried to store, the diffraction efficiency drops dramatically. Recently materials with a higher spatial resolution are being looked for.

This work pretends to optimize the standard composition of the PVA/Acrylamide photopolymer, changing its composition in order to improve its spatial resolution. To do this, a chain transfer agent, 4,4 '-azobis (4-cyanopentanoic acid) (ACPA) will be introduced in the photopolymer and its concentration will be modified. Thus, the optimal concentration which gets obtain the maximum diffraction efficiency for high spatial frequencies could be found.

To quantify the improvement that occurs with the inclusion of the ACPA in the PVA/Acrylamide photopolymer, transmission gratings of 2500 lines / mm will be stored (this spatial frequency has been chose because in this type of photopolymers, the diffraction efficiency is reduced by half compared with the gratings with 1000 lines / mm). Moreover, diffraction efficiency obtained with the different concentrations of ACPA will be measured to compare the obtained results.

9131-72, Session PS3

Implementation of an optical AND gate using Mach-Zehnder interferometers

Santosh Kumar, Ajay Kumar, Sanjeev Kumar Raghuwanshi, Indian School of Mines (India)

The article shows the construction of optical AND gate using cascaded MZIs. In this article, first time only MZI are used to construct the gate. The result is verified by proper analysis using MATLAB and OptiBPM software. The objective of our work is to explore the usefulness of MZI and to make optical switches.

9131-73, Session PS3

Hermite-Gaussian beams with self-forming spiral phase distribution

Alexander A. Zinchik, Yana B. Muzychenko, National Research Univ. of Information Technologies, Mechanics and Optics (Russian Federation)

Spiral laser beams is a family of laser beams that preserve the structural stability up to scale and rotate with the propagation. Properties of spiral beams are of practical interest for laser technology, medicine and biotechnology. Researchers use a spiral beams for movement and manipulation of microparticles. Spiral beams have a complicated phase distribution in cross section.

This paper describes the results of analytical and computer simulation of Hermite-Gaussian beams with self-forming spiral phase distribution.

In the simulation used a laser beam consisting of the sum of the two modes HG TEMnm and TEMn1m1. The coefficients n1, n, m1, m were varied. Additional phase depending from the coefficients n, m, m1, n1 imposed on the resulting beam. As a result, formed the Hermite Gaussian beam phase distribution which takes the form of a spiral in the process of distribution. For modeling was used VirtualLab 5.0 (manufacturer LightTrans GmbH).

The simulation results were verified experimentally.

For the synthesis of spiral beams used two spatial light modulators. Collimated beam of He-Ne laser was passed through them. One of them was working in transmission and distributed of the amplitude of the spiral shaped beam. The second modulator working in reflection mode and formed the spatial distribution of the phase shift setting from 0 to 2pi at each point, respectively. The resulting intensity distribution recorded with a digital camera. The results obtained in the experiment corresponded to the theoretical intensity distribution.

9131-74, Session PS3

Theoretical and experimental analysis of the propagation of sinusoidal signals in Bacteriorhodopsin films

Salvador Blaya, Manuel Candela, Pablo Acebal, Luis Carretero, María Gomariz, Roque Madrigal, Antonio Fimia, Univ. Miguel Hernández de Elche (Spain)

Recently, a great amount of saturable absorbers have been used to obtain slow-light. Among them, it has been reported slow and fast light in biological thin films and solutions of Bacteriorhodopsin (bR). The mechanism of the resulting slow light process in this system can be equally explained by a temporal variation of the absorption (saturable absorption) or by coherent population oscillations (CPO). Recently, in relation to the saturable absorption theory, we performed a rigorous study of the dynamic photoinduced processes of thick bacteriorhodopsin films, taking into account all the physical parameters, the coupling of rate equations with the energy transfer equation, and the effect of temperature change for the analysis of the propagation of sinusoidal pulses. This numerical analysis taken into account six states of the photocycle and the corresponding equations of the two level model were also obtained, observing that this approximation in thick bacteriorhodopsin films describes the propagation of sinusoidal pulses in a qualitative form. In order to obtain analytical expressions of the propagation of pulses in bacteriorhodopsin films a two-level saturable absorption model for bacteriorhodospin has been developed. Time delay, fractional delay and the distortion of pulses have been theoretical analyzed for sinusoidal pulses without the use of a pump beam (near zero background intensity) as a function of parameters such as intensity, frequency of the pulse and life time of the M state. Finally, the corresponding experimental study of the propagation of the sinusoisal pulses has been performed and it has been demonstrated the concordance between the theoretical model and the experiments.

9131-75, Session PS3

Modeling of diffraction from fractal objects with VirtualLab

Yana B. Muzychenko, Alexander A. Zinchik, Sergey C. Stafeev, National Research Univ. of Information Technologies, Mechanics and Optics (Russian Federation)

This paper describes opportunities in modeling of diffraction from fractal objects with variable transmittance and/or phase shift with VirtualLab. The program code is integrated in the software and allows to investigate diffraction fields from fractal gratings and zone plates with different order, scaling factor and fractal dimension. The randomness and correlation coefficient between phase/amplitude and spatial characteristics of the object can also be specified.

Modeling and study of light interaction with fractals is a subject of great importance from two points of view. First, some information on the physical properties of fractal objects may be extracted from Fraunhofer diffraction, such as fractal dimension and scaling factor. Second, the diffraction on fractal objects may create new wave front types which may lead to development of new optical elements with enhanced characteristics.

The results of modeling of diffractals – diffraction fields from fractal objects in Fraunhofer and Fresnel regions are discussed. The influence of the fractal object characteristics on the diffraction field is analyzed.

9131-76, Session PS3

Comparison of kinoform synthesis methods for image reconstruction in Fourier plane

Pavel A. Cheremkhin, Nikolay N. Evtikhiev, Vitaly V. Krasnov, Liudmila A. Porshneva, Vladislav Rodin, Sergey N. Starikov, National Research Nuclear Univ. MEPhI (Russian Federation)

Kinoform is synthesized phase diffractive optical element which allows to reconstruct image by its illumination with plane wave. Kinoforms are used in image processing systems. For tasks of kinoform synthesis iterative methods had become wide-spread because of relatively small error of resulting intensity distribution. There are articles in which two or three iterative methods are compared but they use only one or several test images. The aim of this work is to compare iterative methods by using many test images of different types. Images were reconstructed in Fourier plane from synthesized kinoforms displayed on phase-only LCOS SLM. Quality of reconstructed images and computational resource of the methods were analyzed.

For kinoform synthesis four methods were implemented in programming environment: Gerchberg-Saxton algorithm (GS), Fienup algorithm (F), adaptive-additive algorithm (AA) and Gerchberg-Saxton algorithm with weight coefficients (GSW). To compare these methods 50 test images with different characteristics were used: binary and grayscale, contour and non-contour. Resolution of images varied from 64x64 to 1024x1024. Fullness of non-zero pixels of images ranged from 0.008 to 0.89. Quantity of phase levels of synthesized kinoforms was 256 which equals to number of phase levels of SLM LCOS HoloEye PLUTO VIS. Under numerical testing it was found that the best quality of reconstructed images provides the AA method. The GS, F and GSW methods showed worse results but roughly similar between each other. Execution time of one iteration of the analyzed methods is minimal for the GS method. The F method provides maximum execution time.

Synthesized kinoforms were optically reconstructed using phase-only LCOS SLM HoloEye PLUTO VIS. Results of optical reconstruction were compared to the numerical ones. The AA method showed slightly better results than other methods especially in case of gray-scale images.

9131-77, Session PS3

Generation of keys for image optical encryption in spatially incoherent light aimed at reduction of image decryption error

Sergey N. Starikov, Pavel Cheremkhin, Nikolay N. Evtikhiev, Vitaly V. Krasnov, Vladislav Rodin, National Research Nuclear Univ. MEPhI (Russian Federation)

At present time methods of optical encryption are actively developed. The majority of existing methods of optical encryption use not only light intensity distribution, easily registered with photosensors, but also its phase distribution which require application of complex holographic schemes in conjunction with spatially coherent light. This leads to complex optical schemes and low decryption quality. To eliminate these disadvantages it is possible to implement optical encryption using spatially incoherent illumination which requires registration of light intensity distribution only. However this applies new restrictions on encryption keys: Fourier spectrum amplitude distribution of encryption key should overlap Fourier spectrum amplitude distribution of image to be encrypted otherwise loss of information is unavoidable. Therefore it seems that best key should have white spectrum. On the other hand due to fact that only light intensity distribution is registered, spectra of image to be encrypted and encryption key always have peaks at zero frequency and their heights depend on corresponding total energy. Since encrypted image contains noise, ratio of its average spectrum energy to noise average energy determines signal to noise ratio of decrypted image. Therefore ratio of amplitude at zero frequency to average spectrum amplitude (RZA) of encryption key defines decrypted images quality.

For generation of encryption keys with low RZA method of direct search with random trajectory (DSRT) was used. To estimate impact of key RZA on decrypted images error numerical experiments were conducted. For experiments keys with different RZA values but with same energy value were generated and used. Numerically simulated optical encryption and decryption of set of test images was conducted.

Results of experiment demonstrate that application of keys with low RZA generated by DSRT method leads to up to 20% lower error in comparison to keys generated by means of uniform random distribution.

9131-78, Session PS3

Design of single layer subwavelength diffractive optical element (G-Fresnel) for spectrum splitting and beam concentration

Abbas K. Hasan, Philippe Gérard, Univ. de Strasbourg (France); Pierre Ambs, Univ. de Haute Alsace (France); Patrick Meyrueis, Univ. de Strasbourg (France)

There is an increasing demand for optical elements having the functionality of hybrid devices like the combination of a Fresnel lens and a diffraction grating to obtain a wavelength separation and a beam concentration. These new devices can be used in many applications such as optical spectrometers, optical precision measurement systems and diffractive optical systems for enhancing the efficiency of third generation photo voltaic solar cells. There is also a growing need for developments of a cost-effective technology to fabricate compact optical devices. Therefore the motivation of our project is to find a new model of G-Fresnel taking into account the utilization of the electromagnetic theory for analyzing its behavior rigorously.

In this paper, a novel method is proposed and employed to design G-Fresnel (i.e. grating and Fresnel lens) that has only one structure layer with sub wavelength feature, and that focuses and separates different wavelengths at the same focal

distance. The performance is investigated based on the rigorous electromagnetic theory by using two methods: Finite Difference Time Domain (FDTD) for the study of the near field and Angular Spectrum Method (ASM) for the study of the propagation in the far field.

The design follows several steps. The first step uses an optimization algorithm to find the Fresnel lens profile that is able to minimize the longitude achromatic aberration and focus several wavelengths in same focal point with high diffraction efficiency. The second step consists in summing the product profile of the Fresnel lens with the grating profile that has the characteristics that give high diffraction efficiency in only one order of diffraction. The last step is transforming the product profile into sub wavelength features.

We use the thickness optimization algorithm to prepare different profiles of the Fresnel lens designed with different wavelengths for the same Fresnel number. Adding the thickness that gives a phase shift of 2m pi (where m is real number) in each profile for the predetermined wavelength does not affect the lens performance. By computing the minimum error between the thickness of different wavelengths and by taking the average, we can get the profile of a Fresnel lens that can focus different wavelengths at the same focal point with high efficiency. In order to achieve high diffraction efficiency gratings, we have to design a grating with a period larger than several wavelengths and an angle smaller than five degrees.

We are processing the accumulated thickness that gives a phase shift higher than 2 pi and kept the continuous profile of the G-Fresnel gives a phase shift of only 2 pi and it is then transformed into sub wavelength structures.

The simulation of this device is done rigorously by using the free FDTD software “Meep” (developed by the Massachusetts Institute of Technology) for fields inside the G-Fresnel and for a distance of few wavelengths behind the G-Fresnel. When the field arrives to the steady state then the field just past the G-Fresnel interface can be propagated to a chosen observation plane using angular spectrum method .

The verification of our G-Fresnel model with different profiles of sub wavelength structures and focal distances shows good performance of diffraction efficiency and high resolution through a broad band of the visible spectrum. This promising model of G-Fresnel can be used in many applications.

9131-79, Session PS3

Novel Dielectric Totally Internally Reflecting Concentrator (DTIRC) design for uniform illumination

Sina Babadi, Roberto Ramirez-Iniguez, Tuleen Boutaleb, Firdaus Muhammad-Sukki, Siti Hawa Abu-Bakar, Glasgow Caledonian Univ. (United Kingdom); Tapas Mallick, Univ. of Exeter (United Kingdom)

The Dielectric Totally Internally Reflecting Concentrator (DTIRC) has been developed in the past for wireless infrared Communications and solar energy applications [1] [2]. This paper proposes a new version of DTIRC that can be combined with a light emitting diode (LED) as a first or secondary optic to provide uniform illumination within a circular area with a desired radius. First, a brief introduction about the structure and the main characteristics of the traditional DTIRC is presented. Next, the software simulation work and the main results on the illumination properties of the integrated traditional DTIRC with the LED are discussed before presenting a design approach to optimise the DTIRC for uniform illumination. The analysis of the optimised design is provided afterwards. A summary and conclusions are provided at the end of the paper. The results from this work show that, with an optimised DTIRC, it is possible to achieve a uniformity of illumination of over 95%.

9131-80, Session PS3

Accuracy of photonic-based intra-oral scanner evaluated using micro-CT technology

Michel Fages, Alban Desoutter, Paul Tramini, Jacques Raynal, Frédéric J. G. Cuisinier, Univ. Montpellier 1 (France)

The objective of the study is to develop a novel strategy based on the micro computed tomography (micro-CT) technology, to evaluate the accuracy of photonic-based intra-oral scanners used for optical print in dentistry.

According to literature, several teeth are manually prepared with different designs, to receive different prosthetic reconstructions: onlays (1), peripheral crowns (2), endocrowns (1). Each tooth is scanned using micro-CT.

Files are processed using NRecon and Avizo software. Adobe Photoshop and Image J software are used to measure different regions of interest of the teeth.

So several distances are recorded for each teeth prepared. For the peripheral crowns the height of the preparation (HP1 and HP2), the circumference of the preparation (CP1, CP2), the width of the cervical line (CL1, CL2). For one of those two teeth the differences in height between the cups and fossa funds of the occlusal face are raised (PF). For the endocrown the width of the cervical walk is measured (CW), the depth of the cavity is so measured at three different points (DC). For the onlay depths boxes will be measured (DB) as well as their length (DL) and width (DW).

Thus the majority of the characteristics representing a clinical reality of dental preparations are identified.

Then an optical impression is taken for each tooth using dental intraoral scanner. The 3D images obtained are measured at the same location than the micro CT images.

The results are compared and statically analyzed.

9131-81, Session PS3

Limits of advanced modulation formats for transition in fiber optic telecommunication systems to increase speeds from 10, 40, 100 Gbps to higher bit rates

Michal Lucki, Rajdi Agalliu, Richard Zeleny, Czech Technical Univ. in Prague (Czech Republic)

The update of fiber optic telecommunication systems to increase their transmission rates from 10 Gbps ,40 Gbps, to 100 Gbps and higher is an actual topic. Some modulations cannot perform at higher bit rates because of hardware limits. In addition, transition to higher rates often requires solving the problem of Polarization Mode Dispersion and nonlinear effects, such as Four Wave Mixing that can strongly affect transmission at speeds starting at 10Gbps, causing increase in Bit Error Rate. The margin created few years ago for so-called future use, in many cases appears as not sufficient at present. However, in practice, there is a strong will to maximize the use of existing infrastructure, including lasers, fibers, topology, as well as of the frequency grid. On the other hand, there are techniques that enable optimizing transmission by more advanced modulations, using more effectively the available bandwidth, and reducing the symbol rate, at the same time solving the problem of dispersion and polarization governing.

In this paper we investigate limits of intensity and phase modulation formats used in optical communications. Non-Return to Zero, Return to Zero, Chirped Return to Zero, Carrier-Suppressed Return to Zero, Binary Phase Shift Keying, and Quadrature Phase Shift Keying including the most actual solutions, such as Polarization Division Multiplexing Quadrature Phase-Shift Keying, are investigated in terms of spectral efficiency, Bit Error Rate to find the limits for selected

topologies and spectral grids in Dense Wavelength Division Multiplexing. It has been shown that phase modulation formats have brought many advantages over intensity formats. Differential Phase-Shift Keying and mainly Differential Quadrature Phase-Shift Keying offer improvements in Bit Error Rate and transmission reach, among others. We answer questions about when it is more suitable to coarsen the grid, and when to transit to other modulation etc. There are practical conclusions about when it is possible to pass from 10 Gbps to much higher bit rates.

We study the potential increase of efficiency of Wavelength Division Multiplexing. We investigate the performance of Polarization Division Multiplexing Quadrature Phase Shift Keying, Polarization Division Multiplexing Differential Quadrature Phase Shift Keying in very high speed optical systems that are promising even for terabit transmission. The modulation format use coherent detection which benefits in estimated reach, spectral efficiency, Optical Signal to Noise Ratio tolerances, chromatic dispersion tolerances, and maximum differential group delay tolerance. Advanced polarization government and coherent detection solves as well the problem of Polarization Mode Dispersion. There are conclusions about Optical Signal to Noise Ratio limits of different options of Quadrature Phase Shift Keying and other formats, their immunity to chromatic dispersion, Polarization Mode Dispersion, Four Wave Mixing, among others. For some modulation formats, it is possible to additionally suppress half of their spectral content by applying an appropriate filtering technique preserving the information content.

The simulation results are obtained using OptSim environment employing Time Domain Split Step method. The split step method performs the integration of the fiber propagation equation. The monitors used are eye diagrams, Bit Error Rate, Optical Signal to Noise Ratio, Q-factor. We include the simulation setups and schemes of the transceivers.

9131-82, Session PS3

Simulation and properties of highly nonlinear multilayer optical structures using the transmission line method

Nikolaos Moshonas, National Technical Univ. of Athens (Greece); Gerasimos K. Pagiatakis, School of Pedagogical and Technological Education (Greece); Panagiotis Papagiannis, National Technical Univ. of Athens (Greece); Stylianos P. Savaidis, Nikolaos A. Stathopoulos, Technological Educational Institute of Piraeus (Greece)

Successive dielectric layers that are deposited on dielectric or metallic substrates form multilayer structures that can be deployed in a diverse range of polymeric-devices. Typical examples of such devices are the OLEDs (organic light-emitting diodes) and the OPVs (organic photovoltaics) as well as inorganic ones like DBRs (distributed Bragg reflectors), which are commonly used in VCSELs (Vertical Cavity Surface Emitting Lasers). The calculation of light-wave emission, absorption, refraction and transmission through these structures has been thoroughly analyzed in the last years by using the transfer matrix method (TMM) and recently, the transmission line method (TLM).

It is common practice, in the analysis of multiple layer devices like the ones above, to neglect the presence of nonlinear phenomena. This is mainly due to the fact of their small size and the weak nonlinearity of the materials used. However, the existence of strong third order nonlinear optical susceptibility could seriously affect the properties of a device of even that size. This is not just an interesting conjecture. Due to the progress in organic materials we can find many examples of polymers doped with dyes, organometallic compounds and other combinations, that present impressive third order nonlinear properties and a reported ease of fabrication; thus they could be used to build the layers. In this work we analyze the effect of strong nonlinearity of the third order to the performance of such a device.

In order to study the above discussed nonlinear problem we use the TLM, a well known 1D analysis model that has been used successfully in the analysis of interference problems, though, considering multilayer structures with linear materials. However, the involvement of materials' nonlinearity in the under consideration multilayer structure will increase the complexity of the interference phenomena; hence the necessary adaptation of the model to ensure its applicability is also demonstrated. Since optical multilayer structures with index nonlinearity have not been thoroughly analyzed so far, the application of TLM appears to be useful for the evaluation of power-dependent phenomena such as the devices' wavelength-spectrum shift or the change in spectral reflectivity and transmittance that we observed. More particularly, TLM presents an increased flexibility that allows the simulation of interference effects including index nonlinearity, whereas provides a unique physical insight in comparison with other methods. In this paper, the necessary modifications are applied on TLM in order to simulate optical multilayer structures with nonlinear refractive index and/or nonlinear extinction coefficient. Moreover, the influence of power-dependent phenomena on conceptual optical devices will be assessed using the proposed model.

9131-84, Session PS3

Computational test bench and flow chart for wavefront sensors

Úrsula V. Abecassis, Davies W. de Lima Monteiro, Luciana P. Salles, Euller T. S. Borges, Rafaela Stanigher, UFMG (Brazil)

Adaptive Optics is a multidisciplinary topic with a growing number of applications, from ophthalmology to astronomy, each with their respective requirements. There are, to date, many methods, algorithms, components and devices that can be combined in a vast variety of ways for a wavefront-sensor design in Adaptive Optics. There is also an increasing number of didactic books, scientific papers and websites that assist one through the meanders of wavefront sensing, control and actuation. Nevertheless, they often tackle a specific subject or are organized in a sequential structure of general topics, short of displaying in a straightforward fashion how elements can be chosen to work together. Most groups indeed have the knowledge to make suitable decisions, but for a newcomer, the realm of available options is often fuzzy, from device to system level. In this context, we have envisioned a chart that will be useful to aid the visualization of possible choices and how they relate to each other.

We will focus on wavefront sensing and propose a method to display the available options, from wavefront generation to error analysis, aiming to assist in decision making and in organizing a testbench for simulation and optimization of a device or sensing system. This is based on a flow chart branching downwards and laterally, linking together only structurally feasible options. This detector sub-block of an Adaptive Optics system alone features such numerous pathways that we limit ourselves to detail just a few of the possible tracks to illustrate how one can couple simulation codes and tools to design a system and preview its performance. The chart is flexible enough to accommodate new developments on devices and codes. As the chart is communally extended to actuation and control, and its branches are cooperatively populated with simulation models, a more complete mapping of possible systems will result. We will present simulation results that include the effect of several components, including the sampling plane, photodetectors and electronic circuitry on wavefront reconstruction.

9131-34, Session 8

Design of N-band multilayer antireflection coatings

Francesco Chiadini, Univ. degli Studi di Salerno (Italy); Vincenzo Fiumara, Univ. degli Studi della Basilicata (Italy); Antonio

Scaglione, Univ. degli Studi di Salerno (Italy)

Several methods have been introduced to design dielectric multilayers working as antireflection coatings. The goal of these methods consists in determining the architecture of the multilayer, i.e. in finding out the refractive index and the thickness of each layer of the multilayer structure, which, mounted atop a given substrate, makes reflection low in a given band. In this connection it is worth to note that several techniques have been developed and are currently under investigation to tune the refractive index of optical materials during their fabrication in order to realize multilayer structures with a given sequence of refractive indices [1]. However, to the best of our knowledge, all the proposed methods deal only with the design of dielectric multilayers exhibiting an antireflection behavior in a single band.

We introduced a general analytical synthesis method (based on the classical Riblet method) of quarter-wave multi-section structures which, in principle, works whatever the requested reflection spectrum may be [2]. Given the refractive indices of the materials between which the multilayer is inserted, the input parameters of our design procedure are the number of layers and the desired reflection spectrum. The synthesis method allows the frequency at which the layers must be quarter-wave thick to be determined and the sequence of the refractive indices to be computed so that the reflection spectrum results to be a good approximation to the desired one. Moreover, we showed how our method can be used to design dielectric multilayers working as N-band antireflection coatings. Here, we present some examples confirming the effectiveness of our synthesis procedure in designing dual- and three -band antireflection coatings.

[1] V. Torres-Costa and R. J. Martìn-Palma, “Application of nanostructured porous silicon in the field of optics. A review”, J. Mater. Sci. 45(11), 2823–2838, 2010.

[2] F.Chiadini, V.Fiumara, A.Scaglione, “Synthesis method for N-band multilayer antireflection coatings”, J. Nanophoton., 7, 073097, 2013.

9131-35, Session 8

Observation of self-trapping of optical beams in AA/PVA photopolymer material

Haoyu Li, Yue Qi, James P. Ryle, John T. Sheridan, Univ. College Dublin (Ireland)

We demonstrate theoretically and experimentally that the light can be self-focused and self-trapped in a self-written optical waveguide in a bulk acrylamide/polyvinyl alcohol (AA/PVA) solid photopolymer material volume. The manufacture method, i.e., how to prepare the AA/PVA photopolymer material is detailed. In our experimental observation the refractive index changes induced are permanent. The resulting optical waveguide channel has good physical stability and can be integrated with optoelectronic devices as part of integrated optical systems. The theoretical model developed predicts the formation/evolution of the observed self-written waveguides inside the bulk material. The model involves appropriately discretizing and then numerically solving the paraxial wave equation in Fourier space and the material equation in time space. Experimental results and the predictions of the model are presented and compared.

9131-36, Session 8

Simulating the response of nanostructures under a focused beam

Paul Chevalier, Patrick Bouchon, Riad Haïdar, ONERA (France); Fabrice Pardo, Lab. de Photonique et de Nanostructures (France)

Numerical simulations are important to predict the optical response of nanostructures and are used as a fundamental help for their design. Experimentally these nanostructures can be characterized under focused light.

Here we address the need for simulating the response of nanostructures under a focused beam.

This protocol for simulating the focused response is based on a modal method (P. Bouchon et al., J. Opt. Soc. Am. A, 27(4), 696–702 (2010), B. Portier et al. J. Opt. Soc. Am. A, 30(4), 573-581). As a focused wave could be decomposed into plane waves of different incidences, the focused situation follows from the coherent superposition of the different responses to the individual waves.

By using an apodization (using for instance a Blackman window) of a primary focused beam, we are able to produce realistic focused beams and to determine a base of plane waves to decompose them. This method is flexible as it allows the shape of the desired beam to be easily changed, and is efficient as it preserves the periodic boundary conditions.

This method permits to simulate the concentration of the electric field which is important for the design of non-linear devices, or photo-detectors. We also show that the focal spot can be moved on the surface to different area of interest in order to investigate the specific properties of the simulated structure. Eventually, we also show that it permits to simulate the response of single nanoantennas, and that this response is linked to the angular acceptance of the antenna.

References:

P. Bouchon, F. Pardo, R. Haïdar, & J. L. Pelouard, Fast modal method for subwavelength gratings based on B-spline formulation. JOSA A, 27(4), 696-702 (2010).

B. Portier, F. Pardo, P. Bouchon, R. Haïdar, & J. L. Pelouard, Fast modal method for crossed grating computation, combining finite formulation of Maxwell equations with polynomial approximated constitutive relations. JOSA A, 30(4), 573-581 (2013)

9131-37, Session 8

Sampling of the two-dimensional linear canonical transform

Liang Zhao, Univ. College Dublin (Ireland); John J. Healy, National Univ. of Ireland, Maynooth (Ireland); John T. Sheridan, Univ College Dublin (Ireland)

The two-dimensional non-separable linear canonical transform (2D-NS-LCT) involves a significant generalization of the separable LCT (S-LCT), since it can represent all paraxial orthogonal and non-orthogonal optical systems. Thus the availability of a discrete numerical approximation of the 2D-NS-LCT is important as it permits the modelling of a broad class of optical systems. The continuous 2D-NS-LCTs are unitary, but discretization can destroy this property. In this paper, we discuss the condition on the sampling chosen in the discretization, under which some special cases of the discrete 2D-NS-LCTs are unitary. The results presented here provide a basis for the discussion of the general condition for the discrete 2D-NS-LCT to be unitarity.

9131-38, Session 8

Revisiting Maxwell’s equations: a wave propagation method for electromagnetics in spacetime-varying media

Damian P. San-Roman-Alerigi, David I. Ketcheson, Boon S. Ooi, King Abdullah Univ. of Science and Technology (Saudi Arabia)

Recent publications have demonstrated that there is a wide miscellany of materials whose electromagnetic properties can change at a pace comparable to that of electromagnetic wave oscillation [1, 2]. Novel effects arising from wave propagation in space-time-varying media include trapping, confinement, ultra-short pulse coupling, beam transformation, negative refraction,

eigen–polarization, and the optical Bohm–Aharonov effect [3–12]. This has opened the theoretical possibility to control light in new ways, e.g. Alcubierre's warp drives [13]. In order to study these phenomena, and provide a framework for the modeling and development of novel technologies based on them, we reformulate Maxwell's equations as a system of balance laws, i.e.: ?(?r,t)?q_t+f?^i (?q;?r,t)_x^i = ??(?q;?r,t). Discretization by finite volumes leads to the well known Riemann problem for fluxes between adjacent cells [14]. We extend the high resolution wave propagation algorithms of Clawpack and PyClaw [14, 15], in which the flux difference, in addition to the source, ??, and capacity, ?, are decomposed into eigenvectors of the flux Jacobian. Typical finite difference discretizations discretize hyperbolic and non-hyperbolic terms separately [16]. In the present approach, transient variations in the material, or space, are directly incorporated into convective terms. We show computational results for light trapping in super-luminal refractive index perturbations and light confinement. While our discussion revolves around Maxwell's electromagnetic equations, the methods can be applied to other physical wave phenomena in time-varying media. In our discretization the wave speeds, i.e. the flux Jacobian eigenvalues, turn out to be constant regardless of the material properties. Thus the observed change in velocity a wave experiences when traversing a medium arises from the material's modification of the space's metric, analogous to transformation optics [17, 18].

[1] B. J. Eggleton, B. Luther-Davies, and K. Richardson, Nature Photonics 5, 141 (2011).

[2] D.P.San-Romaán-Alerigi,D.H.Anjum,Y.Zhang,X.Yang,A. Benslimane,T.K.Ng,M.N.Hedhili, M. Alsunaidi, and B. S. Ooi, Journal of Applied Physics 113, 044116 (2013).

[3] A. Kaplan, Optics letters 8, 560 (1983).

[4] C. Ridgely, American Journal of Physics 67, 414 (1999).

[5] P. Piwnicki and U. Leonhardt, Applied Physics B: Lasers and Optics 72, 51 (2001).

[6] N. Rozanov and G. Sochilin, Optics and spectroscopy 98, 441 (2005).

[7] U. Leonhardt, Science (New York, N.Y.) 312, 1777 (2006).

[8] U. Leonhardt and T. G. Philbin, New Journal of Physics 8, 247 (2006).

[9] G. Rousseaux, EPL (Europhysics Letters) 84, 20002 (2008).

[10] F. Belgiorno, S. L. Cacciatori, G. Ortenzi, V. G. Sala, and D. Faccio, Physical Review Letters 104, 140403 (2010),

[11] S. L. Cacciatori, F. Belgiorno, V. Gorini, G. Ortenzi, L. Rizzi, V. G. Sala, and D. Faccio, New Journal of Physics 12, 095021 (2010).

[12] F. Belgiorno, S. Cacciatori, G. Ortenzi, L. Rizzi, V. Gorini, and D. Faccio, Physical Review D 83 (2011), 10.1103/PhysRevD.83.024015.

[13] I. Smolyaninov, Physical Review B 84, 2 (2011).

[14] R. J. LeVeque, International Journal for Numerical Methods in Fluids 40, 93 (2002).

[15] D. I. Ketcheson, K. Mandli, A. J. Ahmadia, A. Alghamdi, M. Q. de Luna, M. Parsani, M. G. Knepley, and M. Emmett, SIAM Journal on Scientific Computing 34, C210 (2012).

[16] I. Faragó, A. Havasi, and R. Horváth, Central European Journal of Mathematics 10, 137 (2011).

[17] U. Leonhardt, New Journal of Physics 8, 118 (2006).

[18] J. B. Pendry, D. Schurig, and D. R. Smith, Science (New York, N.Y.) 312, 1780 (2006).

9131-39, Session 9

The parabasal thin element approximation for the analysis of the diffractive optical elements

Huiying Zhong, Site Zhang, Frank Wyrowski, Friedrich-Schiller-Univ. Jena (Germany)

Analysis of diffractive optical elements (DOEs) can be handled by rigorous as well as numerical methods. The rigorous approach for analysis of DOEs is Maxwell solvers, which start from the Maxwell equations and search the solutions satisfying the boundary conditions, e.g. Fourier Modal Method (FMM) or Finite Element Method (FEM). However, the numerical efforts increase rapidly and become impractical as the feature size of structure increase, especially for three-dimensional structures. The approximate methods to analyze DOEs are mainly based on geometrical optics, which requires the feature size should be large enough compared with the working wavelength. The thin element approximation is such an efficient algorithm. However, the thin element approximation is only valid under the condition of normal illumination. We hereby extend an algorithm, which is called the parabasal thin element approximation, to include the non perpendicular illumination. More specifically, the thin element approximation is valid for paraxial incident beam, while the parabasal thin element approximation is valid for parabasal beam. The divergence angle of parabasal beam is as small as paraxial beam and the main direction is either parallel to the optical axis or not. In this presentation, we present the valid region, basic idea and applications of the parabasal thin element approximation. All the simulations are based on field tracing and done with the optical software VirtualLab.

9131-40, Session 9

Generalized source method for modeling nonlinear diffraction in planar periodic structures

Martin Weismann, Univ. College London (United Kingdom) and Photon Design (United Kingdom); Dominic F. G. Gallagher, Photon Design (United Kingdom); Nicolae-Coriolan Panoiu, Univ. College London (United Kingdom)

We present a new numerical method for the exact analysis of second-harmonic generation (SHG) in two-dimensional (2D) diffraction gratings with arbitrary profile made of non-centrosymmetric optical materials. Our method extends the recently introduced generalized source method (GSM), which is a promising and highly efficient alternative to the conventional Fourier modal method, to quadratically non-linear diffraction gratings. The proposed method can be described as a two-stage algorithm. Initially, the electromagnetic field at the fundamental frequency, ?, is computed in order to obtain the second-harmonic polarization using the known second-order non-linear susceptibility tensor ?^(2). Then the optical field at the second-harmonic frequency Ω=2? is computed using this polarization density as an additional source term in the GSM. We show how to integrate this source term into the GSM framework without changing the structure of the basic algorithm. This allows for the use of a fast iterative solver for the governing linear system of equations. Therefore, the significantly improved algorithm performs with the same computational efficiency as the original GSM, making it particularly suitable for thin grating structures with moderately high refractive index contrast. We use the proposed algorithm to investigate a doubly resonant mechanism that leads to the enhancement of SHG in a 2D crossed GaAs grating mounted on top of a GaAs slab waveguide. This non-linear optical grating is placed on a silica (SiO2) substrate. We design the optical device such that slab waveguide modes at the fundamental and second-harmonic are simultaneously excited and phase matched by the grating. We also illustrate the impact of this simultaneous phase matching on the diffraction efficiencies at the second harmonic. The numerically obtained resonance frequencies show good agreement with analytically computed resonance frequencies of the uncoupled slab waveguide modes. Our results suggest that the proposed numerical method is a powerful tool to design and investigate ultra-compact efficient photonic devices for non-linear optical signal processing at the optical chip scale.

9131-41, Session 9

Fourier Modal Method for crossed gratings with Kerr-type nonlinearity

Subhajit Bej, Jani Tervo, Jari Turunen, Yuri Svirko, Univ. of Eastern Finland (Finland)

Fourier Modal Method (FMM), also known as the Rigorous Coupled Wave Approach (RCWA), [1, 2] is a very well-known method for numerical modeling of diffraction gratings. In the past, it has been implemented both for linear and crossed gratings made of linear optical materials. As discussed in [2], if we consider correct rules of Fourier factorization, this method is relatively faster and consumes less memory as compared to other standard grating modeling methods. For 1D-gratings, FMM has also been extended to the third-order nonlinear materials by Laine and Friberg using an approach based on an iterative linear model [3]. In this method, they solve the nonlinear propagation equation inside the Kerr media iteratively. A somewhat similar approach adopted with another standard grating modeling method namely 'Differential method' was proposed by N. Bonod et al. [4] for the analysis of metallic lamellar gratings. Here we extend the method introduced in [3] to crossed gratings made of arbitrary isotropic materials with third-order nonlinearity. Third-order susceptibility tensors of such media can be represented in terms of effective linear susceptibility of anisotropic but optically linear medium as discussed in [5]. We solve the grating-diffraction problem by making use of the iterative approach with FMM for crossed gratings for arbitrary anisotropic materials [6]. Here anisotropy in the material is induced by light. We also discuss how the symmetries of the effective linear permittivity tensor can be exploited to speed up the computation when one considers normal incidence of light. In general, third order susceptibility of a Kerr medium is a fourth rank tensor comprising of 81 independent elements. However, isotropic materials possess high degree of spatial symmetry and the number of independent elements is much reduced [5]. Several numerical experiments are performed to demonstrate the accuracy as well as the versatility of our numerical technique. Resonance waveguide gratings [7] made of isotropic cubic nonlinear materials (Silicon-Nitride) are investigated numerically using this technique. These devices are extremely sensitive to refractive index mismatch between the grating material and its surroundings. A polarization-sensitive shift of resonance peak with variation of light intensity is numerically demonstrated. This is expected as the refractive index of the grating material also includes a nonlinear part which depends on the intensity of light.

[1] E. Noponen and J. Turunen, J. Opt. Soc. Am. A 11, 2494 (1994).

[2] L. Li, J. Opt. Soc. Am. A 14, 2758 (1997).

[3] T. A. Laine, and A. T. Friberg, Opt. Commun. 159, 93 (1999).

[4] N. Bonod, E. Popov, and M. Neviere, Opt. Commun. 244, 389 (2005).

[5] R. W. Boyd, Nonlinear Optics, Academic Press, London, (1992).

[6] L. Li, J. Opt. A: Pure Appl. Opt. 5, 345 (2003).

[7] S. S. Wang, and R. Magnusson, Appl. Opt. 32, 2606 (1993).

9131-42, Session 10

Comparison of a new dye with Erythrosin B in an AA/PVA based photopolymer material utilising the NPDD model

Yue Qi, Haoyu Li, Univ. College Dublin (Ireland); Jean P. Fouassier, Jacques Lalevée, Univ. de Haute Alsace (France); John T. Sheridan, Univ. College Dublin (Ireland)

Photosensitizers or dyes often act as the initiator in photopolymer materials and are therefore of significant interest. The properties of the photosensitizer used strongly influences grating formation when the material layer is exposed holographically. In this paper, the ability of a recently synthesized dye, D_1, to sensitise an acrylamide/polyvinyl alcohol (AA/PVA) based photopolymer is examined and the material performance is characterised using an extended Non-local Photopolymerization Driven Diffusion (NPDD) model. The results obtained are then compared to those for the corresponding situation when using a Xanthene dye, i.e., Erythrosin B (EB), under the same experiment conditions. The results indicate that, in comparison with EB, the non-local effect is greater when this new photosensitizer is used in the material. Analysis indicates that this is the case because of the dyes weak absorptivity and the resulting slow rate of primary radical production.

9131-43, Session 10

Spatial frequency response of a volume hologram recorded in a ZrO2 nanoparticle-dispersed acrylate photopolymer film containing chain transfer agents

Jinxin Guo, Ryuta Fujii, Yasuo Tomita, The Univ. of Electro-Communications (Japan)

The photopolymerizable nanoparticle-polymer composites (NPCs) have thus far shown their excellent performance in practical applications, such as holographic data storage, nonlinear optics and neutron optics. Specifically, for such holographic applications, a high spatial frequency material response is necessary, as it is the response to high spatial frequencies that determines the resolution and data storage capabilities. However, it is known that the spatial frequency response of a recorded hologram in multi-component photopolymers including NPCs and holographic polymer-dispersed liquid crystals exhibits a reduction in refractive index modulation at high spatial frequencies. In order to overcome this drawback, an addition of chain-transfer agents (CTAs) may be useful as done for all-organic photopolymers to suppress their nonlocal response characteristics. In our work, we investigate the effect of CTAs on the spatial frequency response in NPCs. Here we employ various chain-transfer agents with three different thiol groups in a photopolymerizable ZrO2 nanoparticle-(meth)acrylate polymer composite. A range of CTA concentration is carried out, in order to explore the most effective material combination used in the examination of spatial frequency response. The significant improvement in spatial frequency response of NPCs through the addition of a CTA with the most appropriate concentration is presented.

9131-44, Session 10

Characterization of photopolymerizable nanoparticle-(thiol-ene) polymer composites for volume holographic recording at 404 nm

Masaru Kawana, Jun-ichiro Takahashi, Satoru Yasui, Yasuo Tomita, The Univ. of Electro-Communications (Japan)

Since 2002 we have developed a holographic nanocomposite material, the so-called photopolymerizable nanoparticle-polymer composite (NPC), where inorganic or organic nanoparticles are uniformly dispersed in monomer capable of radical chain photopolymerization. The inclusion of nanoparticles increases the saturated refractive index modulation (?nsat) and the material recording sensitivity (S) that exceed the required minimum values of 0.005 and 500 cm/J, respectively, for holographic data storage (HDS) media. At the same time the mechanical and thermal stability of recorded volume holograms can be improved with the dispersion of inorganic nanoparticles. Recently, we have introduced the use of thiol-ene photopolymerizations that

proceeded via a step-growth radical addition mechanism. We demonstrated that shrinkage reduction as low as 0.4% was possible with ?n_sat and S as high as 0.01 and 1615 cm/J, respectively, at a grating spacing of 1 ?m and a recording intensity of 5 mW/cm2 in the green (532 nm). This result was obtained by using NPCs with 25 vol.% silica nanoparticles and the stoichiometric mixture of secondary dithiol and allyl triazine triene together with an Irgacure 784/BzO2 initiator system. In this work we report on the characterization of volume holographic recording in such thiol-ene-based NPCs at a wavelength of 404 nm by using a highly coherent blue diode laser. We investigate the photopolymerization dynamics and their influences on holographic recording performance for two types of blue-sensitive initiator systems (Irgacure 784/BzO2 and Darocure®TPO) at their varying concentrations. We employed a real-time Fourier-Transform infrared spectroscopy and a differential scanning calorimeter for the photpolymerization measurement. We monitored the buildup of a plane-wave volume grating during two-beam recording at 404 nm and a recording intensity of 5 mW/cm2. The recorded volume grating in a 10-micron-thick NPC film had its grating spacing of 1 ?m. It is found that Darocure®TPO provides larger values for ?n_sat and S than those with Irgacure 784/BzO2, satisfying the requirement for HDS media with Darocure®TPO. On the other hand, it is found that shrinkage reduction with these two initiator systems at 405 nm is not as effective as with Irgacure 784/BzO2 at 532 nm. We discuss such a strong dependence of shrinkage on writing beam wavelength.

9131-45, Session 10

GPU accelerated holographic microscopy for the inspection of quickly moving fluids for applications in pharmaceutical manufacturing

Nazim Dugan, James P. Ryle, John J. Healy, Bryan M. Hennelly, National Univ. of Ireland, Maynooth (Ireland)

Digital holographic microscopy is suitable for the detection of microbial particles in a rapidly flowing fluid since in this technique the focusing can be carried out as post processing of a single captured image. This image, known as a digital hologram, contains the full complex wave front information emanating from the object which forms an interference pattern with a known reference beam. Post processing is computationally intense and it constitutes a bottleneck for real time inspection of fast moving scenes. In the current work, GPU computation is used to accelerate the post processing of the holographic images captured by digital holographic microscopy. In this procedure there are five stages with different time scales: 1) Capturing the image with a fast digital camera, 2) transferring the image to the GPU memory, 3) GPU pre-processing for deciding if the image is worth processing, 4) GPU processing for autofocus and investigating the morphology of detected particles, 5) transferring useful information back to the host computer. Recent NVIDIA GPUs allow overlapping of data transfers with the computation and they can transfer data in both directions simultaneously. However, the different time scales associated with these five different stages of the procedure make it harder to design a pipe line overlapping all these stages. We design a strategy with individual CPU threads for the described stages of the procedure and with different CUDA streams for the GPU involving stages. With appropriate buffers and synchronized accesses for different threads, the delay times between these stages can be minimized and the overlapping of the stages can be carried out as much as possible. Multiple GPU cards can be used with this strategy in order to enable the investigation of the rapid moving fluids in real time or withminimal time delay.

9131-46, Session 10

Application of photo-thermo-refractive glass as a holographic medium for holographic collimator gun sights

Sergey Ivanov, Aleksandr Angervaks, Alexander Shcheulin, National Research Univ. of Information Technologies, Mechanics and Optics (Russian Federation)

Photo-thermo-refractive glass (PTR glass) is a prominent material of optics and optoelectronics. Its use is still rising in a various fields of science and technology. In this work we use PTR glass for creation of holographic optical elements (HOE) forming the image of reticle pattern in holographic collimator gun sights (HCGS). The main advantages of PTR glass use for HOE recording and its working principles in HCGS scheme are discussed.

Compare to widely used classical collimator sights, HCGS have some advantages based on the physical properties of holographic media. They do not have a view field restriction because of ocular physical dimensions; they can be used even with partially damaged or soiled aperture. Optical scheme of HCGS prevents rifleman disclosure due to absence of stray reflections. High diffraction efficiency of HOE allows getting bright reticle patterns; aperture of HCGS has high transparency, without background coloring caused by antireflection coatings.

HCGS used at present have some disadvantages because of utilization thin holographic media, which are vulnerable to set of external actions. Therefore it requires protective coating layers of glass to prevent damage of the holographic media; furthermore optical scheme of such sight needs additional elements to compensate thermal shift of reconstructing wavelength.

The use of PTR glass allows us to simplify the optical scheme of HCGS due to removal of above mentioned elements. PTR glass has high chemical and mechanical stability, non-hygroscopic, and holograms recorded on this material are stable at temperatures up to 400C. Usage of highly-selective volume phase holograms permits to improve the quality of the reticle pattern and decrease production complexity and cost.

The advantages of PTR glass use to create holographic gun sight are demonstrated both theoretically and experimentally. Images of reticle patterns prototypes for several focusing distances are obtained using PTR glass.

9131-85, Session PS

Non-periodic multilayer optics for high-resolution X-ray imaging microscope

Phillipe Troussel, D. Dennetiere, CEA, DAM (France); F. Delmotte, Institut d'Optique LCFIO, CNRS (France); P. Høghøj, Xenocs SA (France); M. Krumrey, Physikalisch-Technische Bundesanstalt (Germany)

With regards of the Laser Megajoules french facility (LMJ), our laboratory is developing advanced time-resolved High Resolution X-ray Imaging (HRXI) diagnostics in order to probe dense plasmas.Shrapnel and X-ray loading on this laser imposed to place any HRXI as far away from the source as possible. Grazing incidence X-ray microscopes are the best solution to overpass this limitation. These imagers combine therefore grazing X-ray microscope and camera. We designed imaging microscopes, mainly with a long working distance (> 25 cm) and high spatial resolution (5-20 μm typically) observing a large field of view (1 - 3 mm). All of them are composed of single or multi-toroidal(s) mirror(s).

To observe a large field of view, X-ray microscope consists of two similar off-axis toroidal mirrors mounted one behind the other into a Wolter-type geometry [1]. We present a first microscope working at 0.6° grazing angle which achieved a 5 μm spatial resolution over a 1mm field of view. Its mirrors were coated by non-periodic (depth graded) multilayer coatings,

developed in collaboration with LCFIO, allowing a high reflectivity up to 12 keV.

To increase the bandwidth of reflectivity or to provide broadband X-ray reflectance at grazing incidence, we have developed a similar microscope, working at a lower grazing angle (0.45°) in order to obtain high reflectivity in the 1-22 keV range energy band. The design of the microscope is discussed, in particular aberrations and their minimization. The realization of the optical coating mirror: a stack of non-periodic layers (between 0.8 nm and 4 nm) is presented and also the different steps concerning the thickness layer calibration, till to obtain a rear plane spectral reflectivity at high energy. This microscope has the possibility to select a spectral bandwidth by using a monochromatic third mirror. This mirror (Gobel mirror) permits to increase the effective aperture and field of view. It is coated by high quality layer stacks with laterally graded thickness for monochromatic radiation. The multilayer deposition has been carried out on the deposition machine of Xenocs Society (France). The mirror and subnanoscale layers characterization were made mainly at the Physikalisch Technische Bundesanstalt (PTB) laboratory at the synchrotron radiation facility Bessy II [2].

References:

[1] Ph. Troussel et al., Review of Scientific Instruments, vol. 76, Mai 2005

[2] M. Krumrey, G. Ulm. Nuclear Instruments and Methods A 467 (2001) 1175

9131-86, Session PS

Optical design of power-saving backlight module with external illuminance

Yi-Chin Fang, National Kaohsiung First Univ. of Science and Technology (Taiwan)

This research propose the concept of Light Guide Film(LGF) at the back side of Back Light Unit(BLU). This new design may induce the exterior light ,then improve the power-saving of existent BLU. Two design models are reseated:One is design for 14 inch LCD monitor of notebook computer,which might improve 21% compared to traditional one. Another is designed for 3.5 inch LCD for mobile phone display ,which might improve 15% compared to traditional one.

Modern displays are required to be much thinner and thinner with best colour gamut. LED play the role at such the kind of modern display light source thanks to its power consumption and the most important , outstanding colour gamut. In backlight modules, the light guide plate (LGP) is a key component in reducing the cost and easier access to develop LGPs on its own.

At present, LEDs have not yet been widely applied to large-size bottom lighting. For some common smaller size edge lighting applications, the three colors of red, blue and green first undergo optical mixing in the light guide structure or in the optical mixing area, then enter the backlight module, and are applied to various kinds of edge lighting structures.

We have manipulated the pattern distribution of the micro features to obtain the required optical characteristics. Two light guide plate (LGP) of 14 inch dimension using an LED light source and 3.5 inch LED BLU are used as an example for the study of integrated LGPs.[1-3]

Conference 9132: Optical Micro- and Nanometrology

Tuesday - Thursday 15–17 April 2014 • Part of Proceedings of
SPIE Vol. 9132 Optical Micro- and Nanometrology V

9132-1, Session 1

Optical frequency comb profilometry using a single-pixel camera *(Invited Paper)*

Yoshio Hayasaki, Quang Duc Pham, Utsunomiya Univ. (Japan)

Fast and high accuracy profilometry of a long-depth object such as large-scale facilities are nowaday becoming very essential for many industrial applications. An optical mode-locked frequency comb laser produces a series of optical pulses separated in time by the round-trip time of the laser cavity and the spectrum of such a pulse train approximates a series of Dirac delta functions, which are equally separated by the repetition rate of the laser. By using a frequency comb femtosecond laser, the refractive index and thickness can be determined by using spectrally resolved single- or two-color interferometry, and phase measurement, profilometry, and tomography of the objects can also be carried out by sweeping the comb interval frequency and using scanning interferometry. Particularly, exploiting periodic peroperty of the optical laser pulses, the precise and wide dynamic range absolute distance measurement can be achieved without any ambiguity by time-of-flight method that calculated the distance via interpulse time and sweeping the comb interval frequency. By resolving the coherent fringe the distance with higher accuracy also can be determined. The accuracy less than an optical fringe of the distance measurement can be obtained with the combination of the time-of-flight and coherent fringe-resolved techniques. Other well-known approaches are intermode beats modification of the optical frequency comb and methods exploiting the radio-frequency domain of a frequency comb femtosecond laser. Technically, the object's profile can be absolutely determined by point-by-point measering the distance of all object's points, but it will be very time consuming and the accuracy is limited by the need to mechanically scan. We demonstrate an optical frequency comb profilometry implemented with the frequency comb femtosecond laser, an optelectronic intefererometer in radio frequecny region, and a single pixel camera without any mechanical movements. An experiment setup was composed of a Ti:Sapphire femtosecond laser with a carrier envelope phase (CEP) stabilization and a repetition rate of fR = 76MHz, 1GHz photo-receivers for detecting an object and a reference waves, a spatial light modulator (SLM) for a spatially modulation of the object wave using a random pattern, and electric circuits for a phase difference between both waves. A plane mirror was used as a target object to evaluate the accuracy the proposed method. The profile of the object was reconstructed then the accuracy was evaluated by calculating the root mean square (RMS) error. In this case, because the original object was considered to be a perfect flat, the RMS error was simply calculated from all measured points and their average depth. The present accuracy was 2.6μm for 4 x 4 measurements at 988 MHz. The frequency can be detected an object with depth smaller than 15.2 cm without any 2ϖ ambiguity. We firstly demonstrate the optical frequency comb profilometry without a mechanical scanning for an object with cm-order depth. The profilometer was constructed with the combination of the optical frequency comb and a single pixel camera.

9132-2, Session 1

Dynamic and uniaxial profilometry by polarization camera

Shuhei Shibata, Fumio Kobayashi, Daisuke Barada, Yukitoshi Otani, Utsunomiya Univ. (Japan)

Many methods for noncontact three-dimensional profilometry have been proposed by using a stereo method such as a moire and a grating projection. However it is difficult to apply a deep hole or step height because grating pattern is hard to observe in the shadow portion. We propose a dynamic measurement of three-dimensional surface shape using contrast detection of uniaxial detection by a polarization camera, which is made pixel polarizers attached on CCD sensor. A polarizing grating is generated in spatially using a quarter wave plate and a spatial light modulator (SLM) which is projected onto a sample. Intensity reflected from sample is captured by the polarization camera. All distance information of z-direction can be determined by calculated contrast of projected polarizing grating pattern that can be calculated in real-time by 4 stepping phase shifting technique using 4 adjacent pixels of spatially different polarizer array. The three-dimensional coordinate is calculated relationship Gauss distribution of measuring contrast. A shadow less measurement of the object's area is archived by using a uni-axial system. Surface profiles are measured to demonstrate this method.

9132-3, Session 1

Comparison of areal measurements of the same zone of etched Si and hydroxyapatite layers on etched Si using different profiling techniques

Mohamed Guellil, Paul C. Montgomery, Pierre Pfeiffer, ICube (France); Bruno Serio, Lab. Energétique Mécanique Electromagnétisme (France)

In the area of micro and nano surface roughness measurement, characterization using several techniques can be helpful to better understand the performance of each technique and to improve the overall measurement precision. This is all the more true when the surface structure deviates from a homogeneous and flat surface to one that is heterogeneous and rough. In the results of materials analysis presented in the literature, where several techniques have been used on the same sample, the measurements are more often from different places. Measuring exactly the same area with different techniques in practice is not easy, despite improvements in individual profiling techniques and methods of marking. Such studies are of great interest in order to characterize and to understand important new materials today such as semiconductor alloys and graphene for silicon technologies, or biomaterials such as hydroxyapatite for use in human implants.

In this work, two types of samples based on a silicon wafer were made by marking them using a photolithographic mask and etching so as to be able to identify and measure exactly the same area. The mask was designed with different geometries varying in size for rapid and efficient localization of sample features varying from mm2 toμm2. The first sample consisted of the bare silicon wafer with a pattern consisting of different sized numbered square features with a depth of about 2.4 μm. The second sample was a rough layer of hydroxyapatite deposited from a solution of simulated body fluid (SBF) on a similarly etched silicon wafer. The same zone of several squares on the two samples were analyzed by interference microscopy (a Leitz-Linnik research microscope and a Zygo NewView 7200 commercial microscope), AFM (Park XE70) and SEM.

The 2D cross sectional profiles and 3D views from the different results were then compared using different analytical measurement tools (MountainsMap, a LabView based laboratory-developed program and Zygo and Park proprietary software). While the general shapes of the measured microstructures were similar, several differences revealed some interesting measurement limits and artifacts of each technique. For example, the average measured depth of the bare silicon squares varied from 2.28 μm to 2.48 μm between the techniques. These variations were due to instrumentation calibration errors, probe/surface interactions and differences in measurement procedures between the software used. In addition, artifacts were also particularly visible on edge

features, consisting either of unmeasured points (Zygo) or a rounding of the edges due to probe/source interactions (Leitz-Linnik and AFM systems).

One interesting result of the work was the confirmation that in practice it is indeed remarkably difficult to carry out measurements in exactly the same place, due to problems in finding the right marking technique for a given sample, in finding the same area, in positioning the 2D profiles and in comparing results using the different analytical software tools. Nonetheless, the general conclusion is that such a study is very useful for providing a better understanding of each measurement technique and for providing more precise measurements of surfaces that are difficult to measure.

9132-4, Session 1

Remote laboratory for phase-aided 3D microscopic imaging and metrology

Meng Wang, Yongkai Yin, Zeyi Liu, Wenqi He, Dong He, Peng Xiang, Shenzhen Univ. (China)

It's always believed that innovation and communication are critical for scientific community. Remote laboratory can make a unique technique belonging to some scientists available for others, which provide a bridge between innovation and communication. Meanwhile, with the development of information technology, data transmission and remote control become more and more convenient, which benefits the setting up of remote laboratory a lot. In this paper, we report a work supported by a joint Sino-German research project "Remote Laboratory for Optical Micro Metrology". A remote laboratory for phase-aided 3D microscopic imaging and metrology is built, which consists of two major components, including the network-based infrastructure for data management and the remote access, and the local experimental system for phase-aided 3D microscopic imaging and metrology. A scientist or an engineer could remotely control the 3D microscopic metrology system to acquire desirable 3D data. Metadata gained in the measurement will be recorded and stored into data base automatically. Then the scientists can take remote access or analysis to the data via internet anytime and anywhere.

The network-based infrastructure of the remote laboratory does not built from scratch. The virtual network computer (VNC) is introduced to remotely control the host computer. Considering the security of remote access, the host computer is hidden behind a proxy server to make it invisible from outside. All the outside contact is handled by the proxy server and all the communication will use a secure shell protocol (SSH) channel to improve the security. In addition, the fingerprint is also used for authentication with an optical joint transform correlation (JTC) system. Data storage and management are handled through the open source project eSciDoc, which is an e-Research environment developed specifically for use by scientific and scholarly communities to collaborate globally and interdisciplinary.

The 3D microscopic imaging and metrology system works on the principle of phase-aided active stereo (PAAS), which aims to reconstruct the surface profile of micro objects accurately. Due to the limited field of view and self-occlusion of solid, single measurement could only get a partial 2.5D range image of the object. Thus a two-axis rotating stage is employed to change the orientation of the object. The two axis of rotation will be calibrated in advance, so the range images of different viewpoints can be registered automatically. Once the surface of the object is measured over all, all registered range images will be merged into a complete, non-redundant 3D model.

9132-5, Session 1

3D-optical measurement system using a new vignetting aperture procedure

Engelbert Hofbauer, Hochschule Deggendorf (Germany) and Hofbauer Optik Mess- & Prüftechnik (Germany); Felix Friedke M.D., Hochschule Deggendorf (Germany) and Hofbauer Optik Mess-& Prüftechnik (Germany); Thomas Stubenrtauch, Roland Maurer M.D., Benjamin Pastötter, Hochschule Deggendorf (Germany)

Using the classical autocollimator principle, there are several restrictions in order to get a large measurement range by increasing measurement distance simultaneously. There are also some shading effects and therefore nonlinearity in the edges of the measurement range, caused by non uniform illumination of the reticle in the object plane. Furthermore it is not possible to use an autocollimator as a sighting telescope. Sighting telescopes themselves are not able to readout in an electronic way by an easy and simple measurement process.

A newly developed measuring procedure uses vignetting to evaluate angles and angle changes without influence of the measurement distance. Further on the same procedure enables to get digital readout and therefore better automatisation by electronical evaluation of the signal for using as sighting telescope. The fully possible readout by a simple 3-D reflector will provide the user with measurement results of six degrees of freedom.

The vignetting field stop procedure will be described. First considering artificial vignetting the theoretical basics from geometric-optical view are represented. Second the natural vignetting with photometric effects will be considered. The distribution of intensity in the light spot in the image plane, the so called V-SPOT, is analytically deduced as a function of different measured variables.

Intensity shifts within the V-SPOT are examined in dependence of different effects by numeric simulation. These effects are geometrical-optical influences, the spatial distribution of the luminous intensity in dependence of the beam angle as well as the distribution of Luminance in the object plane.

On these basics the theoretical investigations regarding measuring Range, accuracy / linearity as well as resolution are examined. The theoretical investigations are compared with experimental results and deviations will be discussed.

Different Principles of measurements will be shown and discussed. Some physical effects can already be corrected by optical-mathematical calibration procedures to get a high linearity for high precision small angle measurements and sighting telescope measurements.

9132-6, Session 2

Characterization of surface and sub-surface defects with optical scattering *(Invited Paper)*

Weiguo Liu, Xi'an Technological Univ. (China)

Surface defects (SDs) and sub-surface defects (SSDs) appear during the fabrication process such as the single point diamond turning (SPDT) or the magneto-rheological finishing (MRF) of optical surfaces. Based on experimental investigation of the microstructure of the finished surfaces, a simplified columnar model was established for the analyses of the SSDs, and a pseudo-periodic model was applied for the analyses of the SDs. Focused on the models, scatter behaviors of the defects were analyzed. Approaches including the Rayleigh-Rice expression, the vector perturbation theory, and a modified vector perturbation theory were adopted for each of the defect model to validate the theories in describing the scatter behaviors of the SD and SSD. Numerical results were obtained to discuss the feasibility of applying the optical scattering behaviors to characterize the defects.

9132-7, Session 2

Measurement comparison of goniometric scatterometry and coherent Fourier scatterometry

Bernd Bodermann, Johannes Endres, Physikalisch-Technische Bundesanstalt (Germany); Nitish Kumar, Peter Petrik, Technische Univ. Delft (Netherlands); Mark-Alexander Henn, Physikalisch-Technische Bundesanstalt (Germany)

Scatterometry is an indirect measurement technique reconstructing the dimensions and geometry of the structures under test from the measured scatterograms by applying inverse rigorous calculations. Various scatterometric methods have been established utilizing different properties of the diffracted light for the reconstruction. Typical measurement systems use goniometric, reflectometric, spectrocscopic or ellipsometric configurations for measuring the diffracted optical far field.

In this paper we will focus on two different scatterometric measurement methods: a goniometric DUV scatterometer and a coherent scanning Fourier scatterometer.

In the first case the light intensity and polarization state of the diffracted optical far field is measured at different angels of incidence (AOI). The typically high angular resolution and high dynamic range together with a wide scope of AOI's provide sufficient information for the reconstruction of the structure parameters under the condition that enough diffraction orders are available. However, the measurement in most realizations is restricted to non conical diffraction and the diffraction pattern has to be scanned in a sequential manner.

In scanning coherent Fourier scatterometry the illumination spot of a spatially coherent laser source is scanned over the sample within one period of the grating. The resulting interferogram of the first and zero diffraction order is recorded. This method extends the conventional coherent Fourier Scatterometry (CFS) by using the principle of temporal phase-shifting interferometry. It has been shown that under certain conditions the improvement in sensitivity is more than fourfold compared to incoherent optical scatterometry [1].

We will present a comparison between these two methods by analyzing the measurement results on a silicon wafer with 1D gratings having periods between 300 nm and 600 nm. The measurements have been performed with PTB's goniometric DUV scatterometer [2] and the coherent scanning Fourier scatterometer at TU Delft [3]. Furthermore we will give intermediate results about the benefits and limitations of these methods. Moreover for the parameter reconstruction of the goniometric measurement data we apply a Maximum likelihood estimation, which provides the statistical error model parameters directly from measurement data [4].

[1] N. Kumar ; O. El Gawhary ; S. Roy ; V. G. Kutchoukov ; S. F. Pereira, et al., "Coherent Fourier scatterometry: tool for improved sensitivity in semiconductor metrology", Proc. SPIE 8324, Metrology, Inspection, and Process Control for Microlithography XXVI, 83240Q (2012)

[2] M. Wurm, S. Bonifer, B. Bodermann, J. Richter: Deep ultraviolet scatterometer for dimensional characterization of nanostructures: system improvements and test measurements, Meas. Sci. Technol. 22 (2011)

[3] S Roy, N. Kumar, S F Pereira, H. P. Urbach., "Interferometric coherent Fourier scatterometry: a method for obtaining high sensitivity in the optical inverse-grating problem", Journal of Optics, Vol. 15, 075707 (2013)

[4] M. Henn, H. Gross, F. Scholze, M. Wurm, C. Elster, and M. Bär, "A maximum likelihood approach to the inverse problem of scatterometry," Opt. Express 20, 12771-12786 (2012).

9132-8, Session 2

Inspection technique of latent flaws on surface of fine polished glass substrates using Stress-Induced Light Scattering Method

Yoshitaro Sakata, Kazufumi Sakai, Kazuhiro Nonaka, National Institute of Advanced Industrial Science and Technology (Japan)

The fine polishing technique, e.g. Chemical Mechanical Polishing treatment (CMP), is one of the most important techniques in the glass substrate manufacturing. However, mechanical interaction, e.g. friction, occurs between the abrasive and the surface of substrates. Therefore, latent flaws are formed in the surfaces of glass substrates depending on the polishing condition. In the case of the cleaning process of the glass substrate in which the latent flaws existed, latent flaws become obvious because glass surfaces were eaten away by chemical interaction of cleaning liquid. Therefore, latent flaws are the cause of decrease the yield of products. In general, non-destructive inspection techniques, e.g. light scattering method, foreign matter on the surface of glass substrates. Though, it is difficult to detect the latent flaws by these method, because these are closed. The present authors propose a novel inspection technique of latent flaws which occurred by the fine polishing technique, using light scattering method with stress concentration (Stress-Induced Light Scattering Method; SILSM). SILSM is possible to classify and separately detect latent flaws and particles on the surfaces. Samples are deformed by the actuator and stress concentrations are occurred around the tip of latent flaws. By photo-elastic effect, the refractive index of around the tip of latent flaws is changed. And then, changed refractive index is detected by cooled CCD camera as the light scattering intensity. In this report, applying SILSM to glass substrates, latent flaws on the surface of glass substrates are detected non-destructively, and the usefulness of SILSM is evaluated as novel inspection technique of latent flaws.

9132-9, Session 2

Development of a scatterometry reference standard

Bernd Bodermann, Physikalisch-Technische Bundesanstalt (Germany); Bernd Loechel, Helmholtz-Zentrum Berlin für Materialien und Energie GmbH (Germany); Frank Scholze, Gaoliang Dai, Johannes Endres, Physikalisch-Technische Bundesanstalt (Germany); Juergen Probst, Max Schoengen, Helmholtz-Zentrum Berlin für Materialien und Energie GmbH (Germany); Michael Krumrey, Physikalisch-Technische Bundesanstalt (Germany); Poul-Eric Hansen, Danish Fundamental Metrology Ltd. (Denmark); Victor Soltwisch, Jan Wernecke, Physikalisch-Technische Bundesanstalt (Germany)

Scatterometry is a common technique for dimensional characterisation of nanostructures in the semiconductor industry. Currently this technique is limited to relative metrology for process development and process control. Although the high sensitivity of scatterometry is well known, it is not yet applied for absolute measurements of critical dimensions (CD) and quality control due to the lack of traceability. Within a project of the European Metrology Research Programme [1] we aim to establish scatterometry as traceable and absolute metrological method for dimensional measurements. This requires an in-depth understanding and quantification of the measurement process and of experimental and numerical limitations as well as the approximations, which usually have to be applied for efficiency reasons. To reduce systematic measurement deviations and to enable a reliable measurement uncertainty budget for scatterometric measurements we investigated both experimentally and by numerical simulations the influences of different tool or sample specific limitations like the plane wave approximation, the influence of a limited interaction area and of line edge roughness. For the

experimental investigations we applied different scatterometry methods like goniometric scatterometry, EUV scatterometry, GISAXS, spectroscopic ellipsometry and Mueller polarimetry. Based on these results measurement uncertainty budgets are estimated for different scatterometry methods using linear approximations for a maximum likelihood approach to analyse the described measurement data.

In a second step the transfer of traceability into industrial applications is supported by the realisation of suitable scatterometry reference standard samples within this project. Two different standards based either on Si or on SiO2 are currently developed. They are manufactured by e-beam lithography. The etched gratings will have periods down to 50 nm and will contain areas of reduced density to enable AFM measurements for comparison. We present first characterisations of the grating quality. Structure details like line edge and line width roughness and edge angles are measured by AFM, optical, EUV as well as X-Ray scatterometry and spectroscopic ellipsometry. Finally we discuss the final design and aimed specifications of standard samples, which are currently developed to face the tough specifications for future technology nodes in lithography.

[1] http://www.ptb.de/emrp/ind17.html, http://www.euramet.org

9132-10, Session 2

Retrieving complex coherence using spatial intensity correlation

Rakesh K. Singh, Vinu R. V., Anandraj Sharma M., Indian Institute of Space Science and Technology (India)

Propagation of coherent light through scattering medium generates spatially fluctuating field. Such field arises from a complex interference effect and produces a speckle pattern. Though, speckle considered as noise in some applications but useful in several other applications. For example, statistical property of the speckle field is used for diagnosis of the scatterer and in imaging application. For the complex Gaussian random field such as laser speckle, the cross-covariance of the intensity distribution, i.e. fourth order correlation, is proportional to the square of the second order correlation. Though, this method is useful to determine amplitude of the coherence but phase information of the coherence function is lost.

In this paper, we propose a new method to retrieve the complex coherence by using the spatial intensity correlation with help of off-axis holography technique. Significance of our work lies with its ability to recover the complex coherence from intensity of the laser speckle in a single shot. The speckle field for which coherence needs to be measured is called 'object' speckle. To apply the holography principle, an independent reference speckle with known coherence function is used. This reference speckle field with known coherence distribution is synthesized by illuminating an independent scattering surface with an off-axis coherent point source. The coherence function of the reference speckle is a complex quantity with uniform amplitude and linear phase term. The linear phase term of the reference coherence function is attributed to the off-axis illumination and explained by the van Cittert-Zernike theorem based on spatial averaging.

Two speckles, namely object and reference, fields are coherently superposed and cross-covariance of the intensity distribution of the resultant speckle is digitally obtained. Here cross-covariance of the intensity is obtained by spatial averaging by taking advantage of the spatial ergodicity. Interference fringes exist in the cross-covariance of the intensity of the resultant speckle. This interference fringe results due to superposition of the complex coherence of the object and reference speckle fields. The off-axis geometry for superposition of the two speckle fields is important for experimental implementation of our proposed idea. This geometry modulates fringes of the intensity correlation with properly selected carrier frequency in such a way that Fourier spectrum of the 'object' coherence field gets separated from the central background or dc. The complex coherence of the object speckle field is retrieved using the Fourier fringe analysis. Application of the proposed method is experimentally demonstrated by measuring the complex coherence of the different 'object' speckle fields at the Fourier plane. The object speckle fields at the Fourier plane are generated by apertures of different sizes at the scattering plane. For comparison purpose, coherence of the 'object' speckle fields are analytically calculated using the van Cittert-Zernike theorem. Good match between experimental and analytical results confirms accuracy of our method.

9132-11, Session 3

Micro/nano-grating metrology *(Invited Paper)*

Huimin Xie, Xianglu Dai, Chuanwei Li, Tsinghua Univ. (China); Zhanwei Liu, Beijing Institute of Technology (China); Dan Wu, Minjin Tang, Tsinghua Univ. (China)

Optical metrology has been greatly developed and widely used for deformation measurement due to its advantages of non-contact, full field and high accuracy. With the rapid progress of microelectronic industry and micro/nano material engineering, developing adaptive measurement method has become an urgent requirement. From the available literatures, the grating-based optical metrology has been successfully applied to the deformation measurement in the micro/nano scale. These methods include the scanning moiré method, geometric phase analysis (GPA) and grid method which can realize the micro/nano-deformation measurement under the high-resolution microscopes. In addition, in order to realize an effective and high accuracy measurement, the high-quality grating plays a key role in the application of the above mentioned methods. In this report, some new grating fabrication methods were proposed with aid of the advanced micro-fabrication techniques, such as electron beam lithography (EBL), focused ion beam (FIB), nanoimprint lithography (NIL) and soft lithography.

This report mainly focuses on the recent development of our research group in the following aspects: (1) grating fabrication technique based on FIB; (2) grating fabrication technique with NIL; (3) grating fabrication technique with soft lithography; (4) microscopic deformation measurement of metal material by scanning electron microscope (SEM) moiré method; (5) the residual stress measurement of MEMS by the SEM moiré method; (6) a three-dimensional (3D) shape detection method based on a modified SEM moiré method; (7) the scanning tunneling microscope (STM) and atomic force microscopy (AFM) moiré methods and applications.

From our study, we can conclude: the EBL, FIB, NIL and soft lithography are qualified to fabricate the micro/nano gratings effectively, and own a good potential for the further application; the scanning moiré method based on the micro/nano gratings shows the superiorities of large measurement area, high precision, no requirement for preparing reference grating as well as real-time measurement; In addition, a new 3D topography detection method is developed in combination of the stereovision technology with the scanning moiré method under SEM, micro 3D shape of the tested sample surface can be measured by tilting the specimen grating with the specific angles.

9132-12, Session 3

Advanced metrology for the 14 nm node double patterning lithography

Damien Carau, STMicroelectronics (France) and CNRS LTM (France); Régis Bouyssou, Christophe Dezauzier, STMicroelectronics (France); Maxime Besacier, MINATEC (France); Cécile Gourgon, CEA-LETI (France)

Critical dimension and overlay measurements have become a key challenge in microelectronics process control, and the weight of metrology in the success of a patterning technique is increasing as the complexity of lithography for the latest

technology nodes. For the 14 nm node, the limit of scanner resolution can be overcome by the double patterning technique, which requires a maximum overlay error between the two reticles of few units of nanometers. The current approach in the measurements of critical dimension and overlay is to treat them separately, but it has become much more complex in the double patterning context, because they are no longer independent. In this paper, a strategy of an original common measurement is developed.

Towards an innovative methodology using scatterometry to measure simultaneously overlay and critical dimension.

The overlay value is the misalignment error between two printed layers. There are two usual techniques: the classical image-based method and the diffraction-based one that acquires the first diffraction orders intensities directly related to overlay.

In this study, the scatterometry technique has been used to do a common measurement for critical dimension and overlay in one target. The metal level has been chosen for its very tight specification. Thanks to this original approach, it will be possible to measure the line widths and the line spaces of the two expositions before the second etch process. The main advantage of the method developed in this paper is that the second lithography step can be reworked if the line spaces exceed the specifications.

The study shows that the spectral Mueller Matrix elements have to be used in the scatterometry optimization because the gain in overlay sensitivity is significant. Moreover a strategy has been implemented to decorrelate parameters of the fitting model in order to find the unique physical solution.

Verification: correlation with classical overlay methods.

Diffraction-based and image-based overlay targets have been placed very close to the scatterometry targets in order to compare the results. Indeed the line spaces are directly linked to the overlay value.

A study has been led to select the best diffraction-based and image-based overlay targets in terms of precision and accuracy. An algorithm based on the rigorous coupled wave analysis has been developed in order to get the theoretical response of the potential targets for the diffraction technique. The overlay sensitivity of the optimized measurement recipes for the two kinds of techniques have been verified thanks to induced overlay wafers.

Besides, it is possible to correlate the results with another method, which consists in measuring line spaces and line widths by top-view scanning electronic microscopy after the complete etch process.

The optimization of the new scatterometry method is ongoing and it will soon provide information to correct the double patterning lithography step by regulation loops.

9132-13, Session 3

Optical measurements of selected properties of nanocomposite layers with graphene and carbon nanotubes fillers

Zofia Lorenc, Leszek Salbut, Anna Paku?a, Ma?gorzata Jakubowska, Marcin Sloma, Grzegorz Wróblewski, Warsaw Univ. of Technology (Poland)

Thin layers of carbon nanotubes or graphene - based composite materials have a big potential for current engineering. Main features of those materials, such as high conductivity, very good transparency, high elasticity, outstanding mechanical resistance to bending, stretching, etc. create a possibility of using them in printing electronics to produce electrodes in flexible screens and light sources.

In the paper the methodology and results of the spectral transmission characteristic of a different layers are presented and discussed. The samples contained different deposited layers with various thicknesses and different amounts of graphene flakes and carbon nanotubes as the nanocomposite fillers.

Additionally, the measurement results of thickness and surface micro-topography of the deposited layers are presented. The correlation between measured parameters and optical properties of the layers under test is determined and discussed.

The presented measurement methodology and the results obtained could be helpful in assessment of producing process repeatability and for the future research, development and application of flexible carbon electrodes based on nanocomposite materials.

9132-14, Session 3

Comparative scanning near-field optical microscopy studies of plasmonic nanoparticle concepts

Patrick Andrae, Martina Schmid, Helmholtz-Zentrum Berlin für Materialien und Energie GmbH (Germany); Paul Fumagalli, Freie Univ. Berlin (Germany)

Nanoparticles show a strong electric-field enhancement which can be exploited for nanoscale devices. The enhancement is related to geometry, e.g., shape, distance, volume, and design parameters, e.g., material, oxidation layer, shells. To investigate the effects of nanoscale optics the improvement and techniques of scanning near-field optical microscopy (SNOM) will be presented.

Nanoparticle clusters can be characterized by far field transmission (T) and reflection (R), which is measured on the same area. The absorption (A) can be calculated via A = 1 - (∑R + ∑T) with integrating R and T over all scattering angles. SNOM techniques distinguish also between illumination or collection mode and reflection or transmission measurement. This opens the door to answering two questions: whether there is near-field absorption and how it can be quantified. Quantitative analysis can prove difficult without knowing the absolute number of incident photons. To overcome this challenge, the evaluation of the potential for extraction of the absorption from simultaneous measurements of reflection and transmission is shown. This allows us to make defined statements about the nanoparticle interactions. Therefore, a setup is presented which includes different light sources: LASERs and a white light source that can also detect a spectral near field enhancement for sunlight applications.

We will discuss how near field absorption is affected by different measurement strategies. Additionally, we calibrate the white light source with an additional spectrometer before coupling into the glass probe. Our results with SNOM techniques will be used to evaluate nanoparticles with a view to further efficiency increases of ultra-thin film CIGSe cells. Therefore, the well characterized particles will be embedded into a complete nanoscale optoelectronic device with optimized far-field scattering properties and near-field enhancement between the glass substrate and the absorber layer of the solar cell directly.

9132-15, Session 3

Investigation of the influence of the scanning probe on SNOM near-field images using rigorous simulations including the probe

Markus Ermes, Stephan Lehnen, Karsten Bittkau, Reinhard Carius, Forschungszentrum Jülich GmbH (Germany)

To investigate light propagation and near-field effects above structured surfaces and layers in detail, scanning near-field optical microscopy (SNOM) is a powerful tool providing the measurement of the near-field intensity. These measurements can be combined with rigorous solving of Maxwell's equations - in our case via the Finite-Difference Time-Domain (FDTD) method - to gain more insight into light propagation and absorption inside the sample, which is not accessible via

experiment. However, we find differences between the intensity distribution obtained via experiment and that observed in the simulation at a constant distance of 20nm above the surface, which corresponds to the typical surface-to-tip distance in the experiment. A first explanation was given by topographic artifacts [Proc. SPIE 8789, 87890I (2013)].

To better understand the interaction between sample and tip in regard to light propagation, we include the near-field tip in high-resolution FDTD simulations of different structures, with the position of the tip resulting from the previously presented results. While there is a visible difference in the overall light distribution of the system, caused by the tip, the relative intensity at the position of the tip is shown to be in very good agreement to the intensity in a system without the tip. This has been found for many tip positions along the surface of the structure. This result is applicable to many systems in different fields of research which use SNOM measurements for obtaining information about near-field effects of samples.

As an example, we show an application in the area of thin-film photovoltaics, where light scattering textured surfaces are used to increase the path length of photons in a wavelength region where the thickness of the absorber layer is (much) thinner than the absorption length of the material. By this path length enhancement, photons are much more likely to be absorbed, which leads to a better overall performance of the device.

9132-17, Session 4

Investigation of error compensation in CGH-based form testing of aspheres

Stephan Stuerwald, Nicolai Brill, Fraunhofer-Institut für Produktionstechnologie (Germany); Robert Schmit, RWTH Aachen University (Germany)

A range of new photonic technologies and applications require optical elements such as aspheric lenses or mirrors with challenging specifications. A key issue for these optical elements is the surface quality, and especially the surface form which is crucial for the optical functionality.

Interferometric form testing using computer generated holograms is one of the main full-field measurement techniques. Currently, typical form deviations in the region of several tens of nanometres occur in case of the widely used computer generated hologram (CGH) based interferometric form testing. Deviations occur due to a non-perfect alignment of the computer generated hologram (CGH) relative to the transmission sphere (Fizeau objective) and also of the asphere relative to the testing wavefront. Thus, measurement results are user and setup dependent which results in a lack of reproducibility of the form errors. When aligning the CGH, the spatial frequency of the fringe pattern is minimised by an operator, however the ideal position cannot be known exactly by the operator as the position of minimum spatial fringe density is usually not unique.

Up to date various methods for improving the measurement performance of interferometric form testing have been investigated, but the correlations between form measurement errors and misalignment have been primarily characterised for specific experimental setups only. No general theoretical method exists however which allows a general and holistic approach to error subtraction which is valid and can be adapted to every measurement setup.

The scientific and technical objectives of this paper comprise the development of a comprehensive theoretical approach to explain and quantify the experimental errors due to misalignment of the computer generated hologram in an optical form testing measurement system. A further step is the programming of an iterative method to realise a virtual optimised realignment of the system on the basis of Zernike polynomial decomposition which should allow the calculation of the measured form for an ideal alignment and thus the subtraction of the alignment based form error. Different analysis approaches are investigated with regard to the final accuracy and reproducibility. To validate the theoretical models a series of systematic experiments is performed with hexapod-positioning systems in order to allow an exact and reproducible positioning of the optical, CGH-based setup. This will result in a comprehensive error correcting algorithm based on Zernike decomposition methods, which allows subtraction of the erroneous alignment induced form deviation.

The experimental system is also utilized for the validation of the correlation coefficients of Zernike coefficients and misalignment. Based on these correlations, different optimization methods are applied for an iterative realignment to the best position of the specimen towards the CGH. The most challenging is to find an adequate method to obtain a better final accuracy of the form testing system by subtraction of a weighted set of specific Zernike coefficients with eliminating real form error.

9132-18, Session 4

Interferometric sensors based on sinusoidal optical path length modulation

Holger Knell, Markus Schake, Markus Schulz, Peter Lehmann, Univ. Kassel (Germany)

The accuracy in interferometric measurement is based on accurate phase estimation. In length measuring interferometry either homodyne or heterodyne principles are applied. Homodyne interferometry uses stabilized lasers and polarization optics, whereas in heterodyne interferometry a frequency shift in one arm of the interferometer leads to sinusoidal modulated interference signals. In addition, phase shifting interferometry uses a linear path length change in order to modulate the interference signal. An alternative to all these principles is based on a sinusoidal modulation of either the reference or measurement arm of an interferometer in order to periodically modulate the phase of the interference signal. Periodic modulation can be easily performed by an oscillating reference mirror in a Michelson or Linnik interferometer. If a micro-optical sensor head is used also the optical path length of the measuring arm of the interferometer can be modulated with frequencies of several kHz. As an advantage, this kind of modulation is fast and much less demanding with respect to the optical components needed compared to the above mentioned modulation techniques.

In this contribution we introduce different sensors which are based on sinusoidal path length modulation. First, a fiber optic sensor in combination with a bending beam driven by a piezoelectrical crystal allows a pointwise measurement with nanometer resolution. The microoptical probe head focuses near infrared light onto the object under investigation by use of a graded index lens. Integrating a reference surface into the probe head leads to a very robust common-path configuration. Alternatively, we built a sensor based on a line scan camera and a long working distance microscope objective. The microscope objective is equipped with a self assembled Michelson interference module. This module comprises a piezoelectrically actuated reference mirror which modulates the optical path length in the reference arm of the interferometer. A surface section of 2 mm length is imaged onto the CCD line which comprises 1000 pixels. Hence, the sensor is capable of measuring 1 million data points per second.

For both sensors similar electronics and signal processing algorithms can be applied. An important prerequisite of high accuracy measurements is a proper synchronization of the signal driving the actuator with the analog-to-digital-converter, which digitizes the interference signal. The sections of the phase modulated signals, which show a nearly linear phase change can be analyzed by use of a discrete Fourier transform (DFT). This leads to a data rate of twice the excitation frequency. If a Hilbert transform signal processing is applied the time dependent phase of the interference signal can be reconstructed over longer intervals leading to a data rate which is finally limited by the frequency of the AD converter.

In combination with appropriate mechanical scanning axes such sensors can be used for microstructure measurement. As an example we present measurement results related to sinusoidal calibration specimens and precision machined surfaces.

9132-19, Session 4

Reconstruction-free wavefront measurements with enhanced sensitivity

Thomas Godin, FEMTO-ST (France); Michael Fromager, Emmanuel Cagniot, ENSICAEN (France); Marc Brunel, CORIA (France); Kamel Aït-Ameur, ENSICAEN (France)

Wavefront measurements are nowadays a ubiquitous tool in many fields of fundamental and applied research such as adaptive optics, refractive surgery or laser material processing. In adaptive optics for instance, the aim is to characterize optical aberrations induced by atmospheric turbulences or eye defects in order to correct them. Several methods have thus been efficiently developed to record wavefronts, from interferometric techniques [1] to the modal decomposition of the probe laser beam [2], but the most widespread technique undoubtedly remains the Shack-Hartmann (SH) sensor [3] and lots of efforts have been focused on improving its sensitivity over the last decades. It has been shown recently that the sensitivity of nonlinear effects measurement techniques such as Z-scan could be dramatically enhanced using a continuous Positive Sensitive Detector (PSD) [4], which is a device able to monitor the position of a beam centroid with a nanometer-scale precision without any discretization of the incident beam. Here, we advantageously use PSD instead of CCD sensors, which are used in all SH sensors, in order to reach high accuracy and sensitivity. Our device allows to observe wavefront distortions usually undetectable using standard SH with the advantage of being low-cost and easy-to-implement [5]. We present a series of advantages compared to SH sensors using computer-generated holograms to simulate various phase profiles and we show that our technique has the ability to fully characterize sharp phase variations and discontinuities thanks to a continuous recording of the exact wavefronts without using any reconstruction process. To the best of our knowledge, it is the first time that such an improvement is reported [6]. This technique is thus proved to go beyond the classical limitations of SH and allows to consider original prospects in the field of wavefront measurements.

[1] S. Velghe et al., Opt. Lett. 30, 245 (2005).

[2] C. Schulze et al., Opt. Express 20, 19714 (2012).

[3] B. Platt and R. Shack, J. Refract. Surg. 17, S573 (2001).

[4] T. Godin et al., Opt. Lett. 36, 1401 (2011).

[5] T. Godin et al., Patent pending n° FR13 53065.

[6] T. Godin et al., Submitted to Appl. Opt. (2013).

9132-20, Session 4

Ray-based calibration for the micro optical metrology system

Yongkai Yin, Meng Wang, Ameng Li, Xiaoli Liu, Xiang Peng, Shenzhen Univ. (China)

In this paper, a quantitative 3D microscopy system based on phase-aided active stereo technique (3DM-PAAS) is presented to accurately characterize the surface topography of micro objects with complex topology and geometry. The proposed system is consisted of a CCD camera and a digital projector mounted on a platform of stereo microscope. Comparing with other optical systems used in the macro field, 3DM-PAAS has some particular characteristics including small field of view and short depth of field due to the large numerical aperture. The aberrations of the 3DM-PAAS would mainly come from spherical aberration and coma instead of field curvature and distortion.

One of the most important issues for optical metrology is how to calibrate the system to achieve a high accuracy measurement. Several calibration methods for micro imaging systems based on traditional stereo vision model have been investigated previously. These methods attempted to refine system calibration by modifying the imaging model and introducing some new calibration parameters. However, it seems not for sure on the issue what the exact imaging model of the 3DM-PAAS is and how to correct the system aberration for the 3DM-PAAS.

In this paper, we present a ray-based calibration method for the 3DM-PAAS, which relies on a fact that image pixels actually record the ray intensities impinging on the photo-sensitive elements of the camera. The idea is that if we could establish the mapping relationship between the incoming rays with respect to corresponding image pixels on the photo-sensor of the detector, it would be possible to exactly determine the imaging process and the influence of aberrations in an implicit form. This idea could be also valid for a projector because the function of a projector can be regarded as an inverse process of imaging. Keep this idea in mind the ray-based calibration could be executed by following steps: First, a planar calibration target is placed on several unknown positions within the measurement volume of the 3DM-PAAS. The target positions can be estimated with the help of collinear constraint. Meanwhile, the reference points of the calibration target can be transformed into a unified coordinate system with the known pose parameters. Then the correspondence between the reference points on the target and the pixels on the camera/projector is established. For camera, the correspondence comes from the reference point of designed pattern. While for projector, the correspondence is determined with the help of absolute phase extracted from the fringe images. Finally the ray corresponding to every pixel can be determined by line fitting with different reference points on the calibration target which can be seen by identical pixel. After calibration, the surface topography can be reconstructed accurately by computing the intersections of rays which are determined by the corresponding pixels between the camera and the projector. The validity and accuracy of proposed calibration approach is demonstrated with a group of experiments.

9132-21, Session 5

Optical design of a Vertically Integrated Array-type Mirau-based OCT system

Johann Krauter, Tobias Boettcher, Wolfgang Osten, Institut für Technische Optik (Germany); Wolfram Lyda, TWIP Optical Solutions (Germany); Nicolas Passilly, Luc Froehly, Sylwester Bargiel, Jorge Albero, Stephane Perrin, Justine Lullin, Christophe Gorecki, FEMTO-ST (France)

Skin cancer is the most diagnosed type of cancer. While an early treatment usually offers good therapy prospects, effective diagnosis techniques are required. Today traditional biopsy is still the reference diagnostic technique, which has the drawback of a long diagnosis time and invasiveness. In recent years, new optical system based on optical coherence tomography were developed for early diagnostics of skin cancer. But as these systems are still bulky and expensive, they're still available at specialized hospitals only.

Therefore we present the optical design of a Vertically Integrated Array-type Mirau-based OCT System (VIAMOS), which will allow non-invasive 3D optical biopsies of skin for early diagnostics of skin cancer. The VIAMOS system constitutes a miniature, low cost, full-field optical coherence tomography system combining swept-source OCT, phase-shifting interferometry and MOEMS technologies. It will provide 3D tomograms of human skin from a measurement volume of 8 x 8 x 0.5 mm? with an axial and transverse resolution of about 6 µm. The swept-source will be realized as a miniaturized, MEMS-based wavelength-tuning Fabry-Perot Interferometer and a near-infrared superluminescent diode resulting in a linewidth of approximately 1 nm and a scanning range of 50 nm. The wafer stacked measurement device consists of 4 x 4 Mirau-Interferometer channels with movable reference mirrors to realize heterodyne detection and will be fabricated by means of MOEMS technologies. The signal detection will be realized using a fast new developed smart camera chip, which features 4 x 4 multiple regions of interest and on-chip signal processing. In this contribution, we present the optical design of the sensor

and provide results of an extensive stray light analysis of the system.

9132-22, Session 5

Optical diffraction tomography: accuracy of an off-axis reconstruction

Julianna Kostencka, Tomasz Kozacki, Warsaw Univ. of Technology (Poland)

Optical diffraction tomography is an increasingly popular method that allows for reconstruction of a three-dimensional refractive index distribution of a semi-transparent sample using multiple measurements of an optical field transmitted through the sample for various illumination directions. The process of assembly of the captured data is usually performed with either of two methods: filtered backprojection (FBPJ) or filtered backpropagation (FBPP) tomographic reconstruction algorithm. The former approach, although conceptually very simple, provides an accurate reconstruction for the object regions located close to the plane of focus. However, since FBPJ ignores diffraction, its use for spatially extended structures is arguable. According to the theory of scattering, more precise restoration of a 3D structure shall be achieved with the FBPP algorithm, which unlike the former approach incorporates diffraction. It is believed that with this method one is allowed to obtain a high accuracy reconstruction in a large measurement volume exceeding depth of focus of the imaging system. However, some studies have suggested that a considerable improvement of the FBPP results can be achieved with prior propagation of the transmitted fields back to the object centre, which supposedly enables reduction of errors due to approximated diffraction formulas used in the FBPP algorithm. In our view this finding casts doubt on quality of the FBPP reconstruction in regions located far from the rotation axis. The objective of this paper is to investigate limitation of the FBPP algorithm in terms of an off-axis reconstruction and compare its performance with the FBPJ approach. Moreover, in this work we propose some modifications to the FBPP algorithm that allow for more precise restoration of a sample structure in off-axis locations. The research is based on extensive numerical simulations supported with wave-propagation method.

9132-23, Session 5

Time-frequency spectroscopic analysis in optical coherence tomography for technical objects examination

Marcin Str?kowski, Maciej Kraszewski, Micha? Trojanowski, Jerzy Plucinski, Gdansk Univ. of Technology (Poland)

Optical coherence tomography (OCT) is one of the most advanced optical measurement techniques for complex structure visualization. The OCT provides 2D and 3D images of the inner structure of scattering materials and objects with micrometer resolution. The measurements are performed in non-contact and non-destructive way. Although, the OCT is mainly applied in medical diagnostics there is a vast range of non-medical applications. The advantages of OCT have been used for surface and subsurface defect detection in composite materials, polymers, ceramics, non-metallic protective coatings, and many more. Our research activity has been focused on time-frequency spectroscopic analysis in OCT. It is based on time resolved spectral analysis of the backscattered optical signal delivered by the OCT. The time-frequency method gives spectral characteristic of optical radiation backscattered or backreflected from the particular points inside the tested device. This provides more information about the sample, useful for further analysis. Nowadays, the applications of spectroscopic analysis for each of composite layers characterization or tissue recognition have been reported. During our studies we have found new applications of spectroscopic analysis. We have used this method for thickness estimation of thin films, which are under the resolution of OCT. Also, we have combined the spectroscopic analysis with polarization sensitive OCT (PS-OCT). This approach enables to obtain a multiorder retardation value directly and may become a breakthrough in PS-OCT measurements of highly birefringent media. In this work we present the time-frequency spectroscopic algorithms and their applications for OCT. Also the theoretical simulations and measurement validation of this method are shown.

9132-24, Session 5

Limited-angle optical microtomography for biological samples

Arkadiusz Kus, Wojciech Krauze, Ma?gorzata Kujawinska, Warsaw Univ. of Technology (Poland)

Currently there is a strong demand on 3D analysis of biological objects especially when anti-cancer treatment is taken into account. This can be achieved with optical diffraction tomography, where projections are gathered by means of digital holography. There are two technical solutions of this method. The first and most straightforward implementation is based on the rotation of the sample. However, very often it is impossible to rotate a sample due to its shape or dimensions, e.g. cells in a Petri dish or a flow chamber. In this case, in order to tomographically analyze an object, it is necessary to alter the angle of its illumination. The process of reconstruction of such objects using only a small number of projections within a limited angle is in general the same in all approaches. Firstly, the required projections must be acquired and this imposes requirements on the measurement setup. Usually the change of the angle of the incident light is realized mechanically – by rotating a mirror or a prism, depending on a configuration. This introduces unwanted and detrimental vibrations that either limit the possible speed of rotation, or impose restrictions on quality of the mechanical parts. As a result it most often leads to a relatively long acquisition time and makes it difficult to analyze dynamic processes in biological samples. What is more, if the rotating mechanism is chosen to be very precise, the final setup is neither compact, nor mobile. We present a solution, which handles these limitations by means of spatial light source multiplexing. The concept is based on the amplitude division of an incident wavefront into sub-sources and thus is a setup with no moving elements. It allows gathering data from 90° angle range. This at the same time is the minimum angular span of projections for the limited-angle algorithms to work with. To reconstruct a 3D distribution of refractive index of an object under study, a second step is necessary: reconstruction of the gathered projections. However, since only a limited amount of data is acquired, standard algorithms, such as Filtered Back Projection, cannot be applied. Applying standard reconstruction procedures would result in characteristically distorted distribution of refractive index. In order to compensate for these distortions we propose to use Data Replenishment Algorithm. It works iteratively, which means that in each step the reconstruction is improved compared to the previous one, until some maximum quality level is reached, after which the reconstructions are only worse. In order to accelerate these calculations we apply certain a priori knowledge that depends on the objects under study.

9132-25, Session 5

Effects of axial scanning in confocal microscopy employing adaptive lenses (CAL)

Nektarios Koukourakis, Technische Univ. Dresden (Germany); Markus Finkeldey, Ruhr-Univ. Bochum (Germany); Moritz Stürmer, Albert-Ludwigs-Univ. Freiburg (Germany); Nils C. Gerhardt, Martin R. Hofmann, Ruhr-Univ. Bochum (Germany); Ulrike Wallrabe, Albert-Ludwigs-Univ. Freiburg (Germany); Jürgen W. Czarske, Andreas Fischer, Technische Univ. Dresden (Germany)

Conventional confocal microscopes apply a rigid setup of an illuminating lens, which creates the focus, and a collecting lens, which focusses the light originating in the focal plane through the pinhole. Usually, mechanical scanning is required to obtain the axial information. This scanning is time consuming and requires high-precision mechanical positioning-systems, which can be very expensive. In this contribution we introduce the usage of electrically tunable liquid lenses in confocal microscopy. This combination potentially leads to a high tuning speed. The numerical aperture of liquid lenses generally is low. Thus we use a combination with a microscope objective of high numerical aperture (NA=0.55) to create an adequate high-quality tunable system. The focal length of the system can be tuned by applying a voltage to the adaptive lens. The axial tuning range is around 900 μm, but can be adjusted to the desired needs by changing the lens combination. Commonly adaptive lenses suffer of hysteresis and environmental effects, which make the relation between the applied voltage and the resulting focal length ambiguous. To compensate for these effects the employed lenses incorporate pressure sensors that open up the possibility to control the focal-length, as the pressure within the lens behaves linearly to the refractive power. This increases the reliability and accuracy of the lens and thus of the whole microscope. In our experiments it proved to be beneficial to use a second adaptive lens, placed in the detection path. Using this lens enables shifting the confocal plane and easily adjusting the setup and compensating misalignments. Additionally the two-lens architecture allows using defocusing methods resulting to an increase in lateral and axial contrast. The proposed combination surpasses the need for mechanical axial scanning and also increases the flexibility of the setup.

9132-26, Session 6

Phase aided 3D imaging and modeling: dedicated systems and new case studies

Yongkai Yin, Dong He, Zeyi Liu, Xiaoli Liu, Xiang Peng, Shenzhen Univ. (China)

In this presentation, we shall talk about dedicated systems and new case studies of phase aided 3D imaging and modeling techniques. The dedicated 3D digitizing systems will be described by ranging from single sensor to measurement network composed of multiple node sensors. The working principles and calibration techniques for both single sensor and sensor network are discussed in details. Furthermore, some new case studies using the sensor network based on 3D node sensors will be presented to demonstrate the effectiveness of these 3D digitizing systems. The first case study is an approach for automatic inspection of the crusible. The second case study involves in cultural heritage digitalization from which high quality 3D color models of movable cultural heritages are obtained successfully using dedicated 3D sensor systems. The third case study will illustrate how the measurement network based on 3D node sensors can be applied for 3D photo booth, which reflects one of new application areas in cultural sector.

9132-27, Session 6

A benchmark system for the evaluation of selected phase retrieval methods

Christian Lingel, Malte Hasler, Tobias Haist, Giancarlo Pedrini, Wolfgang Osten, Institut für Technische Optik (Germany)

In comparison to classical phase measurement methods like interferometry and holography, there are many phase retrieval methods which are able to recover the phase of a complex valued object without the necessity of a reference wave. Due to the large number of different methods, iterative as well as non-iterative ones, it is hard to find the method which is appropriate for a given application or object.

Therefore, we see the need to develop a benchmark system which is suitable for quantitatively comparing different phase retrieval methods. We propose a system which is based on different criteria, some of which can be calculated by analyzing the phase retrieval result compared to the original object. Other criteria evaluate less the performance of the given phase retrieval method but rather the outer features, like the complexity of the optical setup which is required to acquire the necessary intensity images.

Without any claim of completeness we choose 13 different criteria consisting of the RMS error, the PV value and the correlation between the original phase/intensity and the reconstructed. Besides these criteria we analyze the behavior of repeatability for a given noise in the intensity measurements. While the above mentioned criteria judge directly the reconstructed object, we also consider factors which give an estimate about the complexity of the actual measurement of the intensities like the number of images which are needed for the phase retrieval algorithm. In addition we evaluate the possibility of automation, the time consumption of the measurement procedure and the complexity of the optical setup itself (how many lenses, how to align).

For testing the benchmark system we use a software which is suitable, first, to simulate the acquisition process of the intensity measurements, second, to run the phase retrieval algorithm itself and, third, to calculate the values of the benchmark criteria.

Having determined the values of the different criteria we assign points for every criterion which can be weighted by importance and are summed up resulting in an overall benchmark score. This final score can be used to compare different phase retrieval methods and by having a closer look at the single criteria it is possible to analyze the strengths and weaknesses of the method.

We will show the detailed proceeding of calculating the benchmark value by means of a selected phase retrieval method and a phase only object (USAF target). We have to emphasize that the results strongly depend on the object.

9132-28, Session 6

Size measurement of a pure phase object

Kamel Ait-Ameur, Michael Fromager, ENSICAEN (France); Marc Brunel, Univ. de Rouen (France)

The detection of a transparent object is a technical challenge since phase objects yield only poor contrast if they are imaged on an intensity basis. For performing quantitative measurement the image contrast has to be enhanced. For that, we can exploit additional information on phase or polarisation modifications of the laser probe beam (LPB) crossing through the phase object.

We propose a simple method for determining the size of a transparent object based on the reshaping of a laser probe beam which is initially Gaussian in shape. For a given ratio between the size of the incident beam and that of the phase object, the diffracted laser probe beam is transformed in the far-field region into a hollow beam. The detection of the intensity dip in the beam centre is made with a simple photodiode. In practice, the spatial reshaping of the LPB is monitored through the resulting changes in the power transmitted by a pinhole and a stop (opaque disk) set in the far-field of the phase object under study. For convenience, the latter in the experiment is realised by a Spatial Light Modulator (SLM: Holoeye Pluto-NIR). We have considered the influence of various parameters which are the lateral and longitudinal sizes of the phase object, and the pinhole and the stop distances from the phase object under study. The experiment has demonstrated the feasibility of our method and can be extended for the detection of microscopic phase objects.

The potential of the proposed technique for quantifying the nanoscale change of the phase object under study could be very useful to study the morphology dynamics of living cells membrane which represents the biophysical properties and health state of the cell.

9132-29, Session 6

Optimum phase retrieval using the transport of intensity equation

Juan Martinez-Carranza, Konstantinos Falaggis, Tomasz Kozacki, Warsaw Univ. of Technology (Poland)

The quantitative phase mapping of complex objects using intensity only data has gained an increased interest in many technological areas ranging from biology to engineering. A common solution to quantitative phase measurements are interferometric techniques [1], which require coherent illumination. Nevertheless, coherent illumination is related with the speckle pattern generated by the roughness of the surface under study, and therefore, obtaining an accurate phase estimate becomes increasingly difficult. An alternative to interferometry are Transport of Intensity Equation (TIE) [2] based techniques, which relate linearly the phase of an object to the intensity distribution in the Fresnel region, and thereby retrieve quantitatively the phase of a sample. Besides this, TIE solvers belong to a family of deterministic Phase Retrieval Techniques, which retrieved the phase directly from the measured intensity while giving a unique solution plus an additive constant [3,4]. For this reason, the TIE has found a variety of applications [5–9] as in Transmission Electron Microscopy, X-ray imaging, optical microscopy, astronomy, and others. The principle of TIE approaches is based on the relation between the actual phase and the longitudinal variations of the intensity. The latter can be obtained using the measured intensities, i.e. taking a series of intensities measurements along the propagation axis. The accuracy of the axial derivative is subject to the separation between the measurement planes, the Signal to Noise Ratio (SNR) in the captured intensities, and the actual object phase distribution. Despite the tremendous effort made over the last decade [3,10–12] to improve the accuracy in the estimated axial intensity derivate, current available methods succeed this with limited degree of success. In this work, a quantitative analysis of the error in estimated axial derivative is develop in order to derive criteria for the optimum separation among planes that minimize the error in the axial derivative for given the number of planes and SNR. It is later shown that these method is significant more accurate than available methods proposed in the literature. It is further shown, that the plane separation that minimizes the error in the axial intensity derivative is not identical with the plane separation that minimizes the error in the retrieved phase. Nevertheless, the previous developed framework can be extended for a given TIE solver to account for this difference in order to derive expressions for the optimum plane separation that minimizes the error in the calculated phase. It is shown that such techniques can be applied successfully in practice providing TIE based phase reconstructions with improved accuracy. The success of these optimum plane separation strategies have been demonstrated by experiment using a wide range of phase objects, level of noise, and number of measurement planes. The results of this work enable new insights in the system design of TIE based measurement systems and enable accurate phase reconstructions with a reduced the number of planes.

1. J. C. Wyant, “Computerized interferometric surface measurements [Invited].,” Appl. Opt. 52, 1–8 (2013).

2. K. A. Nugent, D. Paganin, and T. E. Gureyev, “A Phase Odyssey,” Phys. Today 54, 27 (2001).

3. T. E. Gureyev, A. Roberts, and K. a Nugent, “Partially coherent fields, the transport-of-intensity equation, and phase uniqueness,” J. Opt. Soc. Am. A 12, 1942 (1995).

4. M. Langer, P. Cloetens, J.-P. Guigay, and F. F. Peyrin, “Quantitative comparison of direct phase retrieval algorithms in in-line phase tomography,” Med. Phys. 35, 4556 (2008).

5. F. Roddier and C. Roddier, “Curvature sensing and compensation: a new concept in adaptive optics.,” Appl. Opt. 27, 1223–1225 (1988).

6. F. Roddier, “Wavefront sensing and the irradiance transport equation,” Appl. Opt. 29, 1402–1403 (1990).

7. E. D. Barone-Nugent, A. Barty, and K. A. Nugent, “Quantitative phase-amplitude microscopy I: optical microscopy.,” J. Microsc. 206, 194–203 (2002).

8. D. Pelliccia and D. M. Paganin, “X-ray phase imaging with a laboratory source using selective reflection from a mirror,” Opt. Express 21, 9308 (2013).

9. K. Nugent, T. Gureyev, D. Cookson, D. Paganin, and Z. Barnea, “Quantitative Phase Imaging Using Hard X Rays.,” Phys. Rev. Lett. 77, 2961–2964 (1996).

10. M. Soto and E. Acosta, “Improved phase imaging from intensity measurements in multiple planes,” Appl. Opt. 46, 7978 (2007).

11. R. Bie, X.-H. Yuan, M. Zhao, and L. Zhang, “Method for estimating the axial intensity derivative in the TIE with higher order intensity derivatives and noise suppression.,” Opt. Express 20, 8186–91 (2012).

12. B. Xue, S. Zheng, L. Cui, X. Bai, and F. Zhou, “Transport of intensity phase imaging from multiple intensities measured in unequally-spaced planes.,” Opt. Express 19, 20244–50 (2011).

9132-30, Session 6

Digital holography to light field

Anand Krishna Asundi, Zou Chao, Nanyang Technological Univ. (Singapore)

Holography uses wave (physical) optical principles of interference and diffraction to record and display images. Interference allows us to record the amplitude and phase of the optical wave emanating from an object on a film or recording medium and diffraction enables us to see this wave-field, i.e. the amplitude and phase of the object. Visually this corresponds to both perspective and depth information being reconstructed as in the original scene. Digital Holography has enabled quantification of phase which in some applications provides meaningful engineering parameters. There is growing interest in reconstructing this wavefield without interference. Thus the increased research in Transport of Intensity Equations (TIE) which uses two or more defocused images to reconstruct the phase. However both these ideally require the use of coherent illumination.

The alternate school of thought emerges from the computer scientist group who primarily deal with ray optics. In a normal imaging system all rays emerging from an object point into are focused to a conjugate image point. Information of ray direction is lost and so to the perspective and depth information. A light field image is one that has information of both amplitude and direction of rays fanning from any object point and thus provides perspective (or what could be termed as phase) of the object wave as well. It would thus be possible to extract phase as we know it from this albeit for a coherent illumination case.

9132-31, Session 7

Measurement of the surface shape and optical thickness variation of a polishing crystal wafer by wavelength tuning interferometer

Yangjin Kim, The Univ. of Tokyo (Japan); Kenichi Hibino, National Institute of Advanced Industrial Science and Technology (Japan); Ryohei Hanayama, The Graduate School for the Creation of New Photonics Industries (Japan); Naohiko Sugita, Mamoru Mitsuishi, The Univ. of Tokyo (Japan)

Recently there has been interest in measuring objects with more than one optical surface. This leads to a multitude of interference fringe patterns from the various cavities which are formed in the beam path and the complexity of the problem increase with the number of surfaces. In this case, phase shifting by varying the optical path length of the reference beam is no longer suitable, because the interference signals from all the surfaces involved will change at the same temporal rate as the phase is shifted, and thus cannot be separated from

each other. Therefore, the multiple beam interference noise will severely degrade the accuracy of the measurement.

In this presentation, we start with categorization of the conventional phase shifting algorithm and Yves Surrel's characteristic polynomial theory and improve the Surrel's 2N – 1 algorithm to new 3N – 2 and 4N – 3 algorithms. And as a verification experiment, the optical thickness variation and surface shape of a Lithium Niobate wafer for a solid Fabry-Perot etalon during the polishing process were measured simultaneously by wavelength scanning Fizeau interferometer with a new phase shifting algorithm. The wafer contacted to a supporting glass parallel plate generates eleven different interference fringes overlapped on the detector. Wavelength scanning interferometry separates in frequency space interference signals associated with different optical paths.

According to Yves Surrel's characteristic polynomial theory, conventional N bucket algorithm has its roots in the characteristic diagram with their argument of integer multiple of unit phase shift amount. Surrel's 2N – 1 algorithm has its double roots in the characteristic diagram and have the insensitivity to phase-shift miscalibration. The new 3N – 2 algorithm and 4N – 3 algorithm allocate the triple roots and quadruple roots in the characteristic diagram respectively. As a result 3N – 2 algorithm and 4N – 3 algorithm have the insensitivity to the phase shift error up to the second and the third degree respectively. The previous described three algorithm consists of window function and discrete Fourier transformation. We will discuss about each window function against the frequency detuning noise.

In experiment, the optical thickness variation and surface shape of a Lithium Niobate wafer of 74 mm diameter and 4 mm thickness were measured simultaneously by wavelength scanning Fizeau interferometer with a new 4N – 3 phase shifting algorithm. The wafer contacted to a supporting fused silica glass parallel plate whose diameter is 80 mm and thickness is 16.5 mm generates eleven different interference fringe patterns overlapped on the detector. The air gap distance was adjusted to 28.5 mm, approximately three times the optical thickness of a Lithium Niobate wafer. Finally, the ratio of air gap distance, the optical thickness of a Lithium Niobate wafer and a supporting fused silica glass parallel plate is about 6:2:5. By fine tuning of a laser diode and recording the interference images at equal interval, we could separate the frequency of the optical thickness variation and the surface shape of a Lithium Niobate wafer with uncertainty of 5 nm PV.

9132-32, Session 7

Metrology of undoped double-sided polished silicon wafer: sur-face, thickness and refractive index profile measurements

Ki-Nam Joo, Chosun Univ. (Korea, Republic of); Ho-Jae Lee, Korea Institute of Industrial Technology (Korea, Republic of)

The purpose of metrology for an arbitrary silicon (Si) wafer is to obtain the geometrical features such as surface and thickness profiles accurately. In current wafer metrology, several types of inspection technologies based on capacitive sensors and optical inter-ferometry have been widely used. Among them, optical interferometry is preferred be-cause it can measure the entire wafer surface as it is typically used in surface metrology. However, these optical techniques only get the optical dimensional parameters, by the nature of the light, and assume that the refractive index of the wafer is preliminary known and uniform. Even, near-infrared (NIR) interferometry to inspect a Si wafer needs high cost for a NIR CCD camera.

In this investigation, we propose a cost effective technique to obtain the surface, the thickness and the refractive index profile of an undoped double-side polished (DSP) Si wafer at once. This technique is based on well-known low coherence scanning interferometry (LCSI) and spectrally resolved interferometry (SRI) using a NIR light around 1 ?m wavelength, which can go through an undoped Si wafer and a typical visible CCD camera. The main role of LCSI is to measure 3D profiles of geometrical features and refractive indices while SRI can obtain the nominal optical thickness of the double-sided polished Si wafer, which can be used preliminary knowledge for scanning range of LCSI as well. The measurement part consists of a DSP Si wafer and a measurement mirror and the detection area is divided into two; one is no wafer region and the other involves the wafer in the optical path. From the correlograms captured by two regions, the geometrical thickness and the group refractive index of the wafer can be extracted. Moreover, the additional technique to calculate the phase refractive index of the wafer using dispersion effect in the correlogram is applied. As the experimental results, the optical thickness, the geometrical thickness, the group refractive index and the phase refractive index profiles were successfully obtained and the mean values over the entire wafer surface were 1869.6 ?m, 490.45 ?m, 3.8121 and 3.516, respectively. Compared to the reference values of the group refractive index and the phase refractive index of the Si wafer, the deviations were 0.055 and 0.04, caused by the position error of the scanning stage.

9132-33, Session 7

Quantitative estimate of laser-induced refractive index changes in the bulk of various transparent materials

Alexandre Mermillod-Blondin, Arkadi Rosenfeld, Max-Born-Institut für Nichtlineare Optik und Kurzzeitspektroskopie (Germany); Thomas Seuthe, Markus Eberstein, Fraunhofer-Institut für Keramische Technologien und Systeme (Germany); Jörn Bonse, Bundesanstalt für Materialforschung und -prüfung (Germany); Moritz Grehn, Technische Univ. Berlin (Germany)

Focusing an ultrashort laser pulse in the bulk of a transparent solid induces a permanent refractive index change on a micrometric to submicrometric scale. Displacing the sample with respect to the laser beam enables direct writing of phase objects in 3 dimensions. This promotes ultrashort pulse laser sources as unique microprocessing tools, as no other available technology enables single step, 3-dimensional microstructuring.

The direct inscription of various embedded micro photonic structures such as waveguide arrays or 3d splitters was already demonstrated. Invisible embedded marking or long term data storage are also good examples of applications that rely on direct 3D laser writing.

In all the aforementioned examples, the efficiency of the microstructures critically depends on the magnitude of the laser-induced refractive index changes. However, a precise measurement of the laser-induced refractive index change is extremely challenging. Existing refractometry techniques are well suited to characterize the refractive index distribution on a plane surface. Carrying out investigations inside the volume with conventional refractometry methods implies sample cleaving, a destructive and time consuming process. Quantitative phase contrast microscopy (QPCM) techniques offer a better alternative for in-situ, non invasive, quasi instantaneous refractive index measurements. QPCM methods usually involve the acquisition of several frames slightly defocused with respect to the plane of the specimen. If the precise amount of defocusing between the different images is well known, an estimation of the 2D refractive index map of the specimen can be obtained by applying the transport of intensity equation. Other QPCM methods based on digital holography require solving the Huygens-Fesnel integral to obtain the refractive index distribution. Recently, Popescu et al implemented a method combining the advantages of phase shift interferometry with the spatial resolution of microscopy. This new method, called SLIM, involves placing a two dimensional spatial light modulator in the Fourier plane of a phase contrast microscope. By controlling the amount of phase shift between the direct and diffracted light, one can measure optical path differences with a sub nanometric precision, without cumbersome calculations.

We applied SLIM to the characterization of ultrashort pulse laser-induced phase objects (such as microdots and lines) in

the volume of various transparent materials. We imprinted the microstructures by focusing a 70 fs duration laser pulse with a 0.45 numerical aperture microscope objective. The results obtained in fused silica confirm previous estimates performed with refractometry. Thanks to its ease of use, SLIM enabled us to explore various laser inscription regimes in a wide range of transparent materials.

9132-34, Session 7

Spectral properties of molecular iodine absorption cells filled to saturation pressure

Jan Hrabina, Martin Sarbort, Ondrej Cip, Josef Lazar, Institute of Scientific Instruments of the ASCR, v.v.i. (Czech Republic)

The absorption cells - optical frequencies references – represent the crucial part of setups for practical realization of the meter unit – highly stable laser standards, where varied laser sources are frequency locked to the selected absorption transitions. Furthermore, not only in the most precise laboratory instruments, but also in less demanding interferometric measuring setups the frequency stabilization of the lasers throught the absorption in suitable media ensure the direct traceability to the fundamental standard of length. We present the results of measurement and evaluation of spectral properties of molecular iodine absorption cells filled to saturation pressure of absorption media. A set of cells filled with different amounts of molecular iodine was prepared and an agreement between expected and resulting spectral properties of these cells was observed and evaluated. The cells made of borosilicate glass instead of common fused silica were tested for their spectral properties in greater detail with special care for the absorption media purity – the measured hyperfine transitions linewidths were compared to cells traditionally made of fused silica glass with well known iodine purity. The usage of borosilicate glass material represents easier manufacturing process and also significant costs reduction but a great care must be taken to control/avoid the risk of absorption media contamination. An approach relying on measurement of linewidth of the hyperfine transitions is proposed and discussed.

The authors wish to express thanks for support to the grant projects from the Grant Agency of CR, project GPP102/11/P820, Academy of Sciences of CR, project: RVO:68081731, Ministry of Education, Youth and Sports of CR, project: CZ.1.05/2.1.00/01.0017, European Social Fund and National Budget of the Czech Republic, project: CZ.1.07/2.4.00/31.0016 and Technology Agency of CR, projects: TA02010711, TA0101995, TE01020233. The support of GRAM (CNRS-INSU) and of DGA/ANR (N°11 ASTR 001-01) are gratefully acknowledged by the french team.

9132-42, Session PS3

Polymer waveguide sensor with tin oxide thin film integrated onto optical-electrical printed circuit board

Jung Woon Lim, Seon Hoon Kim, Jong-Sup Kim, Jeong Ho Kim, Yune Hyoun Kim, Ju Young Lim, Young-Eun Im, Jong Bok Park, Swook Hann, Korea Photonics Technology Institute (Korea, Republic of)

The gas sensors are of importance for a variety of environmental, industrial, medical, scientific and even domestic application. Apart from sensor systems merely providing an alarm signal, it is frequently required to obtain accurate real-time measurements of the concentration of a particular target gas, often in a mixture of other gases. The sensor system for gas detection is highly desirable to provide on-line monitoring of the chemical composition of gas emitted from combustion facilities, in order to minimize air pollutions, and maintain the concentrations of dangerous gaseous species within the limits stipulated by regulations.

In recent years, these gas monitoring sensors using electronic and optical device have been mainly studied. Optical sensors exhibit clear advantages over other sensor technologies (chemical, electrical, micromechanical) owing to the high sensitivity and immunity to electromagnetic interference that they can offer.

Optical fiber-based and waveguide sensors are developed as optical sensor using optical properties. Recent developments on the integration of polymer waveguides for use in waveguide sensors have demonstrated the potential of cost-effectively. Further integration of sensors device using polymer waveguide onto optical-electrical printed circuit board (PCB) can allow the formation of low-cost, highly-sensitive sensing devices for use in a wide range of applications.

Several groups have reported the design and fabrication of waveguide optical sensor application. However, these devices were all made by planar lightwave circuit (PLC) technology. Compared with the complex fabrication process and corresponding high cost of silica-based optical sensor chips such as PLC devices, polymer-based optical sensor chips using nano imprint lithography (NIL) are attractive because they are relatively simple to process and have shown promise for use in low-cost devices.

Tin oxide (SnO2), one of the semiconductor metal oxide film has drawn considerable interest because of their good electrical conductivity and optical property. SnO2 has been widely studied for gas sensor . It has a high reactivity to reducing gases at relatively low operating temperatures and an easy absorption of oxygen at its surface due to the natural non-stoichiometry. Most SnO2 sensors are operated on the basis of the modification of the elecrical properties. However, SnO2 sensors have some darwbacks which, in some cases, limit their use in practice. In particular, their operation principle and high operating temperature lead to high power consumptions and the difficulty to be exploited in combustible and liquid environment. The use of optical waveguides with SnO2 material could enable to overcome these drawbacks.

In this paper, we proposed and fabricated optical sensor module integrated into optical-electrical PCB for gas detection based on polymer waveguide with SnO2 thin film. Their potential application as gas sensors are confirmed through computational simulation using the two dimensional finite-difference time-domain (2-D FDTD) method. Optical-electrical PCB was integrated into VCSEL, photodiode and polymeric sensing device was fabricated by the nano-imprint lithography technique.

9132-43, Session PS3

Metrology of micro-optical components quality using direct measurement of 3D intensity point spread function

Stephane Perrin, Maciej Baranski, Nicolas Passilly, Luc Froehly, Jorge Albero, Sylwester Bargiel, Christophe Gorecki, FEMTO-ST (France)

High-resolution miniature imaging systems require high quality micro-optical elements. Therefore, it is essential to characterize their optical performances in order to optimize their fabrication. Usually, basic evaluation of micro-optical elements quality is based on the measurement of their topography since their optical properties are largely defined by their shape. However, optical characteristics have to be derived from the measured geometry using optical propagation algorithms. An alternative method is the direct measurement of their optical properties. Unlike topography measurement, it allows characterization of high numerical aperture components. Moreover, it can be applied to single elements but also to optical systems composed of several microlenses. The most popular method of direct optical measurement concerns the wavefront measurement that is complicated when it concerns micro-optical elements. In this work, we propose a simple method based on the measurement of the 3D

intensity point spread function (IPSF). IPSF is defined by the 3D shape of the focal spot generated by the micro-element. The direct characterization of focusing response through the measurement of PSF allows very precise estimation of micro-structures quality. The considered method consists in imaging different slices of the focal volume generated by the focusing component. It is easier to implement than wavefront-based methods since it is less affected by probing beam quality and less demanding in terms of alignment accuracy. The employed setup is simple and requires only a microscope objective and a camera that are moved along the propagation axis. It allows, depending on the configuration, characterizing both transmissive and reflective micro-optical components. If additional data analysis is performed, the wavefront or the 3D topography can be calculated from the IPSF data. Moreover, the Strehl ratio and the radius of curvature of the optical element can be also calculated. The advantages of this technique are demonstrated on micro ball lenses and micro-mirrors.

9132-44, Session PS3

Raman spectroscopy of nanostructured silicon fabricated by metal-assisted chemical etching

Igor Iatsunskyi, Odessa I.I. Mechnikov National Univ. (Ukraine); Stefan Jurga, Adam Mickiewicz Univ. (Poland); Valentyn Smyntyna, Nickolay Pavlenko, Valeriy Myndrul, Odessa I.I. Mechnikov National Univ. (Ukraine); Anastasia Zaleska, Odessa I.I. Mechnikov National University (Ukraine) and Odessa II Mechnikov National Univ (Ukraine)

In recent years, silicon nanostructures have been extensively studied both theoretically and experimentally to realize their possible applications. For instance, silicon nanowires (Si NWs) exhibit novel chemical and physical properties due to their dimensions at the nano-scale, and offer great potential in the fields of electronics, photonics, chemical sensors and biological systems. Current interest focuses on the band-gap expansion of Si nanocrystals compared with that of bulk materials based on the quantum confinement effect. Si nanostructures with various morphologies have been fabricated using several methods, such as electrochemical etching, plasma-assisted chemical vapor deposition, sputtering, laser ablation etc. Recently, a new method, termed metal-assisted chemical etching, has been developed, which is relatively simple compared to the electrochemical method. The method does not need an external bias and enables a formation of uniform PS layers more rapidly than the conventional methods.

Raman spectroscopy, as a fast, convenient, nondestructive, and highly sensitive probe of local atomic arrangements and vibrations, has been widely used to characterize the properties of nanomaterials including nanocrystals, nanowires and microcrystalline structures. The localization and lattice vibration properties of various low-dimensional semiconductor nanomaterials have been successfully yielded by the aid of detailed analyses of significant size-dependent red-shift and asymmetric broadening when the nanocrystal size is reduced to nanometer scale.

In this work, we present a detailed experimental and theoretical Raman investigation of nanostructured silicon with different nanocrystal sizes and structures. We demonstrated experimentally that for Si nanostructures smaller than 20 nm, the quantum confinement effect is dominant for the peak shift and line broadening. Depending on morphological parameters it should be taking into account such factors as mechanical stresses, heating and Fano scattering.

9132-45, Session PS3

Sub-kHz traceable characterization of stroboscopic scanning white light interferometer

Ville Heikkinen, Metrologie und Akkreditierung Schweiz (Finland); Ivan Kassamakov, Univ. of Helsinki (Finland); Anton Nolvi, Tor Paulin, University of Helsinki (Finland); Jeremias Seppä, Antti Lassila, MIKES Mittatekniikan keskus (Finland); Edward Hæggström, Univ. of Helsinki (Finland)

Scanning white light interferometry (SWLI) is an established methodology for non-destructive testing of MEMS/NEMS. In contrast to monochromatic interference microcopy SWLI can unambiguously resolve surfaces featuring vertical steps. Oscillating samples can be measured using a stroboscopic SWLI (SSWLI) equipped with a pulsed light source.

For measurements of static samples the lateral and vertical scales of the SSWLI can be calibrated using transfer standards with calibrated dimensions such as line scales, 2D gratings, gauge blocks and step height standards. However, traceable dynamic characterization of SSWLI requires a transfer standard providing precise traceable periodic movement.

A transfer standard based on a piezo-scanned flexure guided stage with capacitive feedback was designed and manufactured. The trajectories of the stage motion for different amplitude and frequency settings were characterized with ~2 nm standard uncertainty using a symmetric differential heterodyne laser interferometer (SDHLI). The transfer standard was used to characterize quasidynamic measurements across the vertical measuring range of the SSWLI, 100 μm. Dynamic measurement properties were characterized using a sinusoidal vertical trajectory with 2 μm amplitude and 50 Hz frequency. The motion amplitude 2408 nm measured with the SSWLI was 6 nm smaller than the amplitude measured with SDHLI. The repeatability of SSWLI expressed as experimental standard deviation of the mean was 11 nm.

A traceable method to characterize the capacity of the SSWLI to perform dynamic measurements at sub-kHz frequencies was demonstrated.

9132-46, Session PS3

Three-dimensional surface reconstruction by combining a pico-digital projector for structured light illumination and an imaging system with high magnification and high depth of field

Audrey Leong-Hoi, Univ. de Strasbourg (France) and ICube (France); Bruno Serio, Univ. Paris Ouest Nanterre La Défense (France) and Lab. Energétique Mécanique Electromagnétisme (France); Patrice Twardowski, Paul Montgomery, Univ. de Strasbourg (France)

A prototype has been developed of a Structured Illumination Microscopy (SIM) system using a miniature projector (pico DLP) to project sinusoidal fringes onto the sample surface that is to be measured, a digital camera for image acquisition and applying the three-step phase shifting algorithm together with the absolute phase retrieval method. This method consists of first determining the typical relative phase of the pattern projected onto the sample surface, by projecting a series of images of three sinusoidal fringe patterns with an offset of $2\varpi/3$ rad between each pattern. However the relative phase shows discontinuities because of the phase shifts. These discontinuities are then removed, not by unwrapping the relative phase, but by projecting another series of three fringe patterns onto the sample. The discontinuities in phase are thereby identified, thus allowing the calculation of the absolute phase, which contains the information of the object surface height.

By using an imaging system composed of a magnifying glass and a relay lens, instead of a conventional microscope objective, the microscope allows reconstructions of 3D surfaces of objects with a 10x magnification, a numerical aperture of 0.065 and a lateral resolution of 5.6 μm, according to the Rayleigh criterion and using an average wavelength of 0.6 μm (incoherent light). An image processing algorithm has been developed to reduce the noise in the acquired images by averaging the intensities of the same pixels in successive images, so as to improve the signal to noise ratio before applying the reconstruction algorithm and optimize the reconstruction method.

Compared with interference microscopy and confocal microscopy that have a shallower depth of field per single XY image due to the higher numerical aperture of the objective, the microscope developed achieves a depth of field of more than 70 μm and thus requires no vertical scanning, which greatly reduces the acquisition time.

Although the system at this stage does not have the same performance as interference microscopy or confocal microscopy in terms of axial and lateral resolution, it is nonetheless faster and cheaper. One possible application of this SIM technique would be to first reconstruct in real-time parts of the object that are to be observed before performing higher resolution 3D measurements with interference microscopy or confocal microscopy.

As with all classical optical instruments, the lateral resolution is limited by diffraction. Work is being carried out with the prototype SIM system in order to be able to exceed the limits in the lateral resolution and thus achieve super resolution.

9132-47, Session PS3

Optical device for precision inspection of MOEMS by Moiré inteferometry

Saïd Meguellati, Univ. Ferhat Abbas de Sétif (Algeria)

The development of microoptical and micromechanical systems requires fabrication of micro components, there is need to find new measurement techniques for characterisation and testing. Fortunately, optical inspection systems which have the particularity to be non-destructive and non-contact diagnostics provide an ideal way to validate and verify product quality.

The reduction of systems size, for a specific use, has become a necessity to the economy of matter, energy and volume, and consequently, the miniaturization of components is required. Characterisation and testing of these micro components requires adapted and increasingly powerful techniques of control. This study will focus on the application of optical measuring techniques in micro-measurements. The accuracy of components geometry is parameter which influences the precision of the function. Moiré topography is full-field optical technique in which the contour and shape of object surfaces is measured by means of geometric interference between two identical line gratings. The technique has found various applications in diverse fields, from biomedical to industrial, scientific applications, and miniaturized instrumentation for space applications. In many industrial metrology applications, non contact and non-destructive shape measurement is a desirable tool for, quality control and contour mapping. This method of optical scanning presented in this paper is used for precision measurement deformation or absolute forms in comparison with a reference component form, of optical or mechanical micro components, on surfaces that are of the order of mm2 and more. The principle of the method is to project the image of the source grating on the surface to be inspected, after reflection; the image of the source grating is printed by the object topography and is then projected onto the plane of the reference grating to detect defects.

The optical device used allows the magnification dimensional surface up to 1000 times the surface inspected, which allows easy processing and reaches an exceptional nanometric imprecision of measurements. According to the measurement principle, the sensitivity for displacement measurement using moiré technique depends on the frequency grating, for increase the detection resolution. This measurement technique can be used advantageously to measure the deformations generated by constraints on functional parts and the influence of these variations on the function. It can also be used for dimensional control when, for example, to quantify the error as to whether a piece is good or rubbish. It then suffices to compare a figure of moiré fringes with another previously recorded from a piece considered standard, which saves time, money and accuracy. This method of control and measurement allows real time control; speed control and the detection resolution may vary depending on the importance of defects to be measured.

9132-48, Session PS3

Spectral ellipsometry studying of iron's optical and electronic properties

Yevheniia Chernukha, Vasyl Staschuk, Olena Polianska, National Taras Shevchenko Univ. of Kyiv (Ukraine); Olexsandr Oshtuk, Taras Shevchenko National Univ of Kyiv (Ukraine)

Iron's optical and electronic properties were investigated on bulk sample at the room temperature. The sample's surface was explored across a broad spectral range ?=0,23 - 2,8?m (h?=0,44 - 5,39 eV) by the Beatty's spectral ellipsometry method. While an experiment was carried out ellipsometry parameters ? and ? were measured near the principle angle of incidence. The dispersive dependences of optical conductivity ?(h?), refractive index R(h?) and permittivity ?(h?) were calculated using these parameters and was used the published data of iron's optical conductivity in liquid state[1] and amorphous metallic alloy Fe78Si10B12 [2].

The optical conductivity was calculated using the published data of the iron's density of electronic states in crystalline [3], amorphous [4] and liquid [5] states. The comparison of the experimental and theoretical curve shows good coordination, but the maxima in optical conductivity spectrum positioned at different energies. It means the indirect transition's model describe the optical conductivity of Fe only in the first approximation.

According to two-band model defined collisions frequency ?s of slowly relaxing, related to the 4s-electron states. Calculated plasma frequency ?s 4s-electron conductivity and optical conductivity limits ?s and ?d, respectively, 4s and 3d-electrons and contribute to the infrared (IR) spectrum of interband transitions ?, plasma frequency ?d and relaxation frequency ?d 3d-electrons. The results are similar to the literature data [6].

References:

[1] Guschyn V.S. et.al. Bulletin of Academy of Sciences of the USSR 46, 58-62 (1986) (in Russia)

[2] Yu. V. Knyazev et.al. Optics and Spectroscopy. 107 (5), 708–712 (2009)

[3] Rudolf Zeller. Computational Nanoscience: Do It Yourself! 31, 419-445 (2006)

[4] M.Gradhand et.al. Phys.Rev.B 77, 134403-1 – 134403-11 (2008)

[5] Takeo Fujiwara, Yukito Tanabe. J. Phys. F: Metal Phys. 9 (4), 73-75 (1979)

[6] Staschuk V.S. et. al. Bulletin of Taras Shevchenko National University of Kyiv, Series Physics. 21, 35-37, (1980)

9132-49, Session PS3

Fingerprint authentication via joint transform correlator and its application in remote access control of a 3D microscopic system

Wenqi He, Hongji Lai, Meng Wang, Zeyi Liu, Yongkai Yin, Xiang Peng, Shenzhen Univ. (China)

We present a fingerprint authentication scheme based on the optical joint transform correlator (JTC) and further describe its

application to the remote access control of a network-based remote laboratory, which is purposely built to share a unique 3D microscopy system based on phase-aided active stereo technique (3DM-PAAS) of our realistic laboratory in Shenzhen University with our project partners in Stuttgart University. In this article, we focus on the involved security issues, mainly on the verification of various visitor identities of the system. By making full use of the JTC-based optical pattern recognition and matching technology as well as a famous cross-platform software, virtual network computer (VNC), we are able to achieve the ultimate aim of hierarchical authentication and access control for any remote visitors (authorized or not). Specifically to say, when a remote visitor attempts to access our 3DM-PAAS, a user password is first mandatory required, which is followed by a fingerprint collection. Then the hash value of the user password together with the collected fingerprint are sent to the server (in our laboratory) relying on the secure shell protocol (SSH), which is introduced to guarantee the security of the communication channel. In the server side, an automatic verification procedure is then activated, by comparing the received hash value with all the authorized hash values, the server can directly deny this remote access request or pick up the corresponding authorized fingerprint for further verification. Note that the aforementioned authorized hash values and authorized fingerprints are all previously stored in the database of the server. In the second-level certification, the received fingerprint and the authorized one are separately written into a spatial light modulator (SLM) side by side to form the input of an optical JTC architecture, and in the output plane a correlation peak means a success verification, the sever will immediately sent back an instruction to authorize the remote visitor access to our 3DM-PAAS by the VNC with a corresponding permission. Here, we should emphasize that different remote visitors are assigned with different-level access permissions in advance and these mapping relationships are also pre-stored in the serve's database. In a word, we proposed a two-factor (password and fingerprint) hierarchal authentication method to manage the remote access to the 3DM-PAAS in our realistic laboratory with the help of the VNC and SSH.

9132-50, Session PS3

Traceable mechanical properties measurement of silicon nanopillars using contact resonance force microscopy

Sai Gao, Uwe Brand, Physikalisch-Technische Bundesanstalt (Germany)

Nano-objects, including nanowires, nanotubes, nanoparticles, nanopillars, and many more, are currently used in various industry fields to improve the properties and functionality of everyday products, such as glass, steel, cement, coatings and easy-to-clean ceramics. Quantitative determination of the mechanical properties of nano-objects therefore plays an important role to understand and control the mechanical performance of the final components.

Due to their outstanding spatial resolution, especially in lateral aspects, atomic force microscopes (AFMs) have long been used for topography measurements of nano-objects. In the past ten years, the capability of AFMs to measure and sensing small forces (down to several tens of pN) has been utilized to perform mechanical properties measurement of nano-objects. Many different AFM based measurement approaches to measure the mechanical properties of nano-objects have been published, such as AFM based beam-bending techniques[1], AFM based nano-indentation method [2], contact-resonance force microscopy (CR-FM) [3] and various others. However, the measurement results show a large scatter and a lack of traceability.

Traceable mechanical measurements using AFMs demands that the mechanical performance of AFM cantilevers in use, especially their normal spring constant, be carefully calibrated. For this purpose PTB has developed an "active reference spring (ARS)" method based on a well-developed MEMS nano-force transducer, which features direct and in-situ determination of the spring constant of cantilevers with an uncertainty less than 5 % for cantilevers with stiffness ranging from 0.1 N/m to 50 N/m.

With the calibrated AFM cantilever, the mechanical properties of silicon nano- / micro-pillars with thicknesses from 70 nm to 500 nm and diameters from 200 nm to 2000 nm have been measured based on the CR-FM method. First results will be presented in this paper.

This research is supported by the European Union by funding the European Metrology Research Programme (EMRP) project "Traceable measurement of mechanical properties of nano-objects (MechProNo)".

Reference

[1] Sriram Sundararajan, Bharat Bhushan, Development of AFM-based techniques to measure mechanical properties of nanoscale structures, Sensors and Actuators A 101 (2002) 338-351

[2] Marcel Lucas, Ken Gall and Elisa Riedo, Tip size effects on atomic force microscopy nanoindentation of a gold single crystal, J. Appl. Phys. 104 113515 (2008)

[3] D C Hurley, M Kopycinska-Müller, A B Kos and R H Geiss, Nanoscale elastic-property measurements and mapping using atomic force acoustic microscopy methods, Measurement Science and Technology 16 (2005) 2167–2172

9132-51, Session PS3

Tilt angle measurement with a Gaussian-shaped laser beam tracking

Martin Sarbort, ?imon Rerucha, Petr Jedlicka, Ondrej Cip, Josef Lazar, Institute of Scientific Instruments of the ASCR, v.v.i. (Czech Republic)

We have addressed the challenge to carry out a stabilization of the angular tilt of a laser guiding mirror, which is intended to route a laser beam with a high energy density. Such an application required good angular accuracy as well as large operating range, long term stability and absolute positioning.

We have designed an instrument for such a high precision angular tilt measurement based on a triangulation method where a laser beam profile is reflected off a movable mirror (that is subject to the stabilization) and detected by an image sensor. As the angular deflection of the mirror causes a change of beam spot position, the principal task is to measure the position on the image chip surface. We have employed a numerical analysis of the intensity pattern, which uses the nonlinear regression algorithm for two position detection methods. The first method detects the Gaussian intensity profile of the laser beam; the latter uses a periodic spot pattern generated by a diffraction grating inserted into the beam path. Both methods are principially very similar, the nonlinear fitting of known beam profile allows the methods for position assesment wih better precision well below the pixel resolution of the chip.

The feasibility and performance were tested on the basis of mathematical and numeric modeling. The simulation indicated, that the method with single spot could reach precision of 0.15 microradians; the method with a periodic pattern could reach precision of 0.4 of nanoradians.

The method with the Gaussian beam was used in the experimentation. The experimental results indicate that the assembled instrument achieves a measurement error of 0.12 micro radian in the range ± 0.6 degrees over the period of one hour, while the mirror to image chip distance were approximately 1 meter and chip size was 12x16mm. The resulting dynamic range is approximately 10^5, the real boundaries are function of the mirror-image chip distance. Considering the use of the grating-generated pattern, the dynamic range could be enhanced approximately by the factor of 20 (considering 20 spots in the pattern with good intensity contrast).

9132-52, Session PS3

Development of a laser-speckle-based measurement principle for the evaluation of mechanical deformation of stacked metal sheets

Clemens Halder, Thomas Thurner, Mathias Mair, Technische Univ. Graz (Austria)

Stacks of metal sheets are widely used in electrical motors, transformers and generators to reduce for eddy current loss in their magnetic circuit. During their design process these electrical machines are optimized for their cost-performance ratio and/or their weight with respect to its given application area, and so the mechanical behavior of the laminated sheet stacks becomes more and more important to be considered during the mechanical and fatigue design of these electromechanical systems.

This work describes the development of a contactless measurement principle based on digital speckle photography for evaluating mechanical deformation states on stacked laminated metal sheet structures. With the help of this measurement method which is able to measure displacements and subsequently strain of individual layers of stacked metal plates, new mathematical simulation models for describing the non-linear mechanical behavior of these stacked metal structures are parameterized and verified.

The measurement setup consist of one or two laser sources illuminating investigation sections on the specimen, which are imaged by telecentric objectives and digital CMOS cameras. Since laser speckle patterns from laminated sheet stacks differ from speckles obtained from standard technical surfaces, the data acquisition and signal processing techniques for standard speckle photography is modified in order to acquire information on relative displacements between individual layers within mechanically loaded sheet metal stacks in a robust and accurate manner. Specialized image template sets and template sizes are used throughout the speckle pattern correlation analysis with underlying mathematical models of the investigated structure for properly limiting the degree of freedom of the evaluated speckle dynamics.

Real world experiments for stacked metal sheets under defined mechanical loads will verify the quality and performance of the newly developed measurement method.

9132-53, Session PS3

A dual-styli micro-machined system for precise determination of the thickness of free-standing thin films

Sai Gao, Physikalisch-Technische Bundesanstalt (Germany)

Free-standing thin membranes have now been widely applied in various research and industrial fields. Rapid advances in micro-fabrication techniques have already enabled that micro-fabricated free-standing membranes made of different materials with thicknesses ranging from a few microns down to less than 100 nm can be realized. In the mean time, quality control of these functional micro-membranes demands that the membrane thickness, which is one of the key parameters of thin membranes, can be precisely determined.

To date, there already exist tremendous membrane thickness methods, which could work well under certain conditions (e.g. applicable only for limited materials, thickness range, sensitivity/uncertainty). Unfortunately, however, there is a lack of a universal membrane thickness measurement method, which could measure thin membranes, especially micro-fabricated membranes of various materials (e.g. from metal to polymer) with small size (i.e. < 0.01 mm2) and wide thickness variation (e.g. from approx. 10 μm down to about 100 nm).

To fulfill the aforementioned demand in this field, a traceable membrane thickness measurement system is presented in this paper. It utilizes a pair of micro-machined nano-force transducers to actively detect the top and bottom surface of a free-standing micro-machined membrane. Thanks to the high force sensitivity (down to sub-Nanonewton) and a relatively large movement range (up to 30 μm) of the MEMS transducers in use, the proposed thickness measurement micro-system is capable of measuring membranes with small open aperture and membrane thicknesses up to 50 μm. In addition, the in-plane movement of the MEMS-transducers is measured in real-time by a self-developed fiber-interferometer with nanometric resolution, which is traceable to the SI unit.

Design and construction of the miniature thickness measurement system are detailed in this paper, including the first measurement results, which prove the feasibility of the proposed measurement system.

9132-54, Session PS3

Automatic digital filtering for the accuracy improving of a digital holographic measurement system

Marcella Matrecano, Lisa Miccio, Istituto Nazionale di Ottica (Italy); Anna Persano, Fabio Quaranta, Consiglio Nazionale delle Ricerche (Italy); Pietro Siciliano, Istituto per la Microelettronica e Microsistemi (Italy); Pietro Ferraro, Istituto Nazionale di Ottica (Italy)

With the advent of charged coupled devices (CCDs) with smaller pixel sizes, high speed computers and greater pixel numbers, digital holography (DH) became a very feasible technology which offers new possibilities for a large variety of applications.

For example, digital holographic microscopy (DHM) is an important tool in optical metrology where it is increasingly urgent the request of higher performance for full 3D, large field of view, high resolution imaging and real-time analysis.

In this context, it presents numerous advantages such as the direct access to the phase information, numerical correction of optical aberrations and the ability of a numerical refocusing from a single hologram. Furthermore, as an interferometric method, DHM offers both a no-destructive and no-contact approach to very fragile objects combined with flexibility and a high sensitivity to geometric quantities such as thicknesses and displacements.

These features recommend it for the solution of many imaging and measurements problems, such as microelectro-optomechanical systems (MEMS/MEOMS) inspection and characterization.

In this work, we propose to improve the performance of a DH measurement system, through digital filters. In other words, we have developed an automatic procedure, inserted in the hologram reconstruction process, to selectively filter the hologram spectrum. The purpose is to provide very few noisy reconstructed images, thus increasing the accuracy of the conveyed information and measures performed on images. Furthermore, improving the image quality, we aim to make this technique application as simple and as accurate as possible.

The obtained results demonstrated that our method allows not only to remove the noisy spatial frequencies, without sacrificing the information content, but it is also fully tunable to the spectrum under investigation. Compared to conventional filtering techniques, our method is perfectly adapted to every analyzed sample, while not requiring any manual adjustments, because it is completely automatic. This leads not only to a great improvement in the precision of the entire measurement and monitoring system but also to a considerable reduction in the analysis time, making the method suitable for real-time applications.

These features permit to increase the images quality and the accuracy of the measurements taken from them, making our technique highly applicable for quantitative phase imaging in MEMS analysis.

9132-55, Session PS3

Common-path configuration in Total Internal Reflection Digital Holography Microscopy

Marcella Matrecano, Alejandro Calabuig, Melania Paturzo, Pietro Ferraro, Istituto Nazionale di Ottica (Italy)

Total Internal Reflection holographic microscopy (TIRHM) is a relatively recent microscopy technique used to image and study surface processes. It incorporate evanescent wave surface profiling with digital holographic microscopy. In particular TIRHM uses a prism as sample substrate in the object arm of a Mach–Zehnder digital holographic microscope. TIRHM is a technique especially suitable to study surface properties with direct applicability in characterizing cellular adhesion, as well as other biological applications and nano-metrics in general.

Anyway, because of the TIR prism's geometry, the acquisition plane is at a sizeable incline with respect to the object one. This implies that in the reconstruction step it is necessary to take into account this anamorphism for an accurate result.

In this work we propose and compare two different approaches to correct tilted plane anamorphism. In the first case, a simplified three-dimensional (3D) formulation of the angular spectrum method (ASM) is proposed. It allows to generate the entire stack of propagated images in a single shot. Starting from this dataset and through simple masking operations, we are able to obtain an en face reconstruction.

In the second approach, a numerical cubic phase plate (CPP) is included into the reconstruction process of digital holograms with the aim to enhancing the depth-of-focus of optical imaging system. The idea comes from the practice of placing a special phase plate in the aperture stop of an incoherent optical system. Here we investigate how the CCP works for coherent light imaging systems in TIRHM.

Theoretical formulations of the two approaches are supported by experimental evidences. In particular, these proposed procedures are applied to digitally process the holograms of differently tilted objects. The obtained results show that the proposed strategies allow to correct effectively the anamorphism of holograms recorded on an inclined plane.

9132-56, Session PS3

Active angular alignment of gauge block in system for contactless gauge block calibration

Zdenek Buchta, Martin ?arbort, ?imon Rerucha, Václav Hucl, Martin Cí?ek, Josef Lazar, Ondrej Cíp, Institute of Scientific Instruments of the ASCR, v.v.i. (Czech Republic)

This paper presents a method for active angular alignment of gauge block implemented in a system for automatic contactless calibration of gauge blocks designed at ISI ASCR. The system combines laser interferometry and low-coherence interferometry. The optical setup combines a Michelson interferometer and a Dowell interferometer, placed in the reference arm of the Michelson interferometer. In this case, the contactless measurement of the absolute gauge block length is done as a single-step operation without any change in optical setup during measurement, giving complete information of the gauge block length. The contactless method employing light for the object length measurement eliminates the measurement error caused by a mechanical interaction between the object and the measurement setup. On the other hand, the precise measurement is conditioned by perfect alignment of the block-shaped object (gauge block) to the measuring beam. If the axis of the gauge block is not parallel with the beam axis, the result of the measurement is influenced by a cosine error. Elimination of the cosine error requires employing of a powerful control technique ensuring the proper object positioning in the experimental setup during its length measurement.

For the gauge block position analysis, the designed algorithm takes advantage of the large beam used for the gauge block length measurement. At the output of the Dowell interferometer, a commercially available USB CCD camera is installed. When the gauge block is placed into the holder, the control software takes a picture from the camera and does the analysis of the image section which shows interference of the HeNe radiation presented in two beams reflected on a bottom and a top surface of the gauge block.

The image analysis employs the "flooding technique" working with gray scale images. In the first step, the value of the mean intensity in the investigated area is determined. Then, the value is used as a threshold separating areas of higher and lower intensity. The resulting image is then analyzed again to identify of areas representing interference fringes - minor areas are regarded to be a noise and they are not taken into account. Finally, the image analysis procedure gives a number of identified interference fringes in the longitudinal and lateral direction. If the number is greater than 1 or if the number of interference fringes cannot be evaluated, the software readjusts the voltage on an adequate PZT transducer built into the gauge block holder to optimize the gauge block position in the system. For each image, several X and Y sections are analyzed for clear identification of all interference fringes and their orientation. For cases of gauge blocks with shape imperfections, the number of iterations is limited to 10. Then, the software carries out the length measurement or marks the gauge block as defective.

The algorithm for gauge block alignment to the measuring beam axis, in combination with the specific gauge block holder, is able to compensate the gauge block lateral and longitudinal tilt up to 0.141 mrad.

9132-57, Session PS3

In-beam tracking refractometry for coordinate interferometric measurement

Miroslava Hola, Josef Lazar, Ond?ej ?íp, Zdenek Buchta, Institute of Scientific Instruments of the ASCR, v.v.i. (Czech Republic)

We propose to extend the principle of compensation of the fluctuations of the refractive index of air through monitoring the optical length within the measuring range of the displacement measuring interferometer. The concept is derived form a tracking refractometry evaluating the refractive index of air in the beam axis coinciding with the positioning interferometer. Application of this approach in multiaxis positioning and measurement mans to compromise the principle of spatial unity of the displacement measuring laser beam and the beam of the tracking refractometer. In this contribution we evaluate the level of uncertainty associated with the spatial shift of these two beams. Consequently the nature of the fluctuations of the refractive index of air in laser interferometry is investigated and discussed with the focus on potential applications in coordinate measuring systems and long-range metrological scanning probe microscopy systems.

The authors wish to express thanks for support to the grant projects from the Grant Agency of CR, project GPP102/11/P820, Academy of Sciences of CR, project: RVO:68081731, Ministry of Education, Youth and Sports of CR, project: CZ.1.05/2.1.00/01.0017, European Social Fund and National Budget of the Czech Republic, project: CZ.1.07/2.4.00/31.0016 and Technology Agency of CR, projects: TA02010711, TA0101995, TE01020233.

9132-58, Session PS3

Asymmetric polarization-based frequency shifting interferometer for microelectronics

Seung Hyun Lee, MinYoung Kim, Kyungpook National Univ. (Korea, Republic of)

In these days, semiconductor manufacturing technologies focus on high precision and miniaturization of electronic and mechanic components, and their assembly in one package. Final products, made by these fine manufacturing technologies, have been much more complex than before. The in-line inspection for the product manufacturing requires precise inspection technology adequate for specified quality control in the manufacturing. According to this manufacturing technological trend, semiconductor packing technologies have been widely developed also because of increasing degree of integration of semiconductor. One of major packing technologies is CSP(chip scale package)/SIP(system in package) technology to assembly the semiconductor die and electronics on micro PCBs.

In these processes, flux plays a critical role in the process dynamics of BGA/CSP package assembly. A vast range of defects in final assembly can be traced back to poor flux or paste deposition. For example, some of the defects in the final assembly derive from poor flux alignment with respect to the intended pads, insufficient thickness/amount of the flux material, excessive amount of flux, or from smearing. The detection of these pass/fail types of defects (attribute data) at an early stage of the process reduces the assembly cost significantly. Moreover, many manufacturers would agree that it is important to control the process of flux deposition by means of relevant measured variables to detect trends and prevent defects from occurring. This requires a system that is able to measure the key variables of the process (variable data). By providing real-time information on key process parameters, manufacturers can take corrective action and prevent scrap and production loss.

For this purpose, in this paper a polarization-based frequency shifting interferometer is proposed for three dimensional flux inspection in microelectronics manufacturing. FSI(frequency shifting interferometer) system, one of most promising optical surface measurement techniques, generally result in superior optical performance comparing with other three dimensional measuring methods as its hardware structure is fixed in operation and only the light frequency is scanned in a specific spectral band without vertical scanning of the target surface or the objective lens. FSI system collects a set of images with interference fringes by changing the frequency of light source illuminated on target objects. Then, it transforms intensity data of acquired image into frequency information, and calculates the height profile of target objects with the help of frequency analysis based on FFT(fast Fourier transform).

The normal FSI system is good performance about specular surface(like semiconductor die). But, if there are transparent objects(like flux) on the surface, their optical polarization characteristics usually make the observed interference fringes degraded. When illuminated light reflects on the flux or penetrates the flux, the direction of polarization of light rotates depending on the polarization characteristic of the flux. The rotation of direction of polarization causes difficulty in measurement. So, a PFSI (Polarization-based Frequency Shifting Interferometer) system is proposed, which applies the polarization analysis method to the conventional FSI system.

First, the PFSI system is proposed for robust measurement to flux. It consists of tunable laser for light source, ?/4 plate in front of reference mirror, ?/4 plate in front of target object, polarizing beam splitter, polarizer in front of image sensor, polarizer in front of the fiber coupled light source, ?/2 plate between PBS and polarizer of the light source. Using the proposed system, low contrast problem of interference fringes due to polarization rotation of acquired fringe image can be solved by using polarization technique. Also, light distribution of object beam and reference beam can be controlled. So, reflected light intensities of the reference beam and object beam can be made similar for conspicuous interference signals.

Second, using PFSI system, the height of flux and the height of die of flux bottom side can be measured in the same system. In case of measuring the height of the flux, the multi-layer reflections are generated in the surface and bottom side of flux. Three interference signals are observed when transparent flux is deposited on the PCB surface; the interference signal A of the reflected light on the reference mirror and the reflected light on the flux surface, the interference signal B of the reflected light on the reference mirror and the reflected light on the flux bottom side, and the interference signal C of the reflected light on the flux surface and the reflected light on the flux bottom side. By light penetrates the flux, Signal A and signal B have different polarization characteristics. By controlling the polarization of the system, the height of flux and the height of bottom side of flux can be measured simultaneously.

Third, the signal processing acceleration method for fast height calculation is proposed for the PFSI, based on parallel processing architecture, which consists of parallel processing hardware and software called GPU(Graphic Processing Unit) and CUDA(Compute Unified Device Architecture). As a result, the processing time reaches into tact time level of real-time processing.

Finally, the proposed system is evaluated in terms of accuracy and processing speed through a series of experiment and the obtained results show the effectiveness of the proposed system and method.

9132-59, Session PS3

Automated multi-point analysis with multi-angle photometric spectroscopy

Travis C Burt, Marcus Schulz, Jeff Comerford, Cameron Bricker, Andrew R. Hind, David L. Death, Agilent Technologies Australia (Australia)

Reflection (R) and transmission (T) are fundamental measurements available for characterizing bulk optics and optical coatings. Historically the complete characterization of optical materials and coatings for precision optics has been largely accomplished on the basis of normal and near normal incidence measurements due to the experimental simplicity of such an approach. This simplicity, however, is not without compromise. Normal incidence transmission measurements are typically conducted in the sample chamber of a spectrophotometer whilst near normal reflectance measurements require the use of a suitable reflectance accessory. A consequence of this approach is that there is never any guarantee that reflectance and transmission measurements are made from exactly the same patch on the sample due to sample repositioning during the significant changes in instrument configuration between R and T measurements.

Multi-angle Photometric Spectroscopy (MPS) measures the reflectance and/or transmittance of a sample across a range of angles (?i) from near normal to oblique angles of incidence (AOI). A recent development by Agilent Technologies, the Universal Measurement Spectrophotometer (UMS) combines both reflection and transmission measurements from the same patch of a sample's surface in a single automated platform for angles of incidence in the range 5°≤|?i|≤85° (i.e. angles on either side of beam normal noted as +/-).

We describe the use of MPS on the UMS with rotational (?) and vertical (z) sample positioning control. MPS(?i,??z) provides for automated unattended multi-angle R/T analysis of samples (up to 20 pieces, 1 inch round) or mapping of single samples (up to 8 inch round). Examples are provided which demonstrate reduced cost-per-analysis in high volume testing as well as spatial spectroscopic information obtained on large diameter samples.

9132-35, Session 8

Single-shot two-channel Talbot interferometry using checker grating and Hilbert-Huang fringe pattern processing

Krzysztof Patorski, Maciej Trusiak, Krzysztof Pokorski, Warsaw Univ. of Technology (Poland)

Diffraction efficiency and image processing enhanced two-dimensional Talbot shearing interferometry providing phase object derivative information in two mutually orthogonal directions is proposed. The properties of the Talbot

interferometer using amplitude checker grating [1] are studied and its performance is compared with a common configuration based on the cross-type amplitude Ronchi grids [2]. Besides the light output gain further setup attractiveness is related to conducting the automatic fringe pattern analysis guided by recently introduced Hilbert-Huang processing for single exposure two-dimensional grating interferometry [3]. The checker grating self-image deformed by the object under test is resolved into two linear fringe families running in +/-45 deg directions with respect to checker grating lines. Next the separated fringe sets are filtered using automatic selective reconstruction aided by enhanced fast empirical mode decomposition and mutual information detrending. Finally the Hilbert spiral transform is implemented to retrieve phase maps representing first derivatives of the object phase distribution. Efficient adaptive digital filtering enables analysis of complex patterns without resorting to coherent spatial filtering resulting in complicated and bulky experimental setups [2]. Numerical and experimental studies corroborate the robustness and versatility of the proposed approach.

1. A. Bhattacharya and R.S. Sirohi, Appl. Opt. 36 (1997), 3745-3752.

2. N. Sun, Y. Song, J. Wang, Z.-H. Li, and A.-Z. He, Appl. Opt. 51 (2012), 8081-8089 and references therein.

3. M. Trusiak, K. Patorski, and K. Pokorski, Opt. Express, accepted for publication.

9132-36, Session 8

Displacement measurement with intracavity interferometry

Josef Lazar, Miroslava Hola, Institute of Scientific Instruments of the ASCR, v.v.i. (Czech Republic); Antonín Fejfar, Jirí Stuchlík, Jan Kocka, Institute of Physics of the ASCR, v.v.i. (Czech Republic); Jindrich Oulehla, Ondrej Cip, Institute of Scientific Instruments of the ASCR, v.v.i. (Czech Republic)

We propose and demonstrate a dispacement measurement method based on a detection of an optical standing wave generated within a passive resonant Fabry-Perot cavity. The technique allows evaluating a position of a photodetector moving along the beam axis by detecting the interference maxima and minima of a standing wave. A coherent laser source is locked to a resonant optical frequency of the cavity. Stabilization of the laser to the cavity may be considered as a referencing of the atmospheric wavelength to the mechanical length of the cavity. Experimental verification of the principle shows a good sensitivity to the pattern of the standing wave. The low-loss transparent photodetector reduces partially the quality of the cavity but its motion does not influence the resonance optical frequency. Reduction of losses was achieved thanks to a design as an optimized set of interference layers acting as an antireflection coating.

The authors wish to express thanks for support to the grant projects from the Grant Agency of CR, project GPP102/11/P820, Academy of Sciences of CR, project: RVO:68081731, Ministry of Education, Youth and Sports of CR, project: CZ.1.05/2.1.00/01.0017, European Social Fund and National Budget of the Czech Republic, project: CZ.1.07/2.4.00/31.0016 and Technology Agency of CR, projects: TA02010711, TA0101995, TE01020233.

9132-37, Session 8

A more robust and flexible approach to Laterally Chromatically dispersed, Spectrally encoded Interferometry (LCSI)

Tobias Boettcher, Marc Gronle, Florian Mauch, Wolfgang Osten, Institut für Technische Optik (Germany)

Multiple systems based on different measurement methods are available for optical topography measurements. Many of them are point sensors that require an axial and lateral mechanical scan and therefore lack in terms of speed, flexibility or precision.

Chromatic confocal spectral interferometry (CCSI) is a hybrid measurement method for fast topography measurements without mechanical axial scan. The CCSI method combines the advantages of the interferometric gain and accuracy of spectral interferometry with the robustness and high lateral resolution of confocal microscopy. A one shot measurement is achieved by using chromatically separated foci in the object space and a spectral detection of the broad band signal.

However, this method still yields a single-shot measurement of one single point only. It requires lateral scanning, which induces uncertainty of the overall topography measurement. In this context the Laterally Chromatically dispersed, Spectrally encoded Interferometer (LCSI), a new concept of a single-shot line sensor based on spectral interferometry has been presented [1]. In this design, the spectral separation by a blazed grating leads to an illuminated line of about 1mm length, where every point is spectrally encoded. Thus, the interference signal depends on both, the lateral position and the optical path difference (OPD) induced by the height profile of the specimen. The OPD is usually retrieved from the derivative of the phase term of the signal. In LCSI, for all n pixels of the spectrometer, this derivation leads to a differential equation, in which both, the surface profile as well as its derivative appear as unknowns. The resulting set of linear equations for a single shot measurement therefore features n equations and 2n unknowns. It can be solved, if a raw estimation on the monotonicity of the phase evolution can be derived from a priori information. Based on first order taylor approximation, one gets n-1 additional equations, leading to a underdetermined system of linear equations. At least one additional equation is needed to retrieve a solution. While a solution to this problem based on the integration of some a priori knowledge has been demonstrated before, it is the intent of this contribution to elaborate on possibilities to solve this problem without any a priori information.

The possibility to use a second, slightly shifted measurement as well as an option to introduce a second light source in order to gather the missing information is investigated.

[1] Gronle, M. et al., Laterally chromatically dispersed, spectrally encoded interferometer, Applied Optics 50, 23, 4574-4580 (2011).

9132-38, Session 8

Suppression of frequency noise of single mode laser with unbalanced fiber interferometer for subnanometer interferometry

Radek ?míd, Martin Cí?ek, Bretislav Mikel, Institute of Scientific Instruments of the ASCR, v.v.i. (Czech Republic); Josef Lazar, Institute of Scientific Instruments of the ASCR (Czech Republic); Ondrej Cip, Institute of Scientific Instruments of the ASCR, v.v.i. (Czech Republic)

Generation of the length etalons and measurement of length of passive Fabry-Perot cavities or their displacement is limited by vibration of mirrors, thermal fluctuations, speed of lock-loops and by the noise and by the linewidth of the laser source. The linewidth of the laser should be below the linewidth of the passive cavity modes to lock the laser to the cavity. For typical 100 mm long Fabry-Perot cavity with finesse from 2000-100000s we can reach MHz to kHz linewidth of the cavity modes which corresonds to 10-11-10-8 relative uncertainty or 1pm-1nm accuracy.

We are presenting a method of noise suppression of laser diodes by unbalanced Michelson fiber interferometer. The unstabilized laser source is represented by compact planar waveguide external cavity laser module ORION (Redfern Integrated Optics, Inc.) working at 1040.57 nm with < 3 kHz linewidth. We built Michelson interferometer with 1 km fiber spool in one arm of interferometer based on SMF-28 fiber

spool to suppress the frequency noise by fast PI control loop up to 33 kHz of laser injection current modulation. The noise in the control loop will be shown and was measured by two independent methods and compared. Results were similar and clearly showing that the laser noise within the laser linewidth was suppressed in favor of higher Fourier frequencies. We were able to decrease the noise level by -60 dBc/Hz up to 1.5 kHz noise frequency of the laser.

9132-39, Session 8

Mapping a vibrating surface by using laser self- mixing interferometry

Roberto Ocaña Pérez, Teresa Molina, AIDO Instituto Tecnológico de Óptica, Color e Imagen (Spain)

The laser-diode self-mixing technique is a well-known, powerful, very simple and low cost interferometric technique. The typical structure of a laser-diode self-mixing device is made up of a laser-diode, collimation lens and processing unit. In the literature one can find numerous examples of target displacement, fluid flow, velocity, distance and vibration measurements. Regarding vibration measurements, the self-mixing effect has been mainly applied to measure amplitude and frequency in isolated points but it is difficult to find real applications in which this technique is applied to measure the vibrating behavior of a complete surface. The reason for this is due to the speckle pattern that is produced when a laser beam is scattered by a real rough surface. When scanning a surface, speckle introduces large changes in the intensity of the scattered signal captured by the photodiode that drives it sometimes to saturation and thereby failing when measuring the amplitude of the vibration. By programming simple algorithms it is possible to overcome this problem. Here we present measurements of fast vibrating titanium loudspeakers up to 6.8 Khz that show the nodal behavior in the micrometer range. We demonstrate that the limit in the frequency range is set by the sample frequency of the data acquisition device. Results are compared with different optical techniques for mapping vibrating surfaces such as laser triangulation.

9132-40, Session 8

Investigation of baseline measurement resolution of a Si plate-based extrinsic Fabry-Perot interferometer

Nikolai A. Ushakov, Leonid B. Liokumovich, St. Petersburg State Polytechnical Univ. (Russian Federation)

In the last two decades industry and academia are drawing an increasing attention to the optical sensors based on the extrinsic Fabry-Perot interferometers (EFPI). Sensors demonstrating high sensitivity to measurands (temperature, strain, pressure and other physical quantities) and utilizing a miniature sensing elements are designed [1]. Systems based on EFPI generally register an absolute value of cavity length L, unlike the most of the interferometric optical sensors, which in some tasks can suffer from an uncertainty of initial value of the measured quantity.

One of the most promising ideas of measuring L is based on the registration of the EFPI spectral transfer function and its approximation with known analytical function. Various concepts of such approximation were developed and implemented, demonstrating an achievement of baseline measurement resolution about tens picometers [2]. Most of the previous propositions of EFPI sensors utilized an air-gap based sensing element. We propose to place a media with high refractive index inside the cavity, providing greater reflectivities of the mirrors and a smaller optical loss due to reduction of the beam broadening inside the cavity. Hence, one can expect higher accuracies of baseline measurement of such wafer-based interferometer.

Silicon, with its refractive index about 3.5 in 1.55 um spectral band, on the one hand, is an ideal material for investigation of such EFPI scheme, and on the other hand, is widely used in MEMS devices, where precise absolute measurement of geometrical sizes may be important.

Proposed EFPI scheme was tested experimentally. A polished silicon plate of width from 50 to 500 micrometers was squeezed between two fiber FC connectors inside a hollow ceramic tube. This provided refractive coefficients about 16% and divergence of the light beam inside the interferometer less than 3 degrees (instead of 4% and 11 degrees, respectively for air-cavity EFPI). Spectral function I(?) of the interferometer was measured using optical sensor interrogator NI PXIe 4844. The interferometer baseline was found by approximating the measured spectral function with an analytical expression given by proper Airy function S(?,L) (reflectivities, light beam divergence and Si dispersion were taken into account). Therefore, the interferometer baseline L was found as a value at which a minima of residual norm between measured spectrum I(?) and analytical expression S(?,L) for EFPI spectral function was obtained. Signal processing method was similar to the one proposed in [2] and was implemented in LabVIEW, enabling real time measurements of Si wafer thickness.

For Si plates with widths from 50 to 500 microns the standard deviation of interferometer baseline measurement was in the range [5; 15] picometers on temporal intervals about 5 minutes.

1. Fang, Z., Chin, K. K., Qu, R., Cai, H., John Wiley & Sons, Inc., Hoboken, New Jersey, 395-426, (2012).

2. N. Ushakov, L. Liokumovich, A. Medvedev, Proc. SPIE 8789, 87890Y (2013).

9133-1, Session 1

Si-based plasmonic and graphene modulators *(Invited Paper)*

Volker J. Sorger, Zhuoran Li, Sarah K. Pickus, Chenran Ye, The George Washington Univ. (United States)

One of the key devices that convert electronic signals into high bit-rate photonic data is the electro-optic modulator (EOM). Its on-chip design plays an important role for the integration of electronic and photonic devices for various types of applications including photonic computing and telecommunication. Recently, indium tin oxide (ITO) and graphene have attracted significant attention primarily due to their extraordinary electro-optic properties for the design of ultra-compact EOMs to handle bandwidth and modulation strength trade-off. Here we experimentally demonstrate a high-performance ITO-EOM in a plasmonic silicon-on-insulator hybrid design. Results show that ITO is capable of changing its extinction coefficient by a factor of 136 leading to 3?-short devices with an extinction ratio of about 1dB/?m. Further numerical device optimizations demonstrate the feasibility for an extinction ratio and on-chip insertion loss of about 6 dB/?m and 0.25 dB, respectively, for a sub-wavelength compact (0.78 ?) EOM design using ITO. Utilizing graphene as an active switching material in a similar ultra-compact plasmonic hybrid EOM design yields enhanced light-matter interaction, in which extinction-ratio is 9 times larger than the insertion-loss for a 0.78 ? short device. Both ITO and graphene EOMs are capable of broadband operations (>500 nm) since no resonator is deployed.

9133-2, Session 1

Hybrid III-V/silicon lasers *(Invited Paper)*

Peter Kaspar, Christophe Jany, Alban Le Liepvre, Alain Accard, Marco Lamponi, Dalila Make, Guillaume Levaufre, Nils Girard, François Lelarge, Guang-Hua Duan, III-V Lab. (France); Jean-Marc Fédéli, Ségolène Olivier, Antoine Descos, Badhise Ben-Bakir, Sonia Messaoudène, Damien Bordel, Sylvie Menezo, CEA-LETI (France)

Silicon photonics is currently attracting scientists of various fields by the prospect of low-cost, compact circuits that combine photonic and microelectronic elements on a single chip. Notably, in the communication market it can address a wide range of applications from short-distance data communication to long-haul optical transmission. However, in order to fully exploit the advantages of photonic integration, a practical integrated light source is required. Since silicon and germanium-based sources are still in their infancy, hybrid approaches using III-V semiconductor materials are currently pursued by several research laboratories in academia as well as in industry. We will briefly review some of the various approaches and then focus on devices based on a vertical optical mode transfer between silicon-on-insulator (SOI) waveguides and guides formed in bonded III-V semiconductor layers.

In our approach of hybrid III-V/silicon integration, unstructured indium phosphide (InP) dies or wafers are bonded, epitaxial layers facing down, on an SOI waveguide circuit wafer. This step does not require precise alignment. Then the InP growth substrate is removed, and the III-V epitaxial film is processed. III-V waveguides are formed, aligned by lithography on top of SOI waveguides, and tapers are introduced in a way that forces the fundamental mode to pass from one layer to the other. This mode transfer guarantees a good confinement factor in the gain material and allows for efficient light amplification. On the other hand, it allows the use of mature silicon photonics components such as Bragg mirrors, waveguide couplers, ring resonators, arrayed waveguide gratings (AWG), etc.

In this paper we will outline the fabrication process of our hybrid components based on wafer bonding. We will present some of the most interesting results from devices such as wavelength-tunable lasers and AWG lasers. The good performance demonstrates that an efficient mode transfer can be achieved between III-V and silicon waveguides and encourages further research efforts in this direction.

9133-3, Session 1

Resonance energy transfer: a new paradigm for improving energy efficiency in hybrid PVs and LEDs *(Invited Paper)*

Pavlos G. Lagoudakis, Univ. of Southampton (United Kingdom)

No Abstract Available

9133-4, Session 1

Nonlinear silicon organic hybrid (SOH) photonics *(Invited Paper)*

Juerg Leuthold, ETH Zürich (Switzerland); Christian Koos, Wolfgang Freude, Robert Palmer, Dietmar Korn, Luca Alloatti, W. Heni, Karlsruher Institut für Technologie (Germany); Christian Schindler, Fachhochschule Jena (Germany); David Hillerkuss, Karlsruher Institut für Technologie (Germany)

Organic materials combined with strongly-guiding silicon waveguides open the route to a new nonlinear photonic platform – the silicon organic hybrid platform. This platform has already proven its versatility in demonstrating 100 GHz bandwidth electro-optic modulators, lowest power liquid crystal phase modulators or all-optical nonlinear devices. In this paper we first review the platform and then comment on our most recent results with SOH modulators demonstrating 100 Gbit/s operation with femtojoule per bit operation or liquid-crystal phase-shifters with voltage-length product as low as VϖL = 0.06 Vmm.

9133-5, Session 2

Towards a strained germanium micro-bridge laser *(Invited Paper)*

Richard Geiger, Paul Scherrer Institut (Switzerland); Martin J. Süess, Christopher B. Bonzon, ETH Zürich (Switzerland); Jacopo Frigerio, Giovanni Isella, Daniel Chrastina, Politecnico di Milano (Italy); Jérôme Faist, Ralph Spolenak, ETH Zürich (Switzerland); Hans C. Sigg, Paul Scherrer Institut (Switzerland)

Tensile strain is an exciting option to induce a direct band gap in germanium (Ge) for the realization of a semiconductor laser compatible with silicon-microelectronics. It could enable the integration of on-chip optical interconnects and the implementation of ultimate powerful opto-electronic circuits and devices without the complexity of combining silicon (Si) with the popular but chemically incompatible group III-V laser materials. However, the required strain levels are enormous (> 4.5% is needed for uniaxially applied stresses) but, as will be shown, can regularly be realized using a novel top-down micro fabrication tech-nology applied on wafer scale.

We will describe the recently developed technology [1,2] to strain semiconductor layers and will discuss the progress and remaining challenges for realizing an efficient Ge-laser for integration in Si-CMOS technology.

1. Minamisawa, R. A. et al., Nat Comms 3, 1096 (2012).
2. Süess, M. J. et al., Nature Photonics 7, 466 (2013).

9133-6, Session 2

Optimized design of an electrically pumped germanium laser

Mathias Prost, Institut d'Électronique Fondamentale (France) and STMicroelectronics (France); Moustafa El Kurdi, Abdelhamid Ghrib, Sébastien Sauvage, Institut d'Électronique Fondamentale (France); Frederic P. Aniel, Institut d'Electronique Fondamentale (France); Nicolas Zerounian, Institut d'Électronique Fondamentale (France); Isabelle Sagnes, Grégoire Beaudoin, Lab. de Photonique et de Nanostructures (France); Frédéric Boeuf, Charles Baudot, STMicroelectronics (France); Philippe Boucaud, Institut d'Electronique Fondamentale (France)

Germanium is a promising candidate to provide a monolithic integration of a laser source for silicon photonics. This material is fully compatible with CMOS production environment thus making possible a large-scale integration for future on-chip photonic devices. The key to obtain optical gain in germanium is to combine n-type doping, to reduce the splitting between the conduction indirect and direct valleys and to lift the valence band degeneracy by introducing tensile strain.

We present a design of a germanium-based laser under electrical injection with enhanced performances. We choose to use a double heterostructure between germanium and the injection barrier layers (Ge/Si or Ge/GaAs), which provides a homogenous injection inside the n-type doped germanium. This structure helps to fulfill the population inversion more easily. We use finite element simulations of electrical transport to study different kinds of double heterostructures in order to evaluate the necessary current density to provide optical transparency of germanium. The effect of doping concentration, band discontinuities and strain amplitude on the optical transparency is studied. Highly-doped capping layers help to reduce the current density threshold, but it remains very high (850kA/cm2). The use of tensile-strained germanium is essential to reduce this threshold. For a biaxial strain of 1.25%, it is reduced by two decades with a moderately doped germanium layer.

Furthermore we propose a realistic structure that can achieve lasing condition. The proposed waveguide design can operate under electrical injection with a strained germanium layer. The strain is transferred through a silicon nitride stressor. We show that under-etching can enhance the strain in the germanium layer. Depending of the topology, these structures could provide a tensile strain from 0.3 to 0.8% for the germanium inside a thicker stack of capping layer.

9133-7, Session 2

New strategies to improve Eu light emission in SI-based matrices

Giorgia Franzò, Istituto per la Microelettronica e Microsistemi (Italy); Gabriele Bellocchi, Univ. degli Studi di Catania (Italy); Simona Boninelli, Maria Miritello, Fabio Iacona, Istituto per la Microelettronica e Microsistemi (Italy)

A promising approach to obtain light emission from Si-based materials is represented by rare earth (RE) doping. Among the different rare-earths, a considerable attention has been devoted to Eu, because it can exist as divalent and trivalent ion and both of them can act as emission centers in the visible range when incorporated in a suitable host matrix.

In this work we have studied the structural, chemical and optical properties of Eu-doped Si oxycarbide (SiOC) and SiO2 thin films synthetized by RF magnetron sputtering. These matrices are fully compatible with Si technology; moreover SiOC presents itself an emission in the visible related to the presence of Si-C bonds and we can therefore hypothesize that an energy transfer from the matrix to Eu ions could occur increasing the emission efficiency of the RE.

When Eu is incorporated in a SiO2 matrix, we observe light emission from both Eu2+ and Eu3+ ions, owing to a proper tuning of the thermal annealing process used for the optical activation of the rare earth. However, the photoluminescence efficiency of both ions remains relatively low and quite far from the requirements for technological applications, mainly due to the extensive formation of Eu-containing precipitates. A detailed study by transmission electron microscopy allowed us to analyze and elucidate the clustering process and to find suitable strategies to minimize it. We found that the substitution of the SiO2 matrix with a SiOC film allows to obtain a very bright light emission centered at about 440 nm from Eu2+ ions. In fact, SiOC is able to efficiently promote the Eu3+-Eu2+ reduction; furthermore, Eu ions are characterized by an enhanced mobility and solubility in this matrix, and as a consequence, Eu precipitation is strongly reduced. Through a control of the annealing conditions and by varying the Eu concentration, it is possible to obtain a continuous shift in the 400-600 nm range of the luminescence peak. Moreover, our data demonstrate that an increase of the luminescence intensity at 440 nm accounting for about a factor of 15 can be obtained in Eu-doped films in comparison with undoped SiOC. We have also found evidences of the occurrence of an energy transfer mechanism between the SiOC matrix and the Eu2+ ions which, by increasing the efficiency of photon absorption for exciting wavelengths shorter than 300 nm, further contributes to increase the optical efficiency of Eu-doped SiOC layers. Finally, by growing on a Si substrate a bi-layer structure composed of two SiOC films doped with different Eu concentrations, it has been possible, through a proper choice of the annealing conditions, to take advantage of the dependence of the photoluminescence peak position on the Eu concentration, so that an intense white emission has been obtained at room temperature.

All of these findings constitute a relevant progress towards the realization of efficient Si-based white light sources, which can be of great interest for applications in photonics or in solid-state lighting.

9133-9, Session 2

Erbium-doped spiral amplifiers with 20 dB gain on a silicon chip

Sergio A. Vázquez-Córdova, Edward H. Bernhardi, Kerstin Wörhoff, Sonia M. García-Blanco, Markus Pollnau, Univ. Twente (Netherlands)

We report the fabrication and optical characterization of long, spiral-shaped erbium-doped aluminum oxide (Al2O3:Er3+) channel waveguides for achieving high overall signal amplification on a small footprint. Al2O3:Er3+ films with Er3+ concentrations in the range between 0.44?3.1?10^20 cm-3 were deposited by reactive co-sputtering onto standard, thermally oxidized silicon substrates [1] and ridge channel waveguides were structured into the films by chlorine-based reactive ion etching [2]. Spiral-shaped waveguides were designed to operate in single mode at both, the pump and signal wavelengths. In the current design, each spiral waveguide occupies an area of 1 cm2. Background propagation losses were quantified by analyzing on an infrared picture the intensity decline of scattered light along the propagation direction of the spiral-shaped waveguides. Typical background propagation losses at 1320 nm are (0.2±0.1) dB/cm for TE mode excitation.

For the gain measurements, a commercially available, pigtailed diode laser at 976 nm was employed as the pump source. By use of a fiber-based wavelength-division multiplexer, pump and signal were combined and the fiber end was directly butt-coupled to the waveguide. The erbium-doped waveguide amplifiers were characterized in the small-signal-gain regime with a launched signal power of 0.6 μW at the peak-gain wavelength of 1532 nm in Al2O3:Er3+. Signal enhancement was detected with an InGaAs detector via lock-in amplification,

or separately with an optical spectrum analyzer. Several spiral-shaped waveguides were studied for each doping concentration. A maximum of 20 dB of internal net gain was measured for a 24.5-cm-long spiral waveguide with an Er3+ concentration of 0.95?10^20 cm-3. Similar results were obtained for a shorter spiral of 12.9 cm length with an Er3+ concentration almost twice as high (2.1?10^20 cm-3). Samples with lower concentration exhibited lower gain because of insufficient pump absorption, while samples with higher concentration showed less gain because of migration-accelerated energy transfer up-conversion and, more importantly, a fast quenching process. Agreement of the experimental results with the advanced amplifier model [3] recently developed in our group is observed over a large concentration range. This result confirms that our model is a suitable tool for the design of Al2O3:Er3+ waveguide amplifiers.

[1] K. Wörhoff, J.D.B. Bradley, F. Ay, D. Geskus, T.P. Blauwendraat, and M. Pollnau, "Reliable low-cost fabrication of low-loss Al2O3:Er3+ waveguides with 5.4-dB optical gain", IEEE J. Quantum Electron. 45, 454-461 (2009).

[2] J.D.B. Bradley, F. Ay, K. Wörhoff, and M. Pollnau, "Fabrication of low-loss channel waveguides in Al2O3 and Y2O3 layers by inductively coupled plasma reactive ion etching", Appl. Phys. B 89, 311-318 (2007).

[3] L. Agazzi, K. Wörhoff, and M. Pollnau, "Energy-transfer-upconversion models, their applicability and breakdown in the presence of spectroscopically distinct ion classes: A case study in amorphous Al2O3:Er3+", J. Phys. Chem. C 117, 6759-6776 (2013).

9133-10, Session 2

Rare earth silicon oxynitrides for silicon light emitting devices

Joan Manel Ramírez, Univ. de Barcelona (Spain); Jacek Wojcik, McMaster Univ. (Canada); Yonder Berencén, Bernat Mundet, Univ. de Barcelona (Spain); Peter Mascher, McMaster Univ. (Canada); Blas Garrido Fernandez, Univ. de Barcelona (Spain)

Solid state lighting provides several advantages compared to incandescent lamps or fluorescent tubes as it offers a competent technology platform with superior energetic efficiency and reduced greenhouse gas release [1]. Nowadays however, the vast majority of multicolour displays and LEDs consist of discrete devices made from expensive epitaxial GaN-related compounds that emit in the blue or UV with a wavelength converting phosphor coating. Also, alternative device technology platforms such as organic LEDs are becoming increasingly important, offering good efficacy and high performance in large area displays. However, these technologies are still expensive and require several fabrication steps when integrating the electronic drivers. In that line, Silicon-based LEDs have become an attractive platform as it offers full integration capabilities using only the CMOS technology. Rare earth-doped Silicon LEDs in particular, although still far from commercial lighting devices in terms of efficacy, present better Lumens per dollar ratio and higher versatility of implementation as they do not require phosphor coatings. Therefore, a much simpler pixel cell is foreseen as only a rare-earth doped active layer is needed, providing an ideal scenario to compete with organic LEDs as large area displays [2].

In this work, we perform a comprehensive study of rare-earth doped Silicon LEDs by using three different dopants (Ce, Tb and Eu) in different silicon oxynitride matrices. The electrical properties and the transport mechanisms as a function of the matrix composition will be discussed, as well as the optical properties such as the luminous efficacy, colour rendering index, colour temperature and external quantum efficiency of devices. Finally, more complex device architectures using a multilayer approach will be proposed to enhance device performance and reliability.

[1] E. Fred Schubert and Jong Kyu Kim, Science 308, 127 (2005).

[2] T. Roschuk, J. Li, J. Wojcik, P. Mascher, and I. D. Calder, Silicon nanocrystals 2010 WILEY-VCH Verlag GmbH & Co. KGaA, Weinheim

9133-11, Session 3

Ge/Si avalanche photodiode

Léopold Virot, STMicroelectronics (France); Laurent Vivien, Institut d'Électronique Fondamentale (France); Yann Bogumilowicz, Jean-Michel Hartmann, CEA-LETI-Minatec (France); Jean-Marc Fedeli, CEA-LETI (France); Delphine Marris-Morini, Eric Cassan, Institut d'Électronique Fondamentale (France); Charles Baudot, Frédéric Boeuf, STMicroelectronics (France)

It has been previously shown that Ge on Si Separate Absorption Charge Multiplication (SACM) avalanche photodiodes can compete with their III-V counterparts. By benefiting from the low multiplication noise of Si and the high absorption efficiency of Ge at telecom wavelength, such photodiodes offer high performances in terms of bandwidth and sensitivity. We present here mesa-type vertically illuminated Ge/Si SACM avalanche photodiodes fabricated on 200mm wafers fabrication line. The primary responsivity of the photodiode is estimated over 0.2A/W at 1550nm and gain over 30 is achieved. The reproducibility of such photodiode with the employed process is very good and makes it clear candidate for high performance applications with a reduced cost compared to III-V equivalents.

9133-12, Session 3

impact of optical crosstalk on monolithic integrated SOA-PIN for access network

Kamel Merghem, Lab. de Photonique et de Nanostructures (France); Christophe Caillaud, Nicolas Chimot, III-V Lab. (France); Anthony Martinez, Guy Aubin, Lab. de Photonique et de Nanostructures (France); Mohand Achouche, III-V Lab. (France); Abderrahim Ramdane, Lab. de Photonique et de Nanostructures (France)

Optical networks have emerged as a solution to constantly increasing throughput demands. New generations of high speed passive optical networks at 10 Gb/s are currently being deployed and the next generation at higher bit rates (25 and 40 Gb/s) is under study. High sensitivity photodectectors like avalanche photodiodes (APD) and optically preamplified detector are key components for next generation access network to meet the optical budget at 25 and 40 Gbit/s.

The major limitation with optical networks is crosstalk, which results from optical network and devices imperfections (imperfect filtering or wavelength routing, optical reflections, ...). In this case, optical components are prone to intra-channel and inter-channel crosstalk depending on the coherence and the wavelength difference of the signal and interferers. The impact of optical crosstalk limits devices performances. In this investigation, we study the effect of crosstalk on a new preamplified SOA-PIN detector which integrates monolithically a semiconductor optical amplifier (SOA) and a high speed photodiode. This detector, which presents both a high responsivity of 148 A/W and a wide 3-dB electrical bandwidth (50 GHz), is very attractive for future high speed short reach links. We first compare SOA-PIN performances with a reference APD detector at 10 Gbit/s under controlled optical crosstalk. In the following, performances of the SOA-PIN detector at 40 Gbit/s are investigated and, in particular, the power penalty in the presence of optical crosstalk.

9133-13, Session 3

4-channel photonic integrated transceiver for access networks

Stanislaw Stopi?ski, Warsaw Univ. of Technology (Poland) and Technische Univ. Eindhoven (Netherlands); Pawel Gdula, Michal M. Nawrot, Pawel Szczepa?ski, Warsaw Univ. of Technology (Poland); Xaveer J. M. Leijtens, Technische Univ. Eindhoven (Netherlands); Ryszard Piramidowicz, Warsaw Univ. of Technology (Poland)

Currently observed trends in research and development of optical telecommunication networks show that the standards are changing dynamically. The increase of bandwidth requirements, driven by broadening of service offer and number of users forces dynamic evolution of the access systems. Simultaneously, the obvious trend to reducing the installation and maintenance costs results in increased requirements for more compact, energy saving and cost-optimized elements, with higher efficiency and reliability.

The solution for the above mentioned demands is anticipated in the photonic integration technologies, which in the past few years have been a field of extensive studies, including both development of fabrication processes as well as design tools and environment. As a result, nowadays two semiconductor platforms, based on indium phosphide (InP) and silicon compounds, offer access to the multi-project wafer (MPW) runs, in which complex, application specific photonic integrated circuit (ASPIC) can be fabricated.

In this work a 4-channel, wavelength division multiplexed (WDM) transceiver for application in optical access systems is presented. It was designed in a generic approach and two versions of the devices were manufactured in MPW runs. The fabrication process makes use of an InP technology and supports following building blocks: deeply and shallowly etched waveguides, semiconductor optical amplifiers (SOAs), electro-optic phase modulators (EOPM) and PIN diodes.

The transmitter part makes use of four SOA sections (500 ?m of length) in Fabry-Perot resonators. Single wavelength generation is granted by a filtered feedback scheme of operation, as part of the power is coupled out of the resonator, filtered by integrated AWG (arrayed waveguide grating) multiplexer and fed back to the laser cavity. The output CW signal is driven by Mach-Zehnder modulators and multiplexed by another AWG to a single waveguide. The modulators are built with MMI (multi-mode interference) power splitters/couplers and phase shifters (2.3 mm of length). The receiver part is constructed with four PIN diodes and an AWG demultiplexer. All of the AWGs have the channel spacing of 200 GHz (1.6 nm) and the central wavelength ?c = 1550 nm. The chips have the dimensions of 4.6 mm x 4.0 mm and were anti-reflection coated.

The fabricated samples were characterized with respect of their applicability to fiber-optic communication systems. Single wavelength operation of lasers was recorded with the output CW power of -8.7 dBm and side mode suppression ratio over 40 dB. The threshold current for all four lasers is around 20 mA. Multi-channel operation was also observed with the power imbalance up to 3.7 dB and SMSR better than 40 dB. The measured static extinction ratio of modulators reaches 42 dB and the driving voltage is V_{ϖ} = 4.9 V.

The transceiver presented in this work combines the advantages of the InP technology, such as low power consumption, multichannel operation and integration of transmitter and receiver functionality in a single chip. It is complemented with reasonably good optical properties of the device, such as spectral characteristics of the lasers and extinction ratio of the modulators. Altogether, this makes this device suitable for application in modern access networks.

9133-14, Session 3

Design, integration and testing of a compact FBG interrogator based on a AWG spectrometer

Andrea Trita, Univ. Gent (Belgium); Garrie Vickers, Optocap Ltd. (United Kingdom); Iker Mayordomo, Fraunhofer-Institut für Integrierte Schaltungen (IIS) (Germany); Dries Van Thourhout, Univ. Gent (Belgium); Jan P. Vermeiren, Xenics NV (Belgium)

A novel, very compact interrogator for Fiber Bragg Grating (FBG) sensors is designed and demonstrated based on an optimized Arrayed Waveguide Grating (AWG) filter with 128 channels

The AWG response is tailored such to achieve large cross-talk between the output channels, which allows simultaneous detection of multiple FBG peaks, using centroid signal processing techniques, without constraints on the minimum FBG peak spectral width.

The measured interrogator resolution is 2.5 pm and the total measurement range is 50nm. The device is fabricated in Silicon on Insulator (SOI) platform, and has a footprint of only 2.2 x 1.5 mm.

The integration with 128 pixel InGaAs array is made by Au stud flip-chip bonding. The spectrometer signals are further integrated and processed in a Readout circuit (ROIC) based on an integrating transimpedance amplifier.

The external electronics are based on a small footprint CPLD for the ROIC sequence, ADC operation and temperature control of the PIC and SLED.

The wireless part is controlled with a microcontroller taking care about the wireless communication and the wireless power management.

The complete embedded unit, including temperature controlled SLED, circulator and all fiber optic splices, is realised in 100 mm diameter 7 mm thick premold, which can be embedded together with the fiber chain.

9133-15, Session 3

Fully CMOS compatible photonics integrated on silicon substrates

Zhiyong Li, Institute of Semiconductors (China); Xi Xiao, Wuhan Research Institute of Posts and Telecommunications (China); Anastasia Nemkova, Yude Yu, Jinzhong Yu, Institute of Semiconductors (China)

Photonic integrated circuits on silicon substrates can be fully compatible with CMOS processes, which is recently presented and demonstrated by the help of 8-inch commercial foundries in Chinese homeland. The effects of CMOS processes on SOI based photonics are estimated for improving fabrication of on-wafer testable silicon photonics. The measurements on fully CMOS photonic integrated circuits are shown too, which includes highly efficient light coupling with insertion loss of ~2 dB between grating waveguides and optical fibers, high-speed optical modulation with 3-dB bandwidth of almost 40 GHz and reverse bias of less than 4 V, and 4-port low power consumption optical switching with cross-talk of less than -20 dB and extinction ratio of more than 15 dB.

Except that, a novel idea in this work shows that a depletion mode PN junction based optical modulator is also can be operated as a high-speed photodiode under a special reverse bias of 5 - 9 V, at a broad wavelength arrange covering C-band, which means that there is no need to employ other special fabrication processes in CMOS foundries, for an example of special dopants such as Si+ or Au+ in optical waveguides, or other materials such as germany or III-V hybrid on silicon substrates for optical detectors. The optical detection in this novel photodiode benefits from the resonance of a microring or microdisk, which enhances the electronic field intensity of

propagating modes in SOI waveguides. The optical signals with data rates of more than 3.35 Gbit/s are transformed into electronic outputs, observed on screen of a sampling oscilloscope. And this function can also be used to monitor wavelength drift of a micro-resonator at different reverse biases. These results indicate a potential alternative to traditional information transportation technology in optical fiber communication systems, and novel optical interconnects on/off chips in future.

9133-16, Session 4

Packaging challenges for integrated silicon photonic circuits *(Invited Paper)*

Nicola Pavarelli, Jun Su Lee, Peter A. O'Brien, Jun Su Lee, Tyndall National Institute (Ireland)

Cost effective packaging of silicon photonic devices presents a significant bottleneck to commercialisation of the technology. One way of addressing this packaging challenge is to use techniques that have been developed by the electronics industry and which also benefit from the use of advanced electronics assembly equipment. Even packaging processes such as fibre coupling can benefit from this approach, along with the hybrid integration of devices such as electronic components (eg. modulator driver ICs). In this presentation, we will present developments made by our group towards achieving scalable fibre and electronic packaging processes that rely on electronic assembly techniques such as flipchip assembly. We will also provide an overview of packaged prototypes being developed within our group for telecom and sensing applications and how these packaging technologies are now being made available to users through the ePIXfab foundry service.

9133-17, Session 4

Active polarization independent coupling to silicon photonics circuit

Jan Niklas Caspers, Univ. of Toronto (Canada); Lukas Chrostowski, The Univ. of British Columbia (Canada); Mohammad Mojahedi, Univ. of Toronto (Canada)

As an alternative to polarization diversity for integrated silicon photonics circuits, where the circuit is duplicated two times for the two orthogonal fiber polarization modes, we propose to use an on-chip active polarization controller for recovering a single TE polarization. Our realized system consists of a 2D grating coupler which serves as the input to a Mach-Zehnder Interferometer (MZI). The MZI was realized using two 2x2 adiabatic couplers.

We couple a number of linear polarization states from a polarization maintaining fiber (PMF) into the silicon photonics circuit using a focusing 2D-grating coupler. A linear polarization state propagating in a PMF has a degree of freedom in terms of the orientation of the electric field (the angle ? in the Poincaré-sphere), or equivalently the amplitude distribution between the fast and slow mode of the PMF. In a 2D-grating coupler, the light is coupled into the TE-mode of two silicon waveguides independent of its input polarization. The polarization state of the light in the PMF determines the waveguide into which the light is coupled, as opposed to the waveguide polarization. Thus a 2D-grating coupler can be considered as a converter of the polarization degree of freedom to an amplitude distribution between the two waveguides. Thermal tuning of an MZI can then be used to couple an arbitrary power distribution of two waveguides into a single output waveguide.

For fabrication, we used e-beam lithography and reactive ion etching (RIE) to define the 2D-grating couplers, the adiabatic 2x2 couplers and the silicon waveguides, using a 220 nm thick SOI wafer. The output of the MZI was coupled to PMFs using two focusing 1D-grating couplers and then measured. For ease of fabrication, the lengths of the two arms of the MZI have an offset of 100 μm and thermal tuning was achieved using a stage-mounted Pelletier element.

A number of linear polarization states were coupled to the 2D grating couplers and the output of the 1D-grating couplers was measured. It was faster to change the input polarization state than to tune the temperature of the sample. Therefore, we opted to heat our sample to a temperature T and set the wavelength of the laser at 1.55 μm. We then adjusted the input polarization state using a ?/2 and ?/4 until we obtained a maximum extinction ratio between the two outputs. By repeating this experiment at different temperatures, we were able to get maximum coupling to a specific 1D-grating coupler for more than 20 linear polarization states. We achieved > 31 dB extinction independent of the input polarization and the standard deviation of the output of the grating coupler 1 was less than 0.62 dB.

We also used the device in the reverse direction (the 2D-grating as output, one 1D-grating as input) and showed that it is possible to tune the output polarization continuously between the two orthogonal fiber polarization by heating the sample.

In summary, we have experimentally demonstrated the possibility of coupling an arbitrary linear polarization state from a fiber to the TE-mode of a single waveguide in an integrated silicon photonics circuit with less than 0.62 dB standard deviation and an extinction ratio larger than 31 dB. Thus, the device can serve as an alternative to polarization diversity to reduce the footprint of integrated circuits. Our device can also be used, in reverse, to create an arbitrary output polarization state; moreover, if a modulator is used instead of thermal tuning, more advanced schemes of information encoding using polarization would become available.

9133-18, Session 4

A transfer matrix description of fibre-coupling into the silicon-on-oxide platform for integrated photonic circuits using polarization diversity couplers

Lee B. Carroll, Dario Gerace, Ilaria Cristiani, Lucio C. Andreani, Univ. degli Studi di Pavia (Italy)

In order to support the development of complete models of integrated circuits, we develop a transfer matrix description of a Polarization Diversity Coupler, which is a low-cost, CMOS-compatible, and industrially scalable device capable of coupling light from an elliptically-polarized telecom fiber-mode into Silicon-on-Insulator (SOI) waveguides. A Polarization Diversity Coupler is essentially a square section of a Photonic Crystal Array matching the footprint of the nearly normally incident fiber-mode, which acts to diffract that mode, with high efficiency, into two (nearly) orthogonal SOI waveguides leading away from the coupler and towards the rest of the photonic circuit. Using just two independent variables, we develop a transfer matrix description of this coupling that accurately describes the polarization dependence of the coupling efficiency into these two waveguides, and so also the mean coupling efficiency (polarization-averaged) and the polarization dependent loss. The two variables in the transfer matrix are fitted to 3D finite difference time domain (3D-FDTD) simulations of CMOS-compatible Polarization Diversity Couplers designed for the standard 220nm SOI platform. Our simple matrix description follows the results of these 3D-FDTD calculations over a 20dB range of coupling efficiency, and also perfectly fits the magnitude and trigonometric form of the calculated oscillatory polarization dependent losses. Combining our transfer matrix for the Polarization Diversity Coupler with existing transfer matrices of other integrated active and passive components, such as filters, semi-conductor optical amplifiers (SOAs) and Mach-Zehnder modulators (MZMs), allows the ensemble transfer matrix for entire photonic circuits, such as passive optical networks (PONs), to be developed. The transfer matrix description can even be extended to describe the losses in coupling efficiency due to fibre misalignment with respect to the fixed geometry of the lithographically-etched Polarization

Dependent Coupler. This will be a useful input for optimizing alignment procedures in industrially-scaled packaging of Si-photonic circuits.

9133-19, Session 4

Adiabatic optical bus for long-range coupling between silicon photonic waveguides

Anthony P. Hope, Thach G. Nguyen, Andrew D. Greentree, Arnan Mitchell, RMIT Univ. (Australia)

Arguably the most important element within integrated circuits is the quality of interconnects. With proposed devices increasing in complexity and the density offered by CMOS fabrication, strong and reliable connections between functional blocks is a key to the success of these technologies. We present a new, planar approach that enables robust coupling between arbitrary pairs of well separated waveguides across a chip, potentially bypassing intermediate waveguides and structures. This new technique presents opportunities for waveguide routing and device topologies that cannot be achieved using traditional evanescent coupling.

Thin ridge silicon waveguides, support a guided TM mode, but this mode leaks power from the waveguide core appearing as unguided TE radiation. This loss mechanism arises due to polarisation conversion that occurs at the ridge sidewalls [1] and can be controlled through interference between these sidewalls and underlying unbound TE slab radiation modes [2]. We have shown that this loss mechanism can be used as a transfer path, as the radiation modes are common to all waveguides etched into the slab. This provides an exciting possibility of performing long range transfer between multiple waveguides without restricting the geometry to nearest neighbour interactions [3].

Strong excitation of radiation modes can be problematic. Light may leak into other devices and sidewall roughness can incur scattering losses and affect the modal properties. These issues are resolved by suppressing the excitation of this radiation by using a counter-intuitive adiabatic technique referred to as Coherent Tunnelling Adiabatic Passage (CTAP) [4]. The advantage of CTAP being that although the slab radiation modes can be used for long-range communication, they are never occupied, and hence the transport is insensitive to the loss mechanisms affecting the radiation modes.

Using EigenMode Expansion (EME) simulations we demonstrate control over the strength of the TM/TE coupling by placing semi-radiating waveguides on a common slab. The slab walls are truncated to track a single discrete TE radiation slab mode. Moving the waveguide provides periodic coupling due to the sinusoidal nature of the slab mode. With a method for controlling the TM/TE interaction, a suitable counter-intuitive coupling sequence can be realised.

This paper will present our insights into the key challenges and current progress towards the fabrication of these proposed devices in a standard planar CMOS processing setting. This new coupling platform shows promise in realising some of the unusual topologies required for quantum optics experiments that have only been conceivably possible in 3D fabrication through the use of optical fibres or direct write technologies. Some of these opportunities and the steps towards their realisation will also be discussed.

[1] T. Nguyen et al., PTL. 21, 486–488 (2009)

[2] N. Dalvand et al., Opt. Express 19, 5635–5643 (2011)

[3] A. P. Hope et al., Opt. Express 21, 22705-22716 (2013)

[4] A. D. Greentree et al., Phys. Rev. B 70, 235317 (2004)

9133-21, Session 5

Chip-scale microresonator frequency combs and femtosecond pulse generation *(Invited Paper)*

Tobias J. Kippenberg, Ecole Polytechnique Fédérale de Lausanne (Switzerland)

No Abstract Available

9133-22, Session 5

Demonstration and analysis of Pockels effect in strained silicon

Pedro A. Damas, Xavier Le Roux, Eric Cassan, Delphine Marris-Morini, Nicolas Izard, Institut d'Électronique Fondamentale (France); Alain Bosseboeuf, Institut d'Électronique Fondamentale (France); Thomas Maroutian, Philippe Lecouer, Laurent Vivien, Institut d'Électronique Fondamentale (France)

Silicon photonics is being considered as a key integration platform for the future, mainly for the reduction of photonic system costs and the increase of the number of functionalities on the same integrated chip by combining photonics and electronics. Moreover, silicon is also a promising material for a wide range of nonlinear optical processes due to its strong optical confinement and large third order nonlinearities. Several impressive works have been reported in the last few years including wavelength and format conversions, signal regeneration, time-division demultiplexing, modulation instability, tunable delay.

However, silicon is a centrosymmetric crystal which inhibits second-order nonlinear optical effects. Nevertheless, this limitation can be overcome by depositing a stress overlayer (typically SiN) on silicon to strain the crystal lattice and break its symmetry. In this case, Pockels effect is enabled, allowing light modulation in silicon at speeds that are not limited by carrier transport and driven at much lower power consumption.

In the present work, we experimentally demonstrate the Pockels effect in a silicon waveguide strained by a SiN overlayer deposited by PECVD. For the referred device, we measured a nonlinear coefficient chi(2) = 146 pm/V, corresponding to a change of effective index of neff = 1.9E-5 under a voltage of 30V.

To complement this study, we also propose a new atomistic model on how the strain effects in the silicon lattice relate to the chi(2) coefficient, arising from the deformation of the crystal lattice. This model allows us to formulate a figure of merit which can be used to simulate and compare the strain effects on the optical phenomena in different structures. This opens the door for a wide variety of parameter optimization and performance improvements of the strained devices.

9133-23, Session 5

Quasi-phase-matched four-wave-mixing of optical pulses in periodically modulated silicon photonic wires

Spyros Lavdas, Univ. College London (United Kingdom); Jeffrey B. Driscoll, Richard R. Grote, Richard M. Osgood, Columbia Univ. (United States); Nicolae-Coriolan Panoiu, Univ. College London (United Kingdom)

We demonstrate that the conversion efficiency (CE) of quasi-phase-matched (QPM) four-wave-mixing (FWM) of optical pulses propagating in periodically modulated silicon photonic nanowires is significantly enhanced as compared to that achievable in uniform waveguides. Our analysis is based on a comprehensive theoretical model that accurately describes the propagation of optical pulses in silicon photonic

nanowires whose transverse cross-section varies adiabatically along the waveguide. In particular, phenomena such as free-carriers generation, two-photon absorption, and self-phase modulation, as well as modal frequency dispersion up to the fourth-order, are taken into account. Due to its relevance to practical applications, the main focus of our work has been on characterizing the extent to which the waveguide and optical pulse parameters, including the pulse width (T), peak power (P), and the second- (?2) and fourth-order (?4) dispersion coefficients, affect the FWM CE. In particular, we have considered a seeded QPM FWM configuration in which a pump pulse with Pp=200 mW, Tp=500 fs, ?p=1.8 ?m, ?2,p<0, and ?4,p<0 and a seeded signal with Ps=Pp/10=20 mW, Ts=500 fs, and ?s=1.59 ?m are launched and co-propagate in a silicon nanowire with sinusoidally modulated width. To achieve efficient FWM, the average width of the waveguide (w0=805 nm) is designed so that the pump and the signal have the same group velocity, whereas the period of the modulation of the width (?=2.96 mm) is chosen to cause the pump, signal and idler (?i=2.074 ?m) pulses to be phase-matched. Our numerical simulations demonstrate that under these circumstances a CE-enhancement of 21 dB, as compared to the case of a constant width waveguide, can be achieved. We anticipate that the results of this work will inspire future experimental studies of nonlinear optical signal processing and light amplification at chip scale and guide the design of novel ultra-compact nonlinear photonic devices.

9133-24, Session 5

Nonlinear response of SiGe waveguides in the mid-infrared

Luca Carletti, Christelle Monat, Ecole Centrale de Lyon (France); Pan Ma, Barry Luther-Davies, The Australian National Univ. (Australia); Darren D. Hudson, Steve J. Madden, David J. Moss, The Univ. of Sydney (Australia); Mickael Brun, Pierre R. Labeye, Sophie Ortiz, Sergio Nicoletti, CEA-LETI (France); Christian Grillet, Ecole Centrale de Lyon (France)

The mid infrared (mid-IR, wavelength range between 2 and 10?m) is of great interest for a huge range of applications such as medical and environment sensors, security, defence and astronomy.

Silicon-on-insulator (SOI) has recently attracted significant interest as a potential material platform for integrated optical devices for the mid-IR. However, the increasing absorption of the silica cladding layer of the SOI platform at wavelengths above 3.5?m may become an issue for applications. Furthermore, it has recently been shown that, under some experimental conditions, e.g. using picosecond pulses, nonlinear losses in the mid-IR can be significant. The free carriers generated by multi-photon absorption can have an important effect due to free-carrier absorption (FCA) and thus limit some applications for which a strong nonlinear response is required, such as supercontinuum generation. It is therefore crucial to explore other material platforms. In this context, SiGe alloys on Si have been suggested as an advantageous alternative platform to SOI for mid-IR since lower propagation losses and higher nonlinear response have been predicted. We have already demonstrated SiGe waveguides with record low propagation losses, which range between 1.5dB/cm at a wavelength of 3.25?m and 0.5dB/cm at 4.75?m. The waveguides were obtained depositing 1.4μm Si0.6Ge0.4 layer by reduced pressure-CVD on a 200mm silicon wafer and structured by reactive ion etching to realize the waveguide core. The ridge is then encapsulated with a 12μm silicon cladding layer. In this work we experimentally measure the nonlinear transmission and self-phase modulation (SPM) of our SiGe/Si waveguides using picosecond pulses at wavelengths between 3 and 5?m. Asymmetric and blue-shifted SPM spectra associated with a drop in the waveguide transmission as the input intensity increases indicate a strong impact of FCA induced by multi-photon absorption process. The nonlinear parameters of SiGe are estimated by fitting the experimental results to standard theory.

9133-25, Session 5

Self pulsation and chaos in sequence of ring resonators

Massimo Borghi, Mattia Mancinelli, Lorenzo Pavesi, Univ. degli Studi di Trento (Italy)

Silicon microresonators are the main building blocks of optical networks on chip. This is due to their capability to route narrowband WDM channels at sub-nanosecond speed rate with exceptionally low losses. Sequences of coupled resonators are also attracting due to their applications as optical buffers and delay lines. The most implemented configurations are the Coupled Resonator Optical Waveguide (CROW) geometry and the Side Coupled Integrated Spaced Sequence of Resonators (SCISSOR) geometry. It is well known that, at high powers near 1550 nm, significant Two Photon Absorption (TPA) can occur. TPA activates thermal and free carrier nonlinearities in silicon, which in turn may switch the resonator state from stable to bistable and even self pulsed as the excitation power increases. The periodic self pulsing of a single cavity has received growing attention in the last years, but only few theoretical works exist on the dynamics of a sequence of coupled resonators. Most models focus only on Kerr type nonlinearities, neglecting thermal and free carrier effects, which are dominating at continuos wave (CW) operation. In this work, we studied theoretically and experimentally the instabilities of a SCISSOR integrated on a Silicon On Insulator (SOI) wafer under thermal and free carrier nonlinearities. We showed that the effect of the cavity coupling is to add a new turbolent regime which was lacking in isolated resonators. Even if optical turbolences, in isolated rings, have been theoretically predicted under Kerr nonlinearities, the extremely small ratio between the Kerr and the thermo optic coefficient have precluded any direct experimental observation. Here, the optical intra cavity feedback overcomes this limitation, enabling the instauration of chaotic regimes in presence of thermal effects. The influence of the input power and of the input wavelength on the onset of chaotic oscillations is investigated with the tool of the reconstructed phase space density. To systematically study how the device parameters modify the power threshold for chaos and the distribution of the regions of instability, we modeled a three cavity system. Starting from standard temporal coupled mode theory, we performed a stability analysis which allows to map the maximum Lyapunov exponent as a function of the input power and the key device parameters. Precise configurations, which maximize the stability of the chaotic regions and the complexities of the associated output waveforms, are found. Furthermore, we discussed how we could implement the chaotic signals as a seed for the generation of all optical random bit sequences. To overcome the main limitation of the device, which is the slow time variation of the signal seed (MHz regime) set by the thermal inertia, we show how the engineering possibilities of silicon photonics can be used to realize a more complex network which combines the turbolences of four SCISSOR to obtain a new seed with an increased high frequency content.

9133-26, Session 6

40 Gbit/s silicon modulators fabricated on 300 mm SOI wafers

Delphine Marris-Morini, Institut d'Électronique Fondamentale (France); Charles Baudot, STMicroelectronics (France); Jean-Marc Fédéli, CEA-LETI (France); Diego Perez-Galacho, Gilles Rasigade, Institut d'Électronique Fondamentale (France); Sonia Messaoudène, CEA-LETI (France); Aurélie Souhaité, STMicroelectronics (France); Melissa Ziebell, Institut d'Électronique Fondamentale (France); Pierrette Rivallin, Ségolène Olivier, CEA-LETI (France); Paul Crozat, Institut d'Électronique Fondamentale (France); David Bouville, Institut d'Electronique Fondamentale (France); Sylvie Menezo, CEA-LETI (France); Frédéric Boeuf, STMicroelectronics (France); Laurent

Vivien, Institut d'Électronique Fondamentale (France)

We present experimental results of silicon modulators based on carrier depletion fabricated on 300mm-SOI wafers available in large-scale microelectronic foundries. Mach Zehnder modulators based on 950 μm-long phase shifters using lateral pn diode or interleaved diodes have been characterized. A 3 dB optical bandwidth of 20 GHz is obtained for the interdigitated phase shifter while 26 GHz is obtained for the lateral pn phase shifter. This difference can be explained by larger capacitance and access resistance of the interdigitated diodes phase shifter. However these values indicate a proper design of the diode design (RC contribution) and RF electrodes. Both devices have been demonstrated working at 40 Gbit/s with extinction ratio of 8 dB. Total on-chip losses were 4.9 dB for the Mach Zehnder modulator based on the lateral pn diode phase shifter and 4 dB for the interdigitated diode phase shifter, at the high speed operating point. Ring modulators are also working at 40 Gbit/s, with 3 dB extinction ratio. This last result is mainly limited by the EDFA operating wavelength required for the high-speed measurements. Further optimization to still increase device performances will be discussed.

9133-27, Session 6

A silicon Mach-Zehnder comb switch for low power operation in on-chip optical data communications

Luis Sanchez, Antoine Brimont, Univ. Politècnica de València (Spain); Sergio Lechago, Amadeu Griol, Universitat Politecnica de Valencia (Spain); Pablo Sanchis, Univ. Politècnica de València (Spain)

High speed operation and low power consumption are the driving forces behind using silicon photonic technology for boosting on-chip optical data communications in next generation data centers and high performance computing systems. Under this scenario, optical switching is one of the core functionalities in which minimizing the power consumption per single switch is especially important. In this work, a silicon comb switch based on an asymmetric Mach-Zehnder interferometric (MZI) structure is proposed and experimentally demonstrated for low power operation. The asymmetry, which is based on introducing a length difference between the MZI arms, is exploited to achieve a comb switching performance thus reducing the power consumption per channel with respect to a conventional symmetric MZI-based switch. For the experimental validation, a silicon switch to operate in ITU standard channels 33 to 36 has been designed and fabricated. Active performance is achieved by means of the thermo-optic effect. The optical signals of the four input wavelengths are multiplexed and externally modulated with a lithium niobate modulator. The modulated signals are then demultiplexed, decorrelated by applying different delays between them, multiplexed back and injected in one of the ports of the silicon switch. The output switched signals are finally coupled out of the chip and separated with a demultiplexer for simultaneously measuring the eye diagram and bit error rate (BER) for each channel. Error free performance is demonstrated through the four channels at bit rates of 10, 20 and 30 Gbits/s showing therefore the potential for reaching up to 120Gbit/s data stream switching performance. Furthermore, a power penalty below 0.5dB is measured as the bit rate increases from 10Gbit/s to 20Gbit/s. The power consumption improvement is also analyzed as a function of the bit rate and experimentally demonstrated.

9133-28, Session 6

Ge quantum-well waveguide modulator at 1.3 um

Mohamed Said Rouifed, Delphine Marris-Morini, Papychaya Chaisakul, Institut d'Électronique Fondamentale (France); Jacopo Frigerio, Giovanni Isella, Daniel Chrastina, Politecnico di Milano (Italy); Samson Edmond, Xavier Le Roux, Jean René Coudevylle, David Bouville, Laurent Vivien, Institut d'Électronique Fondamentale (France)

Silicon photonics has generated an increasing interest in recent years as both microelectronics and telecommunications can benefit from the development of low cost and high performance solutions for high-speed integrated optical links. For short distances and high volume applications, energy consumption of the optical transmitter and receiver is a major concern. Ge rich Ge/SiGe quantum wells (QW) are of particular interest to achieve compact, efficient and low power consumption electro-absorption modulators. In this paper we report performances of Ge quantum well (QW) waveguide modulator working at 1.3 μm. The structure was grown by Low-Energy Plasma-Enhanced Chemical Vapor Deposition (LEPECVD) . An operating wavelength of 1.3 μm was obtained by the use of strain engineering. The active region consists of 20 Ge/Si0.25Ge0.65 QW's on Si0.21Ge0.79 relaxed virtual substrate (VS). 3μm width and 50μm long device was fabricated and characterized. Extinction Ratio (ER) up to 6 dB is obtained. ER of 4 dB with insertion loss of 3dB is also demonstrated. We studied also the integration of the modulator on Silicon-On-Insulator (SOI) platform, by the reduction of the buffer thickness. We performed some simulations using eigenmode expansion method to study the coupling between the Si waveguide and the Ge/SiGe QW active region, in order to design an integrated modulator on SOI. High ER (7.7 dB) and low insertion loss (4 dB) can be achieved using 10 QW in the active region. The energy consumption is estimated as low as 59fJ/bit.

9133-29, Session 6

Ultra-compact modulators using novel CMOS-compatible plasmonic materials

Viktoriia E. Babicheva, Technical Univ. of Denmark (Denmark); Nathaniel Kinsey, Gururaj V. Naik, Marcello Ferrera, Purdue Univ. (United States); Andrei V. Lavrinenko, Technical Univ. of Denmark (Denmark); Vladimir M. Shalaev, Alexandra Boltasseva, Purdue Univ. (United States)

We analyze several multilayer structures with alternative plasmonic materials to be utilized in ultra-compact, CMOS-compatible plasmonic modulators. Various materials are studied as constituent building blocks of the investigated geometries including different dielectrics (silicon nitride, silicon, zinc oxide) and plasmonic materials such as transparent conducting oxides (TCOs) and titanium nitride. The usage of titanium nitride in modulator configurations allows achieving significantly increased modulation depth. Furthermore, transparent conducting oxides may serve as a dynamic element, and the efficient modulation is achieved by tuning the carrier concentration in a transparent conducting oxide layer into and out of the plasmon resonance with an applied electric field. The resonance significantly increases the absorption coefficient of the modulator, which enables larger modulation depth. Numerous modulator layouts are investigated and the typical trade-off between compactness and propagation loss is analyzed. We define figure of merit and discuss results for the absorption coefficient and mode size as functions of the carrier concentration in the TCO layer. We show that an extinction ratio of 46 dB/μm can be achieved, allowing for a 3-dB modulation depth in only 65 nm at telecommunication wavelength. We investigate the integration of the best performing modulator with plasmonic waveguides, and analyze its performance in terms of coupling losses and integration possibilities. The proposed approach is based on cost-effective planar fabrication processes and therefore multilayer structures can be integrated with existing plasmonic and photonic waveguides as well as novel semiconductor-based hybrid photonic/electronic circuits. The ability to easily integrate with existing semiconductor systems could enable new devices for applications in on-chip optics, sensing, optoelectronics, data storage, and information processing.

9133-30, Session 7

High-density silicon optical interposer for inter-chip interconnects *(Invited Paper)*

Takahiro Nakamura, Yutaka Urino, Photonics Electronics Technology Research Association (Japan); Yasuhiko Arakawa, The Univ. of Tokyo (Japan)

One way to overcome the bandwidth bottlenecks in computer systems is to realize high-speed and low-power-consumption bus systems. For realizing these bus systems, the Photonics-electronics convergence system that we proposed is an important concept for inter-chip interconnects. Specifically, our concept is based on the technique of "System in Package (SiP)," in which a number of bare LSI chips are enclosed on a single silicon optical interposer. Therefore, it will be useful for reducing size and supporting multiple functions. We have developed the high-density silicon optical interposer and their composed optical devices for the Photonics-electronics convergence system. In this paper, we present these composed optical devices, such as silicon modulator, germanium (Ge) photodiode, and light source integration, and a high-density silicon optical interposer integrated with them.

Compact and high-speed EO/OE converters are necessary to achieve a high-density silicon optical interposer. For an EO converter, we have developed a forward-biased pin-diode Mach-Zehnder modulator, which has side-wall grating waveguides on 250-?m-length phase shifters, with a pre-emphasis modulation method. This combination can realize high modulation efficiency at high speed. We achieved 50 Gb/s operation in push-pull configuration. For a high-efficiency and high-speed OE converter, we have developed a silicon waveguide-integrated PIN Ge photodiode with a low dark current density and low-applied-bias-voltage operation. The fabricated PIN Ge-PDs showed good photoresponsivity and low dark current density with high speed operation of 40 Gb/s. To minimize the total length and hence losses of waveguide lines on the interposer, the on-chip sources can be located near the modulators. In our case, butt-coupled arrayed lasers are integrated on a silicon substrate of SOI with a passive alignment technique and flip-chip bonding, to provide enough optical output power for power splitting, and to facilitate heat dissipation for high power operation.

The silicon optical interposer was fabricated on a 4.7 mm ?4.5 mm substrate based on each component device, which was adjusted at 20-Gbps operation. A trident SSC array, a 1?4 optical splitter, an optical modulator array, and a PD array were all monolithically integrated onto a single silicon substrate. A 13-channel arrayed LD chip was integrated onto the substrate as a hybrid structure, and these optical components were optically linked to each other via the silicon optical waveguide array. The eye data of the PD output on the silicon optical interposer was measured at 20-Gbps NRZ with a 27-1 pseudo-random binary sequence (PRBS) via the 1?4 optical splitter. The clear eye opening was achieved and it suggests that the optical links were capable of data transmission at 20 Gbps. The bit error rates (BER) for the 20-Gbps PRBS were measured. We confirmed that the BER was less than 10-12 when the PD input power was more than -5 dBm. Error-free transmission at 20 Gbps via the 1?4 optical splitter was therefore successfully achieved. The total footprint was 0.0677 mm2 per channel, meaning that we could achieve a bandwidth density of 30 Tbps/cm2 with a channel line rate of 20 Gbps.

9133-31, Session 7

Ge quantum well optical interconnection integrated on bulk silicon

Papichaya Chaisakul, Delphine Marris-Morini, Univ. Paris-Sud 11 (France); Jacopo Frigerio, Daniel Chrastina, Politecnico di Milano (Italy); Mohamed-Said Rouifed, Univ. Paris-Sud 11 (France); Stefano C. Cecchi, Politecnico di Milano (Italy); Paul Crozat, Univ. Paris-Sud 11 (France); Giovanni Isella, Politecnico di Milano (Italy); Laurent Vivien, Univ. Paris-Sud 11 (France)

We propose and experimentally validate an innovative approach to monolithically integrate Ge quantum well photonic interconnections on silicon substrates. We experimentally show that Ge-rich Si1-xGex virtual substrates (VS) can act as a passive optical waveguide on which a low temperature (< 450°C) high quality epitaxial growth of Ge quantum wells can be performed, realizing active optical planar circuitry on a bulk silicon wafer. As a proof of concept, the photonic integration of a passive Si0.16Ge0.84 waveguide and two Ge/SiGe multiple quantum well (MQW) active devices, an optical modulator and a photodetector, was realized by using a single epitaxial growth step. A Si0.16Ge0.84 VS was engineered to meet the two conflicting requirements of (i) being a waveguide with minimized optical loss at the operating wavelength of the quantum-confined Stark effect (QCSE) modulator based on Ge/Si0.16Ge0.84 MQWs (Ge mean fraction of ~ 92%), and (ii) forming a VS with minimized lattice mismatch to the MQW stack to ensure a high quality epitaxial growth. We will present low-voltage and broadband Ge quantum well interconnects integrated on bulk silicon chips, confirming that Ge quantum well interconnects are feasible for low-voltage broadband optical links integrated on silicon chips. Our approach can be extended to any kind of Ge-based optoelectronic devices working within telecommunication wavelengths as long as a suitable Ge concentration x is selected for the Ge-rich Si1-xGex VS.

9133-32, Session 7

Microring based ratio-metric wavelength monitor on silicon

Ao Shen, Bing Yang, Ting Hu, Ting ge Dai, Zhejiang Univ. (China); Chen Qiu, Huawei Technologies Co., Ltd. (China); Yu bo Li, Yinlei Hao, Xiaoqing Jiang, Jianyi Yang, Zhejiang Univ. (China)

An integrated high-resolution ratio-metric wavelength monitor is demonstrated on SOI platform. The device consists of a reconfigurable demultiplexing filter based on cascaded thermally tunable microring resonators and Ge-Si photodetectors integrated with each drop channel of the resonator. The microring resonators are supposed to achieve specific resonant wavelength spacing to form the "X-type spectral response" between adjacent channels. The ratio of the dropped power between adjacent channels varies linearly with the wavelength in the "X-type spectral" range thus the wavelength can be monitored by investigating the dropped power ratio between two pre-configured resonant channels. The functional wavelength range and monitor resolution can be adjusted flexibly by thermally tuning the resonant wavelength spacing between adjacent rings, an ultra-high resolution of 5pm or higher are achieved while the resonant spacing is tuned to 1.2nm. By tuning the resonant wavelength synchronously, the monitor can cover the whole 9.6nm free spectral range with only two ring channels. The power consumption is as small as 8 mW/nm. We also demonstrate the multi-channel monitor that can measure multi-wavelength-channel simultaneously and cover the whole FSR by preset the resonant wavelengths of every microring resonators without any additional power consumption. The improvements to increase the resolution are also discussed.

9133-33, Session 7

Fabrication of high-density pitch adapters by laser ablation

Francisco Rey-García, Consejo Superior de Investigaciones Científicas (Spain) and Univ. de Santiago de Compostela (Spain); Carmen Bao-Varela, Eliseo Pérez, Univ. de Santiago de Compostela (Spain); Pablo Rodríguez, The Univ. of Manchester (United Kingdom) and Univ. de Santiago de Compostela (Spain); Abraham Gallas, Univ. de Santiago de Compostela (Spain);

Germán F. De La Fuente Leis, Consejo Superior de Investigaciones Científicas (Spain)

High Energy Physics experiments make extensive use of microstrip silicon sensors for tracking purposes [1]. The high granularity of the modern detectors makes the connection between the segmented sensor channels and the readout electronics very complex. Furthermore, due to the mismatch between the sensor pad pitch and the electronics a direct connection is not possible in most of the cases. To solve this problem, customized pieces known as “pitch adaptors” need to be produced.

Usually, in industry, a metallic layer with thickness ranging from 1 to 5 ?m is deposited onto a glass or ceramic substrate. Later this metallic layer is segmented through a photolithographic process, making a bus of electric channels where each one carries the electric signal from one sensor channel to a dedicated readout channel in a readout ASIC (Application Specific Integrated Circuit) [2]. This photolithographic process implies the manufacturing of masks and several steps, including resin deposition and chemical etching. This is thus a slow and expensive method, for prototyping stage. A new method for the fabrication of pitch adapters in which the high-density metal traces are manufactured by means of laser ablation of the metal layer deposited on top of a substrate is presented [3].

The laser-ablation method induced desorption process [4], performed on a previously metal-evaporated substrate. Glass, polymeric (kapton) ceramic (Al2O3) and silicon materials were explored as substrates with different metallization configurations. These substrates were irradiated with a nanosecond Nd:YVO4 laser (Powerline E, Rofin) emitting at a wavelength of 1064 nm. The laser equipment used provides CAD-like software that allows cutting different shapes.

This procedure is faster, simpler and cheaper than photolithography for prototyping or low volume production. A metal-on-glass prototype has been successfully manufactured, tested electrically, bondability and metrology. Results were consistent with high quality PA’s produced through photolithography [2].

9133-34, Session 7

An inter- and intra-chip optical interconnect using a hybrid plasmonic leaky-wave nano-antenna

Vahid Ebrahimi, Leila Yousefi, Mahmoud Mohammad-Tahri, Univ. of Tehran (Iran, Islamic Republic of)

Recently photonic integrated circuits (PIC) have attracted researchers because of their different applications and advantages in optical networks, coherent transceivers, lab-on-chip, and etc. Albeit the electric circuits which are connected to each other by via, different parts of a PIC should be connected through optical interconnect. In the past few years, researchers among the world have proposed different methods to implement optical interconnect such as polymer waveguide, fiber ribbons, fiber image guide, and free space methods based on lens and mirrors. In the waveguide methods, an optical waveguide is used to connect different part of a chip together. This method can be used only for inter-chip connection, and where all elements are on the same layer. On the other hand, free space optical interconnect uses free space for receiving and transmission of optical signal. Various free space interconnect methods have been proposed such as free space method with lens, mirrors, lasers, splitters and modulators.

In this paper, a new method is proposed to provide inter and intra-chip optical interconnect at the standard telecommunication wavelength of 1550 nm. The proposed interconnect method consists of two novel hybrid plasmonic leaky-wave nano-antennas as transmitter and receiver. The antennas are fed by a plasmonic waveguide carrying the optical signal. This structure is a highly directive nanoantenna with 14.6dBi directivity. For increasing the efficiency of communication links between two interconnect, the directivity of leaky-wave antenna is increased by optimizing the slot configuration. Since the plasmonic waveguides are lossy, the optical signal is first coupled from a silicon waveguide to the hybrid plasmonic waveguide by a coupler with 70% (1.5 dB) coupling efficiency at the standard telecommunication wavelength of 1550 nm. The proposed structure has two important advantages over the previously developed interconnect methods. First, it has a planar structure which makes it fully integrable with the photonic ICs and second, its capability to be used both as inter-chip and intra-chip optical interconnect. The Fluquet theorem and the theory of surface plasmons are used to obtain an analytical model for design purposes, and the method is verified by a 3-dimensional full-wave numerical analysis.

9133-35, Session 8

Subwavelength silicon nanophotonics *(Invited Paper)*

Pavel Cheben, Jens Schmid, Dan-Xia Xu, Jean Lapointe, Siegfried Janz, Martin Vachon, Shurui Wang, National Research Council Canada (Canada); Robert Halir, Alejandro Ortega-Moñux, Carlos A. Alonso Ramos, Juan Gonzalo Wangüemert-Pérez, Iñigo Molina-Fernández, Univ. de Málaga (Spain); Aitor V. Velasco, Maria Luisa Calvo Padilla, Univ. Complutense de Madrid (Spain); Przemek John Bock, Canadian Microelectronics Corp. (Canada); Daniel Benedikovic, Milan Dado, Jarmila Müllerová, Univ. of ?ilina (Slovakia)

A new class of silicon photonic structures and devices have emerged exploiting refractive index engineering by subwavelength gratings. By etching an array of gaps of a pitch smaller than the Bragg resonance length into a silicon waveguide, a nanostructure is formed with an effective index controlled by the grating duty ratio. This way, a wide range of synthetic material refractive indexes can be obtained, thereby circumventing the fundamental constraint of a limited number of materials available in silicon photonics. We discuss the principles, design, fabrication and applications of subwavelength nanostructures in silicon photonics. We show that subwavelength engineering is advantageously used to increase the minimum feature size in photonic circuit design to 100 nm or more, compatible with deep-uv 193 nm lithography typically used in silicon photonic foundries. Practical examples will be presented, including recent advances in high efficiency fibre-chip edge couplers and surface grating couplers, polarization splitters and rotators, dispersion engineered colorless MMI and directional couplers, microspectrometer chips and wavelength multiplexers for data interconnects.

9133-36, Session 8

Filters for passive optical networks (PON) in silicon

Celio A. Finardi, Leandro T. Zanvettor, Ctr. de Tecnologia da Informacao Renato Archer (Brazil); William S. Fegadolli, California Institute of Technology (United States); Antonio C. Gozzi, Roberto R. Panepucci, Ctr. de Tecnologia da Informacao Renato Archer (Brazil)

Fiber-to-the-home (FTTH) strategies are relying on PON (Passive Optical Network) technology due to cost effectiveness (maintenance and operation). Silicon photonics, on the other hand, is emerging as a viable platform for high-volume and high-integration optical front-end devices which could lead to low-cost photonics solutions. There are challenges when trying to meet the technical requirements for PON applications, according to the ITU G.984.5 standard. These requirements have high bandwidth (tens of nm) both downstream (1490 nm and 1550 nm) and upstream (1310 nm), in order to meet emerging applications such as VoD, HDTV, e-Learning, interactive games, to name a few. A key component which assigns the download signal to the ONT and collects the

upload signal from the ONT is a triplexer or WDM filter, which handles in an appropriate way the information in the carrier wavelengths. Our work presents the design of WDM filters for wavelength division multiplexing based on silicon photonics technology for ONT – GPON. The chosen approach is based on the combination of directional couplers (DC) and sections of silicon nanowire with high reflective Bragg gratings. The designs are based on the published specifications from IMEC´s SOI passive foundry technology. The modeling of devices requires waveguide parameter extractions which were carried out using Lumerical Inc.´s Mode tool. To simulate wavelength behavior we used Phoenix Soft ASPIC tool. The layout of the structures was implemented parametrically using the IPKISS open source software platform, developed by Gent University. Devices with nanotaper for edge coupling as well as grating couplers (centered at 1520nm) were tested. The ability to produce high quality reflective Bragg gratings is a challenge in different fabrication technologies. We will present our initial results for photonic integrated circuits (PICs) fabricated by standard CMOS photolithography at the IMEC - foundry through the Europractice consortium, and also through electron-beam lithography. Devices with different coupling parameters were tested, and also a set of grating couplers. Optical measurements were carried out with Amonics ASE light source with bandwidth from 1260-1650nm, and Yokogawa OSA, as well as with an Agilent tunable laser with power meter. Optical coupling is carried out with nanopositioners from Thorlabs with lensed fibers from JaTecnologia for edge coupling, or using standard cleaved fibers for grating coupling. Measured 3-dB bandwidths greater than 30 nm were obtained at 1490 nm and also at 1550 nm, in compliance with ITU requirements. Work is ongoing to package devices using in-house v-groove fiber-array technology.

9133-37, Session 8

A novel wavelength multiplexer/ demutiplexer based on side-port multimode interference coupler

Shile Wei, Jian Wu, Beijing Univ. of Posts and Telecommunications (China); Lingjuan Zhao, Institute of Semiconductors (China); Jifang Qiu, Zuoshan Yin, Beijing Univ. of Posts and Telecommunications (China); Rongqing Hui, The Univ. of Kansas (United States)

Various structures, such as directional couplers, Mach-Zehnder interferometers, arrayed waveguide gratings and multimode interference (MMI) couplers have been proposed to realize MUX/DMUX in the 1.31/1.55 ?m wavelength window. Among them, MMI couplers based on self-imaging are attractive for wavelength splitting due to their advantageous properties of compact size, low excess loss, large fabrication tolerance, etc. Till now, the most compact wavelength splitters based on the principle of MMI coupling used slot waveguides with an MMI section of 119.8 ?m on SOI substrate, and asymmetrical multi-section structures on InP wafer. Disadvantages still exist for these two novel structures. For the slot waveguides structure proposed by J. Xiao, the length of the device is still several times longer than the beat length of the two lowest order modes guided by the MMI waveguide. Meanwhile, with restricted interference structure, the gap between two output waveguides (channels for 1.55 ?m and 1.31 ?m) is much less than the width of the MMI section, thus increasing the difficulty of fabrication. For the asymmetrical multi-section structures proposed by C. Yao, the simulated crosstalk is only 12 dB at 1.31 ?m wavelength with an unacceptable simulated insertion loss of -1.46dB. Besides, the output signal from the 1.31 ?m-channel consists of a large fraction of high order modes. Therefore, the single output loss is expected to be high. In addition, the device structure is asymmetric and unable to be utilized as 1.31/1.55 ?m multiplexers in FTTH communication. The basic working principle of the side-port MMI demultiplexer is based on the self-imaging effect in the multimode section, where the input field profile is reproduced in single or multiple images due to phase of guided modes changing at one side of the multimode section at periodic intervals along the propagation direction of the multimode waveguides. Mackie first described the side-port MMI demultiplexer with the same principle as J. Xiao's. So, the length is very long.

In this paper, a novel side-port multimode interference coupler based 1.31/1.55 ?m wavelength MUX/DMUX with a much reduced device size is demonstrated and analyzed. The gap between two output waveguides (channels for 1.55 ?m and 1.31 ?m) is equal to the width of the MMI section so that S-bends are not necessary, thus relaxing its fabrication accuracy requirement. In addition to SOI, the principle and idea of the design can be applied to various material platforms, such as ?-? integrated circuits (InP or AsGa) and PLC guides. It can also be used to split wavelengths other than 1.31/1.55 ?m. The device can be monolithically integrated with other devices proposed earlier.

9133-38, Session 8

Optomechanical excitation in a WGM ring resonator vertically coupled to a bus waveguide

Fabio Turri, Fernando Ramiro-Manzano, Univ. degli Studi di Trento (Italy); Mher Ghulinyan, Georg Pucker, Fondazione Bruno Kessler (Italy); Lorenzo Pavesi, Univ. degli Studi di Trento (Italy)

In this work we report on the characterization, in the near IR range, of the optomechanical properties of a free-standing Whispering Gallery Mode resonator fully integrated on a silicon chip. The system consists of a 100 ?m diameter SiN ring resonator vertically coupled to a buried SiON bus waveguide. The nominal gap between the ring and the waveguide is of 300?m. The ring indeed, is connected to the pillar by six thin rays (0.6?m width – 0.4?m thickness); this cause the ring to have good mechanical quality factor but bad dissipation properties. Different mechanical vibrations of the ring have been demonstrated. The response of the device, investigated over a wide range of coupled optical powers, shows a dependence of the mechanical deformation of the ring on the optical excitation power. Three main power ranges have been found. In the low power regime, the weak optical probe has been used to characterize the mechanical eigenmodes of the ring. At higher powers (second regime) a direct optical excitation of the mechanical modes has been achieved. Optomechanical coupling has been clearly observed with typical out-of-plane vibrations associated to the particularity of the vertical coupling. An upper threshold of the power has been found for this regime: above this threshold a complex thermomechanical excitation of the ring is observed (third regime). Moreover, in the regime of high powers the ring shows an unstable mechanical deformation, oscillating with a periodic pattern between two configurations. These movements of the ring can be well described as self-vibrations of the system. The main parameters of this vibration can be tuned. An increase/ decrease in the coupled power returns a larger/shorter period: a wide range of period values has been covered, from few ?s to tens of s. During the experiment the laser has been placed on the blue shoulder of the resonance and it has been observed that a variation in the detuning causes a change in the shape of the vibration: the system can be pushed to stay more in a configuration or in the other, i.e. the fraction of period spent by the system in a configuration or in the other depends on the detuning. To confirm the mechanical movement of the ring a specific set up has been implemented: a visible laser probe has been sent towards the ring and the light scattered by the ring has been collimated and detected. With the ring excited by the IR source through the bus waveguide, a variation in the amplitude of the visible scattered light has been observed, confirming the mechanical movement. The different behaviour of the system at high powers is associated to new mechanical properties arising from a complex interplay between the heating of the ring material and the mechanical deformation due to the optical pump-related radiation pressure.

9133-39, Session 9

A complete design flow for silicon photonics

James F. Pond, Lumerical Solutions, Inc. (Canada); Chris Cone, Mentor Graphics Corp. (United States); Lukas Chrostowski, The Univ. of British Columbia (Canada); Jackson Klein, Lumerical Solutions, Inc. (Canada); Jonas Flueckiger, The Univ. of British Columbia (Canada); Amy Liu, Dylan McGuire, Xu Wang, Lumerical Solutions, Inc. (Canada)

Broad adoption of silicon photonics technology for photonic integrated circuits requires standardized design flows that are similar to what is available for analog and mixed signal electrical circuit design. We have developed a design flow that combines mature electronic design automation (EDA) software with optical simulation software.

An essential component of any design flow, whether electrical or photonic, is the ability to accurately simulate large scale circuits. This can be particularly important for photonic circuits because the routing to connect different components requires the introduction of additional waveguide sections, as well as waveguide bends and crossovers which affect the overall circuit performance. The circuit simulations must rely on compact models that can accurately represent the behavior of each component. The compact model parameters must be extracted from physical level simulation and experimental results.

We show how large scale circuits can be simulated in both the time and frequency domains, including the effects of bidirectional and, where appropriate, multimode and multichannel photonic waveguides. We also show how active, passive and nonlinear individual components such as grating couplers, waveguides, splitters, filters, electro-optical modulators and detectors can be simulated using a combination of electrical and optical algorithms, and good agreement with experimental results can be obtained. We then show how parameters, with inclusion of fabrication process variations, can be extracted for use in the circuit level simulations. Ultimately, we show how a multi-channel WDM transceiver can be created, from schematic design to tapeout, using key features of EDA design flows such as schematic driven layout, design rule checking and layout versus schematic.

9133-40, Session 9

How the new optoelectronic design automation industry is taking advantage of preexisting EDA standards

Kevin Nesmith, Silicon Integration Initiative, Inc. (United States); Susan Carver, Silicon Integration Initiative (United States)

With the progress in advanced process nodes down to the 5nm to 7nm levels, the Electronic Design Automation (EDA) industry looks to be coming to the end of advancements, as the size of the silicon atom becomes the limiting factor. Or is it? The commercial viability of mass-producing silicon photonics is bringing about the Optoelectronic Design Automation (OEDA) industry. With the science of photonics in its infancy, by adding these circuits to the ever increasingly complex electronic designs, this will allow for many new generations of growth while bringing great advancements in process design methodologies, low power, reducing thermal output, increasing communication throughput, and adapting new manufacturing requirements. Learning from the past 50 years of EDA's mistakes and missed opportunities, this industry is starting with electronic standards and extending them to become photonically aware. By adapting the use of preexisting standards into this relatively new industry allows for easier integration into the present infrastructure and faster time to market.

OpenAccess, the EDA's de facto standard database for electronic designs, is actively being extended into the photonics realm, allowing for fully integrated optoelectronic designs. Extending OpenAccess has been a good review on finding what standard practices have been overlooked with the electronic implementations. By standardizing on more of these regularly used methodologies, we are making OpenAccess even more interoperable between design environments.

Further work comprises to insure foundry adoption by including their specific needs in the photonics extension. To do this, more existing standards are being borrowed from the EDA industry. By implementing the Open Process Specification (OPS), this allows a standard way for foundries to create Process Design Kits (PDKs) that work hand in hand with the design engineers' OpenAccess databases. The OPS file format is in an easy to use XML/XSD format allowing users direct access to the data from many 3rd party tools and scripting languages. OPS, also includes a standard way to define Pcells that support any vendor specific language in a generic way which allows for multiple vendor support in one PDK deliverable.

This article will review the work Silicon Integration Initiative's Silicon Photonics Technical Advisory Board (SP-TAB) has been doing to advance this very popular database and other electronic standards to the photonics realm, thus allowing for a second generation of advancements in the design automation industry.

9133-41, Session 9

Modeling of PN interleaved phase shifters for high speed silicon modulators

Diego Perez-Galacho, Delphine Marris-Morini, Eric Cassan, Laurent Vivien, Institut d'Électronique Fondamentale (France)

Silicon photonics is nowadays a promising technology for next generation of high-speed optical communications, since it allows for CMOS compatibility and reduced costs when considering massive production. These are requirements for applications like fiber-to-the-home (FTTH), where the cost of the transceiver should be reduced, and optical interconnects, where CMOS compatibility is a must. In this scheme, proper design of silicon modulators is a key point. In order to achieve modulation in silicon technology, free-carrier plasma dispersion (FCPD) effect using either carrier accumulation, carrier injection or carrier depletion in different diode configuration has been widely discussed in literature. Due to their high efficiency and high bandwidth, modulators based on carrier depletion in PN interleaved junctions are of particular interest. Although several experimental demonstrations of such modulators have been reported in the literature [1-3] the modeling of this structure is still a challenge because of properties varying in the 3 directions of the space. In this work, we discuss the modeling of such PN interleaved junctions phase shifters. Different approximations, giving different simulation models are presented and compared. The models vary from fully analytical, where the electrical and optical structures are approximated by analytical functions, to more exact where neither electrical nor optical structures are approximated. Comparison and discussion on the models presented are provided, as well as comparison against experimental data.

[1]: D. Marris-Morini et al, Optics express, 21, 22471 (2013)

[2]: Z-Y. Li et al, Optics express, 17, 15947 (2009)

[3]: X. Xiao et al, Optics express, 20, 2507 (2012)

9133-42, Session 9

Analysis of a polarization-independent cross-slot structure using Fourier Modal Method

Somnath Paul, Jani Tervo, Seppo Honakanen, Univ. of Eastern Finland (Finland)

A cross-slot geometry [1-2] can be depicted as two identical horizontal slot waveguides situated side by side on a same substrate, having a narrow lateral separation, i.e. a vertical slot

between them. A symmetric cross-slot structure can also be viewed as four parallel rails of the same length and identical square cross sections, with each of them having an equal distance from the nearest ones. Considering the direction of wave propagation along the z-axis, the cross section of these four rails forms a 2 by 2 symmetric square array in the x-y plane. The high index rail material is chosen as Silicon, and the low index slot material is selected to be Titanium dioxide ensuring a high index contrast across the slot-rail boundaries. Owing to the waveguide geometry and configuration, along with the aid of the continuity of the normal component of the electric displacement vector across the rail-slot interfaces, both the TE and TM polarized guided modes are equally enhanced and confined within the vertical and horizontal slots, respectively. The structure is optimized for the above mentioned rail dimension with the Fourier Modal Method [3-4], and the optimized slot width is found to be 50 nm. The bottom up fabrication of the nanometer scale horizontal slot (filled with titanium dioxide) is proposed to be done with an atomic layer deposition (ALD) technique. The ALD is a unique deposition method resulting in conformal growth of highly uniform thin films with atomic level control of the film composition and thickness. The 50 nm wide vertical slot can be achieved with electron beam lithography (EBL) followed by reactive ion etching (RIE). The filling of the vertical slot region is also proposed to be done with the ALD method, which reduces the scattering loss by smoothening the surface roughness inherently associated with the RIE [5].

References:

[1] J. V. Galan, P. Sanchis, J. Garcia, J. Blasco, A. Martinez, and J. Marti, “Study of asymmetric silicon cross-slot waveguides for polarization diversity schemes,” Appl. Opt. 48, 2693-2696, 2009.

[2] A. Khanna, A. Säynätjoki, A. Tervonen, and S. Honkanen, “Control of optical mode properties in cross-slot waveguides,” Appl. Opt. 48, 6547-6552, 2009.

[3] J. Tervo, M. Kuittinen, P. Vahimaa, J. Turunen, T. Aalto, P. Heimala, and M. Leppihalme, ”Efficient Bragg waveguide-grating analysis by quasi-rigorous approach based on Redheffer’s star product,” Opt. Commun. 198, 265-272, 2001.

[4] L. Li, “Formulation and comparison of two recursive matrix algorithms for modeling layered diffraction gratings,” J. Opt. Soc. Am. A, 13, 1024-1035, 1996.

[5] T. Alasaarela, D. Korn, L. Alloatti, A. Saynatjoki, A. Tervonen, R. Palmer, J. Leuthold, W. Freude, and S. Honkanen, ” Reduced propagation loss in silicon strip and slot waveguides coated by atomic layer deposition,” Opt. Express, 19, 11529-11538, 2011.

9133-20, Session PS3

Large-scale characterization of silicon nitride-based evanescent couplers at 532nm wavelength

Tom Claes, Roelof A. Jansen, Pieter Neutens, Bert Du Bois, Philippe Helin, Simone Severi, Paru Deshpande, Pol Van Dorpe, Xavier Rottenberg, IMEC (Belgium)

Recently, the photonics community has a renewed attention for silicon nitride [1], [2], [3]. When deposited at temperatures below 650K with plasma-enhanced chemical vapor deposition (PECVD) [4], it enables photonic circuits fabricated on-top of standard complementary metal–oxide–semiconductor (CMOS) electronics. Silicon nitride is moreover transparent to wavelengths that are visible to the human eye and detectable with available silicon detectors, thus offering a photonics platform for a range of applications that is not accessible with the popular silicon-on-insulator platform.

However, first-time-right design of large-scale circuits for demanding specifications requires reliable models of the basic photonic building blocks, like evanescent couplers, which couple power between multiple waveguides. While these models typically exist for the silicon-on-insulator platform, they still lack maturity for the emerging silicon nitride platform. Therefore, we meticulously studied silicon nitride-based evanescent couplers fabricated in our 200mm-wafer facility. We produced the structures in a silicon nitride film deposited with low-temperature PECVD, and patterned it using optical lithography at a wavelength of 193nm and reactive ion etching. We measured the performance of as much as 250 different designs at 532nm wavelength, a central wavelength in the visible range for which laser sources are widespread. For each design, we measured the progressive transmission of up-to 10 cascaded identical couplers, yielding very accurate figures for the coupling ratio and loss.

This paper presents the trends extracted from this vast data set, and elaborates on the impact of the couplers’ parameters on their insertion loss and coupling ratio. Additionally, it extends the treatment of standard evanescent couplers, and presents the design and characterization of symmetrical evanescent couplers that couple power at both sides of a bus waveguide.

We think that the large-scale characterization of evanescent couplers presented in this paper, in excellent agreement with the simulated performance of the devices, forms the basis for a component library that enables accurate design of silicon nitride-based photonic circuitry.

[1] C. H. Henry, R. F. Kazarinov, H. J. Lee, K. J. Orlowsky, and L. E. Katz, “Low loss Si3N4-SiO2 optical waveguides on Si,” Appl. Opt., vol. 26, no. 13, pp. 2621–2624, Jul. 1987.

[2] S. Romero-García, F. Merget, F. Zhong, H. Finkelstein, and J. Witzens, “Silicon nitride CMOS-compatible platform for integrated photonics applications at visible wavelengths,” Optics Express, vol. 21, no. 12, p. 14036, Jun. 2013.

[3] D. J. Moss, R. Morandotti, A. L. Gaeta, and M. Lipson, “New CMOS-compatible platforms based on silicon nitride and Hydex for nonlinear optics,” Nature Photonics, vol. 7, no. 8, pp. 597–607, Jul. 2013.

[4] a Gorin, A. Jaouad, E. Grondin, V. Aimez, and P. Charette, “Fabrication of silicon nitride waveguides for visible-light using PECVD: a study of the effect of plasma frequency on optical properties.,” Optics express, vol. 16, no. 18, pp. 13509–16, Sep. 2008.

9133-43, Session PS3

Influence of waveguide structure on Y-branch splitting ratio

Dana Seyringer, Catalina Burtscher, Fachhochschule Vorarlberg (Austria)

Splitting and combining of multiple optical beams plays an important role in integrated optics. The most obvious way is to use a cascade of one-by-two waveguide branches (so called Y-branches) because these splitters are polarization and wavelength independent, i.e. one device can be used to split optical signals in the whole operating wavelength window. However, the processing of the branching point, where two waveguides start to separate, is technologically very difficult. This generally leads to an asymmetric splitting ratio causing non-uniformity of the split power over all the output waveguides. Although it does not have a significant influence on the splitting properties of 1x2 or 1x4 Y-branches it becomes a dominant factor in the splitting of the 1x16, 1x32 or 1x64 optical signals, leading to a huge rise of the variation in the splitting ratio. Furthermore, such splitters are rather large compared to other splitting approaches.

In this paper we will show that not only processing of branching points strongly influences splitting properties of the device but also the used waveguide structure itself. We will show that optimizing this structure the asymmetric splitting ratio of the optical signal can be drastically suppressed - to one fourth of the original value. This is very important particularly for 1x16, 1x32 or 1x64 Y-branches where the variation in the splitting ratio is very high. Consequently, such splitting ratio improvement leads to the insertion loss reduction; another important splitting parameter. Additionally, based on these results we were also able to reduce the size of the designed Y-branch splitters.

9133-52, Session PS3

Hot eletron-based electrolumiscence from silicon-rich silicon nitride/oxide multilayer light emitting devices

Bernat Mundet, Yonder Berencén, Joan Manel Ramírez, Univ. de Barcelona (Spain); Josep Monserrat, Carlos Domínguez, Ctr. Nacional de Microelectrónica (Spain); Blas Garrido Fernandez, Univ. de Barcelona (Spain)

The development of an efficient Si-based light emitting device has been the cornerstone of intense investigations since the end of last century. This finding would allow the monolithic integration of both electronic and photonic components, which circumvents the current microelectronic bottleneck (i.e. interconnection problems and heat dissipation). Among the variety of Si-based luminescent materials, silicon-rich silicon dioxide (SiOx) and silicon-rich silicon nitride (SiNx) have been the most used in terms of either hosts for rare earth ions or luminescent itself. Although, SiOx present better optical properties than SiNx, the optimal trade-off between electrical and electroluminescent properties is attained by combining both materials.

In this work, we demonstrate the electroluminescence and device operation lifetime enhancement by using an adequate multilayer gate stack design based on both SiOx and SiNx materials, in comparison to a conventional single layer gate stack. In particular, this device design favors the hot-electron injection and thus the electroluminescence by impact excitation. In addition, this multilayer gate stack approach allowed us to separately study the electrical and electroluminescence processes underlying on the physical mechanisms.

9133-57, Session PS3

Optical power distribution through fractal routing

Roelof A. Jansen, Tom Claes, Pieter Neutens, Bert Du Bois, Philippe Helin, Simone Severi, Pol Van Dorpe, Paru Deshpande, Xavier Rottenberg, IMEC (Belgium)

Several applications in integrated optics require an equal distribution of power from a single input port among many photonic components, whether they be projection components or sensors. One method of achieving such a system is through using progressively more tightly coupled evanescent couplers to route power from a single feeding line [1]. While very compact, this approach requires careful design and characterization of evanescent couplers, and is vulnerable to process variations as the ratio of coupling has a non-linear relation to the couplers' gap size.

Fractals are self-similar objects where each section is geometrically similar to its parent. It is well known that fractals are widely present in nature, and they also find applications in various fields [2]. In this paper we propose to use a fractal approach for spreading power evenly over an area using micro-machined photonic waveguides.

In the fractal development, the same 1x2 multimode interference (MMI) coupler splits the power at each fractal stage. This provides several advantages. First, only one power splitter design is needed. Second, MMI's are well known, and more robust to process tolerances than evanescent couplers [3]. Third, they are symmetrical, and therefore provide a theoretically perfect power distribution independent of the fractal depth.

We demonstrate a fractal routing system using MMIs, constructed using recursive techniques. The design contains a 6-deep fractal structure feeding 64 until cells, each containing a 1-to-64 splitter tree to give a total of 4096 outputs. For this demonstrator a chip area of 30mm2 is covered. These designs have been manufactured at imec with a nitride film deposited with plasma-enhance chemical vapor deposition (PECVD), using deep ultra-violet optical lithography (193nm) and reactive ion etching in a 200mm platform optimized for generic photonic applications, which has the added advantage of allowing processing on CMOS substrates. Characterization of the components used at 532nm, as well as a complete fractal system is presented.

We therefore demonstrate that a fractal routing provides a novel way to evenly distribute photonic power over a large area.

[1] J. Sun, E. Timurdogan, A. Yaacobi, E. Shah Hosseini, M. R. Watts, "Large-scale nanophotonic phased array," Nature Letter, Nature 493, 195–199 (10 January 2013)

[2] S. JAMPALA, "Fractals: classification, generation and applications", Circuits and Systems, 1992., Proceedings of the 35th Midwest Symposium on, Page(s): 1024 - 1027, vol.2, 09 Aug 1992

[3] L. B. Soldano, E. C. M. Pennings, "Optical Multi-Mode Interference Devices Based on Self-Imaging : Principles and Applications" , Journal of Lightwave Technology, Vol. 13, No. 4, April 1995

9133-58, Session PS3

Microcrystalline and nanocluster-embedded SiGe-based near-infrared photodetectors deposited by laser-assisted deposition system

Ching-Ting Lee, Min-Yen Tsai, National Cheng Kung Univ. (Taiwan)

In view of the high absorption of CO2 laser by the germane (GeH4) and silane (SiH4) reaction gases [1][2], the laser-assisted plasma enhanced chemical vapor deposition system (LAPECVD) was designed to equip external CO2 laser with the conventional plasma enhanced chemical vapor deposition system (PECVD). Since both the CO2 laser and plasma were simultaneously utilized to decompose the SiH4 and GeH4 reaction gases in the designed LAPECVD system, more Si sources and Ge sources could act as nucleation seed in the deposited SiGe films. Consequently, microcrystalline and nanocluster-embedded SiGe films could be obtained. The microcrystalline and the nanoclusters in the SiGe films deposited using the LAPECVD system were observed by the high resolution transmission electron microscopy. The composition of the deposited SiGe films as a function of the CO2 laser power was examined using an energy-dispersive spectrometer (EDS). The Ge composition in the SiGe films increased with an increase of CO2 laser power. The carrier concentration and carrier mobility of the deposited SiGe films were measured using Hall measurement at room temperature. Carrier mobility more than 60 cm2/V-s at a carrier concentration at an order of 1014 could be obtained. Furthermore, the carrier mobility increased with increasing the CO2 laser power. The obtained high performance SiGe films were used as the absorption layer of p-Si/i-SiGe/n-Si near infrared photodetectors deposited on glass substrates using the designed LAPECVD system. The photoresponsivity and the quantum efficiency of 0.47 A/W and 68.5% were respectively obtained in the SiGe-based near infrared photodetectors. Moreover, the photoresponsivity and quantum efficiency were further improved with an increase of the CO2 laser power.
This work was supported by the National Science Council of Taiwan, Republic of China and the Advanced Optoelectronic Technology Center of the National Cheng Kung University.

9133-59, Session PS3

Efficient split-step time-domain modeling for multi-ring waveguide all pass and add/drop filters

Youngchul Chung, Kwangwoon Univ. (Korea, Republic of)

Ring resonator waveguide devices are widely used for optical filters or delay devices. There have been several analysis approaches such as transfer matrix methods or finite-difference

time-domain (FDTD) methods. The transfer matrix method provides efficient and accurate time-harmonic solutions for various ring waveguide devices such as a CROW (Coupled Resonator Optical Waveguide) or a CRR (Coupled Ring Reflector). The FDTD method provides time-domain solutions for the whole ring waveguide structure directly from Maxwell's equations. Even though the FDTD gives us comprehensive time-domain solutions including transient responses, it consumes large amount of computation time.

In this paper, an efficient split-step time-domain model (SS-TDM) for the ring resonator waveguide devices is presented. In the SS-TDM, the bus and ring waveguides are divided into a number of small subsections having equal length. In the first step, the forward/reverse waves in all the waveguides (bus and ring waveguides) are updated to incorporate the attenuation/gain and phase accumulation through a section during a time step. In the next step, the directional coupling effects between the adjacent waveguides are taken into consideration. The appropriate boundary conditions in the bus and ring waveguides are applied at every time step. The above steps are repeated for the required time window. The accuracy of the SS-TDM is checked by comparing the phase and delay responses as a function of wavelength calculated from the SS-TDM with the transfer matrix analysis results for a single-ring resonator APF. For the phase calculation, the continuous wave with varying wavelengths are launched into the single-ring APF and the output phase is measured for each wavelength. Then the delay time is calculated from the derivative of the phase as a function of wavelength.

The time-domain model is applied to analyze the optical pulse transfer characteristics through single-, double-, and triple-ring APF's. In the single-ring APF, the pulse delay increases as the coupling ratio decreases. On the other hand, the pulse shape distortion becomes worse as the coupling ratio decreases, which comes from the reduction of bandwidth for lower coupling ratio. As the number of rings are increased with optimum coupling ratios, the delay time is found to scale with the number of rings. For the single-ring, double-ring, and triple-ring APF with 100GHz free spectral range, the delay is 140ps, 280ps, and 408ps, respectively. The pulse transfer characteristics through the single-ring and apodized quadruple-ring APF for the chirped pulse are also studied. It is observed that the bandwidth of the APF should be wide enough to minimize the pulse shape distortion especially in the case of the chirped input pulse. The pulse transfer characteristics through the single-ring and double-ring ADFs (Add/Drop Filter) are also studied. The two-dimensional OCDMA (Optical code division multiple access) simulation through an encoder/decoder composed of cascaded add/drop filters connected with delay lines is also performed and some examples are shown. In the above 2-D OCDMA encoder, the code is encoded through the shuffling of wavelengths and phases. With these examples it is shown that the split-step time-domain model is useful to efficiently analyze the pulse transfer characteristics through a variety of ring resonator waveguide devices in detail.

9133-61, Session PS3

Germanium nano-heteroepitaxy on silicon

Hui Ye, Yourui Huangfu, Wenbo Zhan, Xu Fang, Zhejiang Univ. (China)

Heteroepitaxy of Ge on Si is very important for the fabrication of optoelectronics devices nowadays. Ge/Si system is often considered as a prototype for heteroepitaxy growth research. Germanium quantum dots can be used as light sources or even in quantum computing. However, fabricating Ge nanodots faces some challenges, such as improving the homogeneity of size and distribution of dots, decreasing the defect density and achieving a high areal density. The Stranski–Krastanov (S–K) growth of Ge dots on Si uses the 4.2% lattice mismatch between Si and Ge, while high-quality Ge films grown on Si need to eliminate the lattice difference without introducing misfit dislocations. Integration of high-quality Ge films on Si can be used for innovative microelectronic technologies, silicon photonics, as well as highly efficient photovoltaic technologies. Many methods have been developed for heteroepitaxy of Ge dots and films on Si during the past few decades. Indeed, growing Ge on Si substrates with nanoscale patterns is the most promising way. For Ge dot growth, there are nanosphere lithography, electron beam lithography, extreme ultraviolet interference lithography and holographic techniques. For Ge film growth, there are selective epitaxial growth (SEG), epitaxial necking, epitaxial lateral overgrowth (ELO) and aspect ratio trapping (ART) techniques.

As conventional lithography technology is very expensive and has limitations of characteristic size on nanoscale, porous alumina membrane (PAM), with lithography-free hexagonal-aligned patterns, has been widely used for the purpose of fabricating nanoscale materials. We adopted ultrathin free-standing PAM as an etching mask to perform pattern transferring. It can transfer cost-effective, centimeter-scale, sub-100 nm nanopatterns on Si. The variety of pore sizes and aspect ratios are adequate to support lattice-mismatched heteroepitaxy. We transferred the patterns of PAM to pits and SiO2 windows on Si substrates for dot and film growth, respectively. Then, we investigated the epitaxial growth of Ge on Si substrates with these patterns. We successfully achieved high-density hexagonal ordered Ge dots on Si substrates with nano-pits transferred from PAM. Furthermore, high-quality selective epitaxial Ge films on Si with different sizes of SiO2 windows were realized. The defects of SEG and ELO of Ge films grown on these nanopatterns were observed with XTEM and HR-TEM measurements. Ge films with low dislocation densities were achieved by etching the Si surface into Si pits to increase the intermixing of Ge–Si. EPD tests confirm two orders of magnitude lower dislocation densities of SEG Ge compared to directly grown Ge. The shadow-etching technique successfully transferred patterns size from 60 to 20 nm. In 20 nm-scales, we experimentally proved the theoretical prediction of Luryi, that defect-free Ge films can be achieved due to the rapid decay of strain energy density as well as the intermixing of Ge–Si.

9133-62, Session PS3

Low-frequency noise quality testing of germanium concentrator photovoltaic cell with very high efficiency

Zdenek Chobola, Miroslav Lu?ák, Jiri Vanek, Brno Univ. of Technology (Czech Republic); Radim Barinka, Solartec s.r.o. (Czech Republic)

The defects are the natural sources of the excess current and the excess noise and they are responsible for the changes of several measurable quantities. Physical processes in electronic devices can give a useful piece of information on the device reliability provided there is a correlation with failure mechanisms.

This paper deals with comparisons of noise spectroscopy, I-V characteristic and microplasma detection of germanium concentrator photovoltaic (CPV) cell with very high efficiency. Efficiency reaches to 38%. We studied two groups with different technologies (A and B). Each group had 10 samples.

In concentrating photovoltaic a large area of sunlight is focused onto the solar cell with the help of an optical device. By concentrating sunlight onto a small area requires less photovoltaic material to capture the same sunlight as non-concentrating photovoltaic. From these follows smaller space requirements. The optical system comprises standard materials but concentrating light, however, requires direct sunlight rather than diffuse light, limiting this technology.

The noise voltage spectral density was measured in forward biased voltage. The noise voltage being picked up across a load resistance RL=100 ?, at a band mean frequency of 1 kHz and bandwidth of 20 Hz.

When high electric is applied to PN junction with some technological imperfections like dislocation in PN junction or crystal-grid defect causing non-homogeneity of parameters it produces in tiny areas of enhanced impact ionization called

microplasma. Microplasma produced noise, which has random spectrum in frequency range.

Light emission is exhibited in full spectrum range. The whole process is observed with a special CCD camera in a dark special cryogenic box. CCD camera G2-3200 with low noise Kodak chip KAF-3200ME is used for measuring.

The article compares the results from noise spectroscopy, I-V characteristic and microplasma. The evidence suggests that the best results are reached by a group A.

9133-63, Session PS3

Boxlike filter response based on a multimode microdisk resonator

Qingzhong Huang, Juguang Chen, Zhan Shu, Ge Song, Jinsong Xia, Huazhong Univ. of Science and Technology (China); Jinzhong Yu, Institute of Semiconductors (China) and Huazhong Univ. of Science and Technology (China)

We have demonstrated boxlike filter response in a multimode microdisk resonator (MDR) evanescently side-coupled with two bus waveguides. It is revealed that the boxlike filtering is generated by the constructive interference between two indirectly coupled whispering-gallery modes in the MDR. Using nanofabrication processes, multimode MDRs were fabricated and then characterized on a silicon-on-insulator platform. Flat-top passband filtering is observed experimentally with a 3-dB bandwidth of 0.65nm, and an out-off band rejection of 27.10dB. Multimode MDR provides new approach for optimizing the optical filtering device in wavelength division multiplexing systems.

9133-64, Session PS3

Photonic integrated circuit for a mid-IR heterodyne spectrometer

Anton I. Ignatov, Moscow Institute of Physics and Technology (Russian Federation); Mikhail S. Nikitin, JSC "Shvabe-Photodevice" (Russian Federation); Alexander V. Rodin, Moscow Institute of Physics and Technology (Russian Federation) and Space Research Institute (Russian Federation)

Laser heterodyne spectroscopy (LHS) is a powerful method for remote analysis of spectra of atmospheres of the Earth and other planets. The method combines high spectral resolution with high sensitivity. Thus it enables not only studying atmospheric chemical and isotopic bulk composition, but also altitude profiling of minor constituents and even Doppler measurements of the wind speed.

LHS is based on the analysis of beating of a broadband weak IR radiation under study, mixed with an intense, highly stabilized reference radiation of a laser (local oscillator, LO). Then radiofrequency spectra of the beating are analyzed instead of optical-frequency incoming signal.

To date, most of working LH spectrometers have been based on free space optics. Signal and LO beams are combined with, e.g., plate beamsplitters. Alternatively, single mode fiber or integrated optics may be used. Integrating of different optical components as well as detector in a single chip will reduce sensitivity to vibration and thermal effects and decrease size and weight of the spectrometer, making it suitable for space missions. Also waveguides or fibers act as spatial filters matching wavefronts of signal and LO beams when detecting their beating.

Only a few LH spectrometers based on fiber/integrated optics have been implemented, based on silica fibers for near IR and based on hollow waveguides for mid-IR. Integrated and fiber mid-IR optics are being developed rapidly, but effective enough solutions, as for near IR, are not found so far, in particular for waveguides, fiber and waveguide splitters. In this work we present a waveguide beam combiner that is a key element of a PIC for the LH spectrometer under development.

We propose a PIC for mid-IR (lambda = 5.8–10.5um) LH spectrometer, based on semiconductor integrated optics. When choosing waveguides' parameters the requirements are single mode behavior, large cross section, low bend losses. These requirements and known to be contradictory: a single mode waveguide with large cross section must be low contrast which leads to high bend losses. Miniaturization of a PIC of the spectrometer is limited by minimal curvature radii of waveguides and by the requirement of strong enough damping of higher (leaking) modes.

The proposed PIC for the spectrometer is based on single mode (two mode if taking into account mode polarization) rib waveguides made of pure GaAs on the substrate of Al0.3Ga0.7As. Combining of signal and LO radiation from two waveguides in a single waveguide is made with a directional coupler. The size of the PIC is about 20mm x 4mm, cross section of waveguides is 20um x 20um. Computer simulations show that the power splitting ratio of the directional coupler is almost the same for the quasi-TE and quasi-TM modes (for the directional coupler transferring 10% of power of the quasi-TE mode from one waveguide to the other the corresponding fraction for the quasi-TM is between 7.8% and 9.5%). The simulated overall power losses (bend losses and losses in materials of the waveguides and the substrate) are less than 12% for the signal radiation and less than 45% for the LO radiation.

9133-44, Session 10

Coupling light to whispering gallery mode resonators *(Invited Paper)*

Daniele Farnesi, Museo Storico della Fisica e Centro Studi e Ricerche Enrico Fermi (Italy); Giancarlo C. Righini, Museo Storico della Fisica e Ctr Studi e Ricerche Enrico Fermi (Italy); Andrea Barucci, Simone Berneschi, Francesco Chiavaioli, Franco Cosi, Stefano Pelli, Silvia Soria, Cosimo Trono, Istituto di Fisica Applicata Nello Carrara (Italy); Davor Ristic, Maurizio Ferrari, Istituto di Fotonica e Nanotecnologie (Italy); Gualtiero Nunzi Conti, Istituto di Fisica Applicata Nello Carrara (Italy)

Full exploitation of the unique properties of high quality factor micro-optical whispering gallery mode (WGM) resonators requires a controllable and robust coupling of the light to the cavity, either for fundamental investigations or even more for practical applications. Fiber tapers are ideal phase-and-mode-matched couplers and are typically used for lab demonstrations in silica based micro-resonators or for exciting higher order mode WGMs. Prism-based coupling basically adapts to any material and offers improved robustness and reliability for the implementation of devices based on larger resonators. We present the results of our studies on alternative methods based on integrated waveguides and special optical fibers. We focus on approaches involving different waveguide types and configurations and various resonators. We also consider a new method based on fiber gratings for improved robustness in biosensing applications.

9133-45, Session 10

Efficient lasing in Nd:GdVO4 depressed cladding waveguides produced by femtosecond laser writing

Hongliang Liu, Feng Chen, Shandong Univ. (China); Javier R. Vázquez de Aldana, Univ. de Salamanca (Spain)

The Nd:GdVO4 crystal is a widely used gain medium for lasing. Waveguides can confine light in compressed volume, in which high light intensities can be reached. As a result, waveguide lasers may possess reduced lasing thresholds and comparable efficiencies with respect to the bulk systems. In this work, we reported on the waveguide lasers at 1064 nm in femtosecond

laser written depressed cladding waveguides in Nd:GdVO4 crystals.

The Nd:GdVO4 sample was cut into dimension of 8?4?2 mm3. The focused laser beam (120fs, 795 nm, 1kHz repetition rate) scanned the crystal at a constant velocity of 500 ?m/s in the direction paralleled to the 4-mm edge at 150 ?m beneath one of an 8?4 mm2 surfaces, creating a number of low-index tracks. The fabricated structures with diameters of 150 and 30 ?m (WG1 and WG2) guided both TE and TM polarized modes with good transmission property. The propagation losses of TM modes for WG 1 were determined to be as low as ~0.7 and 1.0 dB/cm by the back-reflection method, respectively. The maximum refractive index change ?n for the cladding waveguides was estimated to be 2?10-3 with measurement of the N. A. of the waveguides.

A tunable cw Ti:Sapphire laser, generating a polarized light pump beam at 808 nm, was used as the pump source for the waveguide laser system. At room temperature, the central wavelength of the laser emission from the cladding waveguide was 1064.5 nm, which corresponded to the main fluorescence of 4F3/2?4I11/2 transition in the Nd3+ ions, with a FWHM of ~ 0.6 nm.

From the linear fit of the experimental data, for waveguide WG1 in the Nd:GdVO4 crystals, the maximum output power and lasing thresholds were PWG1,TM ≈ 0.57 W, PWG1,TE ≈ 0.51 W, PTM,th ≈ 190 mW and PTE,th ≈ 195 mW, respectively. Meanwhile, the extracted slope efficiencies of these waveguides were ?WG1,TM ≈ 68% and ?WG1,TE ≈ 63%, corresponding to optical-to-optical conversion efficiency of ?WG1,TM ≈ 55% and ?WG1,TM ≈ 49%, respectively. In addition, the slope efficiency of 68% was close to the quantum defect limit between pump and laser photons of 76%. As for the depressed cladding waveguide WG2, the slope efficiencies were ?WG2,TE ≈ 43% and ?WG2,TM ≈ 36% with maximum output power of 0.35 W and 0.3 W, respectively, which were corresponding to optical-to-optical conversion efficiency of ?WG2,TM ≈ 33% and ?WG2,TM ≈ 26%.

The maximum output power of waveguide WG1 reached 0.57W when the launched power climbs at 1.03 W, which was the largest output power acquired in the depressed cladding waveguide in Nd-doped crystals at the same pumping power to our knowledge. In addition, the diameters of depressed cladding waveguides were comparable to those of multimode fibers suggesting possibility to construct efficient fiber-waveguide laser systems for integrated photonic applications.

9133-46, Session 10

Three port optical circulators with ring resonators

Dirk Jalas, Alexander Y. Petrov, Manfred Eich, Technische Univ. Hamburg-Harburg (Germany)

Optical circulators are devices that can separate incoming and outgoing optical waves. They are important building blocks for photonic systems. Circulators relying on magneto-optical effects can be considerably reduced in footprint by using resonators to increase the interaction between the light wave and the magneto-optical materials. So far, there have been two proposals for such resonator concepts. The first being a photonic crystal defect coupled to three waveguides. The waveguides excite an even and an odd mode in the resonator and create by that a standing wave pattern that is non-reciprocal and creates the desired circulator effect. The second approach is a ring resonator which is side-coupled to two waveguides here each incoming optical wave excites either a clockwise or a counter-clockwise travelling wave which have due to the magneto-optical material different resonance frequencies which again creates the desired circulator properties. Both concepts have advantages, the photonic crystal defect offers more bandwidth compared to the ring resonator but it is difficult to produce such a photonic crystal from a material with strong magneto-optical effect such that the concept so far has only been shown to work in 2D simulations. On the other hand the magneto-optical ring resonators have already been successfully shown in experiment. Here, we present concept that has the same bandwidth efficiency as a photonic crystal circulator but which relies on a ring resonator and thereby is experimentally much easier to realize. We achieve this by side coupling three waveguides to the ring resonator. The desired standing wave pattern which recreates the photonic crystal type circulator spectrum is realized by exciting both the clockwise and counter-clockwise traveling wave through a Bragg reflector. We will present full 3D FEM simulations to prove the validity of this concept.

9133-47, Session 10

Suspended photonic waveguide arrays for submicrometer alignment

Tjitte-Jelte Peters, Marcel Tichem, Urs Staufer, Technische Univ. Delft (Netherlands)

This paper presents the development of suspended and mechanically flexible optical waveguide arrays, which play a key role in a new concept for photonic alignment. This alignment concept aims to provide the small tolerances required by planar chip-to-chip coupling of Photonic ICs (PICs) with a mode field diameter (MFD) in the micrometer range and consists of two steps. In the first step the PICs are passively assembled on a common substrate and then secured, hereby aligning the waveguides with limited precision (<5μm). In the second step, high precision photonic alignment is achieved using alignment functions integrated on one of the PICs. To this end, the PIC is provided with three main functions: mechanically flexible waveguide structures, integrated microactuators and a securing mechanism. The free end of the suspended waveguide array is positioned by the microactuators in order to align the waveguides of both PICs. When the coupled light is maximized (using active alignment), the waveguide array is finally secured in its optimal position. The main expected advantages of the approach are improved precision, higher levels of automation and improved yield.

In this paper the modeling and fabrication results of flexible waveguide structures are presented. The partly flexible waveguides are created on a PIC with Si3N4-core/SiO2-cladding configuration on top of silicon. The flexible part consists of multiple parallel Si3N4 cores embedded in a cladding of SiO2 which, at their free ends, are connected by a crossbar. This flexible part is created by etching through the complete 16μm thick SiO2 cladding by reactive ion etching (RIE). Then, the waveguides and crossbar are released by plasma etching of the silicon.

One of the problems we faced was fracturing of the thin and long waveguide structures. One cause is the high intrinsic stress level due to the thick SiO2 and Si3N4 layer stack. With a step-wise etching process, waveguide structures were successfully released. Design proposals and design rules for optimal waveguide design are deduced from this analysis. We have designed flexible waveguide arrays with 2 and 4 coupled beams, various lengths (250, 500, 750 and 1000μm) and various widths (18, 26 and 34 μm). These dimensions result in a beam stiffness ranging from 1.3 to 156 N/m (out-of-plane) and 1.6 to 700 N/m (in-plane). These stiffness values are well compatible with the forces that can be generated by on-chip actuators like thermal actuators, and will enable the travel range as required by the limited precision of the course alignment step.

9133-48, Session 10

Optical coupling between pairs of waveguides made in lithium niobate crystals by means of femtosecond laser writing

Gustavo A. Torchia, Enrique G. Neyra, Ctr. de Investigaciones Ópticas (Argentina)

During the last decade, femtosecond laser writing in optical

materials has shown a remarkable increase in the number of scientific and technological works published in internationals journals. Some advantages of this technique can be pointed as: one step process, possibility of 3D recorded, low cost and easy to implement on a wide range of materials. This technique also offers different optical circuit fabrication with applications in various technological fields ranging from photonics to medicine among others. In this work we study the optical coupling between pairs of waveguides fabricated by femtosecond laser writing technique. In particular, these structures are constructed by written single tracks above the optical breakdown threshold so called type II structures. The study of this coupling has been carried out both experimentally as well as by simulations based on a technique known as "beam propagation method "(BPM). For the last, we have used commercial software (RSoft) and its particular tool, BeamProp. The waveguides were fabricated by using a micro-machining system based on a Chirped Pulse Amplification (CPA) femtosecond laser by Spectra Physics (USA). In this work, we explore the variation of the light intensity at the output from each pair of waveguides, as a function of separation between them and considering a resultant refractive index profile for these guiding structures. Good agreement for simulations and experiments has been obtained in this work. The results presented in this paper can be a suitable tool for optimize the design of optical circuits for technological purpose.

9133-49, Session 11

Wavelength tuning speed in semiconductor ring lasers using on-chip filtered optical feedback

Guy Verschaffelt, Mulham Khoder, Romain Modeste Nguimdo, Vrije Univ. Brussel (Belgium); Xaveer J. M. Leijtens, Jeroen Bolk, Technische Univ. Eindhoven (Netherlands); Jan Danckaert, Vrije Univ. Brussel (Belgium)

Wavelength tunable and switchable lasers are widely used in telecommunication networks as they allow flexible wavelength division multiplexing, fast optical signal routing, and all-optical signal processing.

Semiconductor ring lasers nowadays are promising sources in photonic integrated circuits because they do not require cleaved facets or mirrors to form a laser cavity. They are interesting from a nonlinear dynamics point of view due to the existence of two counter propagating modes (clockwise and counterclockwise modes) that interact with each other. Moreover it is possible to achieve switching between the two directions.

In this work, we characterize the wavelength switching speed of a wavelength tunable semiconductor ring laser using filtered optical feedback. This switching occurs in the two directions simultaneously. The wavelength of the semiconductor ring laser in our approach is controlled on-chip by a filtered optical feedback section which consists of two arrayed waveguide gratings, four semiconductor optical amplifier gates and passive waveguides to connect the components together. The two arrayed waveguide gratings are used to split/recombine light into different wavelength channels. The semiconductor optical amplifiers are placed in the feedback loop in order to control the feedback strength of each wavelength channel independently. The switching is achieved by changing the currents injected in the semiconductor optical amplifiers. The device's fabrication was done in the framework of JePPIX. As in our device the wavelength tuning elements (semiconductor optical amplifiers) are placed outside the laser cavity, the refractive index in the main cavity is not changed when we tune the wavelength. Therefore the emitted wavelength will be more stable than when the tuning elements are inside of the laser cavity.

Experimentally, we measure the wavelength switching speed by modulating the injection current of one gate with a square wave signal while a second gate is biased with a constant injection current. We then record the time-trace of the intensity emitted in each wavelength mode. We observe a wavelength transition time of 5 ns. However, we also notice a non-negligible delay in the switching process. This delay time is not constant, but varies from one switching event to another. In order to have a more detailed analysis about this delay time, a statistic analysis is done for a large number of switching events. We discuss the transition time, the delay time and the different parameters which have an effect on them.

Numerically, we use a two-directional mode rate-equation model of semiconductor ring lasers extended with Lang-Kobayashi terms to take into account the effect of optical feedback. Spontaneous emission noise terms are also included in the model. From these simulations we notice that increasing the feedback strength allows us to decrease the switching time. The simulations also demonstrate that the wavelength transition time and the delay can be further decreased by controlling the phase in the feedback section. We also simulate the effect of the noise on the switching process where we show that both the transition and delay time are dependent on the noise. The numerical results are in good agreement with the experimental results.

9133-50, Session 11

Misalignment tolerant edge-couplers for hybrid integration of semiconductor lasers with silicon photonics parallel transmitters

Sebastian Romero-García, Bahareh Marzban, Saeed Sharif Azadeh, Florian Merget, Bin Shen, Jeremy Witzens, RWTH Aachen (Germany)

Hybrid integration of prefabricated III-V lasers diodes with sub-micrometric silicon photonic waveguides suffers from a tradeoff between alignment tolerance and coupling efficiency. In this work, we demonstrate integrated edge-coupling devices that substantially alleviate this problem by means of a balanced distribution of the laser power between two on-chip single mode SOI waveguides. The device is comprised of two main sections. First, an input array of five thin waveguides routed in parallel to the chip edge allows the propagation of two guided super-modes with an expanded profile. The second section (multimode interference section) is designed to achieve a quadrature phase relation between the ground and first order modes and equally distribute the input power in two individual output waveguides. With this coupling device, a horizontal misalignment of the laser results in a variation in the relative phase of the light coupled in the two output waveguides while maintaining a high total coupling efficiency and a balanced power splitting. The relaxed alignment tolerances enable passive assembly of the lasers with pick-and-place tools. Furthermore, the efficient splitting of the power between waveguides is particularly convenient in applications such as optical interconnects with parallel transmitters. Here, the device design is discussed and experimental characterization of the fabricated structures with a lensed fiber and a Fabry-Pérot laser is presented. The devices have been fabricated with 193nm DUV optical lithography and are compatible with mainstream CMOS technology. The best device in terms of horizontal misalignment exhibits an excellent 1 dB loss horizontal misalignment range of 3.8 μm with excess insertion losses below 3.1 dB (in addition to the 3dB splitting). The back-reflections have also been assessed to be below -20 dB. Finally, the practical feasibility of integrating the coupling devices with Fabry-Pérot lasers is further investigated in a parallel silicon photonics transmitter based on linear MZI modulators.

9133-51, Session 11

Towards low noise class-A Hybrid III-V/ silicon laser

Nils Girard, Ghaya Baili, Pascale Nouchi, Daniel Dolfi, Thales Research & Technology (France); Alban Le Liepvre, Mickael

Faugeron, Frederic van Dijk, Guang-Hua Duan, III-V Lab. (France)

For some stringent applications such as radar technologies, the implementation of optical links for signal transmission requires lasers with extremely low noise levels, over a wide frequency range, typically from 100 kHz to 40 GHz. It has been recently demonstrated that Class-A dynamics in semiconductor lasers lead to a Relative Intensity Noise (RIN) level limited only by the shot noise over a wide frequency bandwidth. Class-A dynamics are obtained when the photon lifetime in the cavity is larger than the carrier lifetime within the active medium. Unfortunately, a drastic reduction of the laser volume is needed for such radar systems. In this context, the Silicon-On-Insulator (SOI) platform is a promising technology to implement low noise class-A lasers with extended cavity, by integrating an active gain medium with low loss Si-waveguides.

In this paper, we report on a first design of extended cavity hybrid III-V/silicon laser. An active section (InP) bonded on a SOI wafer generates the light which is coupled in the Si waveguides by two tapers. The cavity is closed by two Bragg reflectors and filtered by two ring resonators which have a slightly different Free Spectral Range (FSR) to obtain the Vernier effect. Thus the filtering bandwidth is narrow enough (~1nm) to obtain a single frequency operation. At 20°C, the laser has a threshold current around 20mA and an output power above 10mW. The narrow bandwidth of the ring resonator provides us a side mode suppression ratio (SMSR) up to 55dB while the Vernier effect allows 45 nm tunability. Our RIN measurements exhibit a noise floor lower than -165 dB/Hz except at specific frequencies. A first noise peak is indeed observed at 1.5 GHz, corresponding to relaxation oscillations, and reveals that our laser is still class-B. A second noise peak around 14 GHz corresponds to the laser free spectral range.

We will also describe new designs with cavity length up to a few centimeters and a better control of cavity losses. Special filters are also engineered to guarantee a single longitudinal mode operation. Calculation results will be presented to demonstrate that those hybrid III-V/Si lasers could reach the class A dynamics.

9133-8, Session 12

Electrical and electroluminescence properties of silicon nanocystals/SiO2 superlattices

Julian López-Vidrier, Yonder Berencén, Bernat Mundet, Sergi Hernández, Univ. de Barcelona (Spain); Sebastian Gutsch, Daniel Hiller, Albert-Ludwigs-Univ. Freiburg (Germany); Philipp Löper, Ecole Polytechnique Fédérale de Lausanne (Switzerland); Manuel Schnabel, Stefan Janz, Fraunhofer-Institut für Solare Energiesysteme (Germany); Margit Zacharias, Albert-Ludwigs-Univ. Freiburg (Germany); Blas Garrido Fernandez, Univ. de Barcelona (Spain)

In the last 20 years, many efforts have been focused on the determination of carrier transport through silicon nanocrystals (Si-NCs) embedded in dielectric matrices. Because of their band-gap dependence on size, the emitting or absorbing energy ranges can be tuned within the visible spectrum. Novel layer deposition approaches, such as the superlattice (SL) one, allow for the fabrication of size-controlled arrays of these nanostructures within different dielectric matrices, the most employed one being SiO2. Nevertheless, SiO2-based matrices are highly insulating systems, making the transport between Si-NCs strongly dependent on the barrier layer thickness. Different studies have been carried out on the electrical and electro-optical properties of such systems, but no systematic correlation between them has been reported so far.

We present a study on the electrical and electroluminescence (EL) properties of n-i-p type devices containing SiOx/SiO2 SLs deposited on Si substrates. The stoichiometry of the silicon-rich layers, their thickness and the SiO2 barrier thickness were varied from sample to sample, allowing for the study of Si-NCs size and spatial distribution on the EL properties. In all sample configurations, a trap-assisted transport mechanism (Poole-Frenkel type) was predominant at moderate fields (~2-5 MV/cm). The threshold voltage for conduction was found to be strongly dependent on the SiO2 barrier thickness and the Si excess, and to decrease for thinner barrier layers and higher Si excesses. The EL spectra are interpreted in terms of the SiOx/SiO2 SL characteristics, and it is concluded that more efficient emission is observed for samples presenting higher threshold voltages, i.e. thick barrier layers and low Si excesses.

9133-53, Session 12

High-frequency sub-wavelength thermal IR source

Floria Ottonello Briano, KTH Royal Institute of Technology (Sweden); Pauline Renoux, Univ. of Iceland (Iceland); Fredrik Forsberg, Hans Sohlström, KTH Royal Institute of Technology (Sweden); Snorri Ingvarsson, Univ. of Iceland (Iceland); Göran Stemme, Kristinn B. Gylfason, KTH Royal Institute of Technology (Sweden)

On-chip spectroscopy, mid-IR silicon photonics, and near-field thermal imaging all require integrated IR sources. Recent studies have shown that sub-wavelength structuring of thermal sources can enhance radiation and allows control of the polarization, the coherence, and the wavelength of the emission [1,2].

We present the design, fabrication, and characterization of an integrated sub-wavelength thermal IR source, and show experimentally, for the first time, that its small size makes it suitable for high frequency operation. For that, we introduce an innovative method to characterize the frequency response of fast thermal IR sources.

Our thermal IR source consists of a 50 nm thick Pt wire in a four-wire configuration. The emitting area is 1?3 ?m^2. The source lies on a 220 nm thick Si island supported by SiO2. The thermal isolation of the island, and so of the source, can be regulated by varying the etching of the underlying SiO2. The thermal isolation influences the source temperature and its time response.

Applying a current to the source causes a temperature increase proportional to the square of the current itself and a consequent broadband thermal emission. Our source reaches 690 K with a current of 35 mA. The temperature increase (?T) is reflected in a resistance increase according to R=R_0+R_0 ?ΔT, where ? is the temperature coefficient of resistance of Pt thin films. When ?T varies with the applied current, the I-V relation becomes non-linear.

Simulations predict that the maximum frequency at which the current variation modulates the source temperature is 100 MHz [3]. However, high frequency optical IR measurements are limited by the frequency response of available IR detectors. Therefore, we take advantage of the nonlinear I-V relation and electrically characterize the source thermal frequency response. We observe the voltage, both across our thermal source and across a reference bulk resistor of same resistance, with a spectrum analyser. If the resistance of the tested device varies with the applied current, a third harmonic appears in the detected voltage. Only our IR source, and not the reference bulk resistor, exhibits such behaviour, indicating that the source's thermal response is fast enough to follow the current. This way, we demonstrate that the operation frequency range of the source spans from DC up to at least 10 MHz, the limit of our signal generator.

References

[1] J.-J. Greffet, R. Carminati, K. Joulain, J.-P. Mulet, S. Mainguy, and Y. Chen, "Coherent emission of light by thermal sources", Nature, vol. 416, pp. 61-64, Mar. 2002.

[2] Y. Au et al., "Thermal radiation spectra of individual subwavelength microheaters", Physical Review B, vol. 78, pp. 085402-1-5, Aug. 2008

[3] P. Renoux, S. Jónsson, L. J. Klein, H. F. Hamann, and S. Ingvarsson, "Sub-wavelength bolometers: Uncooled platinum

wires as infrared sensors", Optics Express, vol. 19, pp. 8721-8727, Apr. 2011

9133-54, Session 12

Strong infrared photoluminescence and electroluminescence from black silicon formed by femtosecond laser irradiation

Quan Lu, Jian Wang, Fudan Univ. (China); Jie Yang, Dandan Chen, Fei Xu, Shanghai Univ. (China); Zuimin Jiang, Fudan Univ. (China)

Si-based materials have great scientific and commercial interest. However, band-to-band optical transitions in Si have a low efficiency because of its indirect band gap. There have been great efforts over the several decades to obtain technologically viable and efficient light emission from silicon both in the visible and infrared regions of the spectrum. In the visible regions, porous Si, Si/SiO2 superlattices and Si nanopaticles in SiO2 have been the main emphasis. In the infrared region, erbium doped devices, Si/Ge system, FeSi2 and defects in Si formed by plastic deformation offer potential routes. Recently, black silicon (b-Si) has been receiving a great deal of attention due to its interesting physical properties and promising potential technological applications in the field of light emitting. A lot of papers have reported photoluminescence (PL) from b-Si, but very few were on the PL in infrared region and also very few mentioned electroluminescence (EL) from b-Si or structures of similarity to b-Si. To get strong PL or EL in infrared region in Si-based materials still remains a big challenge.

In this work, b-Si was formed by femtosecond laser irradiation on the surface of Si substrates in SF6 ambient. This fabrication process can both introduce shallow and deep levels into Si band gap as luminescence centers and form an n+-p junction in the b-Si. Strong infrared PL was observed for the first time from the sample treated by rapid thermal annealing at the temperatures above 500 °C. The PL properties with annealing temperature were studied. The PL peak energy changes from 0.78 to 0.84 eV (1.59 to 1.48 ?m) with increasing the annealing temperature from 500 to 1200 °C, showing a tunable property. The PL is attributed to the dislocation-related (D1) luminescence. The characteristics of D1 PL, including excitation power dependence as well as temperature dependence of D1 PL, were studied systematically. Also strong infrared EL was observed at room temperature (RT) from the n+-p junction LEDs. EL spectra exhibit only the D1-related emission band and do not contain any peaks that are typically observed from crystalline Si. At a 1000 mA forward current the emitted light is 15.6 mW giving an external quantum efficiency (EQE) of about 2% at RT, which is higher than the previous EQE results of infrared EL from Si-based material. The integrated intensity of D1-related EL increased monotonically and significantly as the measured temperature increased, implying that the device could possibly be applicable as light emitters at RT for optical fiber communication systems.

9133-55, Session 13

Characterization of PECVD Silicon nitride photonic components at 532 and 900 nm wavelength

Pieter Neutens, IMEC (Belgium); Ananth Z. Subramanian, Univ. Gent (Belgium); Mahmud Ul Hasan, Chang Chen, Roelof A. Jansen, Tom Claes, Xavier Rottenberg, Bert Du Bois, Kenny Leyssens, Philippe Helin, Simone Severi, IMEC (Belgium); Frédéric Peyskens, Ashim Dhakal, Univ. Gent (Belgium); Paru Deshpande, IMEC (Belgium); Roel G. Baets, Univ. Gent (Belgium); Pol Van Dorpe, IMEC (Belgium)

On-chip photonic elements have the potential to serve as platform for data transmission applications. Also for biophotonic sensing applications, waveguides and integrated resonators have been proposed as sensing platforms. However most effort has been put in the development of silicon based photonic components for telecom wavelengths. Although silicon waveguide based optical elements have already been used for biosensing [1], they require expensive sources and detectors. Moreover, applications based on Raman spectroscopy or fluorescence often require the use of visible or near infrared wavelengths. Silicon nitride offers a very attractive photonic platform for the development of high-performance low-loss photonic component for wavelengths in the visible and near infrared wavelength regime [2], where silicon behaves as a semiconductor and as a consequence suffers from large free carrier absorption. In addition, the deposited SiN films can be seamlessly integrated with mainstream silicon CMOS chips, providing cheap integrated detectors and the possibility of large-scale parallelism.

In previous publications, waveguides and resonators were fabricated in low-pressure chemical vapour deposition (LPCVD) silicon nitride [3-4], mainly due to the very low material losses in the wavelength range of interest and very good uniformity across the wafer while maintaining a reasonably high refractive index. However LPCVD is a high temperature process and cannot be employed in the back-end-of-line of a CMOS chip, preventing CMOS integration of SiN photonics. At imec, we developed and optimized a 200 mm CMOS compatible process to fabricate nanoscale SiN strip waveguides on silicon based on a low temperature SiN PECVD process and 193 nm DUV lithography. This resulted in wafer-scale homogeneous waveguide properties and low propagation losses.

In order to confirm the low loss performance of the developed PECVD nitride recipe, various test structures were fabricated both in our 200 mm wafer facility by DUV lithography as well as by ebeam lithography on smaller scale. Propagation losses and bend losses were both measured at 532 and 900 nm wavelength, revealing sub 1dB/cm propagation losses at both wavelengths for single mode operation. Also a large set of ring resonators was fabricated for 900 nm operation and measured.

The data presented in this paper shows that the fabrication of CMOS compatible, low temperature PECVD nitride waveguide structures is huge step forward in the development of functional photonic circuits on chip.

[1] C. F. Carlborg et al., A packaged optical slot-waveguide ring resonator sensor array for multiplex label-free assays in labs-on-chips, Lab Chip 10, 281-290 (2010).

[2] S. Romero-Garcia et al., Silicon nitride CMOS-compatible platform for integrated photonics applications at visible wavelengths, Opt. Express 21, 14036-14046 (2013).

[3] E. S. Hosseini et al., High Quality Planar Silicon Nitride Microdisk Resonators for Integrated Photonics in the Visible Wavelength Range, Opt. Express 17, 14543-14551 (2009).

[4] M. Melchiorri et al., Propagation losses of silicon nitride waveguides in the near-infrared range, Appl. Phys. Lett. 86, 121111 (2005).

9133-56, Session 13

Polymer and composite polymer slot waveguides

Marianne Hiltunen, VTT Technical Research Ctr. of Finland (Finland); William S. Fegadolli, California Insitite of Technology (United States); Hugo L. R. Lira, Instituto de Estudos Avançados (Brazil); Petri A. Stenberg, Univ. of Eastern Finland (Finland); Jussi A. Hiltunen, Sanna M. Aikio, VTT Technical Research Ctr. of Finland (Finland); Vilson R. Almeida, Instituto Tecnológico de Aeronáutica – ITA (Brazil); Pentti Karioja, VTT Technical Research Ctr. of Finland (Finland)

The optical field is confined and enhanced in the low refractive index material in the slot waveguide structure [1,2]. Originally, the slot waveguide structure was based on silicon. The demonstrated silicon slot waveguides work at near infrared wavelength due to the fact that silicon is not transparent at visible range. In the sensing applications, visible wavelengths are often preferable. Also disposable sensor chips are desirable,

because reusability might require complicated cleaning procedures. Therefore, we investigate potentially low-cost method to realize polymeric slot waveguide sensor chips working at visible wavelength.

Polymeric slot waveguide structure, which pushes the mode field towards the surrounding media, was designed and characterized. The nanoimprinting technique, which enables reproducible high-throughput fabrication of waveguides, was used to fabricate the integrated Young interferometers, which consist of either one slot or three slots in on arm. The slot Young interferometer operation is based on the phase difference produced by two waveguide arms, one with 5 mm long slot section and another one of a regular ridge waveguide. The operation of the slot Young interferometer was demonstrated at 633 nm wavelength by measuring the phase shift with water and glucose solution. Total length of the interferometer was 30 mm, and the distance between two arms was 70 μm. Short distance between the sensing and reference arm improves the readability of interferogram. In order to improve the sensitivity and blocking the water absorption to the polymer, the waveguide was further coated with thin Al2O3 layer.

References:

[1] V. R. Almeida, Q. Xu, C. A. Barrios and M. Lipson, Opt. Lett. Vol. 29, 1209 (2004).

[2] M. Hiltunen, J. Hiltunen, P. Stenberg, J. Petäjä, E. Heinonen, P. Vahimaa and P. Karioja, Opt. Lett., Vol. 37, 4449, (2012)

9134-1, Session 1

Green nanophotonics for future datacom and Ethernet networks *(Invited Paper)*

Dieter H. Bimberg, Technische Univ. Berlin (Germany) and King Abdulaziz Univ. (Saudi Arabia); Dejan Arsenijevi?, Gunter Larisch, Technische Univ. Berlin (Germany); Hui Li, Technische Universität Berlin (Germany); James A. Lott, Philip Moser, Holger Schmeckebier, Philip Wolf, Technische Univ. Berlin (Germany)

The use of Internet has increased and continues to increase exponentially, mostly driven by consumers. Thus bit rates in networks from access to WDM and finally the computer clusters and supercomputers increase as well rapidly. Their cost of energy reaches today 5-6 % of raw electricity production. For 2023 a cross over is predicted, if no new “green” technologies or “green” devices” will will reduce energy consumption by about 15 %/y. In this presentation two distinct approaches for access and computer networks are described based on nanphotonic devices to reduce power consumption in the next decade.

9134-2, Session 1

Recent advances in photonic crystal lasers: from near infrared to THz frequencies *(Invited Paper)*

Jean-Michel Lourtioz, Xavier Checoury, Raffaele Colombelli, Institut d’Électronique Fondamentale (France)

During the last twenty years, remarkable progress has been accomplished in the understanding of photonic crystal physics and in photonic crystal fabrication (PhC) leading to impressive demonstrations of key functionalities for applications to sensing, all optical processing and photonic integrated circuits in general. PhC resonators can exhibit record Q over V ratios, and myriad designs are now available to build such resonators in various materials and at various wavelengths. Thanks to the control of the spontaneous emission and to the enhancement of light matter interactions, compact PhC lasers with ultra small footprints have been achieved at near infrared showing ultra-low thresholds and ultrafast dynamics. Using surface-emitting structures with metallo-dielectric PhCs, single-mode laser output with a nearly diffraction-limited laser beam has been obtained from quantum cascade lasers (QCL) at THz frequencies.

Yet, the “glory” of PhC lasers has still to come. It is only in the last few years that the issues linked to the very nature of PhCs lasers, namely the poor heat sinking, the large non radiative recombination of carriers at the walls of the PhC etched holes, the poor efficiency on an electrical injection into the tiny laser structures and their difficult interfacing with the outside world have been partially addressed. These issues have hindered for a long time the possible use of PhC lasers for applications, since stable room temperature CW operation could not be achieved and the output power levels were limited to few nanowatts. The achievement of efficient laser emission from electrically pumped two-dimensional PhC lasers was (and still remains) a serious challenge.

In this invited talk, we shall present an overview of recent advances in the field of photonic crystal lasers with prospects of using them in system experiments and in demonstrators. This will include PhC waveguide lasers and PhC Raman microsources at near-infrared wavelengths as well as PhC quantum cascade lasers at THz frequencies.

9134-3, Session 1

Sub-threshold relaxation dynamics of a quantum dot laser

Cheng Wang, Institut National des Sciences Appliquées de Rennes (France); Benjamin Lingnau, Eckehard Schoell, Kathy Lüdge, Technische Univ. Berlin (Germany); Jacky Even, Institut National des Sciences Appliquées de Rennes (France); Frédéric Grillot, Télécom ParisTech (France)

Directly modulated quantum dot (QD) laser is a promising candidate for the next generation high-speed optical networks. However, it is well-known that the intrinsic modulation bandwidth is drastically limited by the low differential gain, the large gain compression factor and the slow carrier capture into the QDs [1]-[3]. In this work, we investigate for the first time the sub-threshold relaxation dynamics of an InAs/InP (001) QD laser. The laser exhibits a modulation efficiency of 0.35 GHz/mA1/2 and a K-factor of 1.7 ns. When reducing the pump current slightly below threshold, the QD laser’s resonance frequency unexpectedly re-increases, while that of a commercial quantum well (QW) laser keeps decreasing. This typical resonance behavior is attributed to the Pauli blocking of the excited state (ES) as predicted in [4], in which the rate equation model takes into account the intradot carrier dynamics in the ground state (GS) and in the ES. As an extension, simulations in this work show quantitative agreements with the measured resonance behavior. In addition, the damping factor offset is dominated by the product of the Pauli blocking and the carrier escape rate from the GS to the ES, in contrast to the sole carrier effective lifetime in the QW laser case. The offset value is found to be inversely proportional to the carrier relaxation lifetime (?ES_GS), decreasing from 40 GHz for ?ES_GS =5.0 ps down to 1.5 GHz for ?ES_GS =100 ps. The theory is also supported by other experiments with reported offset values ranging from 1.7 GHz up to 17.0 GHz [5]-[10]. Finally, it is found that both the resonance frequency and the 3-dB modulation bandwidth decrease almost linearly with the increased ?ES_GS, while large ?ES_GS values induce a parasitic-like roll-off in the modulation response.

[4] Cheng Wang et al., J. Quantum Electron. 48, pp. 1144, 2012.

9134-4, Session 1

The effect of slow passage in the pulse-pumped quantum dot laser

Grigorii S. Sokolovskii, Ioffe Physico-Technical Institute (Russian Federation); Muayyad Abu Saa, Vrije Univ. Brussel (Belgium) and Arab American Univ. (Palestinian Territory, Occupied); Jan Danckaert, Vrije Univ. Brussel (Belgium); Vladislav V. Dudelev, Anton G. Deryagin, Innokenty I. Novikov, Mikhail V. Maximov, Ioffe Physico-Technical Institute (Russian Federation); Alexey E. Zhukov, St. Petersburg Academic Univ. (Russian Federation); Victor M. Ustinov, Ioffe Physico-Technical Institute (Russian Federation); Vladimir I. Kuchinskii, Ioffe Physico-Technical Institute (Russian Federation) and Saint Petersburg Electrotechnical Univ. “LETI” (Russian Federation); Wilson Sibbett, Univ. of St. Andrews (United Kingdom); Edik U. Rafailov, Univ. of Dundee (United Kingdom); Evgeny A. Viktorov, Univ. Libre de Bruxelles (Belgium) and National Research Univ. of Information Technologies, Mechanics and Optics (Russian Federation); Thomas Erneux, Univ. Libre de Bruxelles (Belgium)

In recent years, quantum-dot (QD) semiconductor lasers attract significant interest in many practical applications due to their advantages such as high-power pulse generation because to

the high gain efficiency. In this work, the pulse shape of an electrically pumped QD-laser under high current is analyzed. We find that the slow rise time of the pulsed pump may significantly affect the high intensity output pulse. It results in sharp power dropouts and deformation of the pulse profile. We address the effect to dynamical change of the phase-amplitude coupling in the proximity of the excited state (ES) threshold. Experimentally, the studied QD-laser structure was MBE-grown on a GaAs substrate. The active region included five layers of self-assembled InAs QDs. The structure was processed into 4um-wide mesa-stripes. The 1.5 to 2.5mm-long lasers with high- and antireflection coatings on the rear and front facets lase either at GS (~1265nm) or simultaneously at GS and ES (~1190nm). Under 30ns pulse pumping, the output pulse shape strongly depends on pumping amplitude. At lower currents, which correspond to the ground state (GS) lasing, the pulse shape mimics that of the pump pulse. However, at higher currents the pulse shape becomes progressively unstable. The instability is greatest when in proximity to the secondary threshold which corresponds to the beginning of the ES-lasing. After the slow rise stage, the output power sharply drops out. It is followed by a long-time power-off stage and large-scale amplitude fluctuations. In our numerical simulations, we explain these observations by the dynamical change of the alpha-factor in the QD-laser. In semiconductor lasers, alpha-factor serves for characterization of the phase-amplitude coupling that has been a subject of intensive research for decades and has led to a vast amount of literature. In QD-lasers, both numerical simulations and experiments for simultaneous GS/ES-lasing reveal dramatic increase of the alpha-factor near the ES-threshold. In order to describe the experimental observations, we exploit the delay differential equations model. It supports multimode generation what is essential to describe the effect. The pulse of the pump current in our modeling consists of the 5ns rise, followed by a constant plateau and 5ns fall. The alpha-factor is considered as linearly-increasing during the rise stage and constant after that. Such a slow variation of the control parameters is found to have significant effect on multi-scale dynamical phenomena. In particular, the slow passage through a Hopf bifurcation is featured by a significant delay when the system changes from slowly varying steady state to slowly varying oscillation as lasing modes do not start generation simultaneously, but appear sequentially with the increase of pump. In turn, the change of the alpha-factor leads to significant shifts in the position of the lasing modes. Therefore the power dropout is explained as a sharp transition from the maximum gain mode operation to an operation with a number of modes. The modeling is in excellent qualitative agreement with the experimental observations and reveals the role of the slow passage through the Hopf bifurcation.

9134-5, Session 1

Multistate lasing phenomenon in p-doped and undoped InAs/InGaAs quantum dot lasers

Vladimir V. Korenev, Artem V. Savelyev, St. Petersburg Academic Univ. (Russian Federation); Alexey E. Zhukov, St. Petersburg Academic Univ. (Russian Federation) and Ioffe Physico-Technical Institute (Russian Federation); Alexander I. Omelchenko, St. Petersburg Academic Univ. (Russian Federation); Mikhail V. Maximov, Ioffe Physico-Technical Institute (Russian Federation) and St. Petersburg Academic Univ. (Russian Federation)

Long-wavelength InAs/InGaAs quantum dot (QD) lasers emitting via QD ground state (GS) optical transitions near the wavelength of 1.3 mkm are the promising light sources for a wide range of practically important applications, from optical coherence tomography and aesthetical surgery to fiber amplifiers pump and ultrafast data transmission. In particular, for the pump of fiber amplifiers sufficiently high output power, which corresponds to the GS optical transitions of QDs, is needed. However, with the increase of injection the new line, which corresponds to the excited state optical transitions (ES) of InAs/InGaAs QDs, appears in the lasing spectrum (near the wavelength of 1.2 mkm). The multi-state lasing takes place. Moreover, above the multi-state lasing threshold the useful emission from GS of InAs/InGaAs QDs tends to decrease or even quenches at sufficiently high injection. The series of possible reasons has been proposed, such as self-heating effects, asymmetry in charge carrier distribution within quantum dots, the growth of homogeneous broadening and the growth of internal losses with the increase of injection. Moreover, recently proposed de-synchronization of carrier capture into QDs can also strongly affect maximal GS-power and the current of GS-lasing quenching. It was shown that even the low variation of hole-to-electron capture rate ratio (h-factor) leads to the significant variation of GS-lasing power. However, the ways to increase the output power component corresponding to ground states of QDs were not found yet. In this work, we have shown for the first time both experimentally and theoretically, that the usage of modulation p-doping of laser`s active region allows to increase the maximum output power emitted via GS optical transitions of QDs as well as the range of injection currents, in which multi-state lasing phenomenon takes place. Moreover, the maximal temperature, at which lasing via GS of InAs/InGaAs QD exists, was increased practically by 50C in the case of p-doped samples. In order to study this phenomenon in details we have proposed an analytical model based on the system of rate equations for the photons in laser`s active region and for charge carriers in QDs, which also takes into account the hole-to-electron capture rate ratio (h-factor). The model predictions are in qualitative agreement with the experimental results for self-assembled InAs/InGaAs QDs. Analytical expression for the maximal power of GS-lasing was obtained in terms of the proposed model. The presence of multi-state lasing in InAs/InGaAs QD lasers having sufficiently short cavities, which was experimentally observed in p-doped samples and was absent in undoped samples, is also described in terms of the proposed model.

9134-6, Session 2

High-speed modulation of transverse-coupled-cavity VCSELs *(Invited Paper)*

Fumio Koyama, Hamed Dalir, Tokyo Institute of Technology (Japan)

We review our recent study on the high-speed modulation of transverse-coupled-cavity VCSELs with a bow-tie shape oxide aperture. The noticeable modulation-bandwidth enhancement can be exhibited owing to “photon-photon resonance effect”.

The vertical-cavity surface-emitting laser is a key light source in energy-efficient and high-speed optical interconnects in data centers and supercomputers. VCSELs have various merits such as low power consumption, ultra-fast modulation, low threshold current, small-foot print and low-cost in mass-fabrication. There still remain key challenges such as higher speed modulation of over 40Gbps with low power consumption for energy-efficient data center photonics. The intrinsic modulation speed is limited by the resonance frequency of VCSELs. We proposed the bandwidth enhancement of VCSELs with a transverse coupled cavity, which shows a bandwidth extension thanks to “photon-photon resonances”. A record 3-dB bandwidth of 29 GHz was realized for a 980nm multi-mode transverse coupled cavity (TCC) VCSEL with a bow-tie shape oxide aperture. Also, we realized a quasi-single mode transverse-coupled cavity VCSEL with a smaller bow-tie shape aperture, which makes current injection unnecessary in a feedback cavity. We demonstrated the modulation-bandwidth enhancement of a quasi-single mode VCSEL with a passive optical-feedback-cavity. The 3-dB modulation bandwidth can reach at 27GHz, which is 3 times larger than a conventional VCSEL without optical feedback. Clear eye opening of large signal modulations at 36Gbps was obtained. The modeling and future prospect toward the bandwidth enhancement beyond 40GHz will also be presented.

In addition, we demonstrated the lateral integration of an ultra-compact electro-absorption modulator incorporating the bow-tie-shape oxide aperture. We obtained a low driving voltage lower than 400mVpp. Our ultra-compact modulator integrated VCSEL can boost the modulation speed far beyond the direct

modulation bandwidth with low-power consumption for use in next-generation computing and communication networks.

9134-7, Session 2

Spin-controlled ultrafast vertical-cavity surface-emitting lasers

Henning Höpfner, Ruhr-Univ. Bochum (Germany); Markus Lindemann, Ruhr-Univ Bochum (Germany); Nils C. Gerhardt, Martin R. Hofmann, Ruhr-Univ. Bochum (Germany)

Spin-controlled semiconductor lasers are highly attractive spintronic devices providing characteristics superior to their conventional purely charge-based counterparts. In particular, spin-controlled vertical-cavity surface emitting lasers (spin-VCSELs) promise to offer lower thresholds, enhanced emission intensity, spin amplification, full polarization control, chirp control and ultrafast dynamics. Most important, the ability to control and modulate the polarization state of the laser emission with extraordinarily high frequencies is very attractive for many applications like broadband optical communication and ultrafast optical switches.

We present a novel concept for ultrafast spin-VCSELs which has the potential to overcome the conventional speed limitation for directly modulated lasers by the relaxation oscillation frequency and to reach modulation frequencies significantly above 100 GHz. The concept is based on the coupled spin-photon dynamics in birefringent micro-cavity lasers. By injecting spin-polarized carriers in the VCSEL, oscillations of the coupled spin-photon system can by induced which lead to oscillations of the polarization state of the laser emission. These oscillations are decoupled from conventional relaxation oscillations of the carrier-photon system and can be much faster than these. Utilizing these polarization oscillations is thus a very promising approach to develop ultrafast spin-VCSELs for high speed optical data communication in the near future.

Different aspects of the spin and polarization dynamics, its connection to birefringence and bistability in the cavity, controlled switching of the oscillations, and the limitations of this novel approach will be analysed theoretically and experimentally for spin-polarized VCSELs at room temperature.

9134-8, Session 2

Dynamics of long-wavelength VCSELs subject to dual-beam optical injection

Pablo Perez, Univ. de Cantabria (Spain); Ana Quirce, Vrije Univ. Brussels (Belgium); Antonio Consoli, Univ. Politécnica de Madrid (Spain); Angel Valle, Ignacio Noriega, Luis Pesquera, Univ. de Cantabria (Spain); Ignacio Esquivias, Univ. Politécnica de Madrid (Spain)

Distributed feedback lasers (DFB) subject to two-frequency optical injection exhibit various nonlinear dynamics including locking, periodic and chaotic oscillations. Recent work on vertical-cavity surface-emitting lasers (VCSELs) subject to dual-beam optical injection has also demonstrated period-one nonlinear dynamics that has been used to generate microwave signals with frequencies corresponding to the frequency differences between the two lasers that are injected into the VCSEL.

In this work we report an experimental and a theoretical study of the nonlinear dynamics of a 1550 nm single transverse mode VCSEL subject to two-frequency orthogonal optical injection. Different behaviors include irregular and periodic dynamics in the orthogonal polarization and periodic dynamics in both linear polarizations. We report an analysis of the generated high-frequency microwave signal found when the VCSEL is emitting only in the orthogonal polarization. Good agreement is found between our experimental and theoretical results.

9134-9, Session 2

Experimental and theoretical analysis of limit cycle bistability in a free-running VCSEL

Martin Virte, Emeric Mercier, Vrije Univ. Brussel (Belgium) and Supélec (France); Krassimir Panajotov, Vrije Univ. Brussel (Belgium) and Institute of Solid State Physics (Bulgaria); Marc Sciamanna, Supélec (France)

Laser diodes typically behave like damped oscillators: they are generally expected to only show damped relaxation oscillations toward a stable fixed point. In vertical-cavity surface-emitting lasers (VCSELs), the picture appears to be quite different as polarization dynamics can be experimentally observed including bifurcations to self-pulsation and even chaos [1, 2]. Physically, the circular geometry of VCSEL makes the polarization selection very weak and, thus, the additional degree of freedom can enable complex dynamical behavior in the laser diode.

We recently demonstrated that the San Miguel, Feng and Moloney (SFM) model provides a unifying framework and an accurate qualitative description of these polarization dynamics. However this framework still contains some dynamical features that have never been observed. In particular, among the predictions of the SFM model: three consecutive Hopf bifurcations could appear on the same elliptically polarized steady-states for increasing injection current [3]. This would result in the coexistence of two distinct limit cycles, oscillating around the same elliptical polarization, with different frequencies. Here we experimentally observe such bistability of limit cycles, and demonstrate a convincing qualitative agreement with the theoretical prediction of the SFM model. We therefore provide a new dynamical confirmation of the SFM model validity and bring new light on dynamics of VCSELs.

[1] M. Virte, H. Thienpont, K. Panajotov, M. Sciamanna, Nature Photon. 7, 60-65 (2013).

[2] M. Virte, K. Panajotov, M. Sciamanna, Phys. Rev. A 87, 013834 (2013).

[3] F. Prati, P. Caccia, M. Bache and F. Castelli, Phys. Rev. A 69, 033810 (2004)

9134-10, Session 2

Wavelength controlled VCSELs emitting in the 1310nm waveband

Alexei Sirbu, Ecole Polytechnique Fédérale de Lausanne (Switzerland); Alexandru Mereuta, Andrei Caliman, BeamExpress S.A. (Switzerland); Vladimir Iakovlev, Dalila Ellafi, Zlatko Mickovi?, Elyahou Kapon, Ecole Polytechnique Fédérale de Lausanne (Switzerland)

Among different approaches of long-wavelength vertical cavity emitting laser (VCSEL) fabrication, wafer fusion represents now a well-established technique for producing state of the art device performance in the 1310 nm wavelength band. Recent advancements of this technology demonstrate a new, low power consumption alternative to distributed feedback (DFB) lasers for 40 Gbps Ethernet single-fiber multi-channel coarse wavelength division multiplexing (CWDM) transmission. Compared with DFBs, VCSELs have net advantages of lower operation currents and lower cost, but there is still one potential issue of VCSELs for CWDM applications that is related to wavelength setting. This is because emission wavelength in VCSELs is set by the thickness of the cavity that includes the InP –based active region and part of top and bottom AlGaAs-GaAs distributed Bragg reflectors (DBRs). Consequently, VCSEL emission wavelength is dependent on epitaxial growth thickness tolerances of active and DBR stacks as well as on thickness non-uniformities across the wafer.

For particularly useful CWDM VCSEL systems at the 1270/1290/130/1330nm grid, we have found that typical

values of 1% growth thickness tolerance and 1% thickness non-uniformity result in a yield of devices fitting the CWDM slots below 50%. In case of 1% non-uniformity of the DBR stop band center across the wafer, the emission wavelength non-uniformity of fabricated devices is considerably larger than the accepted CWDM wavelength variation slot of 6.5 nm at room temperature. In addition, we show that about 1% thickness tolerance of layer constituting the VCSEL structure is mainly responsible for the off-set of the average emission wavelength relative to the center of the CWDM slot. To solve these problems, we have developed a fabrication procedure with much improved yield, relying on the high flexibility of the wafer fusion approach. The procedure includes in particular (i) selecting the DBR components to fit the active region emission properties determined during the wafer assembley process; and (ii) the use of wet chemical etching with 1nm accuracy based on oxidant/etching cycles of the cavity layer. Applying different variations of this technique we reach wavelength setting yield of devices from a VCSEL wafer of more than 90%.

9134-11, Session 3

Monolithically integrated InP-based modelocked ring laser systems *(Invited Paper)*

Erwin A. Bente, Valentina Moskalenko, Sylwester Latkowski, Meint K. Smit, Technische Univ. Eindhoven (Netherlands)

In this paper we will present results achieved on monolithically integrated semiconductor modelocked ring lasers operating around 1550nm and fabricated in the standardized InP based technology platform of the COBRA research institute. The ring lasers are passively modelocked using a saturable absorber. The integration technology allows for the combination of passive ridge waveguides and active elements such as optical amplifiers, saturable absorbers and electro-optic phase modulators on a single InP chip. For integrated modelocked lasers this means that the repetition rate of the laser, which is determined by the cavity length, is decoupled from the length of the amplifier and the saturable absorber. Also the relative position of the amplifier, saturable absorber and output coupler can be varied and we have demonstrated that this can be used to have increased control of the laser operation. Furthermore by reducing the length of the amplifier the amplitude noise properties of the laser can be reduced. Spectrally, the output from a modelocked laser is a comb of optical frequencies. Recently we have observed a record width of the frequency comb of a quantum well ring laser operating at a 20 GHz repetition rate. The optical coherent comb around 1542 nm had a 3 dB bandwidth of 11.5 nm. A minimum pulse width of 900 fs was observed using a step-heterodyne technique to characterise the phase and intensity profiles. We will discuss a possible application of such comb sources in the area of gas sensing. For this application two frequency combs with slightly different frequency spacings can be used. Requirements on the stabilisation of the output frequencies from the laser will be discussed and as well as possible solutions to achieve this e.g. using an electro-optics phase modulator in the ring cavity.

9134-12, Session 3

Revisiting the physics of mode locking in lasers

Germán J. de Valcárcel, Univ. de València (Spain); Franco Prati, Univ. degli Studi dell'Insubria (Italy); Auro M. Perego, Univ. degli Studi dell'Insubria (Italy) and Univ. de València (Spain)

Haus Master Equation (ME) is a milestone in the study of laser mode locking. Its simplicity and its accounting for the main features of laser pulses (like their shape and duration) explains its enormous success. As a drawback that status has led to a situation in which more refined treatments of light-gain interaction seem to be superfluous. Yet, placing the existing theory inside a sounder physical basis is the only way to ascertain its validity limits, as well as to make new predictions and explain some of the deviations observed in the experiments.

Here we present a new ME for mode locking, derived rigorously from the laser Maxwell-Bloch equations, which take into account the coherent features of light-gain interaction. As a main consequence, our derivation shows that, even if gain is very slow, its evolution on the fast time scale of laser pulses must be considered, unlike in Haus approach. There are two key points in the derivation. First, the medium polarization is adiabatically eliminated in a refined way in order to account for the finite bandwidth of the active medium. The coherence of the field-gain interaction can be described till the desired precision through a series expansion in powers of a smallness parameter, whose square is the inverse of the number of cavity longitudinal modes falling inside the gain line. A consistent truncation of the series, retaining a parabolic approximation for the gain line, leads to the appearance of gain variations occurring on time scale of the order of the pulse duration. Second, the wave equation is solved taking into account group velocity variations inside the gain medium, which allows a better definition of the cavity round-trip time (hence of the detuning between the modulation frequency and the cavity free spectral range). An important feature of our ME is that, unlike Haus ME, the pulse dynamics is sensitive to the sign of the modulation detuning. The new ME contains Haus ME as a particular case, when the fast variations of gain are neglected, and is just slightly more complex from the mathematical viewpoint. This allows for reasonably fast numerical integration.

We have performed preliminary numerical simulations of active mode locking with the new ME. Using realistic parameter values for both semiconductor and solid state gain media, we observe three main effects not described by Haus ME: (i) pulses display skewness, (ii) they tend to form before the minimum loss point, and (iii) the pulse structure varies in a complex way as a function of the modulator detuning. All these effects are more pronounced the longer is the cavity, and for parameters suitable for semiconductor lasers. The stability of pulses with respect to both pump level and modulator detuning, as well as the influence of noise, are being investigated.

To the best of our knowledge, this is the first attempt to formulate a coherent ME for actively mode locked lasers. Coherent effects manifest both in the shape and in the dynamics of the pulses.

9134-13, Session 3

Regular and turbulent dynamics in Fourier domain mode locked lasers

Svetlana Slepneva, Ben O'Shaughnessy, Bryan Kelleher, Tyndall National Institute (Ireland) and Cork Institute of Technology (Ireland); Stephen P. Hegarty, Tyndall National Institute (Ireland); Andrei G. Vladimirov, Cork Institute of Technology (Ireland) and Weierstrass-Institut für Angewandte Analysis und Stochastik (Germany) and Tyndall National Institute (Ireland); Guillaume Huyet, Cork Institute of Technology (Ireland) and Tyndall National Institute (Ireland)

Fourier Domain Mode Locked Lasers (FDMLL) are novel frequency swept sources that have enabled Optical Coherent Tomography to achieve acquisition speed up to several MHz. A FDMLL consists of a fiber ring cavity with intracavity tunable filter that is modulated synchronously with the cavity round trip time so that the optical line stores an entire frequency sweep that is re-amplified by a semiconductor amplifier.

We experimentally investigated the properties of a FDMLL emitting a 100nm wide spectrum around 1.3mm with a tuning speed of 10kHz. The laser output was analysed using a high frequency detector and a 12GHz real-time oscilloscope. In addition, we developed a delayed homodyne technique to recover the temporal evolution of the phase over the entire spectral range and to enable the measurement of the instantaneous linewidth.

The laser output was studied as a function of the detuning

of the drive frequency of the filter away from the resonant frequency and a pronounced asymmetry was observed with respect to filter wavelength sweep direction. In one direction, we observed mode hopping between frequency-swept solutions due to the detuning or fibre dispersion, while opposite direction was associated with a chaotic regime. Measurements showed that the optical linewidth for both regimes is larger than the free spectral range similar to that observed in long cavity ring laser. In particular, the frequency-swept solutions involve about 1000 modes while the chaotic regime involves about a million of modes.

Theoretically the dynamics of the FDMLL was described by a set of delay differential equations for the electric field envelope and carrier density. The analysis of these equations was made and, in analogy with spatial extended systems, we showed that the mode-hopping between frequency swept solutions is associated with a sub-critical Turing instability while the chaotic regime is closely related to a modulation instability.

9134-14, Session 3

Wider-frequency combs generation, noise reduction, and repetition rate tuning in quantum-dot mode-locked lasers

Tatiana Habruseva, Aston Univ. (United Kingdom) and Cork Institute of Technology (Ireland) and Tyndall National Institute (Ireland); Dejan Arsenijevi?, Dieter H. Bimberg, Technische Univ. Berlin (Germany); Stephen P. Hegarty, Tyndall National Institute (Ireland); Guillaume Huyet, Cork Institute of Technology (Ireland) and Tyndall National Institute (Ireland) and National Research University of Information Technologies, Mechanics and Optics (Russian Federation)

We describe the technique allowing for generation of low-noise wider frequency combs and pulses of shorter duration in semiconductor quantum-dot mode-locked lasers (QD-MLLs). Firstly, we compare experimentally noise stabilization techniques in monolithic QD-MLLs. We discuss the benefits of electrical modulation of the laser absorber voltage (hybrid mode-locking), combination of hybrid mode-locking with optical injection seeding from the narrow linewidth continues wave master source and optical injection seeding of two coherent sidebands separated by the laser repetition rate. For this study all measurements were performed on the same device, a 40 GHz InAs/GaAs QD-MLL, under the same temperature and bias conditions.

All studied techniques resulted in the significant timing jitter reduction compared to passively MLL and allowed tuning of the device repletion rate. With hybrid mode-locking we achieved a 14-times jitter reduction and laser repetition rate tuning over the 10 MHz range, however, it did not affect device phase noise and pulse chirp. Both hybrid mode-locking with optical injection seeding and coherent sidebands injection allowed laser repetition rate tuning, jitter reduction, and also resulted in the phase noise reduction and red-shifted narrowed optical spectrum. With coherent sidebands injection the lowest jitter of 121 fs and the widest frequency tuning range of 342 MHz were achieved. Hybrid mode-locking with optical injection-seeding also had similar outcomes with 240 fs integrated jitter and RF frequency tuning over 167 MHz range.

The modal linewidth reduction and optical spectrum red shift with sidebands injection-seeding were exploited to generate high quality wider frequency combs. We used a chain of two 10 GHz QD-MLLs made from the same wafer and cleaved together. First, QD-MLL was stabilized via sidebands injection-locking. Then, two modes apart from the injection wavelength were filtered from the laser1 optical spectrum and coupled into the second QD-MLL. Outputs from the both lasers were recombined resulting in a wider optical spectrum due to the consequent spectral red-shifts of the devices. This wider frequency comb resulted in pulses of shorter duration.

9134-15, Session 3

Interaction of optical breathers in mode-locked lasers and passive fiber cavities

Andrei G. Vladimirov, Weierstrass-Institut für Angewandte Analysis und Stochastik (Germany); Dmitry V. Turaev, Imperial College London (United Kingdom); Sergey Zelik, Univ. of Surrey (United Kingdom)

Short optical pulses (dissipative solitons) generated by mode-locked lasers have numerous scientific, medical, and technological applications. In the experiments with fiber lasers a transition from fundamental to harmonic mode-locking regime and/or to a regime with two or more closely packed pulses forming a pulse bound state can take place with the increase of the pump parameter. In this presentation we investigate theoretically physical mechanisms responsible for such kind of transitions. We consider a model of a standard silica fiber cavity where the dissipative interaction and formation of optical breathers were recently studied experimentally and a model of passively mode-locked fiber laser based on the generalized complex Ginzburg-Landau equation. We study the effect of periodic modulation resulting from dispersion management and self-pulsing instability on the weak local interaction of well separated optical dissipative solitons via their exponentially decaying tails. We develop a general theory of a weak interaction by deriving analytically a set of ordinary differential interaction equations governing the slow time evolution of the inter-soliton time spacing and their phase differences in the course of interaction. Analytical results obtained using the interaction equations were found to be in a good agreement with those of direct numerical integration of the model equations. We show that although the interaction of stationary optical dissipative solitons can be very weak, under a periodic perturbation optical breathers start to emit slowly decaying dispersive waves which lead to a drastic enhancement of their interaction and formation of new types of bound states corresponding to different soliton oscillations synchronization regimes. Finally the effect of finite population inversion relaxation time on the optical dissipative soliton interaction and a transition to harmonic mode-locking is discussed.

9134-16, Session 4

Laser dynamics providing enhanced modulation bandwidth *(Invited Paper)*

Ivo Montrosset, Paolo Bardella, Politecnico di Torino (Italy)

The objective of this invited paper is to compare quantitatively the small and large signal dynamic characteristics of lasers presenting enhanced modulation bandwidth. In order to compare the different laser cavities we present first the simulation analysis we performed in order to determine the enhanced modulation bandwidth condition of each laser before to compare their dynamic results. Considerations for each laser on the difficulties to obtain such operation condition in the simulations will conclude the presentation.

9134-17, Session 4

Multi-wavelength emission using compact semiconductor ring laser with filtered optical feedback

Mulham Khoder, Romain Modeste Nguimdo, Jan Danckaert, Vrije Univ. Brussel (Belgium); Xaveer J. M. Leijtens, Jeroen Bolk, Technische Univ. Eindhoven (Netherlands); Guy Verschaffelt, Vrije Univ. Brussel (Belgium)

Laser diodes that emit multiple wavelengths simultaneously are needed in a range of applications including wavelength division multiplexing, high speed optical networks, optical instruments testing, optical sensing and tera hertz generation. Several

approaches have been proposed to achieve multi-wavelength emission using different laser systems, such as fiber lasers, solid-state lasers and external cavity laser diodes. Although these systems show exceedingly good performance, they tend to be bulky and expensive. In this work we report on an integrated approach to obtain multi-wavelength emission from a semiconductor ring laser based on on-chip filtered optical feedback.

Semiconductor ring lasers have the advantage that light can be easily coupled with other optical devices and the input / output waveguides via directional couplers. This facilitates their monolithic integration with other optical components, such as delay lines, splitters, and detectors providing therefore flexibility and compactness. Moreover, no thermal control of the wavelength emission is needed and therefore the device can be in principle fast. As ring lasers can support lasing in the clockwise and counterclockwise propagating modes, and it is possible to achieve switching between the two directions. This makes semiconductor ring lasers interesting as devices for all-optical switching in networks.

The device consists of a semiconductor ring laser, two arrayed waveguide gratings and four semiconductor optical amplifiers. The different components are connected by passive waveguides. Light at the semiconductor ring laser's output is coupled to the arrayed waveguide gratings by a directional coupler. The filtered optical feedback is realized by employing the two arrayed waveguide gratings to split/recombine light into different wavelength channels. Semiconductor optical amplifier gates are placed in the feedback loop in order to control the feedback of each wavelength channel independently. The tuning in this approach will be done outside the main laser cavity. As a result there is no change in refractive index in the main ring laser cavity. Therefore, the wavelength stability is improved. The number of emitted wavelengths depends on the number of the biased gates. Multi- wavelength emission can be achieved and tuned by pumping several gates simultaneously with suitable injection currents.

Experimental observations have shown that the effective gain (which includes the effects of material gain, losses, and feedback) is the key parameter that has to be balanced using the feedback in order to achieve multi-wavelength emission. This can be achieved by tuning the injection current in each amplifier which will change the feedback phase and strength. We can select the number of emitted wavelengths by changing the number of semiconductor optical amplifiers being pumped. We can tune the emitted wavelengths by changing the currents injected in each of the optical amplifiers. Numerical simulations are performed using a two-directional mode rate equation model of the semiconductor ring lasers extended with Lang–Kobayashi terms to take into account the effect of optical feedback. Numerical results reproduce the experimental results and show the effects of feedback phase and strength on the multi-wavelength emission.

9134-18, Session 4

Bifurcation to chaos and extreme events in a laser diode with phase-conjugate feedback

Emeric Mercier, Andreas Karsaklian Dal Bosco, Delphine Wolfersberger, Marc Sciamanna, Supélec (France)

Phase-conjugate optical feedback (PCF) - i.e. an optical feedback where the phase of the optical field is conjugated before it re-enters into the laser cavity - has been largely used as a way to stabilize and reduce the linewidth of laser emission but is also known to generate complex dynamics including self-pulsation and chaos [1]. In contrast to the large number of theoretical works available, there have been only few experiments reporting on nonlinear dynamics in the past thirty years. Most importantly, experiments so far have not addressed the peculiarities of the PCF dynamics in comparison with dynamics observed from conventional optical feedback (COF). In this contribution, we report experimentally and theoretically on two chaotic dynamics that relate to the peculiar dynamical properties of a laser diode with PCF. First, we find a chaotic dynamics that resembles the so-called low-frequency fluctuations (LFF) of a laser diode with COF, i.e. the output power shows abrupt dropouts at randomly distributed time-intervals followed by a slower recovery. Although the LFF in PCF shows similar statistical properties to those observed in the LFF in COF, they originate from a distinctively different bifurcation scenario. Increasing the PCF strength the laser diode shows successive bifurcations to time-periodic solutions at the frequency of the external cavity and multiples (also called 'external-cavity modes' or ECMs). These self-pulsing ECMs are the fundamental dynamical solutions of the PCF laser system and no steady state is possible anymore for large feedback strength [2]. Following the destabilization of several such ECMs to chaotic attractors, the dynamics shows a transition to a global attractor connecting the chaotic ECMs and that explains the sequence of power dropouts and recoveries. In addition we show how the bifurcations on these self-pulsing ECMs generate dynamics with extreme events, i.e. pulses with peak intensities well above the average value of the peaks in the output power and that show properties similar to the rogue waves in hydrodynamics [3]. This is the first demonstration of such temporal extreme events in a time-delayed optical system, and we show how the time-delayed feedback impacts on the number and properties of the extreme events.

[1] J.S. Lawrence and D.M. Kane, Phys. Rev. A 63, 033805 (2001).

[2] M. Virte, A. Karsaklian Dal Bosco, D. Wolfersberger, and M. Sciamanna, Phys. Rev. A 84, 043836 (2011).

[3] D. R. Solli, C. Ropers, P. Koonath, and B. Jalali, Nature 450, 1054 (2007).

9134-19, Session 4

Harmonic fundamental self-pulsations from a laser diode using phase-conjugate optical feedback

Delphine Wolfersberger, Andreas Karsaklian dal Bosco, Emeric Mercier, Marc Sciamanna, Supélec (France)

Thanks to the band-gap engineering of quantum confined semiconductor materials and the development of semiconductor-based saturable absorber mirrors, recent years have seen the development of compact and low-cost external-cavity laser diodes generating pulses at several tens of GHz [1]. The physics of the bifurcation leading to self-pulsation leads however to an intrinsic limitation: the fundamental repetition rate is fixed to and limited by the external-cavity round-trip time. This is true in general for the self-pulsating solutions of several time-delayed laser system including self-pulsation from the so-called passive Ikeda nonlinear cavity and external-cavity mode beating or mode locking in the external-cavity laser diode. Solutions to overcome this fundamental limit to the self-pulsation frequency so far rely on either external modulation or complex colliding pulse schemes. By contrast, we demonstrate here that an external-cavity diode laser may generate fundamental self-pulsating dynamics at harmonics of the external-cavity frequency, when a phase conjugate mirror replaces the conventional mirror. As is known from theory [2], a laser diode with phase conjugate external feedback supports a single stationary solution that bifurcates to self-pulsating dynamics of increasing frequency when increasing the amount of light reflected back to the laser diode. The self-pulsation frequency then increases in step of the external-cavity frequency as one increases the feedback strength. We provide here the first experimental evidence of such harmonic external-cavity fundamental self-pulsation. Our experiment uses an 850 nm edge-emitting laser with a self-pumped ring-cavity photorefractive phase conjugator. As a proof-of-concept, we generate experimentally a self-pulsating dynamics at twice and three times the fundamental external-cavity frequency, but numerical simulations also predict stable higher harmonics. The stability of the harmonic self-pulsations strongly depends on both the amount of feedback and the external-cavity length.

[1] E. Avrutin, J.H. Marsh and E.L. Portnoi, IEE Proc. Optoelectron. 147, 251-278 (2000).

[2] M. Virte, A. Karsaklian Dal Bosco, D. Wolfersberger, and M. Sciamanna, Phys. Rev. A 84, 043836 (2011).

9134-20, Session 4

Experimental study of the complex dynamics of semiconductor lasers with feedback via symbolic time-series analysis

Taciano Sorrentino, Univ. Federal Rural do Semi-Árido (Brazil); Andrés Aragoneses Aguado, Sandro Perrone, Univ. Politècnica de Catalunya (Spain); Daniel J Gauthier, Duke University (United States); Maria Carme Torrent, Cristina Masoller, Univ. Politècnica de Catalunya (Spain)

We study experimentally the spiking output of a semiconductor laser with optical feedback from an external reflector. Close to the lasing threshold moderate feedback levels induce apparently random spikes in the laser output intensity, which become more frequent as the laser pump current is increased. This dynamics has been referred to as low-frequency-fluctuations (or intensity dropouts) and has attracted a lot of attention in the last decades, not only because of potential applications of optical chaos, but also, because the mechanisms triggering the dropouts involve the interplay of nonlinearity, time-delay and noise, which are ubiquitous in nature.

For the analysis of the sequences of dropout events we use a popular symbolic method, known as ordinal analysis [1, 2] that considers the relative order in which the dropouts occur. The sequence of inter-dropout intervals is transformed into a sequence of symbolic ordinal patterns.

We unveil a hierarchical and clustered organization of ordinal patterns, with a well-defined structure of the probabilities of occurrence. Simulations of the Lang and Kobayashi model are in good agreement with the observations. To the best of our knowledge, in spite of the large attention that the LFFs have attracted over the years, ours is the first demonstration of an organized symbolic structure underlying the sequence of apparently random intensity dropouts.

Most importantly, we identify a minimal model (a modified circle map modelling spike correlations in sensory neurons), which displays the same symbolic organization, i.e., the same hierarchy and clusters of probabilities of patterns. The validity of this minimal model is further confirmed by analyzing the intensity dropouts when the laser is periodically forced (via direct pump current modulation).

Since the modified circle map is a generic model of forced oscillators, we envision that the underlying symbolic structure found here could be observed in many other dynamical systems. In particular, our results could be yield light on the firing patterns of biological neurons. Establishing a direct connection between these different dynamical systems can offer new perspectives, both, in photonics and in neuroscience. Our results suggest that optical neurons inspired by biological ones could be built using semiconductor lasers, and could provide a controllable set up to mimic neuronal activity. Our findings could also pave the way for novel neuro-inspired optical computing devices.

[1] Bandt, C., Pompe, B. Permutation entropy: a natural complexity measure for time series. Phys. Rev. Lett. 88, 174102 (2002).

[2] Aragoneses, A., et al. Distinguishing signatures of determinism and stochasticity in spiking complex systems. Sci. Rep. 3, 1778 (2013).

9134-21, Session 5

Laser research on an InP-based generic integration platform *(Invited Paper)*

David J. Robbins, Willow Photonics Ltd. (United Kingdom)

In Europe a number of technology platforms for generic integration are being created for the fabrication of photonic integrated circuits (PICs); in Silicon, www.photonfab.eu, in passive dielectrics such as TripleX www.lionixbv.nl/mpw.html, and in Indium Phosphide, www.paradigm.jeppix.eu., and generic platform technology for InP based photonics has recently taken the first steps towards commercialised through brokering organisations such JePPIX, www.jeppix.eu . It offers a range of calibrated building blocks from which application specific PICs can be built and allows simplified, reduced cost access to a standardised technology, but presently only InP based platforms, as introduced in [1] and the focus of this paper, allow the integration of optical gain blocks; the essential feature of a semiconductor laser. The operation wavelength is constrained by the platform, usually C-band, but in the near future we also expect other wavelengths in the 1.3μm-2.0μm range to be addressed using novel quantum wells, quantum dots and selective area growth technology.

A frozen platform technology may not seem an ideal starting point for novel laser research, but for what may be appear to be lost in epitaxial and process flexibility, as this paper will show, much more is gained through a new found ability to build up complex circuits quickly to deliver new and interesting laser based functionality using composite building blocks such as MMIs and AWGs. For example, starting from platform building blocks such as a reflector (which may for example be a DBR, reflective MMI design or a simple facet), and amplifier building block to provide gain, and passive waveguides of various geometries plus the connections required to build a circuit from them, integrated semiconductor lasers of various types can be assembled. The ready integration of novel sources with other circuit functionality can immediately address a wide range of applications for example in telecoms, datacoms, fibre based sensing systems.

In this paper we describe a number of recent PIC developments leading to novel lasers on generic InP platforms. Structures range from the fabrication of simple Fabry-Perot lasers with novel reflectors, through tuneable DBR lasers, multi-wavelength comb lasers, filtered feedback lasers, picosecond pulse lasers and ring lasers, and fast switching wavelength selectable lasers.

Reference: [1] M. Smit, X. Leijtens, E. Bente, J. Van der Tol, H. Ambrosius, D. Robbins, M. Wale, N. Grote, and M. Schell, “Generic foundry model for InP-based photonics,” IET Optoelectron., 5, 5, p. 187, 2011

9134-22, Session 5

Emission regimes in a distributed feedback tapered master-oscillator power-amplifier at 1.5 μm

Mariafernanda Vilera Suárez, José Manuel Garcia Tijero, Antonio Consoli, Santiago Aguilera, Pawel Adamiec, Ignacio Esquivias, Univ. Politécnica de Madrid (Spain)

Integrated master-oscillator power amplifiers driven under steady-state injection conditions are known to show a complex dynamics resulting in a variety of emission regimes. We present experimental results on the emission characteristics of a 1.5 μm distributed feedback tapered master-oscillator power-amplifier in a wide range of steady-state injection conditions, showing different dynamic behaviors. The study combines the optical and radio-frequency spectra recorded under different levels of injected current into the master oscillator and the power amplifier sections. Under low injection current of the master oscillator the correlation between the optical and radio-frequency spectral maps allows to identify operation regimes in which the device emission arises from either the master oscillator mode or from the compound cavity modes allowed by

the residual reflectance of the amplifier front facet. The quasi-periodic occurrence of these emission regimes as a function of the amplifier current is interpreted in terms of a thermally tuned competition between the modes of the master oscillator and the compound cavity modes. Under high injection current of the amplifier section, two different alternating regimes appear: a stable regime with a single mode emission at the master oscillator frequency, and an unstable regime in which the undamped relaxation oscillations result in strong peaks in the radio-frequency spectra as well as multiple frequencies in the optical spectra.

9134-23, Session 5

Physical properties of GaAsBi/GaAs-based quantum well near-infrared lasers

Igor P. Marko, Shirong Jin, Konstanze Hild, Zahida Batool, Stephen J. Sweeney, Univ. of Surrey (United Kingdom); Peter Ludewig, Wolfgang Stolz, Kerstin Volz, Philipps-Univ. Marburg (Germany)

GaAsBi is a new material system having several interesting properties promising for the development of near infrared lasers with suppressed losses. Adding bismuth (Bi) atoms into a standard III-V material system provides strong band gap (Eg) shrinkage allowing a wide spectral coverage and a significant increase of the spin-orbit split-off energy (?SO). It is therefore possible to realize a condition when ?SO>Eg and the dominant Auger process, where the annihilation energy of an electron-hole pair is transferred to a hole excited to the spin-orbit split-off band (CHSH process), is suppressed [1]. This would greatly reduce the threshold current, improve the temperature performance and minimize the system energy requirement. If ?SO>Eg, Inter Valence Band Absorption (IVBA), whereby a photon is reabsorbed through excitation of an SO-electron to the heavy hole band causing an increased optical loss is also expected to be suppressed. Thus, the development of bismide alloys has recently attracted much interest leading to substantial improvements in material quality and demonstration of first electrically pumped GaAsBi lasers [2].

Here we report on the temperature dependent properties of electrically pumped GaAsBi/(Al)GaAs quantum well (QW) lasers. The devices are grown by MOPVE [2] and contain GaAsBi QWs with up to 4.4% Bi and (Al)GaAs barriers. The 2.2% Bi lasers showed operation above room temperature with a wavelength of 947 nm at 295K. The lowest room temperature threshold current density was measured to be 1kA/cm2. The 4.4%Bi laser exhibits lasing up to 180K at a wavelength of 1039nm. Direct measurement of temperature dependence of the radiative part of threshold current and high hydrostatic pressure measurements indicate that at this stage laser performance is dominated by non-radiative recombination related to defects. Further discussion of the potential of this new material system for laser applications will be discussed at the conference.

[1] S. J. Sweeney and S. R. Jin, J. Appl. Phys. 113, 043110 (2013); S. J. Sweeney, Patent No. WO2010149978 (2010).

[2] P. Ludewig et al., Appl. Phys. Lett. 102, 242115 (2013).

9134-24, Session 5

Small linewidths 76x nm DFB-laser diodes with optimised two-step epitaxial gratings

Olaf Brox, Frank Bugge, Anna Mogilatenko, Erdenetsetseg Luvsandamdin, Andreas Wicht, Hans Wenzel, Götz Erbert, Ferdinand-Braun-Institut (Germany)

Compact light sources with small linewidths at 76x nm are attractive for applications such as molecular oxygen spectroscopy (760 nm) and atomic clocks (767 nm potassium D2 line). Ridge waveguide (RW) DFB laser diodes with an internal grating offer compactness combined with large conversion efficiency and excellent beam profiles. In this work we present DFB lasers diodes with emission wavelengths in the 76x nm range and focus on fabrication process and design of the internal gratings formed by a two-step epitaxial process.

The gratings are fabricated after the first epitaxial growth which ends with an InGaP (90 nm), GaAsPy (thickness d) and InGaP (20 nm) layer sequence. Second order gratings with periods in the order of 23x nm are defined by laser interference lithography and successive wet chemical etch steps. After surface cleaning the epitaxial overgrowth follows. For the analysis of the buried structures and the optimization of the etching and regrowth conditions we applied scanning transmission electron microscopy (STEM) using a high angle annular dark-field (HAADF) detector.

DFB grating functionality is achieved with periodical index variations caused by the patterned GaAsPy layer. The band edge of this layer shifts towards higher energies with enhanced P concentration y and lowers the absorption loss. As a drawback the critical layer thickness reduces which makes it difficult to obtain reasonable grating coupling strengths. We aim for coupling strengths in the order of 2/cm to achieve high power, single mode and small linewidths operation of RW DFB lasers. The impact of the P concentration y and the layer thickness d on the optoelectronic performance of DFB laser diodes has been studied. Vertical structures with various y- and d-values are grown and laser diodes are processed into 100 µm wide and 1 mm long uncoated broad-area (BA) devices. Best performing devices have been found for y = 25 % and d = 13 nm without disturbing the grating functionality.

The optimized layer structure is applied to manufacture RW DFB laser diodes with stripe widths of 2.2 µm. The facets of 1.5 mm long DFB devices are coated to obtain power reflectivities of 0.95 and below 1E-3 for the rear and front side, respectively. Devices are mounted p side up on C mount and measurements are performed under continuous wave (cw) conditions. Optimized RW DFB laser diodes show outstanding optoelectronic characteristics in terms of slope efficiency (0.9 W/A), linewidths (11 kHz) and lifetime (> 5000 hours at 100 mW). Details will be presented at the conference.

9134-25, Session 5

Simulations and analysis of beam quality improvement in spatially modulated broad area edge-emitting devices

Mindaugas Radziunas, Weierstrass-Institut für Angewandte Analysis und Stochastik (Germany); Muriel Botey, Ramon Herrero, Univ. Politècnica de Catalunya (Spain); Kestutis Staliunas, Univ. Politècnica de Catalunya (Spain) and Institució Catalana de Recerca i Estudis Avançats (Spain)

Edge emitting broad area semiconductor (BAS) lasers and amplifiers are robust, compact and highly efficient devices for generation of high power beams. However, the spatial and temporal quality of these beams usually is rather low. For a beam quality improvement we propose to use the semiconductor media with a properly chosen longitudinal and lateral periodic modulation of the gain and index, what can be realized, e.g., by a periodic structuring of the electrical contact. Nemely, the ratio of the squared lateral modulation period to the longitudinal one should be approximately equal to the half of the optical field wavelength in semiconductor.

First, we consider the propagation of optical beams along periodically modulated BAS amplifiers. Once the beams are small and are not able to imply a significant gain saturation, their propagation along the longitudinal axis of the amplifier can be described by the linear 1+1-dimensional Schroedinger equation with a periodic potential in both coordinates. By expanding the optical field to a few Bloch modes we reduce the model to a system of ODEs. Its analysis gives us a deep understanding of the impact of different model parameters (modulation depth and periods, amplifier length, linewidth enhancement factor, etc.) to the amplification and the spatial (angular) filtering of the beam. Particularly, we show how

a proper choice of modulation parameters implies not only a strong reduction of the emission divergence, but also an additional amplification of the emitted field.

Next, we simulate numerically the propagation of small and moderate beams along periodically modulated BAS amplifiers. In this case we use the 1+2-dimensional traveling wave model which describes the spatial-temporal dynamics and nonlinear interactions of the optical fields, induced polarizations and carrier density. Even though due to the gain saturation the gain and index modulation amplitudes at different spatial positions of the BAS device are different, the obtained results (compression of the emission divergence) are in a good agreement with the linear model analysis. Finally, our first simulations of the periodically modulated BAS lasers could also show a significant compression of the time averaged far fields.

9134-26, Session 6

Picosecond pulse generation in GaN-based laser diodes *(Invited Paper)*

Ulrich T. Schwarz, Katarzyna Holc, Thomas Weig, Helge Höck, Klaus Köhler, Joachim Wagner, Fraunhofer-Institut für Angewandte Festkörperphysik (Germany)

We explore the use of GaN-based laser diodes (LDs) for the short pulse generation in the violet to blue spectral range. We develop edge-emitting multi-segment LDs for picosecond pulse generation both with and without external cavity. Pulses with pulse duration below 10 ps and peak power above 10 W were achieved from single LDs with bow-tie waveguide geometry. These pulse trains of short, intense pulses are generated by gain-switching or self-Q-switching. To generate even shorter pulses below 1 ps, the group velocity dispersion of the semiconductor waveguide has to be compensated in an external cavity. With a Littman-Metcalf configuration we achieve sub-picosecond pulses with 1 GHz repetition rate. Possible applications include spectroscopy, sensors, bio-photonics, laser-micro-fabrication, nonlinear, and quantum-optics.

Three topics which are specific to GaN-based LDs and relevant for short pulse generation will be discussed: absorption and carrier lifetime in the absorber in the presence of the quantum confined Stark effect, Auger effect, and perturbations of the inhomogeneously broadened gain spectra.

Absorption and carrier lifetime in the absorber section of a multi-section LD are given by the band profile in the active region. The strong piezoelectric field in the quantum wells causes a reduction of the transition matrix element and a wavelength shift. As consequence, absorption is minimal at flat-band conditions, usually at a small negative bias voltage. Absorption increases for large reverse bias voltages due to Franz-Keldysh effect, i.e. absorption in the barriers. Carrier lifetime in this regime is given by tunneling times between quantum wells and barriers. For these short carrier lifetimes and large absorption at large reverse bias, the LD operates in self-Q-switching regime with a pulse repetition rate in the few GHz range. Carrier dynamics between pulses is dominated by spontaneous recombination. Because the carrier density remains equal or larger than the threshold carrier density of a LD with transparent absorber, the Auger effect has an impact on the repetition rate in self-Q-switching mode.

For stable mode-locking in an external cavity, not only compensation of group velocity dispersion, but also a broad and smooth optical gain spectrum is a precondition. While gain spectra of GaN-based LDs are broad (e.g. 25 meV homogeneous and 50 meV inhomogeneous broadening for a violet LD), they are usually not smooth. Interaction of the waveguide mode with substrate modes causes a modulation of the gain spectra. Rough sidewalls, cracks or other irregularities along the ridge waveguide cause a spectral variation of losses, while indium fluctuations of the quantum well result in spectral variation of gain. The result is a gain spectrum with fluctuations of the order of 1/cm between longitudinal modes of the laser diode chip. The magnitude of the fluctuation depends on the substrate, epitaxial growth, and processing, and is a characteristic “finger print” of an individual laser diode. These irregularities of the optical gain spectrum not only affect the longitudinal mode spectrum of the LD chip, but also the dynamics of the LD in the external cavity during mode-locking operation.

9134-27, Session 6

Rate-equation analysis of longitudinal spatial hole burning in high-power semiconductor lasers

Ting Hao, Junyeob Song, Paul O. Leisher, Rose-Hulman Institute of Technology (United States)

For high-power semiconductor lasers, asymmetric reflectivities of facets are employed in order to improve slope efficiency. Cavity lengths of these laser diodes have been increased to better distribute heat in order to increase output power. However, these two methods result in an inhomogeneous longitudinal profile of photon density, which leads to a non-uniform gain profile and is typically referred to as longitudinal spatial hole burning (LSHB). In this work, we developed a model to self-consistently calculate the longitudinal photon density distribution, carrier density distribution and gain distribution in a high-power semiconductor laser. The calculation is based on modified rate equations and a finite difference method is used to solve the differential equations. Newton’s method is employed to obtain final results with residual error below 10^-6. We demonstrate that LSHB is expected to limit the maximum achievable output power of semiconductor lasers having cavity lengths in excess of several mm. This work differs from prior work in the area in that the model developed is employed to analyze the differential power conversion efficiency and power scalability added (or lost) per incremented increase in cavity length. The results are expected to be useful in the optimization of high power semiconductor laser designs.

9134-28, Session 6

973nm wavelength stabilized hybrid ns-MOPA diode-laser system with 15. 5W peak power and a spectral linewidth below 10 pm

Nghiem T. Vu, Andreas Klehr, Bernd Sumpf, Hans Wenzel, Goetz Erbert, Günther Tränkle, Ferdinand-Braun-Institut (Germany)

There is an increasing demand for ns-pulsed, high-peak power, and narrow spectral line width light sources. Among other applications, the detection of atmospheric gases, e.g. H2O, using differential absorption LIDAR (DIAL) requires peak powers in the 10 W range and emission line widths adapted to the line-broadening of the substances under study (about 0.1 cm-1, i.e. 10 pm at 973 nm). The pulse widths should be in the ns-range at repetition rates of some 10 kHz.

In this work, a master oscillator power amplifier (MOPA) system suitable for the generation of optical pulses with a width of 8 ns, a peak power of 15.5 W, and a narrow spectral line width will be presented. The master oscillator (MO) is a 973 nm DFB laser operated in continuous wave mode. At 35°C the threshold current is Ith = 36 mA and the output power reaches 430 mW at current of 750mA. The device operates single mode over the whole current range with a spectral line width below 10 pm and a side-mode suppression ration (SMSR) better than 55 dB. The power amplifier with integrated modulator has a total length of 6 mm consisting of a 2 mm long RW section with a ridge width of 4 um as modulator section (denoted PP) and a 4 mm long gain-guided tapered section (denoted TS) with a full taper angle of 6°. The front and rear facets were passivated and anti-reflection-coated with reflectivity R ≤ 5x10-4. Normally, the PP absorbs the injected CW beam of the DFB laser when CW biased. However, if a current pulse with a defined width ?tPP, (in this experiment ?tPP ≤ 8 ns at f = 25 kHz) is injected, it becomes transparent and the beam can pass. The generated optical pulse is subsequently amplified in the subsequent section (TS), which

is also operated pulsed to reduce the amplified spontaneous emission (ASE). The pulses have ?tTS =15 ns, f= 25 kHz and peak currents up to 18 A. By adjusting the delay time between the current pulses injected into the PP and TS, an optical pulse with a width of 8 ns and a pronounced optical peak power plateau of 15.5 W is obtained. The rise and fall times are 1.3 and 1.8 ns, respectively. The ASE of about 1.3 W is observed only at the beginning and end of the current pulses injected into the amplifier

The spectral properties are measured by using an optical spectrum analyzer (OSA) with a spectral resolution of 10 pm and a dynamic range of 60 dB (Advantest Q8384). It remains constant at all output power levels of the MOPA system for fixed current into the MO. Adjusting the current injected into the MO leads to a continuous tuning range of about 1 nm with a spectral line width ≤ 10 pm and a SMSR of more than 40 dB. The spectral properties of the MOPA system, as well as the shape of optical pulses, peak power and the ASE will be presented.

9134-29, Session 6

Generating a high-brightness multi-kilowatt laser by dense spectral combination of volume Bragg grating stabilized single-emitter laser diodes

Haro Fritsche, Ralf Koch, Bastian Kruschke, DirectPhotonics Industries GmbH (Germany); Fabio Ferrario, DirectPhotonics Industries (Germany); Andreas Grohe, Silke Plueger, Wolfgang Gries, DirectPhotonics Industries GmbH (Germany)

Generating high power laser radiation with diode lasers is commonly realized by geometrical stacking of diode bars, which results in high output power but poor beam parameter product (BPP). The accessible brightness in this approach is limited by the fill factor, both in slow and fast axis. By using a geometry that accesses the BPP of the individual diodes, generating a multi kilowatt diode laser with a BPP comparable to fiber lasers is possible.

We will demonstrate such a modular approach for generating multi kilowatt lasers by combining single emitter diode lasers.

Single emitter diodes have advantages over bars, mainly a simplified cooling, better reliability and a higher brightness per emitter. Additionally, because single emitters can be arranged in many different geometries, they allow building laser modules where the brightness of the single emitters is preserved.

In order to maintain the high brightness of the single emitter we developed a modular laser design which uses single emitters in a staircase arrangement, then coupling two of those with polarization combination to generate one base module. Those modules generate up to 160 W with a BPP better than 7.5 mm mrad. For further power scaling wavelength stabilization is crucial. The wavelength is stabilized with just one Volume Bragg Grating (VBG) in front of a module providing the very same feedback to all of the laser diodes. This results in a bandwidth of < 0.5 nm and a wavelength stability of better than 250 MHz over one hour.

Dense spectral combination with dichroic mirrors and narrow channel spacing allows us to combine multiple wavelength channels, resulting in a multi kilowatt laser module with a BPP better than 7.5 mm mrad, which can easily coupled into a 100 µm fiber and 0.15 NA. In this paper we will demonstrate a high brightness laser module with 2 kW output power out of a 100 µm fiber.

9134-30, Session 6

Optical characterization of of GaSb and InAs-substrate-based type II quantum wells for long-wavelength mid-infrared interband cascade lasers

Filip Janiak, Marcin Motyka, Grzegorz Sek, Krzysztof Ryczko, Mateusz Dyksik, Jan Misiewicz, Wroclaw Univ. of Technology (Poland); Robert Weih, Matthias Dallner, Sven Höfling, Martin Kamp, Julius-Maximilians-Univ. Würzburg (Germany)

Mid-infrared semiconductor lasers are continuously increasing their application range within during the last years including for instanceespecially gas sensing for detection and control of the presence or concentration of harmful gases like CO2, SOx, NH3, and many others. Type II GaSb and InAs-based quantum well system interband cascade lasers (ICLs) with the type II quantum wells as the active region areis potentially able to cover spectrally the range of 2 to 8 µm, and beyond, and are is possible to be easily integrated into a photonic sensor unit. for gas detection.

Hereby, we present optical studies of a set of such GaSb and InAs-substrate-based structures predicted for interband cascade lasers (ICL) with type II quantum well active region structures. First of all, photoluminescence and modulated reflectivity spectra (photoreflectance) have been measured in the range of the interband transitions and then confronted with the energy level calculations in the eight-band kp model to verify the electronic structure. Quantum wells Structures emitting in a broad range from below 3 to above 9 ?m have been investigated. The studies are focused on

The focus will be on the type II – “W” shaped quantum wells (ICL active region)the active region optimization optimizations aimed at maximizing the optical transition oscillator strength via tailoring the electronic structure and the strain and wave function engineering. There will be covered such issues as the band offsets importance, its sensitivity to the layers composition, the active optical transition intensity versus various structure parameters and external factors as temperature or electric field, and the predominant carrier loss mechanisms

Acknowledgements

The work has been mainly was supported by theperformed with the EC within Project WideLase No. 318798 of the 7th Framework Program. J.M. acknowledges the support wihitn the and by the COPERNICUS Award of the Foundation for Polish Science and Deutsche Forschungs Gemeinschaft. F.J. acknowledges the support from Polish Ministry of Science and Higher Education from the subsidy for Faculty of Fundamental Problems of Technology .

9134-31, Session 7

Directly modulated photonic crystal wavelength-scale cavity lasers *(Invited Paper)*

Shinji Matsuo, NTT Photonics Labs. (Japan)

The reduction of active volume of the laser is important to employ the device into the computercom applications such as chip-to-chip and on-chip interconnects. The introduction of the photonic crystal (PhC) wavelength-scale cavity as a laser cavity is important to reduce the active volume because PhC provides a high-Q factor with small cavity. However, its poor thermal conductivity due to air-bridge structure is critical problem to use the device in practical application. Furthermore, air-bridge structure with thin slab layer is difficult to fabricate a p-i-n diode structure. To solve these problems, we employ an ultra-compact embedded active region that we call a lambda-scale embedded active-region PhC laser or LEAP laser. This structure enables us to improve the thermal conductivity because thermal conductivity of InP layer is 10 times larger than

that of InGaAsP layer. In addition, we can expect to improve the quantum efficiency because both photon and carrier are well confined within wavelength-scale active region. We have also developed an electrically driven LEAP laser, which operates under room-temperature continuous-wave conditions. A lateral current injection structure is fabricated by using Si ion-implantation and Zn thermal diffusion into undoped InP layer. The threshold current is 4.8 ?A, which is the lowest threshold current reported for any laser. We also describe the dynamic characteristics of the laser. The LEAP laser exhibits a maximum 3-dB bandwidth of 16.2 GHz and the modulation current efficiency factor is 2.0 GHz/?A0.5, which is four times that of a vertical cavity surface emitting laser (VCSEL). The device is directly modulated by a 10-Gbit/s non return to zero (NRZ) signal with a bias current of 25 ?A, resulting in energy cost of 5.5 fJ/bit. This is the smallest operating energy for any laser. These results indicate that the LEAP laser is highly suitable for use as a transmitter in computercom applications.

9134-32, Session 7

Comparison of spatial antiguided mechanism in single-emitter VCSELs and VCSEL arrays

Tomasz Czyszanowski, Maciej Dems, Robert P. Sarzala, Technical Univ. of Lodz (Poland); Krassimir Panajotov, Vrije Univ. Brussel (Belgium); Elyahou Kapon, Ecole Polytechnique Fédérale de Lausanne (Switzerland)

Anti-guided mode schemes provide larger side mode suppression ratio (SMSR) than any other waveguiding schemes. The anti-guided optical apertures are defined by low refractive index island (single emitter) or islands (array). To increase the emitted power in the single mode regime two approaches are used: single low refractive index aperture encircled by concentric rings of higher refractive index or multiple low refractive index islands. The concentric rings and islands are periodically distributed to meet the resonant condition of the lateral mode. Increase of the size of the single emitter or increase of the number of array emitters together with increase of thermal focusing occurring under CW operation deteriorate the single mode emission. Hence it is crucial to determine which approach provides more efficient discrimination mechanism.

We apply the optical three dimensional, fully vectorial Plane Wave Admittance Method combined with electro-thermal model based on Finite Element Method and perform an exhaustive analysis of the modal gain of all confined modes as a function of the lateral geometrical parameters such as aperture sizes (single emitter) and distance between emitters (array).

We show that both approaches reveal periodic dependence of large modal gains and large SMSR with the change of the aperture size and distance between the emitters. Finally we provide the explanation for the competition between the lateral modes and analyse the modes evolution driven by the change of the lateral parameters in both designs.

This work is supported by the Polish National Science Centre, project DEC-2012/06/M/ST7/00442

9134-33, Session 7

Volume holographic grating stabilized 780nm VECSEL

Gavin N. West, Alec C. Sills, Paul O. Leisher, Rose-Hulman Institute of Technology (United States)

Diode-pumped lasers have become attractive sources for high brightness/high power applications due to their inherent beam quality and efficient power scaling capabilities. Emerging applications are placing ever-greater requirements on the properties of the diode pump. For example, low quantum defect operation of many solid-state lasers can be achieved by directly pumping the upper energy level of the gain medium. The associated absorption feature is typically narrower than the spectral linewidth of typical broad area edge-emitting diode lasers, making diode pumping challenging. Vertical external cavity surface emitting laser (VECSEL) arrays offer the potential to deliver high pump powers at much lower cost than traditional edge emitting devices. In this work, we report on the development of an optically-pumped narrow linewidth 780 nm VECSEL which utilizes a volume holographic grating (VHG) to stabilize the emission spectrum. The VECSEL cavity departs from the traditional design through the use of a lens and planar mirror, such that the pump light can be introduced surface normal (thus ensuring compatibility with 2D scaling to large arrays). The measured spectral width is stabilized to <0.15 nm FWHM (well-matched to the VHG reflective bandwidth) for a wide range of cavity configurations and mode volumes. These results will be applied to 2D array configurations for power scaling and are expected to enable dramatic improvements in the availability of low-cost pump sources for a variety of laser systems.

9134-34, Session 7

Pulsed high-power yellow-orange VECSEL

Emmi L. Kantola, Tomi Leinonen, Sanna Ranta, Miki Tavast, Mircea Guina, Tampere Univ. of Technology (Finland)

Many important medical applications, such as dermatology, eye surgery and various imaging methods, can benefit from the availability of practical and cost-effective yellow-orange lasers. In addition, high-power yellow-orange lasers are also needed in astronomy for laser guide star adaptive optics in earth-based telescopes. In many of the medical applications, pulsed operation is preferred because it can decrease damage to healthy tissue and/or improve overall results in comparison to CW operation. For example, in photocoagulation related eye surgery the ideal pulse width is in the order of 1 μs. Laser guide stars would also benefit from a pulsed high power yellow-orange laser with pulse widths in the microsecond range.

Frequency doubled vertical-external-cavity surface-emitting lasers (VECSELs) have recently emerged as a promising solution for generating high-brightness light in the yellow-orange range. They are compact, power scalable and can maintain good beam quality even when emitting several watts of output power and thus provide a viable alternative to complex and expensive dye and solid state lasers. Furthermore, VECSELs can be conveniently modulated to produce pulse widths down to a few hundred nanoseconds by modulating the pump laser. In addition to the functionality required by the applications, pulsed operation decreases the thermal load on the gain chip, ultimately enabling to increase power and system efficiency compared to continuous wave operation.

We report on the development and realization of the first pulsed high-efficiency intracavity frequency doubled VECSEL emitting around 587 nm. The VECSEL included a MBE grown semiconductor gain chip with an active region comprised of 10 GaAs-based quantum wells. For efficient thermal management the gain chip was capillary bonded to a diamond heat spreader, which was further attached to a water-cooled copper mount. The gain chip was employed in a V-shaped cavity that included a birefringent filter and an etalon for wavelength tuning and linewidth narrowing. The fundamental emission wavelength was frequency doubled using a critically phase matched lithium triborate (CPM LBO) crystal in an intracavity configuration. The pulsed operation was achieved by direct modulation of the 808 nm laser used to pump the gain chip. The operation temperature of the gain chip mount was in the range of 21 °C.

The frequency doubled output was measured for two different pulse widths: ~1 μs and 0.57 μs. The repetition rate was kept constant at 10 kHz. The maximum peak output power measured for both pulse widths was ~14 W, which is a 61 % improvement in power compared to the CW measurement (8.5 W) made at the same coolant temperature. The CW power was also thermal rollover limited, whereas the power curves for the pulsed measurements did not show any thermal rollover and the maximum output power was in fact limited by the available

peak pump power. The optical-to-optical conversion efficiencies for the two pulse widths were 20 % and 21 %, respectively. In comparison, the calculated conversion efficiency for CW operation was 14 %. The pulse widths were limited by the long rise time of the pump laser driver and its specifications.

9134-35, Session 8

Emission properties from nanolasers during transition to lasing *(Invited Paper)*

Weng W. Chow, Sandia National Labs. (United States)

The emission characteristics of nanolasers are investigated, using a fully quantized laser theory. The active medium is treated as consisting of inhomogeneously-broadened semiconductor quantum dots embedded in a quantum well. Threshold behaviors, in terms of intracavity intensity, coherence time and second order correlation function are computed during nonlasing to lasing transition. Comparisons are made between a conventional nanolaser configuration and when approaching unity-spontaneous-factor or few-quantum-dot situations. A motivation for the study is to contribute to discussions involving recent nanolaser experiments, in particular, those relating to thresholdless lasing.

9134-36, Session 8

Absolute and relative refractory periods in a micropillar laser with saturable absorber

Foued Selmi, Rémy Braive, Isabelle Sagnes, Grégoire Beaudoin, Robert Kuszelewicz, Sylvain Barbay, Lab. de Photonique et de Nanostructures (France)

We present experimental and theoretical results on the nonlinear dynamics of semiconductor micropillar lasers with intracavity saturable absorber in the excitable regime. The excitable regime is characterized by an all-or-none type of response to an input perturbation: when the perturbation amplitude is below the excitable threshold, the system remains in its quiet, stable state; when the perturbation exceeds the excitable threshold, a calibrated response pulse is emitted. It is believed to have great potential for fast neuromorphic optical processing, in addition to being also interesting for the study of nonlinear wave propagation. Fast excitable, neuron-like, dynamics is experimentally evidenced with response times in the 200ps range. We also show the presence of an absolute and a relative refractory periods in this system, analog to what is found in biological neurons but with several orders of magnitude faster response times. The absolute refractory period is the amount of time after a first excitable pulse has been emitted during which it is not possible to excite the system anymore. The relative refractory period is the time after a first excitable pulse during which an inhibited response is emitted and has been often overlooked in optical systems. Both these times are of fundamental importance regarding the propagation of stable excitable waves, and in view of designing spike-time based optical signal processing systems. The experimental results are well described by a simple model of a laser with saturable absorber.

9134-37, Session 8

Square-wave emission and dissipative vectorial solitons in a vertical-cavity surface-emitting laser using polarisation degree of freedom

Julien Javaloyes, Univ. de les Illes Balears (Spain); Mathias Marconi, Massimo Giudici, Stephane Barland, Institut Non Linéaire de Nice Sophia Antipolis (France); Salvador Balle, Univ. de les Illes Balears (Spain)

We study theoretically and experimentally the combined effects of polarization-selective optical feedback and of crossed-polarization re-injection in a vertical-cavity surface-emitting laser. We show that the application of polarization-selective optical feedback, which induces an effective dichroism in the system, allows to generate a robust and regular square-wave output signal in each polarization component. The period of the square-wave signal is determined by twice the re-injection delay. We analyze the regularity of the induced modulation as a function of laser bias current, dichroism and of the levels and delays of re-injection and feedback, thus revealing the robustness of the square-wave emission in the parameter space. For a different set of parameters, we also report experimental evidence that the VCSEL can emit light in the form of temporal dissipative solitons. These solitons exploit the vectorial nature of the electromagnetic field, and arise as polarization slips in which the emission orientation performs a cycle while the intensity remains almost constant and can be interpreted as dark-bright soliton. The large temporal aspect-ratio of the cavity enables the experimental observation of independent solitons coexisting with bounded states of soliton molecules within the same round-trip. While the formers evolve independently as evidenced by their uncorrelated random walks, the latter evolve as rigid bodies.

9134-38, Session 8

Beyond the standard approximations: an analysis leading to a correct description of phase instabilities in semiconductor lasers

Lionel Gil, Gian Luca Lippi, Univ. de Nice Sophia Antipolis (France)

Our analysis is based on the propagation equation for the electric field, the energy balance equation and the material susceptibility which connects the time Fourier transform of the polarization P to that of the electric field. This allows us to introduce the full description of the semiconductor material response, without making any assumptions on the polarization terms which interact with previously selected modes of the cavity, not included here. Our description makes use of the derivatives of the susceptibility c(w,N), with its separate real and imaginary contributions, thus taking into account the full material response without any assumptions on their contributions to separate mixing terms which couple individual modes, common in alternative approaches based on a modal expansion. Neither the Rotating-Wave Approximation nor the Slowly Varying Envelope Approximations are performed in our model, we apply a multi-scale analysis to the set of equations to obtain a description in terms of physical variables (electric field and carrier density) which evolve on equivalent time scales. A linear stability analysis of the resulting equations provides the expression for the eigenvalue associated with phase symmetry and shows the existence of a phase instability [1] characterized by phase gradients, whose existence does not necessarily imply amplitude gradients [2]. As such, we can associate the ensuing dynamics with that reported experimentally in Multiple-Quantum-Well semiconductor lasers [3], where a quasi-perfect antiphase dynamics regime has been observed. The numerical integration of the equations of our model convincingly shows that a pure phase instability can occur, in the absence of an amplitude modulation, and that this instability evolves into one with mixed phase-amplitude character (i.e., with a residual modulation of the amplitude) depending on the regime of operation of the laser, as remarked in [3]. Notice that since our model does not project the electric field onto a set of cavity modes, its amplitude (or total intensity) automatically includes all the cross-terms which are normally neglected in a modal description, due to their high beat frequencies. As such, we can speak of a true antiphase dynamics. Experiments conducted on quantum-dot lasers [4] have shown the existence of a dynamics compatible with our predictions. Finally, we remark that the phase instability plays the role of a dynamical noise. This result

opens up new questions on the role of quantum noise sources, intrinsic to any laser (and in particular to semiconductor lasers), relative to those of dynamical origin.

[1] T.B. Benjamin and J.E. Feir, The disintegration of wave trains on deep water. Part 1. Theory, J. Fluid Mech. 27, 417 (1967).

[2] B.I. Shraiman, A. Pumir, W. van Saarloos, P.C. Hohenberg, H. Chaté and M. Holen, Spatiotemporal chaos in the one-dimensional complex Ginzburg-Landau equation, Physica D 57, 241 (1992).

[3] L. Furfaro, F. Pedaci, M. Giudici, X. Hachair, J. Tredicce and S. Balle, Mode-Switching in semiconductor lasers, IEEE J. Quantum Electron. 40, 1365 (2004).

[4] Y. Tangui, J. Houlihan, G. Huyet, E.A. Viktorov, and P. Mandel, Phys. Rev. Lett. 96, 053902 (2006).

9134-39, Session 9

Cavity solitons in vertical-cavity surface-emitting lasers *(Invited Paper)*

Mustapha Tlidi, Univ. Libre de Bruxelles (Belgium)

A drift instability of the cavity solitons induced by a regular time-delayed feedback, which provides a robust and a controllable mechanism, responsible for the appearance of a spontaneous motion has been predicted [1]. Previous works revealed that when the product of the delay time and the rate of the feedback exceeds some threshold value, cavity solitons start to move in an arbitrary direction in the transverse plane [1,2,3]. In these studies, the analysis was restricted to the specific case of nascent optical bistability described by the real Swift-Hohenberg equation with a real feedback term.

In this communication, we study the role of the phase of the delayed feedback and the carrier lifetime on the motion of cavity solitons in broad-area vertical-cavity surface emitting laser (VCSEL) structure, driven by a coherent externally injected beam. This simple and robust device received special attention owing to advances in semiconductor technology. We show that for certain values of the feedback phase cavity soliton can be destabilized via a drift bifurcation leading to a spontaneous motion in transverse plane [4,5]. Furthermore, we demonstrate that the slower is the carrier decay rate in the semiconductor medium, the higher is the threshold associated with the motion of cavity solitons. Our analysis has obviously a much broader scope than semiconductor cavities and could be applicable to large variety of optical and other systems.

[1]M. Tlidi, A.G. Vladimirov, D. Pieroux, and D. Turaev, Phys. Rev. Lett. 103, 103904 (2009).

[2]M. Tlidi, E. Averlant, A. Vladimirov, and K. Panajotov, Phys. Rev. A 86, 033822 (2012).

[3]S. V. Gurevich and R. Friedrich, Phys. Rev. Lett. 110, 014101 (2013).

[4]K. Panajotov and M. Tlidi, Eur. Phys. J. D 59, 67 (2010).

[5]A. Pimenov, A. G. Vladimirov, S. V. Gurevich, K. Panajotov, G. Huyet, and M. Tlidi, Phys. Rev. A (2013) in press.

9134-40, Session 9

Buffering optical data with topological localized structures in semiconductor laser

Bruno Garbin, Julien Javaloyes, Giovanna Tissoni, Stephane Barland, Univ. de Nice Sophia Antipolis (France)

Localized states can form in nonlinear optical systems either in the dimension transverse to propagation, or on the contrary along the propagation dimension. In both cases, they have been observed in systems with or without phase symmetry. Systems with phase symmetry include for instance lasers with saturable absorber, in which localized states have been observed both along the propagation direction (in mode locked lasers) or in the transverse dimention (coupled broad area VCSELs or VCSELs with dispersive optical feedback). Localized states in systems with coherent forcing (ie, without phase symmetry) have also been observed along the tranverse dimension (broad area semiconductor amplifier with forcing) or in nonlinear fiber ring cavity with coherent injection.

In this contribution, we demonstrate a new kind of temporal topological localized structures. We build on the notion of excitability in a laser with optical injection. In this case, excitable pulses are homoclinic orbits connecting the locked state to itself after well defined excursion in phase space corresponding to the relative phase between forcing and slave laser which first unlocks and then locks again. Putting such a system inside a feedback loop and building on the analogy between delayed dynamical systems and spatially extended systems, we show that many independent homoclinic connections can exist and be stable in the pseudo space associated to the delay loop. We show that we are able to control and store up to two bytes of information, each bit being a 2pi phase slip of the slave laser with respect to the master laser. Each bit has a duration of approximately 100ps (detection limit) and the practical limit of the number of bits lets us envision much larger optical data buffering capacity.

9134-41, Session 9

Phase-bistable 1D-structures induced by space periodic injection in VCSELs

Germán J. de Valcárcel, Univ. de València (Spain); Cristián Fernández-Oto, Mustapha Tlidi, Univ. Libre de Bruxelles (Belgium); Krassimir Panajotov, Vrije Univ. Brussel (Belgium) and Institute of Solid State Physics (Bulgaria); Kestutis Staliunas, Univ. Politècnica de Catalunya (Spain) and Institució Catalana de Recerca i Estudis Avançats (Spain)

Above the locking point of a laser with injected (monochromatic) signal, the phase of the laser is locked to that of the master laser: the phase response of the slave laser is mono-stable. Yet, transforming that situation into a phase-bistable one could be interesting for pattern formation since the typical patterns associated to each case differ in general. Unfortunately the classic parametric driving (at the second harmonic of the oscillators' frequency), which leads to that phase bistability in a variety of nonlinear oscillators, is useless in laser systems owed to their very narrow gain line. Yet, "rocking" has been proposed as a general mechanism in physics of dynamical systems, whereby a phase-invariant oscillatory system is converted into a phase-bistable one. Unlike the parametric driving, rocking is effective in lasers because it is resonant, or nearly resonant, with the laser emission frequency. Two types of rocking have been introduced so far, and both involve the modulation of a monochromatic driving so that the sign of its amplitude alternates (periodically or even randomly) either in time or in space [G. J. de Valcárcel and K. Staliunas, Phys. Rev. Lett. 105 (2010) 054101]. A simple experimental implementation of spatial rocking consists of interfering two tilted monochromatic beams at the gain medium, which is a slight modification of the usual laser with injected signal setup. The interference fringes must have a small spatial period, relative to the diffraction length of the system. Both temporal and spatial rocking has been demonstrated experimentally, although the latter was shown in a small aspect ratio system – just a couple of transverse modes.

In this communication we propose and demonstrate analytically and numerically the feasibility of spatial rocking in a VCSEL –a system with a huge number of degrees of freedom. VCSELs are already established as a very convenient system for excitation of spatial patterns, both extended and localized (spatial solitons). The motivation of our research is that spatially rocked VCSELs, due to the imposed phase bistability, can show even more rich pattern formation, and that patterns can be better controllable.

We show the effect of spatial rocking in VCSELS by simulating the well-established mean-field model for injected VCSELs [M. Brambilla, L.A. Lugiato, F. Prati, L. Spinelli, and W.J. Firth, Phys. Rev. Lett. 79 (1997) 2042], trivially modified by the transverse

spatial variation of the injection and for realistic parameter values. For proper values of the injection parameters phase-bistable states occur and a variety of phase bistable patterns are found. Such patterns are rolls, phase domains and phase (dark ring) solitons, which are the typical patterns in phase-bistable systems. Last but not least, we also show the role of spatial rocking to stabilize the spatial patterns in VCSELs. It is well known that the free running VCSELs show a complicated spatio-temporal dynamics, which can be stabilized by means of, e.g. external diffraction gratings. We also show that the spatial rocking stabilizes the chaotic dynamics of VCSELs in time, whereas maintaining the possibility to obtain spatial patterns in space.

9134-42, Session 9

Soliton bound states in semiconductor disk laser

Evgeny A. Viktorov, Univ. of ITMO (Russian Federation) and Univ. Libre de Bruxelles (Belgium); Mantas Butkus, Univ. of Dundee (United Kingdom); Thomas Erneux, Univ. Libre de Bruxelles (Belgium); Craig J. Hamilton, Graeme P. A. Malcolm, M Squared Lasers (United Kingdom); Edik U. Rafailov, Univ. of Dundee (United Kingdom)

The state of multiple bounded solitons was first theoretically predicted as a possible solution in a nonlinear Schrödinger and Ginzburg-Landau equation. The state is also known as a soliton molecule and attracts a wide interest in nonlinear and laser optics [1]. So far the soliton bound soliton states were only demonstrated in fiber lasers. Here we report what we believe is the first demonstration of a temporal soliton bound state in semiconductor disk laser (SDL). Optically pumped SDLs are often considered as a potential alternative for the modelocked vibronic lasers where high kW level peak powers are in high demand for driving various nonlinear processes like bio-photonic imaging, frequency conversion, supercontinuum generation and others. A breakthrough in the lower repetition rate potentially will position SDLs in much higher demand for applications where Ti:Sapphire has been the first choice laser source for high peak power and sub-100 MHz repetition rate.

The laser was passively mode-locked using a quantum dot based semiconductor saturable absorber mirror (QD-SESAM) and was operated at record-low repetition rate of 85.6 MHz overcoming short carrier lifetime limitations. Two mode-locking regimes were observed where the laser would emit single or closely spaced double pulses (soliton bound state regime) per cavity round-trip. The pulses in soliton bound state regime were spaced by discrete, fixed time duration.

For the experiment, a multi-folded cavity was formed around the quantum well based gain medium with a total cavity length of 1.76 m. Saturable absorber with a peak absorption at 967nm was based on InGaAs quantum dot structures and served as one of the cavity end mirrors. The gain chip was pumped with 14 W of 808 nm light and produced 360 mW average output power. The TEM00 mode output beam was vertically polarized. Fundamental mode-locking and bound state regimes were observed by changing the pulse fluence on the SESAM. A fast photo detector and an oscilloscope were used to record a trace of pulses.

In soliton bound state regime, the time separation between individual pulses was 1 ns and the pulse pairs were separated by the cavity round-trip time of 12 ns. Radio frequency spectrum measurement yielded a narrow spectral line at 85.6 MHz and a number of harmonics indicating a stable mode-locked operation. The autocorrelation method was used to measure the pulse duration of 60 ps. Optical spectrum centred at 988.5 nm was strongly modulated, what is typical for soliton bound state. Fundamental regime with single pulse per cavity round trip featured similar characteristics in terms of the pulse duration and the optical spectrum width.

We use a system of delay differential equations to model the dynamics of our device. The theoretical model shows that such regime of bounded pulses with well-defined discretely locked phases between the soliton multiplets is indeed possible given a large difference between alpha factors in gain material and SESAM.

[1] P. Grelu and N. Akhmediev, “Dissipative solitons for mode-locked lasers,” Nature Photonics, vol. 6, pp. 84-92, 2012.

9134-43, Session 9

Cavity solitons in a medium-size VCSEL

Etienne Averlant, Univ. Libre de Bruxelles (Belgium) and Vrije Univ. Brussel (Belgium); Krassimir Panayotov, Vrije Univ. Brussel (Belgium); Thorsten Ackemann, Univ. of Strathclyde (United Kingdom); Mustapha Tlidi, Univ. Libre de Bruxelles (Belgium)

Localized structures, or Cavity Solitons (CSs) have been experimentally observed in broad area (100 micrometer diameter) [1, 2] and in a smaller area (40 micrometer diameter) Vertical-Cavity Surface-Emitting Laser (VCSEL) under optical injection [3]. Such structures can be generated using a writing beam, or spontaneously arise when a control parameter is swept forward and backwards [3] (see [2] for review on this issue).

We experimentally investigate the spontaneous formation of CSs in a medium size (80 micrometer diameter) VCSEL. Bistability being ensured by the optical injection, we swept optical injection power to generate and erase CSs in the near field of the VCSEL. A single and multi-peaked CSs are generated [4] this way.

This device is now used to check theoretical predictions about the delay-induced motion of localized structures [4-7]. Preliminary results on the spontaneous motion of the localized structures in the presence of a delayed feedback will be discussed.

[1] Barland, S., Tredicce, J. R., Brambilla, M., Lugiato, L. A., Balle, S., Giudici, M., Maggipinto, T., Spinelli, L., Tissoni, G., Knödl, T., et al, cavity solitons as pixels in semiconductor microcavities, Nature 419(6908), 699 (2002).

[2] Barbay, S., Kuszelewicz, R., and Tredicce, J. R, Cavity solitons in vcsel devices, Advances in Optical Technologies 2011, 628761 (2011).

[3] Hachair, X., Tissoni, G., Thienpont, H., and Panajotov, K, Linearly polarized bistable localized structure in medium-size vertical-cavity surface-emitting lasers, Phys. Rev. A 79, 011801 (Jan 2009).

[4] Averlant, E., Tlidi, M., Thienpont, H., Ackemann, T., and Panajotov, K., Experimental observation of localized structures in medium size vcsels, Optics Express (submitted)(2013).

[5] Tlidi, M., Vladimirov, A. G., Pieroux, D., and Turaev, D., Spontaneous motion of cavity solitons induced by a delayed feedback, Phys. Rev. Lett. 103, 103904 (Sep 2009).

[6] Tlidi, M., Averlant, E., Vladimirov, A., and Panajotov, K., delay feedback induces a spontaneous motion of two-dimensional cavity solitons in driven semiconductor microcavities, Phys. Rev. A 86, 033822 (Sep 2012).

[7] Panajotov, K. and Tlidi, M., Spontaneous motion of cavity solitons in vertical-cavity lasers subject to optical injection and to delayed feedback, The European Physical Journal D 59(1), 67 (2010).

9134-57, Session PS3

Superfocusing of high-M2 semiconductor laser beams: experimental demonstration

Grigorii S. Sokolovskii, Ioffe Physico-Technical Institute (Russian Federation); Vasileia Melissinaki, Foundation for Research and Technology-Hellas (Greece); Vladislav V. Dudelev, Sergey N. Losev, Ksenya K. Soboleva, Ekaterina D. Kolykhalova, Anton G. Deryagin, Ioffe Physico-Technical Institute (Russian Federation); Evgeny A. Viktorov, Univ. Libre de Bruxelles (Belgium) and National Research Univ. of Information Technologies, Mechanics

and Optics (Russian Federation); Vladimir I. Kuchinskii, Ioffe Physico-Technical Institute (Russian Federation) and Saint Petersburg Electrotechnical Univ. "LETI" (Russian Federation); Maria Farsari, Foundation for Research and Technology-Hellas (Greece); Wilson Sibbett, Univ. of St. Andrews (United Kingdom); Edik U. Rafailov, Univ. of Dundee (United Kingdom)

Focusing of the multimode laser diode radiation is probably the most significant problem that hinders expansion of the high-power semiconductor lasers in many cutting-edge applications. Generally, the 'quality' of laser beams is characterized by so-called 'beam propagation parameter' M2, which is defined as the ratio of the divergence of the laser beam to the diffraction-limited divergence (i.e. the divergence of the 'ideal' Gaussian beam for which M2=1). Therefore, M2 determines the ratio of the beam focal-spot size to that achievable by focusing the 'ideal' Gaussian beam by the same optical system. Typically, the beam propagation parameter M2 for the high-power broad-stripe laser diodes takes the value of 20-50. Thus the focal-spot size for such lasers is typically one or even two orders of magnitude higher than diffraction-limited value. In order to overcome this limitation, recently we proposed a method of the 'interference' focusing of the multimode semiconductor laser radiation. The idea of such a 'superfocusing' relies on the technique developed for generation of Bessel beams with laser diodes which is based on utilization of a cone-shaped lens (axicon). With traditional focusing of multimode radiation, different curvatures of the wave-fronts of various modes lead to a shift of their focal points along the optical axis that causes increase of the focal-spot size with increasing M2. In contrast, formation of the Bessel beam with axicon relies on the 'self-interference' of each mode thus eliminating the main reason for increase of the focal-spot size. For experimental demonstration of the proposed technique, we used broad-area laser diodes with M2 of 20-30 and emission wavelength in ~1um range. Utilization of the axicons with apex angle of 140deg enabled demonstration of the order of magnitude decrease of the focal-spot size compared to what could be achieved by the 'ideal' optical system with a unity numerical aperture. Significant problems for demonstration of the superfocusing in our experiments was the divergence of the laser diode beam when collimated on the axicon and the rounded shape of the axicon tip (which is unavoidable for commercial axicons). Any of these may result in corruption of the Bessel beam and significant increase of the width of its central lobe. The elegant solution for both of these technical problems was utilization of the micro-axions produced on the tip of the 100um optical fiber with the super-resolution 3D laser printing. The fiber axicons used in our experiments featured the rounded area of the tip as small as ~10um in diameter. Combined with the fiber-output beam 'auto-collimation' feature this enabled demonstration of 2-4um focused laser 'needle' beams with nearly 100um propagation length generated from multimode laser diode beams with M2 values of 20 to 30.

9134-58, Session PS3

Critical slowing down in polarization switching of vertical-cavity surface-emitting lasers

Yu-Heng Wu, Yueh-Chen Li, Wang-Chuang Kuo, Tsu-Chiang Yen, National Sun Yat-Sen Univ. (Taiwan)

Vertical-Cavity Surface-Emitting Lasers (VCSELs) have many advantages in many applications. However, Since the cavity anisotropy, the polarization instability is often observed in experiments. A celebrated example is VCSEL's polarization switching (VPS), which means that the polarization switches to the orthogonal polarization at a specific bias current called PS current. If the PS current of increasing and decreasing bias current process are different, it shows a polarization switching hysteresis loop (PSHL). VPS has been studied extensively in dynamical and theoretical studies. In most studies the VPS was ascribed to thermal effect. Therefore, the thermodynamic characteristic of VPS is an important research. In recent studies of VCSELs, critical slowing down (CSD) were used to explain the turn-on delay of semiconductor lasers and the VPS. Nevertheless, the earlier studies investigated the dynamical case, which differ from the static case. This research investigated the critical slowing down in polarization switching (PS) of VCSELs. The VCSEL operated at 850 nm and behaved PSHL in this study. The experiments were performed by step-function current injection in two types: step-up and step-down. In the case of step-up, the initial current was set at lower than PS current, below threshold current, and no current injection for 10 min. After 10 min, the injection current was turned to a final current which is higher than the PS current. The emission of VCSEL still polarized in X-direction at this current. After a relaxation time (?r), the output switched to Y-polarization. For lower initial current case, the range of ?r was from several second to approximate 1000 s, which shows a time divergence with current decreasing. The relationship between Relaxation time and final current in this experiment resembles CSD. For the cases of initial current below threshold and no current injection, there is no divergence behavior in the relationship between ?r and final current. These results show that the mechanism in the case which set the initial current below threshold and which no current injection initially are similar but quite different from the case of lower initial current. In the case of step-down, it was similar to the case of step-up, but the initial current was set at higher than PS current and down to a current lower than PS current. After the current down to a lower current, the output still stay at Y-polarization for a relaxation time, and then the output switched to X-polarization. The result shows a time divergence with current increasing and resembles CSD. The critical current (Ic) of two step-function current experiment are compared. The PS in this experiment is a static case. Moreover, we also find that the divergence of ?r follow a power law and the critical exponent was measured in these experiments. These results contribute to the understanding of the mechanism of CSD in VPS.

9134-59, Session PS3

Enhancement of the low-frequency response of a reflective semiconductor optical amplifier slow light-based microwave phase shifter by using forced coherent population oscillations

Aidan Meehan, Michael J. Connelly, Univ. of Limerick (Ireland)

The field of slow and fast light (SFL) has been a growing area of interest over the past decade. Microwave phase shifters based on SFL have been used to demonstrate applications such as true time delays and tunable filters. Semiconductor optical amplifiers (SOAs) have been extensively researched for use as SFL elements. They can be used to control the group velocity of an amplified signal by adjusting the optical input power and the SOA bias current. One of the most common methods to obtain slow and fast light effects in an SOA is by using coherent population oscillations (CPO). CPO can be achieved by injecting a sinusoidally modulated optical signal into an SOA. As a result the active region carrier density is modulated at the beat frequency (i.e. the modulation frequency) between the sidebands and the carrier frequency. This in turn leads to a change in the group index and so the beat signal at the SOA output is phase shifted relative to the input beat signal. The coupling of energy from the carrier to its sidebands is dependent on the input optical power, bias current and modulation frequency and enables the beat signal gain to reach levels substantially higher than the device's optical gain. However at modulation frequencies below the inverse of the carrier lifetime, the beat signal gain (defined as the ratio of the output to input beat signal powers) is low leading to poor signal-to-noise ratio. The beat signal gain at low frequencies can be greatly enhanced by using forced coherent population oscillations (FCPO), which involves simultaneously modulating the optical power and the SOA current at the same frequency. In this paper we experimentally demonstrate the enhancement at low frequencies (0.5 - 2 GHz) of an SFL based microwave phase shifter using FCPO in a commercially available reflective semiconductor optical amplifier (RSOA). The device used is

a tensile-strained bulk 1550 nm device incorporating a 2.5 GHz current driver circuit. The input light signal is a directly modulated 1550.8 nm DFB laser. A network analyser is used to provide the modulating signal to the laser and current driver and also to measure both the beat signal gain and the phase shift experienced by the beat signal. With no current modulation applied the received electrical power after photo-detection varies linearly from -43 dBm at 0.5 GHz to -40 dBm at 2.0 GHz. When current modulation is applied the beat signal electrical power ranges from -31 dBm to -40 dBm over the same frequency range. Across this range of frequencies it is possible to obtain a controllable phase shift of up to 35 degrees.

9134-60, Session PS3

Characterization of the working parameters of a long-wavelength VCSEL

Pablo Perez, Angel Valle, Univ. de Cantabria (Spain); Ignacio Noriega, Instituto de Fisica de Cantabria, Univ de Cantabria-CSIC (Spain); Luis Pesquera, Univ. de Cantabria (Spain)

We report on measurements of the working parameters of a 1550-nm vertical-cavity surface-emitting laser (VCSEL), including those that describe the polarization behavior of the device. Simple expressions for the laser linewidth and laser power as a function of the bias current are used in a first stage. A simple relation between the laser linewidth and the bias current is derived and used to extract the differential carrier lifetime at threshold. Our VCSEL exhibits abrupt polarization switching when increasing the bias current, from the higher to the lower frequency polarization mode. Effective dichroism and birefringence values at the switching point are then used for extraction of the polarization-dependent parameters of the VCSEL. Spontaneous emission fraction is evaluated from the comparison of the theoretical and experimental polarization-resolved ligh-current characteristics. The obtained values of spin-flip rate and spontaneous emission fraction of our device are larger than those typically used for the theoretical modelling of these devices.

9134-61, Session PS3

Wideband model of a reflective tensile-strained bulk semiconductor optical amplifier

Michael J. Connelly, Univ. of Limerick (Ireland)

Reflective semiconductor optical amplifiers (RSOAs) have shown promise for applications in wavelength division multiplexed passive optical networks and in fiber ring mode-locked lasers. Polarization insensitive SOAs can be fabricated using tensile-strained bulk material and a conventional rectangular cross section waveguide. The introduction of the appropriate amount of tensile strain can be used to compensate for the different confinement factors experienced by the waveguide TE and TM modes. There is a need for models that can be used to predict RSOA static characteristics such as the dependency of the signal gain on bias current and input optical power, the amplified spontaneous emission spectrum and the noise figure. In this paper we extend our prior work on non-reflective SOAs to develop a static model that includes facet reflections. The RSOA is a commercially available device, which comprises an undoped tensile-strained (0.15% strain) InGaAsP active region sandwiched between two InGaAsP separate-confinement heterostructure layers and operates in the 1550 nm. The active waveguide length is 400 microns including an 80 micron input taper. The input facet has very low reflectivity and the back facet has a reflectivity of 0.88. The active region material conduction band is a modelled by a parabolic function of momentum. An axial approximation, including strain effects, which results in a 3x3 Hamiltonian is used to obtain the light-hole, heavy-hole and split-off valence bands. The quasi-Fermi levels are obtained by numerically solving charge neutrality equations for the conduction and valence bands. From the band structure, associated transition matrix elements and Fermi-levels, the polarisation, carrier density and wavelength dependent gain and additive spontaneous emission are calculated; which also includes the intraband lifetime through the use of a sech shaped lineshape function. The spatial evolution of the amplified signal and spontaneous emission photon rates are modelled by travelling wave differential equations that include polarisation dependent material gain, optical confinement factors and material loss coefficients. These differential equations are solved numerically by using a finite difference technique, subject to the boundary conditions at the amplifier input and back facets, in conjunction with a carrier density rate equation. The latter equation includes the total spontaneous emission, Auger recombination rates, the amplified signal and spontaneous emission. In the model 64 spatial sections are used. The wavelength dependence of the amplified spontaneous emission is obtained by using 256 spectral slices over a range of 1400 to 1650 nm. Model parameters that are difficult to calculate or measure, such as the Auger recombination coefficient and intraband lifetime, are estimated by fitting the predicted output spontaneous emission spectrum to polarization resolved spontaneous emission spectrum measurements for various bias currents, using Levenberg-Marquardt least-squares fitting. The model results, including signal gain dependency on wavelength, bias current and input optical power show excellent agreement with experiment. The use of such a wideband model enables the effects of changes in the RSOA waveguide geometry and strain to be evaluated and thereby is an aid in optimising device performance.

9134-62, Session PS3

Experimental investigation of elliptically polarized injection-locked VCSELs

Hong Lin, Bates College (United States); Pablo Perez, Angel Valle, Luis Pesquera, Univ. de Cantabria (Spain)

Polarization properties of vertical-cavity surface-emitting lasers (VCSELs) are interesting from both a fundamental and an applied point of view. Polarization switching (PS) between linear polarizations of the VCSEL can appear when changing the bias current of the free-running device. Also PS appears when the VCSEL is subject to orthogonal optical injection in which the injected field has a linear polarization that is orthogonal to that of the free-running VCSEL. In this situation interesting nonlinear dynamics appear, one of which is the existence of an injection-locked solution for which the two linear polarized modes of the VCSEL lock to the master laser frequency [1]. This situation has been theoretically predicted and corresponds to an elliptically polarized injection-locked (EPIL) state [1].

In this work we make an experimental investigation of the dynamics of a long-wavelength single-transverse mode VCSEL when subject to orthogonal optical injection. The free-running VCSEL emits a linearly polarized beam in the so called “parallel” direction. The polarization of the injected light is perpendicular to this state and is termed “orthogonal” polarization. We observe the EPIL state when the frequency of the orthogonal injected light is near the frequency of the parallel polarization. The EPIL region is measured in the frequency detuning-injected power plane. The results on the nonlinear dynamics of both linear polarizations around the EPIL states will also be presented.

[1] M. Sciamanna, K.Panajotov, Phys. Rev. A 73, 023811 (2006).

9134-63, Session PS3

An adaptive stepsize controlled solver for the dynamic WDM semiconductor optical amplifier response

Christos Vagionas, Aristotle Univ. of Thessaloniki (Greece); Jan Bos, PhoeniX Software (Netherlands)

Semiconductor Optical Amplifiers (SOA) have been extensively used in optical networks and high-speed switches and are recently combined in flip-flops, RAM cells and RAM banks. Building-up SOA-based circuits of increasing complexity with multi-wavelength signals co- or counter-propagating calls for accurate yet efficient time-dependent numerical models supporting large input patterns for system performance evaluation.

Rate equation based models normally discretize the SOA into segments to account for the spatial distribution of the carrier density and photon fluxes within the SOA along its length over time, resulting in a system of coupled differential equations, which can become quite large when material gain is to be calculated accurately over a broad spectrum. Solving such a system by explicit time stepping, the standard approach, requires dense time sampling to remain stable as the time step is limited by the time it takes for photons to propagate from one segment to the next.

Implicit time discretization schemes for stiff systems of coupled differential equations allow one to make accuracy restricted instead of, much more stringent, stability restricted time steps. This at the cost of having to solve a system of equations at each time step. To the authors knowledge this additional cost has so far prevented the application of such schemes for solving dynamic SOA response models. Applying multigrid reduces this cost to the same complexity as that of an explicit time step with a larger constant.

For the second order accurate implicit midpoint rule combined with a simple step doubling scheme as adaptive step size controller, bits are resolved in O(10) steps independent of the bitrate and pulse shape for typical required accuracies. For a SOA discretized into 32 segments and 32 frequency bins for the ASE resolution, our current multigrid solver solves each time step in about 0.1 seconds on a standard PC.

9134-64, Session PS3

A finite-difference time-domain algorithm for simulating light propagation in anisotropic dynamic gain media

Ahmad Al-Jabr, King Abdullah Univ. of Science and Technology (Saudi Arabia); Mohammed Alsunaidi, King Fahd Univ. of Petroleum and Minerals (Saudi Arabia); Boon S. Ooi, King Abdullah Univ. of Science and Technology (Saudi Arabia)

We report a time-domain algorithm to simulate the propagation of light in anisotropic dynamic gain media. This problem has not received much attention in literature due to the challenge of incorporating the active material properties in the rate equations to model the gain dynamic of semiconductor lasers. Typically, active materials are approximated as isotropic media. In this work, we present an algorithm that handles anisotropy and gain at the same time. The main idea behind this algorithm is to separate calculations of Maxwell's equations into layers. In each layer, variables are solved independently. In this case, we will face four calculation problems that are difficult to handle at once. We need to calculate population difference to get gain, polarization, flux densities and electric fields. Therefore, we have separated the calculation of each one into a separate layer that is independent of the other layers, and thus limiting the calculation effort.

The loop of the FDTD can be summarized as follows. First, the polarization can be calculated by knowledge of previous electric fields, population difference and flux densities. By knowledge of polarization, the population difference can updated using the rate equations. There are two models used to describe laser action and they are the two-level system and the four-level system. Whatever laser model is used it is included through the rate equations. With population difference and polarization determined, we can calculate the flux densities. Electric fields can be calculated easily by dividing flux densities by relative permittivity. In anisotropic media, the coupling of polarization fields puts strain on the FDTD algorithm as they should to be calculated at the same time instant. This leads to having too many variables to solve. The coupling problem is solved by updating the values of each polarization field through the general algorithm reported previously. The polarizations need to be averaged around each point to take care of the location mismatch appears in anisotropic FDTD. Finally, incorporating the rate equations makes it a ready algorithm for anisotropic dynamic gain medium. The algorithm is verified against theory by comparing amplification and absorption of light at certain wavelengths as it propagates. Also, the change in population difference is tested for low, medium and high pumping. The importance of this work is then emphasized by numerically studying the propagation of light anisotropic in gain media. Differences between TE and TM modes are analyzed.

9134-65, Session PS3

Two semiconductor ring lasers coupled by a single-waveguide for optical memory operation

Guy Van der Sande, Werner Coomans, Lendert Gelens, Vrije Univ. Brussel (Belgium)

Semiconductor ring lasers are semiconductor lasers where the laser cavity consists of a ring-shaped waveguide. SRLs do not require cleaved facets or gratings for optical feedback and are thus particularly suited for monolithic integration. SRLs are also highly scalable, making them ideal candidates for key components in photonic integrated circuits. SRLs can generate light in two counterpropagating directions between which bistability has been demonstrated. Hence, information can be coded into the emission direction. This bistable operation allows SRLs to be used in systems for all-optical switching and as all-optical memories. For the demonstration of fast optical flip-flop operation, Hill et al. [1] fabricated two SRLs coupled by a single waveguide. Nevertheless, the literature shows that a single SRL can also function perfectly as an all-optical memory [2]. We raise the question whether coupling two SRLs to realize a single optical memory has any advantage over using a solitary SRL, taking into account the obvious disadvantage of a doubled footprint and power consumption. To provide the answer, we numerically study the dynamical behavior of semiconductor ring lasers coupled by a single bus waveguide. To model the single waveguide coupled SRLs, we use the rate equation model for a solitary SRL as in [3] and modify it to comply with our coupling configuration.

The coupling through a single waveguide changes the symmetry properties of the global system compared to those of a solitary SRL. Only one of the two counterpropagating modes of each SRL is fed through to the other SRL, and only one of the modes in each SRL receives input from the other SRL. When both SRLs are operating unidirectionally this leads to globally symmetric and asymmetric states, with respectively equal and unequal power at the outputs in steady state. We provide a detailed analysis of this multistable landscape of the coupled system, analyze the stability of all solutions and relate the internal dynamics in the individual lasers to the field effectively measured at the output of the waveguide [4]. We consider both weakly and strongly coupled devices. The coupling is weak when the coupling amplitude between the SRLs is smaller than or comparable to the backscattering amplitude. This means that the coupling to the other SRL has to be weaker than or comparable to the reflective coupling between the counterpropagating modes inside each SRL. We show which coupling phases generally promote instabilities

and therefore need to be avoided in the design. Regarding all-optical memory operation, we demonstrate that there is no real advantage for bistable memory operation compared to using a solitary SRL. An increased power suppression ratio is found to be mainly due to the destructive interference of the SRL fields at the low power port. Also, multistability between several modal configurations remains unavoidable.

[1] M. T. Hill et al., Nature 432, 206 (2004).

[2] L. Liu, et al. Nature Photon. 4, 182 (2010).

[3] L. Gelens et al., Phys. Rev. Lett. 102, 193904 (2009).

[4] W. Coomans et al., Phys. Rev. A 88, 033813 (2013).

9134-66, Session PS3

Cascadable excitability in optically injected microdisks

Thomas Van Vaerenbergh, Koen Alexander, Martin Fiers, Pauline Mechet, Joni Dambre, Peter Bienstman, Univ. Gent (Belgium)

All-optical spiking neural networks would allow high speed parallelized processing of time-encoded information, using the same energy efficient computational principles as our brain. As the neurons in these networks need to be able to process pulse trains, they should be excitable.

Using simulations, we demonstrate class I excitability in optically injected microdisk lasers, and propose a cascadable optical spiking neuron design. The neuron has a clear threshold and an integrating behavior. In addition, we show that the optical phase of the input pulses can be used to create inhibitory, as well as excitatory perturbations. Furthermore, we incorporate our optical neuron design in a topology that allows a disk to react on excitations from other disks. Phase tuning of the intermediate connections allows to control the disk response. Additionally, we investigate the sensitivity of the disk circuit to deviations in driving current and locking signal wavelength detuning. Using state-of-the-art fabrication techniques for microdisk laser, the standard deviation of the lasing wavelength is still about one order of magnitude too large.

Finally, as the dynamical behavior of the microdisks is identical to the behavior in Semiconductor Ring Lasers (SRL), we compare the excitability mechanism due to optically injection with the previously proposed excitability due to asymmetry in the intermodal coupling in SRLs, as the latter mechanism can also be induced in disks due to, e.g., asymmetry in the external reflection, while we expect that the excitability due to optical injection will also appear in optically injected SRLs with symmetric intermodal coupling. In both cases, the symmetry between the two counter-propagating modes of the cavity needs to be broken to prevent switching to the other mode, and allow the system to relax to its initial state after a perturbation. However, the asymmetry due to optical injection results in an integrating spiking neuron, whereas the asymmetry in the intermodal coupling is known to result in a resonating spiking neuron. This diversity in excitability for a single optical component paves the way towards heterogeneous optical spiking neural networks, containing neurons of which the computational functionality can in principle be adapted depending on the application.

9134-67, Session PS3

The analytical approach to the description of ground-state lasing phenomenon and to the optimization of InAs/InGaAs quantum dot lasers

Vladimir V. Korenev, Artem V. Savelyev, St. Petersburg Academic Univ. (Russian Federation); Alexey E. Zhukov, St. Petersburg Academic Univ. (Russian Federation) and Ioffe Physico-Technical Institute (Russian Federation); Alexander I. Omelchenko, St. Petersburg Academic Univ. (Russian Federation); Mikhail V. Maximov, Ioffe Physico-Technical Institute (Russian Federation) and St. Petersburg Academic Univ. (Russian Federation)

Long-wavelength InAs/InGaAs quantum dot (QD) lasers emitting via QD ground state (GS) optical transitions near the wavelength of 1.3 mkm are the promising light sources for a wide range of practically important applications, from optical coherence tomography and aesthetical surgery to Raman amplifiers pump and ultrafast data transmission. Moreover, these lasers are the beneficial alternative to the currently used arrays of DFB-lasers (distributed feedback lasers) due to the simplicity of their fabrication. However, the majority of currently existing models of QD lasers emitting via GS optical transitions are numerical and based only on the quantitative analysis of the systems of rate equations for QDs giving only the quantitative description of laser`s operation. This, in its turn, complicates their optimization, analysis of operation and finding of the key parameters affecting main spectral characteristics of QD lasers. In order to solve this problem we have proposed a theoretical model, which allowed us not only to describe the experimental data quantitatively, but also to obtain the analytical expressions for the key spectral characteristics of QD lasers and to take into account inhomogeneous broadening. The analytical expression for the shift between the maximum of lasing spectrum and maximum of distribution function of QDs over the energy was found in terms of the proposed model. Thus, in the case of low homogeneous broadening, lasing spectrum width is defined by only two dimensionless parameters, i.e. by the ratio of dispersion of inhomogeneous broadening to the temperature in energy units and by loss-to-maximum gain ratio. The exact analytical expression for the dependence of lasing spectrum width on output power in the case of high temperature is also provided. It was also shown that there are optimal dispersion of distribution of QDs over the energy and optimal size of laser`s active region, which allow to realize the maximum laser`s efficiency at a given injection current. It is shown that in the case of active regions, which have identical layers of QDs, and at fixed cavity length there is an optimal value of dispersion of inhomogeneous broadening, which realizes lasing spectra of maximal width. The minimization of laser`s energy consumption and possible ways of increasing of lasing spectrum width by variation of active region structure and sizes were also studied in details. It is shown that in the cases, when variation of dispersion of inhomogeneous broadening is complicated due to the technological reasons, the usage of multi-layered structures with intentionally introduced irregularity as an active region allows us to increase lasing spectrum width. The optimal structure, which corresponds to the broadest lasing spectrum, is also found.

9134-68, Session PS3

Semiconductor ring lasers with delayed optical feedback: low-frequency fluctuations

Guy Van der Sande, Lilia Mashal, Romain Modeste Nguimdo, Vrije Univ. Brussel (Belgium); Miguel C. Cornelles-Soriano, Instituto de Física Interdisciplinar y Sistemas Complejos (Spain); Guy Verschaffelt, Vrije Univ. Brussel (Belgium)

Semiconductor lasers subject to external feedback are known to exhibit a wide variety of dynamical regimes desired for some applications such as chaos cryptography, random bit generation, and reservoir computing. Low-frequency fluctuations (LFF) is one of the most frequently encountered regimes. It is characterized by a fast drop in laser intensity followed by a gradual recovery. The duration of this recovery process is irregular and of the order of hundred nanoseconds. The average time between dropouts is much larger than the laser system characteristic time-scales.

Semiconductor ring lasers (SRLs) are currently the focus of a rapidly thriving research activity due to their unique feature of directional bistability. They can be employed in systems for all-optical switching, gating, wavelength-conversion functions,

and all-optical memories. SRLs do not require cleaved facets or gratings for optical feedback and are thus particularly suited for monolithic integration. We experimentally and numerically address the issue of LFF considering a SRL in a feedback configuration where only one directional mode is re-injected into the same directional mode, a so-called single self-feedback.

The experiments are performed on an AlGaInAs/InP-based multi-quantum-well SRL with a racetrack geometry that has been fabricated at Glasgow University. The device is a monolithically integrated four-port SRL, where two access waveguides are coupled to the ring cavity by forming directional couplers with the straight sections. The feedback loop is implemented using lensed fibers connected to two ports of the SRL. The round trip time of the external cavity is approximately 60ns, which is quite long. A semiconductor optical amplifier (SOA) is placed in the feedback loop to control the feedback strength by changing the current in the SOA.

We have observed that the system is very sensitive to the feedback strength and the injection current. In particular, the power dropouts are more regular when the pump current is increased and become less frequent when the feedback strength is increased. In addition, we find two different recovery processes after the LFF power dropouts. The recovery can either occur via pulses or in a stepwise manner. Since LFFs are not specific to SRL, we expect these recovery processes to appear also in VCSELs and edge-emitting lasers under similar feedback conditions.

We perform numerical simulations considering a single longitudinal-mode SRL model (also well-suited for microdisk devices) extended with Lang-Kobayashi terms to account for the feedback. The numerics capture the different behaviors very well. Relying on the well-known representation in the phase space of the carriers versus the round trip phase difference the numerical simulations offer additional insight into the LFF and the different recovery processes observed in the experiments.

9134-69, Session PS3

Analogy between the quantum phase transition and the polarization switching of vertical-cavity surface-emitting lasers

Tsu-Chiang Yen, Yu-Heng Wu, Yueh-Chen Li, Wang-Chuang Kuo, National Sun Yat-Sen Univ. (Taiwan)

The investigations of the phase transition in the polarization switching (PS) of vertical-cavity surface-emitting lasers (VCSELs) were recently reported by the authors. That phase transition was classified to be a second-order phase transition (SOPT) according to the criticalities observed in the experiments. This conclusion is based on that the critical phenomenon is a unique characteristic of the SOPT, which does not exist in the first-order phase transition (FOPT). However, some features of that phase transition also indicate that the VCSEL's PS (VPS) is different from the traditional SOPT, especially, quite different from the phase transition around the laser's threshold current. The later was identified as a typical SOPT. In the conventional phase transition investigations of the laser, the laser's intensity is employed as the order parameter. On the basis of Landau's paradigm of the SOPT, that parameter must evolutes from zero to non-zero values, or vice versa, during the phase transition, corresponding to a transition between a disordered state and an ordered state. Nevertheless, in the VPS, the laser's intensity remains constant before and after the PS, revealing an order-to-order transition and significantly contradicting with the classical SOPT. This constancy in the laser's intensity of both polarizations can be interpreted as that both polarizations correspond to two orthogonal and degenerate ground states of the VCSELs. On the other hand, the laser's transverse modes can be expressed mathematically by orthogonal functions of spatial coordinates. These functions cannot transfer to each other through continuous deformations in geometry. That feature attributes a topological characteristic to the laser's transverse modes. Moreover, the spatial coherence of the laser implements a globally geometric characteristic to the laser's output that the transverse modes and the polarizations must simultaneously be emitted all over the laser's facet. But this global characteristic contradicts with the definition of the order parameter, which presents a local property of the systems in Landau's paradigm of classical phase transitions. The spatial coherence plays an important role in the VPS and it is a quantum effect in lasers. In the researches of the quantum phase transitions (QPT), many investigations focus on transitions between quantum states with distinct topological properties. Two features reveal a similarity between the phase transition in the VPS and QPTs with topological order. First, both belong to the order-to-order phase transitions. Second, before and after the phase transition, two ground states are orthogonal, and are degenerate at the critical point. This report investigated the analogy between the QPT with topological order and the VPS. A detail discussion will be present in the conference, exploring that the VPS has a potential for providing a platform to simulate the QPTs of other physical systems.

9134-70, Session PS3

Ising simulation in polarization switching in vertical-cavity surface-emitting lasers

Yueh-Chen Li, Yu-Heng Wu, Wang-Chuang Kuo, Tsu-Chiang Yen, National Sun Yat-Sen Univ. (Taiwan)

Polarization switching (PS) in vertical-cavity surface-emitting lasers (VCSELs) is considered a phase transition in this paper. Furthermore, Ising simulation is used to model the system of VCSELs' Polarization switching (VPS). VPS has been extensively researched for its applications and dynamical studies. Most of earlier investigations studied VPS by dynamical method and confirmed the thermodynamics plays an important role in VPS. However in our previous research, critical phenomena of VPS including critical slowing down (CSD), scaling law and power law were observed in static case. These critical phenomena usually occur in traditional second order phase transition (SOPT) systems. For instance, ferromagnetism to paramagnetism transition is an order to disorder SOPT. Differing from traditional SOPT, the phase transition in VPS is an order to order phase transition if the intensity of x and y-polarization is considered as order parameter. Based on our observation, Ising model is a proper choice to describe VPS system because it exist a SOPT for temperature and first order phase transition (FOPT) for external field. In our simulation, each lattice on two-dimensional Ising model is mapped on each emitting element on VCSEL's beam. And the magnetic dipole moments of atomic spins, -1 and +1, are considered as the two orthogonal linear-polarized light, x and y-polarization. Monte Carlo method is used to calculate thermodynamical statistics in simulation. In our experiment observation, VPS could be distinguished into two types VPS. One's duration of PS is less than 1 ?s, named fast VPS usually accompanying polarization switching hysteresis loop (PSHL). PSHL means the switching points are different in the increasing and decreasing-current processes. The PS duration of the other VPS (slow VPS) is longer than 100 ms. It is more common to find a VCSEL with slow VPS. In fact, both of the two types VPS could be found in VCSELs made from a same wafer. The simulation results of Ising model with external field shows a qualitative and proper description for two types of VPS. Below the critical temperature, the magnetization changes from -1 to +1 abruptly when the external field changes from being negative to positive. This is a discontinuous change and a sign of a FOPT. Above the critical temperature, the magnetization changes continuously with the modulating-external field. These two cases are analogous to the fast and slow VPS separately. For quantitative analysis, it exist a critical temperature and injected signal for discussing the interaction in VCSELs. Suppose VPS could be illustrated by Ising model with external field. It indicates there are some factors that can't be controlled in VCSELs' fabrication processes. More experiment and simulation results will be presented in the conference.

9134-71, Session PS3

Theoretical investigation of a passively mode-locked semiconductor laser with external periodic forcing

Rostislav Arkhipov, Aleksandr Pimenov, Mindaugas Radziunas, Andrei G. Vladimirov, Weierstrass-Institut für Angewandte Analysis und Stochastik (Germany)

In the present work using a delay differential equation model we investigate the dynamics of a passively mode-locked semiconductor laser with dual frequency coherent optical injection and external periodic RF voltage modulation (VM) applied to the saturable absorber section (hybrid mode-locking). The width of the locking range, where the output pulse repetition rate is synchronized to the frequency of the external signal is calculated numerically and asymptotically in the limit of the small external signal amplitude. The dependence of the locking range on the model parameters and the frequency of the external signal is studied. We demonstrate that locking range increases linearly with the external signal amplitude. In the case of dual mode optical injection our numerical simulations indicate that RF locking is about 10 times smaller than optical locking range. We demonstrated numerically that locking ranges are asymmetric in the case of nonzero linewidth enhancement factors in the gain and absorber sections.

We have found that hybrid mode-locking can be also achieved in the cases when the frequency of the external modulation is approximately twice and half of the pulse repetition frequency of the free-running passively mode-locked laser fP. When the frequency of the external modulation is close to fP, 2fP the locking range has the same value. If the frequency of the external signal is close to fP/2 our theory predicts and experiment confirms that locking range is located within a significantly smaller and strongly asymmetric domain. Possible reasons of the hybrid locking range asymmetry are discussed. This asymmetry is related to the dependence of the pulse repetition frequency fP on the mean absorber relaxation rate, which is changing with the growing modulation amplitude of VM in the absorber section.

9134-72, Session PS3

1550 nm VCSEL-based 0.48 Tb/s Transmission Scheme Employing PAM-4 and WDM for Active Optical Cables

Stella Markou, Aristotle Univ. of Thessaloniki (Greece); Stefanos Dris, Dimitrios Kalavrouziotis, National Technical Univ. of Athens (Greece); Hercules Avramopoulos, School of Electrical and Computer Engineering, National Technical National Technical Univ. of Athens (Greece); Nikos Pleros, Aristotle Univ. of Thessaloniki (Greece); Dimitris M. Tsiokos, Aristotle Univ. of Thessaloniki (Greece) and Ctr. for Research and Technology Hellas (Greece)

The ever increasing demand on cloud and high performance computing applications has exposed the urgent need for the operators to upgrade their data-centers' interconnection capacity beyond 100 Gb/s. Vertical-cavity surface-emitting lasers (VCSEL) operating at 1550 nm were recently reported as the preferable source for optical interconnects that could address the need for modulation bandwidth by directly modulating high speed data with or without multi-level modulation formats. In addition, VCSELs offer low footprint, low operating current and high scalability potential by developing multi-element arrays. Recent research efforts demonstrated data transmission experiments at 100 Gb/s employing 1550 nm VCSEL and four-level pulse amplitude modulation (PAM-4) at 25 Gbaud and VCSEL based parallel optics transceivers achieving up to 480Gb/s by using 24 lasers, each modulated with On-Off-Keying (OOK) data format at 20 Gb/s.

With this paper we investigate the system-level performance of VCSELs when parameterized with true experimental LI-VI data and we propose its deployment as the high speed multi-level optical source in a mid-range active optical cable (AOC) model for rack-to-rack interconnection. The AOC architecture combines a 6-element 1550nm VCSEL array directly modulated with 40 Gbaud PAM-4 data and a wavelength division multiplexer (WDM) in order to implement a transmission link with aggregate traffic of 0.48 Tb/s. The 3 dB modulation bandwidth of the VCSEL was set to 15 GHz based on the experimental specifications of the fabricated VCSEL. Transmission reach exceeded 300 m by deploying a two-tap feed forward equalizer filter at the electrical signal generator. Off-line processing was used for the Bit Error Rate measurements and analysis.

The simulated VCSEL module was parameterized by inserting the experimental LI-VI data and dynamic characteristics of state-of-the-art VCSELs developed by TU Munchen. In practice, the thermal behavior and basic operational characteristics of the fabricated VCSEL were used to study the operation and the thermal performance of the complete AOC model. The VCSELs were initially operated at 20 degC and Bit Error Rate (BER) measurements showed power penalties of 1.5 dB and 3 dB for all 6 data channels at 300 m and 500 m of transmission distance respectively. System performance was also investigated for elevated operating temperatures of the VCSEL module by using the corresponding experimental data. The additional system degradation and BER penalties introduced by the VCSEL operation at 50 degC and 65 degC were also investigated for transmission distances of 300 m and 500 m. Transmission distance limits have been determined based on the link power budget, the receiver sensitivity and the VCSEL output power which for this investigation was rather moderate (2mW). Additional optical power at the VCSEL output can in principle increase or even double the transmission distances described here.

9134-73, Session PS3

Accurate electro-optical characterizations of high-power density GaAs-based laser diodes for screening strategies improvement

Pamela Del Vecchio, Univ. Bordeaux 1 (France) and 3S PHOTONICS S.A.S. (France); Yannick Deshayes, Simon Joly, Univ. Bordeaux 1 (France); Mauro A. Bettiati, François J. Laruelle, 3S PHOTONICS S.A.S. (France); Laurent Béchou, Univ. Bordeaux 1 (France)

High power lasers for the 9xx-nm emission range have attracted strong interest, originally mainly for pumping of erbium doped fiber amplifiers in telecom applications but also because spatial single-mode technology allows to reach the highest brightness levels and conversion efficiency. While excellent reliability levels have already been demonstrated, monitoring of electro-optical parametric evolutions is still of interest in order to evaluate the effectiveness of screening methodologies for accurate selection of weak devices and deep understanding of related failure root causes. In this study, we report on a methodology based on reverse and forward I-V measurements and on Degree of Polarization (DoP) of electroluminescence analysis on chip-on-submount devices for the improvement of screening tests.

The I-V curves are performed at reverse bias up to breakdown voltage (VBR) using both a high current accuracy (< 1pA) and high voltage resolution (< 10mV) at different case temperatures (20-50°C). The DoP of luminescence of such devices, related to strains in materials and effect of shear strain on the birefringence, is calculated from the simultaneous measurement of TE (LTE) and TM (LTM) polarized light emissions.

We observe that application of high reverse voltages occasionally produces significant microplasma (MP) pre-breakdown on reverse I-V characteristics as recently observed in InGaN/GaN LEDs and assumed to be a response of electrically active defects. Comparisons between breakdown voltages and number of MP, and changes of leakage current at

low forward voltage (< 0,1V) are considered. DoP measurements are also analyzed versus temperature. Finally the usefulness of these measurements for effective screening of devices is discussed.

9134-74, Session PS3

Delay signature concealment in chaotic semiconductor ring lasers

Romain Modeste Nguimdo, Guy Verschaffelt, Jan Danckaert, Guy Van der Sande, Vrije Univ. Brussel (Belgium)

Broadband chaotic signals are useful for chaos encryption and for the generation of random bit streams. Often such signals are generated from physical systems subject to delay feedback. However, the appearance of the delay signature in the generated dynamics is not desirable. In chaos encryption, it can allow an eavesdropper to reconstruct the full system while for random bit generation, it can reduce the randomness properties of the generated bitstreams. Typically, the delay time is concealed when it cannot be inferred from the signal using sophisticated statistical methods. In practice, successful time-delay concealment in chaotic lasers requires the delay signature to be hidden in both the intensity and the phase variations. While the concealment of the delay signature in the intensity dynamics can be achieved in Fabry-Perot semiconductor lasers when the delay time is chosen close to the relaxation period of the laser operating with moderate feedback, concealment of such delay signature in the phase dynamics is a more difficult task. Typically, the suppression of the delay signature in the phase dynamics requires more sophisticated architectures which include several lasers or the use of external modulation. In this contribution, we use the autocorrelation and delayed mutual information to investigate different scenarios leading to simultaneous time-delay concealment both in the intensity and the phase dynamics generated from semiconductor ring lasers (SRLs) subject to delayed feedback. As SRLs can sustain two-directional modes, we can consider different feedback configurations. Our results show that, in appropriate conditions, the delay signature can be concealed both in the phase and the intensity dynamics of a single SRL subject to a double or single cross-feedback. We explore the parameter sets for which this concealment is possible. The results show that many scenarios are possible for efficient time-delay concealment. It is found that the mode couplings in SRLs are key for the elimination of the time-delay signature. We also find that delay time concealment can be achieved in such a configuration both for short and long delay lengths. However, for double and single self-feedback configuration, it is found that the delay time can always be inferred from the phase dynamics, while being lost in the intensity dynamics. Further understanding of these results is provided based based on the phase equation of the mathematical model. The fact that such delay signatures can be eliminated in SRLs subject to short feedback opens the possibility of implementing secure communication schemes and random number generators on chip.

9134-75, Session PS3

Bifurcation diagram of an external-cavity semiconductor laser: experiment and theory

Byungchil Kim, Georgia Tech-Lorraine (France); Nianqiang Li, Southwest Jiaotong Univ. (China); Alexandre Locquet, Georgia Tech-Lorraine (France); David S. Citrin, Georgia Institute of Technology (United States); Daeyoun Choi, Georgia Tech lorraine (France) and Georgia Institute of Technology (United States)

The dynamics of external-cavity semiconductor lasers (ECLs) are known to be complex and difficult to control; in view of the rich dynamical behavior as well as the technological importance of these devices, the dynamics have been widely investigated. Nevertheless, there is an almost total lack of experimental BDs available for ECLs due to experimental difficulties.

We present experimental bifurcation diagrams of an external-cavity semiconductor laser (ECL) in the low-to-moderate current injection regime and long-cavity case. Based on the bifurcation cascade behavior, we provide a detailed experimental investigation of the nonlinear dynamics of ECLs and of the robustness of the cascade to changes in the current and cavity length; based on the Lang-Kobayashi model, we identify the dynamical regimes and the bifurcations involved in the cascade, as well as the influence of the current and cavity length on the cascade.

We observe three marked phenomena with increasing current. The first is that alternating stable and unstable regions are still observed, but no longer a systematic cascade involving the successive maximum gain modes (MGMs). The second is that the cascade exhibits interrupted chaotic behavior above a feedback level that decreases with increasing I. When I ~1.7Ith , we cannot observe any stable region in entire bifurcation. The third is that for larger I, longer (though fewer) regions of stable CW emission exist compared to low I.

Also, the dependence of the BD on external cavity length(L) is explored. At a short L, we again observe a cascade of bifurcations, but with significantly longer stable regions during which the laser output power dwells on a single external cavity mode (ECM) before moving into the subsequent unstable regime, itself followed by the next ECM.

In order to validate our interpretation of the experimental results, we have carried out theoretical calculations based on the well known LK model. Despite its simplifications, this model successfully explains our experimental results. Larger current leads to trajectories that explore a larger region of phase space with high magnitudes changes. Also, at low current, the unstable regions typically correspond to low frequency fluctuation (LFF) regime, within which a drift toward the MGM is observed. At larger current, the unstable regions typically correspond to fully-developed CC in which chaotic itinerancy between ruins of ECMs is observed, with no attraction toward the MGM. This explains why we observe numerically that at larger current, either larger are needed to get out of an unstable region and reach the MGM, or the MGM is not reached at all.

Numerical simulations also help us interpret the influence of L on the BD. When L is long, the spectral separation between ECMs is reduced (e.g., 1 GHz~15 cm, 500 MHz~30 cm) in the optical spectrum. Therefore, each participating mode being close in phase space, large-amplitude itinerancy between several modes is easily observed. Indeed, numerical observation of the trajectories on the ellipse shows that the proximity the ECMs impedes the development of independent attractors and thus prevents the existence of a bifurcation cascade.

9134-76, Session PS3

Random bit generation using polarization chaos from free-running laser diode

Martin Virte, Emeric Mercier, Vrije Univ. Brussel (Belgium) and Supélec (France); Hugo Thienpont, Vrije Univ. Brussel (Belgium); Krassimir Panajotov, Vrije Univ. Brussel (Belgium) and Institute of Solid State Physics (Bulgaria); Marc Sciamanna, Supélec (France)

During the last five years, starting with the pioneering work of Uchida et al. [1], optical chaos-based random bit generators (RBG) attracted a lot of attention and demonstrated impressive performances with bit rates up to hundreds of Gbps [2, 3]. However all the suggested schemes used external injection schemes (optical injection or feedback) to turn the lasers into chaos, hence strongly increasing setup complexity.On the other hand, we reported that a laser diode can generate a chaotic output without the need for external perturbation or forcing [4], hence unveiling a highly simplified way to generate an optical chaos at high frequency. However the low dimension and limited number of positive Lyapunov exponent casted doubts about its direct use for chaos-based applications.

Here we make a proof-of-concept demonstration for a Random

Bit Generators based on polarization chaos. We therefore suggest a highly simplified RBG scheme using only a free-running laser and small-bandwidth acquisition electronics and we demonstrate convincing performances with bit rates up to 100 Gbps without unusual or complex post-processing methods. We link these performances to the double-scroll structure of the chaotic attractor rather than the bandwidth of the dynamics, hence bringing new light on the importance of chaos topology for chaos-based applications. In addition our scheme exhibit a strong potential as it enables a low-cost and/or integrated in parallel on-chip scheme.

[1] A. Uchida et al., Nature Photon. 2, 728-732 (2008).

[2] T. Yamazaki and A. Uchida, IEEE J. Sel. Top. Quant. Electron. 19, 0600309 (2013).

[3] X-Z, Li and S-C Chan, IEEE J. Quantum Electron. 49, 829-838 (2013).

[4] M. Virte, H. Thienpont, K. Panajotov and M. Sciamanna, Nature Photon. 7, 60-65 (2013).

9134-77, Session PS3

Fast random bit generation with a single chaotic laser subjected to optical feedback

Nianqiang Li, Byungchil Kim, Georgia Institute of Technology (United States); Vyacheslav N. Chizhevsky, B.I. Stepanov Institute of Physics (Belarus); Alexandre Locquet, M. A. Bloch, David S. Citrin, Georgia Institute of Technology (United States); Wei Pan, Southwest Jiaotong Univ. (China)

Random bit generation (RBG) with chaotic semiconductor lasers has been extensively studied because of its potential applications in secure communications and high-speed numerical simulations. Researchers in this field have mainly focused on the improvement of the generation rate and the compactness of the random bit generators. Recently, experimental investigations have shown that, based on multi-bit extraction schemes, one can extract more than one bit from each sample as long as substantial post-processing is carried out, and even in some cases extract more bits than those are present in the digitized chaotic signal. The number of bits extracted per sample of the chaotic laser intensity has for the most part been chosen heuristically and the randomness of the resulting sequence is determined on the basis of standard statistical tests. However, the important question concerning the upper limit in principle based on information theory of the random bit rate that can be extracted from each sample of the chaotic laser intensity remains largely unexplored.

Here we experimentally demonstrate two approaches for fast RBG based on a semiconductor laser with optical feedback. The post-processing is based in both cases on high-order finite differences of the chaotic signal, and aims at obtaining a highly symmetric distribution that is suitable for fast RBG. In the first approach, the initial data obtained with an 8-bit resolution are transformed into 52-bit floating-point numbers; however, we only extract 4 least significant bits from each sample, leading to a physical random bit generation rate of 160 Gb/s that does not exceed the limit set by information theory. In the second approach, we adopt a transformation of initial data obtained with 8-bit resolution into a 64-bit integer type and then we extract more bits than the resolution of our raw signal, leading to faster physical-based pseudo RBG with a rate of the order of Tb/s, that passes all the standard randomness tests though exceeding the limit set by information theory.

9134-78, Session PS3

Sliding frequency mode-locking in a frequency swept Fabry-Pérot laser

Ben O'Shaughnessy, Svetlana Slepneva, Bryan Kelleher, Cork Institute of Technology (Ireland) and Tyndall National Institute (Ireland); Stephen P. Hegarty, Tyndall National Institute (Ireland); Guillaume Huyet, Cork Institute of Technology (Ireland) and Tyndall National Institute (Ireland); Andrei G. Vladimirov, Weierstrass-Institut für Angewandte Analysis und Stochastik (Germany) and Cork Institute of Technology (Ireland) and Tyndall National Institute (Ireland); Hong Chou Lyu, Karol Karnowski, Maciej Wojtkowski, Nicolaus Copernicus Univ. (Poland)

The acquisition speed and image quality of Optical Coherence Tomography (OCT) has greatly improved with the development of frequency swept sources. The Swept Source OCT (SS-OCT) approach requires low noise lasers that can sweep a wide spectrum (typically > 100~nm) at a high frequency rate (typically 100s of kHz to MHz). The overall performance of a swept source is a trade-off between a few key parameters. Here, we analyse both experimentally and theoretically, the performance of a short cavity frequency swept laser.

The experiments were carried out using a short cavity Axsun laser which is simply described as a Fabry-Perot resonator incorporating an intra-cavity tunable filter. The laser output was coupled to a high-frequency detector and analysed with a 13~GHz real-time oscilloscope and a 26~GHz electronic spectrum analyser. In addition, the temporal evolution of the optical phase was analysed by mixing the output with a narrow linewidth tunable laser. To describe the system theoretically we propose and analyse numerically a new model of a frequency swept laser based on a time-delayed dynamical system. This model describes the temporal evolution of the electric field and the carrier density and demonstrates a very good agreement with the experimental data.

When the central frequency of the filter is unchanging the laser emits CW output and at low tuning speeds, hopping between cavity modes is observed. The frequency of the mode-hops increases with the filter speed until eventually undamped pulsations are observed when the transient time following a mode-hop is of the order of the time between consecutive hops. A periodic pulse train is obtained when the filter is swept towards longer wavelengths and an aperiodic train for the opposite sweep direction. We have found that the periodic pulse train can be described as a sliding frequency mode-locking regime resulting from four-wave mixing.

9134-79, Session PS3

Nonlinear dynamics in semiconductor ring lasers with negative optoelectronic and incoherent optical feedback

Sifeu T. Kingni, Univ. de Yaoundé 1 (Cameroon); Guy Van der Sande, Vrije Univ. Brussel (Belgium); Ilya V. Ermakov, Univ. Catholique de Louvain (Belgium); Jan Danckaert, Vrije Univ. Brussel (Belgium)

Semiconductor ring lasers (SRLs) are very attractive devices in photonic integrated circuits because of the possibility of encoding digital information in the direction of emission. The bistability between the two counter-propagating modes leads to a much richer dynamical behavior than commonly found in other types of semiconductor lasers. Under external perturbations, such as current modulation, optical injection or coherent optical feedback, these lasers as others semiconductor lasers often present instabilities in their optical output. In particular, a semiconductor laser with coherent optical feedback is the archetypical problem that most investigations have focused almost exclusively. It seems to exhibit the richest structure and the most complicated dynamics because both the intensity and the phase of the optical field are subject to delayed feedback. With the success of chaotic synchronization such systems have become prime candidates for chaotic communications. In the scheme of coherent optical feedback, synchronization performance depends on the detuning between the free-running frequencies of the transmitter and the receiver laser. However, for lasers subject to optoelectronic or incoherent optical feedback, the schemes would not require fine tuning

of the optical frequencies because the phase of the laser is a free parameter and therefore not involved in determining the system's dynamics. In this work, we study theoretically the dynamical behavior of two SRLs. One is subject to negative optoelectronic feedback and the other laser is subject to incoherent optical feedback. Relying on asymptotic methods, we are able to reduce the original set of five equations used to describe the dynamical behavior of SRLs with negative optoelectronic feedback or incoherent optical feedback to two equations and one map with time delay valid on time-scales longer than the relaxation oscillations. The equations of the reduced models turn out to be the same for both systems. As we vary the feedback strength at a fixed current, the devices under consideration in this work display both continuous wave operation and a period-doubling route to chaos. The two counter-propagating intensities of both systems exhibit in-phase chaotic behavior for small delay times comparable to the period of relaxation oscillations. For delay times significantly longer than the period of relaxation oscillations, the two counter-propagating modes show in antiphase chaotic oscillations. This anti-phase chaotic regime does not involve carrier dynamics and is a result of the underlying symmetry of the SRL. Thanks to the asymptotic simplification, we showed the topological resemblance of the Poincaré section of semiconductor ring lasers with negative optoelectronic or incoherent optical feedback in the antiphase chaotic regime and a periodically forced Duffing oscillator. Moreover, for long delay times, we find that the counter-propagating intensities of both systems depict the same dynamical behaviors when their feedback strengths are increased.

9134-80, Session PS3

Simulation and geometrical design of multisection tapered semiconductor optical amplifiers at 1.57 μm

JJosé Manuel Garcia Tijero, Luis Borruel, Mariafernanda Vilera, Antonio Consoli, Ignacio Esquivias, Univ. Politécnica de Madrid (Spain)

High power semiconductor lasers for gas measurement in lidar systems require high beam quality, high spectral purity and high conversion efficiency. A multi-section monolithically integrated Master Oscillator Power Amplifier (MOPA) operating at 1.57 μm has been proposed as lidar source in space- borne missions for atmospheric observation of planet earth carbon dioxide distribution. The geometrical design of the tapered amplifier is crucial to achieve the required power and beam quality. In this work we investigate by numerical simulations the role of carrier and temperature effects in the beam quality and in the maximum achievable power for different geometrical designs. The simulations were performed with a Quasi-3D model which solves the complete steady-state semiconductor and thermal equations combined with a beam propagation method. A simple model for the intensity propagation is also employed for an initial selection of the geometrical parameters. The role of the lengths of the different sections and of the taper angle in the device performance is investigated.

9134-81, Session PS3

Pulse repetition-frequency multiplication of passively mode-locked semiconductor lasers coupling to an external passive cavity

Rostislav Arkhipov, Weierstrass-Institut für Angewandte Analysis und Stochastik (Germany); Andreas Amann, Univ. College Cork (Ireland); Andrei G. Vladimirov, Weierstrass-Institut für Angewandte Analysis und Stochastik (Germany)

The problem of mode selection is one of the most important problems in the control of laser radiation parameters. In particular, semiconductor lasers with a fixed and predetermined number of primary modes are of interest for a number of applications. For example, two-colour devices are useful for terahertz generation by photomixing. In order to modify the lasing spectrum the incorporation of a number of scattering centers in the form of slots into the laser cavity are used nowadays.

Passively mode-locked semiconductor lasers as sources of short optical pulses with high repetition rates of a few to hundreds of GHz, have important applications in optical telecommunications, optical sampling, and optical division multiplexing. In the present work using a delay differential equation model, we investigate the dynamics of a semiconductor laser with one active cavity and a second external cold cavity. Our numerical simulations indicate that when the coupling between two laser cavities is strong enough and the round-trip time of the active cavity is an integer multiple of the round-trip time of the cold cavity, the pulse repetition frequency of the laser can be close to the repetition frequency of the external empty cavity. We also demonstrate that the electric field amplitude sensitively depends on the relative phase between the electric fields in both cavities giving rise to resonance behavior. The period and width of these resonances depend on the ratio between the round-trip times and the coupling between the two cavities. The investigated phenomena can found it's application in the optical communications when it is necessary to increase pulse repetition frequency of the laser.

The support of EU FP7 ITN PROPHET is gratefully acknowledged (Grant No. 264687).

9134-83, Session PS3

Coupled-cavity VCSELs: numerical analysis of physical phenomena

Leszek Frasunkiewicz, Maciej Dems, Robert P. Sarzala, Technical Univ. of Lodz (Poland); Krassimir Panajotov, Vrije Univ. Brussel (Belgium) and Institute of Solid State Physics (Bulgaria); Tomasz Czyszanowski, Technical Univ. of Lodz (Poland)

Coupled-cavity (CC) VCSELs were realized for the first time 20 years ago and since then have attracted considerable attention. Recently, they have been used for fast voltage-controlled polarization and intensity modulation and high-speed pulse generation . The in-depth understanding of nonlinear interaction of physical phenomena such as current flow, heating, mode competition, recombination and diffusion of carriers allows to control the operation of CC VCSELs. We present detailed numerical analysis of CW operation of CC VCSEL with different radii of current and optical apertures realized by ion-implantation and wet oxidation. The simulations are supported by experimental verification which allowed determining the unknown structural and physical parameters of the considered CC VCSEL. We investigate the current flow, temperature distribution and optical characteristics under different bias conditions. We determine the ranges of steering currents under which dual fundamental mode operation of short and long waves combined with strong discrimination of higher-order transverse modes appears.

This work is supported by the Polish National Science Centre, project DEC-2012/06/M/ST7/00442, FWO-Vlaanderen project G.0657.09N and OZR-VUB

9134-84, Session PS3

Multimode ring laser with optical injection: statistics and phase dynamics

Gustave François, Stephane Barland, Institut Non Linéaire de Nice Sophia Antipolis (France)

Optical localized structures have recently been observed in a nonlinear fiber ring cavity under the influence of coherent forcing. These structures, which take place along the propagation direction in the neighbourhood of a modulational

instability, are formally analogues of spatial cavity solitons known to exist in broad area vertical cavity surface emitting lasers in an amplifier configuration. The notable difference is that they are localized against dispersion instead of diffraction. One of the key enabling elements for stability of these structures is the fiber geometry, which enables purely single transverse mode operation together with a huge number of longitudinal modes.

In an attempt to leverage the semiconductor nonlinearity towards the generation of temporal localized states, we perform an optical injection experiment in a single transverse mode ring laser with a large number of longitudinal modes. The dynamics of single mode semiconductor lasers with optical injection is widely studied and surprisingly rich dynamics can be found (extreme events among others) in spite of the relative simplicity of the equations used to model it. On the contrary, lasers with injected signal in presence of many longitudinal modes are much less documented outside of well behaved, and therefore to some extent not so complex, mode locked regimes. In this contribution, we analyse experimentally the intensity statistics and phase dynamics of a strongly multimode semiconductor laser with external coherent forcing. In particular, we focus our attention on travelling intensity holes strongly reminiscent of dark solitons which would take place along the propagation dimension of the ring laser.

9134-85, Session PS3

High-precision AlGaAsSb ridge-waveguide etching by in situ reflectance monitored ICP-RIE

Nam T. Tran, Magnus Breivik, Saroj K. Patra, Bjørn-Ove Fimland, Norwegian Univ. of Science and Technology (Norway)

GaSb-based semiconductor diode lasers are promising candidates for light sources working in the mid-infrared wavelength region of 2-5 μm. Using edge emitting lasers with ridge-waveguide structure, light emission with good beam quality can be achieved. The ridge waveguide etch depth plays a key role in laser's characteristics, namely the optical confinement and surface recombination of injected carriers [1, 2]. By creating high index contrast, the light can be well-confined inside the waveguides. This is very critical for high bending loss waveguides like S bend, Y branch and Mach-Zehnder structure. Simulation results show improvement of the light confinement in ridge-waveguide laser and Y-branch waveguide if the refractive index contrast is sufficient enough.

To achieve the best optical and electrical confinement for laser performance, it is desirable to stop etching at the interface between the upper Al0.9Ga0.1AsSb cladding layer and the separate confinement heterostructure (SCH) layer of Al0.31Ga0.69AsSb [3]. A common approach for precise etching is dry etching using endpoint detection. In this paper, an in situ reflectance monitoring with a 675 nm-wavelength laser was used to determine the etch stop with a high accuracy. The etching process can in principle be simulated from the reflectance of the laser structure in question, containing layers of different compositions and thicknesses. However, due to the lack of precise data on the optical properties of these laser materials, a simpler structure consisting of 1.5 μm Al0.9Ga0.1AsSb (cladding) capped by 100 nm of GaSb and grown on GaSb (100) substrate was proposed. The reflectance monitoring was performed on this sample while etching it simultaneously with a laser sample. Finally, the etch depth of the ridge waveguide was confirmed by Scanning Electron Microscopy (SEM). From the reflectance and etch depth measurements, the refractive index of the cladding layer at 675 nm wavelength can be determined and used for simulation of the etching process. Using this method, the etching process can be controlled to provide an endpoint depth precision within ± 10 nm.

REFERENCES

1. H. C. Casey, Jr and M. B. Panish, Heterostructure Lasers, Part B: Material and Operating Characteristics. 1978, Orlando: FL: Academic.

2. L. Redaelli et al, Effect of ridge waveguide etch depth on laser threshold of InGaN MQW laser diodes. Proc. of SPIE, 2012.

3. C.P. Chao et al, Fabrication of low-threshold InGaAs/GaAs ridge waveguide lasers by using in situ monitored reactive ion etching. Photonics Technology Letters, IEEE, 1991. 3(7): p. 585-587.

9134-86, Session PS3

Performance of microwave frequency combs utilizing semiconductor lasers under hybrid optical injections

Cheng-Ting Lin, Yi-Hua Wu, Yu-Shan Juan, Yuan Ze Univ. (Taiwan)

We demonstrate and characterize the microwave frequency combs utilizing hybrid optical injections schemes by precisely varying the operational parameters, injection strength, repetition frequency, and detuning frequency. The nonlinear dynamics of a semiconductor laser (slave laser) injected by hybrid optical injections are investigated numerically. The hybrid injections are realized by a dynamical optical pulse injection combined with a tunable level of DC-offset generated by a traditional cw injection. The dynamical pulse injection scheme is achieved by optical pulse injection to the slave laser from a pulsed laser. The microwave frequency combs generated by hybrid injections are characterized and studied. When the slave laser subjected to only the optical pulse injection from the pulsed laser, microwave frequency combs are generated by the nonlinear dynamics of the frequency-locked states with different locking ratios. Under the fixed operating parameters of detuning frequency ?= 18.0 GHz, a repetition frequency 5.0 GHz, and pulses injection strength ?p = 0.02, rich dynamical states including chaotic pulsations and frequency locked states with different locking ratios are observed by tuning the cw injection strength ?dc. Under pure pulse injection case, the amplitude variation of ±27.3 dB in a 30 GHz range is obtained. By further applying a tunable level of DC-offset to the pulses injected semiconductor laser, the advantages of traditional cw injection and dynamical pulse injection schemes are combined and enhanced. The amplitude variation of the microwave frequency comb of ±3.1 dB in a 30 GHz range is achieved when operating the cw injection strength ?dc = 0.29 in a stable locking state. In addition, the bandwidth enhancement to about 30 GHz is also observed by increased the cw injection strength ?dc = 0.35. Therefore, a 6 times enhancement is obtained from further applying a cw injection strength to the injected laser. The frequency accuracy of the microwave comb is also improved, when changed the parameters of the detuning frequency to 1.5 GHz and the cw injection strength ?dc = 0.29. Consequently, the bandwidth broadening in microwave frequency comb is expected when the cw injection system operating in a stable locking state. Nonlinear dynamics of semiconductor lasers subject DC-offset optical pulse injection is investigated by combined both optical pulse injection and cw injection to the slave laser. The comparison of nonlinear behaviors in different schemes, including pure optical pulse injection, pure optical cw injection, and the combination of DC-offset pulse injection schemes are studied. In this paper, strongly improve the amplitude variation and accuracy of the microwave frequency combs generated utilizing hybrid injections scheme are obtained. Utilizing the system, the microwave frequency combs are smoother and more accurate. Because of the characteristics, the microwave frequency comb can be employed, effectively.

9134-87, Session PS3

Switch-on time of reflective semiconductor optical amplifier submitted to strong optical filtered feedback with long delay

Pascal Besnard, Thierry Chartier, Thanh-Nam Nguyen, Ecole Nationale Supérieure des Sciences Appliquées et de Technologie

(France); Fabienne Saliou, Sy Dat Le, Qian Deniel, Philippe Chanclou, Orange SA (France)

In metropolitan networks, one way to increase the data rates is to introduce Dense Wavelength Division Multiplexing (DWDM) in passive optical network (PON), with distances ranging from a couple of ten's kilometers to several hundred kilometers, at data rates ranging from 1 to 10 Gb/s. A realistic implementation requires achromatic components, for which the provider can fix the operating wavelength in order to have the same type of components in the consumer's home. These achromatic components must be low cost, which implies their ability to be directly modulated. It was recently shown [1] that self-seeded-reflective semiconductor optical amplifier (RSOA) could be the candidate. The RSOA is coupled to a Faraday mirror, which is located at a few kilometers in a central office, giving a Free Spectral Range of the extended cavity of the order of 100 kHz. Its wavelength is fixed on the "red" side of the transmission window of a 100 GHz-wide filter, as it is confirmed by our theoretical approach. It was shown [1] that a direct modulation at a few Gbits/s will stand BER (Bit Error Rate) compatible with the standard of optical telecommunication systems. A few descriptions of filtered optical feedback have been done [2, 3] in the literature. We use a Green Function approach, which enables us to describe the case of long delay and strong optical feedback-coupling (anti-reflection coating of the coupling face of the RSOA). In this communication, we focus particularly on the ability for the coupled device to switch on and off, which is essential for the system. The characteristics of the switch-on time is detailed for such a RSOA submitted to strong filtered optical feedback, using a Green function approach [3]. We discuss how such an RSOA coupled to a so long cavity is a low-cost component for WDM-PON operating at several Gbits/s.

References

[1] Qian Deniel et al., 'Up to 10Gbit/s transmission in WDM-PON architecture using External Cavity Laser based on Self-Tuning ONU', " Optical Fiber Communications Conference, OFC/NFOEC '12.

[2] M. Yousefy and D. Lenstra, "Dynamical behavior of a semiconductor laser with filtered external optical feedback," IEEE J. Quantum Electron., vol. 35, pp. 970–976, June 1999.

[3] Alexander Naumenko et al., "Characteristics of a semiconductor laser coupled with a fiber Bragg grating with arbitrary amount of feedback" IEEE JQE, vol. 39 N° 10 p. 1216 2003.

9134-88, Session PS3

Electro-thermal characteristics of VCSELs: simulations and experiments

Markus Daubenschuez, Univ. Ulm (Germany); Philipp Gerlach, Philips Technologie GmbH (Germany); Rainer Michalzik, Univ. Ulm (Germany)

Vertical-cavity surface-emitting lasers (VCSELs) are established in many technical fields today, in particular optical data communication and sensing. Ongoing research has enabled new applications of high-power sources for thermal material treatment or illumination systems. For continuous optimization it is important to have reliable predictions of the electro-thermal characteristics of such devices and arrays. Several approaches have already been presented in the literature. The main difficulty in electrical modeling is the multitude of heterojunctions in the distributed Bragg reflectors (DBRs). It is an extremely demanding task for every commercial semiconductor device simulator to compute the quasi-three-dimensional (q3D) current density distributions and energy band alignments in a full VCSEL structure including the DBRs and the multi-quantum-well inner cavity. Simplifications are thus necessary.

The model presented in this paper is pragmatic, able to handle q3D geometries, and uses epitaxial growth protocols as direct input. We sub-divide the layer stack of the VCSEL into various blocks containing typically one period of the DBRs or the inner quantum well region. In the longitudinal direction, these blocks are processed with the public domain software SimWindows. The program is capable to calculate 1D energy band alignments and current flows for different voltages and temperatures self-consistently. To handle heterojunctions it has a built-in model based on thermionic emission and tunneling currents. For each block, with its epitaxial target parameters like composition and doping concentration, we thus derive its current-voltage (I-V) characteristic and the local carrier densities. To include temperature dependences, we have extended the material database of SimWindows to cover the required temperature range. In a further step we combine the blocks in a main program to get a linearized q3D model of the VCSEL itself. The lateral conductivities are determined from the mobilities and carrier densities obtained via the longitudinal model. The current distribution inside the entire structure is calculated, based on the electrostatic Laplace equation, with finite differences. Thereby, we can find the dissipated power density distribution and get the internal temperature profile of the VCSEL from a solution of the heat conduction equation, applying appropriate boundary conditions. For various lasers with, e.g., different oxide-defined active diameters or contact configurations, we are able to compute and optimize the I-V characteristics and get information about the current-dependent emission wavelength shift. For the latter, the temperature profile that acts on the refractive indices is weighted by the resonant mode pattern. We will show first results of simulations of different kinds of DBRs. Furthermore, comparisons with experimental VCSEL data will be presented.

9134-90, Session PS3

Comparison of two methods of laser stabilization for optoelectronic oscillators

Patrice Salzenstein, Khaldoun Saleh, Mikhail Zarubin, FEMTO-ST (France); Arseniy S Trushin, Lomonosov Moscow State University (Russian Federation)

The laser wavelength of an Optoelectronic oscillator (OEO) is stabilized onto an optical resonance using a Pound Drever Hall stabilization loop. We compare the advanfages and critical points of this stabilization and another one based on the use of acousto-optic cells to lock the laser on the resonance of the crystal based OEO.

9134-91, Session PS3

Extreme events in a broad-area semiconductor laser with saturable absorber

Foued Selmi, Z. Loghdami, Sylvain Barbay, Lab. de Photonique et de Nanostructures (France)

Extreme events are ubiquitous in nature. In optics, an extreme event is characterized by a rare, intense optical pulse in a given intensity probability density distribution. The study of extreme events and extreme waves has been motivated by the analogy with rogue waves in hydrodynamics that are giant waves recently observed in the ocean and whose formation mechanism is still not well understood. Physically, the analogy is based on the fact that some conservative systems in optics and deep water waves in ocean can be described by the nonlinear Shrödinger equation. Extreme events were also found in dissipative systems, such as fibre lasers. Here we present experimental results of extreme events appearance in broad area semiconductor laser with saturable absorber. Our system is a planar VCSEL cavity with integrated saturable absorber that can be optically pumped with varying pump diameters. An interesting aspect of this system is that it is well known that a single-mode laser with saturable absorber cannot display irregular dynamics and hence extreme events. However, spatial coupling through diffraction can make the system become more irregular. We study this system above the self-pulsing

threshold and show the impact of pump diameter on the pulse intensity statistics. We also analyse the pulse intensity statistics locally and show the appearance of a correlation length smaller than the system size in a 1D line laser.

9134-44, Session 10

InGaAlAs RW-based electro-absorption-modulated DFB-lasers for high-speed applications *(Invited Paper)*

Martin Moehrle, Holger Klein, Carsten Bornholdt, Georges Przyrembel, Ariane Sigmund, Wolf-Dietrich Molzow, Ute Troppenz, Heinz-Gunter Bach, Fraunhofer-Institut für Nachrichtentechnik Heinrich-Hertz-Institut (Germany)

Electro-absorption modulated 10G and 25G DFB lasers (EML) are key components in transmission systems for long reach (up to 10 km) and extended reach (up to 80 km) applications. The next generation Ethernet will most likely be 400 Gb/s which will require components with even higher bandwidth. Commercially available EMLs are regarded as high-cost components due to their separate epitaxial butt-coupling growth process to separately optimize the DFB laser and the electro-absorption modulator (EAM). Alternatively the separate area growth (SAG) technique is used to achieve different MQW bandgaps in the DFB and EAM section of an EML. However for a lot of applications an emission wavelength within a narrow wavelength window is required enforcing a temperature controlled operation. All these applications can be covered with the developed EML devices that use a single InGaAlAs MQW waveguide for both the DFB and the EAM enabling a low-cost fabrication process similar to a conventional DFB laser diode. It will be shown that such devices can be used for 25Gb/s and 40Gb/s applications with excellent performance. By an additional monolithic integration of an impedance matching circuit the module fabrication costs can be reduced but also the modulation bandwidth of the devices can be further enhanced. Up to 70Gb/s modulation with excellent eye openings can be achieved. This novel approach opens the possibility for 100Gb/s NRZ EMLs and thus 4x100Gb/s NRZ EML-based transmitters in future. Also even higher bitrates seem feasible using more complex modulation formats such as e.g. DMT and PAM.

9134-45, Session 10

New regime in optically injected quantum-dot lasers emitting at 1.55 μm: Period doubling of relaxation oscillation

Zhenyu Hao, Pascal Besnard, Schadrac Fresnel, Ecole Nationale Supérieure des Sciences Appliquées et de Technologie (France); Dame Thiam, Ecole Nationale Supérieure des Sciences Appliquées et de Technologie (France) and Institut National des Sciences Appliquées de Rennes (France); Alain Le Corre, Ecole Nationale Supérieure des Sciences Appliquées et de Technologie (France) and Institut National des Sciences Appliquées (France)

Optical injection has been extensively studied for semiconductor lasers [1-4].

Quantum dash mode-locked lasers have been the subject of many investigations owing to their remarkable properties such as: low-noise, high thermal stability and broad gain spectrum. We have recently shown anomalous behavior [5] of single-mode DFB quantum dash laser [6] and of Fabry-Perot quantum dot [7] and quantum dash lasers when they are submitted to optical injection, showing general properties quite different from those observed in conventional structures (CS) like bulk or quantum wells.

Close to threshold (< 1.2), a DFB quantum-dash laser shows 6 regimes: locking, wave-mixing (M1, M2 and M4), relaxation oscillation regime and excitability, while 2 regimes are only observed in CS DFB structures. The CS behavior is then closer to that of an optical amplifier, with the observation of locking or bi-mode regimes.

At moderate pump rate, the Q-Dash structure exhibit mainly locking, wave-mixing and relaxation oscillation regimes. These two last regimes occurred for a narrow range of parameter values of injected power and detuning. In CS, more regimes are observed: wave-mixing (1M, 2M), oscillation relaxation, chaos.

The interesting point is that the damping rate is of the same order in these two structures. Then it is then not the key element to explain the discrepancy in dynamics between these two types of structures (Qdash and CS).

For Q-dash Fabry-Perot structures, close to threshold, contrary to Q-dash DFB laser, there are only three regimes; mainly locking and on small range of parameters, oscillation regime and wave-mixing with additional behavior due to the multimode character of the Fabry-Perot.

The Q-Dot Fabry-Perot laser under study has a different behavior from Q-dash DFB laser and exhibits more regimes when submitted to optical injection.

In this last case, we have observed, for the first time, in a Fabry-Perot Q-Dot structure, period-doubling of the so-called oscillation regime. It leads to a possible period-doubling route to chaos and indicates a stronger gain coupled to a low confinement factor. In this communication, we propose to give a general description of the relaxation-oscillation regime and we will point out the specificity of quantum-dot lasers that permits such an observation. Finally we discuss simulations of map using different assumptions and models to point out the role of high gain (and low confinement factor) and of the damping rate.

References

[1] T. B. Simpson, J. M. Liu, K. F. Huang, and K. Tai, Quantum Semiclassic. Opt. 9, 765–784 (1997).

[2] V. Kovanis, T. Erneux and A. Gavrielides, Opt. Commun. 159, 177–183 (1999).

[3] S. Wieczorek, B. Krauskopf, T. Simpson, and D. Lenstra, Phys. Rep. 416, 1–128 (2005).

[4] S. Blin, O. Vaudel, P. Besnard and R. Gabet, Optics Express 17 11, 9288-9299 (2009).

[5] Z. Hao, P. Besnard, ISPALD, Paris (2013).

[6] F. Lelarge, J. Renaudier, R. Brenot, A. Accard, F. van Dijk et al., IEEE JSTQE, 13, 1 111-124 (2007).

[7] K. Klaime, R. Piron, C. Paranthoen, T. Batte, F. Grillot et al., IPRM, Santa Barbara, USA (2012).

9134-46, Session 10

All optical switching with a dual-state quantum dot laser

Boguslaw Tykalewicz, David Goulding, Bryan Kelleher, Cork Institute of Technology (Ireland) and Tyndall National Institute (Ireland); Stephen P. Hegarty, Tyndall National Institute (Ireland); Guillaume Huyet, Cork Institute of Technology (Ireland) and Tyndall National Institute (Ireland)

The unique properties and rich phenomena found with quantum dot (QD) based semiconductor lasers make them very attractive for dynamic studies. QD based devices show improved performance compared to bulk and quantum well based devices in several dynamical configurations, such as when undergoing optical feedback and when optically coupled. A feature of InAs QD lasers is the ability to simultaneously lase at the ground state (GS) and the excited state (ES) with the precise behaviour dependent on several control parameters such as cavity length, injected current and temperature of operation. In [1] a rate equation model is introduced which reproduces this behaviour and also shows that the intradot timescales strongly affect relaxation times in such lasers. In [2] the authors performed a theoretical study of optical injection in QD lasers lasing simultaneously from the GS and the ES, showing some interesting features including generation of picosecond pulses.

Controllable and robust all-optical switching between the ES and the GS could be of interest for both fundamental science and applications. Most experimental studies heretofore have been done on two section devices [3,4]. We present here an all-optical switching mechanism via optical injection into the GS of a single section device when the free-running behaviour is ES lasing only. The device under test was a single (discrete) mode QD laser. For low injection currents the emitted radiation is GS only. As the current is increased the device undergoes a second threshold (at approximately 2 times the GS threshold) and dual state lasing is obtained. Finally, as the current is further increased one obtains ES lasing only. Injection locked behaviour on the GS could be obtained at all currents examined. Most interestingly, even when the device emitted from the ES only (at ~1215 nm) when free-running, injection from the master laser at the GS (~1300 nm) could completely suppress the ES and allow the device to emit from the GS only. We analyse the switching times between GS and ES and vice versa.

References:

1. M. Abusaa, J. Danckaert, E.A. Viktorov and T. Erneux, Phys. Rev. A Vol.87, 063827, (2013).

2. L. Olejniczak, K. Panajatov, S.Wieczorek, H. Thienpont andM. Sciamanna, J. Opt. Soc. Am. B Vol.27, No.11, (2010).

3. A. Markus, M. Rosetti, V. Cagliari, D. Chek-Al-Kar, J. X. Chen, A. Fiore and R. Scollo, Appl. Phys. 100, 113104, (2006).

4. Hsing-Yeh Wang, Hsu-Chieh Cheng, Sheng-Di Lin and Chien-Ping Lee, Appl. Phys. Lett. 90, 081112, (2007).

9134-47, Session 10

Frequency stabilization of an external-cavity diode laser with offset frequency looking to a stabilized He-Ne laser

Christian Sternkopf, Technische Univ. Ilmenau (Germany); Stefan Göllner, EPC Group (Germany); Eberhard Manske, Technische Univ. Ilmenau (Germany)

This paper describes the technical setup of a PLL coupled external cavity diode laser. Our setup consists of a stabilized He-Ne Laser (SIOS SL03) and a commercial grating stabilized diode laser in Littrow-configuration from Sacher Lasertechnik. Both lasers are arranged in a master-slave setup. The light of the He-Ne Laser (master laser) and the diode laser (slave laser) are optical heterodyne with two beam splitters. Therefore the other part of the light from both lasers can be used for other applications which need a stable frequency. A beat frequency (difference frequency) signal from both lasers is detected with an avalanche photodiode and used for the PLL control loop. Inside the PLL chip a phase frequency detector compares the beat frequency with a reference frequency from a local crystal oscillator. The commercial PLL-Chip ADF4111 is used to compare both frequencies and to generate a control signal. The ADF4111 includes programmable frequency dividers for the reference and the beat signal and a digital phase frequency detector (PFD). The beat frequency of the He-Ne Laser and the diode laser is adjustable from 80 MHz to approx. MHz (depending on the PLL Chip and the photodiode). To create a stable diode laser frequency the control loop hold the beat frequency stable. With this technique, we reach a beat frequency stability about:

(Δf_beat)/f=f_(beat [p-p])/f(474THz) =7??10?^(-12)

However, the absolute and the relative frequency stability of the setup depend just on the frequency stability of the stabilized He-Ne Laser (master laser). This laser is stabilized by the patented two-mode stabilization techniques which reaches a relative frequency stability of:

(Δf_(He-Ne))/f=f_(He-Ne[p-p])/f(474THz) =5??10?^(-9) (24h)

As we can see, the diode laser has almost the same absolute and relative frequency stability as the stabilized He-Ne laser under closed loop conditions. This stability is not as stable as an iodine stabilized external cavity diode laser, but with our setup you don't need an absorption cell with complex control components. Another benefit is the high optical useable output power of our laser setup. It is possible to use the He-Ne Laser output (ca. 0,6mW) and the diode laser output (ca. 5 mW) which prefer this system for multi-channel homodyne interferometry with just one laser source. For the frequency control of the diode laser we just use the piezo drive. We designed an adapted loop filter for a stable closed loop system. The whole loop system consists of commercial components. To find an optimized parameter setup for our control system we try different configurations of frequency divider factors and PLL frequencies in combination with different loop filter configurations. Goal of the experiments was a minimized frequency noise and maximum frequency stability. In the article we detailed describe the optical setup, the control loop and measurement results. We show the frequency stability over many hours and the Allan variance of the setup. Finally we show some problems of the diode laser system in relation of long term frequency stabilization. Because the diode laser is primary designed for spectroscopy applications, it has some drawbacks for user-friendly applications. These problems are pointed and we give some proposals for solutions.

9134-48, Session 10

Time-resolved reconstruction of dynamical pulse trains using multiheterodyne detection

Thomas P. Butler, Boguslaw Tykalewicz, David Goulding, Bryan Kelleher, Guillaume Huyet, Stephen P. Hegarty, Tyndall National Institute (Ireland) and Cork Institute of Technology (Ireland)

Optical Frequency Combs (OFC's) provide an important tool in modern metrology [1], and the detection of the complex spectrum of optical waveforms is of considerable interest both in optical communication systems and for the creation of arbitrary optical waveforms. Unfortunately, existing techniques, such as frequency resolved optical gating (FROG)[2], spectral phase interferometry for direct electric-field reconstruction (SPIDER)[3], or stepped heterodyne methods [4] deal poorly with pulse trains that display dynamic properties [5] (i.e. those that are not ideally periodic). This limitation often stems from a large time averaging of the pulse train, or non simultaneous measurements of the comb under test (CUT). To somewhat overcome these limitations when examining dynamic pulse trains, we have used a multiheterodyne beating technique. This multiheterodyne complex spectrum measurement works by mixing the CUT with another reference comb of known spectral intensity.

By positioning the reference comb with a suitable frequency offset and repetition rate difference, a series of RF beat tones can be produced by mixing the signals on a photodiode. Considering the reference comb as a series of fixed local oscillators, the comb is positioned such that each mode will beat with its two nearest neighbours in the CUT. These paired beat tones can be used to measure the phase difference between the two modes of CUT. In this way, a single real time acquisition of these beat tones can then be examined to provide a simultaneous measure of the entire complex spectrum of the CUT. By applying this technique to very small sections of a larger real time trace, a time-resolved picture of the pulse train can be observed.

This technique has been shown to work on periodic pulse trains formed in a LiNbO3 intensity modulator, by comparing the reconstructions to measurements with a high speed sampling oscilloscope and a high resolution optical spectrum analyser. By applying an RF modulation to the drive signal of the modulator, dynamic pulse trains with varying amplitude and frequency were created. By taking small segments of a real time acquisition (~ tens of nanoseconds), the dynamic structure of these pulse trains can be directly measured. This technique could be well suited to the study of pulse trains produced by mode locked semiconductor lasers.

[1] – A. Klee, J. Davila-Rodriguez, C. Williams and P. J. Delfyett. IEEE J. Sel. Top. Quant. 19, 4 (2013)

[2] – K.W. Delong, R. Trebino, J. Hunter, and W. E. White. J. Opt. Soc. Am. B 11(11), 2206-2215, (1995)

[3] – C. Iaconis, I. Walmsley, Opt. Lett. 23(10), 792-794, (1998)

[4] – D.A. Reid, S. G. Murdoch and L. P. Barry. Opt. Express 18, 19 (2010)

[5] – J. Ratner, G. Steinmeyer, T. C. Wong, R. Bartels and R. Trebino. Opt. Lett. 37, 14 (2012)

9134-49, Session 11

Nonclassical light emission from quantum dots in optical nanocavities *(Invited Paper)*

Frank Jahnke, Univ. Bremen (Germany)

Quantum dots are often considered as the active material for the next generation of semiconductor lasers. By placing the quantum dots in optical microcavities with three-dimensional mode confinement, the emission properties of the active material can be tailored. With a single quantum dot emitter in a high-quality cavity, the ultimate limit of miniaturization is reached.

QDs may be viewed as artificial atoms in which interband transitions between localized electron and hole states provide a strong dipole interaction with the electromagnetic field. Self-organized QDs are embedded structures in which the interaction with phonons and with carriers in delocalized states provides efficient QD carrier scattering processes. These are beneficial for applications in light emitters (LEDs, lasers, quantum light sources) as they facilitate a rapid population of the QD electron and hole states. On the other hand, they can be detrimental for quantum-optical effects due to the introduction of dephasing. Lastly, the Coulomb interaction between the QD carriers leads to configuration interaction. Since the size of QDs is much larger than conventional atoms, the configuration interaction energy is only in the meV range and, hence, a number of configurations (excitons, trions, biexcitons, etc.) can simultaneously contribute in optical and carrier scattering processes.

In this talk, we review the use of QDs in optical microresonators for applications as nanolasers with strongly reduced laser threshold. For a small number of 50-200 QD emitters in a resonator, quantum light emission has been demonstrated [1]. Using individual QDs in high-quality cavities, a transition from photon anti-bunching to stimulated emission in the strong-coupling regime is discussed, which leads to the population of higher rungs on the Jaynes-Cummings ladder.

We present theoretical models for the light-matter interaction [2] as well as for the non-equilibrium carrier dynamics in these systems [3], which take into account the QD configuration interaction (multi-exciton states) as well as the many-body interaction with phonons and carriers in delocalized states. Emission properties of few-QD systems are discussed, which include smooth and gradual transitions from thermal to coherent emission, the occurrence of photon anti-bunching for elevated pump rates, as well as giant photon bunching in connection with light trapping.

[1] J. Wiersig et al., Nature 460, 245 (2009).

[2] S. Ritter et al., Optics Express 18, 9909 (2010), C. Gies et al., Optics Express 19, 14370 (2011), W. Chow and F. Jahnke, Progress in Quantum Electronics 37, 109 (2013).

[3] A. Steinhoff et al., Phys. Rev. B 85, 205144 (2012), K. Schuh et al., Phys. Rev. B 87, 035301 (2013), A.-Steinhoff et al., Phys. Rev. B 88, 205309 (2013).

9134-50, Session 11

Feedback-generated periodic pulse trains in quantum dot lasers

Bryan Kelleher, David Goulding, Tyndall National Institute (Ireland) and Cork Institute of Technology (Ireland); Evgeny A. Viktorov, Univ. Libre de Bruxelles (Belgium) and National Research Univ. of Information Technologies, Mechanics and Optics (Russian Federation); Thomas Erneux, Univ. Libre de Bruxelles (Belgium); Stephen P. Hegarty, Tyndall National Institute (Ireland); Guillaume Huyet, Tyndall National Institute (Ireland) and Cork Institute of Technology (Ireland)

Quantum dot lasers (QDLs) have been shown to have greatly enhanced stability in the feedback configuration thanks to a high damping of the relaxation oscillations and they display different dynamics to those of conventional semiconductor lasers [1]. For low feedback levels the behaviour for both QDLs and conventional devices is a constant output on one of the external cavity modes (ECMs). For high feedback levels in conventional devices one obtains Low Frequency Fluctuations (LFF): sharp dropouts in intensity and subsequent gradual build-ups and LFF has been recognised as a chaotic itineracy of the ECMs [2]. An intriguing but heretofore unobserved phenomenon is a synchronization between the ECMs that could result in a periodic, mode-locked behaviour.

We experimentally examine single mode QDLs at high feedback levels (50% - 80% external cavity reflectivity) with a long delay (approximately 1m). Standard LFF-like traces are conspicuous by their absence. Instead we observe regular pulse-trains with a period equaling the external cavity round-trip time where each pulse features a distinctive broad trailing edge plateau (TEP). More complicated multipulse trains appear at still higher feedback levels. ESA spectra clearly show a multimode phenomenon, and clearly very different to the well-known interpretation of LFF. In fact, the distinctive pulse shape with a TEP is very similar to the recently published strong pulse-asymmetry in two-section, passively mode-locked QDLs where a mode decomposition technique revealed the superposition of different modal groups [3] and we attribute the pulses in our experiment to the same phenomenon: each pulse corresponds to a simultaneous excitation of a number of the ECMs. Thus we conclude that the periodic train is a form of mode-locking of several ECMs provided by the strong optical feedback

While the Lang-Kobayashi model explains the observed dynamics with conventional semiconductor lasers extremely well it is unsuitable for the QDL case, principally because of the high feedback levels and long external cavities typically required for instabilities. We consider instead a model tailored specifically for QDLs with strong optical feedback and find it reproduces the experimentally observed trains extremely well. More complicated patterns with a different number of multiplets suggest the existence of a greater number of phase-shifted modal groups.

[1] D. O'Brien, S.P. Hegarty, G. Huyet, J.G. McInerney, T. Kettler, M. Laemmlin, D. Bimberg, V.M. Ustinov, A.E. Zhukov, S.S. Mikhrin and A.R. Kovsh, "Feedback sensitivity of 1.3 mu m InAs/GaAs quantum dot lasers", Electron. Lett. 39, 1819 (2003).

[2] T. Sano, "Antimode dynamics and chaotic itinerancy in the coherence collapse of semiconductor lasers with optical feedback," Phys. Rev. A 50, 2719--2726 (1994).

[3] M. Radziunas, A. G. Vladimirov, E. A. Viktorov, G. Fiol, H. Schmeckebier and D. Bimberg, "Strong pulse asymmetry in quantum-dot mode-locked semiconductor lasers," Appl. Phys. Lett. 98, 031104 (2011).

9134-51, Session 11

Temperature dependent investigation of carrier transport, injection, and densities in 808 nm AlGaAs multi-quantum-well active layers for VCSELs

Andreas P. Engelhardt, Univ. of Kassel (Germany); Johanna S. Kolb, Philips Research (Germany); Friedhard Römer, Univ. Kassel (Germany); Ulrich Weichmann, Philips Research (Germany); Holger Moench, Philips Technologie GmbH (Germany); Bernd Witzigmann, Univ. Kassel (Germany)

The electro-optical efficiency of semiconductor vertical-cavity surface-emitting lasers (VCSELs) strongly depends on the efficient carrier injection into the quantum wells (QWs) in

the laser active region. However, carrier injection degrades with increasing temperature which limits VCSEL performance particularly in high power applications where self heating imposes high temperatures at the point of operation.

By simulation we investigate the transport of charge carriers in 808nm AlGaAs multi-quantum-well active layers with a particular interest in the temperature dependence of carrier injection into the QWs. The transport simulations follow a drift diffusion model complemented by a customized, energy resolved, semi-classical carrier capture theory. In the active QW layers, the model distinguishes between a bound 2D and an unbound 3D carrier population energetically above the QWs. An additional exchange rate in the local continuity equations describes the transition from the unbound to the bound population and vice versa. QW gain as a function of photon energy, electron and hole density, and temperature was precalculated in the screened Hartree-Fock approximation with underlying band structures from 8x8 k.p-theory. The semiconductor simulation is set up in the framework of the simulation environment Synopsys Sentaurus as a 2D edge emitting laser simulation. This allows setting out-coupling and internal losses and the confinement determining the laser-threshold condition, as well as the emission wavelength to match corresponding results from our experimental VCSEL reference. Using the calculated gain data and the experimental parameters for the threshold condition, the appropriate threshold carrier densities in the QWs for a VCSEL are established in simulation for all transport considerations.

Experimental data for comparison was extracted from oxide-confined, top-emitting VCSEL devices designed for emission at 808 nm. Electro-optical characteristics of the single devices measured over a large range of heat sink temperatures allowed for a temperature dependent extraction of characteristic VCSEL parameters with particular interest in threshold current densities and injection efficiency. For better comparison with simulation results, heat sink temperatures were translated to effective active layer temperatures.

With the combination of gain and transport model we achieve a good description of experimental reference data for the injection efficiency and threshold current density over a large temperature range including the effect of gain detuning. Our simulations show that decreasing injection efficiency with temperature is not solely due to increased thermionic escape of carriers from the QWs. Carrier injection is also hampered by state filling in the QWs initiated from higher threshold carrier densities with temperature. Accordingly, efficient injection is not only affected by the temperature und thus self-heating of a VCSEL device. The QW operating point for laser threshold in terms of the carrier concentration has a significant impact as well because of state filling. As a consequence, also VCSEL properties not directly related to the active layer design like optical out-coupling or internal losses, which determine the threshold carrier density, link the temperature dependent carrier injection to VCSEL mirror design.

9134-52, Session 11

Photonic heterostructure high-contrast grating as a novel polarization control and light confinement system in HCG VCSEL

Marcin Gebski, Maciej Dems, Technical Univ. of Lodz (Poland); Jian Chen, Wang Qijie, Dao Hua Zhang, Nanyang Technological Univ. (Singapore); Tomasz Czyszanowski, Technical Univ. of Lodz (Poland)

In order to obtain low threshold VCSELs, high reflectivity mirrors are crucial in their designs. Typically used Distribute Bragg Reflectors (DBR) provide reflectivity over 99.8 % in the spectral range of 75 nm. It has been shown that High Contrast Gratings (HCG), if properly designed, provide extremely large polarization discrimination as well as 150 nm spectrum of high reflectivity which makes them superior to DBRs and potentially opens a way to the next generation HCG based VCSELs. We present numerical simulations of the 980 nm HCG VCSEL design employing new, HCG based 3D light confinement scheme which enables forming an optical aperture regardless of material system. We show that local modification of design parameters of an HCG forms photonic heterostructure, which confines the optical modes and provides strong polarization control with respect to standard DBR mirror. We investigate the modal characteristics of the 980 nm HCG VCSEL with respect to geometrical parameters of heterostructure HCG (h-HCG), especially the dimension of the optical aperture formed by h-HCG. Finally the optimal design of 980 nm GaAs based VCSEL with h-HCG providing high modal gain and strong higher order modes discrimination is proposed.

9134-53, Session 12

Quantum coherent interactions in semiconductor nano-structure optical gain media operating at room temperature *(Invited Paper)*

Gadi Eisenstein, Technion-Israel Institute of Technology (Israel); Johann P. Reithmaier, Univ. Kassel (Germany)

Quantum coherent light matter interactions take place on time scales which are shorter than the de-phasing time of the material. This condition is fundamental because in such interactions, the electromagnetic field modifies the phase of the electronic wave function and this modification has to be sensed before the phase is randomized.

The de-phasing time of solids, particularly semiconductors operating at room temperature is very fast, generally less than 1ps. This is the reason that most experiments seeking to demonstrate coherent interactions in solids are carried out at cryogenic temperatures which lengthen the de-phasing times. However, cooling the semiconductor is not required if the interaction can be induced and measured on time scales shorter than the de-phasing time. This can be achieved using short pulses and ultrafast characterization techniques. In this paper we report on experiments which use this approach to demonstrate Rabi oscillations and self-induced transparency in electrically driven quantum dash and quantum dot optical gain media operating at 300K.

We study the interaction of a 150 fs pulse propagating along a an InP based nano structure optical amplifier and analyze the complete complex (phase and amplitude) output electromagnetic field with a very high temporal resolution using the cross frequency resolved optical gating (X-FROG) scheme. The experiments yield a direct observation of Rabi oscillations and self-induced transparency. Direct observations of the evolution from classical saturation to a regime where coherent interactions dominate is achieved by characterizing the dependence of input pulse energy and bias of the complex electrical field profile at the output of the amplifier.

A complete understanding of the observed experimental results is obtained from an accompanying numerical analysis that calculates the co-evolution of the electronic state-function together with the electromagnetic field according the Maxwell and Schrödinger equations. The calculations do not utilize the rotating wave approximation enabling to calculate all the fast oscillations of the electromagnetic field and of the electronic state functions.

9134-54, Session 12

Distributed-feedback GaSb-based lasers diodes in the 2.3 to 3.3μm wavelength range

Quentin P. Gaimard, Tong Nguyen-ba, Institut d'Electronique du Sud (France); Alexandre Larrue, Lab. d'Analyse et d'Architecture des Systèmes (France); Laurent Cerutti, Yves Rouillard, Institut d'Electronique du Sud (France); Olivier GAUTHIER-LAFAYE,

LAAS CNRS (France); Roland Teissier, Aurore Vicet, Institut d'Electronique du Sud (France)

Development of a reliable, selective, sensitive, technique for atmospheric trace gas concentrations monitoring is a critical challenge in science and engineering. Tunable single-frequency laser in the 2.3 to 3.3μm wavelength range, working in a continuous regime at room temperature can be used for absorption spectroscopy [1] to identify and quantify several gases such as methane (greenhouse gases) and ethylene (food-processing) which are studied in the IES. We report here on the design and fabrication of 1st to 4th order distributed-feedback (DFB) antimonide-lasers diodes in the 2.3 to 3.3μm wavelength range. This process is applied to all studied structures grown by molecular beam epitaxy (MBE) on GaSb substrate [2].

Electromagnetic modeling helps us to determine the Bragg grating period as well as the global geometry of the structure in order to optimize both modal discrimination and optical power of the lasing mode. The grating is defined by holographic lithography.

Two DFB laser diode designs are proposed and investigated in parallel:

-Side wall corrugation DFB [3]: A corrugation on the lateral sides of the ridge waveguide defined by holographic lithography is transferred by both wet and dry on a hard mask formed by Cr and SiO2, followed by a Cl2/N2 dry etching etching in the III-V heterostructure. Ohmic contact are then evaporated on the top of the waveguide after isolating the rest of the substrate by a Si3N4 thin layer.

-Buried DFB [4]. The MBE growth is stopped at the top of the active region. Then the Bragg grating is etched by Ar sputtering through a SiO2 mask. A regrowth process is performed after the reintroduction of the substrate in the MBE vacuum chamber allowing the growth of the upper cladding layer. Chemical etching of the mesa with fluoro-chromic acid, Si3N4 isolation, and gold contact deposition ends the process.

Finally we will show the results on the fabrication and characterization of the devices.

This work is supported by the ANR NexCILAS international project, ANR MIDAS project, NUMEV labex and RENATECH national Network.

[1] M. Jahjah et al. Applied physique B 2011, 10.1007/s00340-011-4671-4

[2] S. Belahsene et al. Phot. Technol. Letters 2010, 22 (15) 1084.

[3] C. S. Kim et al. Applied Physics Letters 2009, 95, 231103.

[4] K. Utaka et al. Electron. Letters. 1981, 17, 961-963.

9134-55, Session 12

Performance investigation of 112 Gb/s PDM-QPSK long-haul systems employing discrete mode lasers

John O'Carroll, Eblana Photonics Ltd. (Ireland); Vidak Vujicic, Dublin City Univ. (Ireland); Nicolas Brochier, Orange SA (France); Laurent Bramerie, Univ. Europenne de Bretagne (France); Liam P. Barry, Dublin City Univ. (Ireland)

100-Gb/s coherent systems based on polarization-division multiplexed quadrature phase shift keying (PDM-QPSK), with aggregate wavelength-division multiplexed (WDM) capacities approaching 10 Tb/s, are getting widely deployed, due to the benefits provided by coherent detection. Coherent detection offers the advantage of access to the amplitude and phase of the optical electric field in the electronic domain at the receiver. This allows compensation of the channel impairments and enables employment of advanced modulation formats. Higher order modulation formats, such as PDM-QPSK, have more stringent linewidth requirements for lasers used in these systems, compared to systems employing intensity modulation and direct detection. A major challenge is therefore to produce lasers with the requisite performance at low cost. Discrete Mode Laser Diodes (DMLDs) can be designed for narrow linewidth emission and present an economic approach with a focus on high volume manufacturability of semiconductor lasers. DMLDs are monolithic and can use existing telecommunication laser packaging platforms to produce lasers in high volumes; this is not easily achieved with External Cavity Lasers (ECLs) which have more complex packaging requirements.

In this paper the performance of a 112 Gb/s long-haul optical transmission system employing PDM-QPSK is investigated using a range of transmitter lasers with linewidth values ranging from 100 kHz to 5 MHz. A linewidth of 100 kHz was obtained from an External Cavity Laser and linewidths ranging from 200 kHz to 5 MHz were obtained from monolithic semiconductor Discrete Mode Laser Diodes with cavity lengths of 300 μm and 1 mm. A bank of 52 DFB lasers was used at the transmitter to implement a wavelength division multiplexed (WDM) transmission system on a 50 GHz grid, and the device under test was introduced to the setup through a coupler and set to one specific wavelength of the ITU grid. The performance of the system is analysed through experimental measurements and simulations performed by Virtual Photonics Incorporated Transmission Maker (VPI TM). Results are presented for back-to-back operation and after transmission through G.654 pure silica core fiber (PSCF) at distances up to 6930 km. Results obtained for the back-to-back case show a penalty in optical signal-to-noise ratio (OSNR) lower that 1dB at BER= 1 ? 10-3 for 5 MHz DMLD compared to 100 kHz ECL. At the soft decision FEC limit of 2.4 ? 10-2 the penalty at 5 MHz is less than 0.1dB. Degradation in performance with increasing transmission distance was observed, but the BER remains below the soft decision FEC limit even after transmission over 6930 km. A small increase in the BER is measured with increasing linewidth as is to be expected and good correspondence is achieved between experimental and simulations results.

9134-56, Session 12

Time-resolved FTIR study of spectral tuning and thermal dynamics of mid-IR QCLs for application in absorption spectroscopy

Kamil Pier?ci?ski, Institute of Electron Technology (Poland); Dariusz Szabra, Military Univ. of Technology (Poland); Dorota Pier?ci?ska, Institute of Electron Technology (Poland); Miroslaw Nowakowski, Jacek Wojtas, Janusz Mikolajczyk, Zbigniew Bielecki, Military Univ. of Technology (Poland); Maciej Bugajski, Institute of Electron Technology (Poland)

Quantum cascade lasers (QCLs) emitting in the mid-infrared region (~9μm) have been demonstrated to be useful tunable light sources for laser-based absorption spectroscopy. QCLs deliver high power and are capable of lasing at room temperature. The development of effective methods for utilizing these lasers in absorption spectroscopy, especially for the purpose of monitoring atmospheric trace-gas species becomes an important issue. Absorption spectroscopy is an effective method for detecting trace amounts of hazardous substances. Detection can be based on two spectroscopic methods: intra- and interpulse. For both methods, knowledge about the tuning of the QCL's emission frequency is crucial. At the same time, the struggle continues to improve thermal properties of the devices. Both problems can be studied by means of registering time resolved emission spectra.

Characterization of the devices includes Light-Current-Voltage (L-I-V) measurements and time resolved Fourier Transform Infrared (TRS-FTIR) spectroscopy. Temporal resolution of 5 ns available in TRS-FTIR spectroscopy, provides information's about the laser's frequency tuning during different modes of operation, meeting specific requirements of various sensing techniques. Investigated QCLs were designed and fabricated at the Institute of Electron Technology in Warsaw.

The aim of this paper is to show the applicability of these QCLs for laser absorption spectroscopy, as well as to address some of the aspects of thermal management of QCLs. Results include electrical and spectral characterization of the devices.

Time resolved spectra show shift of QCL emission mode towards lower wavenumbers during the pulse. Characteristics were registered at different temperatures of operation and driving conditions. Registered shift rates depend on operating temperature, being the highest at room temperature. Based on spectral tuning results, temperature increase rates for different modes of operations were evaluated, delivering information on thermal dynamics of investigated devices.

9134-82, Session 12

The effect of InP based wide-tunable AMQW laser length on power profile

Hesham M. Enshasy, King Faisal Univ. (Saudi Arabia); Daniel T. Cassidy, McMaster Univ. (Canada)

The effect of the length of wide tunable AMQW laser on its output power is demonstrated in this paper. The InP based AMQW laser is custom designed and fabricated to have a large tuning range. The experimental data showed that the output power profile is not following the traditional behavior of laser diodes. The data showed that the laser length can be categorized in three categories, below transitional length cavity (BTLC), above the transitional length cavity (ATLC), and at the transitional length cavity (TLC). The BTLC and ATLC lengths are not suitable for wide tunable applications however the TLC length is suitable for wide tunable applications and the power profile is closer to the traditional power profile of laser diodes. This type of AMQW laser diodes can be used in many applications.

9134-92, Session PS

Predicting modes of operation in quantum dot mode-locked lasers using a delay differential equation model

Lina Jaurigue, Technische Univ. Berlin (Germany); Frederic Grillot, Ecole Nationale Superieure des Telecommunications (France); Eckehard Scholl, Kathy Ludge, Technische Univ. Berlin (Germany)

Semiconductor passively mode-locked lasers are of broad interest due to their potential applications as sources of ultra-short, high frequency light pulses. In spite of the complex dynamics of such devices, a relatively simple delay differential equation model can reproduce the manifold modes of operation experimentally observed. Using such a model we investigate the modes of operation of passively mode-locked lasers. We calculate key model parameters from experimentally measured quantities and thus are able to reproduce experimentally observed features, such as the onset of fundamental mode-locking, pulse widths and repetition rates. Despite the simplicity of the gain model used within our approach nano-structured lasers, such as quantum-dot lasers, can be effectively described. This enables us to make predictions about device behavior in dependence of operational parameters and allows for device optimization.

9135-1, Session 1

Cryogenic Yb-doped lasers for efficient nanosecond, picosecond, and femtosecond sources *(Invited Paper)*

Darren A. Rand, Daniel E. Miller, Tso Yee Fan, MIT Lincoln Lab. (United States)

Operation of lasers at cryogenic temperatures has been used since the very earliest days of laser development. Generally, operation at low temperatures has been viewed as an undesirable and impractical means to improve laser performance. However, many of the fundamental laser materials properties (thermal conductivity, thermal expansion, dn/dT, saturation intensity and fluence) improve significantly as the temperature decreases. Additionally, many rare-earth-ion-doped solid-state lasers that are quasi-three-level lasers at room temperature become 4-level lasers at cryogenic temperature, leading to more efficient laser operation. The overhead associated with cryogenic cooling has been mitigated over time as cryogenics have become increasingly ubiquitous.

Recent laser demonstrations have taken advantage of the improved properties to scale the power of relatively simple end-pumped lasers to hundreds of Watts of output power and provide performance that is not possible with conventional room-temperature lasers. The improved performance is of particular interest for laser systems that need both high average and high peak powers simultaneously. We provide an overview of cryogenic solid-state lasers, discuss recent demonstrations, and give a perspective on the future of this technology.

9135-2, Session 1

Implications of the temperature dependence of Nd:YAG spectroscopic values for low-temperature laser operation at 946nm

SungJin Yoon, Jacob I. Mackenzie, Univ. of Southampton (United Kingdom)

Despite many papers in the literature on the spectroscopic properties of Nd-doped yttrium aluminium garnet (YAG), there does not appear to be a comprehensive study of the key absorption lines, nor emission lines that terminate in the ground state, i.e. around 900nm. We present our measurements of the key spectroscopic properties over the temperature range of 77K to 300K for Nd3+ ions doped in (YAG).

The effective absorption cross section was determined for both 4I9/2 -> 4F3/2 and 4F5/2 transition bands, employing bright LED sources and an optical spectrum analyser, excellent agreement is obtained with standard approaches reported in the literature. For the emission cross section measurements, we used a non-collinear pump (795 nm Lumics LU0793T040 100 micron fibre) configuration, and a pumping irradiance of <1.5 kWcm^-2 (weak compared to a pump saturation irradiance of ~70kWcm^-2), to minimise amplified spontaneous emission compromising the measured fluorescence spectrum. The entire fluorescence spectrum from 850nm – 1450nm was measured. One note of particular interest for the dominant emission wavelengths around 1064nm and 1061nm (4F3/2 -> 4I11/2) was the switch in their relative strength below 170K. Primarily driven by the Boltzmann occupation factor of the upper level, in addition to the fact that the 1064nm line is comprised of two transitions R2->Y3 and R1->Y2, which overlap at 300K but are well separated at lower temperatures, whereas the 1061nm transition is derived from emission between the R1->Y1 Stark levels.

From room to liquid nitrogen temperature (LNT), the peak absorption cross section around 808nm increased by almost 3 times (7pm^2 -> 18pm^2), in conjunction the bandwidth of this absorption line reduced by the same factor, i.e. 0.3nm FWHM @ 77K. As previously noted by Kaminskii [1] the peak of the absorption line was blue shifted by 0.25nm with respect to 300K.

The fluorescence and lifetime for the 938nm and 946nm lines, originating from R1 and R2 Stark levels of the 4F3/2 manifold and terminating in the Z5 Stark level of the ground manifold 4I9/2, were measured and the effective emission cross section determined by the Fuchtbauer-Ladenburg (F-L) method. The effective emission cross section for 946nm (R1 -> Z5) increased from 3.9pm^2 to 8.4pm^2 over the 300K to 77K range, a significant increase in the potential gain at this wavelength. Moreover due to the relatively large ground state splitting, the thermal population of the Z5 (852cm^-1) Stark level of 0.7% at room temperature, reduces by several orders of magnitude at LNT, thus eliminating reabsorption loss for this transition. The 1061 nm emission cross section increased by 3.5 times (21pm^2 -> 78pm^2) over the temperature range investigated, which may be a potential limitation in terms of parasitic amplified spontaneous emission or laser action, with respect to the weaker 9xx nm transitions.

Capitalising on the lower the threshold and higher gains available we built a cryogenically cooled 946nm laser with better than 60% slope efficiency and 50% optical to optical efficiency with respect to the 808nm absorbed pump. There is tremendous scope for power scaling this laser transition via cryogenic cooling with additional benefits to be gained by significantly improved thermo-optical properties of the YAG host.

1. A. A. Kaminskii, Crystalline lasers: physical processes and operating schemes (CRC Press, 1996).

9135-3, Session 1

Passively Q-switched 2.97 ?m fluoride fiber laser base on a semiconductor saturable absorber mirror

Jianfeng Li, Aston Univ. (China) and Aston Univ. (United Kingdom); Yulian He, School of Optoelectronic Information, University of Electronic Science and Technology of China (China); Hongyu Luo, Yong Liu, Univ. of Electronic Science and Technology of China (China); Bin-bin Luo, Chongqing Institute of Technology (China); Zhongyuan Sun, AIPT, Aston University (United Kingdom); Lin Zhang, Sergei K. Turitsyn, Aston Univ. (United Kingdom)

Pulsed mid-IR fiber lasers attracted intensive attention in recent years due to the potential applications in defense, spectroscopy, medicine and gas sensing. In some specific fields such as material processing, micro surgery and nonlinear optical process, fiber lasers with high peak power are eagerly desired. In this paper, we presented an 1150-nm diode cladding-pumped passively Q-switched Ho3+-doped fluoride fiber laser based on a specifically designed GaAs-based mid-infrared semiconductor saturable absorber mirror (SESAM). Compared with conventional SESAMs operating at short-infrared regime, this mid-infrared SESAM employed a specifically reverse design due to low cost and great heat dissipation. At the launched pump power of 0.202 W, the laser started to oscillate and operate in CW state. As increasing the launched pump power to 0.267 W, Q-switched pulses appeared but with violent amplitude fluctuation. After the launched pump power reached 0.426 W, stable Q-switched pulses was achieved with pulse energy of 0.92 ?J, pulse duration of 6.05 ?s, repetition rate of 22.89 kHz. Further increasing the launched pump power until the maximum value 2.814 W, Q-switched pulses maintained very stably with pulse duration decreasing from 6.05 ?s to 2.72 ?s, repetition rate and pulse energy increasing from 22.89 kHz to 58.17 kHz and from 0.92 ?J to 5.25 ?J which was

only limited by the maximum launched pump power. At this maximum launched pump power, pulse train with average power of 305 mW and peak power of 1.93 W was produced at s slope efficiency of 11.6 % with respect to the launched pump power. The signal-to-noise ratio (SNR) of ~45 dB also indicated the Q-switched pulses were operated at stable regime. The Q-switched pulse train from 5I6 ?5I7 transition operated at a center wavelength of 2968.5 nm with FWHM of 5.6 nm. Additionally, CW operation of the Ho3+-doped fluoride laser was investigated by replacing the SESAM with a broadband Au-coated reflector. At the same launched pump power, the spectrum was slightly shifted to 2976.2 nm with broadened FWHM of 11.5 nm as a result of higher and homogeneous feedback. We have demonstrated a passively Q-switched fiber laser with to date longest emission wavelength of 2968.5 nm and highest pulse energy of 5.25 ?J at this band. Further increase in the energy and reduction in pulse duration are expected by increasing the pump power since the SESAM was not fully saturated, shortening the fiber length and increasing the modulation depth of the SESAM.

9135-4, Session 1

Gain-switched PCF rod type fiber laser

Rok Petkovsek, Vid Agrez, Univ. of Ljubljana (Slovenia); Damien Sangla, Julien Saby, Reynald Boula-Picard, François Salin, EOLITE Systems (France)

1. INTRODUCTION

In comparison to different fiber laser pulsed setups, such as direct diode modulation or Q-switching, the gain switched lasers present the simplest way to produce nanosecond laser pulses. Till now several gain switched setup using rare Yb-doped fibers have been reported with pulse duration in the range of over 100 ns[1-3]. With the appropriate design the pulse duration be lowered as shown recently in [4] and a especially in [5] where the pulse duration of only 66 ns was reached. In this paper we present a gain switched rod type PCF fiber laser. It was pumped by high performance pump system that enables high peak power of the output pulses and high pulse-to-pulse stability.

2. EXPERIMENTAL SETUP

Laser system was based on Yb3+ gain switched rod type fiber laser which was pumped at wavelength of 976 nm. One of the key component of the setup is the high performance pump system based on single emitters diodes incorporating high speed and high current laser diode drivers. It is capable to switch on and off up to 800 W of the pump light within few 10s of ns. The pump system active feedback loop monitors the laser and control the pump pulse duration. Consequently very high pulse to pulse stability can be achieved. Furthermore the active control of cooling system determines the temperature of the pump diode in order to allow efficient absorption at the highest absorption peak of ytterbium. This control enables efficient operation over broad range of repetition rate and pump pulse power. On the other hand the spectrum width of the pump light cannot be efficiently controlled. However the spectrum broadening that appears at higher pump pulse power do not significantly influence the laser operation. As for example the FWHM changes from 4 nm to 7 nm for pump pulse power increase from 200 W to 800 W respectively.

The rod type PCF Yb-doped fiber was 60 cm long and straight polished on one end to enable Fresnel reflection for output coupling. On the other end the rod fiber was angle polished to allow only the reflection from the high reflection mirror. Pump pulses were coupled in to the rod type fiber through the angle polished end.

3. RESULTS

The laser setup was characterized with respect to output pulse duration, peak power, output spectrum and pulse stability. The change of the first three parameters was observed with changing the pump pulse power. Keeping the system parameters the same and changing only the energy of the pumping pulse by increasing the pump pulse power the maximum laser peak power of 3.6 kW was reached. Pulse duration was 48 ns. As the broadband HR mirror was used the spectrum of output pulses depends on pump pulse power. This dependence is related to the spectral shift of the gain curve of the active medium. In the case of ytterbium doped fibers higher pump power and consequently higher inversion in the active medium means that gain maximum is shifted from longer wavelength toward the 1030 nm where the emission cross section is highest. In our case the shift in the central wavelength was approx. 3 nm. The pulse to pulse stability was better than ±1%.

CONCLUSION

A short pulse with duration of 48 ns and peak power of 3.6 kW were obtained from gain switched rod type fiber lasers. According to our best knowledge this the highest peak power obtained from Yb-doped active medium based on oscillator (one stage) only. Further the high performance pump system enables high pulse to pulse stability.

REFERENCES

[1] S. Maryashin, A. Unt, and V. P. Gapontsev, “10-mJ pulse energy and 200 W average power Yb-doped fiber laser.” Proc. SPIE 6102, 61020O1-61020O5 (61,73).

[2] Y. Sintov, M. Katz, P. Blau et al., “A frequency doubled gain switched Yb3+-doped fiber laser,” 719529-719529 (2009).

[3] C. Larsen, D. Noordegraaf, P. M. W. Skovgaard et al., “Gain-switched CW fiber laser for improved supercontinuum generation in a PCF,” Opt. Express, 19(16), 14883-14891 (2011).

[4] V. Agre?, and R. Petkov?ek, “Gain-switched Yb-doped fiber laser for microprocessing,” Appl. Opt., 52(13), 3066-3072 (2013).

[5] C. Larsen, M. Giesberts, S. Nyga et al., “Gain-switched all-fiber laser with narrow bandwidth,” Opt. Express, 21(10), 12302-12308 (2013).

9135-5, Session 1

High-energy actively Q-switched DPSS laser with multi-segmented crystal rod pumped at 885nm

George Tsaknakis, Christos Evangelatos, Alexandros Papayannis, National Technical Univ. of Athens (Greece); Giorgos Avdikos, Raymetrics S.A. (Greece); Dimitris Papadopoulos, Univ. of Ioannina (Greece); Paraskevas Bakopoulos, National Technical Univ. of Athens (Greece); Georgios D. Tzeremes, European Space Agency (Netherlands)

In this paper, we present experimental results of a diode-pumped solid-state laser (DPSSL) operating at 1064 nm that was developed in the frames of the QOMA project (Q-Switched Master Oscillator based on Multidoping Nd:YAG Technology for Optoelectronics Space Applications) funded by the European Space Agency (ESA). The system’s design is based on new laser engineering technologies combining high power pumping of a multi-segmented crystal rod at 885 nm and novel crystal cooling configurations. As active material a multi-segmented Nd:YAG crystal rod (0.1%, 0.23%, 0.6% at Nd) of 54 mm length and 3 mm diameter with 7 mm undoped endcaps on both ends is used. The use of this specific crystal rod configuration ensures a high overall efficiency, in combination with excellent beam quality and high average power due to the low thermal effects and mechanical stresses inside the crystal rod. For actively Q-switched operation, a new Acousto-Optic Modulator (AOM) has been designed and manufactured exclusively for our project’s purposes. AOM’s unique feature is that it exhibits antireflection coating at 946 and 1064 nm (dual AR coating), so it can be applied to laser configurations for the generation at 946 and 1064nm radiation. AR values are less than 0.25% at 946 and 1064 nm and are designed to meet a power density of 500 MW/cm2 based on 10 ns pulse width. The repetition rate was adjusted from 25 kHz down to 100 Hz and the laser energy was measured 2.57 mJ at 1 kHz. The pulse width was measured 33 ns.

The M2 for all repetition rates of operation was measured

at ~1.3 indicating a highly monomode operation. To the best of our knowledge, the measured energy of 2.57 mJ at 1 kHz, preserving an almost Gaussian beam profile, is one the best results published so far, proving that the combination of upper laser level pumping at 885 nm and multi-segmented crystal rod design can reduce the thermal losses inside the crystal rod and restrict the thermal lensing effect extending our recent work on a passively Q-switched cavity [1].

[1] C. Evangelatos, P. Bakopoulos, G. Tsaknakis, D. Papadopoulos, G. Avdikos, A. Papayannis, G. Tzeremes, "Continuous wave and passively Q-switched Nd:YAG laser with a multisegmented crystal diode-pumped at 885 nm," Applied Optics, vol. 52, no. 36, pp. 8795-8801, Dec, 2013.

9135-6, Session 2

CEO stabilised high power frequency combs with diode-pumped solid-state-lasers *(Invited Paper)*

Thomas Südmeyer, ETH Zürich (Switzerland) and Univ. of Neuchatel (Switzerland)

Although ultrafast lasers have already enabled numerous important industrial and scientific breakthroughs, there is still a strong need for further improvements in terms of achievable performance, compactness, and reliability. In this presentation, we will review latest developments in the area of ultrafast laser oscillators and frequency comb generation. The highest average power levels and pulse energy levels of ultrafast oscillators are achieved in the thin disk laser geometry. We review the latest milestones in terms of duration, power and pulse energy and discuss the first carrier-envelope-offset (CEO) stabilized SESAM-modelocked thin disk laser. Moreover, we discuss the first frequency comb stabilization by optical feedback to a semiconductor saturable absorber mirror (SESAM). This new method for opto-optical modulation (OOM) overcomes bandwidth limitations of the standard pump current control and enables a CEO-locked 1.5-μm diode-pumped solid-state laser with ten times lower residual phase noise.

9135-7, Session 2

Carrier-envelope phase stabilized, few-cycle, high-power thin-disk oscillator

Marcus Seidel, Jonathan Brons, Max-Planck-Institut für Quantenoptik (Germany); Fabian Lücking, Vladimir Pervak, Ludwig-Maximilians-Univ. München (Germany); Alexander A. Apolonskiy, Max-Planck-Institut für Quantenoptik (Germany) and Ludwig-Maximilians-Univ. München (Germany); Oleg Pronin, Ludwig-Maximilians-Univ. München (Germany); Thomas Udem, Max-Planck-Institut für Quantenoptik (Germany); Ferenc Krausz, Max-Planck-Institut für Quantenoptik (Germany) and Ludwig-Maximilians-Univ. München (Germany)

The output of a Kerr-lens modelocked (KLM) Yb:YAG thin-disc oscillator delivering 250 fs, 40 W average power, 1.1 ?J pulses has been carrier-envelope phase (CEP) stabilized to sub-300 mrad out-of-loop RMS noise. Moreover, the initial pulse duration was reduced to 10 fs, corresponding to only three optical cycles, by means of a two stage spectral broadening and pulse compression setup. This is the first Yb-based laser system which operates within the few-cycle regime and the first KLM thin-disc oscillator which is CEP-stabilized.

The presented system is capable to replace Ti:Sapphire based oscillators, the working horses in many ultrafast optics laboratories, since it provides comparable CEP-stability and pulse durations but offers about two orders of magnitude more average power and pulse energy, resp. Furthermore, owing to the high peak powers of multiple tens of MW, the presented system grants access to amplifier-free high-field physics. Hence, for instance, attosecond physics or coincidence spectroscopy at MHz repetition rates come into reach. Besides, the low intensity noise of the oscillator (0.2 % - 0.3 % rms) allows to study nonlinear optics unprecedentedly close to the damage threshold of solid state materials.

The first spectral broadening stage consists of an 8 cm long large mode area photonic crystal (PCF) fiber of 35 micron mode field diameter. 30 W of the output of the oscillator described in [1] are coupled into this PCF. Due to self-phase modulation (SPM) the Fourier limit of the pulses is reduced from 250 fs to 13 fs. To compress the pulses, tailored chirped mirrors are employed. A total GDD of ≈-2100 fs2 and a TOD of ≈-1100 fs3 is added to the spectrally broadened pulses, yielding 15 fs pulses at an average power of 20 W.

For additional spectral broadening, the compressed laser pulses are focused with a spherical silver mirror (f = 50 mm) into a 3 mm crystalline quartz plate. SPM leads to a Fourier limit below 6 fs, corresponding to less than two optical cycles at 1030 nm central wavelength. The full compression of these pulses is still in progress. Up to now, a pulse duration of 10 fs has been measured at an average power level of 11 W.

To detect the carrier-envelope offset (CEO) frequency of the compressed oscillator output, a reflection from a fused silica wedge is sent into an f-to-2f interferometer. The CEP is measured with a digital phase detector and controlled with a PI2D servo controller. The generated feedback slightly modulates the diffraction losses of an acousto-optic modulator (AOM) which is placed inside the oscillator. The intracavity AOM approach has been demonstrated for the first time. It does not significantly disturb the modelocking but allows phase control over a bandwidth of tens of kHz. The residual CEP noise is suppressed down to 180 mrad in-loop (1 Hz – 500 kHz). A parallel out-of-loop measurement yields a residual CEP noise of 270 mrad.

[1] O. Pronin et al., Opt. Lett. 36, 4746-4748 (2011)

9135-8, Session 2

Transfer of laser frequency standard stability into rf range

Vadim Polyakov, National Research Univ. of Information Technologies, Mechanics and Optics (Russian Federation); Oleg A. Orlov, D.I. Mendeleyev Institute for Metrology (Russian Federation); Evgeny Viktorov, National Research Univ. of Information Technologies, Mechanics and Optics (Russian Federation)

The idea to improve global positioning systems accuracy by means of optical frequency standards has technological difficulties due to the existing user infrastructure. We need to take a technology that transfers the optical stability to the GPS and GLONASS RF operational range – the L1 – L5 signals (1575.42 MHz, 1227.60 MHz, 1381.05 MHz, 1379.913 MHz, 1176.45 MHz). The today accuracy for the GLONASS signal is 10-13.

The optical frequency comb technology is attractive but rather complicated with a view to space-born or any portable application. As we have a technology for optical standard with doubled Nd:YVO laser locked to iodine cell, we suggest to lock the doubled Nd:YVO laser wavelength to iodine absorption lines and by this mean stabilize the intermode beat signal to provide RF standard.

There was developed a special construction where the laser is mounted in compact rigid case. Such laser design allowed to reduce the influence of external temperature and vibration and to increase relative passive laser frequency stability. The saturated vapor iodine cell is used for the laser locking. Sub Doppler third harmonic technique was used to lock laser frequency onto iodine line.

The laser is Nd:YVO with frequency doubling in external cavity with KTP. Pumped by a laser diode at 808 nm, 300 mW. The cavities are placed on a rigid invar frame, which is temperature controlled by a thermoelectric module. The output light proceeds to the spectroscopic scheme. Locking the Nd:YVO cavity to the doubler cavity allows to transfer the stability to the intermode beat signal.

The doubling cavity has the different length comparing to the Nd:YVO cavity, so it allows to select the single longitudinal mode and aovoid beat influence on locking stability. The Nd:YVO cavity is operating in multimode regime.

We demonstrate the stability of the beat signal between two cavity modes of DPSS lasers in the RF range and discuss the technology of tunable RF standard with 10-15 to 10-16 stability in RF range.

References:

1. Wang-Yau Cheng, Lisheng Chen, Tai Hyun Yoon, John L.Hall and Jun Ye, "Sub-Doppler molecular-iodine transitions near the dissociation limit(523 – 498nm), Optics Letters, vol.27, No 8, pp.571-573, 2002.

2. L. Vitushkin, O. Orlov, "A compact frequency-stabilized Nd:YVO4/KTP/I2 laser at 532 nm for laser interferometry and wavelength standards", Proceedings of SPIE,v.5856, pp.281-286, 2005.

3. L. Robertsson, M. Zucco, and L.-S. Ma, "Absolute frequency measurements of the 532 nm radiation recommended for the realization of the metre", Report BIPM-2003/07.

9135-9, Session 2

Coherence and power thresholds of a continuous-wave laser

Marc Eichhorn, Institut Franco-Allemand de Recherches de Saint-Louis (France); Markus Pollnau, Univ. Twente (Netherlands)

The generation of spectrally and spatially coherent light distinguishes lasers from other sources of electromagnetic radiation. A continuous-wave (cw) laser is defined by a time-independent number of coherent photons in the lasing mode of the resonator. When neglecting the influence of spontaneous emission, one finds that the gain would equal the losses. This approximation is sometimes incorrectly considered as a synonymous definition of a cw laser. In such a situation, the coherent photon number would build up and coherence would manifest itself inside the resonator only when pumping above the laser threshold and the threshold inversion would depend only on the total resonator losses, but be independent of decay channels from the upper laser level i) at other frequencies, ii) non-radiatively, and iii) into other optical modes. None of these implications holds true for any laser that mankind has ever created.

We extend the existing theory of cw lasers by systematically considering spontaneous emission as stimulated emission driven by vacuum fluctuations. The direct consequence is that in a cw laser the gain is smaller than the losses. In a simple rate-equation approach, the laser eigenvalue, defined as the ratio of coherent photons inside the resonator divided by the number of photons replaced by photons coupled in via spontaneous emission during one resonator decay time, emerges as the fundamental parameter describing a cw laser.

When with increasing pump rate the coherent photon number in the resonator mode builds up, two laser thresholds occur. The coherence threshold, above which coherence manifests itself in the resonator mode, is relevant for few-photon sources. At the coherence threshold the gain equals half the losses and the stimulated-emission equals the spontaneous-emission rate. An ideal four-level laser exhibits in average one coherent photon in its mode, which is coupled out of the resonator and replaced by one-half photon each via stimulated and spontaneous emission during the resonator decay time. Previously, Björk, Karlsson, and Yamamoto proposed this point, which they called the quantum threshold, as a general definition of the laser threshold.

Furthermore, we provide a definition of the laser power threshold, at which the laser output power increases significantly, that correctly takes spontaneous emission into account. We show that a cw laser reaches the commonly known "threshold inversion" only at infinitely high pump rate and output power and that the correct laser power threshold is diminished by the fraction of upper-state decay into the lasing mode. We confirm previous predictions of a threshold-less four-level laser. The theory describes all types of lasers of three-level, four-level, or any intermediate nature.

9135-10, Session 2

Resonator modeling by field tracing: a flexible approach for fully vectorial laser resonator modeling

Daniel Asoubar, Friedrich-Schiller-Univ Jena (Germany) and LightTrans VirtualLab UG (Germany); Frank Wyrowski, Friedrich-Schiller-Univ. Jena (Germany); Hagen Schweitzer, Christian Hellmann, Michael Kuhn, LightTrans VirtualLab UG (Germany)

Nowadays lasers cover a broad spectrum of applications, like laser material processing, metrology and communications. Therefore a broad variety of different lasers containing various active media and resonator setups with optical components like aspherical or graded-phase mirrors and lenses, diffractive optical elements, thin film coatings and nonlinear optical components are used to provide high design flexibility. The optimization of such multi-parameter laser setups requires powerful simulation techniques. In literature mainly three practical resonator modeling techniques can be found: Rigorous techniques, e.g. the finite element method (FEM), which are based on the solution of Maxwell's equations with periodic boundary conditions at the cavity edges. These techniques suffer from high numerical effort, resulting in a very restricted computational volume of the resonator cavities. Approximated solutions are based on paraxial Gaussian beam tracing by ABCD matrices, which can simulate optical components introducing quadratic phase terms only. Furthermore the beam propagation technique (BPM) is used to analyze transversal resonator modes. This approach is restricted by the computational effort and the flexibility to simulate a large variety of different optical components. All of these existing approaches have in common, that only a single simulation technique is used for the whole resonator. In contrast we propose a combination of different field tracing techniques within the Fox & Li algorithm to fulfill nowadays requirements in the flexible simulation of complex multi-parameter resonators. In field tracing we use a fully vectorial field representation. It allows the smooth combination of different modeling techniques in different subdomains of the resonator. The work introduces the basic concepts of field tracing in resonators to calculate vectorial, transversal eigenmodes of stable and unstable resonators.

9135-11, Session 3

Ultrafast green-laser exceeding 400 W of average power

Bastian Gronloh, Peter Russbueldt, Bernd Jungbluth, Dieter Hoffmann, Fraunhofer-Institut für Lasertechnik (Germany)

We present the world's first laser at 515 nm with sub-picosecond pulses and an average power exceeding 400 W. To realize this beam source we utilize an Yb:YAG-based infrared laser consisting of a fiber MOPA system as a seed source, a rod-type pre-amplifier and two Innoslab power amplifier stages. The infrared system delivers up to 930 W of average power at repetition rates between 10 and 50 MHz and with pulse durations below 800 fs. The beam quality in the infrared is M? = 1.1 and 1.5 in fast and slow axis. As a frequency doubler we chose a Type-I critically phase-matched LBO crystal in a single-pass configuration. To preserve the infrared beam quality and pulse duration, the conversion was carefully modeled using numerical calculations. These take dispersion-related and thermal effects into account, thus enabling us to provide precise predictions of the properties of the frequency-doubled beam.

To be able to model the influence of thermal dephasing correctly and to choose appropriate crystals accordingly, we performed extensive absorption measurements of all crystals used for conversion experiments. These measurements provide

the input data for the thermal FEM analysis and calculation. We used a Photothermal Commonpath Interferometer (PCI) to obtain space-resolved absorption data in the bulk and at the surfaces of the LBO crystals. The absorption was measured at 1030 nm as well as at 515 nm in order to take into account the different absorption behavior at both occurring wavelengths.

9135-12, Session 3

A 1 kW frequency doubled Yb:YAG CW thin-disk laser

Marwan Abdou Ahmed, Martin Rumpel, Univ. Stuttgart (Germany); Montassir Bouzid, Christian Stolzenburg, Alexander Killi, TRUMPF Laser GmbH & Co. KG (Germany); Michael Moeller, Christian Moormann, AMO GmbH (Germany); Thomas Graf, Univ. Stuttgart (Germany)

Deep penetration welding of copper has been reported to be more efficient when using green laser radiation thanks to the approximately 7-10 times higher absorption of copper in the 500 nm wavelength region in comparison to the near infrared (NIR). In the present contribution we report on the achievement of a 1kW output power at 515 nm suitable for the above mentioned application. This was enabled by highly efficient wavelength and polarization selective grating mirror. This latter is used in Littrow incidence and exhibits diffraction efficiency as high as 99.8% in the -1st diffraction order at a wavelength of 1030 nm. The Yb:YAG disk is pumped with up to 2.7 kW of pump power at 940 nm with a pump spot diameter of 6-7 mm. With a plan HR mirror an output power of 1170W with an optical-optical efficiency of about 60% could be reached. When the grating is inserted into the resonator, as a one to one replacement of the HR mirror, an efficiency of ~ 55% is achieved at the maximum output power of 1050W. The reduction in efficiency results from the additional cavity losses caused by the diffraction grating and by depolarization losses in the disk.

For the second harmonic generation, a 12 mm long LBO crystal was introduced in the laser cavity. A maximum output power of 1045 W at a wavelength of 515 nm could be reached with an optical-optical efficiency of about 40%. The stability of the experimental setup was tested at a pump power level of 2.5 kW over several hours. With this reduced pump power level the system reaches an output power of approx. 930 W at 515 nm, which was constant during the measurement without using a closed loop power control.

9135-13, Session 3

CW Yb-fiber laser with wavelength-variable efficient intracavity frequency doubling in partially coupled enchancement cavity

Sergey Khripunov, Daba Radnatarov, Sergey M. Kobtsev, Aleksey Skorkin, Novosibirsk State Univ. (Russian Federation) and Tekhnoscan-Lab LLC (Russian Federation)

The demonstrated in [1] new approach to intra-cavity frequency doubling of CW fibre lasers is attractive both because it makes possible frequency doubling of relatively broadband radiation and because it features a simplified layout, which does not require an active stabilization enhancement cavity length. The present work has further developed this approach and has also shown for the first time that efficient intra-cavity generation of the second harmonic is still possible when the enhancement cavity is not a 'resonator inside a resonator', but rather only has a certain part shared with the main fibre laser cavity.

In the new proposed layout, the function of the output coupler is performed by an antireflection-coated face of the non-linear crystal used for frequency doubling inside the enhancement cavity. Feedback from the other side of the resonator comes from a mirror-prism combination allowing adjustment of the laser output frequency. The non-linear medium is an LBO crystal with normal working surfaces cut for non-critical phase matching and placed inside the enhancement cavity with a bow-tie geometry.

The following results were obtained with this new configuration: output power maximum of 800 mW at 536 nm when pumped with 6 W at 976 nm; output wavelength tuning range of 521–545 nm with the output power at the edges of this range being 420 and 220 mW respectively. The second-harmonic output beam had a pure TEM00 mode. Spectral width of the fundamental radiation (0.5 nm) did not exceed the phase matching spectral width (1.8 nm) of the non-linear crystal.

Application of partially coupled resonant enhancement cavities opens the possibility to improve the cavity's Q-factor and to simplify the overall laser configuration. This paper also presents details of our experimental study and discusses possible further development of the proposed efficient arrangement for frequency doubling of non-single-frequency CW radiation of fibre laser in enchancement cavity. Additionally, possibilities of automatic wavelength scanning of the second-harmonic radiation within a broad spectral range are also examined.

1. R.Cieslak and W.A.Clarkson, "Internal resonantly enhanced frequency doubling of continuous-wave fiber lasers," Opt. Lett. 36, 1896-1898 (2011).

9135-14, Session 3

High-power CW single-frequency Nd:YVO4/LBO laser quasi-continuously tuneable over a wide frequency range

Daba Radnatarov, Sergey Khripunov, Sergey M. Kobtsev, Vladimir M. Lunin, Novosibirsk State Univ. (Russian Federation) and Tekhnoscan-Lab LLC (Russian Federation)

The present work for the first time reports the development and an experimental implementation of quasi-continuous tuning of a powerful diode-pumped Nd:YVO4/LBO green laser in a broad frequency range. The proposed method allows automatic stitching of consecutive 15-GHz continuous tuning ranges with the precision of the laser output line width (5 MHz), while not relying on a high-precision wavelength meter. Experimentally demonstrated was a 60-GHz-wide quasi-continuous frequency tuning range at the output power and wavelength of 1.4 W and 532 nm, respectively. Earlier on, a similar laser was used to achieve a maximum of 24-GHz tuning range [1].

This publication discusses a ring laser with an intra-cavity etalon actively locked to the output frequency. Continuous laser frequency scanning is done by adjustment of the cavity length with a piezo-actuated cavity mirror. For high-precision joining of adjacent continuous detuning ranges, a reference confocal interferometer is used with FSR = 750 MHz and finesse of 250. A computerised control system stores spectral position of the laser output line with respect to transmission peaks of the reference interferometer and restores it after resetting the positions of the intra-cavity etalon and piezo-actuated mirror. This makes it possible to precisely match the end of a preceding smooth tuning range with the beginning of the next one, thus providing broad hop-free tuning.

The paper additionally touches upon the particulars of the influence of self-suppression of axial mode hopping [2] on the implementation of the proposed method.

The proposed and experimentally demonstrated method of quasi-continuous frequency tuning of a so-called 'single-wavelength' laser in a broad range, not limited by the relatively narrow extent of continuous detuning, opens new opportunities to put these lasers to practical use. Tuning the output laser frequency within a broad region covering tens or even hundreds of GHz, in combination with the possibility of a significantly wider generation spectrum achieved with CW OPO, turns 'single-wavelength' single-frequency solid-state lasers into an incredibly powerful spectroscopy tool featuring high-precision frequency tuning in broad spectral ranges.

1. W.Wang, H.Lu, J.Su, K.Peng. Broadband tunable single-frequency Nd:YVO4 /LBO green laser with high output power. Applied Optics, 52, 2279-2285 (2013).

2. K.I.Martin, W.A.Clarkson, D.C.Hanna. Self-suppression of axial mode hopping by intracavity second-harmonic generation. Optics Letters, 22, 375-377 (1997).

9135-15, Session 3

Linear and nonlinear optical methods for temporal characterization of femtosecond UV pulses

Mohammadhassan Valadan, Davide D'Ambrosio, Felice Gesuele, Raffaele Velotta, Carlo Altucci, Univ. degli Studi di Napoli Federico II (Italy)

A common technique to measure the temporal duration of ultrashort pulses is based on nonlinear processes such as second-harmonic-generation; one of the most used experimental schemes is based on noncollinear autocorrelation. This technique is widely spread in the visible and near infrared while it isn't attractive for the UV frequency range. This is not only due to the lack of suitable nonlinear media; even if some new crystals have been recently synthesized, the resulting second harmonic would be in the vacuum UV (VUV) wavelength range and therefore very hard to be handled in typical optical setups. A viable alternative is Sum-Frequency-Generation or Difference-Frequency-Generation: these parametric processes require an additional auxiliary pulse of comparable and known duration with tunable wavelength. The auto- and cross-correlation techniques can also be based on other nonlinear effects such as Two-Photon Absorption (TPA).

TPA takes place in liquids and bulk materials if the photon energy is larger than half the absorption edge. To utilize this for autocorrelation measurements one has to split the original pulse, and spatially and temporally overlap them in the medium. Both beams individually contribute to a TPA signal whatever their temporal delay, and when superimposed in time they additionally contribute due to the TPA arising by the absorption of one photon from each beam. This additional TPA contribution creates the autocorrelation signal.

Within the nonlinear response of materials to optical fields, TPA can be coupled to SPM and XPM depending on the used pulse intensity. We checked that a pulse intensity window is such that TPA is efficiently occurring whereas XPM and SPM can be substantially neglected. TPA based autocorrelation function has been measured and the information on the pulse duration has been retrieved form the FWHM of the fitted function.

Obviously, rather high peak intensities are required for TPA to occur. This regime is not always available and therefore a characterization of the laser source in a low intensity regime would be interesting too. To perform this kind of experiment TPA is no longer an affordable choice as it would become negligible compared with linear absorption and the signal would be too small to be detected.

For low intensities and for deep UV pulses such as the ones we characterized (260 nm) it is possible to set up an autocorrelator based on a linear optical method: the interferometric autocorrelator. This scheme is a slightly noncollinear interferometer, allowing one to measure the contrast of the interference fringes as a function of the delay between the pulses coming from the two arms. This is a measurement of the pulse coherence time which is strictly related to the pulse length; and for a fully coherent laser pulse the two quantities are equal.

In the saturated regime, experienced when high energy UV pulses are produced, however, one might also suspect a deviation of the generated pulse from the full temporal coherence. It will be interesting to seek for any possible distinction between coherence and pulse duration.

9135-16, Session 4

Ultrafast fiber lasers for mid-infrared frequency combs *(Invited Paper)*

Ingmar Hartl, Deutsches Elektronen-Synchrotron (Germany)

Recently, a number of spectroscopy methods have been developed which utilize the unique properties of frequency comb sources, such as multi-heterodyne spectroscopy or cavity-enhanced comb spectroscopy. There is strong interest to extend those spectroscopy techniques to the molecular fingerprint region, spanning the wavelength range from 3 to 15 μm. Due to the lack of laser materials in this spectral region, frequency conversion techniques must be applied. We report of recent progress in converting highly coherent, stabilized Yb- and Tm-fiber frequency comb sources to the mid-infrared spectral region by methods such as difference frequency generation, synchronously pumped optical parametric oscillators or super-continuum generation in mid-infrared compatible, highly nonlinear fibers.

9135-17, Session 4

Tunable mid-IR parametric conversion system pumped by a high-average-power picosecond Yb:YAG thin-disk laser

Ond?ej Novák, Taisuke Miura, Martin Smrz, Jaroslav Huynh, Patricie Severová, Akira Endo, Tomás Mocek, Institute of Physics of the ASCR, v.v.i. (Czech Republic)

The mid-IR wavelength range has gained increased interest due to its applications in gas sensing, medicine, defense, and others. Optical parametric devices play an important role in the generation of radiation in the mid-IR. Low thermal load of nonlinear crystals promises high average power outputs if powerful pump laser is available. We developed 50-W average power pump laser operating at 100 kHz repetition rate. The pulses of Yb-fiber laser oscillator at 1030-nm wavelength are stretched by a chirped volume Bragg grating (CVBG) from 5 ps to 90 ps and inserted into a cavity of regenerative amplifier with an Yb:YAG thin-disk pumped by a 969-nm wavelength stabilized laser diodes. Pumping of the thin-disk at zero phonon line reduces its thermal load and increases conversion efficiency. We obtained the near diffraction limited beam with power of 52 W before compression. Measured efficiency of CVBG is 88%, which corresponds to the estimated output of 45 W after compression. We are going to increase the average power to 100 W in the near future.

We have proposed a wavelength conversion system generating picosecond pulses tunable between 2 and 3 μm. The seed signal radiation is acquired by the optical parametric generation (OPG) in the first nonlinear crystal. By the OPG the signal and idler pulses are generated. Signal pulse energy is increased in the subsequent optical parametric amplifiers. Each amplification stage consists of the crystal pair in the walk-off compensating arrangement. The wavelength of signal is tunable between 1.6 and 2.1 ?m. The 2.1 -3 ?m tunable source will be the idler beam taken from the last amplification stage. High-average output power in order of tens of watts will be achieved. The KTP, KTA, and RTP crystals are considered for the optical parametric process and its comparison will be given. Numerical studies of thermal effects caused by residual beams absorption will be addressed. The results of preliminary experiments will be presented and discussed. We will discuss the possibilities of increasing the wavelength range in the mid-IR and long-wavelength infrared.

9135-18, Session 4

A DFG-based mid-IR laser system for muounic-hydrogen experiment

Lyubomir I. Stoychev, Istituto Nazionale di Fisica Nucleare (Italy) and The Abdus Salam International Ctr. for Theoretical Physics (Italy); Miltcho B. Danailov, Alexander A. Demidovich, Ivaylo P. Nikolov, Paolo Cinquegrana, Paolo Sigalotti, Elettra-Sincrotrone Trieste S.C.p.A. (Italy); Andrea Vacchi, Istituto Nazionale di Fisica Nucleare (Italy)

The determination of the proton size is among the challenging problems facing fundamental physics. One promising approach is to determine the proton Zemach radius, based on high precision spectroscopy of muonic hydrogen. Measuring the energy difference (3S1 ?1S0) in the muonic hydrogen requires a nanosecond mid-IR laser source tunable around 6785±3 nm, with a linewidth less than 0.07 nm and energy about 0.25 mJ at a repetition rate of 50 Hz (limited by the available muonic hydrogen sources).

A rich variety of NL optics based schemes can be used to generate 6.78 ?m light. There are literature reports of pulse energies reaching and even exceeding the requested 0.25 mJ in the 6.78 ?m range, and others reporting linewidths close to the 0.07 nm requested at this wavelength for the muonic hydrogen experiment. However, a generation of pulses having simultaneously all the parameters needed for the above mentioned experiment has not been demonstrated yet.

In this work, after analysing the specific needs of the muonic hydrogen experiment, and several possible schemes for generating pulses with the requested parameters, we propose and present first experimental results of a very straightforward scheme which to our knowledge has not been considered in the literature and promises to reach all the requested parameters. The scheme is based on direct difference frequency generation (DFG) using a fixed wavelength single-mode Nd:YAG laser and a tunable Cr:forsterite laser pumped by a second Nd:YAG synchronised to the first one. A lamp pumped Q-switched Nd:YAG laser with output energy of 150 mJ is used to pump the Cr:forsterite laser. The latter contains a diffraction grating as an output coupler, allowing to obtain tunable light in the 1.200-1.280 ?m range with an energy per pulse of up to 15 mJ and a line-width of about 8-10 pm. Its pulses are then combined with the pulses at 1.064 ?m of a diode-pumped YAG through a dichroic mirror and sent to the nonlinear crystal in a double pass geometry. The two lasers are triggered through a delay generator allowing to compensate the build-up time of the Cr:forsterite pulse and had a relative timing jitter below 1 ns.

The studies reported here used commercially available LiInS2 crystals. Best results were obtained with two 5 mm long LiInS2 crystals put in sequence where an energy of 80 ?J was generated in a single pass geometry while in double pass scheme the obtained energy was about 60% more (further optimization of the double pass geometry can increase this percentage) without any damage of the crystals bulk and coatings even at prolonged exposures (for all cases the diameters of the pumping beams were 3mm). These results indicate that with an appropriate and quite straightforward scaling of the laser system it is possible to obtain over 2.5 mJ with the commercially available LiInS2 crystals.

9135-19, Session 4

Mid-infrared resonant ablation for selective patterning of thin organic films

Sanjeev Naithani, Univ. Gent (Belgium); Charles Duterte, Multitel A.S.B.L. (Belgium); Marieta Levichkova, Heliatek GmbH (Germany); Arnaud Grisard, Thales Research & Technology (France); David Schaubroeck, imec and University Gent (Belgium); Eric Lallier, Thales Research & Technology (France); Yves Hernandez, Multitel A.S.B.L. (Belgium); Karsten Walzer, Heliatek GmbH (Germany); Geert Van Steenberge, Univ. Gent (Belgium)

The fast growing market of organic electronics, including organic photovoltaics (OPV), stimulates the development of versatile technologies for structuring thin-film materials. Ultraviolet lasers have proven their full potential for patterning single organic layers, but in a multilayer organic device the obtained layer selectivity is limited, since all organic layers show extremely high UV absorption. In this paper we introduce mid-infrared resonant ablation as an alternative approach, in which a short pulse mid-infrared laser can be wavelength tuned to one of the molecular vibrational transitions of the organic material to be ablated. As a result, the technique is selective in respect of processing a diversity of organics, which usually have different infrared absorption bands.

Mid-IR resonant ablation is demonstrated for a variety of organic thin-films, employing both nanosecond (15 ns) and picosecond (250 ps) laser pulses tunable between 3 and 4 microns. The nanosecond experimental set-up is based on a commercial laser at 1064 nm pumping a singly resonant Optical Parametric Oscillator (OPO) built around a Periodically-Poled Lithium Niobate (PPLN) crystal with several Quasi-Phase Matching (QPM) periods, delivering more than 0.3 W of mid-IR power, corresponding to 15 μJ pulses. The picosecond laser set-up is based on a similar architecture, allowing for a direct comparison between both pulse length regimes.

The wavelength of the mid-infrared laser can be tuned to one of the molecular vibrational transitions of the polymer to be ablated. For that reason, the IR absorption spectra of the organic materials used in a typical OPV device were characterized in the wavelength region that can be reached by the laser setups. Focus was on OPV substrate materials, transparent conductive materials, hole transport materials, and absorber materials. The process has been successfully demonstrated for selective thin film patterning, and the influence of the various laser parameters will be discussed.

9135-20, Session 4

Quantum cascade laser tuning by digital micromirror array-controlled external cavity

Pajo Vujkovic-Cvijin, Brian Gregor, Spectral Sciences, Inc. (United States); Alan C. Samuels, Erik S. Roese, U.S. Army Edgewood Chemical Biological Ctr. (United States)

Quantum cascade lasers (QCL) are well-positioned to gain wide acceptance for a broad range of analytical applications, due to their broad tunability in the mid-wave (MWIR) to the long-wave infrared (LWIR) spectral region. In this paper we present an external cavity laser tuning approach based on the use of a digital micromirror array (DMA) spatial light modulator based on MEMS (Micro Electro Mechanical System) technology. The external cavity, containing a plane diffraction grating and a DMA, is coupled to the anti-reflection (AR) coated facet of a QCL gain element by a low-aberration imaging lens. The diffraction grating disperses the output of the QCL gain element across the surface of the DMA, where individually addressable micromirrors reflect the desired wavelength back to the gain element, thereby closing the loop and making the selected wavelength oscillate in the cavity.

The DMA used in our work is a Texas Instruments' (TI) 1024x768 pixel Digital Micromirror Device (DMD), where the original window was replaced by a zinc selenide (ZnSe) IR transparent one. As a part of our previous work on dispersive transform spectrometers in the LWIR, we have developed a unique approach to boost the efficiency of a DMA whose small micromirrors (14μm in the case of the TI DMD) would otherwise make the DMA fairly inefficient in the LWIR. The optical design of our cavity takes into account diffraction on the DMA which is utilized to our advantage to optimize the modulation efficiency.

DMA-based laser tuning is computer-controlled through a high-speed interface by a software package written in LabView. The program makes it possible to tune and lock the laser to any desired wavelength, to scan a spectral region, and to

apply wavelength modulation involving any combination and number of wavelengths. Wavelength calibration was performed by using a high-resolution FTIR spectrometer. AR- coated gain chip produced by AdTech Optics was used, with the manufacturer-estimated tuning range of 50-60 cm-1 around 8.3μm. Our DMA-controlled external cavity laser achieved 48 cm-1 of spectral coverage around the central wavelength of 8.3μm. Having in mind inherent losses on the DMA and other intracavity elements, the 48 cm-1 tuning range indicates strong cavity coupling.

The resulting functionality enables fast (<0.1ms switching time) digitally-controlled, random-access wavelength tuning, high-bandwidth wavelength modulation (~30 kHz modulation rate), and stable wavelength locking of the laser output. All these parameters are highly desirable for majority of spectroscopic sensors based on a LWIR laser source. Additionally, as a benefit of the MEMS DMA technology, our laser contains no moving parts at the macro-scale level, making it mechanically robust and reliable for field use.

With a cavity design that contains several QCL gain elements built into the same cavity (as inspired by our imaging spectrometer designs), it will be possible in the future to cover an extremely wide spectral region with a single laser package. Generally, our fast, wideband, digitally controlled laser tuning technology is also applicable to other tunable lasers including solid-state, diode, gas, and fiber lasers.

9135-21, Session 5

Pulsed kW-peak power and integrated all fiber MOPA single-frequency source at 2050nm

Erik M. Lucas, Keopsys SA (France) and ONERA (France); Guillaume Canat, Laurent Lombard, ONERA (France); Yves Jaouën, Télécom ParisTech (France); Sylvain Bordais, Keopsys SA (France)

High power single-frequency, linearly polarized fiber lasers operating in the first atmospheric transparency window and eyesafe wavelength range of 1.9-2.1 μm are highly desirable for many applications, such as LIDARs or of Optical Parametric Oscillator based on ZGP or GaAs.

If thulium-doped (Tm) fiber laser technology operating in the 1900-2000 nm band is quite mature, there are only few developments in 2000-2100 nm band, especially in the pulsed regime with pulse duration longer than 100ns where the phonons reach steady-state. As the gain by meter of Tm-doped fibers is low in this band, the active fibers need to be longer. It results in a non linearity sensitivity enhancement, particularly stimulated Brillouin scattering (SBS).

Tm-doped fibers accept several absorption bands, thereby there are different available pumping schemes (core pumping at 1550nm, core pumping around 1900nm or clad pumping at 793nm). Each pump scheme has a different population inversion profile along the fiber. We discuss the effects of each pumping scheme on inversion population and efficiency based on a specifically designed simulation tool of fiber amplifier adapted to the pulsed regime.

Using these results we have developed a three stages, linearly polarized, single frequency, master oscillator power fiber amplifier (MOPFA) emitting pulses at 2050nm. SBS threshold is related to the core area of the fiber. As the peak power increased in the different stages, the fibers core areas increased to enhance SBS threshold; the first stage was performed with a 6/130μm fiber for a SBS threshold around 20 W, the second with a 10/130μm fiber for a SBS threshold around 50 W and the third with a 25/400μm fiber for a SBS threshold around 500 W. The SBS threshold of the third stage increased with a particular strain distribution which permitted to gain at least 3 dB on the first SBS threshold. An inconstant strain along the fiber increase the Brillouin gain bandwidth and decrease the Brillouin gain amplitude. Up to 1 kW-peak power of linearly polarized, has been achieved using this MOPFA source.

The total signal gain of up to 55 dB and the maximum average output power of over 33 dBm were demonstrated with a M? = 1.2 and a polarisation extinction ratio > 20 dB. For 20 kHz repetition rate, 110 ns pulses with the energy of 115 uJ were achieved which correspond to 1 kW peak-power. To our knowledge, it is the highest peak power, single frequency beyond 2 μm, pulsed source in Tm-silica fiber to date.

9135-22, Session 5

Fibre laser component technology for 2-micron laser systems

Gary Stevens, Gooch & Housego (Torquay) Ltd. (United Kingdom)

We report on recent developments in fibre laser component technology for use in 2-micron laser systems. A range of 'building block' components have been built to allow novel fibre laser architectures that exploit the advantages of fibre lasers based on Thulium and Holmium.

Fibre lasers operating around 2-microns are becoming widely used in an increasing number of applications, which is driving the need for components that can operate reliably at high powers and also integrate easily with other components. To that end, we have designed and built a range of fused fibre, acousto-optic and magneto-optic devices, that can be readily integrated into a range of novel fibre laser systems.

Research has been carried out into improving fused fibre technology for components operating at 2um wavelengths. This has included testing adhesives and packaging designs to fabricate components specifically suited for use at 2 microns. New manufacturing methods have also led to the development of side coupled feed through combiners with signal losses as low as 0.02dB. Also, high power end-coupled pump couplers have been tested up to a kW at 793nm in 2 micron fibre laser systems and have proven to me reliable. Alongside pump couplers a range of taps, splitters and WDMs have been developed which allows for the implementation of a variety of laser architectures and can provide added functionality to a system.

A range of isolator materials have been tested to find materials with suitably high Verdet constant and low absorption. Several potential material have been identified and integrated into fibre-in, fibre-out (FIFO) and fibre-in, beam out (FIBO) isolators. These isolators have been tested and demonstrate low insertion losses and high isolation (>30dB).

New cell designs and materials for Acousto-Optic devices have been researched, which has led to the development of fibre-coupled Acousto-Optic Modulators (AOM) and allows for the realisation of all fibre Thulium and Holmium Q-switched and pulsed fibre lasers. Novel Acousto-Optic Tunable Filters (AOTF) designs have been realised to produce narrow resolution AOTFs and zero-shift AOTFs.

Finally we present results from a variety of laser architectures that demonstrate the flexibility of these 'building block' components and the increasing maturity of 2-micron fibre laser technology. These include an all fibre Q-switched Thulium laser and a tunable Thulium fibre laser which uses an AOTF as an intra-cavity wavelength selector.

9135-23, Session 5

Devices and pumping architecutes for 2 ?m high-power fiber lasers

Andrea Braglia, Politecnico di Torino (Italy) and OPI Photonics (Italy); Alessio Califano, Yu Liu, Massimo Olivero, Guido Perrone, Renato Orta, Politecnico di Torino (Italy)

Thulium-doped fiber lasers are gaining in popularity since they emit at about 2 ?m, a wavelength particularly interesting for many industrial, sensing and medical applications, and, moreover, in the so-called "eye-safe" spectral region. Despite the many advantages, however, the diffusion of thulium-doped fiber lasers with power emissions high enough to allow practical applications is still hampered by the limited availability of

specific components for such lasers and by the cost of the system, which is mainly dominated by the cost of high power pump diodes. The paper proposes alternative paths to high power emission at about 2 ?m by exploring two complementary approaches, namely the development of high power pump combiners to couple the emission of several multimode pump diodes with the active fiber, and the investigation of new pumping schemes that take advantage of rare earth co-doping in which the emission of a first ion is used to pump the thulium ions. Particularly interesting is the ytterbium-thulium (Yb-Tm) co-doping since it allows exploiting the large power delivered by ytterbium-doped fiber laser. The paper first describes the fabrication and characterization of fused fiber combiners with 7 to 39 input ports for end-pumping of thulium-doped active fibers. Typically, high power Tm-doped fiber laser modules are built using silicate double cladding fibers, pumped in the inner cladding with multimode diodes emitting at wavelengths slightly shorter than 800 nm, which is where the Tm exhibits an intense absorption peak. This solution, however, requires combiners with a large number of input ports because of the not so high efficiency of Tm-doped active materials and the power emitted by the pump diodes (at least in comparison with the pump diodes for high power Yb-doped lasers). Hence the detailed study on the possible rare earth combinations to implement an indirect pumping of thulium ions, and specifically of Yb-Tm co-doping, to take advantage of pump diodes with higher output power and, moreover, with a better cost per emitted watt.

Finally, the paper reports on the preliminary experimental results obtained by combining both approaches. The output of Yb-doped fiber laser is connected to a Tm-doped laser cavity through an ad-hoc combiner that protects from unwanted back-propagating signals and adapts the output of the Yb-doped fiber laser to fill the inner cladding of the Tm-doped active fiber. The Yb lasers is made out of a 20/400 Yb-doped double cladding silicate fiber, while the Tm-doped fiber laser uses a 25/250 double cladding silicate fiber. The Yb-doped laser acting as the pump for Tm-doped laser is capable of emitting about 400 W of power, although in the preliminary tests of the Tm-doped laser it has been limited to around 100 W for heath dissipation problems in both fibers, obtaining about 30 W of output power from the Tm-doped fiber. These results demonstrates that the proposed approach can potentially lead to the development of lasers with power levels suitable for industrial applications, although the setup need further optimization, especially to improve the efficiency.

9135-24, Session 5

Pulsed operation of Tm-doped fiber lasers using piezoelectric-driven microbend applied to elliptical coating fibers

Hajime Sakata, Kenta Kimpara, Kento Komori, Masahiro Tomiki, Shizuoka Univ. (Japan)

We report Q-switched pulse generation in thulium-doped fiber (TDF) lasers by using piezoelectric actuators (PAs) to control the intra-resonator loss. A dynamic microbend caused by the PAs is induced into an elliptical coating fiber (ESF) in a fiber ring resonator. The ESF was fabricated by pressing the acrylic coating of single-mode fibers in an oven. Compared with the untreated circular fiber having a diameter of 240 ?m, the ESF was flattened to have a major width of about 300 ?m. We employed a pair of comb-like plates (CLPs) attached on the PAs in order to bend the ESF from both sides. The output pulse power is improved by tuning the duty-ratio and spatial period of the CLPs, so that the ESF is easily bent and the propagation mode is efficiently coupled to radiation modes around ? = 1.9 μm. The TDF used was a single-clad, single-mode fiber having a core diameter of 9 ?m and a length of 1.5 m. The TDF is pumped by a pigtailed InGaAsP laser diode emitting a wavelength of 1.63 ?m to make use of a pulsed pumping technique as well as to reduce a quantum defect between the pumping and the lasing transitions. The pump light is introduced to the fiber ring resonator via the wavelength division multiplexing coupler. The emission spectra were measured with a combination of a monochromator and a PbS photodetector. The resultant spectra showed that the center oscillation wavelength was typically 1.92 μm. When the pump power was increased to 156 mW, the output pulse showed a peak power of 42.5 W with a pulse width of 1.06 ?s. We expect that the in-fiber Q-switching technique will provide simple laser systems for environmental sensing and medical applications.

9135-25, Session 5

A comparitive study of the fluorescence lifetime of common Tm doped crystals

Jakub W. Szela, Stephen J. Beecher, Jacob I. Mackenzie, Univ. of Southampton (United Kingdom)

Solid state lasers emitting in the 2 μm spectral region are of great interest for medical, scientific and defence applications due to the presence of strong water absorption lines and an increased retinal damage threshold making these lasers ‘eye-safe’. Thulium doped solid state lasers provide a highly efficient method of converting pump light from well established laser diodes at ~800 nm to high brightness output at ~2 μm due to the cross-relaxation process between the 3H4 manifold and the 3H6 manifold, potentially yielding two ions in the 3F4 manifold for every one ion excited into the 3H4 manifold. Here we present an extensive collection of 3F4 fluorescence lifetimes to allow laser engineers to assess the suitability of a gain medium for their chosen application.

Overlap between the emission and absorption cross-sections of an ion can lead to re-absorption of fluorescence, which can in turn be re-emitted, increasing the perceived lifetime. Here we have utilised the ‘pinhole technique’ to mitigate the effects of re-absorption and emission. Pulsed light from a 1.2 W 790 nm laser diode is focussed to a 1.6 mm radius spot on the sample facet; a range of pinholes with diameters between 1.0 and 2.4 mm are used. The host crystals investigated are YAlO3 (YAP), Y3Al5O12 (YAG), YLiF4 (YLF) and KY(WO4)2 (KYW). Lifetimes for Tm concentrations of 1.5, 2.0, 3.0 and 4.0 at.% are measured for YAP, 4.0 and 5.0 at.% for YAG, 2.0, 4.0, 6.0 and 8.0 at.% for YLF and 5.0 at.% for KYW. Concentration quenching is found to strongly affect the lifetime of the 3F4 level in YLF, with lifetimes decreasing from 12 ms at 2 at.% Tm to 9 ms for 4 at.%. YAP however, displays far less lifetime quenching, with 3F4 lifetimes decreasing from 4.3 to 4.1 ms over the same concentration range. YAG displays some lifetime reduction, decreasing from 8.4 to 6.4 ms for 4.0 to 6.0 at.% respectively.

We believe this work to be the most comprehensive study of fluorescence lifetimes in Tm doped crystals to date and provides a useful tool for laser designers.

9135-26, Session 6

Theoretical and experimental studies of ultra-short pulsed laser drilling of steel *(Invited Paper)*

Andreas Michalowski, Robert Bosch GmbH (Germany); Yuan Qin, Nanjing Univ. of Science and Technology (China); Rudolf Weber, Thomas Graf, Univ. Stuttgart (Germany)

The production of small holes with high quality and high aspect ratios in metals with ultra-short laser-pulses gains importance because of the flexibility and quality which are achievable. The creation of a capillary by irradiating the work piece with laser light of high intensity is accompanied by strong local heating, melting and partial vaporization of the material.

Theoretical studies of light absorption inside the bore as well as experimental studies of material transport and ejection mechanisms are presented. Preconditions for the applicability of simple geometrical ray-tracing to describe the absorption inside the hole are discussed theoretically. To examine the applicability of the ray-tracing method, the total absorptance and the absorbed intensity of polarized beams is studied

in several capillary geometries. The ray-tracing results are compared with more sophisticated simulations based on the numerical solution of the Maxwell-equations.

The material transport inside the bore-hole shows significant differences regarding to the drilling strategy which helps to explain the quality advantages of helical drilling. Even though the finished bore-hole shows no burr or deposits of solidified melt, a significant amount of melt is generated during the drilling process if high laser fluence is used. In the frame of this contribution, the drilling strategies percussion drilling and helical drilling are compared in terms of melt transport and burr formation using different diagnostic methods.

Finally an optical concept suitable for high-quality laser-drilling is briefly explained and state-of-the-art laser drills are shown.

9135-27, Session 6

On the applicability of arbitrarily shaped nanosecond laser pulses for high quality high efficiency micromachining

Sasia Eiselen, BLZ Bayerisches Laserzentrum GmbH (Germany) and Friedrich-Alexander-Univ. Erlangen-Nürnberg (Germany); Sebastian Riedel, BLZ Bayerisches Laserzentrum GmbH (Germany); Michael Schmidt, BLZ Bayerisches Laserzentrum GmbH (Germany) and Friedrich-Alexander-Univ. Erlangen-Nürnberg (Germany)

Progressive developments in temporal shaping of short laser pulses offer entirely new approaches at influence and investigate laser-matter-interactions. Commonly used parameters for describing the behavior of short or ultra-short pulses or pulse trains are fluence and intensity. However, fluence does not imply any information about the temporal behavior of energy input during specific pulse duration ? while using the pulse intensity as describing parameter is more meaningful. Nevertheless it still is an averaging over pulse duration and no change in intensity can be determined if the temporal pulse shape changes within a certain combination of pulse duration and pulse energy.

Using a flexible programmable MOPA fiber laser experimental studies on the impact of temporal energy distribution within one single laser pulse in micro structuring applications were therefore carried out. With this laser source a direct modulation of the temporal pulse shape in the nanosecond regime can easily be controlled. Experiments were carried out with moved as well as with un-moved beam resulting in areas and dimples respectively drilling holes. The presented results clearly show that any averaging over pulse duration results in missing information about time-dependent interactions but can in the same time lead to significant differences in ablation results. Thus, resulting surface roughness Sa can be decreased up to 35 % when changing the pulse shape at constant parameters of fluence and pulse peak power at a pulse duration of 30 ns. It can be observed that the combination of an intensity peak and a lower edge within one pulse can lead to increasing ablation efficiency as well as higher ablation quality compared to the commonly used Gaussian-like temporal pulse shape.

9135-28, Session 6

Combination of thermal extrusion printing and ultrafast laser fabrication for manufacturing of 3D composite material scaffolds

Evaldas Balciunas, Laurynas Lukosevicius, Dovile Mackeviciute, Sima Rek?tyte, Vygandas Rutkunas, Vilnius Univ. (Lithuania); Domas Paipulas, Karolina Stankevi?i?t?, Vilnius University (Lithuania); Daiva Baltriukien?, Virginija Bukelskiene, Algis S. Piskarskas, Mangirdas Malinauskas, Vilnius Univ. (Lithuania)

We present a novel method for manufacturing of 3D composite material microstructured scaffolds for cell studies and tissue engineering applications. A thermal extrusion (fused deposition modeling) 3D printer is known to be a simple and low cost table-top device enabling rapid materialization of CAD models out of plastics. Here, “Ultimaker Original” (“Ultimaker, BV”) is employed to produce a centimeter scale (up to few cm) micro-porous (pore size down to < 100 um) scaffold out of biocompatible PLA (poly-lactic acid) material. Such structure can serve as a three-dimensional substrate for cell growth or a biodegradable implant. Ultrafast lasers empower direct structuring in 3D with high spatial resolution and feature definition [1]. In order to take advantage of both techniques, the fabricated object is subsequently immersed inside another polymer bath and direct laser writing (“FemtoLAB” setup by “Altechna R&D, Ltd” employing fs laser “Pharos” by “Light Conversion, Ltd”) is used to refine its inner microstructure by fabricating a fine mesh inside the previously produced scaffold. Femtosecond (< 1 ps pulse width) high repetition (> 100 kHz) light pulses enables processing of photopolymers as well as other photo- or thermally cross-linkable materials (for instance non-photosensitized PDMS, SZ2080 and others) [2]. Thus, the same PLA, another biodegradable polymer PEG-DA (poly-ethylen glycol diacrylate, Mn 258) or hybrid materials like ORMOSILs (SZ2080, IESL-FORTH) and ORMOCERs (Microresist, GmbH) can be applied for the laser lithography. After the wet developing procedure, a composite substance scaffold of distinct periodicities is revealed. Another approach to modify the surface of 3D-printed PLA is presented as well - ablation by femtosecond laser pulses. Such dual-scale (macro-micro) structure’s ingredient material pore sizes and overall porosity as well as geometry can be flexibly tuned by changing 3D printing and laser fabrication parameters or a computer model itself. Investigation of cell proliferation and tissue formation on such artificial scaffold (in vitro) and implantation (in vivo) experiments are currently in progress.

To our best knowledge, this is the first experimental demonstration showing the creation of three-dimensional composite material and discrepant pore size scaffold. Such combination of two emerging additive manufacturing techniques, the 3D thermal extrusion printing and direct laser writing in negative tone photopolymers, enables rapid fabrication of diverse functional micro-featured and integrated devices. In case of larger structures or complex shaped substrates are demanded for practice, the introduced method dramatically increases the fabrication throughput. Thus it saves exploitation time of costly ultrafast laser setup by replacing it with low cost 3D printing equipment. It is believed, that in the very near future the proposed approach will find numerous applications in the fields of biomedicine, microfluidics, micromechanics, integrated microoptics and photonics, as well as interdisciplinary practice of before-mentioned.

[1] M. Malinauskas et al., Ultrafast-laser micro/nano-structuring of photopolymers: a decade of advances, Phys. Rep., http://dx.doi.org/10.1016/j.physrep.2013.07.005 (2013).

[2] S. Rek?tyt? et al., Three-dimensional laser micro-sculpturing of silicone: towards bio-compatible scaffolds, Opt. Express, 21, 17028 (2013).

9135-29, Session 6

Near-field-enhanced, off-resonant laser sintering for additive manufacturing of semiconductor particles and the fabrication of dispersed Au-ZnO-micro/nano hybrid structures

Marcus Lau, Ralf Gregor Niemann, Mathias Bartsch, Univ. Duisburg-Essen (Germany); William O’Neil, Univ. of Cambridge (United Kingdom); Stephan Barcikowski, Univ. Duisburg-Essen (Germany)

Laser sintering of ceramics is known to produce unique 2D and 3D geometries made of metals, insulators, or ceramics [1-4]. But production usually takes long time. We show

that laser process windows can be enhanced and sintering thresholds decrease when gold nanoparticles are attached to the sintering target material. For this we used laser-generated gold nanoparticles adsorbed on zinc oxide microparticles. Examination of gold nanoparticle amount attached to zinc oxide microparticles, scanning speed and laser power gave a coherent picture of gold-enhanced laser sintering. From this we carried out conclusions about mechanism of enhancement. Here off-resonant near-field enhancement of gold nanoparticles might be responsible for the widening of laser process windows [5, 6]. Beside the enhancement in manufacturing, we found laser fabricated micro/nano hybrid ultra-structures [7]. Cross-sectioning of the unsintered and sintered particles via cutting by a focused ion beam showed that after laser treatment gold nanoparticles are embedded into the zinc oxide carrier particles. Therefore not only sintering process window widens by supporting microparticles with gold nanoparticles but also hybrid ultra-structures are fabricated. This might be of particular interest for a variety of applications since semiconductor properties are joint with optical and electrical properties of gold nanoparticles. Due to the received results we carried out conclusions about the mechanism. We assume that off-resonant near-field enhancement is responsible for heat transfer to the carrier material, resulting in a meltdown of the material and subsequent re-solidification leaving the sintered micro/nano hybrid material.

[1] S. Hong, J. Yeo, G. Kim, D. Kim, H. Lee, J. Kwon, H. Lee, P. Lee, S. Ko, Nonvacuum, Maskless Fabrication of a Flexible Metal Grid Transparent Conductor by Low-Temperature Selective Laser Sintering of Nanoparticle Ink, ACS Nano, 2013, 7, 5024-5031

[2] M. Agarwala, D. Bourell, J. Beaman, H. Marcus, J. Barlow, Direct selective laser sintering of metals, Rapid Prototyping Journal, 1995, 1, 26–36

[3] N. Tolochko, Y. Khlopkov, S. Mozzharov, M. Ignatiev, T. Laoui, V. Titov, Absorptance of powder materials suitable for laser sintering, Rapid Prototyping Journal, 2000, 6, 155-160

[4] S. Dudziak, M. Gieseke, H. Haferkamp, S. Barcikowski, D. Kracht, Functionality of Laser-Sintered Shape Memory Micro-Actuators, Physics Procedia, 2010, 5, 607-615

[5] É. Boulais, R. Lachaine, M. Meunier, Plasma Mediated off-Resonance Plasmonic Enhanced Ultrafast Laser-Induced Nanocavitation, Nano Lett., 2012, 12, 4763-4769

[6] N. Crespo-Monteiro, N. Destouches, L. Saviot, S. Reynuad, T. Epicier, E. Gamet, L. Bios, A. Boukenter, One-Step Microstructuring of TiO2 and Ag-TiO2 Films by Continuous Wave Laser Processing in the UV and Visible Ranges, J. Phys. Chem. C, 2012, 116, 26857-26864

[7] M. Lau, R. G. Niemann, M. Bartsch, W. O'Neill, S. Barcikowski, Near-field-enhanced, off-resonant laser sintering of semiconductor particles for additive manufacturing of dispersed Au–ZnO-micro/nano hybrid structures, DOI 10.1007/s00339-014-8270-1

9135-30, Session 6

A brief analysis on pulse front tilt in simultaneous spatial and temporal focusing

Site Zhang, Frank Wyrowski, Robert Kammel, Stefan Nolte, Friedrich-Schiller-Univ. Jena (Germany)

The spatial and temporal behavior of ultrashort pulses has drawn more and more attention. Especially in laser material processing, such spatio-temporal behavior has significant influences. In this paper we present a brief analysis on the pulse front tilt (PFT) in simultaneous spatial and temporal focusing (SSTF) mathematically and in simulations. We apply paraxial field tracing based on the Collins integral for modeling the spatio-temporal focusing process. Using the shift theorem of the Fourier transformation, we present an explanation of the PFT in focus for general input pulses. Next, by assuming a Gaussian lateral pulse shape, an analytical solution for the field distribution at any position in the region is obtained. In this work we take the influence of an initial PFT before focusing into considerations as well and find potential way to control the PFT during the focusing process. We are able to see the influence of the initial PFT and chirp on the pulse behavior during the focusing process in an analytical form. Finally with the optical modeling software VirtualLab we present rigorous simulations of the SSTF to verify our mathematical conclusions.

9135-31, Session 7

Laser-induced forward transfer of silver nanowires networks

Teppei Araki, Osaka Univ. (Japan); Rajesh Mandamparambil, Holst Ctr. (Netherlands) and Technische Univ. Eindhoven (Netherlands); Iryna Yakimets, Jeroen van den Brand, Holst Ctr. (Netherlands); Jinting Jiu, Katsuaki Suganuma, Osaka Univ. (Japan)

Silver nanowires (AgNWs) have got much attention as promising materials for transparent flexible or stretchable electrodes. In recent years research and development on AgNWs have been focused on achieving relatively higher conductivity and solution process compatibility. With the conventional techniques for patterned transfer of AgNWs, it is difficult to envision new flexible design for application in stretchable electronics such as for wearable medical sensors. In order to increase the design freedom and decrease of the material usage maskless additive process is an attractive option. Inkjet printing is a potential technique, however, clogging of nozzle due to long nanowires can cause process reliability issues. Laser induced forward transfer (LIFT) is one of the promising alternative techniques to realize digital additive manufacturing not only for maskless patterned depostion but also for repairing and 3D stacking. Here we report successful additive patterned deposition of AgNWs networks on a polyurethane (PU) substrate by using LIFT. The AgNWs networks are fabricated on a quartz substrate with a dynamic release layer (DRL) by drop casting AgNWs solution air-dried and followed by deposition of a transparent resin. The AgNWs network is illuminated from quartz side and is transferred on to the PU substrate. The DRL absorbs the laser energy and gets ablated enabling the AgNWs transfer onto the substrate. The electrical resistance is measured after the transfer process and is found to be 10^-4 ?cm. The typical dimension of the tracks is in the order of several millimeter long and are fabricated by stacking transferred AgNWs networks. By stitching the transferred spots conductive tracks are fabricated. Stretching experiments are carried out to quantify the electrical resistance of the transferred tracks and found to have stable resistance during cyclic measurement. LEDs are integrated on the stretchable PU substrate with transferred AgNW tracks showing the feasibility of the process.

9135-32, Session 7

Application of lower aliphatic alcohols as reducing agents for increasing efficiency of the LCLD process

Dmitriy V. Semenok, Saint-Petersburg State Univ. (Russian Federation)

At present, development of a single-stage method of application the metal conductors during the printed-circuit boards (PCBs, MPCBs) production without masking plate is one of the acutest tasks for the microelectronics manufacturers in the Pacific Rim.

The use of laser processing technologies has already lead to development of commercial samples of laser beam machines (LPKF ProtoLaser S, U3) applying by chasing method the necessary electric circuits of copper conductors on the glass-fiber laminate of the PC board. Besides, there is a number of laser processing technologies at the prototyping stage, their industrial implementation being awaited in the current decade. In particular, this is metal-organic chemical vapour deposition (MOCVD) [1] method using thermal breakdown of metallo-

organics compounds, laser-induced forward transfer (LIFT) [2] method consisting of induced transfer of substance under the action of shock wave and laser-induced chemical liquid-phase deposition (LCLD) [3] method consisting of laser-induced deposition of metals from salt solutions. This paper is mainly focused on the LCLD method as the one with a number of valuable processing features. The process is performed at room temperature and atmospheric pressure and requires little chemical solution (1 ÷ 2 ml). LCLD uses budget-priced diode lasers (power: 1 ÷ 5 W) of visible range.

This paper has dealt with the formation mechanism of nanosized metal coatings on dielectrics; the coatings were produced using LCLD process. The main idea of laser-induced metal deposition from solution consists of implementation, using the focused laser beam, of chemical micro-reactor where redox reaction would be initiated due to heating of the reaction environment. Due to heating of the metallization solution and development of active catalytic centres on the dielectric substrate, deposition of metal occurs only in the local radiation zone. The composition of the solution (metal salt, reducer, surfactant, activating agent) is the key factor pre-configuring the deposition result. Our experiments of laser deposition on oxide glass, pyroceramics (sitall) and Al2O3-ceramics lead to production of the patented [4] solutions compositions demonstrating high technical and economic figures.

DPSS laser (532 nm) was used in the deposition experiments. The laser power varied from 500 to 1500 mW with the single scanning rate up to 60 ?m/s. The deposited copper structures were studied by the scanning electronic microscopy methods and EDX.

References:

1. Fujimoto E., Sumiya M., Ohnishi T., Lippmaa M. Development of a new laser heating system for thin film growth by chemical vapor deposition //Review of Scientific Instruments – 2012. –V.89. – 9.

2. Pique A., Auyeung R.C.Y., Kim H., Metkus K.M., Mathews S.A. Digital Microfabrication by Laser Decal Transfer // J. Laser Micro/Nanoeng. – 2008. – V. 3. – P. 163 – 169.

3. Kochemirovsky V. A. et al. Laser-induced chemical liquid phase deposition of metals: chemical reactions in solution and activation of dielectric surfaces//Russian Chemical Reviews – 2011. – 9. – 80.

4. Kochemirovsky V. A. et al. Method for laser deposition of copper on dielectric surface // Patent RU2466515C1 (2012).

9135-33, Session 7

Laser processing of thin films for industrial packaging

Michele Sozzi, Univ. degli Studi di Parma (Italy); Adrian H. Lutey, Univ. degli Studi di Bologna (Italy); Annamaria Cucinotta, Stefano Selleri, Univ. degli Studi di Parma (Italy); Pier Gabriele Molari, Univ. degli Studi di Bologna (Italy)

The application of laser based systems for processing, and cutting, of single and multi-layer thin films materials presents a wealth of opportunity for high quality and cost effective product wrapping. This of course introduces a level of physical complexity, previously unseen for the traditional mechanical systems. Thus understanding the thermal behavior of single and composite metallic and plastic materials is fundamental in order to better exploit laser technology in this field.

In this work mono layer thin films materials, as aluminum, polyethylene, polypropylene, and their multi-layer combinations, comprising also aluminum paper material, have been exposed to different laser radiation.

A wide number of samples have been processed with 10 – 12.5 ns, IR and Green, and 500 – 800 ps, IR, laser radiation, at different translating speeds ranging from 50 to 200 mm/s.

High quality incision have been obtained for all the tested materials, within proper experimental conditions. Ablation thresholds have been found to be function of the temporal pulse width. Aluminum threshold have been found to be 20% lower in the picosecond regime compared to the one in the nanosecond regime. Polyethylene and polypropylene films have been processed and completely cut with picosecond laser and relatively low fluences. The efficient processing of multilayer materials was basically subjected to the thickness of the aluminum layer. For these films the removal of non metallic materials layers was governed by the heat conduction from the metallic layer. The use of Green, nanosecond, radiation resulted to be the most efficient way to process multi-layer materials.

The presented results provide the necessary parameters for an efficient cut and processing of the tested materials, for the employment of pulsed laser sources in the packaging industry, allowing the laser to prevail in lieu of more costly and energy intensive methods.

9135-34, Session 7

Application of laser welding for RF and DC connectors

Srinivasulu Sakaram, M. P. Gondalia, J. K. Baria, Space Applications Ctr. (India)

Laser welding of RF connectors & DC feedthru finds potential applications in military and space where environmental conditions require an extremely rugged and reliable weld joint. Present paper is focused on the application of Nd:YAG laser with 1064 nm wavelength for welding of RF & DC connectors with Al6061 and characterisation of weld joint interms of environmental, mechanical & RF leakage tests for possible use in space hardware.

The technological approach involves application of laser beam welding technique to hermetically seal laser weldable RF connector and DC feedthru with Al6061 alloy. Better control on laser welding machine parameters such as pulse to pulse overlap, beam energy helps in the realization of a weld joint with leak rate levels<1x10-7 cc/Sec He. Being low heat affected zone(HAZ), it produces a metallurgical fusion weld in a small localized area at the interface. This development eliminates the mandatory need of Gold plating inside connector holes and use of mechanical fasteners.

The Laser welding system with Nd-YAG laser has been used. The system comprises of Laser power supply, Glove box and a drier unit integrated with necessary electrical and electronic interfacing. Features of Glove box housing includes stage assembly for sample mounting with spring loaded mechanism, provision for Fibre Optic Beam delivery at the work piece and provision for soot sucker among others. The Glove box is continuously purged with High purity 99.999% inert Argon gas also called as carrier gas in order to ensure the controlled environmental conditions of moisture and oxygen ppm levels suitable for laser welding. The samples were prepared with machined surface and were firmly fixed using an in-house developed fixture to prevent relative movement. Weld surface cleaning of Aluminium alloys was performed using a soft tissue brush, followed by Iso Propyl (IP) Alcohol solvent cleaning to remove contamination.

Using optimized laser weld parameters, welding of RF connectors and DC feedthru with Al 6061 flange have been completed. Leak rate of <1x10-7 Std CC/Sec Helium has been demonstrated successfully using sniff leak test method for all the seven samples which indicates good process repeatability.

The laser weld joint has withstood Environmental tests namely Thermal shock +180 C to -70C with dwell time of 10 min for each extreme for total of 500 cycles and Sine & Random Vibration tests and passed the post environ leak tests which is in conformance with MIL-STD-883 requirements. The Mechanical load test on the weld joint showed no failure even at 23.2 Kgf which indicates the robustness of the joint. The microsectioning of the joint indicates the depth of penetration of approximately 287 microns for the optimized laser energy levels. Further the radiography analysis has been carried out which indicates crack free and uniform weld joint.

RF leakage test characterisation of weld joint has been carried out using RS103 test at 5V/m field as per MIL-STD-461/462. The pickup level < 90 dBm was observed from L band to Ku band

range which is generally acceptable specification for low power RF units. Test results are presented.

9135-35, Session 8

Process optimization of LIFT through visualization: towards high resolution metal circuit printing

Merijn P. Giesbers, Holst Ctr. (Netherlands); M. B. Hoppenbrouwers, TNO (Netherlands); Edsger C. P. Smits, Rajesh Mandamparambil, Holst Ctr. (Netherlands)

Laser induced forward transfer (LIFT) is a freeform, additive patterning technique used to deposit high resolution structures from a transparent carrier substrate, with a metal film donor. A laser pulse is used to generate small droplets from the donor material, defined by the spot size and energy of the pulse. Metallic as well as non-metallic materials can be patterned using this method. Being a contactless, additive, digital and high resolution patterning technique, this method enables fabrication of multi-layer circuits, enabling bridge printing, thereby decreasing component spacing. These results show that LIFT is a promising technology that is rapidly developing into a mature manufacturing process.

Here we demonstrate copper droplet formation from a thin film donor. The investigation of the LIFT process is done by shadowgraphy, providing detailed information about the droplet formation. The influence of laser fluence on the formation of droplets is discussed along with a statistical evaluation. A temperature model is used to understand the optimal thickness of the donor film for a reliable transfer process. A detailed angle deviation analysis of the copper droplets during flight is carried out. Optimal settings and donor layer thickness for a reproducible angle of departure are discussed. Furthermore the effect of spacing between donor and receiving substrate on droplet formation is shown, as well as single droplet regimes. This enables industrialization of the process for continuous high resolution (<8?m) conductive lines.

9135-36, Session 8

Metallic coatings obtained by pulsed-laser deposition through a dynamic prism system

Ferran Cambronero-López, Univ. de Santiago de Compostela (Spain); Francisco Rey-García, Spanish National Research Council (Spain); Carmen Bao-Varela, Univ. de Santiago de Compostela (Spain); Germán F. De La Fuente Leis, Spanish National Research Council (Spain); Luis Carlos Estepa, Spanish National Research Council (CSIC)-ICMA (Spain)

The study of the modification and functionalization of materials surface plays an important role in the science materials field. The properties of a high amount of materials have been improved modifying their surfaces. Through a wide range of technologies, a large list of glass, ceramic, polymeric or metallic materials have seen enhanced their durability, strength, hygroscopic, anticorrosive, antibacterial, aesthetic, optical or magnetic properties, amongst other characteristics [1-3]. Pulsed laser deposition (PLD) is a term used for a number of technical variants which refer to the general method of irradiating a target with a laser, generally in vacuum, in order to evaporate its solid components onto a substrate [2]. The scientific literature reports an ample variety of geometrical configurations for PLD processes in order to obtain metallic coatings onto a wide range of substrates [3].

This work presents PLD process based in a dynamic prisms system configuration where the laser beam of a nanosecond pulsed Nd:YVO4 laser (Powerline E, Rofin) emitting at a wavelength of 1064 nm is carried through a couple of prism to a metal target placed onto a vacuum chamber. The second prism is located onto a micrometric platform that allows the displacement of the laser beam along the metal target surface. To develop this technique, metal targets of aluminium and brass were irradiated at high vacuum conditions in order to coat commercial glass substrates parallel placed at defined distance.

The surface microstructure of the films obtained by this mobile prism configuration has been characterized by optical (Nikon MM400) and scanning electron microscopy (SEM). The thickness of the coatings was determined by a compact spectrometer (StellarNet Inc., STE-BW-VIS) provided with commercial available software for the measure of thin films (TFCompanion; SemiconSoft Inc.). Finally, the electrical properties were studied in order to test their application on optoelectronic devices.

9135-37, Session 8

Compensation of low order aberrations with reflective beam shaping system

Wenguang Liu, Qiong Zhou, Dianyu Gu, Zongfu Jiang, National Univ. of Defense Technology (China)

Compensation of low-order aberrations is essential for high power conduction cooled end-pumped slab (CCEPS) laser with high beam quality. With the increase of output power, the peak-to-valley of wave front distortion increase to tens of micrometer, And it's difficult to control the wave front with deformable mirrors which always has limited stroke(<20?m). In this paper, an reflective beam shaping system are designed to shaping the rectangular beam spot to squarer beam spot. The beam shaping system is consisted with two cylindrical mirror and one spherical mirror, all the mirrors are commercial available. And at the same time the beam shaping system can be applied to compensate the low order aberrations in CCEPS with low cost. Simulations of PID control algorithm for actively compensation of low-order aberrations with reflective beam shaping system are presented. It shows that different combinations of defocus, 0 degree astigmatism, 45 degree astigmatism, which is the main contribution of beam aberrations in CCEPS, can be well compensated by variation of distance and rotation angle of mirrors. And the convergence is fast when the control target function is set to a suitable combination of low order Zernike coefficients. For beam with wave aberrations (PV=88?, RMS=18?,Z4=27.Z5=23.Z6=35), the change of distance between mirrors is below 100mm, and the rotation angle about Z axis is below 3 degree, and the wave front distortion are decreased to a low level (PV=0.164?, RMS=0.158?) which can be easily corrected later with DM.

9135-38, Session 8

Interferometric beam shaping

Ali Harfouche, Univ. des Sciences et de la Technologie Houari Boumediene (Algeria); Boualem Boubaha, Univ. des Sciences et de la Technologie (Algeria); Michael Fromager, Kamel Ait-Ameur, ENSICAEN (France)

Many commercial laser systems deliver a beam having a Gaussian intensity profile, however, numerous applications require other intensity profiles (top-hat, hollow beam, Bessel beam,...) which are in general obtained by converting the standard Gaussian beam (GB) through transparent diffractive optical elements (DOE). Laser beam shaping (LBS) by use of DOE's is a topic that has been intensively developed over a long time whether the DOE is programmable or unprogrammable. Although, DOE's are a great help to many LBS problems they have inherent drawbacks which are mainly: (i) a relatively high cost, and (ii) only work for a narrow spectral bandwidth. Recently, we have experimentally demonstrated the LBS ability resulting from the coaxial superposition of two CW coherent Gaussian beams. This technique is classified under interferometric LBS techniques contrasting with the usual ones based on diffraction. In particular, we demonstrate the reshaping of a Gaussian beam into a bottle beam or top-hat beam in the focal plane of a focusing lens [1]. Moreover,

we demonstrate that this concept of interferometric LBS can also work for wide spectral bandwidth, i.e. ultra-short laser pulses (fs). This opens the possibility of changing the spatial distribution of the laser intensity in the focal plane of a converging lens without changing its temporal distribution in the problematic case of ultra-short pulses.

[1] B. Boubaha, D. Naidoo, T. Godin, M. Fromager, A. Forbes, K. Aït-Ameur, "Spatial properties of coaxial superposition of two coherent Gaussian beams", Appl. Opt. 52, 5766-5772 (2013).

9135-39, Session 9

High-peak-power Terahertz-wave generation and sensitive detection using second nonlinear optical effect *(Invited Paper)*

Hiroaki Minamide, RIKEN (Japan)

Intense Terahertz (THz)-wave generation and highly sensitive THz-wave detection were obtained by wavelength conversion with second nonlinear optical susceptibility of LiNbO3 crystals. Maximum peak output of about 50 kW was obtained in an injection-seeded THz-wave parametric generator pumped by post-amplified emission from a microchip Nd:YAG laser. Using the sub-nanosecond pulse duration of the laser proposed herein provides effective mitigation of stimulated Brillouin scattering in LiNbO3, producing higher gain for wavelength conversion between near-infrared (near-IR) pump light and THz waves. Monochromatic THz radiation was obtained in the continuous tuning range of 0.7–2.9 THz. Additionally, highly sensitive THz-wave detection was demonstrated based on up-conversion from THz waves to near-IR light as well as efficient THz-wave generation. The signal generated with non-collinear phase-matching condition showed spectroscopic detection on the screen apart from the LiNbO3 crystal. Highly sensitive detection with minimum energy of about 80 aJ/pulse and a large dynamic range of more than 100 dB were achieved in this experiment.

9135-40, Session 9

Feasibility of real-time geochemical analysis using LIBS (laser-induced breakdown spectroscopy) in oil wells

Mohamed Shahin, Suez Canal Univ. (Egypt)

The oil and gas industry has attempted for many years to find new ways to analyze and determine type of rocks drilled on a real time basis. Mud analysis logging is a direct method of detecting oil and gas in formations drilled, it depends on the "feel" of the bit to decide formation type, as well as, geochemical analysis which was introduced 30 years ago, starting with a pulsed-neutron generator (PNG) based wireline tool upon which LWD technology was based. In this paper, we are studying the feasibility of introducing a new technology for real-time geochemical analysis.

Laser-induced breakdown spectroscopy (LIBS) is a type of atomic emission spectroscopy, It is a cutting-edge technology that is used for many applications such as determination of alloy composition, origin of manufacture (by monitoring trace components), and molecular analysis (unknown identification). LIBS can analyze any material regardless of its state (solid, liquid or gas), based upon that fact, we can analyze rocks, formation fluids' types and contacts between them.

In cooperation with the National Institute of Laser Enhanced Science, Cairo University in Egypt, we've done tests on sandstone, limestone and coal samples acquired from different places using Nd: YAG Laser with in addition to other components that are explained in details through this paper to understand the ability of Laser to analyze rock samples and provide their elemental composition using LIBS technique.

We've got promising results from the samples analysis via LIBS and discussed the possibility of deploying this technology in oilfields suggesting many applications and giving a base for achieving a quantitative elemental analysis method in view of its shortcomings and solutions.

9135-41, Session 9

Feasibility and performance study for a space-borne 1645nm OPO for French-German satellite mission MERLIN

Florian Elsen, Matthias Heinzig, Marie J. Livrozet, Jens Löhring, Jochen Wüppen, Fraunhofer-Institut für Lasertechnik (Germany); Christian Büdenbender, Andreas Fix, Deutsches Zentrum für Luft- und Raumfahrt e.V. (Germany); Bernd Jungbluth, Fraunhofer-Institut für Lasertechnik (Germany)

As part of the French-German satellite mission MERLIN we conducted theoretical and experimental analysis of a pulsed 1645 nm OPO to prove the feasibility of such a device for a space borne laser transmitter for IPDA LIDAR.

Based on the OPO architecture from DLR we conducted numerical simulations to improve the efficiency of the setup and lower the fluence on optical components. In recent experiments the OPO obtained 12.5 mJ pulse energy at 1645 nm from 32.0 mJ of a 1064 nm pump laser with a pulse duration of 24 ns. This corresponds to a quantum conversion efficiency of 60%.

9135-42, Session 9

High-brightness all semiconductor laser at 1.57 μm for space-borne lidar measurements of atmospheric carbon dioxide: device design and analysis of requirements

Ignacio Esquivias, Antonio Consoli, Univ. Politécnica de Madrid (Spain); Michel Krakowski, Mickael Faugeron, III-V Lab. (France); Gerd Kochem, Martin Traub, Fraunhofer-Institut für Lasertechnik (Germany); Juan Barbero, Paola Fiadino, Alter Technology (Spain); Xiao Ai, John G. Rarity, Univ. of Bristol (United Kingdom); Mathieu Quatrevalet, Gerhard Ehret, Deutsches Zentrum für Luft- und Raumfahrt e.V. (Germany)

The availability of suitable laser sources is one of the main challenges in future space missions for accurate measurement of atmospheric CO2. The main objective of the European project BRITESPACE is to demonstrate the feasibility of an all-semiconductor laser source to be used as a space-borne laser transmitter in an Integrated Path Differential Absorption (IPDA) lidar system. We present here the proposed transmitter and system architectures, the initial device design and the results of the simulations performed in order to estimate the source requirements in terms of power, beam quality, and spectral properties to achieve the required measurement accuracy. The laser transmitter is based on two InGaAsP/InP monolithic Master Oscillator Power Amplifiers (MOPAs), providing the ON and OFF wavelengths close to the selected absorption line around 1.57 μm. Each MOPA consists of a frequency stabilized Distributed Feedback (DFB) master oscillator, a modulator section, and a tapered semiconductor amplifier optimized to maximize the optical output power. The design of the space-compliant laser module includes the beam forming optics and the thermoelectric coolers.The proposed system replaces the conventional pulsed source with a modulated continuous wave source using the Random Modulation-Continuous Wave (RM-CW) approach, allowing the designed semiconductor MOPA to be applicable in such applications. The system requirements for obtaining a CO2 retrieval accuracy of 1 ppmv and a spatial resolution of less than 10 meters have been defined. Envelope estimated of the returns indicate that the average power needed is of a few watts and that the main noise source is the ambient noise.

9135-43, Session 9

High-power pressure tuned laser diodes for application in laser spectroscopy of solids

Krzysztof Anders, Anna Jusza, Warsaw Univ. of Technology (Poland); Filip Dybala, Artem Bercha, Witold A. Trzeciakowski, High Pressure Research Ctr. (Poland); Mariusz Klimczak, Institute of Electronic Materials Technology (Poland); Ryszard Piramidowicz, Warsaw Univ. of Technology (Poland)

The continuous research on novel optically active materials for application in modern optoelectronics and, specifically, laser technique stimulates also development of the versatile spectroscopic tools. One of the most important are broadband tunable lasers, enabling precise choice of excitation wavelength and perfect matching with the energy level structure of active ions. Such a matching, together with the precise tuning are extremely important in optical spectroscopy of solids, specifically when investigations of up-conversion phenomena in solid state laser materials are of concern. In-depth characterization of up-conversion effects in active optical materials very often requires optical pump sources operating at unique wavelengths in the near-infrared part of spectrum, not available for titanium-sapphire lasers, typically used in spectroscopic research. Moreover, in many cases, coherent radiation at multiple, unique wavelengths would have to be applied to the sample at once, in a single excitation process, in order to fulfill exact resonant match with consecutive, individual stages of the excitation process.

Pressure-tuned high-power diode lasers simplify this task, such that multiple pressure-tuned laser modules are relatively easily integrated into the measurement set-up and each of them can be set to a unique wavelength in a broad spectral range (720-1850 nm, depending on specific laser chip), at the same time maintaining output power level and geometric parameters of output beam. Pressure tuning of laser diodes is based on a well-known effect of hydrostatic pressure on the lattice constant, and hence the energy-gap of crystals, including semiconductor laser materials. The uniqueness of the method in contained in overcoming of multiple technological and technical obstacles of laser chip mounting schemes (axial strain control), heat dissipation, optical power pick-up scheme (e.g. refractive index changes with pressure and hence does geometry of laser beam).

Widely Tunable Diode Lasers Group at Institute of High Pressure Physics (“Unipress”) mastered this technique [1-4] and now disposes reliable, compact high-power laser diode modules which can be pressure-tuned to a set operating wavelength anywhere between 720 nm up to 1850 nm, depending on specific laser diode chip used. The Unipress team can successfully apply the method specifically to high-power tapered laser diodes, which benefit from their high-brightness output beam feature in the whole pressure tuning range. The above described devices are successfully tested since the beginning of 2013 in the Laboratory of Laser Spectroscopy in the Institute of Microelectronics and Optoelectronics.

In this work we present and discuss the operational parameters of pressure tuned laser diodes developed in the Unipress laboratories together with the first results of research on up-conversion phenomena in thulium, holmium and erbium ions pumped at non-typical wavelengths, which enables investigation of new excitation mechanisms, optimization of the pumping schemes and, in turn, development of new types of solid state lasers.

[1] F. Dybala, A. Bercha, M. Klimczak, B. Piechal, Y. Ivonyak and W. A. Trzeciakowski, Pressure tuning of high-power laser diodes in the 720–1540 nm range, Phys. Status Solidi B 250 (4), pp. 703-707 (2013)

[2] R. Bohdan, A. Bercha, O. Mariani, M. Wojdak, F. Dybala, P. Adamiec, W. Trzeciakowski, J. Weber, M.T. Kelemen, Tuning of the high-brightness tapered laser and its applications, Physica Status Solidi (B) Basic Research, 244 (1), (2007), pp. 213-218

[3] F. Dyba?a, P. Adamiec, A. Bercha, R. Bohdan, W. Trzeciakowski, “Wavelength tuning of laser diodes using hydrostatic pressure”, Proc. SPIE Vol. 4989, 181-189 (2003)

[4] T. Suski, G. Franssen , P. Perlin, R. Bohdan, A. Bercha, P. Adamiec, F. Dyba?a, W. Trzeciakowski, P. Prystawko, M. Leszczy?ski, I. Grzegory, and S. Porowski, “A pressure-tuned blue/violet InGaN/GaN laser diode grown on bulk GaN crystal”, Applied Physics Letters 84, 1236 (2004)

9135-58, Session PS3

Characterisation of birefringence of [111]-cut crystal rod using side-pumping and crystal rotation

Thomas Graupeter, Christoph Pflaum, Friedrich-Alexander-Univ. Erlangen-Nürnberg (Germany)

Birefringence influences the beam quality and output power of high power solid-state lasers. Non-uniform absorption of the pump light inside the crystal and a heat sink only at boundaries cause inhomogeneous distribution of the thermal field inside the laser crystal rod. This distribution leads to inhomogeneous thermal strains and birefringence, due to the photoelastic effect. Analytical models for calculating of birefringence have used the plane stress and plane strain assumptions for an axially symmetric pumped crystal. This leads to an axially symmetric birefringence pattern in case of the [111]-cut crystal. However, the plane stress and plane strain assumptions neglect the shear strains in the axial-radial plane. Full 3D numerical calculations take shear strains into account. Results of the birefringence simulation show a threefold symmetry pattern due to the anisotropic behaviour of the photoelastic tensor, which is contradictory to the ideal use of a radial or azimuthal polarized beam. We analysed a laser rod pumped at three sides with threefold symmetry, in order to reduce the effect of birefringence. The absorption is not axially symmetric anymore in our case. The pump light absorption and consequently the temperature, the strains and birefringence are higher within the crystal in regions where pumping is stronger. If the region having a low birefringence due to the photoelastic effect is more strongly pumped than the rest of domain, the degree of three-fold symmetry of birefringence will be reduced. This means the birefringence is affected by the rotation of crystal around its [111]-axis. Smallest birefringence can be obtained by an optimal rotation with respect to the edges of the crystal. Therefore, the output beam of this laser device is more suitable for generating radial or azimuthal polarizations.

9135-59, Session PS3

The pulsed all fiber laser application in the high-resolution 3D imaging LIDAR system

Cunxiao Gao, Shaolan Zhu, Linquan Niu, Li Feng, Haodong He, Zongying Cao, Xi’an Institute of Optics and Precision Mechanics (China)

An all fiber laser with master-oscillator-power-amplifier (MOPA) configuration at 1064nm/1550nm for the high-resolution three-dimensional (3D) imaging light detection and ranging (LIDAR) system was reported. The seeder of the laser was the directly modulated fiber coupled laser diode, and the large mode area (LMA) double clad fiber was used in the power amplifier. The pulsewidth and the repetition frequence of the laser could be arbitrarily tuned 1ns~50ns and 10kHz~1MHz, and the peak power exceeded 100kW could be obtained with the laser. Using this all fiber laser in the high-resolution 3D imaging LIDAR system, the image resolution of 1024?1024 and the distance precision of ±1.5 cm was obtained at the imaging distance of 1km.

9135-60, Session PS3

First principal study of linear optical properties of ?-Al2O3 using in femtosecond laser applications

Hamza Bennacer, Ctr. de Développement des Téchnologies Avancées (Algeria); Abdelkader Boukortt, Univ. de Mostaganem (Algeria); M. I. Ziane, Ctr. de Développement des Téchnologies Avancées (Algeria)

Since last few years, Ti3+-Al2O3 has become the material of choice in crystal growth for the development of ultra-short laser systems producing very short and powerful pulses using the Chirped Pulse Amplification technique.

To investigate the optical properties of Al2O3 compound, we performed full-potential linearized augmented plane wave (FP-LAPW) calculations based on density functional theory. The modified Becke-Johnson (mBJ) exchange potential approximation is used as the exchange correlation potential to calculate the linear optical properties.

Our results are in good agreement with the experimental data.

9135-61, Session PS3

Cryogenically cooled Pr:$YAlO_3$ laser operating at 747 nm, 662nm, and 622nm wavelengths

Martin Fibrich, Czech Technical Univ. in Prague (Czech Republic) and Institute of Physics of the ASCR, v.v.i. (Czech Republic); Jan Sulc, Helena Jelínková, Czech Technical Univ. in Prague (Czech Republic)

Pr-ions doped YAlO3 laser host is one of the most attractive oxide laser material for efficient stimulated emission in the visible region of the electromagnetic spectrum. It combines its good thermal and mechanical properties with nature birefringent character, so, the thermally-induced birefringence should not degrade the laser performance. Moreover, in comparison with the most prominent Pr-doped fluoride crystals, Pr:YAlO3 exhibits positive value of the temperature coefficient dn/dT allowing to simply employ a microchip laser geometry which is in general very attractive because of its compactness, high efficiency and good beam quality. So, this provide a great potential for realizing compact and efficient laser sources suitable for various applications in industry, spectroscopy, fluorescence microscopy, and medicine.

In this contribution, following our results concerning the first demonstration of green laser emission from the Pr:YAlO3 material reached by the crystal cooling down to the cryogenic temperature, efficient continuous-wave Pr:YAlO3 laser emission in the near-infrared (747 nm), red (662 nm), orange (622 nm) and green (547 nm) spectral range at cryogenic temperature is reported. As a pumping source, 1-W GaN laser diode was used. To minimize the resonator losses, microchip geometry realized by cavity mirrors directly deposited as a dielectric films on the crystal faces has been proposed and employed. The microchip crystal mounted on liquid-nitrogen-cooled copper finger was placed in the vacuum chamber of the cryostat with AR-coated windows for pump and generated radiation. In connection with temperature controller, the crystal temperature was controlled within the 77-300K and respective output characteristics were recorded. The best results were demonstrated for 747 nm wavelength; more than 300 mW of output power with the slope efficiency exceeding 52 % has been extracted from the cryogenically cooled 0.6 at. % doped Pr:YAlO3 active material.

9135-62, Session PS3

Simulation of wavefront reconstruction in beam reshaping system for rectangular laser beam

Qiong Zhou, Wenguang Liu, Zongfu Jiang, National Univ. of Defense Technology (China)

Generally it is difficult to directly measure the beam quality of slab laser by using Hartman sensor. In order to measuring the wavefront of laser beam the cylindrical transmitted beam reshaping system must be used for the rectangular beam of slab laser. However because of thermal deformation of cylindrical mirrors, the result of sensor always contain additional aberration introduced by the beam reshaping system such as defocusing and astigmatism. A new method to calculating the wavefront of slap laser is studied in this paper. The method is based on the ray trace theory of geometrical optics. By using the Zemax simulation software and Matlab calculation software, the wavefront of rectangular beam in beam reshaping system is reconstructed. Firstly, with the x- and y-slope measurement of reshaping beam the direction cosine of wavefront can be calculated. Then, the inverse beam path of beam reshaping system is built by using Zemax simulation software and the direction cosine of rectangular beam can be given, too. Finally, Southwell zonal model is used to reconstruct the wavefront of rectangular beam in computer simulation. Once the wavefront is received, the aberration of laser can be eliminated by using the proper configuration of beam reshaping system. It is shown that this method to reconstruct the wavefront of rectangular beam can evidently reduce the negative influence of additional aberration induced by beam reshaping system.

9135-63, Session PS3

Global gain profiles analysis for Raman+EDFA hybrid amplifiers

Márcia da Mota Jardim Martini, CEFET/MG (Brazil); Maria José Pontes, Moisés R. N. Ribeiro, Univ. Federal do Espírito Santo (Brazil); Hipolito J. Kalinowski, Univ. Tecnológica Federal do Paraná (Brazil)

Different configurations of optimized hybrid amplifiers, made by a Raman amplifier followed by an EDFA, are studied in this work. The performance of different hybrid EDFA+Raman amplifiers is obtained using commercial software. These optimized hybrid amplifier configurations contribute to minimize the energy consumption of the entire transmission system. Raman amplifiers can be used along with the EDFA high output power capacity to add spectral shaping flexibility for broadband applications. We have analyzed four different cases regarding the number of pump lasers. Global gain, noise figure and ripple results indicate the effectiveness of the proposed technique to EDFA gain profile equalization using the pump optimization of the Raman amplifier for a WDM, environment using 8, 16, 32, 64 and 128 channels simultaneously coupled to the input fiber. The performance of optimized hybrid amplifier continues to behave in a predictable manner, even with the inclusion of more one pumping, as with the increase of the number of channels and the consequent increase in the level of input power. It is noteworthy the effect of gain saturation taking place in the EDF stage, while the Raman gain remains nearly unchanged, as the Ps level is increased. However ripple tends increase, but with 32 channels decreases significantly if compared with the obtained results considering 16, 64 and 128 channels. The increased ripple values can be compensated with o significant increased of global gain in the case of two pump lasers. The difference in the increase of global gain as increase to three and four pump lasers is not interesting because the ripple increases about 4 dB. This analysis was performed in order to check the global gain saturation and the changes in the global gain profile that occur due to signal-pump, signal-signal, and pump-pump interactions. The performance of optimized Rman+EDFA hybrid amplifier

continues to behave in a predictable manner (similar profiles), even with the inclusion of more pump lasers or input channels. With the increase of number of pump lasers can be observed that NF decreases approximately 1 dB and although also increases around 1 dB. Multiple input channels allowed the gain characterization of the optimized Raman+EDFA hybrid amplifier in terms of global gain, ripple, and noise figure considering applications for WDM systems. Ripple values smaller than 3.7 dB for 8, 16, 32, 64 and 128 WDM input channels have been found in a 30 nm bandwidth (for wavelength over of 1540 nm) , using two optimized Raman pump lasers, with global gain of approximately 30 dB. It was observed that the signal-pump interactions provide better results for the three pump lasers configuration even noise figure average values be greater than approximately 1 dB. The increase of input channels number provides worse results than the increase of pump laser number it occurs because of the energy transference between the input WDM channels. For the investigated scenario under WDM input signals, the cost effective solutions seems to be the configuration with three pump lasers as it improves the average gain and significantly reduces ripple figures.

9135-64, Session PS3

Latest developments in AlGaInN laser-diode technology

Stephen P. Najda, Piotr Perlin, TopGaN Ltd. (Poland); Tadek Suski, Institute of High Pressure Physics (Poland); Lucja Marona, Mike Bockowski, Mike Leszczynski, P. Wisniewski, Robert Czernecki, G. Tagowski, TopGaN Ltd. (Poland); Scott Watson, Antony Kelly, University of Glasgow (United Kingdom)

The latest developments in AlGaInN laser diode technology are reviewed. The AlGaInN material system allows for laser diodes to be fabricated over a very wide range of wavelengths from u.v., i.e, 380nm, to the visible 530nm, by tuning the indium content of the laser GaInN quantum well. Ridge waveguide laser diode structures are fabricated to achieve single mode operation with optical powers of >100mW in the 400-420nm wavelength range that are suitable for telecom applications. High power operation of AlGaInN laser diodes is demonstrated with a single chip, AlGaInN laser diode 'mini-array' with a common p-contact configuration at powers up to 2.5W cw at 410nm. Low defectivity and highly uniform GaN substrates allow arrays and bars of nitride lasers to be fabricated. GaN laser bars of up to 5mm with 20 emitters, mounted in a CS mount package, give optical powers up to 4W cw at ~410nm with a common contact configuration. An alternative package configuration for AlGaInN laser arrays allows for each individual laser to be individually addressable allowing complex free-space and/or fibre optic system integration within a very small form-factor.

9135-65, Session PS3

Compact Nd:YAG laser operating at 1.06, 1.32, and 1.44um wavelength

Michal Nemec, Jan Sulc, Helena Jelinková, Martin Fibrich, Czech Technical Univ. in Prague (Czech Republic); Karel Nejezchleb, Nickalai Kapitch, Crytur Ltd. (Czech Republic)

The aim of this study was design and construction of a Nd:YAG laser system allowing laser generation in the near-infrared region at three separate switchable wavelengths 1.06, 1.32, and 1.44 um. This integrated multi-wavelength laser system can be useful for application especially in medicine and spectroscopy. We used 1.1 at. % Nd/Y doped Nd:YAG active medium 4 x 102 mm in dimensions with anti-reflection coated faces for 1.06, 1.32, and 1.44 um. The laser crystal was placed along Xe flashlamp into the diffuse pump cavity (the pump pulse duration was 800 us FWHM). The laser system was formed by six mirrors including one output coupler, three rear mirrors, and two dichroic mirrors. These mirrors were specially designed and their characteristics were as follow: HR/T @ 1440/1320 and 1064 nm and HR/T @ 1320/1064 nm. The output coupler reflectivity was 17 %, 80 %, and 82 %, for 1.06, 1.32, and 1.44 um wavelengths, respectively. Particular laser Nd:YAG line selection was realized by adequate shutters. The output laser characteristics in terms of output energy, spatial beam structure, and temporal profile were recorded. For 62 J pumping energy, the obtained output energies were 0.80 J, 0.45 J, and 0.19 J, for 1.06, 1.32, and 1.44 um wavelengths, respectively. Specific absorption properties of the designed wavelengths in water and water vapor together with the sufficient reached energy predetermine this compact Nd:YAG laser system for utilization in medical and industry applications.

9135-66, Session PS3

Er-doped ortho- and metha-phosphate glassy mixtures for 1.54 um laser construction

Jan Sulc, Richard Svejkar, Michal Nemec, Helena Jelínková, Czech Technical Univ. in Prague (Czech Republic); Karel Nitsch, Antonín Cihlár, Robert Král, Institute of Physics of Materials of the ASCR, v.v.i. (Czech Republic); Karel Nejezchleb, Crytur Ltd. (Czech Republic); Miroslava Rodová, Institute of Physics of Materials of the ASCR, v.v.i. (Czech Republic); Martin Nikl, Institute of Physics of the ASCR, v.v.i. (Czech Republic)

In recent years considerable research effort has been focused on the preparation and properties of alkali rare earth phosphate glasses due to their possible application as materials for solid state lasers and scintillators. The Er3+ doped Yb phosphate glasses are actually considered as the best matrix for Yb sensitized Er glass laser. Attention has been paid to both meta-phosphate derived of meta-phosphoric acid (HPO3) and those based on ortho-phosphoric acid (H3PO4). While meta-phosphates vitrifies very easy, alone ortho-phosphates do not form glasses. Ortho-phosphates are able to form glassy mixture with alkali meta-phosphate. The goal of our work was preparation and investigation of Er-doped potassium ytterbium lanthanum ortho- and metha-phosphate glassy mixtures developed as a solid-state laser active medium. The tested samples were prepared by rapid quenching of molten mixture of starting K2CO3, YbPO4, LaPO4, YbPO4 and P2O5. Their cations molar concentration was as follows n(K) = 0.7, n(Yb) = 0.135, n(La) = 0.16 and n(Er) = 0.005 and it was the same in all tested samples. Small amount of LaF3 was added to remove some rest of the adsorbed humidity. The additions of the P2O5 to the individual starting charges were batched so the following compositions of resulting glasses should be obtained: (i) pure meta-phosphate, (ii) mixture of 80 mol% of meta-phosphate and 20 mol% of ortho-phosphate, (iii) mixture of 50 mol% of meta-phosphate and 50 mol% of ortho-phosphate, (iv) mixture of 25 mol% of meta-phosphate and 75 mol% of ortho-phosphate, and (v) pure ortho-phosphate. The glassy samples were prepared in the form of discs about 8 mm in diameter and 2 mm in height. The absorption spectra were measured in broad range from 200 up to 2500 nm to identify possible impurities, mainly the residual OH-absorption and to calculate absorption cross-section for pumping and laser transition 4I15/2->4I11/2 and 4I13/2->4I15/2, respectively. For particular transitions fluorescence spectra and fluorescence decay time were recorded simultaneously. It was found that the fluorescence decay time, corresponding to upper laser level 4I13/2 depopulation, progressively increases with the content of ortho-phosphate in glass composition starting from 2 ms for sample (i) up to 8 ms for sample (iv). The laser action at 1.54 um under 975 nm pulsed laser diode pumping was successfully demonstrated using the sample with the longest upper laser level lifetime.

9135-67, Session PS3

Laser characteristics of TGT-grown Nd,Y-codoped:SrF_2 single crystal

Michal Jelínek, Václav Kubecek, Czech Technical Univ. in Prague (Czech Republic); Liangbi Su, Dapeng Jiang, Fengkai Ma, Qian Zhang, Yuexin Cao, Jun Xu, Shanghai Institute of Ceramics (China)

Fluoride-type crystals (CaF2, SrF_2, BaF2) doped with Nd3+ were forgotten for a long time as laser active media because of very detrimental concentration quenching effect resulting from the aggregation of the Nd3+ active ions. Among them, Nd:CaF2 crystal was found to not be useful because Nd3+ ions tend to cluster at very low concentration, while Nd:BaF2 crystal exhibit unacceptably low transition strengths. Strontium fluoride crystals doped with neodymium ions are promising materials for the development of diode pumped lasers and amplifiers mainly because of the adequate absorption cross-section, broad absorption and emission spectra as well as longer fluorescence lifetime. Recently, a very modest laser operation but resulting from a diode pumping was achieved with a SrF_2 crystal doped with 0.5 % Nd3+ ions.

In this paper we present laser properties of newly prepared TGT (temperature gradient technique) grown Nd,Y:SrF_2 crystals with neodymium concentration of 0.4, 0.65 and 0.8 at%. The noncoated crystal samples 3.5 or 5 mm thick were pumped by a 796 nm laser diode Limo matching the Nd:SrF_2 absorption peak. Several output couplers with reflectivity ranging from 70 to 98 % at the generated wavelength were tested. In the pulsed pumping regime (pulse-duration 2 ms, frequency 10 Hz), the maximum average output power of 75 mW was obtained with the slope efficiency as high as 48% and the optical-to-optical efficiency of 42% with respect to the absorbed pump power. The output beam spatial profile was nearly Gaussian in both axes, oscillations started at the wavelength of 1057 nm. At higher pumping levels, the second emission line at 1050 nm appears corresponding to our fluorescence measurements. Wavelength tuning using birefringent filter from 1048 to 1070 nm is probably given by crystal-field splitting of the 4F3/2 manifold in Nd3+. True-CW laser operation was also successfully obtained at lower pumping level with the maximum output power of 90 mW using output coupler reflectivity of 98%. Fluorescence and lifetime measurements will be reported also.

9135-68, Session PS3

Up-conversion emission properties of thulium-doped low-phonon glasses

Anna Jusza, Krzysztof Anders, Warsaw Univ. of Technology (Poland); Filip Dyba?a, Artem Bercha, Witold A. Trzeciakowski, High Pressure Research Ctr. (Poland); Ryszard Piramidowicz, Warsaw Univ. of Technology (Poland)

High efficiency and low cost have been primary motivators for searching new ways of obtaining short-wavelength, coherent radiation. Research effort in this area generally shows two main streams, one of which focuses on wide band gap semiconductor lasers, while the other on frequency multiplication effects in solid state lasers. An alternative solution may bring solid state lasers pumped by up-conversion processes, which in general result in emission or laser action at wavelengths shorter than those used for pumping. Trivalent thulium is the activator ion, which energy structure in certain conditions specifically favours such multi-photon or multi-ion pumping mechanisms yielding the emission in the UV-VIS part of spectrum. In low phonon glasses and fibers, emissions from 1G4 (480 nm), 1D2 (455 nm), as well as 1I6 (287 nm) excited states have been reported, typically involving ESA-type consecutive absorptions of 650 nm photons (3H6?3F2+3F3, 3F4?1G4, 3H4?1D2, 1G4?3PJ) [1], observed also under multi-wavelength pumping at 1112 nm, 1116 nm and 1127 nm [2]. Lately, laser action at 287 nm in Tm3+:ZBLAN fiber was obtained under consecutive ESA of 1064 nm delivered by an Nd3+:YAG laser [3] – which is to date the shortest wavelength of stimulated emission generated in an optical fiber. Laser experiments with thulium-activated fluoride fibers, however very promising, were all severely hindered with photodarkening effects accompanying excitation of UV-violet radiation in the fibers.

In this work we present the latest results of our research on up-converted short-wavelength emission in low-phonon glasses doped with thulium ions, giving further impact to better understanding the short wavelength optical properties of this system. We examined a set of samples with different activator concentrations in different glassy matrices with respect of excitation channels and short wavelength emission properties. A completely new spectroscopic tools - pressure-tuned multimode semiconductor lasers were used as an excitation sources, enabling experimental determination of optimal pumping wavelengths for thulium ions in glass matrices.

Acknowledgements:

This work has been supported by the National Science Centre, Poland, decision number: DEC-2011/03/B/ST7/01917.

References

[1] J. Y. Allain, M. Monerie, H. Poignant. Blue upconversion fluorozirconate fibre laser, Electronics Letters 26 (1990), 166–168.

[2] S. G. Grubb, K. W. Bennett, R. S. Cannon, W. F. Humer, CW room-temperature blue upconversion fibre laser, Electronics Letters 28 (1992), 1243–1244

[3] R. M. El-Agmy, Upconversion CW Laser at 284 nm in a Nd:YAG-Pumped Double-Cladding Thulium-Doped ZBLAN Fiber Laser, Laser Physics 18 (2008) 1-4.

9135-69, Session PS3

Detectability of penetration depth based on weld pool geometry and process emission spectrum in laser welding of copper

Alp Özmert, Daniel Pütz, Alexander J. Drenker, Fraunhofer-Institut für Lasertechnik (Germany)

Laser welding is a promising joining process for copper interconnections. A key criterion of quality for these welds is the penetration depth. The penetration depth is subject to variations by the nature of the welding process. Online detection of penetration depth enables quality assurance and furthermore welding of joint configurations with tighter tolerances via closed-loop control of the laser welding.

Weld pool geometry and optical radiation of wavelengths between 400-1100 nm emitted from keyhole are investigated with regard to how suitable they are for the detection of penetration depth in laser welding of copper Cu-ETP. Different penetration depths were induced by stepwise modulation of laser power while welding bead-on-plate. The welds have been monitored online with illuminated imaging of the work piece surface and spectrometry targeted at the keyhole. Increase of the weld pool length (in direction of travel) corresponding to increase in penetration depth has been observed while no noticeable change was observed of the weld pool width (transverse to the direction of travel). No significant lines were observed in the spectrum. The radiant power obtained by integrating the spectrum in VIS-region was observed to increase with increasing penetration depth as well.

As future work, with increasing understanding and experimental data, online monitoring by indirectly measuring the penetration depth would be possible.

The research leading to these results has received funding from the European Union Seventh Framework Programme (FP7/2007-2013) under grant agreement no 260153 (QCOALA: Quality Control for Aluminium Laser-Welded Assemblies).

9135-70, Session PS3

Phase formation and densification peculiarities of $Y_3Al_5O_{12}:Nd^{3+}$ during reactive sintering

Denis Y. Kosyanov, Institute for Single Crystals (Ukraine); Sergey V. Frolov, Institute of Applied Optics (Ukraine); Yuriy L. Kopylov, Valeriy B. Kravchenko, Institute of Radio Engineering and Electronics (Russian Federation); Victor B. Taranenko, Institute of Applied Optics (Ukraine); Alexander V. Tolmachev, Institute for Single Crystals (Ukraine); Vladimir L. Voznyy, EDAPS-Laser Ltd. (Ukraine); Roman P. Yavetskiy, Institute for Single Crystals (Ukraine)

Optical ceramics are promising materials for utilization as phosphors, solid state lasers host materials, transparent armor, lamp envelopes, scintillation detectors, etc. Transparent laser ceramics possess several advantages over traditional materials among which there are improved processability, lower cost of fabrication, wider range of compositions, higher doping concentration, larger size of ceramic samples. The development of Y3Al5O12:Nd3+ laser ceramics (YAG:Nd3+) with spectral, lasing and mechanical properties equal to those of single crystals is one of the most significant achievements of the laser materials science in recent years. In this paper we present results of YAG:Nd3+ (4 at. %) transparent ceramics fabrication and characterization of its optical properties.

The processes of phase formation and densification during reactive sintering of YAG:Nd3+ (4 at. %) laser ceramics by reactive sintering using submicron oxide powders have been studied. It has been determined that using of fine yttria powders with a bimodal particle size distribution (D50?160 and 400 nm) can partially overlap the temperature ranges of garnet (1200-1500??) and perovskite phase formation (?1100-1400??), which should provide a competitive advantage of shrinkage over swelling processes. Excluding the swelling effect during densification allows one to produce laser-quality YAG:Nd3+ (4 at. %) ceramics by reactive sintering with in-line optical transmission of about 80 % at ?=650 for a 1 mm thick sample, which is equal to that of YAG single crystals.

9135-71, Session PS3

Safe range gated imaging lidar with a nanosecond frequency doubled Nd:YAG laser

Roberto Ocaña Pérez, Ian Wallhead, Teresa Molina, AIDO Instituto Tecnológico de Óptica, Color e Imagen (Spain)

A gated imaging LIDAR is a device that is able to record three dimensional information by taken two-dimensional pictures. In contrast to conventional scanning LIDARs that record only one point with the range information at the frequency of the scanning mechanism, a gated imaging LIDAR does not need a scanning process for recording the 3D information. In fact, in these devices a configured number of pictures taken at the maximum repetition rate of the system formed by an illumination source producing short pulses and a synchronized camera will provide a 3D image. The heart of the system remains in the synchronization mechanism between the illumination source (a pulsed laser) and the capturing imaging device. The image is captured after a certain delay d is applied between the pulse output and the beginning of the camera exposition. Thus, only objects that are separated from the camera a distance given by c x d/2 are recorded. The depth information of every picture is given by the convolution between the time dependence of the laser pulse and the camera gate and will define the resolution of the 3D picture formed as a set of 2D images.

There are different ways of setup a gated imaging LIDAR including strategies about the algorithms used for the configuration of the gate. In this work we have used a home-made frequency doubled nanosecond pulsed Nd:YAG laser as illumination source, a CCD coupled to a generation II image intensifier and a simple progressive delays set for the camera gate using a pulse delay generator to show the potential of this technique as well as to further determine aspects such as the typical energy per pulse needed or the illumination distribution of the laser source. Surprisingly at low levels of the illumination pulse energy that would satisfy the safety laser class 2 we can resolve objects as far as 690 m.

In order to further explore the performance of the constructed system we have recorded both pictures and videos at different synchronization delays between laser pulse and image capture and using different optical elements to build the spatial distribution of the illumination. The results show a clear discrimination of objects situated at different distances that allow us to use different strategies for the in situ-analysis. The low complexity as well as cost make this technique a potential candidate for further developments with different laser sources , electronic synchronization drivers and image intensifiers as well as for applications with intelligent systems for detection of objects at fixed distances.

9135-72, Session PS3

Modeling of the spectrum in a random distributed feedback fiber laser within the power balance model

Ilya D. Vatnik, Institute of Automation and Electrometry (Russian Federation); Dmitry V. Churkin, Aston Univ. (United Kingdom) and Institute of Automation and Electrometry (Russian Federation) and Novosibirsk State Univ. (Russian Federation)

Last few years more and more attention is given to random distributed feedback (DFB) fiber lasers first reported in [1]. The distinguishing feature of the laser is a feedback created by the extremely weak random distributed Rayleigh backscattering. Power characteristics of the random DFB fiber laser are well investigated, while much less efforts were made to predict and control its spectral properties. In particular, a precise role of the random distributed feedback on formation of the spectrum is not clear.

The simplest model for a description of the random DFB fiber laser is a power balance model describing the evolution of the intensities of the waves over the fiber length. This model includes the Rayleigh backscattering as an energy income to the counter-propagating wave. The model predicts well the power performances of the random DFB fiber laser including the generation threshold, the output power and pump and generation wave intensity distributions along the fiber [2,3]. The results of power modeling within the power balance model are in good agreement with many experiments.

In the present work, we extend the power balance model and modify equations in such a way that they describe now frequency dependent spectral power density instead of integral over the spectrum intensities. Earlier this approach was used to simulate spectral line due to spontaneous Raman scattering in conventional Raman fiber lasers with point reflectors [4]. We calculate the generation spectrum, that is generation spectral densities at each wavelength over the gain spectrum, by using the depleted pump wave longitudinal distribution derived from the conventional power balance model. It's reliable under the threshold, where pump distribution is determined by linear losses rather than by energy transfer to Stokes wave. The numerical simulations can be used to predict random DFB laser spectrum under and near threshold, where nonlinear effect are negligible.

1. S. K. Turitsyn, S. A. Babin, A. E. El-Taher, P. Harper, D. V. Churkin, S. I. Kablukov, J. D. Ania-Castanon, V. Karalekas, and E. V. Podivilov, "Random distributed feedback fibre laser," Nat. Photonics 4, 231–235 (2010).

2. I. D. Vatnik, D. V. Churkin, and S. A. Babin, "Power optimization of random distributed feedback fiber lasers," Opt. Express 20, 28033 (2012).

3. D. V. Churkin, A. E. El-Taher, I. D. Vatnik, J. D. Ania-Castanon,

P. Harper, E. V. Podivilov, S. A. Babin, and S. K. Turitsyn, "Experimental and theoretical study of longitudinal power distribution in a random DFB fiber laser," Opt. Express 20, 11178–11188 (2012).

4. M. Krause and H. Renner, "Numerical calculation of the linewidth of Raman fiber lasers due to spontaneous Raman scattering," AEU - Int. J. Electron. Commun. 59, 502–509 (2005).

9135-73, Session PS3

Micromachining of optical fibers using ultrashort laser pulses

Gediminas Cha?evskis, Domas Paipulas, Vilnius Univ. (Lithuania)

Besides the fact that optical fibers are a driving force of today's telecommunications, they also constantly find many new applications in different fields. Having intrinsic property to guide light in long distances, these devices become promising for use in beam/light delivery purposes as well as in sensor technologies. Indeed, integrating fiber Bragg gratings turned out to be a successful solution for adapting fibers to be used as temperature, stress or pressure sensors. In addition, great efficiency and high damage threshold of fibers replaced flash lamps in many laser pumping systems. Furthermore, medical field also benefits from the use of optical fibers: a flexible endoscope relies on optical fibers for imaging, as well as illumination purposes, fiber light diffusers find their way in photodynamic therapy and etc.

In this work we used a femtosecond micromachining system in order to selectively ablate and create well-defined grooves in a standard optical glass fiber in order to form a homogeneous light diffuser. Ultrashort pulse laser systems are powerful tools for micromachining any material, because they emit high energy pulses, which are able to reach intensities needed to induce nonlinear optical processes when focused. In this experiment, a femtosecond laser system, emitting 1030 nm wavelength, 300 fs duration pulses with a repetition rate of 25-200 kHz was used to fabricate microstructures in the multimode quartz fiber. The sample was translated on the three axis translation stage, which is able to translate samples at the speed of up to 300 mm/s. Several different fabrication algorithms and focusing objectives were examined. We show that it is possible to form diverse V-shaped grooves with variable parameters: groove width can be scaled down to 2 μm while depth can vary from 5 to around 100 μm, depending on the number of algorithm repetitions and other system parameters, such as repetition rate, pulse energy, pulse density, focusing conditions, overlapping of the algorithm lines and etc. In addition, highly rectangular, very low surface roughness (500 nm – 3 um, (RMS)) and variable depth (5 to 100 μm) and width grooves, can be formed with a fabrication times of tens of seconds, and could be suitable for interferometric sensor applications. Furthermore, light scattering properties of micromachined grooves were examined, by forming a periodic array of grooves, coupling the 632 nm wavelength beam of the laser diode into the fiber, and measuring the groove-scattered light intensity. The results show, that a micromachined fiber could have potential to be used as micro fiber light diffuser in medical applications.

9135-74, Session PS3

The velocimetry of melt removing in gas-assisted laser cutting of steel using multichannel pyrometer

Alexander V. Dubrov, Yury N. Zavalov, Vladimir D. Dubrov, Institute on Laser and Information Technologies (Russian Federation)

Sheet-metal laser cutting is the largest, in terms of market of machinery, widespread industrial laser application. An investigation of the dynamics of the laser radiation action on the material for development of monitoring systems is one of the directions of quality improvement in laser technology [1, 2]. The model of gas-assisted laser cutting as shown early belongs to a class of nonlinear equations of Kuramoto Sivashinsky type [3]: melt surface is deformed due to instabilities on the interface with turbulent jet of assisted gas.

Fast temperature oscillation is associated primarily with the local absorption of heat. The steel is characterized by a strong dependence of the coefficient of absorption of radiation from the angle of incidence. As a result, the local variable slope of the surface leads to a modulation of absorption of a focused laser radiation [6], and, therefore, modulation of temperature along the front of the cut is occur. The local temperature inhomogeneity drifted down the front. We can determine the velocity of the melt flow measuring the time of moving of the heterogeneity on the known distance between points of observation.

Experiments were carried out on a laser based machine for cutting metal Trumatic L2530 (TRUMPF Group). CO2-laser is used with output power 1500 W. Sample for cutting is 6 mm- thickness plate of mild steel. Oxygen with pressure of 0.45 MPa was used as assisted gas. Cutting speed was varied in range of (20...40) mm/s. Multichannel pyrometer was used to estimate the velocity of melt removing in gas-assisted laser cutting of steel. Local pulsations of brightness temperature from four areas with diameter of about 0.1 mm each, placed one after the other through 0.6 mm along the front of the cut, were measured. We investigated temporal dynamics of thermal luminosity of melt in gas-assisted laser cutting of steel [4, 5]. The method of determine of velocity of movement of temperature inhomogeneities with the motion of the melt is developed now. The correlation between the brightness temperature pulsations in the neighboring areas was calculated for this purpose. It is shown that pre-frequency filtering data allows finding the velocity of so-called "fast" and "slow" waves, together with the velocity of the melt on the surface.

[1] Norman P., Engström H., Kaplan A. F. H., // J. Phys. D: Appl. Phys. v 41, p 195502 (2001).

[2] Poprawe R., Kunig W., CIRP Annals - Manufacturing Technology, 50(1) pp. 137–140 (2001).

[3] Schulz W., Niessen M., Eppelt U. and Kowalick K., "Simulation of Laser Cutting" In: J. M. Dowden Ed.:, Springer Series in Materials Science Vol. 119, pp.21-70 (2009), 458 p.

[4] Dubrov A.V., Dubrov V.D., Zavalov Y.N., et al. // Appl. Phys. B. 2011. v.105, pp. 537–543.

[5] Dubrov A.V., Dubrov V.D., Zavalov Y.N. et al. // Proceedings of SPIE. 2012. v. 8433, p.84330W.

[6] Kaplan A. F. H. // Appl. Phys. Lett. 2012. v.101, p.151605.

9135-75, Session PS3

Self-start of passively mode-locked ring fibre oscillator as a function of pump power

Sergey M. Kobtsev, Sergey V. Smirnov, Sergey Khripunov, Daba Radnatarov, Sergey V. Kukarin, Aleksey V. Ivanenko, Novosibirsk State Univ. (Russian Federation) and Tekhnoscan-Lab LLC (Russian Federation)

This work presents for the first time the results of study of one of the simplest and most reliable configurations of a ring fibre laser passively mode-locked due to nonlinear polarization evolution. The laser arrangement under consideration comprises a single phase retarding element in contrast to most widely used configurations with several wave plates or two polarization controllers. With the use of numerical simulation based on coupled non-linear Schrödinger equations for orthogonal polarization components, we investigate mode-lock domain in terms of pump power and phase delay introduced by the single polarization control element. Changing pump power, we demonstrate capacity of such a simple cavity layout with only one polarization element to operate in different lasing regimes including generation of conventional laser pulse trains at fundamental repetition rate, generation of double-

scale partially coherent and noise-like pulses and generation of multiple pulses per round-trip. We show sub-domains of laser parameters, which correspond to different lasing regimes and discuss possibility of achieving mode-locking in an "empty" cavity with no polarization controlling elements. An important role of random fibre birefringence for mode locking in such a simple system is considered. Besides the results of detailed numerical study, we also announce experimental results obtained with the use of Er fibre laser with a single polarization controlling element based on electronically driven liquid crystal. Our experimental observations are in good qualitative agreement with simulation results and constitute a platform for creation of new simple, low-cost, and reliable self-starting fibre lasers with ultra-short optical pulses.

9135-76, Session PS3

Photonic jet to improve the lateral resolution of laser etching

Andri Abdurrochman, Univ. de Strasbourg (France) and Univ. of Padjadjaran (Indonesia); Sylvain Lecler, Univ. de Strasbourg (France); Joseph-Joël Fontaine, ICube Lab. (France); Frédéric Mermet, IREPA LASER (France); Patrick Meyrueis, Univ. de Strasbourg (France); Bernard Y. Tumbelaka, Univ. Padjadjaran (Indonesia); Paul Montgomery, Univ. de Strasbourg (France)

In the field of micro-fabrication, many techniques have been developed to decrease the etching size, each with their own advantages, conditions and limitations, not to mention operation/production costs. Those techniques applying laser beams or optical systems are limited by the diffraction limit of the optical heads used. We demonstrate theoretically and experimentally, the use of the photonic jet allows an improvement in the optical resolution to fabricate smaller etching without reducing the wavelength to a visible or ultra-violet beam. We also show the potential of the photonic jet using a nanosecond pulsed near-infrared laser for micro-fabrication. This laser is the most common type of laser used in industrial processing because of the price and the fact that well-packaged sources are available. Their typical spatial resolution in laser etching is limited by the spot size of their focus point at around 25-70 μm. A photonic jet is a high spatial concentration of a beam that emerges in the vicinity of dielectric micro-spheres, which is more than 200 times in intensity, onto a half-wavelength spot. In our experiments, glass micro-spheres (ns = 1.5; diameters of 3.93 ?m, 6.1 ?m (Bangs Lab. Inc.), 22-27 ?m, 32-38 ?m (Cospheric®)) and BaTiO3 micro-spheres (ns = 1.9; diameters of 38-45 ?m, 63-75 ?m, and 75-90 ?m (Cospheric®)) have been used to achieve photonic jets. These micro-spheres are placed on the substrate and a defocused laser beam is used to give a larger beam spot so that several micro-spheres can be illuminated at the same time as well as allowing control of the laser beam fluence. The etching process has been tested on two substrates: silicon wafers, which have a significant absorption at 1064 nm, and glass plates, which have a lower absorption at this wavelength. The smallest marking achieved on silicon is 1.3 ?m of average diameter. Despite the low absorption, etchings have also been achieved on glass using larger micro-spheres. Namely our electromagnetic simulations using the Mie theory in free-space indicate that the larger micro-spheres yield higher intensity concentration that can exceed the laser-induced damaged-threshold (LIDT) of glass. They also push the photonic jet further from the micro-sphere surface and so further inside the substrate. Higher refractive index microspheres could be used to pull the photonic jet nearer to the surface, which would also decrease the spot size of the photonic jet. But, too high refractive index micro-sphere could pull the photonic jet inside the micro-sphere which could cause the micro-sphere to be broken.

The number of pulses, the influence of sphere size and refractive index is analyzed. The shapes of the etched marks are correlated to electromagnetic simulations.

9135-77, Session PS3

Laser-beam modulation to improve efficiency of selecting laser melting for metal powders

Anna Okunkova, Pavel Peretyagin, Yuri Vladimirov, Mikhail Loktev, Marina Volosova, Moscow State Univ. of Technology Stankin (Russian Federation); Sergey V. Fedorov, Moscow State University of Technology "STANKIN" (Russian Federation)

In the work represented the experimental results of laser beam modulation while selective laser melting. First of all the authors considered the possible ways to improve efficiency of the selective laser melting process for metallic powders. The optical diagnostic and experimental work of the process shows the losses of the energy in the melting pool up to 30%. The authors considered all the theoretical and experimental possibilities to reduce the losses on the way of energy fluence. They discovered that the energy loses could be on step when the laser beam heat and melt the powder. This could be consequence of the great thermal gradient in the melting pool because of the Gaussian power density distribution. Nowadays on the market there is almost all equipment produced by important manufactures already had the expander for the laser beam. But the optical diagnostics of the process on the different SLM-machines shows it does not change significantly the situation with loses (EOS M280, CONCEPT LASER M3). These losses lead to throwing-out the non-melted particles from melting pool and that can finally destroy the optics of the machine. The authors considered that the Gaussian power density distribution of the laser beam could be changed by two ways: to flat top and to inverse Gaussian. The model of absorbed power by the powder granules in the melting pool shows that probably inverse Gaussian could demonstrate the optimum steady power density distribution. The authors developed the experimental stand with 200W laser source, scanner, beam expander, beam shaper. The mechanical part of the stands had movable pistons, rakel, electronic components to move them in accordance to the program. As material the authors choose Co-Cr because of its excellent melting properties. By the experimental work were obtained the twenty simple tracks for each of the mode with the different beam velocity and power. Next the examples of the tracks were researched by SEM VEGA 3 LMH on irregularity and inequality. By the image of cross-section the authors have done the conclusion and recommendations about the power density distribution. Optical diagnostic by high velocity camera (700 000x) also gives the important data about the stability of the process, which were discussed.

9135-78, Session PS3

Measurement of energy transfer upconversion in Nd:YAG via the Z-scan technique

Renpeng Yan, Univ. of Southampton (United Kingdom) and Harbin Institute of Technology (China); Jacob I. Mackenzie, SungJin Yoon, Stephen J. Beecher, Univ. of Southampton (United Kingdom)

Nd:YAG is one of the workhorse gain material for many industrial, medical and scientific laser systems. Despite a relatively high quantum defect the spectroscopic properties of the 1064 nm transition enable quite efficient operation, while the lower gain transition around 946 nm, which potentially could be more efficient due to a lower quantum defect, is additionally severely affected by detrimental thermal effects in the host material. One potentially significant parameters that leads to a non-radiative decay channel during laser operation, is energy transfer upconversion (ETU). ETU can have a detrimental effect on the laser performance as an additional source of heat, furthermore reducing the population inversion and lowering the potential gain. Whilst there are

many papers studying the influence of ETU on the quasi-four-level laser performance, both experimental and in simulation, the magnitude of the ETU coefficient from the upper laser level has a significant range of reported values from 5x10-17 to 3x10-16 cm3/s [1, 2], as such its actual impact on performance can be difficult to ascertain with certainty. In this work, we investigate 1at.% Nd:YAG using the z-scan technique to obtain a very sensitive measure of the ETU coefficient, determined to be 4.2+/-0.4 x 10-17 cm3/s with excellent agreement between simulation and experimental data.

The Z-scan technique is a simple method, in which the change in transmission of the sample is measured as it is moved through the focus of a pump laser beam, and correlated to the saturation irradiance. Our experiment used a Ti:sapphire laser tuned to absorption peaks of Nd3+ and focussed to a beam waist radius of 20.6 +/- 0.2 ?m, providing a “uniform” beam throughout our 3.25 mm long 1at.% Nd:YAG sample (deviating <2% from the front to rear of the crystal). When the pump laser was tuned to 808 nm the peak (on axis) irradiance available was 54 kWcm-2, nominally four times the saturation irradiance for this absorption line. A simple spatially dependent steady state model, involving just the ground and upper laser level rate equations has been used to interpret the transmission variation as a function of pump beam irradiance, i.e. the sample position. While ground state bleaching increases the pump transmission with higher irradiance values, ETU has the opposite effect, reducing the amplitude of the highest transmission point at the highest pump irradiance, i.e. at focus. This process provides a surprisingly sensitive measure of the magnitude of the ETU coefficient. We will present a comparison of the value determined in our work and that reported in the literature and discuss the implications for the operation of the weaker laser transitions of Nd:YAG.

1. S. Guy, C.L. Bonner, D.P. Shepherd, D.C. Hanna, A.C. Tropper, B. Ferrand: IEEE J. Quantum Electron. QE-34, 900 (1998)

2. Y. Guyot, H. Manaa, J.Y. Rivoire, R. Moncorg´e, N. Garnier, E. Descroix, M. Bon, P. Laporte: Phys. Rev. B 51, 784 (1995)

9135-79, Session PS3

Er:Cr:YSGG Q-switched laser for pumping mid-IR systems

Helena Jelinková, David Vyhlidal, Miroslav Cech, Jan Sulc, Michal Nemec, Martin Fibrich, Czech Technical Univ. in Prague (Czech Republic)

For coherent pumping of Fe:ZnSe and Fe:ZnMgSe lasers generating giant pulses in mid-infrared part of spectrum (4 – 5 um) the radiation with wavelength ~ 3 um and pulse-length in the range of hundreds of nanoseconds (for room temperature operation) are needed. In our case the Er:YAG Q-switched laser was previously designed and proved for this reason. For more flexibility in pumping of Fe-based mid-infrared materials also new Er:YSGG laser was designed and characterized. The system consists of Er:YSGG active material with the diameter 4 mm and length 100 mm. The plan-parallel open resonator (length 38 cm) was formed by the mirror with reflectivity R~100 % at 2.8 um and output coupler with R=56 % at 2.8 um. The output coupler reflectivity was found as optimal (with regard to output energy) from the tested output couplers with the reflectivity between 30 % to 85 %. As Q-switch the electro-optical shutter - LiNbO3 Pockels cell (LiNbO3 crystal length 30 mm, thickness 5 mm with both end cut at Brewster angle) was used. To support the horizontal polarization generation the CaF2 plan plate was inserted under Brewster angle between the active crystal and output mirror. The applied quarter-wavelength voltage was 2 kV. As result the giant pulses with the energy 53 mJ and length of pulse ~ 100 ns were obtained for pumping energy 24 J. The generated wavelength was measured to be 2.79 um and space structure was close to Gaussian. The output radiation characterization was provided also for the same system in which the Er:YSGG crystal was changed to Er:YAG one with the same dimensions. The threshold pumping values in the case of free-running regime (high voltage on Pockels cell was switched off) for Er:YSGG and Er:YAG laser were 10 times higher for Er:YAG crystal for the same arrangement (output coupler reflectivity ~ 60 %). The maximum output energy and pulse-length in Q-switched regime for Er:YAG laser were 38 mJ and ~110 ns, respectively. From the results follow that the Er:YSGG system with the large output energy is good candidate for pumping of Fe:ZnSe or Fe:ZnMgSe systems. The comparison of results obtained during measurements of both Fe:ZnSe and Fe:ZnMgSe lasers working under pumping by the radiation of Er:YSGG and Er:YAG lasers will be also done.

9135-80, Session PS3

Remotely manageable system for stabilizing femtosecond lasers

Martin ?í?ek, Václav Hucl, Radek ?míd, B?etislav Mikel, Josef Lazar, Ond?ej ?íp, Institute of Scientific Instruments of the ASCR, v.v.i. (Czech Republic)

Setups based on CW lasers locked to optical cavities are widely used in experiments in the field of length metrology of low expansion materials. By determining the wavelength of such locked laser the length of the cavity can be assessed. A stabilized optical frequency comb is often used as a reference for measuring the wavelength in this type of experiments. By locking the repetetition and offset frequencies of the comb to a high-grade radiofrequency (RF) oscillator (GPSDO, H-maser, atomic clock) its relative frequency stability is transferred from the RF domain to the optical output spectrum of the comb. This is usually accomplished using various techniques based on phase-locked loops (PLL). In order to measure temperature dilatations of low-expansion materials it is absolutely necessary to keep the comb in operation as long as possible (one week or even more). It is also necessary to eliminate the human presence in the laboratory to the maximum possible extent. In our contribution we are presenting a remotely managed electronic system for stabilizing offset (fceo) and repetition (frep) frequencies of mode-locked femtosecond lasers. The device is based on a telecommunication-grade PLL integrated circuit (IC) that includes a direct digital synthesizer of the reference signal, high-speed frequency dividers, a digital phase detector, a charge pump and loop-filtering circuits. The IC is accompanied by necessary radiofrequency RF circuits (amplifiers, filters) for preprocessing of the input signals. The RF equipment is controlled by a microcontroller unit (MCU) that allows users to set the parameters of the device remotely using the CAN bus interface (tune the reference frequency, etc.) The MCU serves also for monitoring the voltage output of the PLL. A slow digital second-order controller is implemented in the MCU software. Its task is to improve the long-term stability by maintaining the output voltage of the first-order PLL controller in an ideal working range. Pilot experiments were conducted to stabilize frep and fceo of the optical frequency comb with respect to a precise RF reference, which was a 10MHz GPS-disciplined oscillator. We used an optical frequency comb with frep = 100 MHz and 1 550nm central wavelength. The comb was equipped with an f-2f interferometer for measuring of fceo. Results show that the system is capable of stabilizing the optical frequency comb to better than 10^-11 order relative stability and operate uninterruptedly for 10 days and more.

9135-44, Session 10

Volume Bragg gratings for spectral, angular and temporal control of solid state lasers *(Invited Paper)*

Leonid B. Glebov, CREOL, The College of Optics and Photonics, Univ. of Central Florida (United States)

This presentation is a survey of achievements in holographic optical elements (volume Bragg gratings, VBGs) and phase masks recorded in photo-thermo-refractive (PTR) glass. The presentation includes a brief description of basic properties of PTR glass and main types of VBGs and phase masks recorded in this glass flowed by their main applications. The use of narrow band reflecting VBGs as output couplers in external

resonators for solid state, fiber and semiconductor lasers resulted in dramatic narrowing of emission spectra by three orders of magnitude with minimum power penalty. Transverse chirped VBGs with variable period were successfully used for spectral tuning of lasers. Effective transverse mode selection by both transmitting and reflecting VBGs resulted in dramatic increase of their spatial brightness. Reflecting chirped VBGs with variable period were used for stretching and compression short laser pulses resulting in a decrease of size of compressors by orders of magnitude. VBGs were successfully used for coherent and spectral combining of laser beams. Volume phase masks recorded in PTR glass provide effective conversion of both free space and waveguide modes. Incorporation of phase masks inside of VBGs enabled creation of masks operating in wide spectral range and multiplication of masks within a single glass plate.

9135-45, Session 10

Investigation on thermal behavior of resonant waveguide-grating mirrors in an Yb:YAG thin-disk laser

Martin Rumpel, Benjamin Dannecker, Andreas Voss, Univ. Stuttgart (Germany); Michael Moeller, Christian Moormann, AMO GmbH (Germany); Thomas Graf, Marwan Abdou Ahmed, Univ. Stuttgart (Germany)

We present the experimental investigations of different designs of resonant waveguide-grating mirrors which are used as intracavity folding mirror in an Yb:YAG thin-disk laser. The studied mirrors combines structured fused silica substrates, thin-layer waveguide (Ta2O5), a buffer layer (SiO2) and partial reflectors. The grating period was chosen to be 510 nm to allow resonances at an angle of incidence of ~ 10° for TE polarization. The waveguide layer has a thickness of 236 nm. It is followed by the buffer layer with a thickness of 580 nm and the subsequent alternating Ta2O5/SiO2 layers. The exact coating sequence depends on the two design approaches which were investigated in this work: either introducing different partial reflectors, i.e. stacks of quarter wave layers on top of the waveguide while keeping the groove depth of the grating constant, or increasing the grating depth, while keeping an identical partial reflector. The investigation was focused on the rise of the surface temperature due to the coupling of the incident radiation to a waveguide mode, as well as on the laser efficiency, polarization and wavelength selectivity. It is found that, when compared to the simplest RWG design which consists of only a single Ta2O5 waveguide layer, damage threshold as well as laser efficiency can be significantly increased, while the laser performances in terms of polarization- and wavelength selectivity are maintained. So far, the presented RWG allow the generation of linear polarization with a narrow spectral linewidth down to 25 pm FWHM in a fundamental mode Yb:YAG thin-disk laser. Damage thresholds of 60kW/cm2 have been reached where only 63K of surface temperature increase was observed. This shows that the improved mirrors are suitable for the generation of kW-class narrow linewidth, linearly polarized Yb:YAG thin-disk lasers.

9135-46, Session 10

Wavelength stabilisation of a DFB laser diode using measurement of junction voltage

Abdullah S. Asmari, Jane Hodgkinson, Edmond Chehura, Stephen E. Staines, Ralph P. Tatam, Cranfield Univ. (United Kingdom)

Laser diode temperature characterisation and stability are vital for applications such as spectroscopy and data communication. Laser diode emission wavelength and threshold current are both functions of temperature. The ambient temperature, internal heating by the excitation current and the thermal design of the laser diode package all contribute to the temperature of the laser diode active region.

In a conventional system, laser diode temperature is controlled using a Peltier element with a temperature sensing thermistor. The thermistor is placed at a short distance from the laser diode chip and consequently measures the temperature of the package at that position, potentially introducing a systematic error. Despite the use of good thermal design and a case, a change in ambient temperature may cause a change to internal thermal gradients, resulting in laser diode wavelength fluctuation.

We have developed a novel system to measure the temperature of the laser diode junction via the forward and junction voltage. Initial experimental work suggests that this results in better thermal stability, and hence improved stability of the emitted wavelength, than the conventional thermistor based temperature controller. In this paper, both thermistor- and voltage- controlled systems are compared for long term stability and variable ambient temperatures. For ambient temperature changes in the range 10-30°C, we have demonstrated a wavelength stability of 20pm compared to 40pm for thermistor-based control. The method has been applied to a 1650nm DFB laser diode for use in tunable diode laser spectroscopy (TDLS) of methane and is compatible with TDLS signal processing.

9135-47, Session 10

A hybrid semiconductor-glass waveguide laser

Youwen Fan, Univ. Twente (Netherlands) and MESA+ Research Institute for Nanotechnology (Netherlands); Ruud M. Oldenbeuving, SATRAX B.V. (Netherlands) and Univ. Twente (Netherlands) and MESA+ Research Institute for Nanotechnology (Netherlands); Edwin Klein, XiO Photonics B.V. (Netherlands); Chris Lee, Univ. Twente (Netherlands) and MESA+ Research Institute for Nanotechnology (Netherlands) and FOM Institute DIFFER (Netherlands); Hong Song, Technische Univ. Delft (Netherlands) and Zhejiang Univ. (China); Reza Khan, Herman Offerhaus, Univ. Twente (Netherlands); Peter V. D. Slot, Klaus J. Boller, Univ. Twente (Netherlands) and MESA+ Research Institute for Nanotechnology (Netherlands)

We report on a novel type of laser in which a semiconductor laser is controlled by optical feedback from a glass-waveguide circuit. The circuit comprises micro-ring resonators to provide highly frequency selective feedback for obtaining single-frequency and wavelength tunable operation of the laser. Due to the wide transparency range of glass, the named concept can be applied over a wide spectral region, including the entire visible range (400nm to 2.3 μm), by providing feedback to amplifiers based on different semiconductor materials, such as InGaN, AlGaInP, GaInAsSb. Due to the low loss of glass waveguides, micro-ring resonators with high quality factors and extended feedback path lengths can be employed for enhancing the frequency selectivity and narrowing the spectral laser bandwidth.

We present an experimental characterization of such a hybrid semiconductor-glass waveguide laser for the 1.55 μm wavelength range. The laser is based on an InP optical gain chip and a low-loss (0.06 dB/cm) Si3N4 glass waveguide chip with two sequential high-Q ring resonators of slightly different radii. For maximizing the coupling efficiency through optical mode matching between the diode and glass waveguide chips, the glass waveguide is equipped with an adiabatic tapering. The laser shows a record-narrow spectral linewidth of 24 KHz (measured at 2 mW output). Further enhancing the feedback is expected to further narrow the linewidth, possibly towards the sub-KHz range. By means of thermally changing the refractive index of the micro-ring resonators, the wavelength of the hybrid laser can be tuned over a broad range of 42.3 nm (1534.4 -1576.7 nm), which covers the entire telecommunication C-band. With these properties, InP-glass hybrid laser are, for instance, of great interest in long-haul high-capacity DWDM systems and as phase reference in optical beam-forming networks. Operation in

other wavelengths ranges, based on alternative semiconductor materials, can be of relevance for other applications such as gas sensing or precision metrology.

9135-49, Session 10

Lyot-filter based multiwavelength random distributed feedback fiber laser

Srikanth Sugavanam, Aston Univ. (United Kingdom) and Novosibirsk State Technical Univ. (Russian Federation); Zhijun Yan, Aston Univ. (United Kingdom); Vladimir Kamynin, Andrei S. Kurkov, A. M. Prokhorov General Physics Institute (Russian Federation); Lin Zhang, Aston Univ. (United Kingdom); Dmitry V. Churkin, Aston Univ. (United Kingdom) and Novosibirsk State Technical Univ. (Russian Federation)

Recently, a random distributed feedback (DFB) fiber laser operating via Raman gain and random feedback owing to the Rayleigh backscattering was demonstrated [1]. While the threshold of this laser is relatively high, its efficiency is quite comparable to existing CW lasers [1,2]. Up to date, different configurations of random DFB fiber lasers are demonstrated including cascaded, tunable and multiwavelength. In the present work, a novel simple and robust design of the multiwavelength random DFB fiber laser is demonstrated. The laser is based on an all-fiber Lyot filter [3] thus having only one wavelength selective element contrary to the previously demonstrated multiwavelength generation in scheme based on a set of a large number of individual FBGs [4]. The laser generates multiple wavelengths simultaneously in the whole range of the Raman gain spectral profile. The position of each individual wavelength coincides with the passbands of the Lyot filter. Lines have a typical spectral width within 0.08-0.14 nm range, which is much narrower than the Lyot transmission width of 0.2 nm and much narrower than in previous demonstrations of multiwavelength random DFB fiber lasers. The demonstrated power distribution among different lines is much flatter when compared to the spectral profile of the Raman gain or that of the random DFB fiber laser without any filtering elements or with set of FBGs as wavelength selective elements, with a variation of only 0.5 dB over a 4 nm span. At higher pump power, second Stokes wave is generated, which is also multiwavelength and of flat power distribution among different lines.

The demonstrated flatness and linewidth-narrowing suggests that nonlinear processes play an important role in the formation of generation in multiwavelength random DFB fiber laser and different lines could interact nonlinearly with each other. In particular, each generation line could have its own longitudinal distribution of the power along the power thus decreasing the competition of the different lines for the same pump [4]. However, different lines could be correlated. Note that existence of possible mode correlations in the random DFB fiber laser has been reported recently in [5] that resulted in non-Gaussian intensity statistics similarly to the statistics of conventional Raman fiber lasers [6]. The presented multiwavelength random DFB fiber laser could be used as a test bed for experimental investigation of possible nonlinear interaction and correlations as spectral width of individual line (0.08-0.14 nm being equal to 10-18 GHz) is within the electrical bandwidth of real time oscilloscopes. Moreover, simultaneous measurements of the intensity dynamics in different lines could be of interest as it could reveal directly correlations between different lines.

[1]. S.K.Turitysn et al, Nat. Photonics 4, 231–235 (2010).

[2]. I.D.Vatnik et al, Opt. Express 20, 28033–8 (2012).

[3]. Z.Yan et al, Opt. Lett. 37, 353–5 (2012).

[4]. A. El Taher et al, Opt. Lett. 36, 130–132 (2011).

[5]. S.V.Smirnov et al, Opt. Express 21, 21236-41 (2013).

[6]. D.V.Churkin et al, Opt. Lett. 35, 3288–3290 (2010).

9135-50, Session 11

Thin-disk multipass amplifier for ultrashort laser pulses with kilowatt average output power and mJ pulse energies *(Invited Paper)*

Jan Philipp Negel, Andreas Voss, Marwan Abdou Ahmed, Univ. Stuttgart (Germany); Dominik Bauer, Dirk H. Sutter, Alexander Killi, TRUMPF Laser GmbH & Co. KG (Germany); Thomas Graf, Univ. Stuttgart (Germany)

We report on a Yb:YAG thin-disk multipass amplifier for ultrashort laser pulses delivering an average output power of 1.1 kW which is –to the best of our knowledge- the highest output power reported on such a system so far. A commercial TruMicro5050 laser delivers the seed pulses with an average power of 80 W at a wavelength of 1030 nm, a pulse duration of 6.5 ps and a repetition rate of 800 kHz. These pulses are amplified to 1.38 mJ of pulse energy with a duration of 7.3 ps. To achieve this, we realized a scheme in which an array of 40 plane mirrors is used to fold the seed beam geometrically over the pumped thin-disk crystal. Exploiting the incoming linear polarization, an overall number of 40 double-passes over the disk was realized by using the backpath through the amplifier with the orthogonal linear polarization state. Thermal issues on the disk were mitigated by zero-phonon line pumping at 969 nm directly into the upper laser level and by employing a retroreflective mirror pair. The amplifier exhibits an optical efficiency of 44 % and a slope efficiency of 46 %. The beam quality was measured to be better than M?=1.25 at all power levels. As this system can deliver high pulse energies and high average output powers at the same time without the need of a CPA technique, it can be very suitable for high productivity material processing with ultrashort laser pulses. Furthermore, we will present recent results on nonlinear frequency conversion as well as pulse energy scaling with this system.

9135-51, Session 11

Microfabrication of transparent materials using filamented femtosecond laser beams

Simas Butkus, Valdas Sirutkaitis, Domas Paipulas, Vilnius Univ. (Lithuania)

A great number of articles have been published on glass drilling and cutting applications, however, such systems typically employ high NA focusing conditions, low repetition rate lasers and complex fast motion translation stages. Due to the sensitivity of such systems, slight instabilities in parameter values can lead to crack formations in the samples, severe fabrication rate decrement and poor quality overall results. A microfabrication system lacking the stated disadvantages was constructed and demonstrated in this report. An f-theta lens was used in combination with a galvanometric scanner capable of beam scanning rates up to 2 m/s, moreover, an additional water pumping system that enables formation of variable thickness water films on the samples in real time was constructed. The water acts as a medium where filamentation of the laser pulse appears, which in turn decreases the focal spot diameter and increases fluence prior to impinging on the surface of the sample. Due to strong nonlinear effects (self-focusing, multiphoton absorption, diffraction), the filamented pulse propagates along the z axis with negligible divergence producing strong ablation throughout the cross section of the sample. The strong ablation regime is evident even after several mm of propagation along the z axis, therefore, the application of filamentation entirely eliminates the need for z axis positioning. In addition, strong electron generation in the water and subsequent electron-phonon relaxation induces water boiling and evaporation that enhances debris removal from the samples ablated channels due to pressure gradient formations, moreover, it reduces thermal stress through cooling,

giving better quality end results.

This article demonstrates the application of an IR femtosecond (280 fs) laser with an average power of 4.5 W and variable repetition rate (25 – 200 kHz) towards rapid cutting and drilling of different types of transparent materials (soda-lime glass, Corning Gorilla glass, sapphire). The constructed microfabrication system yielded through holes in all of the stated materials. Holes with 2 mm in diameter were drilled in soda-lime glass (1 mm thick), Corning Gorilla glass (1,1 mm thick) and sapphire (450 ?m thick). The fabrication time for through-hole fabrication for these materials was found to be 40, 120 and 40 seconds accordingly. Moreover, complex-shape fabrication was demonstrated for the stated transparent materials. By varying the repetition rate of the laser, scanning speed, focal position and water film thickness optimal conditions for rapid glass cutting and drilling via filamentation in water were determined. It is worth noting, that fabrication without filamentation was impossible in these materials, due complete shattering of the samples caused by thermal stress.

9135-52, Session 11

Laser emission from Nd:YAG laser waveguides realized by femtosecond-laser writing techniques

Gabriela M. Salamu, Florin C. Jipa, Marian Zamfirescu, Nicolaie Pavel, National Institute for Lasers, Plasma and Radiation Physics (Romania)

The waveguide lasers are of special interest in optoelectronics due to their compact dimensions, low threshold of emission and good output performances. Such optical devices can be fabricated in an existing host by various methods, like thermal ion indiffusion, ion or proton exchange, as well as by proton or ion beam irradiation. Recently, direct writing with a femtosecond (fs) laser has been proved to be a powerful tool for realizing waveguides. Using the direct fs-laser writing technique, two types of tracks can be realized, depending on the material properties and on the fs-laser characteristics. The first kind consists of a single line that is used itself for light propagation and it is specific to glasses and LiNbO3. The second type of writing damages the material inside the inscribed track and causes a stress induced refractive index change in the adjacent region; in this case the light is guided in between two such tracks. Thus, such waveguides were realized in various Nd-laser media, and laser emission at 1.06 microns was obtained using the pumping at 807 nm with Ti:sapphire laser.

In this work we report realization of two-walls type and buried depressed waveguides in Nd:YAG single crystal and polycrystalline ceramics laser media, using the fs-laser writing technique. Laser emission at 1.06 and 1.32 microns was realized under the pump at 807 nm with fiber-coupled diode laser. The inscribing was realized with a fs-laser system (Clark CPA-2101) that yielded pulses at 775 nm with 200-fs duration and 2-kHz repetition rate. The tracks were inscribed in 0.7-at.% Nd:YAG single crystals and in 0.7-at.% or 1.1-at.% Nd:YAG ceramics. Two-wall type waveguides and buried depressed waveguides of square, rectangular, circular or elliptical shapes were realized. The propagation losses, which were measured at 632.8 nm, were in the range of 1.1 to 1.4 dB/cm for the two-wall waveguides, and between 1.0 to 2.2 dB/cm for the buried depressed waveguides. Efficient laser emission was achieved at 1.06 and 1.3 microns. Thus, in the case of the Nd:YAG single crystal (thickness of 5 mm), laser pulses at 1.06 microns with 1.8 mJ energy (optical efficiency of 0.20) and continuous-wave output power of 0.54 W for 3.8 W incident pump power were measured from a buried depressed waveguide of elliptical (120 microns?145 microns) shape. The same waveguide outputted laser pulses at 1.32 microns with 0.4 mJ energy. In the case of Nd:YAG ceramics, laser pulses with 1.5 mJ energy at 1.06 microns were delivered from a 100-microns diameter buried depressed waveguide that was realized in the the 8.0 mm thick, 1.1-at.% Nd:YAG ceramics. A detailed characterization of the laser performances was performed and the results will be presented comparatively. These are the first results on laser emission at 1.06 and 1.32 microns using the pump with fiber-coupled diode lasers of waveguides realized in Nd:YAG by fs-writing technique, and prove the concept of compact laser devices of interest in optoelectronics.

9135-53, Session 11

Strong ion migration in high-refractive index contrast waveguides formed by femtosecond laser pulses in phosphate glass

Toney Teddy Fernandez, Jesús del Hoyo Muñoz, Consejo Superior de Investigaciones Científicas (Spain); Patricia Haro-González, Univ. Autónoma de Madrid (Spain); Belen Sotillo, Univ. Complutense de Madrid (Spain); Margarita Hernandez, Consejo Superior de Investigaciones Científicas (Spain); Daniel Jaque Garcia, Univ. Autónoma de Madrid (Spain); Paloma Fernandez, Univ. Complutense de Madrid (Spain); Concepcion Domingo, Jan Siegel, Francisco Javier Solís Céspedes, Consejo Superior de Investigaciones Científicas (Spain)

Strong ion migrations in phosphate glass was found to be the key source for high refractive index contrast waveguides inscribed with a femtosecond laser. Experiments were focused on a commercial phosphate glass (Kigre QX) containing single and multivalent ions such as Lanthanum, Aluminium, Potassium and Silicon along with optically active trivalent rare-earth ions viz. Erbium, Ytterbium and Cerium. The best waveguide processing window was found for 500 kHz repetition rate, 580 nJ - 700 nJ pulses energies and 40 - 80 μm/s scan speeds. Differential Interference Contrast (DIC) transmission optical microscopy, of the written waveguides, revealed that the refractive index increase of the guiding region has a high contrast with a circular shape. Based on measurements of the NA of waveguides, the positive refractive index change (?n) of the guiding region has been estimated to be 1.5x10-2 (at 1620 nm). X-ray microanalysis was carried out on the best waveguide which was written with 640nJ and 60 μm/s. The compositional map of the waveguides evidenced a quite homogeneous increase of La concentration in the high refractive index region of the order of ~25% (relative to the La conc. in the un-irradiated material). This large enrichment in La was accompanied by the cross migration of K to a nearby low refractive index zone that increases its local concentration by a similar amount. We also saw a smaller depletion of P in the high refractive index zone. Changes in the Al concentration was below experimental resolution. In the case of La-phosphate glasses it has been reported that within the low compositional region 0< La2O3<15mol% the density and refractive index of the glass increase linearly with the La2O3 content (?n per mole fraction of La2O3 ≈ 4.9x10-3) mainly because of the relative mass of the La3+ ions and that the relatively small size of the isolated La-polyhedra can be easily accommodated by the phosphate network. For the observed relative increase of 25% in the La content, a ?n ≈ 1.22 x 10-2 could be predicted, which is in very good agreement with 1.5 x 10-2 value obtained from the NA measurements. Since there is no dilation of the network upon increasing the density at the positive index zone, no stress induced birefringence was observed. This observation was substantiated by the micro-raman measurements showing a (PO2)sym band shift of only 3.5cm-1 and negligible FWHM variation indicating that the La-polyhedra was accommodated within the phosphate network without an strong dilations. Hypersensitive Erbium fluorescence transition 4S3/2?4I5/2 at 544 nm was selected for micro-PL analysis. A spatial variation of the spectral shift indicating a red shift of almost 20 cm-1 was observed suggesting a large increase of covalency, indicative of relatively large local compositional changes (associated to local changes in the La, Al or K contents) in the guiding region totally agreeing to the results from the X-ray microanalysis. These results in general confirm the feasibility of adapting the glass composition for enabling the laser-writing of high refractive

index contrast structures via spatially selective modification of the glass composition.

9135-54, Session 12

Power and energy scaling of Kerr-lens mode-locked thin-disk oscillators *(Invited Paper)*

Oleg Pronin, Ludwig-Maximilians-Univ. München (Germany); Jonathan Brons, Marcus Seidel, Elena Fedulova, Max-Planck-Institut für Quantenoptik (Germany); Alexander A. Apolonskiy, Ludwig-Maximilians-Univ. München (Germany) and Max-Planck-Institut für Quantenoptik (Germany); Vladimir L. Kalashnikov, Technische Univ. Wien (Austria); Vladimir Pervak, Ludwig-Maximilians-Univ. München (Germany); Ferenc Krausz, Ludwig-Maximilians-Univ. München (Germany) and Max-Planck-Institut für Quantenoptik (Germany)

The goal of this talk is to provide a guideline for Kerr-lens mode-locking (KLM) of thin-disk oscillators. This includes cavity design, hard and soft-aperture optimization, handling of thermal effects in intra-cavity optics as well as methods of average power and energy scaling. The main differences and similarities between mode-locking of Ti:sapphire bulk and Yb:YAG thin-disk oscillators are presented and oscillators with different gain media are described. Applications for the developed oscillators such as femtosecond enhancement cavity seeding, regenerative amplifier seeding and their long and short term stability are discussed. Emphasis is put on the suitability of KLM thin-disk oscillators not only for laboratory but also for industrial applications.

9135-55, Session 12

948 kHz repetition rate, picosecond pulse duration, all-PM 1.03 μm mode-locked fiber laser based on nonlinear polarization evolution

Simon Boivinet, Multitel A.S.B.L. (Belgium) and Faculté Polytechnique de Mons (Belgium); Jean-Bernard Lecourt, Yves Hernandez, Multitel A.S.B.L. (Belgium); Andrei A. Fotiadi, Patrice Mégret, Faculté Polytechnique de Mons (Belgium)

We present in this study a PM all-fiber laser oscillator passively mode-locked (ML) at 1.03 μm. The laser is based on Nonlinear Polarization Evolution (NPE) in polarization maintaining (PM) fibers. In order to obtain the mode-locking regime, a nonlinear reflective mirror including a fibered polarizer, a long fiber span and a fibered Faraday mirror (FM) is inserted in a Fabry-Perot laser cavity. In fact the NPE occurs in the long span (100m) of the standard PM fiber (PM980) between the polarizer and the Faraday mirror. In this configuration, CW light cannot oscillate in the cavity because its polarization turned to 90° and it is cut by the polarizer when it is reflected by the FM. In pulsed operation, the light travelling in the PM fiber sustains nonlinear effects leading to an additional rotation of the polarization that can be sufficient for transmission through the polarizer after reflection on the FM.

In this work we will explain the principles of operation of this uncommon laser design that permits to generate ultrashort pulses at low repetition rate. In particular we will focus on the results obtained for 100 m of fiber that allows the achievement of a stable pulsed operation at a particularly low repetition rate of 948 kHz. In this experiment, the measured pulse duration is about 6 ps. To our knowledge this is the first all-PM mode-locked laser based on the NPE with a cavity of 100m length fiber.

Furthermore, the different mode-locked regimes of the laser, i.e. multi-pulse, noise-like mode-locked and single pulse, will be presented together with the ways of controlling the apparition of these regimes. When the single pulse mode-locking regime is achieved, the laser delivers linearly polarized pulses in a very stable way. The laser has accumulated 10 hours of continuous operation without any discontinuity or fluctuation of the mode-locking operation proving the robustness of the design.

Finally, this study includes numerical results which are obtained with the resolution of the NonLinear Schrodinger Equations (NLSE) with the Split-Step Fourier (SSF) algorithm. This modeling has led to the understanding of the different modes of operation of the laser. In particular, the influence of the different parameters (span length, angle of polarization, peak power) on the transmission of the nonlinear mirror is studied.

9135-56, Session 12

Experimental observation of coexisting noise-like pulses and solitons in a passively mode-locked fiber laser

Antoine F. J. Runge, Claude Aguergaray, Miro Erkintalo, Neil G. R. Broderick, The Univ. of Auckland (New Zealand)

Complex dissipative structures are known to abound in ultrafast fiber lasers, and they have attracted significant attention during the past few years. Indeed, it is now well-known that passively mode-locked fiber lasers can support a myriad of outputs, ranging from ultra-stable dissipative solitons to bursts of noise-like (NL) fluctuations and rains of solitons. So far distinct dynamical regimes have been predominantly observed in isolation, and their interrelationships remain nebulous. In this contribution, we report the first observation of complex coexistence of noise-like pulses and stable solitons in a passively mode-locked fiber laser. Significantly, we show that solitons can be spontaneously created from a noise-like burst, and also that their presence maps into an enhancement of the phase coherence of the laser output. The laser used in our experiments is an Erbium-doped fiber laser mode locked using the nonlinear polarization evolution. By suitably adjusting the intracavity polarization controller we are able to excite both soliton and noise-like operation. When the laser is operating in the NL regime, we find that minute adjustment of the polarization controller can give rise to small-amplitude pulses moving away from the main burst, resembling the dynamics of soliton rains. To gain more insight we use the dispersive Fourier transform in order to record the single-shot spectra of the laser output in real time. The results allow us to identify the drifting pulses as solitons. We further use a Michelson-like interferometer to measure the degree of first-order coherence of the output pulse train and note that the observed spectral fringes emerge from the drifting solitons while the rest of the spectrum displays negligible phase-coherence. Our results could lead to improved understanding on the formation and nature of noise-like pulses and their relationship with stable dissipative solitons.

9135-57, Session 12

Extent of parameter variability for different pulses from a passively mode-locked fibre laser

Sergey M. Kobtsev, Sergey V. Smirnov, Sergey V. Kukarin, Aleksey V. Ivanenko, Novosibirsk State Univ. (Russian Federation) and Tekhnoscan-Lab LLC (Russian Federation)

Fibre lasers passively stabilised due to the effect of non-linear polarisation evolution can operate in different regimes featuring one or several pulses on the resonator round trip. In the single-pulse regime, the laser may generate three types of pulses [1], of which two exhibit intra-pulse intensity and phase fluctuations. In the extreme case, these fluctuations decompose each pulse into a wave-packet filled with a stochastic sequence of femtosecond sub-pulses. Such pulses have double-scale temporal structure with different typical time scales of the pulse envelope and internal fluctuations. One important feature of

these double-scale pulses (otherwise often called ‘noise-like’) is that they may carry relatively high energy [2]. The present work for the first time announces the results of investigation into variability of parameters of both double-scale and conventional (‘single-scale’) laser pulses, as well as reports on studies of how efficient frequency doubling of these pulses may be.

The conducted research has shown that different settings of polarisation controllers in passively mode-locked fibre lasers may lead to as many as hundreds of various stable mode locking regimes, in which the pulse parameters, such as duration, energy, and spectrum width, may differ by more than an order of magnitude. Thus in our simulations for 10-m long fiber laser we obtained pulses with duration ranging from 4 up to 80 ps and spectral bandwidth of 1-15 nm. This paper discusses the observed ranges of parameter variability of different pulses and demonstrates the most likely realized mode-locked regimes.

Our theoretical and experimental studies of efficiency of frequency doubling of double-scale and conventional laser pulses in most common types of mode locking operation have established that second harmonic generation can actually be even somewhat more efficient with double-scale pulses as compared to conventional ones of similar energy and duration. Since the energy of double-scale pulses and their long-time stability are potentially higher and they are much easier to obtain in long and ultra-long cavities [3,4], double-scale pulses may constitute an attractive alternative to conventional laser pulses for non-linear spectral transformations and applications where the internal pulse structure does not play a major role: Raman amplifiers, biomedicine, microscopy methods, etc.

1. S.Smirnov, S.Kobtsev, S.Kukarin, and A.Ivanenko. Three key regimes of single pulse generation per round trip of all-normal-dispersion fiber lasers mode-locked with nonlinear polarization rotation. Optics Express, 20 (24), 27447-27453 (2012).

2. S.V.Smirnov, S.M.Kobtsev, S.V.Kukarin, and S.K.Turitsyn, Mode-Locked Fibre Lasers with High-Energy Pulses (InTech, 2011), Chapter 3.

3. W.H.Renninger and F.W.Wise, Dissipative soliton fiber lasers (Wiley-VCH Verlag GmbH & Co. KgaA, 2012), Chapter 4.

4. P.Grelu and N.Akhmediev. Dissipative solitons for mode-locked lasers. Nature Photonics 6(2), 84–92 (2012).

Conference 9136A: Nonlinear Optics and its Applications

Monday - Wednesday 14–16 April 2014 • Part of Proceedings of
SPIE Vol. 9136 Nonlinear Optics and Its Applications VIII; and Quantum Optics III

9136-1, Session 1

Nonlinear integrated photonics for photon generation *(Invited Paper)*

Alex S. Clark, The Univ. of Sydney (Australia)

No Abstract Available

9136-2, Session 1

Domain-engineered PPLN for entangled photon generation and other quantum information applications *(Invited Paper)*

Paulina S. Kuo, National Institute of Standards and Technology (United States); Jason S. Pelc, Hewlett-Packard Laboratories (United States); Oliver Slattery, Lijun Ma, Xiao Tang, National Institute of Standards and Technology (United States)

No Abstract Available

9136-3, Session 1

Efficient four-wave mixing by phase-mismatch switching

Yannick W. Lefevre, Nathalie Vermeulen, Hugo Thienpont, Vrije Univ. Brussel (Belgium)

Nonlinear four-wave-mixing (FWM) interactions enable a wide variety of photonic functionalities, including wavelength conversion, all-optical switching, signal regeneration, and generation of entangled photons. The main challenge in realizing efficient FWM interactions is the so-called phase mismatch between the interacting waves. For large phase-mismatches, the impact of FWM oscillates between gain and loss along the propagation path, effectively disrupting the desired build-up of optical intensity. To achieve efficient FWM interactions the waves either have to be phase-matched, or a quasi-phase-matching (QPM) scheme, such as QPM based on dispersion compensation or modulated nonlinearities, has to be realized. However, these techniques require light-guiding media with specific characteristics. For instance, to realize phase-matching or QPM based on dispersion compensation, the dispersion of the medium should allow one to operate respectively near or around a zero phase-mismatch. Alternatively, QPM based on modulated nonlinearities requires a medium in which the strength of the FWM effects can significantly be modulated.

We propose a more general QPM scheme for enabling efficient FWM interactions in the presence of a large phase-mismatch. The scheme is based on increasing the distance over which there is FWM gain, while simultaneously decreasing the distance over which there is FWM loss. This is achieved by adiabatically alternating between two phase-mismatch values along the propagation path. We discuss in detail how such phase-mismatch switching (PMS) can be employed to achieve QPM of a FWM process, what the requirements are for optimal FWM efficiency, and how the scheme is impacted by nonlinear dispersion as well as optical losses. Additionally, we describe how QPM by PMS can be implemented with a silicon-on-insulator strip waveguide of which the width is adiabatically varied between two values along the propagation path. By means of numerical simulations, we show that such a waveguide can enhance the wavelength conversion by 20 dB after 1 cm compared to a corresponding constant-width waveguide. For a pump wavelength of 1550 nm, PMS enables efficient conversion (>–21 dB) around a target signal wavelength situated anywhere in the entire near-infrared wavelength domain of 1300–1900 nm.

9136-4, Session 1

Quantum dot diode optical parametric oscillator

Silvia Mariani, Alessio Andronico, Univ. Paris 7-Denis Diderot (France); Jean-Michel Gérard, Commissariat à l'Énergie Atomique (France); Ivan Favero, Sara Ducci, Giuseppe Leo, Univ. Paris 7-Denis Diderot (France)

Available telecom laser diodes exhibit limited wavelength tunability, provided by temperature or current control. For example, InGaAs Sample Grating Distributed Bragg Reflector single-mode telecom laser diodes are tunable over ~50 nm for a control current change of 90 mA. Moreover, the present technology for light emission in the 2-3μm range does not fulfil yet market expectations. On the one hand, intersubband quantum cascade lasers are not commercially available for emission below 3 μm, because of severe constraints on epitaxial growth. On the other hand, GaSb laser diodes, which rely on strained quantum wells, exhibit CW operation at room temperature from 2 to 3 μm but are still at the development stage too.

For these reasons, near-infrared electrically pumped sources based on intracavity nonlinear processes are attractive given their compactness and promise of practical application. In this context the AlGaAs family is an appealing material choice due to the large non-resonant quadratic nonlinearity of GaAs (d_{14} ≈ 100 pm/V in the near infrared), its good thermal and mechanical properties, and its mature technology. However, a major difficulty in the fabrication of nonlinear active devices is the need of fulfilling the phase-matching (PM) condition. Since GaAs lacks birefringence, various approaches have been employed to achieve PM in low-loss optical waveguides, including quasi-PM [1], form-birefringence PM [2], and modal PM [3].

Here we propose and model an electrically pumped continuous-wave optical parametric oscillator (OPO) in an AlGaAs waveguide exploiting modal PM. Laser emission from InAs quantum dots (QDs) embedded in the waveguide core is designed to excite a second-order mode at 980 nm. At the OPO degeneracy, this mode is phase matched with two cross-polarized fundamental signal and idler modes around 1960 nm. The main advantage of QDs is related to their ability to trap charge carriers and quench diffusion toward non-radiative recombination centers. For lasers, this entails a strong reduction of lateral diffusion length and surface recombination velocity at etched sidewalls [4]. At variance with quantum wells, this unique property of QD active media allows the fabrication of deeply etched narrow-stripe (2-3 μm) laser diodes with threshold currents comparable to those of broad area devices [5]. We show that the possibility to exploit such narrow deeply etched ridge waveguides provides a useful and efficient degree of freedom - the ridge width - to ensure phase matching. This is a crucial point for the experimental demonstration of such devices. With our design, we calculate good transport properties (transparency threshold current around 20 A cm^{-2}), high conversion efficiency (? = 407% W^{-1} cm^{-2}), and low doping-induced losses (? = 0.1 cm^{-1} for the pump mode and ? = 0.4 cm^{-1} for both generated modes).

[1] M. Oron et al., Proc. SPIE 8240, paper 82400C (2012).

[2] A. Fiore et al., Nature 391, 463 (1998).

[3] S. Ducci et al., Appl. Phys. Lett. 84, 2974 (2004).

[4] S. A. Moore et al., IEEE Photon. Technol. Lett. 18, 1861 (2006).

[5] J. P. Reithmaier and A. Forchel, C. R. Physique 4, 611 (2003).

9136-5, Session 1

Indirect transitions of a signal interacting with a moving refractive index front

Michel Castellanos Munoz, Alexander Y. Petrov, Manfred Eich, Technische Univ. Hamburg-Harburg (Germany); Liam O'Faolain, Univ. of St. Andrews (United Kingdom); Juntao Li, Sun Yat-Sen Univ. (China); Thomas F. Krauss, The Univ. of York (United Kingdom)

The dynamic manipulation of light can be achieved by interaction of a signal pulse propagating through or reflected from a refractive index front. Both the frequency and the wave vector of the signal are changed in this case, which is generally called an indirect transition. We have developed a theory to describe such transitions in integrated photonic crystal waveguides. Through indirect transitions the following effects can be envisaged: large frequency shifts, light stopping and order of magnitude pulse compression and broadening without center frequency shift. All effects can be potentially realised with a small refractive index modulation of 0.001.

For experimental realisation we have used slow light photonic crystal waveguides in silicon. The refractive index front was obtained by free carriers generation with a switching pulse co-propagating with the signal in the same slow light waveguide. The group velocities of the signal and the front could be varied arbitrarily by choosing the right frequencies of the signal and switching pulses. The indirect transition was unambiguously demonstrated by considering two situations: front overtaking the signal and the signal overtaking the front. In both cases a blue shift of the signal frequency was observed. This blue shift can only be explained by the occurrence of the expected indirect transition and not by a direct transition without wave vector variation.

9136-6, Session 2

Development and perspectives of high repetition rate attosecond sources *(Invited Paper)*

Arnold Cord, Miguel Miranda, Piotr Rudawski, J. Guo, C. M. Heyl, Esben W. Larsen, Eleonora Lorek, Johan Mauritsson, Lund Univ. (Sweden); Jan Matyschok, Oliver Prochnow, Thomas Binhammer, VENTEON Laser Technologies GmbH (Germany)

No Abstract Available

9136-7, Session 2

Longitudinal mode-filling to cancel SBS in fully-fibered MOPAs dedicated to the production of high-energy nanosecond pulses

Alain Jolly, CEA/CESTA (France) and ALPhANOV (France); Fikri Serdar Gokhan, Hasan Kalyoncu Univ. (Turkey); R. Bello, Pascal Dupriez, ALPhANOV (France)

We present an original study dedicated to the comprehensive analysis of longitudinal mode – filling issues, aiming to the reduction of Stimulated - Brillouin - Scattering (SBS) effects in single - mode fibers. This involves fairly generic interests for the development of robust and low cost MOPA designs with no requirement of active electro – optical phase modulation, as more usually encountered, using fully - fibered architectures to produce highly energetic pulses with pulse durations in the nanosecond range. The basics of our work refers to proper management of the characteristics of laser - diode seeders, either using Distributed Feedback (DFB) or Fiber – Bragg Gratings (FBG) with different values of the fiber length, in combination with chirp effects due to large current transients.

We demonstrate the effectiveness of the optimization of the number of contributing longitudinal modes with properly defined mode – spacing in the spectral density of power, in order to amplify highly energetic pulses from single – pass, Large – Mode - Area (LMA) YDFAs. Depending upon the seeding option and selected mode – field area, for pulse - widths in the range of 5 to 500ns, the SBS threshold has be displaced from about 10 μJ up to some fraction of mJ. On another step, given a bandwidth of interest to specify the output pulse – shape in the typical ranges of about 1 – 2 GHz up to nearly 50GHz, we discuss the trade - off between the attainable SBS cancellation - limits and multimodal noise fluctuations due to mode - competition and hole burning in the strip of semiconductor. This aims to further generation of energetic pulses with properly controlled pulse – shape envelopes, which may still be required in a number of applications.

9136-8, Session 2

Laser-induced microwave generation with nonlinear optical crystals

Caterina Braggio, Univ. degli Studi di Padova (Italy) and Instituto Nazionale de Fisica Nucleare (Italy); Francesco Borghesani, Univ. degli Studi di Padova (Italy); Giovanni Carugno, Istituto Nazionale di Fisica Nucleare (Italy); Federico Della Valle, Univ. degli Studi di Trieste (Italy); Giuseppe Ruoso, Istituto Nazionale di Fisica Nucleare (Italy)

We will talk about measurements of microwave generation at a frequency of approximately 5 GHz accomplished by irradiating a nonlinear crystal (KTP) with a home-made, infrared laser at 1064 nm.

The irradiation of the crystal with a train of short laser pulses produces a time-dependent polarization in the crystal as a consequence of optical rectification. This process gives origin to the emission of microwave radiation that can be transferred to any receivers, either a cavity or a waveguide, without the bandwidth limitation of photodetection.

We have previously investigated both microwave and second harmonic generation as a function of the laser intensity and of the orientation of the laser polarization with respect to the crystallographic axes of KTP.

New results that match our model will be presented involving also different type of crystals (ZnSe, LBO, LNO). Measurements of the microwave emission with the crystals and receiver kept at cryogenic temperature (77 K) will also be presented, that allow to analyze the microscopic origin of the dipolar emission.

We will also report on a novel electro-optic device meant for the diagnostics of high repetition-rate laser systems, which is based on this phenomenon. The device is cost-effective and overcomes bandwidth limitations of state-of-the-art detection techniques. The active element of the device is a nonlinear crystal mounted inside a microwave receiver (i.e. a coaxial waveguide). The emitted radiation is detected in the time domain by an oscilloscope directly or through heterodyne techniques and allows measurements of laser pulse intensity and repetition frequency of the pulses.

9136-9, Session 2

Optical flip-flop memory and routing operation based on polarization bistability in optical fiber

Pierre-Yves Bony, Julien Fatome, Massimiliano Guasoni, Elie Assémat, Stéphane Pitois, Dominique Sugny, Antonio Picozzi, Hans-Rudolf Jauslin, Univ. de Bourgogne (France)

The repolarization of an optical wave without loss of energy is a fundamental physical process that finds important applications in photonics.

Considering the counter-propagating interaction of two distinct optical beams injected at both ends of an optical fiber, it has been shown that an arbitrary polarization state of a signal beam is attracted toward a specific state of polarization (SOP), which is determined by the SOP of the counter-propagating pump beam injected at the fiber output. The generally accepted point of view is that the injection of a pump beam at the fiber output is a prerequisite for the existence of the phenomenon of polarization attraction.

However, our last results show that the optical beam can indeed self-organize its own polarization state by means of a counter-propagating configuration in which the incident signal nonlinearly interacts with its own backward replica generated at the fiber output. More precisely, we report the theoretical prediction and experimental observation of bistability and the associated hysteresis phenomenon in the state of polarization of a light beam propagating in a 4-km long telecommunication optical fiber. This process occurs in a counter-propagating configuration in which the incident forward optical beam nonlinearly interacts with its own Bragg-reflected replica. Experimental monitoring of the hysteresis shows a high robustness, wide opening and sharp transitions in the hysteresis cycle that have contributed to provide two proof-of-principles of optical processing. In particular, a polarization-based flip-flop optical memory has been demonstrated in which set/reset polarization spikes imprinted onto the input signal allows us to permanently load or erase ON/OFF robust states on the output signal in a perpetual manner in such a way to create a dual-state memory. Finally, a 10-Gbit/s switching operation was reported based on this polarization bistability that enables to route data packets on demand along two orthogonal polarization channels.

9136-10, Session 2

Speed gradient control on Josephson junction of optical soliton and surface plasmon

Evren Karakaya, Kaan Guven, Ozgur Mustecaplioglu, Koç Univ. (Turkey)

Plasmonics encompasses the science and technology of plasmons which are the collective oscillations of electrons mainly in metals. In particular, the coupling of plasmons with photons give rise to a hybrid quasiparticle known as the surface plasmon-polariton (also called surface plasmon), which can propagate along metal surfaces. As a result, light can couple to, and propagate through structures that are much smaller than it's wavelength. As the research on the interaction of light with metallic structures matures as a well-established technology, the coupling of surface plasmons to different light sources are being investigated, with the motivation that controlling surface plasmons offer the potential for developing different types of SP-integrated nanophotonic devices. In particular, the coupling between SPs and confined light modes are widely investigated.

A recent proposal is based on the resonant interaction between the SPs on a metal surface and co-propagating soliton in a nonlinear dielectric medium. Under a classical formulation, this system exhibits rich nonlinear dynamical features where the interaction depends on the soliton amplitude; as such it may be utilized to manipulate the SP propagation. Coupling surface plasmons (SPs) to optical solitons in nonlinear (Kerr type) dielectric waveguides has been proposed as an effcient way to control them. This system offers periodical soliton-SP conversion, non-adiabatic switching and hybridized soliton-plasmon bound states. As an additional feature, it has been shown that the system is akin to the bosonic Josephson-junction of Bose-Einstein condensates so that similar and different nonlinear Josephson junction features may be realized in this optic-plasmonic system.

While this was an exciting analogy, surface plasmons are subject to strong dissipative effects in the host metal and perfect Josephson junction is a too idealized model. Recently, the dissipative effect has been taken into account to introduce a more reliable representation of the practical system, where it has been found that robust dynamical phases can be achieved despite the presence of the dissipation by expansion of the Hopf bifurcations to stable limit cycles. Remarkably, it is also examined that the dissipation can bring some benefits if it could be introduced under control.

Based on this motivation, we employ a standard dynamical analysis of the system in the phase space representation, and investigate how dissipation mechanisms and other model parameters affect the phase-space landscape. In particular, our objective is to explore controlled population transfer from soliton photons to surface plasmons subsystem. For this purpose, we employ the speed gradient method known as a unified approach to solving nonlinear control problems. The method to control the behavior of the system by varying the spatial distance between the metal and the waveguide is examined. Our results can contribute to effcient control over plasmon dynamics and excitations.

9136-39, Session PS1

Field-enhanced nonlinear properties of organic nanofibers

Oksana Kostiu?enko, Jacek Fiutowski, Jonathan R. Brewer, Horst-Günter Rubahn, Univ. of Southern Denmark (Denmark)

To induce controllable local field enhancement effects on nanostructures, which were used to modify a second harmonic generation in the nanofibers, several periodic arrays of metal square-nanostructures (100 x 100 ?m2) were fabricated on the top of a 70 nm gold surface using electron-beam lithography, metal deposition, and lift-off. The lateral dimensions of the nanostructures (side length 450 nm) and the pitch distance (750 nm) of the arrays were chosen to achieve the strongest SPP resonances and thus the strongest local field enhancements in the wavelength range of 790 nm. To obtain second harmonic signals from a single nanoaggregates, a laser-scanning microscope built on the basis of an inverted fluorescence microscope (Nikon Eclipse TE 2000U),was used. As an illumination source, a broadband, pulsed Ti:Sapphire laser (Spectra Physics Tsunami, sub 100 fs pulses, rep. 82 MHz, maximum energy per pulse 8 nJ) was exploited, with a center wavelength between 750 and 820 nm. During the sample illumination, the emitted light was simultaneously detected via a photomultiplier in photon counting mode. Morphology effect evaluation, topography and profile measurements have been performed using Atomic Force Microscope.

9136-44, Session PS1

Multi-modes of four-waves mixing at non-collinear interaction of laser beams in medium with cubic nonlinear response

Vyacheslav A. Trofimov, Igor E. Kuchik, Nikita V. Levitskiy, Lomonosov Moscow State Univ. (Russian Federation)

We develop an explicit solution of problem describing non-collinear four-waves mixing in medium with cubic nonlinear response. This solution is carried out for set of Schrodinger equations using plane wave approximation for both the case of phase matching and phase mismatching of interacting waves.

This solution allows to do full analysis of four-wave interaction modes in dependence of the problem parameters. We have shown, in particular, an existence of bistable mode for energy conversion from pump waves to signal wave under certain conditions. In general case, there are greater than 10 various modes of four-wave interaction.

Knowledge about these modes are very important for spectroscopic experiment results understanding using four-waves mixing because its result depends on them..

9136-45, Session PS1

Control of soliton pattern through continuous external injection

Alioune Niang, Foued Amrani, Mohamed Salhi, Hervé Leblond, Univ. d'Angers (France); Andrey K. Komarov, Institute of Automation and Electrometry (Russian Federation); François Sanchez, Univ. d'Angers (France)

Soliton interaction has now a long history since the initial papers in the middle 80's which concerned conservative solitons. With the emergence of fiber lasers, and in particular double-clad fiber lasers, there was a revival on soliton interaction in the framework of dissipative solitons. Indeed, in passively mode-locked high power fiber laser, a large number of solitons can coexist in the cavity when operating in the anomalous dispersion regime. As a general rule, the number of solitons in passively mode-locked fiber lasers increases when the pumping power grows. Many different soliton patterns have been reported independently of the exact mode-locking mechanism revealing some universal properties. The resulting solitons distribution in fiber laser is a direct consequence of their interactions which can be repulsive or attractive or both at different scales. Attractive interaction is responsible of bound states. Repulsive interaction is responsible of the well-known harmonic mode-locking (HML). In many HML fiber lasers, a continuous wave (cw) component is present in the optical spectrum suggesting that this component could play an important role in the HML mechanism. It has been recently shown theoretically that a small cw component allows to control the nature and the strength of the soliton interaction. Based on this prediction and on the role of the cw component in the HML, we have decided to conduct several series of experiments on a passively mode-locked fiber laser injected with an external cw component. In this communication we will demonstrate experimentally that a passively mode-locked fiber laser can be forced to operate in HML regime by means of an external cw component. Starting from different initial soliton distributions, we will show that: (i) the external cw component can force the laser to change its operating regime, (ii) under specific injection conditions the laser operates in the harmonic mode-locking regime and (iii) the effect of the injected cw signal is reversible and reproducible.

9136-46, Session PS1

Instantaneous frequency measurement of microwave signals in optical range using "frequency-amplitude" conversion in the ϖ-phase-shifted fiber-Bragg grating

Anvar A. Talipov, Oleg G. Morozov, Marat R. Nurgazizov, Pavel E. Denisenko, Aleksandr A. Vasilets, Kazan State Technical Univ. (Russian Federation)

In this article we offered a new radio photonics method for the instantaneous frequency measurement of microwave signals, based on the generation of a two-frequency laser radiation with a difference frequency equal to the measured, and the "frequency - amplitude" conversion in the ϖ-phase-shifted fiber Bragg grating. Key features of the method is the using the specific conversion of two-frequency radiation in the ϖ-phase-shifted fiber Bragg grating allowed us to obtain measuring characteristics, that are independent of the fluctuations of the optical carrier in two sub-ranges: 0.3 - 3 GHz in the passband of the FBG and 3 - 30 GHz in its reflection band.To reduce the measurement inaccuracy caused by temperature fluctuations of the spectral characteristics of system elements an additional monitoring channel were applied, based on a four-frequency narrow-band measurement method without the use of phase analysis. The advantage of this approach is the ability of the measurement in a band up to 300 MHz with narrow-band low-noise photodetector.

For practical realization a setup was assembled. Setup consists of the laser LDI-DFB 1550-20/50-T 2-SM3-FA-CWP, source Superlum SLD Pilot- 4, the oscilloscope Agilent InfiniiVision 7000, random waveform signal generator AFG3000, multimeter, MZM JDS Uniphase OC- 192 Modulator, stabilized power supply PSS-1, the spectrum analyzer FTB 5240-S, an optical splitter, a circulator, FBG, the photodiode LSIPD-A75. The conversion coefficient "frequency-amplitude" for the frequency 2 GHz of first sub-range was 2.35. by pass, for the frequency 8 GHz of the second sub-range - 0.28 by reflection. The resulting data are in good agreement with the coefficients, taken us for a theoretical verification.

9136-47, Session PS1

Engaging new dimensions in nonlinear optical spectroscopy using auxiliary beams of light

Jack S. Ford, David S. Bradshaw, David L. Andrews, Univ. of East Anglia (United Kingdom)

By applying a sufficiently intense beam of off-resonant light, simultaneously with a conventional excitation source beam, the efficiencies of one- and two-photon absorption processes may be significantly modified. The nonlinear mechanism that is responsible, known as laser modified absorption, is fully described by a quantum electrodynamical analysis. The origin of the process, which involves stimulated forward Rayleigh-scattering of the auxiliary beam, relates to higher order terms which are secured by a time-dependent perturbation treatment. These terms, usually inconsequential when a single beam of light is present, become prominent under the secondary optical stimulus – even with levels of intensity that are moderate by today's standards. Distinctive kinds of behaviour may be observed for chromophores fixed in a static arrangement, or for solution- or gas-phase molecules whose response is tempered by a rotational average of orientations. In each case the results exhibit an interplay of factors involving the beam polarisations and the molecular electronic response. Special attention is given to interesting metastable states that are symmetry forbidden by one- or two-photon absorption. Such states may be accessible, and thus become populated, on input of the auxiliary beam. For example, in the one-photon absorption case, terms arise that are more usually associated with three-photon processes, corresponding to very different selection rules. Other kinds of metastable state also arise in the two-photon process, and measuring the effect of applying the stimulus beam to absorbances of such character adds a new dimension to the information content of the associated spectroscopy. Finally, based on these novel forms of optical nonlinearity, there may be new possibilities for quantum non-demolition measurements.

9136-48, Session PS1

Pre-determination of the gap location on an electromigrated gold nanowire by second-harmonic generation

Marie-Maxime Mennemanteuil, Jean Dellinger, Alexandre Bouhelier, Lab. Interdisciplinaire Carnot de Bourgogne (France)

Electromigration is a technique largely used in molecular electronics to create molecular-scale gap. When a voltage difference is applied across a gold nanowire, a physical motion of the ions is induced by a momentum transfer of the electrons to the atoms, which eventually leads to the rupture of the nanowire. The location of the failing point is poorly controlled and typically occurs at a structural defect of the nanowire. In this study, we seek to develop an innovative imaging technique to pre-determine the location of the rupture when a nanowire is electrically stressed.

Our approach relies at evaluated second-order nonlinear susceptibility of the nanowire and its electron transport characteristics. The change of the nanowire morphology during the electromigration process is spatially followed by recording

the second harmonic generation (SHG) together with the evolution of the differential conductance ∂i/∂v, dictating the electronic transport. We image the local SHG response and the ∂i/∂v signal for each position of the nanowire when raster scanned through the focus of a femtosecond pulsed laser beam. Defects along the nanowire are recognized in SHG images as high intensity spots. These spots are correlated with a reduced differential conductance in the ∂i/∂v image. Temperature is a key factor in the electromigration process. Temperature is affected on a one hand by the current flow in the nanowire and in the other hand by the energy deposited by the laser when focused on the defects. The evolution of the SHG response and the amplitude of the differential conductance are followed during the electromigration. The gap obtained after the rupture of the nanowire is characterized by a very strong SHG response, which corresponds spatially to SHG spots and the conductance minima recorded before the failure of the nanowire. Using this imaging protocol, the position of the rupture can be predetermined. This is a necessary step for controlling the electromagnetic environment of the gap by a subsequent structuring around the failing point.

The research leading to these results has received funding from the European Research Council under the European Community's Seventh Framework Program FP7/2007–2013 Grant Agreement no 306772.

9136-49, Session PS1

Observation of large-Kerr nonlinearities in atomically thin MoS2

Felice Gesuele, Raffaele Velotta, Carlo Altucci, Mohammadhassan Valadan, Univ. degli Studi di Napoli Federico II (Italy)

Molybdenum disulphide (MoS2) is a two-dimensional layered material that has recently attracted increasing interest due to its electronic and optical properties. For instance, it has been demonstrated that with decreasing the layer number, the indirect band gap, which lies below the direct gap in the bulk material, shifts upwards in energy by more than 0.6 eV. This leads to a crossover to a direct-gap material in the limit of the single monolayer. Interestingly, the MoS2 monolayer emits light strongly with an increase in luminescence quantum efficiency by more than a factor of 10^4 compared with the bulk material.

Strategies similar to those applied for other two-dimensional materials like graphene can be used to obtain single layer MoS2 by mechanical or chemical exfoliation as well as CVD growth. The possibility of facile production of single layer and its direct-gap semiconductive behaviour makes MoS2 highly promising material for integration in photonics devices. Moreover recently, T. Heinz and co-workers [Nanoletters (2013) 13, 3329-3333] demonstrated that atomically-thin MoS2 single-layers or multilayers composed of a odd number of layers exhibit an unexpectedly strong SHG emission with a maximum of intensity for the single layer.

Here we present the first observation of large Kerr nonlinearities in solution processed MoS2 by means of broadband z-Scan spectroscopy.

Sample of MoS2 were chemically exfoliated in solution of ethanol and water. Atomic force microscopy along with Raman characterization has been employed to retrieve the distribution of sizes (of the order of hundreds of nanometers) and layers (from 1 to 4).

A modified z-Scan setup was employed for the measure of spectral nonlinear refractive index n2 and absorption coefficient ? of the MoS2 solution. We employ femtosecond supercontinuum white light as ultrafast source for characterize our samples. A referenced couple of high speed and linear Si-array were employed to measure change in transmittance in the open and closed aperture configuration.

We find that the third order nonlinear refractive index n2 is wavelength dependent and follows the MoS2 absorbance spectrum. It shows clear resonances, relative to the exciton transitions. At single layer resonance it shows resonant values larger more than two orders of magnitude of typical bulk semiconductor values.

Time-resolved femtosecond broadband transient absorption measurements are ongoing in order to estimate the occurrence of thermal effects. At the same time micro-four wave mixing and z-scan micro-spectroscopy will be employed to quantitative estimate the ?(3) coefficient in function of the layer number.

We argue that the creation of excitons and their vertical confinement as well as their large binding energies in atomically thin MoS2 are at the origin of the huge third order nonlinearity in analogy to a well-known effect discovered in 1D systems.

Our findings, although preliminary, demonstrate the potential of MoS2 as nonlinear material for low-cost integration into optoelectronic devices.

9136-50, Session PS1

Nonlinear picosecond pulse transformation in large-core microstructured fibers

Alexandra Pasishnik, S.I. Vavilov State Optical Institute (Russian Federation); Stanislav O. Leonov, Bauman Moscow State Technical Univ. (Russian Federation)

Supercontinuum (SC) generation is described by the maximum optical power of 50 W in continuous-wave regime while taking place in a fiber with a core of less than 5 μm in diameter. However, further energy increase appears to be difficult because of the material damage when the fiber tip is under the impact of extremely high-power launching radiation.

The process of SC generation in a large-core microstructured fiber initiated by picosecond laser pulses has not been studied sufficiently so far. Under these circumstances it becomes relevant to explore nonlinear optical power converters based on multi-mode large-core microstructured fibers and commercially available low-cost solid-state picosecond lasers as well.

We investigated both theoretically and experimentally nonlinear picosecond pulse conversions (pulses with a duration of 2 ps originated from ytterbium solid-state laser) in microstructured fibers made from silica glass having a core of 8-12 μm in diameter. The ratio of the air hole diameter to the structure pitch was equal to 0.95 in order to provide optimal power concentration in a core. Pump wavelength was 1030 nm. Zero dispersion wavelengths for fundamental and higher-order modes were located in the normal dispersion region. The average optical power delivered to the fiber turned out to be 1.8 W, pulse repetition rate – 200 kHz, corresponding to pulse energy of 9 μJ and peak power of 4.5 MW.

During the experiment we have attained SC generation with the energy conversion efficiency up to 100%. Minimum threshold of SC generation and simultaneously maximum spectral broadening were observed in the fiber with a core of 8 μm in diameter. Moreover, spectra of SC obtained for the other samples had nearly identical properties: under the power level of approximately 0.9 W anti-Stokes and Stokes isolated peaks appeared at wavelengths of 800 nm and 1450 nm respectively. Further optical power increase resulted in the SC spectrum covering more than an octave (from 400 to 1800 nm).

From the theoretical analysis of phase-matching condition we have concluded that main mechanisms leading to SC spectrum formation is the process of four-wave mixing (FWM) occurring in the higher-order mode (mentioned isolated peaks) and broadening caused by stimulated Raman scattering in the spectral range 1030-1400 nm. We have also investigated temporal development of nonlinear scenario by cutting the fiber length from 5 to 0.5 m.

Additionally, the origin of secondary radiation and broadening of spectral peaks is discussed. In order to initiate the generation process in the gain spectral channels made by the pump it is necessary to have suitable spectral noise as a source. As regards to stimulated Raman scattering it is ensured by spontaneous scattering. But there is a need for another resource if deal with FWM. In presented microstructured fibers the nonlinear parameter ?P = 110-145 1/m. Despite a comparatively large core size this circumstance guarantees

significant self-phase modulation process due to a high peak power. Self-modulation, in turn, broadens the initial pump spectrum up to tens of nanometers in FWHM that serves as a source to initiate FWM.

9136-51, Session PS1

Plasmon-solitons in nonlinear metal slot waveguides: bifurcations at low power

Wiktor Walasik, Institut Fresnel (France) and Aix-Marseille Univ. (France); Yaroslav V. Kartashov, ICFO - Institut de Ciències Fotòniques (Spain); Gilles Renversez, Institut Fresnel (France) and Aix-Marseille Univ. (France)

Merging the fields of nonlinear optics and plasmonics attracted a lot of attention in recent years (Kauranen & Zayats, Nature Photonics, 2012). Some of the devices combining these two domains were designed to create sub-wavelength light beams (Feigenbaum & Orenstein, Opt. Lett., 2007) or nonlinear switches (Smirnova et al. Phys. Rev. A., 2013). Recently, we have demonstrated that plasmon-soliton waves can be generated at low power in realistic planar configurations made of a semi-infinite nonlinear dielectric covered by a buffer linear dielectric film and a metal layer in contact with an external medium (Walasik et al., Opt. Lett., 2012; Walasik et al., Phys. Rev. A, 2014). This result motivates the present work dedicated to a configuration of a metal slot waveguide with a nonlinear dielectric core. In this work the nonlinearity is located in a finite size dielectric layer and it is of a focusing Kerr type like in chalcogenide glasses or hydrogenated amorphous silicon which are seen as promising materials for nonlinear integrated photonics (Eggleton et al., Nature Photonics, 2011; Lacava et al., Appl. Phys. Lett., 2013).

We find the stationary nonlinear solutions in these one-dimensional metal/nonlinear dielectric/metal structures using two new semi-analytical models based on Maxwell's equations. The first model extends the approach proposed for dielectric waveguides (Fedyanin & Mihalache, Z. Phys. B, 1982.) to metal slot nonlinear waveguides. It uses a simplified treatment of the Kerr nonlinear term where only the transverse component of the electric field is taken into account. The second model extends the approach used for a semi-infinite nonlinear medium (Yin et al., Appl. Phys. Lett., 2009) to a more complex case where the nonlinear medium has a finite size and therefore it requires the treatment of two nonlinear interfaces. This last method is more accurate because it provides an exact treatment of the nonlinearity.

We classify the types of the solutions of this structure as: symmetric, antisymmetric, or asymmetric. We obtain the nonlinear dispersion relations for the structure. A rich dispersion relation with modes bifurcations, including for higher order nonlinear modes is obtained. In the previous studies of plasmon-solitons in slot waveguides (Feigenbaum & Orenstein) the stress was put on the sub-wavelength localization of the 2D waves due to the slot waveguide structure (in transverse direction) and nonlinear effects (in lateral direction). However the nonlinear effects were not taken into account in the transverse direction which did not allow to observe the bifurcation effects and higher order nonlinear modes. Thanks to the versatility of the models we developed asymmetric structures are also studied.

We have also studied the influence of the nonlinear core width on the lowest/first Hopf bifurcation occurring in the symmetric slot waveguide. We show that the increase of waveguide width causes a drastic shift of the bifurcation point to lower powers that should allows to observe it experimentally. Two configurations based on realistic material parameters are proposed. The first one possesses a nonlinear dielectric core made of a photostable chalcogenide glass. In the second configuration the core is made of hydrogenated amorphous silicon. Both materials have sufficiently high damage thresholds (a few GW/cm2) and low two-photon absorptions at 1.55 □m which make them good candidates to be used in possible experiments.

9136-52, Session PS1

Multimode interference in a z-cut periodically poled MgO-doped lithium niobate crystal with a planar waveguide using single-pass second-harmonic generation

Junhee Park, Tai-Young Kang, Jeong-ho Ha, Han-Young Lee, Korea Electronics Technology Institute (Korea, Republic of)

We present the characteristics of multimode interference (MMI) in the single-pass second harmonic generation of a distributed Bragg reflector (DBR) tapered laser radiation. The blue light source was realized by quasi-phase matching (QPM) in a periodically poled MgO-doped lithium niobate planar waveguide. The pump laser was a single-frequency DBR tapered diode laser with a wavelength of 920 nm. The diode laser consists of a 6-mm-long DBR tapered diode laser with a sixth-order surface grating. The ridge waveguide of the tapered laser diode is 4 um wide and 2 mm long and consists of a 1-mm-long unpumped DBR section and a 1-mm-long pumped ridge section. The tapered section is 2 mm long with a taper angle of six degrees.

The output from the DBR tapered diode laser was collimated in the fast axis using an aspherical lens. In addition, additional cylindrical lens was used to collimate the laser beam in the slow axis. A half-wave plate was positioned behind the collimation lens because of the different polarization of the pump source. The laser beam was focused with a cylindrical lens in the slow and fast axes, respectively, which were chosen based on a simulation result in order to maximize the coupling efficiency into the waveguide facet and achieve the maximum conversion efficiency. The pump output power was 3.0 W from the DBR tapered diode laser and NIR power was achieved in 2.45 W in front of planar waveguide facet,.

Blue light was obtained from a planar waveguide with a poling period of 4.33 ?m at room temperature. The dependence of the wavelength conversion efficiency on the temperature tuning showed an asymmetric sinc2 shape. In addition, not only the fundamental but also multimodes (first and second mode) were simultaneously generated in a QPM tolerance curve, and it results from multimode interference in the second harmonic wave.

9136-53, Session PS1

Investigation of the separate optical nonlinear contributions of the core and cladding materials of silicon photonics slotted waveguides

Weiwei Zhang, Samuel Serna, Institut d'Électronique Fondamentale (France); Nicolas Dubreuil, Institut d'Optique Graduate School (France); Eric Cassan, Institut d'Electronique Fondamentale (France)

The nonlinear properties of slotted silicon photonic waveguides filled with third-order nonlinear polymers (NP) is quantitatively studied by properly calculating the effective nonlinearity susceptibilities separately associated to the core and cladding regions, respectively. The adopted approach circumvents the frequent approximation that the introduced NP dominates the nonlinear behavior of the slotted waveguide and the correlated unverified assumption that light confinement into the slot allows neglecting two-photon absorption (TPA) in silicon. Metrics of slotted hybrid waveguides are investigated by analyzing TPA and carriers effects with the nonlinear wave propagation method. To do so, the X(3) properties of the silicon and NP (taken as DDMEBT) layers are considered as a starting point, including for each the refractive index, the Kerr index, and the two-photon absorption (TPA) factor of merit (FOM=n2/Beta_TPA.lambda), respectively. A full-vectorial mode solver is then used to calculate the mode profiles for silicon strip

and slot waveguides, from which the effective complex susceptibilities coming from the core and cladding regions are obtained. A possible first-order investigation of the light slowing down factor is achieved by sweeping the light group index in the solved nonlinear equation in the assumption that the lateral mode profile is roughly preserved.

The waveguide dimensions, e.g. width, heights, and slot width, have been swept and the detailed related results will be presented. To summarize, it is predicted that the waveguide effective FOM for silicon slotted waveguides can be typically maintained above 3.8 in most of situations, meaning a 4.4 improvement with respect to silicon strip waveguides.

9136-54, Session PS1

Linear electro-optical scattering from ferroelectric nanocrystals

Duc Thien Trinh, Ecole Normale Supérieure de Cachan (France) and Hanoi National Univ. of Education (Viet Nam); Vasyl V. Shynkar, Joseph Zyss, Ecole Normale Supérieure de Cachan (France)

We report a measurable linear electro-optical scattering response from individual ferroelectric (KTiOPO4) nano-crystals. The newly developed Pockels Linear Electro-Optical Microscopy (PLEOM) [1-3] is used in this context to map the second-order susceptibility ?(2) of non-centrosymmetric materials with a high sensitivity due to stabilized interferometric homodyne detection. The random spatial orientation of single nano-crystals (with an average size of 100 nm), together with the orientation of the electric dipole moment of ferroelectric domains can be jointly inferred from the intensity polarization plot and the phase of the linear electro-optical response. Down-scaling the electro-optic response to nanocrystals opens-up new applications towards sub-diffraction electro-optic nano-labels for nonlinear microscopy with applications to nano-sciences and biophotonics. By using a low power He-Ne laser source and a low intensity level of the illumination beam, PLEOM bears the potential of a new low-cost non-invasive imaging method in biology, especially relevant for sensitive samples.

9136-55, Session PS1

Nonlinear optical characterization of crystal structure and growth of metal-organic frameworks

Stijn Van Cleuvenbergen, Katholieke Univ. Leuven (Belgium); Monique A. Van der Veen, Technische Univ. Delft (Netherlands); Thierry Verbiest, Katholieke Univ. Leuven (Belgium)

In the past two decades, the synthesis of metal-organic frameworks (MOFs) has drawn a great deal of attention because of their high promise for applications (gas storage, catalysis...) and their synthetic flexibility. [1] Although a lot of promising structures have been determined, the rational design of MOFs to come to predictable structures under specific conditions is still hindered by the limited understanding of the underlying crystal growth process. [2]

We propose time-resolved second-harmonic scattering (SHS) as an alternative to the traditional techniques to study crystallization in MOFs. Since the second-harmonic response is inherently sensitive to symmetry and organization, it is ideally suited to study crystalline materials. [3, 4] In the earliest stages of crystallization the technique is equivalent to hyper-Rayleigh scattering and can detect the formation of the very first MOF bonds, clusters and nuclei, as well as determine the response and symmetry of these structures. [5] Subsequently, when these structures grow increasingly larger, constructive and destructive interference between different points give rise to an angle-dependent signal, exactly as in linear scattering. [6] In this phase, rigorous analysis allows determining relevant parameters such as size, symmetry and even shape and of the growing crystallites. [7]

Time-resolved SHS allows following the complete crystal growth process in situ on all relevant length and time scales, providing information on morphology and crystallinity simultaneously. This opens the way to a better fundamental understanding of the crystallization in MOFs and a more conceptual approach towards true rational design. It goes without saying that this technique is applicable on other systems as well and could be a true asset for the entire crystal community.

References

1. S.T. Meek, A. Greathouse, M.D. Allendorf, Adv.Mat. 23, 249 (2011).

2. R.E. Morris, Chem. Phys. Chem 10, 327 (2009).

3. M.A. Van der Veen, F. Vermoortele, D.E. De Vos, T. Verbiest, Anal. Chem. 84, 6378 (2012).

4. S. Van Cleuvenbergen, G. Hennrich, P. Willot, G; Koeckelberghs, K. Clays, T. Verbiest and M.A. Van der Veen, J. Phys. Chem. C 116 12219, (2012).

5. K. Clays, A. Persoons, Phys. Rev. Lett. 66, 2980 (1991).

6. N. Yang, W.E. Angerer, A.G. Yodh, Phys. Rev. Lett. 87 103902, (2001).

7. A.G.F. de Beer, S. Roke, Phys. Rev. B 79 15420, (2009).

9136-56, Session PS1

Effect factors of temperature measurements by femtosecond time-resolved CARS

Yang Zhao, Sheng Zhang, Zhibin Zhang, Zhiwei Dong, Deying Chen, Zhonghua Zhang, Yuanqin Xia, Harbin Institute of Technology (China)

Time-resolved femtosecond coherent anti-Stokes Raman spectroscopy (fs-CARS) is utilized to measure the premixed methane/oxygen/nitrogen flame temperature at atmospheric-pressure. The measurements are performed using the CARS signal of the nitrogen molecule in the first few picoseconds after the initial in-phase excitation (from 200 fs-3 ps). The theory of the time-resolved fs-CARS is presented briefly (The theory model is presented in detail by Lucht et al. Appl Phys Lett 89, 251112 (2006)). The theoretical results of the time-resolved fs-CARS are used to extract temperatures by comparing them with time-resolved fs-CARS experimental signals. The procedure for fitting theoretical spectra to experimental spectra is explained. The parameters for Raman transition are obtained from the Sandia CARS spectral-fitting code. Arbitrary scaling factors for ratio of resonance and non-resonance are used to match the experimental signal with the theoretical spectrum. The least-square fit is used for obtaining the best-fit results. In the process of fitting, the interval of temperature (the assumptive best-fit temperature) is from 100 K to 10 K and the interval of arbitrary scaling factor is from 0.1 to 0.001. The experimental results show good agreements with theoretical ones. The results of temperature measurement present a good repeatability. Laser parameters are very important for accurate temperature measurements. The effects of laser parameters on temperature measurements are discussed. The laser parameters include delay time between the pump and Stokes (?), laser pulse shape, pulse duration, central wavelength of the pump/probe pulses (?p) , and laser pulse's timing jitter. The theoretical spectra with the laser parameters which are the same as actual ones are used to fit the theoretical spectra with the laser parameters which are different from the actual ones. Laser parameters in our measurements are shown as follows. Laser pulse shape is Gaussian. ? is 0 fs. ?p is 675 nm. Pulse duration is 40 fs. Laser parameters in our discussion are shown as follows. Laser pulse shape is hyperbolic secant and Lorentz, respectively. ? is from -60 fs to +60 fs. ?p is from 650 nm to 700 nm. Pulse duration is from 40 fs to 100 fs. In 2000K, variations of ? lead to less than 5% error and while variations of the other three parameters lead to less than 1% error. Timing jitter is added to the pump/probe pulses and Stokes pulses.

The results indicate that the error led by timing jitter of Stokes pulses is bigger the error by pump/probe pulses'. In 2000K, the results indicate that timing jitter of 10% lead to less than 2% error for temperature measurements. In the higher temperature measurement, the impact of the error in laser parameters is greater. Based on the above analysis, we can estimate the effects of laser parameters on temperature measurements.

9136-57, Session PS1

Ultra-compact NAND/NOR/XNOR all-optical logic gates based on a nonlinear 3x1 multimode interference coupler

Mohd Zubir Mat Jafri, Mehdi Tajaldini, Univ. Sains Malaysia (Malaysia)

Highly miniaturized multimode interference (MMI) coupler based on nonlinear modal propagation analysis (NMPA) is presented. This method is a novel design and potential application for optical NAND, NOR and XNOR logic gates for Boolean logic signal processing devices. Crystalline polydiacetylene is used to allow the appearances of nonlinear effects in low input intensity and ultra- short length for controling the MMI coupler as an active device to access light switching due to its high nonlinear susceptibility. We consider an 10?33 ?m2 MMI structure with three input and one output. Notably, the access facets are single- mode waveguides with 500 nm width. The center input contributes to control the light propagation in MMI by intensity variation whereas others could launch by particular intensity when they are ON and zero for OFF. Output intensity is analyzed in various sets of inputs to show the capability of Boolean logic gates, the contrast between ON and OFF is calculated on different kind of mentioned gates to present the efficiency. Good operation in low intensity and highly short coupler is observed because of NMPA method based on finite difference method (FDM) mode solver. Furthermore, nonlinear effects may be realized through the modal interferences. More efforts to achieve the high contrast in this ultra-compact dimension is a purpose of future works.

9136-58, Session PS1

Influence of photonic crystal fiber manufacturing inaccuracies on supercontinuum generation

Marek Napierala, Zbigniew Ho?dy?ski, Michal Szymanski, Michal Murawski, InPhoTech Ltd. (Poland) and Military Univ. of Technology (Poland); Pawel Mergo, Univ. of Maria Curie-Sklodowska (Poland); Pawel Marc, Leszek R. Jaroszewicz, Military Univ. of Technology (Poland); Tomasz Nasilowski, InPhoTech Ltd. (Poland) and Military Univ. of Technology (Poland)

The properties of photonic crystal fibers (PCFs) can be easily modified and tailored for a specific application by changing air-hole size, spacing or even arrangement. An example of such application is supercontinuum (SC) generation, which takes advantage from adequately designed dispersion characteristics and high nonlinearity. However, whilst the cross-section of PCFs can be freely designed, and the characteristics modeled, the fiber fabrication imposes limits on what can be manufactured and with which accuracy. If the fiber has low tolerance to the manufacturing inaccuracies, the fabricated fiber may exhibit characteristics different from the expected ones.

To show how the fabrication imperfections influence the SC generation we have manufactured a four series of nonlinear PCFs with slightly changed structural parameters (i.e. air-hole diameters and lattice constant). Each fiber series has been fabricated from one preform and had zero dispersion wavelength (ZDW) close to 1064 nm. We have investigated a change of the nonlinearity and dispersion characteristics in these fibers caused by variation of structural parameters. The generation of SC has also been measured when pumped at the wavelength of 1064 nm. We provide the comparison of evolution of SC generation and different nonlinear effects in fabricated fibers.

The results show that fibers with similar designs may provide very different SC characteristics since even small changes of structural parameters may result in the shift of ZDW from one side of the pumping wavelength to the other side. Due to the extensive content of experimental research performed for different PCFs, our paper indicates how to design a fiber to be tolerant to the fabrication inaccuracies and to obtain the desired SC characteristics.

9136-59, Session PS1

Experimental demonstration of optical XOR and XNOR gates for differential phase modulated data

Ravikiran Kakarla, Deepa Venkitesh, Indian Institute of Technology Madras (India)

All optical logic gates play a key role in implementing an optically transparent network where the node functionalities are performed in the optical domain, to reduce latency and power consumption. In this paper we present the experimental demonstration and details of optimization of all optical XOR/XNOR gate using four-wave mixing (FWM) in Semiconductor Optical Amplifier (SOA) for 10 Gbps Differential Phase Shift Keyed (DPSK) data.

Two DPSK modulated signals at carrier frequencies ?_1 and ?_2; phases ?_1 and ?_2 and a continuous wave pump at frequency ?_cw and phase ?_cw are allowed to undergo FWM in a non-linear SOA to generate additional frequency components. The phase of the generated FWM idler corresponding to the frequency ?_1+?_2-?_cw given by ?_1+?_2-?_cw, corresponds to the XOR operation in DPSK format. Light from a Distributed feed back laser and tunable laser source are combined and phase-modulated using a pseudo-random bit sequence. The bit sequences in the two carrier wavelengths are separated in time by propagating through a sufficient length of Single Mode Fiber; the data is combined with a CW pump from a tunable laser and allowed to undergo non-degenerate FWM in a nonlinear SOA. The relative spacing between the pump and the signal wavelengths and their polarization states are optimized to yield maximum conversion efficiency in the desired idler. The XOR output is further propagated through a delay-line interferometer (DLI) to obtain XOR and XNOR outputs in the two ports of the DLI, in the OOK format. Electrical extinction ratio of better than 7.2 dB, contrast ratio of better than 8 dB and amplitude modulation of less than 1dB is observed for data at 10 Gbps, for wavelengths separations of up to 2 nm between the signals.

9136-60, Session PS1

Cross-absorption as a limit to heralded silicon photon pair sources

Chad A. Husko, Alex S. Clark, Matthew J. Collins, The Univ. of Sydney (Australia); Alfredo De Rossi, Sylvain Combrié, Gaelle Lehoucq, Thales Research and Technology (France); Isabella Rey, Univ. of St. Andrews (United Kingdom); Thomas F. Krauss, The Univ. of York (United Kingdom); Chunle Xiong, Benjamin J. Eggleton, The Univ. of Sydney (Australia)

In recent years integrated waveguide devices have emerged as an attractive platform for scalable quantum technologies [1]. In contrast to earlier free-space investigations, one must consider additional effects induced by the media. In amorphous materials, spontaneous Raman scattered photons act as a noise source [2]. In crystalline materials two-photon absorption (TPA) and free carrier absorption (FCA) are present at large intensities. While initial observations noted TPA affected

experiments in integrated semiconductor devices, at present the nuanced roles of these processes in the quantum regime is unclear. Here we experimentally demonstrate that cross-TPA (XTPA) between a classical pump beam and generated single photons imposes an intrinsic limit on heralded single photon generation, even in the single pair regime. Our newly developed model is in excellent agreement with experimental results.

The single photons are generated via spontaneous four-wave mixing (SFWM) where two pump photons annihilate to create entangled signal and idler photons. The key insight of this work is losses by XTPA between a pump photon and a signal or idler photon limit efficiency of SFWM in silicon.

We perform two different experiments: (i) coincidence-to-accidental ratio (CAR) and (ii) heralded g(2)(0) correlation measurements to characterise the single photon sources. We employ two photonic crystal waveguide (PhCW) devices displaying inherently different nonlinear absorption processes, namely TPA in silicon (Si) and three-photon absorption (ThPA) in gallium indium phosphide (GaInP) to determine the role of nonlinear loss in photon pair generation [3].

In summary, we describe the interaction of probabilistic photon generation with multi-photon processes in both the generation and collection of single photons. Using experiment and model, we have shown that TPA imposes an intrinsic limit on photon generation. The implications of this result are absolutely critical to single photon sources exhibiting TPA, such as silicon.

REFERENCES

[1] J. L. O'Brien, A. Furusawa and J. Vu?kovi?, "Photonic quantum technologies," Nat. Photon. 3, 687-695 (2009).

[2] Q. Lin, F. Yaman and G. Agrawal, "Photon-pair generation in optical fibers through four-wave mixing: Role of Raman scattering and pump polarization," PRA 75, 023803 (2007).

[3] C. Husko*, A. Clark*, M. J. Collins, A. De Rossi, S. Combrié, G. Lehoucq, I. Rey, T. F. Krauss, C. Xiong, and B. J. Eggleton, "Multi-photon absorption limits to heralded single photon sources," Scientific Reports (accepted, to appear) (2013) *Equal contribution.

9136-61, Session PS1

NLSE-based model of a random distributed feedback fiber laser

Sergey V. Smirnov, Novosibirsk State Univ. (Russian Federation); Dmitry V. Churkin, Aston Univ. (United Kingdom) and Institute of Automation and Electrometry (Russian Federation) and Novosibirsk State Univ. (Russian Federation)

Recently, a new type of a random laser – random distributed feedback fiber laser – was demonstrated [1]. The random feedback in the laser is provided by the Rayleigh backscattering in an optical fiber core. The laser has a well-localized smooth optical spectrum having a width much less than the spectral width of the gain profile. These features are usually attributed to a coherent random feedback, however initially it was claimed that the laser operates via incoherent random feedback. Interestingly, the power balance equation set in which the Rayleigh scattering is included as an average energy feedback (i.e. as an incoherent feedback) describes well the power performances of the laser [1]. That means that the incoherent nature of the feedback could define the power balance in the laser. At the same time, correlation properties of the Rayleigh scattering are well known [2]. Potentially, spectral properties of the random DFB fiber lase generation could be affected by the coherent properties of the feedback, however there is no any theoretical description or a model describing the spectral properties of the random DFB fiber laser. All these make a question of type of the random feedback in the random DFB fiber laser intriguing.

In this work we propose a NLSE-based model of power and spectral properties of the random DFB fiber laser [1]. The model is based on coupled set of non-linear Schrödinger equations for pump and Stokes waves with the distributed feedback due to Rayleigh scattering. The model considers random backscattering via its average strength, i.e. we assume that the feedback is incoherent. In addition, this allows us to speed up simulations sufficiently (up to several orders of magnitude). We found that the model of the incoherent feedback predicts the smooth and narrow (comparing with the gain spectral profile) generation spectrum in the random DFB fiber laser. The model allows one to optimize the random laser generation spectrum width varying the dispersion and nonlinearity values: we found, that the high dispersion and low nonlinearity results in narrower spectrum that could be interpreted as four-wave mixing between different spectral components in the quasi-mode-less spectrum of the random laser under study could play an important role in the spectrum formation. Note that the physical mechanism of the random DFB fiber laser formation and broadening is not identified yet.

In addition, using the proposed model, we investigate temporal and statistical properties of the random DFB fiber laser dynamics. Interestingly, we found that the intensity statistics is not Gaussian. The intensity auto-correlation function also reveals that correlations do exist. The possibility to optimize the system parameters to enhance the observed intrinsic spectral correlations to further potentially achieved pulsed (mode-locked) operation of the mode-less random distributed feedback fiber laser will be discussed.

References

1. S. K. Turitsyn et al. "Random distributed feedback fibre laser," Nat. Photonics 4(4), 231–235 (2010).

2. M. D. Mermelstein et al. "Rayleigh scattering optical frequency correlation in a single-mode optical fiber," Opt. Lett. 26, 58-60 (2001).

9136-62, Session PS1

Resonant modes of plasmonic nano-antenna

Olivier Demichel, Marlene Petit, Benoit Cluzel, Alexandre Bouhelier, Univ. de Bourgogne (France)

Charges oscillations in materials -also called plasmons- allow to confine the electromagnetic field in deep sub-wavelengths domains (down to ?/100) in the vicinity of the surface. This confinement is coupled to a large enhancement in the electric field amplitude which allows to efficiently couple propagating waves with structures at the nanometer scale. This coupling is the essence of any antenna device and plasmons in metallic structures (like Au, Ag ..) have resonnances in the visible range making nowadays possible the realization of nano-antenna for visible light.

Furthemore, as plasmons induce a strong localized electric field, non linear processes (such as second harmonic generation, two photon luminescence (TPL) and so on..) are likely to happen. The efficiency of non linear processes evolves as the squared of the local electromagnetic power. Mapping the TPL signal of a nanostructure is thus a nice approach to access to the electric field distribution of plasmonic modes in nanostructures.

Here, we show that the TPL mapping of gold nanorods depending on the nanorod length allows to 'easily' find structures which are resonant for the excitation wavelength. We spatially modulate the excitation beam polarization in order to excite both even and odd plasmonic modes. Simulations are in quite good agreement with experimental datas. Simulations allow to access to the shapes and polarisation states of the resonant modes depending on the nanorod lengths and on the spatial polarization distribution of the excitation beam. Furthermore, we analyze the angular distribution of back-scattered light depending on excited modes, and we show that the spatial modulation of the excitation beam allows to control the scattering directions of nano-antennas.

9136-63, Session PS1

Multipolar nonlinear light-matter interactions with Gaussian vector beams

Mikko J. Huttunen, Jouni Mäkitalo, Godofredo Bautista, Martti Kauranen, Tampere Univ. of Technology (Finland)

The light-matter interaction (LMI) for nanostructures is often analyzed in terms of the electric and magnetic Mie multipoles. Excitation with a homogeneous plane wave is usually assumed and then the various multipoles arise from field retardation across finitely-sized nanoparticles even when the microscopic LMI is dipolar. This has important implications, e.g., for second-order nonlinear optics, which is electric-dipole-allowed only in non-centrosymmetric materials. In this paper, we show that similar effects can arise from focused excitation with vectorial beams. More specifically, we show that surface second-harmonic generation (SHG) can be analyzed in terms of multipolar contributions while the microscopic LMI is dipolar, leading to strongly asymmetric nonlinear emission in the forward and backward directions.

We demonstrate this by measuring SHG emission into reflected and transmitted directions from silicon nitride thin films with isotropic surface symmetry. A homogeneous and thin sample was chosen, since traditional scalar treatments predict symmetric emission. Therefore, the asymmetric emission can be related to the Mie-type multipoles due to the finitely-sized and vectorial excitation. When the vector nature of light is taken into account, the total electric-field distribution has, in addition to the transverse part, also a longitudinal part. Interestingly, the longitudinal part has different parity compared to the transverse part with respect to the interaction with the sample, giving rise to multipole effects. Indeed, a five-fold difference in the transmitted and reflected emissions was measured when numerical aperture of 0.8 was used to create focused vector excitation.

Our results suggest that separation of the surface and bulk responses, which have dipolar and multipolar character, respectively, may be even harder than thought. In addition, the longitudinal field becomes stronger when light is confined to dimensions comparable to wavelength. Therefore, the effects could be useful for tailoring nonlinear LMIs at the nanoscale, such as in waveguides or optical antennas.

9136-64, Session PS1

Delay-based reservoir computing using semiconductor ring lasers

Romain Modeste Nguimdo, Jan Danckaert, Guy Verschaffelt, Guy Van der Sande, Vrije Univ. Brussel (Belgium)

Reservoir computing (RC) is a computation tool for information processing inspired by the way that the brain processes the information. It can potentially perform computationally hard tasks such as pattern recognition, time series prediction and classification at which the brain excels. Unlike traditional computers where the processing of information is typically handled sequentially, the RC concept is based on the computational power associated with complex nonlinear transient motion developed in a high dimensional nonlinear system. It was shown recently that its architecture can be drastically simplified by replacing the entire reservoir which usually consists of a large number (100 - 1000) of randomly connected nonlinear dynamical nodes by a single dynamical nonlinear node subject to delayed-feedback. In this latter configuration, the delay plays a crucial role: on one hand, it brings the nonlinear node (reservoir) to an infinite dimension and on the other hand, it is used to form the virtual nodes which replace the real nodes in complex networks. Since then delay-based RC concept is increasingly receiving reawakened interest, both numerically and experimentally either to better understand the concept or to further improve the overall performances of such systems. In particular, delay-based RC schemes operating at high bit rates or achieving parallel computation have been proposed using semiconductor lasers with all-optical feedback. However, the RC systems based on delay dynamics discussed in the literature are designed by coupling many different stand-alone components (e.g. long delay fibers, external mirrors, polarization controllers, semiconductor lasers etc..) which lead to bulky, lack of long-term stability, non-monolithic systems. These drawbacks motivate to investigate devices designed in a compact way and integrated on chip. Semiconductor ring lasers (SRLs) or microring lasers appear as promising candidates since they are scalable and can be easily implemented on chip. Furthermore, the fact that several feedback configurations can be achieved allows for more variability in the system design. Due to the existence of two counter propagating modes interacting both linearly and nonlinearly fashion, it is not easy to make a quick estimate of their computational power. In this contribution, we numerically investigate the computational performances of SRLs considering different feedback configurations including double and single cross- and self-feedback configurations. We consider a time series prediction task as benchmark to explore different parameter sets for good performance. In addition we discuss the effect of noise on the RC performances. The results indicate that acceptable results i.e. small prediction errors can be obtained for any of the configurations, providing suitably chosen parameters. Specifically, the feedback strengths can be adjusted such as to obtain good performances below and above the laser threshold currents.

9136-65, Session PS1

Spatial extreme events in a photorefractive single-feedback system

Nicolas Marsal, Vianney Caullet, Delphine Wolfersberger, Marc Sciamanna, Supélec (France)

Rogue waves are extreme events occurring in systems where many waves are present. They are characterized by long tails of their probability density functions (PDF) due to their very low probability of occurrence. Such rare and intense events are originally observed in open ocean in form of freak waves. Their origin is still a matter of debate but a large interest has grown in the last years for observing their appearance in different physical contexts such as in liquid Helium, acoustic turbulence, microwaves cavities, laser fiber systems...

More specifically in optics, despite the large theoretical interest and experimental demonstrations [1] focused mainly on fibers (one dimensional temporal events) and thin Kerr-type media (1D or 2D spatial events) an experimental evidence of spatial extreme events in a bulk photorefractive system is still lacking.

To that aim, we investigate experimentally a photorefractive pattern forming single feedback system. This configuration is known to generate a rich variety of transverse patterns (from rolls and hexagons to dodecagons) and has been extensively investigated in the context of pattern formation control. Here, we consider a different situation far above the primary instability threshold corresponding to the appearance of a stationary Turing pattern (corresponding to the well-known spatial modulational instability). Consequently, the system is in a “turbulent” regime where no stable regular patterns appear but strong spatio-temporal instabilities arise. The observation of the near field intensity distribution of the backward beam with a CCD camera shows the appearance of high peaks whose intensities are well above the average intensity of the whole modulated beam. In many aspects, those peaks are similar, and represent the spatial counterpart of what is known as rogue waves in hydrodynamics and in one dimensional optical temporal fiber systems.

Different statistical criteria are used to demonstrate that those peaks are extreme. First, we study for different input intensities the probability density function of each peak on the near field images. We show that the statistics deviates from a Gaussian distribution and possesses long tails that prove the presence of extreme events. Secondly, we measured that the highest amplitude peaks go beyond the “abnormality factor” criterion for rogue events (larger than 2 times the significant peak height that correspond to the mean value of the intensities of

the third more powerful peaks) used in ocean waves. Finally, we emphasize that the intensity is not the only parameter that influences the appearance of rogue spatial peaks. A nonlocal coupling is induced in the system by precisely tilting the feedback mirror. Such a mechanical action is known to induce advection effect in single feedback systems, leading to the formation of convective instabilities. For our study, the advection effect created by the misalignment influences the PDF and consequently can be used as a control parameter for the observation of extreme events.

[1] D. R. Solli, C. Ropers, P. Koonath, and B. Jalali, "Optical rogue waves," Nature, vol. 450, no. 7172, pp. 1054–1057, 2007.

9136-66, Session PS1

Femtosecond pulse distortion induced by Tamm plasmon polaritons in a metal/photonic crystal system

Boris I. Afinogenov, Lomonosov Moscow State Univ. (Russian Federation); Vladimir O. Bessonov, Lomonosov Moscow State Univ. (Russian Federation) and A.N. Frumkin Institute of Physical Chemistry and Electrochemistry (Russian Federation); Andrey A. Fedyanin, Lomonosov Moscow State Univ. (Russian Federation)

1. Introduction

Tamm plasmon-polaritons (TPP) in photonic crystals (PC) are optical analogues of electronic density localization at the boundary of periodic atomic potential [1] and appear as electromagnetic field localization at the boundary of photonic crystal and metal [2]. Unlike surface electromagnetic waves and surface plasmon-polaritons (SPP) Tamm plasmon-polaritons do not have phase-matching conditions for in-plane wave vector, thus TPP can be excited for any angle of incidence [2].

Ultrafast dynamics of SPP was intensively studied last years [3-4]. Ultrafast measurements can provide information about lifetime and excitation dynamics of the TPP which is of the great fundamental interest and on the other hand is useful for the creating brand new devices for controlling the light.

2. Samples and setup

The studied samples consisted of 6 pairs of ZrO2/SiO2 (average thicknesses 110 nm and 145 nm respectively) quarter-wavelength layers with SiO2 layer on top, deposited on quartz substrate using thermal evaporation. The resultant structure was covered by a 30-nm-thick gold. As a reference sample 30-nm-thick gold film on quartz substrate was used. As a source Ti:Sapphire laser with pulse precompressor was used, providing 30 fs pulses with 80 MHz repetition rate. Polarization of incident light was controlled with a wideband half-wavelength plate. Temporal profiles of femtosecond pulses, reflected from the Au/PC sample and gold film, were obtained using noncollinear intensity cross-correlation measurements. Spectra of reflected pulses were controlled by spectrometer.

3. Experimental results

Experimental cross-correlation function of pulse reflected from reference sample is in an excellent agreement with Gaussian fit. Spectrum of the light, reflected from the gold film demonstrates no features. In the spectrum of light, reflected from the sample, dip was observed, associated with the excitation of the TPP. After tuning the laser the way that pulse spectrum overlaps with the TPP resonance centrally, cross-correlation functions for the reflected pulses were measured. Temporal profiles of ultrashort pulses are distorted in the presence of the TPP. Tails on the trailing edges in cross-correlation functions arise. Tail of TM polarized pulse was approximated with function y = y0 + exp(-x/?), where ? corresponds to the lifetime of TPP, which was found to be 30 fs.

4. Conclusions

It is shown that temporal profile of femtosecond laser pulses reflected from Au/PC system is modified in the presence of Tamm plasmon-polariton. Lifetime of TPP was estimated at 30 ± 1 fs from fitting the tail of cross-correlation function of TM polarized pulse with exponential function.

5. References

[1] I.E. Tamm, JETP 3, 34 (1933).

[2] M. Kaliteevski et al. Phys. Rev. B 76, 165415, (2007).

[3] A. S. Vengurlekar, A. V. Gopal, and T. Ishihara, App. Phys. Lett. 89, 181927 (2006).

[4] P. Vabishchevich, V. Bessonov, F. Sychev et al., JETP lett. 92, 575 (2011).

9136-67, Session PS1

Modeling Kerr frequency combs using the Lugiato-Lefever equation: A characterization of the multistable landscape

Pedro Jose Parra-Rivas, Vrije Univ. Brussel (Belgium) and Consejo Superior de Investigaciones Cientificas (Spain); Damia Gomila, Consejo Superior de Investigaciones Científicas (Spain); Manuel A. Matias, Consejo Superior de Investigaciones Cientificas (Spain); Stephane Coen, The Univ. of Auckland (New Zealand); Lendert Gelens, Vrije Univ. Brussel (Belgium); Francois Leo, Univ. Gent (Belgium)

Optical frequency combs can be used to measure light frequencies and time intervals more easily and precisely than ever before, opening a large avenue for applications. Traditional frequency combs are usually associated with trains of evenly spaced, very short pulses. More recently, a new generation of comb sources has been demonstrated in compact high-Q optical microresonators with a Kerr nonlinearity pumped by continuous-wave laser light. These combs are now referred to as Kerr frequency combs and have attracted a lot of interest in the last few years.

Kerr frequency combs can be modeled in a way that is strongly reminiscent of temporal cavity solitons (CSs) in nonlinear cavities. Temporal CSs have been experimentally studied in fiber resonators and their description is based on a now classical equation, the Lugiato-Lefever equation, that describes pattern formation in optical systems.

The work presented here consists of three main parts. Firstly, we perform a theoretical study of the correspondence between the CSs and patterns with frequency combs. It is known that the CSs appear in reversible systems that present bistability between a pattern and a homogeneous steady state through what it is called a homoclinic snaking structure. In this snaking region, single and multi-peak CSs coexist with patterns and homogeneous solutions, creating a largely multistable landscape. We study the changes of the homoclinic snaking for different parameter regimes in the Lugiato-Lefever equation and determine the stability and shape of the frequency combs through comparison with the underlying CSs and patterns. Secondly, we include third order dispersion in the system and study its effect on the multistable snaking structure. For high dispersion strengths the CS structures and the corresponding Kerr frequency combs disappear. Finally, we consider the effects of small size resonators and discuss how the previous scenarios change when the cavity size decreases.

9136-68, Session PS1

Precise crystal temperature measurement in process of nonlinear frequency conversion of laser radiation

Andrey Baranov, Moscow Institute of Physics and Technology (Russian Federation) and NTO "IRE-Polus" (Russian Federation); Oleg A. Ryabushkin, Aleksey V. Konyashkin, Moscow Institute of Physics and Technology (Russian Federation) and NTO "IRE-Polus" (Russian Federation) and Institute of Radio Engineering and Electronics of RAS (Russian Federation)

At present rapid growth of laser technology demands spectrum broadening of laser sources. One of the perspective solutions of this problem is nonlinear frequency conversion of laser radiation in nonlinear-optical crystals such as LiNbO3, Li3BO4, KTiOPO4 etc. Multiple harmonic generation or parametric generation of laser radiation in such dielectric crystals can be realized. The process of frequency conversion is nonlinear and as follows the intensity of converted wave grows quadratically with pump intensity. Crystals applied in nonlinear optics usually have small optical absorption coefficients. However its heating can be considerable when high-power is involved. It is essential that conversion efficiency depends on phase difference between interacting electromagnetic waves. It means that for efficient conversion these waves should be phase matched. Thereby crystal temperature is crucial parameter because refractive indices that specify phase velocities of interacting waves depend on temperature. We have recently introduced novel method for crystal temperature measurement during its interaction with laser radiation. It is well known that all nonlinear-optical crystals possess piezoelectric properties. When external radio-frequency electric field is applied to the crystal a piezoelectric resonances can be observed when exciting frequency corresponds to one of the crystal intrinsic vibration mode frequencies. At first piezoelectric resonance frequency dependence on temperature is calibrated when crystal is heated uniformly without laser radiation influence. Then crystal equivalent temperature change caused by laser heating is determined directly from revaluation of measured frequency shift of piezoelectric resonance, provided that its dependence on crystal uniform temperature is known. It was shown that frequencies of piezoelectric resonances linearly depend on crystal uniform temperature. Also for the case of linear optical absorption the crystal equivalent temperature during interaction with laser radiation linearly changes with power. However substantially nonlinear behavior of crystal equivalent temperature was observed during phase matched nonlinear frequency conversion process. Optical absorption coefficients are different for interacting waves and wave's intensities are nonuniform along light propagation direction. Consequently temperature distribution inside crystal, which is nonuniform either, influence conversion efficiency. It is obvious that uniform crystal heating by laser radiation can be easily compensated with help of external thermostat temperature adjusting. However crystal nonuniform temperature distribution is much harder to compensate. The phenomenon of crystal nonuniform longitudinal heating could lead to efficiency saturation at values much lower than 100 percents. We conducted experiments of equivalent temperature measurement of PPLN crystal in process of second harmonic generation. Nonlinear dependence of PPLN equivalent temperature on pump power was observed near crystal phase matching temperature. True temperature tuning curves of the crystal itself rather than thermostat were measured. Decrease of equivalent crystal temperature that corresponds to the maximum value of second harmonic power was observed with pump power increase. We introduce combined numerical model of crystal heating in process of second harmonic generation together with second harmonic generation in case of crystal nonuniform temperature distribution. This model explains both nonlinear behavior of crystal equivalent temperature at phase matching and temperature tuning curves distortion in terms of longitudinal temperature gradient inside crystal caused by absorption of pump and generated laser radiation.

9136-69, Session PS1

Synthetic diamond as a new material for on-chip nonlinear wavelength converters

Nathalie Vermeulen, Vrije Univ. Brussel (Belgium); John E. Sipe, Univ. of Toronto (Canada); Lukas G. Helt, Macquarie Univ. (Australia); Hugo Thienpont, Vrije Univ. Brussel (Belgium)

The emergence of synthetic diamond, an artificial material that closely resembles its natural variant, has enabled photonics researchers to start exploiting the unique optical properties of diamond for various applications. Furthermore, over the past few years significant progress has been made in the fabrication of several diamond-based waveguide structures, paving the way to the realization of on-chip diamond-based photonic devices. Diamond waveguides have already been successfully deployed in quantum optical applications, whereby the nitrogen-vacancy centers in the diamond host material serve as individual quantum bits. They are also promising structures for Raman lasing applications. Although the diamond Raman lasers realized thus far all rely on free-space cavities containing a bulk laser crystal, recent numerical simulations show that on-chip diamond waveguide Raman lasers could also exhibit excellent lasing characteristics.

In this conference paper we consider the use of diamond waveguides for another important photonic functionality, namely that of nonlinear wavelength conversion based on Kerr or Raman-resonant four-wave mixing. To realize on-chip nonlinear wavelength converters, researchers initially focused on silicon nanowaveguides, as they enable the use of high-precision manufacturing based on the mature CMOS technology, while exhibiting strong nonlinearities combined with tight light confinement. Furthermore, silicon waveguides allow phase matching the conversion processes both through dispersion engineering and through "automatic" quasi-phase-matching, a new concept that we introduced earlier on. A major drawback of silicon, however, is that it is plagued by strong nonlinear losses at wavelengths below 2.2 microns. To circumvent these nonlinear losses while adhering to CMOS-compatible materials, amorphous silicon nitride waveguides were soon identified as an alternative medium for realizing on-chip wavelength converters. However, it is hard to downscale the waveguide cross-sections below 1 micron^2 due to the modest refractive index of silicon nitride. Furthermore, automatic quasi-phase-matching cannot be exploited here since this phase matching technique requires the nonlinear medium to be crystalline rather than amorphous.

To a large extent, diamond combines the best of silicon and silicon nitride systems. It is a CMOS-compatible material with a Raman gain almost as high as that of silicon, and a Kerr coefficient that is of the same order of magnitude as that of silicon nitride. The relatively high refractive index of diamond allows the use of nanoscale waveguide cross-sections, and the material is free from nonlinear losses even at very short wavelengths down to the ultraviolet. Finally, diamond waveguides offer the same phase matching possibilities as their silicon counterparts.

In this conference paper we predict the performance of diamond waveguide structures for FWM-based wavelength conversion. We investigate both diamond ring converters operating in the near-infrared/mid-infrared and converters covering the ultraviolet/visible domain. We show that, by properly designing the waveguide geometries, high-performance wavelength conversion with dispersion-engineered phase matching and efficiencies above -10dB can be attained over a bandwidth of several tens of THz. Furthermore, we numerically demonstrate that also outside the dispersion-engineered spectral region significant conversion efficiencies can be established by means of "automatic" quasi-phase-matching. Finally, we make a performance comparison between diamond converters and those based on silicon and silicon nitride.

9136-70, Session PS1

Self-action effects in semiconductor quantum dots

Alexander M. Smirnov, Vladimir S. Dneprovskii, Maria V. Kozlova, Lomonosov Moscow State Univ. (Russian Federation); Arseniy R Kanev, Lomonosov Moscow State University (Russian Federation)

Self-diffraction from an induced 1D, 2D and 3D transient photonic crystal has been discovered in the case of resonant excitation of the excitons (electron – hole transitions) in CdSe/ZnS quantum dots (highly absorbing colloidal solution) by powerful beams of mode-locked laser with picosecond pulse duration. Self-diffraction arises for two, three and four laser beams intersecting in the cell with colloidal CdSe/ZnS quantum dots (QDs) due to the induced 1D, 2D and 3D dynamic photonic

crystals respectively. Additionally the bleaching of exciton transition provokes the creation of transparency channel and laser beam's self-diffraction at the induced circular aperture. The physical processes that arise in CdSe/ZnS QDs and are responsible for the observed self-action effects are discussed.

Nonlinear optical effects in QDs are of great interest both for their fundamental properties and important possible application in science and engineering: optical limiting, saturable absorbers for Q-switched and mode-locked lasers, optical switching, etc.. The efficiency of nonlinear optical devices depends on the values of nonlinear changes of absorption and/or refraction. The magnitude of these nonlinearities becomes resonantly enhanced in the spectral vicinity of the absorption edge.

The goal of our work is the investigation of nonlinear optical processes that arise in the case of resonant excitation of the allowed basic exciton transitions of colloidal CdSe/ZnS QDs that lead to self-diffraction effects. Self-diffraction is the self-action effect of light beams that spread in the medium with properties depending on the light intensity. Two types of self-diffraction process may arise in resonantly absorbing QDs. I. In the case of efficient nonlinear absorption (bleaching of the basic exciton transition) the high-power laser beam may create the transparency channel, and thus its self-diffraction may arise at induced aperture. II. Two, three or four powerful intersecting laser beams in absorbing or transparent nonlinear medium induce 1D, 2D and 3D transient photonic crystals respectively due to periodic modulation of absorption and/or refraction and their self-diffraction at created photonic crystals may arise.

Self-action processes in the case of powerful picosecond laser pulse interaction with resonantly excited excitons in colloidal CdSe/ZnS QDs were explained by different processes. A transparency channel and an induced photonic crystals arise as a result of coexisting and competing processes: saturation of the fundamental exciton transition and the red Stark shift of the exciton absorption spectrum. At high excitation either an electron or a hole can be trapped at the surface of QD, this results to appearance of spatially separated charge and hence the emergence of induced electric field which leads to the red Stark shift of the absorption spectrum. Saturation and Stark effects are characterised by different dynamic properties. The relaxation time of the induced electric field, which arises when a carrier is captured by the QD surface is about 5-10 ns; the relaxation time of excited excitons is shorter than 1ns. The relaxation time of excited excitons has been measured by probe technique of an induced 1D photonic crystal.

9136-72, Session PS1

Magnetic-field induced effects in optical second-harmonic generation from magnetic three-layer structures

Tatyana V. Murzina, Irina A. Kolmychek, Victor L. Krutyanskiy, Alexander A. Klevtsov, Lomonosov Moscow State Univ. (Russian Federation)

Composite planar magnetic structures are being studied for quite a time and are known to demonstrate a number of exciting phenomena such as oscillatory exchange coupling through non-magnetic spacers, giant magnetoresistance, enhanced and strongly modified magneto-optical effects, etc. At the same time, not much research has been done in the field of the nonlinear optics. At the same time, it may provide unique information on the properties of multilayer structures. This is especially valid for the particular case of optical second harmonic generation, which is known for its high sensitivity to the main properties of buried interfaces that are hardly available by other experimental techniques.

In this work we present the experimental results on magnetic-field induced effects in optical second harmonic generation (SHG) from planar magnetic three-layer structures of the composition CoFe/nonmagnetic spacer/CoFe of the thicknesses 10 nm/1-2 nm/10(20) nm. The nonmagnetic spacer is alimunum or alumina oxide. Different coercitivity of the ferromagnetic (FM) layers allows for the existence of antiferromagnetic structure, or magnetic toroid moment, for a definite range of the external magnetic field values.

For the SHG experiments the radiation of a femtosecond Ti-sapphire laser operating at 800 nm wavelength was used, the second harmonic radiation was detected in transmission or in reflection from the samples. We measured the SHG intensity magnetic hysteresis loops for the angles of incidence from zero to 50 degrees counted from the normal to the film surface. Linearly or circularly polarized fundamental radiation was used, while linearly polarized SHG was detected. We show experimentally and by model calculation that the observed SHG hysteresis contain necessarily both linear and quadratic in magnetization M components, including those attributed to the interlayer exchange interaction. We also prove that the latter contribution is much more pronounced for circularly polarized pump beam.

This conclusion is made on the base of consecutive analysis of the experimental data for two types of samples. A pronounced asymmetric shape of the magnetic hysteresises of the SHG intensity that appear at different geometrical conditions for the samples with dielectric or metal nonmagnetic spacers proves the role of the quadratic in M SHG components. It is worth to note that commonly in SHG such nonlinear sources are neglected.

We also compare the linear and nonlinear magneto-optical measurements in order to judge on the particular behaviour of magnetic interfaces, which is possible for the SHG studies. The discrepanc? between these two types of measurements reveal peculiarities of the interfaces magnetization.

9136-73, Session PS1

Electrical nonlinear response of a photomixer for applications in ultrafast measurements

Florin L. Constantin, Ctr. National de la Recherche Scientifique (France)

The optoelectronic heterodyne conversion is a well-established technique with applications in frequency conversion, high-speed communications and high-resolution spectroscopy. The experimental setup based on two continuous-wave near-infrared lasers and a photomixer provides a competitive THz source in terms of fabrication technology, spectral purity, broadband modulation and frequency tuning. The design of the photomixer is based on a low-temperature-grown GaAs layer connected with interdigitated electrodes at the driving point of a planar spiral antenna, whose extremities are wire-bonded to a microwave line and electrically addressed with a bias-t. Optical coupling between free-space THz-waves and antenna is performed with a silicon lens. This paper discusses nonlinear current-voltage response of the photomixer within a new analytical model accounting the empirical dependences of carrier lifetime on laser power and electrical bias and of combination-generation processes on photomixer geometry. The second-order electrical nonlinearity of the photomixer is a key parameter addressed by microwave and THz-wave rectification. The measurements of its dependences on the laser power and on the voltage bias are compared with the model.

High-speed direct-current amplitude modulation of THz-waves generated with the photomixer will be presented for the first time. THz-wave modulation index dependence on the modulation voltage and on the photomixer electrical nonlinearity is experimentally investigated and compared with the model. Moreover, THz-wave heterodyne detection technique using as local oscillator the lasers detuned by a THz frequency gap will be presented. Photomixer nonlinearity allows frequency mixing and the low-frequency signal is measured and compared with the model. In addition, this approach allows time-resolved measurements of a dual pulse frequency optical beat by asynchronous optical sampling technique with a THz-wave source that will be presented for the first time.

9136-74, Session PS1

Near-infrared CW OPO in an AlGaAs waveguide

Cécile Ozanam, Marc Savanier, Univ. Paris 7-Denis Diderot (France); Loïc Lanco, Lab. de Photonique et de Nanostructures (France); Alessio Andronico, Ivan Favero, Sara Ducci, Giuseppe Leo, Univ. Paris 7-Denis Diderot (France)

The quest for an electrically pumped monolithic version of the optical parametric oscillator (OPO) is still open half a century after its original demonstration. Recently, orientation-patterned GaAs in the mid-IR has undergone important progress with high-power OPOs exhibiting thresholds of ≈2kW in the pulsed regime and ≈7W in the continuous-wave (CW) regime. [1,2] However, the transposability of this approach to near-IR integrated platform is hindered by large scattering losses at short wavelengths, and by the lack of GaAs-based high-power pump lasers around 2 μm. Therefore the route to a fully integrated tunable semiconductor source of near-IR light remains very ambitious.

In this challenging context, here we demonstrate the first integrated near-infrared OPO in III-V semiconductor waveguide. This nonlinear device is based on a selectively oxidized GaAs/AlAs heterostructure, the same “AlOx” technology that is at the heart of VCSEL fabrication.

The heterostructure and waveguide design allows for type-I form-birefringent phase matching, with a TM00 pump around 1 μm and TE00 signal and idler around 2 μm. Form birefringence is induced in the waveguide core by creating a sub-wavelength periodic stack, where GaAs is alternated with oxidized Al-rich AlGaAs (AlOx). [3,4] Thanks to the high non-resonant chi^(2) of GaAs, the relatively weak guided-wave optical losses, and the fabrication of unconventional monolithic SiO2/TiO2 dichroic Bragg mirrors (6 bi-layers deposed onto non-uniform end facets), we observe a threshold of 210 mW at degeneracy in the CW regime, with a single-pass-pump doubly resonant scheme. For such a continuous-wave pump power, corresponding to an intensity of 0.8?107W/cm2, we can estimate a two-photon absorption of 0.19 cm-1, which is negligible with respect to the linear absorption at pump wavelength.

Further improvement can be achieved by adopting a double-pump-pass scheme [5] and, in a more fundamental way, by further optimizing the waveguide optical losses. The latter are induced by a not entirely mastered AlAs oxidation process and are of two distinct types: Rayleigh-like scattering at signal and idler wavelength (alpha≤ 1cm-1), due to the interface roughness between GaAs and AlOx layers; and absorption at pump wavelengths (alpha≈ 3cm-1), due to volume defects in the GaAs layers adjacent to the aluminum oxide.

This result marks a milestone for integrated nonlinear photonics and represents a significant step toward the goal of a monolithic OPO.

We acknowledge the financial support from the Laboratoire d’Excellence SEAM of Sorbonne Paris Cité, under the DOLPHIN project.

[1] A. Grisard et al., Opt. Mat. Expr. 2, 1020 (2012).

[2] M. Oron et al., Proc. SPIE 8240, 82400C (2012).

[3] J. M. Dallesasse et al., Appl. Phys. Lett. 57, 2844 (1990).

[4] A. Fiore et al., Nature 391, 463 (1998).

[5] J. E. Bjorkholm et al., IEEE J. Quantum Electron. QE-6, 797 (1970).

9136-75, Session PS1

A novel observation of two state behavior in the instability-induced supercontinuum generation of exponential saturable nonlinearity

Nithyanandan Kanagaraj, Pondicherry Univ. (India)

Supercontinuum generation (SCG) is the phenomenon of generating ultrabroad band spectrum has been the subject of intense research in the last few decades. Owing to its potential application in diverse field such as frequency metrology, optical coherence tomography, ultra-short pulse compression, sensor technique, fiber characterization etc., the SCG in the modern days has been recognized as the “White-light laser”. The physics underlying SC generation is now generally well understood; the primary mechanism of generating broadband source is identified as soliton fission (SF) and modulational instability (MI) . Former is the well-known mechanism of generating high quality broadband spectrum driven by the soliton dynamics. Latter is the MI induced SCG (MI-SCG), where the initial dynamics are governed by the noise, which lead to the breakup of the pulses similar to the case of SF. In principle, each material possesses an upper power threshold at which the nonlinear response of the medium saturates, such medium is refereed as the saturable nonlinear medium (SNL) . The power threshold at which nonlinear response of the medium saturates is known as the saturation power. Lyra et al, reported the different functional form of the SNL, out of which ESN is observed to generate the broadest spectrum at relatively shorter distance than the known kind of SNL. Thus, we study the MI induced SCG in the ESN system and report the novel two state behavior in the SCG. We identify and discuss the salient features of ESN and its cutting edge over the other functional form of saturable nonlinearities. An exact dispersion relation is obtained using LSA and the MI analysis is performed. Unlike the conventional Kerr type nonlinearity, the critical modulational frequency (CMF – frequency corresponding to the instability window) does not monotonously increases, rather behaves in a way, such that the increase in power increases the CMF up to the saturation power, and further increase in power decreases the CMF. This is due to the fact that the effective nonlinearity in ESN follows in a unique such that there exist two different powers at which the nonlinearity register same value. Because of which, the MI spectrum is identical at two different powers (i,e) input power (P) above and below saturation power (Ps). Following the MI analysis, we study the SCG numerically using split-step Fourier method. The evolution of spectral bands is studied for different input power and it is observed that the spectrum is nearly identical at two different input powers, corresponding to the constant nonlinear factor. Also, the maximum enhancement of SCG (SCG at shortest distance) is observed only at P = Ps and for all combination of powers the SCG gets inevitable suppressed. This we observe as the unique feature of ESN system and represent as the two state behavior in the SCG. Thus we brings to the light that the dynamics of SCG in ESN are indeed unique and o?ers rich information which could be useful in many applications.

9136-76, Session PS1

High performance and energy efficient RF photonic notch filter using on-chip stimulated Brillouin scattering

David A Marpaung, Blair Morrison, Ravi Pant, Benjamin J. Eggleton, The University of Sydney (Australia)

Microwave photonics (MWP) is a field that primary deals with the generation, distribution, and processing of high speed radio frequency (RF) signals using photonic techniques and components. Photonic technologies enable RF signal processing with low-loss, broad bandwidth, enhanced flexibility, and immunity to electromagnetic interference. For the last 25 years, MWP systems have relied on discrete fiber-based components, but recently there is a growing interest in exploiting photonic integrated circuits in these systems. This so-called integrated microwave photonics (IMWP) approach promises advantages in the reduction of size, weight, power, and cost of MWP systems. Thus far, IMWP has largely been limited to linear optical processing. It is attractive to examine the potential of nonlinear optics in integrated platform for microwave signal processing. Here, we focus on harnessing on-chip stimulated Brillouin scattering (SBS) for high performance RF photonic notch filtering.

Harnessing stimulated Brillouin scattering (SBS) in nanophotonic devices has recently attracted significant interest due to its great potential for realizing tunable slow light, optical frequency comb, and RF photonic signal processor in a compact footprint. For typical RF photonic applications, the amount of SBS gain required is relatively high. For instance, creating an RF photonic notch filters with a moderate 20 dB suppression will require an SBS anti-Stokes spectrum with the same amount of absorption. Realizing such a high SBS gain/absorption in a short chip-scale device has been proven challenging due high pump power required, which might lead to adverse effects such as material degradation or even damage to the device. Thus, to elegantly harness the low SBS gain from on-chip low-power devices to function in real-life applications is highly desired and will represent a technological breakthrough.

In this paper, we report a reconfigurable RF photonic notch filter with an ultra-high suppression (>55 dB), achieved using very low on-chip SBS gain (<1 dB) and pump power (<10 mW). Furthermore, the filter exhibited a high resolution (3-dB bandwidth of 40 MHz), combined with ultra-wide frequency tuning (1-20 GHz) and flexible bandwidth reconfiguration (resolution tuning of 31-77 MHz), achieved by tuning the pump frequency and power. To our knowledge, this is the highest overall performance demonstrated for any on-chip RF photonic filter. This filter shows competitive performance to state-of-the-art integrated electrical RF filters in terms of resolution and suppression, with a key advantage of a 20-fold enhancement in tuning range.

High performance and power efficiency in our filter were achieved by implementing a simple yet powerful RF photonic signal processing scheme that creates anomalously high suppression RF notch filter from virtually any kind of optical resonance, irrespective of its type (gain or absorption), or its magnitude. In this scheme, an electro-optic modulator (EOM) was used to generate an RF-modulated dual-sideband (DSB) signal with tunable relative amplitude and phase. The complex (magnitude and phase) response of an optical resonant filter was then used to tailor the relative amplitude and phase of these sidebands, to create a destructive interference at a specific RF frequency to leading to a notch with an ultra-high suppression.

9136-11, Session 3

Broadband mid-IR frequency conversion and quantum photonics in monolithic semiconductors *(Invited Paper)*

Amr S Helmy, Univ. of Toronto (Canada)

No Abstract Available

9136-12, Session 3

High-yield second-harmonic generation from mid-infrared to near-infrared regions in silicon-organic hybrid plasmonic waveguides

Jihua Zhang, Xinliang Zhang, Wuhan National Lab. for Optoelectronics (China); Eric Cassan, Institut d'Électronique Fondamentale (France)

After a wide range of attractive applications in the telecom-band for optical communications, silicon nanophotonics has also recently raised a great interest for mid-infrared (IR) applications due to the low inherent loss of silicon and broad application fields in this wavelength range. Especially, principles and devices based on nonlinear frequency conversion to bridge the mid-IR-to-near-IR gap have been intensively studied. These works were mainly based on the third-order nonlinear four-wave mixing (FWM) in silicon. For example, spectral translation of a signal at lambda=2440 nm to the telecom band at lambda=1620 nm was realized based on FWM in silicon wires. However, the conversion efficiency may be increased by using nonlinear materials with larger nonlinear susceptibilities or lower-order nonlinear processes with larger efficiencies. Plasmonic based nonlinear devices also open up opportunities for further improving the performance of nonlinear processes and scaling down the sizes.

In this context, we report the theoretical investigation of the quadratic nonlinear property of a silicon-organic hybrid plasmonic waveguide with a thin polymer layer deposited on top of a silicon slab and covered by a metal cap. Due to the hybridization property of the waveguide modes, efficient phase-matched second harmonic generation (SHG) from mid-infrared (~3.1?m) to near-infrared wavelength windows (~ 1.55 ?m) is achieved with small fabrication-error sensitivity (225nm< tolerated waveguide width < 378 nm) and large bandwidth (100nm). The SHG yield is as large as 8.8% for a pumping power of only 100 mW.

9136-13, Session 3

All-optical generation of surface acoustic waves in a silica optical microwire

Jean-Charles Beugnot, FEMTO-ST (France) and Univ. de Franche-Comté (France); Sylvie Lebrun, Lab. Charles Fabry (France) and Univ. Paris-Sud (France); Gilles Pauliat, Institut d'Optique Graduate School (France) and Univ. Paris-Sud (France); Vincent Laude, Hervé Maillotte, FEMTO-ST (France) and Univ. de Franche-Comté (France); Thibaut Sylvestre, Univ. de Franche-Comté (France) and FEMTO-ST (France)

The complex and intriguing dynamics of light-sound interactions in tiny optical waveguides have recently witnessed a renewed interest because of their experimental realization in emerging key areas of modern optics [1]. Among other microdevices, silica micro or nanowires are the tiny and as-yet underutilized cousins of optical fibres [2]. These hair-like slivers of glass enable enhanced nonlinear optical effects and applications not currently possible with comparatively bulky optical fibers. Although fiber tapers have helped greatly improve optical Kerr effect and stimulated Raman scattering in the framework of supercontinuum generation and wavelength conversion, Brillouin scattering in these tiny waveguides has never been observed yet.

In addition to standard stimulated Brillouin scattering (SBS), here, we demonstrate the generation of a new class of surface acoustic waves in a subwavelength-diameter silica microwire and term this new effect as surface acoustic wave Brillouin scattering (SAWBS). Using numerical simulations based on electrostriction [3] and experimental results, we show that SAWBS results from the stimulated optical excitation of Rayleigh-type surface-ripple waves propagating at a velocity of 3400 m/s along the optical microwire surface and giving rise to new useful RF sidebands around 6 GHz in the scattering spectrum. As these new acoustic resonances are strongly sensitive to microwire surface, SAWBS opens new interesting opportunities for various sensor applications but also in other domains such as telecommunications, microwave photonics and plasmonics.

[1] Bahl, G., Zehnpfennig, J., Tomes, M. & Carmon, T. "Stimulated optomechanical excitation of surface acoustic waves in a microdevice," Nature Communications 2, 403 (2011).

[2] Tong, L. Gattass R. R. and Ashcom J. B. "Subwavelength-diameter silica wires for low-loss optical wave guiding," Nature 426, 816–819 (2003).

[3] Laude V. and Beugnot, J.-C. "Generation of phonons from electrostriction in small-core optical waveguides," AIP Advances 3, 042109 (2013).

9136-14, Session 3

Supercontinuum generation in hydrogenated amorphous silicon waveguides at telecommunication wavelengths

Jassem Safioui, Univ. Libre de Bruxelles (Belgium); François Leo, Bart Kuyken, Shankar K. Selvaraja, Roel G. Baets, Univ. Gent (Belgium) and IMEC (Belgium); Philippe Emplit, Univ. Libre de Bruxelles (Belgium); Gunther Roelkens, Univ. Gent (Belgium) and IMEC (Belgium); Serge Massar, Univ. Libre de Bruxelles (Belgium)

Recently, hydrogenated amorphous silicon (a-Si-H) waveguides have attracted a lot of attention. Its larger band-gap than crystalline silicon gives a lower two-photon absorption (TPA) and a significantly higher figure of merit (FOM > 2) at telecom wavelengths. Therefore, the demonstration of several nonlinear functions such as parametric amplification, frequency conversion and all-optical signal processing became feasible. In this work, we demonstrate supercontinuum (SC) generation in a-Si-H waveguides at telecommunication wavelengths using short picosecond pulses (FWHM≈1.2 ps). We investigate the SC in waveguides of different cross section ranging from 500?220 nm2 to 800?220 nm2, which changes the dispersion of the waveguide. Correspondingly we observe large changes in the bandwidth of the SC, since it is 300 nm wide in 500?220 nm2 waveguides and reaches 550 nm in 800?220 nm2 waveguides.

Following the spectrum evolution versus power, we observe that self-phase modulation, modulation instability, and dispersive wave generation are the main processes responsible for the SC generation in all these waveguides.

The major drawback of this material at telecommunication wavelengths is optical degradation which has been reported in some experiments when injecting high pump power into 500?220nm2 waveguides. In the wider waveguides, which produce the broader SC, degradation seems to be very low at this pulse width, since the SC bandwidth remains constant even after one hour of continuous exposure to the high power pulse train.

Finally a comparison with crystalline silicon waveguides of similar geometry will also be made.

9136-15, Session 3

Opportunities for Raman wavelength conversion with silicon microdisks

Iterio Degli-Eredi, Nathalie Vermeulen, Hugo Thienpont, Vrije Univ. Brussel (Belgium)

In recent years, the use of nonlinear optics to enable all-optical wavelength conversion in waveguide structures has gained widespread interest in different application domains. In the field of integrated nonlinear optics, silicon-on-insulator (SOI) is one of the most promising material systems because of the possibility to mass-manufacture SOI structures with the mature CMOS technology and because of silicon's high Raman optical nonlinearity. In Raman-based wavelength converters, a signal input is converted to an idler output in the presence of a pump through Coherent anti-Stokes Raman scattering (CARS). This process benefits from the tight light confinement in SOI structures, and when using SOI microrings or SOI microdisks, one has the additional advantage that the light is resonantly enhanced in these structures. In comparison with microrings where the light is guided by a ring-shaped waveguide, microdisks have the extra asset that the light modes have typically smaller propagation losses, leading to higher cavity enhancement factors.

One of the main issues of using CARS for wavelength conversion is the dispersion-induced phase mismatch that deteriorates the efficiency of the conversion process, as the newly generated idler is sequentially amplified and depleted depending on the dephasing with the other waves involved in the process. We have shown earlier on that an appropriate method to overcome this issue in silicon microrings, is using the concept of "automatic" quasi-phase matching (QPM). In QPM, the nonlinearity is 'switched off' periodically in the regions of the structure where the idler is depleted. Only the dephasing between the waves is then compensated in those regions, thus leaving the idler intensity unaffected there. Hence, the waves travel through subsequent nonlinearly active and passive layers, which result in a net idler gain. Since the nonlinear susceptibility of CARS for transverse electric (TE)-polarized light is dependent on the angle between the crystal axes and the light polarization in <100>-grown uniform silicon microrings, the light modes experience alternating nonlinearly active/passive regions, while propagating along the uniform rings. If the correct ring radius is chosen such that the nonlinearly active/passive regions along the propagation path of the mode correspond to the idler gain/depletion regions that normally occur due to the phase mismatch, QPM is "automatically" achieved.

In this paper, we numerically investigate whether this "automatic" QPM concept for Raman wavelength conversion can be applied to silicon microdisks instead of microrings. We show that, for each wavelength involved in the nonlinear process, we can excite the proper light mode for which the "automatic" QPM concept is obtained in the microdisk, and find that we can achieve wavelength conversion efficiencies close to 0 dB at input pump powers as low as a few mWs.

9136-16, Session 4

Ultra-weak interactions of temporal cavity solitons observed over astronomical distances *(Invited Paper)*

Miro Erkintalo, Univ. of Auckland (New Zealand); Jae-Kyung Jang, EO Technics Co., Ltd. (Korea, Republic of); Stuart G. Murdoch, Stephane Coen, The Univ. of Auckland (New Zealand)

No Abstract Available

9136-17, Session 4

Giant breathers in nonlinear fiber optics

Benoit Frisquet, Bertrand Kibler, Guy Millot, Univ. de Bourgogne (France)

The nonlinear wave propagation has been an intense subject of research for scientists since the 1960s, in particular by using a universal model of nonlinear science, the nonlinear Schrödinger equation (NLSE), with applications to plasma waves, deep water waves, optics and quantum condensates. Recently, nonlinear fiber optics has proved the existence of other nonlinear waves: the soliton on finite background (or breather) predicted in systems governed by NLSE since more than 25 years. These localized waves evolving on a continuous background are considered the simplest models of the growth and decay of isolated steep wave events (rogue waves) in many nonlinear dispersive systems. But although their first observations were confirmed in different domains of nonlinear science during the last years, including hydrodynamics and plasma physics, no experiment has been performed in order to reveal synchronized interactions between these first-order periodic solutions of the NLSE. We report here a novel optical fiber-based test bed to excite the formation of two breathers that collide during propagation. In particular we have used the spectral shaping of an optical frequency comb to synthesize tailored modulated initial conditions of the continuous wave. We show that controlling the phase and group velocity differences between breathers is required to their efficient collision and the emergence of a giant localized wave. Our high quality pulse characterization in optics has allowed us to compare the resulting wave form to the theoretical description of the collision given by higher order solutions of the model. Our work confirms that one can now consider the collision of breather waves as an alternative to describing giant rogue

waves. A first experimental proof of the control of such an interaction between complex waves is also of fundamental importance for testing theories of nonlinear wave dynamics in cross-disciplinary research.

9136-18, Session 4

Spatio-temporal stability of 1D Kerr cavity solitons

Pedro Jose Parra-Rivas, Vrije Univ. Brussel (Belgium) and Instituto de Física Interdisciplinar y Sistemas Complejos (Spain); Lendert Gelens, Vrije Univ. Brussel (Belgium); François Leo, Univ. Gent (Belgium) and IMEC (Belgium); Damia Gomila, Manuel A. Matias, Instituto de Fisica Interdisciplinar y Sistemas Complejos (Spain); Stephane Coen, The Univ. of Auckland (New Zealand)

The Lugiato-Lefever equation (LLE) has been extensively study since its derivation in 1987, when this mean-field model was introduced to describe nonlinear optical cavities. The LLE was originally derived to describe a ring cavity or a Fabry-Perot resonator with a transverse spatial extension and partially filled with a nonlinear medium but it has also been shown to be applicable to other types of cavities, such as fiber resonators and microresonators.

Depending on the parameters used, the LLE can present a monostable or bistable input-output response curve. A large number of theoretical studies have been done in the monostable regime, but the bistable regime has remained widely unexplored. One of the reasons for this was that previous experimental setups were not able to works in such regimes of the parameter space. Nowadays the possibility of reaching such parameter regimes experimentally has renewed the interest in the LLE.

In this contribution, we present an in-depth theoretical study of the different dynamical regimes that can appear in parameter space, focusing on the dynamics of localized solutions, also known as cavity solitons (CSs). We show that time-periodic oscillations of a 1D CS appear naturally in a broad region of parameter space. We provide the first experimental evidence of this oscillatory regime of operation of this temporal 1D CS. More than this oscillatory regime, we theoretically report on several kinds of chaotic dynamics. We show that the existence of CSs and their dynamics is related with the spatial dynamics of the system and with the presence of a codimension-2 point known as a Fold-Hopf bifurcation point. Although several of the dynamical regimes were out of reach for our experimental setup using a fiber resonator, such operation regions can become accessible by using other devices such as microresonators, for instance widely used for creating optical frequency combs.

9136-19, Session 4

Strong nonlocal interaction stabilizes cavity solitons with a varying size plateau

Cristian Fernandez Oto, Mustapha Tlidi, Univ. Libre de Bruxelles (Belgium); Daniel Escaff, Univ. de Los Andes (Chile); Marcel G. Clerc, Univ. de Chile (Chile); Pascal Kockaert, Univ. Libre de Bruxelles (Belgium)

Cavity solitons are localized light peaks in the transverse section of nonlinear resonators. These structures are usually formed under a coexistence condition between a homogeneous background of radiation and a self-organized patterns resulting from a Turing type of instabilities. In this issue, most of studies have been realized ignoring the nonlocal effects.

Non-local effects can play an important role in the formation of cavity solitons not only in optics such as liquid crystal and meta-materials but also in various out of equilibrium systems such as populations dynamics and plant ecology [1,2,3]. Depending on the choice of the nonlocal interaction function, the nonlocal coupling can be strong or weak. When considering strong interaction, the non-local function decays slower that an exponential [4]. In this case, the interaction between fronts is controlled by the whole non-local interaction function. However, when considering a weak type of coupling, front interaction is described by the asymptotic behavior of the tail of one front around the position of the other.

On the other hand, experiments on liquid crystals and on photorefractive materials show a strong non-local response mediated by Lorentzian Kernel [5,6]. Recently we have shown that this type of nonlocal coupling strongly affects the dynamics of fronts connecting two homogeneous steady states and leads to the stabilization of cavity solitons with a varying size plateau [7].

In this communication, we consider a ring passive cavity filled with a Kerr medium like a liquid crystal or left-handed materials and driven by a coherent injected beam. We show that cavity solitons resulting for strong front interaction are stable in one and two-dimensional setting out of any type of Turing instability. Their spatial profile is characterized by a varying size plateau. For fixed values of the dynamical parameters, their size varies strongly as a function of the injected field intensity. We show that, in some limits, this kind of cavity solitons can be explain by fronts interaction. Our results can apply to large class of spatially extended systems.

References

[1] M. G. Clerc, D. Escaff, and V. M. Kenkre, Phys. Rev. E 82, 036210 (2010).

[2] M. Tlidi, R. Lefever, and A. Vladimirov, Lect. Notes Phys. 751, 381 (2008).

[3] L. Gelens, G. Van der Sande, P. Tassin, M. Tlidi, P. Kockaert, D. Gomila, I. Veretennicoff, and J. Danckaert, Phys. Rev. A 75, 063812 (2007).

[4] D. Escaff , Eur. Phys. J. D 62, 33(2011).

[5] X. Hutsebaut, C. Cambournac, M. Haelterman, J. Beeckman, and K. Neyts, JOSA B, 22, 1424 (2005)

[6] A. Minovich, D.N. Neshev, A. Dreischuh, W.Krolikowski, and Y.S. Kivshar, Opt. Lett. 32, 1599 (2007).

[7] C. Fernandez-Oto, M.G. Clerc, D. Escaff, and M. Tlidi, Phys. Rev. Lett., 110, 174101 (2013).

9136-20, Session 4

Spatial polarization domain-wall solitons

Maïté Swaelens, Simon-Pierre Gorza, Pascal Kockaert, Univ. Libre de Bruxelles (Belgium); Stephane Coen, The Univ. of Auckland (New Zealand); Marc Hälterman, Univ. Libre de Bruxelles (Belgium)

In nonlinear Kerr media with anomalous dispersion, it is well known that bright solitons are related to modulational instability. In the same way, Haelterman et al. predicted the existence of a new kind of soliton related to the Berkhoer and Zakharov modulational instability that occurs in the normal dispersion regime of propagation. Such structures can be formed when cross-phase modulation is higher than self-phase modulation. They consist in the transition between two do- mains of opposite circular polarizations, and were therefore named “polarization domain wall solitons” (PDW). The existence of PDW has experimentally been demonstrated in the temporal domain in 1999 by Pitois et al.

Up to now, however, the domain-wall soliton has not yet been observed in the spatial domain, probably because its observation requires a medium exhibiting a strong negative instantaneous nonlinear refractive index (n2). In this work, we propose to make use of colloidal semiconductor quantum dots (CSQD), as they can present the required strong negative n2. Although the crystalline structure of semiconductors is not isotropic, the use of CSQD ensures isotropy on a macro- scopic scale, which in turns implies that cross-phase modulation effects are two times higher than self-phase modulation.

The geometry of our system is as follows : two orthogonally polarized beams are copropagating side by side so that the soliton is formed at their boundary. The numerical simulations that were performed in order to determine the experimental

conditions enabling the observation of the spatial PDW soliton have shown that the formation of spatial PDW is possible even with initial condition far from ideal, i.e. with a sharp initial transition between the two polarization components and Gaussian shape for the beam the domain wall is inscribed on.

9136-21, Session 5

Extreme pulse compression and deep-UV generation in gas-filled hollow-core PCF *(Invited Paper)*

KaFai Mak, Max-Planck-Institut für Physik (Germany); John C. Travers, Max-Planck-Institut für die Physik des Lichts (Germany); A. Ermolov, Max-Planck Institut für Physik (Germany); F. Tani, Shinmaywa Industry Co., Ltd. (Japan); Philipp Hoelzer, Max-Planck-Institut für die Physik des Lichts (Germany); Amin Abdolvand, Medical Research Council (United Kingdom); Nicolas Y. Joly, Philip St. John Russell, Max-Planck-Institut für die Physik des Lichts (Germany)

The unique properties of kagomé-style hollow-core photonic crystal fiber (kagomé-PCF) make it an excellent platform for the study of ultrafast nonlinear optics in gases. Not only is the optical loss relatively low across a broad transmission window, but the anomalous waveguide dispersion is also comparable in magnitude to the normal dispersion of many filling gases at pressures of a few atmospheres. The result is a simple system that combines pressure-tunable dispersion with significant optical nonlinearity. By virtue of its small and hollow core, nonlinear effects such as SPM-induced spectral broadening of fs pulses can be investigated at energies (≈100 nJ to 100 ?J) that would cause damage in conventional solid-core PCF, but in most cases are below the values needed in hollow capillaries. Pulse energies in the aforementioned range are available in current state-of-the-art high brightness and high repetition rate fiber and thin-disk lasers. Furthermore, the ability to pump in the anomalous dispersion regime and excite intense low-order solitons (N = 1-10) leads to interesting dynamics, such as soliton self-compression and the related generation of dispersive radiation. Recent examples of the use of gas-filled PCF include the scaling of conventional SPM-induced spectral broadening and subsequent chirped-mirror-based pulse compression to intermediate energies, compressing a 103 fs, 10 ?J pulse at 800 nm down to 10.6 fs; the use of the initial stage of soliton self-compression to directly obtain few-cycle pulses, compressing an input 24.3 fs pulse down to 6.8 fs; and the efficient generation of dispersive waves when the self-compressing soliton is perturbed by higher-order dispersion, resulting in a tunable source of visible to vacuum-UV light when pumping at 800 nm.

9136-22, Session 5

Controlling modulation instability using an incoherent low-amplitude seed

Thomas Godin, Duc Minh Nguyen, Shanti Toenger, Yves Combes, Benjamin Wetzel, Thibaut Sylvestre, FEMTO-ST (France); Goëry Genty, Tampere Univ. of Technology (Finland); Frédéric Dias, Univ. College Dublin (Ireland); John M. Dudley, FEMTO-ST (France)

Modulation instability (MI) corresponds to the exponential growth of a low-amplitude noise on an incident continuous-wave or quasi-CW pump and underlies fundamental nonlinear processes such as in fiber supercontinuum (SC) generation [1]. The spectral and noise properties of MI-driven SC have been shown to be extremely sensitive to the presence of a low-amplitude co-propagating seed. However, all previous studies have been carried out using highly coherent seed and pump [2]. Here we report the seeding of MI with a partially-coherent external seed and study the influence of the seed bandwidth on the broadening dynamics and show a strong resonance phenomenon at peak MI gain. Specifically, we use broadband ASE to seed picosecond MI in a highly nonlinear fiber and we observe resonant enhancement of the MI spectral width as well as noise reduction as the seed wavelength is swept across the peak of the MI gain curve. Using a dispersive time-stretching technique, we record the shot-to-shot spectral fluctuations of the output spectra and reveal improvement in noise properties directly. We also performed numerical simulations to illustrate the influence of the seed on the MI structure and excellent agreement with experimental results is found. Moreover, by increasing the ASE seed bandwidth we studied the influence of the effective coherence time of the seed on the MI spectral and noise properties. This has allowed us for the first time to show that the seed coherence is a critical factor in observing seeded MI; the resonant effects described above only when the seed coherence time is longer or comparable to the pump pulse duration [3]. These results provide new insights into the dynamics of MI in general, and show that the specific use of a seed can have a strong effect on MI spectral properties.

[1] G. Genty and J.M. Dudley, IEEE J. Quantum Electron. 45, 187 (2009).

[2] K.K.Y. Cheung et al., Opt. Lett. 36, 160 (2011).

[3] D.M. Nguyen et al., Submitted to Opt. Lett. (2013).

9136-23, Session 5

Tunable stimulated Brillouin scattering in hybrid polymer-chalcogenide tapered fibers

Jean-Charles Beugnot, FEMTO-ST (France); Raja Ahmad, Martin Rochette, McGill Univ. (Canada); Vincent Laude, Hervé Maillotte, Thibaut Sylvestre, FEMTO-ST (France)

Chalcogenide-glass fibers offer a unique set of optical properties presenting an excellent platform for development of highly nonlinear optical devices for all-optical signal processing and mid-infrared applications [1]. In addition to providing broadband and orders of magnitude larger nonlinear gain in telecommunication bands with respect to the conventional single-mode silica fibers [2], chalcogenide-based fibers allow for the achievement of supercontinuum sources covering wavelength up to 10 μm in the mid-infrared region. Enhanced stimulated Brillouin scattering (SBS) has also been evidenced in chalcogenide optical fibers and in photonic chips. SBS is of particular interest because it has important implications in various fields ranging from slow light to optical fiber sensors and lasers. On the other hand, it can be detrimental to other specific applications such as parametric signal processing by limiting the transmitted optical power. Here we demonstrate both the control and the reduction of SBS using polymer-coated chalcogenide (As2Se3) tapered optical fibers with sub-micrometer waists over a length of a few centimeters. We show that the SBS frequency shift can be widely tuned over a broad radio-frequency range by varying the core diameter of the optical microwire. In addition, it is observed that the hybrid polymer-As2Se3 optical microwires enable a strong Brillouin linewidth broadening up to 125 MHz and a higher SBS power threshold compared to standard chalcogenide optical fibers, as the result of damping of acoustic waves in the polymer cladding. Thanks to their robustness and desired optical properties, hybrid PMMA-As2Se3 microwires are promising candidates for the development of the ultimate compact nonlinear fibered optical devices.

[1] B. J. Eggleton, B. Luther-Davies K. Richardson, "Chalcogenide photonics", Nature Photonics 5, 3, 141– 148 (2011).

[2] R.Ahmad & M. Rochette, "High efficiency and ultra broadband optical parametric four-wave mixing in chalcogenide-PMMA hybrid microwires," Opt. Express 20, 9572-9580 (2012).

9136-24, Session 5

Normal dispersion modulation instability in an As2Se3 chalcogenide hybrid microwire

Thomas Godin, Yves Combes, FEMTO-ST (France); Raja Ahmad, Martin Rochette, McGill Univ. (Canada); Thibaut Sylvestre, John M. Dudley, FEMTO-ST (France)

Modulation instability (MI) in an optical fiber manifests itself by the exponential growth of a low-amplitude noise or signal on a quasi-CW pump and is associated with the appearance of two parametric sidebands. MI has been shown to be a key mechanism in noise-driven processes such as supercontinuum (SC) generation in the long-pulse regime [1] and is most commonly studied in the anomalous dispersion regime of an optical fiber, although its observation in the normal regime has been reported previously in a silica photonic crystal fiber [2]. We report here the first observation of MI in the normal dispersion regime of a tapered As2Se3 hybrid microwire with far detuned sidebands located at wavelengths around 2 μm and 3.5 μm. Chalcogenide glasses are a promising material in the field of mid-infrared (MIR) broadband SC generation as they exhibit impressive nonlinear optical properties: a nonlinear refractive index 1000? larger than silica and a wide transmission window in the MIR [3]. We use here a tapered microwire made up of an As2Se3 core (3.6 μm diameter in the wire region) and a polymer cladding which is pumped at a wavelength of 2620 nm. When increasing the pump power, we clearly observe the emergence of the two MI sidebands located at ±30 THz from the pump, which corresponds exactly to the value derived using the microwire dispersion coefficients [4]. This observation has been confirmed using numerical simulations based on a stochastic nonlinear Schrödinger equation (NLSE) model. These results show the potential of chalcogenide nanowires for far-detuned mid-infrared frequency conversion with potential applications in sensing at new wavelengths and for entangled photons pair generation.

[1] J. M. Dudley, et al., Rev. Mod. Phys. 78, 1135-1184 (2006).

[2] J. D. Harvey, et al., Opt. Lett. 28, 2225-2227 (2003).

[3] B. J. Eggleton, et al., Nat. Photon. 5, 141-148 (2011).

9136-25, Session 5

Temporal localized structures in a photonic crystal fiber resonator

Lyes Bahloul, Univ. des Sciences et de la Technologie Houari Boumediene (Algeria); Mustapha Tlidi, Univ. Libre de Bruxelles (Belgium); Lynda A. Cherbi, Univ. des Sciences et de la Technologie Houari Boumediene (Algeria)

Temporal localized structures are nonlinear pulses that have been theoretically predicted [1] and experimentally observed in fiber ring resonator [2]. These studies have been limited to fiber cavity with group-velocity dispersion restricted to the second order.

In this communication, we consider the effects of high orders dispersion on the dynamics of temporal localized structures in photonic crystal fiber resonator pumped by a continuous wave of power. We assume a single mode optical fiber, the free propagation of light along the fiber is described by the nonlinear Schrödinger equation (NLS) in which the propagation constant is expanded up to the fourth order in a Taylor series. The NLS is supplemented by appropriate resonator boundary conditions. This analysis leads to the generalized Lugiato-Lefever model. This mean field approach is valid in the double limit of high cavity finesse and the nonlinear cavity phase shift must be much smaller than unity. Furthermore, we assume that the length of the cavity is much shorter than the characteristic dispersion lengths of the field. Finally, we assume that the optical field maintains its polarization as it propagates along the fiber. We therefore neglect polarization instabilities. The inclusion of the fourth dispersion allows the modulational instability to have a finite domain of existence delimited by two pump power values [3,4].

We show that temporal localized structures exhibit a motion with a constant velocity [4]. This regular drift is induced by a broken reflection symmetry mediated by third-order dispersion.

We focus the analysis on both bright and dark temporal localized structures. They consist of asymmetric moving peaks or dips in a uniform background of the intensity profile. The number of the moving localized structures and their temporal distribution is determined solely by the initial conditions. We characterize this motion by computing the velocity of bright and dark temporal localized structures. Without fourth order dispersion dark localized structures do not exist.

Finally, a weakly nonlinear analysis allows us to estimate analytically the threshold of the appearance of bright localized structures in the vicinity of the first threshold associated with the modulational instability.

REFERENCES

[1]A.J. Scroggie et al., Chaos, Solitons and Fractals, 4, 1323 (1994).

[2]F. Leo et al., Nature Photonics, 4, 471 (2010).

[3] M. Tlidi, et al. Opt. Lett. 32, 662 (2007); M. Tlidi and L. Gelens, Opt. Lett. 35, 306 (2010).

[4]M. Tlidi, L. Bahloul, L. Cherbi, A. Hariz, and S. Coulibaly, Phys. Rev A, 88, 035802 (2013).

9136-26, Session 6

High-speed multiphoton imaging *(Invited Paper)*

Jeffrey A. Squier, Colorado School of Mines (United States)

No Abstract Available

9136-27, Session 6

Airy beams propagation in optically induced photonic lattices

Bojana M. Bokic, Univ. of Belgrade (Serbia); Falko Diebel, Westfälische Wilhelms-Univ. Münster (Germany); Dejan Timotijevic, Aleksandra Piper, Univ. of Belgrade (Serbia); Martin Boguslawski, Westfälische Wilhelms-Univ. Münster (Germany); Dragana M. Jovic, Institute of Physics (Serbia); Cornelia Denz, Westfälische Wilhelms-Univ. Münster (Germany)

Airy beams are a well-known type of accelerating optical beams [1]. Unlike ordinary optical wave fronts, Airy beams show an accelerated transverse intensity distribution which remains invariant along their parabolic trajectories [2]. The ballistic-like properties of the Airy beam qualified it for various applications ranging from particle trapping along curved paths [3] and self-bending plasma channels [4] to ultrafast self-accelerating pulses [5] and Airy light bullets accelerating in both transverse dimensions and in time [6]. Over the years, higher dimensional Airy beams have been systematically investigated, particularly in the field of optics and atom physics. In terms of experimental realization, optics provides a fertile ground to directly observe and study the properties of such non-spreading localized waves in detail. One of the interests of these beams is their potential for applications in nonlinear optics: nonlinear interaction of light with some material and a study of accelerating beam dynamics inside nonlinear media. Formation of accelerating self-trapped optical beams has been proposed employing different self-focusing nonlinearities, ranging from Kerr to quadratic nonlinearities, and also using an optically induced refractive-index potential [7, 8].

We analyze theoretically and experimentally how an optically induced photonic lattice affect and modify acceleration of Airy beams. Various conditions for the propagation and existence of Airy beams are considered. Acceleration control of Airy beams using different lattice defects is also investigated. We consider

how the positive and negative defects influence the beam diffraction as well as reduction of beam acceleration. Modifying refractive index change, as well as defect size, the acceleration can be reduced to the point of creating a beam that propagates similar to discrete beams or Airy defect modes.

Our analysis provides a very good tool for manipulation and controlling Airy beam acceleration and self bending properties, as well as appropriate conditions for the formation of discrete and surface waves or additional class of defect modes. A similar method can be used for control of other accelerating beams, such as parabolic beams.

REFERENCES

[1] G.A. Siviloglou, J. Broky, A. Dogariu, and D. N. Christodoulides, Phys. Rev. Lett. 99, 213901 (2007).

[2] G. A. Siviloglou, J. Broky, A. Dogariu, and D. N. Christodoulides, Opt. Lett. 33, 207 (2008).

[3] J. Baumgartl, M. Mazilu, and K. Dholakia, Nat. Photonics 2, (2008) 675–678.

[4] P. Polynkin, M. Kolesik, J. V. Moloney, G. A. Siviloglou, and D. N. Christodoulides, Science 324, (2009) 229–232.

[5] A. Chong, W. H. Renninger, D. N. Christodoulides, and F. W. Wise, Nat. Photonics 4, (2010)103–106.

[6] D. Abdollahpour, S. Suntsov, D. G. Papazoglou, and S. Tzortzakis, Phys. Rev. Lett. 105, (2010) 253901.

[7] I. Kaminer, M. Segev, and D. N. Christodoulides, Phys. Rev. Lett. 106, 213903 (2011).

[8] Zhuoyi Ye, Sheng Liu, Cibo Lou, Peng Zhang, Yi Hu, Daohong Song, Jianlin Zhao, and Zhigang Chen, Opt. Lett. 36, 3230 (2011).

9136-28, Session 6

AlGaAs microdisks for SHG in the telecom range

Silvia Mariani, Alessio Andronico, Univ. Paris 7-Denis Diderot (France); Aristide Lemaître, Lab. de Photonique et de Nanostructures (France); Ivan Favero, Sara Ducci, Giuseppe Leo, Univ. Paris 7-Denis Diderot (France)

Nonlinear frequency conversion can be very efficient in Whispering Gallery Mode (WGM) semiconductor microresonators, thanks to high optical confinement and a good modal overlap. Moreover, the 4bar crystallographic symmetry, characteristic of GaAs compounds, together with a circular geometry, provides effective quasi-phase matching (QPM) without the need of domain inversion. [3]

In this framework, some experimental studies have been recently published reporting on Second Harmonic Generation (SHG) in GaAs WGM microcavities [1, 2]. However, GaAs does not allow working with a Fundamental Frequency (FF) mode in the telecom range, since the second harmonic photons energy exceeds the gap energy and two photon absorption losses are high up to 1800 nm. With the outlook of new technological applications, it would be interesting to work with a pump wavelength in the third telecom window.

Here we report on the design, fabrication and characterization of Al_0.4Ga_0.6As microdisks suspended on a GaAs pedestal, conceived for SHG with a FF wavelength around 1550 nm [4]. For a microcavity with optimal radius (R=1.866 μm) and thickness (h=150 nm), a nonlinear conversion efficiency of 10^{-3}/mW is expected when both FF and SH waves are resonant in the cavity and fulfill the QPM condition Delta m = m_{SH} - 2m_{FF} = ±2 (m being the mode azimuthal order).

The microdisks fabrication has required a specific technological development, especially for the challenging control of the geometrical parameters due to the uncertainties related to wet chemical etching. To investigate the spectral properties of a first generation of microdisks, we started with a series of linear measurements [4]. WGM excitation and sample optical characterization were carried out via evanescent coupling with a silica tapered fiber, at both FF and SH, by using two different CW external-cavity tunable laser diodes, emitting in the 1500-1600 nm and in the 755-785 nm range, respectively. By doing so, we were able to observe a TE-polarized mode at lambda_{FF}=1508.9 nm with an intrinsic quality factor Q_{FF}=1.43x10^4 and a TM-polarized mode at lambda_{SH} =767.6, with an intrinsic quality factor Q_{SH}=4.9x10^2. The discrepancy between lambda_{FF} and 2lambda_{SH} was due to a non-optimal disk radius, which has been fixed in a second generation of disks. By endowing the experimental layout with an accurate temperature control, the latter is currently being used to spectrally superpose the phase-matched resonant modes. Finally, fabrication progress allowed to considerably improve the quality factors and the fiber-disk coupling efficiency, and to observe SHG around 775 nm.

[1] P. S. Kuo et al., Opt. Lett. 3, 3580 (2009).

[2] P. S. Kuo and G.S Solomon, Opt. Express 19, 16898 (2011).

[3] Y. Dumeige and P. Feron, Phys. Rev. A 74, 063804 (2006).

[4] S. Mariani et al., Opt. Lett. 38, 3965 (2013).

9136-29, Session 6

All-optical vortex switching in reconfigurable optically-induced nonlinear waveguide arrays

Falko Diebel, Univ. of Münster (Germany); Daniel Leykam, The Australian National Univ. (Australia); Martin Boguslawski, Patrick Rose, Cornelia Denz, Westfälische Wilhelms-Univ. Münster (Germany); Anton S. Desyatnikov, The Australian National Univ. (Australia)

Discrete low dimensional photonics structures, such as coupled waveguide arrays, represent an important building block for various types of integrated all-optical light guiding and switching architectures. Nonlinear materials are essential to provide the possibility of controlling light with light itself.

One versatile way to realize highly-nonlinear discrete photonics structures is optical induction [1]. This method allows reversibly fabricating tunable refractive index landscapes with high nonlinear response even at modest power levels and thus provides a versatile platform to study a multitude of fundamental linear and nonlinear effects [2–4].

In this contribution, we present a new type of ring-shaped coupled nonlinear waveguide structures that allow power-controlled switching the topological charge of a discrete vortex. In the linear regime a discrete vortex-bearing beam propagates in a stable way through a discrete refractive index structure while its phase singularity periodically changes sign, resulting in the flipping of the vortex charge. Incorporating the strong nonlinear response of the used photorefractive material, the vortex beam power controls the frequency of the flipping. Above a critical power, the charge reversal is suppressed.

To experimentally realize such a coupled waveguide structure, we take advantage of the optical multiplexing method [5] which opens access to a wider class of photonic structures to optical induction, such as variable arrays of coupled waveguides as present here. In particular, we use an incoherent superposition of multiple nondiffracting Bessel beams at arbitrary transverse positions. Each Bessel beam induces a single waveguide. We control the coupling strength between the waveguides through their separation.

With the presented work we introduce an array of coupled nonlinear waveguides that enables power-controlled switching the topological charge of a discrete optical vortex. The all-optical switching of this quantized charge will find applications in optical computing and information processing technologies.

References:

[1] N. K. Efremidis, S. Sears, D. N. Christodoulides, J. W. Fleischer, and M. Segev, “Discrete solitons in photorefractive optically induced photonic lattices,” Phys. Rev. E 66(4), 1–5 (2002).

[2] F. Lederer, G. I. Stegeman, D. N. Christodoulides, G. Assanto, M. Segev, and Y. Silberberg, “Discrete solitons in optics,” Phys. Rep. 463(1-3), 1–126 (2008).

[3] M. Segev, Y. Silberberg, and D. N. Christodoulides, "Anderson localization of light," Nat. Photonics 7(3), 197–204, Nature Publishing Group (2013).

[4] P. Rose, M. Boguslawski, and C. Denz, "Nonlinear lattice structures based on families of complex nondiffracting beams," New J. Phys. 14(3), 033018 (2012).

[5] M. Boguslawski, A. Kelberer, P. Rose, and C. Denz, "Multiplexing complex two-dimensional photonic superlattices.," Opt. Express 20(24), 27331–27343 (2012).

9136-30, Session 6

Parallel generation of fast random bits based on optoelectronic phase-chaos systems

Romain Modeste Nguimdo, Vrije Univ. Brussel (Belgium); Pere Colet, Consejo Superior de Investigaciones Científicas (Spain); Jan Danckaert, Vrije Univ. Brussel (Belgium)

Random bits, completely unbiased and unpredictable are highly desired for numerous of applications including encryption, stochastic modeling, and online gaming and lotteries. Typically, these random bits can be generated using physical systems. However, in practice random bit generation rate in such systems is limited by the system component capabilities such as the detection bandwidth, electronic digitization and post-processing circuitry. To increase such rates, multi-bit anolog-to-digital convertors (ADCs) are often used although the effect of such operation in the system entropy is still unclear. An alternative way to increase the bit generation consists in implementing physical parallel random bit generators and interleave them to form a single bit-stream with the overall cumulative bit rate. In this contribution, we model the performance of an optoelectronic phase-chaos system operating with telecom components to generate random bits. The key component of the system is differential delay, namely the system is subject to two delay times which differ in an amount much larger than the autocorrelation time. This is implemented by a delay loop and an imbalanced Mach-Zhender modulator. Our results indicate that considering multi-bit ADCs only the least significant bit is further digitalized. We also show that the system can be extended to have several chains in parallel each with a Mach-Zhender modulator, each chain being used to produce a sequence of random bits. If the differential delays of the Mach-Zhenders differ by an amount larger than the autocorrelation time of the chaotic dynamics, the output of the different chains is uncorrelated and therefore can be used for parallel generation of statistically independent random bit-streams. These results are further verified through the computation of the binary crosscorrelation and binary mutual information between the parallel bit-streams. In addition, we also find that a sequence constructed by interleaving the parallel bit-streams also pass all the NIST tests for randomness. Based on the least significant bits which can be included in the sequence and the number of the parallel branches which can be implemented, we show that bit rates up to Tb/s can be achieved.

9136-31, Session 7

High-power femtosecond fiber lasers based on self-similar pulse evolution *(Invited Paper)*

Frank W. Wise, Cornell Univ. (United States)

No Abstract Available

9136-32, Session 7

Vector solitons in harmonic mode-locked erbium-doped fiber lasers

Tatiana Habruseva, Aston Univ. (United Kingdom); Mkhitar Mkhitaryan, Department of General and Applied Physics, Moscow Institute of Physics and Technology (Russian Federation); Chengbo Mou, Aston Institute of Photonic Technologies, Aston University (United Kingdom); Aleksey G. Rozhin, Sergei K. Turitsyn, Sergey V. Sergeyev, Aston Univ. (United Kingdom)

Mode-locked fiber lasers (MLFLs) are attractive sources of short pulses. Typically, MLFLs operate at repetition rate in the order of a few to tens of MHz due to the relatively long laser cavity. Higher repetition rates can be achieved in passively MLFLs by increase of the pump power resulting in harmonic mode-locking. Single wall carbon nanotubes (CNTs) films have attracted much attention as a laser saturable absorber material due to their ultrafast recovery time and polarization insensitivity. Harmonic mode-locked fiber lasers based on CNTs are stable sources of sub-picosecond pulses at high repetition rates, which can be used in optical communications, metrology, optical sampling or sensing applications. Due to fiber birefringence different types of vector solitons can be formed in such lasers. The polarization insensitivity of CNTs based saturable extends the possibility of studying polarization dynamics in mode-locked lasers.

We constructed fiber laser with 7.8 m cavity length. The ring cavity consisted of a 40 cm long highly erbium-doped gain fiber (LIEKKI 110-4), a single mode fiber with anomalous dispersion, a 99/1 tap, a fiber isolator, a polarization controller (PC), an output coupler, a saturable absorber and a wavelength division multiplexing (WDM) coupler. The gain fiber was pumped at 976 nm by a laser diode via a 980/1550 nm WDM coupler and a PC. We used a single-wall CNTs polymer film embedded between standard FC/APC fiber connectors as a saturable absorber. In experiments, the pump current of the laser diode was increased and various polarization attractors were obtained by varying both the in-cavity and pump PCs for a given pump power.

We demonstrated passively harmonic mode-locked fibre laser with repetition rate tunable between 25 MHz and 326 MHz and over 50 dB sidebands suppression ration up to 11th harmonic. Polarisation dynamics study revealed a range of vector solitons: polarization-locked and polarization-evolving solitons, soliton crystal with polarization switching between two cross-polarized SOPs, etc. The novel operation regimes with a combination of solitons at different frequencies were also demonstrated. State of polarization dynamics of vector solitons can be applied in telecommunications applications in the context of increased capacity in fibre optic telecommunications based on polarisation division multiplexing quadrature phase shift keying and modified coded hybrid subscriber/amplitude/ phase/ polarisation modulation schemes.

9136-33, Session 7

The laminar-turbulent transition in a fibre laser

Dmitry V. Churkin, Aston Univ. (United Kingdom) and Institute of Automation and Electrometry (Russian Federation) and Novosibirsk State Univ. (Russian Federation); Elena Turitsyna, Aston Univ. (United Kingdom); Sergey V. Smirnov, Novosibirsk State Univ. (Russian Federation); Srikanth Sugavanam, Nikita S. Tarasov, Xuewen Shu, Aston Univ. (United Kingdom); Sergey A. Babin, Eugenii V. Podivilov, Institute of Automation and Electrometry (Russian Federation); Gregory Falkovich, Weizmann Institute of Science (Israel); Sergey K. Turitsyn, Aston Univ. (United Kingdom)

In optics, understanding how a system loses coherence, as spatial size or the strength of excitation increases, is a

fundamental problem of practical importance.

In optical fibres with normal dispersion, a coherent monochromatic wave or spectrally narrow packets are linearly stable with respect to modulation instability. In a laser cavity with normal dispersion, it is theoretically possible to overcome wave de-phasing by nonlinear four-wave-mixing and achieve a classical wave condensation forming a coherent state. However, operational regimes in many fibre lasers correspond to very irregular light dynamics and a low degree of coherence. A quasi-CW fibre laser normally generates so many modes (up to 106), that fluctuations in their amplitudes and phases result in a stochastic radiation, which calls for description in terms of wave turbulence

In our experiments, increasing the cavity length or the power of a fibre laser causes the output to pass from a coherent laminar state to a turbulent one. The laminar regime is realized at low power and the turbulent regime at a high pump power. There is a sharp transition in the properties of the laser radiation upon the increase of the power. The optical spectrum width increases by almost twice after the power increases by only 1 percent. In addition, below the transition, the generation is quite stable and intensity fluctuations are small, so the intensity probability density function (pdf) has a sharp narrow peak centred at the mean intensity, as it should for a coherent state. At the transition, the pdf changes form and develops a wide, approximately exponential tail that manifests as a significant probability of high-intensity fluctuations. The transition is also detected as a drop in the background level of the intensity autocorrelation function from a coherent-state level to a stochastic regime

In numerical simulations within NLSE model, we demonstrate that the laminar state is a coherent condensate, and the transition is condensate destruction. Moreover, we identify the mechanism of the loss of coherence. Indeed, in experiment we detected long-living propagating intensity minima both on a stable laminar background and on a strongly fluctuating turbulent background. As these structures live ~100 nonlinear lengths, so they are coherent. In numerical simulations we prove that these coherent structures are dark and grey solitons. Finally, we found that the laminar-turbulent transition is via the appearance, proliferation and clustering of solitons.

This finding could prove valuable for the design of coherent optical devices as well as systems operating far from thermodynamic equilibrium.

References: EG Turitsyna, SV Smirnov, S Sugavanam, N Tarasov, X Shu, SA Babin, EV Podivilov, DV Churkin, G Falkovich, SK Turitsyn, “The laminar-turbulent transition in a fibre laser”, Nature Photonics, 7(10), 783-786, 2013.

9136-34, Session 7

Self-similar pulse-shape mode for femtosecond pulse propagation in medium with resonant nonlinearity

Vyacheslav A. Trofimov, Irina G. Zakharova, Lomonosov Moscow State Univ. (Russian Federation); Swapan Konar, Birla Institute of Technology (India)

We investigate the mode of laser pulse propagation in homogeneous medium with resonant nonlinearity, at which the shape of pulse is self-similar one along some distance of propagation. We take into account a laser pulse frequency detuning from resonant frequency. Both types of sign for frequency detuning are considered. This results in appearance of a refractive index grating which induced self-action of a laser pulse.

We develop analytical solution of corresponding nonlinear eigenfunction problem of laser pulse propagation in medium for multi-photon resonance. This solution is confirmed by computer simulation of an eigenfunction problem for Schrödinger equation with considered nonlinearity.

Using computer simulation, one shows a validity of existence of such kind of laser pulse propagation in a medium with resonant nonlinear response.

9136-35, Session 8

Nonlinear energy deposition in water from fs-laser pulses: effect of the input chirp

Carles Milián Enrique, Ecole Polytechnique (France); Yohann Brelet, Amelie Jarnac, Ecole Nationale Supérieure de Techniques Avancées (France); Vytautas Jukna, Lab. Hubert Curien (France); Aurélien Houard, André Mysyrowicz, Ecole Nationale Supérieure de Techniques Avancées (France); Arnaud Couairon, Ecole Polytechnique (France)

We numerically and experimentally investigate micro-Joule (up to 5 uJ) ultrashort laser pulse propagation in water under tight focusing conditions for a vacuum wavelength of 800 nm. Such pulses easily produce localized and weakly ionized plasmas in condensed media as a result of nonlinear energy deposition mechanisms, i.e., multi-photon absorption (MPA) and avalanche ionization. Plasmas generated in this way are non-homogeneous in space (and time) and therefore may be responsible for the generation of voids (cavitation) and sound waves. An accurate control of the above effects is of great importance for many applications like eye surgery, laser safety, micro-machining, and sub-micro void formation.

Our simulations for pulse propagation and the associated plasma generation integrate numerically the forward Maxwell equation accounting for dispersion, diffraction, Kerr nonlinearity, plasma defocusing, and three sources of loss (linear, multi-photon, and plasma absorption). This is coupled to a rate equation for the electron plasma density derived from Drude model and describing MPA through the Keldysh rate.

Experiments are performed in a 10 cm long cuvette made of BK7 glass, which is filled up with distilled water. Optical pulses of 45 fs in intensity full width at half maximum (FWHM) are provided by a Ti:sapphire Laser operating at 100 Hz and focused down in the water tank by a lens of 7.5 cm of focal length. This set-up ensures time delays in between consecutive pulses which are, in principle, large compared with typical hydrodynamical times (typically 10’s of micro-seconds). Moreover, the wide input beam of 7 mm of FWHM prevents damage to the glass and the early rise (delocalization) of strong nonlinear effects before the focus.

We demonstrate that the tuning of the input pulse chirp provides a simple and effective mechanism to control the distance at which the plasma is generated, its volumetric distribution and the free electron density. In particular, we demonstrate the existence of two optimal values for the input pulse chirp. Whilst one of them maximizes the optical energy deposition (minimum of optical transmission), the other one maximizes the length of the plasma volume along the propagation direction (yet keeping the free electron density nearly constant and maximal). These two scenarios require MPA to be at least as important as avalanche ionization. An overall absorption dominated by avalanche ionization is observed in the cases for which the transmission increases towards the linear limit, corresponding to pulses propagating through the nonlinear focus with large values of chirp. Elongation of the plasma volume is observed close to the minimum of transmission and is associated to the cases in which the pulse temporal compression has not reached yet its maximum at the focal position but peak intensities are big enough for triggering MPA efficiently. Our results are in good agreement with experiments after performing a parametric study of the MPA and electron-ion collision time coefficients.

9136-36, Session 8

Formation of turbulent and laminar generation in quasi-CW Raman fiber laser

Sergey V. Smirnov, Novosibirsk State Univ. (Russian Federation); Dmitry V. Churkin, Aston Univ. (United Kingdom) and Institute of Automation and Electrometry (Russian Federation) and

Novosibirsk State Univ. (Russian Federation)

It was shown recently that the quasi-CW Raman fiber laser may operate under specific conditions in the highly coherent regime analogous to the spectral condensate or the laminar flow and admits the transition to the low coherent lasing similar to the turbulent flow [1]. The mechanism of the observed laminar-turbulent transition in the fiber laser is identified – profileration and clusterization of dark and grey solitons [1]. In the present work we investigate for the first time dynamics of the initial stage of both laminar and turbulent regimes and show how the system loses stochasticity while laminar lasing is developed. Using the model based on coupled nonlinear Schrödinger equations [2] we show that same initial noise conditions can lead to either laminar or turbulent lasing depending on cavity parameters such as fiber dispersion and nonlinearity, fiber Bragg gratings (FBG) dispersion and bandwidth, cavity length. The area of existence of laminar lasing is considered. In the turbulent regime in which there are no mode correlations, huge spectral broadening due to four-wave mixing is observed on each fiber pass. However, each reflection from the cavity mirror balances the generation spectrum in a way that the total broadening factor over the cavity round-trip is equal to unity (i.e. the generation spectrum supports some self-consistent form) in the turbulent regime. The equilibrium is reached typically after few round-trips only. In contrast, in the case of the laminar lasing, spectral narrowing is observed at consequent cavity round-trips. We found that in the laminar regime the generation radiation have two principally different components: narrow-band spectral condensate with pronounced mode correlations and stochastic, turbulent wide-band component of non-correlated waves. Laminar component propagates through optical fiber cavity with minor or with no spectral broadening and thus does not experience loss at FBGs. Turbulent component of the spectrum has a bandwidth constantly increased due to FWM what leads to the turbulent waves filtering-off at each cavity round-trip. As a result, the laminar regime is build-up gradually and asymptotically approach the final laminar spectrum over 50-100 round-trips. The revealed mechanism of laminar regime build-up is essential for creating highly coherent narrow-band laser sources with exceptionally wide spectral range of operation accessible for Raman lasers. Such sources are required for a wide range of applications including telecom, spectroscopy and many others.

References

1. E.G. Turitsyna, S.V. Smirnov et al. “The laminar–turbulent transition in a fibre laser.” Nature Photonics, v. 7, N 10, p. 783 - 786 (2013).

2. D.V. Churkin, S.V. Smirnov, E.V. Podivilon. “ Statistical properties of partially coherent cw fiber lasers.” Optics Letters, v. 35, N 19, p. 3288-3290 (2010).

9136-37, Session 8

Nonlinear mixing and mode correlations in a short Raman fiber laser

Ilya Vatnik, Institute of Automation and Electrometry (Russian Federation); Oleg A. Gorbunov, Institute of Automation and Electrometry (Russian Federation) and Novosibirsk State Univ. (Russian Federation); Dmitriy V. Churkin, Aston Univ. (United Kingdom) and Institute of Automation and Electrometry (Russian Federation) and Novosibirsk State Univ. (Russian Federation)

Full characterization of nonlinear interactions of numerous longitudinal modes in quasi-CW Raman fiber lasers (RFL) is of great interest because it defines the possible correlations in laser radiation and affects the probability of extreme events. In numerical simulations, different models based on NLSE are used to describe the interactions between numerous modes and predict statistical properties of the radiation. However, in all models an unrealistically low number of longitudinal modes (i.e. frequencies) is used [1]. Indeed, most of RFLs demonstrated so far are usually based on long cavities having typical lengths more than several hundreds of meters. As the generation spectrum is quite broad (~ 1 nm), the total number of different spectral components generated in the cavity could be up to hundreds of millions. However, numerical modeling of dynamics and nonlinear interaction of only 216 (or less) of different longitudinal modes is usually performed. This limitation can affect predictions of fine laser radiation properties like deviations of intensity statistics from Gaussian, the probability of extreme events and origin and manifestation of correlations between different laser modes.

In the present paper we experimentally demonstrate a generation in a short Raman fiber laser having 10 000 different longitudinal modes only. We design the laser using 12 meters of commercially available fiber. Note that in previous demonstrations of short RFLs, the custom fibers with high Ge-doped and/or elliptical core were used. Contrary to the recently demonstrated single longitudinal mode DFB Raman laser and short DBR Raman laser [2,3], in the laser under study the number of modes is high enough for efficient nonlinear interactions. Thus, the presented laser could be directly modelled using NLSE-based approaches with real number of modes. Experimentally measured time dynamics reveals the presence of mode correlations in the radiation: the measured extreme events lasts for more than 10 round-trips, that makes the laser an attractive object for investigation.

1. D. V. Churkin and S. V. Smirnov, “Numerical modelling of spectral, temporal and statistical properties of Raman fiber lasers,” Opt. Commun. 285, 2154–2160 (2012).

2. J. Shi, S. Alam, and M. Ibsen, “Highly efficient Raman distributed feedback fibre lasers,” Opt. Express 20, 5082–5091 (2012).

3. A. Siekiera, R. Engelbrecht, A. Nothofer, and B. Schmauss, “Short 17-cm DBR Raman Fiber Laser With a Narrow Spectrum,” IEEE PHOTONICS Technol. Lett. 24, 107–109 (2012).

9136-38, Session 8

Influence of the generated power, measurement bandwidth, and noise level on intensity statistics of a quasi-CW Raman fiber laser

Oleg A. Gorbunov, Institute of Automation and Electrometry (Russian Federation) and Novosibirsk State Univ. (Russian Federation); Srikanth Sugavanam, Aston Univ (United Kingdom); Dmitry V. Churkin, Aston Univ. (United Kingdom) and Institute of Automation and Electrometry (Russian Federation) and Novosibirsk State Univ. (Russian Federation)

Statistical properties of the radiation generated in quasi-CW fiber lasers are studied intensively nowadays, both numerically and experimentally. It was shown that these properties are nontrivial, and intensity dynamics of a quasi-CW fiber laser generating numerous longitudinal modes which was thought to be completely stochastic contain internal correlations. These correlations revealed as non-exponential intensity probability density function (pdf) with increased probability of generation of extreme events having amplitude much higher than an average value. It is important, that intensity statistics could depend on the generation power as it should be obviously related to the nonlinear processes. Moreover, as the optical bandwidth is usually much larger than the measurement bandwidth, the shape of the measured intensity probability density function should be affected by the limited measurement bandwidth as well as measurement noise. These problems, however, remains uninvestigated so far.

In presented paper we have experimentally studied statistical properties of quasi-CW radiation of the Raman fiber laser generating numerous longitudinal modes. The total spectrum width was up to 0,8 nm being much broader than the measurement bandwidth of 25 GHz. We measured intensity pdf and found that it is non-exponential revealing internal mode correlations in the radiation. We found that the statistical properties do depend on power. With power increase, the pdf becomes narrower meaning that the probability of generation of extreme events decreases. In particular, the measured

probability of the generating an event with the 4 times higher than the average intensity decreases exponentially with power. The possible mechanism could be related for less pronounced spectral correlations at higher power, as more intense nonlinear interactions lead stochastization of phases.

It is important that the measurement bandwidth and the level of measurement noise could affect the measured intensity pdf. To check this influence, we developed a simple model of the multimode quasi-CW generation with exponential statistics (i.e. uncorrelated modes) and model the measured intensity pdf of such radiation by varying the measurement bandwidth, noise level and making averaging within fixed time interval, i.e. model measurement process. We found that the slope of the intensity pdf could be changed while varying the measurement bandwidth, but the statistics remains exponential. At the same time, the measurement noise and the width of temporal interval in which the intensity is averaged do not affect the far wing of the intensity pdf, but induce the dip near zero intensities. Such dips are experimentally observed in every measurement. Thus, the experimentally observed fat tails in intensity pdf does not related to measurement issues, and are result of mode correlations in the radiation. At the same time, we found numerically that any spectral correlations between different modes in the central part of the modeled spectrum induce fat tails in pdf, i.e. increase the probability of the generation of extreme events.

9136-40, Session 9

Sensitive THz-wave detector using a quasi-phase-matched LiNbO3 at room temperature

Kouji Nawata, Takashi Notake, RIKEN (Japan); Hideki Ishizuki, Institute for Molecular Science (Japan); Feng Qi, Yuma Takida, Shuzhen Fan, Shin'ichiro Hayashi, RIKEN (Japan); Takunori Taira, Institute for Molecular Science (Japan); Hiroaki Minamide, RIKEN (Japan)

Sensitive THz-wave sensor at room temperature is crucial for most applications such as 2-dimensional real-time imaging and nonlinear phenomena in semiconductors caused by multi-photon absorption, light-induced ionization, and saturated absorption.? LiNbO3 is a promising material for frequency up- and down-conversion because of its high nonlinearity and high resistance to optical damage. However, the angular phase-matching condition between the THz wave and the near-infrared in LiNbO3 restricts the interaction volume during propagation in a crystal.

In this letter, we propose an efficient scheme that two optical waves, the pump and up-conversion signal beams, interacting with the THz wave, propagate collinearly in a slant-stripe-type periodically poled LiNbO3 (PPLN) crystal to achieve effective enhancement for the signal beam. We also demonstrate efficient frequency up-conversion.

A master oscillator power amplifier (MOPA) system (energy: 20 mJ/pulse, pulse duration: 590 ps, wavelength: 1064 nm) consisting of a Nd:YAG microchip laser and a Nd:YAG optical amplifier was used as a pump source for the THz-wave detection. A slant-stripe-type PPLN with an angle of 20° and a grating period of 29.0 um was used. The length and thickness of the PPLN were 15 mm and 5 mm, respectively. The THz-wave source generated monochromatic THz waves with over one kilowatt of peak power and with wide tunability in an injection-seeded THz-wave parametric generator (is-TPG) using a bulk LiNbO3 crystal. Detailed information about the is-TPG has been previously reported.

A minimum detectable energy of 0.3 pJ/pulse at the frequency of 1.6 THz was achieved with the pump energy of 1.8 mJ/pulse in room temperature. The dynamic range of the incident THz-wave energy of 60 dB was demonstrated. Further improving for the sensitivity using longer interaction length in a PPLN crystal was also investigated.

9136-41, Session 9

Second-harmonic generation from a QCL in an AlGaAs waveguide

Cécile Ozanam, Marc Savanier, Univ. Paris 7-Denis Diderot (France); Aristide Lemaître, Lab. de Photonique et de Nanostructures (France); Guilhem Almuneau, Lab. d'Analyse et d'Architecture des Systèmes (France); Mathieu Carras, III-V Lab. (France); Giuseppe Leo, Univ. Paris 7-Denis Diderot (France)

The 2-3μm window combines the advantages of being a covert and eye-safe range and is widely used for a large number of civilian applications including gas sensing, security and medical applications, as well as for military applications. However, the availability of integrated room-temperature on-chip coherent optical sources in this spectral range is limited. In particular the spectral overlap between laser diodes and quantum cascade lasers (QCLs) remains relatively poor, although some devices have already been demonstrated [1,2] and intracavity frequency doubling performed at room temperature [3].

Here we demonstrate quasi-continuous-wave frequency doubling of a QCL radiation in a GaAs waveguide. In the isotropic GaAs, the type I phase-matching condition between the TE fundamental wave (FF) around 4.46 μm and the TM second harmonic (SH) at 2.23 μm is fulfilled by form birefringence [4]. The latter is induced by creating a sub-wavelength periodic stack where two materials of different refractive index are interleaved, and in the present case it suffices to introduce two selectively oxidized Al0.98Ga0.02As layers in the GaAs core of the waveguide. This multilayered GaAs/AlOx core is sandwiched between Al0.8Ga0.2As claddings to ensure vertical confinement via total internal reflection. The lateral confinement is provided by wet etching a ~15 μm wide ridge.

Compared to AlGaAs/AlOx parametric sources with FF wavelength around 1 μm, the smaller number of AlOx layers here is made possible by the smaller amount of form birefringence needed to compensate for the lower material dispersion at long wavelengths. Reducing the use of AlOx is beneficial in terms of guided-wave optical losses, which are mainly due to scattering at AlOx/GaAs interfaces [5].

Preliminary measurement revealed unambiguously SH generation, since the power of the TM polarized SH field depends quadratically on the power of the TE polarized FF. So far the external SH power was limited to a few nW by the fact that, due to fabrication tolerances, we had to use the width of the waveguide ridge as a coarse phase-matching parameter, which results in multimode horizontal confinement and non-optimal coupling between the laser beam and the fundamental guided mode.

We are currently characterizing the efficiency of the converter, which we predict as high as ~670% W-1cm-2. Finally, we are designing new samples that should result in a higher SH power through a better input coupling.

[1] W. Bewley et al., Optics Express 20, 20894 (2012).

[2] A. Bismuto et al., Semiconductor Science and Technology 27, 045013 (2012).

[3] A. Vizbaras et al., Physica Status Solidi (C) 9, 298 (2012).

[4] A. Fiore et al., Nature 391, 463 (1998).

[5] C. Ozanam et al., "Towards an AlGaAs/AlOx near-IR integrated OPO", submitted (2013).

9136-42, Session 9

2.6 um to 12 um tunable ZGP parametric master oscillator power amplifier

Tobias Traub, Photonik-Zentrum Kaiserslautern e.V. (Germany); Gregor Anstett, Fraunhofer-Institut für Optronik, Systemtechnik und Bildauswertung (Germany); Guido Göritz, GWU-Lasertechnik Vertriebsges.mbH (Germany); Johannes A. L'huillier, Photonik-Zentrum Kaiserslautern e.V. (Germany)

Coherent sources of mid-IR radiation are of great interest for a variety of applications, like IR-MALDI, trace-gas detection or time-resolved IR spectroscopy. Tunable systems are often desirable to permit access to particular spectral regions, most prominently the atmospheric windows at 3-5 um and 8-12 um.

While direct mid-IR emission is making great progress with the quantum cascade laser there is no alternative to OPO/OPA systems if the desired application needs a tunable coherent light source and millijoule pulse energies. The most prominent nonlinear crystal for mid-IR OPO/OPAs is zinc germanium diphosphide (ZGP), due to its high nonlinearity of 70 pm/V, relative robustness and wide transmission.

We present a tandem optical parametric oscillator (OPO) with subsequent optical parametric amplification (OPA). The output wavelength is widely tunable from 2.6 um to 12 um or 4000 cm-1 to 833 cm-1.

The pump source of this system is a Nd:YAG laser, which provides 10 ns pulses at a wavelength of 1064 nm. This emission is used to pump a type-II phase-matched KTP-based OPO. The OPO is operated at degeneracy and produces two orthogonally polarized rays both at a wavelength of 2128 nm. Back reflection of the pump in combination with type-II phase matching leads to a narrow bandwidth even at degeneracy and so the spectral width is below 6 nm (FWHM) for both polarizations. The pulse energy for the combined output is 150 mJ, which corresponds to a conversion efficiency of 33.3 %.

The horizontally polarized beam is used to pump a type-I phase-matched ZGP-based OPO. A 15 mm long ZGP crystal is used in a 17 mm long flat-flat OPO cavity. This setup leads to a low OPO threshold of 2 mJ. Pumped at 70 mJ the maximum output energy was achieved at 4.2 um and was 17.5 mJ for signal and Idler combined. The conversion efficiency of this stage was 25%.

The ZGP OPO tuning range is very large and it seamlessly covers the Mid-IR from 2.6 um up to 12 um. This is the largest tuning range achieved in ZGP, to the best of our knowledge.

The energy output of the OPO can be further increased by optical parametric amplification (OPA) in an additional stage. As pump for the OPA serves the vertically polarized output of the KTP OPO which was unused so far. The amplification behavior for various input energies is investigated and at 4.2 um maximum Mid-IR pulse energy of 22 mJ could be obtained.

9136-43, Session 9

Frequency doubling into the yellow spectral range with tunable DBR-RW diode lasers

Roland Bege, Andre Kaltenbach, Christian Fiebig, Gunnar Blume, David Feise, Alexander Sahm, Mirko Fischer, Frank Bugge, Katrin Paschke, Ferdinand-Braun-Institut (Germany)

For medical-technical and biologic applications laser-based devices are of interest which serve as compact and user-friendly tools. Diode lasers provide laser light of high power and at the same time excellent brightness for sensor technology, analysis and spectroscopy. However, diode lasers in the yellow spectral range from 550 to 600 nm have not been sufficiently developed, yet. Therefore, the second harmonic generation (SHG) of infrared laser light ranging from 1100 to 1200 nm is an appropriate approach. Periodically poled crystals which utilize quasi-phase matching are the first choice for SHG in order to be easily integrated on micro-optical benches allowing devices of small dimensions.

We demonstrate the conversion of laser light from 1120 nm to 560 nm with magnesium doped LiNbO3 (ppLN:MgO) crystals. Ridge waveguide diode lasers with nearly diffraction limited beams (M? < 1.3) are used to deliver infrared pump powers of more than 500 mW. They are stabilized by an internal DBR grating. The wavelength of the diode lasers can be tuned by more than 2 nm by means of heating the passive DBR section without suffering severe output power losses. Hence, we are able to vary the wavelength of the frequency doubled laser light over more than 1 nm. Adapting the crystal's temperature preserves phase matching of SHG while wavelength tuning. Ridge waveguide crystals are used for frequency doubling to gain high conversion efficiencies. So we could achieve a second harmonic power of 85 mW for a pump power of 430 mW at a wavelength of 560 nm. Since the lateral mode of the fundamental is confined in the ridge waveguide, a beam quality of the frequency doubled laser light similar to the fundamental is generated.

9136-80, Session 11

High-performing SPS based on native NIR-emitting single colour centers in diamond *(Invited Paper)*

Paolo Traina, Istituto Nazionale di Ricerca Metrologica (Italy); Daniele Gatto Monticone, Univ. degli Studi di Torino (Italy) and Istituto Nazionale di Fisica Nucleare (Italy) and CNISM Sezione di Torino (Italy); Ekaterina V. Moreva, Istituto Nazionale di Ricerca Metrologica (Italy); Jacopo Forneris, Univ. degli Studi di Torino (Italy) and Istituto Nazionale di Fisica Nucleare (Italy) and CNISM Sezione di Torino (Italy); Mattia Levi, Univ. degli Studi di Torino (Italy); Konstantin Katamadze, Institute of Physics and Technology (Russian Federation); Giorgio Brida, Ivo P. Degiovanni, Emanuele Enrico, Giampiero Amato, Luca Boarino, Istituto Nazionale di Ricerca Metrologica (Italy); Paolo Olivero, Univ. degli Studi di Torino (Italy) and Istituto Nazionale di Fisica Nucleare (Italy) and CNISM Sezione Torino (Italy); Marco Genovese, Istituto Nazionale di Ricerca Metrologica (Italy)

Single-photon sources (SPS) play a key-role in many applications, spanning from quantum metrology [1, 2], to quantum information [3, 4] and to the foundations of quantum mechanics [5]. Although an ideal SPS (i. e. emitting indistinguishable, single photons “on-demand”, at a high repetition rate) is far from being realized due to real-world deviations from the ideality, much effort is currently devoted to improving the performance of real sources [6].

With regards to the emission efficiency, it appears natural to employ sources that are in principle deterministic in the single-photon emission (single quantum emitters such as single atoms, ions, molecules [7], quantum dots [8] or color centers in crystals [9-13]), as opposed to probabilistic ones (usually heralded SPS based on parametric down-conversion) [14, 15].

We present an overview of our preliminary results concerning a work-in-progress NIR pulsed single photon source based on single quantum emitters, namely color centers in diamond. They are particularly promising because of a narrow emission line (tipically less than 5 nm), a shorter excited state lifetime with respect to NV centres (1~2 ns compared to 12 ns) allowing a ten-fold photon emission rate upon saturation, and the fully-polarized emission.

[1] G. Brida et al., Laser Phys. Lett. 3, 115-123 (2006);

[2] S. V. Polyakov and A. L. Migdall, J. Mod. Opt. 56(9), 1045-1052 (2009);

[3] R. Thew and N. Gisin, Nature Photon. 1, 165-171 (2007);

[4] J. L. O’Brien et al., Nature Photon. 3, 687-695 (2009);

[5] M. Genovese, Phys. Rep. 413, 319-396 (2005);

[6] S. Scheel, J. Mod. Opt. 56, 141-160 (2009);

[7] B. Lounis and W. E. Moerner, Nature 407, 491 (2000);

[8] Z. L. Yuan et al., Science 295, 102 (2002);

[9] A. Zaitzev, Phys. Rev. B 61,12909 (2000);

[10] D. Steinmetz et al., Appl. Phys. B 102, 451–458 (2011);

[11] I. Aharonovich et al., Phys. Rev. B 81, 12120 (2010);

[12] D.A. Simpson et al., Appl. Phis. Lett. 94, 203107 (2009);

[13] E. Wu et al., Optic express, 14, 1296 (2006);

[14] T. Zhong et al.,, Optics Letters 35, 1392 (2010);

[15] G. Brida et al., Appl. Phys. Lett. 101 (22), 221112-221112-4 (2012).

9136-81, Session 11

Single rare-earth ion in a crystal as a spin qubit *(Invited Paper)*

Roman L. Kolesov, Kangwei Xia, Petr Siyushev, Rolf Reuter, Rainer Stöhr, Mohammad Jamali, Tugrul Inal, Jörg Wrachtrup, Univ. Stuttgart (Germany)

Rare-earth (RE) ions doped into optical crystals are known to be extremely good quantum memories with decoherence times in the range of a minute [1]. However, their full-scale usage in quantum information processing requires an optical access to the electron and/or nuclear spin of a single RE ion. Here, we present the results of an experimental investigation of the properties of a single electron spin of cerium ion (Ce3+) doped in a YAG crystal. Individual Ce3+ ions were isolated in an ultrapure YAG crystal by means of confocal microscopy. The detection of single fluorescent ions is confirmed by photon anti-bunching, spectral, and lifetime measurements. Ce3+ ions appear to be quite bright optical emitters, comparable to quantum dots and nitrogen-vacancy (NV) center in diamond, with the detection count rate as high as 2x10^5 photons/sec. Their excited state electron spin exhibits coherent dynamics under excitation with circularly polarized light even at room temperature revealed as optically detected Larmor precession of the excited state spin [2]. Thus, Ce3+ ion shows strong prospects for realization of spin-photon entanglement in a rare-earth based system. At cryogenic temperatures, the ground-state electron spin can be efficiently prepared in a well-defined state by means of optical pumping with a circularly polarized light. The state of the electron spin can be read out all-optically and can be manipulated by microwave radiation similar to the NV center in diamond. We have observed high-contrast optically-detected magnetic resonance (ODMR) of a single Ce3+ electron spin. The following spin properties are measured: 1) spin-lattice relaxation time T1=5-6ms, 2) ODMR width is around 12MHz, 3) and decoherence time T2=250ns. Latter is defined primarily by the hyperfine interaction with the dense bath of 27Al nuclei. We also show that decoherence time can be extended almost 4 orders of magnitude to reach 2ms (almost T1 limit) by using dynamic decoupling microwave pulse sequences (CPMG sequence with as many as 24000 pulses in our case). Decoherence time can be further extended by isolating cerium ions in low-spin host crystals. This is confirmed by our preliminary results on the excited state dynamics (optically detected Larmor precession) of cerium-doped YSO (yttrium silicate) nanocrystals.

[1] G. Heinze et al. PRL 111, 033601 (2013)

[2] R. Kolesov et al. PRL 111, 120502 (2013)

9136-82, Session 11

Quantum state reconstruction of a qubit system by weak values

Mirko Cormann, Bertrand Hespel, Yves Caudano, Univ. of Namur (Belgium)

In the standard approach of quantum measurements, only real-valued probabilities are accessible grandeurs in a direct relationship with the complex amplitudes of a wavefunction. To determine the complete quantum state of a system, we must perform different projection measurements on many identical copies. A post-processing fit of the measured probabilities to the unknown quantum state estimates finally the complex wavefunction [1, 2]. Recently, a new technique has been considered to determine the complex probability amplitudes describing the quantum state of a particle by a direct measure, in which the measurement outcome is directly connected to the complex amplitudes [3, 4]. It is based on the measurement of a weak value of an observable [5]. Weak values are usually defined in the framework of weak interactions of two systems (a quantum system and a meter), combined with conditional

measurement of the meter based on the post-selection of the final state of the quantum system.

In our research, by measuring weak values of an observable in a two-qubit system, we determine directly the density matrix of the polarization state of an entangled photon pair produced by the nonlinear process SPDC (type I spontaneous parametric down-conversion). This direct measurement of the density matrix is an alternative technique to the generally used state tomography [2]. Although our experiments are performed on photons, the model is valid for any two-qubit state. We show that the application of different quantum gates and projection measurements of the two-qubit system allows us to bring the real and the imaginary parts of weak values of the Pauli operator ?z in a direct relationship with measurable probability amplitudes. Furthermore, we point out the essential role of the post-selection in our method, as our measurements of weak values are modeled theoretically without applying the weak measurement approximation in our calculations.

[1] U. Fano, Rev. Mod. Phys. 29, 74–93 (1957)

[2] “Photonic State Tomography”, Advances in Atomic, Molecular, and Optical Physics, Elsevier, Volume 52, Pages 10 –442 (2005)

[3] J. S. Lundeen, B. Sutherland, A. Patel, C. Stewart, and C. Bamber, Nature, 474, 188–191 (2011)

[4] J. Z. Salvail, M. Agnew, A. S. Johnson, E. Bolduc, J. Leach, and R. W. Boyd, Nature Photonics 7, 316 –321 (2013)

[5] Y. Aharonov, D. Z. Albert, and L. Vaidman, Phys. Rev. Lett. 60, 1351–1354 (1988)

9136-83, Session 11

Optimized QKD BB84 protocol using quantum dense coding and CNOT gates: Feasibility based on Probabilistic Optical Devices

Amor Gueddana, Moez Attia, Rihab Chatta, SUP’COM (Tunisia)

In this work, we simulate a fiber-based Quantum Key Distribution Protocol (QKDP) BB84 working at the telecoms wavelength 1550 nm with taking into consideration an optimized attack strategy. We consider in our work a quantum channel composed by probabilistic Single Photon Source (SPS), single mode optical Fiber and quantum detector with high efficiency. We show the advantages of using the Quantum Dots (QD) embedded in micro-cavity compared to the Heralded Single Photon Sources (HSPS).

Second, we show that Eve is always getting some information depending on the mean photon number per pulse of the used SPS and therefore, we propose an optimized version of the QKDP BB84 based on Quantum Dense Coding (QDC) that could be implemented by quantum CNOT gates.

We evaluate the success probability of implementing the optimized QKDP BB84 when using nowadays probabilistic quantum optical devices for circuit realization. We use for our modeling an abstract probabilistic model of a CNOT gate based on linear optical components and having a success probability of sqrt (4/27), we take into consideration the best SPSs realizations, namely the QD and the HSPS, generating a single photon per pulse with a success probability of 0.73 and 0.37, respectively. We show that the protocol is totally secure against attacks but could be correctly implemented only with a success probability of few percent.

9136-84, Session 11

The study of reducing the effect of detector saturation on ghost imaging

Ruiqing He, Nanjing Univ. of Science and Technology (China); Qian Chen, Nanjing Univ. of Science and Technology (China); Wenwen Zhang, Jing Shu, Nanjing Univ. of Science and Technology (China)

Ghost imaging is a widely studied imaging method in recent years. The key principle of ghost imaging or quantum imaging is the correlation between the signal and reference light, but in practical applications, for the sampling depth limited the bucket detector may be in saturation state, which will reduce the correlation of the two beams. The methods of reducing the effect of saturation on ghost imaging are presented for two kinds of bucket detectors, the CCD array and PIN photo-diode / APD(Avalanche Photo Diode). The simulations show that these methods are useful and qualities of ghost image can be increased.

9136-85, Session 12

2D spatial measurement of the Einstein-Podolsky-Rosen paradox in twin images *(Invited Paper)*

Paul-Antoine Moreau, Fabrice Devaux, Eric Lantz, Univ. de Franche-Comté (France)

In 1935, Einstein, Podolsky and Rosen (EPR) proposed a “gedanke experiment” in which two entangled particles were considered [1]. They showed that even if the particles are well separated in a way that they cannot exchange information, they can exhibit both perfect position and momentum correlations. Spontaneous Parametric Down Conversion (SPDC) generates entangled photons whose behavior is close to the original state described by EPR [2].

We demonstrate here EPR entanglement using images provided by two cameras. The quantum state involved in the demonstration is generated by SPDC in a BBO crystal using a type II phase matching configuration. The U.V. pump at 355 nm generates signal and idler photons that are filtered at the degeneracy (710 nm) using narrow-banded interference filters.

Full field images are obtained from EMCCD cameras (Electron-Multiplying CCD) in a photon counting regime. Because of the stochastic gain of the Electron-Multiplying register, a thresholding process is applied on the grey-level images. In order to make the detection process to be consistent, the fluence of the SPDC is maintained at a low value, around 0,15 photons per pixels. As a consequence, the probability that two photons impact the same pixel during the exposure time is negligible. Binary images are then used without any post-selection, and the near and far field standard deviations involved in the Heisenberg inequality test are obtained by computing the cross-correlation function the images provided by the synchronized cameras [3]. In contrast with previous 1-D demonstrations [2], we ensure the consistency of the demonstration by using the whole intensity of the SPDC in both near and far fields. We obtained former results using a single camera [3,4]; in that case however the spatial separation of the images was not total and the violation of the Heisenberg uncertainty principle was only of a factor 4. We report here a violation by a factor 585 on one of the transverse spatial dimensions and 33 in the other obtained on 800 images. The quantum nature of the correlation was verified by controlling the sub-shot noise nature of the intensities fluctuations.

The violation of the Heisenberg inequalities for the inferred quantities has thus been demonstrated for the whole system involving the two spatial transverse dimensions. This demonstration of one of the most fascinating phenomena of quantum mechanics is made in the form closest to its original formulation.

To our knowledge, our results correspond to the highest degree of paradox ever obtained with an EPR state, whatever the domain considered.

[1] A. Einstein et al., Phys. Rev., 47, 777-780 (1935).

[2] J. C. Howell et al., Phys. Rev. Lett. 92, 210403 (2004).

[3] F. Devaux et al., Eur. Phys. J. D 66, 192 (2012).

[4] P.-A. Moreau et al., Phys. Rev. A, 86, 010101 (2012).

9136-86, Session 12

Nonlinear optics in graphene for quantum optics applications

Andrew Fraine, Olga Minaeva, David S. Simon, Gregg S. Jaeger, Alexander V. Sergienko, Boston Univ. (United States)

The development of graphene technology has rapidly advanced in the past decade thanks to new approaches to fabrication and development of various graphene-integrated platforms [1, 2]. Due to its unique electrical properties, graphene offers an alternative solid-state environment to explore nonlinear optical processes. Access to strong optical nonlinearity is a requirement for many quantum information protocols [3]. For example, a quantum key distribution protocol using coherent states is proposed that relies on weak single-photon cross phase modulation that is traditionally achieved with atomic systems in the regime of electromagnetically induced transparency (EIT) [4, 5]. Although EIT offers the largest possible single-photon phase shifts due to strong atomic resonances, practical limitations such as strict frequency constraints, cumbersome atomic configurations, and a limited opportunities for integrating with fiber communication networks.

Several demonstrations of the large broadband nonlinearity have been presented, but the interaction volumes are typically limited by the thickness of the single layer of carbon atoms [6, 7]. To fully exploit the large available nonlinearity, planar waveguide structures coupled to graphene can be exploited to maximize the light-matter interaction. Solid-state nonlinear materials such as graphene have the advantage of exploiting modern nanotechnology techniques to engineer both the material and geometric properties such as doping levels, electrical gating, and embedding graphene in slot waveguides [8]. We demonstrate the opportunity afforded by graphene to engineer the optical nonlinearity making use of the broadband ultrafast optical properties, remarkably strong nonlinear coefficient, and unique plasmonic characteristics.

1K.S. Novoselov et al., Science 22 Vol. 306 no. 5696 pp. 666-669 (2004)

2K.P. Loh et al., Nature Photonics 5, 411-415 (2011)

3W.J. Munro et al., New J. Phys. 7 137 (2005)

4B.T. Kirby et al., Phys. Rev. A 87, 053822 (2013)

5D.S. Simon et al., arXiv 1305.3975 (2013)

6E. Hendry et al., Phys. Rev. Lett. 105, 097401 (2010)

7H. Zhang et al., Optics Lett. Vol 37, Issue 11 (2012)

8Z. Lu et al., JOSA B, Vol. 29, Issue 6 (2012)

9136-87, Session 12

Position-dependent photon operators in the quantization of the electromagnetic field in dielectrics at local thermal equilibrium

Mikko Partanen, Teppo Häyrynen, Jani Oksanen, Jukka Tulkki, Aalto Univ. School of Science and Technology (Finland)

During the last few decades, the research of quantum optical processes in lossy media has generated a wealth of information on the quantization of the electromagnetic field in dielectrics and especially in layered structures. The vector potential and electric field operators obey the well-known canonical commutation relation for an arbitrary choice of normal mode functions, but the same does not hold true for the commutation relations of the ladder operators. The anomalous commutation relations of the ladder operators have been studied e.g. by by Barnett emph{et al.} [Phys. Rev. Lett. 77, 1739 (1996)] and Aiello [Phys. Rev. A 62, 127 (2000)] but no clear resolution for the anomalies was found although it was argued that the anomalies were irrelevant as long as the field commutation relations and classical field quantities were well defined. However, according to very recent suggestions, the ladder operators and their commutation relations might in fact relate to measurable quantities [Collette et al., Proc. of SPIE Vol. 8772, 87721D (2013)].

We propose a new approach to formulate the field operators in a lossy medium based on defining position dependent photon ladder operators that obey canonical commutation relations. The introduced position dependent ladder and photon number operators have a very clear physical interpretation and they give new insight to the local photon number balance, the formation of the local thermal equilibrium, and the optical energy transfer. We apply the introduced position dependent photon number operator to simple layered geometries and show that this can result in position dependent and oscillating photon number expectation values. Furthermore, we investigate how energy is transferred between bodies coupled through the interfering optical fields and how the thermal equilibrium is formed. We also discuss the possibility to realize a measurement for detecting the predicted photon number oscillations.

9136-88, Session 12

Optical four-wave mixing and generation of squeezed light in an optomechanical cavity driven by a bichromatic field

Germán J. de Valcárcel, Rafael Garcés, Univ. de València (Spain)

Since the seminal papers by Fabre et al. and Mancini and Tombesi on the generation of quadrature and intensity optical squeezing associated to the well known bistability of the classic pendular cavity model, a lot of literature has been devoted to characterize and search new regimes where those quantum features emerge in optomechanical cavities. Recently the effects of using a bichromatic optical drive have begun to be studied in the case where the two driving frequencies are red- and blue-detuned with respect to the cavity frequency by the mechanical oscillator frequency. Such a scheme however does not lead to squeezing itself but conditioned under output measurements. However if either the cavity is highly detuned or the optomechanical coupling is quadratic instead of linear, the same type of driving has been shown to produce squeezing, which is large for the mechanical oscillator but quite moderate for the optical field. Finally related driving schemes, now consisting of a strong monochromatic field with weak sidebands again separated by twice the mechanical oscillator frequency have been proposed, which produce high levels of mechanical squeezing, related to the parametric excitation of the mechanical oscillations.

Here we propose to use a type of modulated driving consisting of two components, whose beat note is not related to the frequency of the mechanical oscillator. As we will show a bifurcation exists for the input power at which the (non-injected) mid-frequency becomes generated due to four-wave mixing of the drive frequencies. For fixed detuning between the (non-injected) mid-frequency and the cavity frequency, that bifurcation happens at two values of the injected intensity (it has the shape of a tongue in the injection intensity-detuning plane), so that the non-injected frequency becomes generated between them. At those thresholds (which are static bifurcations, unlike the parametric instability of the mirror motion) high levels of optical squeezing –ideally perfect– are predicted, which do not depend critically on the temperature of the device. Approximated expressions for the squeezing level, validated by a complete Floquet theory treatment and by numerics, are derived.

9136-89, Session 12

Quantum information with optical photons in hybrid molecule-superconducting qubit system

Sumanta Das, Anders S. Sorensen, Univ. of Copenhagen

(Denmark); Sanli Faez, Leiden Institute of Physics (Netherlands)

We propose a novel hybrid system consisting of a molecule and a superconducting qubit which allows quantum state read out and entangling the superconducting qubit with optical photons. In our scheme we make use of the tunability of the narrow transition of an organic molecule which inside an optical slot-waveguide can have a large coupling to a single guided mode [1]. The organic molecules can have a large permanent dipole moment that give rise to a large linear stark co-efficients [2]. A cooper-pair box (CPB) qubit [3] if placed near the slot-waveguide can create a large electrostatic field variation while hopping between its two states. This field in presence such big stark coefficient lead to a molecule-CPB coupling strength of almost hundreds of MHz. For successful realization of our scheme one needs strong coupling regime in such hybrid system. We attain this in two different techniques depending on how we want to harness it. For optical determination of the qubit state, strong coupling is obtained by moving away from degeneracy point while driving the CPB with a coherent source. A coupling strength of the order of [(molecule-qubit coupling)^2/qubit transition frequency] is achieved with this approach. A flip in the state of the qubit in this case creates a shift of the emission line of the molecules by few line- widths. A frequency tunable few photon pulse send into the slot-waveguide, will interact with the molecule and get reflected or transmitted depending on the state of the CPB. By collecting the photons we get a direct optical read-out of the qubit state. For entanglement and other quantum information related work however, this regime of strong coupling is unsuitable, as the dressed CPB will have strong decoherence being away from its charge degeneracy point. Hence for quantum information processing we propose the use of an exotic system of two dipole interacting molecules inside the slot waveguide coupled to a non-driven CPB operating at the charge degeneracy point. In this approach the achieved molecules-CPB strong coupling [(molecule-qubit coupling)^2/ natural line-width] allows a direct entangling scheme where the energy of the outgoing photons is entangled with the state of the superconducting qubit. As superconducting qubits are known to be highly sensitive to absorption of optical photons our scheme is ideally suited to interface light with superconducting systems since it can be done with very few photons (on the order of 1 to 100). It is worth noting that the strong coupling regime of our work can be useful to study various other quantum effects in such novel hybrid molecule-CPB system. For example, effects like nonlinear photon-photon interactions, storage and manipulation of quantum information either in the context of quantum computation or quantum simulation.

[1] Q. Quan, I. Bulu, M. Lon?ar, Phys. Rev. A 80, 011810(R) (2009).

[2] C. Brunel et al., J. Phys. Chem. A, 103, 2429 (1999).

[3] Y. Makhlin, G. Schön, A. Shnirman, Rev. Mod. Phys. 73, 357 (2001).

9136-100, Session PS1

Nearly deterministic loading of a single cesium atom in a magneto-optical trap and in a microscopic optical tweezer by feedback control

Bei Liu, Junmin Wang, Wenting Diao, Jieying Wang, Gang Jin, Jun He, Shanxi Univ. (China)

Based on our realization of nearly complete transferring cold cesium (Cs) atoms from a magneto-optical trap (MOT) to a microscopic far-off-resonance optical tweezer back and forth, we investigated the possibility for nearly deterministic loading a single Cs atom in the microscopic tweezer. We can count atoms trapped in the MOT or the tweezer by efficiently collecting laser-induced fluorescence (LIF) photons on an avalanche photodiode. When cold Cs atoms prepared in the MOT are nearly complete transferred into the microscopic tweezer, the LIF photon counting can be used to trigger some processes. If we have only one atom in the tweezer, no action is needed; if two or more than two atoms in the tweezer, we noted that the red-detuned light-assisted-collision (LAC) has been utilized to remove atoms from the tweezer two by two, so ~ 50% probability was achieved to load a single atom in the tweezer (depending randomly on initially transferred even or odd atoms in the tweezer). Here we employ a blue-detuned LAC process, which will remove atoms from the tweezer one by one until only one atom stays. By only adopting this feedback path, we can achieve ~78% probability for loading a single atom in the tweezer. We never observed two or more than two atoms in the tweezer.

To suppress the zero atom probability, we also adopt another feedback path: the controllable atomic adsorption and desorption. Blue light from a LED array can efficiently induce fast release of the adsorbed Cs atoms on inner surface of a quartz ultra-high vacuum (UHV) cell. The atomic adsorption and desorption processes can be conveniently manipulated by switching on and off the blue LED array. So the loading rate of our Cs MOT can be fast controlled via the adsorption and desorption processes. If finally we have no atom in the tweezer, this blue-light induced atomic desorption quickly increases the Cs atomic density in the MOT region to an appropriate level, and allows the MOT quickly to trap a single atom than to transfer near completely into the tweezer.

By combining above-mentioned two feedback paths, we can achieve ~ 99% probability for loading a single atom in the tweezer. Up to now, to our best knowledge, this is the highest probability for a single atom loading in a microscopic optical tweezer. This two-path feedback control scheme may be extended to load a small-size tweezer array with exact single atom trapped in each site simultaneously. This is very important to implement an addressable multiple qubits system for demonstrating quantum register and quantum processor.

9136-90, Session 13

Recovery of qubit coherence by noise-eater technique *(Invited Paper)*

Miroslav Gavenda, Lucie Celechovska, Miloslav Dusek, Radim Filip, Palacky Univ. Olomouc (Czech Republic)

We propose quantum noise eater for a single photonic qubit and experimentally verify its performance for recovery of a superposition carried by a dual-rail photonic qubit. A coherent but randomly arriving photon penetrating into single rail of this system causes a change of its state, which results in an error in subsequent quantum information processing. We theoretically prove and experimentally demonstrate a conditional full recovery of the superposition by the quantum noise eater.

During an elementary noise impact, the dual-rail photonic qubit is influenced by a single photon from coherent noise in only one rail.

Similarly to the noise eater technique for laser light, a partial detection of number of photons in optical beam is exploited, however with single photon resolution. Moreover, differently to that technique, measured information is used to conditionally herald only the cases when at most one photon is present. The photon is subtracted using a linear optical device that with nonzero probability spatially separates an incoming two-photon state into two single photon states followed by a detection of one of the photons. If a photon is subtracted then only one photon remains in the dual-rail qubit. When the signal and noise photons are fully coherent, this linear-optical version of the noise eater technique can optimally reach the perfect recovery of qubit superposition, irrespective of the probability of the noise impact.

The experimental setup was built using fiber optics that allow us to simply control transmissivities of the beam splitters via variable-ratio couplers.

The main part of the setup is a balanced Mach-Zehnder (MZ) interferometer.

Signal and noise photons were created by type-I degenerate spontaneous parametric downconversion in a nonlinear crystal pumped by a continuous laser (413-nm). All used detectors

were Perkin-Elmer single-photon counting modules.

We have measured visibilities without the action of noise eater and with the action of noise eater. Without the action of noise eater the visibility lineary increases with T (increasing ratio of signal) whereas with the action of noise eater the visibility increases to unity (theory) and is independent of T.

Details of calculations and extension to two-photon noise can be find on arXiv:1308.0831.

9136-91, Session 13

High-resolution characterization of quantum bi-photon sources with classical difference frequency generation

Andreas Eckstein, Guillaume Boucher, Univ. Paris 7-Denis Diderot (France); Aristide Leamître, Lab. de Photonique et de Nanostructures (France); Pascal G. Filloux, Ivan Favero, Giuseppe Leo, Univ. Paris 7-Denis Diderot (France); John Sipe, Univ. of Toronto (Canada); Marco Liscidini, Univ. degli Studi di Pavia (Italy); Sara Ducci, Univ. Paris 7-Denis Diderot (France)

Non-classical light sources based on three- or four-wave mixing are ubiquitous in modern quantum optics. For instance, spontaneous parametric down-conversion (SPDC), in which one pump photon decays into a “signal” and an “idler” photon, is widely employed to generate squeezed vacuum or single photon pair states. Spectral correlations between the generated photons determine the shape of their joint spectral density. Advances in integration and miniaturization of optical devices require the development of rapid testing techniques to characterize spectral properties of these devices in view of mass production.

We demonstrate a method for spectral characterization of non-classical photon pair produced by SPDC or four-wave mixing using difference frequency generation (DFG): a CW laser beam is injected as seed into the signal mode to stimulate the generation of photon pairs. The DFG output spectrum is, as the corresponding SPDC marginal spectrum of this mode, determined by pump spectrum and phasematching properties of the source, but it is also pre-conditioned to the seed laser’s wavelength. By sweeping the seed wavelength, we measure a seed/output spectral correlation function of the DFG process.

Although DFG can in very good approximation be treated as a classical process, with a coherent pump, seed and output beams, its spectral correlation function is equal to the joint spectral density of a photon pair from the SPDC process, with the advantage of a significantly higher photon flux.

In comparison, SPDC implies small signal and idler photon numbers, necessitating frequency resolved single photon coincidence detection to investigate bi-photon spectral correlations [1-3]. The use of DFG allows us to obtain the joint spectrum with a linear detector, such as an optical spectrum analyzer, rather than a single photon detector, thus greatly simplifying and accelerating the characterization of quantum photonic devices.

In a measurement of a semiconductor SPDC source’s [4] joint spectrum, our approach boosts spectral resolution by an order of magnitude compared to state-of-the-art, whilst reducing the measurement time. The results clearly show spectral features of SPDC in an optical cavity caused by the natural reflectivity of the semiconductor waveguide’s end facets. This effect has been theoretically predicted [5], but only our approach features simultaneously the spectral resolution and signal-to-noise ratio necessary to observe it within a reasonable measurement duration.

Beside the unequivocal technological advantages of this approach, these results are of fundamental interest in the study of quantum optics, as they demonstrate that quantum correlations of photon pairs generated by parametric fluorescence can be directly identified through a “classical” experiment [6].

[1] Y.-H. Kim and W. P. Grice, Optics Letters 30, 908 (2005).

[2] W. Wasilewski, P. Wasylczyk, P. Kolenderski, K. Banaszek, and C. Radzewicz, Optics Letters 31, 1130 (2006).

[3] M. Avenhaus, A. Eckstein, P. J. Mosley, and C. Silberhorn, Opt. Lett. 34, 2873 (2009).

[4] A. Orieux et al., Phys. Rev. Lett. 110, 160502 (2013).

[5] Y. Jeronimo-Moreno, S. Rodriguez-Benavides and A. U’Ren, Laser Phys. 20, 1221–1233 (2010).

[6] M. Liscidini and J. Sipe, ‘Stimulated Emission Tomography’ to appear in PRL (2013).

9136-92, Session 13

Slow light in evanescently-coupled optical cavities containing quantum dots

Emre Ergecen, Middle East Technical Univ. (Turkey)

Ability to tune the group velocity of a light pulse is of great importance for optical communication applications and realization of quantum information processing. Tunability of group velocity can be achieved by using either optical or electronic resonances. Tunability of an optical resonance depends on the change in refractive index of the cavity material. However, since electro-optical coefficients of non-engineered materials are quite small, the tuning range of optical resonances by electric field is narrow. This makes tuning by electric field impractical for most applications. Quantum dot (QD) coupled to a photonic crystal cavity is a useful hybrid system exhibiting nonlinear features. In this work, we analyze the use of quantum dot - optical cavity hybrid systems to engineer nonlinear waveguides susceptible to electric fields. We start by theoretically analyzing the optical pulse propagation at low-photon number excitation limit in a periodically arranged strongly coupled quantum dot - photonic crystal system. A one dimensional periodic array of evanescently coupled photonic cavities (coupled resonator optical waveguides) containing non-interacting quantum dots allows us to tune the group velocity and the bandwidth of the pulse by adjusting the detuning between the cavity resonance frequency and QD energy splitting. Tunable group velocity can achieved by applying an external electric field which will result in an increase the QD energy splitting because of DC Stark effect. We also show that, using this approach, light pulses can be slowed down or stored by compressing the pulse bandwidth adiabatically and reversibly. Adiabatic bandwidth compression can be achieved by slowly increasing the QD-cavity detuning when the light pulse is inside the coupled resonator optical waveguide. The energy splitting and the coupling constant after applying electric field is calculated by using perturbation theory for two level systems. With our approach, nonlinear materials highly susceptible to electric fields can be engineered in low-excitation regime.

9136-93, Session 13

Generation of correlated photon pairs in micro/nano-fibers

Xiaoying Li, Liang Cui, Cheng Guo, Tianjin Univ. (China); Yuhang Li, Z. Y. Xu, Lijun Wang, Tsinghua Univ. (China); Wei Fang, Zhejiang Univ. (China)

The micro/nano-fibers (MNFs) have been extensively investigated owing to their potential usefulness as building blocks in future micro- or nanometer-scale photonic components or devices. In addition to the characteristics of small footprints, relatively large evanescent field, and strong near-field interaction, the MNFs also have the properties of the miniaturized modal area, engineerable dispersion, large available length, low wave-guiding loss, and easy connection to a standard fiber optical system. More applications of MNF, including optical nonlinear effects and atom manipulation, have been explored in recent years. However, the application of MNF in generating quantum light has not been reported yet. In this presentation, we demonstrate a source of quantum correlated

photon pairs via spontaneous four wave mixing (SFWM) in a 15 cm long MNF for the first time.

The MNF is drawn from SMF-28 single mode fiber (SMF), and the dispersion property of the air-cladding MNF is usually determined by its diameter. To obtain photon pairs at about 1310 and 850 nm, respectively, we fabricate a 15 cm long MNF with diameter of about 0.9 mum using a taper-drawing workstation. The MNF is then pumped by a homemade mode-locked laser system, which is based on the Yb-doped fibers. The central wavelength of pump pulses launched into the MNF can be changed within the range of 1031-1051 nm by using a transmission grating, and the full width at half maximum of pump is about 1.5 nm.

We first observe the generation of the individual signal and idler photons via SFWM by using single photon detectors (SPDs), SPD1 and SPD2, respectively. When the central wavelength of the pump and the detected signal and idler photons are about 1031.8, 1310 and 851 nm respectively, we record the counting rate of each SPD by varying the pump power P_a. For the results measured by each SPD, we fit the measured data N with the second-order polynomial function $N=s_1P_a+s_2P_a^2$, where the coefficients s_1 and s_2 are respectively determined by the strengths of Raman scattering (RS) and SFWM. We find the quadratic part $s_2P_a^2$ dominate, showing the phase matching condition of SFWM is satisfied. We then verify the quantum correlation of photon pairs by measuring the coincidence and accidental coincidence rates of the two SPDs for the signal and idler photons originated from the same and adjacent pulses, respectively. The results show the coincidence-to-accidental ratio of 530 for a photon production rate of about 0.002 (0.0005) per pulse in the signal (idler) band can be obtained. Moreover, we analyze the spectral information of the signal photons in the wavelength range of 1270-1610 nm. The result reveals that the bandwidths of the photon pairs are much greater than the theoretically expected value due to the inhomogeneity of the MNF, and experimental observation illustrates that the spectrum of RS in MNF is different from that in conventional optical fibers and photonic crystal fibers. Our investigation shows that the MNF is a promising candidate for developing the sources of quantum light in micro- or nanometer-scales, and the spectral property of photon pairs can be used to non-invasively test the diameter and homogeneity of the MNF.

9136-94, Session 13

Two-photon polarization spectra with Cs-133 6S_1/2-6P_3/2-7S_1/2 and Rb-87 5S_1/2-5P_3/2-4D_5/2 ladder-type atomic system: Autler-Townes splitting and laser frequency locking to excited-state transition

Junmin Wang, Baodong Yang, Jie Wang, Huifeng Liu, Jun He, Shanxi Univ. (China)

Based on our realization of a two-color magneto-optical trap (TC-MOT) with a ladder-type cesium (Cs) 6S_1/2 - 6P_3/2 - 8S_1/2 (852nm+794nm) system [Optics Express, Vol.20 (2012) p.11944], we aim to extend the TC-MOT to a ladder-type Cs 6_S1/2 - 6P_3/2 - 7S_1/2 (852nm+1470nm) system, and further to explore the possibility for employing the four-wave mixing process in the TC-MOT to generate 852nm + 1470nm quantum correlated photon pairs. Because the 852nm photons allow quantum information storage and readout with Cs atomic ensemble and the 1470nm photons allow low-loss transmission in a telecom fiber network, so the 852nm + 1470nm quantum correlated photon pairs are basic resources for implementing the quantum network or the distributed quantum information processing. For doing so, we investigated a possible method for frequency stabilizing 1470nm diode laser to Cs 6P_3/2 - 7S_1/2 excited-state transition with Cs vapor cell by extending the polarization spectroscopy (PS) to the two-color polarization spectroscopy (TCPS). The physical essences of the PS and TCPS are the unsymmetrical atomic populations on the Zeeman sublevels of ground state for the PS and those of the intermediate excited state for the TCPS due to optical pumping. We characterized the TCPS signals of a ladder-type Cs 6S_1/2 - 6P_3/2 - 7S_1/2 (852nm+1470nm) system experimentally and observed the Autler-Townes splitting (ATS). We also performed a comparison between TCPS and the double-resonance optical pumping (DROP) spectroscopy. By employing the radio-frequency modulation sidebands from the outcome of a fiber-pigtailed waveguide-type electro-optical modulator (EOM) for a precise frequency calibration, we measured the ATS as a function of the 852nm laser intensity. The modulation sidebands also provided us a method to offset locking the 1470nm laser to Cs 6P_3/2 - 7S_1/2 excited-state transition via the TCPS with an adjustable detuning (changing the modulation frequency on the EOM).

9136-95, Session 14

A photon-pair-emitting laser diode *(Invited Paper)*

Fabien Boitier, Claire Autebert, Adeline Orieux, Univ. Paris 7-Denis Diderot (France); Aristide Lemaître, Elisabeth Galopin, Lab. de Photonique et de Nanostructures (France); Christophe Manquest, Carlo Sirtori, Ivan Favero, Giuseppe Leo, Sara Ducci, Univ. Paris 7-Denis Diderot (France)

Photonics is playing a central role in the development of quantum information technologies. In this context, electrically driven sources of non-classical states of light have a clear advantage over optically driven ones in terms of portability, energy consumption and integration. Semiconductor materials are an ideal choice to achieve extremely compact sources of non-classical light states; for example, an entangled-light-emitting diode has been demonstrated exploiting the bi-exciton cascade of a quantum dot [1]. Two key issues towards large scale applications are room temperature operation and the compatibility with existing telecom network; indeed photonic devices operating around 1.55 μm are crucial components to enable quantum links between distant nodes. Despite its non-deterministic nature, Spontaneous Parametric Down-Conversion (SPDC) stays the most widely process used to produce photon pairs. The AlGaAs platform, thanks to its direct band gap, presents an evident interest for the electrical injection [2]. In order to deal with the isotropic structure of this crystal, several solutions have been proposed to achieve second-order nonlinear optical conversion in AlGaAs waveguides [3–6]; among these, modal phase matching, in which the phase velocity mismatch is compensated by multimode waveguide dispersion, is one of the most promising to monolithically integrate the laser source and the nonlinear medium into a single device [7, 8]. Here we present an electrically injected AlGaAs source emitting photons pairs at telecom wavelength and operating at room temperature. The device is based on type-II intracavity SPDC in an AlGaAs laser diode and generates pairs at 1.57 μm. The active medium is a quantum well inserted in the core of the structure. Two Bragg mirrors provide both a photonic band gap vertical confinement for the laser mode —a Transverse Electric Bragg mode— and total internal reflection claddings for the photon-pairs modes —one TE00 and one TM00. The laser characteristics and the nonlinear optical behavior are investigated within the same device; the tunability curves of the laser emission and of second harmonic signal intersect at room temperature. The demonstration of photon pair emission is done via time-correlation measurements, giving an internal conversion efficiency higher than ~ 10?9 pairs/pump photon [9]. Our device, based on conventional diode laser fabrication processing, let envision the use of III-V semiconductors for a widespread diffusion of quantum communication technologies.

[1] C. L. Salter et al., Nature 465, 594 (2010).

[2] R. Horn et al., Physical Review Letters 108, 153605 (2012).

[3] A. Fiore et al., Nature 391, 463 (1998).

[4] X. Yu et al., Journal of Crystal Growth 301, 163 (2007).

[5] L. Lanco et al., Physical Review Letters 97, 173901 (2006).

[6] J. P. Van der Ziel et al., Applied Physics Letters 25, 238 (1974).
[7] A. Orieux et al., in CLEO : Science and Innovations (2012).
[8] B. J. Bijlani et al., Applied Physics Letters 103, 091103 (2013).
[9] F. Boitier et al., submitted.

9136-96, Session 14

All optical Zitterbewegung analog in single-photon cavity dynamics

Ali W. Elshaari, Sata Lahiwel, Anas Elgaood, Tatweer Research (Libyan Arab Jamahiriya)

Here we propose an all optical analog of Zitterbewegung (ZB) effect. ZB was initially predicted by Schrödinger as resulting solution of the Dirac equation for relativistic fermions like electrons. In recent years there has been an increased interest in quantum effects on different physical platforms. Particularly, attempts has been made to demonstrate ZB on both classical and quantum levels using spintronic, trapped ions, ultracold atoms, and photonic crystal. In this work we predict the emergence of ZB effect for an optical Q-bit on Silicon photonic platform. The work delivers a fully analytic quantum mechanical treatment, in addition to finite difference time domain (FDTD) simulations of the cavity QED equations. The simulation uses a Jayens-Cummings-like model to describe the cavities-field interactions. The resulting (ZB) oscillation resembles [Rabi] vacuum oscillation in atom-cavity systems, with single photon changing its position state as a function of time. Confining photons into nano-scale cavities enhances the Purcell factor which intern can lead to cavity-photon-material coupling and improve the optical density of modes. The proposed cavity configuration allows superposition of bosonic eigenstates for the photons that are coupled interchangeably between the cavities in both weak and strong coupling regimes. Various coupling parameters and different Q-factors and lifetimes in the cavity modes are discussed with emphasis on their relation to the ZB effect. Different Gedanken experiments are performed to pave the way for experimental realization, and application to different platforms. The present work will have great impact on Quantum information processing for creating coherent superposition eigenstates, as building blocks for Quantum computation.

9136-97, Session 14

Compact saturation absorption spectroscopy set-up for atomic physics experiments

Archana G. Hegde, Manipal Univ. (India); S. Pradhan, Bhabha Atomic Research Ctr. (India)

Doppler free spectroscopy technique, particularly saturation absorption spectroscopy plays a critical role for frequency reference as well as laser frequency stabilization in various atomic physics experiments. Since many of these experiments requires complicated optical layout, a compact saturation absorption spectroscopy set-up with few optical components will ease out the experiments on hand. Recently, the various attributes of pump-probe spectroscopy has been studied in presence of a DC and an oscillating magnetic field for frequency scanning as well as generating a dispersion signal for frequency stabilization [1, 2].

We have studied various optical lay-outs for pump-probe spectroscopy with a motivation for development of compact set-up with improved flexibility. Our simple experimental set-up allows us to change the pump-probe ratio arbitrarily. The optical arrangement allows magnetic field driven frequency scanning and phase sensitive detection using atomic energy level modulation. The results and comparisons of different optical lay out for pump-probe spectroscopy set-up will be presented.

[1] “Magnetic field modulation spectroscopy of Rubidium atoms”, S. Pradhan, R. Behera and A.K. Das, Pramana-J. Phys., 78, 585 (2012).
[2] “Magnetoassisted pump-probe spectroscopy of cesium atoms”, S. Pradhan and B. Jagatap, J. Opt. Soc. Am. B, 28, 398 (2011).

9136-98, Session 14

Nanometric surface probing with ultra-cold atoms

Murtaza Ali Khan, European Laboratory for Non-Linear Spectroscopy (Italy) and Karlsruhe School of Optics (Germany); Florian Schaefer, European Lab. for Non-linear Spectroscopy (Italy); Wolfram H. P. Pernice, Karlsruhe School of Optics (Germany); Francesco Saverio Cataliotti, European Laboratory for Non-Linear Spectroscopy (Italy)

We present latest results on the development of a new experimental setup to study the regime of strong light-matter interaction. In the final setup a sample of cold Rb-87 atoms will we prepared close to an Atom Chip. The Atom chip serves to both, the preparation of the cold atom cloud and as a supporting structure for photonic structures. We strive to study the strong interaction between the cold atoms and light coupled to the photonic structure and their interaction with the Si chip itself.

Cold and ultra-cold atoms have made a number of important contributions to improve over understanding of fundamental physics, quantum information, quantum interferometry [1] and many other related fields.

On the other hand light-matter interaction is a basic tool in physics research and application that is gaining importance day by day. Modern production techniques such as electron beam lithography nowadays already offer the possibility to create highly functional photonic structures within Silicon wafer substrates that give us high control on photonic fields. We want to combine the available techniques to precisely control, both, light fields and cold atoms clouds, in order to study the new phenomena when the two of them step into close interaction.

Acknowledgements:

The current project is financed by, FP7 collaborative project MALICIA”light-matter interface in absence of light”, Murtaza Ali Khan is supported by Doctorate Euro-photonics Erasmus Mundus program, the experimental apparatus is based at European Laboratory for Non-Linear Spectroscopy (LENS), University of Florence. The Atom Chip is fabricated at Karlsruhe School of Optics (KSOP), Karlsruhe Institute of Technology.

References:

[1] I. Herrera, J. Petrovic, P. Lombardi, L. Consolino, S. Bartalini, and F.S. Cataliotti, “Degenerate quantum gases manipulation on Atom Chips”, Phys. Scr. T147 (2012)
[2] Wolfram H.P. Pernice, Chi Xiong and Hong X. Tang, “High Q micro-ring resonators fabricated from poly crystalline aluminum nitride films for near infrared and visible photonics”, Vol. 20, No. 11. OPTICS EXPRESS 12261 (2012)

9136-99, Session 14

Towards continuous-variable quantum key distribution with multi-mode entangled states of light

Vladyslav C Usenko, Laszlo Ruppert, Radim Filip, Palack? Univ Olomouc (Czech Republic)

Quantum key distribution (QKD) has its goal in developing the methods (protocols) allowing two trusted parties to share a secure key which they can lately use for confidential communication through classical channels using one-time pad cryptographic system. Early developments in the field

were based on the discrete-variable information encoding and decoding from the state parameters of the two-level quantum systems (qubits) or entangled qubit pairs, represented by single or entangled photons in the typical optical implementations. Contrary to that the recently developed continuous-variable (CV) protocols are based on the use of multi-photon states of light and are supposed to improve the applicability of QKD with the bright pulses, being more stable against loss in the communication channels and at the same time less demanding in terms of the experimental equipment. Typically the CV QKD protocols are based on the homodyne measurement of the quadrature observables of light, which are similar to the position and momentum operators of a particle in quantum mechanics. Similarly to the discrete-variable protocols, the CV QKD protocols can be realized using either preparation and measurement of the states or using bipartite entangled states, which are measured by the two remote parties. In the latter case the bits, which are then used for distillation of a secure key, are generated during the measurement. The states, typically used for this purpose, are the twin-beam states, being quadrature-entangled and having Gaussian quadrature probability distributions. This allows using the well-established security proofs for the Gaussian CV QKD protocols allowing security analysis based on covariance matrix formalism. At the same time, the homodyne detection may be intrinsically multi-mode, when a local oscillator used as a phase reference for the measurement of a quadrature consists of different spectral, spatial or other types of modes. This is not an issue in the other tasks of CV quantum information processing, such as quantum teleportation, quantum metrology etc. However, it may have strong influence on the security of CV QKD, especially when the trusted parties are not aware of the multi-mode structure of their measurement. Thus, we first study the case of the multi-mode measurement of the single-mode entangled source, which effectively means additional security-breaking side-channel loss prior to detection. Moreover, the entangled states may be as well multi-mode, which is observed in particular in the case of the bright squeezed vacuum (BSV) states of light. In this case we show the positive effect of the mode balancing on the side of the source or mode selection on the side of detection. We also demonstrate the impact of the limited knowledge of the trusted parties about the structure of the protocol on its security. Finally, we consider the case of the heavily multi-mode states with fluctuating energy per mode and show the positive effect of increasing number of the modes, which leads to averaging of the Gaussian entanglement of the states and stabilization of the key rate. The result opens a promising pathway towards the realization of CV QKD with the multi-mode states of light.

9137-1, Session 1

Triplet sensitized conjugated polymers for use in solar cells *(Invited Paper)*

Hugo A. Bronstein, Univ. College London (United Kingdom); Rolf Andernach, Hendrik Utzat, Stoichko Dimitrov, Martin J. Heeney, James Durrant, Imperial College London (United Kingdom)

The short distance (~20 nm) a singlet exciton can diffuse in an organic solar cell has resulted in the need for complex, poorly understood bulk heterojunctions. Here we present the synthesis and characterization of a conjugated polymer suitable for use in organic solar cells where the singlet excitons are sensitized into triplet excitons. Covalent attachment of a small amount of heavy metal containing porphyrin into the polymer allows efficient intersystem crossing of the singlet excitons on a conjugated polymer backbone into triplet excitons. The long lifetime of the triplet exciton potentially allows it travel further, and thus for the creation of an efficient bi-layer organic solar cells.1,2 This talk will focus on the synthesis of the novel conjugated polymer, and its photophysical characterization that demonstrates the presence of triplet excitons on the polymer backbone. Organic solar cell data using the triplet sensitized polymer will then be discussed.

9137-2, Session 1

Multijunction polymer solar cells and water splitting *(Invited Paper)*

René A. J. Janssen, Technische Univ. Eindhoven (Netherlands)

No Abstract Available

9137-3, Session 1

Design parameters and ordering effects in poly(benzo[1,2-b:4,5-b']dithiophene-thieno[3,4-c]pyrrole-4,6-dione) (PBDTTPD) and analogs for efficient solar cells

Pierre M. Beaujuge, King Abdullah Univ. of Science and Technology (Saudi Arabia)

Among Organic Electronics, solution-processable ϖ-conjugated polymers are proving particularly promising in bulk-heterojunction (BHJ) solar cells with fullerene acceptors such as PCBM.[1] In the past few years, we have found that varying the size and branching of solubilizing side-chains in ϖ-conjugated polymers impacts their self-assembling properties in thin-films. Beyond film-forming properties, nanoscale ordering in the active layer governs material and device performance. For example, in poly(benzo[1,2-b:4,5-b']dithiophene–thieno[3,4-c] pyrrole-4,6-dione) (PBDTTPD), TPD substituents of various size and branching impart distinct molecular packing distances (i.e., ϖ–ϖ stacking and lamellar spacing),[2] varying degrees of nanostructural order in thin films,[2] and preferential backbone orientation relative to the device substrate.[3] These structural variations have been found to correlate with solar cell performance, with power conversion efficiencies ranging from 4% to 8.5%.[2-4] In parallel, discrete backbone modifications in PBDTTPD can impact polymer backbone conformations and self-assembly,[5] and various ring-substituents directly appended to the ϖ-conjugated backbone can induce morphological effects and may also affect polymer performance in BHJ solar cells with PCBM.[6] Our recent developments emphasize how systematic structure-property relationship studies impact the design of efficient polymer donors for BHJ solar cell applications.

[1] P. M. Beaujuge, and J. M. J. Fréchet, JACS 2011, 133, 20009.

[2] C. Piliego, T. W. Holcombe, J. D. Douglas, C. H. Woo, P. M. Beaujuge, and J. M. J. Fréchet, JACS 2010, 132, 7595.

[3] C. Cabanetos, A. El Labban, J. A. Bartelt, J. D. Douglas, W. R. Mateker, J. M. J. Fréchet, M. D. McGehee, and P. M. Beaujuge, JACS 2013, 135, 4656.

[4] J. A. Bartelt, J. D. Douglas, W. R. Mateker, A. El Labban, C. J. Tassone, M. F. Toney, J. M. J. Fréchet, P. M. Beaujuge, and M. D. McGehee, 2013, Submitted.

[5] J. Warnan, C. Cabanetos, A. El Labban, M. R. Hansen, C. Tassone, M. F. Toney, and P. M. Beaujuge, 2013, Submitted.

[6] J. Warnan, A. El Labban, C. Cabanetos, E. Hoke, C. Risko, J-L. Brédas, M. D. McGehee, and P. M. Beaujuge, 2013, Submitted.

9137-4, Session 1

Morphologically controllable photophysical properties of heterogeneous polymer blend films used in organic solar cells

Xiaotao Hao, Shandong Univ. (China)

Conjugated polymer-based blend nanocomposites have gained worldwide attention in recent years due to their potential application in efficient and low-cost solar cells. The photophysical properties of the electron donor and acceptor critically affect the efficiency of organic photovoltaic (OPV) devices, and these properties are strongly dependent on the morphology of the thin organic films that are constructed. The morphology that a given material adopts is in turn strongly dependent upon a range of experimental parameters, including film formation method, solvent, miscibility of blended materials, any annealing conditions used, characteristics of the substrate, as well as the organic material itself. [1?2]

In this work, time-resolved confocal fluorescence microscopy and structured illumination microscopy are applied to the study of the nanomorphology of blend films of poly (3-hexylthiophene) (P3HT) and [6, 6]-phenyl C61-butyric acid methyl ester (PCBM).[3?4] These measurements confirm the presence of an emissive region around the crystalline regions of PCBM indicating the presence of a layer that inhibits charge separation between the polymer and the large PCBM-rich regions. We show here that structured illumination microscopy is a viable method of gaining additional information from these weakly emitting films.

We also reported the influence of the alkyl side-chain length of poly(3-alkylthiophene) (P3AT) on the charge transfer properties of P3AT:PCBM hybrid films. The effect of annealing on the morphology of P3AT:PCBM has been investigated through atomic force microscopy. Surface topography is dramatically affected by thermal annealing. The charge transfer behavior was studied systematically via absorption, steady-state and time-resolved fluorescence measurements. We interpret the fluorescence properties in terms of the strong intermolecular interactions among the individual polymer chains and interactions between P3AT and PCBM.

References:

(1) X.T. Hao, N.Y. Chan, T.A. Smith, D. E. Dunstan, J. Phys. Chem. C, 2009, 113, 11657.

(2) X.T. Hao, L.J. McKimmie, T.A. Smith, J. Phys. Chem. Lett., 2011, 2, 1520.

(3) X.T. Hao, N.Y. Chan, C. Hecker, N. Tanigaki, T.A. Smith, Macromolecules, 2010,43,10475.

(4) X.T. Hao, L.M. Hirvonen and T.A. Smith, Meth. Appl. Fluor., 2013,1, 015004/1-8.

9137-5, Session 1

Room-temperature solution-processed transition metal oxides as efficient carrier extraction layer for high-performance organic solar cells

Feng-Xian Xie, Xin-Chen Li, Chuan Dao Wang, Wallace C. H. Choy, The Univ. of Hong Kong (Hong Kong, China)

An essential aspect in designing efficient and stable organic solar cells (OSCs) is the engineering of interfacial carrier transporting layers between the organic layer and metal electrodes. Among various materials available for interfacial layers, transition metal oxides (TMOs) have great potential owing to their wide range of energy level aligning capabilities. Bearing the compatibility with large-area, low-cost, high-throughput production and all-solution technology, we propose a one-step method to synthesize low-temperature solution-processed TMOs such as molybdenum oxide and vanadium oxide for hole transport layers through the synthesis of hydrogen molybdenum bronze and hydrogen vanadium bronze. Interestingly, the hydrogen metal oxide bronzes (HMOs) are dispersed uniformly and stably into water-free solvents which are particularly beneficial to the device stability and processing. With low temperature treatment or even at room temperature, the TMO films with small amount oxygen vacancies exhibit high film quality and desirable electrical properties. Through the analysis of UPS and XPS results, we identify the importance of oxygen vacancies for TMOs as HTL. Notably, the synthesized HMOs can be dispersed uniformly and stably into water-free solvents. By using our TMOs to make OSCs with polymer blend of P3HT:PCBM, the power efficiency (PCE) reaches 4% (vs 3.7% for PEDOT:PSS control device) and PCE of 7.75% using polymer blend of PBDTTT-C-T:PCBM (vs 7.24% for the corresponding PEDOT:PSS control device) [1]. Recently, we have achieved solution process of TMOs at room temperature [2] and the PCE performance can reach about 8% in inverted OSCs with polymer blend of PBDTTT-C-T:PCBM as the active layer. Consequently, the results of our newly-synthesized TMOs demonstrate that oxygen vacancy plays an essential role for TMOs as effective HTL for applications on organic electronics.

[1] F. Xie, W.C.H. Choy, C. Wang, X. Li, S. Zhang, J. Hou, “Low-temperature Solution-Processed Hydrogen Molybdenum and Vanadium Bronzes for Efficient Hole Transport Layer in Organic Electronics”, Adv. Mat., vol. 25, pp.2051–2055, 2013.

[2] X.C. Li, W.C.H. Choy, F. Xie, S. Zhang and J. Hou, “Room-Temperature Solution-Processed Molybdenum Oxide as Hole Transport Layer with Ag Nanoparticles for Highly Efficient Inverted Organic Solar Cells”, J. Mater. Chem. A, vol. 1, pp.6614-6621, 2013.

9137-6, Session 2

Influence of buffer layers on energy-level alignment in organic thin-film solar cells *(Invited Paper)*

Takeaki Sakurai, Fu Wei, Tetsuya Miyazawa, Shenghao Wang, Katsuhiro Akimoto, Univ. of Tsukuba (Japan)

In organic solar cells (OSCs), an interface exists between the organic molecules and the electrode made of an inorganic material; the electrical properties of this interface affect the performance of the devices. One of the methods used to improve the electrical properties of an interface is to introduce a buffer layer between the organic molecules and the electrode. In small molecule based OSCs, bathocuproine (BCP) is used well as a buffer layer between C60 and metal cathode to improve the device efficiency. Nevertheless, the lifetime and the stability of the device with BCP buffer layer are not good for the practical application. In order to acquire the reliability of the devices over a long period, the development of a new buffer layer is necessary. To obtain the strategies for the development of the effective buffer layer, we have investigated the electronic structures at the interfaces between C60 and a large variety of organic semiconductors by means of synchrotron based in-situ ultraviolet photoelectron spectroscopy (UPS). Ag deposited Si (100) wafers were used as substrates. The C60/buffer/Ag heterostructures were formed by depositing buffer materials on Ag and subsequently depositing C60 onto buffer/Ag stack layer in a step-by-step way in a vacuum deposition chamber. A series of perylene derivatives (PTCDA, PTCDI and PTCBI), TCNQ derivatives (TCNQ and F4TCNQ) and pyridine based acceptor molecules (BCP, TPBi and TAZ) were applied as buffer layers. For all buffer/Ag stack structures, the LUMO level of buffer layers almost accords with Fermi level of Ag, that is, electron is easily transferred from the Ag electrode to the buffer layers due to the disappearance of the electron injection barrier. In contrast, the electron injection barrier height between LUMO of C60 and LUMO of buffer materials correlates with the work function of the buffer/Ag stack structures (?buff). For the specimens whose ?buff is higher than 4?eV (perylene and TCNQ derivatives), energy level of HOMO of C60 shifts towards higher binding energy with decreasing substrate ?buff, that is, the energy barrier height varies with changing the ?buff. On the other hand, for the specimens whose ?buff is below 4 eV (BCP, TAZ and TPBi), energy level of HOMO of C60 is fixed at 1.9 eV with respect to the Fermi level, and the electron injection barrier height between LUMO of C60 and LUMO of buffer materials turns to be zero. Thus, it is important to select buffer/Ag heterostructure with low work function in order to maintain good electric contact near Ag cathode. The more detailed physical mechanism about the energy level alignment (charge transfer, gap states, and dipole layer formation) and the strategy of the development of an effective buffer layer will be shown using integer charge transfer model [1]. [ref.1] S.Braun et al., Adv.Mater. 21 (2009) 1450.

9137-7, Session 2

Thieno[3,2-b]thiophene based diketopyrrolopyrrole and isoindigo polymers for high performance OFET and OPV applications

Iain Meager, Raja Shahid Ashraf, Iain McCulloch, Imperial College London (United Kingdom)

Organic Photovoltaics (OPV) and Field Effect Transistors (OFET) have made a large amount of progress in recent years towards matching the performance, stability and cost effectiveness of their inorganic counterparts. Diketopyrrolopyrrole (DPP) is a well established structural motif for the organic semiconducting materials, thieno[3,2-b] thiophene flanked DPP polymers were previously shown by our group as an excellent candidate material for such applications with impressive efficiencies in solar cells devices and mobilities in transistors.1 Through careful design of the nature of the alkyl chain we demonstrate a route towards improved solubility, molecular weight, polydispersity index as well as a wider range of accessible comonomer units2 combined with state of the art post-polymerisation techniques this leads to increased short circuit currents (Jsc) and power conversion efficiencies (PCE). Further improvements to both OFET and OPV performance are demonstrated using a new method of synthetic design where systematically moving the alkyl chain branching position further away from the polymer backbone leads to dramatic improvements in device performance. Most noticeably the OPV efficiency jumps from around 5% to in excess of 7%, with improvements showing an interesting correlation to increased crystallinity of the polymer material.3 The high performing nature of the fused heterocyclic thieno[3,2-b]thiophene building block is also demonstrated for the first time as the flanking unit in analogous isoindigo polymers. The thieno[3,2-b] thiophene isoindigo has many structural similarities to the previously described DPP polymers, however, unlike DPP the electron rich flanking units are fused to the electron deficient core giving an increased coplanarity along the polymer backbone favourable for charge transport properties. The new isodindigo unit was copolymerised with a range of comonomer units (thiophene, benzothiadiazole, bithiophene) to afford a

new series of high performance ladder-type polymers with very narrow optical band gaps and broad red-shifted absorption profiles. When used as the active layer in OFET devices impressive ambipolar performance was observed with electron mobilities > 1 cm2 / Vs.4

References

[1] H. Bronstein et al, J. Am. Chem. Soc. 2011, 133 (10), pp 3272–3275

[2] I. Meager et al, Macromolecules. 2013, 46 (15), pp 5961–5967

[3] I. Meager et al, J. Am. Chem. Soc. 2013, 135 (31), pp 11537–11540

[4] I. Meager et al, 2014, Manuscript in preparation.

9137-8, Session 2

Fullerene-free organic solar cells exploiting long-range exciton energy transfer

Kjell Cnops, IMEC (Belgium) and Katholieke Univ. Leuven (Belgium); Barry P. Rand, Princeton Univ. (United States) and IMEC (Belgium); David Cheyns, IMEC (Belgium); Bregt Verreet, Princeton Univ. (United States) and IMEC (Belgium); Max A. Empl, Paul L. Heremans, IMEC (Belgium) and Katholieke Univ. Leuven (Belgium)

In order to increase the power conversion efficiency (PCE) of organic photovoltaic devices, the spectral absorption range should be broadened while retaining efficient harvesting of generated excitons. This requires the use of multiple complementary absorbers, usually incorporated either in tandem cells[1,2] or in cascaded heterojunctions.[3,4] We present a simple three-layer device structure comprising a sexithiophene (6T) donor and two non-fullerene acceptors, chloroboron subphthalocyanine (SubPc) and chloroboron subnaphthalocyanine (SubNc). In this device architecture long-range exciton energy transfer is exploited in order to enhance the photocurrent generation.

Both SubPc and SubNc are traditionally used as donor materials. Using them as acceptor in bilayer devices with a 6T donor, we realize PCE values of 4.7% and 6%, respectively, both higher than previously reported values for fullerene-free devices. The high photocurrent generation in these devices is attributed to the strong absorption in visible light of the non-fullerene acceptors. In addition, high open-circuit voltages are realized due to the improved energy level alignment between the frontier molecular orbitals at the donor-acceptor interface. In the three-layer device the photocurrent originates from all three complementary absorbing materials, resulting in a quantum efficiency above 75% at wavelengths between 400 nm and 720 nm. With an open-circuit voltage close to 1 V, this leads to a remarkable PCE of 8.4% for a fullerene-free organic solar cell.

Using photoluminescence quenching experiments we demonstrate that an efficient two-step exciton dissociation mechanism is active in the three-layer device. First, excitons generated in the outer SubPc layer are transferred to the middle SubNc layer by long-range Förster resonance energy transfer. Subsequently, the transferred excitons dissociate at the 6T / SubNc heterojunction. In this energy relay cascade architecture the SubNc layer thus functions simultaneously as an energy acceptor for excitons generated in the SubPc layer, and as a charge acceptor at the interface with 6T. By fitting the experimental photoluminescence data, using numerical exciton density simulations, a Förster radius of 7.5 nm was obtained for exciton energy transfer from SubPc to SubNc. This indicates that the interlayer energy transfer process is very efficient and the excitons can be transferred over much larger distances compared to the normal diffusion process in a single layer. Utilizing this long-range exciton harvesting process, the multilayer cascade structure thus forms an important alternative device architecture to improve the performance of organic solar cells beyond that of conventional donor-fullerene systems.

[1] Cheyns, D., Rand, B. P. & Heremans, P. Organic tandem solar cells with complementary absorbing layers and a high open-circuit voltage. Appl. Phys. Lett. 97, 033301 (2010).

[2] You, J. et al. A polymer tandem solar cell with 10.6% power conversion efficiency. Nat. Commun. 4, 1446 (2013).

[3] Cnops, K., Rand, B. P., Cheyns, D. & Heremans, P. Enhanced photocurrent and open-circuit voltage in a 3-layer cascade organic solar cell. Appl. Phys. Lett. 101, 143301 (2012).

[4] Ichikawa, M., Takekawa, D., Jeon, H.-G. & Banoukepa, G. D. R. Cascade-type excitation energy relay in organic thin-film solar cells. Org. Electron. 14, 814–820 (2013).

9137-9, Session 2

Plasmonic-electrical effects of metal nanoparticles for highly-efficient organic solar cells

Wallace C. H. Choy, Feng-Xian Xie, Di Zhang, Wei E. I. Sha, Xin-Chen Li, Baofu Ding, The Univ. of Hong Kong (Hong Kong, China)

Optical effects of the plasmonic structures and materials effects of the metal nanomaterials have recently been individually studied for enhancing performances of organic solar cells (OSCs). In this work, differently, the effects of plasmonically induced carrier generation and enhanced carrier extraction of the carrier transport layer (i.e. plasmonic-electrical effects) in OSCs are investigated. We propose and demonstrate enhanced charge extraction in TiO2 as a highly efficient electron transport layer by the incorporation of metal nanoparticles (NPs). While OSCs using pristine TiO2 can only operate by UV activation (< 400 nm, otherwise poor S-shape J-V characteristics are exhibited), efficient device performance is demonstrated by using Au NPs incorporated TiO2, at a plasmonic wavelength (560-600 nm) far longer than the originally necessary UV light. By optimizing the amount of Au NPs doped into TiO2, the performances of OSCs with various polymer active layers are enhanced and efficiency of 8.74% is reached [1]. In order to understand the fundamental physics, an integrated optical and electrical model (i.e. a multiphysics model), which takes into account hot carrier tunneling probability and extraction barrier between TiO2 and active layers, is introduced here. From experimental and theoretical studies, we attribute the enhanced charge extraction under plasmonic wavelength illumination to the strong charge injection of plasmonically excited electrons from NPs into TiO2. The mechanism favors better energy alignment at the TiO2 interface which facilitates carrier transport in OSCs. Recently, we also find that the TiO2-metal NPs composite can enhance the carrier accumulation which can fill the trap states in TiO2 and thus improve the electrical conduction of TiO2 and thus improve the device performances of OSCs [2]. The work can contribute to new approaches and knowledge to utilize plasmonically electrical nanostructures in organic optoelectronic devices for enhancing device performances.

[1] D. Zhang, W.C.H. Choy, F. Xie, W.E.I. Sha, X. Li, B. Ding, K. Zhang, F. Huang, and Y. Cao, “Plasmonic-electrically Functionalized TiO2 for High Performance Organic Solar Cells”, Adv. Funct. Mat., DOI: 10.1002/adfm.201203776.

[2] F.X. Xie, W.C.H. Choy, W.E.I. Sha, D. Zhang, S. Zhang, X. Li, C.W. Leung, J. Hou, “Enhanced Charge Extraction in Organic Solar Cells through Electron Accumulation Effects Induced by Metal Nanoparticles”, Energy Environ. Sci., vol. 6, pp.3372 – 3379, 2013.

9137-10, Session 2

Highly-conductive silver nanowire networks via purposeful wire functionalization as transparent top electrode for organic photovoltaics

Franz Selzer, Nelli Weiß, David Kneppe, Ludwig Bormann,

Christoph Sachse, Nikolai Gaponik, Lars Müller-Meskamp, Alexander Eychmüller, Karl Leo, Technische Univ. Dresden (Germany)

Small molecule based organic photovoltaics are a promising technology for future processing in high throughput roll-to-roll coating machines. Therefore flexible and transparent electrodes suitable for large area processing on temperature sensible plastic films with low sheet resistance and high transmittance are required. The commonly used Indium Tin Oxide (ITO) shows high performance on rigid substrates like glass. Due it's brittleness and very high process temperatures (400°C) ITO can not be used on plastic films. Percolative networks made of silver nanowires (AgNWs) is a flexible alternative showing comparable opto-electrical performance to ITO. Usually they are deposited from solution, followed by post-annealing at temperatures up to 200°C for approximately one hour. The annealing step, which is necessary to obtain highly conductive AgNW electrodes and the solvents involved in the deposition limit the versatility of this type of electrode and do not allow the direct deposition as top contact onto evaporated small molecule devices. Here we present a novel spray-coated AgNW mesh showing high opto-electrical performance although processed at very low temperatures below 100°C on top of a small molecule solar cell. We investigate different types of wire functionalization and the consequences on typical network parameters of AgNWs like sheet resistance and transmittance. By comparing all investigated materials under different circumstances like varying concentration, etc. and with the help of scanning electron microscopy as well as atomic force and optical transmission microscopy high-performance AgNW electrodes are processed at 30°C showing sheet resistance values of less than 50 Ohm/sq at transmittance values greater than 80%. Finally, the successful implementation as transparent top electrode for high-performance organic p-i-n type solar cells is demonstrated.

9137-11, Session 3

Optical gain and losses in organic lasers *(Invited Paper)*

Thomas J. Riedl, Bergische Univ. Wuppertal (Germany)

No Abstract Available

9137-12, Session 3

Bose-Einstein condensation of exciton-polaritons in a polymer filled microcavity at room temperature *(Invited Paper)*

Rainer F. Mahrt, Thilo Stoeferle, IBM Research – Zürich (Switzerland)

No Abstract Available

9137-13, Session 3

Threshold reduction by multidimensional photonic confinement in metal-organic microcavities

Andreas Mischok, Robert Brueckner, Technische Univ. Dresden (Germany); Christoph Reinhardt, Technische Univ. Dresden (Germany) and McGill Univ. (Canada); Markas Sudzius, Vadim G. Lyssenko, Hartmut Froeb, Karl Leo, Technische Univ. Dresden (Germany)

Due to their geometry, optical microcavities allow strong confinement of light between the mirrors and promise single mode operation at lowest possible lasing thresholds. Nevertheless, such devices exhibit losses not only due to parasitic absorption of the active or mirror layers, but especially via outcoupling of leaky modes waveguided perpendicularly to the emission direction. Addressing these loss channels requires multi-dimensional photon confinement, e.g. by adding lateral structures to effectively trap photons in the laser mode.

In this work, we present an organic microcavity facilitating the highly fluorescent blend of the matrix material Alq3 doped by 2wt % with the laser dye DCM, sandwiched between high quality dielectric distributed Bragg reflectors. For future electrical contacting, a silver layer of 40 nm thickness is added next to the active layer. This highly conductive layer leads to the formation of Tamm-Plasmon-Polaritons (TPP), replacing the original cavity mode and shifting its resonance to the red. To avoid even higher parasitic absorption introduced by such contacts, the silver layer is structured on the micrometer-scale using photolithography, yielding seperated areas supporting either original cavity mode or red shifted TPP-resonances. This separation leads to a strong spatial trapping of the modes to only their resonant regions on the sample and can in turn be exploited to achieve complete three-dimensional confinement of photons and effectively reduce lateral loss channels.

In elliptic holes produced in the metal layer, we observe the formation of Mathieu-Modes, which are in excellent agreement with theory, leading to an increased photon lifetime and a reduction of the lasing threshold by six times. Facilitating triangular cuts in the silver layer, more complex standing modes develop in the system, allowing a precise optimization of the mode volume and reducing the threshold even further down to one order of magnitude below the threshold of an unstructured organic cavity.

These results show that the introduction of absorptive metals, needed for the realization of an electrically driven laser, can be harnessed to reduce leaky modes and in turn improve the characteristics of the device.

9137-14, Session 3

Three-dimensional organic microlasers

Nina Sobeshchuk, Ecole Normale Supérieure de Cachan (France) and Univ. of Informational Technologies, Mechanics and Optics (Russian Federation); Clément Lafargue, Stefan Bittner, Joseph Lautru, Severin Charpignon, David Ulbricht, Ecole Normale Supérieure de Cachan (France); Igor Y. Denisyuk, Univ. of Informational Technologies, Mechanics and Optics (Russian Federation); Joseph Zyss, Melanie Lebental, Ecole Normale Supérieure de Cachan (France)

The research on microcavities and -lasers has mostly focused on flat (two-dimensional, 2D) cavities, which means structures with a thickness in the order of the wavelength [1]. In contrast, three-dimensional (3D) cavities with dimensions of the same order of magnitude in all three directions have scarcely been investigated. Here we present first results on fabrication and characterization of three-dimensional organic microlasers.

For obtaining the 3D structures, it was reasonable to use the well-known SU8 photoresist as a resist designed for production structures with high aspect ratio. Different organic dyes in the concentration 0.5%wt were introduced directly within the monomer. The film deposition on a silicon/silica or glass wafer was implemented by spin-coating. The film thickness was monitored by the viscosity of the resist and the spin-coating mode. After a prebake, the cavity shapes were defined by a single UV exposure step. Cylindrical cavities of various shapes with thicknesses in the range of 20-150 μm were successfully fabricated. SEM pictures showed good quality structures with perpendicular/parallel faces, smooth surfaces and few defects.

The microlasers were pumped one at a time by a pulsed frequency doubled Nd:YAG laser (532 nm,10 Hz, 500 ps) impinging perpendicularly to the substrate plane. The size of the pump beam was chosen such that the whole cavity was covered. The lasing emission was collected by a lens that could be positioned in an arbitrary direction and transferred to a spectrometer.

We investigated cavities with square cross section and strip

cavities with a lateral extension in the range of 50-200 μm. All investigated microcavities showed multimode lasing. Typically, the spectra consist of one or several series of equidistant resonances. Since the size of the cavities is very large compared to the wavelength, it is useful to consider them as ray-dynamical systems [1, 2]. In the ray-dynamical limit, the cavities can be considered as 3Dphoton billiards, and many properties of the resonators can be linked to the dynamics of the classical billiard. In particular, the free spectral ranges (FSRs) of the resonance series correspond to the optical lengths of periodic ray trajectories in the corresponding billiard. We found that the periodic orbits sustaining the lasing emission depend sensitively on the shape and ratio between the height and the lateral size of the cavities. In addition, images of the lasing cavities and far-field emission diagrams were collected to understand the relation between the cavity shape and the periodic orbits preferred by the lasing modes. This would allow engineering cavities with specific spectral and emission properties as a function of their shape.

References

[1] M. Lebental, N. Djellali, C. Arnaud, J.-S.Lauret, J. Zyss, R. Dubertrand, C. Schmit, and E. Bogomolny,"Inferring periodic orbits fromspectra of simply shaped microlasers," Phys. Rev. A, vol. 76, p.023830, 2007.

[2] E. Bogomolny, N. Djellali, R. Dubertrand, I. Gozhyk, M. Lebental, C. Schmit, C. Ulysse, and J. Zyss,"Trace formula for dielectric cavities ii : Regular, pseudo-integrable, and chaotic examples," Phys. Rev. E,vol. 83, p.036208, 2011.

9137-15, Session 3

Integrated vertical microcavity using a nanoscale deformation instead of sidewalls for strong lateral confinement

Lijian Mai, IBM Research - Zurich (Switzerland); Fei Ding, Leibniz-Institut für Festkörper- und Werkstoffforschung Dresden (Germany); Thilo Stöferle, Armin W. Knoll, Bert-Jan Offrein, Rainer F. Mahrt, IBM Research - Zurich (Switzerland)

Optical cavities are important for many applications including lasing and in cavity quantum electrodynamics (cQED) for the enhancement of light-matter interaction between the optical field and single emitters. A high degree of light-matter interaction is also crucial for the development of single-photon devices, which represents the ultimate goal in terms of efficiency. In order to increase the degree of interaction, an increase in the quality factor (Q) and a simultaneous decrease in the mode volume (V) is required.

We report on the experimental realization of a vertically emitting optical microcavity which achieves lateral mode confinement without using pillar or mesa structures. Instead, the confinement is induced using a nano-scale Gaussian-shaped deformation embedded in the cavity, as proposed in [1]. This reduces light scattering compared to pillars with sidewall roughness or sharp material interfaces from mesas, and therefore retains a high Q even for strong lateral confinement down to wavelength dimensions. Solid state cavities containing a perylene-diimide dye-doped polystyrene film with a mode volume V < 0.4 ?m3 and a quality factor Q > 1000 of a single mode have been fabricated. These measured values match closely with the results of 3D finite-difference time-domain (FDTD) simulations of the corresponding structures. In order to prove the coupling of the microcavity to the embedded emitters, the samples were also probed by time-resolved microphotoluminescence. An enhancement of the spontaneous emission rate by a factor of 3.5 has been observed at room temperature.

The sample was made using focused ion beam milling (FIB) of a Si substrate and Bragg reflectors were deposited on the milled substrates by sputtering Ta2O5 and SiO2.

[1] F. Ding et al., Phys. Rev. B 87, 161116 (R) (2013)

9137-31, Session PS2

Tunable color emission from cascaded amplified spontaneous emissions in organic thin films

Kin Long Chan, Kok-Wai Cheah, Hong Kong Baptist Univ. (Hong Kong, China)

Semiconducting (conjugated) polymer draws much attention nowadays as it is a promising possible application. With increasing emission efficiency, excited emission such as ASE (amplified spontaneous emission) and lasing have been achieved. Lasing emission form solid films containing semiconducting polymer also draws lots of attentions as promising gain materials in lasing application. In this research, the gain media in optical amplifiers will be studied. The color of light emission can be continuously tuned from blue; white to green will be demonstrated.

This work aims at getting tunable color emission of ASE with two different color ASE spectra that have near-equal spectral profile. Two materials, Poly (9, 9-di-n-dodecylfluorenyl-2, 7-diyl) (PFO) and Poly [(9, 9-di-n-octylfluorenyl-2, 7-diyl)-alt-(benzo[2,1,3]thiadiazol-4,8-diyl)] (F8BT) were selected. The correspond peaks of PFO and F8BT are at 450 nm and 575 nm respectively, and the full width half maximum are 5 nm and 10 nm. Therefore they are suitable to combine to give broaden-range of color in ASE. PFO thin film is first deposited onto a glass substrate, then a high transmittance optical clear adhesive (over than 80 % transmittance in visible range) was added as a spacer that separate it from the F8BT thin film. The cascaded films successfully demonstrated when pumped by 355 nm third harmonic laser from YAG-Nd. The CIE achieved is from (0.42, 0.55) to (0.18, 0.11) and a comparable threshold.

In conclusion, we demonstrate the color of light emission can be continuously tuned from blue, white to green. The method we used here also indicates a potential way to tailoring the emission spectra of organic light emitting devices.

9137-32, Session PS2

Oxadiazole- and triazole-based highly-efficient thermally activated delayed fluorescence emitters for organic light-emitting diodes

Jiyoung Lee, Katsuyuki Shizu, Hiroyuki Tanaka, Hiroko Nomura, Takuma Yasuda, Chihaya Adachi, Kyushu Univ. (Japan)

The use of thermally-activated delayed fluorescence (TADF) is an effective way of harvesting singlet and triplet excitons. TADF emitters are promising next-generation materials for organic light-emitting diodes (OLEDs) because they can realize high electroluminescence efficiency without heavy metals (H. Uoyama et al., Nature 2012, 492, 234-238). In a TADF emitter, triplet excitons are converted into singlet ones to emit delayed fluorescence. Molecules with a small energy gap between the lowest singlet excited state (S1 state) and the lowest triplet state (T1 state), ΔEST, can exhibit efficient reverse intersystem crossing by harvesting thermal energy.

We developed highly-efficient TADF emitters containing 2,5-diphenyl-1,3,4-oxadiazole (OXD) or 3,4,5-triphenyl-4H-1,2,4-triazole (TAZ) electron acceptor and phenoxazine (PXZ) electron donor moieties (J. Lee et al., J. Mater. Chem. C, 2013, 1, 4599-4604). The strong electron-accepting ability of oxadiazole/triazole and the electron-donating ability of phenoxazine lead to small ΔEST. Oxadiazole-based compounds PXZ-OXD and 2PXZ-OXD showed green emission, while the triazole-based ones PXZ-TAZ and 2PXZ-TAZ exhibited sky-blue emission. The donor–acceptor–donor-type compounds 2PXZ-OXD and 2PXZ-TAZ showed more efficient TADF and higher photoluminescence quantum yields (PLQYs) than the donor–acceptor-type molecules PXZ-OXD and PXZ-TAZ. When doped into a host material, the 2PXZ-OXD displayed a high PLQY of 87%. The contributions from the prompt and delayed

components to the PLQY (87%) were estimated to be 76.6% and 10.4%, respectively. Time-resolved photoluminescence measurements of the doped film showed that the delayed component increased with increasing temperature from 8K to 200K, suggesting that 2PXZ-OXD showed TADF. 2PXZ-OXD thus effectively converts T1 states into S1 states and realizes the high PLQY. From the fluorescence and phosphorescence spectra measured at 8K, ?EST of 2PXZ-OXD was determined to be 0.15 eV. To evaluate the potential of 2PXZ-OXD in OLEDs, we fabricated an OLED containing 2PXZ-OXD as a green emitter. The OLED exhibited an EQE of 14.9%, which exceeds those obtained with conventional fluorescent emitters. This high EQE comes from the efficient generation of TADF in 2PXZ-OXD.

9137-33, Session PS2

Colloidal quantum dot lasers on ultra-thin glass for flexible photonics

Caroline N. Foucher, Benoit Guilhabert, Nicolas Laurand, Martin D. Dawson, Univ. of Strathclyde (United Kingdom)

Colloidal quantum dots (CQDs) are promising nanomaterials for the fabrication of photonic devices. They have high photoluminescence efficiency and broad absorption spectra. Furthermore, they are compatible with solution processing techniques and their emission can be tuned over a wide range of wavelengths by changing their size and/or composition. Consequently, CQDs are being used in devices and applications that include bio-imaging, displays, LEDs and lasers.

Interest in flexible photonic devices, which are not constrained by rigid substrates but can be bent or flexed, has been growing recently. So far, thin films of (what can be) solution-processed light-emitting materials, e.g. CQDs, are combined with entirely polymeric substrates and structures to enable such devices. Here, we introduce a new format of flexible CQD laser that does not rely solely on polymers but uses also ultra-thin glass membranes. Glass offers advantageous characteristics compared to polymers in terms of thermal stability, resistance to UV light, transparency and gas barrier properties whilst maintaining mechanical-flexibility if it is made thin-enough (<100 μm). While a limited number of optical elements utilising thin glass have been recently reported for display applications, this is to our knowledge the first demonstration of a laser on flexible glass.

The CQD lasers reported here are optically pumped vertical–emitting devices based on a distributed feedback cavity. The structure consist of a thin film of CdSe/ZnS CQDs deposited on top of a <50-μm-thick nanostructured epoxy layer, itself lying on a 30-μm-thick glass membrane. Gain-switched lasers of 5 ns pulse duration emitting at 610 nm with <500-μJ/cm2 average threshold are demonstrated. The mechanical flexibility of the devices is also tested: bending the laser enables a continuous and reproducible wavelength tuning over 18 nm.

9137-34, Session PS2

Organic semiconductor distributed feedback laser as excitation source in Raman spectroscopy using free-beam and fibre coupling

Xin Liu, Sergei Lebedkin, Karlsruher Institut für Technologie (Germany); Timo Mappes, Carl Zeiss AG (Germany) and Karlsruher Institut für Technologie (Germany); Sebastian Köber, Christian Koos, Manfred M. Kappes, Uli Lemmer, Karlsruher Institut für Technologie (Germany)

Enabled by the broad spectral gain and the efficient energy conversion in the active material, organic semiconductor lasers are promising for spectroscopic applications and have been recently applied for high resolution absorption and transmission spectroscopy. Relying on distributed feedback (DFB) resonators, it allows the simple fabrication of laser devices with narrow bandwidth and low laser threshold, both being favorable for Raman spectroscopy. Here, we present the application of organic semiconductor DFB lasers as excitation sources in Raman spectroscopy via free space as well as fibre coupling.

The organic semiconductor tris(8-hydroxyquinoline) aluminum (Alq3) doped with the laser dye 4-(dicyanomethylene)-2-methyl-6-(p-dimethylaminostyryl)-4H-pyran (DCM) forms a very efficient and stable Foerster energy transfer system and was chosen as the active gain material for our laser devices. To match the Alq3:DCM red emitter, we applied a glass grating with a one dimensional corrugation period of 400 nm as the second order distributed feedback resonator. After the cleaning procedure, Alq3 and 2.3 % by weight of DCM were thermally co-evaporated in a high vacuum chamber with a thickness of 210 nm onto the glass grating substrate. An encapsulation was achieved by bonding a glass lid through ultraviolet curable optical adhesive. The organic DFB laser exhibits a slope efficiency of 7.6 % and a laser threshold of 28 nJ pulse-1 at an pump area of 540 μm ? 425 μm. The life time of the organic semiconductor laser is an issue in general and especially for Raman measurements requiring long integration times. We thus investigated the laser degradation characteristic through monitoring the excitation power while maintaining the pump pulse energy constant. The laser emission from one pumped spot of the organic semiconductor laser decays only 10 % within 30 min at a pump pulse energy of 3.2 μJ pulse-1 and a high repetition rate of 10 kHz. This stability of one single pumped spot is sufficient to meet the demands of Raman spectroscopy.

In the free space configuration, the laser emission of an encapsulated organic semiconductor laser is guided directly into an inverted confocal microscope. Employing this configuration we investigated the Raman spectra of sulfur (S8) and cadmium sulfide (CdS). The collected Raman signals were analyzed and recorded by a spectrograph connected to a liquid-nitrogen-cooled CCD-Camera. Furthermore, we fabricated a spectrally tunable organic semiconductor DFB laser to optimize the Raman signals for a given optical filter configuration. We show that the proposed organic DFB laser can replace a bulky helium-neon (He-Ne) gas laser in this Raman spectroscopy setup.

In the fibre coupling configuration, the organic laser is guided into a confocal microscope through a multi-mode optical fibre with a coupling efficiency of 70 %. Our novel fibre-coupled organic laser provides a portable laboratory Raman system. Using rhodamine 6G as analyte we verified the efficiency of the fibre-coupled organic semiconductor DFB laser in surface-enhanced Raman scattering (SERS) measurements.

We foresee the application advantages due to the high tunability of organic semiconductor lasers. Furthermore, integration of organic lasers in lab-on-chip devices could enable miniaturized Raman detection schemes for biomedical analysis.

9137-35, Session PS2

Enhancement of power conversion efficiency in solution processed organic photovoltaic devices by embedded plasmonic gold-silica core-shell nanorods

Xiaoyan Xu, Terence K. S. Wong, Xiao Wei Sun, Nanyang Technological Univ. (Singapore)

The active layer thickness of bulk heterojunction (BHJ) organic photovoltaic (OPV) devices is typically of order 100nm because the exciton diffusion length is much shorter than the absorption length in organic semiconductors. As a result, enhancement of light absorption is crucial to increase the power conversion efficiency (PCE) of OPV devices. In this presentation, we demonstrate the enhancement of light absorption in both solution processed polymer-fullerene and small molecule-fullerene BHJ OPV devices by incoporating gold-silica (Au-SiO2) nanorods in the active layer. The polymers studied include regioregular poly(3-hexylthiophene) (P3HT) and the low bandgap polymer, poly[2,6-(4,4-bis-(2-ethylhexyl)-4H-cyclopental[2,1-b:3,4-b']dithiphene)-alt-4,7-(2,1,3-benzothhiadiazole)] (PCPDTBT). For the small

molecule-fullerene device, 7,7'-(4,4-bis(2-ethylhexyl)-4H-silolo[3,2-b:4,5-b']-dithiophene-2,6-diyl)bis(6-fluoro-4-(5'-hexyl-[2,2' bithiophene]-5-yl)benzo[c][1,2,5]thiadiazole) (p-DTS(FBTTh2)2) was used. Each of these donor materials was blended with donor such as [6,6]-phenyl-C61-butyric acid methyl ester (PC60BM) or [6,6]-phenyl-C71-butyric acid methyl ester (PC70BM) at a fixed weight ratio in either chlorobenzene or dichlorobenzene with the processing additive 1,8 octanedithiol. Au-SiO2 core-shell nanorods synthesized by a seed-mediation method were added to the blend solution at different percentage of the total donor/acceptor weight. The Au-SiO2 nanorods had a typical inner core and a silica shell. The sizes of Au-SiO2 nanorods for polymer-fullerene OPV and small molecule-fullerene OPV are different. Au-SiO2 nanorods for polymer-fullerene OPV have the length and diameter of core around 109 nm and 34 nm respectively and silica thickness around 10 nm while Au-SiO2 nanorods for small molecule-fullerene OPV have the length and diameter of core around 92 nm and 40 nm respectively and silica thickness around 9 nm. Their two localized surface plasmon resonance peaks overlap well with the absorption spectra of the donor:acceptor blends. OPV devices were fabricated by spin coating the active layer onto poly(3,4-ethylene-dioxythiophene):poly(styrenesulph onate) (PEDOT:PSS) on indium tin oxide glass followed by evaporation of the calcium/aluminum cathode. Under AM 1.5G illumination at 100mWcm-2, the optimized ITO/PEDOT:PDD/P3HT:PC71BM/Ca/Al and ITO/PEDOT:PSS/PCPDTBT:PC71BM/Ca/Al devices with 1 wt% Au-SiO2 nanorods showed a PCE improvement relative to control device of 9.3% (to 3.42%) and 20.8% (to 4.11%) respectively. For the ITO/PEDOT:PSS/p-DTS(FBTTh2)2:PC71BM/Ca/Ag device, the PCE improvement relative to control was 24.2% (to 8.01%). Additional optical characterization was carried out to investigate the absorption enhancement mechanism and the role of the nanorods in facilitating light trapping within the active layer.

9137-36, Session PS2

Probing bulk transport and the energetic disorder of amorphous semiconductors in a thin-film transistor configuration

Wai Yu Sit, Cyrus Y. H. Chan, Shu-Kong So, Hong Kong Baptist Univ. (Hong Kong, China)

Thin film transistors (TFTs) can be used to determine the bulk-like mobilities of amorphous semiconductors. We investigated different organic hole transporting layers (HTs), e.g. Spiro-TPD, 2TNATA, NPB, TPD and TCTA, which are commonly used in organic light-emitting diodes (OLEDs). With a non-polar polymer, polystyrene (PS) as gate dielectric layer, the TFT mobilities of these hole transporters are found to be in good agreement with the time-of-flight (TOF) mobilities. On the other hand, when SiO2 was used as the gate dielectric layer, the TFT mobilities are 1-2 orders lower than that of TOF mobilities. We also performed temperature dependence experiments between 200K and 400K. The interfacial energetic disorder was around 74meV when PS was used as the gate dielectric. However, when SiO2 was used, the energetic disorder was enlarged to around 90meV. Instead of using hole transporting layers, we further tested host materials of OLEDs such as BAnF derivatives for holes and electrons transport. We further investigate the material consumption in TFTs by performing thickness dependence measurements of NPB in TFTs using PS as the gate dielectric. Following the analysis model presented by Dinelli et al, we found that only 8nm of NPB is sufficient for TFTs to achieve TOF mobilities. TOF technique requires 2?m to 10?m in order to obtain a clear transit time signal. However, OTFT needs only 8nm to complete the film and achieve TOF mobilities. This study can have wide applications in the transport characterization of amorphous organic semiconductors especially reducing the material consumption.

9137-37, Session PS2

Subbandgap absorption and photoconductivity in polymer-fullerene bulk heterojunction

Mark Khenkin, Vladimir Malov, Lomonosov Moscow State Univ. (Russian Federation); Alexey R. Tameev, A.N. Frumkin Institute of Physical Chemistry and Electrochemistry (Russian Federation); Andrey G. Kazanskii, Lomonosov Moscow State Univ. (Russian Federation)

An improved understanding of basic processes in a polymer bulk heterojunction (BHJ) initiated upon irradiation is essential for progress in organic photovoltaics. Absorption in the subbandgap range is very weak; nevertheless, it is of fundamental importance for revealing the processes of generation of charge carriers in a donor-acceptor blend of the bulk heterojunction. Researches in BHJ solar cell structures performed so far by photothermal deflection spectroscopy and photoconductive spectroscopy have left many questions regarding the optical transitions that lead to the absorption in this spectral range. This is partly the result of the controversy within the scientific community over how to explain, understand and describe the photophysics and photochemistry of such materials.

In the report, we present experimental data on absorption in subbandgap spectral range measured by constant photocurrent method (CPM) and spectral dependences of photoconductivity for various electron donor polymers (P3HT, PCDTBT, PTB7) and their BHJ blends with the fullerene derivative PC71BM, an electron acceptor. The mixing of the conjugated polymer and PC71BM results in increase of photoconductivity by one order of magnitude and shift of photoconductivity spectrum edge toward low energy. In visible range, the blend of PTB7 and PC71BM possesses the highest photoconductivity among all the others BHJ under study. For each BHJ, the spectra of photoconductivity and absorption measured by CPM were found to be somewhat different. The finding indicates that the photoconductivity spectra of the donor–acceptor blends are limited in use to obtaining their absorption spectra in subbandgap range. The issue of using absorption spectrum of BHJ in subbandgap range to derive information about their band structure is considered.

9137-38, Session PS2

Light-controlled vector polyphotochromism

Irakli Chaganava, Institute of Cybernetics (Georgia); George Kakauridze, Institute of Cybernetics (Georgia); Barbara N. Kilosanidze, Institute of Cybernetics (Georgia); Yuri Mshvenieradze, Institute of Cybernetics of the Georgian Technical University (Georgia)

Phenomenon of vector polyphotochromism was observed in some high-efficient polarization-sensitive materials dependent on the radiant exposure when material was illuminated with linearly polarized actinic light. The phenomenon has purely vector nature, since under probing by unpolarized light, the transmission spectra of the irradiated and unirradiated area of the material are practically identical. However, an essential change in the transmission spectrum of the material was observed by placing the irradiated area between crossed polarizers when the orientation of the axis of induced anisotropy was of 45 degrees relative to the axes of the polarizers. The dispersion of photoanisotropy was studied at different exposure values. Kinetic curves of the photoanisotropy were obtained for wavelength of 532 nm and 635 nm of probing beam for different values of exposure (30, 60 and 250 J/cm?) with linearly polarized actinic light (457 nm). The dispersion curves of the photoanisotropy were obtained for these values of exposure showing an anomalous behavior for exposures above of 30 J/cm?. This phenomenon was observed in specially

synthesized organic materials based on azo dyes introduced in a polymer matrix. We discuss path for enhancement of this phenomenon. An explanation of this phenomenon is presented based on chromatic polarization. The difference between optical densities was obtained for polarized light with a wavelength of 532 nm and 635 nm at different exposures, which makes the prospect the dynamic polarization spectral filters controlled by light and the spectrally selective dynamic polarization holographic gratings to be created.

9137-39, Session PS2

Computational design of small organic dyes with strong visible absorption by controlled quinoidization of the thiophene unit

Sergei Manzhos, National Univ. of Singapore (Singapore); Wei Han Tu, Anderson Junior College (Singapore); Yi Yin Tan, Raffles Girls' School (Singapore)

Availability of small organic dyes with strong solar absorbance would go a long way towards the development of economically viable dye-sensitized solar cells. We present a computational Density Functional Theory (DFT) and Time-Dependent DFT (TD-DFT) study of possibilities of rational design of small dyes with a significant solar absorbance.

We first show that small thiophene-containing molecules can achieve a stronger solar absorbance when the conjugation order is changed and show that this is due to the interaction of the thiophene with an electron withdrawing group. We establish a correlation between the change in the BLA (bond length alternation) and the amount of redshift of the absorption spectrum achieved by changing either functional groups or the conjugation order. The strongest BLA change (from about -0.03 to about +0.1) from aromatic to quinoid character of the thiophene unit is achieved by changing the position of the methine unit separating the thiophene from the cyanoacrilyc anchoring group. We show that it is possible to achieve the quinoidization and a similar magnitude of the redshift by sidechain functionalizations.

We then present rational design of phenothiazine dyes by controlled quinoidization of the thiophene unit by choosing the electron withdrawing group. We systematically study the effect of several functional groups including pseudo- and (for the first time) super- halogens. A super-halogen unit induced the strongest quinoidization (in terms of BLA) of all functional groups tried.

Given the known sensitivity of the BLA of the thiophene unit and of the absorption spectrum of molecules with a significant charge transfer character in the corresponding electronic transition to longe-range effects, we compared results obtained with the most commonly used B3LYP functional and the range-separated CAM-B3LYP. CAM-B3LYP provide a wider range of BLA changes and a better match to the experimental spectrum of the reference dye, yet the trends computed with both functionals were similar.

As a result of this study, we propose a new dye where a fumaronitrile unit induces an increase in the bond length alternation and a concurrent red shift in the absorption spectrum vs. the parent dye 3-(5-(3-(4- (Diphenylamino) phenyl) -10-octyl-10H-phenothiazin-7-yl) thiophen-2-yl)-2-cyanoacrylic acid. The visible absorption peak is predicted at 520 nm, in CH2Cl2 vs. 450 nm for the parent dye. The LUMO and HOMO levels of the new dye are suitable for injection into TiO2 and regeneration by available redox shuttles, respectively.

9137-40, Session PS2

P3HT:PCBM:pentacene inverted polymer solar cells with roughened Al-doped ZnO nanorod array and photoelectrochemical treatment

Hsin-Ying Lee, Hung-Lin Huang, National Cheng Kung Univ. (Taiwan)

The organic solar cells have attracted much attention because they possess many advantages, including low cost, lightness, flexibility, easy fabrication, and large area. In this work, the P3HT:PCBM:pentacene (1:0.8:0.065 by weight) inverted polymer solar cells with roughened Al-doped ZnO (AZO) nanorod array were fabricated. The pentacene doping could modulate the hole and electron mobility in the active layer and the optimal hole-electron mobility balance (uh/ue=1.000) measured by using the space-charge-limited current (SCLC) method was achieved as the pentacene doping ratio of 0.065 by weight. The 100-nm-long AZO nanorod arrays were formed as the carrier collection layer and the carrier transportation layer of the inverted polymer solar cells using the combination technique of the laser interference photolithography method and the wet etching process. Because the AZO nanorod array was prepared using the wet etching process, more defects could be formed on the sidewall surface of the AZO nanorod. In this work, the photoelectrochemical (PEC) treatment was used to passivate the surface of the AZO nanorod. According to the XPS spectra, the Zn(OH)2 was formed on the surface of the PEC-treated AZO nanorod, which could reduce the carrier recombination path in the inverted polymer solar cells. Compared with the inverted polymer solar cells without PEC treatment, the short circuit current density and the power conversion efficiency of the P3HT:PCBM:pentacene (1:0.8:0.065) inverted polymer solar cells with roughened AZO nanorod array and photoelectrochemical treatment were increased from 14.56 mA/cm2 to 15.26 mA/cm2 and 5.45% to 5.89%, respectively. The enhancement in the performance of the inverted polymer solar cells with PEC treatment could be attributed to that the PEC treatment could effectively decrease the defects on the surface of the AZO nonorod.

This work was supported from the National Science Council of Taiwan and Ministry of Economic Affairs of the Republic of China under contract no. TDPA 101-EC-17-A-08-S1-204.

9137-41, Session PS2

Bistable memory device based on DNA biopolymer nanocomposite

Yi-Tzu Lin, Ting Yu Lin, Yu-Chueh Hung, National Tsing Hua Univ. (Taiwan)

Deoxyribonucleic acid (DNA), as one kind of biopolymer, has recently emerged as an attractive optical material, showing promise in making versatile optoelectronic devices. In the present study, we report the fabrication and characterization of DNA biopolymer nanocomposite with tunable conductivities and the application in bistable memory device. DNA nanocomposite consisting of DNA biopolymer and silver nanoparticles is synthesized using a phototriggered method. The nanocomposite exhibits tunable conductivities when exposed to UV light under different periods of time. The electrical conductivity is suggested to be dependent on the quantity and the distribution of silver nanoparticles formed in DNA biopolymer. In addition, a memory device based on DNA biopolymer nanocomposite is demonstrated. The operation of different conductivity states can be adjusted by the concentration of nanoparticles. The device shows bistability of current, and presents a stable write-read-erase cycle. Detailed performance of the DNA-based memory device will be presented and discussed.

9137-42, Session PS2

Transparent superhydrophobic thin film composed of nanoparticles and bio-based polymer and transparent slippy liquid infused surface with antifrosting

Kengo Manabe, Shingo Nishizawa, Seimei Shiratori, Keio Univ. (Japan)

Studies about anti-frosting have been researched as the application of superhydrophobicity, however it is generally accepted that superhydrophobic surface have low anti-frosting property because large surface area by micro/nano topography provides a lot of spots where frost can form. On the other hand, Slippy Liquid Infused Surface (SLIPS) can repel various liquid and have ability to prevent frost formation by slipping fog. SLIPS film which can prevent frost formation needs high transmittance as frost is caused by differences of temperature between opposite sides on glass windows and lens. The film is fabricated by dropping lubricant oil on superhydrophobic film. The superhydrophobic film as an underlayer of lubricant oil needs transparence to fabricate it. However the superhydrophobic film has relief structure as mentioned-above and causes to decrease transmittance. Therefore, we firstly fabricated anti- reflective (AR) film with min. surface roughness to deliver superhydrophobic performance by Layer-by-Layer (LBL) method. The development of multilayer thin films with nanopores containing biomolecules has attracted much attention in material and surface science as one of the optical applications and surface wettability control via LBL (Layer-by-Layer) self-assembly method. Especially, the previous studies indicated that films composed of nanoparticle or nanofibers can demonstrate low refractive index. Also, chitin nanofibers (CHINFs) have attracted much attention because of their high mechanical strength. The shells of crustaceans are expected to be particularly useful for materials applications, because they are made from mineral salts, protein, and chitin; it is known that mineral salts can be removed using HCl, and proteins can be removed using NaOH. The CHINFs surface is transformed from chitin to chitosan by deacetylation, which results in a positive charge on the CHINFs, due to the presence of amine groups. In this study, anti-frost film with high transmittance was fabricated by improvement of hydrophobic underlayer of SLIPS. We fabricated films with low refractive index and antireflective property by using LBL and functionalized it by fluoroalkylsilane via gas phase method as the underlayer. The antireflective film with nanopores composed of nanoparticle and bio-based polymer by LBL showed that the highest transmittance was 97% and the lowest refractive index was 1.20. After adding hydrophobic performance by gas-phase process, the film demonstrated that the highest transmittance was 97%, the lowest refractive index was 1.23 and the water contact angle is 153°. In addition, we fabricated transparent SLIPS film by putting a drop of lubricant oil (Krytox GPL 103) on the films and the highest transmittance of this SLIPS film was 98%. Also, anti frosting test was conducted by comparing the glass substrate, the LBL superhydrophilic film, superhydrophobic film and SLIPS film. This result showed that the transparent SLIPS film easily can slip fog and prevent frost formation because of small thermal change of the films and it would be applied to medical devices such as endoscopic camera lens.

9137-43, Session PS2

Optical Properties of Type-II Nanorods: ZnO/PVK Coaxial Heterostructure

Chi-Pin Chiu, Wei-Hsuan Lai, Shih-Shou Lo, Feng Chia Univ. (Taiwan)

Inorganic-organic hybrid type-II nanorods heterostructure had been fabricated using ZnO nanorods and poly(N-vinylcarbazole)(PVK). The structural and optical properties of the ZnO/PVK heterostructure were detail investigated. The scanning electron microscopy (SEM) image of ZnO/PVK displayed certain amounts of PVK can be seen clearly on the ZnO surface. An obvious peak located at 490 cm-1 was found in the Raman spectra due to the effectively covalence bond between ZnO and PVK. A broad blue emission band at wavelength 420 nm and visible emission at 560 nm was observed in the room temperature photoluminescence spectra. When the heterostructure was annealed at 350 oC 1h, the blue emission band 420 nm disappeared and a blue-shift visible emission located at 520 nm was obtained because the organic shell layer PVK had been burned out. The blue-shift of visible emission can be attributed to the effectively bond of ZnO and PVK. The physical mechanism of the as-synthesized nanorods was discussed. The new inorganic-organic hybrid nanostructure has the potential application for light-emitting diodes, photovoltaic and optical sensors.

9137-44, Session PS2

In-depth analysis of solvent effects on bulk heterojunction solar cell performance

Reihaneh Zohourian Aboutorabi, Mojtaba Joodaki, Ferdowsi Univ. of Mashhad (Iran, Islamic Republic of) and Sun Air Research Institute (Iran, Islamic Republic of); Kosar Shahbazi, Sun Air Research Institute (Iran, Islamic Republic of)

In order to fabricate high performance polymer solar cells, donor:acceptor mixture must be prepared using a proper solvent. Since solubility of C60, as a truly cost effective acceptor, is very limited in common solvents, finding a suitable solvent can enhance the Poly(3-hexylthiophene):C60 (P3HT:C60) based solar cell performance in terms of short circuit current (JSC), fill factor (FF) and consequently power conversion efficiency (PCE). The formation of C60 aggregates and P3HT crystallinity depend on the selection of proper solvent. These two factors influence several electrical and optical properties of the cell. In this work, 1,2-Dichlorobenzene (the most common solvent) and a mixture of 1-Chloronaphtalene and Chlorobenzene (Cl-naph:CB) and 1-Methylnaphtalene Chlorobenzene are chosen as two alternative solvents for preparing P3HT:C60 films and simulation is performed to understand how these solvents influence the solar cell behavior. The performance of a P3HT:PCBM cell prepared with ODCB is also considered for comparison. A numerical model is employed to simulate the operation of different cells mentioned. In order to model the finite slope of I-V curve in large forward bias, the effect of voltage dependent series resistance is also considered. The model accepts several input parameters including exciton generation rate (G), the difference between P3HT HOMO and C60 LUMO energy levels (Eg), electron and hole mobility (?n and ?p), exciton mobility, electron-hole pair distance (a), exciton decay rate (kf), static interfacial dielectric constant (?r), active layer thickness, temperature, etc. To determine the estimated values of unknown input parameters, an optimization algorithm is used. Firstly, the code input parameters' possible ranges of variation are determined using calculations based on others' experimental researches. Then, an optimization algorithm is performed to find the value of each parameter, fitting the cell I-V curves. The results are compared with conventional solar cell model and it is shown that the traditional model may not be an accurate analysis tool to understand solar cell behavior. The series resistance (Rs) and shunt resistance (Rsh) can be estimated using current-voltage data; these two parameters can be used to intuitively understand how each solvent may affect the cell performance. Simulation results indicate that a suitable solvent mainly improves the cell performance by changing 3 determinative parameters which are G, ?n and ?p; It is shown that every 20% increase of G would increase JSC by almost 20%. This amount of increase could be achieved using a proper solvent. The solvent may also affect other parameters such as a and kf. Although parameters such as Eg and ?r are very crucial in determining PCE, they cannot be effectively improved changing the solvent. It is reported that the cell prepared by Cl-naph:CB performs better than other cells. Considering our results, this can be attributed to its larger G, ?n and ?p. It also

has the least Rs among all other cells (which is caused by its higher mobility-carrier density product). This work gives experimentalists an idea of how they should select a solvent. The results can also be generalized to find a proper solvent for other active layer materials.

9137-45, Session PS2

Synthesis of high-surface-area titanium dioxide by sol-gel process for DSSC

Ari H. Ramelan, Sayekti Wahyuningsih, Suharyana Suharyana, G. Juliana, A. R. Khoirunisa, R. Suryana, E. Pramono, Univ. Sebelas Maret (Indonesia)

The semiconductor layer is a very important part of the dye-sensitized solar cell as it gives a high surface area for dye adsorption which gives rise to high currents. Therefore, different synthesis routes need to be explored to try and optimize this component of the DSSC. The work presented in this paper is the characterization of TiO2 nanocrystals that have been synthesized for application as the working electrode for the dye-sensitized solar cells. This synthesis has good potential for scaling-up DSSC manufacture as no pressure is required and there is good control of the particle size and crystalline structure due to the low reactivity of the titanium tetrachloride (TiCl4) precursor used. In the present research work we report the synthesis of TiO2 nanoparticles by Sol-Gel technique. The characterization of particles was carried out by XRD, SAA, SEM and TEM techniques. The importance and applications of these nanoparticles for solar cells are also discussed in this work.

In this work, titanium dioxide (TiO2) nanoparticles having enhanced surface area were synthesized by mixing of 6 gram of Pluronic PE 6200 and 76 ml methanol with vigorous stirring for 30 minutes to initiate micelle structure. Then 3.5 ml of TiCl4 was slowly added the solution under stirring for 30 minutes. The solutions were then aged for 7 days at 40 - 45oC in a furnace until dry gel was formed. The TiO2 dry gels were then calcined at 600oC for 4 hours with a heating rate of 5oC/minute to remove the block copolymer and promote crystallization.

A fine mesoporous structure was formed for as-prepared TiO2 after calcination at 400?C and the average pore diameter was about 8 nm. The porous TiO2 products possess mixing phases of anatase and rutile. Phase transformation from anatase to rutile occurred when the samples were calcined. The phase transition temperature is sensitive to the silicon content. The particle size of ? 45 nm remained constant upon calcinations from 400 to 800? C. The specific surface area was increased up to 65% compared to regular TiO2 samples that were prepared by the similar sol-gel procedure. The porous TiO2 nanostructures exhibited enhanced photocatalytic performance to decompose methylene blue under UV irradiation.

9137-46, Session PS2

High-transmittance and barrier properties of thin-film encapsulations for top-emission organic light-emitting diodes

Yong-Qiang Yang, Yu Duan, Xiao Wang, Ya-Hui Duan, Ping Chen, Dan Yang, Feng-Bo Sun, Kai-Wen Xue, Jilin Univ. (China)

This paper reported a room-temperature thin film encapsulation (TFE)process based on low temperature atomic layer deposition Al2O3 layer for top-emission organic light-emitting devices (TEOLEDs).The barrier characteristics of H2O-based O3 based Al2O3 films were investigated. O3-based Al2O3 TFE showed lower WVTR of 8.7?10-6 g/m2 day and longer continuous operation lifetime of 2 folds compared to the device of with H2O-based Al2O3 TFE under identical environmental and driving conditions. Furthermore, it was found that the refractive index of O3-based Al2O3 was lower to H2O-based Al2O3., substantially increased efficiencies are expected for metal based top electrodes. This factor would be still a desired improvement for optimizing enhanced light extraction.

9137-47, Session PS2

Top-emitting OLED encapsulated with hybrid organic-inorganic structure formed by ALD/MLD method

Xiao Wang, Yu Duan, Yongqiang Yang, Jilin Univ. (China)

We investigate the optical and barrier properties of thin-film encapsulations (TFEs) for top-emitting organic light-emitting diodes (TOLEDs). TFEs were fabricated by stacking multiple pairs of inorganic and organic layers, the inorganic and organic moisture barrier layers were prepared by Atomic layer deposited (ALD) Al2O3 and molecular layer deposition (MLD) alucone,respectively.

Here, Alucone MLD using trimethylaluminum (TMA) and ethylene glycol (EG) is employed together with Al2O3 ALD using TMA and H2O to deposit films. ALD Al2O3 coatings are efficient barriers against gases and vapors. Al2O3 coatings are, however, brittle and straining them to generate defects that impair barrier properties. Alucone layers can improve the smooth of ALD-grown Al2O3film. Furthermore, ALD/MLD alloy films can be deposited that have an adjustable organic-inorganic composition. Therefore, these alloys have tunable properties that may be useful for designing light out-coupling for TOLEDs. In this study,, by carefully adjusting the thickness of organic-inorganic films, we can get an optimized light extraction of TOLEDs. The ALD/MLD alloy barrier film maintained not only the high moisture barrier strength but also the good optical performances.

9137-48, Session PS2

Physical properties and application of type-II nanorods: ZnO/PVK coaxial heterostructure

Wei-Hsuan Lai, Chi-Fang Chiu, Shih-Shou Lo, Feng Chia Univ. (Taiwan)

Type-II semiconductor have both valence and conduction bands of the core that are either both lower or higher than those of the shell. The spatial separation of charge carrier and confinements leads to several characteristic differences from type-I semiconductor. Similar to staggered quantum wells, photoexcitation of type-II semiconductors results in charge separation of one type charge carrier is the core and the opposite sign charge carrier in the shell. Type-II semiconductor also provide interesting opportunities for tuning carrier-carrier interactions in structures, which is an important capability for such application as lasing [1], nonlinear optics and photovoltaics types of type-II semiconductor [2-3].

Inorganic materials offer the potential for a wide range of electronic properties (enabling the design of metals, semiconductor, and insulator), dielectric, substantial mechanical hardness, and thermal stability. However, organic molecules, on the other hands, can provide high fluorescence efficiency, large polarizability [4], plastic mechanical properties, ease of processing, and structural diversity.

Today, organic-inorganic hybrid materials represent a new class of materials that may combine desirable physical properties characteristic of both organic and inorganic components within a single composite. Organic-inorganic hybrid nanomaterials have recently attracted great attentions due to the appealing possibility of synergetic properties exploiting the best of both components. In particular, blends of semiconductor nanocrystals and conjugated polymers outstand as candidates to obtain materials tailored for applications in, light-emitting devices and photovoltaics.[5-6] In comparison to organic emitters, semiconductor nanostructure have a number of advantages such as high photostability, broad spectral range of light absorption, and narrow emission line width. The

conduction properties of closely packed NC films are on the other hand poor, making inefficient the electrical pumping of nanostructure. An evident approach to overcome this difficulty is to produce a composite material where the nanostructures provide their efficiency luminescence and a conducting polymer provides efficienct charge conduction. From a technology view-point, such an organic-based nanocomposite material offers the potential for efficient which is compatible with the colloidal chemistry of nanocrystal. However, the effective design of tailored optoelectronic properties remains challenging because the photophysics of the organics-inorganic hybrid materials, which include charge separation and Dexter and Foster energy energy transfer.

In this study, we designed a new inorganic-organic (ZnO-PVK) hybrid heterostructure (Type-II) nanorods. The structural and optical properties of as-synthesized nanorods were detail investigated.

9137-49, Session PS2

AZO electrodes deposited by atomic layer deposition for OLED fabrication

Benoit Dugrenil, Lab. d'Analyse et d'Architecture des Systèmes (France); Isabelle Séguy, Lab. d'Analyse et d'Architecture des Systèmes (France) and Univ. de Toulouse (France); Hsin-Ying Lee, National Cheng Kung Univ. (Taiwan); Thierry Camps, Lab. d'Analyse et d'Architecture des Systèmes (France); Yu-Chang Lin, National Cheng Kung Univ. (Taiwan); Jean-Baptiste Doucet, Lab. d'Analyse et d'Architecture des Systèmes (France) and Univ. de Toulouse (France); Ying-Shuo Chiu, National Cheng Kung Univ. (Taiwan) and Institute of Microelectronics (Taiwan); Ludovic Salvagnac, Elena Bedel-Pereira, Lab. d'Analyse et d'Architecture des Systèmes (France) and Univ. de Toulouse (France); M. Ternisien, Univ. Paul Sabatier (France); Ching-Ting Lee, National Cheng Kung Univ. (Taiwan) and Institute of Microelectronics (Taiwan); Veronique Bardinal, Lab. d'Analyse et d'Architecture des Systèmes (France) and Univ. de Toulouse (France)

Transparent conducting oxide (TCO) films are widely used as electrodes in various optoelectronic devices, including flat panel displays (LCDs and OLED), light emitting diodes and photovoltaic devices. The dominant material used as TCO film is Indium Tin Oxide (In2O3:Sn, ITO), due to its low resistivity and high transmittance in the visible spectral range [1]. However, the cost of using indium is high due to its scarce characteristic and it can degrade the performance of OLEDs due to indium diffusion into the organic layers [2]. Therefore, AZO (ZnO:Al) is a favorable material as an alternative TCO owing to its low cost, nontoxic, and relative abundance. In this work, we present a comparative study of optimized AZO electrodes deposited by Atomic Layer Deposition (ALD) [3] with commercial ITO in terms of structural, optical and electrical properties. Furthermore, AZO-based OLEDs are shown to present a much lower threshold voltage as well as higher emission efficiency than ITO ones. Finally, we have investigated the interest of a localized micro-scale electrode patterning to further improve current injection in these devices.

[1] Y. Igasaki, H. Kanma, Appl. Surf. Sci., vol. 169-170, 508 (2001)

[2] F. So and D. Kondakov, Adv. Mater., 3762–3777, 22 (2010)

[3] H.S. Lee et al, Journal of Applied Physics Letters, vol. 107; 1 (2010)

9137-50, Session PS2

Amplified spontaneous emission of glass forming DCM derivatives in PMMA films

Aivars Vembris, Univ. of Latvia (Latvia); Elmars Zarinsh, Riga Technical Univ. (Latvia) and Univ. of Latvia (Latvia); Valdis Kokars, Riga Technical Univ. (Latvia)

One of the well-known red light emitting laser dyes is 4-(dicyanomethylene)-2-methyl-6-(4-dimethylaminostyryl)-4H-pyran (DCM). Amplified spontaneous emission (ASE) had been widely investigated of DCM molecules or its derivatives in polymer or low molecular weight matrix. The main issue for these molecules is aggregation which limits doping concentration in matrix. Lowest ASE threshold values within concentration range of 2 and 4 wt% were obtained.

In this presentation we will show ASE properties of three original DCM derivatives in poly(N-vinylcarbazole) (PVK) at various concentration. Two of the derivatives are the same DCM dye with replaced butyl groups at electron donor part with bulky trytiloxyethyl groups and with (DWK-1) and without (DWK-1TB) replaced butyl group at pyran part by terc-butyl group. These groups do not influence electron transitions in the dye but prevent aggregation of the molecules. Third derivative (DWK-2) consists of two equal donor groups with the attached trytiloxyethyl groups.

Photoluminescence quantum yield (PLQY) almost not changing on DWK-1 and DWK-1TB concentration up to 10wt%. At the same time DCM molecules PLQY starts to decrease from 1 wt% and at 10 wt% it is three times less in comparison with 1 wt% sample. Bulky trytiloxyethyl groups prevent aggregation of the molecules thus decreasing interaction between dyes and numbers of nonradiative decays.

Increases of dye density in matrix without lose in PLQY results in low ASE threshold energy. Two orders of magnitude lower ASE threshold energy was obtained in the sample with DWK-1 and DWK-1TB in comparison to the lowest threshold energy of the sample with DCM molecules.

Influence of the molecule structure on PLQY and ASE threshold value in the doped thin films with various concentrations will be discussed.

Acknowledgment:

This work has been supported by the European Social Fund within the Project No. 1DP/1.1.1.2/13/APIA/VIAA/018.

9137-51, Session PS2

Surface potential, ionization energy, and morphology of organic layer of indandione derivatives with various thickness

Raitis Grzibovskis, Aivars Vembris, Univ. of Latvia (Latvia)

More often in different electronical devices organic compounds are used instead of inorganic due to lower cost and easier production. In most cases organic layer thickness in the device is up to 100nm. Impact of the interface between electrode and organic layer become important at such thickness of active layer. This can lead to the shift of ionization energy of compounds and values obtained from bulk layers can no more be used. It is important to evaluate the effect of interface on the energy level of the layer. Additional impact on the energy level could be due to different morphology of the layer, for example, polycrystalline or amorphous films.

In this work we have studied thickness influence on the energy level change of two organic compounds containing the same active part - 2-(4-[N,N-dimethylamino]-benzylidene)-indane-1,3-dione. Quantum chemical calculation shows that both molecules have the same molecule ionization energy. While one compound molecules are flat and tend to form polycrystalline film, other compound molecules contain bulky trityloxyethyl group and can form amorphous thin film from solution. Depending on their film forming properties, different sample preparation methods were used- thermal evaporation in vacuum for one compound and spin-coating for other. All samples were made on ITO covered glass substrate.

Information about energy level of the system can be obtained from surface potential and directly measuring molecule ionization energy. Surface potential was measured using Kelvin probe technique and ionization energy was obtained from photoelectron emission spectroscopy in vacuum. Images of the

sample surface was obtained by scanning electron microscope (SEM).

Correlation between surface potential and ionization energy and morphology of thin films depending on thin film thickness will be discussed.

Acknowledgment: This work has been supported by the Latvia-Lithuania-Taiwan cooperation project „Synthesis and studies of organic electroactive materials for effective and reliable optoelectronic devices"

9137-52, Session PS2

Photoelectrical properties of indandione fragment containing azobenzene compounds

Janis Latvels, Aivars Vembris, Raitis Grzibovskis, Univ. of Latvia (Latvia)

Organic thin films with semiconducting properties have been intensively studied in nowadays due to very promising applications in organic electronics. Among organic semiconductors, group of indandione fragment containing azobenzene compounds are good candidates for use in design of photovoltaic devices due high absorption coefficient in visible light range (up to 106 cm-1). Attached bulky trityloxyethyl or triphenylsilyl groups facilitate amorphous structure formation from solution thus enables to develop flexible systems with low production costs.

Determination of energy levels of organic compounds in thin solid films is necessary to obtain efficient heterojunction which is critical for high efficient photovoltaic devices.

In our work photoelectrical properties and ionization energy of azobenzene compounds containing indandione fragment were studied.

Ionization energy of molecules in thin films was studied by photoelectron emission measurement in vacuum. Electron affinity potential was obtained by combining ionization energy of molecules and optical band gap.

A number of methods are possible to apply for energy gap characterization of organic molecules in solid state. In case of organic crystals and amorphous state charge carriers are not quasi-free electrons and holes. Electronically relaxed hole and electron determines optical band gap EGOpt, which could be obtain from absorption spectra of compound.

The electronically and vibrationally relaxed state difference of holes and electrons corresponds to adiabatic energy gap EGAd what in its turn correlates with the value of threshold energy of photoconductivity ETh. The ETh can be estimated from the quantum efficiency of photoconductivity ?(h?), which was used for calculation of electron affinity potential.

The typical sandwich-type structure of the samples for the measurements was used where the layer of organic material is sandwiched between two electrodes on the glass substrate. The samples were fabricated by spin-coating method.

Acknowledgment:

This work has been supported by the European Social Fund within the Project No. 1DP/1.1.1.2/13/APIA/VIAA/018.

9137-53, Session PS2

Electrical and Electro-optic Characterization of Nonlinear Polymer Thin Films on Silicon Substrate

Stefan Prorok, Technische Univ. Hamburg-Harburg (Germany); Marvin Schulz, Technische Univ Hamburg-Harburg (Germany); Alexander Y. Petrov, Manfred Eich, Technische Univ. Hamburg-Harburg (Germany); Jingdong Luo, Alex K. Y. Jen, Univ. of Washington (United States)

Nonlinear electro-optic polymers have attracted a considerable amount of attention in the last couple of years. It has been shown that combined with slotted silicon waveguides these materials can be used to build compact electro-optic modulators with very small footprints and large modulation bandwidth. However up to now the full potential of this approach could not be realized. It has been found that the electro-optic coefficients in slotted waveguide structures are significantly lower than those found in thin films on ITO coated glass substrates. Studying the underlying physical effects of this behaviour directly in slotted waveguide structures is challenging. Slotted waveguides have typical slot widths of 200 nm and below. Furthermore the slotted waveguides are usually modelled as parallel plate condensers neglecting effects such as etching roughness, field enhancements at edges and slanted etching facets.

In order to investigate the interplay between silicon and nonlinear polymer we have measured the electro-optic coefficients in thin polymer films on a plain silicon substrate using the Teng-Man method. Compared to direct characterization of electro-optic polymers in slotted waveguide structures thin films on silicon substrates offer a better control of the experimental conditions. At the same time substrates coated with a polymer film of thickness below 200 nm are similar to a slotted waveguide in terms of interface- and geometric properties. Taking into account multiple reflections we show that, in contrast to commonly used low refractive index substrates, high refractive index substrates allow us to measure both electro-optic coefficients at the same time. The electro-optic coefficients are presented as a function of the applied poling field and the results are compared to measurements on indium tin oxide coated glass substrates.

9137-55, Session PS2

Investigation of self-assembled monolayer formation using infrared-reflection-absorption-spectroscopy

Sabina Hillebrandt, Tobias Glaser, Ruprecht-Karls-Univ. Heidelberg (Germany) and InnovationLab GmbH (Germany); Annemarie Pucci, Ruprecht-Karls-Univ. Heidelberg (Germany) and InnovationLab GmbH (Germany) and Ruprecht-Karls-Univ. Heidelberg (Germany)

Charge injection barriers caused by a misalignment of energy levels are a major concern in organic semiconductor devices. One possibility to improve charge carrier injection is the application of an additional layer at the interface between the contact and the organic semiconductor. Self-assembled monolayers (SAMs) have proven to form stable and well defined layers on various contact materials. Depending on their molecular dipole they can lower or raise the work function of a material and are therefore very well suited as injection layers.

Since SAMs can be processed from solution they form a relevant material for printed organic electronics. The orientation of the SAM and thus properties like the interface dipole and work function shift are influenced by various parameters such as concentration of the molecule in solution, immersion time and purity of the solution or substrate.

Infrared-reflection-absorption-spectroscopy (IRRAS) is a very sensitive tool to measure changes in the orientation of SAMs on metal substrates. We performed IRRAS measurements on SAMs consisting of perfluorinated decanethiol (PFDT) on evaporated gold substrates to probe the orientation, ordering and quality of the SAMs. Due to the molecular dipole of PFDT, the formation of the monolayer leads to an increase of the work function of the sample. We performed Kelvin-probe measurements to determine the work function shift and to correlate this shift to the orientation of the molecules.

By systematic variation of immersion time and concentration focusing on low exposures (given by the product of immersion time and concentration), we were able to reconstruct the process of layer formation. Taking into account realistic printing

circumstances we also investigated the impact of oxygen in solvent and substrate on the layer formation process.

9137-56, Session PS2

Spectral studies of 1-tert-butyl-7-(4-chlorophenyl)-3-phenylpyrazolo[3,4-b] pyrrolo[3,4-d]pyridine-6,8(3H,7H)-dione

Cindy J. Valencia Caicedo, Efrain Solarte-Rodriguez, Univ. del Valle (Colombia); Alfredo Perez, Univ del Atlántico (Colombia); Jairo Quiroga, Univ. del Valle (Colombia)

The search for new molecules having pharmacological properties and also exhibit optical properties that allow control them or use them to trigger biochemical processes in cells or biological tissues using light, is one of the most important challenges of photochemistry and biophotonics of this century. Likewise, in the field of solutions to energy problems, finding molecules or nanoscale molecular aggregates to improve the processes of energy transfer and facilitate the production of clean and renewable energy, is seen as one of the most important steps attack and solve these problems from the most fundamental level. The pyrazole nucleus has shown interesting pharmacological properties as antianxiety, antypiretic, analgesic and anti-inflammatory agents, but also as antibacterial and antifungal active ingredients. Some pyrazole-containing compounds such as the pyrazolo[3,4-b]pyridines are interesting fused heterocycles, because they exhibit diverse biological and light emitting properties. Continuing with our current studies on the synthesis and characterization of fused pyrazolopyridine derivates, herein we describe the optimization of a reaction protocol to obtain new pyrazolo[3,4-b]pyrrolo[3,4-d]pyridines via Aza-Diels-Alder reactions starting with aminopyrazoles and using N-substituted maleimides as dienophiles. The structure these new molecules and their spectroscopic properties were determined via elemental analysis, mass spectroscopy and UV-VIS fluorescence spectrometry. Optical studies were performed using a high resolution all optical fiber 4000 channels OceanOptics® spectrophotometer and blue LASER and Blue LED as light sources. The molecular samples were prepared following the here described protocol and analytic grade THF (Tetrahidrofurano) was used as solvent.

9137-16, Session 4

Emitter orientation as key parameter in OLEDs *(Invited Paper)*

Tobias D. Schmidt, Univ. Augsburg (Germany)

No Abstract Available

9137-17, Session 4

Design of highly luminescent and stable benzophenone-based molecules for OLEDs displaying efficient thermally-activated delayed fluorescence

Sae Youn Lee, Takuma Yasuda, Chihaya Adachi, Kyushu Univ. (Japan)

It is well-known that benzophenone possess high intersystem crossing (ISC) efficiency and small singlet–triplet exchange energy (?EST). However, benzophenone itself is difficult to apply in organic light-emitting diodes (OLEDs) because of its intrinsic low photoluminescence efficiency (PLQE) at room temperature and instability in redox reactions. In this study, we designed new benzophenone-based butterfly-shaped molecules to achieve high thermally activated delayed fluorescence (TADF) efficiency. To obtain a high efficiency of TADF, rather small ?EST between S1 and triplet excited (T1) levels should be necessary for light-emitting materials which can be attained by small orbital overlapping between the highest occupied molecular orbital (HOMO) and the lowest unoccupied molecular orbital (LUMO). Based on this conception, we demonstrated TADF-OLEDs employing the newly designed benzophenone derivatives (4,4'-bis{3-(9H-carbazol-9-yl)}methanone (Cz2BP), 4,4'-bis{3-(9H-carbazol-9-yl)-9H-carbazol-9-yl}methanone (CC2BP), 4,4'-bis{4-(10H-phenoxazine-10-yl)}methanone (Px2BP), 1,4-bis{4-(10H-phenoxazine-10-yl)benzoyl}benzene (pPx2BP2), and 1,3-bis{4-(10H-phenoxazine-10-yl)benzoyl}benzene (mPx2PB2) can achieve high external electroluminescence quantum efficiencies from deep-blue to red emission. Our molecular design for the benzophenone derivatives allows spatial separation of HOMO and LUMO on the donor and acceptor fragments, respectively, leading to exceptionally small energy difference between S1 and T1 (?EST?<?0.10?eV) using the TD-DFT/B3LYP/6-31G(d,p) method. In addition, a high electrochemical stability of benzophenone derivatives were confirmed by cyclic voltammetry (CV). Photoluminescence quantum yields of co-deposited films of host : benzophenone derivatives were found to be 35.9-72.7%. Moreover, transient PL properties of host : benzophenone derivatives co-deposited films has been further studied over a wide range of temperature from 150 to 300K and confirmed the temperature dependent fluorescence intensity which promoted by strong thermal energy in high temperature. TADF-OLEDs using benzophenone derivatives as emitting materials showed relatively high external quantum efficiencies ranging from 14.7 to 4.2% in a whole visible light region.

9137-18, Session 4

Molecular-scale simulation of electroluminescence in a multilayer white OLED

Murat Mesta, Technische Univ. Eindhoven (Netherlands); Marco Carvelli, Rein J. de Vries, Harm van Eersel, Technische Univ. Eindhoven (Netherlands) and Philips Research Labs. (Netherlands); Jeroen J. M. van der Holst, Technische Univ. Eindhoven (Netherlands); Matthias Schober, Mauro Furno, Björn Lüssem, Karl Leo, Technische Univ. Dresden (Germany); Hans-Peter Löbl, Philips Research (Germany); Reinder Coehoorn, Philips Research Nederland B.V. (Netherlands) and Technische Univ. Eindhoven (Netherlands); Peter A. Bobbert, Technische Univ. Eindhoven (Netherlands)

In multilayer white organic light-emitting-diodes (OLEDs) the electronic processes in the various layers should be concerted such that efficient, stable and colour-balanced electroluminescence can occur. The interplay of these processes, namely, injection and transport of charge carriers as well as generation, diffusion and radiative decay of excitons is rather complex. Understanding functioning of white OLEDs can be improved by performing computer simulations with experimentally validated models. Here we show that it is feasible to carry out Monte Carlo simulations [1] including all of these molecular-scale processes. Injection and transport of the charge-carriers are modelled as a hopping process with Miller-Abrahams rates in a spatially correlated energy landscape, and diffusion of excitons as Förster resonance energy transfer. The simulated current density and emission profile of a hybrid multilayer OLED combining red- and green-emitting phosphorescent layers with a blue-emitting fluorescent layer are shown to agree well with experiment. The experimental emission profile was obtained with nanometre resolution from the measured angle- and polarization-dependent emission spectra. Both the measurement and the simulation results indicate that the light generation occurs in regions of a few nanometres thick. The simulations also demonstrate the crucial role of exciton transfer from green to red and the efficiency loss due to excitons generated in the non-emitting interlayer between the green and blue layers. The perpendicular and lateral confinement of the exciton generation to regions of molecular-scale dimensions revealed by this study, demonstrate

the necessity of molecular-scale instead of conventional continuum simulation.

[1] M. Mesta et al., Nature Mater. 12, 652 (2013).

9137-19, Session 4

Improvement of power efficiency and reduction of blur effect in OLED with micro-lens array films by reducing substrate thickness

Chun-Che Ma, Yi-Jiun Chen, Li-Jen Hsiao, Hoang Yan Lin, National Taiwan Univ. (Taiwan)

This study demonstrates that attaching micro-lens array films (MAFs) on the substrate and reducing the substrate thickness of OLED can significantly increase the power efficiency, while simultaneously reduce image blurring. Using a point source model, the power efficiency enhancement and reduction of blur effect are respectively discussed in three different regions of the MAFs attached substrate: partially reflecting region, transmitting region, and light guiding region of micro-lens. According to the equations, derived with regard to the substrate thickness and the displacement from the point source and based on geometric relations corresponding to different regions, reducing the substrate thickness will result in different levels of enhancement for power efficiency in different regions.

Our 3D bottom emitting OLED model, based on Monte-Carlo ray-tracing method, in which the emitting layer, consisting of ensembles of mutually incoherent dipole radiators with random isotropic distribution, is originally sandwiched between the hole transport layer (HTL) and the electron transport layer (ETL). To simplify the model, the HTL and ETL layers are merged into one equivalent organic layer, with the emission layer (EML) at the bottom of the ETL/HTL organic layer. Assuming negligible micro-cavity effects, the surface emission is approximately Lambertian while the edge emission is comprised of discrete substrate reflections and leaky waveguide modes.

The parameters of the OLED structure from cathode to anode were set as followed: the reflectivity and absorptivity of the silver cathode is set as 85.85% and 14.15%, respectively. The thickness of HTL (nHTL = 1.795), ETL (nHTL = 1.724), ITO (nITO = 1.896), glass: BK7 (nGlass = 1.519 at wavelength of 550 nm), and MAF: PET (nPET = 1.575), PMMA (nPMMA = 1.494) are 60 nm, 130nm, 100 nm, 700 ?m, 100 ?m and 8.3 ?m, respectively. Micro-lenses are set to be 10 ?m in diameter, 5 ?m in height and 1 ?m in the gap of each micro-lens in a rectangular arrangement.

By comparing OLED with MAFs and bare OLED, the overall enhancement ratio of power efficiency is 1.46, which can be further improved to 1.78 by reducing the substrate thickness from 700 ?m to 50 ?m, and the blur-length is reduced from 942 ?m to 165 ?m. The simulation results demonstrate the possibility of applying MAFs to OLED for higher power efficiency without image degradation in display and lighting applications.

9137-20, Session 4

Improved designs for p-i-n OLEDs towards the minimal power loss of devices

Dashan Qin, Hebei Univ. of Technology (China)

Organic light emitting diodes (OLEDs) have been successfully made the middle-sized displays of mobile phones. Whereas, the low-yield, high-power loss, and poor stability of OLED panels are still remaining as the obstacles to the fast growth of the OLED industry, especially for the lighting application. The p-i-n OLEDs have been widely recognized as the promising method to circumvent these bottleneck factors, due to the unique merit of the doping techniques to offer low-power loss.

In p-i-n OLEDs, the frequently used n-doped electron transport layers (n-ETL1, such as n-BCP, n-Alq3.) possess markedly lower conductivities but markedly higher capabilities of injecting electrons into ETL such as BCP, Alq3, as compared to another class of n-doped ETL (n-ETL2, e.g., n-NTCDA, n-PTCDA, n-C60). Thus, in order to minimize the electron loss, we provide the structure of uniting double n-doped layers (n-ETL2/ n-ETL1/ ETL). See Chin. Phys. Lett. 27(11), 117801 (2010).

In p-i-n OLEDs, the hole current injected from the single p-doped hole transport layer (HTL) into the neighbouring neat HTL must be limited, because the higher conductivity p-doped HTL has the higher lying, highest occupied molecular orbital (HOMO) level of the host material, leading to a larger hole transport energy barrier (?B) across the interface with the neighbouring HTL. Therefore, in order to minimize the hole loss, we suggest the structure of uniting two p-HTLs, p-HTL1/p-HTL2/HTL. The p-HTL1 possesses high-lying HOMO level and thereby high conductivity, decreasing the ohmic loss in the hole conduction; the p-HTL2 features a low-lying HOMO level, reducing the interficial ?B. See Phys. Solidi Status A, 210(6), 1157-1162 (2013).

9137-21, Session 5

Highly-efficient organic light-emitting devices patterned via photolithography *(Invited Paper)*

Simonas Krotkus, Technische Univ. Dresden (Germany); Fabian Ventsch, Daniel Kasemann, Technische Univ. Dresden (Germany) and Institut für Angewandte Photophysik (Germany); Simone Hofmann, Karl Leo, Malte C. Gather, Technische Univ. Dresden (Germany)

Photolithography is a mature, high resolution and parallel patterning technique, which is scalable to large area substrates and has fully developed protocols for registration between multiple processed layers. More importantly, it has a fully established infracstructure used in the inorganic semiconductor industry, as well as for liquid crystal display color filter patternning, where photolithography is considered a standard technology. However, to this date, its application in structuring organic semiconductors is rather limited due to incompatibility of photolithographic processing steps with the majority of organic materials. Namely, significant damage has been shown to occur in organic films, induced by the standard photoresists and organic or water-based solvents used for the pattern transfer, developing, etching or lift-off steps.

In this contribution, we present a modified bilayer photolithographic patterning approach [1] and test its compatibility with organic light emitting diode (OLED) technology. Our method consists of using a polymer layer for the lift-off in hydrofluoroether (HFE) solvents, in combination with commercial photoresist/solvent to allow pattern transfer. Compatibility of small molecule OLEDs with processing step in HFEs is demonstrated by dipping samples into HFE7100 solvent and measuring the change of the devices electrical and optical performance, as well as long term stability. Moreover, state-of-the-art p-i-n electroluminescent structures, comprising the phosphorescent emitter Ir(ppy)3 doped into a double matrix, were photolithographicaly structured and compared to reference pixels defined via shadow mask. No significant dentrimental effect of our patterning approach was observed, which allows us to demonstrate OLEDs with state-of-the-art performance structured via photolithography.

[1] H. Kleemann, A. A. Zakhidov, M. Anderson, T. Menke, K. Leo, and B. Lüssem, “Direct structuring of C60 thin film transistors by photo-lithography under ambient conditions,” Org. Electron., vol. 13, no. 3, pp. 506–513, Mar. 2012.

9137-22, Session 5

A new route to harvest triplets for high-efficiency organic light-emitting diodes *(Invited Paper)*

Chihaya Adachi, Hajime Nakanotani, Kyushu Univ. (Japan)

Electroluminescence in OLEDs is based on the radiative recombination of excitons formed from injected hole and electron carriers with the branching ratio of three triplet excitons and one singlet exciton. Thus, it is crucial to harvest triplet excitons, and the use of molecules exhibiting high efficiency phosphorescence such as Ir(ppy)3 resulted in nearly 100 % internal efficiency. Although Ir complexes are a promising material in OLEDs, a method to achieve high efficiency using a wide variety of fluorescence molecules would be of great value. Here we report a novel pathway for high efficiency fluorescence-based OLEDs that use the delayed fluorescence materials as a host.

9137-23, Session 5

Fully solution processed multi-photon OLEDs for white-light emission

Stefan Höfle, Alexander Schienle, Christoph Bernhard, Uli Lemmer, Alexander Colsmann, Karlsruher Institut für Technologie (Germany)

We present multi-photon emitting OLEDs where white light emission was achieved by stacking blue and yellow OLEDs utilizing an intermediate charge carrier generation layer (CGL) for monolithic device interconnection. With respect to future printing processes for organic optoelectronic devices, all functional layers were deposited from solution. The CGL comprises a low-work function zinc oxide layer that was applied from solution under ambient conditions and at moderate processing temperatures, and a high-work function interlayer that was realized from various solution processable metal oxides or PEDOT:PSS derivatives. Since every charge carrier generates two photons, the luminance and the current efficiency of the stacked OLED at a given device current density exceed the luminance and current efficiency of the single OLED devices, hence reducing the electrical device stress.

9137-24, Session 5

Simulation of advanced OLED light-extraction structures with novel FEM methods

Lin Zschiedrich, JCMwave GmbH (Germany); Horst J. Greiner, Philips Technologie GmbH (Germany); Jan Pomplun, JCMwave GmbH (Germany)

We present novel numerical techniques for the simulation of the light outcoupling from modern organic light-emitting diodes (OLED). For the spatial discretization we use the finite element method which we apply in the frequency domain as well as in the time domain (Discontinuous Galerkin Method). To model the quasi-infinite extension of the OLED in the horizontal directions we apply a recently proposed approach based on the Floquet transform [1]. Thick layers are efficiently discretized by a plane wave expansion which we combine with the Finite Element Method by the domain decomposition method [2]. We benchmark the new simulation tools for highly efficient state of the art OLED light extraction structures [3].

The design and optimization of advanced light extraction structures for OLEDs require accurate simulations of the light outcoupling process based on full-wave Maxwell's equations. Modern OLEDs are characterized by a multi-scale structure comprising nanostructures of sub-wavelength dimension as well as optically thick layers with a thickness of many wavelengths. For example, a corrugated cathode or other sub-wavelength structurings are used to inhibit light trapping within the OLED. Other prominent examples are micro lens arrays of several wavelength diameter on top of an high-index intermediate layer.

The rigorous, full-wave simulation of the light outcoupling from such a modern OLED is still a numerical challenge for the following reasons: The complex geometrical features need an accurate discretization. The singular-like field profiles at metallic interfaces necessitates a fine discretization of the electromagnetic field in certain regions. It is required to account for the quasi-infinite dimension of the OLED in the horizontal direction in combination with thick layers.

The finite element copes well with the complex geometry and the singular-like field profile within the structured layer and the emitting layer. However, the infinitely periodic structure in the horizontal direction requires additional modeling steps. We will show that a brute-force truncation of the OLED to numerically feasible computational domain results in an prohibitive large error, since the light outcoupling at distant positions from the dipole source is strongly underestimated. We have recently shown that this can be overcome by novel Floquet transform techniques [1]. Together with the above mentioned domain decomposition method an accurate simulation of highly efficient OLED light extraction structures becomes possible. We will give a comprehensible introduction to our novel calculation methods and illustrate their application by means of an example taken from the literature [3].

Taken from the literature [3]

[1] Zschiedrich L., Greiner H., Burger S. "Numerical analysis of nanostructures for enhanced light extraction from OLEDs" Proc. SPIE Vol. 8641 (2013) 86410B, (Light-Emitting Diodes: Materials, Devices, and Applications for Solid State Lighting XVII, DOI: 10.1117/12.2001132), and is made available as an

[2] Schädle A., Zschiedrich L., Burger S. "Domain decomposition method for Maxwell's equations: Scattering off periodic structures", Journal of Computational Physics, In Press, Corrected Proof, Available online

[3] Yamae, K. Tsuji, H. Kittichungchit, V. "Highly Efficient White OLEDs with over 100 lm/W for General Lighting" SID Symposium Digest of Technical Papers, Volume 44, Issue 1, pages 916–919, June 2013

9137-25, Session 5

Correlating the transition dipole moment orientation of phosphorescent emitter molecules in organic light-emitting diodes (OLEDs) to basic material properties

Arko Graf, Philipp Liehm, Technische Univ. Dresden (Germany) and Univ. of St Andrews (United Kingdom); Caroline Murawski, Simone Hofmann, Karl Leo, Technische Univ. Dresden (Germany); Malte C. Gather, Technische Univ. Dresden (Germany) and Univ. of St. Andrews (United Kingdom)

The efficiency of OLEDs is currently mainly limited by their low outcoupling efficiency resulting from total internal reflection at the different interfaces within the device and from coupling to waveguided and plasmon modes. Most known methods to enhance the light extraction are based on adding additional refractive structures, e.g. micro-lens arrays or scattering layers. On the molecular scale, the emission pattern of each molecule in the emissive layer of the OLED can be described as an oscillating dipole. The orientation of the associated transition dipole moment strongly affects the amount of light lost to total internal reflection as well as to waveguided and plasmonic modes. Therefore, an alternative way of increasing light extraction is to use emitting molecules with horizontally oriented transition dipole moments. Simulations indicate that the external quantum efficiency can be increased by a factor of 1.5 in an OLED with exclusively horizontal instead of isotropic dipole orientation. Recently, the average dipole

orientation of the Iridium-based phosphorescent emitters Ir(ppy)3, Ir(ppy)2(acac), and Ir(MDQ)2(acac) was studied in detail [1-5]. While the transition dipole orientation of Ir(ppy)3 was found to be isotropic, non-isotropic and preferentially horizontal orientation was observed for Ir(ppy)2(acac) and Ir(MDQ)2(acac).

Here, we compare the orientation of the emissive dipole moment of seven Iridium-based emitter molecules by measuring the angle dependent spectral radiant intensity of the transverse magnetic polarized emission from OLEDs comprising these emitters. These data are compared to the intensity calculated by a multilayer simulation method that includes a parameter describing the average dipole orientation. By varying the orientation parameter in the simulation, the least square error between simulation and experiment is minimized and thus the actual orientation is determined. Surprisingly, amongst the emitters studied, isotropic orientation is by far the exception; most emitters show a considerable degree of horizontal orientation. To better understand this observation and to identify ways of predicting transition dipole orientation of emissive molecules, we calculate the permanent dipole moment of the most abundant isomer of each emitter using density functional theory. In combination with the size of the molecules, the permanent dipole moment yields a parameter that correctly predicts –at least for the emitters investigated here whether the average transition dipole moment is isotropic or horizontal. Possible explanations for this correlation are discussed.

[1] Flämmich M., Frischeisen J., Setz D. S., et al., Organic Electronics 12, 1663 (2011).

[2] Kim S., Jeong W., Mayr C., et al., Advanced Functional Materials 23, 3896 (2013).

[3] Penninck L., Steinbacher F., Krause R., Neyts K., Organic Electronics 13, 3079 (2012).

[4] Liehm P., Murawski C., Furno M., Lüssem B., Leo K., Gather M. C., Applied Physics Letters 101, 253304 (2012).

[5] Murawski C., Liehm P., Leo K., Gather M. C., Advanced Functional Materials 10.1002/adfm.201302173 (2013).

9137-26, Session 6

X-ray imaging sensor arrays on foil using solution processed organic photodiodes and organic transistors *(Invited Paper)*

Abhishek Kumar, Date Moet, Jan-Laurens van der Steen, Ashutosh Tripathi, Francisco Gonzalez Rodriguez, Joris Maas, Holst Ctr. (Netherlands); Matthias Simon, Walter Reutten, Alexander Douglas, Philips Research Nederlands (Netherlands); Rob Raaijmakers, Philips Healthcare Nederlands (Netherlands); Pawel E. Malinowski, Kris Myny, Imec (Belgium); Umar Shafique, University of Waterloo (Canada); Ronn Andriessen, Paul Heremans, Gerwin Gelinck, Holst Ctr. (Netherlands)

We demonstrate imaging sensor arrays fabricated on foil using organic photodiodes and thin film transistors. We used spin-coating of typical photovoltaic polymer blends for fabrication of organic photodiodes having absorption peak in the green light which matches the typical X-ray detector scintillator output wavelength (~550 nm). The imaging arrays consist of 32x32 pixels with pixel size of 1x1mm2 and 200x200um2 based on pentacene TFTs and an QQVGA(160x120 pixels) imager with pixel size of 126x126um2 based on amorphous oxide TFTs. The accurate reproducibility of shadow images of the objects demonstrates excellent potential of these arrays for imaging. Furthermore, the low dark leak signal observed in our organic photodiodes makes them ideal for the low dose medical X-ray imaging applications. We also demonstrate that the crosstalk is insignificant despite the fact that the photodiodes are non-patterned and form a continuous layer in the array. The semi-transparent top electrode is also a continuous layer above the photodiodes in the array. Further on top we used a thin flexible barrier to encapsulate the entire stack to protect it from degradation due to moisture ingress. Since both photodiodes as well as TFTs are fabricated on foil with processing temperatures below 150° C , these imaging sensors can be flexible, rugged and light weight, thereby offering unique advantages over conventional amorphous silicon based imaging sensors on rigid substrates. Further, by combining with a scintillator layer on top of the arrays, we show the potential of these arrays for the X-ray imaging applications.

Keywords: X-ray imaging sensor, flexible imaging sensor, organic photodiode, organic thin-film transistors, crosstalk, amorphous oxide thin-film transistors, dynamic read-out

9137-27, Session 6

Chemical modified single-walled semiconducting carbon nanotubes

Nebras E. Al-Attar, Univ. College Dublin (Ireland); Ilona Kopf, Silvia Giordani, Trinity College Dublin (Ireland); James H. Rice, Univ. College Dublin (Ireland)

Single-walled carbon nanotubes (SWCNT) possess optical and electronic properties that can be potential tailored by the addition of a chemical group via covalent bonding to the nanotube thereby altering the conjugative network and creating changes in the electronic structure of the SWCNT. Surface-enhanced Raman (SERs) spectroscopy enables the imaging of single molecules.

SERs from single molecules possess random fluxing or blinking in the SERs intensity as a function of time. The study of such blinking processes has the potential to inform on the electronic structure of the molecule and how it interacts with its local environment [1].

SWCNTs with chemical groups covalently to the SWCNT surface were investigated using surface-enhanced Raman (SERs) spectroscopy at the single nanotubes level assessing the impact of such altering of the nanotube on the blinking process and in turn its interaction with the local environment.

Previous studies [1-3] have shown that SWCNT's at the single molecule level can be studied using SERs. These studies have shown that 'blinking' in SERs intensity occurs for SWCNT at the single/few molecule level. These studies have shown that the SERs blinking obeys the power-law in common with other materials for related processes.

We studied specifically SWCNTs and SWCNTs that have been chemically treated to improve their purity and also to alter the structure of the nanotube surface via covalently attaching carboxylic acid groups. Excitation of the nanotube samples at wavelengths in resonance with metallic and also semiconductor nanotubes was undertaken. Temporal fluctuations of SERs of purified and oxidised SWCNTs have been observed for both excitation wavelengths. These spectral features were assigned to arising from Raman scattering from single and few carbon nanotube molecules.

We studied both the spectral features and also the SERs blinking rates. The effect of chemical introduction of carboxylic acid moieties to the surface of the nanotubes was seen to tentatively reduce the temporal fluctuations in the SERs spectra. In addition both the power density and thickness of the silver substrate dependence on the Tangential modes G-band and disorder-induced feature D-Band have been studied for both highly purified and oxidised SWCNT.

REFERENCES

1. N. Ai, W. Walden-Newman, Q. Song, S. Kalliakos, S. Strauf. ACS Nano. 5, 2664-70 (2011).

2. N. Al-Alttar, I. Kopf, K. Flavin, E. Kennedy, S. Giordani, J.H Rice. Chem. Phys. Lett., 568–569, 95–100, 2013.

3. N. Al-Alttar, E. Kennedy, I. Kopf, S. Giordani, J.H. Rice, Chem. Phys. Lett., 535, 146-151, 2012

9137-28, Session 6

Lanthanide complexes with fluorinated aromatic carboxylates for visible and near-infrared luminescence

Valentina V. Utochnikova, Lomonosov Moscow State Univ. (Russian Federation) and Lebedev Physical Institute (Russian Federation); Alena S. Kalyakina, Alexey Y. Grishko, Lomonosov Moscow State Univ. (Russian Federation); Alexander A. Veber, A. M. Prokhorov General Physics Institute (Russian Federation); Rik Van Deun, Univ. Gent (Belgium); Stefan Bräse, Karlsruher Institut für Technologie (Germany); Natalia Kuzmina, Lomonosov Moscow State Univ. (Russian Federation)

The luminescence of trivalent lanthanide ions, which can be effectively sensitized by organic ligands, has long ago found its wide application in different areas of human activity. Recently the accent in lanthanide coordination compounds (Ln CCs) luminescent properties investigation was shifted from visible to near infrared (NIR) spectral range. Despite a wide research carried out in this respect NIR luminescence efficiency of Ln CCs is still very low, and to achieve higher values there remained a lot of questions, which can only be answered at parallel fundamental investigation of their luminescence features and testing of new material testing for practical applications.

Among the possible reasons of low NIR luminescence efficiency is that excited low-lying emissive states of NIR-emitting lanthanide ions efficiently undergo vibrational quenching even by C-H groups. One of the possible ways to avoid it which has already proved its effectiveness [1] is ligand fluorination. Elimination of C-H groups from the structure should also give a positive impact on lanthanide ion luminescence in the visible range.

Lanthanide coordination compounds (Ln=Pr, Nd, Sm, Eu, Gd, Tb, Dy, Er, Tm, Yb) with carboxylates (HCarb = pentafluorobenzoic acid, tetrafluorobenzoic acid, trifluorobenzoic acid, nitrotetrafluorobenzoic acid, ? tetrafluoroterephtalic acid) were synthesized and completely characterized. Almost all of them exhibited luminescence in visible or NIR spectral range. They have also appeared to be highly soluble and exhibited good film-forming properties, and thus answer all the requirements to the luminescent compounds – precursors of new luminescent materials.

[1] P.B. Glover, A.P. Bassett, P.Nockemann, B.M. Kariuki, R. Van Deun, Z. Pikramenou, Chem. Eur. J., 13(22), 2007, 6308

9137-29, Session 6

IR spectroscopic studies of charge transfer in organic semiconductors

Sebastian Beck, Ruprecht-Karls-Univ. Heidelberg (Germany) and InnovationLab GmbH (Germany); David Gerbert, Univ. Heidelberg (Germany) and InnovationLab GmbH (Germany); Christian Krekeler, InnovationLab GmbH, Heidelberg (Germany) and Institute for High-Frequency Technology, Technische Universität Braunschweig (Germany); Tobias Glaser, Ruprecht-Karls-Univ. Heidelberg (Germany) and InnovationLab GmbH (Germany); Annemarie Pucci, Ruprecht-Karls-Univ. Heidelberg (Germany) and InnovationLab GmbH (Germany) and Ruprecht-Karls-Univ. Heidelberg (Germany)

Charge transfer (CT) in organic semiconductors is essential for all kinds of applications but its basic mechanisms are still under severe discussion. In this study we want to introduce a new approach for the qualitative and quantitative analysis of CT in doped organic semiconductors and at interfaces by means of in situ infrared (IR) spectroscopy. For typical examples we used hole transport materials such as 4,4´-bis(N-carbazolyl)-1,1´-biphenyl (CBP) and p-dopants such as molybdenum oxide (MoO3) which were deposited via thermal evaporation onto a silicon substrate. To achieve doped layers the dopant and the matrix material were evaporated simultaneously, whereas stacked layers were obtained by subsequent evaporation steps.

In the spectra of the doped layers, additional absorption bands appear in the mid IR range. These can be assigned to the charged matrix molecules that arise due to electron transfer to the acceptor molecules. The charged molecules exhibit different absorption bands, as the charge transfer leads to a change in bond length and bond strength of the molecules. Our results very well agrees with density functional theory (DFT) calculations of the vibrational spectra of both, charged and non-charged molecules. By fitting the spectra of the doped layers as a superposition of the vibrational oscillators of neutral and charged species, we were able to quantify the amount of charged matrix molecules and to determine the doping efficiency of the investigated system.

The formation of CBP cations was also observed during deposition onto MoO3 layers and vice versa.

Financial support by BMBF (project MESOMERIE) is gratefully acknowledged.

9137-30, Session 6

Optical and Topographic Changes in Water-Responsive Patterned Cholesteric Liquid Crystalline Polymer Coatings

Jelle E. Stumpel, Dirk J. Broer, Technische Univ. Eindhoven (Netherlands); Cees W. M. Bastiaansen, Technische Univ. Eindhoven (Netherlands) and Queen Mary Univ. of London (United Kingdom); Albert P. H. J. Schenning, Technische Univ. Eindhoven (Netherlands)

In this work, we present an optical sensor which can respond towards different kinds of (basic) analytes. Analytes in the gas phase as well as in solution are tested. The sensor is composed of a hydrogen-bonded cholesteric liquid crystal polymer which is designed in a fashion to respond towards the target analyte. Initially, this inkjet-printed polymer film selectively reflects green light; the working principle is similar to the one of a Bragg reflector. However, when a basic analyte compound is present, it can disrupt the hydrogen bonds in the network, leading to formation of carboxylate salts. Furthermore, the molecular degree of order of the cholesteric material lowers, resulting in a loss of the green reflection. Since the carboxylate salt is hygroscopic, it will absorb water from the solution or air, leading to swelling of the material. With this swelling, the cholesteric organization of the polymer network returns. Due to the increase in thickness (i.e. the helical pitch becomes greater), red light is reflected, which can be clearly observed by the naked eye. The optical sensor is not cross-sensitive to water vapor. Without presence of the analyte, the sensor is not hygroscopic and water will not be absorbed. Therefore, these responsive coatings have great potential as battery-free optical sensors in for instance the food packaging industries.

9138-1, Session 1

The effect of HDR images on privacy: crowdsourcing evaluation

Pavel Korshunov, Ecole Polytechnique Fédérale de Lausanne (Switzerland)

The ability of High Dynamic Range (HDR) imaging to capture details in high-contrast environments, making both dark and bright regions clearly visible, has a strong implication on privacy. However, the extent to which HDR affects privacy when is used instead of typical standard dynamic range (SDR) imaging is not yet clear. In this paper, we investigate the effect of HDR on privacy via crowdsourcing evaluation using Microworkers platform. Due to the lack of standard privacy evaluation dataset, we have created HDR images of people of varying gender, race, and age, shot indoor and outdoor and under different lighting conditions. We evaluate the tone-mapped versions of these images, obtained by several popular tone-mapping algorithms, using subjective privacy evaluation methodology applied in the crowdsourcing context. The results of the experiments demonstrate a significant loss of privacy when even tone-mapped versions of HDR images are used compared to typical SDR images shot with a standard exposure.

9138-2, Session 1

An automated approach for tone mapping operator parameter adjustment in security applications

Lukas Krasula, Czech Technical Univ. in Prague (Czech Republic) and Univ. de Nantes (France); Manish Narwaria, Patrick Le Callet, Univ. de Nantes (France)

High Dynamic Range (HDR) imaging has been gaining popularity in recent years. Different from the traditional low dynamic range (LDR), HDR content tends to be visually more appealing and realistic as it can represent the dynamic range of the visual stimuli present in the real world. As a result, more scene details can be faithfully reproduced. As a direct consequence, the visual quality tends to improve. HDR can be also directly exploited for new applications such as video surveillance and other security tasks. Since more scene details are available in HDR, it can help in identifying/tracking visual information which otherwise might be difficult with typical LDR content due to factors such as lack/excess of illumination, extreme contrast in the scene, etc. On the other hand, with HDR, there might be issues related to increased privacy intrusion. Therefore, it will be interesting to investigate if an HDR content (displayed on an HDR screen) reveals more information as compared to the LDR scene(s) obtained using different Tone Mapping Operators (TMOs) and adjusted for the regular LDR screen. Several scenes from HDR security video were selected and presented to subjects on HDR display and on regular LDR display using different TMOs. The purpose of the study was to determine, if the use of HDR displays in security application brings any advantage, from the security/privacy point of view, compared to much cheaper solution using TMO. The results are reported.

The submission is intended for the special track “HDR Imaging and Privacy Intrusion”.

9138-3, Session 1

Automatic face recognition in HDR imaging

Manuela Pereira, Juan-Carlos Moreno, Hugo Proenca, Antonio M. G. Pinheiro, Univ. da Beira Interior (Portugal)

The gaining popularity of the new High Dynamic Range (HDR) imaging systems is raising new privacy issues caused by the methods used for visualization. HDR images require tone mapping methods for an appropriate visualization on conventional and non-expensive LDR displays.

These visualization methods might result in completely different visualization raising several issues on privacy intrusion. In fact, some visualization methods result in a perceptual recognition of the individuals, while others do not even show any identity. Although perceptual recognition might be possible, a natural question that can rise is how computer based recognition will perform using tone mapping generated images?

In this paper, a study where automatic face recognition using sparse representation is tested with images that result from common tone mapping operators applied to HDR images. Its ability for the face identity recognition is described. Furthermore, typical LDR images are used for the face recognition training.

9138-4, Session 1

Exposure control for HDR video

Martin Bürker, Christoph Rößing, Daimler AG (Germany); Hendrik P. A. Lensch, Eberhard Karls Univ. Tübingen (Germany)

High Dynamic Range (HDR) video is a continuous stream of HDR images. The generation of HDR images requires several Low Dynamic Range (LDR) images with different exposure times, increasing the overall frame rate beyond the capability of most cameras. A relatively new sensor gives the possibility to acquire two LDR images at the same time, which allows the camera to produce enough HDR images for a steady video.

We propose an algorithm to determine the exposure times for HDR video by adapting them to the current lighting. To get optimal results, each pixel should be acquired with the highest possible signal-to-noise ratio - ideally in all exposures. Since this is only possible for very narrow dynamic ranges, the algorithm has to find the best trade-off for all pixels. In the case of two LDR images the short exposure should deal with the bright parts of the scene, while the long exposure should captures the dark parts.

To divide the pixels in bright and dark sets, the algorithm estimates how the histogram of the - for example - short exposure would look like if it were taken with the long exposure time. When this histogram is subtracted from the original (long) histogram, the result contains those pixel values, that were not, or not sufficiently, captured by the long exposure and can be used to adjust the long exposure time by standard (single) exposure control algorithms. The same procedure leads to an optimized short exposure time.

The histogram for another exposure is estimated by rearranging the bins. Each bin contains values from its floor to the beginning of the next bin. Since these borders vary with the exposure time they have to be recalculated, taking into account the non-linearity of the camera. This step requires to transform the histogram form digital values to a linear domain like the irradiance domain, by applying the inverse camera response curve and normalizing with the exposure time. Unfortunately, the bin borders of the old and new histogram do not align in general. Hence the remapping has to interpolate between the given bin values. The new histogram is then transformed back into the original domain, so the histograms can be subtracted.

The subtraction takes away what part of the dynamic range was already covered, while allowing the histograms to “overlap” if possible. On the other hand, if the dynamic range of the scene is to large to be sufficiently captured with two exposures, the algorithm still finds the setting that best suits the majority of all pixels.

The algorithm has been compared with state-of-the-art algorithms for HDR imaging. It proves to have similar results in mean squared error to a ground truth gained from real-world

data. Furthermore this algorithm is capable to run during the capturing process of a video, since it doesn't require additional exposures than those taken anyway.

It's possible to use the same technique for more than two exposures, estimating and subtracting all histograms from each other, although such sensors are not available, yet.

9138-5, Session 2

Comparative study of fusion algorithms and implementation of new efficient solution

Amine Besrour, SUP'COM (Tunisia) and Univ. de Technologie Troyes (France); Hichem Snoussi, Univ. de Technologie Troyes (France); Mohamed Siala, Fatma Abdelkefi, SUP'COM (Tunisia)

Although High Dynamic Range (HDR) imaging has been the subject of significant researches over the past years, the goal of acquiring the best cinema-quality HDR images of fast-moving scenes using an efficient merging algorithm has not yet been achieved. In fact, through the years, many efficient algorithms have been implemented and developed. However, they still not efficient yet because they do not treat all the situations or because they have not enough speed to ensure fast HDR image reconstitution. The most recent and efficient algorithms are the Sony and AMP ones. For the Sony architecture, they use a back-illuminated sensors disposed inversely of the front-illuminated in order to get lighter and clearer pictures. Their fusion algorithm is based on the View-DR technology. With this newly developed algorithm, all the electrons, which are converted from the captured light, are fully used by the imager, which is quite different from DynaView and other Wide-D technologies deployed in the industry that drop about half of these electrons. Though its high quality and the efficiency of the solution, it still a mechanically weak and hard to construct. For the AMP algorithm, the key aspect remains in the use of data pixels from the brightest, the most exposed sensor as possible. Although this technique provides better final images than the Sony pictures, the solution still cumbersome and the fusion algorithm is not well optimized yet. Indeed, it does not treat all the test cases and it could be faster, more powerful and optimized. In this paper, we will present a full comparative analyze and study of the available fusion algorithms. Also, we will implement our personal algorithm which can be more optimized and faster than the existed ones and we will present still pictures from the acquired HDR images, tonemapped with various techniques. For this, we will implement an algorithm which takes in consideration the level saturation of the neighboring pixels and consider the right decision. This analyze will provide faster and more efficient results in terms of quality and brightness. Also, by taking in consideration all the possible situations, this solution will automatically eliminate some treatments without time lost. As result, this technique and this study will be more optimized and more competent than the old ones.

9138-6, Session 2

Using full-reference image quality metrics for automatic image sharpening

Lukas Krasula, Karel Fliegel, Czech Technical Univ. in Prague (Czech Republic); Patrick Le Callet, Univ. de Nantes (France); Milo? Klima, Czech Technical Univ. in Prague (Czech Republic)

Image sharpening is a post-processing technique employed for the artificial enhancement of the perceived sharpness by shortening the transitions between luminance levels or increasing the contrast on the edges. The greatest challenge in this area is to determine the level of perceived sharpness which is optimal for human observers. This task is complex because the enhancement is gained only until the certain threshold. After reaching it, the quality of the resulting image drops due to the presence of annoying artifacts. Despite the effort dedicated to the automatic sharpness estimation, none of the existing metrics is designed for localization of this threshold. Nevertheless, it is a very important step towards the automatic image sharpening. In this work, possible usage of full-reference image quality metrics for finding the optimal amount of sharpening is proposed and investigated. The intentionally over-sharpened "anchor image" was included to the calculation as the "anti-reference" and the final metric score was computed from the differences between reference, processed, and anchor versions of the scene. Quality scores obtained from the subjective experiment were used to determine the optimal combination of partial metric values. Five popular fidelity metrics - SSIM, MS-SSIM, IW-SSIM, VIF, and FSIM - were tested. The performance of the proposed approach was then verified in another subjective experiment.

9138-7, Session 2

Effect of using different cover image quality to obtained robust selective embedding in Steganography

Karwan A. Abdullah, Naseer Al-Jawad, Alan A. Abdulla, The Univ. of Buckingham (United Kingdom)

This paper is aimed to investigate the use/effect of different quality cover image in Steganography and test that using bitplane analysis in term of robustness against some active attacks such as gamma, statistical filters, and linear spatial filters. The secret message is embedded in higher bitplane, i.e. in other than 1st Least Significant Bit (LSB), in order to resist any active attacks. The embedding process is performed in three major steps: First step, the embedding algorithm is selectively identify a useful areas (blocks) for embedding based on its lighting condition. Second step is to nominate the most useful blocks for embedding based on their entropy and average. Third step is to select the right bitpalne for embedding. This kind of block selection made the embedding process scatters the secret messages randomly around the cover image. Different test has been performed for selecting a proper block size and this is related to the nature of the used cover image. Our proposed method is suggesting a suitable embedding bitplane as well as the right blocks for the embedding. Experimental results demonstrate that different image quality used for the cover images will have an effect when the stego image is attacked by different active attacks. Although the secret messages are embedded in higher bitplane, but the stegos images cannot be recognized visually.

9138-8, Session 3

Refocusing capabilities in a miniaturized multi-channel multi-resolution imaging system using a tunable lens

Lien Smeesters, Gebirie Y. Belay, Heidi Ottevaere, Youri Meuret, Hugo Thienpont, Vrije Univ. Brussel (Belgium)

Inspired by nature, we are interested in an optical imaging system which combines the multi-channel design of the compound eyes of insects and the refocusing capability of the human eye in one compact configuration. Refocusing multi-channel imaging systems are nowadays only commercially available in bulky and expensive designs since classical refocusing mechanisms cannot be integrated in a miniaturised configuration. At wafer-level, the neighbouring lenses in multi-channel systems are made within the same substrate, making their movements limited. Our goal is to design a low-cost, compact refocusing two-channel imaging system. One channel is able to capture a wide field-of-view (FOV) image (2x40°) of a surrounding with a low angular resolution (0.078°), whereas a detailed image of a small region of interest (2x7.57°) can be obtained with the high angular resolution channel (0.0098°). Moreover, to solve the lack of refocusing in miniaturised multi-channel imaging systems, we investigated the use of a voltage tunable liquid lens in the high angular resolution channel.

In this paper, we first study the working principle, optical quality and tunability of a commercial voltage tunable liquid lens. To be able to model the voltage tunable liquid lens, we performed several characterisation measurements. For different applied voltages, the focal length and wave aberrations of the lens where measured using a transmitting Mach-Zehnder interferometer working at 632.8nm. Our main focus in this paper is on the design of a compact high resolution refocusing imaging system which captures a detailed image with a limited FOV. This design is obtained by the combination of a tunable lens with four aspheric lens surfaces. We analysed and optimised the configuration with Code V optical design software in which we used the modulation transfer function (MTF) and transverse ray aberration (RMS spot size) as merit functions. After the fabrication of the passive lenses with ultra-precision diamond tooling, the high resolution refocusing system was tested in a proof-of-concept demonstrator. Its optical performance is determined by imaging a USAF 1951 resolution chart through the passive and tunable lenses on a commercial CMOS camera sensor. The resolving power, optimal object distance and depth-of-field (DOF) of both demonstrator and simulations correspond well, which confirms the reliability of the optical imaging model and the developed tunable lens model in Code V. At the end of this paper, we discuss the integrated design of the refocusing two-channel imaging system. Both channels were designed with corresponding inter-lens distances, thicknesses and image distance so they can be easily integrated in a wafer-level manufacturable design. The simulated wide FOV and high angular resolution optical channels show a diffraction-limited performance ensuring a good overall image quality. We can conclude that the insertion of a tunable lens in a multi-channel imaging system improves the DOF compared to current state-of-the art published compact imaging systems. Moreover, the wafer-level refocusing multi-channel design can also form the basis of an advanced three-dimensional stacked image sensor, where different image processing algorithms can be simultaneously applied at the different images on the image sensor.

9138-9, Session 3

Time-delay compensation for stabilization imaging system

Yueting Chen, Zhihai Xu, Qi Li, Huajun Feng, Zhejiang Univ. (China)

The spatial resolution of imaging systems for airborne and space-borne remote sensing are often limited by image degradation resulting from mechanical vibrations of platforms during image exposure. The captured images can be blurred and distorted due to the degradation of the modulation transfer function (MTF). A straightforward way to overcome this problem is to actively stabilize the optical axis or drive the focal plane synchronous to the motion image during exposure. This kind of stabilization imaging system usually consists of digital image motion estimation and micro-mechanical compensation. Motion estimation is accomplished by an auxiliary high-speed array camera with sub-pixel precision real-time image registration algorithms (e.g. gray-scale projection correlation algorithm). During the integration time of the prime imaging CCD, a sequence of images can be obtained by the auxiliary array camera. Inter-frame image displacements are estimated by image correlation algorithms. The measured motion is then used by a controller. The controller immediately drives a tip-tilt mirror stage to compensate the optical axis jitter thus to ensure a stable image in focal plane.

The performance of such kind of visual servo stabilization imaging system is closely related to precision of motion estimation and measurement time delay. The time delay discussed in this paper is caused by acquisition period of the auxiliary array camera, image processing time and control time. The image processing time and control time is relatively much less than the acquisition period of the auxiliary camera. Large time delay results in larger phase delay between motion estimation and micro-mechanical compensation, and leads to larger uncompensated residual motion and limited bandwith. The paper analyzes the time delay caused by image acquisition period and introduces a time delay compensation method based on SVM (Support Vector Machine) motion prediction. The main idea to cancel the time delay is to predict the current image motion from delayed measurements. A support vector machine based method is designed to predict the image motion, because SVM is a supervised learning method and has a strong capacity to solve nonlinear regression problems. Firstly, hundreds of image motion vectors are obtained to train the SVM model. The model has a dozen inputs and one output. The output is the predicted current motion vector and the inputs are a sequence of motion vectors measured lately. Secondly, the trained model is used to predict the current image motion. The inputs of the model are repeatedly updated in a FIFO (First In, First Out) approach. The predicted motion is then used to drive the piezo actuated tip-tilt mirror to compensation current image motion.

A prototype of stabilization imaging system has been implemented in the lab. The auxiliary camera is a Mikrotron MC1302 high speed CMOS camera. To analyze the influences of time delay on system performance and to verify the proposed time delay cancelation method, comparative experiments over various frequencies of vibration are taken. The experimental results show that, the accuracy of motion compensation and the bandwith of the system can be significantly improved with time delay cancelation.

9138-10, Session 3

Proof-of-concept demonstration of a miniaturized three-channel multiresolution imaging system

Gebirie Y. Belay, Heidi Ottevaere, Vrije Univ. Brussel (Belgium); Youri Meuret, Katholieke Univ. Leuven (Belgium); Hugo Thienpont, Vrije Univ. Brussel (Belgium)

Multichannel imaging systems have several potential applications such as multimedia, surveillance, medical imaging and machine vision, and have therefore been a hot research topic in recent years. Such imaging systems, inspired by natural compound eyes, have many channels, each covering only a portion of the total field-of-view of the system. As a result, these systems provide a wide field-of-view (FOV) while having a small volume and a low weight. Different approaches have been employed to realize a multichannel imaging system. We demonstrated that the different channels of the imaging system can be designed in such a way that they each can have different imaging properties (angular resolution, FOV, focal length). The first channel possesses the largest angular resolution (0.0096°) and narrowest FOV (7°), whereas the third channel has the widest FOV (80°) and the smallest angular resolution (0.078°). The second channel has intermediate properties. Therefore, with such an imaging system, it is possible to obtain general information of a surrounding environment with the wide FOV (third) channel while inspecting a small region of interest in detail with the high resolution (first) channel. Such a multiresolution capability allows different image processing algorithms to be implemented on the different segments of an image sensor. For example, a motion detection algorithm could be implemented on the wide FOV channel for event awareness, whereas a face detection algorithm could be implemented on the high resolution channel.

Using optical ray-tracing software (CODE V), we have designed a miniaturized multiresolution imaging system that contains three channels each consisting of four aspherical lens surfaces fabricated from PMMA material through ultra-precision diamond tooling. Moreover, baffles and aperture stops fabricated from Titanium and Aluminum based metal alloy through metal additive manufacturing are part of the integrated imaging system. The baffles avoid crosstalk between the neighboring channels and the aperture stops limit the light getting through the system. The integrated imaging system is assembled by connecting the four PMMA plates containing the four aspherical lens surfaces, the baffles and the aperture stops plate through capillary columns. This paper presents the experimental proof-

of-concept demonstration of the integrated imaging system using a commercial CMOS sensor and gives an in-depth analysis of the obtained results. The performance of the imaging system was evaluated at different object distances for different types of objects to be imaged, starting from the USAF plate (for the depth of field determination) up to slanted edge targets (for MTF determination) and different pictures displayed on the source laptop (for visual inspection). Experimental images captured with the three channels are compared with the corresponding simulated images. The experimental MTF of the channels for a slanted edge target is smaller than the simulated MTF due to various factors like misalignment of the assembled components, crosstalk between the channels and fabrication errors. This multichannel multiresolution approach opens the opportunity for low-cost compact imaging systems that can be equipped with smart imaging capabilities.

9138-11, Session 3

Imaging objects behind a partially-reflective surface with a modified time-of-flight sensor

Dave Geerardyn, Maarten Kuijk, Vrije Univ. Brussel (Belgium)

Depth images can nowadays be captured with different methods. The best known are stereovision, structured light, continuous-wave time-of-flight and pulsed time-of-flight (range-gating). For distance measurements, the time-of-fights (TOF) methods have already proven a good working operation. Continuous-wave and pulsed time-of-flight are nowadays used in different applications. Pulsed time-of-flight techniques are slow and mostly used in combination with a scanning mirror, which makes them not well suited for imaging purposes. Continuous-wave time-of-flight techniques are much faster and more suited for imaging purposes, but cannot be used behind partially-reflective surfaces. In commercial applications, both TOF methods require specific hardware which cannot be exchanged. In this paper, we discuss the transformation of a continuous-wave time-of-flight (CWTOF) sensor to a pulsed time-of-flight (PTOF) camera, which is able to make an image and measure the distance of an object behind a partially-reflective surface, like the air-water interface in swimming pools when looking from above. We first created our own PTOF depth camera, based on an in-house designed CWTOF CMOS sensor. We added extra components to make it suitable for both CWTOF and PTOF. When visualization is wanted from objects behind partially-reflective surfaces, CWTOF will give a weighted average of the distances between the objects and the surfaces. We thus need the PTOF to get distance information from these objects, but in combination with the fast, multi-pixel properties of the CWTOF to be able to achieve a decent image resolution. We describe the necessary hardware components for a normal TOF camera and compare it with the specifically adapted elements which makes it a range-gating depth imager. Afterwards, the perceived image of a given scene was modeled by Matlab and commercial ray-tracing software. We simulated the distances and images of an object, positioned behind a partially-reflective surface. To achieve a high resolution, the light source was modeled as a pulsed laser which generates intense, low-jitter, nanoseconds pulses. The different objects were modeled according to the Phong reflection model. The ray-tracing software allowed us to study the rays emitted by the light source, reflected and refracted by the objects, focused by a wide-angle lens and captured by the detector. These rays were exported to Matlab, where we created a virtual image. Subsequently, optical path lengths were calculated for every pixel and transferred into time delays, which we used to simulate the pulse deformations. These deformations are studied and interpreted to achieve the depth information. To test the applicability of our system, various light sources and different wavelengths were used for these simulations. To verify our model with the commercial existing systems, a 850nm near-infrared light-emitting diode and laser diode was used. To expand this principle to other applications, the model was also tested with 520nm green laser diodes. The latter wavelength can be applied for objects positioned underwater. As a result, this can be applied in drowning-people detection systems for swimming pools. Moreover, these 3D cameras can be easily installed on the ceiling instead of the more difficult installation in the sidewalls of the swimming pool.

9138-12, Session 3

Ambient light-sensitive display of multimedia content on mobile handsets

Eran A. Edirisinghe, Asmaa H. A. Al-Marhoubi, Dhammike S. Wickramanayake, Loughborough Univ. (United Kingdom)

The quality of experience of viewing multimedia content on a mobile handset will depend significantly on ambient light incident on the display screen. At present the mobile device's Ambient Light Sensor (ALS) readings are utilised by multimedia players to automatically adjust the illumination and contrast settings of multimedia device in an attempt to quickly adapt to changing viewing conditions and to thus enable improved quality of experience.

However the above approach has two main drawbacks. First, the sensitivity of the adjustments made to the content will heavily depend on the latency of operation and angle of sensitivity of the ALS. Our investigations using the latest mobile handsets revealed that the speed and sensitivity of operation of state-of-the-art ALSs is not sufficient to cater for the above need. Second, changing the illumination level and/or contrast will not improve the quality of experience as doing so could directly result in fully underexposed or overexposed regions in the image.

In the proposed work the first drawback is addressed by modelling the ambient light distribution in the environment based on a fixed number of readings obtained when the device was moving slowly or kept stationary. This model is used to predict ALS readings in real-time and allowing them to be corrected as necessary when the ALS responds later, due to latency. The creation of the illumination model of the environment needs the calculation of distance between readings. This is done by sensor fusion that uses the accelerometer, gyroscope and velocity meter readings of the mobile handset. The proposed work addresses the second drawback by adopting an extended version of the local histogram equalisation based image enhancement approach proposed by us in [1], in which the predicted and subsequently corrected ALS readings are used to instantaneously enhance image quality.

We present details of mathematical modelling of ambient illumination in an environment in which a mobile phone is situated. We demonstrate the accuracy and speed of ALS reading updates that can be achieved via this model, supported by frequent updates done via the actual ALS readings. The use of the above values in automatically driving the local histogram equalisation based approach presented previously by us in [1] is explained. An implementation on a mobile handset that uses the Android OS is used to present results and carry out a detailed evaluation.

[1] Léonce, A, Wickramanayake, DS, Edirisinghe, EA, Hsu, T-I (2012) High Dynamic Range video transmission & display using standard dynamic range technologies, Proceedings of SPIE - The International Society for Optical Engineering, 8436, ISSN: 0277-786X. DOI: 10.1117/12.922851.

9138-22, Session PS3

Spread-space spread spectrum video watermarking authentication based on double random phase encoding technique

Shi Liu, Changliang Guo, Univ. College Dublin (Ireland); Bryan M. Hennelly, National Univ. of Ireland, Maynooth (Ireland); John T. Sheridan, Univ. College Dublin (Ireland)

In this paper we present an imperceptible watermarking

procedure to embed copyright information into digital video using optical Double Random Phase Encoding (DRPE) technique. This proposed process utilizes the capability of the optical DRPE to spread the energy of information throughout both the space and spatial frequency domain. The watermark information takes the form of 1D barcode arrays and is encrypted separately into optical speckle noise. Then the encrypted watermark array is inserted into the chosen frame of the host video. In the case of blind detection integration, over the y-axis, can be used to strengthen the energy of the barcode and extracts the original information without access to the original host images. Simulations are performed on different types of compressed video and the feasibility and the robustness of the proposed method is demonstrated.

9138-24, Session PS3

Chalcogenide glass applied to molding process with good thermal stability

Ju Hyeon Choi, Young-Jun Jang, Jeong-Ho Kim, Hye-Jeong Kim, Korea Photonics Technology Institute (Korea, Republic of)

An interest of chalcogenide glass has been increased because of their use in preparing optical lenses in range of 3-12 ?m. With recent advance in less costly uncooled detector technology, moldable lens using chalcogenide glass has drawn a great deal of attention. In this study, amorphous Ge-Sb-Se chalcogenide was prepared by a standard melt-quenching technique. Melted chalcogenide glass for moldable lens should have unique thermal mechanic properties in order to be applied to molding process. Specifically, the Ge:Sb ratio were controlled in order to find out the most stable glass forming area.

Thus, the optical, thermal and thermo mechanical properties to find out right composition were characterized by IR transmission spectroscopy, DSC (Differential Scanning Calorimeter) and TMA (Thermo Mechanical Analysis), respectively. The moldability of chalcogenide glass was characterized through transcription properties of the mold's surface. The relations between thermal properties and the moldability were studied using thermal properties such as Tg and Tx as function of mean coordination number i.e composition ration between Ge and Sb. In addition, both IR transmittance and x-ray diffraction patterns of the molded chalcogenide glass lens were evaluated to verify the compositional and structural stability of the glass material under the given molding conditions. Finally, the preferential Ge:Sb ratio in Ge-Sb-Se based chalcogenide glasses was selected for producing moldable lenses.

9138-25, Session PS3

Precise dispersion equations of absorbing filter glasses

Steffen Reichel, Ralf Biertümpfel, SCHOTT AG (Germany)

The refractive indices versus wavelength of optical transparent glasses are measured at a few wavelengths only. In order to calculate the refractive index at any wavelength (besides the measured ones), a so-called Sellmeier series is used as an approximation formula of the wavelength dependent refractive index. Typically, a 3 term Sellmeier representation is sufficient. Such a Sellmeier representation (dispersion equation) assumes an absorbing free (= loss less) material. In optical transparent glasses this assumption is valid since the absorption of such transparent glasses is very low. However, optical filter glasses (color glass) have often a rather high absorbance in certain regions of the spectrum. In addition color glass (absorbing filter glass) is manufactured by precise controlling the transmittance at specific wavelength (the "filter curve"). The refractive index of filter glasses is not as precise as for optical glasses, like e.g. N-BK7. This is because for optical filter glass it is very difficult to precisely control both transmittance and refractive index.

But optical filter glasses are becoming more and more important as elements in sophisticated optical designs. Therefore, the exact description of the wavelength dependent function of the refractive index is essential for an optimized design. For example digital cameras use an IR cut filter to ensure good color rendition and image quality. In order to reduce ghost images by reflections and to be nearly angle independent absorbing filter glass is used. Such absorbing filter glass is for example blue glass BG60 from SCHOTT. Nowadays digital cameras improve their performance and so the IR cut filter needs to be improved. To be specific one topic is the accurate knowledge of the refractive index versus wavelength (dispersion) of the used glasses for the optical design, including the optical filter glass. But absorbing filter glass is not loss less as needed for a Sellmeier representation. In addition it is very difficult to measure it in the absorption region of the filter glass, which is for example for blue glass in the range of 700nm to 1000nm. Besides the absorption region it is more important to precisely describe the refractive index in the high transmission region – but here the refractive index in the blocking region must be known.

We have focused a lot of effort on measuring the refractive index at specific wavelength for absorbing filter glass – even in the absorption region. The different measurement methods and the resulting data will be described. In addition we estimate the use of a Sellmeier representation for typical filter glasses. It turns out that in most cases a Sellmeier representation can be used even for absorbing filter glasses. Finally Sellmeier coefficients for the approximation of the refractive index (dispersion equations) will be given for different filter glass types. These are NIR cut filter glasses (Schott BG type), IR cut filter glasses (Schott KG type), neutral density filter glasses (Schott NG type), and longpass filter glasses (Schott RG type).

9138-26, Session PS3

Transformation of a omnidirectional images

Vasiliy P. Lazarenko, Sergey N. Yaryshev, EVS Ltd. (Russian Federation)

This paper presents the algorithm designed for omnidirectional CCD TV cameras. Omnidirectional camera is a vision system providing a 360° panoramic view of the scene. The image taken from omnidirectional camera is distorted. In order to correct the distortion of the image or make it easy to view, we need to transform it. Using presented algorithm, we able to make the transformation of the omnidirectional image.

The algorithm for transforming of omnidirectional image consists of several steps. At the first step we must form a matrix depending on what we want to see in the end. For example, we want to create a virtual pan-tilt-zoom camera. We must specify the following parameters: resolution, field of view, rotation and tilt angles. After that, we create the virtual plane in object coordinate system, which will correspond to this virtual camera. As a result, we have a matrix of 3d points in object coordinates system.

At the second step we need to transform the coordinates of points in the object coordinate system to the camera coordinate system. In order to translate the coordinates, we need to know the imaging function of our system. This function determines the relationship between the coordinates of the object-space coordinates and the corresponding pixel point. In our previous work we use the fisheye projection model and we got positive results. But how accurate this projection model? In order to find the exact function, we need to calibrate the omni-directional camera. After studying methods of calibration of omnidirectional cameras, we chose a technique developed by Davide Scaramuzza. This method assumes that the imaging function, which manages the relation between pixel point and the corresponding 3D point in object-space, can be described by a Taylor series expansion, whose coefficients are the parameters to be estimated. After calibration we use this estimated function. As a result we have a matrix of calculated pixel points, that corresponding to our virtual plane.

In the last step we use the computed coordinates of the points to display the image of virtual camera.

9138-27, Session PS3

Study of irradiance distribution in optical equisignal zone

Anton A. Maraev, National Research Univ. of Information Technologies, Mechanics and Optics (Russian Federation); Aleksandr S Vasilev, ITMO University (Russian Federation); Alexandr N. Timofeev, National Research Univ. of Information Technologies, Mechanics and Optics (Russian Federation)

Nowadays means of optical-electronic remote control are widely used in industry, construction, geodesy, etc. They enable to achieve high performance and accuracy while positioning elements under control at large distance. There are instruments based on optical equisignal zone (OEZ) which can perform this task.

Such a system contains a searchlight forming the base plane, and a receiver, which determines its position relative to the base plane. The base plane is created by two light sources (e.g. LEDs) modulated with different frequencies. Their fluxes are condensed on the edge of a splitting prism, thus halves of original sources compose one light source on the edge. The prism reflects these fluxes in the same direction. Thus irradiance of two fields divided by the base plane is formed in the plane of the sensor. The difference between fluxes coming on the plane of the sensor (so-called differential flux) results in the signal of the receiver, indicating the direction the receiver is to move. The receiver is attached to an element under control so that it becomes possible to keep the element in a required position.

It is known that air refraction caused by temperature gradient leads in one of the largest error in optical-electronic systems. Considering that rays are bended by heated atmosphere in a different way according to their wavelength, it is possible to found the position of each ray on the sensor. So applying light sources of different wavelength would enable to attenuate air refraction influence using a special processing algorithm, and thus to reduce the error of positioning. since the larger the difference of wavelengths is, the more precisely the difference in position of rays may de determined, it is recommended to use pairs of light sources with the difference between wavelengths as large as possible (e.g. a blue/UV source and red/IR one). Characteristics of the base plane are necessary for setting requirements for an optical system of the searchlight when using two wavelengths.

In the paper we consider distribution of irradiance in the field of analysis and its dependence on quality of the edge of the splitting prism. Sensitivity of the system near the projection of the base plane on the sensor and the shape of the base plane are studied.

9138-28, Session PS3

Architectural textured surfaces panels for optical purposes

Gonçalo M. Furtado Cardoso Lopes, André A. Chaves, Univ. do Porto (Portugal)

A multidisplinary project is being developed at the University of Porto, using a multidisciplinary research, with input from interaction design, architecture and engineering.

The object of research is the study of structures and textured panels for modular architectural surfaces, especially for interiors, modelled and manufactured with computer support and the subsequent assembly of its various components. Each panel will have a size of 20x20cm, and their combination will results in a wall panel similar to traditional Portuguese wall tiles. The aim of this research is to create a multimedia interface actuated by various human senses.

The research emphasizes an methodological approach that is both scientific and artistic, which later results are both academic and business. The modular components are produced in composite materials, such as paper, using a binder of high performance epoxy resin (transparent bicomponent).

Technological elements used include electronic devices (sensors and actuators, fiber optics, processor type as “arduino”, circuit boards with electronic application of optical fibers) that enables the reception and emission of sensory stimuli. We are currently conducting experiments on materials and technologically advanced devices, such as optical fibers and sensory technology, by performing small prototypes designed to test solutions conceived within the aim of project.

The expected result includes a prototype versatile and innovative (aesthetic and functional), capable of applying to different spatial contexts interiors. Its performance allows, given the visual and tactile aspects, the playfulness of such spaces.

9138-13, Session 4

Adaptive reconstruction of Gabor transformed holograms

Kartik Viswanathan, Patrick Gioia, Orange SA (France); Luce Morin, Institut National des Sciences Appliquées (France)

We provide an analysis of the pruning of wavelet coefficients for view-point based degraded reconstruction of holograms. Using the good time-frequency localization of the Gabor wavelets, we identify methods to prune the wavelet transformed hologram for compression, based on the position of the viewer. For a setup containing limited number of view-points, we establish that view-dependent pruning techniques form a viable method of efficient hologram compression for 3D video using multi-view data.

9138-14, Session 4

Impact of packet losses in scalable 3D holoscopic video coding

Caroline Conti, Luís Ducla Soares, Paulo Nunes, Instituto Univ. de Lisboa (Portugal) and Instituto de Telecomunicações (Portugal)

Holoscopic imaging, also known as integral imaging, became a prospective glassless 3D technology to provide more natural 3D viewing experiences to the end user. Additionally, holoscopic systems also allow new post-production degrees of freedom, such as controlling the plane of focus or the viewing angle presented to the user. However, to successfully introduce this technology into the consumer market, a display scalable coding approach is essential to achieve backward compatibility with legacy 2D and 3D displays. Moreover, to effectively transmit 3D holoscopic content over error-prone networks, e.g., wireless networks or the Internet, error resilience techniques are required to mitigate the impact of data impairments in the user quality perception. Therefore, it is essential to deeply understand the impact of packet losses in terms of decoding video quality for the specific case of 3D holoscopic content generated by microlens arrays, notably when a scalable approach is used. Moreover, it is also important to study how the various coding configurations (e.g., the number of 2D views used in lower layers and the view generation parameters) influence the decoding quality in the presence of data losses.

In this context, this paper studies the impact of packet losses when using a three-layer display scalable 3D holoscopic video coding architecture previously proposed, where each layer represents a different level of display scalability (i.e., L0 - 2D, L1 - stereo or multiview, and L2 - full 3D holoscopic). For this, a simple error concealment algorithm is used, which makes use of inter-layer redundancy between multiview and 3D holoscopic content and the inherent correlation of the 3D holoscopic content to estimate lost data. Furthermore, a study of the influence of the number of 2D views used in lower layers and the view generation parameters on the performance of the used error concealment algorithm is also presented.

9138-15, Session 4

Efficient Holographic Image Compression based on the JPEG 2000 architecture empowered by arbitrary wavelet decompositions and directional transforms

Tim Bruylants, David Blinder, Heidi Ottevaere, Adrian Munteanu, Peter Schelkens, Vrije Univ. Brussel (Belgium)

With the advent of modern computing and imaging technology, the use of digital holography became practical in many applications such as microscopy, interferometry, non-destructive testing, data encoding, and certification. In this respect the need for an efficient representation technology becomes imminent. However, the characteristics of these holographic recordings differ significantly from that of regular natural imagery, because it represents a recorded interference pattern that mainly manifests itself as additional high-frequency information. Since regular image compression schemes are typically based on a Laplacian frequency distribution, they are unable to optimally represent such holographic data. However, unlike most image codecs, the JPEG 2000 standard can be readily tuned to efficiently cope with images containing such alternative frequency distributions by enabling the arbitrary wavelet decomposition of Part 2 of the standard. As such, by applying the packet decomposition, it can already significantly improve the compression performance for off-axis holographic images over that of regular image compression schemes. Moreover, extending JPEG 2000 with directional wavelet transforms results in even higher improvements in its compression efficiency. Extending the standard to support directional filtering would only require additional signaling the filter directions, and would not impact any other existing functionality. In this paper, we show how the arbitrary wavelet decomposition feature, combined with these directional wavelet transforms, allows for the efficient compression of microscopic off-axis holographic imagery at lossy-to-lossless bit-rates. For generating results, we make use of a JPEG 2000 compliant codec framework. The results demonstrate that combining both the packet decomposition structure and the directional wavelet transforms can significantly improve the compression efficiency for microscopic off-axis holograms.

9138-16, Session 4

Maximizing optical efficacy and color gamut in projection applications by combining four laser wavelengths

Roberto Ocaña Pérez, Ian Wallhead, AIDO Instituto Tecnológico de Óptica, Color e Imagen (Spain)

Laser projection devices should be designed to maximize their luminous efficacy and color gamut. This is for two main reasons. Firstly, being either stand alone devices or embedded in other products, they could be powered by battery, and lifetime is an important factor. Secondly, the increasing use of lasers to project images calls for a consideration of eye safety issues. The brightness of the projected image may be limited by the Class II accessible emission limit. There is reason to believe that current laser beam scanning projection technology is already close to the power ceiling based on eye safety limits. Consequently, it would be desirable to improve luminous efficacy to increase the output luminous flux whilst maintaining or improving color gamut for the same eye-safe optical power limit.

Here we present a novel study about the combination of four laser wavelengths in order to maximize both color gamut and efficacy to produce the color white. Firstly, an analytic method to calculate efficacy as function of both four laser wavelengths and four laser powers is derived. Secondly we provide a new way to present the results by providing the diagram efficacy vs color gamut area that summarizes the performance of any wavelength combination for projection purposes. The results indicate that the maximal efficacy for the D65 white is only achievable by using a suitable combination of both laser power ratios and wavelengths.

9138-17, Session 4

Photorefractive phase-conjugation digital holographic microscopy

Huang-Tian Chan, Xin Yu Wong, Yang-Kun Chew, Ming-Tzung Shiu, Chi-Ching Chang, MingDao Univ. (Taiwan)

In this work, we propose an innovative method for digital holographic microscopy we name it as Photorefractive Phase-Conjugation Digital Holographic Microscopy (PPCDHM) technique based on the phase conjugation dynamic holographic process in photorefractive BaTiO3 crystal and the retrieval of phase and amplitude of the object wave were performed by a reflection-type digital holographic method. Both amplitude and phase reconstruction benefit from the prior amplification by Mutually Pumped Conjugation (MPPC) as they have an increased SNR. The interest of the PPCDHM is great, because its hologram is created by interfered the amplified phase-conjugate wave field generated from a Photorefractive Phase Conjugator (PPC) correcting the phase aberration of the imaging system and the reference wave onto the digital CCD camera. Therefore, a precise three-dimensional description of the object with high SNR can be obtained digitally with only one hologram acquisition. The method requires the acquisition of a single hologram from which the phase distribution can be obtained simultaneously with distribution of intensity at the surface of the object. The idea shows in this work that, for the first time to the best of our knowledge, the combination of the phase conjugation of object wave generated by a photorefractive BaTiO3 crystal and reconstruction hologram by digital holographic microscopy method that is possible to obtain the quadratic phase compensated 3D imaging of several micro-structured samples. The proposed combination of digital and photorefractive holography could open up new era and applications for digital holography for example for imaging through scattering media in biomedical applications.

9138-18, Session 5

Survey on texture analysis using LBP techniques

Sergio A. Orjuela Vargas, Wilfried Philips, Univ. Gent (Belgium)

Differentiating regions based on texture is an important task in computer vision. Particularly, applications like quality inspection of material surfaces require algorithms capable of differentiating similar textures. In many empirical studies, LBP techniques have shown to be successful for texture characterization. The main advantages of these techniques are the robustness against illumination changes and the low requirements for implementation. LBP techniques codify the intensity changes around each pixel in an image with a label. Each label, which is known as the LBP-code, is computed based on a series of comparisons between the intensity values of pairs of pixels in the neighborhood of a center pixel. Commonly, the pixels on the image are labeled by using a look up table where the input is a codified string number, resulting from the comparison of the intensities in the neighborhood. Similar versions of intensity variations in the neighborhood can be labeled with the same LBP-code. Then, a histogram, called the LBP-histogram, of the occurrences of the LBP-codes on each image is used as a feature to characterize the global texture of the image. We present in this paper a survey of LBP techniques. We start by briefly discussing the origins of the LBP technique and the first LBP extensions. Then, we discuss LBP techniques based on circular neighborhoods. Afterwards, we discuss LBP techniques for multi-resolution analysis. Next, other techniques based in binary patterns are discussed. We also compare the techniques in terms of their capabilities for differentiating fine changes of texture. The difference

between two LBP-histograms is evaluated by quantifying their divergence of the distributions using probability distances. We use the square root of twice the Jensen-Shannon entropy, which comply with the requirements of a metric. Our database is composed of images that exhibit progressive changes in texture. We particularly quantify the square root of twice the Jensen-Shannon entropy between the LBP-histograms of a changed texture and the original. We make use of a database, which consists of images exhibiting transitional changes of texture. The progressive change in texture with respect to the original is represented with a monotonic change in the metric. Appropriate statistics can be computed if using several sample images of each progressive texture change. Then, we are interested in identifying from a set of LBP techniques, those that ensure a monotonic relationship of the texture changes with the metric while offer a clear distinction between the sets of measures corresponding to consecutive texture changes. Besides, we prefer those techniques where the ratio between the measure variation of each particular texture change and all measures is minimal. Therefore, we quantify the degree monotonicity of the metrics as function of the texture change, the ratio between the variability of measures corresponding to each texture change and the variability of measures for all measures as well as the separation between measures of consecutive texture changes. The results of this approach can be of use for further research in similar applications where fine changes in texture need to be differentiated.

9138-19, Session 5

Texture descriptor approaches to level set segmentation in medical images

Jimena Olveres, Rodrigo Nava, Univ. Nacional Autónoma de México (Mexico); Ernesto Moya-Albor, Univ. Panamericana (Mexico); Boris Escalante-Ramírez, Univ. Nacional Autónoma de México (Mexico); Jorge Brieva, Univ. Panamericana (Mexico); Gabriel Cristóbal, Consejo Superior de Investigaciones Científicas (Spain); Enrique Vallejo, Hospital Ángeles Pedregal (Mexico)

Medical image analysis has become an important tool for improving medical diagnosis and planning treatments. It involves volume or still image segmentation which plays a critical role in understanding image content by facilitating extraction of the anatomical organ or region-of-interest. Also it may help towards the construction of reliable computer-aided diagnosis systems. In recent years, level set methods have emerged as a general framework for image segmentation; such methods are mainly based on gradient information and provide satisfactory results. However, the noise inherent to the images and the lack of contrast information between adjacent regions hamper the performance of the algorithms, thus, others proposals have been suggested in the literature. For instance, characterization of regions as statistical parametric models to handle the evolution of level sets. In this paper we study the influence of texture on a level-set-based segmentation. In addition to image gray level values, we propose the use of different texture descriptors such as the Hermite transform and local binary patterns for characterizing object regions. The resulting features are incorporated into the level set model to improve organ segmentation. We assess several algorithms on different medical images modalities and compare their performance using standard Hausdorff distance.

9138-20, Session 5

Knee cartilage segmentation using active shape models and local binary patterns

German A. Gonzalez, Boris Escalante-Ramírez, Univ. Nacional Autónoma de México (Mexico)

Segmentation of knee cartilage has been useful for opportune diagnosis and treatment of osteoarthritis (OA). This paper presents a semiautomatic segmentation technique based on Active Shape Models (ASM) which uses Local Binary Patterns (LBP) to describe the surrounding texture of femoral cartilage. The proposed technique is tested on a 16-image of magnetic resonance database of different patients and it is validated through Leave-One-Out method. We compare this technique (ASM-LBP) with ASM algorithm proposed by Cootes and the results show that ASM-LBP has better performance and average Dice Simmilarity Coefficient (DSC) values than ASM by Cootes in whole cases. Furthermore, we add a routine which improves the robustness versus two principal problems: oversegmentation and inicialization.

9138-21, Session 5

Sparsity optimized compressed sensing image recovery

Sha Wang, Yueting Chen, Huajun Feng, Zhihai Xu, Qi Li, Zhejiang Univ. (China)

Compressed sensing (CS) is an emerging framework stating that sparse signals which have a concise linear representation on an appropriate basis can be exactly recovered from a number of linear projections considerably lower than the Shannon-Nyquist Theorem required. This means that instead of sensing an image using millions of pixels to obtain high resolution, the image can be sensed directly in compressed form. Sampling a relatively small number of projections depends on the actual sparsity of the image. Image sparsity depends on the representing basis and among which, the overcomlete dictionary are the better one and they are very suitable to sparsely describe images. The performance of sparse recovery using compressed measurements improves when the dictionaries learned from training data rather than predefined dictionaries. Training overcomplete dictionaries which facilitate a sparse representation of the image leads to state-of –art results in image restoration. When training the dictionary, the training sparsity of the trained images should be specified first. Then the trained dictionary will be used in the reconstruction stage and the recovered sparsity of the recovered image should be set as well. We find that the recovered sparsity has significant effects on the image reconstruction properties.

To further improve the compressed sensing image recover accuracy, in this paper, we proposed a method which is mainly by optimal estimation of the recovered sparsity according to the given sparsity of the trained dictionary and with the optimized sparsity to control the reconstructing method, and better reconstruction results can be achieved successfully. Our method mainly includes three main procedures. Firstly, forecasting the possible sparsity range by analyzing our large test data to obtain a possible sparsity set. We find that the possible sparsity are always 3-5 times of the sparsity specified in the dictionary training. Secondly, to precisely estimate the optimal recovered sparsity, we only choose several samples randomly from the compressed sensing measurements and using the sparsity candidates in the possible sparsity set as the dictionary parameters to reconstruct the original image patches. As the several samples are randomly chosen from the original measurements, the reconstruction results are credible. Thirdly, choosing the sparsity corresponding to the best recover result as the optimal sparsity and adopting which to be the control parameter in dictionary based compressed sensing image reconstruction. As the training sparsity can be specified according to the RIP (Restricted Isometry Property) condition, when given the training sparsity, the optimal sparsity can be estimate from one of the three candidates in the possible sparsity set. Therefore, the estimation computation cost is relatively small and the reconstruction result can be much better than the traditional compressed sensing method. The experimental results show that, the peak signal-to-noise ratio (PSNR) index of the recovered images which adopting our estimation method can be higher up to 4dB compared to the traditional method without the sparsity estimation.

9139-15, Session PS3

Automatic 2D to 3D video conversion implemented for real-time applications

Volodymyr Ponomaryov, Instituto Politécnico Nacional (Mexico); Eduardo Ramos-Diaz, Univ. Autónoma de la Ciudad de Mexico (Mexico); Victor Gonzalez-Huitron, Instituto Politécnico Nacional (Mexico)

Disparity map (DM) estimation is one of the principal problem in 3D viewing but still a very difficult problem for rendering 3D perception in images precisely. DM enhancement can open a wide variety of novel research topics and applications, such as virtual view synthesis, high performance imaging, image/video segmentation, object recognition, environmental surveillance, remote education, industrial inspection, 3DTV, etc.

There are a number of manual techniques that are currently used in DM reconstruction, such as hand drawn object outlines manually associated with an artistically chosen disparity value; a semiautomatic outlining with corrections made manually by the operator, etc. Such manually and semiautomatic methods could produces high quality disparity maps but there are very time consuming and expensive. In automatic techniques, literature distinguishes between local and global methods. Local methods such as block matching or optical flow estimation define the constraints for small regions surrounding the pixel of interest for which correspondences in another view is searched. Global methods define constraints for the entire image in the form of a coast function, which is then minimized by means of global optimization such as graph cuts, belief propagation or simulation annealing.

Hardware implementation of an automatic 3D color video generation based on 2D real video sequences is presented in this paper. The proposed framework includes neighboring frames processing using the following blocks: CIELab color space conversion, wavelet transform, edge detection using HF sub-bands (HL, LH and HH), color segmentation via k-means on a*b* color components, up-sampling, disparity estimation, adaptive post-filtering, and finally, the anaglyph 3D generation. Edge detection is implemented as follows: for each wavelet sub-band, the Donoho threshold is computed, then each sub-band is binarized with its respective threshold, next, the sub-band images are added. Disparity map (DM) estimation is realized employing the following procedure: in left stereo image, the windows with different sizes are used according to information obtained from binarized sub-band image, distinguishing different texture areas into LL sub-band image. Once the different window sizes are found, the stereo matching is computed between two LL sub-band images: left and right. Finally, up-sampling is employed in order to obtain the DM. Adaptive post-processing procedure is based on median filter and k-means segmentation in a*b* component plane where for each from four clusters the median filtering is used in 11 x 11 processing window. The SSIM and QBP criteria are used in order to justify the performance of the proposed procedure. Numerous simulation results confirm that novel approach appears to perform better than other state-of-art techniques. The proposed technique has been performed on the DSP TMS320DM648, Matlab's Simulink module over a PC with Windows 7 and using graphic card (NVIDIA® Quadro® K2000) demonstrating that the proposed approach can be applied in real-time processing mode.

9139-16, Session PS3

Image resolution enhancement using edge extraction and sparse representation in wavelet domain for real-time applications

Volodymyr Ponomaryov, Herminio Chavez-Roman, Victor Gonzalez-Huitron, Instituto Politécnico Nacional (Mexico)

The images and video sequences that register from radar, optical, medical and other sensors and that are presented on high-definition television, in electron microscopy, etc. are obtained from electronic devices that use a variety of sensors. Therefore, pre-processing technique that permits enhancement of image resolution should be used. This step can be performed estimating a HR image from measurements of an LR image that were obtained through a linear operator that forms a degraded version of the unknown HR image, which was additionally contaminated by a noise. In most applications, the degraded operator can be treated as a subsampling procedure that should be inverted to restore an original image size. Therefore, this problem usually should be treated as an ill-posed problem.

A number of approaches have been proposed to use in the design of SR algorithms. The nearest neighbor algorithms use interpolation on the closest pixels. It is also possible to use bilinear interpolation, the bi-cubic interpolation algorithm, or the Lanczos interpolation that is superior in comparison with their classic counterparts. There exist a number of fuzzy logic methods and techniques based on the spline technique. Simple interpolation-based methods such as bilinear or bi-cubic interpolation tend to produce HR images with jagged edges; this is a common effect of many SR algorithms.

The predominant challenge of this study is to employ an approach that uses wavelet transform space, accounting for both spatial and spectral wavelet pixel information to enhance the resolution of a single image that can also be expanded to video sequences. This paper presents the design a novel framework in the image resolution enhancement from a single input image employing the wavelet domain techniques. The principal idea of proposed approach in super-resolution (SR) consists of using edge preservation procedure and mutual interpolation between the input low-resolution (LR) image and the HF sub-band images performed via the Discrete Wavelet Transform (DWT). In the designed SR procedure, the LR image is used in the sparse representation for the resolution-enhancement process, employing a 1-D interpolation in the given angle directions; following, the computations of the new samples along all oversampled rows, columns or diagonals are found, estimating the missing samples. Finally, pixels are performed via the Lanczos interpolation. To preserve more edge information, it has been proposed an extraction step of the edge HF sub-bands that employs the first level in the DWT decomposition from an input image. The differences between the LL sub-band image and LR input image is used in the intermediate process to correct the estimated HF component, generating a significantly sharper reconstructed SR image.

Additionally, the novel framework employs a denoising procedure by using the Non-Local Means for the input LR image.

An efficiency analysis of the designed and other state-of-the-art filters have been performed on the DSP TMS320DM648 by Texas Instruments through MATLAB's Simulink module and on the video card (NVIDIA® Quadro® K2000), showing that novel SR procedure can be used in real-time processing applications.

Experimental results have confirmed that designed framework outperforms existing SR algorithms in terms of objective criteria (PSNR, MAE and SSIM) as well as in subjective perception, justifying better image resolution.

9139-17, Session PS3

An automatic lesion detection using dynamic image enhancement and constrained clustering

Jean M. Vianney-Kinani, Alberto J. Rosales-Silva, Francisco J. Gallegos, Instituto Politécnico Nacional (Mexico); Alfonso Arellano, Instituto Nacional de Neurología y Neurocirugía (Mexico)

In this work, we present a fast and robust practical tool for detection of lesions with minimal user interaction to assist clinicians and researchers in radiosurgery planning and assessment of the response to the therapy. Particularly, a fuzzy image enhancement is performed on T1 weighted magnetic resonance (MR) images so as to facilitate a better segmentation that leads to a clear-cut detection. First, we establish a fuzzy system that performs the intensity transformation through the implication method, then, the scalar output obtain from this system is used to separate the healthy structures from the unhealthy ones using constrained fuzzy clustering, and finally with minimal user interaction, the lesion contour is outlined through the level set methods, thus turning the algorithm into an indispensable tool for the spatially localized radiotherapy planning and response assessment, which is typically done manually in current clinical practice. Another key advantage of this lesion detection pipeline is the simultaneous use of features computed from the intensity properties of the image in a cascading pattern which makes the computation fast, robust and self-contained. We empirically validate our algorithm with large scale experiments using both clinical and synthetic brain lesion datasets, and an 88%–95% overlap performance of the proposed algorithm was attained with an emphasis on robustness with respect to different and heterogeneous lesion types, and its efficiency in terms of computation time.

9139-18, Session PS3

Dual-wavelength diffraction phase microscopy

Mohammadreza Jafarfard, Ctr. for 3D Nano Optical Imaging System (Korea, Republic of)

We introduce and experimentally demonstrate a single shot dual-wavelength diffraction phase microscopy (DW-DPM) with the highest stability and speed of measurement to solve ambiguity of phase by separately measuring both the refractive index (RI) and the sample thickness. Using common path interfrometery, it provides sub-nanometer temporal stability and because of single shot measurement its speed is in order of millisecond. The setup is quiet simple to be manipulated and need just a few optical components more than a conventional microscope. The potential of this technique for the simultaneous measurement of RI and morphology is demonstrated by accurate measurement of two kind of known samples.

9139-20, Session PS3

Feature selection gait-based gender classification under different circumstances

Azhin T. Sabir, Naseer Al-Jawad, Sabah A. Jassim, The Univ. of Buckingham (United Kingdom)

This paper proposes Gender classification based on human gait features and investigates the problem of two variations; clothing (wearing coats) and carrying bag condition as addition to the normal gait sequence. The feature vectors in the proposed system are constructed after applying wavelet transform. Three different sets of feature are proposed in this method. First, Spatio-Temporal distances that are dealing with the distance of different parts of the human body (like feet, knees, hand, Human Height and shoulder) during one gait cycle. The second and third feature sets are constructed from approximation and non-approximation coefficient of human body respectively. To extract these two sets of feature we divided the human body into two parts; upper and lower body part, based on the golden ratio proportion. The second set extracted from wavelet level three low frequency sub-band and the third set of feature is extracted from wavelet high frequency sub-bands.

In this paper, we have adopted a statistical method for constructing the feature vector from the above sets. The dimension of the constructed feature vector is reduced based on the Fisher score as a feature selection to optimize their discriminating significance. Finally k-Nearest Neighbor is applied as a classification method. For testing the performance of our method we used CASIA B gait database that composes gait sequences of 124 subjects, which are unequally distributed (i.e. Contains 31 females and 93 males).

From the gender point of view, this database has imbalanced number of subjects. To overcome this problem, we proposed a way for testing the performance by selecting randomly equal subset of males and females. Different experiments run separately and repeated many times (for each time different training set is generated and used) to cover the entire subjects in the database and to make the achieved result more reliable compared with the existing approaches.

The proposed method is tested based on three different modules of human gait; normal sequences, carrying bag sequences, and wearing-coat sequences. All the three modules are classified based on normal walking sequences as a training set. Experimental results show that fusing the three mentioned sets of feature offer significant results by achieving recognition rate (97.6%, 90.1%, and 87.4%) for (normal, carrying bag, and wearing-coat) gait sequences respectively.

The performed results confirm that normal walking sequences provide better performance as compared to wearing-coat and carrying bag sequences, because of two reasons; First, clothes and carrying conditions are affect the human gait features and they change human body module. Second, in this experiment we used more realistic way by using only normal gait sequences as training for the three modules. Experimental results show that our approach is providing more realistic scenario and better performance compared with the existing approaches.

9139-21, Session PS3

Software architecture as a freedom for 3D content providers and users along with independency on purposes and used devices

Razia Sultana, Andreas Christ, Hochschule Offenburg (Germany); Patrick Meyrueis, Univ. de Strasbourg (France)

The improvements in the hardware and software of communication devices have allowed running Virtual Reality (VR) and Augmented Reality (AR) applications on those. Nowadays, it is possible to overlay synthetic information on real images, or even to play 3D on-line games on PDAs, smart phones or some other mobile devices. Hence the use of 3D data for business and specially for education purposes is ubiquitous. Due to always available at hand and always ready to use properties of mobile phones, those are considered as most potential communication devices. The total numbers of mobile phone users are increasing all over the world every day and that makes mobile phones the most suitable device to reach a huge number of end clients either for education or for business purposes. There are different standards, protocols and specifications to establish the communication among different communication devices but there is no initiative taken so far to make it sure that the send data through this communication process will be understood and used by the destination device. Since all the devices are not able to deal with all kind of 3D data formats and it is also not realistic to have different version

of the same data to make it compatible with the destination device, it is necessary to have a prevalent solution. The proposed architecture in this paper describes a device and purpose independent 3D data visibility any time anywhere to the right person in suitable format. There is no solution without limitation. The architecture is implemented in a prototype to make an experimental validation of the architecture which also shows the difference between theory and practice.

9139-22, Session PS3

Comparative study of Internet cloud and cloudlet over wireless mesh networks for real-time applications

Kashif A. Khan, Qi Wang, Chunbo Luo, Xinheng Wang, Christos Grecos, Univ. of the West of Scotland (United Kingdom)

Mobile cloud computing is receiving world-wide momentum for ubiquitous on-demand cloud services for mobile users provided by Amazon, Google etc. with low capital cost. However, Internet-centric clouds introduce WAN delays that are often intolerable for real-time applications such as video streaming. One promising approach to addressing this challenge is to deploy decentralized mini-cloud facility known as cloudlets to enable localized cloud services. When combined with local wireless connectivity, a wireless cloudlet is expected to offer low cost, high performance cloud services for the users.

Nevertheless, insightful and numerical comparison of the two different cloud networking architectures (cloudlet and the Internet cloud) for real-time applications is still largely missing in the literature. In this work, we implement a realistic framework that comprises both a popular Internet cloud (Amazon Cloud) and a real-world cloudlet (based on Ubuntu Enterprise Cloud) for mobile cloud users in a wireless mesh network. We employ and focus on real-time video streaming over the HTTP/HTTPS standard as a typical application, and perform a comprehensive comparative analysis and empirical evaluation of the application's performance when it is delivered over the Internet cloud and the cloudlet respectively. The study quantifies the influence of the two different cloud networking architectures on supporting real-time video streaming. We also enable movement of the users in the wireless mesh network and investigate the effect of user's mobility on mobile cloud computing over the cloudlet and Amazon cloud respectively. Furthermore, the paper analyzes the advantages and disadvantages of both cloud networking architectures, and investigates optimized integration and cooperation of Internet clouds and cloudlets for business-oriented cloud services through quality of service awareness and traffic engineering.

9139-23, Session PS3

Empirical evaluation of H.265/HEVC-based dynamic adaptive video streaming over HTTP (HEVC-DASH)

Iheanyi C. Irondi, Qi Wang, Christos Grecos, Univ. of the West of Scotland (United Kingdom)

Real-time HTTP streaming has gained global popularity for delivering video content over the Internet. In particular, the recent MPEG-DASH (Dynamic Adaptive Streaming over HTTP) standard enables on-demand, live, and adaptive Internet streaming in response to network bandwidth fluctuations. Meanwhile, emerging is the new-generation video coding standard, H.265/HEVC (High Efficiency Video Coding) promises to reduce the bandwidth requirement by 50% at the same video quality when compared with the current H.264/AVC standard. However, little existing work has addressed the integration of the DASH and HEVC standards, let alone empirical performance evaluation of such systems.

This paper presents an experimental HEVC-DASH system, which is a pull-based adaptive streaming solution that delivers HEVC-coded video content through conventional HTTP servers where the client switches to its desired quality, resolution or bitrate based on the available network bandwidth. Previous studies in DASH have focused on H.264/AVC, whereas we present an empirical evaluation of the HEVC-DASH system by implementing a real-world test bed, which consists of an Apache HTTP Server with GPAC, an MP4Client (GPAC) with openHEVC-based DASH client and a NETEM box in the middle emulating different network conditions. We investigate and analyse the performance of HEVC-DASH by exploring the impact of various network conditions such as packet loss, bandwidth and delay on throughput and video quality. Furthermore, we compare the Intra and Random Access profiles of HEVC coding with the Intra profile of H.264/AVC when the correspondingly encoded video is streamed with DASH. Finally, we explore the correlation among the quality metrics and network conditions, and empirically establish under which conditions the different codecs can provide satisfactory performance.

9139-24, Session PS3

Network-aware scalable video monitoring system for emergency situations with operator-managed fidelity control

Tawfik A. Al Hadhrami, James M. Nightingale, Qi Wang, Christos Grecos, Univ. of the West of Scotland (United Kingdom)

In emergency situations, the ability to remotely monitor unfolding events using high-quality video feeds will significantly improve the incident commander's understanding of the situation and thereby aids effective decision making. This paper presents a novel, adaptive video monitoring system for emergency situations where the normal communications network infrastructure has been severely impaired or is no longer operational. The proposed scheme, operating over a rapidly deployable wireless mesh network, supports real-time video feeds between first responders, forward operating bases and primary command and control centres. Video feeds captured on portable devices carried by first responders and by static visual sensors are encoded in H.264/SVC, the scalable extension to H.264/AVC, allowing efficient, standard-based temporal, spatial, and quality scalability of the video.

A three-tier video delivery system is proposed, which balances the need to avoid overuse of mesh nodes with the operational requirements of the emergency management team. In the first tier, the video feeds are delivered at a low spatial and temporal resolution employing only the base layer of the H.264/SVC video stream. Routing in this mode is designed to ensure fair use of all nodes across the entire mesh network. In the second tier, whenever operational considerations require that commanders or operators focus on a particular video feed, a 'fidelity control' mechanism at the monitoring station sends control messages to the routing and scheduling agents in the mesh network, which increases the quality of the received picture using SNR scalability while conserving bandwidth by maintaining a low frame rate. In this mode, routing decisions are based on reliable packet delivery with the most reliable routes being used to deliver the base and lower enhancement layers; as fidelity is increased and more scalable layers are transmitted they will be assigned to routes in descending order of reliability. The third tier of video delivery transmits a high-quality video stream including all available scalable layers using the most reliable routes through the mesh network ensuring the highest possible video quality.

The proposed scheme is implemented in a proven simulator, and the performance of the proposed system is numerically evaluated through extensive simulations. We further present an in-depth analysis of the proposed solutions and potential approaches towards supporting high-quality visual communications in such a demanding context.

9139-25, Session PS3

Scene-based nonuniformity correction using multiframe registration and iteration method

Jianle Ren, Qian Chen, Guohua Gu, Xuelian Yu, Danping Li, Nanjing Univ. of Science and Technology (China)

In this paper, an improved scene-based nonuniformity correction(NC) algorithm for infrared focal plane arrays(IRFPAs) using multiframe registration and interation is proposed. This method estimates the global translation and iterates between several adjacent frames. Then mean square error between any two properly registered images is minimized to obtain nonuniformity correction parameters. The detailed method includes three main steps: First, we assume that brightness along the motion trajectory is constant, and a linear detector response and model the nonuniformity of each detector with a gain and a bias. Second, several adjacent frames are used to compute relative motion of any two adjacent frames. Here we use the Fourier shift theorem, their relative translation can be obtained by calculating their normalized cross-power spectrum. We choose N adjacent frames, so the total number of iteration is N*(N+1)/2. Then the mean square error function is defined as the corresponding difference between the two adjacent corrected frames, and it is minimized making use of the least mean square algorithm. The use of correlation of adjacent frames sufficiently, together with iteration strategy between them, can get fast and reliable fixed-pattern noise reduction with low few ghosting artifacts. We define the algorithm and present a number of experimental results to demonstrate the efficacy of the proposed method in comparison to several previously published methods. The performance of the proposed method is thoroughly evaluated with clean infrared image sequences with synthetic nonuniformity and real infrared imagery.

9139-26, Session PS3

Visible projection of the near-infrared fluorescence image by a novel positioning system

In Hee Shin, Korea Photonics Technology Institute (Korea, Republic of); Seok-ki Kim, National Cancer Ctr. (Korea, Republic of); Joo Beom Eom, Jae Seok Park, Hyeong Ju Park, Korea Photonics Technology Institute (Korea, Republic of); In-Kyu Park, Chonnam National Univ. Medical School (Korea, Republic of); Byeong-Il Lee, Korea Photonics Technology Institute (Korea, Republic of)

Although near infra-red fluorescence (NIR) imaging has many advantages in sentinel lymph node(SLN) mapping and cancer detection, it shows a serious drawback that NIR cannot be detect by the naked eye without any detectors. This limitation further disturbs accurate SLN detection and adequate tumor resection resulting in the presence of cancerous cells near the boundaries of surgically removed tissues.

To overcome the drawback of the conventional NIR imaging method, a novel NIR imaging system that it can make the NIR fluorescence image visible to the naked eye as NIR fluorescence image detected by a video camera is processed by a computer and then projected back onto the NIR fluorescence excitation position with a projector using conspicuous color light has been developed recently.

In this paper, we implemented a phantom experiment to evaluate the performance of the developed NIR fluorescence projection system by use of the Indocyanine Green (ICG). Also, we applied the developed NIR fluorescence projection system in normal mouse model to confirm the usefulness of the system in clinical field. In normal mouse mode, a BALB/c nude mouse was prepared to be applied and 0.25mg/ml stock solution of the ICG was injected through a tail vein of the mouse.

From the application in normal mouse model, we could confirm that the injected ICG stayed in the liver of the mouse and verify that the projection system projected the ICG fluorescence image at the exact location of the ICG by performing laparotomy of the mouse.

From the experimental results, we could confirm that the NIR fluorescence projection system can make it possible to visualize the invisible NIR fluorescence image and to realize that SLN mapping and cancer detection in clinical surgery.

9139-27, Session PS3

Adaptive skin segmentation via feature-based face detection

Michael J. Taylor, Tim Morris, The Univ. of Manchester (United Kingdom)

Varying illumination can have significant effects on the apparent colour of skin, which can be damaging to the efficacy of any colour-based segmentation approach. We attempt to overcome this issue by presenting a new adaptive approach, capable of generating skin colour models at run-time. Our approach utilises a Viola-Jones feature-based face detector in a moderate-recall, high-precision configuration to sample faces within an image, with an emphasis on avoiding potentially harmful false positives. Determined empirically, these results tend to be overestimates of actual face sizes, and will typically contain some background information, so we define subregions within them that we can be confident represent only faces, from which we extract pixels as candidates to build our skin colour model. Prior to this, however, the candidates must be filtered in order to eliminate uninteresting features that can reasonably be expected to appear in our subregions. Thankfully, these features will typically share a common trait - extreme intensity. Features such as facial hair, nostrils, and inner eyes (irises and pupils) tend to be dark, and have low intensities, whereas features such as teeth, outer eyes, and reflective glasses or jewellery are usually much brighter than skin, and have high intensities. Based upon this knowledge, the filtration of these features consists of establishing the standard deviation of the luma (the weighted RGB intensity sum) of the extracted pixels, and then rejecting any that are, therefore, considered to be outliers. Now with a set of pixels that we can confidently consider to be representative of skin within the given image, we train a Gaussian function to model the skin colour in the normalised rg colour space. Operating within the normalised rg space affords us several benefits. Firstly, given that it represents colour components merely by their proportions in the given colour, rather than by their independent intensity, it is inherently resistive to the effects of illumination variation. Secondly, and importantly for the purposes of efficient, run-time modelling, it allows us to reduce the dimensionality of our modelling problem from a 3D space to a 2D space. The choice of a two-dimensional Gaussian function as our modelling method is similarly ideal. Because our given set of “skin” pixels can only ever be considered, at best, a mere subset of all actual skin pixels within the given image, the capacity a Gaussian function has to interpolate skin colours not necessarily represented by our extracted and filtered set is extremely useful. Additionally, unlike a number of other training processes, a Gaussian function needs only our positive samples in order to be built, which is beneficial because it is not possible to establish true negative samples at run-time using a methodology such as ours. Once the parameters of our Gaussian function (simply in terms of mean and covariance matrix) have been determined, the probability (on a 0.0 - 1.0 scale) that any pixel within the given image represents skin can be calculated, and when used in conjunction with a probability threshold (typically 0.5), all pixels can be classified, and skin successfully segmented. The results of implementing this process have been extremely encouraging. It has been tested using a wide variety of input images, with different environments, various lighting conditions, and the numbers of subjects ranging from just one to several dozen, and in comparison to several other pixel-based techniques, the overall accuracy of our approach has proven to be highly competitive, and often outstanding.

9139-28, Session PS3

The wide-area retrievals of temperature in life space from multidata set fusion

DongYeob Han, Chonnam National Univ. (Korea, Republic of)

Heat wave is one of the phenomena stemmed from abnormal climate caused by climate change. This phenomenon which occurs strongly and frequently worldwide recently has been threatening the heath-vulnerable classes in the urban and suburb area. To reduce the damage from the heat wave, the current research attempts to perform data assimilation between high-resolution images and ground observation data based on middle infra-red satellite imagery. We use an integrated approach involving compilation of both spatial and non-spatial data from government agencies and institutions, application of spatial and temporal analyses using remote sensing data. Seven major land-use categories (Built-up, Road, Agriculture (green house, paddy fields, and dry fields), Field of construction work, Vegetation (forests), Wasteland and Water bodies) were obtained based on the topographic data, satellite imagery, and cadastral information. The four land-uses were selected as the most strongly areas affected by heat waves according to the survey of National Emergency Management Agency. The near real-time temperature retrievals of selected areas are performed and analyzed using thermal data from smartphone temperature sensor, Landsat, and MODIS imagery. And, this paper also includes the relation between NDVI and ground weather observation data from Korea meteorological administration. In the future, we will estimate the precise wide area temperature of life space and promote the application of the heat/health watch/warning system.

9139-29, Session PS3

Moving targets tracking on a mobile infrared platform and its real-time application on GPU

Chen Peng, Qian Chen, Weixian Qian, Nanjing Univ. of Science and Technology (China); Zhuang MIAO, Science and Technology on Low-Light-Level Night Vision Laboratory (China); Xiao-yi Jing, East China Institute of Photo-Electronics (China)

In the vision from a mobile infrared platform, the background scene keeps changing due to the moving camera, which results in more background clutter and noise. In this condition, it is difficult to track the target rely on brightness or gradient information. In this paper, we present a new tracking algorithm which segments the moving target according to the difference of velocity field between the target and background. In the proposed algorithm, the phase correlation method is introduced to transform two adjacent frames into one coordinate to remain a relatively static background. And then the improved Horn-Schunck optical flow is calculated in the tracking window to estimate the velocity field of the target. Finally we introduce the particle filter algorithm to estimate the location of the target, which has a more robust performance by optimizing the transition probability of particles with features of optical flow. Our algorithm can be organized in parallel processing mode enabled for GPU. By parallel computing, our algorithm is computationally efficient that it can work in real time. Experimental results show that the proposed algorithm can track the infrared target in real time on a moving platform.

9139-1, Session 1

Deriving video content type from H.265/HEVC bitstream semantics *(Invited Paper)*

James M. Nightingale, Qi Wang, Christos Grecos, Univ. of the West of Scotland (United Kingdom); Sergio R Goma, Qualcomm Inc (United States)

As network service providers seek to improve customer satisfaction and retention levels, they are increasingly moving from traditional quality of service (QoS) driven delivery models to customer-centred quality of experience (QoE) delivery models. QoS models only consider metrics derived from the network, whereas QoE models also consider metrics derived from within the video sequence itself. Previous studies have shown that video content type plays a major role in QoE modelling. Various spatial and temporal characteristics of a video sequence have been proposed, both individually and in combination, to derive methods of classifying video content either on a continuous scale or as a set of discrete classes. QoE models can be divided into three broad categories, full reference, reduced reference and no reference models. Due to the need to have the original video available at the client for comparison, full reference metrics are of limited practical value in real-time adaptive video applications. Reduced reference metrics often require metadata to be transmitted with the bitsream, while no reference metrics typically operate in the decompressed domain at the client side and require significant processing to extract spatial and temporal features.

Notably, little existing work has addressed content type classification in the context of the new H.265/HEVC standard, which employs new coding structure that is significantly different from the current H.264 and previous standards. This paper proposes a heuristic, no reference approach to video content classification which is specific to H.265/HEVC encoded bitstreams. The H.265/HEVC encoder makes use of both spatial characteristics to determine partitioning of coding units and temporal characteristics to determine the splitting of prediction units. We derive a novel function that approximates the spatio-temporal characteristics of the video sequence by using the weighted averages of the depth at which the coding unit quadtree is split and the shape and depth of prediction unit splitting to estimate spatial and temporal characteristics respectively. Since the video content type of a sequence is determined by using high level information parsed from the video stream, spatio-temporal charachertistics are identified without the need for full decoding and can thus be utilised in a timely manner to aid decision making in QoE oriented adaptive real time streaming. Comparisons with well-known spatio-temporal methods of determining content type show our method to correlate well with a mean accuracy of 78%.

9139-3, Session 1

The novel optical flow tracking technology for moving targets under complex background

Lei Liu, Zhijian Huang, Nanjing Univ. of Science and Technology (China)

With the continuous development of science and technology, infrared imaging technology has played an important role in national defense, medical, transportation and other areas. The tracking technology of small infrared target is an important branch of infrared imaging technology, which has not only very important scientific research value, but also has broad application prospect in the military and civil area.

Nowadays, different algorithms have been proposed for infrared target tracking. However, under complex backgrounds, such as clutter, varying illumination, and occlusion, the traditional tracking method often loses the real infrared small target.

To cope with these problems, firstly we have studied three infrared target tracking algorithms to enhance the tracking performance according to the characteristics of the small target in infrared images, namely, Mean shift algorithm, Optical flow method and Particle filter method. The basic principles and the implementing procedure of these algorithms for target tracking are described. Secondly, infrared small target tracking software is developed by a human-computer interaction interface created by MFC in VC++ combined with many functions in OpenCV so as to realize these three tracking algorithms. Lastly, a performance assessment conclusion is made by analyzing the experiment results. The experimental results show that,

compared with the traditional algorithm, the presented method greatly improves the accuracy and effectiveness of infrared target tracking under complex scenes, and the results are satisfactory. It is of great significance for actual application of small infrared target tracking technology.

9139-4, Session 1

New boundary effect free algorithm for fast and accurate image arbitrary scaling and rotation

Leonid Bilevich, Leonid P. Yaroslavsky, Tel Aviv Univ. (Israel)

A new fast DCT-based algorithm for accurate image arbitrary scaling and rotation is described. The algorithm is free from boundary effects characteristic for FFT-based algorithm and ensures perfect interpolation with no interpolation errors.The algorithm is compared with other available algorithms in terms of the interpolation accuracy, computational complexity and suitability for real time applications.

9139-5, Session 1

Comparative analysis of real-time video streaming for 3D cloud video games using different virtualization technologies

Adedayo A. Bada, Jose Alcaraz-Calero, Qi Wang, Christos Grecos, Univ. of the West of Scotland (United Kingdom)

The usage of virtualization clearly maximizes the efficient utilization of the huge resources available in cloud infrastructures. This has led to a more user-centric hardware customization of servers by means of the usage of various virtualization technologies like Xen, KVM, VMware and VirtualBox etc. The deployment of such technologies has brought new challenges in the virtualized systems in terms of security, performance, isolation, etc. One clear challenge is the ability to cope with demanding visual communication tasks such as 3D graphics rendering which is essential in many popular real-time video applications. Currently, the emulated video cards available in the virtualized systems typically are unable to provide high quality 3D videos in real-time as against physical graphics adapters. Furthermore, computational resources, high network bandwidth requirement, and low power 3D graphics adaptors of most client devices pose a big challenge to render 3D videos in real-time on the client for cloud scenarios.

It is imperative to systematically investigate the factors that affect the overall performance of real-time 3D video streaming in a cloud gaming environment. This paper describes a comprehensive empirical performance evaluation of the physical/virtual architecture implemented in a cloud environment based on OpenStack. Different virtualization technologies and virtual video cards have been used for carrying out this analysis and also various 3D benchmarks tools have been utilized in order to analyse the optimal performance in the context of 3D online gaming applications. This study highlights 3D video rendering performance under each type of hypervisor when factors like Network I/O, Disk I/O, Memory usage and Virtual disk format are explored in the cloud environment. Comparisons of these factors under well know virtual display technologies such as VNC, Spice and Virtual 3D adaptors reveals the strengths and weaknesses of the various hypervisors with respect to 3D video rendering and streaming.

9139-19, Session 1

Real-time system for early video smoke detection to improve fire protection in rolling stocks

Sergio Saponara, Luca Pilato, Luca Fanucci, Univ. di Pisa (Italy)

Using video and image processing to detect fire smoke is an innovative technique for fire protection or monitoring system. Nowadays this technology is adopted for manufacturing plants, wide storage areas and surveillance of wide forests or natural sites.

All the above systems are integrated in a CCTV network, using visible spectrum cameras. Vision-based smoke detection systems have not been proposed yet for fire protection and monitoring in rolling stocks. Aboard trains typically gas-based smoke and fire sensors, working punctually, are adopted. Introducing a vision-based early smoke detection system, thanks to the observation of the whole area, will reduce the response time for fire suppression.

A vision-based smoke detection system, operating on-board trains, has several challenges with respect to those operating in wide plants or forests or storage areas. Indeed, in passenger trains there are many visual obstacle like seats, baggage and moving people. There are also fast luminosity change and out-windows trouble.

Our approach is supporting the fire protection system already installed on rolling stocks, and using local sensors, with a video smoke detector which exploits video surveillance cameras already available on-board the train. To this aim an algorithm is proposed exploiting temporal, spatial and chromatic characteristics of the reference scenario.

Particular features extracted and analyzed by our algorithm are:

- Motion
- Color
- Pixel Intensity Distribution
- Blob Size and Geometric Distribution
- Blob Motion
- Persistence of Localized Smoothness Area
- Space and Time Overlap Alarm Zones

The entire processing flow, described hereafter, has been designed in a modular way. Any step can be replaced with a more efficient or precise one but with increased complexity. This way the desired trade-off between algorithmic accuracy and complexity can be found.

The main innovative contents of the processing flow described in the paper with respect to the state of the art are:

a) Hybrid Motion detection method with Single Difference and Background Subtraction and adopting self adaptive thresholds

b) Boundary Extraction with closed 8-connectivity guaranteed.

c) Persistent Smoothness Condition Management, with its simplicity and effectiveness

The proposed algorithm has been successfully verified with several video set and its implementation complexity fully characterized.

While standard fire sensors need about one minute to reveal fire disaster, the proposed video-based smoke detection requires only a few seconds for every position of fire generation aboard a train.

9139-6, Session 2

Refocusing from a plenoptic camera within seconds on a mobile phone *(Invited Paper)*

Oscar Gomez-Cardenes, José Gil Marichal-Hernandez, Fernando L. Rosa González, Jonas Philipp Lüke, Juan José Fernández-

Valdivia, José Manuel Rodríguez Ramos, Univ. de La Laguna (Spain)

Refocusing a plenoptic image by digital means and after the exposure has been thoroughly studied in the last years, among others by Ren Ng and Todor Georgiev, but few efforts have been put into real time implementation in a constrained environment such as that provided by current mobile phones and tablets, although some companies have announced they are conducting their efforts in this direction.

In this work we address the aforementioned challenge demonstrating that a complete focal stack, comprising 31 refocused planes from a (256x16)^2 plenoptic image, can be achieved within seconds by a current SoC mobile phone platform.

The election of an appropriate algorithm is the key to succeed. In a previous work we developed an algorithm, the fast approximate 4D:3D discrete Radon transform, that performs this task with linear time complexity, O(n), where others obtain quadratic, O(n^2), or linearithmic time complexity, O(n log n). Moreover, that algorithm does not requires complex number transforms, trigonometric calculus nor even multiplications nor float numbers. It elaborates on the multi scale approach pioneered by Götz and Druckmüller; Brady; and Brandt in the context of 2D Hough/Radon transform, but extrapolate it so that it can tackle the 4D plenoptic images as input and give directly as result its 3D focal stack.

Our algorithm has been ported to a multi core ARM chip on an off-the-shelf tablet running Android. In a powerful PC a sequential implementation can hardly remain inside the limit of seconds, hence a careful implementation exploiting parallelism at several levels has been necessary to assure that we remain within seconds in spite of having a much less powerful processor. The final implementation takes advantage of multi-threading in native code to exploit coarse parallelism by having as many cores as available working in different parts of the image. But there is also a lot of fine grain parallelism that can be exploited in a SIMD way, using ARM NEON general-purpose SIMD engine, by realizing that each task can compute the directions of the previous stage and next stage data, and computations associated with those data, with a SIMD multiply-accumulate strategy that works exclusively on packs of unsigned short integers. The memory footprint is under control partially as a consequence of the ability to work exclusively on half precision integers.

As a result our current implementation completes the refocusing task within seconds for a 16 megapixels plenoptic image with microlenses arranged in a rectangular grid, much faster than previous attempts running on powerful PC platforms or dedicated hardware.

The times for the different stages of the digital refocusing are given for a variety of environments within Android ecosystem, from the Mediatek SoCs to the strongest chipsets of Exynos and Snapdragon line of products. We will consider, on future works, to carry out experiments on GPU implementation on Tegra product.

9139-7, Session 2

A low-cost real-time embedded platform for car's surrounding vision system

Sergio Saponara, Giacomo Fontanelli, Luca Fanucci, Emilio Franchi, Univ. di Pisa (Italy)

The use of cameras for automotive applications is growing rapidly, probably because among all the car safety technologies that are spreading, those that stimulate the sight are considered the most immediate and reliable from the drivers. For this reason, a lot of manufacturers are trying to develop solutions always more advanced in this direction, offering technologies for the obstacle's detection, brake assist and some other products to improve vision.

However, the proposed systems are expensive and equipped only on high-end vehicles. Among all the dangerous situations that can be encountered while driving, the most frequent is the one determined by the blind spots: the driver is unable to see all the zones around the vehicle, so some actions can reveal itself source of unwanted accidents. To face this issue the design and the implementation of a flexible and low-cost embedded system for car's surrounding vision is presented in this work. The target of the proposed multi-camera vision system is to provide in real-time the driver with a better view of the objects that surround the vehicle during maneuvering. The purpose of the project is also to develop a low-cost product, so that it can spread even in the low-end of the automotive market.

Fish-eye lenses are used to achieve a larger Field of View (FOV) but, on the other hand, introduce radial distortion of the images projected on the sensors. Using low-cost cameras there could be also some alignment issues. Since these complications are noticeable and dangerous, a real-time algorithm for their correction is presented. Then another real-time algorithm, used for merging 4 camera video streams together in a single view, is described.

The two algorithms have been implemented on a platform equipped with 4 cameras with Aptina MT9V128 sensors, capable of producing video streams at 30 frames/s with PAL resolution, and 4 fish-eye lenses with 173° FOV. The four video streams are combined into a single video stream, always with PAL resolution, using a development board Texas Instruments TVP5154 EVM equipped with a 4-channel multiplexer. The resulting video stream is divided into four quadrants, each of which is coupled to a camera. The quad video stream is then processed through a further development board, Texas Instruments DM642 EVM, equipped with a DM642 DSP at 720 MHz. Roughly 2MB of total memory are required to run the code.

Experimental results are reported obtained when using the proposed algorithms and the relevant implementing platform for a car's parking application scenario.

The discontinuities between the different cameras are perceivable, also because of the difference in brightness and color between the zones. This defect can be eliminated by performing a more accurate calibration of the fish-eye correction algorithm and applying a some kind of interpolation. However, if you consider that the system requires about 2MB of memory to be run, and that the DSP DM642 at 720 MHz is used for about 40% of its total power, the results are satisfactory and leave margins of qualitative improvement or further reduction of the cost, scaling on lower-frequency processors like the Texas Instruments DM368, which is an ARM926 processor at 400 MHz.

9139-8, Session 2

HDR-ARtiSt: a 1280x1024-pixel adaptive real-time smart camera for high-dynamic range video

Pierre-Jean Lapray, Barthélémy Heyrman, Dominique Ginhac, Univ. de Bourgogne (France)

Standard cameras capture only a fraction of the information that is visible to the human visual system. This is specifically true for natural scenes including areas of low and high illumination due to transitions between sunlit and shaded areas. When capturing such a scene, many cameras are unable to store the full Dynamic Range (DR) resulting in low quality video where details are concealed in shadows or washed out by sunlight. The imaging technique that can overcome this problem is called HDR (High Dynamic Range) imaging.

This paper describes a complete smart camera built around a standard off-the-shelf LDR (Low Dynamic Range) sensor and a Virtex 6 FPGA board. This smart camera called HDR-ARtiSt (High Dynamic Range Adaptive Real-time Smart camera) is able to produce a real-time HDR live video color stream by recording and combining multiple acquisitions of the same scene while varying the exposure time. This technique appears as one of the most appropriate and cheapest solution to enhance the dynamic range of real-life environments. HDR-ARtiSt embeds real-time multiple captures, HDR processing, data display

and transfer of a HDR color video for a full sensor resolution (1280 ? 1024 pixels) at 60 frames per second. The hardware implementation on the Virtex 6 shows relatively low hardware resources occupation (about 17% of the device) and a maximum frequency of 125 MHz.

The main contributions of this work are:

(1) Multiple Exposure Control (MEC) dedicated to the smart image capture from the sensor with alternating three exposure times. The MEC evaluates dynamically the adequate exposure times from frame to frame using the histograms and the number of low-level and high-level saturated pixels of each captured frame. Exposure times are evaluated according the following principle: fewer than 10% of the pixels must be saturated at high-level for the short exposure time (respectively at low-level for the long exposure time). If too many pixels are saturated, the exposure time is decreased for the subsequent short exposure captures (respectively increased for the long exposures). Finally, the middle exposure time is linearly computed from the two other exposures.

(2) Multi-streaming Memory Management Unit (MMMU) dedicated to the memory read/write operations of the three parallel video streams, corresponding to the different exposure times. This MMMU continuously manages the storage of 3 frames, the oldest frame being systematically replaced with the new acquired frame. The MMMU is able to capture and store the current stream of pixels from the sensor, and delivers simultaneous 2 pixel streams previously stored to the HDR creating process. With such a memory management, we avoid waiting for the capturing of new 3 frames before computing any new HDR data. Once the initialization is done, our system is synchronized with the sensor framerate (i.e. 60 fps) and is able to produce a new HDR frame for each new capture.

(3) HRD creating by combining the video streams using a specific hardware version of the Devebec's technique, and Global Tone Mapping (GTM) of the HDR scene for display on a standard LCD monitor.

9139-9, Session 2

Gait recognition based on Kinect sensor

Mohammed H. Ahmed, Naseer Al-Jawad, Azhin T. Sabir, The Univ. of Buckingham (United Kingdom)

This paper presents gait recognition based on the human skeleton and trajectory of joint points captured by Microsoft Kinect sensor.

Two sets of dynamic features are extracted during one gait cycle; the first is Horizontal Distance Features (HDF) that is based on the distances between (Ankles, knees, hands, shoulders), the second set is the Vertical Distance Features (VDF), this set provides significant information of human gait that extracted from the height of (hand, shoulder, and ankles) during one gait cycle. Another feature is added to the second set of features, which is triangle created based on hip-center and distance between ankles. These two sets of feature are difficult to be extracted based on gait silhouette accurately, therefore the Kinect sensor is used to determine the precise measurements. The two sets of feature are separately tested and then fused to create one feature vector.

A database has been created in house to perform our experiments; this database consists of sixteen males and four females. For each individual 10 videos have been recorded, each recording includes in average two gait cycles. The Kinect sensor is used here to extract all the skeleton points, and these points are used to build up the feature vectors mentioned above.

K-Nearest Neighbor is used as a classification method based on Cityblock as a distance function. We tested our system by using each set of feature vector separately and then combine both in one set. When HDF used alone the recognition rate achieved is 56%, while VDF provided 83.5% recognition accuracy. When fusing both of the HDF and VDF as one feature vector, the recognition rate increased to 92%, experimental results show that vertical distance features provide significant result.

The result is outperforming the existence technique, for the following reasons; first adding a new set of feature that depends on the vertical feature rather than horizontal feature, moreover these feature cannot be extracted for a traditional gait silhouettes accurately, second getting the extracted features using Kinect sensor point are very precise when compared to these technique that uses tradition camera for getting the human gait.

9139-10, Session 3

Comparison of two real-time hand gesture recognition systems involving stereo cameras, depth camera, and inertial sensor

Nasser Kehtarnavaz, The Univ. of Texas at Dallas (United States); Matthias F. Carlsohn, Computer Vision and Image Communication (Germany); Kui Liu, The Univ. of Texas at Dallas (United States)

This paper presents a comparison of two real-time hand gesture recognition systems. One system utilizes a pair of stereo cameras while the other system utilizes a combination of a depth camera and an inertial sensor. The latter system is a multi-modality system as it utilizes two different types of sensors. These systems have been previously developed in the Signal and Image Processing Laboratory at the University of Texas at Dallas and the details of the algorithms deployed in these systems are reported in [1] and [2]. In this paper, a comparison is carried out between these two real-time systems in order to examine which system performs better for the same set of hand gestures under realistic conditions.

The codes for these systems are written in C both running in real-time on a PC platform having a quad core 1.7GHz processor and 4G of memory. The input images in the stereo camera system are captured by the stereo webcam Novo Minoru, which is an inexpensive stereo webcam. The input data in the fusion system are captured by a Microsoft Kinect camera and a wireless inertial sensor made in the ESSP Lab at the University of Texas at Dallas [3]. The wireless inertial sensor is tied to a subject's wrist.

For comparison, the five single hand gestures that appear in the Microsoft. MSR Action Recognition Dataset [4] are considered. These gestures include 3D and movements made by a single hand. For the multi-modality system, 8-12 HMM states were used as this system uses a HMM classifier to recognize hand gestures based on both the depth camera and the inertial sensor signals. The 3-axis accelerometer and the 3-axis gyroscope signals from the wireless inertial sensor and the 3-axis {X, Y, Z} gradient or position difference signals from the Kinect camera were captured simultaneously to form the observation sequence O = {O1, O2, ..., OT} of the HMM classifier.

The recognition results obtained indicate that the multi-modality system outperforms the stereo system. This is attributed to the fact that the sensors in the multi-modality system act in a complementary manner compensating for each other's errors or deficiencies. Example video clips of these systems operating in real-time can be seen at the websites [6] and [7].

[1] Liu, K., and Kehtarnavaz, N., "Real-time robust vision-based hand gesture recognition using stereo images," Journal of Real-Time Image Processing, online since Feb 2013, print to appear later.

[2] Liu, K., Chen, C., Jafari, R., and Kehtarnavaz, N., "Fusion of inertial and depth sensor data for robust hand gesture recognition," under review IEEE Sensor Journal.

[3] "http://www.essp.utdallas.edu/"

[4] "http://research.microsoft.com/en-us/um/people/zliu/actionrecorsrc/"

[5] Johnson, M., "Capacity and complexity of HMM duration modeling techniques," IEEE Signal Processing Letters, 12(5), 407-410, 2005.

[6] "http://www.youtube.com/watch?v=jYg7U2UYeZo"

[7] "http://youtu.be/GSQrExl81mo"

9139-11, Session 3

3D filtering technique in presence of additive noise in color videos implemented on DSP

Volodymyr Ponomaryov, Hector Montenegro-Monroy, Alfredo Palacio-Enriquez, Instituto Politécnico Nacional (Mexico)

Image filtering has a wide field of applications such as image processing, computer vision, telecommunications, medicine, satellite imaging, robots etc., where the main objective of the denoising procedure is to detect, filter or remove undesired noise from a color image and videos. Noise affects not only the performance of an image in a specific task but also its perceived quality. The most common type of noise encountered in practice is the additive noise that is generally assumed to be a stochastic Gaussian process. Efficient filtering should be performed by obtaining a valid weighting procedure for the pixels in the vicinity of a central one that should be denoised. An important difference between image and color videos filtering is that in videos it is possible to use previous (and/or future) frames for better pixel denoising in the actual frame. However, when two or more frames are processed together for noise removal it should be compensated local motions between different frames, because in other case they can introduce motion blur and ghosting artifacts. Fuzzy-based filters for the reduction of additive noise and other kinds of noises in color videos have been successfully applied. The advantage of fuzzy approach is in the efficient preservation of image features, such as edges, chromaticity characteristics, texture and fine details, while corrupted pixels are being filtered. Several promising filtering procedures have been developed over the past five years, demonstrating good performance quality. These algorithms have shown sufficiently good performance results in removing additive noise, exhibiting good preservation of edges, textures, sharpness and the chromatic properties of the filtered color image or videos. Among them are the better techniques: 3D-LLMMSE, WMVCE, RFMDAF, FDARTF_G, VBM3D, NLM, etc.

The novel fuzzy filtering scheme for the filtering of color videos contaminated by additive Gaussian noise is proposed. A special characteristic of fuzzy filters is their self skill to adapt based on local image data. The novel framework employs three filtering stages: spatial similarity filtering, interframe denoising via compensation of the local motions in neighboring frames, and finally spatial post-processing smoothing. The difference with other state-of-the-art filtering methods is that the novel approach analyzes basic and several related gradient values between neighboring pixels into a 7 X 7 sliding window in the vicinity of a central pixel in each of the RGB channels. Following, the similarity measures using the designed fuzzy logic rules between the analogous pixels in the RGB color bands are taken into account during the denoising. The designed fuzzy rules are used to preserve the image features (textures, edges, chromatic properties, etc.). In the second stage, two neighboring color video frames are analyzed together where the probabilistic local motions between neighboring frames should be estimated via block matching procedure, finding these motions in eight directions, finally permitting to increase the volume of processing data in denoising procedure. In this stage, the edges and smoothed areas in a current frame are distinguished for final post-processing smoothing. Numerous simulations results confirm that this novel 3D denoising filter appears to perform better than other state-of-the-art methods, among them the filters mentioned above in terms of objective criteria (PSNR, MAE, NCD and SSIM) as well as subjective perception via human vision system in the different color video sequences.

An efficiency analysis of the designed and other mentioned filters have been performed on the DSP TMS320DM648 by Texas Instruments through MATLAB's Simulink module, showing that the novel 3D fuzzy filter can be used in real-time processing applications.

9139-12, Session 3

Parallel multithread computing for spectroscopic analysis in optical coherence tomography

Michal Trojanowski, Maciej Kraszewski, Marcin Strnkowski, Jerzy Plucinski, Gdansk Univ. of Technology (Poland)

Spectroscopic Optical Coherence Tomography (SOCT) is an extension of Optical Coherence Tomography (OCT). It allows gathering spectroscopic information from particular, scattering points inside the sample. It is based on time-frequency analysis of interferometric signals. Such analysis requires calculating hundreds of Fourier transforms while performing a single A-scan, instead of one, as in traditional SD-OCT (Spectral Domain OCT). Additionaly further processing of acquired spectroscopic information is needed. This significantly increases the time of computations required. During last years, application of graphical processing units (GPU's) was proposed to reduce computation time in OCT by using parallel computing algorithms. GPU technology can be also used to speed-up signal processing in SOCT. However parallel algorithms used in classical OCT need to be revised, because of different character of analysed data. Classical OCT requires processing of long, independent interferometric signals for obtaining subsequent A-scans. The difference with SOCT is that it requires processing of multiple, shorter signals, which differ only in a small part of samples. We have developed new algorithms for parallel signal processing for usage in SOCT, implemented with NVIDIA CUDA (Compute Unified Device Architecture). We present details of the algorithms and performance tests for analysing data from in-house SD-OCT system. We also give a brief discussion about usefullnes of developed algorithm. Presented algorithms may be useful for researchers working with OCT, as they allow to reduce computation time and are step toward real-time signal processing of SOCT data.

9139-13, Session 3

Simultaneous edge sensing compression and encryption for real-time video transmission

Nazar Al-Hayani, Naseer Al-Jawad, Sabah A. Jassim, The Univ. of Buckingham (United Kingdom)

Video compression and encryption are essential requirements in multimedia applications and video conferencing in particular. Applying both techniques simultaneously for real-time transmission is a challenging task where optimizing output size and quality are essential. In this paper we are proposing a wavelet based dynamic edge sensing in order to encrypt the low frequency sub-band edges while compressing the high frequency sub-bands. This work is aims to improve the security of the encryption and enhance the computational performance for both encryption and compression. Both encryption and compression are based on edges extracted from the wavelet high frequency sub-bands. Although the spatial domain edge detection approach for compression and encryption is discussed in the literature, but the wavelet transform provides dynamic edges detection which makes the compression ratio dynamic and moreover, provides an approach to a selective encryption.

The compression algorithm includes two major steps, Reference Frame (RF) encoding and non-Reference Frame (n-RF) encoding. A wavelet transform to level 2 will be applied to the sequence of video frames. The compression is applied on the high frequency sub-bands of level 1 and 2. The high frequency sub-bands are subdivided to a certain number of blocks of size 16x16 and DCT is applied for each block. Each sub-divided block will be quantised and is considered to be a vector. These vectors will be used to construct a codebook. Then this codebook will be send through the transmitter. This method will be applied for RF only. For the n-RF, the vector quantization method will be applied, but this time the matching criteria will

be applied on the corresponding blocks of the RF codebook and the n-RF codebook before applying DCT to the RF.

The encryption is applied to the low frequency sub band of level 2. The encryption algorithm utilises the chaotic logistic map combined with sine map to scramble the wavelet coefficients of the edges extracted from the low frequency sub-band. These edges are mapped from the high frequency sub-bands using different threshold. The encryption analysis was performed based on two different analyses; in terms of attack complexity and PSNR analysis. The total number of possible combinations of significance coefficients permutations constructed from wavelet sub-bands of level 2 is ≈?10?^99, which is greater than the number of possible permutations of AES. Thus making a brute force attack on The AES key is more efficient than trying to reshuffling the scrambled blocks of our proposal encryption.

The proposed method was applied on different videos. Each video contains 100 frames on average. The frame size of these videos is (256 x320) pixels. During our experiments we have converted all images to grayscales. Six different videos of different nature were used in our tests. Experimental results show that the proposed algorithms have the following features; rapid (average execution time is 0.45 sec for encryption and compression excluding IO operations) and best performance in term of PSNR (average of 30+ db) with higher compression ratio (between 0.18 and 0.27) compared to stand alone DCT and DWT.

Conference 9140: Photonics for Solar Energy Systems

SPIE. PHOTONICS EUROPE

Monday - Wednesday 14–16 April 2014 • Part of Proceedings of SPIE Vol. 9140 Photonics for Solar Energy Systems V

9140-1, Session 1

Light trapping and solar energy harvesting in thin film photonic crystals *(Invited Paper)*

Sajeev John, Univ. of Toronto (Canada)

Photonic crystals are widely known for their light-trapping capabilities. This is often associated with the occurrence of a photonic band gap or other suppression in the electromagnetic density of states [1-3]. This enables guiding of light on an optical micro-chip and unprecedented forms of strong-coupling between light and matter. In the past, practical applications of these effects have focused on information technology. More recently, an important opportunity has emerged in the area of energy technology. This arises from light-trapping in the higher bands of a photonic crystal, where the electromagnetic density of states is enhanced rather than suppressed. This enables unprecedented strong absorption of sunlight in a material with weak intrinsic absorption [4].

We describe designs of 3D photonic crystal silicon-based solar cells that enhance the overall absorption of sunlight using architectures consisting of less than 1 micron (equivalent bulk thickness) of silicon. These crystals trap light through a parallel-to-interface negative refraction (PIR) effect and other optical resonances that occur over a broad angular and frequency range [4]. These 3D photonic crystals exhibit an enhanced electromagnetic density of states, consisting of slow group velocity modes, in which the flow of energy is transverse to the depth of a thin film of material. In the case of a modulated nanowire photonic crystal solar cell, it is possible to absorb roughly 75% of all available sunlight in the wavelength range of 400-1100 nm, using one micron of silicon [5, 6]. In the case of conical nano-pore silicon photonic crystal, roughly 85% of all available sunlight is absorbed [7] and power conversion efficiency in the range of 17.5%-22.5% is predicted [8]. With combined plasmonic and photonic crystal light trapping, the fraction of absorbed sunlight exceeds 90% [9]. The power conversion efficiencies of these sub-micron photonic crystals rival those of present-day solar cells using up to 300 microns of silicon. These photonic crystals offer additional opportunities for solar spectral reshaping to rival and possibly surpass the Shockley-Queisser power conversion efficiency limit.

References:

1. S. John, Physical Review Letters 58, 2486 (1987)

2. E. Yablonovitch, Physical Review Letters 58, 2059 (1987)

3. S. John, Physical Review Letters 53, 2169 (1984)

4. A. Chutinan and S. John, Physical Review A 78, 023825 (2008)

5. G. Demesy and S. John, J. Applied Physics 112, 074326 (2012)

6. A Deinega and S. John, J. Applied Physics 112, 074327 (2012)

7. S. Eiderman, S. John, A. Deinega, J. Applied Physics 113, 154315 (2013)

8. S. Deinega, S. Eyderman, S. John, J. Applied Physics 113, 224501 (2013)

9. K. Le and S. John, Optics Express Vol. 22, Issue S1, pp. A1-A12 (2014), DOI:10.1364/OE.22.0000A1

9140-2, Session 1

Photonic nanostructures for light trapping *(Invited Paper)*

Thomas F. Krauss, The Univ. of York (United Kingdom)

We introduce a novel approach for designing the rich Fourier spectra required for high efficiency broadband light trapping in solar cells and show how these structures can be employed to achieve performance close to the Lambertian limit

9140-3, Session 1

Quasicrystalline light harvesting nanophotonic structures for crystalline silicon thin-film solar cells

Jolly Xavier, Jürgen Probst, Philippe Wyss, David Eisenhauer, Veit Preidel, Helmholtz-Zentrum Berlin für Materialien und Energie GmbH (Germany); Franziska Back, Eveline Rudigier-Voigt, SCHOTT AG (Germany); Christoph Hülsen, Bernd Löchel, Bernd Rech, Christiane Becker, Helmholtz-Zentrum Berlin für Materialien und Energie GmbH (Germany)

Novel light trapping schemes are inevitable for the efficiency-enhancement in thin film Si solar cells. While periodic nanophotonic structures rely on coherent light trapping based on wave interference with pronounced resonant properties depending on the lattice parameters, random light trapping structures have the benefit of wide angle and broadband spectral absorption. Here we bring together the advantages of both in a single platform by implementing higher symmetry quasicrystalline nanophotonic structures as broadband light harvesting scatterers for thin-film crystalline Si solar cells. Photonic quasicrystalline structures combine the short range disorder leading to the absence of translational periodicity in real space but with an inherent tunable long range order resulting in a dense Fourier spectrum with defined higher symmetry diffraction patterns. Here, we investigate crystalline silicon nanostructures in 2D ten-fold quasicrystalline symmetry with the effective nearest neighbor distance of about 650nm. We use nanoimprint-lithography for patterning sol-gel coated on glass substrates in the designed transversely quasicrystalline geometry, ensuring a cost-effective, large-area nanopatterning. After analyzing the scattering and transmission properties of these quasicrystalline-structured substrates, the transversely ten-fold symmetry quasicrystalline silicon nanoarchitectures are prepared on these textured substrates by high-rate silicon film evaporation, solid phase crystallization and chemical etching. We present the far-field diffraction patterns and SEM images confirming the designed higher order symmetry of the fabricated nanophotonic quasicrystalline light scatterers for light harvesting. We further present our investigation on absorption-enhancement for a spectrum of light for varying angle of light incidence in these fabricated higher symmetry crystalline Si architectures in comparison to a planar Si thin film of same thickness. The presented transversely quasicrystalline nanophotonic poly-Si nanoarchitectures reveal their emphatic influence in enhancing the light trapping for new generation economically viable thin-film solar cells.

9140-4, Session 1

Complex photonic crystals structure to enhance optical light trapping in thin film 2nd-generation solar cells

Loic Lalouat, Ding He, Romain Peretti, Guillaume Gomard, Christian Seassal, Emmanuel Drouard, Institut des Nanotechnologies de Lyon (France)

The efficiency of 2nd generation solar cells, constituted of thin absorbing layers, is limited by both the absorption efficiency and carrier recombination issues. Integrating novel light trapping schemes enables the optimization of the absorption efficiency in the active layers with a strongly reduced thickness, which could also lead to higher carrier collection efficiency. Photonic crystals (PCs) have a great potential to enhance absorption thanks to their so-called slow Bloch modes. If a strictly mono-periodic PC enables to achieve high absorption in limited spectral range, it has been reported than a small amount of controlled disorder on the PC parameters can increase more

the integrated absorption.

In this communication, we first investigated numerically the mechanism responsible for this improvement through a simple case: a 200nm ultra-thin film of hydrogenetad amorphous silicon (aSi) deposited on glass. Thanks to a 3D Finite Difference Time Domain (FDTD) method, we analyzed several kinds of perturbation (according to group theory) in light of band folding mechanism in k-space.

The enhanced absorption in the supercell is thus the results of a better coupling of incident light in a larger number of modes in spectral range of interest. A clear understanding of this phenomenon enables us to demonstrate that introducing a control amount of disorder in the PC enables to overcome the integrated absorption of an optimized monoperiodic PC.

Thanks to this analysis of disorder effect, experimental results obtained on samples prepared by E-Beam lithography are analyzed. At last, we numerically investigated this absorption enhancement for more realistic solar stack (i.e. with back metal and conducting layer) in the case of 1μm thick crystalline silicon (cSi).

9140-5, Session 1

A comparison of scattering and non-scattering antireflection designs for back contacted polycrystalline thin-film silicon solar cells in superstrate configuration

Daniel Lockau, Helmholtz-Zentrum Berlin (Germany) and Zuse-Institut Berlin (Germany); Martin Hammerschmidt, Konrad-Zuse-Zentrum für Informationstechnik Berlin (Germany); Jan Haschke, Helmholtz-Zentrum Berlin (Germany); Mark Blome, Konrad-Zuse-Zentrum für Informationstechnik Berlin (Germany); Florian Ruske, Helmholtz-Zentrum Berlin (Germany); Frank Schmidt, Zuse-Institut Berlin (Germany); Bernd Rech, Helmholtz-Zentrum Berlin (Germany)

A new generation of polycrystalline silicon thin film solar cells is currently being developed in laboratories, employing a combination of novel laser or electron beam based liquid phase crystallization (LPC) techniques and single side contacting systems [1-3]. The lateral grain size of these polycrystalline cells is in the millimeter range at an absorber thickness of up to 10 microns.

The main benefit of the above mentioned absorbers in terms of implementation of optical designs is that front and back surface are very well separated. Depending on the applied conditions, the LPC process can even yield a flat rear surface and therefore facilitates the implementation of a separate rear side optical system. Additionally employing a back side contacting system adds even more freedom to fine tune the optics at the front side of the cell (incident / substrate side) but introduces an absorber interface which needs good passivation. To achieve a good trade-off between optical performance and recombination losses, the electrical properties need to be considered when designing the front side optical system.

In this contribution we present a comparative simulation study of several 1D, 2D and 3D nano-optical designs for the substrate / illumination side interface to the several micrometer thick back contacted LPC silicon absorber material. The compared geometries comprise multilayer coatings, gratings with step and continuous profiles as well as combinations thereof. Using the transfer matrix method and a finite element method implementation [4] to rigorously solve Maxwell's equations, we discuss anti-reflection and scattering properties of the different front interface designs in view of the angular distribution of incident light. To compare their light trapping potential we study internal scattering properties and escape losses. Combining the generation rates from optical simulation with electrical device simulations, we further monitor the influence of front side geometry, surface and volume recombination mechanisms on the solar cell performance for selected geometrical designs.

References:

1. Amkreutz, D., et al. (2011). Prog. Photovolt. Res. Appl., 19, 937–945.

2. Haschke, J., et al. (2013). Sol. Energy Mater. Sol. Cells, 115, 7–10.

3. Dore, J., et al. (2013). "Progress in Laser-Crystallised Thin-Film Polycrystalline Silicon Solar Cells". In: PVSC, 2013 39th IEEE.

4. Burger, S., et al. (2008). In: Integrated Photonics and Nanophotonics Research and Applications, p. ITuE4, OSA. doi:10.1364/IPNRA.2008.ITuE4

9140-6, Session 2

Optical management of exciton radiative decay in organic solar cells

Gregory Kozyreff, Univ. Libre de Bruxelles (Belgium); Diana C. Urbanek, Jordi Martorell, ICFO - Institut de Ciències Fotòniques (Spain)

Despite great advances towards the achievement of efficient organic solar cells, it becomes increasingly difficult to improve from current device performance with today's molecules of choices, such as P3HT and PCBM. This may indicate that one is gradually reaching the efficiency limit afforded by these molecules. In this presentation, we suggest to consider a class of molecules, which, unlike the usual ones, have a large fluorescence quantum yield, q, defined as the ratio of the radiative loss rate to the total exciton loss rate. In that case, the main decay channel of excitons is radiative. Hence, since organic solar cells are extremely thin and fluorescence is affected by nearby boundaries, there is hope, in theory, to increase the diffusion length of excitons. This is in line with Shockley and Queiser (SQ) famous thermodynamic theory, which shows that a large fluorescence quantum yield is necessary to maximize power conversion efficiency [1]. Note, however, that the SQ theory applies primarily to non-organic semi-conductor devices.

In order to increase the excitation lifetime and diffusion length, one must properly design the device architecture. The parameters at hand are, mainly the thicknesses and indexes of refraction of the various layers making up the solar cell: transparent electrodes, holes and electron blocking layers, donor and acceptor materials. The present approach, therefore, is purely optical and does not rely on molecular engineering.

Using well-known formulas for the radiative decay rate of molecule derived by Chance, Proc and Silbey [2], and by Wasey et al. [3] for anisotropic materials, we determined the fluorescence decay rate of excitons in a bilayer geometry and included it in a transport equation. Thus, we determined the diffusive currents as a function of the device architecture for parallel, perpendicular, or randomly oriented excitons.

For thin cells, the EQE can be factorized as a product ?A ?D(q), where ?A is an absorption efficiency and ?D(q) is a diffusion efficiency. By optimizing the architecture for a unit fluorescence quantum yield q=1, we found a dramatic improvement with respect to the non-radiative case, q=0, for all exciton orientations. The largest increase in exciton lifetime can be estimated as the fifth power of the index contrast between the photoactive material and the neighboring layers and is found for perpendicular excitons [4].

[1] W Shockley and H. Queisser, J. App. Phys 32 (1961) 510-519

[2] R Chance et al., Adv. Chem. Phys. 37(1978) 1-65

[3] J Wasey et al., Opt. Commun. 183 (2000) 109 - 121

[4] G Kozyreff et al., Opt. Express 21 (2013) A336-A354

9140-7, Session 2

Organic solar cells improvement with quantum dots, up-converters and MoO3 hole transport layers

Marc Jobin, Cedric Pellodi, Haute école du paysage, d'ingénierie

et d'architecture (Switzerland)

We report on the power conversion efficiency (PCE) enhancement for organic solar cells (OSCs) based on several approach. A standard cell composed of an indium tin oxide (ITO) anode, a P3HT/ PCBM active layer, a PEDOT:PSS hole transport layer and an aluminum cathode is used as a reference to compare the effects of the following three modifications.

Firstly, CdSe quantum dots (QDs) are used to take advantage of the multiple electron generation (MEG), and to enhance the light absorption. Under the control of infrared spectroscopy, CdSe QDs are washed with hexanoic acid in order to remove the ligand, which is an insulator and so decrease the OCSs efficiency. QDs are not used to replace the donor material (PCBM) but directly incorporated into the P3HT:PCBM with different concentration. OCSs with P3HT:PCBM:QDs active layer shows an efficiency increasing with the QDs concentration, but a lower efficiency than the reference cell. It's assumed that the lower performances are due to the QDs ligand, which is not completely removed by the washing procedure.

Secondly, NaYF4 up conversion (UC) particles are incorporated into a TiOx sol-gel to form an additional layer used to convert low energy photons (near IR, 980nm) to higher energy photons (blue and green). OCSs with UC layer showed a PCE up to 2.3% which is 0.9% higher than the reference cell. The PCE enhancement is both attributed to the IR light absorption and to the better electron transport between the active layer and the cathode, due to the TiOx electrical properties. Variable temperature (80K-300K) photoluminescence has been used to interpret the optical process taking place on the NaYF4 crystals when embedded in TiO2.

Finally, MoO3 layer is used to replace the PEDOT:PSS layer as holes transport layer (HTL). This layer is deposed either by thermal evaporation or by spin coated sol-gel solution. We found evaporation better in terms of thickness control and reproducibility. It has been demonstrated that the PEDOT:PSS HTL can be replaced by MoO3, and the thickness of this MoO3 layer strongly affects the PCE of the cell. The maximum PCE of 1.4% was obtained with for thickness of 40nm.

9140-8, Session 2

Variable temperature photocurrent characterization of quantum dots intermediate band photovoltaic devices

Edson Garduno-Nolasco, Mohamed Missous, The Univ. of Manchester (United Kingdom); Jaroslav Ková?, Miroslav Mikolá?ek, Martin Florovi?, Daniel Donoval, Slovak University of Technology, Institute of Electronics and Photonics (Slovakia)

The efficiency of Photovoltaic devices based on semiconductors material systems is limited by a number of recombination processes in the material bandgap. The main issue for enhancing the efficiency is to reduce the recombination phenomena and to extend the absorption wavelength range. Silicon, with a bandgap of 1.1 eV, is an excellent option in this respect. However, its thermal stability is not ideal for high temperature operation conditions. GaAs on the other hand is an excellent option for applications under high temperature conditions because of its proven thermal stability. By inserting InAs Quantum Dots in a GaAs host semiconductor structure, new energy levels can be generated. These new levels result in the enhancement of the wavelength absorption. Thus, the key objective of this work is to design a material based on GaAs semiconductor with extended absorption wavelength within the infrared range.

In this work we extend our previous characterisation of these material systems by studying variable temperature photocurrent spectroscopy. A series of GaAs/InAs quantum dots (QDs) structures grown using Molecular Beam Epitaxy and having different doping profiles (in between the dots) were used for in-depth studies of their performances as a function of temperature as potential devices for intermediate band cells. The comparison of the variable temperature results with the standard GaAs system are presented, as well as the analysis of the inter-dot doping effect for these InAs/GaAs material system.

9140-9, Session 2

Substrate-less photovoltaic devices containing silicon nanocrystals in SiC

Julian López-Vidrier, Sergi Hernández, Univ. de Barcelona (Spain); Philipp Löper, Ecole Polytechnique Fédérale de Lausanne (Switzerland); Manuel Schnabel, Fraunhofer-Institut für Solare Energiesysteme (Germany); Marica Canino, Marco Allegrezza, Consiglio Nazionale delle Richerche (Italy) and Istituto per la Microelettronica e Microsistemi (Italy); Lluís López-Conesa, Sònia Estradé, Francesca Peiró, Univ. de Barcelona (Spain); Stefan Janz, Fraunhofer-Institut für Solare Energiesysteme (Germany); Caterina Summonte, Consiglio Nazionale delle Richerche (Italy) and Istituto per la Microelettronica e Microsistemi (Italy); Blas Garrido Fernandez, Univ. de Barcelona (Spain)

Silicon nanocrystals (Si-NCs) have become a very promising material for the optoelectronics industry, as their electronic properties can be tuned thanks to the quantum confinement effect. The control of the NC size is therefore crucial, and it can be achieved through novel deposition processes such as the superlattice (SL) approach. By decreasing their size, Si NCs present a higher band gap energy, which allows for absorption of the high-energy photons from the solar spectrum with less thermalisation and thus higher light-conversion efficiency in a photovoltaic device

We present a structural and electro-optical study of a set of 30x Si0.85C0.15/SiC SLs with varying Si0.85C0.15 thickness, deposited on Si substrate by means of plasma-enhanced chemical-vapour deposition. After deposition, all wafers were annealed at 1100 °C to induce the Si excess precipitation and consequent formation of nanocrystals. The SL structures were investigated by means of energy-filtered transmission electron microscopy and Raman scattering, to confirm the presence of Si nanoaggregates and evaluate their crystalline degree. Membrane structures were prepared by locally removing the Si substrate, thus avoiding any influence of the wafer substrate. Afterwards, selective contacts to the intrinsic Si-NC/SiC layer were prepared from p- and n-type a-SixC1-x:H. Finally, thin ITO layers were sputtered on both the front and the back of the p-i-n cell, which guarantees good transparency and electrical contact. Optical microscopy and light-beam induced current techniques were employed to verify that light-conversion took place within the membrane area. An I(V) characterization, in dark and under illumination, revealed the PV properties of the material. Finally, a spectral response study was performed on the active membrane area, allowing us to determine the role of Si-NCs in the light-conversion of solar radiation.

9140-10, Session 3

The photonic solar cell: system design and efficiency estimations *(Invited Paper)*

Oliver Höhn, Tobias Kraus, Fraunhofer-Institut für Solare Energiesysteme (Germany); Ulrich T. Schwarz, Fraunhofer-Institut für angewandte Festkörperphysik (Germany); Benedikt Bläsi, Fraunhofer-Institut für Solare Energiesysteme (Germany)

Increasing the efficiency of solar cells by a restriction of the maximal angle of emission has been proposed for several times. Typically, this is achieved by applying a directional selective filter on top of the solar cell. This filter leads to a reflection of emitted light under certain angles back into the cell, where it then can be reabsorbed. A system where the emission process itself is inhibited for certain angles (Photonic Solar Cell) is in principle a better system, because then absorption respectively reflection losses in the filter can be suppressed as the emission in fact does not take place.

In this contribution, we focus on a Photonic Solar Cell, where the cell and the filter are combined in one single optoelectronic device. This means that the solar cell itself has a photonic structure or is implemented into a Photonic Crystal. The interesting question is how such a device could look like and how it performs. Here, design concepts for Photonic Solar Cells are shown and simulated optically. An interesting system could be an integration of a solar cell as defect layer into a thin film stack. To get an idea of the potential of such systems, the emission out of a Photonic Solar Cell has to be compared to the emission out of a standard solar cell. Therefore, a scattering-matrix-formalism is used. First estimations of the possible system efficiencies in terms of detailed balance calculations are given as indication of the system quality.

9140-11, Session 3

Novel light-trapping concepts for crystalline silicon solar cells using diffractive rear side structures

Johannes Eisenlohr, Nico Tucher, Alexander Bett, Hubert Hauser, Jan Benick, Jan Christoph Goldschmidt, Benedikt Bläsi, Martin Hermle, Fraunhofer-Institut für Solare Energiesysteme (Germany)

Periodic dielectric nanostructures for the rear side of silicon solar cells are a promising possibility to enhance the path length of near infrared light in the weakly absorbing silicon bulk material. Especially for very thin crystalline silicon solar cells such novel light trapping concepts are essential to realize high short circuit current densities.

We have realized two kinds of diffractive rear side structures. First, hexagonal sphere gratings that are produced by a self-organized growth process using spin coating, and second, binary gratings produced via nano-imprint lithography. Both process chains are potentially scalable to large areas.

To integrate these gratings into crystalline silicon solar cells without any negative side-effects on the electrical properties we introduce an additional very thin dielectric layer of Al2O3, that passivates the surface electrically but has a negligible influence on the optical properties. The nano-imprinted gratings are realized in an additional amorphous silicon layer behind the passivation layer. The hexagonal sphere gratings are also deposited on the passivation layer. Thus we aim for electrically thin and flat but optically thick and rough solar cells.

For both grating types we proved the absorption enhancement in the silicon bulk due to the rear side grating compared to a planar reference wafer. We measured absorption enhancements corresponding to a potential photo current gain of 1.5 mA/cm2 for sphere gratings (cell thickness 100 μm) and 1.6 mA/cm2 for nano-imprinted crossed gratings (cell thickness 200 μm).

To show the absorption enhancement also on solar cell level, we are currently developing a process chain for contact formation that allows a local opening of the nano-imprinted gratings and subsequent deposition of metal contacts. We use a photolithographic process with subsequent wet-chemical and plasma etching. The rear side structure that consists of three materials (Al2O3, a-Si, SiO2) can be opened by hydrofluoric acid (removal of SiO2 and Al2O3) and SF6-plasma (removal of a-Si).

Alongside the technological integration of the light trapping structures into complete solar cells we also further investigate the fundamental optical properties of diffractive structures by optical measurements and by wave optical simulations using rigorous coupled wave analysis. We compare state-of-the-art light trapping concepts like pyramidal front side textures in combination with a rear side mirror with our novel concepts. We show that diffractive rear sides in combination with planar antireflection coatings can compete with the light trapping properties of pyramidal structures. For very thin solar cells our simulations show even higher photo current densities. Additionally the diffractive rear sides potentially exhibit electrical advantages due to the electrically flat surfaces. A further point of this work is the optical interaction of the front and rear surface. We investigate the light paths for different front surface antireflection structures like pyramids, planar coatings and black silicon in combination with diffractive rear side structures. In this regard we present optical absorption measurements and compare these to our simulations. We evaluate the different potential photo current gains and relate these to the Lambertian limit (4n2-limit) valid for completely randomizing structures.

9140-12, Session 3

Tuning light coupling to waveguide modes in thin-film silicon solar cells

Michael Smeets, Ulrich W. Paetzold, Vladimir Smirnov, Karsten Bittkau, Matthias Meier, Forschungszentrum Jülich GmbH (Germany); Dirk Michaelis, Christoph A. Waechter, Fraunhofer Institut für Angewandte Optik und Feinmechanik (Germany); Reinhard Carius, Uwe Rau, Forschungszentrum Jülich GmbH (Germany)

High efficiency thin-film silicon solar cells require advanced light-trapping concepts in order to absorb as much as possible of incident light in the optically thin absorber layer of the solar cells. The state-of-the-art light-trapping concepts apply randomly textured front contacts of transparent conductive oxides and metal back contacts in order to scatter incident light and thereby enhance the light path inside the absorber layers. Recently, an alternative concept named “plasmonic reflection grating back contacts” was introduced in literature. It applies plasmon-enhanced diffraction at the periodically textured Ag back contact in thin-film silicon solar cells to couple incident light to leaky waveguide modes and thereby enhancing the absorption in the absorber layers. In first studies, the potential of plasmonic reflection grating back contacts to couple light to waveguide modes was demonstrated in prototype solar cells showing an improved light-trapping effect compared to the state-of-the-art random textured thin-film silicon solar cells.

In this contribution, we study in depth the light-trapping effect of prototype thin-film solar cells made of hydrogenated amorphous silicon in substrate configuration applying plasmonic reflection grating back contacts. The light-trapping effect in these devices is caused by light coupling to leaky waveguide modes which are supported by the silicon absorber layers. By changing the unit cell and the corresponding periodicity of the plasmonic reflection grating back contact, the spectral and angular dependence of the light coupling to leaky waveguide modes is tuned. The resulting impact on the light trapping effect is analyzed spectrally by spectral response measurements with a resolution below 3 nm as well as reflectance measurements for various angles of incidence. The conclusions drawn from our study provide new routes for the design of next generation’s plasmonic reflection grating back contacts which can further improve the light trapping in thin-film solar cells.

9140-13, Session 3

Imperfect geometric shapes of complex gratings as solar absorbers with highly optical performance

Nghia Nguyen-Huu, Michael Cada, Dalhousie Univ. (Canada); Jaromír Pi?tora, V?B-Technical Univ. of Ostrava (Czech Republic)

This paper describes a numerical investigation on the optical absorptance in the visible and near infrared regions of an optimal solar absorber with a consideration of its different geometric shapes that could be occurred in micro/nanofabrication processes. The solar absorber based on a one-dimensionally complex silicon (Si) structure comprising a single-layered Si grating on top of an Si substrate. The optical absorptance spectra of the solar absorber with considered imperfect geometries such as tiny features attached to the top and the bottom of sidewall gratings are analyzed. The results have shown that the grating structure with attached

nanoscale features exhibits higher average absorptance (92%) than the perfect grating (89%). Additionally, this absorptance enhancement is also investigated by calculating magnetic field, energy density, and Poynting vector distributions. This study has proved that the imperfect geometries of nanograting structures should be taken into consideration in the simulation and fabrication processes since they have significantly attributed the cause of absorptance enhancement.

9140-14, Session 3

Diffraction gratings patterned on titania electrodes to improve light harvesting in dye solar cells

Carmen López López, Alberto Jimenez Solano, Silvia Colodrero, Reyes Ortiz, Mauricio E. Calvo, Hernán R. Míguez, Consejo Superior de Investigaciones Científicas (Spain) and Instituto de Ciencia de Materiales de Sevilla (Spain)

The use of gratings as an efficient diffractive optical element was investigated for high performance of DSCs. Diffraction gratings were formed on the TiO2 nanocrystalline electrode by a soft-lithographic approach that uses a polymeric composite based on vinyl and hidrosilane end-linked polymer, called “hard PDMS” (h-PDMS) as stamp. The pattern-transfer fidelity is evidenced by an atomic force microscopy study of the surface of the polymer and their porous TiO2 counterpart. Energy carried of reflected diffracted modes were measured for various wavelengths and compared with the theoretical data obtained through a model based on a rigorous coupled wave analysis (RCWA). From this results, we noticed that the energy carried by efficiently back diffracted modes is typically on the order of a few percents of that of the incoming beam, and hence photocurrent enhancements of similar magnitude are expected, in good agreement with our experimental observations. In this regard, we gather consistent experimental evidence by measuring the I-V curves and the incident photon to collected electron efficiency (IPCE). The behaviour of the cells is also investigated under different illumination conditions.

9140-15, Session 4

Photon management with luminescent materials and photonic structures *(Invited Paper)*

Jan Christoph Goldschmidt, Stefan Fischer, Benjamin Fröhlich, Johannes Gutmann, Barbara Herter, Clarissa Hofmann, Janina Löffler, Fraunhofer-Institut für Solare Energiesysteme (Germany); Frank C. J. M. van Veggel, Univ. of Victoria (Canada); Sebastian Wolf, Fraunhofer-Institut für Solare Energiesysteme (Germany)

Luminescent materials allow for changing the spectral composition of light, while photonic crystals allow for changing the light’s spatial distribution due to spectral selective reflection and local field enhancement. This paper highlights the recent progress of how these effects can help increasing photovoltaic device efficiencies.

A special focus of this work is on upconversion, the generation of one high energy photon out of at least two lower energy photons. With upconversion, otherwise lost sub-bandgap photons can be converted into photons that can generate a current in a solar cell. Recently, we reported an enhancement of the short-circuit current density of an upconverter silicon solar cell device by 13.1mA/cm2 due to upconversion at a solar concentration of 210 suns, measured with a sun simulator. The used upconverter material was ??NaYF4 doped with 25% Er3+, synthesized at the University of Bern, Switzerland. The upconverter was embedded in the polymer perfluorocyclobutyl (PFCB), at Heriot-Watt University, United Kingdom, with a powder to polymer concentration of 75.7 w/w%. Although this constitutes a very good result, the potential relative increase of the solar cell efficiency was only 0.19%. Hence, further means to increase upconversion are necessary.

Photonic structures can increase the local irradiance on the upconverter, thus increasing absorption and, due to the non-linearity of upconversion, also the upconversion quantum yield (UCQY). Secondly, the photonic structures change the local photonic density of states, which can be used to amplify wanted radiative transitions and suppress others. This can be realized by embedding the upconverter into a cavity formed by amorphous silicon carbide (a-SiC) multi-layer structures, resonant to the wanted upconversion emission at 980 nm, placed in an appropriate distance of another a-SiC structure, which is highly reflective at the excitation wavelength of 1523 nm. Our simulations show that the internal UCQY can be more than tripled this way. For these simulations, an optical model of the photonic structure environment was coupled to a rate equation model of the Er3+doped ??NaYF4material.

In a first experimental realization of such a structure with Er3+doped ??NaYF4 nanoparticles the biggest enhancement of upconversion luminescence was observed when the upconverter material was placed on top of one a-SiC multi-layer structure reflective at 980 nm on top of one structure reflective at 1523 nm. For a complete structure with an additional a-SiC multi-layer structure reflective at 980 nm on top of the upconverter followed by the two other structures, an enhancement in comparison to the reference without any photonic structures was found, which was, however, lower than for the incomplete cavity. A possible explanation is parasitic reflection in the top structure. The observations are currently being confirmed in new sets of measurements with a larger number of samples.

In the next step, the integration of different upconverter materials directly into photonic multi-layer systems of TiO2 and poly-methyl-methacrylate (PMMA) will be investigated, with the goal of increased absorption, due to more upconverter material bearing layers, and with optimization also in regard to the efficient out-coupling of upconverted photons.

9140-16, Session 4

Organic upconverters embedded in a Bragg structure

Clarissa Hofmann, Barbara Herter, Johannes Gutmann, Janina Löffler, Stefan Fischer, Sebastian Wolf, Fraunhofer-Institut für Solare Energiesysteme (Germany); Roland Piper, Nicholas J. Ekins-Daukes, Neil Treat, Imperial College London (United Kingdom); Jan Christoph Goldschmidt, Fraunhofer-Institut für Solare Energiesysteme (Germany)

Upconversion presents a possibility to exploit sub-bandgap photons for current generation in solar cells. Upconverter photons that carry the energy of at least two sub-bandgap photons can be absorbed by the solar cell. Hence, using upconversion, the Shockley-Queisser efficiency limit can be overcome. Especially for semiconductor materials with a large bandgap, upconversion has a high potential for improving solar cell performance. Although several works could measure an increase of short circuit current density due to upconversion for solar cell upconverter devices, the overall effect is still small. Current investigations focus on improving the upconversion quantum yield (UCQY) of promising upconverter materials, such as ? NaYF4:Er3+ and a number of organic upconverter materials. We already showed theoretically that embedding the upconverter material into a photonic structure can increase UCQY by a factor of 1.8. Two major effects of photonic structures contribute to this result: firstly, the locally increased irradiance within the structure improves UCQY due to the non-linear nature of upconversion; secondly, the variation of the local photonic density of states can increase wanted radiative transitions and suppress others.

In this work we investigate the promising approach of embedding an upconverter directly into the layers of a Bragg-like multi-layer structure. As theoretical analysis the effect of a locally increased irradiance is simulated, using the scattering matrix method. The local photonic density of states is obtained from calculations of the eigenmodes of the photonic crystal

using the plane wave extension method. The simulation results will subsequently be coupled with a rate equation model of the upconversion dynamics to determine the influence of the photonic structure on the UCQY. The simulation parameters will be optimized for maximizing UCQY.

The optimized structure from the simulation will be produced out of stacked layers of TiO2 and polymethylmethacrylate (PMMA), the latter doped with the upconverter material. In this work we investigate the organic upconverter materials platinum tetraphenyltetrabenzoporphyrin (PtTPBP) as sensitizer and rubrene, perylene or diphenylanthracene (DPA) as emitter. Via spin-coating of PMMA, dissolved in toluene as low refractive index material and TiO2-sol as high refractive index material, stacks will be formed. The thickness of the single subsequent layers can be controlled by the concentration of the solution as well as the speed of rotation. We already successfully produced similar stacks, where instead of the upconverter an organic dye was used as a dopant. The spin-coating production process was optimized, so that stacks with up to 29 layers could be produced that show high spectral selective reflectivity. The optical properties of the formed upconverter Bragg-structures will also be determined via photoluminescence measurements. As a reference, samples consisting only of the same number of doped PMMA layers will be used. In the next step quantum yield measurements will be carried out and again be compared to measurements on reference samples.

9140-17, Session 4

Trivalent rare-earth ions as photon down-shifter for photovoltaic applications

Franziska Steudel, Fraunhofer-Ctr. für Silizium-Photovoltaik (Germany); Sebastian Loos, Fachhochschule Südwestfalen (Germany); Bernd Ahrens, Stefan Schweizer, Fraunhofer-Ctr. für Silizium-Photovoltaik (Germany) and Fachhochschule Südwestfalen (Germany)

Solar modules have a poor response in the blue and near ultraviolet spectral range due to thermalization losses and absorption in the glass and the front contact layer. The approach to optimize the low external quantum efficiency in the short-wavelength spectral range by application of a down-converter was introduced in 1979 by Hovel et al. [1]. For an ideal down-converter, Trupke et al. [2] estimated an increase in efficiency of a silicon solar cell with a band gap of 1.1 eV from 30% to 37%.

Here, rare-earth doped borate glasses are investigated for their potential as down-converting cover glass of CdTe solar cells. Note, that CdTe solar cells have a poor response in the ultraviolet and blue spectral range due to absorption in the CdS buffer layer having a band gap of 2.4 eV. The following trivalent rare-earth ions are analyzed in detail: Sm3+, Eu3+, and Tb3+. These ions provide strong absorption bands in the ultraviolet / blue spectral range and an intense emission in the red (Sm3+ and Eu3+) or green (Tb3+) spectral range. The gain in short-circuit current density of a CdTe solar cell is calculated for different rare-earth ion concentrations. The calculations are based on the rare-earth's absorption coefficients as well as their photoluminescence quantum efficiency. For Sm3+, the PL quantum efficiency depends significantly on the doping concentration. Finally, the potential of doubly-doped borate glasses, i.e. the glasses are doped with two different rare-earth ions, is investigated.

[1] H. J. Hovel, R. T. Hodgson, and J. M. Woodall, "The effect of fluorescent wavelength shifting on solar cell spectral response," Solar Energy Materials 2, 1, 19–29 (1979).

[2] T. Trupke, M. A. Green und P. Würfel, "Improving solar cell efficiencies by downconversion of high-energy photons," Journal of Applied Physics 92, 3, 1668–1674 (2002).

9140-18, Session 4

Rate equation analysis of nanocrystal-enhanced upconversion in neodymium-doped glass ceramics

Ulrich Skrzypczak, Charlotte Pfau, Martin-Luther-Univ. Halle-Wittenberg (Germany); Gerhard Seifert, Martin-Luther-Univ. Halle-Wittenberg (Germany) and Fraunhofer-Ctr. für Silizium-Photovoltaik (Germany); Stefan Schweizer, Fraunhofer-Ctr. für Silizium-Photovoltaik (Germany) and Fachhochschule Südwestfalen (Germany)

Rare-earth ions embedded in glassy matrices are promising materials for photon upconversion processes, e.g. to convert near infrared light to frequencies above the band gap of a solar cell to make it available for electrical power generation. One strategy to optimize the efficiency of such upconversion processes is to embed the active ions in a host matrix with minimal losses to non-radiative relaxation. We have recently shown for the model system of Nd3+ in fluorochlorozirconate (FCZ) glass that a uniform growth of BaCl2 nanocrystals inside such glasses can decrease the probability of multi-phonon relaxation (MPR) drastically, leading to a huge increase in upconversion intensity for monochromatic illumination.

To identify the key processes which may enhance or diminish the total upconversion efficiency, we have developed a comprehensive description for the optical dynamics of Nd3+ in FCZ glass ceramics based on a rate equation system including ion-photon, ion-phonon, and ion-ion interactions. An effective medium approach is utilized to account for the Nd3+ located in BaCl2 nanocrystals or the FCZ glass bulk, respectively. The numerous parameters required to enable a reliable numerical simulation of the processes were obtained from theoretical approaches like Judd-Ofelt theory, as well as from experimental studies of luminescence decay after femtosecond excitation at various wavelengths and luminescence spectra under cw illumination at 800 nm wavelength.

This rate equation model enables a convenient, self-consistent description of all time-resolved and cw experiments on samples with different neodymium concentration. On this basis, the power dependence of upconversion spectra could be simulated in reasonable agreement with the experimental result for 800 nm cw illumination. Currently, the rate equation system is extended to the simulation of spectrally continuous irradiation, e.g. sunlight, which will allow us to predict the efficiency of an upconverting bottom layer in a suitable solar cell.

9140-19, Session 5

Front and rear decoupled texturing in nano-crystalline silicon-based solar cells *(Invited Paper)*

Olindo Isabella, Dane N. P. Linssen, Fai Tong Si, Miro Zeman, Technische Univ. Delft (Netherlands)

Improving the conversion efficiency of thin-film silicon solar cells is a delicate interplay between spectral utilization, materials processing and light management. For enhancing the photo-current density generated by the solar cell, the spectral absorptance of the absorber layer must be enlarged. This means that the spectral losses due to reflectance and supporting layers have to be minimized. In this respect, light management techniques play an important role. In particular, combining light scattering at textured interfaces with efficient rear reflector enables enhanced light coupling in the absorber layers.

In this contribution we report our recent studies on light management applied to nano-crystalline silicon solar cells. We analysed the effect of decoupled texturization between front and rear side on the absorptance of the absorber layer. At the front side, we considered high aspect ratio pyramidal features for anti-reflective effect and enhanced light in-coupling, while

at the rear side we took into account shallower pyramidal features for effective light scattering. The novelty of our study lies in the optical modelling of the complete p-i-n solar cell structure based on nc-Si:H and in the analysis of its spectral performance by means of the excited wave-guided modes. A 3-D Maxwell solver based on finite element method was used for the simulation of absorptance and reflectance spectra, while an iterative method based on the calculation of poles of the Fresnel coefficients was deployed for sampling the excited wave-guided modes.

Our study comprised three simulation phases, in which the thickness of the intrinsic nc-Si:H layer was kept constant to 2 μm. Firstly, an ample parameters space was investigated. Varying period, height and duty cycle of both front and back side textures, we could rank the three most promising structures to be used later on. In the second phase, we especially focussed on the metallo-oxide interface at the back side. Regardless the simulated geometrical structure, we found that the insertion of doped layers based on nc-SiOx:H with the concurrent usage of an appropriate back transparent conductive oxide (TCO) resulted in the minimization of plasmonic losses in the silver rear reflector. In the third phase we finally optimized the thickness of the front TCO.

Our best simulated solar cell structure showed an implied photo-generated current density equal to 35.65 mA/cm2, which is +3.40% higher than the value predicted by Tiedje-Yablonovitch limit calculated for the same thickness and in the wavelength range between 300 nm and 1200 nm. This enhancement was ascribed to the optimized decoupled front and back side texturization, which increased the light in-coupling at long wavelengths. In fact, by sampling the resonance peaks of the nc-Si:H absorptance on a dispersion-relation diagram, we found that all of them were related to wave-guided modes concurrently excited by the front and the back textures.

9140-20, Session 5

Optical simulation of photonic random textures for thin-film solar cells *(Invited Paper)*

Karsten Bittkau, Andre Hoffmann, Forschungszentrum Jülich GmbH (Germany)

Many types of thin-film solar cell demand advanced light-trapping concepts, in order to overcome the limitations from the weak absorptance near the band gap. Mostly, random textures are incorporated that scatters incoming light diffusely prolonging the effective light path in the absorber layer. As an alternative, periodic structures like gratings or photonic crystals incorporated at different interfaces of the device are investigated by several groups. The optical design of optimized textures is often done by rigorous optical simulations.

We recently demonstrated that a simple scalar approach sufficiently describes angular resolved scattering in transmission and reflection inside the absorber material. We found that pure random textures scatter light most efficiently in reflection at the back contact, whereas two-dimensional periodic structures show their highest diffraction efficiencies in transmission.

We demonstrate that by the combination of both, periodic structure and random texture conformally incorporated at the front and back contact, the high diffraction efficiency in transmission still dominates the light scattering, but the resonance is much broader due to the random structure. The light scattering at the back contact still shows the broad angular distribution around large angles like the random texture without periodic structure. The combined photonic random texture, therefore, benefits from both resulting in optimal transmission and reflection properties.

Starting with a randomly textured ZnO:Al layer, that is well-known to provide high-efficiency microcrystalline silicon solar cells, we add a two-dimensional periodic structure with optimized period and height on top of the random texture by applying the scalar approach. The significant improvement of quantum efficiency is verified by Finite-Difference Time-Domain simulations taking into account real layer stack properties. The thus optimized structure outperforms pure periodic and random structures.

9140-21, Session 5

Optimized nano-textured interfaces for thin-film silicon solar cells: identifying the limit of randomly textured interfaces

Klaus Jäger, Dane N. P. Linssen, Olindo Isabella, Miro Zeman, Technische Univ. Delft (Netherlands)

In difference to common crystalline silicon solar cells, which have a thickness of around two hundred micrometers, thin-film silicon solar cells are only few micrometers thick, i.e. the amount of material required for production is drastically reduced. At such thicknesses, however, light is not efficiently absorbed in the absorber layer.

Thus, light management techniques are instrumental for maximizing the absorption of the incident light in the absorber layer of thin-film silicon solar cells. Besides anti-reflective coatings on the front side and reflectors at the backside, nano-sized structures are the most common light management tools.

The most investigated nano-sized textures are either metallic or dielectric nanoparticles and nanotextures that can be incorporated within the solar cells with various techniques. Since they can easily be manufactured on large scale, randomly nano-textured interfaces are the most common type of nanotextures used in thin-film silicon solar cells. For maximal absorption of light in the absorber layer it is crucial to develop nanotextures with morphologies that are optimized for the thickness and optical properties of the absorber layer.

In the past we developed an optimization procedure that allows us to generate and investigate optimized nanotextures for thin-film silicon solar cells. This procedure consists of three building blocks: first, the Perlin algorithm with that we can generate nanotextures with well-controlled statistical surface parameters. Secondly, a fast and accurate optical model based on the scalar scattering theory that can predict the angular and spectral scattering properties of nano-textured surfaces between arbitrary materials. Thirdly, the simulated annealing algorithm that we use as optimization tool for finding the optimized nanotextures. Our optimization procedure was already successfully tested for thin-film single junction solar cells that used amorphous silicon as absorber material [1].

In this contribution we will apply our optimization procedure to thin-film solar cells made from nanocrystalline silicon, which, due to its lower bandgap, is used in multi-junction devices where solar cells with different band gaps are stacked onto each other for a better utilization of the solar spectrum. To estimate the maximal gain in implied photo-generated current density that can be expected from using randomly nano-textured interfaces, we will perform a parameter study where we treat the vertical and lateral feature sizes of the nanotextures and the absorber layer thickness as independent variables. We will correlate the statistical surface parameters of the generated nanotextures to the implied photo-generated current density, where we are especially interested in the influence of the surface angle distribution. We will investigate both layer-by-layer conformal and front-rear decoupled nano-textured interfaces.

We further will perform rigorous calculations using the Finite Element Method in order to compare the performance of optimized random nanotextures with that of optimized periodic structures. We will put our results in the framework of the classical 4n2 absorption enhancement limit in order to estimate the maximal gain in absorption that can be expected from random nanotextures in thin-film solar cells.

[1] K. Jäger, M. Fischer, R.A.C.M.M. van Swaaij, and M. Zeman, Opt. Express 21, A656 (2013).

9140-22, Session 5

Tailoring randomly rough textures for light trapping in thin-film solar cells

Piotr Kowalczewski, Marco Liscidini, Angelo Bozzola, Lucio C. Andreani, Univ. degli Studi di Pavia (Italy)

High efficiency thin-film solar cells require strong and broad-band light trapping. In this regard, randomly rough textures are particularly promising as intrinsically broad-band scatterers. Yet, the description of realistic rough topographies is complicated, which makes the optimization of such textures difficult. In this work, we study rough interfaces with a simple model of Gaussian roughness, which is able to describe the optical properties of the state-of-the-art rough substrates (Neuchâtel and Asahi-U), commonly used in thin-film solar cells. In our approach, rough interfaces are described by only two statistical parameters: the root mean square (RMS) deviation of height and the lateral correlation length.

The optical properties of solar cells with rough interfaces are modelled with Rigorous Coupled-Wave Analysis, with the roughness described by the stair-case approximation. As a figure of merit we use the short-circuit current density calculated with the AM1.5G spectrum. In this framework, we demonstrate that optimized rough textures allow approaching the Lambertian Limit of absorption.

We explain these results by a detailed analysis of the Angular Intensity Distribution and haze of the light transmitted through the roughness, showing a clear correlation between the optical properties of the interface and absorption enhancement in the active layer. We also compare crystalline and microcrystalline silicon solar cells to investigate the role of light-trapping as a function of the properties of the energy band gap.

Although absorption in the structure with an optimized rough texture approaches the theoretical light-trapping limit, this requires large and sharp surface features which, in turn, may cause electrical losses at the interface, mainly due to the voids/cracks created during the fabrication process. We demonstrate, however, that a combination of a rough interface and a diffraction grating allows achieving strong and broad-band absorption enhancement also with a shallow roughness. Therefore, such a hybrid interface may be beneficial for the electrical properties of the interface.

Typically, light-trapping strategies documented in the literature are presented with an underlying assumption that each absorbed photon contributes to the photocurrent. Yet, diffractive nanostructures may have a strong impact on electrical properties, including increased surface recombination and losses in the highly doped regions. We address this trade-off between optical and electrical performance of solar cells by transferring the photogeneration rate obtained from the optical model to the commercially available device simulator (Silvaco Atlas). Then, solution of the drift-diffusion equations gives energy conversion efficiency of a textured cell.

Optimizing the parameters of the electrical simulator (i.e., simulation grid) significantly reduces the computational cost, and gives a possibility to explore a wide range of parameters, such as surface recombination velocity, junction depth, or doping level.

This coupled electro-optical modelling allows simultaneous optimization of both optical and electrical properties of solar cells with rough interfaces, and provides a clear route to design high efficiency solar cells with a micron-scale absorbing layer.

9140-23, Session 5

Opto-electronic properties of different black silicon structures passivated by thermal ALD deposited Al2O3

Martin Otto, Martin-Luther-Univ. Halle-Wittenberg (Germany); Matthias Kroll, Thomas Käsebier, Friedrich-Schiller-Univ. Jena (Germany); Xiaopeng Li, Martin-Luther Univ. (Germany); Benjamin Gesemann, Martin-Luther Univ. Halle-Wittenberg (Germany); Kevin Füchsel, Fraunhofer-Institut für Angewandte Optik und Feinmechanik (Germany); Johannes Ziegler, Martin-Luther Univ. (Germany); Alexander N. Sprafke, Martin-Luther Univ. Halle-Wittenberg (Germany); Ralf B. Wehrspohn, Fraunhofer-Institut für Werkstoffmechanik (Germany)

Black silicon (b-Si) structures offer improved light absorption but require appropiate surface passivation for photovoltaic applications. Here, we compare the opto-electronic performance of different wet and dry etched b-Si structures passivated by thermal ALD deposited Al2O3.

9140-35, Session PS2

Morphology of active layer and devise performance of polymer/ZnO BHJ solar cells

Nataliya V. Babayevskaya, Oksana O. Matvienko, Yuri N. Savin, Alexander V. Tolmachev, Valerey V. Vashchenko, Institute for Single Crystals (Ukraine)

A bulk heterojunction (BHJ) photovoltaic (PV) device on the base of hybrid films consisting from the photosensitivity polymer (donor) and semiconductor nanocrystals (NC) (acceptor) are attract attention as an alternative of Si based energy sources. The spatial arrangement of nanocrystals in photoactive layer is crucial for the PV device performance. By modifying the physical or chemical properties of the nanocrystal surface with the surface ligand molecules (interface modifiers, IMs), the phase separation in polymer-NC can be controlled and the performance of blend hybrid photovoltaic cells can be improved significantly.

Among a large number of types of conjugated molecules perspective as IMs attention draw the perylene imide (PI) dyes which are used widely in solid-state dye-sensitized solar cells (DSSC). In contrast with other organic semiconductors PIs show high electron mobility, specific carrier injection-tuning properties, have a large molar absorption coefficients, and excellent photo and thermal stabilities. The chemical modification of the PIs by introducing corresponding substituents at the N-positions and/or at the bay core positions can result in optimized electronic and optical properties, controlled solubility, appearance of a surface active properties. In spite of the fact that many cited works are devoted to the PI dyes application in DSSCs the study of effect of PI dyes as IMs on photovoltaic properties was discussed in limited cases. The key issue for the fabrication of efficient BHJ photovoltaic devices in addition to the charge transfer properties is the morphology control (the dispersion or phase segregation of nanoparticles in polymer matrix of the BHJ active layer. Such control can be realized by a ligand modification of nanoparticle surface by means of application of corresponding a surfactant dyes, in particular PI dyes.

The present study is devoted to effect of new interface modifiers, IMs (substituent perylen imide dyes with a different number of alkyl-octyl substituents and naphthyl phosphonic acid (NPA)) on the active layer morphology and photovoltaic properties of polymer/ZnO BHJ solar cells.

It was demonstrated that IMs can to control the phase separation in MEH-PPV/nc-ZnO blend films and influence on photovoltaic properties of BHJ solar cells. It is determined that all studied IMs decrease the fluorescence lifetime quenching and increase the quenching efficiency owing to favorable position of their energy levels respect to polymer MEH-PPV and ZnO nanocrystals ones. It is shown the presence of alkyl substiuents in PI induce the homogeneous distribution of nc-ZnO with IM(PI1) and a random distribution of a small-size aggregates of nc-ZnO with IM(PI2). For BHJ photovoltaic cell the most device performance was obtain when IM(PI2) was used.

9140-36, Session PS2

Characterization of silicon nanoparticles (Si-nps) embedded in a silicon-nitride matrix by spectroscopic ellipsometry

Jean-Paul Gaston, Céline Eypert, HORIBA Scientific (France)

Silicon nanoparticles (Si-nps) show different optical properties than bulk silicon. A strong correlation has been established between the particle size and the band-gap. These particular properties offer potentialities of application in optoelectronics, silicon based memories and third generation solar cells where nanoparticles embedded in a dielectric matrix are used to enhance the photovoltaic effect.

The approach consists in reducing the losses of single band-gap solar cells, namely the ability to absorb photons with energies less than the band-gap and the losses by thermalization of the photons with energies higher than the band-gap. Thus, varying the particle size enables to optimize the absorption of light. In another hand, a precise determination of the optical properties of these nanoparticles is required for a better optimization of the efficiency of the resulting solar cells. From this point of view Spectroscopic Ellipsometry represents a technique of choice for the characterization of the optical and structural properties of these layers.

Silicon-Rich silicon Nitride (SRN) layers with silicon excess deposited on silicon substrate were prepared by remote controlled ECR-PECVD. These SRN layers were obtained by the deposition of a mixture of pure silane (SiH4) and ammonia (NH3) on a silicon substrate. The gas flow ratio NH3/SiH4 gives the silicon excess amount with regard to Si3N4 stoichiometry. The samples are then annealed in order to induce the crystallization of the Si-nps in the SRN layers.

The ellipsometric measurements were carried out with a UVISEL spectroscopic ellipsometer in the visible range [1.5–6.5 eV]. The analysis of the ellipsometric experimental data aimed at the determination of the layers thicknesses, volume fractions and the optical properties of the Si-nps. The analysis has been undertaken over two steps. The first one focused the attention on the determination of the thicknesses of the SRN Layers and the volume fractions of the Si-nps by using the Bruggeman Model also refereed to as EMA (Effective Medium Approximation)

In the second step, the thicknesses and the volume fractions have been fixed as obtained form the first step and a Tauc-Lorenz dispersion formula has been used to refine the optical properties of the silicon nano-particles

9140-37, Session PS2

Post-hydrogenation of amorphous hydrogenated silicon films modified by femtosecond laser irradiation

Mark Khenkin, Andrey Emelyanov, Andrei G. Kazanskii, Lomonosov Moscow State Univ. (Russian Federation); Pavel Forsh, Lomonosov Moscow State Univ. (Russian Federation) and Russian Research Ctr. Kurchatov Institute (Russian Federation); Oleg Kon'kov, Ioffe Physicotechnical Institute (Russian Federation); Martynas Beresna, Mindaugas Gecevicius, Peter G. Kazansky, Univ. of Southampton (United Kingdom)

Tandems of amorphous (a-Si:H) and nanocrystalline (nc-Si:H) hydrogenated silicon are widely applied for photovoltaics. Laser crystallisation of a-Si:H films allows to optimise tandems manufacturing process due to avoiding multiple deposition stages and precise localisation of laser induced modification. The main issue limiting the employment of this technology is hydrogen out-diffusion which accompanies laser processing. Hydrogen is used to passivate dangling bonds in a-Si:H structure and at a-Si:H/c-Si interface, thus it is a key factor determining films quality for photovoltaics. Here we report our study of evolution of hydrogen content in femtosecond laser crystallised a-Si:H films and its recovery of by post-hydrogenation procedure.

a-Si:H films were deposited by conventional PECVD method from silan and argon gas mixture. Laser processing was performed with Yb:KGW laser system (?= 1030 nm, ? = 300 fs) with different laser fluences (30-155 mJ/cm2). After the treatment films were exposed to hydrogen plasma for 1 hour.

Raman spectroscopy revealed that crystalline volume fraction in modified films gradually increases with laser fluence and reaches maximal value of 70 %. Constant photocurrent method (CPM) was used as suitable tool for studying photoconductivity of films with a complex structure. It was found that before hydrogen plasma treatment CPM spectra of studied films had "a-Si:H"-like lineshape until the high crystallinity (> 60 %) was reached. This behavior is evidence of low photoconductivity of modified part of the films, because the total photoconductivity value is determined by contribution of a-Si:H part remaining after the crystallisation. However for films exposed to hydrogen plasma after laser treatment the shape of CPM spectra gradually changes from "a-Si:H"-like to "nc-Si:H"-like with increase of films crystallinity. This result points that films' photosensitivity was restored by hydrogen incorporation in their structure.

9140-38, Session PS2

Effective enhancement of conversion efficiency for a-Si thin-film solar cell using patten-array dendritic silver nanostructure

Wei-Hsuan Lai, Chi-Pin Chiu, Feng Chia Univ. (Taiwan); Der-Jun Jan, Wei-Hsiu Hsu, Institute of Nuclear Energy Research (Taiwan); Shih-Shou Lo, Feng Chia Univ. (Taiwan)

Pattern-array dendritic silver nanostructure has been fabricated by a laser interference lithography technique and electrochemistry process. The morphology of the Ag nanostructure can be well controlled by the reaction time. When the proposed structure was used in the solar cell. The back-reflector of solar cell can be well designed by various Ag nanostructures and periods. For an as-fabricated 1D periodic Ag nanostructure substrate with period 1 um, a 7% increase in conversion efficiency of a-Si thin-film solar cell is obtained due to enhanced near-field coupling, and that the path length enhancement than the single transparent conductive layer. The scattering cross section of the silver nanostructure is sensitive of the thickness, which provides additional tunability in the design of dendritic silver array.

9140-39, Session PS2

Tunable phenylenevinylene dimer and trimer molecules for light harvesting antennas

Delower Bhuiyan, Callaghan Innovation (New Zealand); Nicola Winch, Gerald J. Smith, Victoria Univ. of Wellington (New Zealand); Sebastiampillai G. Raymond, Robert D. Breukers, Andrew J. Kay, Callaghan Innovation (New Zealand); Trevor A. Smith, The Univ. of Melbourne (Australia)

In photosynthesis plants capture energy from sunlight using an "antenna" assembly of chromophores, notably chlorophyll. This antenna relays the energy to reaction centers where it is converted to chemical energy. There is considerable interest in mimicking this phenomenon using synthetic chromophores in thin polymer films for application in solar cells. In this case the function of the chromophore antenna is to absorb diffusely-distributed photons and convey the excitation energy to solar-electrical energy conversion sites.

To develop novel materials for such an antenna system requires an understanding of the excitation energy transfer

(EET) processes. These EET processes are dependent on the intramolecular conformations of the component chomophores and the macrostructural molecular architecture of the antenna system. Promising materials for antenna systems include poly-(para-phenylenevinylene) (poly-PV), and its derivatives such as poly-(2-methoxy-5-(2-ethyl-hexoxy)-1,4-phenylene vinylene) (MEH-poly-PV).

In this paper we focus on PV-based antenna systems with regard to the photophysics of the individual chromophore dimers and trimers, and the energy transfer characterristics of these chromophores in different molecular environments. The fluorescence quantum yields and lifetimes of two substituted PV dimers were found to vary substantially in solvents covering a range of polarities and viscosities. The fluorescence yield in such environments gives insights into the non-radiative photon-loss pathways, which would reduce the net efficiency of PV molecules in antenna systems. Losses are related to both the viscosity and polarity of the medium, and can be explained in terms of the higher energy absorbed photons populating Franck-Condon states, these relax directly by twisted intramolecular charge transfer “funnels” in the excited state potential energy surface, from where they non-radiatively cross to the ground state.

9140-40, Session PS2

Direct-pulsed laser interference texturing of ZnO:Al front contact layers for light trapping in a-Si:H/μc-Si:H solar cells

Sven Ring, Sebastian Neubert, PVcomB (Germany); Florian Ruske, Helmholtz Zentrum Berlin (Germany); Bernd Stannowski, PVcomB (Germany); Frank Fink, Hochschule fuer Technik und Wirtschaft (Germany); Rutger Schlatmann, PVcomB (Germany)

In Si thin film photovoltaics, texturing of the front contact layers is a common way to increase cell efficiency. We present results on direct pulsed laser interference texturing of ZnO:Al for the application as light-scattering front contact for silicon thin film solar cells. The samples were fabricated on 3.2 mm low iron glass which have been coated with a ZnO:Al layer. Micro diffraction gratings of 20 micron diameter with smoothly shaped grooves and a period of 860 nm have then been written using single pulses of a 355 nm picosecond laser using a two-beam interference setup. The groove depth depends on the local laser intensity, and reaches up to 120 nm. At too high pulse energies, the grooves vanish due to surface melting of the ZnO:Al. The fast scanning stage and the high repetition rate laser of a laser scribe system have been used to write grating textures of several cm? size in ZnO:Al films with a surface coverage of about 80%. A typical laser written grating texture in a ZnO:Al film showed a haze value of 9% at 700 nm. Light scattering of the grating texture sets in for ?< P, as expected from the simple grating equation for grating textures in air. The total transmission of the film was not deteriorated compared to the film before texturing, while the sheet resistance increased moderately by 15%. In particular, a strong darkening of the ZnO thin film, which has been reported previously for nanosecond laser pulses, cannot be observed for picosecond UV-laser pulses. A-Si:H/μc-Si:H tandem solar cells have then been deposited on the laser textured ZnO:Al front contacts layers, using PVcomB’s standard tandem deposition processes, based on a p-i-n/p-i-n stack in an AKT 1600 PECVD system. The i-layer thickness of the top and bottom cell was 290 nm and 1750 nm, respectively. The back contact, consisting of an 80 nm thick ZnO:Al layer and a 200 nm thick silver layer, was deposited using DC-magnetron sputtering. Cells of 1 cm? size were defined by laser scribing after back contact deposition. These cells using the laser grating textured front contact reach an efficiency of 11 %. The short circuit current density reaches 11.0 mA/cm?, which is an increase of 19% as compared to reference cells on planar ZnO:Al. The open circuit voltage of the laser textured cells is not reduced as compared to the reference cell, indicating similar device quality of the Si grown on the different substrates. This approach allows to write textures in ZnO:Al films that have been deposited under conditions not suitable for wet chemical texturing. The method can be improved further by using 2D periodic patterns and optimizing the groove pitch, and may be applicable also to other solar cell technologies.

9140-41, Session PS2

Reactive pulsed-laser deposition of amorphous hydrogenated silicon thin films for solar cell applications

Maria Kandyla, Athanasios Mellos, Michael G. Kompitsas, National Hellenic Research Foundation (Greece)

Amorphous hydrogenated silicon (a-Si:H) thin-film solar cells achieve power conversion efficiencies up to 12% and take advantage of the existing infrastructure of the silicon industry, therefore they are of high technologic interest. Moreover, amorphous silicon is cost-effective compared to crystalline silicon and it is only needed in small quantities for thin-film solar cell production on rigid or flexible substrates. Pulsed laser deposition (PLD) is a simple, versatile, and cost-effective technique for the deposition of a-Si:H layers.

We employ reactive pulsed laser deposition for the fabrication of a-Si:H solar cells in the p-i-n configuration for increased efficiency, because the short minority-carrier lifetime in a-Si:H, especially in the doped varieties, requires electric field assistance for efficient collection of photogenerated carriers. We irradiate silicon targets by a large number of laser pulses produced by a Q-switched Nd:YAG laser system (10 ns pulse duration, 355 nm wavelength) in hydrogen atmosphere. Varying the PLD parameters, such as the laser fluence, number of pulses, substrate temperature, and hydrogen pressure, we optimize the morphology, structure, electric conductivity, and optical properties of the a-Si:H layers for maximum efficiency.

IR transmission measurements on a-Si:H thin films deposited on silicon substrates indicate Si-O, Si-Si, and Si-H bonds. From the transmission peaks originating from Si:H bonds we estimate the amount of hydrogen in the films. The hydrogen content of the films increases linearly with the PLD hydrogen pressure up to a certain point. Beyond the PLD hydrogen pressure of 15 Pa, excessive hydrogen removes H atoms from the surface of the films and the final hydrogen content decreases.

From optical transmission and reflection measurements in the wavelength range 300 – 1200 nm, we are able to determine the optical bandgap of the films. The optical bandgap increases with increasing hydrogen pressure during deposition, until it reaches a maximum value (at 15 Pa) and then starts decreasing, ranging from 1.5 – 2.5 eV. The presence of hydrogen in a-Si:H films is known to passivate Si dangling bonds, which create midgap electronic states. Therefore, by the reduction of these states, the optical bandgap increases. In agreement with the IR transmission data, the reduction of the hydrogen content of the a-Si:H films beyond the PLD hydrogen pressure of 15 Pa results in a decrease of the bandgap.

Electrical measurements obtained at room temperature by the Van der Pauw method, reveal that the conductivity of the films increases with the PLD hydrogen pressure up to the value of 15 Pa, upon which the conductivity starts decreasing, in agreement with the IR and optical data. Passivation of the Si dangling bonds by the incorporated hydrogen is known to improve the electrical properties of a-Si:H films.

The samples structure was studied by X-ray diffraction (XRD). We observe that the amorphous phase prevails, but the crystallinity of the films is improved by increasing the hydrogen pressure during deposition up to the pressure value of 15 Pa.

9140-42, Session PS2

Cu2ZnSnS4 semiconductor materials based on Cu, Sn, and ZnS by using a sequent sulfurization process

Chi-Pin Chiu, Wei-Hsuan Lai, Shih-Shou Lo, Feng Chia Univ. (Taiwan)

In this study, Cu–ZnS–Sn layers were fabricated using the co-evaporation method and the co-evaporation films were transformed into CZTS films by using the sulfurization process at a high-temperature, 550 oC. The influence of sulfurization time on the Raman, photoluminescence, structure and conductivity of CZTS thin-film are studied in detail.

The CZTS thin film was developed using a Cu, Sn, and ZnS co-evaporation process and a sequent sulfurization process, and a proposed formation path of the CZTS thin-film is presented. In this experiment, the detection secondary phase that cannot be distinguished only using XRD-based techniques was demonstrated. The result indicates the potential of the Raman scattering technique in detection and in-depth resolved analysis of secondary phases for CZTS thin-film. A narrow direct band gap of 1.2 eV was obtained for the compound CZTS, which was confirmed using PL measurement. The EDS and Hall measurement confirmed the p-type electrical behavior can be achieved in the CZTS thin-film with Cu-poor and Zn-rich condition. The CZTS thin-film shows potential for application for solar cells.

9140-43, Session PS2

Fabrication of Ag nanostructure via laser interference lithography and electrochemical process for solar cell appliction

Shih-Shou Lo, Wei-Hsuan Lai, Feng Chia Univ. (Taiwan)

Silicon is the materials of choice for photovoltaic applications due to its low cost, nontoxicity and abundance in nature However, the efficiencies of such silicon thin-film cells at the moment are low compared to wafer-based silicon cells because of the relatively poor light absorption. Therefore, thin-film silicon solar cells require light trapping for high performance. Because a-Si thin-film solar cells are only a few microns thick, standard method of increasing the light absorption, which used surfaces textures that are typically around 10 microns in size for wafer-based cells [1]. However, for thin-film solar cells, which may have a thickness of only 1-2 ?m, such textures are not suitable. A way of achieving light trapping in thin-film solar cells that has emerged recently is the use of scattering from metal nanoparticles [2-3].

Recently, it has been demonstrated that metal nanoparticles fabricated by laser lithography, metal deposition process and annealing process.[4] Laser lithography has been a nearly ideal nanofabrication tool for these studies since it can produce surface confined nanoparticles with fixed interparticle spacing in a massively parallel manner. As a consequence, laser lithography derived nanoparticles do not aggragate and behave optically as N weakly coupled nanoparticles rather than as an array of strongly coupled focus on sensing mechanisms involving local refractive index changes and/or medicated optical responses. Furthermore, laser lithography allows for the easy manipulation of the nanoparticles size [5]. Surface plasmon resonance in metallic nanoparticles is currently being exploited for a variety of application subwavelength photonic [6] and solar cell [7]. The appeal of surface plasmon excitations or such applications typically arises from the large electromagnetic field enhancement near the metal surface, and the dependence of the resonance wavelength on the nanoparticle's size, shape and local dielectrics environment. In this study, we report such an effective 7% enhancement of conversion efficiency in an a-Si thin-film solar cell semiconductor via excitation of surface plasmon resonance in dendritic Ag with periodic pattern-array structure deposited by electrochemical process on an ITO substrate.

9140-45, Session PS2

Metamaterial photonic crystals for photovoltaic applications

J. Ricardo Mejía-Salazar, Brayan F. Diaz, Nelson Porras-Montenegro, Univ. del Valle (Colombia)

We have performed a theoretical study of 2D metamaterial photonic crystals composed by metamaterial cylindrical rods. Numerical calculations were performed by means of the well known finite difference time domain technique. As a result, we have observed a superior electromagnetic field localization in this type of systems when compared with its conventional plasmonic photonic crystal counterpart, which constitutes itself as an alternative to enhance the light-matter interaction for applications in sensors and photovoltaic cells. On the other hand, we have performed a comparative analysis of the excited Mie plasmon-polariton modes in this type of systems with analytical results corresponding to a single metamaterial cylinder, obtaining a very good agreement.

9140-46, Session PS2

Structures used in optical fibers that increase the collection of solar radiation used for indoors lighting

Tania Nicte Mata Mata, Univ. Autónoma de Nuevo León (Mexico); Gustavo Rodriguez Morales, UNIVERSIDAD AUTONOMA DE NUEVO LEON (Mexico) and FACULTAD DE INGENIERIA MECANICA Y ELECTRICA (Mexico); Norma P. Puente, Univ. Autónoma de Nuevo León (Mexico)

In recent years it has been looking for a renewable energy under the power with which we have now is not a permanent resource in the future will be insufficient. In this paper pretends use the solar energy for the indoors illumination, different methods has been evaluated for a better capture and distribution of the daylight, some researchers have proposed optical devices for the capture of the sunlight like solar modules, mirrors, fiber, optical tubes, etc. But for transportation has been chosen the optical fiber as previous studies have shown that the fiber is effective in the uniform distribution and able to tolerate the heat. There have been studies of solar radiation global and then focus in Mexico about the spots of intense solar radiation located geographically, a study of the months and hours where a maximum radiation is obtained. In this work we study this new technology through optical devices capable of collect the daylight, located in specific points of high intensity of solar radiation, that way can be transported for the optical fiber. The first step of this new technology is with some optical devices that captures the daylight, could be for a mirror arrangement or solar modules, once the light is concentrated for this devices, the light will be refracted inside the fiber with an special optical geometry, which consist of a conical aperture inside and the light can be transported, distributed and used for illumination. Through a program is calculated the path of light, and once the light beam enters the optical fiber is simulated with possible angles caused by the incident beam and vertex angles hollow conical opening of the fiber, showing that a certain value of angles the light can't be refracted and reflected, also was evaluated the refraction index of the air, core and cladding of the optical fiber looking for the light inside the fiber have a total internal reflection, once the light inside the fiber get a total internal reflection will show that doesn't have lost and can be used for illumination. It has been proposed a second conical aperture for ensure that a double opening can have more light and can be distributed along the fiber; with this new system will reduce the consume of electricity and will be an excellent alternative of the environment.

9140-47, Session PS2

Computational optimization of triangular and honeycomb lattice structured tapered nanoholes for enhanced light trapping in thin-film Si solar cells

Jolly Xavier, Helmholtz-Zentrum Berlin für Materialien und

Energie GmbH (Germany); Sven Burger, Konrad-Zuse-Zentrum für Informationstechnik Berlin (Germany); Philippe Wyss, Daniel Lockau, Helmholtz-Zentrum Berlin für Materialien und Energie GmbH (Germany); Martin Hammerschmidt, Konrad-Zuse-Zentrum für Informationstechnik Berlin (Germany); Bernd Rech, Helmholtz-Zentrum Berlin für Materialien und Energie GmbH (Germany); Frank Schmidt, Konrad-Zuse-Zentrum für Informationstechnik Berlin (Germany); Christiane Becker, Helmholtz-Zentrum Berlin für Materialien und Energie GmbH (Germany)

For an optimized light harvesting while using diverse periodic photonic light-trapping architectures in low cost thin film crystalline Si solar cells, it is also of prime importance to tune the features of their lattice point basis structure. In view of this, tapered nanoholes would be of importance for envisaged better light incoupling due to graded index effect and also from the point of fabrication feasibility. Using a 3D finite element modeling software, here we computationally investigate the basis structural influence of triangular as well as honeycomb lattice structured experimentally feasible tapered air nanoholes in a 400nm thick crystalline Si absorber. In addition to giving convergence of measurements for both these structures considering a rectangular computational domain, for the case of triangular lattice structures we also give our results of convergence using a hexagonal computational domain. The former may be of greater interest for achieving a maximum tapering angle and a large diameter of the nanoholes in the direction of incidence. For a wavelength rage of 300 to 1100nm, we present the computed results on light absorption of the engineered Si nanoholes for diverse effective pitches ≤ 1000nm for an intended fill fraction. For the studied triangular as well as honeycomb lattice structured nanoholes, we observe that in comparison to the cylindrical nanoholes, the tapered nanoholes perform better in terms of light trapping in textured Si thin films. In particular, we rigorously study the influence of side wall angle of the tapered nanoholes in Si thin film for the optimized absorption enhancement. A comparison of our computed results with a few experimental measurements is also done to support our computational findings for optimization of the tapered nanoholes. Further we extend our study on these array of optimized tapered nanoholes for optical path length and optical efficiency enhancement in a single junction thin film crystalline Si solar cell.

9140-49, Session PS2

Doping effect on optical band gap and structural properties of tin oxide and zinc oxide

Naziha Kesri, University (Algeria)

ZnO and SnO2 are inexpensive metal oxides when they are deposited by simple techniques. They belong to the important family of transparent conducting oxides (TCO) of high optical band gap that combine low electrical resistance with high optical transparency in the visible range of the electromagnetic spectrum and important emission band in the UV spectra. The optical band gap can be tuned by doping with suitable metal and/or nonmetals making the possibility to get intermediate bandgaps.

Currently, zinc oxide and tin oxide thin films are intrinsically n-type semiconductors. Origin of n-type conductivity could be the existence of native point defects, structural defects, n-type doping by appropriate atoms and the source of such conductivity is still in debate. However, in order to fully use SnO2 and ZnO potential for the fabrication of optoelectronic devices, access to p-type of highly controlled properties is desirable. But ZnO and SnO2 have asymmetric doping limitations, i.e., they have a tendency to become n-type rather than p-type. Recently increasing attention has been paid to get p-type for both SnO2 and ZnO and cheaper solar cell as a p-n junction.

In this work, undoped and Cu-doped zinc oxide thin films have been deposited onto glass substrates by spray pyrolysis technique. By the same technique, undoped and Zn-doped tin oxide thin films have been deposited onto glass. The two doping atoms could give p-type conductivity and act significantly on band gap. The precursor solution is formed mainly by zinc acetate and copper chloride for ZnO and by tin chloride and zinc acetate or zinc chloride for SnO2. The substrate temperature was fixed at 450°C and we vary [Cu/[Zn] or [Zn/[Sn] ratios, calculated on atomic percent in the starting solution, from 0 to 30%. We report structural results of the films using X-ray diffraction. All Cu-doped ZnO films are polycrystalline with wurtzite phase and preferential orientation along (002) direction. The diffractive peaks of samples, which corresponded to (110), (101) and (211) of standard SnO2 powder, indicated that the samples were polycrystalline rutile structure. While copper incorporation affects stronghly lattice parameters in Cu-doped ZnO, zinc doping remains SnO2 rutile parameters almost constants. The optical measurements of the crystalline ZnO and SnO2 thin films were carried out at room temperature using Cary 500 UV-VIS-NIR spectrophotometer in the wavelength range from 300 to 2500 nm. Swanepoel's envelope method was employed to evaluate the optical constants such as the refractive index n, extinction coefficient k, and absorption coefficient ? from reflectance spectra. The thickness of the films was determined from interference fringes of transmission data measured over the visible range and the optical band gap was obtained from the dependency of absorption coefficient on photon energy. For Cu-doped ZnO, it can be seen that the band gap first decreases as the Cu/ (Cu+Zn) atomic ratio increases. However, higher ratios increase Eg. The measured band gap values of the films were between 3.17 and 3.26 eV. For Zn-doped SnO2, the measured optical band-gap was found to be ranged from 3.8 to 3.7 eV.

9140-24, Session 6

10% efficiency solar thermophotovoltaic systems using spectrally controlled monolithic planar absorber/emitters

Hiroo Yugami, Makoto Shimizu, Asaka Kohiyama, Tohoku Univ. (Japan)

In solar thermophotovoltaic (STPV) generation systems, the thermal radiation from emitters heated by the high temperature solar absorbers is converted into electricity at a photovoltaic (PV) cell. The STPV system has some advantages against PV generation system. For instance, it is possible to control the thermal radiation spectrum of the emitter. The PV cell generally has the inherent sensitive region where an incident photon excites an electron. Therefore, the enhancement of the thermal radiation at the sensitive region of the PV cell increases the generation efficiency.

Theoretically, the STPV system efficiency reaches up to 85% and 45%, considering Carnot efficiency and using an emitter which emits monochromatic radiation, respectively. However, the experimental STPV system shows lower efficiency than theoretical one. For example, in case of using unstructured Tungsten emitters at a concentration of 4000 suns and GaSb PV cell, the net efficiency of STPV system is about 2% . The low system efficiency is mainly caused by a large amount of heat loss from the high-temperature absorber/emitter system.

The purpose of this study is to achieve a high-efficiency STPV generation system using a monolithic planar absorber/emitter. The superiority of the maximum temperature on the monolithic planar absorber/emitter is estimated by using spectral and thermal properties of components in the STPV system. Using the full configuration of the STPV system, the system efficiency about 10% is achieved in this study.

9140-25, Session 6

Optimisation of textured tandem solar absorber performances using a genetic algorithm approach

Lucie Gaouyat, Alexandre Mayer, Univ. of Namur (Belgium); Frederic Mirabella, ArcelorMittal Liège (Belgium); Olivier Deparis, Univ. of Namur (Belgium)

Solar absorbers are classified into six types [1]. Most commonly, the “tandem absorber” type is used, which consists of CERMET (CERamic-METal) layers topped with Anti-Reflective (AR) layers. On the other hand, a promising alternative to the tandem design is the use of a stand-alone textured metallic substrate, which is justified by absorption enhancement due to light trapping effect. Our study first reports on the theoretical performances of an optimally textured aluminium substrate. In addition, we study the combination of both approaches, i.e. conformal tandem absorber layers deposited on a textured substrate. Starting with the stand-alone substrate, the chosen texture was a “waffle-like” periodic corrugation of reversed truncated pyramids, which was defined by four geometrical parameters. A genetic algorithm approach was used in order to optimise simultaneously both the solar absorptance (?) and the thermal emittence (?) (at 100°C). The optimisation was performed over a broadband wavelength range, from 300 nm to 15 µm. The optimized stand-alone textured substrate exhibited ?=81.1% and ?=4.5%. In a second step, the use of conformal tandem absorber layers on the textured aluminium substrate was modelled following the same approach. The tandem stack introduced two additional parameters in the optimisation. Experimental values of refractive indexes of NiCrOx cermet layer and SnOx AR layer were determined by UV-visible- and IR-spectroscopic ellipsometry. A six-parameter optimisation is on-going, the result of which will be presented at the Conference. All optimised performances will be compared to a flat reference. Better opto-thermal performances are anticipated, hopefully reaching the market state-of-the-art.

[1] C.E. Kennedy, NREL technical report, July 2002.

9140-26, Session 6

New light-trapping concept by means of several optical components applied to compact holographic 3D concentration solar module

Ayalid M. Villamarín Villegas, Instituto Holográfico Andaluz, S.L. (Spain); Francisco J. Pérez López, Instituto Holográfico Andaluz S.L. (Spain); Antonio Calo López, Hugo J. Rodríguez San Segundo, Instituto Holográfico Andaluz, S.L. (Spain)

A new light-trapping concept is presented, which joins broad bandwidth volume reflection holograms working together with three other optical components: specifically designed three-dimensional (3D) cavities, Total Internal Reflection (TIR) within an optical medium, and a highly reflective surface. This concept is applied to design and develop low concentration photovoltaic (CPV) and solar thermal modules reaching a concentration factor of up to 3X. Higher concentrations are feasible for use in concentrated solar power (CSP) devices. The whole system is entirely made of polymeric materials (except for the solar cells or fluid carrying pipes), thus reducing weight and cost by up to 40%. The module concentrates solar light onto the solar cells – or fluid carrying pipes – with no need for active tracking of the sun, covering the whole seasonal and daily incident angle spectrum while it also minimizes optical losses. In this work the optical characteristics and performance of the multiplexed volume reflection holograms registered in dicromated gelatine film (DCG) are analysed. The holograms can reach high diffraction efficiencies (98%). Thanks to specifically designed raw material, coating and developing process specifications, also very broad selective spectral bandwidth (higher than 250 nm) and angular bandwidth (+15º) per grating are achieved. The hologram with these features was optimized to use silicon solar cells, thus trapping the energy in the spectral region from 500 nm to 1100 nm. However, other holographic designs for other semiconductor devices or for fluid heating are feasible. The 3D shape, the optical quality of both hologram and reflective surface, the TIR effect and the correct coupling of all the components are key to the high performance of the concentration solar module.

9140-27, Session 6

Spectral splitting planar solar concentrator: experimental testing of a design aiming at dye sensitized solar cells

Pascal Blain, Céline Michel, Lionel Clermont, Fabian Languy, Univ. de Liège (Belgium); Marc Décultot, University of Liège (Belgium); Serge Habraken, Univ. de Liège (Belgium); Cédric Lenaerts, Karl Fleury-Frenette, University of Liège (Belgium); Denis Vandormael, SIRRIS (Belgium); Jérôme J. D. Loicq, Univ. de Liège (Belgium)

In this paper we present a new design concept for solar concentrator based on waveguiding and spectral splitting of light. Planar solar concentrators allow guiding incident light onto spatially separated solar cells [1]. Our idea consists in spectrally assign parts of the incoming flux to cells with suited spectral responses. By comparison with MJ cells, it has the advantage of enabling the independent control of output power of each junction. Moreover different and/or unmatched lattice solar cells could be used at the same time.

This concentrator is based on sunlight coupling in the waveguide by diffractive elements and refractive ones [2]. Sunlight impinges an array of blazed diffraction gratings combined with asymmetric cylindrical lenses. This optical element couples light into the waveguide. The waveguide consists in a transparent slab with aluminum coated V-shaped grooves. These V-grooves are placed at the focal points (lines) of the cylindrical lenses. Thanks to the diffraction grating, the optical design enables the spectrally broadened focalized first order diffracted light to be split into two beams by the V-grooves. Both beams cover two different spectral domains and aim opposite directions. Those beams undergo total internal reflection on both sides of the slab and exit through the waveguide edges. Meanwhile, the unwanted 0th order, which essentially contains thermal infrared responsible of heating problems, crosses right through the slab. Overheating issues are thus reduced.

One practical application of that concentrator is to guide sunlight to dye sensitized solar cells. A design is proposed to redirect sunlight to N3 (UV/Vis conversion) and SQ2 (NIR conversion) dye cells. After the description of the concept and the design, we will present the experimental characterization of the optical elements of the concentrator and evaluate their efficiencies. The theoretical optical efficiency of that concentrator concept reaches 82%.

[1] J.H. Karp, et al., “Planar micro-optic solar concentrator,” Opt. Express 18 (2), 1122-1133 (2010).

[2] C. Michel, et al., “Optical study of a solar concentrator for space applications based on a diffractive / refractive optical combination”, Solar Energy Materials and Solar Cells (2013), http://dx.doi.org/10.1016/j.solmat.2013.08.04

9140-28, Session 6

Investigation of spectral impacts on the performance of a concentration device using a Fresnel lens combined with a double junction cell

Jérôme J. D. Loicq, Univ. de Liège (Belgium); Nicolas Galante, Facultes Univ. Notre Dame de la Paix (Belgium); Tanguy Thibert,

Marie-Laure Hellin, Fabian Languy, Serge Habraken, Univ. de Liège (Belgium)

This experimental study was carried out within the context of high concentration photovoltaics.

The paper presents the results of an experimental investigation relating to the quantification of the impacts of the chromatic effect on the performance of a double junction GaInP/GaAs solar cell. Chromatic effects are the result of material dispersion caused by the refractive optics component. This study aims to evaluate the effect of the spectral modification of the incident beam on the whole solar concentrator system performance. Such considerations are fundamental in producing a highly accurate design, with which to achieve the best possible system performance. Efficiency is evaluated within the vicinity of the focus of a Fresnel lens designed for concentration. On the optical axis, rays with different wavelengths are not focalized at the same points. The spectral content of the beam depends, therefore, upon the position of the cell along the optical axis. It is assumed that spectral content modification may have an impact on cell performance and, as a consequence, on system efficiency as a whole. Efficiency of the optical Fresnel lens and of the cell were evaluated in relation to spectral content modification.

9140-29, Session 7

Solar highways: core-shell nanowires for high-efficiency, low-cost photovoltaics *(Invited Paper)*

Erik C. Garnett, Beniamino Sciacca, Sander Mann, Sebastian Oener, FOM Institute for Atomic and Molecular Physics (Netherlands)

The ideal solar cell would convert light into electricity in an infinitely small volume. Such a structure not only limits material usage but also relaxes carrier diffusion length requirements and maximizes the output voltage. Here we describe a novel solar cell geometry consisting of a metal nanowire covered by an ultrathin semiconductor layer, which shows extreme light absorption enhancement.[1] Using both Mie theory and finite difference time domain simulations, we show that inserting a metal core into a semiconducting nanowire dramatically improves absorption in two ways: (1) increasing the total number of spectrally overlapping resonances and (2) maximizing absorption per resonance by satisfying the critical coupling condition. The additional freedom provided by independent tuning of metal core diameter and shell thickness provides the ability to enhance absorption in both polarizations. Using full-field simulations we show that these outstanding optical properties are robust against geometrical perturbations such as changes in cross-sectional shape. We begin experimental work with a model system consisting of a silver nanowire core and cuprous oxide shell. These core-shell nanowires are synthesized at low temperature in solution and here we will present high-resolution transmission electron microscopy images and selected area electron diffraction patterns proving that the core-shells are single-crystalline with atomically sharp and epitaxial interfaces. We will show spatially-resolved, single nanowire optical measurements (reflection, scattering, absorption) taken using an integrating sphere and compare the results to theoretical predictions. Finally, we will show that this same core-shell geometry can be combined with anodic alumina templates to make vertical arrays of core-shell nanowires.

[1] S.A. Mann and E.C. Garnett, Nano Letters, 13, 3173, (2013).

9140-30, Session 7

Ultraviolet curing nanoimprint green lithography using water-repellent film derived from biomass for solar cells devices

Satoshi Takei, Toyama Prefectural Univ. (Japan); Kenta Ito, Toyama Prefectural Univ (Japan); Gaku Murakami, Richell Corp. (Japan); Tsutomu Obata, Yoshiyuki Yokoyama, Toyama Industrial Technology Center (Japan); Kigenn Sugahara, Toyama Industrial Technology Center (Japan) and Toyama Prefectural Univ (Japan); Wataru Mizuno, Junji Sumioka, Toyama Industrial Technology Center (Japan); Masayuki Fujii, Richell (Japan); Tetsuro Okada, Toyama Prefectural Plastic Industries Association (Japan)

Nanopatterning of an ecofriendly water-repellent film derived from biomass using an ultraviolet curing nanoimprint green lithography was investigated. Developed sugar-related organic compounds with liquid glucose and trehalose derivatives derived from biomass produced high-quality imprint images of pillar patterns with a 100-500 nm diameter. Ecofriendly antiglare film with liquid glucose and trehalose derivatives derived from biomass was indicated to achieve the real refraction index of 1.45 to 1.53 at 350 to 800 nm, low imaginary refractive index of <0.004 and low volumetric shrinkage of 5.9 % during ultraviolet irradiation. A distinctive bulky glucose structure in sugar-related organic compounds was considered to be effective for minimizing the volumetric shrinkage of the water-repellent film during ultraviolet irradiation, in addition to suitable optical properties and water-repellent property for the surface of solar cells devices.

9140-31, Session 7

Study of plasmonic nanoparticle arrays for photon management in solar cells

Sabrina Juechter, Sarah-Katharina Meisenheimer, Fraunhofer-Institut für Solare Energiesysteme (Germany); Thomas Fix, Univ. de Strasbourg (France) and iCube Lab. (France); Hubert Hauser, Christine Wellens, Fraunhofer-Institut für Solare Energiesysteme (Germany); Ulrich T. Schwarz, Fraunhofer Institut für Angewandte Festkörperphysik (Germany); Benedikt Bläsi, Fraunhofer-Institut für Solare Energiesysteme (Germany)

Photon management is of increasing importance for solar cells, as thinner cells and higher efficiencies should be achieved simultaneously. The use of metallic nanostructures revealing plasmonic effects is one promising concept [1]. In this way, light trapping can be improved by scattering and diffraction of incident light at the plasmonic particles. This leads to increased internal path lengths and thus an enhancement in absorption.

Different approaches to fabricate plasmonic nanostructures are available [1]. In literature, most often results from self-organized metal particles can be found. These irregular structures show resonances for different wavelengths and also suffer from parasitic absorption as a result of the varying dimensions of the particles [2]. The parasitic absorption can be minimized by realising regularly ordered particles. Our fabrication process, suitable to meet these requirements, is based on interference lithography (IL), UV-nanoimprint lithography (UV-NIL) and lift-off. We use IL for the realization of master structures. This process allows patterning of nanostructures on areas up to one square meter. Combining IL with NIL as a replication technique, the process chain is very flexible in shapes, sizes and arrangements [3] and has the potential to be up-scaled. In the UV-NIL process, a flexible silicone stamp, which was replicated from the master structure, is pressed into a UV-curing resist. While maintaining the pressure, the resist is cross-linked using UV light. A plasma etching step is applied to remove the residual resist layer. Afterwards, the substrate is coated with a thin metal layer and finally a lift-off process is carried out. This results in metallic nanoparticles arranged in a regular pattern on

the substrate.

We show experimental results of disk shaped particles arranged in a crossed grating with 300 nm period and elliptical particles arranged in a hexagonal grating with a lattice space distance of 300 nm. These two particle arrays were characterised optically on glass and on silicon substrates. Due to the alignment of the elliptical particles, the spectral position of the resonance peak depends on the polarization. This enables switching between different effective particle sizes by changing the polarization direction. In this way, the size dependence of the plasmonic resonance on metal particles can be investigated. Furthermore, it is possible to switch "on and off" the plasmonic resonance in the spectral region of weak absorption in silicon. Optical measurements of the particles are compared to wave optical simulations using rigorous coupled wave analysis (RCWA). From this, a promising particle configuration for use in solar cells is deduced.

[1] H.A. Atwater and A. Polman, Nature Materials, 9, 205-213, 2010

[2] E.-C. Wang et al, IEEE Journal of Photovoltaics, 3, 267-270, 2013

[3] S. Jüchter et al, Proc. of SPIE, 8438, 84380S, doi: 10.1117/12.922214, 2012

9140-32, Session 7

CIGS/organic single-junction and tandem hybrid solar cells

Manuel Reinhard, Uli Lemmer, Alexander Colsmann, Karlsruher Institut für Technologie (Germany)

Copper indium gallium diselenide (CIGS) solar cells are the most efficient thin film photovoltaic devices. In this work, we investigate CIGS/organic hybrid solar cells comprising semi-transparent metal top electrodes and wide-band gap organic semiconductors as buffer layer. Depositing the organic semiconductors from solution, we fabricate Cd-free CIGS solar cells exhibiting about the same efficiency as their fully inorganic counterparts comprising CdS, and significantly higher open-circuit voltages as compared to buffer-free devices. Although the organic molecules do not cover the CIGS surface homogeneously, their use enables prolonged charge carrier lifetimes according to impedance spectroscopy measurements.

Combining wide and narrow band gap absorbers in tandem solar cells is a promising approach to improve the energy conversion of sunlight. We therefore present hybrid tandem devices comprising monolithically connected copper indium gallium diselenide (CIGS) bottom cells and polymer top cells. The thin polymer:fullerene bulk heterojunction absorber layers were transferred onto the rough CIGS surface by a soft-contact lamination technique. Sputtered or solution deposited top-cathodes complete the tandem devices with enhanced open circuit voltages.

Finally, we present copper indium gallium diselenide (CIGS) solar cells incorporating solution-deposited transparent top cathodes. The utilized highly conductive polymer blend and the silver nanowire mesh exhibit excellent transparency in the near-UV region and form pinhole-free, homogeneous layers.

[Appl. Phys. Lett., 103 (2013) 143904; Appl. Phys. Lett. 102 (2013) 063304; Org. Electron. 14 (2013) 273-277]

9140-33, Session 7

Theoretical insights into multibandgap hybrid perovskites for photovoltaic applications

Jacky Even, Laurent Pédesseau, Institut National des Sciences Appliquées de Rennes (France); Claudine Katan, Institut des Sciences Chimiques de Rennes (France)

Following pioneering works [1], the 3D hybrid perovskites CH3NH3PbX3 have recently been shown to drastically improve the efficiency of Dye Sensitized Solar Cells (DSSC) [2]. It is predicted to open "a new era and a new avenue of research and development for low-cost solar cells ... likely to push the absolute power conversion efficiency toward that of CIGS (20%) and then toward and beyond that of crystalline silicon (25%)" [3]. We have theoretically investigated the crystalline phases relevant for photovoltaic applications [4]. Our findings reveal the dramatic effect of spin orbit coupling (SOC) on their multiple band gaps, sizably smaller for tin than for lead based materials. Critical electronic states and optical absorption are thoroughly investigated. Effective masses, a key parameter for hole transport, are also inferred. Besides inversion of band edge states, their physical properties show a close match to conventional semiconductors.

[1] A. Kojima et al, J. Am. Chem. Soc. 131, 6050 (2009), M. M. Lee et al, Science 338, 643 (2012), H-S. Kim et al, Sci. Rep. 2, 591 (2012).

[2] J. Burschka et al, Nature, 499, 316 (2013), J. H. Heo et al, Nature Photonics 7, 487 (2013), M. Liu et al, Nature 501, 395 (2013), S. D. Stranks et al, Science 342, 341 (2013). G. Xing et al, Science 342, 344 (2013).

[3] N. G. Park, J. Phys Chem. Lett. 4, 2423 (2013). H. Snaith, J. Phys Chem. Lett. 4, 3623 (2013).

[4] J. Even et al, J. Phys. Chem. Lett. 4, 2999 (2013), Phys. Status Solidi RRL (2013), Phys. Rev. B 86, 205301 (2012).

9140-34, Session 7

Analysis of a novel decagonal semiconductor nanowires for solar cell applications

Mohamed Hussein, Mohamed F. Hameed, Zewail City of Science and Technology (Egypt); Nihal F. F. Areed, Zewail City of Science and Technology (Egypt) and Mansoura Univ. (Egypt); Salah S. Obayya, Zewail City of Science and Technology (Egypt)

A lot of innovation introduced in the semiconductor industry has successfully led to solar cell designs with higher conversion efficiencies through the use of inexpensive materials and processes. Recently, III–V semiconductor-based nanowire (NW) solar cells have attracted the interest of many researcher all over the world. In this regard, semiconductor nanostructures form a promising ingredient for next generation solar cells with higher energy conversion efficiencies and lower cost. The natural abundance of silicon, lack of toxicity, and compatibility with mature integrated-circuit fabrication techniques are advantages in recruiting silicon-based nanostructured solar cells for ambitious future energy harvesting. As a consequence of their low reflection and strong broadband absorption, vertically-aligned silicon nanowire arrays (NWAs) can be used as an antireflection coating or as an active layer in the solar cells. In particular, silicon NWAs with radial p-n junctions can provide advantageous optoelectronic properties that manifest silicon quality requirements with low cost cells.

One of the main goals in studying NW solar cells is the determination of the most suitable geometry for achieving maximal efficiencies. It has been proved by many theoretical and experimental studies that the NWAs with well-defined geometric parameters such as diameter, length, and filling ratio exhibit a much more efficient light absorption in the solar spectrum. The Si NWAs can have much lower reflectance than silicon thin films and the overall absorption efficiencies of the Si NWAs proved inferior to silicon thin films of the same thickness. In this study, a novel design of decagonal semiconductor NW is proposed and analyzed for solar cell applications. The optical properties are numerically investigated by using 3D finite difference time domain method. The suggested design consists of vertical Si semiconductor NWs arranged in a decagonal shape with a large Si NW embedded in the core region. The effect of the height, core radius as well as the number and radii of Si NWs, are studied with regard to the wavelength of the incident wave. The structural parameters of each NWA are optimized to maximize the ultimate efficiency. Moreover,

the ultimate efficiency is used to evaluate the light absorption capability of the Si NWAs for solar cell application.

In this study, the absorptance, reflection and transmission are calculated as a function of height, core radius and the radii of Si NWs to determine how the perfect-absorption limit is approached. The Shockley–Queisser limit, or detailed balance limit, which refers to the calculation of the maximum theoretical efficiency of a solar cell made from a single pn junction is calculated by examining the amount of electrical energy that is extracted per incident photon. The numerical simulations are investigated for improving the ultimate efficiency of the NW within the wavelength range from 300 nm to 1100 nm. The proposed semiconductor NW design shows efficiency of 38 % which enhances the ultimate efficiency over the previous work by 7.5 %. It is expected that such nanowires are potentially excellent optoelectronic materials candidates for efficient photovoltaic devices.

9141-1, Session 1

Imagers based on organic photodiodes *(Invited Paper)*

Paul L. Heremans, IMEC (Belgium); Date Moet, TNO (Netherlands); Pawel E. Malinowski, IMEC (Belgium); Abishek Kumar, Medizinische Univ. Wien (Austria); Jan-Laurens van der Steen, Holst Center (Netherlands); Kris Myny, IMEC (Belgium); Gerwin H. Gelinck, Holst Ctr. (Netherlands)

Organic photodetectors are formed by a heterojunction of a donor and an acceptor organic semiconductor. Depending on the selected materials, the quantum efficiency can be optimized for specific wavelengths, ranging from ~350 nm to near infrared (~1000 nm). They can be formed as thin-film diodes on top of an active matrix of read-out engines in many possible technologies. Silicon read-out circuitry can be used, but also thin-film transistors (TFT) on glass or even plastic substrates. This opens the way to non-planar focal plane arrays with high resolution and high speed.

We will show in this presentation the state of the art in organic photodetectors as well as imagers based on organic TFT backplanes and oxide TFT backplanes, on 25 ?m thick plastic film. We will also discuss potential application examples.

9141-2, Session 1

Performance analysis of a large photoactive area CMOS line sensor for fast, time-resolved spectroscopy applications

Elena Poklonskaya, Daniel Durini, Melanie Jung, Olaf Schrey, Adrian Driewer, Werner Brockherde, Bedrich J. Hosticka, Holger Vogt, Fraunhofer-Institut für Mikroelektronische Schaltungen und Systeme (Germany)

Since developed, photomultiplier tubes (PMT) and charge coupled devices (CCD) have been extensively used in many scientific fields such as microscopy and emission spectroscopy due to their high sensitivity, high speed of detection and low noise behavior. Once established themselves as a standard detector technology in the field of emission spectroscopy the PMT still could not fully satisfy the market demands. Offering extremely high sensitivity in the ultra-violet (UV) region and the possibility for the time- resolved measurements (TRM), PMT can detect only one signal at distinct position in the spatially distributed spectrum,therefore lots of PMT's are needed to equip a universal spectrometer.

On the other hand, CCD line sensors,which have been recently employed in hybrid emission spectrometers due to their ability to detect the entire spectrum simultaneously, require multiple integrations to pick up the information from the indispensable emission lines.

In spark emission spectroscopy application, numeric atomic and ionic lines are excited and emitted during the spark plasma discharge. However, only a certain amount of these lines contains the information about the desired element. Time-resolved spectroscopy measurements give the possibility to define a right time window for the collection of the photogenerated charges belonging to each emission channel (gate integration).

CCD sensors do not have the ability of time-resolved measurements, random pixel addressing and non-destructive readout. CMOS approach on the other hand can be a good alternative to CCD. A lateral-drift field photodector (LDPD) based CMOS line sensor offers the possibility of time gating accompanied by non-destructive readout and charge accumulation over several cycles, which enhances the signal-to-noise ratio (SNR).

In this work we characterize developed CMOS line sensor by means of the photon-transfer method (PTM) and based on the EMVA 1288 standard. A test array with several different 5-pixel test clusters was fabricated using the 0.35 ?m LV/HV CMOS process with an LDPD and a specially designed UV-enhanced silicon-nitride passivation. The length of the pixel photoactive area is 200 ?m. The distance between the n-wells of the neighboring pixels is 5.5 ?m for a 10 ?m pixel pitch. The LDPD yielded 43 pA/cm2 of dark current at room temperature defined to the entire pixel area, 66.100 e- of saturation capacity, a responsivity of 520 V/?J/cm2 for ?=525 nm of impinging radiation, and a sensitivity of 17.3 ?V/e-.

The transfer time is a major concern during the development of a CMOS line sensor due to the extra long photoactive area, which introduces difficulties in the collection and transport of the charge carriers. For the developed LDPD pixel transfer time equals to 6 ?s under illumination 905 nm and the irradiance of 714 W/m2 was obtained.

A new CMOS line sensor consisting of 368 pixels, each with the length of 200 μm, is currently fabricated. It will be characterized in the next two months and the results will be presented at the conference and described in the conference paper.

9141-3, Session 1

A 270?1 Ge-on-Si photodetector array for sensitive infrared imaging

Amir Sammak, Technische Univ. Delft (Netherlands); Mahdi Aminian, Ecole Polytechnique Fédérale de Lausanne (Switzerland); Lin Qi, Edoardo Charbon, Lis K. Nanver, Technische Univ. Delft (Netherlands)

A CMOS compatible Ge photodetector fabricated on Si substrates has in the past been shown to be suitable for infrared sensing even in Geiger mode for photon-counting at room temperature. This paper focuses on implementations of the technology for the fabrication of imaging arrays with high reproducibility and yield. The process involves selective chemical vapor deposition (CVD) of a ~ 1-?m-thick n-type Ge crystal on a Si substrate at 700°C, followed by deposition of a nm-thin Ga and B layer-stack (so-called PureGaB) all in the same deposition cycle. The PureGaB layer fulfills 2 functions: for the first the Ga forms an ultrashallow p+n junction on the surface of Ge islands that allows highly-sensitive infrared photodiode-detection in the Ge itself, and secondly, the B-layer is a barrier layer that protects the Ge/Ga from oxidation when exposed to air as well as from spiking during metallization.

The Ge is deposited in 5?5 μm2 windows that are opened by plasma-etching through a 1-?m-thick SiO2 using soft-landing on the Si surface. The windows are arranged in an array of 270?1 with a spacing between neighboring windows of 5 μm. A design for patterning the surrounding oxide is developed to ensure a uniform selective growth of the Ge crystalline islands so that the wafer surface remains flat over the whole array. This design delivers a pixel size of 10x10 μm2 giving a fill-factor of ~ 25%. An Al metallization is used to contact each of the photodiodes to metal pads located outside the array area. A new process module has been developed for removing the Al metal on the Ge-islands to create a PureGaB-only front-entrance window without damaging the ultrashallow junction. Thus the sensitivity to front-side illumination is maximized. Electrical I-V characteristics are, to our knowledge, the best reported in literature with ideality factors of ~1.1 with Ion/Ioff ratios of 10E8. The uniformity is good and the yield is more than 95% over the whole array.

9141-4, Session 1

Design and characterization of a readout circuit for FET-based THz imaging

Suzana Domingues, Daniele Perenzoni, Matteo Perenzoni, David Stoppa, Fondazione Bruno Kessler (Italy)

Terahertz (THz) focal plane arrays based on CMOS field-effect transistors (FET) detection have been successfully demonstrated, but so far the reported system performances are not adequate for a commercial THz camera. Typically there is a signal-to-noise ratio (SNR) degradation when readout circuits are connected to the FET detectors.

In fact, while the FET detector itself has an intrinsic good noise performance, the extremely weak output signal (several microvolts) produced by the absorbed THz power makes signal amplification necessary. Therefore, readout circuits designed in a noise-efficient way are expected to bring a further progress towards a high-performance THz camera.

Targeting the development of a practical THz camera, a switched-capacitor integrator readout circuit for FET-based THz detectors was fabricated in a 0.13 μm standard CMOS technology. It is directly connected to the FET drain terminal and provides a better SNR as the number of accumulation cycles increase, without the need of large capacitance values. The readout circuit total area is 26 x 139 μm2, and it was implemented below the bowtie THz antenna connected between the FET gate and source terminals, which occupies and area of 150 x 150 μm2. In this way, the designed circuit is suitable for implementation in pixel arrays due to its compact size and small power consumption below 20 μW.

A full characterization of the system main parameters was done, including responsivity, noise equivalent power (NEP) and SNR values. THz measurements around 300 GHz show a good output signal linearity up to 200 accumulation cycles (which means a gain of 400 times), and a SNR improvement after each operation cycle.

In order to find the optimum bias point of the FET detector, responsivity and NEP curves in function of the gate-to-source voltage (VGS) for an arbitrary number of 200 accumulation cycles have been measured for different operating clock frequencies. A responsivity peak of 37.3 kV/W was obtained with a clock frequency of 200 kHz, which leads to 500 measurements per second with on-off modulation of the source. A minimum NEP of 5.45 nW/√Hz was obtained with a 400 kHz clock frequency, while at 200 kHz clock frequency the NEP is 6.93 nW/√Hz. A test structure containing only a FET detector and a bowtie THz antenna was used to evaluate the impact of the readout circuit in the FET THz detection.

9141-5, Session 1

Comparison of gate driven and source driven FET structures as THz detectors

Muhammad Ali, Matteo Perenzoni, Fondazione Bruno Kessler (Italy)

Several test structures of 300 GHz detectors based on Field Effect Transistors (FET) are implemented in 0.18 um CMOS technology on the principle of distributed resistive self-mixing. In literature, these detectors have been mainly configured as Gate Driven (GD), when the THz signal is applied between gate and source of a single device, and as Source Driven (SD), when the signal is applied between the source terminals of two properly connected devices. However, a real comparison requires the fabrication of proper test structures on the same substrate with similar boundary conditions.
In this work, a total of 4 FET test structures comprising of GD and SD configurations with different gate widths were designed, fabricated and measured for comparison purposes in terms of responsivity, bandwidth and noise. Each structure is accompanied by an on-chip bow-tie antenna sized on the simulated impedance of the detectors. The detectors have been characterized by a measurement setup comprising a frequency-tunable THz source and a lock-in amplifier. Measurement results indicate the potential of using both these FET configurations as THz detectors in imaging applications, highlighting the pros and cons of each configuration. A normalized frequency sweep analysis at an optimized gate bias voltage of 500mV shows that the SD FET is more broadband in nature as compared to its GD counterpart. On the other hand, results show that the GD structures are twice as much more responsive than the SD structures for the same channel width and length, making the choice a trade-off between high sensitivity and broadband operation. The measurements also indicate, as expected from the detector impedance, that FET structures with smaller widths show higher voltage response than the those with smaller widths for a given channel length. These structures will be used in future developments for a THz imaging application.

9141-6, Session 1

Ultralow power high-dynamic range color pixel embedding RGB to r-g chromaticity transformation

Michela Lecca, Leonardo Gasparini, Massimo Gottardi, Fondazione Bruno Kessler (Italy)

The present work describes a color pixel topology that converts the three chromatic components from the standard RGB space into the normalized r-g chromaticity space. This conversion is implemented with high-dynamic range and with no dc power consumption. The pixel is intended to become the basic building block of a CMOS color vision sensor, targeted to ultra-low power applications, such as human machine interfaces, gesture recognition, and face detection. In this framework, skin color is a highly discriminative visual feature [1],[2], that allows to detect the image area of interest and thus to reduce the computational burden of any further processing algorithm [3]. The use of the r-g coordinates is advantageous as a way of providing robustness against variations of the light intensity, caused for instance by shadows. Currently, by using a commercial RGB camera, the color conversion from RGB to r-g coordinates suffers of inaccuracy, especially in those regions of the image with low-light intensity. The proposed pixel overcomes this problem thanks to the auto-exposure capability, that ensures the same accuracy over a very large range of light intensity, up to about 120dB.

Experimental results showed a significant improvements in performance, especially in outdoor applications with uncontrolled lighting conditions.

References

[1] S. Bianco, F. Gasparini, and R. Schettini (2013). Computational strategies for skin detection. In Proc. of the 4th CCIW, Springer-Verlag, 199-211

[2] M. Soriano, S. Huovinen, B. Martinkauppi and M. Laaksonen (2000): Skin Detection in Video under Changing Illumination Conditions. Proc. 15th ICPR, Vol 1, 839-842.

[3] D. Chai and N. Ngan King (1999). “Face segmentation using skin-color map in videophone applications.” Circuits and Systems for Video Technology, IEEE Transactions on, 9.4: 551-564.

9141-8, Session 2

Global shutter imagers for industrial applications *(Invited Paper)*

Guy Meynants, CMOSIS bvba (Belgium)

Global shutter image sensors offer significant advantages over rolling shutter imagers but their implementation needs careful consideration. Each pixel needs a storage element on which the signal is stored after the exposure period. For a fixed pixel size this memory element will reduce the fill factor. Microlenses or backside illumination can compensate for this. An important specification is the parasitic light sensitivity or shutter efficiency

of the pixel. This is a measure how insensitive the memory cell in the pixel is to light. Depending on the pixel architecture, this may be especially difficult in combination with backside illumination. Other important pixel performance parameters related to pixel architecture are read noise and dark current.

In this paper we will review global shutter pixel architectures, compare their performances and discuss possible future developments. We discuss the issues related to global shutter pixels for backside illumination and how the most advanced CMOS image sensor process technologies can offer new approaches.

9141-9, Session 2

A 65k pixel, 150k frames-per-second camera with global gating and micro-lenses suitable for fluorescence lifetime imaging

Samuel Burri, François Powolny, Ecole Polytechnique Fédérale de Lausanne (Switzerland); Claudio E. Bruschini, Ecole Polytechnique Fédérale de Lausanne (Switzerland) and Ctr. Hospitalier Univ. Vaudois (Switzerland); Xavier Michalet, Univ. of California, Los Angeles (United States); Francesco Regazzoni, Technische Univ. Delft (Netherlands); Edoardo Charbon, Ecole Polytechnique Fédérale de Lausanne (Switzerland) and Technische Univ. Delft (Netherlands)

This paper presents our work on an 65K pixel single photon avalanche diode (SPAD) based imaging sensor realized in a 0.35?m standard CMOS fabrication process. At a resolution of 512 by 128 pixels the sensor is read out in 6.4?s to deliver over 150k black and white frames per second.

The individual pixel has a size of 24x24?m? and contains the SPAD with quenching and gating circuitry along with a memory element. The array of pixels is row-addressable and data is sent out of the chip on 128 lines in parallel at a frequency of 80MHz. The system is controlled by an FPGA which generates the gating and readout signals and can be used for arbitrary real-time computation on the frames from the sensor. The system is connected to a computer through USB.

The pixels are composed of the SPAD element and 12 transistors. Three of them are used to implement the fast gating circuitry and four for a NMOS memory element. The gating signals are distributed across the chip through a balanced tree to minimize the signal skew between the pixels. The active area of the chip is 5% and can be significantly improved with the application of a micro-lens array. A micro-lens array, for use with collimated light, has been designed and its performance is reviewed in the paper.

Among other high-speed phenomena the gating circuitry capable of generating illumination periods shorter than 5ns can be used for Fluorescence Lifetime Imaging (FLIM). In order to measure the lifetime of fluorophores excited by a picosecond laser the sensors' illumination period is synchronized with the excitation laser pulses. A histogram of the photon arrival times relative to the excitation is then constructed by counting the photons arriving during the sensitive time for several positions of the illumination window. The histogram for each pixel is afterwards transferred to a computer where software routines extract the lifetime at each location with an accuracy better than 100ps. We show results for fluorescence lifetime measurements using different fluorophores with lifetimes ranging from 150ps to 5ns.

9141-10, Session 2

Characterization of single-photon avalanche photodiodes in CMOS 150nm technology

Hesong Xu, Fondazione Bruno Kessler (Italy); Lucio Pancheri, Univ. degli Studi di Trento (Italy); Leo H. C. Braga, David Stoppa, Fondazione Bruno Kessler (Italy)

Over the last few years, Single-Photon Avalanche Photodiodes (SPADs) integrated within standard CMOS technologies have been proposed for different time-resolved imaging applications such as fluorescence lifetime imaging microscopy, 3-D imaging and ?-ray detection in Positron Emission Tomography systems. These applications require large arrays of SPADs monolithically integrated with processing electronic circuits, tailored for the specific system needs. The optimization of such sensor arrays call for a thorough understanding of how the SPAD technological and geometrical parameters affect their performance. To this end, a complete experimental characterization of CMOS SPADs with different sizes and geometries is essential to develop reliable models of the devices, which can then be used for the design of the application-specific sensor arrays and related circuit.

In this contribution we present a test chip designed for the characterization of two different types of SPADs in 150nm CMOS technology. Each type of SPADs is implemented in two different shapes (circular and square) as well as four sizes (5, 10, 15 and 20?m diameter). In order to obtain a statistical relevant dataset, the test chip includes 20 SPADs for each shape and size, for a total of 320 devices. Each SPAD connected to a passive quenching transistor, a clamping transistor and a voltage comparator can be separately addressed through a decoder. A test PCB provides power supply, bias and reference voltages, while the acquisition was conducted with an external acquisition board.

First measurements have been conducted to characterize the distribution of breakdown voltage, dark count rate (DCR) and photon detection probability (PDP) for different SPAD shapes and sizes. We found that the average breakdown voltage slightly decreases with SPAD size, while the uniformity is improved in larger area device.

The DCR of the devices, which represents the main noise source, is strongly affected by defects and impurities in silicon. At low excess bias voltage, the experimental results show a shape-independence of DCR, as circular and square SPADs with similar size have approximately the same distribution. In square devices, the measured DCR as a function of excess bias voltage exhibits a sudden increase over 5V excess bias voltage. This is likely caused by early breakdown in the SPAD corner.

The PDP as a function of wavelength at different excess bias voltages was measured using a wide spectrum light source and a monochromator. We observed that PDP is dependent on device area, and is strongly reduced in small devices. The behavior is due to the presence of dead zone near the guard ring, which was previously assumed to be active area in the data analysis. Finally, PDP non-uniformity was measured using a LED source and a diffuser to obtain uniform illumination. Measurement results showed that PDP non-uniformity is lower than 1%.

9141-11, Session 2

Comparative analysis of high-performance infrared avalanche Hg1-xCdxTe and InxGa1-xAsyP1-y heterophotodiodes

Mikhail S. Nikitin, JSC "Shvabe-Photodevice" (Russian Federation); Viacheslav A. Kholodnov, Albina A. Drugova, Institute of Radio Engineering and Electronics (Russian Federation); Galina V. Chekanova, JSC "Shvabe-Photodevice" (Russian Federation)

Technology of infrared (IR) avalanche photodiodes (APDs) gradually moves from simple single element APD to 2D focal plane arrays (FPA). Spectral covering of APDs is expanding continuously from classic 1.3 μm to longer wavelengths due to using of narrow-gap semiconductor materials like Hg1-xCdxTe. Developers and manufacturers of different optical communication, measuring and 3D thermal imaging systems do have great interest in modern APDs. Heteroepitaxial structures

InxGa1-xAsyP1-y and Hg1-xCdxTe became major infrared detector materials for fabrication of high-performance APDs. Significant improvement in material growth technology results in progress in IR APD technology. Nowadays perspective APDs with separate absorption and multiplication regions can be realized on multilayer heteroepitaxial structures both InxGa1-xAsyP1-y and Hg1-xCdxTe. To create the best performance optimally designed avalanche heterophotodiode (HAPD) it is necessary to carry out detailed theoretical analysis of basic features of generation and multiplication of charge carriers in proper heterostructure. Optimization of HAPD properties requires comprehensive estimation of HAPD's pixel performance depending on pixel's multi-layer structure design, layers' doping, distribution of electric field in the structure and operating temperature. Objective of the present work was to develop general approach for analytical description of basic processes in HAPDs and compare performance of HAPDs based on InxGa1-xAsyP1-y and Hg1-xCdxTe.

9141-12, Session 2

Photodetector based on GaSb with deep quantum well Al(As)Sb/InAsSb/AlAsSb grown by MOVPE for the 0.9-2.0 micrometeres spectral range

Igor A. Andreev, Maya P. Mikhailova, Gleb G. Konovalov, Edward V. Ivanov, Yury P. Yakovlev, Ioffe Physico-Technical Institute (Russian Federation); Eduard Hulicius, Alice Hospodková, Jirí Pangrác, Markéta Zíková, Institute of Physics of the ASCR, v.v.i. (Czech Republic)

We report design and study of photodetectors based on n-GaSb/p-GaSb with deep 20 nm AlSb/5 nm InAs(0.84) Sb(0.16)/20 nm AlSb quantum well and cap p-GaSb layer with 0.5 micron thickness. Heterostructures were grown on n-GaSb:Te (100) substrates by MOVPE in an AIXTRON200 machine. Samples under study had round mesa with 500 microns photosensitive diameter. The luminescent and photoelectrical properties of GaSb-based heterostructures with deep Al(As)Sb/InAsSb/Al(As)Sb quantum well were studied. Intense superlinear luminescence and enhance of the optical power were observed in dependence on drive current in the spectral range of 0.6-0.8 eV at T=77K and T=300K.

Spectra of photosensitivity and current–voltage characteristics were investigated at 77-300 K. Spectral response of the photodetector was studied at the photovoltaic mode in the range of 0.9-2.0 microns with maximum sensetivity at lambda=1.55 micron (T=300K). High quantum efficiency 0.6-0.7 and detectivity D*(lamda max)= (5-7) ?10^10 W^(-1)? cm? Hz^(1/2) were achieved at room temperature.

Zero bias resistance R0=?U/?I=2-6 kOhm (300?) and R0=10-60 MOhm (77?) were found. Current sensitivity was evaluated as high as 0.75-0.88 A/W for the maximum spectral range at 1.55 micron. The photodetectores demonstrate the capacitance as low as ?=2.0-5.0 pF at reverse bias U= ?1 V. The speed of response is estimated at t (0.1–0.9)=100–200 ps. The photodetector bandwidth of 2-3 GHz was reached. These quantum well photodetectors are prospective for heterodyne spectroscopy and information technology.

This work is in part supported by the Russian Foundation for Basic Research and Prezidium of Russian Academy of Science Program.

Keywords: photodetector, deep quantum well, broad bandwidth, nanoheterostructures

9141-62, Session PS1

Near-field and complex-field time-stretch transform

Peter T. DeVore, Brandon W. Buckley, MohammadHossein Asghari, Daniel R. Solli, Bahram Jalali, Univ. of California, Los Angeles (United States)

The time-stretch dispersive Fourier transform enables high-throughput acquisition of optical spectra in single-shot measurements by performing an analog Fourier transform and stretching the signal to facilitate capture with high-speed electronics. The coherent time-stretch transform adds complex-field detection so that spectral amplitude and phase can be measured in the temporal near field, i.e., without a strict dispersion requirement. Full-field spectra are recovered via temporal interferometry on waveforms dispersed in the temporal near field. Real-time absorption spectra including both amplitude and phase information are acquired at 37 MHz

9141-64, Session PS1

FBG sensor for temperature-independent high-sensitive pressure measurement with aid of a Bourdon tube

Srimannarayana Kamineni, Vengal Rao Pachava, Sai Shankar Madhuvarasu, Kishore Putha, National Institute of Technology, Warangal (India)

A temperature independent high sensitive pressure sensing system using fiber Bragg grating (FBG) and 'C' shaped bourdon tube (CBT) is demonstrated. The sensor is configured by firmly fixing the FBG (FBG1) between free and fixed ends of the CBT. Additional FBG (FBG2) in line to the FBG1 is introduced which is shielded from the external pressure, tend to measure only the ambient temperature fluctuations. The CBT has an elliptical cross section where its free end is sealed and the fixed end is open for subjecting the liquid or gas pressure to be measured. With the application of pressure, the free end of CBT tends to straighten out results in an axial strain in FBG1 causes red shift in Bragg wavelength. The pressure can be determined by measuring the shift of the Bragg wavelength. The experimental pressure sensitivity is found to be 66.9 pm/psi over a range of 0 to 100 psi. The test results show that the Bragg wavelength shift is linear corresponds to change in applied pressure and well agreed with the simulated results. This simple and high sensitive design is capable of measuring static/dynamic pressure and temperature simultaneously which suits for industrial applications.

9141-65, Session PS1

Fiber-Bragg grating seismic sensor using inverted spring-mass system

Dinakar Dantala, Kishore Putha, Vengal Rao Pachava, Srimannarayan Kamineni, National Institute of Technology, Warangal (India)

An attempt was made to design the fiber Bragg grating seismic sensor using an inverted spring-mass system. The sensor is configured by using a vertical spring loaded with some weight over its head provides damped motion of the spring with respect to the seismic vibration (P-wave) in axial direction, such that the arrangement of weight on the spring provides free motion only in one direction that is parallel to the base. One end of the FBG is attached to spring coil while other end is fixed to a supporting bar placed parallel to the spring on the same base. An interrogation system is developed using Single mode multimode single mode (SMS) to monitor the Bragg wavelength shift of FBG in terms of power variation corresponding to the seismic vibration. It allows replacement of the bulk OSA by a simple photo detector along with circuitry. Thus it enables low-cost measurement and fast response in real time applications. The measured electrical signal from the detector is fed into the data acquisition system which monitors the seismic vibration (ground shaking) of earth or vibration manually developed from the machinery. The sensor is attached on the specially designed vibrator to study the response for seismic vibration at various frequencies and amplitudes. The experimental results show that

the proposed sensor is capable of measuring the vibrations of frequency over the range of 2-20Hz. It is evident from the results that the sensor is highly sensitive at 7.5Hz represents the resonance frequency of the designed sensor system. The resonance frequency and the range of the frequency can be optimized by changing the spring parameters or suspended load and also the position of the FBG attached between the spring and support.

9141-66, Session PS1

An all-fiber vacuum sensor based on thermo-optics' effect in vanadium-doped fiber

Ziga Matjasec, Denis Donlagic, Univ. of Maribor (Slovenia)

This paper introduces an all-optical, fiber-optics vacuum sensor, which takes advantage of the thermo-optics effect within the vanadium-co doped single-mode fiber. The vanadium-doped fiber was produced by the modified chemical vapor deposition (MCVD) using a flash vaporization doping process, where the fiber's core was co-doped with the vanadium. The presented sensor can be applied in various industrial applications, where the vacuum measurements are needed.

This sensor utilizes a high-power, 980 nm pump-diode, capable to generate up to 300 mW of optical power and a short section of highly absorbed vanadium-doped fiber, with the absorption up to 12 dB/cm at 980 nm. Due to spectral absorption properties of vanadium ions in silica, the absorbed optical power emitted by 980 nm source is mostly converted via a non-radiative relaxation process into the heat within the vanadium-dope fiber. The relaxed heat rises the fibers temperature and changes the fibers core refractive index and thus change the optical path length of the fiber. The heat transfer between the heated optical fiber and surrounding gas depends mostly on the gas pressure. The 980 nm source operates in pulse mode therefore the vanadium-doped fiber is continuous heated and self-cooled. Further, the vanadium doped-fiber is inserted into a Fabry-Perot interferometer which forms, in combination with DFB laser diode at 1550 nm, a high coherence interferometer for optical path length measurement, while the absorption of vanadium–doped fiber at 1550 nm remains low. The time constant and absolute modulated optical path of the step response, when the fiber is heated/cooled, can be directly correlated with the gas pressure. The time constant is independent of the pump-diode's optical power, while the absolute modulated optical path also depends on the pump-diode's output optical power and should thus be compensated.

The sensor was built into a standard ISO-KF flange and tested on vacuum chamber. The vacuum measurements down to 10^-5 mBar were demonstrated in practice, where the 1 cm long section of vanadium-doped fiber was inserted into a Fabry-Perot interferometer. The all-optical vacuum sensor allows for a remote and fully dielectric measurement of a gas pressure and can be used in various industrial applications.

9141-67, Session PS1

Defects monitoring of a beam based on dynamic distributed strain

Rong-mei Liu, Nanjing Univ. of Aeronautics and Astronautics (China); Zelun Li, Chongqing Univ. of Science and Technology (China); Farhad Ansari, Univ. of Illinois at Chicago (United States)

Structural health monitoring (SHM) in-service is a very important and definitely demanded for safely working of structures, especially detection of damage locations. Most of the structural damage is manifested by cracks. In recent years, a number of optical fiber–based techniques have been applied in monitoring of cracks since optical fiber sensors have the advantages of immunity to electrical and electro-magnetic interference, geometric compatibility for distributed sensing etc. Since the damage location cannot be pre-specified, monitoring the local strain information all over the structure is required. One of the most applicable approaches for distributed optical fiber sensing is based on the Brillouin backscattering. Various approaches based on Brillouin fiber optic sensors have been proposed for detection of cracks in structures. However, most of the studies were fulfilled by applied static load on the structures. Strain singularity along the sensors would imply the damages location. In practice, the structures, such as large-span bridges are subjected to dynamic load mostly. Therefore, capture of vibrated strain on a beam based on Brillouin frequency shift (BFS) was experimentally studied. In order to obtain the dynamic response rapidly, a new BOTDA method using amplitude transfer of BFS was applied hereby. At the level of spatial resolution of 10 cm and the sampling interval of 5 cm of the BOTDA system, a sampling frequency for dynamic strain of about 14 Hz was achieved. For the first modal natural frequency of the most of large structures, the sampling frequency would be high enough. A beam of 15-m span with simulated cracks was applied in the study. Free vibration experiments were carried on the beam by using commercial BOTDA sensor system to record the distributed dynamic strain. Crack detection from the captured distributed vibrated strain was studied. Wavelet analysis was applied to orient the crack.

9141-68, Session PS1

Luminescent optical fibers with silver molecular clusters and semiconductor quantum dots for detection of ultraviolet and visible radiation

Darina Agafonova, Alexsandr I. Sidorov, St. Petersburg Electrotechnical Univ. LETI (Russian Federation) and National Research Univ. of Information Technologies, Mechanics and Optics (Russian Federation); Elena V. Kolobkova, Alexsandr I. Ignatiev, Nikolay V. Nikonorov, National Research Univ. of Information Technologies, Mechanics and Optics (Russian Federation)

Molecular clusters (MC) of metals (Mn, where M = Ag, Au, Cu, n = 1-15) have intense luminescence in the visible region of spectrum. Spectral characteristics of excitation and luminescence of MC depend on clusters size and host composition. Luminescence of MC can be used for spectral radiation conversion in fluorescent lamps, light-emitting diodes, solar cells and for development of photonic devices.

Semiconductor quantum dots (QDs) occupy a special place among the luminescent low-dimensional structures. Varying QDs size during synthesis one can control the spectral characteristics of excitation and luminescence. It makes possible to synthesize optical glass-ceramics with desired properties.

Optic fibers doped with MC and QDs are of interest, because they allow combining merits of material with fiber-optics technology. It can be used in design of sensor systems and photonic devices. Luminescent optical fibers with spectral conversion are demanded for creation of sensitive elements in fiber-optic sensors for different parts of optical spectrum. Also they can be used for detection of electrical charge.

This work presents results of investigation of silica and fluorophosphate optical glasses and fibers with Ag-MC and CdS(Se) QDs. Optical properties of the materials are defined. The silica optical fibers doped with Ag-MC have an excitation spectrum in the range of 200-530 nm and luminescence spectrum in the range of 500-800 nm. The fluorophosphate optical fibers doped with CdSxSe1-x (x=0.4-0.6) QDs have an excitation spectrum in the range of 200-700 nm and luminescence spectrum in the range of 830-1000 nm. It is show that spectral conversion of radiation enhances sensitivity of fiber-optic sensors of electric arc and spark. The reason is effective excitation of waveguide modes, reduced signal losses and effectively matched spectra of optical signal and spectral sensitivity of a silicon photodetector.

It is shown that luminescence of Ag-MC and QDs can be

used for temperature measurements. Dependence of integral luminescence intensity has almost linear temperature dependence in the region 20-250oC for the fluorophosphate fibers based on glasses with CdS and CdSxSe1-x QDs. Temperature sensitivity of luminescence intensity for glasses and fibers with Ag-MC is 2-3 times greater compared to materials with QDs and 4-30 times greater compared to published results for materials with rare-earth ions (Nd3+, Er3+, Eu3+, Yb3+). Studied glasses and fibers can be used for construction of sensitive elements of temperature fiber optic sensors.

9141-69, Session PS1

Lubricant oil condition monitoring using a scattering-free single-wavelength optical scheme

Anna G. Mignani, Leonardo Ciaccheri, Andrea A. Mencaglia, Istituto di Fisica Applicata Nello Carrara (Italy); Giuseppe Adriani, Alessandro Paccagnini, Massimo Campatelli, Mecoil Diagnosi Meccaniche S.r.l. (Italy); Heidi Ottevaere, Hugo Thienpont, Vrije Univ. Brussel (Belgium)

Nowadays, a precise assessment of lubricant oil condition encompasses time-scheduled off-line sampling and further analyses in specialized laboratory for tribology. A more modern approach of preventive and predictive maintenance relies on online devices capable of real time monitoring the onset of lubricant oil degradation. For this scope, technologically simple and low-cost devices for online sensing are requested to be coupled to a stand-alone web-connected data logger. Therefore, the oil condition is continuously and remotely checked in order to trigger a service intervention only when the oil degradation exceeds a planned threshold. This monitoring approach optimizes oil sampling, and, consequently, maintenance costs.

Optical spectroscopy, especially absorption and fluorescence, demonstrated effectiveness for monitoring the most important indicators of lubricant oil condition, namely total acid number (TAN), water content and metals. Also, a chromatic technique based on transmitted light intensity at RGB wavelengths was proposed for the online assessment of TAN and total contamination index.

This paper presents an innovative optical scheme for the monitoring of TAN. A set of lubricant oils with different ageing conditions were measured in the visible and near-infrared spectral ranges by means of diffuse-light absorption spectroscopy. This technique allows for obtaining a scattering-free spectroscopic information, and is particularly suitable to analyze turbid lubricant oils. Then, depending on the brand of the lubricant oil being used, an effective model for TAN prediction was created which made use of a narrow wavelength band only. This measuring scheme is precursor of implementing a low-cost LED-based optical setup for online use.

9141-70, Session PS1

Sensitivity-enhanced Immunoplasmonics for biomarker detection

Yoochan Hong, Minhee Ku, Eugene Lee, Jin-Suck Suh, Dae-Sung Yoon, Jaemoon Yang, Yonsei Univ. (Korea, Republic of)

When the metal nanoparticles meet incident light having longer wavelength than size of the nanoparticles, surrounded electromagnetic field of nanoparticles were enhanced, as a result, the surface plasmon which is surrounding nanoparticles is also strongly resonated. These phenomena is termed as localized surface plasmon resonance (LSPR), and recently, LSPR-based nanobiosensing technology was extensively researched and developed as a technique for highly sensitive, label-free, and flexible sensing techniques for the detection of biomarkers. Herein, we developed distinct sensing techniques based on LSPR for detection of enzymatic activity and expression level of respective biomarkers. First of all, we have measured extinction change of a number of gold nanorods for detection of proteolytic activity. To enhance the detection sensitivity of biomarkers, we have developed a sensor system that was composed of silver nanocubes, biomarker specific aptamer, and single nanoparticle's scattering spectrum measurement system. The silver nanocubes have high figure of merit value, so the changes of LSPR signal can be certainly detected, in addition, aptamer is known as a new class of capturing agent and have been attracted tremendous attention as a replacement of antibody. Moreover, scattering spectrum measurement system for single nanoparticle has been known as a method with maximized sensitivity for biomolecular detection. Collectively, we verified capability of sensor system we manufactured for biomarker detection using whole cell lysates, and the sensor system shown excellent ability for selective, specific, and sensitive detection of biomarker.

Acknowledgement: This research was supported by the National Research Foundation of Korea (NRF) funded by the Ministry of Education, Science and Technology (2012R1A1A2006248) and a grant from the National R&D Program for Cancer Control, Ministry for Health and Welfare, Republic of Korea (1220100).

9141-71, Session PS1

Monitoring of the molecular structure of lubricant oil using a FT-Raman spectrometer prototype

Valentin Ortega Clavero, Hochschule Offenburg (Germany) and Univ. de Strasbourg (France); Andreas Weber, Werner W. Schröder, Dan Curticapean, Hochschule Offenburg (Germany); Nicolas Javahiraly, Patrick Meyrueis, Univ. de Strasbourg (France)

The determination of the physical state of the lubricant materials in complex mechanical systems is highly critical from different points of view: operative, economical, environmental, etc. Furthermore, there are several parameters that a lubricant oil must meet for a proper performance inside a machine. The monitoring of these lubricants can represent a serious issue depending on the analytical approach applied.

The molecular change of aging lubricant oils have been analyzed using an all-standard-components and self-designed FT-Raman spectrometer. This analytical tool allows the direct and clean study of the vibrational changes in the molecular structure of the oils without having direct contact with the samples and without extracting the sample from the machine in operation.

The FT-Raman spectrometer prototype used in the analysis of the oil samples consist of a Michelson interferometer and a self-designed photon counter cooled down on a Peltier element arrangement. The light coupling has been accomplished with a conventional 62.5/125 ?m multi-mode fiber coupler. The FT-Raman arrangement has been able to extract high resolution and frequency precise Raman spectra, comparable to those obtained with commercial FT-Raman systems, from the lubricant oil samples analyzed. The proposed instrument prototype has no additional complex hardware components or costly software modules. The mechanical and thermal irregularities influencing the FT-Raman spectrometer have been removed mathematically by accurately evaluating the optical path difference of the Michelson interferometer. This has been achieved by producing an additional interference pattern signal with a ? = 632.8 nm helium-neon laser. It enables the FT-Raman system to perform reliable and clean spectral measurements from the analyzed oil samples.

9141-72, Session PS1

Polyaniline nanoskein for Redox-specific optical nanoprobe

Seungyeon Hwang, Yoochan Hong, Jihye Choi, Seungjoo Haam, Dae-Sung Yoon, Jin-Suck Seo, Jaemoon Yang, Yonsei Univ. (Korea, Republic of)

In the process of nanoparticles synthesis, various surfactants are used for water solubility of the nanoparticles. In general, various surfactants have been used for the increase of water-solubility of the synthesized biomedical nanoparticles. However, excess surfactants during a synthetic process can induce a significant cytotoxic effect toward organisms or tissues. For this reason, we tried to design a synthetic process of nanoparticles that there were no surfactants, and we successfully synthesized water-soluble nanoparticles without any surfactants, named as polyaniline nanoskein (PANS), as a nanoprobe for biomedical applications. The PANS were synthesized using polyaniline by heating and cooling at diverse solvents, such as benzyl ether and n-methyl-2-pyrrolidone. To confirm the chemical structure of PANS, first of all, Fourier transform infrared spectra were measured, and the shapes of 2-D and 3-D structures for PANS were also confirmed via transmission electron microscopic and scanning electron microscopic images, respectively. The unique property of polyaniline, which is reversibility of color change as varying its doped state, is also shown in PANS. To demonstrate this characteristic, absorbance spectra were recorded as varying the pH of the surrounding solution, from pH 1 to 10. The PANS also showed a better potential for Raman agent than bulk polyaniline, and a near-infrared photothermal agent because of its high absorbance in near-infrared region. Collectively, in this work, we verified that PANS has a possibility of nanoprobe for biomedical applications as a photothermal and Raman agent, and to conclude, the PANS can sensitively and effectively detect redox state of surrounding environment. Acknowledgement: This research was supported by the National Research Foundation of Korea (NRF) funded by the Ministry of Education, Science and Technology (2012R1A1A2006248) and a grant from the National R&D Program for Cancer Control, Ministry for Health and Welfare, Republic of Korea (1220100).

9141-73, Session PS1

Research remote laser methods for radionuclides monitoring

Sergey V. Kascheev, Valentin V. Elizarov, Alexander S. Grishkanich, Victor G. Bespalov, National Research Univ. of Information Technologies, Mechanics and Optics (Russian Federation); Sergey K. Vasil'ev, Emergency Technical Ctr. of Rosatom (Russian Federation); Dmitriy N. Redka, Saint Petersburg Electrotechnical Univ. "LETI" (Russian Federation); Alexander P. Zhevlakov, National Research Univ. of Information Technologies, Mechanics and Optics (Russian Federation)

Laser sensing can serve as a highly effective method of searching and monitoring of radioactive contamination. Its advantages over traditional, such as physico-chemical (sampling), or the standard radiometric (radiometers and spectrometers): remote, possibility of continuous areal and profile scanning with simultaneous determination of a wide range radioactive elements and compounds, as well as highly sensitive and fast detection

The first method of remote detection a radionuclide in atmosphere was elaborated. Its essence consists in definition the Sr90 and ?s137concentration by excitation and registration of fluorescence at wavelength of * = 0.347?7.0 um at laser sensing.

The Nd:YAG (355 nm, 100 Hz) beam extended by optical system up to 50 cm diameter was directed to the radionuclide contamination zone where excited the cesium and strontium atoms. Receiving optical collected diffused fluorescent radiation which reached two blocks of interference filters. First filtering block selected the band of 0.4?0.5 um. Fluorescence lines *1 = 455.528 nm (Cs line 5p66s 2S 1/2 - 5p67p 2P° 3/2), *2 = 460.733 nm (Sr line 5s2 1S 0- 5s5p 1P°1) and *3 = 852.113 nm (Cs line 5p66s2S 1/2 - 5p66p 2P° 3/2), *4 = 894.347 nm (Cs line 5p66s 2S 1/2 - 5p66p 2P° ?) were selected in the second one. The radiation selected in blocks comes in the photoreceiver - cooled high-sensitivity CCD.

However, preliminary results of investigation show the real possibility to register Cs137 and Sr90 with concentration at level of 1013-1015 cm-3 (concentration of radioactivity for extreme of emergency situations (more 10Bk/m3)) up to 100 m distance from the contaminated object. So, registration of slightly contaminated fields by fluorescence spectroscopy is difficult.

The second method experiments were carried out under the Raman-scattering circuit. Thus Nd:YAG laser pulses (266 nm, 20 mJ, 6 ns, 100 Hz) were focused in a chamber with different radionuclides (U235O2 , U238O2). Back scattering, anti-Stocks radiation got on USB2000 compact spectrometer (Ocean Optics) and received spectrum was further processed on a computer. In the course of the experiment were resolved Stocks Raman spectral lines of the isotope shifts U235O2 and U238O2. Preliminary results of investigation show the real possibility to register the leakage of a radionuclide with concentration up to 108-109 cm-3 on a safe distance (100 – 500 m) from the contaminated object.

9141-74, Session PS1

Analyzer for measurement of nitrogen oxide concentration by ozone content reduction in gas using solid state chemiluminescent sensor

Vladimir P. Chelibanov, Gennady G. Ishanin, Leonid N. Isaev, National Research Univ. of Information Technologies, Mechanics and Optics (Russian Federation)

Role of nitrogen oxide in ambient air is described and analyzed. New method of nitrogen oxide concentration measurement in gas phase is suggested based on ozone concentration measurement with titration by nitrogen oxide. Research of chemiluminescent sensor composition are carried out on experimental stand. This stand consists of ozone scrubber for ozone removal from the sample, ozone generator, reactor for interaction between ozone and nitrogen oxide, optical module for ozone concentration measurement.

Optical sensor composition was investigated in experimental stand. The sensor produced on the base of solid state non-activated chemiluminescent composition is applied as ozone sensor. Composition is put on the surface of polymer matrix with developed surface. Sensor compositions includes gallic acid with addition of rodamine-6G.

Chemiluminescent lighting is result of interaction between ozone and chemiluminescent composition and it is analytical signal of gas analyzer. Absorption, fluorescence and Raman spectrums were analyzed during chemical reaction between ozone and optical sensor chemical composition. These spectrums were got before luminescence light appearance. They allowed to make conclusion about multi step process of interaction and, in particular, about step responsible for accumulation of luminescence emitters.

Model of interaction process between sensor composition and ozone has been developed, main products appeared during reaction are identified. The product determining the speed of luminescense appearance is found. This product belongs to quinone class. Then new structure of chemiluminescent composition was suggested, with absence of activation period and with high stability of operation.

Experimental model of gas analyzer was constructed and operation algorithm was developed. Algorithm includes the steps of purge, ozone zeroing, base signal measurement (NO absent is the analyzed gas – NO zeroing), the measurememtn of ozone reduction after interaction with sample containing NO.

Testing of gas analyzer was carried out in laboratory and in the monitoring station within long period. Comparison with different producers gas analyzers also was done. Necessary data about transfer function linearity, zero and span drift, sensor resource and stability were obtained.

It was demonstrated that developed NO measuring instrument would be applied for monitoring purposes of ambient air.

Conclusions:

1. It is discovered the way of product formation, which precede chemiluminescence light appearance in solid state chemiluminescent sensor. It is discovered that reaction of product accumulation (quinones) are responsible for induction period.

2. “Dark” mechanism of quinone synthesis is suggested with addition of nanosize particles of DEGUSSA P-25 in ozone sensor composition.

3. Technology of non-activated chemiluminescent sensors preparation is suggested. These sensors will be applied in optical module of titrometric nitrogen oxide analyzer.

4. New method and measuring instrument of nitrogen oxide measurement is suggested based on optical solid state chemiluminescent sensor of ozone reduction.

9141-75, Session PS1

Spectral calibration of coded aperture snapshot spectral imaging

Wang Jianwei, Qunbo Lv, Yangyang Liu, Linlin Pei, Lulu Qian, Academy of Opto-Electronics (China)

Abstract: Coded aperture spectroscopy allows for large extended sources to be efficiently coupled into dispersive pectrometers by replacing the traditional input slit with a patterned mask.Spectral calibration is trerequisite for spectroscopy to obtain the spectrum information exactly.In this papper,we described the spectral calibration’s principle and metheds of coded aperture snapshot spectral imaging,and then gived the result of the experiment using a monochromatic extended source,at last we compared the accuracy between different methods(the one is directly,another one is indirectly).The results indicate that the primary factors influencing spectral calibration’s precision are three reasons:measure precision of imaging area,precision of relative radiometric calibration and precision of standard spectrum.

9141-76, Session PS1

Micro-resonators based on integrated polymer technology for optical sensing

Pauline Girault, Jonathan Lemaitre, Mohammed Guendouz, Nathalie Lorrain, Luiz Poffo, Ecole Nationale Supérieure des Sciences Appliquées et de Technologie (France); Michel Gadonna, Ecole Nationale Supérieure des Sciences Appliquées et de Technologie (France) and Télécom Bretagne (France); Dominique Bosc, Ecole Nationale Supérieure des Sciences Appliquées et de Technologie (France)

Over the last decades, the growing need for compact sensors and without markers that allow rapid and inexpensive reliable detection of various substances, induces a significant research of new technological solutions.

In this context, the aim of this work is to improve sensors based on easily integrated micro-resonator (MR) component in integrated optics. MRs can act as highly sensitive and selective functions in many areas such as health and food. They can offer the advantage of significantly small size as well. In a sensor based on MR, the interaction between the molecules to be detected and the evanescent wave induces an intensity change and/or a shift of the specific resonance wavelength (d?) with the refractive index variation (dn) due to the molecules. Thus, the sensitivity of the function can be given by d?/dn, expressed in nm/RIU (Refractive Index Unit). In this study, we analyse the different ways to optimize this interaction and to increase the sensitivity. These works take place in the objective to reach sensitivities that could be as high as 104 and even 105 nm/RIU.

In this work, we have first designed and achieved the fabrication of submicronic gap ring-waveguides (from 0.5 to 1.0 μm), with new couple of polymers and, by the way, we confirm our forecasts about the resolution that can be achieved with UV (i-line) photolithography. Thanks to these results, MRs have been just fabricated with refractive index contrast up to 0.16 at 1550 nm. First results show excellent drop filtering response (-20 dB) and are in concordance with theoretical study. Then, the resonator will be assessed with different molecules in order to evaluate the performances of the sensor. Moreover, we will also discuss different options to improve the sensitivity of sensors based on MRs.

9141-77, Session PS1

Precise piezoelectric resonance laser calorimetry of crystals

Aleksey V. Konyashkin, Oleg A. Ryabushkin, Moscow Institute of Physics and Technology (Russian Federation) and NTO “IRE-Polus” (Russian Federation) and nstitute of Radio Engineering and Electronics of RAS (Russian Federation)

At present, output powers of CW fiber lasers reach 10 kW in single-mode and more than 100 kW in multimode regimes. Devices for measuring such high values in wide wavelength range are usually based on thermal principle of operation and suggest complete conversion of radiation into heat. We have recently introduced novel method for laser power low-loss measurement with beam quality retaining. It is based on weak heating of an optically transparent bulk piezoelectric resonator by transmitted radiation. Main idea is to use frequency temperature dependence of piezoelectric resonances excited in crystal. Piezoelectric resonances can be observed by measuring the response of crystal sample to the applied external electric field. Electric field of the varying radiofrequency affects the piezoelectric crystal, which is placed in unclamped manner between two strip electrodes and is connected in series with the load resistor. For each value of the electric field frequency the amplitude and the phase of the voltage on the resistor are measured by the lock-in amplifier.Temperature calibration of resonance frequency Rf is performed during uniform crystal heating. So each Rf value of selected resonance corresponds to certain temperature T. In wide temperature range Rf linearly depends on T with piezoelectric resonance thermal coefficient Kprt. Crystal temperature change caused by optical absorption is also proportional to laser power P. Dependence of resonance frequency shift on incident power ?Rf(P)=KproP is clarified. Extrapolation of this dependence allows direct measurement of any unknown power by detecting frequency shift and taking into account measured value of piezoelectric resonance optical coefficient Kpro. Obviously, ability to measure powers in both wide dynamic and wavelength ranges depends on crystal resonator optical absorption properties. Fortunately optical absorption and heat transfer coefficients of crystal can be precisely measured using novel modification of laser calorimetry technique based on implementation of crystal equivalent temperature concept. Employing piezoelectric resonances the crystal equivalent temperature change caused by optical absorption can be expressed as ??eq(P)=?Rf(P)/Kprt or in linear case ??eq(P)=(Kpro/Kprt)P=?P, here ? is optothermal coefficient. Novel calorimetry approach suggests determination of optical absorption and heat transfer coefficients by solving nonstationary heat conduction equation using measured time parameter ? of equivalent temperature kinetics ?eq(P,t) of the crystal, heated by laser radiation. Crystal’s ?eq kinetics is directly measured using resonance frequency shift ?Rf dependence on time when the laser power is switched on. Characteristic time constant ? of crystal ?eq kinetics during laser heating is determined using exponential fitting: Rf(t)=[Rf(0)-Rf(P)]exp(-t/?)+Rf(P), where Rf(P) is stationary resonance frequency value corresponding to laser power P. Equivalent temperature stationary value

is ?eq(P)=T0+?Rf(P)/Kprt, where T0 is crystal temperature at P=0. Then heat transfer coefficient is obtained h=(mc)/(S?) where m is crystal mass, c is specific heat capacity, S is crystal total surface area. Optical absorption coefficient is also calculated: ?L=hS? where L is crystal length. Introduced calorimetric metrology was verified in experiments with several nonlinear-optical crystals (SiO2, LiB3O5, LiNbO3, KTiOPO4) using

CW Yb-doped fiber laser.

9141-78, Session PS1

Optic-electronic sensor for measuring the deformations of the axle at the radiotelescope

Igor Konyakhin, Tatyana V. Turgalieva, Renpu Li, National Research Univ. of Information Technologies, Mechanics and Optics (Russian Federation)

Nowadays the new radio astronomy instruments are designed and several radiotelescopes are modified at many countries.

There is a necessity to realise the accuracy angle position between con-struction axes of radiotelescope. The research in the millimetre wave range re-quires the few (no more 2 arc. seconds) deviation the position of elevation and azi-muth axes.

A weight of the main mirror causes to the three dimension deformation on roll, yaw and pitch angles of the elevation axle relatively the theoretic line. At re-sult the orientation of a parabolic mirror axis on elevation angle and azimuth angle is not equal to values, which are set by the electric turn drive system at the axle bearings.

Autocollimation semi-active optic-electronic semsors are used for the measuring the three dimension deformation.

The first metrology problem is the measuring the roll angle deformation. The autocollimation method for measuring the roll angle is realised if the aperture of the optic path is more 100 mm. But the system for deformation measurements must be positioned into elevation axis with small diameter (40 mm and smaller). Disadvantages of the existing method for measuring the roll angle can be avoided with using the new type of the anamorphic glass prism as the part of the autocolli-mation reflector.

The second problem is the measuring of yaw and pitch angle deformations. The ordinary reflector for autocollimation sensor as plane mirror can not be com-posed with anamorphic component. The special triple mirror with invariant line as the elevation axis direction is proposed.

The autocollimator is installed on the bearing of the elevation axle as a rigid base and the triple mirror and anamorphic system as the special reflector is positioned into the elevation axle.

The autocollimator includes the light emission diode (LED) as source of radiation with aperture mark, objective and the receiving CMOS matrix analyzer. The video-frame from matrix is calculated by the digital microprocessor.

The autocollimator includes the light emission diode (LED) as source of radia-tion with aperture mark, objective and the receiving CMOS as matrix analyzer. The video-frame from matrix is calculated by the digital microprocessor.

The light beam from autocollimator passes through anamorphic system, triple mirror and anamorphic system again. The autocollimator objective projects the im-age of mark after transformation by the anamorphic system and triple mirror to the CMOS matrix. The digital microprocessing system determines the coordinates and parameter of the image mark form, which conclude the information about measur-ing roll angle. The information about yaw angle and pitch angle is the coordinates of the image center.

The parameter of the image mark form is the difference of the angle coeffi-cients and for two contour lines on the image.

The measuring value of the roll angle is calculated by the equations relatively the anamorphic coefficient.

The measuring value of the yaw angle and pitch angle are calculated by the equa-tions relatively values of angles between sides of the triple mirror.

As result the computer and physical modeling of the reflector as composition of the triple mirror with anamorphic system have shown an opportunity of realization the thee dimension angle sensor system with necessary parameters.

9141-79, Session PS1

Precise optical differential thermometer sensor based on interferometric measurement of thermal expansion

Michal Lucki, Leos Bohac, Richard Zeleny, Czech Technical Univ. in Prague (Czech Republic); Marcela Davidkova Antosova, Vocational Technical College and Engineering School for Elektrotechnics (Czech Republic)

Knowing a thermal expansion coefficient and measured exact thermal expansion, it is possible to design a very sensitive sensor measuring temperature differential. A Michelson interferometer is used to determine temperature changes. It measures linear expansion on a copper rod as a change in length in response to a change in temperature. Based on obtained interferograms and the known value of thermal expansion coefficient, temperature change can be calculated. The accuracy of the procedure can be determined by using the exact differential method based on the measurement errors for linear expansion, and initial length. The contribution of this paper is the employment of Michelson interferometer to obtain design a very sensitive differential thermometer measuring with the accuracy of one thousandth degree Celsius. It results from the achieved precision of measuring the optical path length difference in the range of hundreds nanometers.

The sensor is also suitable for measuring small amplitudes or small oscillation's frequency that require a noninvasive and noncontact method. The overall accuracy of Michelson interferometer is half of used wavelength, which is 632.8 nm. The optical path length difference corresponding to one fringe is equal to value of half-wavelength. The value of half-wavelength multiplied by the number of interference fringes is equal to thermal expansion of investigated object. The measured object is a copper rod terminated with a dielectric mirror. Heating of the copper rod is done by a coil.

Thermal expansion of the copper rod affects the position of a mirror placed at its end and causes changes to optical path length. The measuring beam is guided to the investigated copper rod. Thermal expansion of the copper rod affects the position of the mirror placed at its end and causes changes to the optical path length in a measuring arm. An additional phase shift between both arms causes changes to the distribution of interference fringes that are counted and monitored. Information about the amount of fringes is stored in a computer and is used to calculate the change in optical path length. A number of fringes passing through the aperture in an observation plane is proportional to thermal expansion of the rod.

To an approximation with regard to measurement, the change in optical length of an object due to thermal expansion is related to a temperature change by a linear expansion coefficient, which is defined as linear expansion due to a change in temperature with respect to initial length of an object. Based on measured thermal expansion and knowing the nominal value of thermal expansion coefficient, which is constant for a given material, we specify the differential between initial and final temperature.

The advantage of this sensor is its precision and noncontact procedure. The experimental results confirmed the high accuracy of this optical method. The measurements require performing some supplementary measurements, such as that of initial length of the rod. The experiment showed demands for mechanical stability of a free space arrangement as well as the importance of many aspects.

9141-80, Session PS1

Hydrocarbon halo-laser spectroscopy for oil exploration needs

Sergey V. Kascheev, Victor G. Bespalov, Valentin V. Elizarov, Alexander S. Grishkanich, Evgeniy A. Makarov, National Research Univ. of Information Technologies, Mechanics and Optics (Russian Federation); Sergey A. Bogoslovsky, Alexander A. Il'insky, All Russia Petroleum Research Exploration Institute (Russian Federation); Alexander P. Zhevlakov, National Research Univ. of Information Technologies, Mechanics and Optics (Russian Federation)

We discuss some advances in equipment sensitivity for the techniques of remote laser spectroscopy and Raman lidar which sufficiently enlarge their applications. Our Raman lidar is an active, airborne laser remote sensing instrument with ultraspectral resolution (?/? ? > 1000)

Unlike Raman spectroscopy, CARS employs multiple photons to address the molecular vibrations, and produces a signal in which the emitted waves are coherent with one another. As a result, CARS is orders of magnitude stronger than spontaneous Raman emission.

Chamber filled by mixture of such gases and air served as the simulator of hydrocarbon halo was irradiated by femtosecond Ti:Sapphire and nanosecond Nd:YAG lasers pulses. A pump beam of frequency ?p (Ti:Sapphire, 800 nm, 30 fs, 0,2 mJ, 50Hz) and a probe beam at frequency ?pr (Nd:YAG, 1064 nm, 8 ns, 60 mJ, 50 Hz) were focused in a chamber. These beams interact with sample and generate a coherent optical signal at the anti-Stokes frequency (?pr+?p-?S) (fig.1). The anti-Stokes signal (? = 656 nm for CH4 and ? = 658 nm for C3H8) is resonantly enhanced when the frequency difference between pump and Stokes beams (?p-?S) coincides with the frequency of Raman resonance, which is the basis of technique's intrinsic vibrational contrast mechanism.

Spectra were registered with use of the USB2000 compact optical fiber spectrometer (Ocean Optics). Back scattering anti-Stocks radiation got on a spectrometer and received spectrum was further processed on PC. Pressure of methane and propane chosen as indicator substances of hydrocarbon deposits was made ~ 0.01 Torr in 0.2 m-length chamber that was corresponded to 10m-thickness of an real halo with concentration at level of 5•1012 cm-3, i.e. 200 ppb, for each of these gases (fig.2). Since Ti:Sapphire laser has a wide spectrum, the coherent anti-Stock scattering of radiation occurs from corresponding Fourier-components of pump (? = 800 nm) and Stocks signal (? = 1064 nm), removed on Stocks shift size of researched gases. Therefore it was possible to observe an occurrence of new components about 650 nm, various for different HHG (fig.1), in anti-Stock scattering spectrum.

Method CARS allows to realize measurement of the concentration level is 3-10 molecules and determine hydrocarbons in real atmosphere with presence of impurities.

As estimations have shown the reliability of HHG detection can exceed 80 % at the integration method of seismic prospecting and laser remote sensing in CARS circuit with the use of Nd:YAG laser (1064 nm, 3J, 8 ns, 100 Hz).

9141-81, Session PS1

Performance of near-infrared fluorescence sensing probe for target-guided surgery method of sentinel lymph node

Byeong-il Lee, Korea Photonics Technology Institute (Korea, Republic of) and National Cancer Ctr. (Korea, Republic of); In Hee Shin, Hyeong Ju Park, Jea Seok Park, Joo Beom Eom, Korea Photonics Technology Institute (Korea, Republic of); Seok-ki Kim, National Cancer Ctr. (Korea, Republic of)

With the development of fluorescence signal detector, in vivo biological sensing and imaging has been investigated non-invasively. In addition, recently, the clinical application of near infrared (NIR) indocyanine green (ICG) is used as contrast agent of sentinel lymph node (SLN) localization. Therefore, the high-efficiency fluorescent sensing probe is required for detection of fluorescent signals at SLN with high intensity. Also, phantom and small animal experiments are applied to verify the performance of sensing probe.

In this paper, we suggest a NIR fluorescence sensing probe for target-guided surgery system which was composed of a NIR CCD camera (Guppy Pro F-031B), LED excitation light source (760?), band-pass filter (830 ?) and operational software. Optically designed mirror holes and lens were applied to enhance of the efficiency of fluorescence in the sensing probe.

Uniformity of exposed LED light on target location at the distance of 50 cm and 100 cm were 69% and 80% respectively. Thermal noise from the light source was measured using IR thermometer for 1 hour after water cooling was equipped. Thermal changes were recorded within 10% variation at 22 Celsius. A home-made phantom was prepared in 3 % concentration of Intralipid (diluted with water). The fluorescence signal intensity was measured depending on the phantom position.

Recently, the use of fluorescent dyes in the near-infrared (NIR) region with high penetration becomes possible to observe the real-time location of the disease, and movement. So the NIR fluorescent sensing probe has been applied for pre-clinical, clinical studies. In particular, the detection module and high-efficiency light sources are necessary to detect the fluorescence signal in vivo. In this study, NIR fluorescence sensing probe was integrated in order to establish the target-guided method of SLN.

9141-82, Session PS1

Optoelectronic complex for separation of mineral objects of small size, that are moving through zone of analysis

Nikita A. Pavlenko, Elena V. Gorbunova, Aleksandr N. Chertov, Valery V. Korotaev, National Research Univ. of Information Technologies, Mechanics and Optics (Russian Federation)

The current state of the mining industry is characterized by a continuous depletion of mineral resources. And the traditional technologies of extraction and enrichment are often unable to provide the profitability of deposits development.

Thus, development of new and the improvement of existing systems for mineral raw materials separation are becoming increasingly important.

The optical sorting method is the most promising in terms of improving the structure of optical sorters, complexification and alteration the data processing algorithms, increasing efficiency in the use of this method as well as expanding the scope of application for optical sorters.

Existing optical sorters have a number of shortcomings relating to both schemes of lighting and registration of mineral objects as well as used algorithms of grayscale and color images processing. As a result, there are great difficulties with:

– determination of optimal separating thresholds and differential thresholds when configuring work parameters of optical sorter;

– estimation of close color tints between mineral samples when sorting;

– sorting low-contrast minerals;

– reconfiguration of sorter for separating transparent and semitransparent mineral samples after separating non-transparent mineral samples.

This paper deals with the description of the optoelectronic complex which is intended for study of separation possibilities of moving mineral samples (non-transparent as well as semitransparent and transparent) by an analysis of their optical

parameters. This complex, in fact, is a prototype of an optical sorter and it is designed for work with objects ranging in size from 1 mm to 20 mm, because the separation of such mineral samples by optical sorting method usually presents the greatest difficulties.

The main feature of proposed optoelectronic complex is its design in the form of a few building blocks. Mentioned design allows transforming of the measurement scheme under the optical properties of various minerals. The optoelectronic complex consists of a feeder system with conveyor belt, few LED lighting blocks, and image registration block based on line scan camera. The ability to change the background color and lighting spectrum is also provided. The mutual arrangement of complex's building blocks for various types of mineral samples is determined on the basis of proposed design method.

Experimental studies were conducted using various samples of feldspars. Control of optoelectronic complex and visualization results are implemented using LabVIEW.

9141-83, Session PS1

Self-amplified CMOS image sensor using a current-mode readout circuit

Patrick M. Santos, UFMG (Brazil) and CEFET/MG (Brazil) and Univ. de Lyon/Institut des Nanotechnologies (France); Davies W. de Lima Monteiro, UFMG (Brazil); Patrick Pittet, Univ. de Lyon/Institut des Nanotechnologies (France)

The feature size of the CMOS processes decreased during the past few years and problems such as reduced signal excursion have become more significant in voltage-mode pixels, even though the integration of more functionality inside the pixel has become easier. This work makes a contribution on both sides: the possibility of a high signal excursion range using current-mode circuits together with functionality addition by making signal amplification inside the pixel. The pixel architecture is quite similar to the classic 3T voltage-mode pixel, but a very small modification was made to integrate a transconductance amplifier providing a current as an output. The matrix with these new pixels will operate as a whole large transistor outsourcing an amplified current that will be used for signal processing. This current is controlled by the intensity of the light received by the matrix, modulated pixel by pixel during the readout time. The output current can be controlled by the biasing circuits to achieve a very large range of output signal levels. It can also be controlled with the matrix size and this permits a very high degree of freedom on the signal level, although it must be accompanied with careful observation of current densities inside the integrated circuit. In addition, the matrix can operate at very small integration times. Its applications would be those in which the pixel size (and so, the resolution) is not so important, but fast imaging processing and high signal amplification are required, such as UV image sensors. Simulation results will be presented to support: operation, control, design, signal excursion levels and linearity for a matrix of pixels that was conceived using this new concept of sensor.

9141-85, Session PS1

Tomographic wavefront retrieval by combined use of geometric and plenoptic sensors

Juan T. Trujillo-Sevilla, Univ. de La Laguna (Spain); Luis F. Rodríguez Ramos, Instituto de Astrofísica de Canarias (Spain); Juan J. Fernández-Valdivia, José G. Marichal-Hernández, José Manuel Rodríguez Ramos, Univ. de La Laguna (Spain)

The plenoptic sensors are usually used for the acquisition of the Lightfield of a scene; from that frame, a variety of results can be obtained: refocus at will, all-in-focus image, depth map, 3D stereo image, integral 3D, synthetic aperture,... However, an equally important and original feature in this kind of sensors is the ability to extract tomographical wavefront phases, a 3D map of the refractive index changes. This characteristic has great applicability in fields such as medical microscopy and adaptive optics for extremely large telescopes.

In plenoptic sensors, a microlens array is placed at the focus of the objective lens and the sensor becomes the focus of the microlens. The major disadvantage of the plenoptic sensor is its loss of optical resolution over what would be the same optical system without microlenses, which now depends on the diameter of the used microlenses. The final definition of the images built from the plenoptic frames matches the number of microlenses arranged in the focal plane.

Meanwhile, the geometric sensor, a new variety of the classic curvature sensor, significantly recovers at full optical resolution the wavefront phase at the pupil of the telescope or the imaging system. However, it lacks the ability to measure the tomographic wavefront phase, unlike the plenoptic sensor. In this sense they are complementary.

In a combined use of the two sensors, for example by placing the plenoptic sensor in a defocused plane, the final resolution of the phase maps obtained by the plenoptic sensor depends on the number of pixels allocated to each microlens, whereas in the geometric sensor this definition coincides with the number of microlenses arranged. Therefore, increasing one definition is the decrease in the definition in the other. In this sense they are also complementary.

In this paper we will show laboratory results related to the combined use of the geometric and the plenoptic sensor: firstly both of them will be used at the same time but individually and watching the same turbulence, secondly the plenoptic sensor will be placed in a defocused plane of the objective lens. A comparison between the wavefront phase maps obtained using the two possible combining possibilities will be shown.

9141-86, Session PS1

The effects of BRDF on the laser range profile

Yanhui Li, Zhensen Wu, Lu Bai, Xidian Univ. (China)

A backscattering model of average signal power function for laser radar range imagery obtained by a short pulse laser for the target is presented in this paper. This model can analyze the laser range profile (LRP) which relates the average power seen by the receiver with laser pulse, target shape, optical scattering properties of surface material, incidence angle and other factors. Simulation of the laser range profiles of a number of different coarse targets is given. Based on the results of the simulated model and theoretical analysis, the different targets can be identified. The optical scattering property of the material is characterized by bidirectional reflectivity distribution function (BRDF). The BRDF can be measured or obtained by building up a theoretical model. Different materials have different BRDF and LRPs of different material have different peak value. In this case, comparing LRPs of different targets can estimate not only the shape of targets but also the characteristic of target surface. The model can be used for demonstration of LiDAR image and can also be used to generate library of model data sets for automatic target recognition.

9141-88, Session PS1

Evaluation of thermal exposure on absorbing objects with digital holographic interferometry method

Pavel Bodienkov, Boris Manuchin, Olga Vladimirov Andreeva, National Research Univ. of Information Technologies, Mechanics and Optics (Russian Federation)

The effect of exposure on absorbing objects results in an increase in temperature of an object and also changes in its

optical and physical characteristics. In case of low absorbing objects these changes are reasonably small and, as a rule, inhomogeneous. This is why their evaluation is difficult problem that warrants special methods for solve it. These objects include imagining material for optical recording of information (photomaterials) and different types of biological objects: from cellular medication to tissue samples.

Evaluation of target exposure with different powers and types, low-absorbing in visible region, is sufficiently effective when visible emission (light) is used as sensing emission, since in this case well-developed methods of optical diagnostics can be utilized not only for quantative evaluations, but also for visualization of passing process.

The digital holographic interferometry method that is used in our current work is now widely applied for researching of temporal dynamics of objects transformation at different processes. Authors used constructed hardware and software, which allow to detect and control phase changes of transparent objects with temporal dimension not less than 100 ms during a long time.

Samples of imaging polymer material for volume holography «Difphen» which is solid solution of organic dye phenanthrenequinone(PQ) uniformly distributed in polymethylmethacrylate (PMMA), were used as a subject of research. Samples are made in the shape of plane-parallel disks, diameter is 40 mm and thickness (2÷4) mm. The expose emission ?=473 nm is situated in absorbing region of PQ. It is a beam of solid state DPSS laser which diameter is 3 mm and power about 50 ???. The part of the sample that was exposed the radiation became discolored and heated up. Discoloration process passes in localized area of emission influence (exposed area), while temperature of the exposed area increased and spread to unexposed area by heat transfer.

Sensing emission ?=532 nm is used for observation of the process of spreading of the temperature. In this part of spectrum sample is not photoresponsive.

The running of experiment consisted of registering interferogramms, which represent distribution of emission phase that had past the sample on the surface of the sample at the present sampling time: the phase portrait of the sample in the stable form before the start of exposure; in the process of exposure; after the stop of exposure. The change of the phase of sensing emission on the surface of the sample can be evaluated quantitatively, if it is known that the difference of the phases between two neighboring fringes is 2ϖ. The change of the refraction index for the sample that is 4 mm wide is Δn=1.3?10-4, which equals the change of the temperature about 20 ? for this material. Consequently, the field of the temperature gradient in the sample can be calculated at any moment of observation of the spading of warmth effect.

In the result we show possibility of applying digital holographic inerferometry method for evaluation of thermal exposure on low-absorbing objects, including objects with photo-induced changes of refraction index.

9141-90, Session PS1

Self-mixing diode laser interferometry for velocity measurements of different targets

Alexandra S. Alexandrova, Univ. of Liverpool (United Kingdom) and Cockcroft Institute (United Kingdom); Vasilis Tzoganis, Univ. of Liverpool (United Kingdom) and Cockcroft Institute (United Kingdom) and RIKEN Nishina Ctr. (Japan); Carsten P. Welsch, Univ. of Liverpool (United Kingdom) and Cockcroft Institute (United Kingdom)

Gas targets are used for a number of accelerator based experiments as well as for beam diagnostic purposes. In the case of supersonic gas jets, they combine low internal temperatures with high directionality and as a result they are very interesting as experimental targets in different fields of science. For the optimisation and verification of the properties of such monitor it should be characterised with high accuracy, in particular with regards to its velocity and density profile. In these applications, gas jet velocities can be up to 2,000 m/s and inhomogeneously distributed across the jet. However, all currently used methods for such characterisation are either not reliable or require a powerful laser system.

A diode laser velocimeter based on the laser self-mixing method is currently being developed by the QUASAR Group as an easy-to-build and compact solution when compared to alternative measurement techniques. The technique seems a promising way for a complete characterisation of the gas jet parameters. The laser velocimeter could provide in-detail information about velocity, density and temperature of any jet with micrometer-resolution. Such a sensor would allow for unambiguous measurements from a single interferometric channel, and could be installed even in radiation-exposed environments.

In this contribution, the heterodyne principle and design of the laser diode velocimeter are first discussed. The laser velocimeter is a self-aligning device, based on the self-mixing method where the laser is both a transmitter and receiver of the signal. It should be pointed out that laser self-mixing is usually used for measurements of low velocities and vibrations. The here-presented theoretical analysis shows the possibility to extend these measurement capabilities also to high velocities by altering the design.

In this contribution experimental results from measurements with different targets, including white paper and fluids, are presented. The initial calibration and verification of the accuracy of the method was done on a set-up which allows velocities of up to 50 m/s. The set-up for testing the sensor allows investigations into the limitation of the method as well as into the amount of feedback which is needed for a detailed study of a gas jet. In order to verify the possibility of using the velocimeter as a flow sensor, measurements of local velocities were performed on fluids with externally-imposed flow profiles.

The experimental results show that the velocity of a white paper target can be measured with an accuracy better than 2% and micrometer spatial resolution over a velocity range from 0.5 mm/s to 50 m/s. The sensor's capability to measure higher target velocities is discussed.

9141-91, Session PS1

Compact microring resonator sensor based on three-trenched channel plasmonic waveguide

Ahmed Heikal, Mohamed F. Hameed, Zewail City of Science and Technology (Egypt) and Mansoura Univ. (Egypt); Salah S. Obayya, Zewail City of Science and Technology (Egypt)

In this paper, compact three trenched channel plasmonic microring resonator sensor (TTC-PMRS) on a silicon-on-insulator substrate is proposed and analyzed. The three trenched waveguide is composed of three metal-gaps-silicon structure, where the optical energy is greatly enhanced in the narrow gaps. The full vectorial finite difference frequency domain method is used to numerically analyze the device optical characteristics as a biochemical sensor. As the optical field in the proposed structure has a large overlap with the upper-cladding sensing medium, the sensitivity is very high compared to other dielectric microring resonator sensors. A typical sensitivity of 700 nm/RIU is obtained with a figure of merit 21. The proposed (TTC-PMRS) has a compact size and high sensitivity and can be integrated in an array form on a chip for highly-efficient lab-on-chip biochemical sensing applications.

9141-13, Session 3

Toward large-area roll-to-roll printed nanophotonic sensors

Pentti Karioja, Jussi A. Hiltunen, Sanna M. Aikio, Teemu Alajoki, Jarkko Tuominen, VTT Technical Research Ctr. of Finland (Finland); Karl Böhlen, Rene Hauser, 3D AG (Switzerland); Martin D. B. Charlton, Univ. of Southampton (United Kingdom); Arjen Boersma, TNO Science and Industry (Netherlands); Peter Lieberzeit, Univ. Wien (Austria); Thorsten Felder, Momentive Performance Materials (Germany); David Eustace, Renishaw Diagnostics Ltd. (United Kingdom); Eliav I. Haskal, Philips Research Nederland B.V. (Netherlands); Samuli Siitonen, Ville Kontturi, Nanocomp Oy Ltd. (Finland)

Polymers have become an important material group in fabricating discrete photonic components and integrated optical devices. This is due to their good properties: high optical transmittance, versatile processability at relative low temperatures and potential for low-cost production. Recently, nanoimprinting or nanoimprint lithography (NIL) has obtained a plenty of research interest. In NIL, a mould is pressed against a substrate coated with a moldable material. After deformation of the material, the mold is separated and a replica of the mold is formed. Compared with conventional lithographic methods, imprinting is simple to carry out, requires less-complicated equipment and can provide high-resolution with high throughput. Nanoimprint lithography has shown potential to become a method for low-cost and high-throughput fabrication of nanostructures.

We show the development process of nano-structured, large-area multi-parameter sensors using Photonic Crystal (PC) and Surface Enhanced Raman Scattering (SERS) methodologies for environmental and pharmaceutical applications. We address these challenges by developing roll-to-roll (R2R) UV-nanoimprint fabrication methods. Our development steps are the following: Firstly, the proof of concept structures are fabricated by the use of wafer-level processes in Si materials. Secondly, the master molds of successful designs are fabricated, and they are used to transfer the nanophotonic structures into polymer materials using sheet-level UV-nanoimprinting. Thirdly, the sheet-level nanoimprinting processes are transferred to roll-to-roll fabrication. In order to enhance roll-to-roll manufacturing capabilities, silicone-based polymer material development was carried out. In the different development phases, Photonic Crystal and SERS sensor structures with increasing complexities were fabricated using polymer materials in order to enhance sheet-level and roll-to-roll manufacturing processes. In addition, chemical and molecular imprint (MIP) functionalization methods were applied in the sensor demonstrators. In this paper, the process flow in fabricating large-area nanophotonic structures by the use of sheet-level and roll-to-roll UV- nanoimprinting is reported.

9141-14, Session 3

Exploiting the phase properties of Bloch surface waves on photonic crystals for efficient optical sensing

Francesco Michelotti, Alberto Sinibaldi, Riccardo Rizzo, Aleksei Anopchenko, Univ. degli Studi di Roma La Sapienza (Italy); Norbert Danz, Peter Munzert, Fraunhofer-Institut für Angewandte Optik und Feinmechanik (Germany); Emiliano Descrovi, Politecnico di Torino (Italy)

Optical sensors exploiting Bloch surface waves (BSW) at the truncation edge of one dimensional photonic crystals (1DPC) have been proposed as a valid alternative to surface plasmon resonance (SPR) operating in the Kretschmann-Raether configuration for label-free optical biosensing [1]. The main advantages of BSW with respect to SPR are in that their dispersion can be almost arbitrarily tuned in wavelength, momentum and polarization (TE or TM) by changing the 1DPC materials and geometry. Typically, the resonances the BSW show are much sharper than SPR due to the reduced absorption losses, resulting in a possible increase of resolution [2]. Moreover in fluorescence applications the signal intensity doesn't suffer from quenching in proximity of the metal layer [3].

To reduce the BSW resonance width and increase the resolution it is desirable to work with 1DPC with as small losses as possible. However this makes that the BSW observed in a single polarization reflection scheme are shallow and difficult to track in a sensing experiment. We recently showed that it is possible to increase the performance of optical biosensors by exploiting the phase characteristics of BSW around the resonance and operating in an ellipsometric configuration at fixed angle and wavelength of operation [2].

Here we report on the practical implementation of an angularly resolved ellipsometric optical biosensing scheme based on BSW sustained by tantalia/silica multilayers. The angular resolution is obtained by a focused illumination at fixed wavelength and detecting the angular reflectance spectrum by means of a CMOS array detector. Experimental results obtained by using several tantalia/silica multilayers with different structure and operating at different wavelengths will be reported, showing that the resolution can be routinely pushed below 2x10-7RIU/Hz1/2.

References

[1] M. Shinn, W.M. Robertson, Sensors and Actuators B, 105, 360 (2005).

[2] A. Sinibaldi, R. Rizzo, G. Figliozzi, E. Descrovi, N. Danz, P. Munzert, A. Anopchenko, F. Michelotti, Optics Express, 21, 23331 (2013).

[3] M. Ballarini, F. Frascella, F. Michelotti, G. Digregorio, P. Rivolo, V. Paeder, V. Musi, F. Giorgis, E. Descrovi, Appl. Phys. Lett., 99, 043302 (2011) .

9141-15, Session 3

Gas sensing using SiON and polymeric 2D photonic crystal chemical sensors

Arjen Boersma, Milan Saalmink, Renz J. van Ee, Ralph S. A. Stevens, TNO Science and Industry (Netherlands); Martin D. B. Charlton, Michael E. Pollard, Univ. of Southampton (United Kingdom)

Photonic Crystals (PhC) are very attractive for application in chemical sensors since their optical properties can be changed when exposed to analytes. In addition, their responses are equally reliable on areas as small as a few μm2 to mm2. The major challenge in the development of photonic crystal sensors is the production of these periodic structures on an industrially relevant scale. E.g., (inverse) opal sensors have a limited application due to the complex manufacturing process. Alternatively, photonic crystal slabs can be made from semiconductors by various etching processes. In this paper we present the modeling, design and manufacturing of both SiON and polymer PhC sensor chips for the detection of formaldehyde at ppm level.

Accurate designs of PhC structures in materials such as SiON and polymer composites can steer the in and out coupling of the light from the PhC regions. The refractive index of these materials must be high to enhance the optical response. The SiON chips were manufactured by e-beam lithography, and could be used as such. However, this nanostructured wafer was also used as an Nano Imprinting Lithography (NIL) master for the manufacturing of identical structures in a high refractive index polymer composite. The manufacturing of these nanostructures in polymer materials opens the way for mass manufacturing of the sensor chips.

Polymer materials in general have a relatively low refractive index (< 1.7). The use of nanoparticles can enhance this value. In this project, the composite material for the polymer chips consisted of TiO2 nanoparticles dispersed in a UV curing polymer matrix. Although refractive indices up to 1.8 were

feasible by changing the amount of nanoparticles in the composition, values of 1.7 were used in order to ensure good processability of these materials into the PhC structures, using an adapted NIL process.

After manufacturing of the PhC chips, these were functionalised with chemical receptors, that will capture the formaldehyde molecules and subsequently change their refractive index. This change in refractive index of the thin conformal layer inside the holes of the PhC will lead to a shift in the outcoupled light. The thickness of this receptor layer is very critical in the performance of the sensor: too thin will results in low sensitivity; too thick will effectively block the holes. The thickness could be well tuned by a combination of a suitable patterned deposition technique and droplet size.

The chips with the functionalised layers have been exposed to formaldehyde and the shift in the outcoupling of the light from the PhC patch was monitored during and after exposure. It was measured that both chips showed a distinct change in optical behaviour upon absorption of the formaldehyde. Two measurement techniques were used for the characterization of the performance: 1) an adapted ellipsometer in which changes in intensity of reflected light was assessed, and 2) a optical set-up that projected the outcoupled light from the PhC patches onto a CCD camera.

9141-16, Session 3

Optimization of a radiative membrane for gas sensing applications

Anthony Lefebvre, Salim Boutami, MINATEC (France); Jean-Jacques Greffet, Henri Benisty, Institut d'Optique Graduate School (France)

Optical gas sensing relies on the absorption of a targeted gas at a specific wavelength. Key components for non-dispersive infrared sensors are a radiation source, an optical filter, a gas cell and an infrared detector. Most gases of interest (CO2, CO, CH4...) absorb in the mid-infrared, from 3 to 10 microns, and their concentration can be obtained from Beer-Lambert law. When it comes to engineering a cheap, portable and low-power sensor, incandescent sources are more suitable than expensive quantum cascade lasers and inefficient light-emitting diodes. Using standard MEMS technology, such sources of radiation have already been created in the form of free standing circular micro-hotplates. This paper deals with the design of these membranes in order to maximize their wall-plug efficiency. Constraints from specifications are taken into account, including available energy per measurement and maximum power delivered by the electrical supply source. The main drawback of these membranes is the power lost through conduction to the substrate, not converted in (useful) radiated power. If the membrane temperature is fixed by technological requirements, radiative flux can be favored by increasing the membrane radius. However, given a finite amount of energy, the bigger the membrane, the shorter the time it can be turned on. This clearly suggests that an optimum can be found, both in terms of efficiency and signal-to-noise ratio. Using simulations based on a spatio-temporal radial profile, we demonstrate how to optimally design such membrane systems, and provide an insight into the thermo-optical mechanisms governing this kind of devices, resulting in a non-trivial design with a substantial benefit over existing systems. To further improve the performances of the source, we also consider tailoring the membrane stack emissivity to privilege the infrared signal to be sensed as well as to maximize energy efficiency.

9141-17, Session 3

Quartz-enhanced photoacoustic spectroscopy with antimonide compounds in very compact systems

Nguyen Ba Tong, Mariem Triki, Quentin Gaimard, Yves Rouillard, Aurore Vicet, Univ. Montpellier 2 (France)

The development of compact optical sensor for trace gas species is more and more interesting for diverse fields of applications such as environmental monitoring, industrial process control and medical diagnostics. Quartz Enhanced Photoacoustic Spectroscopy (QEPAS) [1] has been proved to be an attractive tool for selective and sensitive detection and quantification of molecular trace gas since its invention in 2002. This technique has shown a large range of applications with compact and cheap setups, based on the use of a commercial quartz tuning fork (QTF) as an efficient acoustic transducer. The optical energy absorbed by the gas results in a periodic thermal expansion which gives rise to a weak acoustic pressure wave. This pressure excites a resonant vibration of the QTF thereby generating an electrical signal via piezoelectric effect.

We present in this paper measurements made by QEPAS technique with antimonide laser diodes emitting at 2.3 μm and 3.3 μm fabricated by IES. These measurements are dedicated to environmental purposes, such as methane detection and ethylene control. Two demonstrators will be presented: a laboratory bench and a brand new compact setup. The detection limits of the demonstrators were evaluated: for example, measurements of methane diluted in dry nitrogen led to a threshold detectivity of 100 ppbv at 3.38 μm [2]. Some key points of the QEPAS setup will be simulated and discussed.

9141-18, Session 4

Current trends in technologies for microsystems in bio-microanalyses

Leandro Lorenzelli, Fondazione Bruno Kessler (Italy)

Technologies for fabrication of micro devices and systems continue to progress and diversify due to the rising demands for miniaturization and performance enhancement coming from a number of applications of paramount interest in the context of the societal challenge. Microsystems for bio-microanalyses (e.g. Micro Total Analysis Systems, Lab on Chip, Point of Care devices), and more in general all the devices that provide fast and low cost methods for biological screening by combining microelectronics, microfluidics with physical, bio-chemical, and optical sensors on a compact substrate like a chip or a cartridge, envisage an increasing range of powerful applications for test in medical diagnostic and in the agrofood sector also.

In fact, as in the medical screening procedures, quality control at Hazard Analysis and Critical Control Points (HACCP) in the food and beverage industry demands a large volume of tests and the associated costs are significant. The development of fast, sensitive, multiplexing and automated analyses technology could aid the industry in the depreciation of the overheads and at the same time it could satisfy consumers' demand for safety with new devices for quality control certified food and beverages.

This talk aims at focusing challenges and solution proposals for developing microsystems by providing a review of the state of the art of microfluidics and sensor technologies for lab on chip with specific reference to relevant case studies in food/beverage analysis.

9141-19, Session 4

Optical transmission measurements for in-line monitoring of turbid oil-water emulsions

Philipp Metz, Christian-Albrechts-Univ. zu Kiel (Germany); Katja Dopf, Markus Aichholz, Boris Riedel, Uli Lemmer, Karlsruher Institut für Technologie (Germany); Barbara Freudig, Clifton Zimmermann, Optimags Dr. Zimmermann GmbH (Germany); Martina Gerken, Christian-Albrechts-Univ. zu Kiel (Germany)

Optical transmission measurements are attractive for in-line monitoring in the processing of oil-water emulsions as they are simple, contact free, and fast. Examples of oil-water

emulsions are body lotions, pharmaceutical crèmes, or dairy products. These typically exhibit a high scattering coefficient due to the difference in refractive index between the oil and the water. The visible turbidity of milk, e.g., is attributed mainly to the fat content. We focus on oil-water emulsions that appear "white", i.e., they exhibit a low absorption coefficient at the measurement wavelength. For absorbing media the concentration may be calculated directly from the optical transmission following the logarithmic dependence given in the Lambert-Beer law. Due to multiple scattering events in oil-water emulsions, these exhibit a nonlinear relationship between the attenuation and the oil concentration. We demonstrate that for increasing oil content in oil-water emulsions the attenuation first increases, then levels out, and finally even decreases for a fat content of 60%. Therefore, the measurement is ambiguous for a fat content around 50%. For skim oil-water emulsions with a fat content of below 20% optical transmission measurements show high sensitivity. We set up a prototype system employing simple single-wavelength optical transmission measurements through a defined measurement volume as a method for in-line fat content monitoring of oil-water emulsions. Using experiments and ray-tracing simulations we evaluate system optimization. The emitter optics as well as the wavelength choice in the near infrared were found to be of little influence. The solid angle of detection should be maximized in order to collect more light to reduce the signal-to-noise ratio at the detector. Additionally, absorbing measurement volume boundaries enhance the sensitivity. Single-wavelength optical transmission measurements allow for fast, simple, and contact free registration of deviations or malfunctions in the process enabling quick reactions and short down-times.

9141-20, Session 4

Formaldehyde sensor using non-dispersive UV spectroscopy at 340nm

John J. Davenport, Jane Hodgkinson, Cranfield Univ. (United Kingdom); John R. Saffell, Alphasense (United Kingdom); Ralph P. Tatam, Cranfield Univ. (United Kingdom)

Formaldehyde is a volatile organic compound that exists as a gas at room temperature. It is hazardous to human health causing irritation of the eyes, nose and throat, headaches, limited pulmonary function and is a potential human carcinogen. Sources include incomplete combustion, numerous modern building materials and vehicle fumes. At the time of writing, methods for detecting formaldehyde gas that are simple, reliable and inexpensive are limited.

Here we describe a simple method for detecting formaldehyde using low resolution non-dispersive UV absorption spectroscopy. A two channel system was developed, making use of a strong absorption peak at 339nm and a neighbouring region of negligible absorption at 336nm as a reference. Using a modulated UV LED as a light source and narrow laser-line filters to select the desired spectral bands, a simple detection system was constructed specifically targeted at formaldehyde. Filters were tilted, taking advantage of their off-axis behaviour to tune their central transmission wavelengths to specific formaldehyde features. This removed the requirement for components such as gratings and CCD arrays commonly featured in optical spectrometers.

By paying particular attention to sources of noise, a minimum detectable absorbance of 1.65?10-5AU was achieved (as $\Delta I/I0$). The system was tested with formaldehyde finding a limit of detection of approximately 1.5ppm for a 195mm gas cell, with a response time of 20s. The dominant performance limitation is currently unwanted temperature fluctuations of the UV LED, which we believe result in changes to its emission spectrum.

9141-21, Session 4

Chalcogenide planar waveguides for chemical sensing in the mid-infrared

Duk-Yong Choi, Pan Ma, Yi Yu, Xin Gai, Zhiyong Yang, Steve J. Madden, Barry Luther-Davies, The Australian National Univ. (Australia)

Chalcogenide glasses (ChGs) are a promising platform for chemical or biochemical optical sensors because of their wide transparency in the mid-infrared (MIR) between 4000-400cm-1 (2.5–25?m), which includes most of the important range for vibrational spectroscopy. In addition ChG planar waveguides can be compact, highly reproducible, and be integrated with sources and detectors as well as microfluidic systems [1]. As a result, ChG waveguides are being developed as optical sensors for the mid-infrared (MIR); however, to date their capabilities have been demonstrated only in the near infrared (NIR) [2] partly due to the scarcity and poor performance of MIR optical components. Recently, this has started to change, thanks to the development of some key elements. In particular, quantum cascade lasers (QCLs), HgCdTe and InSb focal plane array cameras, and quantum well infrared photo-detectors have all become commercially available and also affordable. Obtaining low loss waveguides in the MIR has been another recurring theme. As wavelengths get longer it becomes much more difficult to find a suitable combination of materials and processes that are transparent and even those that are, have to be almost completely free from common contaminants such as C, H or O as these introduce strong absorptions within the transmission band.

In this paper we report the structure, fabrication, and characteristics of ChG waveguides for optical sensing in the MIR. The studied waveguides were made using Ge11.5As24Se64.5 glass film as the rib-type core on a Ge11.5As24S64.5 bottom cladding, and this composite provided a refractive index contrast of about 0.4. We employed a conventional photolithography and dry etching to define the structure, and aimed to evaluate what losses can be achieved and how they may be affected by contamination that occurs during processes. The best waveguides, which included 10nm thick fluorocarbon polymer as a top coating, had losses for the TE-mode averaging < 0.5dB/cm over the whole measurement range from 3–7.4?m (3000-1350cm-1). However, around 3.4?m these increased to about 0.8dB/cm due to hydrocarbon contamination on the waveguide surfaces that could not be removed by either wet chemical or plasma cleaning. Beyond 7?m the losses started to increase as the TE mode approaches cut-off and due to the presence of the fundamental C-F absorption band of the fluorocarbon coating. The lowest loss of 0.3dB/cm was observed near 5?m where there is generally fewer absorption bands present in any of the most likely contaminants. The capabilities of these waveguides for spectroscopy were demonstrated by measuring the absorption spectrum of soluble ferric ferrocyanide (Fe7(CN)18, Prussian blue) in dimethyl sulphoxide (DMSO) solvent placed on the waveguide surface. Strong absorption peak of the C-N stretching vibration was measured at 4.8?m, which matches well with a reference spectrum [3].

[1] J. J. Hu, et al., Opt. Express 15, 2307 (2007).

[2] A. Ganjoo, et al, J. Non-Cryst. Solids 352, 584 (2006).

[3] Pawel J. Kulesza, et al., Anal. Chem. 68, 2442 (1996).

9141-22, Session 4

Application of temperature-dependent fluorescent dyes to the measurement of microwave absorption in water

Oleksandr Popenko, Nataliia Kuzkova, Andrey Yakunov, National Taras Shevchenko Univ. of Kyiv (Ukraine)

It is known that influence of electromagnetic millimeter waves (MW) on biological objects is different from the usual heat

wave of other bands. The physical nature of this phenomenon is still unclear. In order to implement adequate physical model is an actual definition of "non-thermal effect" that require precise temperature measurement of irradiated objects. High-sensitivity temperature sensors (thermocouples, thermistors, etc.) making perturbations in the investigated samples, affect the local temperature and heat transfer characteristics in a given place. Although less accurate, optical methods are more convenient for registration of temperature changes in small volumes.

To determine temperature changes in water caused by the MW absorption we used an optical non-contact method, which is based on the existence of the fluorescence intensity temperature dependence of organic dyes. It was measured the local temperature rise in the capillary, placed inside a rectangular waveguide, in which MW propagate. We have chosen two dyes with opposite temperature effects: Rhodamine 6G (R6G) and Rhodamine C (RC).

Established that in most cases, the temperature rise is making destructive contribution to the fluorescence yield. With the growth of temperature, increases the frequency and energy of molecules collisions in solution as well as the amplitude of internal molecular vibrations, leading to an increase in non-radiative relaxation of the excited levels, and thus fluorescence quenching. Along with temperature quenching of the dye solution potential following mechanisms that increase the overall yield of fluorescence with increasing temperature. In particular, some organic molecules in aqueous solution tend to form associated complexes: dimers, trimers, etc., where fluorescence quantum yield is much lower than in the individual molecules. At sufficiently high concentrations the fluorescence spectrum is formed as a superposition of the spectra of individual molecules and their associates. Some associates divided into separate molecules with increasing temperature which is accompanied by a relative increase in fluorescence intensity.

Preliminary measurements showed that fluorescence temperature dependence of the RC solution corresponding to the first scenario, R6G – to the second, and in the range of 20 – 40 degrees the relative intensities approximated by a linear function. Two fluorescent sensors were used for measurement of temperature increment caused by microwave absorption at 47 GHz. Taking into consideration the calibration dependences, the local temperature increase in the capillary at 20 mW absorbed power was 7 degrees in both cases.

Our method can be applied in medical and biotechnological techniques using microwave irradiation.

9141-23, Session 4

UV spectroscopy determination of aqueous lead and copper ions in water

Mohd Zubir Mat Jafri, Chun Ho Tan, Hwee San Lim, Yow Chong Moo, Univ. Sains Malaysia (Malaysia)

Lead (Pb) and copper (Cu) ions are very common pollutants in water which have dangerous potential causing serious disease and health problems to human. Lead is toxic to many organ of the body, and prolong exposure to lead ions will caused serious brain and nervous system damage. Low quantity of copper ions are required for body metabolism, however excessive copper ions intake will caused anemia, tissue injury and liver damage. In normal tap water regulation, concentration was limited to 0.015 mg/L (15 ppb) for lead and 1.3 mg/L (1300 ppb) for copper.

Heavy metal ions such as lead and copper are commonly determined using chemical reagent method and atomic absorption spectroscopy-graphite furnace. Those method can archive high accuracy but it required to be operate by well-trained technician and expensive. Thus, the aim of this paper is to determine lead and copper ions in aqueous solution using direct UV detection without using any additional chemical reagent. The UV light source used in this project is deuterium lamp with JAZ Spectrometer.

This technique used direct absorption method and it allows the determination of both lead and copper ions from range 0.2 mg/L to 10 mg/L using UV wavelength from 210 nm to 230 nm. The method was successfully applied to synthetic sample with high regression coefficient. In this study, we found that lead ions have a very obvious peak near 215 nm. However, copper ions does not have a significant peak but shows respond at the wavelength ranged from 215 nm to 230 nm. We also tested this technique on tap water from various location at Penang, Malaysia and river water in Penang.

In conclusion, this technique have some advantages over the chemical method, it is a much simpler and non-destructive technique without the need of preparing the chemical reagent. In future works, this technique will be simplified into a more portable device with lower cost using UV LED, fiber optic, photodiode and PIC controller.

9141-24, Session 5

Analysis of the intrinsic refractometric sensitivity of optical fiber plasmonic sensors

Christophe Caucheteur, Valérie Voisin, Patrice Mégret, Univ. de Mons (Belgium)

Optical fiber refractometers coated by a nanoscale gold layer constitute a miniaturized counterpart to the Kretschmann prism and enable the exploitation of surface Plasmon resonance (SPR) for accurate (bio)chemical sensing purposes. Different configurations including the use of etched or side-polished optical fibers, long period fiber gratings and tilted fiber Bragg gratings have been reported by the past, presenting similar performances in terms of refractometric sensitivity in a small range of surrounding refractive index (SRI) values.

In this paper, for the first time to the best of our knowledge, we analyze the impact of the gold coating and optical fiber cladding thicknesses on the cladding modes distribution. We focus more particularly on the SPR mode (cladding mode resonance that couples to the SPR wave at the metal layer-surrounding medium interface) and its subsequent refractometric sensitivity. We clearly figure out that the optimum gold thickness for SPR generation lies in the range between 30 and 70 nm. We also report that a decrease of the cladding diameter from 125 μm to 80 μm enhances the refractometric sensitivity by ~20 %. Theoretical investigations obtained with a finite-difference complex mode solver in cylindrical coordinates are corroborated by experimental data. We make use of tilted fiber Bragg gratings (TFBGs) photowritten in the core of a standard singlemode silica fiber to individually interrogate the cladding modes. TFBGs couple light to the fiber cladding in reflection and present a comb-like amplitude transmitted spectrum composed of the core mode resonance (so-called Bragg resonance) and several tens of cladding mode resonances. The Bragg resonance provides temperature-insensitivity while each cladding mode resonance finely probes a given range of surrounding refractive index values. TFBGs were coated with gold using a standard sputtering process. Depositions were made in two steps with the fiber rotated by 180° between both depositions to ensure a relatively uniform gold thickness all around the fiber cross-section. Transmission spectra were measured using an optical vector analyser from Luna Technologies that was chosen for both its high wavelength resolution (1.25 pm) and fast scanning rate (a few s to cover the full TFBG spectrum). Experiments conducted on gold-coated TFBGs immersed in calibrated liquids finally show that their ultimate refractometric sensitivity is of the order of 550 nm/RIU (refractive index unit).

9141-26, Session 5

Limit of detection comparison for surface wave biosensors

Riccardo Rizzo, Fraunhofer-Institut für Angewandte Optik und Feinmechanik (Germany) and Univ. degli Studi di Roma La Sapienza (Italy); Francesco Michelotti, Univ. degli Studi di

Roma La Sapienza (Italy); Norbert Danz, Fraunhofer-Institut für Angewandte Optik und Feinmechanik (Germany)

Sensors utilizing surface plasmon resonance (SPR) are established as the method of choice in label-free optical biosensing [1]. A variety of optical approaches including imaging, angularly and spectrally resolved resonance tracking can be applied to read the transducers information. Previously, surface waves propagating at the boundary of truncated photonic crystals have been suggested [2] to be applied in plasmon-like configurations. In contrast to plasmons such Bloch surface wave sensors feature the possibility to optimize the resonance, i.e. to tune its position and width as the most important parameters.

The option to engineer the resonance requires defining a merit function for optimization. The recently discussed 'figure of merit' (FoM) [3] can be used as such quantity and Bloch surface wave sensors, based on the FoM values, have been shown to potentially beat SPR sensors [4]. The derivation of the FoM does not consider measurement noise which will limit the sensor's performance and govern the 'limit of detection' (LoD) as the quantity of interest for any application.

Starting from a simplified model of angular resonance analysis the effect of noise on the extracted resonance position is qualitatively analyzed. This allows one to define a LoD taking all key parameters of the surface wave sensor, i.e. resonance depth, width, sensitivity and sampling, into account. These parameters are dealt with in an angularly resolved measurement scheme. The resulting LoD will be discussed in comparison to the FoM. Sample BSW designs as well as experimental results on the characterization of BSW sensors will be reported and compared to SPR.

References

[1] J. Homola, Chem. Rev. 108 (2008) 462

[2] M. Shinn, W.M. Robertson, Sens. Act. B 105 (2005) 360

[3] A. Sinibaldi, R. Rizzo, G. Figliozzi, E. Descrovi, N. Danz, P. Munzert, A. Anopchenko, F. Michelotti, Optics Express, 21, 23331 (2013)

[4] A. Sinibaldi, N. Danz, E Descrovi, P. Munzert, U. Schulz, F. Sonntag, L. Dominici, F. Michelotti, Sens. Act. B 174 (2012) 292

9141-27, Session 5

TiN/Au bilayers for temperature measurement in plasmonic sensors

Karl Fleury-Frenette, Jurij Hastanin, Cédric J. M. Lenaerts, Univ. de Liège (Belgium)

Au/TiN bilayers were investigated as plasmonic sensing elements to be used in combination with a single Au layer in order to discriminate the influence of temperature on the surface plasmon resonance from those originating from changes in the probed medium refractive index. Titanium nitride features high thermo-optical coefficients one order of magnitude higher than those of gold over most of the wavelength range where it can support surface plasmon resonance. Some Au/TiN bilayers offer the potential for a significantly enhanced temperature sensitivity in comparison to a single gold layer that could eventually be exploited to determine the relative contributions of temperature and change in the probed medium refractive index on the surface plasmon resonance occurring at the interface of a nearby single gold layer where these contributions can be of comparable amplitude. In order to illustrate this point, the complex refractive indices of TiN and Au as a function of temperature between 20° and 50°C were first obtained from TIRE (Total Internal Reflection Ellipsometry) measurements on single layers over the spectral range 350 nm – 800 nm. From these results, the Au/TiN bilayer thickness configuration providing a 1°C-sensitivity in water for the TIRE measurement scheme was determined. Then, TIRE measurements on an Au single layer and the selected Au/TiN bilayer were carried out with water and a water-glucose solution as probed media over the range 20° to 50° C. Both TIRE phase difference and amplitude ratio spectral curves were fitted simultaneously in order to retrieve the temperature and refractive index of the liquids at this same temperature using the previously determined layers refractive index data. The liquids refractive indices at 633 nm were compared to values measured using a critical angle refractometer.

9141-28, Session 5

SPR detection method for the thickness of metal thin film

Qinggang Liu, Chao Liu, Tianjin Univ. (China); Xue Yu, Tianjin University (China); Meiou Liu, Geng Sun, Tianjin Univ (China)

The evanescent wave, occurred when the incident light generates total internal reflection on the interface between glass and metallic film, can raise the surface plasmon (SP) on the metallic film. SP and evanescent wave can resonate under certain angle of incidence when they have the same frequency and wave number. In this case, the power of reflection beam decreases dramatically, and the resonance peak appears in the reflection spectroscopic. The positions of resonance peaks are different when the refraction indexes of medium on the metallic film or the thicknesses of the metallic film are different. In the experiments utilizing the technology of reflected light with prism to measure the concentration, we found that metal film thickness of prism side had an immediate impact on reflectivity and reflection phase of incident light. Therefore, the research of SPR phase detection for measuring nanoscale thickness of metal film had been considered. It is found by our research that the method of SPR phase detection could be used to measure nanoscale thickness of metal film, which provided a novel means to calculate the value of thickness through figuring up the relative offset of interference fringes with the TM-polarized and TE-polarized wave of film-substrate step and then fitting the formulate representing the relation between phase variation and metal film thickness. The simulation and testing results indicated that the accuracy with the range of film thickness between 30 and 80 nanometers is not more than 0.33 nm. Moreover, this method has some advantages such as non-contact, high precision and simple mechanism.

9141-29, Session 6

Novel design of dual-core microstructured fiber with enhanced longitudinal strain sensitivity

Lukasz Szostkiewicz, InPhoTech Ltd. (Poland); Tadeusz Tenderenda, InPhoTech Ltd. (Poland) and Military Univ. of Technology (Poland); Marek Napierala, InPhoTech Ltd. (Poland); Michal Szymanski, Military Univ. of Technology (Poland); Michal Murawski, InPhoTech Ltd. (Poland) and Military Univ. of Technology (Poland); Piotr Lesiak, Warsaw Univ. of Technology (Poland); Pawel Mergo, Univ. of Maria Curie-Sklodowska (Poland); Pawel Marc, Leszek R. Jaroszewicz, Military Univ. of Technology (Poland); Tomasz Nasilowski, InPhoTech Ltd. (Poland) and Military Univ. of Technology (Poland)

Constantly refined technology of manufacturing increasingly complex photonic crystal fibers (PCF) leads to new optical fiber sensor concepts. The ways of enhancing the influence of external factors (such as hydrostatic pressure, temperature, acceleration) on the fiber propagating conditions are commonly investigated in literature. On the other hand longitudinal strain analysis, due to the calculation difficulties caused by the three dimensional computation, are somehow neglected. In this paper we show results of such a 3D numerical simulation and report methods of tuning the fiber strain sensitivity by changing the fiber microstructure and core doping level. Furthermore our approach allows to control whether the modes' effective refractive index is increasing or decreasing with strain, with the possibility of achieving zero strain sensitivity with

specific fiber geometries. The presented numerical analysis is compared with experimental results of the fabricated fibers characterization. Basing on the aforementioned methodology we propose a novel dual-core fiber design with significantly increased sensitivity to longitudinal strain for optical fiber sensor applications. Furthermore the reported fiber satisfies all conditions necessary for commercial applications like good mode matching with standard single-mode fiber, low confinement loss and ease of manufacturing with the stack-and-draw technique. Such a fiber may serve as an integrated Mach-Zehnder interferometer when highly coherent source is used. With the optimization of single mode transmission to 850 nm, we propose a VCSEL source to be used in order to achieve a low-cost, reliable and compact strain sensing transducer.

9141-30, Session 6

Impact of hydrostatic pressure on modulation instability processes in a birefringent microstructured fiber

Karol Tarnowski, Alicja Anuszkiewicz, Jacek M. Olszewski, Wroclaw Univ. of Technology (Poland); Pawel Mergo, Univ. of Maria Curie-Sklodowska (Poland); Bertrand Kibler, Univ. de Bourgogne (France); Waclaw Urbanczyk, Wroclaw Univ. of Technology (Poland)

Optical fibers can be used as active and passive elements of fiber-optic sensors for measuring a variety of physical parameters. This sensing technology employs different mechanisms based on linear interaction of external physical/chemical parameters with guided light. Recently an alternative approach has been proposed exploiting the recent achievements in nonlinear optics [1-3]. It uses a direct sensitivity of nonlinear frequency processes to external factor. The operation principle of such sensors relies upon tracking the wavelengths generated by the nonlinear frequency conversion processes under different environmental conditions (temperature, pressure etc.).

In our work we investigated an impact of hydrostatic pressure on scalar and vector modulation instabilities (MI) in a microstructured birefringent optical fiber. Basing on analytical predictions one can expect higher sensitivity of the vector MI compared to the scalar MI. Our experimental results confirm a possibility of measuring hydrostatic pressure by tracking a position of vector modulation instability bands. In order to better understand the observed phenomenon we performed numerical simulations based on the coupled nonlinear Schrödinger equations. The results of simulations are in good agreement with the measurements and show that the polarization-dependent vector nonlinear processes are better suited for pressure sensing applications than the scalar nonlinear processes. An important advantage of the presented nonlinear fiber optic sensor over linear sensors based on Bragg gratings or long period gratings is no need for fiber preprocessing.

Presented work was supported by Polish-French POLONIUM Program. K. Tarnowski acknowledges Foundation for Polish Science START Program.

[1] J. R. Ott, M. Heuck, C. Agger, P. D. Rasmussen, O. Bang, Opt. Express 16, 20834-20847 (2008).

[2] M. H. Frosz, A. Stefani,O. Bang, Opt. Express 19, 10471-10484 (2011).

[3] B. Gu, W. Yuan, M. H. Frosz, A. P. Zhang, S. He, O. Bang, Opt. Lett. 37, 794-796 (2012).

9141-31, Session 6

Reflective polarimetric vibration sensor based on temperature-independent FBG in HiBi microstructured optical fiber

Karima Chah, Univ. de Mons (Belgium); Christophe Caucheteur, Univ. de Mons (Belgium) and F.R.S.-FNRS Research Associate (Belgium); Patrice Mégret, Univ. de Mons (Belgium); Sanne Sulejmani, Thomas Geernaert, Francis Berghmans, Hugo Thienpont, Vrije Univ. Brussel (Belgium); Marc Wuilpart, Univ. de Mons (Belgium)

Fiber optic sensors outperform traditional sensor technologies in fields such as structural health monitoring, vibration and seismic activity monitoring, intrusion detection, and many other applications. Their key advantages include electromagnetic interference immunity, lightweight, small size, multiplexing capabilities, low power consumption, corrosion and high temperature resistance. To meet the demand of more and more challenging optical sensors a new generation of optical fibers, the so-called microstructured optical fibers (MOFs), has appeared. These fibers are composed of a structure of holes surrounding a solid core, which offers a unique design flexibility to optimize their waveguide properties for specific applications. In particular, the design can be optimized to strongly reduce the cross-sensitivity of a sensor to parasitic physical parameters like temperature variations, as is the case for the sensor presented here. Our sensor is based on a Bragg grating inside a temperature independent highly birefringent MOF with a high transverse strain sensitivity, to evaluate vibrations by a polarimetric measurement of the reflection spectrum. This technique takes advantage of the stress-induced phase shift between the two orthogonally polarized fiber Eigen modes. It consists in coupling linearly polarized light through one arm of an optical coupler (50:50) in the sensing optical fiber in which a highly reflective fiber Bragg grating is inscribed. The reflected power is analysed with a polarization analyser. The optical fiber is crushed by a mechanical transducer designed to transform the vibration into a mechanical stress transversal to the fiber's axis. The vibration therefore induces a change of the phase modal birefringence that varies in time at the same frequency. In this study we show that standard single-mode fibers do not provide stable measurements, the conventional polarization-maintaining fibers lead to a significant cross-sensitivity to temperature whereas the highly birefringent microstructured optical fiber, show temperature independent (up to 120°C) and repeatable vibration measurements.

9141-32, Session 6

Improving of the sensitivity of the evanescent field sensor based on microstructured-core PCF

Lynda A. Cherbi, Samy Touzene, Issam Hadouche, Abderahmane Bellil, Univ. des Sciences et de la Technologie Houari Boumediene (Algeria)

In this work, we were able to improve the sensitivity of a biosensor - evanescent mode type and thus contribute to the design of a bacteria sensor in water by choosing an appropriate microstructure of Photonic crystal fiber(PCF) . We modeled with the finite element method several configurations of PCF whose both the core and the cladding are microstructured and based on polymers materials. We were able to increase the overlap between the electromagnetic field and the material to be analyzed in the hole, compared to previous works, by using a PCF whose the core is constituted of 19 holes of diameter of 0.874 μm and a pitch of 1.5 microns. The diameter of the core is 32 microns. The cladding is constituted of 18 holes of 6 microns diameter and the pitch is 6.4 microns. The cladding is made from the polymer(PMMA- polymethyl methacrylate) . It noted the improvement of the sensitivity parameter r% of the fiber sensor especially around 1050nm. This allowed us to conclude that the increase of the number of holes in the PCF's core has significantly improved the sensitivity of the fiber which makes it the best candidate for use as a sensor to analyze specific substances in the water introduced into these holes by using the micropumps. Then, several structures of PCF have been proposed to consider another way of analyzing the liquid by the PCF-sensor by expanding the evanescent field to the outside of PCF and immerse it in the liquid to be analyzed, by tuning

the PCF's geometry and materials, where it was found the enhancement of the evanescent field that significantly improves the sensitivity of the obtained sensor.

9141-33, Session 6

Highly-sensitive biological sensor based on photonic crystal fiber

Shaymaa I. H. Ibrahim, Mohamed F. Hameed, Zewail City of Science and Technology (Egypt) and Mansoura Univ. (Egypt); Salah S. Obayya, Zewail City of Science and Technology (Egypt)

This paper introduces a numerical analysis of a highly sensitive, easy-to-fabricate photonic crystal fiber (PCF) biological sensor. The proposed biological sensor is based on surface plasmon resonance (SPR). The SPR-based sensor is currently one of the most commercially preferred sensors due to its simplicity, robustness and high sensitivity without the need to molecular labels. Photonic crystal fiber sensors are now a subject of intense study as the current fabrication technologies enables both mass production and integration of the sensors.

The proposed sensor design consists of six slots that contain the analyte with their surfaces metalized to enable the excitation of the SPR modes. The core of the PCF is made of silica with circular air holes of different or similar diameters that can support light guidance. The Silica is also used as a background material. The central air hole is made to enable the phase matching between the guided PCF mode and the SPR mode by tuning the characteristics of the fundamental core mode. The phase matching between the core mode and the excited SPR mode is very sensitive to the refractive index change in the analyte.

To enhance the sensitivity, optimization of metal thickness, diameters of the air holes at the core circumference, the position and the diameter of the central air hole has been carried out to achieve high sensitivity up to 3000 RIU/nm for wavelength interrogation. However, changing the diameters independently so that we have two different diameters for the holes, we are able to obtain a dual channel sensing capability utilizing both ?HE?_11^x and ?HE?_11^y modes. The sensitivities of both channels are high up to 2600 RIU/nm and 3000 RIU/nm, respectively. In our investigations, the effects of the geometrical parameters and metal type on the sensor sensitivity are studied in detail to produce more efficient sensing capabilities.

The numerical analysis of the proposed sensor structures is carried out using a full vectorial finite element method (FEM) with perfectly matched layer (PML). With FEM, the cross section of the structure is divided into triangles to accurately model the curved and circular boundaries. The PML is used as boundary conditions to correctly find the propagation characteristics of the leaky modes supported by the SPR-PCF sensor. The fabrication of the proposed sensing structures should be straight forward process as the core consists of only circular holes with relatively large diameters.

9141-34, Session 7

Trends and future of Fiber Bragg Grating sensing technologies: tailored Draw Tower Gratings (DTG(r)s) *(Invited Paper)*

Eric Lindner, FBGS Technologies GmbH (Germany)

Fiber Bragg Gratings (FBGs) are today commonly used in different sensing applications. The requirements of the fiber and FBG characteristics are very diverse and strongly depending on the application and the used measurement technology. In this presentation we will give an outlook about the current and future trends of the use of Fiber Bragg Gratings in sensing applications. Furthermore we will discuss how the use of Draw Tower Grating (DTG(r)) technology enables the production of tailored FBG sensing fibers for these applications.

9141-35, Session 7

Peak detection in fiber-Bragg grating sensors using a fast phase correlation algorithm

Alfredo Lamberti, Steve Vanlanduit, Ben De Pauw, Francis Berghmans, Vrije Univ. Brussel (Belgium)

The fiber Bragg grating sensing principle is based on the exact tracking of the peak wavelength location in function of the sensor state. Several peak detection techniques have already been proposed in literature. Among these, conventional peak detection methods such as the maximum detection algorithm (MDA), do not achieve a very high precision and accuracy. This is in particular the case when the Signal to Noise Ratio (SNR) and the wavelength resolution are poor, or when the peak shape is deformed. On the other hand, recently proposed algorithms like the cross-correlation demodulation algorithm (CCA), are more precise and accurate but require a significantly higher computational effort.

To overcome these limitations, we have developed a novel fast phase correlation algorithm (FPC) which has the same accuracy and precision as the CCA, but is at the same time considerably faster. This paper presents the FPC technique and analyzes its performances for different SNR and wavelength resolutions. Using simulations and experiments, we compare the FPC with the MDA and CCA algorithms. The FPC detection capabilities were as precise and accurate as those of the CCA and considerably better than those of conventional peak detection methods. The computational time of the proposed fast FPC is up to 50 times lower than CCA, making the FPC a valid candidate for future implementation in real-time systems.

9141-36, Session 7

Monitoring of reinforced composites processed by microwave radiation using fiber-Bragg gratings

David Barrera, Univ. Politècnica de València (Spain); Inma Roig, AIMPLAS - Technological Institute of Plastics (Spain); Salvador Sales, Univ. Politècnica de València (Spain); Rudolf Emmerich, Fraunhofer-Institut für Chemische Technologie (Germany)

The well-known advantages of optical fiber sensors make them suitable for embedding into fiber-reinforced composite materials. These materials require the use of strict conditions to obtain a reproducible polymerization process. In conventional thermal processing, energy is transferred to the material from the surfaces while in microwave processing the energy is supplied by an electromagnetic field directly to the material. This results in rapid heating throughout the material thickness with reduced thermal gradients. The use of microwave radiation is a technical alternative for the non-homogeneous heating of the fiber-reinforced composite materials with the conventional processing and reduces the processing time. In this paper a comparison between the conventional processing and the microwave processing of carbon fiber-reinforced composites has been performed. Fiber Bragg Gratings have been used for on-line monitoring with the aim of a better understanding of the residual stress and distortions induced during the processing.

The samples are composed of a total of 21 unidirectional carbon prepregs layers. To obtain the residual stress along the samples the sensors are placed both in the direction of the carbon fibers and perpendicular to them. A total of 10 strain FBG sensors are used in each of the samples distributed in two different layers. Additionally, there are two FBG sensors used for temperature monitoring. For conventional processing, the samples are placed inside an oven at 180ºC during 3 hours. For microwave processing, a robotic arm equipped with a microwave antenna is used.

The measured residual strain in both processing techniques is lower in the parallel direction of the carbon fibers. The

measured residual strain values in the perpendicular direction to the carbon fibers are larger than in parallel direction but slightly smaller in microwave processing. Finally, small samples from the center of the laminates are used to study the glass transition temperature. The obtained values are similar in both curing processes.

9141-37, Session 7

Vibration monitoring of carbon fiber composites by multiple fiber optic sensors

Massimo Olivero, Alberto Vallan, Guido Perrone, Politecnico di Torino (Italy); Daniele Tosi, Univ. of Limerick (Ireland); Wei Chen, Politecnico di Torino (Italy)

The research here presented takes root into the large demand for in-line structural health monitoring of carbon-reinforced-composites (CRC), which require low-cost and minimum invasive sensors to track fatigue and predict the onset of cracks and failures. Fiber optic sensors (FOS) represent a viable technology in monitoring the vibrations of CRC crafts (e.g. frames of race cars, lightweight mechanic components, sporting goods) due to a number of advantages such as the inherent low form factor of optical fibers that makes them ideal as embedded sensors, the immunity from electromagnetic disturbances and the multiplexing capability.

Most common FOS for strain and vibration rely on the mature fiber Bragg grating (FBG) technology, which works well in terms of reliability and integration of multiple sensors, but it might not represent the best solution in the case of low-level, high-frequency strain, or in the case of budget-limited applications.

The aim of this work is the comparison of the FBG technology with a simple vibration-measurement system based on the detection of polarization rotation in a standard optical fiber, applied to the dynamic structural monitoring of CRC items for the automotive industry. A CRC test plate in a 4-layer configuration was equipped with FBG and polarimetric fiber sensors (PS) that were embedded during the fabrication process. The plate was then mechanically stressed by applying static and dynamic loads while monitoring the sensors response, in order to compare -highlighting pros and cons- the two sensor types.

The system for acquisition of the FBG data relies on the standard interrogation scheme that performs the analysis of the FBG reflection peak. Its practical implementation is realized by a custom-developed interrogation unit, fabricated by off-the-shelf optoelectronic components integrated with a micro-controller. The instrument can yield up to 5 kdata/s and, through Gaussian interpolation of the measured spectra, it can detect shifts of the FBG spectra with a resolution well below 1 pm.

The PS is made of standard telecom fiber coiled into the plate and excited by a pigtailed laser diode. The state of polarization (SOP) of the light entering the sensing fiber, adjustable by a polarization controller, undergoes a rotation while traveling the fiber subjected to vibration. At the output of the sensing fiber, a polarizer and a photodiode provide a signal dependent on the change of SOP, which can then be correlated to the vibration of the host structure.

The test plate was fastened and then subjected to vibrations applied by a computer-controlled shaker. The applied force was calibrated by a load cell, which also served as a reference sensor. Vibrations in the range 5-30 Hz and different loads were applied.

The outcome of the comparison is that both sensors can easily detect vibrations in the range of interest, with a minimum sensitivity below 1kg of applied weight. The FBG requires signal processing (Gaussian fitting) to detect small vibrations, but it yields better results in terms of noise and fidelity to the applied stress. The polarimetric sensor requires that the polarizer and the photodiode are placed close to the sensing fiber, in order to avoid spurious noise related to the propagation outside the embedded fiber, but, beside the reduced complexity and cost, it is likely more effective for detection of high frequency, since the interrogation system has virtually no limitations on the data sampling rate.

9141-38, Session 7

Optical backscatter reflectometer to study the response of cascaded FBGs embedded in fibre reinforced polymer composites during flexural tests

Damien Kinet, Univ. de Mons (Belgium) and Multitel (Belgium); Didier Garray, Sirris (Belgium); Alexey V. Faustov, Univ. de Mons (Belgium); François Narbonneau, Multitel A.S.B.L. (Belgium); Patrice Mégret, Christophe Caucheteur, Univ. de Mons (Belgium)

Optical fibre sensors (OFS) have attracted considerable attention over the last decades due to their ability to measure strain in the host structure at multiple locations. Lightweight, compactness, high mechanical resistance, electromagnetic immunity are some of the fibre Bragg grating (FBG) characteristics that make it a prime candidate as a sensor in various fields. One of them is composite materials. Their high mechanical resistance coupled with a small weight comparatively to metallic materials make them very useful in the aircraft and railway industries, reducing energy consumption and CO2 emissions. However, there is a need to know the internal strain state inside this material when it is subject to external perturbation to prevent sudden breakages. In this context, embedding FBG sensors inside polymeric composite structures is of high interest to perform in-situ monitoring from the curing stage of the polymer throughout the structure life cycle until breakdown.

In this paper, we present two different sensors configurations. For the first one, as classically done, we embed a high number of very short FBGs (1mm long) written at different wavelengths distributed every 15 mm along a unique optical fibre. This FBGs network is placed straight along the length of the sample between two layers of a composite material. The latter is manufactured by the hand lay-up technique by stacking together 8 layers of plain weave carbon fabrics. Dimensions of the sample are 300x39x3.15 mm (LxWxH). The second configuration, much more challenging, consists in several samples of ~3 mm long uniform FBG sensors, written at the same Bragg wavelength, cascaded every ~10 cm along a unique low macrobending sensitive singlemode optical fibre. We embed these ones in different fibre reinforced polymer (FRP) composites (glass, G, and carbon, C). The manufacturing technique is the same as for the first configuration. The only difference between GFRP and CFRP being the number of layers (16 and 8 respectively). The dimensions of the samples are roughly 250x80x3 mm (LxWxH). Sensors positioning was realized to obtain, at the end of the curing process, a mapping of the internal strain distribution inside the sample. In this work, we use an Optical Backscatter Reflectometer (OBR4400) from Luna Technologies to follow the amplitude spectral evolution (with the main focus on the Bragg wavelength displacement) of our FBGs when composite samples are subject to bending (both 3 and 4 points). This interrogator presents decisive advantages for our application such as high-speed interrogation and high spatial resolution (less then 50 ?m). The tunable laser source can sweep a wavelength range from 1525 nm to 1625 nm at a speed up to 100 nm/s so that the measurement itself takes less then one second. This measurement is followed by signal processing steps to recover the spectrum of each grating independently from the others and so to retrieve the strain distribution inside composite materials. As the same equipment is used for the two FBGs sensors distributions, we compare them in terms of metrological performances.

9141-39, Session 7

Optical fiber embedding into thermal spray coating promises new smart materials design able to operate under harsh environment

Yi Duo, Univ. de Technologie de Belfort-Montbéliard (France); Pierre Pfeiffer, Univ. de Strasbourg (France); Sophie Costil, Univ. de Technologie de Belfort-Montbéliard (France); Bruno Serio, Univ. Paris Ouest Nanterre La Défense (France)

Although a large number of fiber optic sensors have been developed, it is observed that the applications have materialized slowly especially in the areas of mechanical and thermal sensors where they are still too often ignored by engineers. In certain areas related to defense and aerospace, the development of fiber optic sensors could lead in manufacturing and large-scale commercialization. New sensor applications in the automotive industry, medical and multi-media for example, require the availability of integrated and communicating sensors, light, which can operate in harsh environments and immune to noise sources from magnetic and electrostatic electrical origin. In this case, engineers could find benefit with the use of optical fiber sensors. They offer a unique perspective for control applications such as in vivo temperatures in medical therapy or during magnetic resonance imaging examination for instance. Thermal spray coating can be applied to build multi-layered system with sensors placed within the layers. Fiber optic embedded sensors can be used to measure physical parameters during the elaboration process of the system or to obtain information on its structural integrity in service. In this study, techniques for embedding fiber optic in ceramics layers have been investigated with the aim of making fiber optic sensors.

We will show embedding characteristics, the first results of optical attenuation change during the elaboration and finally the strength of the mechanical adhesion of the fiber embedding.

9141-40, Session 8

Terbium-doped gadolinium oxysulfide (Gd2O2S:Tb) scintillation-based polymer optical fibre sensor for real time monitoring of radiation dose in oncology *(Invited Paper)*

Elfed Lewis, Sinead O'Keefe, Denis McCarthy, Univ. of Limerick (Ireland); Peter Woulfe, John Cronin, Galway-Mayo Institute of Technology (Ireland); Mark Grattan, Alan Hounsell, Belfast City Hospital (Ireland); Dan Sporea, Laura Mihai, National Institute for Lasers, Plasma and Radiation Physics (Romania); Anand P. Santhanam, N. Agazaryan, Univ. of California, Los Angeles (United States)

A novel extrinsic optical fibre X-ray and gamma ray dosimeter for biomedical applications is presented. The primary focus of the sensor is to measure medical level doses of ionising X-ray and gamma radiation. The scintillation material in the fabricated sensor tip delivers a visible light signal (540 nm) upon exposure to ionising radiation and the resultant low level scintillating light is coupled to a commercially available PMMA (poly methyl methacrylate) plastic optical fibre, which guides it towards a distal fluorescent optical spectrometer located at up to 30 m from the point of measurement. In this way the measurements can be performed from within the LinAc Control area.

The Detector is an Ocean Optics Fluorescent spectrometer which is capable of measuring the low level light signal from the sensor and hence converts the ionising radiation energy to measurable arbitrary optical intensity units. Initial testing at multiple clinical locations has shown the scintillating optical fibre X-ray and gamma ray dosimeter exhibits an acceptable sensitivity upon excitation from a clinical LinAc. Further examinations of the sensor have revealed acceptable low end resolution (capable of detecting cGy dose levels) and repeatability of measurement for various levels of clinical level ionising X-ray energy (typically in the range 4 to 20 MV). The sensor is also capable of detecting electron beams delivered from the LinAc (6 to 22 MeV). Additionally, with the use of a different phosphor powder particle diameter the sensor is capable of measuring electron energies in a range as low as 50keV to 140keV.

Repeated tests in three separate clinical locations have demonstrated that the sensor has excellent repeatability of measurement for a wide range of tests (less than 0.7% of fsd for repeated dose and less than 3% for dose rate within its operating range). Further microscopic investigations of the sensor coating are ongoing which will lead to an optimisation of the sensor geometry e.g. positioning of the coating, coating width and composition of the scintillation material/ epoxy mixture.

9141-42, Session 8

High-sensitivity metal oxides-coated long-period fiber grating sensors for humidity monitoring in high-energy physics applications

Gaia Maria Berruti, Marco Consales, Univ. degli Studi del Sannio (Italy); Michele Giordano, Anna Borriello, Univ. degli Studi di Napoli Federico II (Italy); Salvatore Buontempo, CERN (Switzerland); Giovanni Breglio, Univ. degli Studi di Napoli Federico II (Italy); Paolo Petagna, CERN (Switzerland); Alajos Makovec, The Univ. of Debrecen (Hungary); Andrea Cusano, Univ. degli Studi del Sannio (Italy)

This contribution deals with a feasibility analysis for the development of fiber optic humidity sensors to be applied in high-energy physics (HEP) applications, and in particular in experiments actually running at the European Organization for Nuclear Research (CERN).

In particular, our multidisciplinary research group has been recently engaged in the development of high-sensitivity Long Period Fiber Gratings (LPGs) sensors coated with finely tuned thin layer (typically 100-200nm thick) of hygrosensitive metal oxides for relative humidity (RH) monitoring at temperature below 0°C as well as in presence of strong ionizing radiations.

Different oxides have been investigated (e.g. SnO2 and TiO2) in order to achieve a good control on the optical (low loss) and geometrical (thickness and azimuthally/longitudinal uniformity) characteristics of the overlays for the LPG.

In particular, here we report the results obtained during a deep experimental campaign (carried out in the laboratories of CERN) where the RH detection characteristics of metal oxide-coated LPG sensors were analyzed in the RH range 0-80% and in the temperature range -10-25°C. Preliminary results evidenced the amazing sensitivity of the fabricated devices, especially in correspondence of low value of RH (in the range 1-20%), where it reaches values thousands of times higher than that achieved with Polymide-Coated Fiber Bragg Grating (FBG) sensors characterized by coating thicknesses hundred times higher [1]. This is also accompanied by a much faster responses.

The effects of ionizing radiations on the sensing performance of the fabricated devices were also investigated. In particular, as a first preliminary result, we found that the excellent RH sensing features of the realized LPG sensors are preserved even after exposure to a 10KGy dose of gamma ionizing irradiation. Exposures to progressively higher doses of radiations are currently in progress to define the applicability limits, however obtained results are very interesting and envisage good perspectives for an effective exploitation of LPG technology for RH monitoring in high energy applications.

References

[1] G. Berruti et al., Radiation hard humidity sensors for high

energy physics applications using polymide-coated Fiber Bragg Gratings sensors, Sensor. Actuator. B 177 (2013) 94

9141-43, Session 8

On a possible method to measure the radial profile of the photoelastic constant in step-index optical fibers

Sophie Acheroy, Royal Belgian Military Academy (Belgium); Thomas Geernaert, Francis Berghmans, Vrije Univ. Brussel (Belgium); Patrick J. Merken, Royal Belgian Military Academy (Belgium); Heidi Ottevaere, Hugo Thienpont, Vrije Univ. Brussel (Belgium)

Photoelasticity is a well-known experimental technique used to study stress and strain distributions in a transparent material. It relies on the analysis of stress-induced birefringence in the material. The stress-optic law establishes the link between applied stress and induced birefringence. It uses the photoelastic constant as material dependent coefficients. We discuss a measurement method that aims to determine the radial distribution of the photoelastic constant C in an optical fiber.

The technique uses a polarizing microscope and mechanical loads externally applied to the fiber under test. These loads axially stress the fiber. The radial distribution of C(r) is obtained from the measurement of the retardance profile of a transversely illuminated fiber. To determine the full-field retardance profile of the fiber we apply the Sénarmont compensation method. The inverse Abel transform of the retardance divided by the photoelastic coefficient yields the radial stress-distribution of the axial stress in the fiber. Hence measuring the retardance profile as a function of the applied mechanical load allows deriving the photoelastic coefficient. We therefore measure the retardance profile of a transversely illuminated fiber for different values of axial load applied to the fiber and we compute the inverse Abel transform in order to derive the radial distribution of C(r).

The inverse Abel transform is very sensitive to noise and produces overshoots in the center of the fiber due to numerical artefacts. Therefore we also explore numerical methods to smoothen the shape of the retardance and hence lower the overshoots in the shape of C(r). The artefacts can be lowered by decreasing the noise level of the measured retardation profile. To achieve this, the algorithm to compute the retardance profile R(y) and the inverse Abel transform of that profile have to be optimized. For that purpose we also demonstrate the effects of a low-pass filter applied on the shape of R(y) to filter out the noise of the retardation profile. The influence of the low-pass filter on the final shape of C(r) is carefully analyzed to avoid loss of information.

We applied our method to glass step-index fibers with different core dimensions. The first results suggest that C may not be constant across the fiber and that the mean absolute value of C is slightly larger for glass fibers than for bulk fused silica. This can, for example, influence the accuracy with which one is able to predict the response of optical fiber sensors used for measuring mechanical loads.

9141-44, Session 8

EFPI sensor utilizing optical spectrum analyzer with tunable laser: detection of baseline oscillations faster than spectrum acquisition rate

Nikolai A. Ushakov, Leonid B. Liokumovich, St. Petersburg State Polytechnical Univ. (Russian Federation)

In the last two decades industry and academia are drawing an increasing attention to the optical sensors based on the extrinsic Fabry-Perot interferometers (EFPI). Sensors demonstrating high sensitivity to measurands (temperature, strain, pressure and other physical quantities) and utilizing a miniature sensing elements are designed [1].

One of the most promising ideas of measuring L is based on the registration of the EFPI spectral transfer function and its approximation with known analytical function. Various concepts of such approximation were developed and implemented, demonstrating an achievement of baseline measurement resolution about tens picometers [2]. Another merit of this approach is registration of the absolute baseline value. The main disadvantage of this technique is that it provides only one sample per acquisition of the EFPI spectral function.

From the other point of view, optical spectrum analyzers based on the tunable lasers capture each spectral point at a discrete time moment, hence, providing an ability to obtain the measurand values with a much higher sample rates (proportionally to the point number in the registered spectrum of the interferometer). Therefore, introducing EFPI spectral function (considering low-finesse cavity) as I(?,t)=Acos(4ϖnL(t)/?) and taking into account temporal dependency of tunable lasers wavelength ?(t), variations of interferometer baseline during the spectrum acquisition can be extracted using standard phase (or frequency) detection procedure.

The approach of registering the baseline oscillations faster than the spectrum acquisition rate is the following: at first, EFPI spectral function I(?) is measured, then with respect to ?(t) dependence, represented as I(t). The second step is to estimate the mean cavity length during the spectrum acquisition L0 by approximating measured spectrum by analytical expression S(?)=Acos(4ϖnL0/?) using approach proposed in [2]. After that the analytic signal x(t) for I(t) is calculated, and the desired baseline fluctuations L(t) can be estimated as [arg{x(t)}-arg{S(?(t))}] ?(t)/4ϖn.

The proposed approach was implemented experimentally. The examined interferometer was formed by the fixed fiber FC connector and an external mirror placed at several hundred microns from the fiber end and attached to a PZT oscillating at frequencies from 10 to 500 Hz with amplitude from 5 nm to 100 nm. Spectra measurements were performed with optical sensor interrogator NI PXIe 4844. Signal processing was realized in LabVIEW, providing operation in a real-time mode. The limit on the frequency of registered interferometer baseline fluctuations is determined by the speed of the laser wavelength tuning Vs, refractive index of the media inside the cavity (air in our case), mean cavity length and central wavelength ?0: fmax=2nL0?Vs/?0^2.

1. Fang, Z., Chin, K. K., Qu, R., Cai, H., John Wiley & Sons, Inc., Hoboken, New Jersey, 395-426, (2012).

2. N. Ushakov, L. Liokumovich, A. Medvedev, Proc. SPIE 8789, 87890Y (2013).

9141-45, Session 8

FBG-based biosensor for the concentration measurement of hemoglobin

Libish T. M., Cochin Univ. of Science and Technology (India) and Sree Chitra Thirunal College of Engineering (India); Bobby M. Chirappuram, Vadakedathu P. N. Nampoori, Cochin Univ. of Science and Technology (India); Radhakrishna G. Prabhu, Robert Gordon Univ. (United Kingdom); P. Radhakrishnan, Cochin Univ. of Science and Technology (India)

In this paper, we propose a novel method for measuring the concentration of hemoglobin present in bio-chemical samples. The bio sensor exploits the inherent characteristics of the Fiber Bragg Grating (FBG) which is coated with a biopolymer, deoxyribonucleic acid (DNA). It is well known that hemoglobin reacts with high specificity to DNA material. For increased sensitivity, the fiber with FBG was etched with hydrofluoric acid (HF) prior to coating with the DNA. The etched FBGs are sensitive to an external analyte by evanescent field interaction.

The sensing mechanism is based on the interaction of the hemoglobin with the biopolymer film, which changes the film refractive index and also exerts some stress on the underlying fiber, resulting in a shift in the Bragg wavelength. The stress and RI change induced in the biopolymer film during its interaction with hemoglobin depends on the concentration of hemoglobin present in test samples. Using a real time monitoring set-up, we recorded the Bragg wavelength changes with changes in hemoglobin concentration. By analyzing the Bragg wavelength shift, we calculated the concentration of hemoglobin present in the sample solutions.

Today, the hemoglobin concentration measurement is very important and has significant applications in medical diagnostics, drug discovery, food and biotechnology. Currently analytical techniques like Gas Chromatography- Mass Spectroscopy and High Performance Liquid Chromatography-Mass Spectroscopy are commonly used. But most of these techniques have the disadvantage that they are expensive, time consuming and require skilled technicians to perform the analysis. So, a fiber optic based biosensor will be a promising alternative to the classical analytical methods due to its simplicity, relatively low cost, inherent specificity, ability to perform sensing using a small amount of sample and rapid response.

At present, refractive index sensing based on the etched FBG is an extraordinarily important subject in the bio sensing area which attracts significant research interest. The etched FBGs can be made to detect extremely low concentrations of biochemical target molecules by applying suitable material coatings on their surface. These coatings selectively react with specific target molecules and result in the refractive index change. The presence of a specific target molecule is detected by analyzing the Bragg wavelength shift of the FBG reflection spectra.

The fabrication of the sensor has been carried out using an FBG with Bragg reflectivity at 1564.28 nm before etching. After an HF etching time of 33 minutes, a final blue shift of 0.28 nm in the Bragg wavelength was observed between unperturbed and etched grating with air as external medium. The FBG was then dipped in DNA coating solution for two minutes and withdrawn at a speed slow enough to produce a uniform coating without bead formation. Residual stress after the film deposition was observed which produced a red shift of 0.26nm.

The FBG exhibited a total red shift of approximately 0.112 nm when the hemoglobin concentration was gradually changed from 50 μg/mL to 300 μg/mL. Apart from the red shift, there was a reduction in the reflected power with increasing hemoglobin concentration. The FBG sensor sensitivity was around 0.448 pm/μgmL-1 of hemoglobin in the measurement range.

9141-46, Session 9

OLED integrated silicon membranes for light-modulation devices

David Cheneler, Lancaster Univ. (United Kingdom); Michael Vervaeke, Vrije Univ. Brussel (Belgium); Hugo Thienpont, Vrije Universiteit Brussel (Belgium); Vito Guido Lambertini, Mauro Brignone, Ctr. Ricerche Fiat S.C.p.A. (Italy)

Organic light-emitting diodes (OLEDs) are a maturing technology predominately used to create digital displays in devices such as television screens and mobile phones. However, the range of possible applications for OLEDs is far more significant if they can be integrated into mechanical devices. Modern OLEDs incorporating a simple organic polymer thin film multilayer structure consisting of conductive layers and emissive layers between two electrodes can be formed on most substrates such as glass, metals, and ceramics and even flexible surfaces. This feature makes OLEDs an attractive technology for sensing applications. A number of optical chemical and biological sensors have successfully integrated OLEDs. The OLED is fixed in these devices, and do not exploit their innate compliance and, as of to date, they have not been implemented as a mechanical sensor, except as a light source in flexible waveguides acting as pressure sensors. To this end, the feasibility of incorporating OLEDs into micro-fabricated silicon sensor technology to realise a new generation of functionalised materials for sensor applications was investigated. In this paper, the fabrication of a demonstration unit incorporating a light-emitting organic compliant pressure sensor capable of utilising light modulation as a dynamic force transduction mechanism is described.

The design investigated was a micro-machined flexible circular membrane upon which is deposited multiple layers of organic polymers and the pertinent electrodes forming a light emitting diode. The OLED is encapsulated with an epoxy and a glass layer for protection to extend the life of the device. The glass is coated with an opaque mask except for a small circular opening at the centre. An aperture is axially located above the OLED surface to allow a small amount of light to reach the photon detector. For simplicity, the photon detector in this instance is a light dependent resistor, the output of which is monitored via a standard potential divider circuit. The underside of the membrane has been exposed to nitrogen at a given pressure which causes the membrane and OLED to deflect changing the distance between the OLED and the aperture. This in turn causes a change in the number of photons escaping the aperture and reaching the sensor, changing its response as a function of the applied pressure.

The theoretical output of the OLED with pressure, along with the corresponding output of the monitoring circuitry is given. It is shown that there is good agreement between the theory and the measured experimental results. An interesting design requirement is discussed. Due to the geometry of the deflected membrane and the Lambertian nature of the emission of the OLED, it has been shown that it is necessary to ensure that the light-emitting surface is of a comparable size to the aperture, which has to be in turn much smaller than the membrane. It has been proven that if these conditions are not met, then the system will not function as a pressure sensor as the output is independent of the deflection. When these conditions are met, it is clear that this is indeed a promising sensing technology.

9141-47, Session 9

Enhanced integrated optical resonators for label-free biosensing

Davide Gandolfi, Marta Guarisco, Univ. degli Studi di Trento (Italy); Laura Pasquardini, Cecilia Pederzolli, Mher Ghulinyan, Georg Pucker, Fondazione Bruno Kessler (Italy); Lorenzo Pavesi, Univ. degli Studi di Trento (Italy)

We realized a series of whispering-gallery-mode resonator vertically-coupled to a buried bus waveguide. By using different etching processes, we changed the slope of the outer walls of the resonators, creating disk and wedge structures. Then, we measured their bulk sensitivity and limit of detection by exposing both structures to several water-glucose solutions at different concentrations. This characterization shows enhanced bulk sensitivity and a much lower limit of detection for the wedge resonator, in comparison to standard disk resonators of same dimensions.

From a finite-element modeling, we attributed the first characteristic as a result of the less confined mode profile. The latter characteristic is the combined effect of both higher sensitivity and of higher quality factor. The quality factor is increased thanks to the higher surface quality of the wedge resonator, as reporterd also in several papers.

Moreover, with FEM simulations we optimized the design of the WGM optical cavity, trying to maximize the surface (instead of bulk) sensitivity, which is useful for an optimal label-free biosensing.

In addition, the vertical coupling scheme allows the simultaneous use of multiple excitation wavelengths, from the near infrared to the visible range, which is of great impact in view of an integrated biosensor. We measured and simulated the sensitivity (and limit of detection) of the wedge resonator at a probing laser wavelength of 1540 nm and 780 nm.

Finally, a demonstrative biosensor is used for specific sensing of human thrombin protein. The optical resonator is first silanized and then functionalized with DNA-aptamers. DNA-aptamers can be thought as artificial antibody, and can be realized – in principle – for a huge plethora of proteins (without requiring major modifications in the functionalization procedure, which is crucial for multiplexed analysis). The device is then enclosed in a simple microfluidic chamber, where continuous flow is provided by means of a syringe pump.

Our sensor shows a fast (less than five minutes to saturation) response when exposed to a buffered solution of target proteins. The lowest concentration that we tested, 100nM, is well above our current optical limit of detection. On the contrary, the biosensor does not respond to aspecific protein (bovine serum albumin) solutions, even at concentration as high as 500nM. This result is important because it proves (partially) that a specific biorecognition should be possible even in complex solutions. A more convincing proof will arise from future tests with other classes of proteins.

9141-48, Session 9

Analysis of optimal frequency bias of frequency-lock in passive ring resonator optic gyro

Junjie Wang, Lishuang Feng, Yinzhou Zhi, BeiHang Univ. (China)

The passive ring resonator optic gyro (PROG) has been of great interest in gyro fields for its potential to meet the critical demands of angular velocity sensor function in low cost, small sized, high-precision inertial navigation systems. Whether the PROG works in open-loop mode or close-loop mode, it is based on the real-time frequency trace-and-lock technology. The frequency-lock (FL) accuracy of a PROG, which is closely related to the signal-to-noise ratio (SNR) that corresponds to the frequency bias where the operation point is set, determines the ultimate measurement precision of the gyro system; therefore it is particularly important to choose a proper frequency bias for the PROG to achieve excellent performance. However, there is no detailed guidance of the FL frequency bias for the transmission-type and reflection-type PROGs reported yet. The frequency bias of the PROG is usually realized by phase modulator, acoustic-optic frequency shifter or direct frequency modulation technology. In this paper, the sketch maps of typical transmission-type and reflection-type PROG are described at first. Then the FL accuracy of the PROG limited by the photon shot noise is deducted. Based on the principle that the best performance of the PROG comes from the optimal SNR rather than the highest sensitivity, the relation between the SNR affected by the photon shot noise of the photodetector, sensitivity and the frequency bias is analyzed in detail under Lorentz function approximation for both transmission-type and reflection-type PROGs. The normalized light intensity, photon shot noise, SNR and sensitivity are only related to the frequency bias. The calculated results show that for a transmission-type PROG, the frequency bias at the biggest SNR and the biggest sensitivity equal 0.3536 and 0.2887 of the full width at half maximum (FWHM) of the ring resonator respectively, where an optimal balance between the SNR and the sensitivity can be achieved provided the frequency bias is set in this region. For a reflection-type PROG, the two corresponding frequency biases equal 0.2887Q? and 0.2887 of the ring resonator's FWHM respectively, where Q? is a monotony decrease function of the resonance depth, and their difference relies heavily on the resonance depth of the PROG. The deeper the resonance depth reaches, the larger the difference is. The SNR and the sensitivity change rapidly in the region ranging from 0 to 0.2887, hence once the reflection-type ring resonator is fixed, it is better to find the best FL frequency bias experimentally to achieve the optimal balance between the SNR and the sensitivity. This work provides explicit theoretical guidance for the systematic optimization of the PROG.

9141-49, Session 9

On the possibility of phase measurements in microoptical gyro

Vladimir Y. Venediktov, St Petersburg Univ. (Russian Federation) and Saint Petersburg Electrotechnical Univ. "LETI" (Russian Federation); Yuri V. Filatov, Egor V. Shalymov, Saint Petersburg Electrotechnical Univ. "LETI" (Russian Federation)

Development of comparatively cheap and miniaturized (with the size of several centimeters or less) gyros for the wide range of possible applications is one of the most important tasks in the field of developing the navigation and orientation equipment. For today this area is preoccupied by various kinds of micromechanical gyros. However, these devices are sensitive to linear accelerations and to various kinds of mechanical stress, limiting thus the field of their possible applications. Optical gyros (ring laser gyros and fiber-optical gyros) are free of these limitations, but for various reasons their minimal diameter is limited by some 100-150 mm. Hence during the last decade the main activities in the area of developing the microoptical gyro were concentrated on the other scheme of prospective device, based on the use of passive ring single-mode cavities.

All known approaches to microoptical gyro design with the use of the passive ring cavity are employing the amplitude characteristics of such cavities and their splitting for determining the rotation speed. Our results indicate that one can use the phase retardation characteristics for the same purposes. Such a technique is widely used in fiber-optical gyros, and thus the corresponding approaches and methods can be also used in designing the passive microoptical gyros.

We have considered the ring cavity with single DC, which is similar to the well-known Gires-Tournois interferometer, and have, in particular, analyzed the dependence of phase retardation in such devices upon radiation frequency for various rates of coupling coefficient and of energy dissipation inside the cavity. It was shown that in the ring cavity one can exploit such phase retardation dependence for measuring the Sagnac effect, introduced by cavity rotation and thus to develop in future the variant of passive microoptical gyro, employing the phase measurements instead of amplitude ones.

9141-63, Session 9

Silicon nitride waveguides for on-chip Raman spectroscopy

Ashim Dhakal, Univ. Gent (Belgium); Pieter Wuytens, Frederic Peyskens, Photonics Research Group, INTEC Department, Ghent University (Belgium); Ananth Z. Subramanian, Nicolas Le Thomas, Roel G. Baets, Univ. Gent (Belgium)

The evanescent tail of the guided modes can efficiently excite Raman active molecules located in the cladding of a waveguide. Similarly, a significant fraction of the total emitted Stokes power is evanescently coupled to the same mode. Further, the enhancement effects inherent to the waveguide, alongside with the long interaction length, lead to an increased light-matter interaction, resulting in a higher sensitivity as required by spectroscopic applications, especially in the context of Raman spectroscopy.

We calculate the spontaneous Raman scattering efficiency as a function of silicon nitride strip waveguide dimensions and show that under typical conditions, the over all efficiency is in the order of 10e-8, which is approximately two orders of magnitude higher than in confocal configuration in the free space.

We also report the experimental demonstration of the use of silicon nitride based photonic waveguides in a lab-on-a-chip context for Raman spectroscopy. To the best of our knowledge, this is the first demonstration of Raman spectroscopy using photonic waveguides.

9141-50, Session 10

Measuring the colour of rendering mortars

Yves Govaerts, Wendy Meulebroeck, Ann Verdonck, Vrije Univ. Brussel (Belgium); Michael de Bouw, Belgian Building Research Institute (Belgium) and Artesis Univ. College of Antwerp (Belgium)

When restoring decorative rendering mortars for historic façades, professionals need to determine the colour of these finishes in order to select an appropriate repair mortar. Currently, the appearance of these renders is only assessed from a subjective point of view. To match with the aesthetic aspects of the façade, contractors must constantly adjust their repair mortar composition to avoid a patchwork of different colours, which is detrimental for heritage. This time-consuming (trial-and-error) methodology can be excluded by evaluating 'colour' with an objective numerical approach.

Since a rendering mortar is characterized by its heterogeneous appearance, colour perception is different depending on the field of view. Unfortunately no standardized procedure is available for measuring the colour of artificial stone-like materials. Unlike uniform surfaces, it is not obvious to quantify colour variations derived from the lime-cement paste, the distribution of mineral pigments and their ageing and weathering effects.

Based on recent studies on determining the colour of natural stone (especially granite rocks), this research presents a methodology for measuring the colour of nonhomogeneous rendering mortars.

Two different spectrophotometers were used to measure the colour of 4 mortar samples, each taken from a different location. One of the instruments is frequently used in scientific papers but is a fixed device for laboratory applications (UltraScan XE) and the second one is a portable device (AvaSpec-3648), which is easy to handle in situ. In both cases illuminant D65 and a viewing angle of 10° was used. These instruments have a diffuse illumination geometry, so that the light is uniform distributed on the sample, to simulate outdoor conditions. Spectral reflectance was measured between 360-750 nm with a wavelength interval of 10 nm. The results were displayed in the CIE L*A*B* color space. The mortar samples were derived from early 20th century architectural heritage in Belgium.

The challenge of the research was to define the material-dependent boundary conditions for the measurement. Unknown parameters are the number of measurements, the aperture of the measuring head and the possibility of observing the sample with or without the specular component. The number of measurements was found by measuring 25 points randomly on the sample surface, each time with another aperture area (6, 9 and 25 mm). The cumulative averages of these points converged to a minimum number of measurements. Using fixed parameters, it was possible to determine the most convenient measuring area. Finally, the relevance of the specular component was analyzed by calculating the colour differences (according to CIEDE2000 and CAM02-UCS formula) between L*a*b* values with and minus the specular reflection.

The outcome of the research is indispensable to measure the colour of rendering mortars in situ which allows to propose viable restoration strategies for rendered listed buildings.

9141-51, Session 10

Damage and deterioration monitoring of artwork by data fusion of 3D surface and hyperspectral measurements

Roger Groves, Technische Univ. Delft (Netherlands); Emilio Ribes-Gómez, AIDO Instituto Tecnológico de Óptica, Color e Imagen (Spain)

This paper describes the processing algorithm methodology and preliminary results from a novel optical-based system for the assessment of chemical and mechanical deterioration of artworks. This system has been developed in the FP7 Syddarta Project and is composed of two optical channels: 1) a 3D imaging channel consisting of a Digital Light Projector, a CMOS camera and a Liquid Crystal Tunable Filter, which acquires 3D surface data and multiband information in the visible spectral range; 2) a hyperspectral imaging channel consisting of a MCT camera, an Acousto-Optical Tunable Filter and an infrared light source, which acquires hyperspectral information in the spectral range 900 to 2500 nm. The developed processing algorithms perform the system calibration, damage detection and chemical deterioration analysis. Photometric and geometric calibrations have been implemented. The photometric calibration is based on a white reference and a map of intensities is obtained in order to compensate the acquired images from light variations. The geometric calibration is based on planar homographies. From this, the interior and exterior orientation of the projector and the two cameras are obtained, which is used to map the acquired data of the different sensors into a single reference frame. To acquire the 3D data, a set of phase-shifted fringe patterns is projected on the object which are processed by Fourier transform. To identify mechanical deterioration (e.g. cracks, holes, warping), the acquired 3D cloud of points is meshed and differences in surface normals for a given radius are computed. To analyse the chemical deterioration of the pigments a supervised classification method has been implemented. First of all, spectral data is normalized with the Extended Multiplicative Scatter Correction algorithm. Then, data dimensionality is reduced by applying Principal Component Analysis and classification is done with Support Vector Machine. Results are presented showing the performance of the described algorithms.

9141-52, Session 10

Development of a measurement system for the online inspection of microstructured surfaces in harsh industrial conditions

Thomas Müller, Benjamin Langmann, Eduard Reithmeier, Leibniz Univ. Hannover (Germany)

For the inspection of microstructured surfaces usually microscopic imaging techniques are applied. These techniques require clean measurement conditions. Soilings, such as dust or splashing liquids, can disturb the measurement process or even damage instruments. Since these soilings occur in most manufacturing processes, microscopic inspection is carried out in a separate laboratory.

We present a measurement system which allows for a microscopic inspection and a 3D reconstruction of microstructured surfaces under harsh industrial conditions. The introduced measuring system is used in a grinding wheel dresser. The dimensions of the structure to be measured are in the range of 50 to 500 µm. The measurement system enables precise positioning of the grinding wheel with an accuracy of 5 µm.

The main component of the measurement system is a CCD camera with a high magnification telecentric lens. The magnification is gradually adjustable from 2.5-10x. Thereby, even structures with dimensions in the range of 30 to 50 µm can be measured. Camera and lens are integrated in a waterproof and dustproof enclosure. The inspection window of the enclosure has an air curtain serving as a splash guard.

The workpiece illumination is crucial to get good measurement results. The measuring system includes high-power LEDs, which are integrated in a waterproof enclosure. The light from each source is coupled into a multi-mode fiber and is guided to the workpiece surface. The measurement system also includes a Laser with a specially designed lens system to form an extremely narrow light section on the workpiece surface. A line width of 25 µm can be obtained. The line and the camera with high magnification telecentric lens are utilized to perform a

laser triangulation of the microstructured surface.

Image processing for automatic and high precision positioning of the workpiece was developed. The algorithm is based on a comparison of the camera images with a reference image. Thereby, even small workpiece displacements can be detected. The resolution of the measurement system is 1 µm/pixel. The image processing algorithm generates a displacement signal which is used for placement correction by the machine tool.

The high magnification factor of the telecentric lens leads to a very small depth of field of the imaging system. In order to be able to measure microstructured surfaces with structure heights larger than 100 µm, image fusion techniques need to be applied to obtain sharp images. This paper evaluates focus stacking algorithms for image fusion and compares processing results for high precise measurements.

Some workpieces have surfaces with high variations of surface reflectivity. This can lead to camera images with highly under- and over overexposed image sections. Therefore, an image fusion algorithm was developed which increases the dynamic range of the image and allows for uniform illumination of the camera image.

9141-53, Session 10

Dual-laser vibrometry: Elimination or extraction of pseudo vibrations

Michael L. Jakobsen, Martin J. Bækbo, Steen G. Hanson, Technical Univ. of Denmark (Denmark)

Laser vibrometers can measure angular velocity of a rotating object with high reliability and precision. The angular velocity is measured directly, which means that no information is required about the radius of the object, nor will any minor simultaneous translation of the object affect the measurements.

However, the use of coherent light generally introduces speckles in the field backscattered from the object. The speckles will somehow infiltrate the optical and electronic post processing, and appear as noise in the angular velocity measurements. This noise contribution is called pseudo vibrations. Pseudo vibrations are structured in the sense that they repeat themselves for every revolution of the object. Therefore, when applying spectral analysis to the angular velocity with the intentions to measure physical fluctuations in angular velocity, the pseudo vibrations will occur with its fundamental frequency exactly located at the cycle frequency of the object and with potentially all the corresponding harmonics available within the bandwidth of the system.

Various methods have been introduced to eliminate the pseudo vibrations. The speckles can be forced to decorrelate either by mechanically moving the sensor along the shaft or by adding a volatile liquid film to the surface. The relative changes in the pseudo vibrations can be found by subtracting a reference measurement from the angular velocity measurement. And, the pseudo vibrations can be reduced by averaging the angular velocities from several independent laser vibrometers located at separated positions along the shaft.

We will introduce a method based on two laser vibrometers, simultaneously monitoring the rotating object. They are arranged in such a way that they observe precisely the same path on the surface of the object, but with a slight time delay due to a finite and known angle between the optical axes of the two vibrometers. In other words: The pseudo-vibrations obtained by both laser vibrometers are the same but, they are occur with a known time delay. While, any physical fluctuations in the angular velocity will occur simultaneously in both laser vibrometers. Finally, simple trigonometry can reveal either the physical fluctuations in angular velocity without pseudo vibrations - or pseudo vibrations without fluctuations.

9141-54, Session 10

Smart image sensor using laser targeting: a multiple barcodes application

Muhammad Junaid J. Amin, Nabeel A. Riza, Univ. College Cork (Ireland)

Optical image sensing systems are used in a variety of applications including industrial inspection, product tracking and security systems. Images acquired via these systems require objects of interest to be located within the imaging receiver's depth of field. In case of laser-based barcode imaging, the readability range of barcode locations is limited due to a constant and restricted imager depth of field arising from fixed focal length lenses present in the imaging system. Furthermore, conventional barcode scanners do not provide target specific intelligence to the laser targeting mechanism via programmable beamforming that can add additional capabilities to the overall transmit-receive active (i.e., laser illuminated) imager. Therefore, to the best of our knowledge, proposed is a novel variable depth of field smart image sensor design using intelligent laser targeting for high productivity multiple barcodes reading applications. Sensor smartness comes via the use of an Electronically Controlled Variable Focal-Length Lens (ECVFL) within the laser transmitter and optical imaging receiver. The ECVFL in the receiver allows a flexible depth of field that enables clear image capture over a range of barcode locations. The proposed design overcomes the limitation of conventional imagers comprising fixed focal length lenses having a constant depth of field which restricts barcode readability range. Imaging of a 660 nm wavelength laser line illuminated 95-bit one dimensional barcode is experimentally demonstrated via the smart imager for barcode target distances ranging from 10 cm to 54 cm. The smart sensor captured barcode images are evaluated using a proposed barcode reading algorithm based on peak recognition and thresholding. Experimental results after computer-based post-processing via algorithm application on captured images show a nine-fold increase in barcode target distance variation range (i.e., range variation increased from 2.5 cm to 24.5 cm) when compared to a conventional fixed lens imager. Applications for the smart sensor include industrial multiple product tracking, marking, and inspection systems.

9141-55, Session 10

Development of disaster prevention method using a combination of sensor network technology and photogrammetry

Nao Minakata, Kyoto Univ. (Japan); Satoshi Nishiyama, Okayama Univ. (Japan); Takao Yano, Kyoto Univ. (Japan)

The prediction of slope failures and landslides and the prevention of resultant damages require the establishment of sound slope behavior monitoring technology, but in the case of a rock slope, there have been very few examples to monitor the extensive area-wide behavior of the slope because the following factors make it difficult to monitor the extensive area-wide behavior of the slope:

- As the time between the appearance of a signal symptom and the occurrence of failure is short unlike in the case of landsliding, a slope failure can occur unexpectedly.

- It is difficult to maintain the measurement devices installed on a rock slope.

- The technology to allow the extensive area-wide tracking of deformations and to be able to save the measurement cost is required.

Considering this situation, we have developed a wireless slope monitoring system using MEMS (Micro Electro Mechanical Systems) sensor units. This unit equipped with a radio communication device works as an inclinometer from the remote. Measurement data is transmitted to the base station

using a radio, and it is possible to observe the rock mass behavior with a web browser through the base station. The measurement system is low-cost and simple enough so that the residents living in dangerous areas can use it to mitigate the risk of rock slope disasters. However, it is very difficult to quantitatively evaluate the risk of rock slope from measurement results because it is impossible to know the precise warning criterion of a rock slope failure. We try to monitor rock slope behavior using a combination of measurement system using MEMS sensor units and the warning criterion simulated by photogrammetry. We made the rock sloe model using photogrammetry and simulated the three-dimensional sloe behavior by discontinuous deformation analysis (DDA). The three dimensional model of the rock slope was reconstructed on the display from measurement data using photogrammetry. In the model, the discontinuities on the reconstructed slope model were recognized, and then by changes in the shape of the slope, we tried to determine whether it is in a dangerous condition by using DDA simulation of the slope behavior. As a result of the analysis, the warning criterion was also considered with the arrangement of MEMS sensor units on the slope. This paper presents an example of monitoring of rock slopes using a combination of state-of-the-art instrumentation using MEMS technology and the warning criterion by photogrammetry. This paper argues that the proposed system can serve as an effective method to eliminate worldwide slope hazards.

9141-56, Session 11

Linear electro-optic effect for nuclear magnetic resonance coil

Reina Ayde, Univ. Claude Bernard Lyon 1 (France); Gwenaël Gaborit, IMEP-LAHC (France) and Kapteos (France); Jean Dahdah, Lionel Duvillaret, Kapteos (France); Raphaël Sablong, Anne-Laure Perrier, Olivier Beuf, Univ. Claude Bernard Lyon 1 (France)

Introduction

The use of metallic coaxial cables in Magnetic Resonance Imaging (MRI) could induce local high Specific Absorption Rate (SAR) [1]. Moreover, the possible crosstalk between coaxial cables in multiple-elements array coil decreases image quality. Optical fiber link could be a promising alternative to coaxial cables for MRI to solve definitively these electromagnetic issues. Here, the conversion of the Radio-Frequency (RF) magnetic field into an electric signal by electro-optic (EO) effect was demonstrated and characterized.

Methods

A RF magnetic field Bz is generated using an emission RF coil associated fed by a function generator. The electrical power Pin of the generator ranges from 14 dBm downto -101 dBm at a frequency of 128.2 MHz (proton resonance frequency at 3T). The receiver coil, designed to be resonant at 128.2 MHz, is located in front of the RF emission coil to probe the magnetic field Bz. Thus an electromotive force ? is induced and applied on an electro-optical micro-chip. This latter, consists of a 6 mm length and 7 μm diameter of a X-cut Ti-diffused LiNbO3 waveguide confined between two coplanar electrodes lying on YZ plane and separated by 18 ?m.

A linear polarized optical probe beam (pigtailed DFB laser, ?=1550 μm) is orientated at 45° relatively to extraordinary and ordinary axis of the waveguide. The Eigen refractive indices of the crystal vary linearly with the induced EZ(Bz), lying in between the electrodes. Hence, a modulation of the laser polarization state appears [2]. A quarter wave plate and a polarizer convert this modulation into a variation of optical power. Finally, this latter is converted into an electrical signal using a fast photodiode. A spectrum analyzer states the output signal power Pout.

Results

The linearity of the EO conversion was established. The curve corresponding to measured values Pout (dBm) versus input power Pin (dBm) closely fit to the expected theoretical values (including noise contributions). The linear coefficient of the fitted curve for the measured data is 0.99 between -70 dBm and 14 dBm of input power. The measurement dynamics of the EO waveguide exceeds 100 dB and the minimum detectable field is 0.1 V.m-1.Hz-1/2 . The associated minimum measurable RF magnetic field corresponds to a signal equalizing electronic noise value (-104 dBm) and reaches 3 pT.

Discussion

The EO signal conversion using a Ti:LiNbO3 waveguide with an endoluminal RF coil was experimentally demonstrated. A very good linearity, dynamic and sensitivity were measured. The minimum RF magnetic field detected appears compatible with real MR experiments. Moreover, this EO conversion leads to a better signal to noise ratio than typical galvanic linked NMR coils, which are much more invasive. So, the next step will be to build a fibered and non-invasive probe to perform first phantom MR images.

References

[1] V. Detti et al., “Assessment of radiofrequency self-heating around a metallic wire with MR T1-based thermometry”, Magn. Res. Med., 66 (2), 2011.

[2] L. Duvillaret et al., “Electro-optic sensors for electric field measurements. I. Theoretical comparison among different modulation techniques”, JOSA B, 19 (11), 2002.

9141-57, Session 11

Multiwavelength laser line profile sensing for agricultural crop characterization

Wolfram Strothmann, Arno Ruckelshausen, Hochschule Osnabrück (Germany); Joachim Hertzberg, Univ. Osnabrück (Germany)

Triangulation-based laser line profile sensing is a widely used technique for precise and fast 3D measurement in industrial applications. More recently, it is used for applications in the area of outdoor agricultural sensing as well. However, in many agricultural applications high resolution range data by itself is insufficient. There is also a strong need for local spectral intensity information, e. g. to monitor the crop quality and yield. As a consequence the combination of image-based range scanners with spectral imaging is often necessary. Under varying environmental conditions this is a tedious and error-prone problem, though. In contrast, the novel approach shown here allows capturing range data along with spectral laser reflectance and pixel-wise backscattering information at multiple, selectable wavelengths using a single sensor system. The system consists of multiple continuous wave (CW) line lasers simultaneously captured by a single monochrome imager. A system ready to capture 3 line lasers at 100 Hz was set up. Line lasers at different wavelengths in the visible and NIR range (up to 950 nm) can be combined in accordance with the requirements of a specific application. Consecutively captured images are matched using sum of absolute differences (SAD) in order for tracking relative movement between the sensor system and the analyzed object. This allows normalizing images before the evaluation of reflectance and scattering, thereby reducing the influence of uncontrolled ambient lightning. Furthermore, the SAD-based matching is used for pixel-accurate assembly of range and reflectance information gathered from different laser lines. The described approach allows scanning and matching multiple laser lines (3 for the prototype, though not limited to 3). It captures spectral intensity data and range data at the same time. This has several advantages. First, it allows replacing multiple sensor systems, e. g. range scanner + spectral imaging, by a single system. Second, it can replace high cost (passive) spectral imaging systems by a cheaper laser-based (active) imaging system for applications were only a few known wavelengths are significant for determining the output. The same is valid for applications were only a few wavelengths are evaluated as analyzing the entire hyper-spectral data cube might not be possible in real time. Third, the system as an active imaging system has higher light usage in comparison with passive spectral imaging systems as no filters nor beam splitting optics are applied. This reduces the energy effort for lightning. Fourth, using relative movement and

SAD-based background subtraction, it makes the evaluation of laser-light backscattering not only at laser points but over the entire surface of objects possible. This can be of interest for recent research on applications using laser-light backscattering e. g. for decay detection in fruits. The prototype was set up and successfully tested for a variety of crops including sugar beets, potatoes, fruits, etc., thereby showing feasibility, matching and line assembly. The outcome can be visualized as range images with multiple overlays representing spectral features or as 3D point clouds with additional spectral laser reflectance and backscattering information at multiple, selectable wavelengths available for each point.

9141-58, Session 11

Modeling fluorescence LIDAR transmission for underwater object detection and recognition

Laura Zotta, Stefania Matteoli, Marco Diani, Giovanni Corsini, Univ. di Pisa (Italy)

Fluorescence Light Detection And Ranging (LIDAR) systems have been proven powerful for detecting and recognizing underwater objects in several applications. Fluorescence systems have been employed mainly for detecting and recognizing oil spill and chemicals dissolved in the sea, and to identify phytoplankton species. In a typical fluorescence LIDAR system, the laser source generates a Ultra-Violet (UV) pulse to induce fluorescence spectra that may be exploited to derive chemical-physical information about object material composition useful to recognition. Thus, the fluorescence spectral signal may be considered as a spectral signature typical of each specific object/material.

In this work a model for fluorescence LIDAR system transmission in the water medium both in the presence and absence of an underwater object is proposed. The developed model describes the transmitted laser beam interaction with the underwater object, the bottom, and the water molecules. Specifically, the fluorescence return signals are modeled involving the inelastic backscattering contributions due to Raman scattering by water molecules and fluorescence by water constituents, bottom, and object.

A range of simulations have been performed modeling the situation of an underwater object submerged at different depths within the water column for a variety of system characteristics and water environmental conditions. Simulation results show the model potential and flexibility for reproducing the signals acquired in different operational scenarios on the basis of various system parameters, acquisition geometries, and water environments. The transmission model may be useful to predict the performance of a given fluorescence LIDAR system in specific underwater object detection and recognition applications. Furthermore, the developed model may be exploited in a signal processing chain in order to enable water column effect compensation and extract the signal contribution pertinent to a given underwater object. In the future, the proposed model will be tested by employing measurements acquired both by means of an ad hoc laboratory experimental set-up and in real water scenarios.

9141-59, Session 11

Design of a wind lidar system based on a low-cost laser diode for wind energy applications

Leilei Shinohara, Thorsten Beuth, Maik Fox, Wilhelm Stork, Karlsruher Institut für Technologie (Germany)

In this paper we present the progress of developing a fiber based coherent Doppler wind LIDAR (CDL) system for the predictive control of wind turbine systems (WTS) that we first introduced as a concept in 2012. Faced with increasing overall energy consumption and pressing social expectations, in the name of “renewable and green energy”, wind energy is facing many challenges in development and application. Nowadays larger WTS is set up in difficult to access locations such as offshores. Such locations bring an overhead in the production cost as well as the Operation & Maintenance (O&M) costs. Our objective is to develop a low-cost laser Doppler wind remote sensing system to support the pitch control system of WTS in order to lower the material requirement which leads to a lower production cost, reduce the O&M costs and decrease the price of wind energy in the long term.

Compare to the State-of-the-Art wind LIDAR system, a low-cost shorter coherent length laser system is used. An optical coherent detection method is chosen for the mega-hertz rang Doppler frequency measurement. In order to achieve a multiple range sensing, a multiple length fiber delay line is used.

The current main focusing of our investigations has been laid on the evaluation of a low cost laser diode as the source of the LIDAR system instead of using a high cost fiber laser system, and the optical design of emitting, receiving, and detection system. The shorter coherence length lasers bring a higher phase noise into the detection, which normally is not used for the coherent LIDAR system. However, such a laser can achieve a higher output power with a lower cost which is very important in our application. In order to bring this laser into the LIDAR system, first of all an evaluation of different laser sources is made. Since each measurement is only taken couple ten micro seconds, in such a short period the evaluation result from standard single longitude mode laser diodes with a temperature controller shows couples to dozens meters coherent length which is good for our applications. Furthermore, a laser coherence controller is added into the system to keep the coherence length. The LIDAR system sends a laser beam into the measurement region and scattered by the aerosols which is collected by the receiver. To avoid the system complexity, sending and receiving using the same optics is very common. The sending and receiving beams separate by a circulator or a beam splitter, however the cross talk or the reflection signal lead strong phase noise in our system. In order to reduce the strong influences from the phase noise, we used an off-axis parabolic mirror with a centered hole for superposition of two beams, sending beam through the center hole, parabolic mirror for receiving the scattering signals. By separating the sending and receiving beams, the noise come from crosstalk or beam splitter can be completely avoid. In the paper we are going to discuss the simulation and experiment result by introducing this concept.

9141-60, Session 11

Research Advances of 3D Flash LiDAR Sensor onboard UAV

Guoqing Zhou, Yilong Liu, Jiazhi Yang, Guilin Univ. of Technology (China); Biao Zhang, Guilin University of Technology (China); Xiang Zhou, Guilin Univ. of Technology (China); Rongye Shi, Peking University (China)

In contrast to scanning LiDAR system, the flash LiDAR has no mechanical moving part, and it is featured with weight, small volume, and energy efficiency. This paper presents the advance of a pre-mature of flash LiDAR sensor including laser emtting system, associate with the pulsed Voltage technology, and optical receive system. A complete laser emitting system, including optical system consisted of emitting system and receive system, controlling systems, electro-optic transmitting system and high precise time-interval measurement system, etc., has been designed and implemented. In this paper, the design and spec. of optical system, as well as the design of high precise time-interval measurement which the critical part of the flash LiDAR, has been presented. In the chapter of experiment, some important experiments have been demonstrated, the explain of the results followed. The efficiency of fiber coupling module is 35.2%, and can be raised by enlarging the applied numerical aperture from 0.3 to 0.5. The APD array receives the laser pulse and generates electrical pulse properly, and can be used as a stop signal for time-interval measurement module. The average error of time-interval measurement is

approximately 1ns which means the average measuring error distance is about 15 cm, and the errors are overestimated. Future work on extensive and on-going investigation and investments for a prototype of flash LiDAR system is drawn up as well.

9141-61, Session 11

NIR-LEDs lighting system for enhancing Brix distinction with saving energy to agricultural products

Kwang-Hoon Lee, Dong-Kil Lee, Yang-Gyu Kim, Anjin Park, Won-Gun Jang, Youngsik Park, Korea Photonics Technology Institute (Korea, Republic of)

Generally the halogen lamp is used widely to the light source in a distinction process such as sugar content, acidity content, the browning of fruits as so on in the field of agricultural products because of the wide range of the wave lengths from UV (Ultra Violet) to NIR (Near Infrared) through the visible range. However the halogen lamp is required much of light power, namely high energy will be needed increasingly if we want to take a good accuracy from the distinction process in short time. Additionally all of light range in the lamp is not used to the process. In regarding the reports, NIR light is used mainly to the process and some part of visible light is used. Therefore the existing process, the property distinction of agricultural production, with the halogen lamp induces the wasting energy and lower detection efficiency than total driving lamp power. For these reasons, we suggest a NIR-LED light system to replace the halogen lamp as well as to increase the light efficiency with energy conserving in the sugar content distinction process. The suggested NIR-LED system is consisted of 4 group of light sources substituted in 4-different wave lengths such as 740nm, 780nm, 810nm and 870nm, which wave lengths are optimized to detect the Brix in Melon. In the analysis of sugar content by Brix index with the NIR-LED lamp system, PLSR regression analysis has been used in, and it has a role to extract the correlation between the level of Brix and the lights. To compare the performance of sugar content prediction of Melon by between the lamp systems, we made the suitable calibrating equations for each lamp system. In the simple result, the halogen lamp system produces the Brix with R2(C)=0.67 and SEC=0.50, and the NIR-LED lamp system has Brix with R2(C)=0.53 and SEC=0.60. The quantitative data from comparison shows that the halogen lamp made a good Brix prediction to the NIR-LED light lamp but the point of view of energy saving, NIR-LED lamp was 1/10 as least to the halogen lamp(NIR-LED : 2.5W, Halogen lamp : 25W were consumed in the test).

The International Year of Light 2015: A Unique Opportunity for Photonics

John M. Dudley, Univ. de Franche-Comté, CNRS Institut FEMTO-ST, Besançon, France

A partnership of over 100 scientific societies and organizations from more than 85 countries has successfully led an initiative to have the year 2015 declared the International Year of Light at the United Nations General Assembly. The science and technology of light have revolutionized medicine, have opened up international communication, and are central to linking the cultural, economic and political aspects of the world. Advances in light-based technology are crucial for sustainable development, they open up new educational horizons, they preserve cultural heritage, and address issues of climate change. An International Year of Light will raise public and international political awareness of the importance of light for the future of global society. This presentation will review its goals and planning.

Horizon 2020 and a European photonics partnership for growth and jobs

Wolfgang Boch , European Commission, Directorate General for Communications Networks, Content and Technology, PHOTONICS Unit, Belgium

This talk will start with an overview of Horizon 2020, the new European programme for research and innovation; it will highlight the most significant novel features and what it will mean for photonics research, development and innovation (RD&I) in Europe. In particular the Photonics Public-Private Partnership (PPP) which has recently been launched will play an essential role in determining the research and innovation priorities for future funding rounds. The key objectives of this partnership is to use research excellence, to boost the innovation eco-system to drive Europe's competitiveness, secure industrial leadership in this highly innovative and economically significant global photonics market; thus creating economic growth and jobs.

The speaker will explain what the Public Private Partnership means for those looking for European funding in this area and will illustrate how upcoming funding opportunities will cover the full scope from research to close to the market innovation and will emphasise the need to address the broader value chain.

Large-Scale Integrated Pphotonics for 21st Century Information Technologies

Raymond G. Beausoleil, Hewlett-Packard Labs., United States

Moore's Law has set great expectations that the performance/price ratio of commercially available semiconductor devices will continue to improve exponentially at least until the end of this decade. Although the physics of nanoscale silicon transistors alone could allow these expectations to (almost) be met, the physics of the metal wires that connect these transistors places stringent limits on the performance of integrated circuits. We will describe a Si-compatible global interconnect architecture — based on chip-scale optical wavelength division multiplexing — that could precipitate an "optical Moore's Law" and allow exponential performance gains until the transistors themselves become the bottleneck. Based on similar fabrication techniques and technologies, we will also present quantum approaches to optically-coupled information processors for computation beyond Moore's Law.

First, we will present recent results demonstrating the optical coupling of nitrogen-vacancy color centers to single-crystal diamond resonators, allowing enhancement of the zero-photon transition rate by a factor of 70. This is a first critical step towards large-scale integrated diamond quantum optical networks, but scaling remains a formidable challenge for the development of practical applications of quantum information technology for commercial utilization. Second, it may be possible to harness devices with explicitly quantum coherent behavior to perform reliable classical computations using quantum feedback control. As an initial step toward this goal, we have demonstrated ultrafast switching in microscale nonlinear optical devices fabricated in amorphous silicon.

Nanoparticle-Enabled Endoscopy for Cancer Diagnosis and Interventional Guidance

Brian C. Wilson, Princess Margaret Cancer Centre and Techna Institute, Univ. of Toronto, Canada

Endoscopy is widely used both for cancer detection/localization/staging and to guide local surgical and minimally-invasive treatments. The sensitivity and specificity of conventional endoscopic imaging and its utility and reliability for interventional guidance rely on changes in one or more intrinsic morphological or optical characteristics of the tumor, which can be highly variable depending on the tumor site and stage. Hence, there has been significant interest in the use of exogenous optical contrast agents ("probes") to highlight lesions, particularly early-stage. The ability to target such agents to tumor-expressed biomarkers is an additional potential benefit. Nanoparticle (NP)-based optical probes have a number of different added advantages that include multi-modality and multiplexed imaging and/or enhancement of focal therapies.

As well as providing a status report on NP-based endoscopy, several different technology platforms under development will illustrate the challenges and potential of these approaches. These platforms include: I. surface enhanced Raman scattering (SERS) NPs for biomarker-multiplexed imaging, II. porphyrin-lipid nanovesical ("porphysome") NPs for fluorescence imaging and photothermal therapy dose enhancement, and III. porphysome-contrast photoacoustic imaging for tumor localization and thermal therapy monitoring. The challenges of translating these technologies into first clinical trials include producing the NPs under gmp conditions and implementing practical and cost-effective imaging instrumentation optimally matched to the nanoparticle properties.

This work is supported by the Terry Fox Research Institute and the National Science and Engineering Council of Canada.

From Classical to Quantum Nonlinear Optics in Photonic Structures

John E. Sipe, Univ. of Toronto, Canada

Nonlinear polarizations described by the $\chi(2)$ and $\chi(3)$ susceptibilities are central to many of the phenomena of classical nonlinear optics, including processes as diverse as second harmonic generation and four-wave mixing. These same susceptibilities govern quantum optical processes in which correlated photons are generated, such as spontaneous parametric down-conversion and spontaneous four-wave mixing. We argue that it is useful to address classical and quantum calculations within the same framework, particularly in the integrated optics structures that will be important for quantum information processing "on a chip." When this is done a more unified picture of nonlinear optics, involving both classical and quantum regimes, results; we show how analytical or numerical classical calculations, or even just the results of classical experiments, can immediately be used to predict the behavior of a device in the quantum regime, and how it will scale as parameters are changed. We also show how it is possible to do a "virtual tomography" of the entangled states that would be generated in a quantum experiment by recording the results of a series of easily-performed classical experiments.

Graphene Quantum Nano-Optoelectronics: Fundamentals and Applications

Frank Koppens, ICFO- The Institute of Photonic Sciences, Spain

Optoelectronics and power conversion based on graphene and related 2d materials is one of the most rapidly developing and exciting areas with prospects for commercial applications. These materials have huge potential for an "all-in-one" solution to the challenges of future opto-electronic technologies, banking on a wide palette of unique aspects such as tuneable optical properties, broadband absorption (from UV to THz frequencies), high electrical mobility for ultrafast operation, and novel gate-tuneable plasmonic properties. In addition, graphene is an excellent host for confining and manipulating optical fields at the nanoscale, with potential for new avenues in quantum information processing, imaging, and sensing.

In this talk, we will review both fundamentals and applications associated to the interactions of light with graphene and related 2d materials. Ongoing efforts towards applications are being discussed, addressing the fields of photodetection, optical modulation, nano-photonics, long-wavelength photonics and power conversion.

Biography: Frank Koppens obtained his PhD in experimental nanoscience and quantum computation at the Kavli Institute of Nanoscience, Delft University, The Netherlands. His PhD work includes several breakthroughs on coherent control of single spins in semiconductor quantum dots. After a postdoctoral fellowship at Harvard University, since August 2010, Koppens is a group leader at the Institute of Photonic Sciences (ICFO). He has received the Christiaan Hugyensprijs 2012, the ERC award as well as the ERC proof-of-concept, and is deputy leader of the optoelectronics workpackage of the graphene flagship (1B€ project for 10 years).

The Nano-optoelectronics group of Prof. Koppens focuses on the realization of a variety of novel active and hybrid nano-photonic and plasmonic devices based on graphene and related 2d materials. The aim is to reveal new physical quantum phenomena related to strong interactions between light and matter, mediated by 2d materials, and to develop new applications for sensing, photodetection and nano-scale light processing and switching. In addition, the group merges graphene nano-photonics with other domains such as opto-mechanics, non-linear optics and light-harvesting.

The Butterfly Effect in Laser Diode Dynamics

Marc Sciamanna, Supélec, OPOTEL and LMOPS, France

The discoveries of deterministic chaos and the related butterfly effect have led to a major paradigm shift, overthrowing two centuries in which the Laplacian viewpoint of dynamical systems was dominant. Soon after the invention of the laser, the possibility of observing chaos in a light signal became a topic of great interest. For fifty years semiconductor lasers have however been considered as damped nonlinear oscillators, and therefore could not be driven into temporal chaos unless with the use of an external forcing, e.g. optical feedback or parameter modulation. We review here the history and applications of light chaos and most importantly recent experiments where polarization chaos is reported from a free-running solitary vertical-cavity surface-emitting laser (VCSEL) [1]. Random-like hopping between non-orthogonal elliptically polarized modes is observed in a quantum dot VCSEL and is identified as chaos from the computation of a positive largest Lyapounov exponent and the analysis of the strange attractor correlation dimension. The observation of polarization chaos from a solitary laser diode brings several fundamental questions and leads to interesting new applications. Recent works include the observation of polarization self-pulsation and optical bistability in the route to chaos and the generation of random numbers at very high bit rates from the sampling and processing of the polarization chaotic laser output.

[1] M. Virte, K. Panajotov, H. Thienpont, M. Sciamanna, "Deterministic polarization chaos from a laser diode", Nature Photon. 7, 60-65 (2013).

Pushing the Boundaries of Silicon Photonics

Michal Lipson, Cornell Univ., United States

Photonics on chip enables monolithic integration of optics and microelectronics for applications such as optical interconnects in which high data streams are required in a small footprint. I will provide an overview of recent advances and challenges in the field. As an example of silicon photonics unique capabilities, I will describe ultrahigh speed devices that enable one to change the structure's optical properties on a time scale that is shorter than the photonic time of flight, leading to novel applications such as optical isolators on a silicon chip.